

Sheng-Hong Chen

Hydraulic Structures

 Springer

Hydraulic Structures

Sheng-Hong Chen

Hydraulic Structures

 Springer

Sheng-Hong Chen
Wuhan University
Wuhan
China

ISBN 978-3-662-47330-6 ISBN 978-3-662-47331-3 (eBook)
DOI 10.1007/978-3-662-47331-3

Library of Congress Control Number: 2015939917

Springer Heidelberg New York Dordrecht London
© Springer-Verlag Berlin Heidelberg 2015

This work is subject to copyright. All rights are reserved by the Publisher, whether the whole or part of the material is concerned, specifically the rights of translation, reprinting, reuse of illustrations, recitation, broadcasting, reproduction on microfilms or in any other physical way, and transmission or information storage and retrieval, electronic adaptation, computer software, or by similar or dissimilar methodology now known or hereafter developed.

The use of general descriptive names, registered names, trademarks, service marks, etc. in this publication does not imply, even in the absence of a specific statement, that such names are exempt from the relevant protective laws and regulations and therefore free for general use.

The publisher, the authors and the editors are safe to assume that the advice and information in this book are believed to be true and accurate at the date of publication. Neither the publisher nor the authors or the editors give a warranty, express or implied, with respect to the material contained herein or for any errors or omissions that may have been made.

Printed on acid-free paper

Springer-Verlag GmbH Berlin Heidelberg is part of Springer Science+Business Media
(www.springer.com)

Foreword 1

When my friend Professor Chen Sheng-hong asked me to write a foreword for his book “Hydraulic Structures,” I accepted with great pleasure. From our first encounter 20 years ago at a Beijing technical conference up to now, we have met regularly either in China or in Europe, including a 6-month stay at the Swiss Federal Institute of Technology in Lausanne (EPFL). We have had long discussions, visited construction sites, and design offices and became friends. The results of these common experiences and exchanges in teaching rock mechanics, dam engineering, and related topics progressively entered into Prof. Chen’s teaching and lecture notes.

Since the increase in world population and the quest for a sustainable development enhances the need for dams for flood control, irrigation, and hydro-electric power plants, Chen decided to gather his lecture notes and write a comprehensive book on “Hydraulic Structures.”

From the lecture notes to this book, there was, however, a strenuous and long way to go, and the author is to be congratulated for the issue of his perseverance. This impressive book is a comprehensive manual of “Hydraulic Structures” encompassing all the steps from the preliminary project to design, construction, monitoring, and maintenance. It is written in a clear way, going into detail where required and gives the interested reader numerous historical and bibliographic references.

Engineers dealing with hydraulic structures will appreciate the practical approach of this vast topic. This includes besides numerous types of dam spillways with their gates, rock slopes, and water tunnels. Teachers and students of Dam Engineering will find in this book—fruit of 20 years of research, teaching, and consulting—most valuable help and information about the various design and calculation methods. The different types and possible sophistication of geometrical modeling are given particular emphasis.

In conclusion, Prof. Chen Sheng-hong's "Hydraulic Structures" should be found in every public or private engineering library, in universities, technical schools, administrations, and design offices.

All my best wishes for an interesting and valuable read!

April 2015

Dr.-Ing. Peter Egger
Former EPFL and KIT
(Karlsruhe Institute of Technology) Professor

Foreword 2

My first meeting with Prof. Chen Sheng-Hong was in Lille (France) in 1999. Since that date we succeeded in building a strong cooperation through yearly academic visits, Ph.D. co-supervision, joint papers in international journals and conferences, and the organization of lectures for students and young researchers.

During this long time of cooperation, I highly appreciated the scientific and the engineering quality of the work of Prof. Chen as well as that of his Ph.D. students. This work resulted in significant advances in the (i) development of numerical modeling for fractured rocks including complex issues such as the mechanical behavior of highly fractured rocks, water flow in fractured rocks, pro-mechanical interaction in fractured rocks, reinforcement of fractured rock mass, behavior of fractured rocks under seismic loading, and (ii) the application of advanced modeling in the design of complex hydraulic structures, in particular large dams, under complex mechanical and environmental loading.

During the visit of Prof. Chen to Lille last year (June 2014), he kindly presented me with an advanced draft of his book (Hydraulic Structures). I was greatly impressed by the large area covered by this book, by the scientific and engineering basis of his work, and by the quality of the presentation. It was obvious that this book responded to a high need in the field of hydraulic structures for students, researchers, academic faculties, engineers, and staff involved in the field of different phases of hydraulic structures: project analysis, design, construction, and management with both local and global approaches. Professor Chen conducted a huge state-of-the-art analysis in the field of hydraulic structures and he crossed it with his own academic and professional expertise. This work resulted in this exceptional book, which I believe will be a reference book in the field of Hydraulic Structures. I would like to outline that this book is one of the first in English presenting the thorough Chinese academic and engineering experience in the field of hydraulic structures.

It is my great pleasure and honor to write this foreword and to encourage students, researchers, engineers, and staffs involved in hydraulic structure to keep this book close at hand; they can find significant responses to a wide range of both academic and professional questions.

Thanks to Professor Chen for this great contribution.

May 2015

Prof. Isam Shahrouh
Distinguished Professor, Former Vice-President
University of Lille—Science and Technology

Preface

It has been nearly 40 years since I started the study of hydraulic engineering as an undergraduate student. I still can recall vividly the magnificent impression in the winter of 1980 by a chance of field practicing tour organized by the university, when I first visited one of the most important hydraulic projects in my country at that time—the Danjiangkou Project with a gravity dam at a height of 97 m. In the following three decades, I have continued my profession in the education and consultant related to hydraulic engineering, and witnessed a rapid progress of China in this field. I have been content with my works and contributed the sustainable career passion to the following mutually promote impetuses.

- In an attempt to enlighten and to encourage our students to have a good command of the courses and to be creatively engaged in their career related to hydraulic engineering, I should organize and present appropriate materials in a logical and imaginative way. The students in my classes and field practicing tours, as well as the practicing engineers in the design and construction institutions, also make contribution by asking penetrating questions and demanding constructive and exercisable answers.
- I am fortunate to have the chance to participate in consultant works for more than 30 giant hydraulic projects in China, which is attributable to the fast economy development in the past three decades. For example, accompanied by the continuous consulting service works for the Xiaowan Project with a 294.5m-high arch dam from 1996 until today, covering its abutment excavation and reinforcement, as well as the dam body placement and reservoir operation, I have been growing up, and growing old of course. By these engineering consulting activities, I am also lucky enough to have got acquainted with and made good friends with some field engineers and to have accumulated experiences concerning engineering design, construction, and management.
- These education and consulting experiences provide a vast engineering background for my academic research of hydraulic structures, covering their deformation, stress, stability, seepage control, and reinforcement. In these researches, the structural issues related to the numerical modeling (e.g., FEM,

BEM, CEM), the coupling of strain/seepage/thermal in jointed rock mass and concrete, the feedback analysis and performance forecasting, etc., are explored and exercised. These research experiences, in turn, promote the university education and help to undertake the engineering consultant.

Not very long ago, I perceived that I was losing career energy and passion due to personal reasons; then I was aware that it could be the right time for stepping into a life stage that Bertrand Russell described in his prose entitled “How to Grow Old” that “... gradually the river grows wider, the banks recede, the waters flow more quietly, and in the end, without any visible break, they become merged in the sea.” Therefore, I decided to complete this last academic book concerning hydraulic structures, as a full stop to conclude a phase of active engineering works, afterward the time may come for another new mission designed by God.

This book is designed to provide useful, pragmatic, basic, and up-to-date knowledge and a road map for the design, construction, and management of hydraulic structures. It is aimed primarily at students who are planning to become hydraulic engineers, but it should also appeal to practicing engineers and engineering geologists with several experiences, as well as at postgraduate students and researchers wishing for a comprehensive and straightforward introduction to the current theories and practices with regard to hydraulic structures. In addition, this book will also be a useful reference for relevant contractors and consultants.

The author hopes to provide a logical and imaginative framework for teaching, studying, and exercising the basic principles of the subject that is developed right from the start and is unfolded through elaboration on the topics related to the planning and investigation, the basic theories (e.g., hydrology, geology, environment, economy, material), the prevalent design tool kits (e.g., analysis of actions and their effects), and the design and construction as well as management of typical hydraulic structures (e.g., layout, configuration, safety calibration, modification, foundation treatment, miscellaneous, surveillance, instrumentation, emergency action plan, aging and mitigation). Continuing the spirit of our predecessors, this book is not only about the fundamentals of related engineering knowledge but also on the concept of sharing experience and knowledge of practice engineers, which is reflected in the following distinct features:

- The history and state of the art concerning hydraulic engineering and structures, equally emphasizing on both the world’s and Chinese recent experiences, are elaborated comprehensively in this book (Chap. 1).
- In many cases, a hydraulic project will be of multi-purpose, and the study comprises a large number of matters; some or all of them will influence the selection of the project site and scale, while others will dominate the types, sizes, and locations of the structures. Hence, the entire project must be investigated as a whole before the design requirements for each single structure (e.g., dam) can be firmly established. This book covers and presents many basic and practical concepts as well as techniques for the design and study of multi-purpose hydraulic projects (Chaps. 2 and 3), inclusive of the planning and economic evaluation for the project; the ecology and environment protection

studies and engineering hydrology and geology studies, for the project sites; and the exploration and property studies on the construction materials (concrete, soil, rock).

- It is a basic requirement that the design of hydraulic structures should make allowance for the actions, and when analyzing a given set of actions, it is commonly necessary to employ many techniques. This book has tried to group the various routine calculation techniques for actions in a single chapter (Chap. 4) so that it would not be necessary to discuss the same technique more than once. However, several particular actions such as elastic resistance and uplift diagram will retain in the corresponding chapters.
- In the recent decades, there has been a magnificent progress in the analysis of structural performances under various anticipated actions, ranging from traditional calculation (e.g., gravity method and trial load method) to modern mathematical modeling (e.g., FEM), from traditional physical (e.g., brittle material) modeling to geomechanical and emulating material modeling, and from laboratory testing to systematic field instrumentation and monitoring. This book is particularly heartened by the illustration of these modern and prevalent tool kits for structural analysis, which should be helpful to those who already have some knowledge of the basic concepts (Chap. 5). In doing so, the attempt to balance and complement the theoretical aspects of the subject with practical applications is exercised.
- The book provides and reviews recent advances in important design methodologies related to the reliability theory, the CAD technique, and the optimal theory (Chap. 6). Students and engineers will find use in these new developments. My hope is that after working through the book and recommended references and bibliography, the reader will be ready and able to design hydraulic structures methodically, thoroughly, confidently, and efficiently.
- The book closely links the whole hydraulic project comprising various hydraulic structures in lieu of traditional structure design solely. Rock slopes are geology bodies located on the surface of the earth's crust, which are often parts of or at the vicinity of hydraulic structures. Their failure and deformation will give rise to an important impact on the safety and normal operation of hydraulic projects. Since more and more hydraulic projects built in western China are situated on the deep valleys in this mountainous area, the stability and stabilization study on them are introduced in this book (Chap. 14). Over these years, the role of the management and aging mitigation has expanded beyond the framework of civil concrete structures to meet various needs of hydraulic structures (e.g., concretes in dam body, tunneling, and spillway lining; rocks and soils of dam body and foundation). The challenges are wider covering issues of environmental protection and sustainable development. Recognizing this, I decide that it is timely for the book to be reviewed and updated by management (Chap. 18). This includes the latest standards and practices as well as technologies applicable and useful for handling of issues such as surveillance and monitoring, nondestructive testing, aging scenarios, and mitigation. My belief is that university students

and engineering practitioners should know and understand the basic principles and techniques described in this book.

- I am well aware that hydraulic structure design is mostly about the application of engineering concepts rather than the use of mathematical and mechanical techniques. Therefore, I am convinced that comprehensive design ability for hydraulic structures should be emphasized throughout the book (Chaps. 7–13, 15–17) rather than merely on computational formulas or routine processes. By providing knowledge and engineering examples concerning the assumptions and principles, parameters and criteria, evaluations and modifications, treatments and countermeasures, etc., the book is intended to present more philosophy in the “design” apart from general description of the hydraulic structures and related computations. I strongly expect that individual lecturers will bring in other engineering examples drawn from their own experiences. However, I do hope that they would discuss their engineering examples within the simple framework described in this book.

The courses at Wuhan University which form the basis of this book have been developed jointly with my colleagues over the decades. I am fortunate to have had assistance and encouragement from them and other friends, particularly Profs Tan Guang-ming (Wuhan University, China), Peter Egger (EPFL, Switzerland), and Isam Shahrour (Lille University 1, France) for their general help and suggestions. My special thanks go to my family and confidants for their warm company, loving concern, and steady support, all these were essential for the successful completion of the book. I am grateful to Wuhan University for allowing me the time to write this book. I also thank Mr. Wang HL and Mrs. Xu Q for their help with the production of some of the figures.

Sheng-Hong Chen

Contents

1	Introduction	1
1.1	Hydraulic Projects and Hydraulic Structures	1
1.1.1	Types of Hydraulic Structures	1
1.1.2	Layout of Hydraulic Projects	3
1.1.3	Classification of Hydraulic Projects and Their Design Safety Standards	6
1.2	History of Hydraulic Engineering	7
1.2.1	3000 BC–300 AD	11
1.2.2	300 AD–1800 AD	12
1.2.3	1800 AD–1940 AD	19
1.2.4	1940–End of Twentieth Century	23
1.3	Water Resources and Hydropower Resources in China	34
1.4	Hydraulic Engineering in China	37
	References	38
2	Planning and Design of Hydraulic Projects	41
2.1	Purposes of Hydraulic Projects	41
2.1.1	Flood Control	41
2.1.2	Irrigation	42
2.1.3	Power Generation	42
2.1.4	Navigation	43
2.1.5	Domestic and Municipal Purposes	43
2.1.6	Environment Protection	44
2.1.7	Recreation and Other Purposes	44
2.2	Planning for Hydraulic Projects	45
2.2.1	Tasks and Requirements of Planning	45
2.2.2	Principles of Planning	46
2.2.3	State of the Art and Trends in the Planning	47
2.3	Ecology and Environment Protection	48
2.3.1	Ecological and Environmental Issues in Hydraulic Projects	48

- 2.3.2 Environmental Protection Design for Hydraulic Projects 51
- 2.3.3 Environmental Impact Monitoring and Reviewing for Hydraulic Projects 55
- 2.4 Engineering Hydrology 56
 - 2.4.1 Engineering Hydrologic Issues in Hydraulic Projects 56
 - 2.4.2 Collection of Hydrologic Messages and Data 56
 - 2.4.3 Hydrologic Computation 57
- 2.5 Engineering Geology 61
 - 2.5.1 Engineering Geologic Issues in Hydraulic Projects 61
 - 2.5.2 Geologic Mapping 62
 - 2.5.3 Geologic Exploration and Investigation 64
 - 2.5.4 Regional Tectonic Stability and Earthquake Hazard 73
- 2.6 Location and Exploration for the Sources of Construction Materials 78
 - 2.6.1 Tasks of Construction Material Investigation 78
 - 2.6.2 Requirements in Planning Phase 79
 - 2.6.3 Requirements in Preliminary Phase 79
 - 2.6.4 Requirements in Feasibility Phase 80
- 2.7 Economy Evaluation 80
 - 2.7.1 Tasks of Economy Evaluation 80
 - 2.7.2 National Economy Evaluation 81
 - 2.7.3 Financial Evaluation 82
 - 2.7.4 Integrated Economy Evaluation 82
- 2.8 Phases of Investigation and Design of Hydraulic Projects 83
 - 2.8.1 Phases of Investigation and Design for Water Resources Projects 84
 - 2.8.2 Phases of Investigation and Design for Hydropower Projects 86
- 2.9 Preparation and Compilation of Design Reports 86
 - 2.9.1 General Requirements 86
 - 2.9.2 Contents and Outlines—Specifically for Feasibility Report 87
- References 90
- 3 Study on Material Properties 95**
 - 3.1 General 95
 - 3.2 Rock 101
 - 3.2.1 Basic Physical and Mechanical Properties of Intact Rock 102

3.2.2	Basic Physical and Mechanical Properties of Discontinuity	103
3.2.3	Basic Physical and Mechanical Properties of Rock Mass.	105
3.2.4	Parameter Back Analysis	107
3.3	Soil.	113
3.3.1	Particle Size and Composition	114
3.3.2	Soil Classification and General Characteristics	118
3.3.3	Density of Soil	119
3.3.4	Permeability of Soil	119
3.3.5	Deformation and Strength of Soil	120
3.3.6	Compaction Characteristics of Soil	122
3.4	Concrete	123
3.4.1	Deformation and Strength of Concrete.	125
3.4.2	Density of Concrete	126
3.4.3	Permeability of Concrete	126
3.4.4	Thermal and Its Related Characteristics of Concrete	127
3.4.5	Durability of Concrete.	131
	References.	135

4 Actions on Hydraulic Structures and Their

	Effect Combinations	139
4.1	Definition and Classification of Actions.	139
4.1.1	Definition of Actions.	139
4.1.2	Classification of Actions	139
4.2	Self-weights	141
4.2.1	Self-weight of Concrete Dam	141
4.2.2	Self-weight of Embankment Dam	143
4.2.3	Earth Pressure	143
4.2.4	Silt (Sediment) Pressure.	144
4.3	Thermal Actions	145
4.3.1	Temporal Features of Thermal Action	145
4.3.2	Spatial Features of Thermal Action and Thermal Stress	146
4.3.3	Computation of Thermal Action	150
4.4	Seepage Actions	154
4.4.1	General Concept.	154
4.4.2	Theory and Computation of Seepage Field.	157
4.4.3	Computation of Seepage Force.	162
4.4.4	Remarks	163
4.5	Fluid Actions	164
4.5.1	Hydrostatic Pressure	164
4.5.2	Hydrodynamic Force.	165

4.6	Seismic Actions	183
4.6.1	Earthquake Inertia Force	184
4.6.2	Seismic Hydrodynamic Forces	188
4.6.3	Seismic Dynamic Earth Pressure.	189
4.7	Load (Action Effect) Combinations.	190
4.7.1	Partial Coefficient Method	191
4.7.2	Safety Factor Method	191
	References.	192
5	Analysis of Action Effects for Hydraulic Structures	195
5.1	General	195
5.2	Physical Modeling	196
5.2.1	Principles of Modeling Similitude.	197
5.2.2	Materials	198
5.2.3	Loads on the Model and Loading System	199
5.2.4	Measuring System.	200
5.2.5	Geomechanical Modeling.	200
5.3	Mathematical Modeling	202
5.3.1	Typical Methods for Mathematical Modeling	202
5.3.2	Limit Equilibrium Method of Rigid Body	206
5.3.3	Finite Element Method for Elastic Problems.	223
5.3.4	Finite Element Method for Seepage Problems.	228
5.3.5	Finite Element Method for Thermal and Thermal Stress Problems	230
5.3.6	Finite Element Method for Dynamic Problems	231
5.3.7	Block Element Method	236
5.4	Monitoring Modeling	239
5.4.1	Statistical Modeling.	240
5.4.2	Deterministic Modeling	245
5.4.3	Mixed Modeling.	247
	References.	249
6	Design Criteria and Methods for Hydraulic Structures.	253
6.1	Safety and Reliability Calibration for Hydraulic Structures.	253
6.1.1	Basic Concepts.	253
6.1.2	Principles of Structural Reliability.	254
6.1.3	Partial Safety Factor Method for Hydraulic Structures.	261
6.2	Optimal Design for Hydraulic Structures	268
6.2.1	Basic Concepts.	268
6.2.2	Mathematical Models for Structural Optimal Design	269
6.2.3	Solution of Optimal Problems	271

6.2.4	Optimal Design of Concrete Gravity Dams	272
6.2.5	Optimal Design of Concrete Arch Dams	274
6.3	Computer Aided Design for Hydraulic Structures	276
6.3.1	Basic Concepts	276
6.3.2	Structure of CAD System	276
6.3.3	Development and Application of CAD Technology in the Chinese Hydraulic Engineering	278
	References	281
7	Gravity Dams	283
7.1	General	283
7.1.1	Features and Working Conditions of Gravity Dams	284
7.1.2	Design Theory and Profile of Gravity Dams	288
7.1.3	Layout of Gravity Dam Projects	288
7.1.4	Main Design Tasks for Gravity Dams	292
7.2	Loads and Load Combinations of Gravity Dams	293
7.2.1	Load Computation—With Particular Emphasizing on the Uplift	294
7.2.2	Load (Action Effect) Combinations	298
7.3	Stability Analysis for Gravity Dams	298
7.3.1	Stability Analysis Along Dam Base	299
7.3.2	Stability Analysis Along Deep-Seated Slip Planes	302
7.3.3	Stability Analysis of Bank-Slope Monoliths	306
7.3.4	Engineering Countermeasures for the Improvement of Stability	307
7.4	Stress Analysis for Gravity Dams	309
7.4.1	Purposes and Methods of Stress Analysis	309
7.4.2	Stress Analysis by Gravity Method	310
7.4.3	Influence of Non-load Factors on the Stress Distribution in Gravity Dams	315
7.4.4	Stress Control Standard for Gravity Dams	318
7.5	Profile Design for Gravity Dams	319
7.5.1	Design Principles	319
7.5.2	Basic Profile	320
7.5.3	Practical Profile	320
7.6	Flood Release and Erosion Prevention of Gravity Dams	322
7.6.1	Design of Dam Spillways	323
7.6.2	Crest Profile of Overflow Spillway Dams	327
7.6.3	High-Speed Flow Problems in the Spillway Dam Design	330
7.6.4	Energy Dissipation and Scouring Protection	330

- 7.7 Appurtenant Features of Gravity Dams 343
 - 7.7.1 Materials for Gravity Dams 343
 - 7.7.2 Appurtenant Structures of Gravity Dams 344
- 7.8 Foundation Treatment and Preparation for Gravity Dams 353
 - 7.8.1 Excavation and Clearance 354
 - 7.8.2 Consolidation Grouting 355
 - 7.8.3 Curtain Grouting 356
 - 7.8.4 Contact Grouting 360
 - 7.8.5 Drainage 360
 - 7.8.6 Treatment of Weak Seams and Karst 362
- 7.9 Roller Compacted Concrete (RCC) Gravity Dams 367
 - 7.9.1 Features of RCC Dams 367
 - 7.9.2 History of RCC Dams 368
 - 7.9.3 Design of RCC Dams 369
 - 7.9.4 Construction of RCC Dams 376
- 7.10 Other Types of Gravity Dams 377
 - 7.10.1 Slotted Gravity Dams 377
 - 7.10.2 Hollow Gravity Dams 379
 - 7.10.3 Stone Masonry Gravity Dams 382
- 7.11 Buttress Dams 384
 - 7.11.1 Classification of Buttress Dams 386
 - 7.11.2 Features of Buttress Dams 386
 - 7.11.3 Massive-Head Buttress Dams 387
 - 7.11.4 Flat-Slab and Multi-Arch Buttress Dams 390
 - 7.11.5 Development of Buttress Dams in China 392
- References 393

- 8 Arch Dams 397**
 - 8.1 General 397
 - 8.1.1 Features of Arch Dams 399
 - 8.1.2 Topographic and Geologic Requirements
for Arch Dams 401
 - 8.1.3 Classification of Arch Dams 404
 - 8.2 Loads and Load Combinations 410
 - 8.2.1 Loads 410
 - 8.2.2 Combinations of Action Effects
(Load Combinations) 411
 - 8.3 Stress Analysis for Arch Dams 412
 - 8.3.1 Methods for Stress Analysis 412
 - 8.3.2 Analysis of Foundation Deformation 415
 - 8.3.3 Independent Arch Method 419
 - 8.3.4 Trial Load Method 421
 - 8.3.5 Strength Calibration for Dam Body 426

8.4	Stability Analysis for Dam Abutments	427
8.4.1	Sliding Conditions of Abutment Rock Masses	429
8.4.2	Analysis Methods	430
8.4.3	Limit Equilibrium Method of Rigid Body	431
8.5	Design of Dam Body	436
8.5.1	Arch Dam Layout	436
8.5.2	Procedure and Key Issues in the Design	439
8.5.3	Optimal Design	446
8.5.4	Factors Affecting the Layout	446
8.6	Flood Release and Energy Dissipation of Arch Dams	451
8.6.1	Layout of Flood Release	451
8.6.2	Types of Dam Body Spillways	452
8.6.3	Energy Dissipation and Scouring Protection of Arch Dams	458
8.7	Materials and Structural Elements of Arch Dams	462
8.7.1	Materials	462
8.7.2	Structural Elements	463
8.8	Foundation Treatment	471
8.8.1	Foundation Excavation	471
8.8.2	Consolidation Grouting	472
8.8.3	Curtain Grouting	474
8.8.4	Foundation Drainage	476
8.8.5	Treatment of Large-Scale Discontinuities	477
8.8.6	Prestress Reinforcement	480
8.8.7	Karst Foundation Treatment	481
8.9	Layout of Arch Dam Projects	481
8.10	Stone Masonry Arch Dams	486
8.10.1	Working Features of Stone Masonry Arch Dams	486
8.10.2	Structural Features of Stone Masonry Arch Dams	487
8.11	RCC Arch Dams	488
8.11.1	Layout of RCC Arch Dam Projects	490
8.11.2	Design of RCC Arch Dams	491
8.11.3	Upstream Waterproof and Construction Joints	494
	References	495
9	Embankment Dams	497
9.1	General	497
9.1.1	Design Requirements for Embankment Dams	499
9.1.2	Classification of Embankment Dams	500
9.1.3	Layout of Embankment Dam Projects	503
9.2	Loads and Load Combinations	505
9.2.1	Loads	505
9.2.2	Load Combinations	506

9.3	Seepage Analysis for Embankment Dams	506
9.3.1	Permeable Characteristics of Embankment Materials	506
9.3.2	Hydraulic Method	507
9.3.3	Seepage Failures and Countermeasures	515
9.4	Stability Analysis for Embankment Dams	519
9.4.1	Strength Properties of Soil	519
9.4.2	Stability Analysis Methods and Allowable Safety Factor	520
9.4.3	Test and Selection of Shear Strength Parameters	525
9.5	Stress and Deformation Analysis for Embankment Dams	528
9.5.1	Consolidation and Settlement Analysis	528
9.5.2	Stress and Strain Analysis	532
9.5.3	Cracking Provisions	533
9.6	Basic Profile of Embankment Dams	535
9.6.1	Crest of Dam	535
9.6.2	Width of Crest	536
9.6.3	Slope of Dam	536
9.7	Soil Available and Compaction Standard	538
9.7.1	General Principles in the Selection of Embankment Materials	538
9.7.2	Requirements for Material Design	539
9.7.3	Materials for Anti-seepage Devices	541
9.7.4	Materials for Dam Shell	548
9.7.5	Materials for Filter, Transition, and Draining	551
9.8	Structural Elements of Embankment Dams	551
9.8.1	Anti-seepage Devices	551
9.8.2	Draining of Dam Body	555
9.8.3	Dam Crest and Slope Pitch	558
9.8.4	Filters	561
9.9	Treatment of Dam Foundation	564
9.9.1	Rock Foundation	565
9.9.2	Sand and Gravel Foundation	566
9.9.3	Earth Foundation	576
9.10	Connection of Embankment Dam with the Other Structures	584
9.10.1	Connection of Embankment Dam with Foundation and Abutments	584
9.10.2	Connection of Embankment Dam with Adjacent Concrete Structures	585
9.11	Selection of Embankment Types	588
	References	590

10 Rockfill Dams	593
10.1 General	593
10.1.1 Classification of Rockfill Dams	596
10.1.2 Requirements for Rockfill Dams	597
10.1.3 Design Theory of Rockfill Dams	599
10.2 Profile of Rockfill Dams	599
10.2.1 Elevation of Dam Crest	599
10.2.2 Crest Width and Structural Requirements	600
10.2.3 Slope	600
10.2.4 Zoning of CFRD	601
10.3 Selection of Rockfill Materials and Compaction Standard	603
10.3.1 Quality Requirements for Rockfill Materials	603
10.3.2 Compaction Requirements for Rockfill Materials	604
10.4 Structural Elements of Rockfill Dam	605
10.4.1 Anti-Seepage Devices	605
10.4.2 Slope Protections	608
10.4.3 Toe Slabs, Face Slabs, and Water Stops of CFRD	609
10.5 Foundation Treatments	616
10.6 Type Selection of Rockfill Dams	618
10.6.1 Materials Available	618
10.6.2 Topographic and Geologic Conditions	619
10.6.3 Climatic Conditions	619
10.7 Further Developments and Other Key Issues of CFRD	619
10.7.1 Advantageous of CFRD	620
10.7.2 Layout of Flood Releasing Works and Balance Between Excavation and Placement	621
10.7.3 Layout of DrawDown Tunnels	622
10.7.4 Materials for Dam Body	623
10.7.5 Cracking of Face Slab	627
10.7.6 Resistance Against Earthquake	629
10.7.7 Protection of Cushion Zone	632
10.7.8 Inverse Filtration	633
10.7.9 Quality Control of Rockfill Placement	634
10.8 Hardfill Dams	635
10.8.1 Anatomy and History	635
10.8.2 Major Features in the Design of Hardfill Dams	638
10.8.3 Mixing Proportion Design and Functional Parameters	639
References	640

11	Sluices and Barrages	643
11.1	General	643
11.1.1	Definitions	643
11.1.2	Working Features of Barrages and Sluices	644
11.1.3	Types of Sluices (Fig. 11.1)	645
11.2	Composition of Sluice and Project Layout	648
11.2.1	Sluice Chamber	649
11.2.2	Upstream Transition	650
11.2.3	Downstream Transition	650
11.2.4	Layout of Barrage Project	651
11.3	Size of Intake	652
11.3.1	Regulating Sluices	653
11.3.2	Head Regulators	656
11.3.3	Drainage Sluices	656
11.4	Energy Dissipation and Scouring Protection	657
11.4.1	Features of Energy Dissipation and Scouring Protection	657
11.4.2	Layout of Energy Dissipation and Scouring Protection	657
11.4.3	Stilling Basins	658
11.4.4	Other Issues in the Energy Dissipation and Anti-scouring Design	667
11.5	Under Seepage Control for Barrages and Sluices	669
11.5.1	Creep Line Layout	670
11.5.2	Anti-seepage and Draining Devices	672
11.5.3	Seepage Analysis for Barrage and Sluice Foundation	675
11.5.4	Control of Seepage Failure	680
11.5.5	Bypass Seepage and Its Control	681
11.6	Layout and Structural Design for Sluice Chambers	682
11.6.1	Bottom Floors	682
11.6.2	Piers	689
11.6.3	Gates	693
11.6.4	Parapet Walls	693
11.6.5	Joints and Water Stops	694
11.6.6	Service and Access Bridges	696
11.7	Stability Analysis and Foundation Treatment	696
11.7.1	Loads and Load Combinations	696
11.7.2	Contact Stress and Bearing Capacity	698
11.7.3	Stability Analysis Against Sliding	700
11.7.4	Floatation Computation	701
11.7.5	Settlement Computation	702
11.7.6	Foundation Treatment	702

11.8	Abutment Transition Structures.	707
11.8.1	Type of Abutment Transition Structures.	707
11.8.2	Wing Walls	707
11.8.3	Structure of Retaining Walls	709
	References.	711
12	Shore Spillways	715
12.1	General	715
12.1.1	Types of Separate Spillways.	715
12.1.2	Applicability of Separate Spillways.	717
12.2	Chute (Proper Open Channel or Trough) Spillways.	717
12.2.1	Entrance (Access or Approach) Channels.	718
12.2.2	Control Structures	720
12.2.3	Chutes.	724
12.2.4	Terminal Structures and Outlet Channels	735
12.3	Spillways of Other Types.	736
12.3.1	Side-Channel Spillways	736
12.3.2	Drop Inlet (Shaft or Morning Glory) Spillways.	742
12.3.3	Siphon Spillways	745
12.3.4	Baffled Apron Drop Spillways	747
12.3.5	Culvert Spillways	747
12.4	Emergency Spillways	748
12.4.1	Overtopping Emergency Spillways	749
12.4.2	Flushing Embankment Emergency Spillways	750
12.4.3	Blast Washout Emergency Spillways.	750
12.5	Type Selection and Layout of Spillways	751
	References.	752
13	Hydraulic Tunnels	755
13.1	General	755
13.1.1	Types and Functions of Hydraulic Tunnels	756
13.1.2	Working Features of Hydraulic Tunnels.	758
13.2	Layout of Hydraulic Tunnels	759
13.2.1	Procedure of Layout	759
13.2.2	Longitudinal Profile	760
13.2.3	Gates in the Tunnel.	762
13.2.4	Route of Tunnels	764
13.3	Intakes	765
13.3.1	Types of Tunnel Intakes	766
13.3.2	Components of Tunnel Intakes	768
13.4	Body of Tunnels.	771
13.4.1	Shape of Cross Section	771
13.4.2	Cross-sectional Dimension	772
13.4.3	Lining of Tunnel Body	774

- 13.5 Outlets and Energy Dissipation 781
- 13.6 Countermeasures Against Cavitation to Hydraulic Tunnels . . . 783
 - 13.6.1 Profile Design 784
 - 13.6.2 Aeration Slots 786
- 13.7 Stability of Surrounding Rock Mass During Tunneling 787
 - 13.7.1 Stress Concentration in Surrounding Rock Mass 787
 - 13.7.2 Deformation of Surrounding Rock Mass 788
 - 13.7.3 Stability of Surrounding Rock Mass 788
- 13.8 Structural Analysis of Lining 790
 - 13.8.1 Design Loads and Their Combinations 793
 - 13.8.2 Elasticity Theory for Lining Calculation 800
 - 13.8.3 Structural Mechanics Method
for Lining Calculation 804
- 13.9 Bolt and Shotcrete Supports 804
 - 13.9.1 Principles of Bolt and Shotcrete Supporting 804
 - 13.9.2 Design of Bolting and Shotcrete Support 806
 - 13.9.3 Several Notes on the Bolt
and Shotcrete Supporting 809
- References 810

- 14 Rock Slopes in Hydraulic Projects 813**
 - 14.1 General 813
 - 14.1.1 Classification of Rock Slopes 817
 - 14.1.2 Main Tasks in the Rock Slope Design 819
 - 14.2 Factors Influencing the Stability of Rock Slope 822
 - 14.2.1 Stratum and Rock Characteristics 823
 - 14.2.2 Geologic Structure 823
 - 14.2.3 Rock Mass Structure 824
 - 14.2.4 Action of Water 826
 - 14.2.5 Action of Vibration (Shaking) 828
 - 14.2.6 Slope Shape 830
 - 14.2.7 Geostress 830
 - 14.2.8 Action Due to Other Engineering Structures 832
 - 14.3 Design Criteria for Slopes 832
 - 14.3.1 Absolute Design Standard—Design Code
Specifications 834
 - 14.3.2 Relative Design Standard 835
 - 14.4 Limit Equilibrium Method for Slope Stability Analysis 838
 - 14.4.1 Specifications for Hydraulic Slopes 838
 - 14.4.2 Engineering Application—The Right Reservoir
Bank Landslide (the Pubugou Project) 839

14.5	Numerical Method for Slope Stability Analysis.	840
14.5.1	Finite Element Method	841
14.5.2	Block Element Method	846
14.6	Slope Stabilization	850
14.6.1	Principles in the Slope Stabilization	850
14.6.2	Stabilization Countermeasures	851
	References.	865
15	Hydraulic Steel Gates	869
15.1	General	869
15.1.1	Functions and Components	869
15.1.2	Classification of Gates.	870
15.1.3	Brief History of Hydraulic Gates	873
15.2	Basic Requirements for the Layout of Gates.	874
15.3	Plate Steel Gates.	875
15.3.1	Types of Plate Gates	876
15.3.2	Layout and Structure of the Leaf of Plate Gate.	878
15.3.3	Raising and Lowering Efforts and Hoists.	886
15.4	Radial Gates.	888
15.4.1	Leaf Structure and Layout of Radial Gate	888
15.4.2	Raising and Lowering Efforts and Hoists.	891
15.5	Deep Gates	892
15.5.1	General	892
15.5.2	Deep Plate Gates	893
15.5.3	Deep Radial Gates	894
	References.	895
16	Irrigation and Drainage Works	897
16.1	General	897
16.2	Water Intake Works	898
16.2.1	Types and Features of Water Intake Works and Their Positions	898
16.2.2	Layout of Undammed Intakes.	901
16.2.3	Layout of Lateral Intakes with Water Damming by Barrage.	904
16.3	Aqueducts	911
16.4	Inverted Siphons and Culverts	915
16.4.1	Inverted Siphons.	915
16.4.2	Culverts.	920
16.5	Water Measuring	923
16.5.1	Particular Measuring Devices	923
16.5.2	Measuring by Existing Hydraulic Structures.	927
	References.	927

- 17 Appurtenant Works 929**
 - 17.1 General 929
 - 17.2 Navigation Structures 929
 - 17.2.1 Classification of Navigation Structures 929
 - 17.2.2 Ship Locks. 930
 - 17.2.3 Ship Lifts 940
 - 17.2.4 Selection of Navigation Structures. 945
 - 17.2.5 Location of Navigation Structures 945
 - 17.3 Timber Passing Structures 947
 - 17.3.1 Log Ways 947
 - 17.3.2 Timber Slides 950
 - 17.3.3 Log and Raft Conveyers 951
 - 17.3.4 Selection of Timber Passing Structures 951
 - 17.4 Fish-Passing Structures 952
 - 17.4.1 Classification of Fish-Passing Structures 953
 - 17.4.2 Fish Ladders 954
 - 17.4.3 Fish Locks 958
 - 17.4.4 Fish Elevators 960
 - 17.4.5 Downstream Fish-Passing Facilities. 960
 - 17.4.6 Layout of Fish-Passing Facilities. 961
 - 17.5 Floating Debris Discharging Structures 963
 - References. 964

- 18 Operation and Maintenance of Hydraulic Structures 967**
 - 18.1 General 967
 - 18.2 Hydrologic Observation and Forecasting 967
 - 18.2.1 Water Regime Observation 968
 - 18.2.2 Hydrologic Forecasting 968
 - 18.2.3 Reservoir Operation 970
 - 18.3 Safety Surveillance for Hydraulic Structures. 970
 - 18.3.1 Safety Inspection for Dams 971
 - 18.3.2 Monitoring for Dams. 973
 - 18.3.3 Safety Review for Dams 974
 - 18.4 Instrumentation for Hydraulic Structures 975
 - 18.4.1 Deformation Monitoring 975
 - 18.4.2 Seepage Monitoring 992
 - 18.4.3 Strain/Stress and Temperature Monitoring 996
 - 18.4.4 Automated Measurement Techniques
and Data Acquisition for Dams. 1003
 - 18.5 Remedial Action. 1005
 - 18.5.1 The Need for Remedial Action. 1005
 - 18.5.2 Requirements for Remedial Action 1005
 - 18.5.3 Emergency Action Plans (EAP) for Dams 1006

18.6	Aging of Hydraulic Structures	1008
18.6.1	Nondestructive Examination	1009
18.6.2	Aging Diseases of Hydraulic Structures	1014
18.6.3	Mitigation of Aging	1022
	References.	1026

Chapter 1

Introduction

1.1 Hydraulic Projects and Hydraulic Structures

The major function of a hydraulic project (i.e., water project) is to alter the natural behavior of a water body (river, lake, sea, groundwater) by concentrating its flow fall. It is intended for purposeful use for the benefits of national economy and to protect the environment, including electric power generation, flood control, water supply, silt mitigation, navigation, irrigation and draining, fish handling and farming, ecologic protection, and recreation. It is common that a number of hydraulic structures (i.e., hydraulic works) of general or special purposes are constructed to form a single or integrated hydraulic project to comprehensively serve foregoing purposes. Such a project is known as the water resources project or hydropower project in China, and the latter is primarily for electric power generation in addition to other possible benefits. The general-purpose and special-purpose hydraulic structures which are parts of a hydraulic project can be further divided into main, auxiliary, and temporary structures.

1.1.1 Types of Hydraulic Structures

Hydraulic structures are submerged or partially submerged in water. They can be used to divert, disrupt, or completely stop the natural flow. Hydraulic structures designed for integrated river, lake, or seawater projects are referred to river, lake, and marine water works, respectively. By the features of their actions on the stream flow, main hydraulic structures are distinguished as water retaining structures, water conveying structures, and special-purpose structures.

1. Water retaining structures

Dams (inclusive barrages) are typical water retaining structures that affect closure of the stream and create heading-up afflux. Made of various materials, dams fall into soil and/or rockfill embankment, concrete, reinforced concrete, masonry, and wooden. Of which, the first two are the most prevalent nowadays.

(a) Concrete dams

By the structural features, concrete dams are termed as gravity (massive), buttress, and arch.

A gravity dam is a concrete structure resisting the imposed actions by its weight and section without relying on arch. In its common usage, the term is restricted to solid masonry or concrete dam which is straight or slightly curved in plan. The downstream face of modern gravity dam is usually of uniform slope which if extended would intersect the upstream face at or near the maximum reservoir level. The upstream face is normally of steep uniform slope or vertical with a steep batter (flared) near the heel. The upper portion is thick enough to resist the impact of floating debris and to accommodate a roadway and/or a spillway. The thickness of section at any elevation is adequate to resist sliding and to ensure compressive stresses at the heel under different loading conditions.

A buttress dam depends principally upon the water weight in addition to the concrete weight for stability. It is composed of two major structural elements: a water-supporting deck of uniform slope and a series of buttresses supporting the deck. Buttress dams are customarily further classified according to the deck type: A flat slab dam is one whose deck comprises flat slabs supported on the buttresses; a multi-arch dam consists of a series of arch segments supported by buttresses; and a massive-head buttress dam is formed by flaring the upstream edges of the buttresses to span the spaces between the buttresses.

An arch dam is always curvilinear in plan with its convex side facing headwater. On its vertical cross section, the dam is a relatively thin cantilever slightly curved. An arch dam transmits a major part of the imposed actions to the canyon walls mainly in the form of horizontal thrusts from its abutments.

By the water flow features, concrete dams may be non-overflow and overflow, and the latter releases water through openings (outlets) that can be free overflow and/or submerged under the headwater level, i.e., orifices, deep openings, and bottom outlets.

(b) Embankment dams

Embankment dams are massive fills of natural ground materials composed of fragmented particles, graded and compacted, to resist seepage and sliding. The friction and interlocking of particles bind the material particles together into a stable mass rather than by the use of a cementitious substance (binder). All modern embankment dams have basically trapezoidal cross section with straight or broken contour of upstream and downstream slopes. The topmost edge of the slope is the crest, and the lowermost edge of the slope is the toe or heel. Horizontal portions on the dam slope surfaces are termed as “berms.”

The actions of the impounded reservoir create a downward thrust upon the mass of the embankment, greatly increasing the pressure of the dam on its foundation, which in turn adds force effectively to seal and make the underlying dam foundation waterproof, particularly at the interface between the dam and its streambed.

There are various types of embankment dams. On the basis of the natural ground materials used, earthfill dams are compacted by fine-grained soils accounted for over 50 % of the whole placed volume, whereas rockfill dams are compacted by coarse-grained materials accounted for over 50 % of the whole placed volume. On the basis of section zoning, homogenous and zoned embankment dams may be distinguished, and among the latter category, the term “decked rockfill dams” is used particularly for the rockfill dams employing thin upstream membrane of non-natural materials such as asphaltic concrete, reinforced concrete, and geomembrane.

Embankment dams are commonly constructed as non-overflow. However, small rockfill dams are occasionally allowed for being topped over the crest if the dam crest and downstream face are adequately reverted (Chanson 2009; Manso and Schleiss 2002).

2. Water conveying structures

Water conveying structures are artificial channels cut in the ground and made of either ground materials such as soil and rock (e.g., canals and tunnels) or artificial materials such as concrete and metal (e.g., aqueducts, flumes, siphons, pipelines).

3. Special-purpose hydraulic structures

Special-purpose hydraulic structures are accommodated in a hydraulic project to meet the requirements of:

- Hydroelectric power generation, inclusive power plants, forebays and head ponds, surge towers and shafts, etc.;
- Inland waterway transportation, inclusive navigation locks and lifts, berths, landings, ship repair and building facilities, timber handling structures and log passes, etc.;
- Land reclamation, inclusive sluices (head works), silt tanks, irrigation canals, land draining systems, etc.;
- Water supply and waste disposal (sewerage), inclusive water intakes, catchment works, pumping stations, cooling ponds, water after treatment plants, sewage headers, etc.
- Fish handling, inclusive fish ways, fish locks and lifts, fish nursery pools, etc.

1.1.2 Layout of Hydraulic Projects

A hydraulic project is usually huge and comprises several hydraulic structures erected over an extensive geographic area and is intended to serve large-scale social and economic program. The hydraulic project with retaining structures built on the

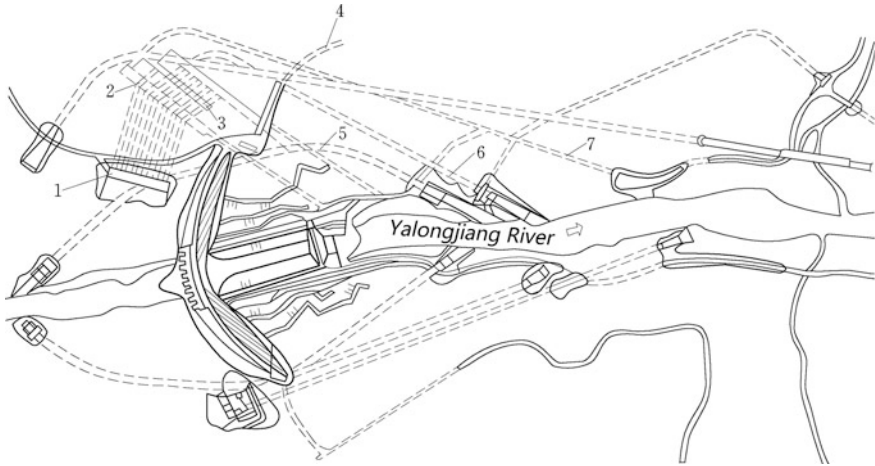


Fig. 1.1 Ertan Hydropower Project (arch dam)—China 1 Power intake, 2 Main machine house, 3 Main transformer chamber, 4 Left bank high way, 5 Number 2 tail race tunnel, 6 Number 1 tail race tunnel, 7 Access tunnel for power house

main stream of a river or canal, which creates afflux head of water, is known as operating under head; otherwise, it would be a headless (non-head) water project. Figures 1.1, 1.2, and 1.3 show three typical water resources and hydropower projects in China.

Fairly number of alternative layout schemes are compared with respect to technology and economy aspects before the final optimal layout scheme is decided, which should facilitate the construction and the management as well as reduce the investment, on the premise of ensuring project safety. The key issues facing the layout of a hydraulic project are as follows:

1. Flood release during service period and river diversion during construction period commonly dominate the project layout. The spillway should attain sufficient discharge capacity; meanwhile, its detrimental effects such as downstream scouring, silt depositing, and disturbance to power plant operation should be avoided or alleviated. The possibility of the reconstruction and reuse of temporary diversion structures as part of permanent flood or silt releasing structures is taken into account in the project layout, too.
2. Power plant should be located at places of easy to access and outgoing power lines. Concrete dam projects usually install power plant at dam toe. Bank power plant or underground power plant is also frequently employed under the situation of narrow river rapids or for the purposes to avoid construction interference and/or to collect more head.
3. Navigation structures (e.g., ship lock and lift) are located on the one or on the both riverbanks, where the flow conditions are advantageous for the upstream and downstream approach and berth of vessels. To avoid the interferences in the

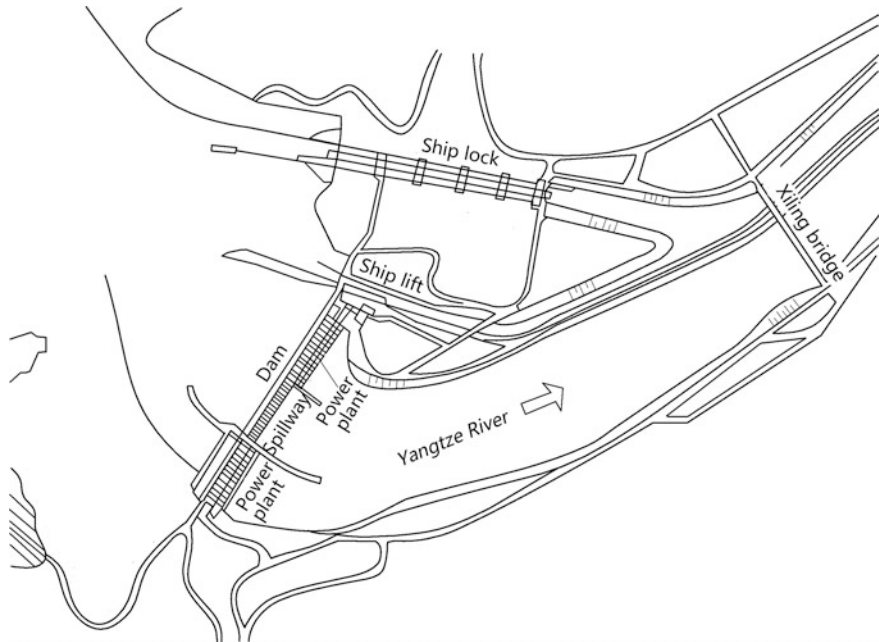


Fig. 1.2 Three Gorges Water Resources Project (gravity dam)—China

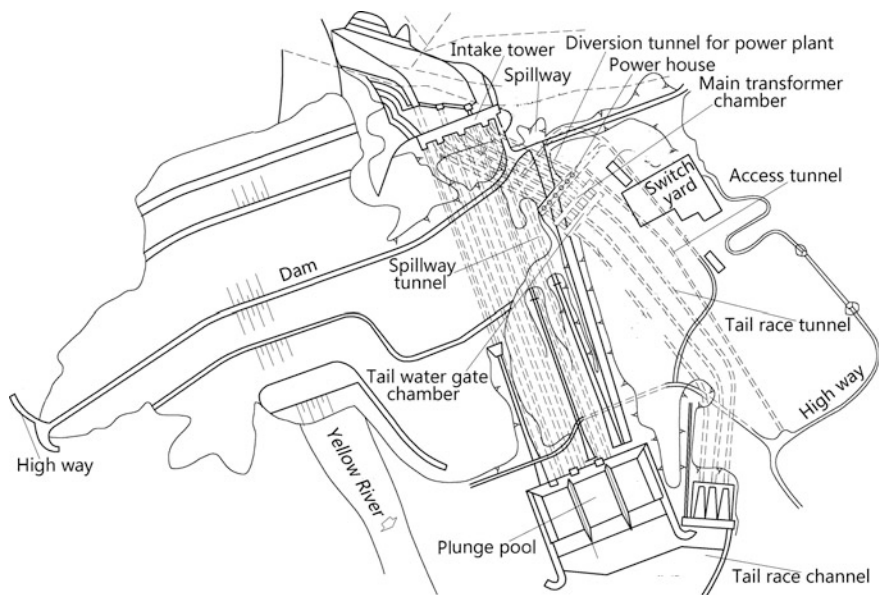


Fig. 1.3 Xiaolangdi Water Resources Project (embankment dam)—China

construction and operation, navigation structures are best to be separated with the intakes and the tailrace channel of the power plant.

4. Silt flushing structures should be layout carefully with respect to the reservoir/pool sedimentation process and the silt protection requirement of the project, of which the intakes of power plant and canal head works are particularly emphasized. It is customarily to provide certain sized bottom outlets as desilting sluices (excluders) for flushing silt, to keep effective reservoir storage capacity and free of silt in front of intakes. The solid gravity dams and arch dams may meet this requirement by providing bottom outlets with low intake elevation and large orifice size. On the contrary, tunnels for releasing flood inflow and flushing silt are demanded for the projects using embankment dams.
5. Dam safety is the most important. Particularly, the serious structural and equipment accidents as well as the civil air defense of dams and power plants should not be overlooked. The major countermeasure is drawing down or emptying reservoirs in time. To meet this requirement, in addition to crest spillway, intermediate and bottom outlets have to be provided to control the reservoir water level as flexibly as possible.

Viewing from the high dams and large power stations in operation or under construction in China, the project layout is often, although not always, focused on flood releasing and powerhouse locating, which may be grouped into several representatives with respect to major dam types, and will be presented in the subsequent corresponding chapters of this book.

1.1.3 Classification of Hydraulic Projects and Their Design Safety Standards

In the first step, water resources and hydropower projects are distinguished as 5 classes in China according to their scales, benefits, and importance in the society and national economy. Secondly, permanent hydraulic structures in the project are classified into 5 grades according to their importance in the project concerned. The higher the structure grade, the higher the design safety standard is stipulated, regarding:

- Flood-resisting ability, e.g., flood standard (recurrence interval), freeboard height, etc.;
- Earthquake-resisting ability, e.g., seismic design standard, earthquake counter-measures, etc.;
- Strength and stability, e.g., material strength, allowable safety factor against sliding, crack prevention requirements, etc.;
- Material type, quality, durability, etc.;
- Operation reliability, e.g., margin of structural size, monitoring instrumentation, etc.

There are two state standards in China for the classification of water resources and hydropower projects with corresponding design safety standards, due to the organization reshuffling history of the state central government: One is mainly adopted by the design institutes belong to the formal Ministry of Water Resources (with entry word of SL), and another one is mainly adopted by those belong to the formal Ministry of Electric Power (with entry word of DL).

1. Classification indices according to SL252-2000 2000 “Standard for classification and flood control of water resources and hydroelectric project” (Tables 1.1 and 1.2)
2. Classification indices according to DL 5180-2003 2003 “Standard for classification and design safety of hydroelectric project” (Table 1.3)
3. Grading of permanent hydraulic structures and flood standards

Permanent structures are classified into 5 grades according to their importance in the project accommodated, both in the design codes of SL252-2000 2000 and DL 5180-2003 2003 (Table 1.4).

The design reference period of permanent retaining structures with grade 1 is stipulated as 100 years, while that of the other permanent structures is 50 years. For particular large-scale projects, the design reference period of permanent retaining structures must be decided after special studies; the design reference period of temporary structures may be decided according to their anticipated service time plus possible construction delay.

The flood standard in terms of recurrence interval for permanent structures is listed in Tables 1.5, 1.6, and 1.7.

DL 5180-2003 also recommends the structural reliability theory for the design of hydraulic structures, and the target reliability index is stipulated to represent the design safety standard. However, where the structural reliability design is not available due to the delay in the design code updating for a certain structure, the determinant design method may have to be employed, and under such circumstances, the allowable safety factor is stipulated to represent the design safety standard. In the application of structural reliability theory, the structural grades 1–5 (Table 1.4) are corresponding to the structural safety grades I, II, and III, respectively.

The other design safety standards for specific structural problems, if any, will be discussed in the subsequent chapters of this book.

1.2 History of Hydraulic Engineering

The history of applying water to the farmland and residences may date back to the dawn of human civilization. The remote history of hydraulic structures concerning when and where irrigation systems and dams were first constructed is not very clear. However, study on ancient Egypt, Iraq (Babylonia), Iran (Persia), India, Sri Lanka (Ceylon), China, Greece, and Roman does confirm that such hydraulic works in these lands were begun thousands of years ago (Jansen 1980).

Table 1.1 Classification indices of water resources and hydropower projects (SL252-2000)

Class	Scale	Flood control			Water logging control	Irrigation	Water supply	Electric power generation
		Gross storage capacity of reservoir (10^8 m^3)	Importance of the cities and industry enterprises protected	Farmland protected ($0.66667 \times 10^3 \text{ ha}$)				
I	Large (1)	≥ 10	Very important	≥ 500	≥ 200	≥ 150	Very important	≥ 1200
II	Large (2)	10-1.0	Important	500-100	200-60	150-50	Important	1200-300
III	Medium	1.0-0.10	Moderate	100-30	60-15	50-5	Moderate	300-50
IV	Small (1)	0.10-0.01	General	30-5	15-3	5-0.5	General	50-10
V	Small (2)	0.01-0.001	N/A	< 5	< 3	< 0.5	N/A	< 10

Table 1.2 Classification indices of barrage (sluice) projects (SL252-2000)

Class	I	II	III	IV	V
Scale	Large (1)	Large (2)	Medium	Small (1)	Small (2)
Flow discharge through barrage (m ³ /s)	≥5000	5000–1000	1000–100	100–20	<20

Table 1.3 Classification indices of hydropower projects (DL 5180-2003)

Class	Scale	Gross storage capacity of reservoir (10 ⁸ m ³)	Installed capacity (MW)
I	Large (1)	≥10	≥1200
II	Large (2)	<10 ≥ 1.0	<1200 ≥ 300
III	Medium	<1.0 ≥ 0.10	<300 ≥ 50
IV	Small (1)	<0.10 ≥ 0.01	<50 ≥ 10
V	Small (2)	<0.01	<10

Table 1.4 Grading of permanent hydraulic structures

Project class	Grade of permanent hydraulic structures	
	Main structures	Auxiliary structures
I	1	3
II	2	3
III	3	4
IV	4	5
V	5	5

Table 1.5 Flood standard for the permanent structures in mountainous and hilly areas

Item		Grade of hydraulic structures				
		1	2	3	4	5
Recurrence interval of design flood (year)		1000–500	500–100	100–50	50–30	30–20
Recurrence interval of check flood (year)	Embankment dams	MPF, or 10,000–5000	5000–2000	2000–1000	1000–300	300–200
	Concrete and masonry dams	5000–2000	2000–1000	1000–500	500–200	200–100

In the Black Desert of modern Jordan, there is a ruin of a dam built between 3000 BC and 4000 BC with some real skill. Egypt claims to have the world’s oldest dam built about 5000 years ago to store water for drinking and irrigation, relating to the founding of Memphis city on the River Nile. The historian Herodotus attributed it to Menes, the first king of the initial Egyptian dynasty.

In Babylonia and Assyria, irrigation technique was extensively booming along the Tigris and Euphrates river valleys as early as 2100 BC and reached its peak later in Sassanian times.

Table 1.6 Flood standard for the permanent structures in plain areas

Item		Grade of hydraulic structures				
		1	2	3	4	5
Reservoir project	Recurrence interval of design flood (year)	300–100	100–50	50–20	20–10	10
	Recurrence interval of check flood (year)	2000–1000	1000–300	300–100	100–50	50–20
Barrage (sluice) project	Recurrence interval of design flood (year)	100–50	50–30	30–20	20–10	10
	Recurrence interval of check flood (year)	300–200	200–100	100–50	50–30	30–20

Table 1.7 Tide standard for the permanent structures in littoral areas

Grade of hydraulic structures	1	2	3	4, 5
Recurrence interval of design tidal level (year)	≥100	100–50	50–20	20–10

The Persians of ancient times recognized well the importance of irrigation to the civilization. By excavating underground water tunnel and gallery systems—Kanats (also called Karez in Baluchistan)—they led water flow down the system and then collected and carried it to the farmlands. Although the origin of Kanats has not been ascertained well, yet in the ruins at Sialak near Kashan, their traces considered to be as much as 6000 years old have been discovered.

Near Lakorian Pass and in the Mashkai Valley in the southern region of Baluchistan (Pakistan), ruins of pre-Aryan dams are found, which shows that there were ancient irrigation systems. In the centuries following the Aryan invasions in the middle of the second millennium BC, irrigation on this subcontinent was boosted. Archeological excavations at Harappa, Mohenjo Daro, and Kot Dijji all revealed the existence of advanced civilizations supported by irrigation systems.

Sri Lanka (Ceylon) also possesses ancient irrigation systems. After their immigration from south Asia subcontinent in the fifth century BC, the Sinhalese engineers established daring precedents in earthfill embankment construction and implemented irrigation systems, which supported a flourishing economy and society until the land was overcome by new invaders (Malayan) in about 1200 AD.

Water resources application in China onsets very early attributable to her brilliant and ancient civilization. Engineers constructed massive canals with levees and dams to channel the water flow for irrigation, as well as locks to allow ships to pass through. Originally, the Chinese solved the problem of ship transportation in the region of river rapids by building dikes with slopes on the banks of the canal. The boats were then manually hoisted up and down the slopes. Later, they discovered that by constructing two dams (as sidewalls) a certain distance apart, the boats could enter the pool created between them where the water level might be slowly raised or lowered down. Vertical grooves were cut into opposite sides of the sidewalls, and tree trunks were fitted horizontally into the grooves, which held the water at the

highest level. This invention is now recognized worldwide as the ancestor of hydraulic gates. The Anfeng Tang (dyke) of 10 m high, the oldest operational embankment dam in China located in the Shouxian County, Anhui Province, was built in 598–591 BC, by Sun Shu'ao, the premier of the State Chu who is respected as the first hydraulic engineer in China. Another important hydraulic engineer in China, Ximen Bao, was credited of starting the practice of large-scale canal irrigation systems during the Warring States Period (481–221 BC). The famous Dujiangyan (weir or barrage), still a functioning hydraulic project today, was built by Li Bing and his son in the Qin dynasty (221–207 BC), which provided irrigation water for the vast rice fields in the prosperous Western Sichuan Plain.

Hydraulic engineering had been highly developed in Europe under the aegis of the Roman Empire where the people were especially creative in the construction and maintenance of aqueducts, for the purposes of supplying water to and removing sewage from their prospered cities. They also used hydraulic mining methods to prospect and extract alluvial gold deposits in a technique known as hushing.

Eupalinos, an ancient Greek engineer, built the tunnel of Eupalinos on Samos in the sixth century BC, which is an important contribution to both civil and hydraulic engineering. It was dug from both ends which required the workers to keep an accurate direction and elevation so that the two tunnel segments met and to maintain a sufficient slope to allow for the flowing of water.

The mechanical power of falling water is a traditional resource used for services and productive purposes in the whole civilization history. However, prior to the widespread availability of commercial electric power, hydropower in ancient period was merely used for irrigation and operation of simple hydraulic machines, such as water mills, textile machines, and sawmills. For example, it was used by the Greeks to turn water wheels for grinding wheat into flour more than 2000 years ago.

According to various well-known literatures (ICOLD 2013; Smith 1971; Jansen 1980; Schnitter 1994; Zhu 1995), the history of hydraulic engineering may be roughly divided into four major stages based on the technique features, which will be summarized in the following subsections.

1.2.1 3000 BC–300 AD

This is a dawn period of hydraulic engineering in the human history featured by embankment dams and their impounding reservoirs mostly for water irrigation, with or partially with (insufficient) spillways or intakes. Ancient Roman dams for drinking and SPA water supply were often combined with other hydraulic structures such as upstream masonry, downstream embankment fill, aqueduct, and canal.

Ruins in ancient India and Sri Lanka provide evidences of how reservoirs and embankment dams were built by early people: It involved the placement of earthfill across streams using materials transported in baskets or other containers. Turning to the most available materials, the ancient dam builders made use of soils and gravels freely. Compaction was accomplished incidentally by the trampling feet of the

carriers. Due to the lack of or only have preliminary understanding of the material mechanics and hydraulics, these works often failed.

Table 1.8 lists several important historical hydraulic structures, particularly the dams, in this period which are recorded exactly by history documents or verified by ancient ruins.

1.2.2 300 AD–1800 AD

This is a period featured by the appearance of masonry and “concrete” dams (gravity, buttress, arch) and embankment dams with steep slopes.

This is also a historical period mostly overlapped by the Christian “Middle Ages” (from 476 AD to 1453 AD) (Hill 1996) and the “Islamic Golden Age” (from the eighth to sixteenth centuries) (Burke 2009). In 711 AD, Spain was conquered by the Muslims, and their rule continued until 1492. Age of autocracy overlapped the whole period in the most eastern dynasties, particularly in China.

Under the rule of a single Islamic Caliphate, different regional hydraulic technologies were assembled into a water management technological complex as “toolkit,” which has a global impact and whose various components developed in different parts of the Afro-Eurasian landmass. These include the canals and dams as well as the qanats from Persia, the water-lifting devices including the noria and the shaduf as well as the screw pump from Egypt, the windmill from Afghanistan, the saqiya with a flywheel effect from Islamic Spain, the reciprocating suction pump and crankshaft—connecting rod mechanism—from Iraq, and the geared and hydraulic driven water supply system from Syria.

Hulagu Khan led his Mongols into Baghdad in 1258 and into Damascus in the second year (1259). They crashed Arabic rule, and most of the ancient public works in that region were reduced to ruin. As a result, the rich farmlands bordering the upper Tigris reverted to desert.

The Renaissance started from the sixteenth century profoundly affected European intellectual life in the early modern period. It initiated in Italy and spread to the rest of Europe. Its influence is still strongly felt in literature, philosophy, art, music, politics, science, religion, and other aspects of intellectual inquiry inclusive hydraulic structures.

The design concepts of the early Spanish dam engineers were conveyed to the colonies in America continent since the sixteenth century. However, it is widely believed that hydraulic projects had been well developed before the conquest of the Spanish. For example, near the Teotihuacan, Mexico, and in the Nepena and Canete valleys in Peru, there are still signs of ancient dams.

Since the 1700s, mechanical hydropower was used extensively for milling and pumping. During the 1700 and 1800s, water turbine development continued.

As the accumulation of engineering expertise, an increasing number of the works built in this period had lasted a long time. Table 1.9 lists several important historical dams in this period.

Table 1.8 Historical hydraulic structures in the period of 3000 BC–300 AD

Year	Name and features	Location	Remark
3000 BC–4000 BC	Jawa Dam	The Black Desert, Jordan	With some real skill already
2950 BC–2750 BC	“Sadd el-Kafara,” a masonry gravity dam, 14 m high	Nile River, Egypt	Arabic name meaning “Dam of the Pagans,” with some engineering expertise already
Around 2100 BC	Nahrwan Canal and Dijail Canal	Diversion from the Tigris River, Babylonia and Assyria	The ruins found at the river near the ancient head works are of massive rubble masonry
1900 BC	Joseph’s Canal, by Prophet Joseph when he was the Grand Vizier to the Pharaoh	Medinet-el-Faiyum, Egypt	For the purpose of irrigating the green fruit gardens of that area by taking off the Nile River
1319 BC–1304 BC	Lake Homs Dam (Quatinah barrage), 7 m high and 20 m wide at base	Syria (during the reign of the Egyptian Pharaoh Sethi)	The oldest operational dam in the world
Around 800 BC	Marib Dam, 3.2 km long, 37 m high, and 152 m wide at base	Wadi Sadd (Saba River), North Yemen (since 1990, a part of the Republic of Yemen)	At a site 5 km upstream of this ancient dam, a new Marib dam was commissioned in 1986
705 BC–681 BC	Ajilah Dam, about 240 m long and at least 3 m high	Khostr River, Mesopotamia (Iraq)	Attributed to the Assyrian King, Sennacherib, to serve his capital city of Nineveh
600 BC	Tunnel of Eupalinos on Samos, dug from both ends	Greece	First known hydraulic tunnel
598 BC–591 BC	Anfeng Tang (dyke or dam), 10 m high	Shouxian County, Anhui Province, China	Embankment. Still in functioning today
539 BC	Diyala dam	A tributary of the Tigris, Persia	Embankment to create diversion works for an extensive water distribution network composed of reportedly 30 canals
505 BC–100 BC	Dams of Kalabalala, 24 m high and about 6 km long	Ceylon	Embankment type
322 BC–298 BC	Sudarsana Dam	India, during the reign of Chandragupta	Embankment. Survived until at least 457 AD

(continued)

Table 1.8 (continued)

Year	Name and features	Location	Remark
240 BC	Gukow Dam, 30 m high and almost 300 m long	Jingshui River, Shansi Province, China	Stone-crib embankment. For the water diversion into the Zhengguoqu Canal
214 BC	Lingqu Canal, part of a historical inland waterway between the Yangtze River Delta and the Pearl River Delta	Xing'an County, Guangxu Province, China	The first canal with ship locks in the world for the purpose of inland waterway transportation
193 BC	Alcantarilla Dam, 20 m high and at least 550 m long	Spain (after the Romans gained control of Toledo)	The oldest dam in Spain and is possibly the earliest Roman dam. Spillways were accommodated
100 BC	Dam of Glanum, approximately 6 m high and 9 m long at crest. It is also known as the "Vallon de Baume Dam"	Southern France, Roman Empire	The oldest masonry arch dam. In 1891 AD, a new arch dam was constructed on the ruins, concealing evidence of this ancient work

Table 1.9 Historical hydraulic structures in the period of 300 AD–1800 AD

Year	Name and features	Location	Remark
Second century	Proserpina Dam, 19 m high and 427 m long. A concrete core sandwiched between two masonry walls	About 6 km north of Merida, Spain	It possesses large capacity spillways. The upstream face is battered steeply, while the downstream masonry face is vertical on which the masonry buttresses were erected to provide resistance against overturning
Second century	Cornalbo Dam, 24 m high and 200 m long. Its cross section is trapezoidal with masonry revetment	Near Merida, Spain	One of the oldest embankments is still operational. The core of the dam was made up of masonry walls forming interconnected boxes filled with stones or clay
Second century	Kasserine dam, 10 m high, about 150 m long at crest. It is remarkable that the dam was curved	217 km southwest of Tunis	A masonry-faced structure with a core composed of earth and rubble. Cut stone blocks with mortared joints were used in the vertical upstream facing, while the downstream side was stepped down from the crest
162	Kaerumataike Dam, 17 m high and 260 m long	On the Yodo River near the Nara, Japan	Earth embankment
270	Shushtar Dam-Bridge, approximately 550 m long	On the Karun River in Khuzestan, Persia (by the King Shapur I)	For the purpose to improve the irrigation projects
Third century	Dam of Homs, 6.1 m high. The thickness varies from 7 m at the top to approximately 20 m at the base	On the River Orontes, Syria (Roman period)	It survived and provided service for seventeenth centuries; until in 1934, a new and larger dam was superimposed on the ancient one. The core of the dam was of basaltic rubble masonry, cemented with mortar. Cut basalt stones were placed on both faces of the dam, and the joints were mortar sealed
459	Kalaweve Dam, about 19 km long	Ceylon	Earthfill embankment to create irrigation reservoir (tank)

(continued)

Table 1.9 (continued)

Year	Name and features	Location	Remark
833	Tashan Yan (barrage), 27 m high	On the Zhangxi creek, Zhejiang Province, China	Masonry gravity type, serving for irrigation
Around 960	Dam on the Rio Guadalquivir, zigzag alignment of about 427 m in total length	Cordova, Spain	The oldest remaining Muslim dam in Spain. In addition to its original functions of water supply and mill operation, the pool created by this rubble masonry dam protected the bridge piers of the Puente Romano (Roman Bridge) from erosion
Around 960	Band-i-Amir Dam, 9 m high and 76 m long, has a downstream slope about 1–1	On the River Kur, Persia	Built entirely of cut stones with mortared joints reinforced by iron bars anchored in lead. It still stands although its function has been impaired by siltation
Around 960	Moti-Talab Dam, 24 m high and 157 m long, has a cross section with a broad crest of 27 m wide	Near Mandya (Mysore), India	Earthfill embankment with steep slopes (2:3 upstream and 1:1 downstream) protected by cut stone facing
Eleventh century	Bhopal reservoir with an area of 650 km ² impounded by two earthfill dams covered on both slopes with immense blocks of cut stone	Bhopal (Madhya Pradesh), India	Evidence of this great pool still remains, and a spillway was excavated in the rock of a hill saddle
Thirteenth century	Almonacid de la Cuba Dam, 29 m high and 85 m long, with a downstream face composed of large stone blocks placed in tiers and set in mortar	On the Rio Aguavivas, about 40 km south of Zaragoza, Spain	The oldest surviving Christian dam in Spain with original spillway at the left abutment. As part of the enlargement, the spillway crest was elevated by a curved weir
1300	Kebar Dam. The constant intrados radius is 38 m, the height is about 26 m, the chord length is 55 m, and the crest thickness is 5 m	On the Kebar River, about 170 km southwest of Tehran, Persia	The oldest known surviving arch dam. Materials used in the construction were cemented rubble masonry with mortared stone block facing

(continued)

Table 1.9 (continued)

Year	Name and features	Location	Remark
1350	Kurit Dam, 60 m high. Later, 4 m was added to the dam height in 1850	Persia	Masonry arch. Even though part of its lower downstream face fell off, it remained the highest dam in the world until the early twentieth century
1384	Almansa Dam, about 14.6 m high and curved to a intrados radius of about 26 m, whose thickness is approximately 10 m at the base and 4 m at the crest	Near the town of Almansa, Spain	Arched gravity dam composed of rubble masonry and regarded as the first known arch dam in Spain. It was enlarged in 1586 and again in the years 1736 and 1921 and is still in sound condition
Fifteenth century	Daimonike Dam, 32 m high	Near Nara, Japan	Earthfill embankment
	Padawiya Dam, 18 km long and approximately 21 m high	60 km northeast of Anuradhapura, Ceylon	Earthfill embankment with slope facing consisted of cut stone
1500	Mudduk Masur Dam, 33 m high	Madras Province, southern India	Embankment whose height was unsurpassed for about 300 years
1594	Alicante Dam, 41 m high. The plan is curvilinear with a crest length of about 80 m and a thickness varies from approximately 20.5 m at the top to 33.7 m at the base	Tibi, Spain	Rubble masonry arch dam, also known by the name of the nearby Tibi village. It was installed with silt excluding system and vertical shaft outlet. Originally, there was no separate spillway. The dam was rehabilitated in 1738, and a side-channel spillway was constructed later. The dam was enlarged in 1943; therefore, its present height is 46 m
Mid-seventeenth century	Eliche Dam. The mean radius is 62.6 m and the crest length is about 70 m. The dam height is 24 m and the arch thickness varies from about 9 m at the top to 12 m at the base	Rio Vinalop, Spain	It is the first true arch dam in Spain, using traditional rubble masonry with cut stone facing

(continued)

Table 1.9 (continued)

Year	Name and features	Location	Remark
Seventeenth century	Ponte Alto Dam, about 5 m high and 2 m thick, with a radius of approximately 14 m	On the River Fersina just east of Trento, Italy	Masonry blocks with unmortared joints. The first masonry arch dam in Italy. In 1752, the addition of a second stage increased the height to 17 m. Subsequent enlargements in 1825, 1847, 1850 and 1887 created a dam of present height of 38 m
1642–1667	Pul-i-Khadju Bridge-Dam, whose slotted weir is about 6 m high, 30 m thick, and 141 m long	Persia	Cut stone blocks masonry built during the reign of Shah Abbas II
1667–1675	St. Ferreol Dam, 36 m high and 780 m long	On the River Laudot, about 50 km southeast of Toulouse, France	It is an earthen embankment having three parallel masonry walls extending the full length of the dam, one at each face and one in the center. The fill between the walls is composed of stones and earth
1714–1721	Oberharz Dam, 22 m high and about 151 m long. It has a width varying from about 16 m at the crest to 44 m at the base	Germany	The first large dam in Germany composed of two stone block face walls confining a central zone of sand
1747	Almendralejo Dam, 170 m long, approximately 20 m high, with a thickness varying from 10 m at the crest to 12 m on the base	About 51 km south of Badajoz, Spain	Rubble masonry buttress dam, also known as the dam of Albuera de Feria. It has survived without any significant deterioration. Successive enlargements increased the height to 23.5 m

1.2.3 1800 AD–1940 AD

This is a period featured by the fast development in techniques for concrete dams, along with the sophisticated application of sciences (e.g., mathematics and material mechanics). Climbing formwork, Portland cement, modern concrete, and multi-purpose reservoirs started to prevail.

Before the mid-nineteenth century, rational theories and criteria for dam design had few acceptance, and problems encountered in construction were ordinarily tackled by trial and error. Take the Puentes Dam on the Rio Guadalentin (Spain) as an example: It is a 50-m-high rubble masonry gravity dam intended to be built on rock foundation. However, after the foundation clearance, a deep crevice was found, and the countermeasure decision was to pile in the alluvial fill under the central portion of the dam. As a result, after 11 years of service, the dam failed in 1802 due to the foundation blew out under reservoir pressure.

After the mid-nineteenth century, the masonry gravity dam design and construction had made important breakthrough. In 1853, Sazilly, a French engineer, advocated that pressures within a gravity dam should be held to specific limits and that the structure should be dimensioned to preclude sliding. The concept of keeping the resultant of forces within the middle third of each horizontal plane was emphasized later by Rankine (1881) of England. The ideas of Sazilly and Rankine showed the way toward rational analysis of gravity dams. The first project accomplished according to the principles proposed by Sazilly was the Furens Dam (France, $H = 50$ m). In 1858, two French engineers, Graeff and Delocre, initiated the process of the selection and subsequently the design of the Furens Dam that would be, for about 10 years, the largest in the world. Located in the vicinity of Rochetaillée, close to Saint Etienne, the construction of the Furens Dam began in 1860 and the first filling took place in 1866. In the stage of design, Delocre initially used the “practical section” proposed by Sazilly, changing the sectional configuration to a polygonal profile.

Mining also gave impetus to the dam construction. Discovery of gold in California (USA) in 1848 led to extensive placer workings which necessitated the use of dams and conduits as a result of the need to impound water for mining operations. Drill and blast mining techniques by miners provided an abundant supply of rock materials for the use in dam construction. The miners used the rock quarry materials to construct water storage dams in remote areas with available mine haul and dump equipment, or even by hand solely. At the beginning, these dams were built with stone-filled log cribs. A later development was the dumped rockfill confined by dry rock walls at the faces and lined with two or more layers of wood planking. One of the highest dumped rockfill dams constructed in the California Sierras (USA) during this earlier period was the Meadow Lake dam of 23 m high.

While these relatively rough works were being practiced by the western USA pioneers, European engineers were engaged in more sophisticated projects in contrast to their crude predecessors. In France, the Zola Dam regarded as the first

“rational arch dam” was completed in 1854. With an unprecedented arch height of 42 m, its stress analysis was firstly carried out by the cylinder method, which looks at an arch dam as a part of vertical cylinder in the water. This rubble masonry structure with cut stone faces is still intact.

Darcy’s Law concerning the rate of seeping water flow through a soil (permeability) was promulgated in 1856 and is still very relevant today. It dictates how and where different types of earth materials (clay, silt, sand, gravel, cobbles, and rockfill) can be used in an embankment dam.

In 1875, the first stage of the Lower San Leandro (Chabot) Dam was completed to serve the communities on the east shore of San Francisco Bay in California (USA). It was built by Anthony Chabot in charge of San Francisco’s first public water supply. A special feature of this earthfill embankment ($H = 35$ m) is a central foundation trench excavated 9 m below the streambed. In the bottom of the trench, three parallel concrete cutoff walls were built, each at 0.9 m thick and 1.5 m high, with about half of this height anchored in the foundation and rest half protruding. The fill contains a core zone which is about 27 m wide at its bottom of the foundation trench. The dam was enlarged in the 1890s, its new height above foundation is 47 m, and its length is 137 m.

Design concept and theory for gravity dams continued to advance. The middle third criterion was being questioned, which had been generally accepted as sufficient guarantee against the overturning of dams. However, several failures (e.g., the Bouzey Dam of France at height of 22 m failed in 1895) demonstrated that uplift and sliding could be of greater concern. Designers began to consider these factors in new projects. As early as 1882, a draining network to reduce uplift had been incorporated into the body of the Vyrnwy Dam in Liverpool (UK). Engineers in the USA firstly took into account of the uplift in the design for the Wachusett Dam in Massachusetts (1900–1906), which gave rise to a fat section of flat slope. The Olive Bridge Dam in New York State (1908–1914), USA, was constructed with drains in the dam body but with none in the foundation. Among the first dams with both dam and foundation drainage were the Medina in Texas (1911–1912), the Arrowrock in Idaho (1914–1915), and the Elephant Butte in New Mexico (1914–1915). Since then, drilling of drainage holes has been commonly exercised for large gravity dams.

The New Croton Dam (also known as Cornell Dam, USA, $H = 91$ m), a gravity dam completed in 1905, was one of the first applications of American Portland cement. In later projects, Portland cement found increasing acceptance.

Series accidents waked up engineers concerning the importance of foundation treatment for gravity dams. The Austin Dam in the Freeman Run Valley, Pennsylvania (USA), failed partially due to the foundation problem on September 30, 1911, destroyed much of the town of Austin, and resulted in the deaths of 78 people (Greene and Christ 1998). A little more recently, in 1928, the failure of the St. Francis dam near Los Angeles, California (USA), also due to the foundation problem, killed hundreds of people (Outland 1963). Since then, foundation stability analysis has become an indispensable task in the safety calibration of gravity dams, considering the possibility of various sliding mechanisms and seepage effects,

which may either take place along the foundation surface and/or involve deep-seated rock fractures.

The design of high arch dams requires more advanced methods for stress analysis. New methods for the analysis of arch dams emerged around the first decade of the twentieth century. In 1889, Vischer and Wagoner described several horizontal arches and only one crown cantilever in the stress check of the Bear Valley Dam (USA, $H = 19.5$ m) and the Sweetwater Dam (USA, $H = 33$ m). But it was unknown to engineers in the other countries until several years later. In 1904, Woodard applied this method second time to the Cheesman Dam (USA, $H = 64$ m); thereafter, the method started to attract the wider interest of dam engineers. In 1905, two US engineers—Wisner and Wheeler—under the request of the Reclamation Service, initiated studies to better understand the load distribution on arch dams. Using an iterative process with respect to the force sharing and the compatibility of displacements among several arch rings and a central cantilever, they obtained the load distribution across the various sections, which led to the conclusion that at higher elevations, the behavior of the arch was decisive, whereas close to the bottom, the cantilever effect prevailed. Noetzli (1921,1922) summarized the situation in a landmark paper by giving relatively simple formulas for calculating the cantilever and the arch actions and then applied his formulations to the design of the Pathfinder Dam ($H = 65$ m, USA), which was completed in 1909, and the Buffalo Bill Dam ($H = 99$ m, USA).

Started from around mid-1920s, the arch dam design and construction had achieved amazing progress attributable to the advancement in material sciences, construction techniques, and well-formulated analysis methods.

The Swiss engineer, Gryuner, tried the American experience in the Montsalvens Arch Dam erected in 1920. His two assistances, Stucky and Gicot, analyzed side cantilevers, apart from the crown one, which enabled to improve the profile of the arch dam in the vertical direction. By 1925, Vogt had shown that the displacement of foundation rock could be estimated approximately using three formulae derived from the Boussinesq's theory of the elastic semi-space. In 1929, Howell and Jaquith, both from the Bureau of Reclamation, formalized comprehensively the calculation method using various arches and cantilevers developed through scattered contributions, as the “trial load method.”

In the 1920s studies using physical models were exercised to analyze arch dams, and experimental centers were established in Portugal (Civil Engineering Laboratory in Lisbon), Italy (ISMES in Bergamo), England (Imperial College), and Spain (Central Laboratory in Madrid). The trial load method underwent its first application which was checked with a model test (scale 1:240) at the University of Colorado at Boulder (USA). The trial load method had been rigorously checked in 1926 with the help of the Stevenson Creek Dam -an 18 m high experimental arch dam near Fresno in California.

Techniques for mixing and placing concrete were undergoing significant changes, too. The Diablo Dam, for example, used a dry mix placed by a belt conveyor suspended from a derrick, with a short tube known as an “elephant trunk” at the discharge end. In the construction of the Calderwood Dam (Tennessee, USA) and

Chute a Caron Dam (Quebec, Canada), use was made of bottom-dump buckets that enabled placing relatively dry concrete in the forms without segregation.

The Danish immigrant engineer Jorgensen (1915) published a paper on the constant angle arch dam in which he showed how to configure an arch dam with a minimum volume at each level by using the cylinder formula and by reducing the radius of curvature in the lower regions where the water pressure is higher. He indicated that the volume of material needed would be a minimum if the central angle remained the same at a value of about 133.6° —hence, his dam designs are called “constant angle dams.” In 1914, in the design of the 52-m-high Salmon Creek Dam in Alaska (USA), Jorgensen abandoned the prevalent constant radius type of arch dam and realized the first constant angle dam, followed by the 84-m-high Lake Spaulding Dam in California in 1919. By 1931, he would state that over 40 constant angle arch dams had been completed. Since then, constant angle dams have been the dominant arch dam type in not too wide valley.

The birth of double-curvature arch dams is mainly attributable to the two arch dams. The Marèges Dam (France, $H = 90$ m) designed by André Coyne was constructed between 1932 and 1935. Coyne cut a 7 m wide portion at dam heel of tensile cracking area, instead of conventional US way to thicken the cantilever base to resist the tensile stress. His genius gave rise to a first step toward double-arch dams. The Osiglietta Dam (Italy, $H = 76$ m) completed in 1939 designed by Nicolai, who bended the upper portion of the dam in the direction of downstream. This creation was enlightened by the laboratory experimental findings during 1935–1939 in the ISMES that such bending might strengthen the upper portion of arch rings. The Osiglietta dam is also the first arch dam in the world having peripheral joint.

Embankment dams started to evolve from the relatively simple homogeneous or two-zoned earthfill into the extremely complex, highly analyzed, well-instrumented, and multi-zoned earthfill and rockfill structures. Rockfill technology was given new impetus in USA. From the 1910s to the 1940s, rockfill dump dams began to exceed 30 m in height. The “dry rock dump” technique in rockfill dam construction developed into the placement of thick single or multiple rockfill lifts in combination with upstream facing of relatively impervious materials (timber, steel, concrete, or asphaltic concrete). In 1924, the Dix River Dam for the water supply of Danville, Kentucky (USA), set a height record of 84 m for rockfill dams. In 1931, the Salt Springs Dam in California (USA) raised the record further up to 100 m.

Earlier of this period, settlement/consolidation behavior of granular materials was not tested, although settlement benchmarks were first installed along the edges of the embankment crest at the Belle Fourche Dam (also known as Orman Dam, USA, $H = 37.4$ m) in 1911. Field and laboratory testing of soil and rock materials began to emerge during the 1920s and early 1930s. In addition to the pioneering works on the topics such as soil permeability by Karl von Terzaghi who is generally considered the father of soil mechanics, others contributed greatly to the evolution of soil and rock testing, too, in the attempt to characterize these materials.

The grading from finer grained materials at the core to coarser grained materials toward the outer slopes was started to be employed in embankment dams, which

demanded the understanding of the filtering actions for preventing soils from “internal erosion” (piping). The research works by Bertram with the assistance of Terzaghi and Casagrande resulted in a paper that is generally given the credit as the first document on filter criteria, in the early 1940s.

Anecdotal evidence from the soil slope failures in the early 1900s suggested that the failure surface is often cylindrical like curvilinear, especially in a homogeneous, isotropic, and cohesive soil mass. In 1916, Pettersson and Hultin proposed a slope stability analysis method of arc to analyze the failure of a quay wall in Goteborg, Sweden. But it did not appear to be introduced to the engineers in the other countries. The method of slices was formally introduced by Fellenius where he divided the sliding soil mass contained within the arc into slices and analyzed their equilibrium by equating the forces and moments to zero.

The world’s first hydroelectric power plant was installed in Cragside, Rothbury (England), in 1870. Industrial use of hydropower started in 1880 in Grand Rapids, Michigan (USA), when a dynamo driven by a water turbine was used to provide theatre and storefront lighting. In 1881, a brush dynamo connected to a turbine in a flour mill provided streetlighting at Niagara Falls, New York (USA). The key breakthrough came when the electric generator was coupled to the turbine, and thus, the world’s first hydroelectric station (of 12.5 kW in capacity) was commissioned on September 30, 1882, on the Fox River at the Vulcan Street Plant, Appleton, Wisconsin (USA), lighting two paper mills and a residence (Edenhofer et al. 2011).

China’s first hydropower station is the Shilongba on the Tanglangchuan River in the city of Kunming, Yunnan Province. The station was put into operation in 1912 and has since provided power to the Kunming city through a 32-km-long power line. Outfitted with two sets of generators manufactured by Germany and Austria, respectively, the power station had an installed capacity of 480 kW when it was completed. One of the generators is still in use, and the station added two 3000 kW generators in the 1950s. The station has supplied more than 1 billion kWh of electricity since putting into operation and is still supplying voltage to nearby residences. Although the Shilongba Hydropower Station has generated less electricity in recent years due to decreased water flow in the river, the station has assumed a relatively new role as tourist attraction. In 2006, this power station was listed as one of the China’s key cultural relics Table 1.10 lists several historical hydraulic structures in the period of 1800AD-1940AD.

1.2.4 1940–End of Twentieth Century

It is an exciting era featured by high concrete and embankment dams as well as giant hydropower plants. Drinking water supply for quickly growing cities required large reservoirs. After the invention of electricity transmission with alternating current, high dams were necessitated for increasing demand of clean and convenient hydropower. Since the 1950s, the increase in the number and height of dams was accelerated around the whole globe, and dams of several types (gravity, arch,

Table 1.10 Historical hydraulic structures in the period of 1800 AD–1940 AD

Year	Name and features	Location	Remark
Around 1800	Meer Allum Dam. The arch thickness is 2.6 m. Each buttress is 7.3 m thick and 12.8 m long	Hyderabad, India	The first true multiple-arch buttress dam of mortared masonry. The spans of the 21 vertical arches vary up to a maximum of 45 m
1839	Yeni Dam, 16 m high and 93 m long. Its crest thickness is 7 m, and base thickness is 9.5 m	Istanbul, Turkey. By the decree of Sultan Mahmut II	A curved masonry gravity structure also known as the Sultan Mahmut Dam
1854	Zola Dam, 42 m high	Aix-en-Provence, France	Rubble masonry. The first arch dam whose stress analysis was rationally carried out by the cylinder method
1882	Vyrnwy Dam	Liverpool, UK	Masonry gravity. A draining network to reduce uplift had been firstly incorporated into the dam body
1892	Tansa Dam, 2.8 km long and 41 m high	Bombay, India	Embankment
1887–1897	Mullaperiyar Dam, 53.66 m high	Kerala, India	Masonry gravity
1902	Aswan Dam, 20 m high and 1951 m long. Enlargement of this gravity dam to a height of 27 m was completed in 1912, followed by a further raise in 1933 to 53 m high	River Nile, Egypt	It was built with quarried granite. Successful operation of the dam was attributable in part to provision of sluiceways in the structure which allowed silt to flow through to the irrigated lands of the lower Nile
1904	Cheesman Dam, at height of 72 m and curved in plan on a radius of 122 m	Colorado, USA	Arched gravity to which, in 1904, Woodard applied crown cantilever method (initiated by Vischer and Wagoner)
1900–1906	Wachusets Dam	Massachusetts, USA	Masonry gravity. Gave firstly the consideration to the uplift in the design, which resulted in fat section
1905	New Croton Dam, 90.5 m high. The last major American cut stone masonry dam	New York, USA	Masonry gravity. While natural cement was used on this project, it was also one of the first applications of American Portland cement
1909	Pathfinder Dam, 65 m high	Wyoming, USA	Masonry arch dam

(continued)

Table 1.10 (continued)

Year	Name and features	Location	Remark
1915	Kensico Dam, 94 m high	New York, USA	Introduced a new era in dam construction by the invention of “cyclopean concrete”
1924	Dix River Dam, 84 m high	Kentucky, USA	Set a height record of rockfill dam
1931	Salt Springs Dam, 100 m high	California, USA	Set a height record of rockfill dam
1931–1936	Hoover (Boulder) Dam, 221 m high and 379 m long on crest. Thickness varying from 13.7 m at the top to 201 m at the base	Colorado River, USA	It is an concrete arched gravity structure set a height record in the world
1935	Marèges Dam, 90 m high	Dordogne River, France	Designed by André Coyne. It initiated the practice of double-arch dams. It also incorporated several innovative features such as the ski-jump spillway
1939	Osiglietta dam, 76 m high	Italy	Designed by Nicolai. It initiated the practice of double-arch dams by bending the upper portion of the dam in the direction of downstream

multiple arch, zoned earthfill or rockfill) continued to mount toward new height until exceeding 250 m. Up to 1939, there were only 11 completed dams higher than 100 m, of which 5 were in Western Europe and 6 were in USA; by 1960, there were already 88 dams higher than 100 m in service throughout the world. New dam height and volume records were set and broken in quick succession.

New dam type, material, construction method, etc., had been developed fast. Some of them had limited influences, and the others, particularly on the aspects of material and construction, have profound influences until today.

Three events are the most worthwhile to be noted for this significant historical period, namely the invention of RCC dams, fast development of rockfill dams, and comprehensive design theory of super-arch dams. These three dam types are prevalent in the construction of modern high dams, particularly on the west southern areas in China.

1. RCC dams

Featured by the dry lean concrete of lower cementitious material and roller compaction construction method, the roller compacted concrete (RCC) dam is one of the most competent type in the design of modern high dam project. Research works on RCC dams started from 1960. The first experiment of RCC was carried out for the cofferdam of the Shimen embankment dam in Taiwan, China ($H = 133$ m). A high gravity dam—the Alpe Gera ($H = 172$ m) in Italy—tried to use the construction technology of embankments to construct the concrete dam in 1963. Later on, this method was quickly developed for dams, cofferdams, and dam rehabilitations in Canada, USA, UK, Pakistan, Japan, and Brazil. By these practices, engineering experience and expertise were accumulated step by step. The Shimajigawa Dam in Japan ($H = 89$ m) and the Willow Creek Dam in USA ($H = 52$ m) belong to the initial batch of RCC dams in the world. The world's highest RCC gravity dam—Longtan ($H = 216.5$ m)—is now erected in China. Since the 1990s, the RCC started to be exercised in the construction of arch dams. Just a bit of later after the construction of the first two RCC arch dams in South Africa (Wolwedans at height of 70 m in 1990, and Knellpoort at height of 50 m in 1989), the first two Chinese RCC arch dams were completed in 1993—the Puding RCC Arch Dam (Guizhou Province, China, $H = 75$ m) and the Wenquanbao RCC Arch Dam (Hebei Province, China, $H = 48$ m)—which became the landmarks of the RCC arch dams in the southern and northern China. They were followed by a series of high RCC arch dams such as the Shapai (Sichuan Province, China, $H = 132$ m) and the Dahuashui (Guizhou Province, China, $H = 134.5$ m).

2. Rockfill dams

The 1940s also initiated the first use of earthfill core and filter materials in the interior section of the rockfill dams, this evolution gave the impetus to the growth of several related disciplines, including soil mechanics, engineering geology, seismology, hydraulics, and instrumentation. Another consequence of this evolution is the invention of larger, faster, more powerful, and more efficient earthwork construction equipments.

High-pressure jet wetting or irrigation flooding techniques were applied to the dry rock dump surfaces—“wet dump” to consolidate and to reduce large post-construction settlements down to acceptable levels. From the 1960s to the present day, rockfill construction shifted from wet rock dump placement in thick loose lifts to compacted rockfill placement in thin controlled lifts using heavy roller compaction. In 1958, the Quoich Dam (UK, $H = 38$ m) became the first rockfill dam using thin controlled lifts by heavy vibration roller compactor. The wet rock dump technique was essentially terminated by around 1965 on large rockfill dams in the world. The New Exchequer Dam (USA, $H = 150$ m) completed in 1966 became the last rockfill dam by the mixed methods of “dry rock dump” technique of thick rockfill lifts and “wet” roller compacted of thin rockfill lifts. From the Foz do Areia Dam (Brazil, $H = 160$ m) completed in 1980, to the Salvajina Dam (Colombia, $H = 148$ m) completed in 1985, until the Aguamilpa Dam (Mexico, $H = 187$ m) completed in 1993, the design and construction techniques of compacted rockfill dams achieved amazing progress. In 1989, the Alberto Lleras Dam, also known as the Guavio Dam erected in Columbia, mounted a record height at 243 m. The highest compacted rockfill dam with central core in China is the Nuozhadu Dam in the Yunnan Province at a height of 261.5 m, completed in 2012. Until now, the highest record of the central core rockfill dam is kept by the Nurek Dam (Tajikistan, $H = 300$ m) completed in 1980. However, the Rogun (Raguni) Dam with a designed height of 330 m in Tadzhikistan is sometimes rated as the highest in the world although it has not been completed so far. The Tarbela Dam on the Indus River, Pakistan, with 142 Million m^3 of earth and rock is keeping the world record of the embankment volume so far.

A remarkable event in the modern rockfill dam construction is the boost of concrete-faced rockfill dams (CFRD). The Cethana Dam (Australia, $H = 110$ m) completed in 1971 established technique landmarks for the modern CFRD. Nowadays, in parallel to concrete arch dam and RCC dam, CFRD is very competent in the selection of dam type in China. The world’s highest CFRD (Shuibuya, $H = 233$ m) is erected in China.

In 1970, the hardfill dam—a kind of symmetrical trapezoidal shaped embankment using low-cost cemented sand and gravel materials and having a concrete impervious face on its upstream face, was proposed by Raphael (1971), as “the optimistic gravity dam.” And later, Londe and Lino (1992) named it as “Faced Symmetrical Hardfill Dam (FSHD).” Nowadays, the European countries commonly name it as hardfill dam, and Japan calls it cemented sand and gravel dam (CSG dam) (Toshio et al. 2003). Actually, it may be looked at as an “intermediate dam” between the concrete gravity type and rockfill type. Since the beginning of the 1990s, with the first application to the cofferdam ($H = 15$ m) in the construction of the Nagashima Dam (Japan), the employment of this dam type has been accelerated. The Cindere Dam (Turkey, $H = 107$ m) completed in 2005 is the tallest hardfill dam in the world at present.

3. Arch dams

The trial load method had revealed that along an arch ring, the arch load is maximum at the crown and minimum at the abutments. Therefore, the curvature should be largest at the crown and minimum at the abutments, to obtain both good stress conditions for the dam body and good stability conditions for the abutments. Gicot is the first who suggested parabola arch ring, and the idea was first realized in the Vieux Emosson Arch Dam (Switzerland, $H = 45$ m) completed in 1955. Famous Chinese parabola arch dams are Ertan ($H = 240$ m), Xiluodu ($H = 278$ m), Xiaowan ($H = 294.5$ m), and Jinping 1 ($H = 305$). Gicot also suggested ellipse arch ring, implemented it in the Les Toules arch dam (Switzerland, $H = 86$ m), and completed in 1963. Representative Chinese ellipse arch dams are the Gaixiaba ($H = 141$ m) and the Jiangkou ($H = 140$ m). Leroy, from Coyne and Bellier, France, suggested logarithmic spiral arch ring and designed the Vouglans Dam (France, $H = 130$ m) that was completed in 1962. The highest Chinese logarithmic spiral arch dam is the Laxiwa ($H = 250$ m).

Due to the relatively conservative conclusions by the Stevenson Creek Test Dam (Engineering Foundation (US) 1927), the enthusiasm in the arch dam construction was cooled down in USA. Since the 1950s, the center of arch dam construction was moved to Europe. The Marèges dam at a height of 90 m on the Dordogne River (France) was constructed between 1932 and 1935. The dam, designed by André Coyne, incorporated several innovative features by the first application of the double curvature and the ski-jump spillway. The Kariba Dam (Zambia and Zimbabwe, $H = 128$ m), 6 orifices of $9.1 \text{ m} \times 9.46 \text{ m}$ in size were installed with the total discharge of $9500 \text{ m}^3/\text{s}$ and the unit flow rate of $176 \text{ m}^2/\text{s}$. The Kariba Dam was also designed by André Coyne in 1955 and completed in 1959. Along with the mounting in the height, the arch dam also had tendency of becoming thinner and thinner. The Tola dam of 90 m high designed by André Coyne was only 2.43 m thick at the base.

However, a somewhat Pollyanna atmosphere in the construction of high arch dams was waked up by a timely warning lesson—the failure of the Malpasset Dam in 1959 (Londe 1987), which brought a lawsuit against more than ten engineers. Arch dam construction suffered a serious setback in the world (Ru and Jiang 1995). For example, the arch dams under construction such as the Contra (Switzerland, $H = 220$ m) and the Kurobe 2 (Japan, $H = 186$ m) were suspended for the reinforcement of abutment rock; the Shimen Arch Dam (Taiwan, $H = 141$ m) was replaced by embankment type. After a series of systematic investigations, it became fully recognized that abutment stratum conditions were critical to the stability of high arch dams. Step by step, the confidence and construction of high arch dam had been recovered. Precedent setting for arch dams since the mid-twentieth century in the world is the Mauvoisin Arch Dam (Switzerland, $H = 237$ m) completed in 1957, the Vajont Arch Dam (Italy, $H = 265$ m) completed in 1960, and the Contra Arch

Dam (Switzerland, $H = 220$ m) completed in 1965. In Soviet Union, the double-curvature concrete arch dam of the Inguri ($H = 271.5$ m) was completed in 1987, which is located 7 km from the Dzhvari Village in a narrow gorge of the Inguri River, Georgia (since 1991, it is an independent country officially named as the Republic of Georgia). In 2012, the Xiaowan Arch Dam (China, $H = 294.5$ m) set a new height record.

Apart from the other areas in civil engineering (e.g., highways, railways, mines), the requirement on the dam foundation and abutments gave strong impetus to the fast progress in the rock mechanics led by Leopold Müller et al., nearly 20 year later than the soil mechanics (Müller et al. 1964). The evolution of soil mechanics and rock mechanics gave rise to the birth and maturation of geotechnical engineering, as an important civil engineering specialty. The use of computers and computer programs for the analysis and design became a routine practice within a fairly short time after they were developed by geotechnical engineers.

According to the statistics by ICOLD, there were only 15 dams higher than 30 m in China up to 1950. Among them, 8 were earthfill or rockfill dams and 7 were gravity dams. Alternatives for dam-type selection at that time were quite limited. After 1950, especially after the economy reform and opening to the outside world initiated around 1980, dam constructions and techniques have achieved great progresses in the country (Jia 2013). Also according to the statistics by ICOLD, averagely 335 dams were completed per year in the world except China from 1951 to 1977, but only altogether 420 dams were built in China during this period. In contrast, according to the incomplete statistics at the end of 2004, there were about 47,500 large dams in the world, of which 26,278 were erected in China that accounted for approximately 55 %. By the end of 2005, there were 130 large dams higher than 100 m in China, of which 9 are higher than 200 m.

Early hydropower plants (HPP) were proliferated of small to medium sized and distributed wherever there was an adequate supply of flowing water and a need for electricity. As the electricity demand grows, the number and size of hydropower plants were increasing. Hydropower plants today span a vast range of scales, from a few watts to tens of GW. The largest projects, the Itaipu in Brazil and Paraguay with 14,000 MW installed generator and the Three Gorges in China with 22,400 MW installed generator, both produce between 80 and 100 TWh/year. The great variety in the size of hydropower plants gives the technology able to meet both large centralized urban energy demands and decentralized rural needs.

Conventionally, hydropower is used to meet mechanical energy needs as well as to provide space lighting and heating and cooling. More recently, hydropower has also been investigated for the use in the electrolysis process of hydrogen fuel production, provided there is abundance of hydropower in a region and a local goal to use hydrogen as fuel for transportation (Yumurtacia and Bilgen 2004). Table 1.11 lists several historical hydraulic structures in the period from 1940 to around the end of the twentieth century.

Table 1.11 Historical hydraulic structures in the period from 1940 to around the end of the twentieth century

Year	Name and features	Location	Remark
1948	Escaba Dam, 83 m high	Tucumán, Argentina	The highest flat slab buttress dam in the world
1954	Malpasset Dam, 66 m high	Reyran River, France	Arch dam. Failure in 1959 waked up dam engineers the importance of the dam abutment stability
1955	Vieux Emosson Dam, 45 m high	Valais, Switzerland	The first parabola arch dam, designed by Gicot
1957	Mauvoisin Dam, 237 m high	Valais, Switzerland	Double curvature
1957	Zeuzier Dam, 156 m high	Valais, Switzerland	Arch dam. Sustained damage from deformation occurred in 1979, due to a change in groundwater arising from the driving of a tunnel nearby. After 4 years of repair, it has been back in operation
1959	Kariba Dam, 128 m high, 24 m thick at base. Six orifices of 9.1 m × 9.46 m are installed	Zambia and Zimbabwe	Arch dam designed by André Coyne whose total discharge is 9500 m ³ /s and unit flow rate is 176 m ² /s
1960	Vajont Dam, 265 m high	Monte Toc, Italy	A landslide in 1963 generated an immense surge wave overtopping the world's highest concrete arch dam at that time
1962	Grande Dixence Dam, 285 m high	Valais, Switzerland	Highest concrete gravity dam in the world
1962	Vouglians Dam, 130 m high	Franche-Comté, France	The first logarithmic spiral arch dam designed by Leroy
1963	Alpe Gera Dam, 172 m high	Lombardy, Italy	It tried to use the construction technology of embankments to place concrete dam, which initiated the practice in RCC dams
1963	Les Toules Dam, 86 m high	Bourg-St-Pierre, Switzerland	The first ellipse arch dam designed by Gicot
1964	Glen Canyon dam, 216 m high and 475 m long. Arch thickness varies from 7.6 m at the crest to 91.5 m at the base	Colorado River in Arizona, USA	The highest arch dam in USA
1965	Contra Dam, 220 m high	Ticino, Switzerland	Double-curvature arch dam

(continued)

Table 1.11 (continued)

Year	Name and features	Location	Remark
1967	Oroville dam, 235 m high with a volume of 61,000,000 m ³	Feather River, USA	Zoned earthfill dam made use of the abundant supply of ideal pervious materials that had been produced by dredgers mining for gold in the flood plain
1968	Daniel Johnson (Manicouagan No. 5) Dam, 214 m high	Quebec, Canada	The highest multi-arch buttress dam in the world. It consists of 13 arches supported by 12 buttresses, with the central arch spanning 161.5 m
1972	Dworshak Dam, 219 m high and 1002 m long	North Fork of the Clearwater River, Idaho, USA	A straight concrete gravity dam with a concrete volume of 4,970,000 m ³
1973	Mica Dam, 242 m high and 792 m long	British Columbia, Canada	An earthfill dam which has a nearly vertical core of glacial till and outer zones of compacted sand and gravel
1976	Tarbela Dam, 143.26 m high	Indus River, Pakistan	The world record for the volume of dam with 142,000,000 m ³ of earth and rock
1979	Kolnbrein Dam, 200 m high	Malta River, Carinthia, Austria	While the reservoir was filling, several cracks appeared in the arch dam and it took more than a decade of repairs before the reservoir could operate at maximum level
1980	Foz do Areia Dam, 160 m high	Paraná, Brazil	Record setting of the CFRD at that time
1980	Shimajigawa Dam, 89 m high	Yamaguchi, Japan	Gravity type belongs to the initial batch of the Japanese RCC—RCC wrapped with thick and high-quality CVC
1980	Nurek Dam, 300 m high	Vaksh River, Tadzhikistan	World's highest rockfill embankment dam
1983	Willow Creek Dam, 52 m high	Oregon, USA	Gravity type belongs to the initial batch of RCC dams with dry lean concrete of low cementitious material (66 kg/m ³)
1984	Itaipu Dam, 196 m high and 7919 m long	Brazil and Paraguay	Combination of gravity, buttress, and embankment sections. It is the highest massive-head buttress dam. It also has the largest annual energy generation in the world (98.2 TWh in 2012)
1986	Kengkou Dam, 56.8 m high and 122.5 m long	Fujian Province, China	The first RCC gravity dam in China. Concrete amount 60, 600 m ³ , of which 42, 000 m ³ is RCC

(continued)

Table 1.11 (continued)

Year	Name and features	Location	Remark
1987	Inguri Dam, 271.5 m high, 10 m thick at the crest and 52 m thick at the altitude 50 m above its base	Inguri River, Georgia	Double-curvature dam had been keeping the world's record of arch dam height until the completion of the Xiaowan Dam (China)
1987	Upper Stillwater Dam, 87 m high	Utah, USA	Gravity type belongs to the initial batch of RCC dams, with dry lean concrete of high cementitious material (240–250 kg/m ³)
1989	Alberto Lleras Dam, 243 m high	Guavio, Columbia	Also known as the Guavio Dam
1989	Knellpoort Dam, 50 m high	Free state, South Africa	One of the first batch of RCC arch gravity dams
1990	Wotwedans Dam, 70 m high	Western Cape, South Africa	One of the first batch of RCC arch gravity dams
1993	Aguamilpa Dam, 187 m high	Tepec, Mexico	Record setting of the CFRD at that time
1993	Wenquanbao Dam, 48 m high	Hebei Province, China	The first RCC arch dam in the Northern China
1993	Puding Dam, 75 m high	Guizhou Province, China	The first RCC arch dam in the southern China
1999	Ertan Dam, 240 m high	Yalongjiang River, China	The first Chinese particular high double-curvature arch dam
2001	Shapai Dam, 132 m high	Sichuan Province, China	The second highest RCC arch dam in the world
2005	Cindere Dam, 107 m high	Turkey	The highest hardfill dam in the world
2007	Dahuashui Dam, 134.5 m high	Guizhou Province, China	The highest RCC arch dam in the world
2008	Shuibuya Dam, 233 m high	Hubei Province, China	The world's highest CFRD
2008	Three Gorges Dam, 181 m high	Yangtze River, Hubei Province, China	Gravity dam, with generator installation of 22,400 MW, it is the world's largest hydropower station
2009	Longtan Dam, 216.5 m high	Guangxi Province, China	The world's highest RCC gravity dam
2009	Guangzhao Dam, 200.5 m	Guizhou Province, China	The world's second highest RCC gravity dam
2009	Laxiwa Dam, 250 m high	Qinghai Province, China	The Chinese highest logarithmic spiral arch dam
2010	Xiaowan Dam, 294.5 m high	Yunnan Province, China	The highest double-curvature arch dam in the world
2010	Pubugou Dam, 186 m high	Sichuan Province, China	Central core rockfill dam, on a riverbed with alluvial deposit of 77.9 m deep, the concrete cutoff wall in the foundation is 82.9 m deep

(continued)

Table 1.11 (continued)

Year	Name and features	Location	Remark
2012	Nuozhadu Dam, 261.5 m high	Yunnan Province, China	The Chinese highest central core rockfill dam
Under construction	Xiangjiaba Dam, 165 m high	Sichuan/Yunnan Province, China	Concrete gravity. With generator installation of 7750 MW, it is the fifth largest hydropower station in the world
Under construction	Xiluodu Dam, 285.5 m high	Sichuan/Yunnan Province, China	Double-curvature concrete arch dam. With generator installation of 13,860 MW, it is the third largest hydropower station in the world
Under construction	Jinping 1 Dam, 305 m high	Sichuan Province, China	Will create the new height record of double-curvature arch dam when it will be completed soon
Under construction	Bakhtiari Dam, 325 m high	Lorestan Province, Iran	Double-curvature concrete arch dam

2012). In addition, there are also the southeast coastal river systems including the Qiantangjiang and the Mingjiang, the northeast international river systems including the Heilongjiang and the Yalujiang, and the southwest international river systems including the Lancangjiang and the Nujiang and the Yaluzangbujiang (Brahmaputra), the northwest international rivers of the Ertix and the Ili. There are also several interior river systems of Tarim and others in the provinces or autonomous regions of Xinjiang, Gansu, Inner Mongolia, and Qinghai.

According to the statistics data, there are more than 50,000 rivers in China with a drainage area of over 100 km². Among them, there are more than 1600 rivers with a drainage area of over 1000 km², 20 rivers with a length of over 1000 km, and 3019 rivers with theoretical hydropower resources of over 10 MW.

The average annual precipitation in China is 648 mm, i.e., about 6190 billion m³ in total. Accordingly, the total amount of annual river runoff in China is about 2711 billion m³. There are 17 rivers having an annual runoff over 50 billion m³, which is ranked at the fifth place in the world after Brazil, Russia, Canada, and USA.

According to the data provided by the State Development and Reform Commission in 2004 (National Leading Group for the Re-check of the National Hydropower Resources Survey 2004), the theoretical hydropower resources in the Chinese mainland are 695 GW, corresponding to an annual energy output of 6083 TWh; the technically exploitable hydropower resources are 542 GW, which are at the first place in the world. Accordingly, China has planned 270 hydropower power stations with installed generator capacity over 300 MW, of which 100 are over 3000 MW and 800 are between 50 and 300 MW. The hydropower resources of the major river basins in China are listed in Table 1.12.

Due to the geographic features of the country, scarce cultivable land and huge population are highly concentrated in the eastern China, while 82.9 % of water and hydropower resources are distributed in the vast western part of the country. The society development, particularly in the middle and lower river reaches with huge population, is often encountered with difficulties to satisfy multiple purposes such as flood control, agriculture irrigation, navigation, water supply, aquaculture, recreation, and ecology and is liable to conflicts among those purposes to some extent in terms of quantity and quality of water consumption, as well as spatial-time allocation. Therefore, China is actually a country in short of water resources: The average water resources per capita is about 2100 m³ and per hectare is about 22,500 m³, which is only 30 and 50 % of the world's level, respectively. In order to give priority to the full use of clean and renewable hydropower resources and meet the electric power demands, the high-quality management, rational exploitation, careful protection, and sustainable utilization of water resources are and will continue to be a strategically paramount issue in the economical and social development of the country.

Table 1.12 Hydropower resources of the major river basins in China

River basin	Theoretical hydropower resources		Technically exploitable hydropower resources		Number of power stations
	Annual energy output		Annual energy output		
	TWh	MW	TWh	MW	
Yangtze	2433.598	277,808.0	1187.899	256,272.9	5748
Yellow	379.413	43,312.1	136.096	37,342.5	535
Pearl	282.394	32,236.7	135.375	31,288.0	1757
Haihe	24.794	2830.3	4.763	2029.5	295
Huaihe	9.800	1118.5	1.864	656.0	185
Northeast river system (Songhuajiang, Heilongjiang, Liaohe, etc.)	145.480	16,820.8	46.523	16,607.4	644 + 26/2
Southeast river system (Qiantangjiang, Minjiang, etc.)	177.611	20,275.3	59.339	19,074.9	2558 + 1/2
Southwest river system (Lancangjiang, Nujiang, etc.)	863.007	98,516.8	373.182	75,014.8	609 + 1/2
River system in Tibet (Yaluzangbujiang)	1403.482	160,214.8	448.311	84,663.6	243
Northwest river system (Ertix, Ili, Tarim, etc.)	363.357	41,479.1	80.586	18,471.6	712
Total	6082.9	694,400	2473.9	541,640	13,286 + 28/2

N.B.: According to the data of the general surveys in 2005

1.4 Hydraulic Engineering in China

Hydraulic engineering in China has gained rapid progress since the 1950s until the end of the 2000s, as has been interspersed foregoing. In the twenty-first century, the hydropower exploitation in China will attain a greater breakthrough by two steps (Peng 2006; Zhu 2009).

The first step was from 2001 to 2010. By the end of 2010, the national hydropower capacity reached 210,000 MW, and the corresponding annual energy output was 650 TWh. The hydropower accounted for about 30 % in the national electric power supply. The 5200 dams higher than 30 m were completed or under construction, of which 145 exceeded 100 m. Among the 450 completed hydroelectric stations larger than 50 MW in generator installation capacity (including 21 pumping storage stations), 100 exceeded 300 MW (including 15 pumping storage stations) and 40 were of especially large scale whose installation capacity exceeded 1000 MW (including 7 pumping storage stations). By the year of 2010, the total reservoir storage capacity reached 1/6 of the river annual runoff of the whole country, which played important role in the flood protection, irrigation, and water supply by covering 0.35 Billion population and 0.033 Billion ha farmland as well as hundreds of large to medium cities including Beijing, Tianjing, Guangzhou, Shanghai, and Wuhan. To meet the development requirements of metropolis cities, a large number of long distance water diversion projects were constructed, and more than 100 large to medium cities relied mainly on the reservoir supply for domestic living and industry, such as the Miyun reservoir for Beijing, the Panjiakou reservoir for Tianjing, and the Shenzhen reservoir for Shengzhen and Hongkong.

The second step is from 2011 to 2050. During this period, under the state policy guidance of exploiting her vast western area, China will nearly complete the exploitation of her hydroenergy potential, and there will be tens of super-large-scale hydropower plants built in the western China. Specially, the Motuo hydropower project, with design installed generator capacity larger than 40,000 MW, will be put into operation. It will become the greatest base of the hydropower in the world. The capacity of electricity transferred from the West to the East will exceed 150,000 MW.

Following the progress in the construction of large-scale water resources and hydropower projects, China has reached international level concerning the research, design, and construction technologies. The largest hydraulic project completed in the world—the Three Gorges project—provides electric capacity of 22,400 MW; the world's highest arch dam (Xiaowan, $H = 294.5$ m), the world's highest concrete-faced rockfill dam (Shuibuya, $H = 233$ m), and the world's highest RCC gravity dam (Longtan, $H = 216.5$ m) are all erected in China. The various giant projects under construction or nearly to be completed such as the Xiluodu, Xiangjiaba, Jingping 1, and Jingping 2 will further give an impetus to push the technologies of water resources and hydropower engineering in China up to a greater height (Table 1.13).

Table 1.13 Large-scale hydropower projects to be constructed during the “twelfth five-year plan” (2012–2017)

River basin	Projects
Jinshajiang	Baihetan, Wudongde, Longpan, Liyuan, Ahai, Longkaikou, Ludila, Guanyingyan, Suwalong, Yebatan, Lawa
Lancangjiang	Cege, Kagong, Rumei, Guxue, Gushui, Wulonglong, Lidi, Tuoba, Huangdeng, Dahuaqiao, Miaowei, Ganlanba
Daduhe	Shuangjiangkou, Jinchuan, Anning, Badi, Danba, Houziyan, Huangjinping, Yingliangbao, Laoyingyan, Zhentouba, Shaping
Upreach of the Yellow river	Ningmute, Maerdang, Chiha, Banduo, Yangqu, Heishanxia
Yalongjiang	Lianghekou, Yangen 1, Yangen 2, Mengdigou, Yangfanggou, Kala
Nujiang	Songta, Maji, Yabiluo, Liuku, Saige

References

- Burke E III (2009) Islam at the center: technological complexes and the roots of modernity. *J World Hist* 20(2):165–186
- Chanson H (2009) Embankment overflow protection systems and earth dam spillways. In: Hayes WP, Barnes MC (eds) *Dams: impacts, stability and design*. Nova Science Publishers, New York, pp 101–132
- Edenhofer O, Pichs-Madruga R, Sokona Y, Seyboth K, Matschoss P, Kadner S, Zwickel T, Eickemeier P, Hansen G, Schlömer S, von Stechow C (eds) (2011) *IPCC (Intergovernmental Panel on Climate Change) special report on renewable energy sources and climate change mitigation*. Cambridge University Press, Cambridge
- Engineering Foundation (US) (1927) *Arch dam investigation: a progress report on the Stevenson Creek Test Dam, Near Fresno, California*. The Foundation, CA
- Greene BH, Christ CA (1998) Mistakes of man: the Austin dam disaster of 1911. *Pennsylvania Geol* 29(2/3):7–14
- Hill D (1996) *A history of engineering in classical and medieval times*. Routledge, New York
- Howell C, Jaquith AC (1929) Analysis of arch dams by trial-load method. *Trans ASCE* 93(1):1191–1225
- ICOLD (2013) *Historical review on ancient dams (bulletin 143)*. ICOLD, Paris
- Intergovernmental Panel on Climate Change (IPCC) (2012) *Special report on renewable energy sources and climate change mitigation*. Cambridge University Press, Cambridge
- Jansen RB (1980) *Dams and public safety, a water resources technical publication*. Water and Power Resources Service (Bureau of Reclamation, US Department of the Interior), Denver
- Jia JS (ed) (2013) *Dam construction in China—a sixty-year review*. China Water Power Press, Beijing
- Jorgensen LR (1915) The constant angle arch dam. *Trans ASCE* 78(1):685–721
- Kollgaard EB, Chadwick WL (eds) (1988) *Development of dam engineering in the United States*. Pergamon Press, New York
- Londe P (1987) The Malpasset dam failure. *Eng Geol* 24(1–4):295–329
- Londe P, Lino M (1992) The faced symmetrical hardfill dam: a new concrete for RCC. *Int Water Power Dam Constr* 44(2):19–24
- Manso PA, Schleiss AJ (2002) Stability of concrete macro-roughness linings for overflow protection of earth embankment dams. *Can J Civil Eng* 29(5):762–776

- Ministry of Water Resources of the People's Republic of China (2000) SL252-2000 "Standard for classification and flood control of water resources and hydroelectric project". China Water & Power Press, Beijing (in Chinese)
- Ministry of Water Resources of the People's Republic of China (2012) China water resources bulletin 2011. China Water & Power Press, Beijing
- Müller L, Fairhurst C (1964) Felsmechanik und Ingenieurgeologie (Rock mechanics and engineering geology), supplementa (book 1). Springer, Wien (in German)
- National Development and Reform Commission of the People's Republic of China (2003) DL 5180-2003 "Classification & design safety standard of hydropower project". China Electric Power Press, Beijing (in Chinese)
- National Leading Group for the Re-check of the National Hydropower Resources Survey (2004) Results of the re-check work of the national hydropower resources survey. China Electric Power Press, Beijing (in Chinese)
- Noetzli FA (1921) Gravity and arch action in curved dams. *Trans ASCE* 84(1):1–60
- Noetzli FA (1922) The relation between deflections and stresses in arch dams. *Trans ASCE* 85 (1):284–307
- Outland CF (1963) Man-made disaster: the story of st Francis Dam. Clark AK, Glendale
- Pan JZ, He J (2000) Large dams in China, a fifty-year Review. China WaterPower Press, Beijing (in Chinese)
- Peng C (2006) 21st century China hydropower engineering. China Electric Power Press, Beijing (in Chinese)
- Rankine WJM (1881) Miscellaneous scientific papers: report on the design and construction of masonry dams. Charles Griffin and Company, London
- Raphael JM (1971) The optimum gravity dam. In: Rapid construction of concrete dams, proceedings of engineering foundation conference. ASCE, New York, pp 221–247
- Ru NH, Jiang ZS (1995) Arch dams—accident and safety of large dams. China WaterPower Press, Beijing (in Chinese)
- Sazilly JA (1853) Note sur un type de profil d'égal résistance proposé pour les murs de réservoirs d'eau. *Annales des Ponts et Chaussées*. 6:191–222 (in French)
- Schnitter NJ (1994) A history of dams: the useful pyramids. AA Balkema, New York
- Smith NA (1971) A history of dams. Peter Davies, London
- Toshio H, Tadahiko F, Hitoshi Y et al (2003) Concept of CSG and its material properties. In: Berga L (ed) Proceedings of the 4th international symposium on roller compacted concrete dams. AA Balkema, Madrid, pp 465–473
- Vogt F (1925) Über die berechnung der Fundament Deformation. *Avhandlingar utgitt av Det Norske Videnskaps Akademi*, Oslo (in German)
- Woodard SH (1904) Lake Cheesman dam and reservoir. *Trans ASCE* 53(2):89–132
- Yumurtacia Z, Bilgen E (2004) Hydrogen production from excess power in small hydroelectric installations. *Int J Hydrogen Energy* 29(7):687–693
- Zhu SA (1995) Technical history of dam engineering. Water Resources and Electric Power Press of China, Beijing (in Chinese)
- Zhu TZ (2009) 20th century river hydropower planning in China. China Electric Power Press, Beijing (in Chinese)

Chapter 2

Planning and Design of Hydraulic Projects

2.1 Purposes of Hydraulic Projects

A hydraulic project may be small or large, simple or complex, and single or multiple purposed, and it should provide the functions to accomplish the optimum development of related water and hydropower resources.

In many cases, the project will be multi-purposed. For this reason, the investigations may comprise a large number of matters, and some or all of them will influence the selection of the project site and scale. Hence, the entire project must be investigated as a whole before the design requirements for each single structure, such as the dam, can be firmly established.

Main aspects of the river development using hydraulic projects, with particular emphasis upon the design requirements for dams and reservoirs, will be presented hereinafter.

2.1.1 Flood Control

Many river basins are frequently suffered from destructive floods and are, therefore, difficult to be used for farming and residence. A very effective way for flood defense is to build hydraulic projects with capacious reservoirs. Many projects (e.g., the Three Gorges Project) owe a good deal or majority of their social and economic benefits to flood control function. Sometimes, hydraulic projects are specially built to fight floods only.

In the design of flood control projects and structures, it should be taken into account that:

- The relation of the cost for flood control with the benefits to be derived through the reduction of cumulative damage should be favorable and in light of public interest, as compared to alternative means for obtaining similar benefits;

- The temporary storage for design and check floods must be sufficient to cut the major peak inflows or to lower down the frequency of minor floods; and
- Flood control must be effective and reliable, and so far as it is predictable, the method of flood control should be automatic rather than manual.

2.1.2 Irrigation

Nowadays, about 230 million hectares of farmlands are irrigated all over the world—as much as 70 % of the water taken from rivers is used for irrigation, of which 75 % never returns back to the streams. In some regions, especially in the Middle East, the Central Asia and northern China, farming without irrigation would be unfeasible at all.

It is customary to distinguish between gravity irrigation and pumping irrigation. The former depends on the head created by dams over the elevation of the farmlands to which the water is delivered. The latter employs powered pumps, so the water can be lifted to any desired elevation, to be distributed later over the ramified system comprised of canals and conduits.

The desired amount of water is stored in reservoirs, and the power for pumps is furnished by hydropower plants that are generally components of multi-purposed hydraulic projects. Most modern China's irrigation systems are supported by multi-purposed hydraulic projects.

For successful irrigation, the supply of water must be adequate at an economically reasonable capital investment per unit of area and must be easy for operation and maintenance.

2.1.3 Power Generation

It is a sad fact that thermal power stations, especially those of coal-burned types, discharge a lot of ash and noxious gases into the atmosphere and foul up large territories. Of these, surplus dioxide is fraught with the gravest consequences. The thing is that it mixes well with water vapors and yields sulfuric acid, which, upon precipitation, poisons water bodies. In recent years, the toxic haze phenomenon frequently occurs in a wide territory across the northern and eastern China, which is mainly blamed for this coal-burned pollution, apart from another major pollution sources from steel and cement industries, city infrastructure construction, and vehicle exhaust.

Although they do not pollute the atmosphere, nuclear power plants present another danger since they produce radioactive wastes that are rather difficult to get rid of. The Fukushima Daiichi nuclear disaster caused by the Tohoku earthquake induced tsunami on March 11, 2011, gives a global warning for the potentiality due to uncontrolled consequences of nuclear power plant accident.

Hydropower stations are sufficiently “clean” enterprises that result in few soil, water, or air pollution. Therefore, they may considerably reduce the overall pollution compared to thermal or nuclear power stations. As far as the pollution problems are concerned, hydropower is extremely attractive.

On a global scale, the unlimited and uncontrolled development of power engineering (nuclear power plants being the most important cause for concern) may, in the long run, upset the thermal balance of the Earth—a fact its consequences to the mankind are very difficult to predict insofar. In this aspect, hydraulic power engineering, which ultimately depends on solar energy (in fact, it merely redistributes the energy released by the Sun) and therefore does not affect the thermal balance of the planet, appears to be an ideal choice.

Where the power generation is targeted in the development of a hydraulic project, the capacity of the power generating equipment and the load demand are closely related to the quantity of water available and the amount of storage provided, which in turn, dictate the height of the dam.

2.1.4 Navigation

River transportation plays an important role in water economy. As a rule, inland water transportation capacity will be raised considerably by building dams and barrages. The point is made that a chain of storage reservoirs improves navigation depths, straightens navigation channels, and ensures the pathway of large ships. Also, the regulated outflow from reservoirs improves navigation conditions in the downstream reaches. In China, most inland waterways depend on major hydraulic projects. Examples are the Yangtze River and the Yellow River waterways.

When a dam is constructed on a large river considering upstream and downstream navigation, it may be desirable to construct ship locks or lifts to provide pathway for vessels over the barrier. Depending upon topographic and geologic conditions, the locks may be the integral components of the dam or entirely separate structures. The functional design criteria are the dimensions of lock chamber or handling trough and the draft of vessels to be accommodated, and the estimated number of vessels passing upstream and downstream at peak periods without excessive delay.

2.1.5 Domestic and Municipal Purposes

Much water is consumed by metallurgical, chemical, wood pulp, and paper industries. Among major industry users are also thermal and nuclear power plants. In many industrially developed regions of China, the demand for water cannot be met by the local water resources solely. To deal with the problem, reservoirs are built to store the most of the local runoff, and large water developments are set up to

divert water from other basins. Most of these water supply systems originate from the reservoirs of multi-purposed hydraulic projects.

Although it constitutes merely about one-tenth of the industrial water consumption, public water supply, which meets the immediate needs of the population, should be taken into account seriously. Consequently, it is hardly surprising that the primary function of quite a number of multi-purposed hydraulic projects is to supply water for domestic daily consumption.

Sometimes, there is a need for the hydraulic project in a region where stream flow either ceases entirely or is reduced to extremely low levels during seasons of the year, and where such natural stream flow is the principal source of water supply for one or more communities, water storage creation for stream flow regulation may be justified apparently.

The quality of the water must be such that it can be rendered portable and usable for domestic and most industrial purposes by economical treatment methods. It should meet state public health standards with regard to bacterial purity, taste, color, odor, and hardness. Control and protection of watershed areas are desirable for municipal water supply reservoirs.

2.1.6 Environment Protection

It might be a selfish but reasonable idea that the important environmental issues are those that the most direct concern to the livelihood and well-being of mankind, and the various other living things are of concern to human to whatever degree their existence is important to his living conditions, i.e., there is a close relation between the important environmental issues and the social needs of human beings.

Among the various beneficial environmental–social effects of hydraulic projects, they may be distinguished as farmland improvement by irrigation, higher standard in flood protection, enhanced water quality and supplying ability for domestic and municipal uses, clean power supply without consumption of fuel, and fishery and recreational development. These benefits, partially measurable in economic terms, are among the principal objectives of a hydraulic project. However, the negative impacts of the hydraulic project on the environment should be never overlooked in the design and construction.

2.1.7 Recreation and Other Purposes

A reservoir might significantly make an excellent site for various recreational facilities and health farms. Sometimes, small reservoirs are built specially for recreation purposes.

Occasionally, a hydraulic project is proposed to regulate the water level in shallow lakes and swamps other than those purposes heretofore enumerated. For

example, the project for the detention or diversion of stream flow to conserve it by transforming surface water to groundwater through the process of infiltration could be planned and constructed. To justify the project economically, however, it must be determined that the soil characteristics will permit infiltration to occur in a desirable quantity.

2.2 Planning for Hydraulic Projects

2.2.1 Tasks and Requirements of Planning

Water resources planning is an important basis for their exploration, development, conservancy, and protection, which falls into river basin planning and regional planning. The former is further divided into river basin comprehensive planning and river basin specialized planning, while the latter is further divided into regional comprehensive planning and regional specialized planning (Jiao et al. 2004; Liu 2006).

Specialized planning means planning for the hydrographical test, flood control, hydropower development, logging control, irrigation, navigation, recreation and tourism, fishery, water and soil conservancy, water resources protection, environment protection, etc., of the river basin or region concerned.

Regional planning should be submitted to river basin planning, and specialized planning should be submitted to comprehensive planning. In China, the comprehensive planning of important rivers and lakes is accomplished by the related local governments under the leadership of the State Council. The approved planning must be executed to the letter; any revisions should be examined and approved by the State Council. Documents of the laws and regulations related to the water resources and hydropower planning in China are as follows: “Flood Control Law of the People’s Republic of China,” “Water Law of the People’s Republic of China,” “People’s Republic of China Land Law,” “Electricity Law of the People’s Republic of China,” “Environmental Protection Law of the People’s Republic of China,” “Law of the People’s Republic of China on Water and Soil Conservancy,” “Forestry Law of the People’s Republic of China,” “Environmental Impact Assessment Law of the People’s Republic of China,” “Regulations of Land Requisition Compensation and Resettlement of Large and Medium Hydropower Project Construction,” as well as the other administrative regulations.

Until 2010, there have been more than 70 years in the history of Chinese planning works for water resources and hydropower resources, and most of the basin comprehensive developments or main river cascade hydropower developments have been approved by the State Council and the related state ministries.

2.2.2 Principles of Planning

- Pay attention to the investigation of water resources and hydropower resources. The optimal development scheme should be completed after the comprehensive comparison resting on necessary topographic survey, hydrologic tests and analyses, geologic exploration and analyses, environmental impact evaluation, and engineering technology demonstration.
- Select mainstay projects of high regulation ability as leading reservoirs and to construct rational cascade development configuration. In this way, the head fall and water runoff may be fully exploited in both the short and long terms.
- Comprehensive utilization of water resources should be carried out in the whole planning process. On the one hand to aim main development purposes and on the other hand the comprehensive requirements such as electric power generation, flood control, sediment interception, navigation, irrigation, water supply, timber floating, fishery, and recreation are studied.
- Land acquisition and reservoir region immigration should be carefully handled and tackled. The comprehensive utilization of water resources should be restricted by the inundation loss, which is an important factor dominating the selection of the planning scheme.
- Care is taken over the protection and recovery of ecological environment system during the whole planning process. The water resources and hydropower development and ecological environment protection should be mutually promoted and coordinated.
- Market oriented in the water resources allocation should be persisted. The normal storage level and installed generator capacity are demonstrated and optimized with respect to the balance of exploitable and market demands, the relation of input and output, as well as the principle of maximum investment pay back.
- Engineering investment and benefits should be elucidated separately for multi-purposed water resources and hydropower projects. The feasibility and rationality of alternative schemes are to be studied. If there is no well-anticipated economic benefits in the near future, staged construction or obligate position for later construction should be considered.
- Very often, limited by the factors related to technology and finance status, basin water resources and hydropower planning cannot reach the goal in one step. As there are development in national economy and society and the progress in technology, the planning philosophy and method will be changed and innovated. Therefore, the approved planning scheme might be subject to revision and supplementation, if necessary.

2.2.3 State of the Art and Trends in the Planning

Exactly speaking, water resources and hydropower planning is related to three major systems including water resources system, energy system, and electric system. Each of them is large and complex with various influencing factors, featured as multi-purposes, multilayers, and indeterminate. Nowadays, the planning of water resources and hydropower development is directed to the techniques such as the multi-objective synthetic optimal selection criteria; solution of the distributed, multilayered, and multi-functioned system; group decision-making model based on process-oriented decision-making; and use of artificial intelligent system (e.g., artificial neural network) and expert system.

Today, hydropower development planning models are readily available in the form of tool kits whose various components are contributed by the scholars all over the world. At the end of the 1980s, by the application of the famous WASP-III (IAEA) (Hamilton and Bui 2001) and MARKAL (IEA) (Loulou et al. 2004; Seebregts et al. 2000) models, the Chinese planning model IRELP/I (Inter-Regional Electric Long-term Planning) was developed, which employed mixed-integer linear programming. With this model, the hydropower planning and the power source planning were for the first time combined in China. The SIRELP (Strengthened Inter-Regional Electric Long-term Planning) model is a strengthened version of the IRELP/I model, which uses several advanced optimization skills to overcome the shortcomings of its predecessor, for addressing hydropower projects with over-year regulation reservoir and huge calculation quantity. The above two models had been employed in the important domestic projects such as the Three Gorges. However, since the mixed-integer linear programming is not theoretically strict for solving nonlinear programming issues, and the dependent on 0–1 variables makes the calculation amount very huge, these models are not able to solve the planning problem for hydropower projects with over-year regulation reservoirs ideally.

To directly seek solutions for both the linear and nonlinear problems by successive approximation, the HELP (Hydropower and Electricity Long-term Planning) model (Dyner and Larsen 2001) developed on the basis of aforementioned predecessors in 1990s is now widely accepted in China due to its technique advantages such as the combination of dynamic programming and linear programming, the abandonment of integer variables, and the ability to make the investment decision and to handle discontinuous variable problems (e.g., numbers of generating units and transmission lines) as well as to optimize operation decisions (Yang and Pu 1993; Yu et al. 1994).

2.3 Ecology and Environment Protection

2.3.1 *Ecological and Environmental Issues in Hydraulic Projects*

The realization that human is an integral part of nature and that his interaction with the fragile ecological systems surrounding him is of paramount importance to his continued survival is prompting a re-evaluation of the functional relationships that exists between the environment, its ecology, and human (Dober 1969).

The needs to store water for use through the period of drought seasons, to supply industry and agriculture water for material goods and foodstuffs, to provide recreational water in ever-increasing amounts, and to meet the skyrocketing electric power demands, all require the construction of hydraulic projects. These projects help human beings, but meanwhile give rise to impacts on ecosystem and environment. Referring to the original environmental setting, hydraulic projects are a new component of the environment. Thus, care should be exercised to coordinate the old and new components of the environment, especially the new hydraulic projects constituting a new water resources system. An increasing concern is the effects of a hydraulic project integrated by several hydraulic structures upon the ecosystems, particularly on the fish, wildlife, and human inhabitants adjacent to the project (Brandon 1987; Golzé 1977; Graf 1999; ICOLD 1992; Oglesby et al. 1972; Thornton 1990; Wetzel 1990).

In the planning phase of any hydraulic projects, an environmental investigation must be implemented to evaluate environmental and ecological impacts of the hydraulic structures and to study proper countermeasures for avoiding or alleviating their adverse effects (United Nations 1990). In any events, the environmental impacts around the construction site areas are not to be overlooked in making a project plan. Philosophically, if well designed, a hydraulic project should reduce the natural hydrological disasters, utilize the water resources more effectively, and provide more harmonious circumstances for the survival and development of human beings and nature. However, it should be admitted that many of these are exceedingly complex and few answers concerning the total impacts of a hydraulic project on its environment are readily available.

1. Environmental benefits from hydraulic projects

(a) Reducing disaster and damage attributable to flood and drought control

A hydraulic project with dam may increase the resisting capability against natural disasters such as flood, water logging, drought, salinization, and alkalization, or reduce the frequency of their occurrences. As a result, it will provide more comfortable and stable circumstances for mankind.

(b) Providing hydropower as a clean energy

For a 2000 MW hydropower project built to replace the thermal power plant in the power system, 5 billion kg of raw coal may be saved annually. Furthermore,

44 million kg of emission of nitric oxides, 1.15 million kg of carbon monoxide, 24 billion kg of sulfur dioxide, and 1.4 billion kg of solid waste also will be cut each year. In addition, a large amount of water for cooling which is the pollution source of heat emission to local water body also will be eliminated.

(c) Improving inland transportation waterway

Water stream is a natural transportation route. Compared with land transportation, it has the advantages of low transportation cost, less or even no land occupation, less or no resettlement, low fuel consumption, less pollution, low noise, suitability for long distance transportation of heavy cargo, and enjoyable ship traveling for tourism.

(d) Protecting the ecological environment and bringing ecosystem in good circulation

The construction of a large reservoir, in general, would improve the local climate and make it turning to the beneficial direction. Through the regulation of water body, the annual average temperature and the extreme lowest temperature would be raised, while the extreme highest temperature would be lowered down. In addition, the relative humidity around the reservoir region and its surrounding areas would be enhanced, which is generally beneficial for crops.

The construction of a large reservoir may also prevent people from pests by controlling water level. As one of good examples, the Hongzehu Lake area in China was one of the historical bases of East Asia locusts. After the construction of the barrage located at the San He (River), 1.64 m of the mean water level of the Lake has been raised. Since 1960, the water level has been maintained at about 12.5 m, so that locusts living below 11.5 m were all submerged. As a result, the occurrence of plagues of locusts has been reduced. Another good example is the elimination of the schistosomiasis parasitized and reproduced through water snails. The situation in favor of the growth of water snails is that the region is submerged in summer and turned to dry land in winter. However, the fluctuation of the water level in the most reservoirs in China is in an opposite way: The reservoir water level in summer is always kept lower for storage of floods, while during winter, the level is commonly kept higher. It creates a situation unfavorable for the growth of water snails.

(e) Improving water quality and water supply capacity

Construction of hydraulic projects with reservoirs of regulating storage could enhance the dilution and self-purification capacities of water body, hence improve the water quality of river and reduce the possibility of saltwater intrusion in the estuary. In China, for example, the Fengman Project and Xin'anjiang Project have greatly improved the water quality of their riverside cities of Harbin and Hangzhou, respectively.

(f) Creating or improving recreational condition

All the large-scale hydraulic projects with reservoirs are able to be developed into recreation places, such as the Xin'anjiang Reservoir and the Three Gorges Reservoir.

Some reservoirs also may improve the downstream recreational sites through the augment of flow in dry season by their regulation. For instance, although the famous Lijiang River flows through the Guilin City lacks water in dry seasons, its recreational condition has been greatly improved by the upstream Qingshitan Project which supplies additional flow in the dry seasons for this beautiful river.

2. Adverse environmental effects caused by hydraulic projects

Human's understanding on the importance of environmental problems has been progressing from unconsciousness to overall concern since the 1970s. A hydraulic project may simultaneously have positive and negative effects on environment as any other kinds of man-made projects. The rational way out is that consideration should be given to all effects and efforts must be made to achieve the maximum positive effects and the minimum negative ones. If attention is called only at one effect either positive or negative, the overall potential benefits of the hydraulic project could not be fully exploited and sometime wrong decision might be made.

The pertinent aspects of the most concern with respect to adverse effects have been well recognized and summarized by scholars (Mattice 1991) such as:

- Over cultivation and reclamation, random deforestation, and other relevant environmental impacts caused by the improper arrangement of resettlement;
- Inundation or damage of historical and archeological sites, of forests and ecological environment for rare fauna or flora, as well as of mineral deposit;
- Loss of wildlife, fish, and aquatic habitats;
- Public health affected by waterborne diseases;
- Cold damage to irrigation and some migratory fish due to the released discharge through thermally stratified reservoirs; and
- Seismic activity, landslide, and other relevant environmental geology problems triggered or induced by reservoir impounding.

Nowadays, several heretofore enumerated detrimental effects may be either partially or nearly completely mitigated. However, it is noting worthy to indicate that the degree of importance of many these effects depends on the existing physical and environmental circumstances at the sites: Some may be so paramount as almost certainly to prohibit the use of the sites for reservoirs; at other sites, the effects may be quite minor and the amount of environmental loss may be easily acceptable, when the project needs are demonstrated.

3. Effects of environment on hydraulic projects

Environment also affects hydraulic projects in many aspects. Adverse effects include earthquake-induced dam failure and landslide, soil erosion in upper reaches

bringing sedimentation into reservoir (Morris and Fan 1998), and scouring of riverbed. Therefore, before the construction of a hydraulic project, attention should be called at the study on the environmental settings around its up- and downstream areas as well as site area, which are considered as components of the system for planning and designing in order to ensure the long-term benefits of the project.

2.3.2 Environmental Protection Design for Hydraulic Projects

To improve environment is one of the main purposes of hydraulic projects. As for their adverse effects, if investigations have been done beforehand and the mitigation measures have been taken, generally they could be reduced to acceptable level (Pan et al. 2000a).

As a recently developed soft science, environmental hydroscience is the knowledge system in applying fundamental sciences for solving the environmental problems encountered in hydraulic engineering. It was introduced into China at the late 1970s (Dudgeon 1995; Zhong and Power 1996) and has been developing increasingly since then.

China has established a set of regulations and specifications for handling the environmental issues related to hydraulic engineering, covering respective phases of planning, feasibility study, project design, construction, operation, retrospective environmental assessment, monitoring network planning, and instrumentation.

1. Environmental impact alternatives

It is demanded to examine alternative dam and reservoir plans to take note of any possibilities for minimizing adverse environmental impacts while accomplishing the major project purposes. The eventual choice of a project plan is made in the consideration of relative accomplishments, expenditure, social effects, economic influences, and environmental impacts.

The following is the commonly employed methodology in China to select alternative plans having different amounts of environmental impacts, with each plan accomplishing the expected objectives.

The first step is to make an examination and inventory of the various important environmental qualities of the stream or stream system under consideration. Environmental factors might be ranked in sequence according to their importance. This inventory would be of the existing conditions, which may be natural conditions in some instances, but more likely may be conditions which have been influenced by human activities up to the present time.

In the second step, the future environmental condition without the project development is estimated: It may be the same as the existing one, or may be improved or degraded? The future environmental condition “without project,” to the extent it can be foreseen, becomes the basis of the comparison of alternative project plans.

Next, an economically optimum project disregarding all environmental impacts except those that can be positively accepted is planned. The evaluation of this alternative plan will show the possibly maximum project accomplishments within the physical conditions and economic limitations. It might be designated as the “economically optimum planning alternative.”

Another alternative plan would be devised wherein an attempt would be made to minimize all important adverse environmental impacts and still produce some portion of the intended project accomplishments. If this “environmentally optimum alternative” indicates greatly reduced accomplishments and/or much increased costs from the above “economically optimum planning alternative,” it may be set aside in favor of a third alternative as described below.

A third alternative plan would be devised whereby a compromise would be made between the above two extreme alternatives, seeking to avoid or to minimize the most important adverse environmental impacts while achieving all or most of the potential project accomplishments of the economically optimum alternative. Since concessions must be made for environment, this plan will probably cost more per unit of accomplishment than the economically optimum plan.

The results of evaluation with respect to the alternative plans would be summarized to show relative amounts of environmental impacts, project accomplishments, expenditures, and the costs incurred. This summary will provide the basis for obtaining agreement and making decision on selecting a “better” plan.

2. Design targets

Design should be devoted to the accomplishment of the following goals:

- Keeping the natural beauty of the surrounding areas;
- Creating aesthetically satisfying structures and landscapes;
- Giving rise to minimum disturbance to the area ecology; and
- Preventing water from contaminants around the reservoir area.

Designer should try to accomplish these targets in the most economical way, through detailed structural considerations, landscape considerations, protective considerations, and construction considerations.

(a) Structural considerations

It goes without saying that the main purpose of any hydraulic structure is that it performs its function. Beyond this, thoughtful considerations should be given to blending the work with the environment and to provide pleasing surroundings. For example, if the work is an embankment dam, several actions can be taken which may prove beneficial to the project environment: A curved axis convex in the upstream direction could be used in lieu of a straight axis to make the reservoir more resemble to a natural lake; the downstream slope of the embankment could be covered with topsoil and seeded to present natural appearance; if it is not possible to reseed the downstream slope of the dam, cobbles and boulders which are indigenous to the area can provide a pleasing protective covering; the materials found in the reservoir area and from adjacent structure excavations are utilized to the maximum extent

practically; and borrow areas located above the reservoir level should have their final slopes flattened to conform with the surrounding area and for easy reseeded.

If it is necessary to excavate rock abutments above the dam crest level, consideration should be given to the use of pre-splitting blast techniques since they leave clean, straight, and aesthetic surfaces.

The diversion schemes should be such that excessive siltation created during construction will not be released into downstream water body. Materials from excavations which are not used in the embankment compaction should be placed in the reservoir area and preferably along the upstream toe of the dam, which may provide additional stabilization of the upstream dam slope.

Buildings used at the work site should blend with their surroundings. Pipelines, power lines, and electrical apparatus would be better to be buried. Where this is not possible, they should be painted to blend with their background.

(b) Landscape considerations

As much as possible of natural vegetation should be left in place. If there exists significant areas of natural beauty near the project, every effort should be made to preserve them. Borrow areas and cut slopes near and above the reservoir area should be revegetated soon after the mission is completed; the topsoil removed from the slopes should always be stockpiled for reuse.

Access roads to the work site during construction should be kept to a rationally minimum, and those who not planned for permanent use after the completion of the work should be obliterated and reseeded. Road relocation near the work site provides an opportunity to eliminate deep cuts in hillsides, use scenic alignments, and provide reservoir viewing locations. Adequate road drainage should be installed and slopes should be so cut that reseeded operations will be convenient (Gray and Leiser 1982).

Erosion control should be started at the beginning of the construction. Roads, cut slopes, and borrow areas should be provided with terraces, berms, or other check structures if excessive erosion is anticipated likely. Exploratory trenches in borrow areas which are not used or are adjacent to the work site should be refilled and reseeded.

Quarry operations and rock excavations should be so performed that the minimum amount of material is removed, and final rock slopes for the completed excavation are shaped to be nice looking.

For projects where power transmission lines will be installed, suggestions from experts and institutions should be taken to alleviate their environmental impacts.

(c) Protective considerations

At locations where accidents or incidents can occur, protective devices and warning systems should be installed. The most dangerous locations at a dam site are near the spillway (especially if it is chute-type), the outlet works, intake tower, and the stilling basins. Siphons are extremely dangerous. In addition, canals often have steep side slopes which prevent climbing out. They should be all fenced off and marked by warning signs.

When the project encompasses the generation of electricity, the problems of providing adequate safety precautions are considerably important and the advice of corresponding experts should be sought.

(d) Construction considerations

The environmental and ecological design requirements provided in the specifications are converted from an document by the designer into a reality by the contractor. The owner should ensure compliance by having competent inspectors and specifications which clearly spell out the construction regulations. Excessive air, water, and dust pollution during construction should be prevented; specifications covering these items should provide a framework for the inclusion of other important environmental provisions. The contractor and his staff should be well informed that this is an important step in the planning, design and construction sequence. The contractor should also institute safety precautions during construction and be encouraged to bring forward any obvious defects in the environmental considerations encountered (Shields and Sanders 1986).

If not intended for permanent use, construction camp site would be better to be placed within the reservoir area below normal water level. All trees, shrubs, and grass land areas which are to be protected should be staked or roped off. Any operations which will affect a large wildlife population should be performed in periods of low wildlife occurrence. The used water going downstream should be muddied as little as possible and be pollution free. Siltation ponds may be needed in extreme cases.

A temporary viewing site showing the completed project and explaining its purposes is helpful in promoting good community relations, which may also be used for the tourism purpose after the completion of the project.

(e) Provisions of water contaminant around the reservoir area

A part of the water used for irrigation and almost all of the water used for industrial and public purposes goes back to rivers. Naturally, this water contains a vast amount of mineral, organic, chemical, and bacterial contaminants which may, unless appropriate measures are taken, kill the fish and waterfowls (Hocutt et al. 1980) and make the water unfit for drinking, recreation, or even for use in various industrial process (Serhal et al. 2009). Apart from contaminated sewage water, a great deal of pollution is caused by petroleum products getting into water from passing vessels and by the leachate of rotting sunken timber.

Nature has endowed the water body in rivers, lakes, and seas with an amazing ability to purify itself by the actions of oxygen, water plants, microorganisms, and solar radiation. In fact, not long ago when pollution was not as serious as it is nowadays, water body could manage its health successfully. Unfortunately, this self-purifying capacity is far from being limitless. To make the situation even worse, the natural purifying capacity may be further weakened due to the slow down of the water flow in reservoirs created by dams. Therefore, much should be done to fight the environmental pollution around the reservoir areas. For instance, the releasing of non-purified wastewater into reservoirs should be totally banned,

and plants and factories are encouraged to adopt closed-cycle operation where the water would be reused after purification, and the hydraulic project should not be promoted without the advice of biologists.

2.3.3 Environmental Impact Monitoring and Reviewing for Hydraulic Projects

In order to build a function of environmental monitoring system, the issues need to be addressed are institutional arrangements within which such a system can be properly established; an effective network within which the components and parameters need to be monitored at different locations; position and frequency of monitoring for different elements in each location; indigenous expertise to carry out the necessary analysis; dissemination of information to potential users; and regular presentation of appropriate information to decision makers in time.

The role of the retrospective environmental impact assessment (EIA) for hydraulic projects is to justify the prediction of the change in the main environmental parameters and the effectiveness of the mitigation measures adopted. Moreover, the new mitigation measures and monitoring process to be adopted in the operation period are proposed. The EIA is accomplished by the identification, predication, and evaluation of the environmental impacts of the project on both the nature and society, and through the comprehensive assessment of the whole project. The public health issue in EIA becomes special concern recently. It is meant to assess the impacts on physical, biologic, and social sub-systems and their interaction with the project. The temporal scope of EIA covers construction stage and operation stage, whereas the spatial scope of EIA cover the project site and the surrounding areas.

Generally, the retrospective EIA of hydraulic projects consists in following aspects:

- To select the levels for assessment. Usually three levels are used, i.e., before construction, impounding stage, and operation stage.
- To determine the main environmental parameters to be investigated.
- Monitoring design and instrumentation.
- Statistics and analysis of data.
- Recommendation of the occurrence and development process as well as the mode of the main impacts on the important parameters.
- Feedback to the original EIA concerning the methods and conclusions.
- Put forward further mitigation measures, monitoring, and management methods.

For some important environmental parameters, the risk analysis and risk management should be carried out.

2.4 Engineering Hydrology

2.4.1 *Engineering Hydrologic Issues in Hydraulic Projects*

Engineering hydrology is an applied earth science which studies the movement, distribution, and quality of water on the earth, including the hydrologic cycle, its process, water balance, precipitation type, and estimation of precipitation.

Engineering hydrology uses hydrologic principles in the solution of engineering problems arising from human exploitation of the water resources. In its broadest sense, engineering hydrology seeks to establish relations defining the spatial (regional, geographic) and the temporal (seasonal, annual) variability of water, with the aim of ascertaining society risks involved in sizing hydraulic structures and projects (Golzé 1977; Pan et al. 2000b; Ponce 1989; Warren and Lewis 2003; Linsley et al. 1949; Zuo et al. 1984). Methods of stream flow measurement, stage discharge relation, unit hydrograph theory, transposition of hydrograph, synthesis of hydrograph from basin characteristics, stream flow routing, flood frequency analysis and attenuation of flood flows, sedimentation, etc., are the most important specified fields in the engineering hydrology.

Engineering hydrology finds one of its greatest applications in the design and operation of hydraulic projects. In the phase of river basin planning, the runoff and flood series of the main stream and tributaries are the basic data for the selection of the layout, the purposes and tasks, the scales and relationships, of the hydraulic projects. In the phase of feasibility study, to specify design parameters of a project, the magnitude of flood flow for safe disposal of excess flow, the minimum flow and quantity of flow available at various seasons, the capacity of reservoir storage, the interaction of the flood and hydraulic structures (e.g., levee, reservoir, barrage, and bridge) are studied based on the corresponding engineering hydrologic data. In the phase of construction, the design flood during the construction period, rating curve at the dam site and power plant site, etc., are necessary for the design of temporary diversion structures and for the arrangement of rational construction schedule, as well as for the rescue and emergency repair during flood seasons. In the phase of service life, the optimal safety operation of the project is also based on the high-quality hydrologic forecasting with regard to the runoff, flood, sediment, and ice conditions (Vide Chap. 18).

2.4.2 *Collection of Hydrologic Messages and Data*

Correct and reliable hydrologic messages and data establish solid base for engineering hydrologic computation and analysis. The main channels for obtaining the hydrologic messages and data are as follows:

- From the hydrology terminal, the distribution of hydrometric stations, gauging stations, and precipitation stations, which have long-term observation data

concerning water level, flow discharge, flow rate, silt, precipitation, evaporation, may be found out.

- Short-term hydraulic survey may be carried out in several important river sections, for the collection of data concerning water level, flow discharge, and silt.
- During the phases of planning, designing, and construction, temporary water gauges are installed at the river sections near the dam site and power plant site, for the observation of water level, flow discharge, and sediment.
- Precipitation data are needed to evaluate factors for use in computing the probable maximum flood (PMF). The major storm over a project basin and its surrounding areas are analyzed with respect to orientation, isohyetal pattern, aerial coverage, total depth, duration, and short-term intensity.
- Through the verification of historical documents and inscriptions on tablets, the hydrologic messages such as historical flood or minimum water level in dry seasons may be obtained.
- By means of archeology, the messages of ancient flood may be collected.
- By means of aerial photographs and satellite remote sense, the messages and data concerning hydrology may be supplemented.

2.4.3 Hydrologic Computation

1. Computation of design runoff

The chronological record of flow is defined as the hydrograph, which is the base for all statistics analysis of the runoff for a river basin. It reveals many characteristics of the runoff of the basin, such as the seasonal distribution of high and low flows, the contribution of groundwater flow, etc. The time unit used in hydrograph is varied with different purposes: Annual discharge is usually used in comparing sequences of high and low years only; monthly flows are the most useful in the reservoir design of multi-purposes.

Arranging the flows for any unit of time in the descending order of magnitude, the percentage of time for which any magnitude is equaled or exceeded may be computed. The resulting array is called a flow-duration curve or cumulative frequency curve. Such curves are useful in determining the relative variability of flow between two points in or not in one basin, approximating the amount of storage, etc.

A mass curve is a plot of the cumulative of the runoff from the hydrograph against time. It is a useful device in the analysis of runoff records.

A storage-draft curve gives the specific storage needed to sustain various draft rates of regulated flow. If storage is unlimited, the curve will approach the available mean flow as an asymptote.

The frequency of occurrence of hydrologic events is a necessary part of the hydrologic studies for hydraulic project design, which may be expressed in either of the following two ways:

- Recurrence interval. It is an average interval expressed in years and does imply that events will be equally spaced in time;
- Probability or percent chance of occurrence in any year. It is computed as the reciprocal of the recurrence interval.

The key data to be analyzed are the annual maxims, or one flood peak event per year. The independent annual flood maxims should be first tabulated in chronological order and improved that each year is represented. Then, the relative magnitudes should be assigned an sequent number.

2. Computation of design flood

Flow is one of major environment conditions entail hydraulic projects—one of the dominant dam safety indices is the magnitude of flood that the dam can withstand. The flood peak, flood volume, and flood hydrograph corresponding to the design criteria for flood control are called the design flood. Determining design flood for a hydraulic project is to predict the flood that may occur during operating period in the future. However, since the flood in the future cannot be forecasted exactly due to the uncertainty of long-term changes in flood, the design flood often has to be determined by using frequency estimation, stochastic simulation, or probable maximum precipitation/flood (PMP/PMF), etc. (Davis 1952; ICOLD 2003; Morri and Wiggert 1972; Sokolov et al. 1976).

If the records of runoff are short and experience with known floods is limited, a design flood should be developed from storm record. As early as in the 1940s, the study on the PMP and PMF were initiated by American engineers (Hershfield 1961; US Weather Bureau 1947). The PMF may be obtained by the PMP via water yield and flow concentration computation. Later, the PMP and PMF are increasingly prevalent in the design of important hydraulic projects. The concepts of PMP and PMF were introduced to China in 1958, and the latter were employed to study the design flood for the Three Gorges Project. The study on the PMP and PMF was emphasized after a rare storm at the upper reaches of the Huaihe River in August, 1975, which resulted in huge losses of life and property. Nowadays, it is widely recognized that the PMP and PMF should be exercised for rechecking important hydraulic projects in the country.

The hydrologic analysis, economic analysis of cost, and benefit analysis, for different dam heights and reservoir capacities, will guide to the choice of the reservoir capacity and the corresponding dependable flow that can be justified. The selected design flow allows some degree of failure, and some deficiencies of water are also permitted.

In USA, the design flood may be selectively used as follows:

- The PMF is applied for extreme important projects, its failure should be absolutely prevented;
- The standard design flood is applied for important projects, huge losses could be resulted in, if failed;
- The flood by recurrence analysis is only used for the projects of minor disaster consequences after failure.

In China, depending on the magnitude of the project and the economic losses caused by overtopping of the dam and the damages to the permanent structures, the flood may have a wide range of recurrence intervals, varying between 10 and 10,000 years. The DL5180-2003 “Classification & design safety standard of hydropower projects” stipulates that, if the failure might result in extreme downstream disaster, grade 1 water retaining structures and spillway structures should use PMF, or recurrence intervals of 10,000 years, as check flood standard.

(a) Reservoir design flood

The volume of flood control storage should be sufficient to impound total or partial runoff from the greatest known flood that has occurred from the controlled area. Storage for flood control may be provided in a single purpose project in which all the capacity, except that for a small pool, is allocated to this purpose. Storage for flood control in a multi-purposed project may be allocated specifically, too, and this flood control storage is usually the top increment in the reservoir and is released as soon as practicably possible after the passing of a flood. Where there is a definite flood season, use of all or part of the flood control storage may be permitted in the dry seasons.

If the reservoir is one member of a reservoir series, it is needed to study the complete operation procedure and economics in selecting the capacity of the reservoir. Flood detention and releasing involve a change in timing of the natural flood hydrograph. With a system of reservoirs, the changes in timing may not necessarily benefit all downstream reaches with equal effectiveness. This is especially true if several floods occur in succession, and before the flood storage can be discharged without causing damage. Detailed operation studies are required to draw the “rule curves” for system coordination and the operation of gates for individual dam.

(b) Spillway design flood

The spillway for a dam project is intended to provide regulating outlet for flood control operation when reservoir levels are above the spillway crest, by which to prevent the dam from overtopping induced damages or failure.

The spillway design flood is the most important flood to be provided for in the design of a hydraulic project. The magnitude and probable recurrence interval of the flood is related to the importance of the project, its functional use, the economic value of the investment, and the potential losses to property and life that would result from total or partial failure of the project.

It does not exist a fixed criterion to establish the relation between the height of dam, the volume of storage, and the factor of safety, to be adopted in the spillway design flood. However, some general standards for the hydrologic design of spillways can be summarized as follows:

- Design the dam and spillway large enough to assure sufficient dam safe unless the coming flood is larger than the PMF.
- Design the dam and appurtenances in such a manner that the structure can be overtopped without failure and without suffering serious damages, if possible.

- Design the dam and appurtenances in such a manner that breaching of the structure from overtopping would only occur at a relative gradual rate, and in this way, the rate and magnitude of downstream flood would be within acceptable limits.
- Drawdown the reservoir level low enough and storage impoundment small enough in time, so that no serious flood hazard would occur to the downstream in the event of breaching.

3. Rate curve at dam site and power plant site

Rate curve at dam site and power plant site of several river sections is required for the project planning, design, construction, and operation. The rate curve before and after the construction is usually not the same; therefore, they should be studied for different cases, respectively. The rate curve also may be influenced by the construction slag deposit and the structural features and become very complicated, which should be studied specially.

4. Water balance computation of reservoir

It comprises the analysis of the inflow, outflow, and losses, which may be important for large- to medium-scale hydraulic projects. The losses including evaporation, leakage, and frozen and their estimation ordinarily make use of indirect methods based on different postulations due to the lack of observation data.

5. Hydrologic forecast

The technique of analysis and estimation, which can determine the hydrologic status in the future via the hydrologic status at earlier and present stages, is named as hydrologic forecast. The hydrologic forecast plays an important role in the safe construction and operation of dams and spillways, and electric power generation (Vide Chap. 18). Hydrologic forecast must have the predicted value and period with satisfied accuracy. The hydrologic forecast generally falls into short-term flood forecast and mid- and long-term hydrologic forecast, according to the forecast period. The theoretical base of short-term flood forecast is the theory of runoff yield and flow concentration. The mid- and long-term hydrologic forecast is generally developed by means of meteorology or statistics.

6. Sedimentation analysis

Rainfall and surface runoff are responsible for the detachment and movement of soil particles on the land surface. These soil particles are referred to as sediments. The study of sediment detachment and movement is an important subject in the engineering hydrology. The subject of sediment movement transcends engineering hydrology to encompass the related field of fluvial geomorphology, sediment transport and deposit, as well as river morphology (Garcia 2008).

Sedimentation is a key issue dominating the service life of reservoir and the benefits of hydropower projects. Sedimentation study comprises the estimation of sediment runoff, sediment particle gradation, position, shape, and speed of reservoir sedimentation, years of erosion and deposition of reservoir balance, and preventive

countermeasures (Brandt 2000). The calculation of reservoir backwater is also an important task in the sedimentation study, which should be taken into account in the evaluation of the reservoir tail rise and its influencing on the reservoir inundation.

2.5 Engineering Geology

2.5.1 Engineering Geologic Issues in Hydraulic Projects

Investigations relating to geology and foundation conditions are essential for the design of hydraulic structures such as dams, spillways, and tunnels (Chen et al. 2000; Golzé 1977; ICOLD 2005; Price 2009; Zuo et al. 1984). Furthermore, various past events have emphasized the necessity for extending investigations to cover the reservoirs and even the areas beyond. In 1963, a landslide occurred at the Vajont Project, Italy, generated an immense surge wave overtopping the world's highest concrete arch dam of the day. This wave left its marks 238 m above the reservoir level and continued downstream into the town of Longarone, resulting in an approximate 2500 fatalities. Within 60s, the Vajont Reservoir was choked with more than 239 million m³ of earth and rock extending from the dam toe toward the reservoir tail for a distance of about 1.61 km. Remarkably, the dam withstood the overpressures to which it was subjected. In the same year, the failure of Baldwin Hills Project located in Los Angeles County, California, USA, provided a lesson of how the combined geologic factors and human activities outside the reservoir area might destroy a conservatively designed homogeneous earthfill dam of 47.2 m high (Scott 1987). The Baldwin Hills Dam is located in a seismically active and unstable region where the Inglewood fault lays 152 m to the west whose branches pass through the reservoir floor and dam abutment. The entire project is situated at the edge of Inglewood Oil Field, its extractions of oil, and gas from deep-seated formations had created a bowl of subsidence, the rim of which enclosed the project. Contemporaneously localized areas within this bowl were experiencing uplift as a result of secondary oil recovery operations which entailed high-pressure re-injection of water into the oil-bearing formations. The long-term effect of these conditions was to depress, tilt, and stretch the reservoir, which created offset and separation along one of the fault branches passing through the reservoir. As a result, a leakage pathway beneath the dam was developed and rapidly enlarged, leading to the complete failure of the dam, which in turn resulted in 5 fatalities and approximately \$15 million of downstream property loss.

Every hydraulic project requires geologic investigation to detect and to evaluate conditions that will affect its design, construction, and operations. It is the responsibility of the engineering geologist to identify geologic conditions which could endanger the hydraulic structures due to significant geologic hazards including landslides, earthquakes, land subsidence, leakage, and the presence in critical locations of liquefiable strata.

Taken in sequence, the geologic investigation is generally accomplished by the following works (Acker 1974; Clayton et al. 1982; Lowe and Zaccheo 1975; Look 2007; Mathewson 1981):

- Canvass of the literatures of reports, maps, and photographs;
- Reconnaissance of the project area to detect geologic conditions which could affect project feasibility;
- Geologic mapping of the dam site, the reservoir site, and the location of the sources of construction materials;
- Subsurface exploration by means of geophysical surveys, drilling, exploratory pits, and/or trenches and/or adits; and
- Foundation evaluation entailing soil and/or rock mechanics studies.

2.5.2 Geologic Mapping

Geologic map for hydraulic projects is frequently the only “as built” drawing of the foundation conditions requiring detailed investigations and is useful in evaluating any stability, settlement, or seepage problems (Casagrande 1961). The map should convey as much information as possible to the designer and researcher so that they will be well informed of the site geology and utilize this knowledge in selecting the location and in the design.

Observation, interpretation, and recordation are the three elements of the geologic mapping. It should be performed under the close supervision of an experienced engineering geologist who is skillful in recognizing and interpreting those geologic features that are important with respect to project safety. The collection, study, and evaluation of foundation data form a continuing program from the time of the preliminary investigation to the design until the completion of the project. In a preliminary geologic mapping, assignment is targeted to provide data necessitated for the selection of the site and the type of dam. However, very often, the type of dam has not been determined in this phase; therefore, the geologic mapping should include information on availability and haul distances for construction materials for various types of dams. In the design stage, geologic mapping is supplemented by subsurface exploration and is, therefore, more accurate and detailed than that performed for the preliminary stage. Geologic features uncovered during construction period should be mapped as soon as possible since they will have an influence on any feedback analysis and redesign (e.g., resloping an excavation, and strengthening a reinforcement) that become necessary due to varied foundation conditions off anticipated. The final geologic maps may also be valuable in settling future claims and may prove to be important documents for the safety inspection and review, as well as for consulting boards of inquiry in the event of a future serious structural accident.

The quality of geologic maps largely depends upon the acuteness of the field observations. The geologist should examine as many outcrops and structural

features as he can, which comprises identifying the rock type, determining discontinuity strike and dip, and structural trends as well as the other significant geologic features.

Gullies, canyons, and streambeds are the natural windows to the subsurface and should be “walked out” and examined. Man-made excavations or openings, such as mine shafts and connecting tunnels, should be observed since they provide important subsurface knowledge. Springs and wells within the reservoir area or in the areas affected by the reservoir should be investigated and pertinent information recorded, since they may contain useful clues concerning the thickness and characteristics of formations, and may also provide an opportunity to obtain hydrologic information such as groundwater level, rock formation permeability, and water samples for chemical analysis. Very often, faults perform as ground water barriers and cause a high phreatic zone along their trend. This wet area can be recognized by springs or strange vegetation.

For hydraulic projects, maps of greater than 1:5000 may be considered to be small scale which could be applied to the problems of general planning such as road and tunnel locations, locations of construction materials, and the description of geological conditions in a reservoir area; large-scale maps are those devoted to the depiction of relatively small surface in great detail and range from about 1:1000 (for a dam site) to about 1:50 (for a rock slope or tunnel). The following list presents the basic geologic documents provided by the geologist in charge of geological surveys: geology investigation reports, physical and mechanical testing reports, geophysical prospecting reports, topographic map (1:200–1:1000), engineering geologic plan (1:200–1:1000), longitudinal and cross sections (1:200–1:1000), adit geologic drawing (1:50–1:100), shaft geologic drawing (1:50–1:100), bare log (drill hole columnar section), stratigraphic column, hydrogeology experimental results and documents, long-term observations of groundwater level, ground water contour, and contour line map of rock roof (potential slip surface).

A new development in the production of engineering geologic documents is the use of computer-aided design/computer-aided manufacturing (CAD/CAM) systems and the geographic information system (GIS). CAD/CAM systems are mostly orientated toward handling vector type of data, whereas GIS systems can handle both the raster data and vector data. Vector data are those that may be described as points, lines, surfaces, and volumes that define an entity object in the CAD/CAM or GIS systems. Raster data have the form of a regular grid or cell structures that jointly define the object, but each cell is a separate entity in the systems. GIS systems normally combine or contain a (limited) CAD/CAM system, a database for the objects and entities with property values, a visualization unit, and a calculation unit able to manipulate the coordinates and properties and statistic routines. The combination of database and visualization makes a GIS system particular handy for engineering geology. For example, it should be possible, if the separate items of data necessary for rock mass classification exist, to ask the GIS system to produce a particular form of rock mass classification for a specified lithology within a given area.

2.5.3 Geologic Exploration and Investigation

Geologic exploration can be broadly distinguished as indirect or direct. The indirect method involves aerial photographic interpretation, geologic reconnaissance, seismic, and geophysical techniques including many electronic “down-the-hole” devices used to correlate physical drill-hole data. The direct method involves drilling holes into the ground and extracting samples for visual identification or laboratory analysis. Although there are many approaches to the problems of identifying soil and rock types and structural features, there is no singular method providing all of the information required for all of the soil and rock types associated with any particular project site. Depending upon the scale of a particular project, a combination of disciplines involving indirect methods in the preliminary phase followed by direct methods for correlation is generally utilized. The direct methods of exploration will be mainly discussed in further detail thereafter in this Chapter, while several typical indirect methods (e.g., non-destructive tests) will be presented in Chap. 18 of this book.

1. Exploration and investigation methods

(a) Boring

A boring is defined as a cylindrical hole drilled into the ground. The primary objective for a properly drilling exploratory program is to obtain information by sample extraction to determine the distribution, types, and properties of the subsurface soils and rock formations at the site. Borings can be excavated by hand (e.g., hand auger), although the usual procedure is to use mechanical equipments.

The required number and spacing of borings for a particular project must be based on judgment and experience. For rock slope engineering, three to five borings on a longitudinal section in the critical direction should be made to obtain main geological section for analysis. Number of other longitudinal geologic sections depends on the extent of stability problem, whose spacing is generally less than 30 m. For complex slopes, apart from longitudinal sections, at least two transverse sections perpendicular to the critical direction should be investigated. For the purpose of stabilization design, the borings should be layout in the area where reinforcement structures may be located.

The additional drill holes are incorporated into a drilling program which takes advantage of knowledge of special conditions revealed during the preliminary investigations. These drill holes become more specifically oriented and increased in number to better define the foundation conditions and determine the foundation treatment scheme.

(b) Geological excavation

In addition to borings, other methods for performing subsurface exploration are test shafts, tunnels (adits), pits, and trenches. Exploratory openings are usually oriented to cross particular geologic features or discontinuities. The number and depth of the openings depend on the soil and/or rock types and the trends of geologic discontinuities such as faults, shears, and prominent joint sets.

Geological excavation provides the best manner for examining the foundation by visual observation of subsurface conditions. They can also be used to obtain undisturbed samples of soil or rock. Backhoe pits and trenches are an economical means of performing subsurface exploration, while shafts and tunnels are more expensive. In many subsurface explorations, backhoe trenches are used to evaluate near surface geologic conditions, whereas shafts and tunnels are employed to investigate deeper subsurface geologic conditions. Geological excavations are also especially useful when performing fault studies, by which the width and elements of attitude (dip, strike, elevation) of the shear zone can be well determined. If there is uncertainty as to whether or not a fault is active, then dateable material must be present in the excavation in order to determine the date of the most recent fault movement. The excavation may also provide space for in situ tests.

(c) Geophysical detect

Geophysical detects are often exercised in the reconnaissance or preliminary phases of a site investigation program to provide information such as the depth of weathering, the bedrock profile, the location of major faults, the groundwater table, and the degree of rock fracturing. The results obtained from geophysical detects are usually not sufficiently accurate to be used in the final design and should preferably be calibrated by putting down a number of boring tests or excavation tests for spot-checking. Use of geophysical techniques involves considerable experience and judgment in the interpretation of results. Common types of geophysical techniques are the electrical methods, seismic methods, electromagnetic methods (geological radar), acoustic methods, gravity methods, borehole TV logger, etc., which will be presented in details in Chap. 18 of this book.

(d) Hydrogeological test

The investigation of groundwater plays an important role in geologic exploration. Hydrogeological tests (e.g., laboratory permeability tests and pumping or packer tests) and borehole hydrogeological observations (e.g., water table in borehole) are conducted to measure the permeability coefficients, groundwater table, flow direction and velocity, as well as the hydraulic relation of different strata, which provide the fundamental information on the site conditions needed for structural stability analysis and drainage design.

2. Reservoir investigation

Study on reservoir geology and environmental geology is attached relatively high importance in countries such as China due to the concentrated population and residences around reservoir areas and the relatively scarce farmland resources in the country. The contents of investigation are varied, depending on the natural and social conditions. The slope stability study on reservoir bank is focused on the large rockfalls, landslides, and unstable rock masses that are located near the proposed project site and may potentially endanger its safety, and on those large landslides that are located although far from the project site yet will potentially affect the local residence and navigation (ICOLD 2002). In the China's central to western

mountainous areas, mudflow is a common natural disaster that will influence the reservoir's environment and needs to be carefully addressed. In some regions, mostly in northern China, bank caving and immersing resulted from reservoir impoundment also need to be controlled. The impact on mineral resources by direct reservoir inundation or by rising of groundwater table must be studied before the decision making. In limestone area, a clear conclusion must be reached before the dam construction on the possibility and amount, if any, of Karst seepage to adjacent valleys or downstream reaches. In some areas, assessment should be made on the variation of groundwater (water table, temperature, and quality) resulted from reservoir impoundment and its impacts (both positive and negative) on the local industrial and agricultural activities as well as people's life. Take the Three Gorges Project as an example. The number of resettled people from its reservoir area is tremendous. As a result, the secondary hazards induced by intensified human activities attributable to the resettlement of millions of people will be one of the most prominent environmental and geological issues for this project. So far, comprehensive and in-depth studies have been carried out covering the topics of reservoir bank stability, induced scouring by clear discharged flow to the downstream riverbed, the impact of intensified bank caving on the levee safety, the impact of water level variation on soil gleization in the Jiangnan alluvial plain, the relationship between the Yangtzi River and the large lakes such as the Dongting Lake and Poyang Lake.

3. Dam foundation investigation

Generally speaking, the objective of engineering geological investigation for dam foundation comprises (ICOLD 1993):

- Define unstable rock masses and the limits for dam foundation.
- Identify various geological defects in terms of their locations, properties, and trends.
- Determine various boundaries for computation.
- Provide geotechnical parameters for competent numerical analyses, and propose principles and methods for the treatment of geological defects.

In the early days, the excavation depth for dam foundation was solely determined through the assessment of foundation rock mass quality based on geologists' experience. Along with the advancement of computational geomechanics (Chen 2006), as well as the testing and measuring techniques in the recent years, a quantitative classification methodology for foundation rock mass has been gradually replacing the traditional qualitative method of rock mass quality assessment systems: The location and top surface of available bedrock are determined with the consideration of the working conditions of hydraulic structures concerned.

(a) Cut slope

Study on the stability of deep cut slopes and on the respective supporting is one of the most arduous jobs in the engineering geological investigation for a work site (Hoek and Bray 1981), since statistics indicates that issues resulted from deep

cut slopes are much more problematic than those caused by other hydraulic structures. The cut slopes may be the dam abutment slopes, the powerhouse slopes, the entrance and outlet slopes of underground caverns (tunnels), the slopes on both sides of stilling basin, the slopes on both sides of spillway, and the ship lock slopes.

The stability of deep cut slopes has attracted increasing attentions in China since the 1980s, and many engineering geology and geomechanical problems concerning cut slope engineering have been successfully solved in the construction of hydraulic projects. The Geheyan Project, for example, has a 110-m-high cut slope at the outlets of power tunnels, and the lower portion of the slope consists of soft shale containing numerous sheared zones, while the upper portion consists of massive and hard limestone. The Tianshengqiao II Project has a cut slope of 370 m high just behind the powerhouse, consisting of alternative layers of sandstone and shale with very complex tectonic structures. Rock mass slip occurred from time to time during the construction. Based on the geological conditions of the slope, comprehensive engineering countermeasures were adopted to stabilize the slope, including anti-slide piles, pre-stressed anchor cables, and unloading. The Three Gorges Project's navigation work comprises of double-lane and five-stage flight ship locks of 1607 m in length. It was totally excavated in a granite mountain with a maximum cut depth of 170 m. In order to guarantee the normal operation of the ship lock gates, it is demanded that the accumulated time-dependent deformation should not exceed 5 mm after the installation of the miter gates. Therefore, assessment of the slope stability and the long-term time-dependent deformation is a crucial technology challenge. Guided by the experts of various fields through extensive and in-depth study, this structure was completed and put into operation successfully in 2003.

(b) Embankment dam foundation

The foundation will limit the choice of embankment type to a certain extent, although such limitations will frequently be modified, considering the height of the proposed dam. The different foundations commonly encountered are as follows:

- **Rock foundation.** Attributable to relatively high bearing capacity and resistance to erosion and percolation, it offers few restrictions as to the type of embankment that can be built upon it. Economy of materials or overall cost will be the ruling factor. The removal of disintegrated rock together with the sealing of seams and fractures by grouting will frequently be undertaken.
- **Gravel foundation.** If well compacted, it is suitable for earth- and rockfill embankments in addition to barrages and low concrete gravity dams. As gravel foundations are frequently subject to water percolation at high rates, special precautions must be taken by providing effective water cutoffs or seals.
- **Silt or fine foundation.** It can be used for earthfill embankments in addition to barrages and low concrete gravity dams, if properly designed. But it is not suitable for rockfill embankments. The main problems are the settlement, the prevention of piping, the excessive percolation losses, and the protection of the foundation at downstream toe from erosion.

- Clay foundation. It can be used for earthfill embankments but require special treatments. Due to the considerable settlement if the clay is unconsolidated and the moisture content is high, clay foundations ordinarily are not suitable for concrete gravity dams and rockfill embankments. Tests of the foundation material in its natural state are normally required to determine the consolidation characteristics of the material and its ability to support the superimposed load.
- Non-uniform foundation. Occasionally, situations may occur where reasonably uniform foundations of any of the foregoing descriptions cannot be found and where a non-uniform foundation comprising rock and soft material must be used. Such conditions can often be overcome by special design and appropriate treatment.

(c) Concrete dam foundation

As the reservoir rises behind a concrete dam, it pushes the dam into the canyon walls and stream floor. To compute the stress and deflection of the dam as well as the abutment reactions, it is necessary to know how much the rock foundation deforms under the combined loads of gravity, water, temperature, and others.

The deformation characteristics of foundation rock for concrete dams are significantly influenced by the density, orientation, extension and aperture of joints and cracks near the loaded bedrock surfaces, and by the compressibility of gouge found within faults and shear zones (Farmer 1968). To evaluate the resistance of the foundation to the forces tending to push the dam downstream wards, it is necessary to know the shear strength along potential planes of weakness. Since the strength of discontinuities and the shearing forces are influenced by the magnitude and direction of the in situ stresses, their measuring is also demanded for determining the foundation deformation and the degree of rock slabbing or relaxation that may occur due to the removal of the overburden rock.

4. Spillway foundation investigation

Geologic exploration for a spillway foundation should begin with the preparation of a geologic map of the spillway and adjacent areas, followed by detailed subsurface exploration (e.g., exploratory drilling or trenching) along the spillway alignment, if necessary.

Although bearing capacity could be important, the weight of ground material removed is often greater than the weight of spillway, so the foundation generally is able to support the spillway structure. However, care must be exercised to ensure that in the foundation, there are no bedding planes, joint sets, fracture systems, or other discontinuities with adverse orientations.

Stability of both cut and natural slopes adjacent to the spillway should be studied with great care, which requires thorough geotechnical analyses taking into account of geologic structures, groundwater conditions, and the mechanical properties of the soil and/or rock. Where deep cuts are made for the spillway, particularly in shales and siltstones, or where there is high tectonic stress, considerable rebound may be anticipated. A good way to handle such rebound is to leave an interval of several

months after excavation to allow the rock to finish rebounding before the concrete placement.

5. Underground work investigation

Underground works in hydraulic projects may be either the tunnels for river diversion, flood release, water conveyance and communication, or the underground caverns for accommodating hydropower plants. Since China's water resources and hydropower development is moving toward her Western territory, the underground works are much more frequently encountered and their types are much more widely varied than ever before. The Tianshengqiao II Project has a water conveyance tunnel of 9.8 km long located in a region with very complicated Karst and geological structure conditions. Various geological problems such as collapse, intrusion of groundwater, crushed zones of faults and rock burst were encountered during the tunneling. The Ertan Project is located in a canyon region of the Yalongjiang River with very high in situ stress. Its underground powerhouse cavern is one with the largest span in China—28.5 m wide and 71.5 m high. The Xiaolangdi Project has 16 tunnels (for diversion, flood releasing, silt releasing, water conveyance, and irrigation) and a giant underground powerhouse (containing six turbine generators). Those works have to be concentrated in the limited area of a mountain on the left bank, due to the constrains in the topography, geology, and hydraulic structure layout.

Since the mid-1980s, many pumped-storage power stations have been constructed in China, such as the Guangzhou Pumped-storage Power Station, the Shisanling Pumped-storage Power Station, and the Tianhuangping Pumped-storage Power Station. A lot of complicated geological problems were encountered during the excavation of their underground works. Similar to slope engineering works, the underground works in hydraulic project are varied in types, scales, and working conditions. Their geological conditions are very different with each other, varying from very hard and intact granites to strongly Karstified carbonate rocks, swelling plastic mudstones, gouge filled fault zones, and alternated rocks, from horizontal strata to strongly squeezed zones to high in situ stress and high geothermal areas. Insofar, a rich expertise has been accumulated concerning the geological and geotechnical investigation and research for long and giant underground works with complicated geological conditions.

(a) Tunnel

Basic questions with answers dependent on geologic conditions are as follows: Can the tunnel be built? Will the portal areas and tunnel body be stable? Will geologic hazards such as raveling or running ground be encountered during the tunneling? Will groundwater be a problem? Will it have to be lined? What kind of support?

The initial step should be the preparation of a geologic map in the vicinity and along the tunnel alignment to determine the physical and mechanical conditions of rock. During exploration drill, water pressure tests (pumping or packer) should be made to determine the permeability of rock. Temporary casing should be installed

in drill holes, so water levels can be monitored. Springs in the area also should be canvassed and measured. These groundwater data are useful for determining how much water will be encountered during tunneling and how the tunneling adversely affects the groundwater environment as well.

(b) Powerhouse

Exploration program for an underground powerhouse should start with a detailed surface geology map and preliminary exploratory drill holes to evaluate the geologic conditions at the underground power plant. During this phase, geologic structures may become evident which would make reorienting or relocating of the underground chamber. To more accurately evaluate underground conditions, exploratory adits for observing the behavior of the rock during excavation, for performing additional rock mechanics tests, and for determining residual stress are necessary.

The kind of support is one of the most important concerns to be decided in light of geological exploration. The modern tendency is to use rock bolt reinforcement for the roof and walls. However, if the rock is closely fractured or too soft to be adequately reinforced by rock bolts, then other support systems such as concrete or steel arches must be installed to reinforce the roof of the powerhouse, which may either be supported on posts or on a rock hunch. If a haunch support is contemplated, the geologist should determine that the rock is suitable for excavation of a haunch and that there are no adverse rock structures which would cause the haunch to fail.

Because underground powerhouses are usually in the dam abutments, water impounding in the reservoir will change the groundwater conditions and can raise groundwater to envelope the powerhouse. Therefore, geologic investigations should indicate rock permeability around the powerhouse. In many instances, a grout curtain as an impermeable envelope around the powerhouse is conventionally employed to protect the powerhouse from groundwater, and a drainage system to collect any seeping water through the curtain is provided. Successful installation of such an anti-seepage system requires thorough knowledge of geologic conditions around the powerhouse.

Geologic problems with a surface powerhouse are considerably different from those of underground. The main geologic problems that generally arise are stability of both cut and natural slopes around the powerhouse, stability of the penstock foundation, adequacy of the foundation, and troubles that might arise from excavating rebound. Groundwater conditions that may affect either the construction or operation of the powerhouse should not be overlooked, too.

Where the groundwater is above the foundation level, particularly in alluvial strata, pumping tests should be made to evaluate the groundwater conditions, for dewatering system design of the foundation.

6. In situ stresses in surrounding rock mass

The virgin or undisturbed in situ stresses are the natural stresses that exist in the ground prior to any excavation, which is an important geologic setting of cut slope,

tunnel, and dam foundation. They determine the boundary and initial conditions for deformation/stress analysis and affect the adjustments in stress that develop when an opening is created (Goodman 1989; Jaeger et al. 2007). The influence of in situ stress on the hydraulic structures should be assessed with the consideration on its magnitudes and attitudes and zoning features, the impacts of the in situ stress on fracturing of various rocks, and the working conditions of the structures concerned. The foundation of various hydraulic structures should fully use the stress transition zone, partially use the stress-release zone, and avoid as far as possible the stress concentration zone. The top of the structure's foundation bedrock should be adjusted appropriately so as to keep the ratio between the stress and the strength of the foundation rocks within a range in which the rocks could only be fractured slightly. The axis of the tunnel should be aligned as parallel as possible or oblique slightly to the maximum principal stress. The surrounding rock mass of underground caverns should be reinforced when it is situated within the stress concentration zone. Full attention should be paid to the stress concentration-induced damages such as rock burst, scaling, and fracturing.

The in situ stress existing in a formation can be decomposed into three principal compressive components, approximately one vertical and two horizontal, which are usually not equal. The vertical stress is attributable to the overburden weight exerting on the top of a formation. The horizontal stresses are the result of the deformation of the rocks plus externally applied tectonic actions. The parameters that affect the magnitude of the in situ stresses include overburden weight, fluid pore pressure, porosity, anomalies in the rock fabric (i.e., natural fractures), rock mechanical properties (such as Poisson's ratio), tectonic activity, temperature changes, and chemical and physicochemical processes such as leaching, precipitation, and recrystallization of constituent minerals. Mechanical processes such as fracture generating and propagation, slip on fracture surfaces, and viscoplastic flow throughout the medium can be expected to produce both complex and heterogeneous states of the stress field.

Topographic conditions also significantly influence the in situ stress. In a deep cut river valley, the in situ stress field is commonly distributed in 4 zones:

- Stress-release zone. Situated in the superficial part of the valley slopes with small magnitudes;
- Stress transition zone. Situated in the shallow part of the valley, ranging in medium magnitude;
- Stable stress zone. Situated in the deep part of the valley slopes, ranging in high magnitude; and
- Stress concentration zone. Situated in the riverbed.

Although some of the simplest clues to stress orientation can be estimated from the knowledge of a region's structural geology and its recent geologic history, quantitative information from stress analysis requires that the boundary conditions are known, and field measurements of in situ stresses are the only true guide for critical structures. During the past 40 years, methods for measuring in situ stresses have been well developed (Goodman 1989). Based on a survey of published

database, it may be confirmed that the vertical in situ stresses measured in the field reasonably agree with simple predictions using the overburden weight of rock. However, horizontal in situ stresses seldom show magnitudes as low as the limiting values predicted by elastic theory, but often vary considerably and depend on geologic history, denudation, tectonics, or surface topography. At shallow depths, there may be a wide variation in values since the strain changes being measured are often close to the accuracy limit of the measuring instruments.

To determine the magnitude and orientation of in situ stresses by the field test using several points, much manpower and material resources are requested. Basically, there are two types of in situ stress measuring methods: One is named as direct, represented by flat jack measurements and hydraulic fracturing, which determines a circumferential normal stress component at particular locations in the wall of a borehole. If sufficient boundary stress determinations are made in the borehole periphery, the local value of the field stress tensor can be determined directly. Another one is indirect, based on the determination of strain changes in the wall of a borehole, or other deformations of the borehole, induced by over coring that part of the hole containing the measuring device. If sufficient strain changes or deformation measurements are made during this stress relief operation, the six components of the field stress tensor can be obtained from the experimental observations using procedures developed from elastic theory. It should be pointed out that the in situ stresses measured in the same geology element commonly present different data by different methods. Even by a same measuring method, the data also display large dispersion. These are mainly attributable to the influence by the factors of faulting, topography, erosion, and denudation, apart from the errors resulted from measuring apparatus.

Based on these field readings, the stress regression method is designed to determine the initial stress field by means of regression method, least squares method, and other modern artificial intelligent methods, for example, artificial neural network (ANN) is a mathematical model often used as a nonlinear data modeling tool to fit the complex relationship between inputs and outputs. Recent research shows that the ANN and FEM can be combined to back analyze the initial stress field using measured in situ stresses before the excavation, whose basic procedure is illustrated as follows (Chen 2006).

- (a) Establish 3D regional FE model with effort to reflect joints, fractures, and terrain;
- (b) Define a set of boundary load combinations corresponding to the regional FE model;
- (c) For each boundary load combination, implement FE analysis to obtain the stresses at the in situ test points;
- (d) The computed stresses at the in situ test points and the corresponding boundary load combinations are grouped into samples for ANN, in which the stresses are inputs and the boundary load combinations are outputs;
- (e) The ANN training is carried out using the samples defined in the step (d);

- (f) Input the in situ test readings of the stresses into the trained ANN leads to the “best guess” of the boundary load combination;
- (g) Apply the “best guess” of boundary load combination to the 3D regional FE model, the initial stress field is back analyzed, which may be used in the excavation calculation of dam foundations, cut slopes, and underground works.

Based on the 13 field test points in the Xiaowan Project, the initial stress field is back analyzed using the procedure described above. Figure 2.1 shows the distribution of the initial stresses whose characteristics coincides with which is well known with regard to the deeply cut valley.

2.5.4 Regional Tectonic Stability and Earthquake Hazard

The shaking of the ground surface during an earthquake is a consequence of seismic waves (stress waves), which are generated by the slip on and/or tip propagation at an exiting fault which causes the sudden release of stress (strain energy) in rock (Hyndman and Hyndman 2009). The motion due to a disturbance at the origin can be split into longitudinal, transverse, and surface waves, of which the latter are most destructive. Focus is the origin from which the earthquake tremor is supposed to start, or a point to which all the earthquake waves converge. Epicenter is the point on the surface above the focus. Earthquakes that produce destructive ground shaking usually are generated by faults in the upper 30 km of the earth’s crust (Richter 1958).

The severity of an earthquake is gauged by the amount of energy released at the focus, is termed as the magnitude which is an index of the earthquake related to the size of the slipped fault area, and is described in a quantitative way in many countries inclusive China by the so-called Richter Magnitude of the earthquake for shallow shocks (GB17740-1999 “General Ruler for Earthquake Magnitude” 1999; ICOLD 2011). The maximum earthquake magnitude encountered is usually smaller than 9.

$$\begin{cases} M = \log_{10} \left(\frac{A}{T} \right)_{\max} + \sigma(\Delta) \\ \sigma(\Delta) = 1.66 \log_{10} \Delta + 3.5 \end{cases} \quad ((2.1))$$

where M = magnitude of earthquake; A = maximum amplitude of horizontal ground motion recorded by a standard seismograph, μm ; T = wave period, second; σ = calibration function correcting for the angular distance Δ from seismometer to epicenter; and Δ = angular distance from seismometer to epicenter, ($^{\circ}$).

The intensity is an identification of the effect severity of ground shaking at a definite point and is described in a short-hand way by the Modified Mercalli intensity number (from 1 to 12), which is correlated with certain classes of observed effects of ground shaking.

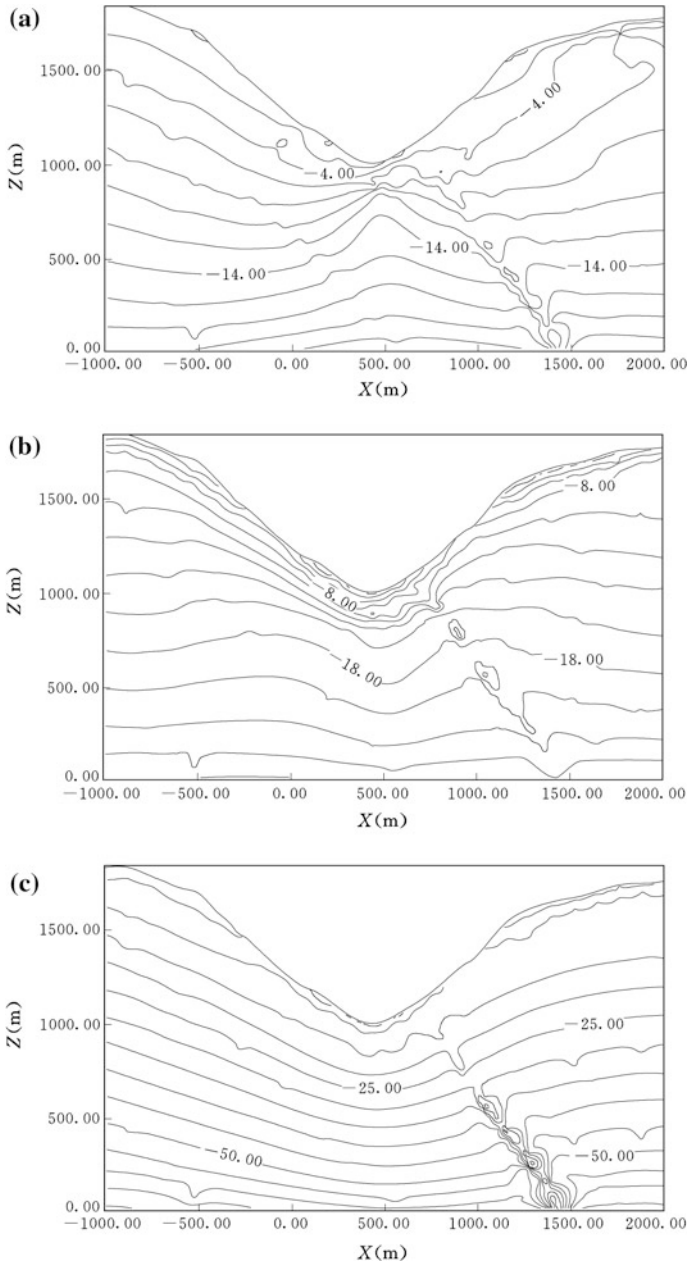


Fig. 2.1 Contours of initial stress of the vertical section along the dam axis (Unit: MPa)—The Xiaowan Project (China, $H = 294.5$ m). **a** Maximum principal stress; **b** medium principal stress; and **c** minimum principal stress

Many regions of the world are subject to potentially destructive earthquakes. The border of the Pacific Ocean is particularly prone to seismic activity where approximately 80 % of the world's earthquakes occur. A second seismic belt runs across northern India into Turkey, Greece, and Italy. In addition, destructive earthquakes also occur in other parts of the world, although much less frequently (ICOLD 1975; Poulos et al. 1985).

The potential hazard to a specific hydraulic project from an earthquake depends on how large the earthquake is and how near the project site to the epicenter. The occurrence of an earthquake in the vicinity of hydraulic structure can cause its damages, or even failure, if the earthquake actions have not been given adequate consideration in the design. Earthquakes of magnitude 5.0 or greater can generate severe ground shaking to potentially damage hydraulic structures. For earthquakes of magnitude lower than approximately 5.0, the ground motion is unlikely to be hazardous due to its very short duration, even though the peak acceleration may be large in the case of very shallow fault slip.

The following are two typical cases of earthquake damages to dams, which are often referred to as lessons in the community of dam engineering.

- Xinfengjiang Dam. This massive-head buttress dam in China was damaged by the magnitude 6.2 earthquake in March 19, 1962. The dam sustained a horizontal crack approximately 10 m below the crest.
- Koyna Dam. This concrete gravity dam was damaged by the south India earthquake in December 10, 1968. This magnitude 6.5 earthquake occurred close to the dam and an accelerograph within the dam recorded a peak acceleration of approximately 0.5 g. The dam sustained a horizontal crack near the upper third point and many of the appurtenances of the dam were also damaged.

It is not possible to predict when and where earthquakes will occur and how large they will be; therefore, considerable judgment is involved in assessing the seismic risk at a specific project site. Most seismic countries have prepared seismic zoning maps to assist designer and builder. These maps normally divide the country into a number of zones of different degrees of seismic hazard. Such zoning maps are employed for the first-level assessment of seismic hazard. In building codes for example, zoning maps are used to regulate the earthquake design of ordinary structures, or facilities.

As a complement to the published zoning maps, a seismic hazard analysis for a specific project site can be conducted by evaluating the magnitude of ground motions from all capable sources (focuses) with the potential for generating strong ground motions at the site. The value of such seismic analysis is the ability to incorporate the latest developments in local seismicity. The analysis is usually carried out in three steps: first, to establish the location and style of faulting of all potential sources and assign each a representative earthquake magnitude; second, an appropriate attenuation relationship is selected as a function of magnitude, faulting mechanism, site-to-source distance, and site conditions; and third, the capable sources are screened based on magnitude and ground motion intensity at the site, to determine the governing source.

1. Regional tectonic stability

Geology- or seismology-related elements often determine the feasibility of the project and strongly influence the planning, design, construction, and operational activities. Therefore, earthquake-related hazards should be identified early in the project investigation and be evaluated continuously in the subsequent stages of hydraulic work design.

Regional tectonic stability studies the presence of faults, active or inactive, and their influences on the design of the hydraulic structure. The study comprises regional tectonic setting analysis, regional tectonic stability analysis, as well as the geologic investigation for the hydraulic project.

Regional tectonic setting analysis is intended to collect the earthquake data and documents of 150–300 km in radius around the project. This may be carried out using “Chinese seismic intensity zoning map (1990)” or GB18306-2001 “Seismic ground motion parameter zonation map in China,” from which the basic intensity at the reservoir and the dam site, as well as the level of seismic bedrock peak horizontal acceleration, may be obtained. DL5073—2000 “Specifications for seismic design of hydraulic structures” stipulates that if the basic intensity is 6 or greater, the special seismic risk analysis and aseismic design are to be carried out for the project with a dam higher than 200 m or a reservoir storage capacity over 10 billion m³; these are carried out for the dam higher than 150 m and located on the area of basic intensity 7 or greater.

Study on the regional tectonic stability and seismic activities are customarily conducted in an area around the project approximately 20–40 km in radius. The study covers:

- Regional geological background, namely regional strata, geological structures, geomorphology, and geological evolution process;
- Features of deep geophysical field and characteristics and intensity of neotectonic movements;
- Distribution of faults and their activities;
- Historic earthquake records;
- Recent seismic observation data and seismic background analyses; and
- Seismic risk analysis and study on the dynamic parameters of earthquakes.

Studies are also made of geologic formations and soil deposits on the work site to assess their possible behavior during earthquake shaking and how they might affect the stability of the hydraulic structure.

The project site should avoid the epicentral region with earthquake magnitude over 6.5, or intensity over 10; the dam, spillways, and power plants should not locate on the active faults and related branching faults.

The Auburn Arch Dam (USA, $H = 210$ m), whose proposals and studies emerged in the late 1960s, and construction work commenced in 1968, involving the diversion of the North Fork American River through a tunnel and the construction of a massive earth cofferdam. Following a nearby earthquake and the

discovery of a seismic fault that underlay the dam site, the project was suspended for fears that the dam's design would not allow it to survive a major earthquake.

China is a country with frequent earthquakes, which are mostly concentrated in the piedmont seismic zones of the Taihangshan and Yanshan mountains in east China, of the Qinhai, Ningxia, and Xinjiang Provinces in west China and of the most areas in southwest China (General Administration of Quality Supervision of the People's Republic of China 2001). Priorities thus should be given to the assessment of regional tectonic stability and seismicity risk when a dam is contemplated in these regions. Taking the Ertan Project as an example, it is located in a north-south trending tectonic zone in Sichuan and Yuannan regions that have very strong tectonic and seismic activities. After years of in-depth study and investigation, the Chinese engineers and researchers identified a relative stable massif (safe island) on which the dam would be located, by ascertaining the characteristics and activities of major faults surrounding the project area.

How the reservoir loading is related to the earthquake triggering is not well understood at present and is still the subject of research (Kerr and Stone 2009). Presumably, it is linked to the extra weight on the earth's crust and possibly also to additional water and water pressure diffused to considerable depth. It is thought that the reservoir loading is just the triggering mechanism to release an existing state of stress in the rock. It is now customary to install one or more seismographs in the vicinity of a new major dam to record shocks having magnitudes in the range of 1.5-3.5, to monitor any change in recurrence interval during and following the impounding of the reservoir.

2. Design criteria and aseismic analysis

The aforementioned studies provide information on the seismic hazard at a proposed project site by giving parameters as to the magnitudes and frequencies of occurrence of earthquakes that can be expected, the likely active faults identified, etc. Based on these, the judgment must then be made to establish appropriate earthquake design criteria for the project.

During earthquakes, a hydraulic structure is excited with vibrating motion due to the ground shaking. The procedure named as pseudo-static method that has commonly been employed for earthquake design is to include in the prescribed loads a constant percent (5, 10, etc.) g of acceleration force and then to proceed with essentially an equivalent static analysis. When the pseudo-static method is used, the difficulties with correlating the equivalent static force to what actually happens during an earthquake, and with knowing what the factor of safety, make it desirable to develop a method of design that is based on dynamic analysis and that relates more closely to the actual behavior of a hydraulic structure during an earthquake (ICOLD 2013). The difficulties with this type of more advanced approach is that all the physical parameters are not known accurately and hence have to be estimated; furthermore, with the present state of the art, the subbase of the structure is commonly given an acceleration which is identical to the entire base, which is not realistic. More recordings of the earthquake motions of hydraulic

structures and their bases are needed, and more research is required on how to model a real structure by means of dynamic analysis using numerical methods such as FEM that take into account the real dynamic properties of the material of which the structure is constructed.

2.6 Location and Exploration for the Sources of Construction Materials

2.6.1 Tasks of Construction Material Investigation

Investigation on natural construction materials is usually concerned with one or two questions, namely is there a sufficient quantity of specified construction material available within a reasonable haul distance, or the more comprehensive question of, what construction materials are available in the area (Golzé 1977). The importance of a thorough construction material investigation to the planning and design of hydraulic projects is apparent: The availability of construction materials often dictates the location and type of the dam which can economically be considered at a contemplated site.

Previously, investigation of natural construction materials was not so important in China, because the dams of that time were small, the dam sites had very favorable conditions, and the reserve of natural construction materials (e.g., sand and gravel, earth material and rock aggregate) is abundant. In the recent twenty years, more and more dams have been constructed in the western China, and the requirements on the environmental and ecological protection are getting higher and higher. As a result, the natural reserve of sand and gravel as well as earth materials in the project area finds itself being harder and harder to meet the demand. Therefore, new sources and types of construction materials, such as processed artificial aggregates, have to be explored.

In China, many types of hard rocks such as granites, basalts, carbonate rocks, metamorphic rocks, and sandstones have been used to process artificial aggregates. Among them, carbonate rocks are most widely employed. Study on the alkali-silica reaction of igneous rock aggregates and the alkali-dolomite reaction of carbonate rock aggregates is essential in the quality assessment of artificial aggregates even though it is expensive, time consuming, and difficult in techniques.

Gravelly soil, weathered residual soil, and their mixed soil have been widely used as impervious earth material. The requirements on the stone materials for high CFRD are quite different from those for traditional rockfill dams.

An efficient investigation can be realized only through proper planning, field, and laboratory works. Generally, the investigation contains several phases normally follows a “learn-as-you-go” procedure and becomes more detailed as the design work progresses and as the project moves from the planning phase to the construction phase.

2.6.2 Requirements in Planning Phase

A thorough search within 20 km distance around the project site should be made. The published geologic maps of the area are most useful in locating possible sources of construction materials, by showing the distribution of various geologic units and brief descriptions of them. Potential sources of construction materials may thus be identified and located, and further studies may be planned. Topographic maps are indispensable to the construction material investigation. Many surface soils are closely related to the type of rock from which they are derived. The agricultural soil survey maps and reports may be of value to the engineer in which items such as soil profile descriptions, ground surface conditions, natural vegetation, drainage, meteorological data, flood danger are included. Aerial photography may reveal material sources that may easily be overlooked by engineers who depend solely on visual ground investigations.

The potential construction materials in an specified area should be directed toward the estimation of the quantities of all types of construction materials available within the area, by which the geologic plan of 1/5000–1/10,000 and distribution plan of 1/50,000–1/100,000 for borrow are provided.

2.6.3 Requirements in Preliminary Phase

The objective of this phase for the material investigation is to locate suitable materials meeting the probable requirements from the type of dam or other work being considered.

This stage includes preliminary drilling, sampling, and testing of the most promising sources in order to verify that adequate quantities of suitable materials are available. A more complete and thorough investigation of existing geologic data, existing quarries and borrow areas, their test results, performance records, and production data is demanded at this phase.

Field studies, including geologic sectional mapping of 1/1000–1/2000, comprehensive geologic plan of 1/2000–1/5000, and borrow area distribution plan of 1/25,000–1/50,000 should be completed for the more promising areas. Limited sampling of selected areas and preliminary testing will provide more reliable data on the areas. New estimation of the volume of materials available should be based on the additional data collected, the volume of materials available should be at least three times of the design requirement, and whose estimation error should be lower than 40 %.

A joint review with planners, designers, and construction specialists is appropriate at this phase. This review brings out questions, new approaches, and suggestions for the final exploration of the construction materials. Frequently, this review provides the basis for narrowing the scope of the study and permits the investigator to concentrate his efforts on the more probable types of materials to be used for the project.

2.6.4 Requirements in Feasibility Phase

The objective of this phase is to confirm the location of adequate quantities of suitable materials for an evaluation of the specific sources of construction materials. It is also important to evaluate the excavation, process, transportation, and environmental impact of the material borrow.

The methods of exploration in this phase may vary locally. Large diameter drilling is probably the most efficient for exploring unconsolidated construction materials. Trenches and test pits excavated by backhoe are also very efficient for exploring unconsolidated deposits. All of these methods permit accurate and detailed logging, which should be accomplished by capable specialists. They should record the usual geologic and soils descriptions, and their observations are of great importance during drilling and sampling. Sufficient amount of material samples should be extracted in for reliable testing. The exploration also should be able to provide data on the issues such as the most suitable materials, methods of excavation, depth of overburden, thickness and uniformity of the materials, and depth to groundwater.

Geophysical methods such as seismic wave and electrical resistivity are not usually needed in exploring materials. However, in many areas, the geophysical methods may be exercised effectively to provide useful data on the borrow areas, such as the groundwater table, the depth to consolidated rock, the degree of fracturing, the density and the modulus of elasticity, etc. Although these may not be able to provide precise values, they are very accurate for a relative determination and are reliable in a qualitative sense.

At this stage, geologic sectional mapping of 1/500–1/1000, comprehensive geologic plan of 1/1000–1/2000, and borrow area distribution plan of 1/10,000–1/50,000 should be completed. The volume of materials available in the area should be at least two times of the design requirement, and whose estimation error should be lower than 15 %.

2.7 Economy Evaluation

2.7.1 Tasks of Economy Evaluation

The economy evaluation for a hydraulic project is to make analysis and demonstration of economic feasibility and rationality of the to-be constructed project, by providing integrated evaluation and suggestions. Aimed to avoid risks to the maximum extent and enhance optimal economic benefits, the economic evaluation is at the kernel in the feasibility study which provides an important basis for decision making (National Development and Reform Commission of the People's Republic of China, Ministry of Housing and Urban-Rural Development of the People's Republic of China [2006](#); Pan et al. [2000c](#)).

The economy evaluation falls into process evaluation and final evaluation. The process evaluation is to make technoeconomic analysis and evaluation for available construction alternatives, after comprehensive comparison and screening, to find out an alternative with the best economic performance for inclusion in the feasibility report. The final evaluation is to make final integrated economic analysis and evaluation, which is the main component of feasibility study and the key to budget project investment (Zhou 2007).

From the 1950s to 1970s, China had been practicing a planned economy on the basis of whole public ownership. In the theories of investment effect, emphasis was put on that the social production and investment effect must follow the particular socialism laws of rigorously planned for proportional development. As a result, the payment period method for justifying alternatives and for selecting hydropower parameters was prevalent. In the early period after the founding of the P. R. China since 1949, goods prices remained stable which did not seriously deviate from their value, a rationally stipulated payment period was capable of reflecting the relative economy indices of hydropower and water resources projects. During this period, because the capital investment was provided gratis by the state in a unified way, time factor was usually not considered in the economic analysis.

From the end-1970s, the state commenced the policy of opening-up and economy reform step by step. The theories of socialist market economy have been established gradually, and the shift from the planned economy to a market economy has been realized. Hence, the theories and methodology for the economic analysis of project decision have entered a flourishing new phase. A series of codes for project economy evaluation have been issued, such as “Tentative Rules for Economic Analysis of Hydropower Project,” “Economic Evaluation Methodology and Parameters of Construction Project,” “Tentative Regulations for the Financial Evaluation of Hydropower Construction Project,” and “Tentative Regulations for the Economic Evaluation of Pumped-storage Power Station.”

The main tasks for economic evaluation may be accomplished through national economic evaluation, financial evaluation, and integrated economic evaluation (Yang and Pu 1993; Yu et al. 1994).

2.7.2 National Economy Evaluation

The national economy evaluation for hydraulic projects, particularly hydropower projects, is to analyze and calculate the net contribution of a hydropower project to the national economy from the point view of comprehensive national economy balancing, so as to allow for evaluating the economic rationality of the project (National Development and Reform Commission of the People’s Republic of China, Ministry of Housing and Urban-Rural Development of the People’s Republic of China 2006).

The national economy evaluation uses the shadow price for each year in the calculation period, follows the “with and without” comparison principle and

emphasizes the overall benefits of electric power system. The costs may be direct or indirect, and the former is referred to the economic value of input calculated with shadow prices, whereas the latter is the cost paid by the society for the project, but not by the project itself. The internal rate of return is the main indicator in the evaluation, and the others may be selective according to the characteristics and actual needs of the project, for instance, the net present value, the net present value rate, etc., with respect to the economy.

2.7.3 Financial Evaluation

The financial evaluation is to analyze and calculate the direct financial benefits and cost of a project, to formulate financial statements, to calculate evaluation indicators, and to investigate profitability and payment capacity as well as foreign exchange balancing, so as to allow for evaluating the financial feasibility. The main indicators are the financial internal rate of return, the investment recovery period, the financial net present value, etc.

Similar to the national economy evaluation, the financial evaluation is mainly implemented by firstly dynamic analysis and secondly static analysis. “Tentative Regulations for the Financial Evaluation of Hydropower Construction Project” issued in 1994 clearly indicates that the calculation period should be ranged from construction to productive operation. The former is the total period of designed construction, including the initial operational period; the latter is usually counted as 20–30 years. For multi-purposed hydraulic projects, it is demanded that the financial evaluation should be made for the two cases of “with and without” investment allocation, the forecast prices based on current prices should be used in the evaluation, the financial basic rate of return is tentatively determined as 12 % for the total investment and 15 % for the capital fund, and the cost and benefits may be linked to the power generation where the special transmission and transformation engineering is tentatively included.

The financial evaluation also comprises sensitivity analysis aimed at investigating the impacts of the main elements on financial indicators (such as sale price to network), so as to forecast the capacity of the project against risks and to further determine whether the project is financially feasible.

2.7.4 Integrated Economy Evaluation

Many large- and medium-sized hydropower projects are of state infrastructure closely related with the social and economical development, and some of their economical factors are difficult to quantification. In order to comprehensively analyze their impacts on the development of society and economy, in addition to the national economy evaluation and financial evaluation, integrated economic analysis

and study also have to be carried out from the macropoint of view, for evaluating the economic rationality and feasibility of the project. The indicators adopted in the evaluation are as follows:

- Total investment and unit functional investment (such as the investment per unit-installed capacity and the investment per unit energy). Comparison is customarily made between hydropower and thermal power projects of similar size.
- Main engineering amount.
- Quantities of reservoir inundation and land excavated or covered by construction, inundation and land occupation per unit function, and proportion of compensation cost for reservoir inundation in the total project investment.
- Quantity of saved fuel.
- Multi-purposed benefits in addition to power generation.
- Reliability and feasibility of power price checking and ratification.

For a particularly important hydropower project, analysis and evaluation should be made with regard to the role and impacts of the project on the national economy in the following aspects:

- The role and function of the project in the country, river basin, and regional economy;
- Adaptability to the state industry policies and productivity distribution;
- Amount of project investment and the financial capability of the state and the region. For a hydropower project requiring a large investment, consideration should be given to the national affordability, and the analysis should be made with regard to the finance, materials, technology, and manpower; and
- Impacts of reservoir inundation and land occupation by the project on the regional society and economy.

For a hydropower project of large scale and requiring long period of initial operation, one of the important economy evaluation supplementary indicators for studying its economic rationality is the proportion of investment before the beginning of benefit generation in the total investment. Usually, it is strongly demanded for a large-sized water resources or hydropower project to start creating benefits with less than the two-thirds of total investment be used up, and the lower, the better.

2.8 Phases of Investigation and Design of Hydraulic Projects

At present, there are two-phased (staged) systems of the investigation and design in China for water resources projects and hydropower projects, respectively. This situation is mainly due to the reshuffling history of the state central government:

One is mainly practiced by the institutes belong to the formal Water Resources Ministry, and another is mainly practiced by those who belong to formal Electric Power Ministry.

2.8.1 Phases of Investigation and Design for Water Resources Projects

The design for water resources projects is a five-phased process including proposal, feasibility study, preliminary design (conceptual design), design of bid, and construction documents design.

1. Proposal for the project

The proposal for the project is normally originated with the desire to satisfy the state's (or a region's) specific needs, objectives, or purposes. The main contents of the proposal for a project comprises the following: the background, aims, and tasks of the project; investigation and necessary exploration regarding the hydrology, geology, ecology, environment, society, and humanities; justification of the necessity of the project; preliminarily verification of the feasibility and rationality; preliminary consideration of the project scale, construction scheme, construction location and time, and layout of the main works; and investing estimation of the project.

Considerable basic data are usually available in the form of maps, aerial photographs, stream flow records, regional geological reports, census statistics, crop yields, market statistics, power loads, previous investigation reports, etc. The designer must evaluate these data, supplement them with rough additional data, and conceive a workable basic proposal that utilizes available resources to meet the needs. This basic proposal may then be compared roughly with alternatives to accomplish the desired purposes on progressively increased or diminished scope and scale. It will be possible, by judgment or cursory study, to eliminate many alternatives so that an approximate final proposal emerges which entails purposes, approximate locations and heights of dams, capacities of reservoirs, spillways, outlets, canals, power plants, and other features, and which minimizes the environmental impact of the project. All these will be refined in the successive design stages.

The proposed project should be consistent with any long-range planning program that may have been adopted for the vicinity. The entire area to be served by the proposed project should be studied to determine whether there will be conflicts with other projects of a similar nature for use of land or water resources, head drops, etc., or whether economies are possible by securing optimum development of resources through joint use (Zhou 2007).

2. Feasibility study

The objective of this phase is to determine the project's feasibility on the base of project proposal. This involves the studies that will permit a sound analysis and

conclusion with respect to the specific engineering economic–environmental considerations. These are primarily:

- That the project is responsive to an urgent present or anticipated social or economic need;
- That the project will adequately accomplish the intended purposes;
- That the class, site, and layout of the project are clearly illustrated based on the major hydrologic and geologic parameters as well as the other major conditions which may be encountered;
- That the engineering construction quantities and period are properly rated and scheduled;
- That the land inundation and acquisition, as well as the indemnifying measures, are studied preliminarily;
- That the services performed through the project and the benefits produced will justify the investment; and
- That the project will cause minimal disturbance to the ecology and environment of the area.

The study should determine that the difficulties inherent in facility sites affecting economy, safety of construction, and quality of operation have been satisfactorily foreseen and that the designs are technically sound, and reasonably representative of the actual structures may be expected to be built after more detailed investigation.

3. Preliminary design (conceptual design)

The preliminary design bridges the gap between the design concept and the design of bid (detailed design). In this phase, the overall project configuration is defined. Schematics, diagrams, and layouts of the project will provide early project configuration, which could be changed or optimized in the following phases. The main features of the preliminary design are as follows:

- More detailed and accurate basic data are required concerning climate, hydrology, topography, geology, materials, economical, and comprehensive requirements;
- More detailed and thorough investigation, exploration, and experiment should be conducted;
- Decisions are made on the issues concerning comprehensive purposes, class of the project and grade of the structures, layout of the project, type and size of the main structures, and layout and type of main electromechanical devices; and
- Decisions on the quantities, methods, schedule, and preliminary budget of the project construction.

4. Design of bid (technical design)

As the extensively developing of bidding system in the engineering construction in China, the Water Resources Ministry stipulated in 1994 that for the projects demanding bidding but had not been commenced, design of bid should be

supplemented after the completion of preliminary design, which is the basis of construction bidding documents and planning. The bidding design is similar to the former technical design intended to further improve the design for an optimal schemes, based on which the preliminary budget is revised, so as to meet the requirements for construction bidding.

5. Construction documentary design

This is a phase where the engineer should completely describe the designed product through solid modeling and drawings, including:

- Foundation excavations and treatments of the structures;
- Drawing of structural configuration and reinforcing steel bars;
- Metal structures and detail drawing;
- Layout and install drawing for electromechanical devices, embedded pieces, pipelines, and electric lines;
- Maintenance and testability provisions;
- Material requirements;
- Reliability requirements;
- External surface treatment and marking; and
- Design life.

In many countries, there is detailed design phase following the preliminary design, which is similar to the construction documentary design phase in China.

2.8.2 Phases of Investigation and Design for Hydropower Projects

The investigation and design of a hydropower project is divided into 4 phases including preliminary feasibility study, which is nearly identical to the feasibility study for water resources projects; feasibility study, which is nearly identical to the preliminary design (conceptual design) for water resources projects; design of bid; and construction documentary design.

2.9 Preparation and Compilation of Design Reports

2.9.1 General Requirements

There are various types of design reports. By rough classification, they are planning reports, research reports, investigation and design reports, consulting (evaluation) reports, safety appraisal reports, etc. By detailed classification, they are outlines of investigation and design, special engineering geology investigation reports, special

test study reports, special demonstration reports of specialized fields, designing alternative comparison reports, consulting (evaluation) reports of specialized fields, appraisal reports of specialized fields, completed (water impounding) safety evaluation reports, summary reports of the survey and design works, staged design and study reports, etc., of which the staged design and study reports are the most important documents in the project demonstration and approval. In the following, the project feasibility report will be taken as an example to show how a technical report is prepared and compiled.

The project feasibility report is generally prepared on completion of the feasibility investigation as a basis for advising the sponsor or owner, the government department, and others who must approve or authorize the project of its merits. To ensure a complete description and record of all essential data, calculations, and conclusions entering into the design, a uniform procedure for the reporting is desirable (Golzé 1977). In China for example, the contents and depth of the project feasibility report are required officially in the design code or specification (e.g., DL/T5020-2007 “Specification for compiling feasibility study report of hydraulic and hydroelectric engineering”).

The report should well describe the project investigations, plans, engineering features, environmental considerations, costs, benefits, and relationships to existing and further developments, problems, and financing. It should contain a general description of the design, including the various factors involved, a copy of the detailed estimate, and a drawing showing the general plan and sections. It also should present definite recommendations, based upon probable accomplishments, regarding feasibility and acceptability under possible means of financing the construction. The conclusions and recommendations should be adequately supported by the investigations, and in such form that, if necessary, the work may be readily reviewed by the responsible authorities.

2.9.2 Contents and Outlines—Specifically for Feasibility Report

In the following, we outline the items that a feasibility report should be generally covered. Although the information listed in the outline is not all necessary for small projects, the greater part of it will be necessitated for the medium to large projects.

1. Location and purposes

- (a) River section, township, range, principal meridian, county, province, nearest city.
- (b) Location in respect to the other features.
- (c) Accessibility.
- (d) Purposes such as amount of storage (live, dead), type of storage (irrigation, flood, power, domestic, etc.), water surface elevations, place where water will be transferred, etc.

2. Summary of project features

- (a) General plans and sections.
- (b) Capacities of storage, spillway, outlet, etc.
- (c) Installed generator capacity.
- (d) Levels of normal storage, maximum storage, minimum storage, etc.
- (e) Maximum height of dam above streambed.
- (f) Estimated expenditure of the whole project, dam, and reservoir.

3. Data for design

- (a) Comprehensive data. Topography; geology; logs of test pits and drill holes; hydraulic data including capacities and requirements, irrigation, flood, power, spillway, outlet, diversion, and area-storage capacity curves for various elevations of water surface; hydrologic data including hydrographs, maximum-recorded flood, inflow design flood, mean annual runoff of drainage basin, and tailwater rate curve; cross sections of streambed; climatic conditions; and borrow areas and aggregate deposits, location, and transportation facilities available.
- (b) Design data for the reservoir. Proposed capacities with corresponding water surface elevations; general dimensions; existing structures affected; nature of land inundation and clearing required; relocations including railroad, highway, telephone lines and optical fiber lines, oil lines, and power lines; and geology including general formations, factors relating to reservoir losses, contributory springs, deleterious mineral, and salt deposits;
- (c) Design data for the dam. Geological features, formations, nature of streambed, and abutments; interpretation of test pits and drill holes; percolation tests; and groundwater.

4. Dam design

- (a) Features entailing the design.
- (b) Water surface elevations, storage capacities, and freeboard.
- (c) Governing dimensions concerning crest width, sectional slopes, height, zoning, crest length, roadway, and base width at maximum section.
- (d) Safety standards (criteria) against percolation, sliding, cracking, etc.
- (e) Cutoff and drainage, including cutoff trench and cutoff wall, grouting requirements; toe drains; and draining holes.
- (f) Appurtenances, including galleries, parapet, and curbs.

5. Outlet works design

- (a) Factors affecting outlet location.
- (b) Requirements on discharges and corresponding water surface elevations; diversion capacities, and water surface elevations.
- (c) Dimensions, materials, linings, etc., of the tunnels and conduits, if any.
- (d) Gate chamber (inclusive dimension, location, accessibility), gates, valves, and pipes (inclusive dimension and elevation).
- (e) Approaches, shafts, adits, plugs, and trash racks.
- (f) Stilling basin and plunge pool.

6. Spillway design

- (a) Requirements and other factors governing design and location.
- (b) Type and description of controlled or uncontrolled, lining, dimension, and elevation.
- (c) Gates (dimension and operation manner).
- (d) Stilling basin and plunge pool (inclusive general description and dimension).
- (e) Approach and discharge channels.

7. Appurtenant works design

Navigation structures, fish ways, log ways, etc., if any.

8. Construction facilities

- (a) Construction layout (inclusive construction camp) and schedule.
- (b) Power available, construction railroad, shipping points, and hauls.

9. Materials and unit prices

- (a) Location of borrows and hauls of natural materials.
- (b) Cement (nearest mill, hauls).
- (c) Railroads, terminals.
- (d) Unit prices.

10. Environmental and ecological protection

- (a) Fish and wildlife protection.
- (b) Recreational development plan.
- (c) Area beautification plan.
- (d) Environmental protection measures during construction.

11. Appendices

The feasibility report of a project should be accomplished by following documents, as parts of the report or as appendices:

- (a) Examination reports for the preliminary study and the corresponding researches of specialized fields, important meeting summaries and memories, and documents of seminars and discussions.
- (b) Certificates, agreements, or the main documents concerning the project comprehensive benefits, reservoir inundation, land occupation, submerge of mineral resources, and environmental evaluation.
- (c) Hydrologic analysis checks, or hydraulic calculation sheets.
- (d) Important reports of geologic investigation and rock and soil tests.
- (e) Reports of hydraulic model tests, structural model tests, and the other tests.
- (f) Reports of the specialized fields concerning construction techniques, layout, and schedule.
- (g) Reports of type selection for electromechanical devices and metal structure equipments.
- (h) Other important reports related to the design and research of the project, if any.

References

- Acker WL III (1974) Basic procedures for soil sampling and core drilling. Acker Drill Company, Scranton
- Brandon TW (ed) (1987) River engineering. Part 1, Design principles, vol 7. Institution of Water and Environmental Management, London
- Brandt SA (2000) A review of reservoir desiltation. *Int J Sedim Res* 15(3):321–342
- US Weather Bureau (1947) Generalized estimates of maximum possible precipitation over the United States East of the 105th meridian, for areas of 10, 200, and 500 Square Miles. Hydrometeorological report no. 23. US Weather Bureau, Washington DC
- Casagrande A (1961) First Rankine Lecture—control of seepage through foundations and abutment of dam. *Géotechnique* 11(3):161–182
- Chen SH (2006) Computational rock mechanics and engineering. China WaterPower Press, Beijing (in Chinese)
- Chen ZA, Sun ZL, Peng TB, Xi QX (eds) (2000) Hydropower engineering in China—engineering geology. China Electric Power Press, Beijing (in Chinese)
- China Earthquake Administration (1999) GB17740-1999 “General Ruler for Earthquake Magnitude”. Standards Press of China, Beijing (in Chinese)
- Clayton CRI, Simons NE, Matthews MC (1982) Site investigation. Halsted Press, New York
- Davis CD (1952) Handbook of applied hydraulics. McGraw-Hill, New York
- Dober RP (1969) Environmental design. Van Nostrand Reinhold Company, New York
- Dudgeon D (1995) River regulation in southern China: ecological implications, conservation and environmental management. *Regulated Rivers: Res Manage* 11(1):35–54
- Dyner I, Larsen ER (2001) From planning to strategy in the electricity industry. *Energy Policy* 29 (13):1145–1154
- Farmer IW (1968) Engineering properties of rocks. E & FN Spon Ltd, London

- Garcia MH (2008) Sediment transport and morphodynamics. In: Garcia MH (ed) ASCE manual of practice 110—sedimentation engineering: processes, measurements, modeling and practice. ASCE, Reston, pp 21–163
- General Administration of Quality Supervision of the People's Republic of China (2001) GB18306-2001 "Seismic Ground Motion Parameter Zonation Map of China". Standards Press of China, Beijing (in Chinese)
- Golzé AR (1977) Handbook of dam engineering. Van Nostrand Reinhold Company, New York
- Goodman RE (1989) Introduction to rock mechanics, 2nd edn. Wiley, New York
- Graf WL (1999) Dam nation: a geographic census of American dams and their large-scale hydrologic impacts. *Water Resour Res* 35(4):1305–1311
- Gray DH, Leiser AT (1982) Biotechnical slope protection and erosion control. Van Nostrand Reinhold, New York
- Hamilton B, Bui DT (2001) Wien automatic system planning (WASP) package—a computer code for power generating system expansion planning (Version WASP-IV). User's manual. Computer manual series 16. IAEA, Vienna
- Hershfield DM (1961) Estimating the probable maximum precipitation. *J Hydraulics Div ASCE* 87 (HY5):99–116
- Hocutt CH et al (eds) (1980) Power plants, effects on fish and shellfish behavior. Academic Press, New York
- Hoek E, Bray JW (1981) Rock slope engineering, 3rd edn. Institution of Mining and Metallurgy, London
- Hyndman D, Hyndman D (2009) Earthquakes and their causes (Chap. 3). In: Natural hazards and disasters, 2nd edn. Brooks/Cole, CA
- ICOLD (1975) A review of earthquake resistant design of dams (Bulletin 27). ICOLD, Paris
- ICOLD (1992) Dams and environment socio-economic impacts (Bulletin 86). ICOLD, Paris
- ICOLD (1993) Rock foundations for dams (Bulletin 88). ICOLD, Paris
- ICOLD (2002) Reservoir landslides: investigation and management—guidelines and case histories (Bulletin 124). ICOLD, Paris
- ICOLD (2003) Dams and floods—guidelines and case histories (Bulletin 125). ICOLD, Paris
- ICOLD (2005) Dam foundations. Geologic considerations. Investigation methods. Treatment. Monitoring (Bulletin 129). ICOLD, Paris
- ICOLD (2011) Reservoirs and seismicity—state of knowledge (Bulletin 137). ICOLD, Paris
- ICOLD (2013) Selecting seismic parameters for large dams—guidelines (revision of Bulletin 72) (Bulletin 148). ICOLD, Paris
- Jaeger JC, Cook NGW, Zimmerman R (2007) Fundamentals of rock mechanics, 4th edn. Wiley-Blackwell, MA
- Jiao Y, Zhang GL, Li DX (2004) China water conservancy advancing to wards modernization—Tenth Five-year Plan. China WaterPower Press, Beijing (in Chinese)
- Kerr R, Stone R (2009) A human trigger for the great quake of Sichun? *Science* 323(5912):322
- Linsley RK, Kohler MA, Paulhus JLH (1949) Applied hydrology. McGraw-Hill, New York
- Liu N (2006) Study on project objective decision making. China WaterPower Press, Beijing (in Chinese)
- Look BG (2007) Handbook of geotechnical investigation and design tables. Taylor & Francis, London
- Loulou R, Goldstein G, Noble K (2004) Energy technology systems analysis programme—documentation for the MARKAL family of models. IEA, Paris
- Lowe J, Zaccheo PF (1975) Subsurface explorations and sampling. In: Winterkorn HF, Fang HY (eds) Foundation engineering handbook. Van Nostrand Reinhold Company, New York, pp 1–66
- Mathewson CC (1981) Engineering Geology. Charles E. Merrill, Columbus
- Mattice J (1991) Ecological effects of hydropower facilities. In: Gulliver J, Arndt REA (eds) Hydropower engineering handbook. McGraw-Hill, New York
- Morris GL, Fan J (1998) Reservoir sedimentation handbook: design and management of dams, reservoirs, and watersheds for sustainable use. McGraw-Hill, New York

- Morris HM, Wiggert JM (1972) Applied hydraulics in engineering, 2nd edn. Ronald Press, New York
- National Development and Reform Commission of the People's Republic of China (2007) DL5020-2007 "Specifications on Compiling Feasibility Study Report of Water Conservancy and Hydropower Projects". China Electric Power Press, Beijing (in Chinese)
- National Development and Reform Commission of the People's Republic of China, Ministry of Housing and Urban-Rural Development of the People's Republic of China (2006) Economic evaluation methods and parameter of construction projects, 3rd edn. China Planning Press, Beijing (in Chinese)
- Novak P, Moffat AIB, Nalluri C, Narayanan R (1990) Hydraulic structures. The academic division of Unwin Hyman Ltd, London
- Oglesby RT, Carlson CA, McCann JA (1972) River ecology and Man. Academic Press, New York
- Pan JZ, He J, An ZY (eds) (2000a) Hydropower engineering in China—immigration and environmental protection. China Electric Power Press, Beijing (in Chinese)
- Pan JZ, He J, Wang RC (eds) (2000b) Hydropower engineering in China—engineering hydrology. China Electric Power Press, Beijing (in Chinese)
- Pan JZ, He J, Zhao YK (eds) (2000c) Hydropower engineering in China—economic planning. China Electric Power Press, Beijing (in Chinese)
- Peng C (2006) 21st century china hydropower engineering. China Electric Power Press, Beijing (in Chinese)
- Petersen MS (1986) River engineering. Prentice Hall, New Jersey
- Ponce VM (1989) Engineering hydrology: principles and practices. Prentice-Hall, New Jersey
- Poulos SJ, Castro G, France JW (1985) Liquefaction evaluation procedure. *J Geotechn Eng ASCE* 111(6):772–792
- Price DG (ed) (2009) Engineering geology—principles and practice. Springer, Berlin
- Richter CF (1958) Elementary seismology. Freeman WH and Company, San Francisco
- Scott RF (1987) Baldwin Hills reservoir failure in review. *Eng Geol* 24(1–4):103–125
- Seebregts A, Kram T, Schaeffer GJ, Seebregts AB (2000) Endogenous learning of technology clusters in a MARKAL model of the Western European energy system. *Int J Global Energy Issues* 14(1–4):289–319
- Serhal H, Daniel BD, El Jamal KJ, Bastin-Lacherez S, Shahrour I (2009) Impact of fertilizer application and urban wastes on the quality of groundwater in the Cambrai Chalk aquifer, Northern France. *Environ Geol* 57(7):1579–1592
- Seymour RT (1978) The aseismic design of concrete dams. *Water Power Dam Constr* 28(1):37–38 (Part one), 28(2):41–46 (Part two)
- Shields FD Jr, Sanders TO (1986) Water quality effects of construction and diversion. *J Environ Eng ASCE* 112(2):211–223
- Sokolov AA et al (1976) Flood flow computation, methods compiled from world experience. The UNESCO Press, Paris
- Thornton KW, Kimmel BL, Payne FE (eds) (1990) Reservoir limnology: ecological perspectives. Wiley-Interscience, New York
- United Nations (1990) Environmental impact assessment. Guidelines for water resources development ESCAP. Environment and development series. United Nations, New York
- USBR (1987) Design of small dams, 3rd edn. US Govt Printing Office, Denver
- Warren V Jr, Lewis GL (2003) Introduction to hydrology, 5th edn. Pearson Education, NJ
- Wetzel RG (1990) Reservoir ecosystems: conclusions and speculations. In: Thornton KW, Kimmel BL, Payne FE (eds) Reservoir limnology: ecological perspectives. Wiley-Interscience, New York
- Yang XT, Pu YJ (1993) Resource economics—economic analysis over optimum resources disposition. Chongqing University Press, Chongqing
- Yu MZ et al (1994) Hydropower planning and management. China WaterPower Press, Beijing (in Chinese)
- Zhong Y, Power G (1996) Environmental impacts of hydroelectric projects on fish resources in China. *Regulated Rivers: Res Manage* 12(1):81–98

- Zhou JP (2007) Practical guide to hydropower engineering investigation and design project manager. China Electric Power Press, Beijing (in Chinese)
- Zuo DQ, Gu ZX, Wang WX (eds) (1984) Geology, hydrology and materials. In: Handbook of hydraulic structure design, vol 2. Water Resources and Electric Power Press of China, Beijing (in Chinese)

Chapter 3

Study on Material Properties

3.1 General

Materials widely used in hydraulic structures are mineral materials such as natural soil, natural stone, inorganic binding material, concrete, and cement mortar; organic materials such as wood, bamboo, asphalt, and geosynthetics; and metal materials such as steel and cooper. The rock, soil, and concrete are the most prevalent materials for the building of hydraulic structures, whose properties, such as density, permeability, deformation, consolidation, and strength, must be explored, tested, and analyzed comprehensively in order to design a hydraulic structure that is safe, feasible, and appropriate for the site conditions (Craig 2004; Goodman 1989; Hudson and Harrison 1997; Jaeger et al. 2007; Mehta and Monteiro 2006; Zienkiewicz 1968; Golze 1977; Liu et al. 2013; USBR 1987; Zuo et al. 1984). Rock and concrete are some times termed as rocklike materials.

1. Density

Density is one of the important engineering properties of rock, soil, and concrete. The density of concrete and soil may be controlled through the selection of aggregate stone and/or compaction effort, by which the deformability as well as the resistance strength in bearing and shearing may be “designed.”

The density of a foundation material becomes crucial when a structure will be placed on alluvium that contains soft or loose soils. The low density soils in foundation may settle significantly when they are loaded and saturated, which in turn may lead to cracking in the structure. Be subjected to an earthquake, a failure also could be triggered due to liquefaction in these low density soils.

The identification of low density soils can be made by normal geologic explorations such as undisturbed sampling, penetration testing, and trenching. Actual measuring of density must be made in the field.

2. Permeability

Permeability is another important property to be assessed, as it will impose direct effects on the design and can represent a significant cost of the hydraulic structure (Hsich and Neuman 1985; Hsich et al. 1985; Louis and Maini 1970).

Study on the permeability property may be accomplished by in situ tests, normally performed in drill holes, and laboratory tests. In situ tests are usually conducted by pumping or packer techniques in single borehole to measure permeability coefficients. Although such tests are valuable for understanding the permeability of materials, a good evaluation of the permeability could be the most difficult task, particularly for fractured rock masses, due to the heterogeneity of most foundations and limitations of test procedures. By the stipulations of three orthogonal sets of fractures in rock masses, triple hydraulic probe was proposed by Louis in 1970 to measure permeability tensor. Later on, cross-hole tests were also proposed by Hsich and Neuman in 1985 for the same purpose.

The concepts of primary permeability and secondary permeability in rock masses are widely accepted nowadays. The former refers to the rock matrix (intact rock) permeability, whereas the latter indicates the rock mass permeability dominated by discontinuities. Usually, the presence of discontinuities in a rock mass gives rise to a much higher value of permeability compared with that of the intact rock matrix. Therefore, in most rock foundation, permeability problems encountered in the hydraulic engineering, the secondary permeability plays much more important role in the cutoff and dewatering design.

For a given soil, the coefficient of permeability is a function of void ratio. The permeability coefficient of the soil depends primarily on the average size of the pores, which in turn is related to the distribution of particle size, particle shape, and soil structure. In general, the smaller of the particles, the smaller average size of the pores and the lower of the coefficient of permeability. The presence of a small percentage of fines in a coarse-grained soil results in a value of permeability significantly lower than the same soil without fines. If a soil deposit is stratified, the permeability parallel to the stratification lifts is higher than that perpendicular to the stratification lifts.

The permeability of concrete depends not only on mix proportions, compaction, and curing, but also on microcracks resulted from the ambient temperature and humidity cycles. It also should be emphasized that the loss of mass by surface wear, the cracking, as well as the leaching of the components of hardened cement paste by soft water or acidic fluids (sulfate attack) would increase the porosity of concrete, which in turn make the concrete more vulnerable to abrasion and erosion. Addition of aggregate to a cement paste or a mortar increases the permeability considerably, the larger of the aggregate size, the greater of the coefficient of permeability is. The explanation as to why the permeability of concrete is higher than the permeability of the corresponding cement paste lies in the microcracks normally appearing in the interfacial transition zone (ITZ) between the aggregate and the cement paste. During the early hydration period, the ITZ is weak and vulnerable to cracking from differential strains between the cement paste and the aggregate particle induced by

drying shrinkage, thermal shrinkage, and externally applied load. These meso- or microscale cracks in the ITZ are too small to be seen by the naked eye, but are larger than most capillary cavities in the cement paste matrix. Later on, the propagation of these cracks establishes the interconnections for seeping water percolation.

3. Deformation modulus

The most useful single description for the mechanical properties of rocklike materials is the complete stress–strain curve under confining, shown in Fig. 3.1, which is obtained using a right cylinder of material sample being confined laterally (σ_3) and compressed in axial direction (σ_1), where the horizontal axis is strain (ϵ_a) and the vertical axis is deviate stress ($\sigma_1 - \sigma_3$). If $\sigma_3 = 0$, the test is called uniaxial. This type of resultant curve, known as the strain-controlled complete stress–strain curve, was first obtained in 1966 for rock, for the purpose to illustrate the very significant effect of the microstructure and the history on its mechanical behavior (Jaeger et al. 2007).

At the very beginning of loading, the curve has an initial portion (OA) which could be concave upward for rock, but could be convex for soil and concrete. This is mainly due to the deficit in the rock specimen preparation—the ends of the cylinder being non-parallel and/or the closing of micro-cracks within the intact rock. After this initial portion, there is a portion of essentially linear behavior (AB). B may be defined as “yield stress,” after this point plastic strain ϵ^p will manifest following the continuous but gentler mounting of the curve along the loading, which is termed as “hardening phase.” The plastic strain may be detected by an unloading–reloading circle, for example, $F \rightarrow Q \rightarrow T$, where the total strain is divided into the components of elastic and plastic, i.e., $\epsilon = \epsilon^e + \epsilon^p$. After the peak stress C, the complete stress–strain curve enters descending post-peak region (CD), which is named as “softening phase.” In this phase, much more plastic strain may be found through unloading–reloading circle, such as $S \rightarrow T \rightarrow U$.

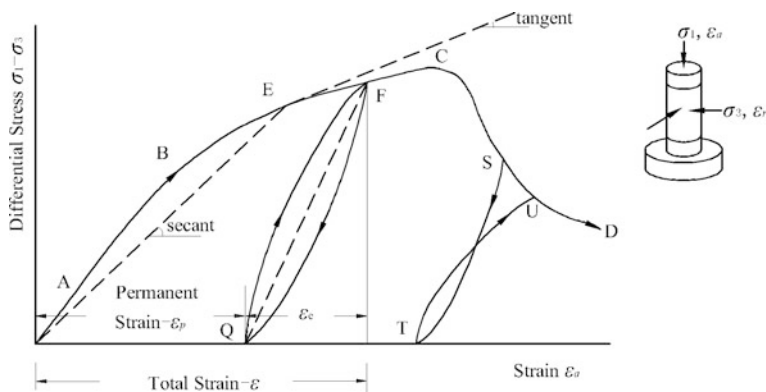


Fig. 3.1 Complete stress–strain curve of rock under confining pressure

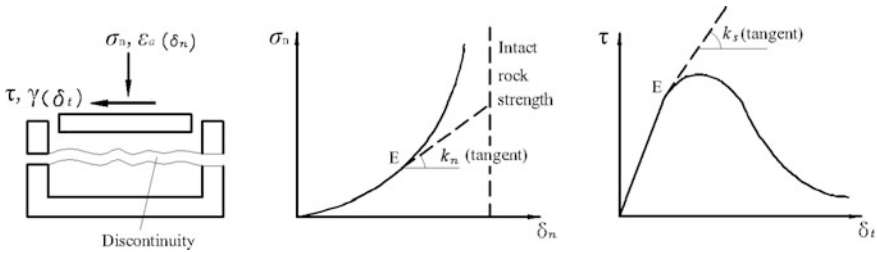


Fig. 3.2 Complete stress–strain curve under direct shear for discontinuity

Another very useful description for the mechanical behavior of rocklike materials is the complete strain–displacement curve under direct shear for discontinuities (joint, fracture, etc.), as shown in Fig. 3.2. In compression, the discontinuity is gradually pushed close, with an apparent limit when its two surfaces are contacted. The stiffness k_n associated with this compression process has strong nonlinearity which gradually increases with the applied normal stress, until reaching a limit associated with the strength of the intact rock/concrete. When a discontinuity is subjected to shear stress, the curve is rather like the complete stress–strain curve for compression of intact rock in Fig. 3.1, i.e., there is an initial shear stiffness, a peak shear strength, and a post-peak failure region.

Although there exist various factors related to loading conditions (e.g., confining stress in triaxial test) and loading rates which influence the shape of the curve, there are always several features important to be indicated from Fig. 3.1 (Fig. 3.2 similar). The first one is the Young’s modulus E of the material, either tangent or secant. The next one is the compressive strength which is the maximum stress that can be sustained. The third one is the steepness of the descending portion of the curve which is an index of the brittleness. If the behavior after the compressive strength is in a form of progressive strain at the same stress level, the material is termed as ductile, and a residual stress may be identified; if a drop in the stress level to zero at the same strain value occurs, the material is brittle. In fact, the real situation is more complicated than these two extraordinary cases because it is usually to have strain-hardening behavior under high confining pressure, while hardening behavior may be less important under low confining pressure.

Regarding to the definition of the Young’s modulus, there are several most commonly used expressions. The tangent modulus is given by the slope of a line drawn tangent to the stress–strain curve at any point, of which the initial tangent is the slope at initial stress. The elastic tangent modulus, which is conventionally named as “elastic modulus” (Young’s modulus), is the slope of any specified linear point (or near linear) on the stress–strain curve, but usually at a specified stress level (such as 50 % for rock) of the maximum or peak stress. The “chord modulus” is given by the slope of a line drawn between two points on the stress–strain curve. The “deformation modulus” is the slope of the line between zero and a specified stress level with respect to the maximum or peak stress (e.g., 40 % for concrete,

one-third for soil), which belongs to “secant modulus.” The “recovery modulus” is the slope of unload line.

In principle, the value of E of intact rock, soil, and concrete can be estimated from the curve relating principal stress difference and axial strain in an appropriate laboratory test. However, due to the effects of sampling disturbance, it is preferable to determine the Young’s modulus E and Poisson’s ratio μ (or G) from the results of in situ tests.

Four basic types of equipments are used in the measuring of in situ deformation modulus:

- Borehole jacks and dilatometers;
- Flat jacks installed in slots cut into rock mass;
- Plate bearing tests; and
- Radial jacking tests.

Expanding against the walls, jacks designed to fit inside exploratory drill hole or slot and associated equipments for measuring dilation can provide qualitative information on the deformability at depths of several hundred meters. Although they are quite useful, they are not sufficiently accurate in hard rock to provide quantitative design data for large hydraulic structures.

Plate bearing test is to apply load increments to a test plate, either in a shallow pit, or at the bottom of a large-diameter borehole, or on the wall of an adit, and to measure the resulted displacements. The value of E is then calculated using the relevant close-form displacement solution.

“Intact rock” is defined in engineering terms as “rock matrix” containing no large-scale fractures. However, on the small scale, it consists of grains with meso- or microstructure governed by the rock-forming processes and geological events, together with water penetration and weathering effects. Significant geological fractures such as faults, joints, bedding planes, and fissures are commonly termed as “discontinuities,” which have many geometrical and mechanical features governing the overall behaviors of the rock mass, particularly the deformation, strength, and permeability. The discontinuities have certain shapes and sizes as well as orientations. The overall geometrical configuration of the discontinuities in the rock mass is termed as “rock structure.” As far as the deformation modulus (and the strength as well) of rock mass is concerned, it can be approached in two ways, i.e., either by computation using the properties of the intact rock and the discontinuities, respectively, or via the direct in situ measuring. Although various theoretical models have been proposed for the computation of deformation modulus and strength (Amadei 1983; Chen and Pande 1994; Pande and Gerrard 1983; Salamon 1968), they are all subjected to the verification and adjustment using data measured through in situ large-scale tests or using engineering analog and back analysis, if possible.

In selecting modulus for the design of soil foundations and embankments, it is necessary, as always, to distinguish between drained and undrained loading. It is also necessary to remember that the modulus is highly nonlinear and values appropriate to the strains in the ground soil should be selected. The modulus, which

is the gradient of the stress–strain curve, may be either tangent or secant: Analysis can be done in one step using secant modulus or in several steps using tangent modulus.

The Young's modulus used in concrete design may be estimated from empirical expressions that assume direct dependence of the modulus on the strength and the density of concrete or concrete grade directly. As a first approximation, this estimation makes sense because the stress–strain behavior of the three components of concrete, namely the aggregate, the cement paste matrix, and the ITZ, would actually be related to the deformation and ultimate strength of the concrete.

For a material subjected to simple axial load, i.e., the confining pressure $\sigma_3 = 0$ in the Fig. 3.1, the ratio μ of the lateral strain ε_r to axial strain ε_a within the elastic range is called Poisson's ratio. It is generally not needed for the conventional design of concrete gravity dams. However, it is required for the structural analysis of tunnels, arch dams, and other statically indeterminate structures.

4. Shear strength

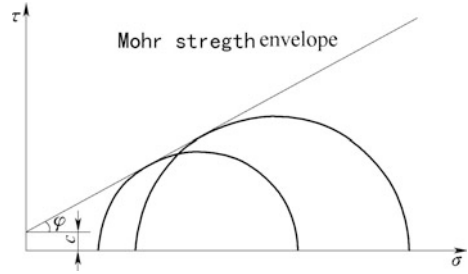
For embankment dams and low concrete dams as well as barrages, the strength of most rock foundations is enough to give rise to no serious foundation troubles. However, weak sedimentary rocks such as shales and siltstones should be carefully investigated to determine their strength due to their low density and high water content.

If the embankment dam or barrage is to be constructed on alluvium foundation that contains deposits of silt and clay, then shear failure potential in the foundation should be studied. In the design of cut rock slopes and rock foundations of high concrete dams, the most important rock mechanics parameter is the shear strength, which is a term used in soil and rock mechanics to describe the magnitude of the shear stress that a soil or rock can sustain. Shear strength is a result of friction and interlocking of particles, and possibly cementation or bonding at particle contacts, and is commonly evaluated in a comprehensive way using experiments, back analysis, and engineering analog (empirical data).

Conventionally, shear strength is evaluated by laboratory tests and in situ tests, of which laboratory tests employ shear box (direct shear test), triaxial, and unconfined (uniaxial) compressive apparatus, whereas in situ tests fall into vane shear and direct shear (Commission on Standardization of Laboratory and Field Tests (ISRM) 1974; Hoek 1990).

The Mohr envelope is primarily a graphic method to represent the results of a series of experiments on the shear of rock/soil under varying external conditions, e.g., triaxial tests under a series of confining pressures (Craig 2004; Duncan and Wright 2005). In any experiments, the maximum and minimum principal stresses, σ_1 and σ_3 , when failure takes place, are assumed to be known, and a Mohr circle for them can be drawn. If the conditions of the test (e.g., confining pressure) are changed slightly, a slightly shifted Mohr circle (Fig. 3.3) will be obtained. The envelope of all such circles, if exists, is the Mohr envelope for the material which is a curve relating normal stress σ and shear stress τ . In practice, only a limited portion of the envelope is available.

Fig. 3.3 Mohr strength envelope



In a definite stress range, prior to the postulation of the principle of effective stress, the shear strength of the material at a point on a particular plane was expressed by Coulomb as a linear function of the normal stress at the same point. Therefore, in the stability analysis, it is generally assumed that the failure of materials may be calibrated using the Mohr–Coulomb criterion, in which the shear strength is expressed in terms of parameters c (cohesion) and φ (angle of shearing friction):

$$\tau_f = c + \sigma \tan \varphi \quad (3.1)$$

where c and φ = total stress strength parameters representing the intercept at vertical coordinate and the slope of the Mohr–Coulomb shear envelope.

In the tests, graphs of shear stress against normal stress and shear displacement are plotted, which is employed to find c and φ corresponding to the peak and residual shear strengths. Peak strength may be defined as the maximum resistance of the sample to the shear force, while the residual strength is the resistance of the failed shear surface after considerable movement, which is adopted selectively in the stability analysis taking into account of the properties of the hydraulic structures. In the selection of strength parameters, the reservoir impounding induced softening should be foreseen, too.

It should be beard in mind that the tests are always not able to simulate well the natural conditions of materials, particularly for the rock masses and discontinuities; therefore, the test data are normally not applied directly. They are subjected to revision taking into account of experimental conditions, representative of the samples, computing methods, and natural conditions.

It is also worthwhile to indicate that laboratory or in situ testing is minimized until the decision on the site of the hydraulic structure has been made.

3.2 Rock

The Earth's outer solid layer, i.e., the lithosphere, is made of rocks of minerals or mineraloids. At a granular level, rocks are composed of grains of minerals held together by chemical bonds. Many rocks contain silica (SiO_2) which forms crystals

with other compounds. The proportion of silica in rocks and minerals is a major factor in determining their name and properties. Over the geologic history, rocks can transform from one type into another, which called the rock cycle. These events produce three general classes of rocks: igneous, sedimentary, and metamorphic.

Rocks have been used by human throughout the civilization history for more than 2 million years, firstly being as tools for hunting and defense and then as a building material for shelters and monuments. Lithic technology marks some of the oldest and continuously evaluated cultures, such as the “Old and New Stone Ages.”

In the modern civil engineering, rocks are generally described in the bore log using the following sequence of terms: drilling information, rock type, weathering, color, structure, rock quality designation (RQD), strength, and defects (Look 2007).

3.2.1 Basic Physical and Mechanical Properties of Intact Rock

The rock unit weight varies from the lowest 18 kN/m³ (e.g., sand stone and limestone) to the largest 30 kN/m³ (e.g., granite and basalt) depending on its type and weathering degree.

The conventional compressive testing with or without confining pressure, in which a short, right cylinder is loaded axially, is one of the most widespread experiments in rock mechanics (Fig. 3.1). This configuration is employed in the studies of strength, long-term creep, as well as elastic behavior. There is approximately a tenfold increase in deformation modulus and uniaxial strength from an extremely weathered to a fresh rock. The geologic age of the rock also may affect the deformation and strength parameters for sedimentary rocks.

The Young's modulus differs considerably for different rock types and at various stages of deformation. In compact igneous rocks, Young's modulus is nearly constant until their failure. The commonly encountered Young's moduli (secant or deformation) and Poisson's ratios of fresh rocks are ranged from 80 GPa (granite porphyry, diorite, basalt porphyrite) to 3.0 GPa (shale, siltstone, conglomerate), and 0.15 (basalt porphyrite) to 0.33 (shale, siltstone, conglomerate). Generally speaking, the higher of the Young's modulus is the lower of the Poisson's ratio would be.

As for the uniaxial strength of intact rock, its variation related to rock types is ranged from the lowest 40 MPa (phyllites) to the highest 170 MPa (rhyolites), according to Hoek and Bray (1981).

Assuming fresh to slightly weathered rock, the shear strength of rock may be ranged from the lowest sedimentary (triassic, coal, chalk) of $c' = 1-20$ MPa and $\varphi' = 25^\circ-35^\circ$ to the highest igneous (granite) of $c' = 30-50$ MPa and $\varphi' = 45^\circ-55^\circ$. Strongly weathered rock can present significantly reduction in shear strengths (Look 2007).

The permeability coefficient k of various intact rocks by laboratory test data available in the literatures ranges from approximately 10^{-3} (cm/s) (glenrose

sandstone) to 10^{-11} (cm/s) (granite and shale) (Farmer 1968; Serafim 1968; Jaeger et al. 2007). The primary permeability of rock (intact) matrix is several orders lower than the secondary permeability in magnitude, due to the influence of discontinuities.

3.2.2 Basic Physical and Mechanical Properties of Discontinuity

There are two fundamentally types of discontinuities, i.e., those who have been simply opened and are termed as “joints,” and those who have been certain lateral movement and are termed as “shear zones” or “faults.” The main features of rock discontinuity geometry may be illustrated as follows.

- Spacing and frequency: Spacing is the distance between adjacent discontinuity intersections with the measuring scan line. Frequency (i.e., the number per unit distance) is the reciprocal of the spacing.
- Orientation (trend): The discontinuity is assumed to be planar whose dip direction (the compass bearing of the steepest line in the plane) and dip angle (the angle that this steepest line makes to the horizontal plane) uniquely define its orientation.
- Persistence: The extent of the discontinuity in its own plane is commonly described using persistence, incorporated with the assumptions regarding the shape of the bounded plane and the associated characteristic dimensions (e.g., discontinuity disks of circular, ellipse, or rectangular).
- Roughness: The surface of the discontinuity is usually uneven, and whose roughness may be defined either by reference to standard charts or mathematically.
- Aperture: It is the perpendicular distance between the adjacent rock walls of the discontinuity, which strongly dominates the nonlinear phenomenon in the deformation and strength parameters of the discontinuity.
- Discontinuity sets: Discontinuities occur for good mechanical reasons with some degree of clustering around preferred orientations associated with the formation mechanisms. Hence, it is convenient to adopt the concept of discontinuity set consisting of parallel or nearly parallel discontinuities.

There is a variety of testing procedures for the mechanical attributes of discontinuities, ranging from the tilt test, through the shear box and standard triaxial procedures, to the sophisticated tests on servo-controlled equipment. Figure 3.2 shows a complete stress–displacement curve in direct shear testing for a discontinuity.

The normal and shear forces applied across a discontinuity can be scaled by the nominal area of the discontinuity to give normal and shear stresses, respectively, which give rise to normal and shear displacements. These displacements are related

to the corresponding stresses by various parameters extensively studied (Barton et al. 1985), of which the combination of the elastic model proposed primary by Goodman et al. (1968), and the Mohr–Coulomb shear strength criterion is the most prevalent in the design of hydraulic structures in many countries inclusive China. The so-called Goodman joint element model simply links the stress increments in conjugate with the displacement increments in a linear form of

$$\begin{cases} d\sigma_n = k_n d\delta_n \\ d\tau = k_s d\delta_t \end{cases} \quad (3.2)$$

where k_n and k_s = coefficients of normal stiffness and tangential stiffness, MPa/m.

Basically, it is assumed that the strength of discontinuities is calibrated by the Mohr–Coulomb criterion Eq. (3.1). To give an example, at unfilled rock joints the friction angle is ranged from $\varphi' = 20^\circ - 27^\circ$ (schists, shale) to $\varphi' = 34^\circ - 40^\circ$ (basalt, granite, limestone, conglomerate).

As for the stiffness coefficients with respect to the joint compression and shear, there is no linear relation mainly due to the closure and shear on the irregular discontinuity surfaces. Among various approximations, Chen et al. (1989) had established a unified stiffness and permeability model which considers the asperities as an evenly “filled” medium. This model applies for both the filled and non-filled discontinuities and is usually termed as “filled model,” viz.:

$$\begin{cases} k_n = k_{n0} \exp(-\xi\sigma_n) \\ k_s = k_{s0} \exp(-\xi\sigma_n) \end{cases} \quad (3.3)$$

where ξ = coupling coefficient; k_{n0} and k_{s0} = initial stiffness coefficients, MPa/m; and σ_n = normal stress on discontinuity (negative for compressive), MPa.

There are interrelations between most of the rock properties, and the flow of fluid through a fractured rock mass is no exception, as it depends on the aperture of the fractures, which in turn will depend on the normal stress exerting across the fractures. In the extreme case at great depth, all the fractures may be effectively closed, so that the primary and secondary permeability are similar. Snow (1969) has proposed the “parallel plate model” which was later improved by Louis (1970), Tsang and Witherspoon (1981), Barton et al. (1985). Attempts on the coupling relationship between normal stress and tangential seepage through the discontinuity were also made by Gale (1982), Raven and Gale (1985). By the “filled model” aforementioned, the discontinuity permeability will be simply related to the normal stress as

$$k = k_0 \exp(\xi\sigma_n) \quad (3.4)$$

where ξ = coupling coefficient; k_0 = initial permeability coefficient of the imagined or real discontinuity filling, MPa/m; and σ_n = normal stress on discontinuity (negative for compressive), MPa.

The parameters in Eqs. (3.3) and (3.4) may be estimated by the routine tests for joints (Chen et al. 1989; Chen 2006).

3.2.3 Basic Physical and Mechanical Properties of Rock Mass

It is widely recognized that there are three basic peculiarities of rock mass compared to soil and concrete:

- Rock mass comprises structural body surrounded by structural planes (geological discontinuities); therefore, the engineering characteristics of rock mass are coded by the material of structural body and various geological discontinuities, and the latter are often dominant.
- The rock mass on which the hydraulic works rest has different stability status varying with stress conditions.
- The changeable characteristics and spatial combinations of structural planes, coupled with different properties and configurations of structural bodies, contribute to great disparity in the mechanical characteristics of rock mass.

Engineers have developed various rock mass classification schemes which are basically a compromise between the use of a complete theory and ignoring the rock properties entirely. All the existing classification schemes consider a few of the key rock mass features and assign numerical values to the classes. The schemes provide a shortcut to the rock mass properties that are more difficult to assess (e.g., the prediction of rock mass deformability) and provide direct guidance for engineering design (e.g., the type and amount of support required for a tunnel).

There are two prevalent classification schemes in the geotechnical engineering community, which were essentially developed for estimating the supporting necessity of tunnels in civil engineering: One is the Q Method by Barton, and another one is the RMR System by Bieniawski (Hudson and Harrison 1997). Attempts also have been made to extend the classification systems, such as to the cut slopes.

However, engineering practices for hydraulic projects demonstrate that any classification systems can only define the overall properties of rock masses within a limited spatial scope. It can by no means include those special geological elements of dominant significance which are difficult to be quantified by statistics, e.g., the low-strength, thin-opening, and gently inclined discontinuities in the dam foundation which control the sliding resistant capacity of the rock mass.

At present, China has promulgated the (GB50218-94) "Standard for Engineering Classification of Rock Masses" (1994), which has two major contents: One is the basic quality classification for rock mass, and the other is the class identification of engineering rock mass. The former is generally applicable to assess the basic

quality of rock mass, while the latter can be employed to revise the basic quality index in conjunction with specific engineering undertakings.

The basic quality index (BQ) of rock mass is given by

$$\text{BQ} = 3R_c + 250K_v \quad (3.5)$$

where R_c = uniaxial compression strength of saturated rock (MPa); K_v = index representing the rock mass integrity in the expression of

$$K_v = \left(\frac{V_{\text{pm}}}{V_{\text{pr}}} \right)^2 \quad (3.6)$$

In which V_{pm} = primary wave velocity of rock mass (km/s) and V_{pr} = primary wave velocity of rock matrix (km/s). Equation (3.5) is subject to the following constraints:

- For a given K_v by Eq. (3.6), if $R_c > 90K_v + 30$, then assuming $R_c = 90K_v + 30$ for the calculation of BQ.
- For a given R_c , if $K_v > 0.04R_c + 0.4$, then assuming $K_v = 0.04R_c + 0.4$ for the calculation of BQ.

The rock mass quality classification is illustrated in the Table 3.1.

In case of difficulty, the parameters R_c and K_v are to be estimated using point load strength index $I_{(s)50}$ and volumetric joint count of rock mass J_v , according to Eq. (3.7) and Table 3.2.

$$R_c = 22.82I_{(s)50}^{0.75} \quad (3.7)$$

In which $I_{(s)50}$ is the point load strength index using cylindrical sample of 50 mm in the diameter.

In the phase of planning or preliminary study, when the test data are in short, the shear strength parameters may be selected according to the geologic condition, rock classification, characteristics of discontinuities, recommendation of design specifications, as well as the data from analogue projects. All these information provide valuable aids to engineers in their evaluation of shear strength parameters.

For the dam engineering, the basic quality index BQ can be used directly. However, the Standard (GB50218-94) requests a revision in BQ for the underground and slope engineering, and the main factors taken into account of in the revision are as follows: groundwater, dominant weak structural plane, and initial tectonic stress. The Standard (GB50218-94) also suggests empirical relationships of the BQ versus physical and mechanical parameters of the rock masses, which are obtained from the statistics analysis relating the classifications and field tests of the 47 typical projects in China.

Table 3.1 Standard for basic quality classification of engineering rock masses

Basic quality grade classified	1	2	3	4	5
Basic quality index BQ	>550	550–451	450–351	350–251	≤250
Qualitative traits of rock mass for basic quality classification	Hard and integral rock mass	① Hard rock/fairly integral rock mass ② Fairly hard rock/integral rock mass	① Hard rock/fairly fissured rock mass ② Fairly hard rock or alternating hard and soft rock/fairly integral rock mass ③ Comparatively soft rock/integral rock mass	① Hard rock/fissured rock mass ② Fairly hard rock/fairly fissured to fissured rock mass ③ Fairly hard rock or alternating hard and soft rock predominated by soft rock/fairly integral to fairly fissured rock mass ④ Soft rock/very fissured rock mass	① Comparatively soft rock/fissured rock mass ② Soft rock/fairly fissured to fissured rock mass ③ Very soft rock/very fissured rock mass

Table 3.2 Relationship between K_v and J_v

J_v (count/m ³)	<3	3–10	10–20	20–35	>35
K_v	>0.75	0.75–0.55	0.55–0.35	0.35–0.15	<0.15

GB 50487-2008 “Code for engineering geological investigation of water resources and hydropower” also recommends shear strength parameters of rock masses and discontinuities for different types of rocks, according to the collected database from the extensive field and laboratory testing carried out in the China’s hydraulic engineering.

Tables 3.3 and 3.4 list a part of the shear strength parameters of rock masses and discontinuities tested in the China’s hydraulic projects, which may be referred to in the early phases of design, too.

Table 3.5 lists the principal values of the permeability tensors for several rock masses obtained from in situ tests and revised according to the geologic conditions. It is clearly shown that the secondary permeability tensor of fractured rock is anisotropic.

3.2.4 Parameter Back Analysis

It is merely theoretically possible using laboratory or in situ tests to obtain a careful interpretation in light of the behavior of rock masses (or soils/concrete) that makes

Table 3.3 Shear strength parameters of rock masses tested in the China's hydraulic projects

Project	Rock formation	Rock type	Weathering degree	Peak strength parameters of rock by direct shear		Peak strength parameters of concrete/rock contact face by direct shear			
				f	c' (MPa)	Compressive strength of concrete (MPa)	f	c (MPa)	ρ
Three Gorges	Presinian system	Porphyritic granite	Slightly weathered	1.7-1.9	1.08-2.06	21.6-38.2	1.33-1.77	1.37-2.49	
			Weakly weathered	0.9-1.83	0.2-2.16	20.1-27.6	1.04-1.43	1.27-1.96	
			Strongly weathered	1.2-1.54	0.3-1.96	-	-	-	
			Totally weathered	0.80-1.14	0.13-0.47	-	-	-	
			Intact	2.26-2.5	4.6-5.2	15.0-26.1	1.13-1.47	1.42-1.96	
Goupitan	P_{1m}	Biocalcarenite	Slightly weathered and intact	1.20-1.82	2.80-6.86	20-30	1.19-1.57	1.10-2.45	
			Ditto	1.38-1.88	1.12-3.40	-	-	-	
			Ditto	1.1-1.26	1.1-1.55	-	-	-	
Shuibuya	P_{1q}^4	Medium-to-thick layer of fine grained limestone	Ditto	2.40	1.50	-	-	-	
			Ditto	1.19	0.98	-	-	-	
			Ditto	1.20	1.01	-	-	-	

(continued)

Table 3.3 (continued)

Project	Rock formation	Rock type	Weathering degree	Peak strength parameters of rock by direct shear		Peak strength parameters of concrete/rock contact face by direct shear		
				f	c' (MPa)	Compressive strength of concrete (MPa)	f	c (MPa)
Yinpan		Massive limestone (containing silt)						
	C _{2h}	Fine sandstone	Ditto	1.91	1.02	-	-	-
	O _{1d} ²	Argillaceous limestone	Ditto	-	-	20.2-25.1	1.36	1.38
	O _{1d} ³⁻²	Sandstone	Ditto	-	-	19.1-24.1	1.21	1.07
	O _{1d} ¹⁻³	Shale	Ditto	1.31	1.12	21.8-23.2	1.40	0.87
	O _{1d} ¹⁻³		Weakly weathered	1.28	1.51	14.1-25.1	1.33	1.03
Geheyan	O _{1d} ³⁻¹	Shale	Slightly weathered and intact	1.49	1.87	-	-	-
			Weakly weathered	-	-	-	1.17	0.64
	ε	Limestone	Slightly weathered and intact	-	-	20	1.60	1.18
Ertan		Shale	Ditto	-	-	20	0.92	0.29
	P	Simaite	Fresh and monolithic	2.05	3.5		1.22-	>0.5
		Meta basalt	Ditto	1.73	2.2	17.5-18.9	1.42	0.2-0.7
		Aphanitic basalt	Slightly weakly weathered	1.23	1.1	15.0-27.3	1.50-	0.45-
							1.55	0.80

(continued)

Table 3.3 (continued)

Project	Rock formation	Rock type	Weathering degree	Peak strength parameters of rock by direct shear		Peak strength parameters of concrete/rock contact face by direct shear		
				f	c' (MPa)	Compressive strength of concrete (MPa)	f	c' (MPa)
Laxiwa	r_5	Granite	Weakly weathered	-	-	-	1.2-1.4	0.95
Longtan	T_2	Argillaceous slate intercalated with sandstone	Ditto	-	-	-	0.85	1.5
		Interbedding of argillaceous slate and sandstone	Fresh	1.21	1.05	-	-	-
		Sandstone	Slightly weathered	1.70	2.74	-	1.30	1.99
			Weakly weathered	-	-	-	0.9	2.4
Danjiangkou	Simian system	Argillaceous slate	Slightly weathered	1.16 ~ 1.29	1.93 ~ 3.58	-	1.1	1.99
		Meta diabase	Weakly weathered	-	-	-	1.0	1.7
			Slightly weathered and intact	-	-	1.27-13.1	1.1-1.2	1.15-1.6
		Meta diorite-porphyrityrite	-	-	6.3-10.9	0.8-1.17	1.12-1.37	
Chlorite micaschist	-	-	1.38-2.06	1.22-1.30	1.44-1.84			

Table 3.4 Shear strength parameters of discontinuities tested in the China’s hydraulic projects

Projects	Types of discontinuity	Numbering	Peak strength parameters by direct shear		Yield strength parameters by direct shear	
			<i>f</i>	<i>c</i> (MPa)	<i>f</i>	<i>c</i> (MPa)
Gezhouba	Silted intercalation of clay stone	202	0.204	0.031	0.19	0.010
		219	0.44	0.031	0.30	0.005
		218	0.23	0.010	0.16	0.005
		213	0.30	0.025	0.24	0.012
		212	0.35	0.034	0.30	0.029
		212	0.54	0.059	0.32	0.020
		131	0.22	0.02	0.20	0.043
		132	0.22	0.015	0.20	0.010
		132	0.28	0.029	0.25	0.023
	Intercalation of clay stone	313	0.48	0.167	0.42	0.105
		313	0.32	0.118	0.26	0.067
		701	0.43	0.049	0.35	0.015
	Brecciform claystone intercalation	113	0.40	0.039	0.36	10.015
307		0.39	0.069	0.39	0.069	
307		0.43	0.059	0.37	0.020	
Datengxia	Silted intercalation	305	0.337	0.021	–	–
	Discontinuous argillic intercalation	304	0.407	0.086	–	–
Tingzikou	Silted intercalation	J13	0.40	0.17	–	–
	Mud-filled fracture	–	0.40	0.19		
	Stratification plane of quartz sandstone/ claystone	–	0.57	0.14	–	–
	Stratification plane of claystone/ siltstone	–	0.50	0.10	–	–
	Stratification plane of sandstone/ argillaceous siltstone	–	0.59	0.40	–	–
	Stratification plane of siltstone/ claystone	–	0.49	0.26	–	–
	Stratification plane of rock-fragment sandstone/claystone	–	0.63	0.55	–	–
Xiaonanhai	Shear zone	406	0.49	0.13	0.41	0.12
	Shear zone	418	0.53	0.16	0.44	0.14
	Shear zone	404	0.44	0.14	0.40	0.11
	Bedding plane	–	0.76	0.25	0.66	0.17

(continued)

Table 3.4 (continued)

Projects	Types of discontinuity	Numbering	Peak strength parameters by direct shear		Yield strength parameters by direct shear	
			f	c (MPa)	f	c (MPa)
Yinpan	Silted intercalation	I-2002	0.29	0.04	–	–
	Silted intercalation	I-3101	0.19	0.02	–	–
	Silted intercalation	I-3202	0.18	0.01	–	–
	Fractured intercalation	II-1103	0.39	0.08	–	–
	Fractured intercalation	II-3103	0.39	0.26	–	–
Shuibuya	Silted intercalation	031	0.22	0.01	–	–
	Stratification plane of shale/siltstone	–	0.39	0.09	–	–
	Shear zone	001	0.55	0.19	–	–
	Shear zone	F205	0.58	0.15	–	–
Gaobazhou	Shear zone	300-1	0.20	0.042	–	–
	Shear zone	259	0.25	0.035	–	–
	Shear zone	201	0.24	0.025	–	–
	Shear zone	301	0.41	0.08	–	–

Table 3.5 Principal values of equivalent permeability tensors

Projects	Position	Rock type	Fracture sets	Principal values of equivalent permeability tensor (10^{-3} cm/s)		
				k_1	k_2	k_3
Xiaowan	Dam foundation	Granitic gneiss (slightly weathered and intact)	3	0.000800	0.000694	0.000139
Longtan	Cut slope on left abutment	Sandstone, clayslate (slightly weathered and intact)	5	0.007983	0.005438	0.005438
Pushihe	Dam foundation	Granite (weakly weathered)	3	0.355	0.143	0.133
Lingnan	Cut slope	Meta sandstone (weakly weathered)	4	0.740	0.287	0.181

up the full-scale hydraulic works. Because to do so, it is highly necessary taking into account of the representative of test samples in view of the forming of slip surfaces, inhomogeneous, and the variation of environmental factors (e.g., water content). The tests results are also influenced by the factors such as sampling method, sample preparation, test method, and test procedure.

Hoek (1990) discussed the difficulties in determining shear strength of rock masses by field or laboratory tests and concluded that the usefulness of the information obtained from these tests in the decision making for parameters would be very limited. Engineers should turn to other means such as establishing empirical criteria, comparing the geotechnical properties of the materials under consideration with those of the similar works whose parameters have been well understood. Among all these approaches, back analysis is an important way to help engineers in determining the deformation and shear strength parameters.

For a large project, some small slope failures would always have been encountered during the construction of roads, excavation of tunnel portals and pits at the borrow areas, etc. Such slope failure itself presents a case for back analysis. Lessons learned from the back analysis of these failures are valuable in assessing the material strength. In fact, reevaluating a small landslide happened during construction is similar to a large-scale direct shear test performed on the same ground materials.

For inactive ancient landslide, the back analysis may be based on the judgment of stability degree and the formulation of the equilibrium equations for the typical section. The solution of these equations provides c and/or ϕ . According to the engineering experiences, when a landslide is in creep compression stage, constant slip stage, and accelerate slip stage, the stability coefficient may be estimated as 1.01–1.10, 1.0, and 0.95–0.98, respectively.

During the construction of a hydraulic project, particularly in the process of the excavation for dam foundation, cut slopes, and tunnels, new geologic features could be revealed, and a lot of monitoring data concerning the stress and displacement in soils and rock masses will provide engineers the messages related to the real state of the structure dominated by the deformation and strength parameters. Using these data coming from the monitoring instruments, both the parameters and the structure designing could be justified and revised by the back analysis, if necessary. One of successful approaches for back analysis of this mission can be established by the FEM combined with the optimum methods, with the help of investigation instruments and the understanding of the construction procedure, as well as the engineering experience (Chen et al. 2001).

3.3 Soil

Soils are aggregates of uncemented or weakly cemented accumulation of mineral particles produced by the weathering of rocks (Acker 1974). They form three-phase systems together with air and/or water in the void spaces (pores) between the particles. Weak cementation can be due to carbonates or oxides precipitated between the particles or due to organic matter. If the products of weathering remain at their original location, they constitute a residual soil. If the products are

transported and deposited in a different location, they constitute a transported soil. The agents of transportation are gravity, wind, water, and glaciers. During transportation, the size and shape of particles can undergo changes and the particles can be sorted into size ranges.

Most natural soils have a density ranged in $1\text{--}2\text{ g/cm}^3$. A large portion of the earth's surface is covered by soils, and they are widely used as construction and foundation materials. Soil mechanics is the branch of engineering sciences that deals with the engineering properties of soils and their behavior under stress. Little of the soil on the Earth is older than the Pleistocene and none is older than the Cenozoic, although fossilized soils are preserved from as far as the Archean.

Soil can exist as a naturally occurring material in its undisturbed state, or as a compacted material for engineering structures and/or foundations. Like other construction materials, soil possesses mechanical properties related to compressibility (deformation), strength, and permeability. For the safe design of hydraulic structures (e.g., embankment dams), it is important to quantify these properties to predict how soils will behave under field actions. Quantification of the mechanical properties of soils is performed using standardized laboratory tests as well as in situ tests. Initially, a dam designer has at his disposal the characteristics of soil materials under natural condition: type of ground material in quarries, their granulometric composition, texture, moisture content at yield and rolling points, permeability coefficient and their density, etc. (Craig 2004; Terzaghi et al. 1996).

3.3.1 Particle Size and Composition

Particle size in soils can vary from over 100 mm to smaller than 0.001 mm. The particle-size analysis of a soil sample involves determining the percentage by mass of particles within the different size ranges. The particle-size distribution of a coarse soil can be determined by the method of sieving—the soil sample is passed through a series of standard test sieves having successively smaller mesh sizes. The mass of soil retained in each sieve is determined, and the cumulative percentage by mass passing each sieve is calculated. If fine particles appear in the soil, the sample should be treated with a deflocculating agent and washed through the sieves. The particle-size distribution of soil is presented as a curve on a semilogarithmic plot as shown in Fig. 3.4, in which the ordinate being the percentage by mass of particles smaller than the size given by the abscissa.

The flatter of the distribution curve, the larger range of the particle sizes in the soil will be; whereas the steeper of the curve, the smaller of the size range will be. A coarse soil is described as well graded if there is no excess of particles in any size range and if no intermediate sizes are lacking. In general, a well-graded soil is represented by a smooth, concave distribution curve (e.g., the curve 1 in Fig. 3.4). A coarse soil is described as poorly graded if a high proportion of the particles have

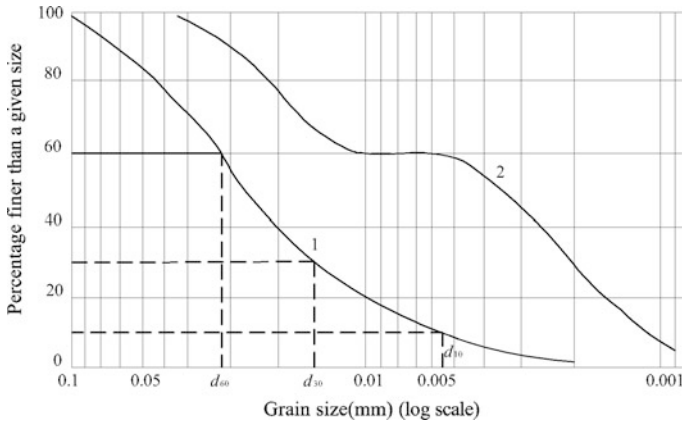


Fig. 3.4 Grain-size distribution of soil

sizes within narrow limits (a uniform soil) or if particles of both large and small sizes are present but with a relatively low proportion of particles of intermediate size, i.e., it might have a combination of two or more well-graded soil fractions; this type of soil is also referred to as a gap-graded soil or step-graded soil (e.g., the curve 2 in Fig. 3.4).

The most important indices used in the soil material design for embankment dams are briefly illustrated as follows.

1. Inhomogeneity (uniformity) coefficient and coefficient of gradation

The inhomogeneity coefficient has high significance for loose soils and is defined as

$$C_u = d_{60}/d_{10} \tag{3.8}$$

where d_{60} and d_{10} = grain sizes showing that there are by weight 60 and 10 % particles of smaller size in the soil, mm.

The coefficient of gradation C_c is defined as

$$C_c = \frac{(d_{30})^2}{d_{10}d_{60}} \tag{3.9}$$

where d_{30} = diameter through which 30 % of the total soil mass is passing, mm.

Generally, a soil is referred to as well graded if C_u is larger than about 4–6 and C_c is between 1 and 3. It is customary to consider that if $C_u \leq 3$, the soil is practically homogeneous. When most of the particles in soil mass are of approximately the same size, i.e., C_u is close to 1, the soil is called poorly graded.

2. Mean-weighted size of particle

For large-grained soils, often used is the concept of mean-weighted size of particles

$$d_{w,m} = \frac{\sum_1^n d_i \Delta p_i}{100} \quad (3.10)$$

where Δp_i = content of fraction of size d_i , %.

Often, $d_{w,m} \approx d_{50}$.

3. Shape of soil grain

The shape of soil grain has effect on various soil properties. In small-grained soils, the shape affects the density and the interaction of minerals with water, and in large-grained soils, it affects the porosity and strength. Quantitatively, shape is determined only for large-grained soils. If $d_3 < d_2 < d_1$, then

$$K_{\text{shape}} = d_3/d_1 \quad (3.11)$$

where d_3 = minimum characteristic grain size, mm; d_1 = maximum characteristic grain size, mm.

With $K_{\text{shape}} = 1$, the shapes are almost spherical or cubic. Soils with $K_{\text{shape}} > 0.3$ are preferred for use in dams.

4. Porosity

Porosity is the ratio of the volume of voids to the total volume of the soil.

$$n = \frac{V_v}{V} \times 100 \% \quad (3.12)$$

where V_v = volume of voids and V = total volume of soil.

The use is often made of the void ratio (e), which is the volume of voids to the volume of solid particles (skeleton), in a unit volume:

$$e = \frac{V_v}{V_s} = \frac{n}{1 - n} \quad (3.13)$$

where V_s = volume of solid particles (skeleton).

If $e \leq 0.5$, the soil is considered to be sufficiently dense, whereas if $e \geq 1$, the soil is loose.

5. Water content

The water content is the ratio of the mass of water to the mass of solid particles (skeleton), in a unit volume:

$$w = \frac{m_w}{m_s} \times 100 \% \quad (3.14)$$

where m_w = mass of water and m_s = mass of solid particles (skeleton)

6. Degree of saturation

The degree of saturation (S_r) is the ratio of the volume of water to the volume of voids, which determines the degree of filling the soil pores with water:

$$S_r = \frac{V_w}{V_v} \times 100 \% \quad (3.15)$$

where V_w = volume of water in voids.

7. Dry bulk density

The dry bulk density (ρ) of soil is the ratio of the mass of solid particles (skeleton) m_s to the total volume V , that is,

$$\rho_d = \frac{m_s}{V} \quad (3.16)$$

Correspondingly, the dry unit weight γ_d is defined as the ratio of the weight of solid particles W_s to the total volume V :

$$\gamma_d = \frac{W_s}{V} \quad (3.17)$$

8. Density index

For sandy and large-grained soils, use is made of the coefficient of density index (D_r), or “relative density” expressing the relationship between the void ratio (e), and the limiting values e_{\max} and e_{\min} . This is due to the fact that as an absolute value, the porosity does not always characterize the density of sandy soils.

$$D_r = \frac{e_{\max} - e}{e_{\max} - e_{\min}} \quad (3.18)$$

where e_{\max} and e_{\min} = coefficients of porosity (void ratios) of extremely loose and dense soils, respectively; e = actual value of porosity coefficient.

9. Threshold moisture of consistency conversion from one form into another

It is known as the consistency limit or Atterberg limit. The upper and lower limits of the range of water content over which the soil exhibits plastic behavior are defined as the liquid limit (w_L) and the plastic limit (w_p), respectively. The difference between w_L and w_p is known as plasticity number (I_p), which helps identify clay material in addition to its granulometric composition:

$$I_p = w_L - w_p \quad (3.19)$$

3.3.2 Soil Classification and General Characteristics

Soil classification is a scheme for the arrangement of soils into various broad groups or subgroups to provide a common language expressing briefly the general usage characteristics without detailed descriptions, each with broadly similar behavior (Casagrande 1948). There are various classification schemes for different purposes: agricultural classification based on how soils support crops, geological classification based on the age of the deposit or the nature of the grains, etc. For hydraulic engineers, the civil engineering classification stipulated in the GB/T50145-2007 “Standard for engineering classification of soil,” which is based on the mechanical properties using simple indices (e.g., grain-size distribution, liquid limit, and plasticity index of soil), is mainly observed.

From the standpoint of hydraulic structures, it is the first thing to distinguish soils depending on the grain size (Grishin 1982): boulder, diameter of particles exceeding 20 cm; cobblestone and round crushed stone, diameter of particles 20–10 cm; large pebble, diameter of particles 10–6 cm; gravel, diameter of particles 40–2 mm; sand, diameter of particles 2–0.05 mm; dust, diameter of particles 0.05–0.005 mm; and clay, diameter of particles smaller than 0.005 mm. In a narrow definition, soils are usually determined by the relative proportion of the three typical kinds of soil particles, called soil “separates”: sand, silt, and clay. Sand and silt are the products of physical and chemical weathering; clay, on the other hand, is a product of chemical weathering but often formed as a secondary mineral precipitated from dissolved minerals.

Clays are well known for their plasticity which depends on the amount of clay fractions ($d < 0.005$ mm) present in soil, on the moisture, and on the properties of minerals constituting these fractions. The clayey soils as foundation materials are characterized by the following general properties inherent to them: The degree of compatibility under load depends on the moisture content; with the increase in moisture content their strength decrease; they swell with the increase in moisture content and shrink when dry; their permeability coefficient is very small; and they have tensile strength due to molecular cohesion between particles of very small diameter. Loess and loess-like soils are characterized by the fact that they, when wetted, settle significantly. Therefore, for the construction of barrages and sluices on loess and loess-like soils, it is necessary that the soil are pre-moistened, and the structure is so designed to adapt the possible large settlements, distortions, etc. Silty soils settle even more (e.g., up to 20 cm/m) and, therefore, their load-resistance capacity is poor.

Non-cohesive soils differ in their properties depending on their formation conditions. Fine top and clay (argillaceous) sands or the so-called quick sands contain 80–96 % fractions of size from 0.25 to 0.05 mm. Fine unconsolidated (loose) sands can have porosity up to 42–50 %. Such sands under vibratory actions can exhibit large subsidence and come into a liquefaction state.

3.3.3 Density of Soil

Soil density, particularly bulk density, is a governing index in the soil compaction operation.

Particle density is equal to the mass divided by the volume of the solid particles, i.e., it excludes pore space and organic material. Soil particle density is typically 2.60–2.75 g/cm³ and is usually unchanging for a given soil. Soil dry bulk density is equal to the dry mass divided by the volume of the soil, i.e., it includes air space and organic materials of the soil volume. A high bulk density is indicative of either good soil compaction or high sand content. Soil dry bulk density is highly variable for a given soil. For example, the bulk density of loam for cultivation is about 1.1–1.4 g/cm³.

Pore space is that part of the open bulk volume not occupied by either mineral or organic matter but occupied by either air or water. There are four categories of pores: Very fine pores <2 μm, fine pores = 2–20 μm, medium pores = 20–200 μm, and coarse pores = 200–0.2 mm

The commonly designed dry density of compacted soils in embankments is ranged from 1.60 (optimal water content $w_{op} = 19\text{--}20\%$) g/cm³ to 1.85 ($w_{op} < 13\%$) g/cm³ for clayey cohesive soils, from 1.95 to 2.35 g/cm³ for non-cohesive soils (e.g., sand gravel, sand, and cobble), and from 1.85 to 2.28 g/cm³ for rockfills (tuff, phyllite).

3.3.4 Permeability of Soil

The coefficient of permeability for coarse soils can be determined by means of the constant-head permeability test. The soil specimen is contained in a Perspex cylinder and rests on a coarse filter or a wire mesh. A steady vertical flow of water, under a constant total head, is maintained through the soil, and the volume of water flowing per unit time may be recorded. For fine soils, the falling-head test can be employed.

The permeability coefficient of soils depends primarily on the average size of the pores, which in turn is related to the distribution of particle sizes, particle shape, and soil structure. There are various formulae for the estimation of the permeability coefficient for soils. For sands, Hazen (1911) showed that the approximate value of k may be given by

$$k = cd_{10}^2 \text{ (cm/s)} \quad (3.20)$$

where d_{10} = effective size in mm, through which 10 % of the total soil mass is passing; c = constant that varies from 1.0 to 1.5.

For coarse-grained soils such as sands and some silts, Kozeny–Carman’s equation gives a good description of the permeability coefficient (Carman 1956; Kozeny 1927)

$$k = \frac{1}{C_s S_s^2 T^2} \frac{\gamma_w}{\mu} \frac{e^3}{1+e} \quad (3.21)$$

where μ = absolute coefficient of viscosity; γ_w = unit weight of water; C_s = shape factor, for granular soils the shape factor is approximately 2.5; S_s = surface area per unit volume of soil solids; e = void ratio; and T = tortuosity, for granular soils T is about $\sqrt{2}$.

For clayey soils, Olsen developed a model to account for the variation of permeability due to unequal pore sizes to explain the variation of the coefficient of permeability with void ratio.

According to various tests results, the permeability coefficients encountered in the applications to embankments are as follows: 1 cm/s for clean gravels, 10^{-2} – 10^{-5} cm/s for sandy soil, and 10^{-8} cm/s for unfissured clays and clay–silts (>20 % clay).

3.3.5 Deformation and Strength of Soil

The coefficient of internal friction of clays is small, e.g., 0.35–0.3 or lower. The extensive use is made of sands having porosity 35–40 % and angle of friction 30° – 35° . Fine top and clay (argillaceous) sands or the so-called quick sands can yield a small angle of repose (3° – 7°) at a moisture content of 13–14 %, which decreases down to 0° at a moisture content of 17–18 %, and have small load-resisting capacity.

One of the basic deformation parameters is the modulus of compression obtained by the confined compression test and defined as

$$E_s = \frac{1}{m_v} = \frac{1+e_1}{a_v} \quad (3.22)$$

where e_1 = initial void ratio; a_v = compression factor, MPa^{-1} ; and m_v = coefficient of volume compressibility, MPa^{-1} .

Within the applied pressure range $p = 100$ – 200 kPa, it may be roughly classified as follows: $E_s < 4$ MPa, high compressibility; $15 \text{ MPa} \geq E_s \geq 4$ MPa, medium compressibility; and $E_s > 15$ MPa, low compressibility.

The deformation modulus (secant) E has a theoretical relationship with E_s as

$$E = \left(1 - \frac{2\mu^2}{1 - \mu}\right) E_s \tag{3.23}$$

The Poisson’s ratio μ for soils is in the range of 0.15 (gravelly soil) \sim 0.25 (hard clay) \sim 0.35 (plastic clay).

The constant modulus presented heretofore is sufficient for the purposes of conventional design of embankment dams and foundations. However, in high embankment dams where numerical methods (e.g., FEM) are exercised for detailed analysis concerning their deformation and stress, more advanced models are demanded to take into account of the nonlinearity in the modulus. Nearly over 40 years, the most popular nonlinear elastic constitutive model is the hyperbola model formulated by Duncan and Chang (1970). The so-called Duncan–Chang model postulates a hyperbolic stress–strain relation Eq. (3.24) obtained from triaxial tests (Fig. 3.5a, b).

$$(\sigma_1 - \sigma_3) = \varepsilon_a / (a + b\varepsilon_a) \tag{3.24}$$

where a and b = constants. b is the reciprocity of the initial modulus of elasticity, while the meaning of the parameter $1/a$ is asymptotical value of the difference between principal normal stresses.

The deduction gives the expression of tangent modulus E_t as

$$E_t = [1 - R_f(1 - \sin \varphi)(\sigma_1 - \sigma_3) / (2c \cos \varphi + 2\sigma_3 \sin \varphi)]^2 E_i \tag{3.25}$$

$$E_i = K p_a (\sigma_3 / p_a)^n \tag{3.26}$$

where R_f = failure ratio; E_i = initial modulus; p_a = atmospheric pressure used to eliminate unit system selecting effect, kN/m^2 ; K and n = modulus number and modulus exponent, and they are dimensionless material parameters.

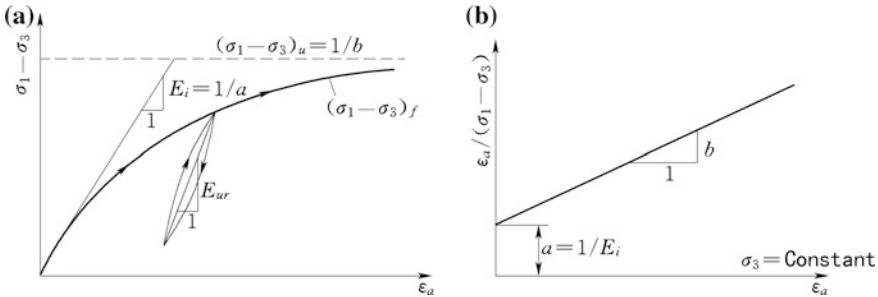


Fig. 3.5 Hyperbola curve of stress and strain. **a** $(\sigma_1 - \sigma_3) \sim \varepsilon_a$ relation; **b** $\varepsilon_a / (\sigma_1 - \sigma_3) \sim \varepsilon_a$ relation

where the soil undergoes unloading/reloading, the tangent modulus is defined as

$$E_{ur} = K_{ur} p_a (\sigma_3 / p_a)^{n'} \quad (3.27)$$

where K_{ur} and n' = unloading–reloading modulus number and modulus exponent.

It is customarily assumed that $K_{ur} = 2K$ and that n' is identical to n .

The initial Poisson's ratio and the tangent Poisson's ratio can be expressed as follows:

$$\begin{cases} \mu_i = G - F \log \left(\frac{\sigma_3}{p_a} \right) \\ \mu_t = \frac{\mu_i}{(1-A)^2} \\ A = \frac{D(\sigma_1 - \sigma_3)}{K p_a \left(\frac{\sigma_3}{p_a} \right)^n \left[1 - \frac{R_f(1 - \sin \varphi)(\sigma_1 - \sigma_3)}{2(c \cos \varphi + \sigma_3 \sin \varphi)} \right]} \end{cases} \quad (3.28)$$

where D , F , and G = material parameters.

Parameters (φ , c , R_f , K , n , D , F , and G) are generally specified for a definite soil using triaxial tests. Attention should be drawn to the fact that, while in a standard triaxial compression test, the confining pressure is always greater than zero, whereas it may be equal to or even less than zero in general finite element analyses. To obtain a numerically stable in the analysis, a set of initial elastic modulus is required for this case.

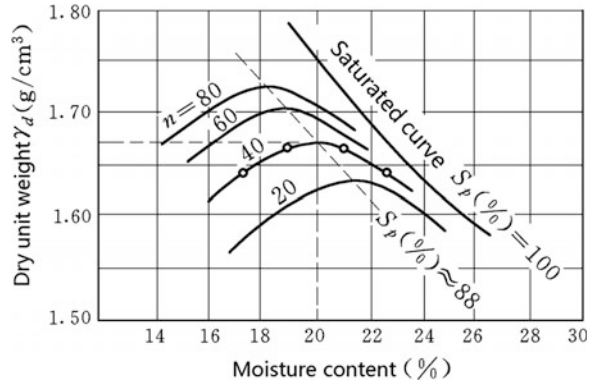
The Duncan–Chang model is successful in analyzing many practical problems and is simple to set up with standard triaxial compression tests. When triaxial test data are not accessible, empirical parameters are also abundantly available in literatures. However, it should be aware of its basic limitations in the application of this model:

- The intermediate principal stress σ_2 is not taken into account;
- Results may be unreliable when extensive failure occurs;
- It does not consider the volume changes due to the changes in shear stress (shear dilatancy);
- Input parameters are not fundamental soil properties, but only empirical values under limited conditions; and
- The model is mainly intended for quasi-static analysis.

3.3.6 Compaction Characteristics of Soil

When a soil is compacted with a constant energy, by adding water step by step, the dry density of the soil increases first attributable to the lubrication effect of water allowing for particle movement. The dry density of soil decreases, however, as the water content is beyond a certain limit because more part of the void in the soil is filled with water which interferes filling of soil particles. Compaction curve is

Fig. 3.6 Compaction curves of cohesive soil



therefore formed like a mountain where the peak point is defined by the maximum dry weight γ_d and the optimum water content w_{op} , as presented in Fig. 3.6.

It is well known that the compressibility of fill materials is gradually reduced as compaction dry density increases. It is also generally known that soils compacted in unsaturated states, especially in the dry side of optimum water content, have a certain skeleton strength composed of suction effect between soil particles. This skeleton strength readily disappears by wetting (saturation) during the first filling of the reservoir, which results in significant settlement (collapse) in the upstream dam shell (Naylor et al. 1986, 1989). Compressibility due to wetting collapse can be easily evaluated by conducting compression tests on saturated samples compacted in the same dry density.

Characteristics of shear strength of compacted soils are almost identical to those of compressibility mentioned above. Strength of compacted soils generally shows a peak on the dry side of the optimum water content. Severe strength reduction, however, is anticipated on the dry side when the fill is submerged, so that dry side compaction should be avoided especially in the upstream fill.

The permeability of compacted soils, on the other hand, has a minimum peak on the wet side of the optimum.

3.4 Concrete

Being the most widely used construction material in hydraulic structures, concrete is a composite material that consists essentially of a binding medium within which are embedded particles or fragments of aggregate. The binder is formed from a mixture of hydraulic cement, flying ash, water, and several kinds of admixtures (ICOLD 2009; Mehta and Monteiro 2006).

Aggregates are the granular materials, such as sand, gravel, or construction, and demolition waste that are used with a cementing medium to produce either concrete or mortar.

Cement is a finely pulverized, dry material which may develop the binding effect as a result of hydration. Cement is called hydraulic when the hydration products are stable in an aqueous environment. The most commonly used hydraulic cement is the Portland cement consisting essentially of reactive calcium silicates which forms the calcium silicate hydrates (C-S-H) primarily responsible for its adhesive characteristics and is stable in aqueous environment.

Apart from aggregates, cement, and water, admixtures are commonly added to the concrete batch immediately before or during mixing. The use of the admixtures in concrete may give rise to a variety of benefits such as to modify the setting and hardening characteristics of the cement paste by chemically influencing the rate of cement hydration, to plasticize fresh concrete mixtures by water-reducing admixtures cutting the surface tension of water, to improve the durability of concrete exposed to cold weather by air-entraining admixtures, and to reduce thermal cracking in mass concrete by mineral admixtures such as pozzolans.

Mortar is a mixture of sand, cement, and water, which is like concrete but without coarse aggregates. Grout is a mixture of cementitious material and fine aggregate, to which sufficient water is added to produce a pouring consistency without segregation of the constituents. Shotcrete is a mortar or concrete that is pneumatically transported through a hose and projected onto a rock surface at high velocity for the purposes of protection and reinforcement.

Concrete has a number of valuable properties: It permits large-scale mechanization of jobs to be performed at highest rates and allows the construction of structures of a variety of shapes and sizes; it has the required strength increasing with time and excellent resistance to water; it has much less requirement on maintenance; and in most codes of practice, the allowable concrete stresses are limited to about 50 % of the ultimate strength, and thus the fatigue strength of concrete is generally not a dominant problem.

Based on unit weight, concrete can be classified into three broad categories: Concrete containing natural sand and gravel or crushed-rock aggregates, generally weighing about 2400 kg/m^3 , is called normal-weight concrete, and it is the most prevalent for hydraulic structures. The term lightweight concrete is used for concrete that weighs less than about 1800 kg/m^3 . Heavyweight concrete, generally used for radiation shielding, is a concrete produced from high-density aggregates and weighs more than 3200 kg/m^3 . The normal-weight concrete in hydraulic structures is subjected to different physicochemical and mechanical actions of either fresh or sea water. Such concrete is called hydraulic concrete which must possess the following properties to ensure stability and long service life of structures: high strength, high density, low permeability, and high water resistance (i.e., corrosion resistance); high abrasion resistance and cavitation resistance; high crack resistance; and good workability.

The property of the place-ability (flow-ability) depends on the composition and water-cement ratio (W/C) of concrete. The so-called settlement (slump) of a standard cone made from a concrete mix serves as an index of flow-ability: The larger settlement of the concrete mix cone after removing the form, the greater flow-ability and place-ability of concrete placed in forms or sections. Use is made of

different types of concrete mixes: dry and low-slump concrete mixes (slump 1–2 cm) demand compaction in sections by vibration for obtaining required strength and are used in massive frames and structures; moderate-slump (slump 2–4 cm) concrete mixes find application in reinforced massive frames; in reinforced concrete structures with up to 1 % reinforcement ratio, consistent concrete mixes of 5–8 cm slump may be required; and 8–12 cm slumps are permitted for even larger proportions of reinforcement.

Concrete mixes of different compositions are used depending on the requirements for concrete, demanded by operating conditions of structures or their elements. Rational selection of composition of concrete consists in obtaining good quality concrete at minimum cost, that is, obtaining long-life and economical concrete. In this respect, the specific consumption of cement for one cubic meter is a key index: It should be possibly minimum for the given concrete grade and for reducing liberation of heat in concrete and the danger of cracking.

Different zones of the concrete dam or of any concrete hydraulic structures operate under different states of stress/seepage/temperature conditions. Therefore, for the purposes of achieving maximum correspondence of concrete grades to the operating conditions and of obtaining maximum economy, the so-called concrete grade zoning is customarily exercised in massive concrete structures.

3.4.1 Deformation and Strength of Concrete

The significance of the elastic limit (strength) in structural design lies in the fact that it represents the maximum allowable stress before the material undergoes permanent deformation. The strength of concrete depends on its proportions related to the grade and amount of cement, the characteristics of stone aggregate, and the amount of added water (i.e., W/C). It also depends on the age of concrete and curing conditions (temperature and moisture). It is useful to divide concrete into three general categories based on uniaxial compressive strength: low-strength concrete, whose compressive strength is lower than 20 MPa; moderate-strength concrete, whose compressive strength is ranged from 20 to 40 MPa; and high-strength concrete, whose compressive strength is higher than 40 MPa. Moderate-strength concrete, also referred to as ordinary or normal concrete, is employed for most hydraulic works.

Exclusive of USA, strength grading of cement and concrete is exercised in China, Europe, and many other countries characterized by the grade for compressive and tensile strengths expressed in MPa. The concrete grade is determined by the uniaxial compression strength of standard cubes (15 × 15 × 15 cm) or by the tensile (rupture) strength. The samples are tested at the age of 28 days in China.

The standards of China (Ministry of Water Resources of the People's Republic of China 2008a, b; Ministry of Housing and Urban-Rural Development of the People's Republic of China 2010) provide for the following grades and corresponding design parameters (Young's modulus, tensile, and compressive strength)

of concrete based on compressive strength in a series of C_{15} , C_{20} , C_{25} , C_{30} , C_{35} , C_{40} , C_{45} , C_{50} , C_{55} , C_{60} .

In addition to strength, the engineer must know the elastic modulus (Young's modulus) E of the material because it significantly influences the rigidity of a hydraulic works. For a material subjected to uniaxial load, the ratio of the lateral strain to axial strain within the elastic range is called the Poisson's ratio and denoted as μ . Poisson's ratio is required for structural analysis of tunnels, arch dams, and other statically indeterminate structures. Although there appears to be no consistent relationship between the Poisson's ratio and the other concrete characteristics such as W/C , curing age, and aggregate gradation, the Poisson's ratio is generally lower in high-strength concrete and higher for saturated concrete and for dynamically loaded concrete. The elastic modulus and Poisson's ratio of concrete are evaluated by experiments for a specific project. In the initial phase of design, the standards of China suggest reference values in relation to the concrete grade. The elastic modulus E of concrete in compression varies from 14 to 40 GPa; for ordinary concrete, the modulus E may be commonly assumed as 20 GPa. The values of Poisson's ratio for concrete generally vary between 0.15 and 0.20, and for ordinary concrete, it may be assumed as 0.167.

3.4.2 Density of Concrete

Concrete density is mainly dependent on the density and grain composition of aggregate, as well as the compaction of the mix. Most natural mineral aggregates, such as sand and gravel, have a bulk density of 1520–1680 kg/m³ and produce normal-weight concrete with approximately 2400 kg/m³, which is subjected to slight variation within a range of 1.5 % following the concrete grade with a same aggregate: It is generally high for high-grade concrete. This variation should be carefully studied, particularly for gravity dam, since the dam body size and corresponding expenditures will be significantly influenced by the concrete density.

3.4.3 Permeability of Concrete

The permeability of concrete depends not only on mix proportion, compaction, and curing, but also on micro- or meso-cracks caused by the ambient temperature and humidity cycles. The permeability coefficients of concrete, which are strongly related to its density, usually vary between 10^{-5} and 10^{-9} cm/s.

Professional judgment in the design of concretes should take into consideration not only the strength, deformation, and permeability, but also its durability, which has serious implications for the life cycle of a structure. Durability of concrete is defined as its service life under given environmental conditions. Generally, watertight concrete endures for a long time. The excellent conditions of the

2000-year-old concrete linings of several aqueducts in Europe built by the Romans are a living testimony to the long-term durability of concrete in moist environments. In general, there is a relationship between strength and durability since low strength is associated with high porosity and high permeability. Permeable concretes are, of course, less durable.

3.4.4 Thermal and Its Related Characteristics of Concrete

1. Thermal characteristics

The temperature rise in a concrete structure due to the hydration process and thermal flow causes temperature variations which in turn produce thermal strain/stress because of the restraint conditions present in the structure. The most adverse effect of the thermal stress is the cracking in the surface lift. On the thin placed concrete lift, the surface temperature is usually controlled by the atmosphere. When the initial temperature of the concrete is higher than the atmosphere temperature, and the surface is not protected, the temperature jump (nonlinear gradient) across the lift joint between old and new concrete could be over 10 °C in the daytime with full sun. While in the night and rainy day, it could be only 2 °C. If the time of placing interval between two lifts is longer, the temperature jump would be even much larger, which will lead to the early age cracking in young concrete. Cracking may also emerge if the mean temperature rising is varied considerably in the different parts of a casted structure. In both cases of early age cracking referred to above, the thermal movement due to hydration is the key clue.

The thermal movement in concrete is governed by a differential equation restrained by initial and boundary conditions (Carslaw and Jaeger 1985), as will be presented in the Chap. 4 of this book [Eqs. (4.19)–(4.21)]. The basic parameters such as the thermal diffusivity α , the thermal conductivity λ dominating the heat flux transmitted through a unit area of a material under a unit temperature gradient, the density ρ , and the specific heat c defined as the quantity of heat needed to raise the temperature of a unit mass of a material by one degree are all dependent on the corresponding parameters of water, cement, and aggregate.

It is conventionally to estimate the thermal diffusivity α using the percentage proportion of concrete and the parameters in Table 3.6 according to

$$\alpha = \frac{\lambda}{c\rho} \quad (3.29)$$

For important projects, all the thermal parameters should be studied by the laboratory tests. In Table 3.7, the thermal parameters of several China's dam projects may be referred to in the initial phases of design.

Table 3.6 Thermal parameters of concrete components for the calculation of concrete thermal diffusivity

Material	Density ρ (kg/m ³)	Thermal conductivity λ [kJ/(m.h. °C)]				Specific heat c [kJ/(kg. °C)]			
		21 °C	32 °C	43 °C	54 °C	21 °C	32 °C	43 °C	54 °C
Water	1000	2.1604	2.1604	2.1604	2.1604	4.1868	4.1868	4.1868	4.1868
Cement	3100	4.4464	4.5929	4.7353	4.8651	0.4564	0.5359	0.6615	0.8248
Quartz sand	2660	11.1285	11.0992	11.0532	11.0364	0.6992	0.7453	0.7955	0.8667
Basalt	2660	6.8915	6.8705	6.85580	6.8370	0.7662	0.7578	0.7829	0.8374
Dolostone	2660	15.5330	15.2609	15.0139	14.3356	0.8039	0.8206	0.8541	0.8876
Granite	2680	10.5047	10.4670	10.4419	10.3791	0.7159	0.7076	0.7327	0.7746
Limestone	2670	14.5282	14.1933	13.9169	13.6573	0.7494	0.7578	0.7829	0.8206
Quartz	2660	16.9105	16.7765	16.6383	16.4751	0.6908	0.7243	0.7578	0.7913
Rhyolite	2660	6.7701	6.8119	6.8622	6.8873	0.7662	0.7746	0.7997	0.8081

Table 3.7 Thermal parameters of several China's dam projects

Project		λ [kJ/(m h °C)]	c (kJ/(kg °C))	ρ (kg/m ³)	a (m ² /h)	Remark
Liujiaxia		10.3410	0.8792	2450	0.00480	–
Sanmenxia		10.1740	1.0760	2450	0.00385	–
Xin'anjiang		11.9324	1.0509	2465	0.00460	–
Gutian		8.3736	1.0048	2450	0.00440	–
Xiaowan		8.4790	1.0470	2500	0.003239	–
Longtan	CVC/RCC	8.7760/9.2700	0.9672/ 0.9672	2450/ 2400	0.003704/ 0.003941	Fine aggregate
Guangzhao	CVC/RCC	8.3850/8.2210	0.9700/ 0.9520	2450/ 2459	0.003600/ 0.003600	Fine aggregate
Three Gorges		10.4670	0.9590	2500	0.003471	–

There is another important parameter β , which is termed as surface exothermic coefficient concerning the concrete/air contact face, which is listed in Table 3.8. It may be found that there is a tight relation with wind speed.

Hydration heat of cement is the propulsion to “warm up” concrete, which may be represented by two kinds of formula:

- Exponent

$$Q(\tau) = Q_0(1 - e^{-m\tau}) \quad (3.30)$$

where $Q(\tau)$ = accumulated hydration heat at age of τ (kJ/kg); Q_0 = total hydration heat; τ = concrete age; and m = constant related to cement and curing temperature.

Table 3.8 Surface exothermic coefficient concerning the concrete/air contact face

Wind speed (m/s)	β [kJ/(m ² h °C)]		Wind speed (m/s)	β (kJ/m ² h °C)	
	Smooth surface	Rough surface		Smooth surface	Rough surface
0.0	18.4638	21.0596	5.0	90.1418	96.7151
0.5	28.6796	31.3591	6.0	103.2465	110.9921
1.0	35.7553	38.6442	7.0	116.0581	124.8922
2.0	49.4042	53.0049	8.0	128.5766	138.4575
3.0	63.0951	67.5750	9.0	140.7602	151.7296
4.0	76.7022	82.2288	10.0	152.6926	165.1274

- Hyperbolic

$$Q(\tau) = \frac{Q_0\tau}{n + \tau} \quad (3.31)$$

where $n = \text{constant}$.

Hydration heat of cement should be tested for a specific project. For moderate-heat Portland cement, the hydration usually does not exceed 210 kJ/kg after three days of hardening and 252 kJ/kg after seven days.

The thermal regime analysis often employs adiabatic temperature rise θ of concrete instead of the hydration heat Q of cement. θ may be obtained either by direct or indirect methods.

For an important project, direct method using thermal rising test facilities on concrete samples is required, and the following formula may be fitted using testing data:

- Exponent

$$\theta(\tau) = \theta_0(1 - e^{-\alpha\tau^\beta}) \quad (3.32)$$

- Hyperbolic

$$\theta(\tau) = \theta_0\tau^\alpha/(\beta + \tau^\alpha) \quad (3.33)$$

More complicated models (e.g., the maturity model) may also be established and employed (Roy et al. 1994).

In short of tested data, indirect method may be employed based on the hydration heat and amount of cement and mixtures, as well as the specific heat and density of them:

$$\theta(\tau) = \frac{Q(\tau)(W + kF)}{c\rho} \quad (3.34)$$

where W = amount cement, kg/m^3 ; c = specific heat of concrete, $\text{kJ}/(\text{kg } ^\circ\text{C})$; ρ = density of concrete, kg/m^3 ; F = amount of mixture, kg/m^3 ; $Q(\tau)$ = hydration heat of cement, kJ/kg ; and k = fraction coefficient, for fly ash $k = 0.25$.

2. Thermal strain/stress characteristics

Under the thermal action, the thermal strain is mainly governed by the coefficient of thermal expansion α , which is defined as the change in unit length per degree of temperature change. Since the thermal shrinkage strain of concrete is controlled by the coefficient of linear thermal expansion of the aggregate which is the primary constituent of concrete, selecting an aggregate with a low coefficient of thermal expansion (e.g., limestone), when it is economically feasible and technologically acceptable, may become a critical factor for cracking prevention in mass concrete. The coefficient of thermal expansion of commonly used rocks and minerals varies from about 5×10^{-6} per $^\circ\text{C}$ (limestones and gabbros) to 12×10^{-6} per $^\circ\text{C}$ (sandstones, natural gravels, and quartzite). The reported values of the coefficient of linear thermal expansion for concrete mixtures with different aggregate types are approximately ranged from 6 to 12×10^{-6} per $^\circ\text{C}$. The coefficient of thermal expansion can be estimated from the weighted average of the components, assuming 70–80 % aggregate content in the concrete mixture.

Primary factors affecting thermal stress for young concrete, apart from degree of restraint and temperature change, are the growth of the Young's modulus $E(\tau)$ with the ongoing of time, which has a basic type of exponent function

$$E(\tau) = E_o(1 - e^{-a\tau}) \quad (3.35)$$

where τ = concrete age; E_o = final modulus when $\tau \rightarrow \infty$; a = constant.

In China, several improved forms, such as that proposed by Zhu (1985), are widely employed.

- Composite exponent

$$E(\tau) = E_o(1 - e^{-a\tau^b}) \quad (3.36)$$

- Hyperbolic

$$E(\tau) = \frac{E_o\tau}{q + \tau} \quad (3.37)$$

Table 3.9 Fitted constants of the Young's modulus expression

Concrete		Hyperbolic		composite exponent		
		E_0 (GPa)	q (d)	E_0 (GPa)	a	b
RCC	Yantan project C15	32.8	8.20	36.07	0.24	0.45
	Three Gorges project C15	35.6	28.00	35.00	0.061	0.70
	Three Gorges project C20	37.9	25.63	38.00	0.065	0.70
CVC	Yantan project C20	35.91	6.46	35.70	0.28	0.52
	Three Gorges project C20	34.25	8.59	34.25	0.24	0.50

The practices in China show that for CVC, composite exponent function has the high precision, whereas for RCC, the hyperbolic function could be better. Table 3.9 lists several fitted constants of the Young's modulus expression, whereas Tables 3.10 and 3.11 list several typical computation and test data of Young's modulus for CVC and RCC, respectively.

It is worthwhile to indicate that the curing temperature has significant effects on the Young's modulus, and various revision methods may be employed (Zhu 1996), if necessary.

Another important factor affecting thermal stress in young concrete is the creep or stress relaxation. They have actually the same mechanism emerged as two phenomena: the former gives rise to a gradual increase in strain with the ongoing of time under a given level of sustained stress, and the latter gives rise to a gradual decrease in stress with the ongoing of time under a given level of sustained strain. Both manifestations are typical of viscoelastic and/or viscoplastic properties of concrete materials, particularly in their young age. The mechanism and expression, as well as the computation, may be referred to the literatures and design handbooks (Bazant 1982; Bazant and Wu 1974; Mehta and Monteiro 2006; Neville et al. 1983; Troxell et al. 1958; Zhou and Dang 2011).

3.4.5 Durability of Concrete

1. Impermeability

Impermeability is a key parameter related to the durability of hydraulic concrete, which is interrelated tightly with the density and cracking resistance. The smaller of the pore size in concrete, the higher is its impermeability. To meet the impermeability requirement, the water–cement ratio W/C must not exceed 0.5–0.55, and care should be taken to avoid separation of concrete mix into layers during handling and placing it in the framework. In China, by impermeability, the concretes are divided into six grades as W_2 , W_4 , W_6 , W_8 , W_{10} , W_{12} . The number indicates the pressure of water (in atmospheres) against which standard samples of concrete can withstand without allowing the water to percolate through them at age of 28, 60 or

Table 3.10 Computation and test data of Young's modulus for RCC

Expression	Yantan project C15				Three Gorges project C15				Three Gorges project C20			
	Test (GPa)	Computation (GPa)	Error (%)		Test (GPa)	Computation (GPa)	Error (%)		Test (GPa)	Computation (GPa)	Error (%)	
Hyperbolic Eq. (3.37)	7d	15.09	15.10	0.06	6.76	7.12	5.32		7.69	8.13	5.72	
	28d	24.63	25.37	3.00	18.84	17.80	5.52		21.02	19.79	5.85	
	90d	30.06	30.06	0.00	28.82	27.15	5.79		29.51	29.50	0.03	
	180d	—	—	—	29.15	30.81	5.69		33.21	33.18	0.09	
Composite exponent Eq. (3.36)	7d	15.09	15.79	4.67	6.76	7.42	9.76		7.69	8.51	10.74	
	28d	24.63	23.76	3.53	18.84	16.33	13.32		21.02	18.55	11.75	
	90d	30.06	30.21	0.50	28.82	26.57	7.81		29.51	29.66	0.51	
	180d	—	—	—	29.15	31.53	8.16		33.21	34.76	4.66	

Table 3.11 Computation and test data of Young's modulus for CVC

Expression		Yantan project C20			Three Gorges project C20		
		Test (GPa)	Computation (GPa)	Error (%)	Test (GPa)	Computation (GPa)	Error (%)
Hyperbolic Eq. (3.37)	7d	19.00	18.67	-1.74	16.10	15.38	-4.47
	28d	28.75	29.18	1.46	24.20	26.21	8.31
	90d	33.50	33.50	0.00	30.80	31.20	1.49
	180d	–	–	–	–	–	–
Composite exponent Eq. (3.36)	7d	19.00	19.17	0.89	16.10	15.99	-0.08
	28d	28.75	28.37	-1.35	24.20	24.43	0.95
	90d	33.50	33.74	0.71	30.80	30.55	-0.81
	180d	–	–	–	–	–	–

90 days may also be applicable with regard to the initial exerting time of head gradients on the hydraulic structure face.

2. Frozen resistance

In cold climate areas, damage to concrete due to freezing and thawing (FT) cycles is one of the major aging problems requiring heavy expenditures for the repair and replacement. Frost damage in concrete can take several forms, and the most common is cracking and spalling of concrete caused by progressive expansion of the cement paste matrix attributable to repeated FT cycles. The ability of concrete to resist the deterioration due to frost action depends on the characteristics of both the cement paste and the aggregate, which is controlled actually by the interaction of several factors, such as the location of escape boundaries, the pore structure of the material (size, number, and continuity of pores), the degree of saturation, the rate of cooling, and the tensile strength of the material. The provision of escape boundaries in the cement paste matrix and modification of its pore structure are relatively easy to implement, the former can be realized by means of air entrainment in concrete, and the latter by the use of proper mix proportions and curing. In China, by frozen damage resistance, the concretes are divided into seven grades as F_{400} , F_{300} , F_{250} , F_{200} , F_{150} , F_{100} , F_{50} . The number indicates the FT cycles after which concrete samples at age of 28 days reduce strength by no excessive of 25 %, 60 or 90 days may also be applicable with respect to the onset time of FT cycle.

3. Abrasion and cavitation resistance

Abrasion of concrete can take place under the action of high-speed water flow carrying solid particles, such as sand, gravel, and pebble, in particular. When severe abrasion conditions exist, it is recommended that, in addition to the use of hard aggregates, the concrete should be proportioned to develop high compressive strength (e.g., at least C_{40}). It is also worthwhile to emphasize that particular care should be exercised to ensure, at least, that the concrete at the surface is of high quality. For example, at least 7 day of continuous moist curing after the finishing of

concrete, delay of the floating and troweling operations until the concrete has lost its surface bleed water, etc.

Competent quality concrete shows excellent resistance to steady flow of clear water; nevertheless, unsteady flow at velocities exceeding 12 m/s may cause severe damage to concrete through cavitation, which is a type of destruction merging in concrete around zones of high vacuum and high flow velocities when the surface of concrete is subjected to “bombardment”—repeated impact of cavitation bubbles which give rise to significant pressures. The best solution lies in removal of the sources of cavitation (e.g., surface misalignments and abrupt changes of slope). The concrete necessitated a resistant to potential cavitation must have sufficient strength (e.g., at least C_{40}). The concrete mix must be prepared using a selected strong filler (grain size not exceeding 30–40 mm) and with W/C ratio not higher than 0.40–0.45.

4. Cracking resistance

Cracking in concrete is commonly resulted from uneven distribution of temperature in it, attributable to the liberation of heat from hydration of cement during setting and hardening, and due to the changes in environmental temperature. As a result, the temperature of concrete placed in the structure mounts firstly and then cools down. The exterior surfaces of the structure cool down quickly and the inner entity cools down at a slower rate. The uneven distribution of temperature gives rise to non-uniform deformations in the structure and, in turn, results in irregular distribution of thermal strain/stress. The maximum value of tensile deformation of concrete, below which no apparent cracks appear, is commonly ranged between 0.00005 and 0.00007.

Since the liberation of hydration heat depends mainly on the mineralogical composition, activity, and other properties of the cement used, the temperature deformation (strain) can be lowered down to allowable values by cutting the temperature rise, in this way to reduce or even to avoid the danger of cracking, by:

- Using low-heat cements;
- Selecting concrete composition with minimum specific ratio of cement;
- Adding surface-active substances and diluents, for example, fly ash and other substances, into concrete mix; and
- Undertaking appropriate construction practices, such as pre- and/or post-cooling.

When considering the problem of crack resistance, it is also necessary to take into account, in addition to temperature deformation, the drying shrinkage deformation of concrete associated with the moisture loss. The maximum linear shrinkage of concrete samples must not exceed 0.3 mm/m at the age of 28 days and 0.7 mm/m at the age of 180 days (the temperature of air is assumed to be equal to 18 °C); the maximum linear elongation of concrete samples (in the swollen state) should not be more than 0.1 mm/m after 28 days of the birth and 0.3 mm/m after 180 days.

Cracks can also appear due to other reasons, such as overloading and irregular settlement, but this is a structural concern which will be addressed in the

corresponding chapters and does not depend directly on the concrete material technology.

5. Chemical deterioration resistance

In concrete, the deterioration processes triggered by chemical reactions involve generally the formation of expansive products in hardened concrete, which can lead to certain harmful effects. The four major scenarios associated with expansive chemical reactions are as follows: sulfate attack (SA), alkali-aggregate reaction (AAR), delayed hydration of free CaO and MgO, and corrosion of steel in concrete (Mehta and Monteiro 2006).

At first stage, expansion may take place without any damage to concrete, but the increasing buildup of the internal stress eventually manifests itself as the serious structural problem by the closure of the expansion joints, deformations and displacements in different parts of the structure, cracking, spalling, etc. SA can also manifest in the form of a progressive decrease in the strength and a loss of mass due to the loss of cohesiveness of the cement hydration products (C-S-H).

After the deterioration, particularly the cracking of the concrete, its permeability increases and the aggressive water penetrates more easily into the interior, thus in turn accelerates the process of deterioration.

A review of the deterioration processes attributable to chemical reactions and their damage mitigations will be further discussed in the Chap. 18 of this book. For more details, readers are referred to the corresponding literatures (Mehta and Monteiro 2006) and design specifications (Ministry of Housing and Urban-Rural Development of the People's Republic of China 2010; Ministry of Water Resources of the People's Republic of China 2008a, b).

References

- Acker WL III (1974) Basic procedures for soil sampling and core drilling. Acker Drill Company, Scranton
- Amadei B (1983) Rock anisotropy and the theory of stress measurements. Springer, Berlin (Germany)
- Barton N, Bandis S, Bakhtar K (1985) Strength, deformation and conductivity coupling of rock joints. *Int J Rock Mech Min Sci Geomechan Abstr* 22(3):121–140
- Bazant ZP (1982) Mathematical models for creep and shrinkage of concrete. In: Bazant ZP, Wittman FH (eds) *Creep and shrinkage in concrete structure*. Wiley, New York
- Bazant ZP, Wu ST (1974) Dirichlet series creep function for aging concrete. *J Eng Mech Div ASCE* 100(EM3):575–597
- Carman PE (1956) *Flow of gases through porous media*. Academic, New York
- Carslaw HS, Jaeger JC (1985) *Conduction of heat in solids* (2nd edn). Oxford University Press, Oxford
- Casagrande A (1948) Classification and identification of soils. *Transact ASCE* 113(1):901–930
- Chen SH (2006) *Computational rock mechanics and engineering*. China WaterPower Press, Beijing (in Chinese)
- Chen SH, Chen SF, Shahrour I, Egger P (2001) The feedback analysis of excavated rock slope. *Rock Mech Rock Eng* 34(1):39–56

- Chen SH, Pande GN (1994) Rheological model and finite element analysis of jointed rock masses reinforced by passive, fully-grouted bolts. *Int J Rock Mech Min Sci Geomech Abstr* 31 (3):273–277
- Chen SH, Wang HR, Xiong WL (1989) Study of the seepage characteristics of joint surface. *J Wuhan Univ Hydraul Electr Eng* 22(1):53–60 (in Chinese)
- Commission on Standardization of Laboratory and Field Tests (1974) Suggested methods for determining shear strength. Document No. 1. Lisbon (Portugal): ISRM
- Craig RF (2004) *Craig's soil mechanics* (7th edn). Spon Press, London
- Duncan JM, Chang CY (1970) Nonlinear analysis of stress and strain in soils. *J Soil Mech Found Div, ASCE* 96(SM5):1629–1653
- Duncan JM, Wright SG (2005) *Soil strength and slope stability*. John Wiley & Sons, New Jersey
- Farmer IW (1968) *Engineering properties of rocks*. E & FN Spon Ltd., London
- Gale JE (1982) The effects of fracture type (induced vs. natural) on the stress-fracture closure permeability relationships. In: Goodman RE, Heuze FE (eds) *Proceedings of 23rd Symposium on Rock Mech*. AA Balkema, Rotterdam (Netherlands) pp 290–298
- Golze AR (ed) (1977) *Handbook of dam engineering*. Van Nostrand Reinhold Company, New York
- Goodman RE (1989) *Introduction to rock mechanics* (2nd edn). Wiley, New York
- Goodman RE, Taylor R, Brekke TL (1968) A model for the mechanics of jointed rock. *J Soil Mech Found Div ASCE* 94(SM3):637–659
- Grishin MM (ed) (1982) *Hydraulic structures*. Mir Publishers, Moscow
- Hazen A (1911) Discussion of “dams on sand foundation” by AC Koenig. *Transact ASCE* 73 (1):199
- Hoek E (1990) Estimating Mohr-Coulomb friction and cohesion values from the Hoek-Brown failure criterion. *Int J Rock Mech Mining Sci Geomech Abstr* 12(3):227–229
- Hoek E, Bray JW (1981) *Rock slope engineering* (3rd edn). Institution of Mining and Metallurgy, London
- Hsich PA, Neuman SP (1985) Field determination of the three dimensional hydraulic conductivity tensor of anisotropic media 1, theory. *Water Resour Res* 21(11):1655–1665
- Hsich PA, Neuman SP, Stiles GK, Simpson ES (1985) Field determination of the three dimensional hydraulic conductivity tensor of anisotropic media 2, methodology and application to fractured rocks. *Water Resour Res* 21(11):1667–1676
- Hudson JA, Harrison JP (1997) *Engineering rock mechanics—an introduction to the principles*. Elsevier Science Ltd., Oxford (UK)
- ICOLD (2009) *The specification and quality control of concrete for dams* (Bulletin 136). ICOLD, Paris
- Jaeger JC, Cook NGW, Zimmerman R (2007) *Fundamentals of rock mechanics* (4th edn). Wiley-Blackwell, MA
- Kozeny J (1927) Ueber kapillare Leitung des Wassers in Boden. *Wien Akad Wiss* 136(2a):271–306 (In German)
- Liu ZM, Wang DX, Wang DG (eds) (2013) *Handbook of hydraulic structure design* (vol 1)—fundamental theories. China WaterPower Press, Beijing (in Chinese)
- Look BG (2007) *Handbook of geotechnical investigation and design tables*. Taylor & Francis Group, London
- Louis C, Maini YN (1970) Determination of in-situ hydraulic parameters in jointed rock. In: *Proceedings of the 2nd international congress, ISRM, Belgrade (Yugoslavia)* pp 235–245
- Mehta PK, Monteiro PJM (2006) *Concrete: microstructure, properties, and materials* (3rd edn). McGraw-Hill, New York
- Ministry of Housing and Urban-Rural Development of the People's Republic of China (2010) GB50010-2010 《Code for design of concrete structures》. China Construction Industry Press, Beijing (in Chinese)
- Ministry of Water Resources of the People's Republic of China (2008a) GB/T50145-2007 《Standard for engineering classification of soil》. China Planning Press, Beijing (in Chinese)

- Ministry of Water Resources of the People's Republic of China (2008b) SL191-2008 «Code for design of hydraulic concrete structures». China Water Power Press, Beijing (in Chinese)
- National Development and Reform Commission of the People's Republic of China, Ministry of Housing and Urban-Rural Development of the People's Republic of China (1994) GB50218-94 Standard for Engineering Classification of Rock Masses. Standards Press of China, Beijing (in Chinese)
- Naylor DJ, Maranha das Neves E, Mattar D Jr, Veiga Pinto AA (1986) Prediction of construction performance of Beliche Dam. *Geotechnique* 36 (3): 359–376
- Naylor DJ, Tong SL, Shahkarami AA (1989) Numerical modelling of saturation shrinkage. In: Pietruszczak, Pande (eds) *Proceedings of 3rd international symposium on numerical models in geomechanics. NUMOGIII*. Elsevier Science Ltd., Amsterdam pp 636–648
- Neville AM, Diger WH, Brooks JJ (1983) *Creep of plain and structural concrete*. Construction Press, London
- Pande GN, Gerrard CM (1983) The behaviour of reinforced jointed rock masses under various simple loading states. In: *Proceedings of 5th ISRM congress*. Brown Prior Anderson Pty Ltd., Melbourne, pp F217–F223
- Raven KG, Gale JE (1985) Water flow in a natural rock fracture as a function of stress and sample size. *Int J Rock Mech Min Sci Geomech Abstr* 22(4):251–261
- Roy DM, Scheetz BE, Sabol S, Brown PW, Shi D, Licastro PH, Idom GM, Andersen PJ, Johanson V (1994) Maturity model and curing technology. National Academy of Sciences, Washington
- Salamon MDG (1968) Elastic moduli of a stratified rock mass. *Int J Rock Mech Min Sci* 5(6):519–527
- Serafim JL (1968) Influence of interstitial water on the behaviour of rock masses. In: Stagg KG, Zienkiewicz OC (eds) *Rock mechanics in engineering practice*. Wiley, London, pp 55–97
- Snow D (1969) Anisotropic permeability of fractured media. *Water Resour Res* 5(6):1273–1289
- Terzaghi K, Peck RB, Mesri G (1996) *Soil Mechanics in engineering practice*. John Wiley and Sons, New York
- Troxell GE, Raphael JM, Davis RE (1958) Long-time creep and shrinkage tests of plain and reinforced concrete. *Proc ASTM* 58:1101–1120
- Tsang YW, Witherspoon PA (1981) Hydromechanical behavior of a deformable rock fracture subject to normal stress. *J Geophys Res* 86(B10):9287–9298
- USBR (1987) *Design of small dams* (3rd edn). US Govt Printing Office, Denver
- Zienkiewicz OC (ed) (1968) *Rock mechanics in engineering practice*. Wiley, New York
- Zhou JP, Dang LC (eds) (2011) *Handbook of hydraulic structure design* (vol 5)—concrete dams. China WaterPower Press, Beijing (in Chinese)
- Zhu BF (1985) The elastic modulus, creep compliance and stress relaxation coefficient of concrete. *J Hydraul Eng* 9:54–61 (in Chinese)
- Zhu BF (1996) On the formula for modulus of elasticity of concrete. *J Hydraul Eng* 3:89–90 (in Chinese)
- Zuo DQ, Gu ZX, Wang WX (eds) (1984) *Geology, hydrology and materials*. In: *Handbook of hydraulic structure design* (vol 2). Water Resources and Electric Power Press of China, Beijing (in Chinese)

Chapter 4

Actions on Hydraulic Structures and Their Effect Combinations

4.1 Definition and Classification of Actions

4.1.1 Definition of Actions

It is a basic requirement that the design of hydraulic structures should make allowance for the actions (Golzé 1977; Liu et al. 2013; USBR 1987; Zhou and Dang 2011; Zuo et al. 1984). The term “actions” means an amount of factors being usually or actually sustained by structures, which result in stress and deflection within structures named as “effects.” Actions may be direct or indirect, the former refers to concentrated or distributed forces, which are conventionally called as “loads”; the latter means the factors inducing extra deformation and restricted stress which are stipulated for the earthquake, thermal variation, etc.

Ever since a long time ago, engineers were used to call the foregoing two types of actions imprecisely as “loads,” e.g., self-weight load, hydrostatic load, seismic load, and thermal load. Although the Chinese GB50199-94 “Unified Design Standard for Reliability of Hydraulic Engineering Structures” stipulates that the term “loads” is replaced by “actions,” with respect to the fact that the design method using safety factor is still employed in many Chinese design codes for various hydraulic structures, as a compromise, the terms “loads” and “actions” will be used in this book in parallel, if no danger of confusing would be led to.

4.1.2 Classification of Actions

The actions can be classified according to their time dependence and spatial variation, effect property to the structure, and occurring frequency (Grishin 1982; Iqbal 1993; Lin 2006; Novak et al. 1990; Wang and Wueng 1990; Wu 1991; Zuo et al. 1995).

1. Classification according to temporal features

(a) Permanent actions

Those who within the design reference period do not vary along time, or the variation is so small that may be overlooked, e.g., self-weight, earth pressure, and pretension force.

(b) Variable actions

Those who within the design reference period vary along time, and the variation is so significant that may be not neglected, e.g., water pressure, uplift, wave pressure, and wind pressure.

(c) Occasional actions

Those who within the design reference period occur in very low probability, with short duration but high magnificent, e.g., water pressure under the check water level (including static water pressure, uplift, and wave pressure) and seismic inertia (inclusive dynamic water pressure).

2. Classification according to spatial features

(a) Fixed actions

They are actions whose position and distribution are fixed, e.g., self-weight of the structure.

(b) Free actions

They are actions whose position and distribution are changeable. In powerhouse, for example, the wheel pressure of the traveling overhead crane depends on the weight of the object lifted and may move along the runway girders.

3. Classification according to the effect features on structure

(a) Static actions

They are actions which do not vary (e.g., self-weight and earth pressure) or only vary slowly (e.g., static water pressure and uplift pressure) as the time goes on.

(b) Dynamic actions

They are actions that vary quickly (e.g., seismic inertia) as the time goes on.

4. Classification in the design method using safety factor

The above classifications are stipulated in GB50199-94 “Unified Design Standard for Reliability of Hydraulic Engineering Structures,” which is intended to promote the design level up to the base of reliability theory. However, insofar a large part of Chinese water resources and hydropower projects are designed using traditional safety factor method, in which instead of “actions,” the term “loads” is used.

(a) Basic loads

Loads exerting on hydraulic structures frequently or in long term, e.g., self-weight loads, water loads under the normal and design flood water levels

(including corresponding static water pressure, uplift, wave pressure, and dynamic water pressure), silt pressure, earth pressure, and ice pressure.

(b) Special loads

Loads exerting on hydraulic structures unusually, e.g., water loads under the check flood water level (including corresponding static water pressure, uplift, and wave pressure) and seismic loads (inclusive of dynamic water pressure).

4.2 Self-weights

Weight of masonry, concrete, or soil is the counterbalancing force to withstand the effect of all the forces enumerated hereinafter. Self-weight is attributable to the gravity, and its magnitude is determined by the density of the materials that constitute the structure, i.e.,

$$G = \gamma V$$

where γ = unit (or specific) weight of the material, kN/m^3 ; V = volume, m^3 .

Regarding the water content, the unit weight further falls into dry unit weight, wet unit weight, and saturated unit weight, particularly for soils. For concrete and masonry materials, the difference in these unit weights is ignored. Buoyant unit weight is used for all the materials submerged under water. Unit weights are decided by tests. In the absence of specific data from laboratory tests, the unit weights of concrete or soil recommended in the DL5077-1997 “Specifications for Load Design of Hydraulic Structures” can be adopted for preliminary design phases. Generally, the gravity of fixed equipments such as service gates and headstock gear sets on a concrete dam should be considered, while the gravity of unfixed equipments such as cars and moving headstock gears are often ignored.

4.2.1 Self-weight of Concrete Dam

In the preliminary design phase, the unit weight of concrete can be stipulated as $\gamma_c = 23.0\text{--}23.5 \text{ kN/m}^3$ related to aggregate type, but the difference in the unit weight of different concrete grade and the unit weight of steel bars are customarily ignored. In the design phases of technical or construction details, the unit weight of concrete should be justified by tests. Self-weight is considered to exert through the centroid of the structure concerned.

Generally speaking, the construction and grouting sequence may affect the manner in which the self-weight of the structure is transmitted to its foundation.

Take concrete arch dam as an example, which is divided by transverse contraction joints in the process of construction and is poured layer by layer. Then, the engineers inject grouting agents through the embedded pipes to seal the joints in low-temperature seasons, for the purpose to ensure arch integrity. This process is named as “arch closure.” Prior to the grouting, the self-weight of the concrete is assumed being transmitted vertically to the foundation by cantilever action. On the contrary, when imposed after the grouting of the joints, the self-weight is assumed to be distributed between vertical cantilever and horizontal arch elements when using trial load method, in much of the same manner as other loads in the stress computation for the arch dam. For double-curvature arch dams, however, the height of the independently poured cantilever block should be limited in order to assure its stability during construction. In the practice, as soon as the dam is poured to a certain height, the engineers ordinarily post-cool the dam then grout the transverse joints.

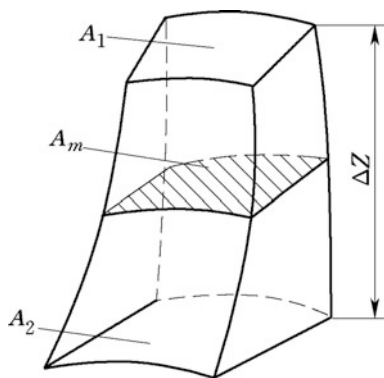
In addition, for a large-scale engineering monographic study for the stability of arch dam according to the construction and operation procedures is sometimes undertaken using numerical methods (e.g., finite element method) taking into account the spatial-time evolution of the fields (seepage, temperature, deformation/stress) related to the real loading history, including the self-weight of course, during the construction and operation periods.

Because the horizontal planes of an arch dam monolith are in the form of fan as shown in Fig. 4.1, the gravity of monolith between the plane A_1 and plane A_2 should be calculated by the Simpson formula as follows:

$$G = \frac{1}{6} \gamma_c \Delta Z (A_1 + 4A_m + A_2) \quad (4.1)$$

where γ_c = unit weight of concrete, kN/m^3 ; ΔZ = height of the dam monolith concerned, m; A_1 , A_2 , and A_m = areas of the top, bottom, and middle planes, respectively, m^2 .

Fig. 4.1 Diagram to the computation of the self-weight of arch dam monolith



Equation (4.1) may be simplified as:

$$G = \frac{1}{2} \gamma_c \Delta Z (A_1 + A_2) \quad (4.2)$$

4.2.2 Self-weight of Embankment Dam

The unit weight of earth- and rockfill is selected depending on the position of water level and phreatic line as follows:

- Dry unit weight γ_d (kN/m³)

$$\gamma_d = (1 - n)G\gamma_w \quad (4.3)$$

- Wet unit weight γ_s (kN/m³)

$$\gamma_s = (1 - n)G(1 + w)\gamma_w \quad (4.4)$$

- Saturated unit weight γ_f (kN/m³)

$$\gamma_f = [(1 - n)G + n]\gamma_w \quad (4.5)$$

- Buoyant unit weight γ' (kN/m³)

$$\gamma' = (1 - n)(G - 1)\gamma_w \quad (4.6)$$

where n = porosity; G = specific gravity; γ_w = unit weight of water, kN/m³; and w = natural moisture content.

4.2.3 Earth Pressure

Where one or two sides of a retaining structure are filled with earth embankment, active earth pressure, passive earth pressure, or earth pressure at rest shall be considered, as the case may be.

- Active earth pressure (kN/m²)

$$p_u = \gamma_s H t g^2 \left(45^\circ - \frac{\phi}{2} \right) \quad (4.7)$$

- Passive earth pressure (kN/m^2)

$$p_u = \gamma_s H t g^2 \left(45^\circ + \frac{\varphi}{2} \right) \quad (4.8)$$

- Earth pressure at rest (kN/m^2)

$$p_u = \gamma_s H \quad (4.9)$$

where γ_s = unit weight of earth, kN/m^3 ; H = overburden depth of embankment, m; and φ = internal friction angle of the earth-or rock fill, ($^\circ$).

4.2.4 Silt (Sediment) Pressure

After the completion of a dam or barrage project, the incoming stream brings silt or sediment into the reservoir. The sediment deposits on the reservoir bed following the general rules that: starting from the region of the reservoir front (backwater end), the velocity of incoming flow is descendent along the stream; thus, the coarse-grained sediment firstly deposits in the reservoir front while the fine-grained silt deposits gradually along the stream till the dam. As the sediment deposits more and more, fine grain of silt may be carried to in front of the dam.

The elevation of sediment deposit against the dam face rises as the time goes on, which should be estimated according to the amount of sediment carried by the river and the defined term of deposit which may be 50–100 years. The amount of deposited sediment can be determined according to the analysis and reference of historical sediment discharge data and the status of soil and water conservancy in the headwater areas around the reservoir. Deposit depth is a complex time-dependent function related to suspended sediment concentration, reservoir characteristics, river hydrograph, and other factors. Although accurate prediction is inhibited attributable to various major uncertainties, relatively reliable data may be available, by the comprehensive studies using appropriate mathematical and physical models based on sufficient field data.

The gradual accumulation of significant deposits of fine sediment, notably silts, against the upstream face of the dam generates a resultant force whose magnitude is a function of the silt depth and the unit weight. The cohesion of silt is commonly neglected. The internal friction angle φ_n of silt deposit depends on the grain diameter, graduation, and particle shape. It is also worthwhile to indicate that in the process of deposit both the unit weight and friction angle will increase gradually. The following data may be referred to in the preliminary design phase: $\varphi_n = 18^\circ$ – 20° for coarse-grained silt accumulated long time; $\varphi_n = 12^\circ$ – 14° for clayey-soil silt; $\varphi_n = 0^\circ$ for very fine silt and clay. It could be interesting to mention that $\varphi_n = 25^\circ$ – 35° were tested from several old Chinese dam projects including the Liujiaxia and the Guanting.

Normally, the silt pressure can be calculated using the earth pressure formulation. For example, the horizontal component of pressure can be expressed as:

$$p_n = \gamma' h_n t g^2 \left(45^\circ - \frac{\varphi_n}{2} \right) \quad (4.10)$$

where p_n = horizontal silt (sediment) pressure on vertical dam face, kN/m^2 ; γ' = buoyant unit weight of the silt, kN/m^3 ; φ_n = internal friction angle, ($^\circ$); and h_n = overburden depth of deposited silt referring the point concerned, m.

- N.B. ① Where the upstream face of the concrete dam is sloping or flared, the vertical silt pressure is calculated similar to the vertical static water pressure;
- ② Horizontal silt pressure is ignored for embankment dams due to their much larger volume and self-weight. However, the self-weight of silt may be taken into account in the stability analysis for the upstream embankment slope and its revetment.

4.3 Thermal Actions

Hydraulic structures operate under variable ambient temperature conditions ever changing in time; as a result, expansion or shrinkage strain will be induced by temperature and moisture changes within the concrete. When the structure is restrained or confined internally or externally, thermal stress will be given rise to. It has been proved that the existence and change of thermal stress is the main scenario of cracking in concrete. The temperature changes are called “thermal action” or “thermal load,” for it indirectly results in deformation and stress within concrete structures.

Thermal action is dependent on the structure type, material properties, construction course including artificial heating or cooling procedure, thermal exchange between the structure and foundation, and fluctuations of the ambient temperature (water, air) during construction and operation period. Thermal action is usually spatial-time-dependent.

4.3.1 Temporal Features of Thermal Action

Generally, the temperature development within concrete of hydraulic structures experiences three stages, as illustrated in Fig. 4.2.

1. Early stage

This is temperature mounting period, initiated from the casting and finished at nearly the end of the exothermic hydration of cement.

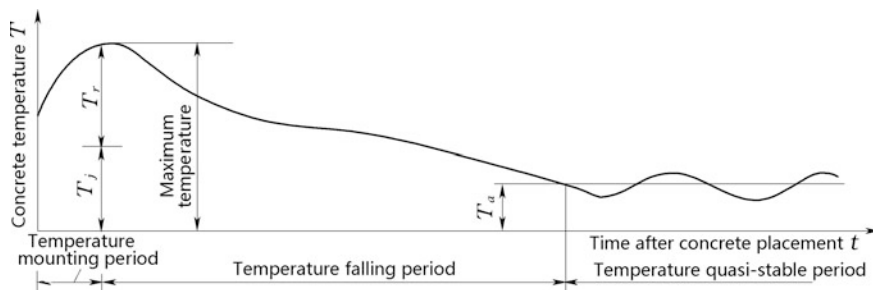


Fig. 4.2 Temperature development process

2. Middle stage

This is temperature falling period, commenced from nearly the end of the exothermic hydration of cement and terminated at the stable temperature. It often takes long time for exothermal concrete to lower its temperature.

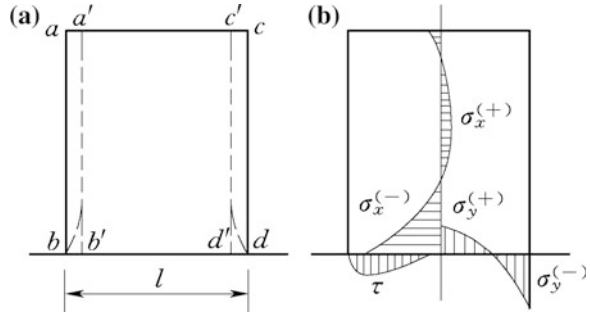
3. Late stage

This is the normal service period after totally cooling down of concrete. The zones underlying the faces (to a depth of 5–6 m from the surface) are exposed to seasonal changes in temperature due to the temperature fluctuations of air and water and solar radiation, which is called as “quasi-stable temperature.” In the portion deeper inside the massive structure, the fluctuations may be ignored and the temperature is stable assumed the mean annual temperature of the locality. For massive concrete structures such as gravity dams, the course reaches stable temperature is quite a long period ranged from several decades to more than one hundred years, if no artificial cooling measures would be carried out during the construction.

4.3.2 Spatial Features of Thermal Action and Thermal Stress

Due to both the development of the Young’s modulus and the thermal action along with the time, thermal stress developed within massive concrete structures also experiences three stages as early stage thermal stress, middle stage thermal stress, and late stage thermal stress. In temperature mounting period, the expansion of concrete lift is restrained by underneath foundation rock or old concrete. This restriction induces horizontal compressive stress, which is of lower level because the Young’s modulus at this stage has far from been fully developed. On the contrary, in the temperature falling period when concrete age exceeds 28d and the Young’s modulus is fairly developed, the shrinkage restriction results in higher horizontal tensile stress, which gives rise to net tensile stress after the offset of early stage compressive stress. If such net tensile stress exceeds the tensile strength of the concrete, undesirable cracking occurs. In addition, the surface radiating or cold snap

Fig. 4.3 Thermal stress due to base temperature difference



during concrete construction produces nonlinear temperature gradient from the surface to the internal portion of massive concrete, which also may cause surface cracking (Fanelli and Giuseppetti 1975; Price 1982; Singh 1985; Tatro and Schrader 1985).

1. Thermal stress due to base temperature difference

(a) Construction period

Supposing a pouring concrete block on the foundation whose placing temperature is T_p , the maximum temperature rise is T_r , the stable temperature is T_f , then the net temperature drop of the concrete block is $T = T_p + T_r - T_f$.

In Fig. 4.3a, $a'b'$ and $c'd'$ define the freely deformed configuration of the block after the uniform temperature drop T ($^{\circ}\text{C}$), and $a'b$ and $c'd$ are the base restricted configuration of the block after the deformation. Under the restraint of base, stresses σ_x , τ , and σ_y manifest at the block bottom (Fig. 4.3b). Where the foundation is rigid, the horizontal stress σ_x giving rise to vertical cracking may be expressed as

$$\sigma_x = E_c \alpha T \tag{4.11}$$

where E_c = Young's modulus of concrete, kN/m^2 ; α = Coefficient of thermal expansion, $1/^{\circ}\text{C}$.

For a high pouring block, at the height of $0.15 l$ from the base (l = pouring block length), the horizontal stress σ_x drops down to 50 % of that at bottom; σ_x is nearly zero at the height of $0.4 l$ above the base.

For non-rigid foundation, instead of E_c , effective Young's modulus E_e is used in Eq. (4.11).

$$E_e = \frac{E_c}{1 + 0.4 \frac{E_c}{E_R}} \tag{4.12}$$

where E_R = Young's modulus of foundation rock, kN/m^2 .

Long intermittent pouring block imposes restraint on new pouring block in a similar way of foundation restraint, but the restraint degree is lower.

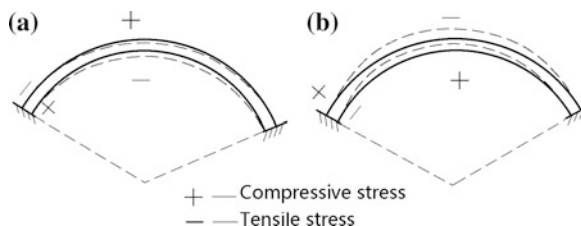


Fig. 4.4 Temperature variation and corresponding deflection/stress of arch dam. **a** Temperature drop; **b** temperature rise

(b) Service period

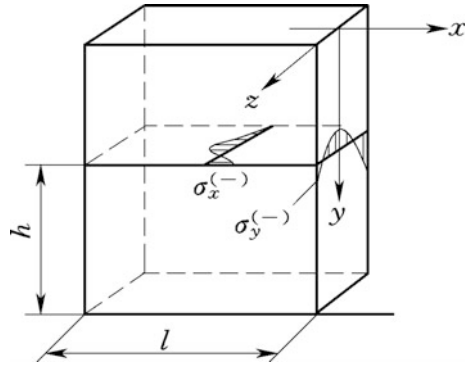
Thermal stress during service (operation) period may be induced by the foundation restraint, too. However, the relative importance of thermal stress during service period is depending on the type of works. For instance, temperature changes during service period, which are usually not important in case of gravity dams, will give rise to important deflection and stress in case of arch dams. The thermal stresses push the arch dam moving upstream during the summer and downstream during the winter. Hence, it cannot be neglected in the course of the design of arch dams.

When the dam temperature drops below the arch closure temperature, the dam axis shrinks and tensions lead to downstream displacement (Fig. 4.4a), which produces additional bending moment and shear force of the same direction and axial force of opposite direction referring to those that induced by the reservoir water pressure. As a result, at arch abutments, the upstream portion is in tension while the downstream portion is in compression, whereas at arch crown the upstream portion is in compression while the downstream portion is in tension. When the temperature rises above its closure temperature, the dam axis expands and compresses lead to upstream displacement (Fig. 4.4b), which produces additional bending moment and shear force of opposite direction and axial force of same direction referring to those that induced by the reservoir water pressure. As a result, at arch abutments, the upstream portion is in compression while the downstream portion is in tension, whereas at arch crown the upstream portion is in tension while the downstream portion is in compression. Generally, temperature drop is disadvantageous to dam strength, while temperature rise is disadvantageous for the stability of dam abutments.

2. Thermal stress due to inside and outside difference in temperature

Another kind of thermal stress will emerge because of the inside and outside difference in temperature after the removal of frameworks. This temperature difference is conventionally defined according to the average temperature of a dam block and the surface temperature (inclusive of framework removal induced temperature drop). For a pouring block of large height and length, the corresponding surface thermal stress is as follows:

Fig. 4.5 Thermal stress due to inside and outside difference in temperature



$$\sigma_x = \sigma_y = \frac{2}{3} E_c \alpha T \quad (4.13)$$

where T = inside and outside temperature difference of the concrete block, °C.

This kind of thermal stress reaches maximum on the surface (Fig. 4.5) and is the major cause of surface cracking. Under the joint influence of foundation restraints, these surface cracks may be further developed into major and penetrated cracks endangering the structure safety.

3. Remarks

Disregarding the effects such as crack formation (matter of early age) and chemical changes due to AAR or aggressive water, the increase of concrete age is in general beneficiary for the overall structural safety. An increase in the elastic modulus leads to a reduction in elastic deformations, and an increase in the strength leads to an increase in structural safety. A long-term prediction for the evolution of material properties should be provided together with a continuous surveillance process.

The volume of concrete may be changed as the time goes on, which can be resulted from mechanical, physical, and chemical processes:

- Temperature change. It has very important effects on concrete structures, of which two distinct phenomena need to be cared over, as has been discussed in the foregoing. One is the hydration of the cement which causes warm up during the hardening, and another is the environmental variation of temperature under the normal service conditions. These temperature variations may lead to cracking in concrete. In both cases, the analysis of the temperature distribution in the structure and of the consequent-induced stresses needs data on the adiabatic temperature rise, conductivity and diffusivity, and specific heat and coefficient of thermal expansion, which have been illustrated in Chap. 3 of this book.
- Volume change. It is mainly due to the moisture variation in concrete and the consequent drying shrinkage. The effect of drying shrinkage of massive concrete reduces rapidly along the thickness and become negligible at a depth of about 0.50 m.

Creep is time-dependent deformation due to sustained load. It is generally accepted that concrete creep is a rheologic phenomenon associated with the gel-like component in the cement paste. Creep phenomenon also can be explained partly in terms of viscoelastic and/or viscoplastic deformation of the cement paste and to the gradual transfer of load from cement paste to aggregate. Creep properties are of particular relevance to understand the mechanism leading to the prediction of potential thermal cracking of mass concrete: The most extensive use of creep data is in the thermal stress analysis for concrete dams (Mehta and Monteiro 2006; Zhou and Dang 2011). Recently, it has been found that some forms of enhanced creep emerge in structures affected by alkali–aggregate reactions and can significantly affect the long-term accumulation of compressive stresses.

Creep effects (short and long term) need to be handled, especially for arch dams. These effects lead to the redistribution of stresses which are evaluated for only by appropriate analysis tools. The effects of increased time-dependent plastic deformation have to be considered and monitored, and countermeasures have to be taken. Therefore, the SL191-2008 “Design code for hydraulic concrete structures” indicates that thermal stress may be reduced considering the creep phenomenon, if such stress is computed simply by the linear elasticity theory.

As conventional countermeasures against cracking, permanent thermal expansion and contraction joints are installed within gravity dams, massive-head buttress dams, and slab buttress dams. Therefore, apart from the thermal control measures during construction, the periodical thermal variation is not necessarily taken into account during the operation period for these types of dams. However, the periodical thermal variation should be taken into account during the operation period for arch dams and multi-arch buttress dams, because they are monolithic (without permanent thermal expansion and contraction joints) and statically indeterminate structures restrained by foundation and abutments. Thermal stress is not considered for embankment dams. However, care should be called at dry cracking and freezing cracking for the impervious membranes of clay.

4.3.3 Computation of Thermal Action

Thermal action or thermal load is defined as temperature change with respect to a definite period, which is generally considered separately for construction period and operation period in the design of hydraulic structures. Construction period comprises the early stage of temperature mounting started from the casting and the middle stage of temperature falling finished at the stable temperature. Operation period is featured by annual temperature fluctuations following the ambient temperature (water, air) and solar radiation.

Thermal action in construction period is a very complex process which has tight relation with the construction technique and environment factors. Numerical methods (e.g., FEM) are customarily employed for the simulation of the thermal action in construction period, which are able to take into account the factors related

to cast procedure, material properties, ambient temperature, artificial cooling, etc. (Chen and Chen 2014; Ishikawa 1991; Malkawi et al. 2003; Zhang and Garga 1996; Zhu 1991, 1998, 2006; Zhu and Cai 1989).

Thermal action in operation period is important for statically indeterminate hydraulic structures (e.g., arch dams). The onset time of thermal action in the operation period is related to the construction technology and environmental factors, too. Conventionally, arch dams are subdivided by transverse joints into a number of blocks for releasing the thermal stresses. These joints will be grouted after the cooldown of dam monoliths, and therefore the onset time of the thermal action in operation period is the grouting seal (closure) and the formation of dam monolith. For pouring without transverse joints (e.g., RCC arch dam), the onset time of the thermal action in operation period is that when the temperature reaches the highest during the construction period. For massive concrete structures, the consideration of annual temperature fluctuation is sufficient, while for the truss or plate structures, sometimes the month temperature fluctuations should be taken into account, too.

1. Truss structures

Due to its small cross section, a linear thermal action distribution along the truss thickness can be assumed and the action may be resolved in terms of mean temperature T_m and temperature gradient T_d along the thickness:

$$T_m = \frac{1}{2}(T_e + T_i) \quad (4.14)$$

$$T_d = T_e - T_i \quad (4.15)$$

where T_i , T_e = temperature of the interior and external surfaces, respectively, °C.

2. Flat plate (slab) structures

Shell structures with ratio of thickness L to curvature radius R smaller than 0.5 may also be treated as flat plate structures (such as the most of arch dams). Thermal action $T(x)$ is commonly resolved into three parts along the thickness (x -direction) of such structures (Fig. 4.6), i.e., mean temperature T_m , average temperature gradient T_d , and curvilinear portion of temperature diagram T_n :

$$T_m = \frac{1}{L} \int_{-\frac{L}{2}}^{\frac{L}{2}} T(x) dx \quad (4.16)$$

$$T_d = \frac{12}{L^2} \int_{-\frac{L}{2}}^{\frac{L}{2}} xT(x) dx \quad (4.17)$$

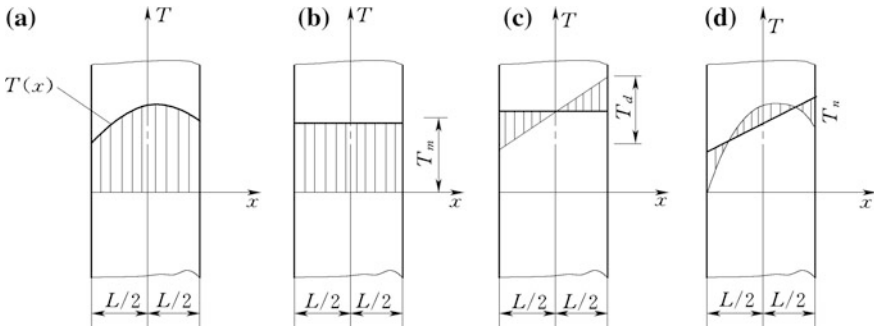


Fig. 4.6 Temperature distribution of flat plate (slab)

$$T_n = T(x) - T_m - T_d \frac{x}{L} \tag{4.18}$$

Mean temperature T_m causes axial deformation while temperature gradient T_d causes bending, which are all necessarily considered in the design, particularly of arch dams. The curvilinear component of the temperature diagram T_n mainly gives rise to superficial cracking and may be usually neglected in the design. However, thermal control and cracking prevention measures should be exercised in the construction, to effectively eliminate the adverse effects of curvilinear temperature action.

Detailed computation procedures for T_m and T_d may be found in the DL 5077-1997 “Specifications for Load Design of Hydraulic Structures.”

3. Massive concrete structures

Temperature regime in a massive concrete may be solved by the heat transfer theory for continuum, both in the construction period and operation period. The thermal action for a specified period is then defined as the temperature difference regarding the end and beginning of the period concerned (Zienkiewicz and Taylor 2005; Zhu 1998).

The governing equation of the temperature $T(x, y, z, t)$ in a structure is formulated on the basis of thermodynamics:

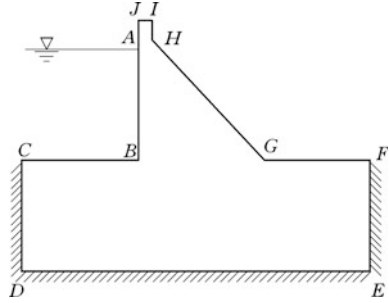
$$\frac{\partial T}{\partial t} = a \left(\frac{\partial^2 T}{\partial x^2} + \frac{\partial^2 T}{\partial y^2} + \frac{\partial^2 T}{\partial z^2} \right) + \frac{\partial \theta}{\partial t} \tag{4.19}$$

where θ = adiabatic temperature rise, ($^{\circ}\text{C}$); a = thermal diffusivity, m^2/h .

The initial condition should be specified as:

$$T = T_0(x, y, z) \quad \text{when} \quad t = 0$$

Fig. 4.7 Boundaries of the temperature regime of a gravity dam



There are basically two types of boundary conditions (Fig. 4.7):

- ① First type boundary [e.g., dam face contacted to reservoir water or foundation base, (ABCDEF) in Fig. 4.7]

$$T = T_b \tag{4.20}$$

For the dam face contacted to reservoir water directly, T_b is the water temperature.

- ② Second type [e.g., dam face exposed to air, (FGHJA) in Fig. 4.7]

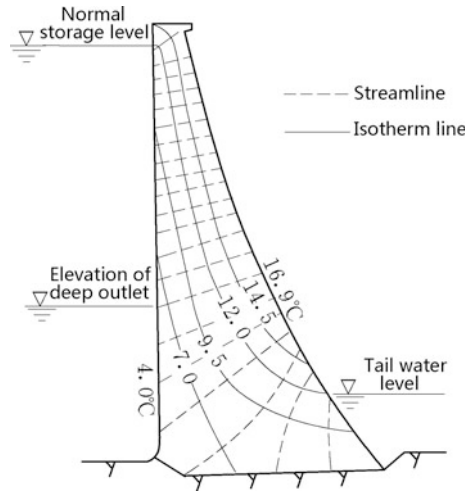
$$\lambda \frac{\partial T}{\partial x} l_x + \lambda \frac{\partial T}{\partial y} l_y + \lambda \frac{\partial T}{\partial z} l_z = -\beta(T - T_a) \tag{4.21}$$

where $l_x, l_y, l_z =$ normal direction cosines of the boundary surface; $T_a =$ temperature of the water or air, °C; $\lambda =$ thermal conductivity, kJ/(m h °C); $\beta =$ surface exothermic coefficient, kJ/(m² h °C).

Based on Eqs. (4.19)–(4.21), the numerical method such as FEM may be formulated for the solution of complex thermal problem. However, the reliability and applicability of such a mathematically perfect solution are strongly dependent on the rationality in the evaluation of the thermal parameters related to the material, the real construction schedule, as well as the ambient factors such as the spatial-time variation of air temperature and reservoir water temperature, of which the latter (i.e., T_b) was quite complicated. Nowadays, sufficient experiences have been accumulated (Zhu 1998) for a good understanding of the reservoir water temperature in the majority China’s rivers (in temperate zone only). Empirical formula, numerical computation, and engineering analog analysis are all available in the corresponding design specifications and handbooks for the estimation of the reservoir water temperature (Zhou and Dang 2011).

After a long service period, the temperature fluctuations inside massive concrete caused by the ambient temperature (water, air) and solar radiation can be overlooked. Figure 4.8 shows such a steady temperature field of a gravity arch dam, which satisfies the Laplace equation as

Fig. 4.8 Steady temperature field of a gravity arch dam



$$\frac{\partial^2 T}{\partial x^2} + \frac{\partial^2 T}{\partial y^2} + \frac{\partial^2 T}{\partial z^2} = 0 \tag{4.22}$$

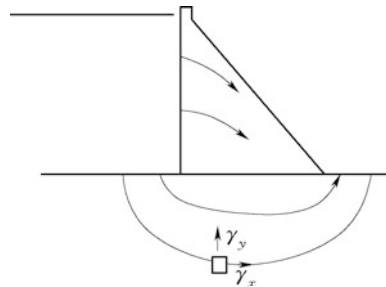
The numerical solution for the governing Eqs. (4.19)–(4.21) will be discussed in Chap. 5 of this book.

4.4 Seepage Actions

4.4.1 General Concept

The foundation and dam materials (concrete, rock, soil) are pervious to a certain extent, and seepage will occur attributable to the up- and downstream head differences. Figure 4.9 shows the seepage path within and under a gravity dam.

Fig. 4.9 Seepage path within and under a gravity dam



Permeability characteristics depend on the distribution, shape, and orientation of the porosity, cracks, and discontinuities of materials. For the lower pervious material such as concrete, it will take a long time (maybe several decades or even longer) to form a stable field of seepage, if there do not exist serious cracks and holes resulted from construction defects. On the contrary, attributable to large quantities of joints, fissures, and other structural faces, which are usually high permeable, foundation rock will take a much shorter time to form a stable field of seepage.

The water permeated into the materials builds up pore water pressure (Casagrande 1961; Cedergren 1989; Harz 1949; Keener 1950). The load due to such pore water pressure exerting on the pervious dam is not a kind of boundary traction but instead a kind of volumetric force. Since the calculations in a volumetric way are relatively complicated, it is often simplified as boundary tractions, i.e., the “uplift,” for the convenience of calculation and analysis. Another reason for the use of uplift lies in the fact that discontinuities in foundation rock and construction joints in dam concrete are often weak faces dominating the water percolation, consequently the uplift action may be postulated as a interstitial water pressure having characteristics of boundary traction. Traditionally, only the pore water pressure which exerts upward on a horizontal dam base or a horizontal section within the dam is named as “uplift.” Nowadays, uplift is commonly defined as the resultant effective component of interstitial water pressure perpendicular to any plane, e.g., the dam/base interface, construction joints, or discontinuities within the underlying rock. However, this term and definition are not applicable in the tunnel or slope projects. The uplift in the dam engineering is generally divided into two components as “seepage pressure” and “buoyant pressure.” The uplift offsets a part of the self weight of dam, and therefore it is unfavorable to the stability against sliding and the strength control. Although the buildup of pore water pressure and affected factors are quite complicated, after several decades of observation and research, they are understandable and may be controlled well.

The hydraulic head diminishes along the seepage path due to head loss. The residual head at any position is then termed as seepage pressure, which is dependent on the water level difference, and distributes linearly or in a form of curvilinear along the plane concerned, with an intensity of $\gamma_w H$ at the dam heel and zero at the dam toe.

If the position of the plane considered is located below the tailwater level, the buoyant pressure is defined identical to the hydrostatic pressure corresponding to the tailwater depth over the position concerned. The buoyant pressure distributes uniformly along the dam base plane with an intensity of $\gamma_w H_2$.

Another concept related to the seeping water is the excess pore pressure and effective stress, particularly for soils. The importance of the forces transmitted through the soil skeleton from particles to particles was recognized in 1923 when Terzaghi presented the principle of effective stress transmitted through the soil skeleton only (Craig 2004)

$$\sigma = \sigma' + p \quad (4.23)$$

where p = pore water pressure or seepage pressure; σ = total stress; σ' = effective stress.

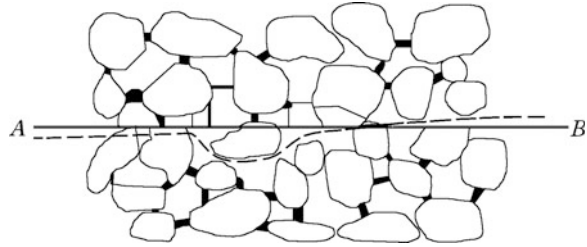
The just completed concrete dam manifests no seepage and usually $p = 0$. After a term of service when a portion of dam and foundation are saturated, the pore water pressure is built-up.

In the embankment dam design, the principle of effective stress is important in which the pore water pressure is denoted as u instead of p . A soil can be visualized as a skeleton of solid particles enclosing continuous voids which contain water and/or air. For the range of stresses usually encountered in practice, the individual solid particles and water can be considered incompressible. Air, on the other hand, is highly compressible. When a force is applied in a fully saturated soil, at beginning it may be resisted partially by inter-particle forces and partially by the increased pressure of the pore water above the static value due to the deformation of solid skeleton. The component of pore water pressure above the static value u_s is known as the “excess pore water pressure” u_e , i.e., $u = u_s + u_e$. The reduction of excess pore water pressure as drainage takes place is described as “dissipation.” As the excess pore water pressure dissipates, the effective stress increases, accompanied by a corresponding reduction in volume. When the dissipation of excess pore water pressure is completed, the increment of total stress will be carried entirely by the soil skeleton. This phenomenon is called “consolidation.”

For dam concretes and foundation rocks, the transient state process of built-up and dissipation of excess pore water pressure are normally not considered, i.e., $p = u = u_s$.

The very fact that water seeps through material pores arises another question—effective area on which the water pressure exerts at, which is quantified as effective area coefficient of uplift a_2 . Figure 4.10 illustrates the microstructure of porosity materials under electron microscope. It seems that the uplift pressure only exerts at the porosity part on the horizontal section A–B, and the space occupied by soil grains exerts no pressure. Therefore, it might be inferred that the area on which uplift pressure exerts should be a fraction smaller than 1.0 correlated with the porosity. However, the fact ascertained by experiments is that a_2 is nearly identical to 1.0. This paradox was solved by a series of extensive researches since the 1930s by Terzaghi, Leliavesky, Harza, McHenry, Creager, Гищина, and so on (Grishin 1982). A credible explanation is actually based on an irregular horizontal section fluctuated around the straight section A–B (broken line in Fig. 4.10). After the 1960s, the conclusion that $a_2 = 1.0$ is world widely accepted in design specifications.

Fig. 4.10 Microstructure of porosity materials



4.4.2 Theory and Computation of Seepage Field

The permeability study relies on the solution of hydraulic potential or water head function $H(x, y, z)$ using either theoretic, experimental, or engineering analog methods.

Theoretic and experimental methods make use of the principles in the fluid dynamics. For example, the steady-state permeability theory for pervious continuum comes from the directly analog of fluid dynamics of continuous flow (Featherstone and Nalluri 1995).

1. Governing equation

According to the Darcy’s law, the components of seepage velocity may be written as (Zienkiewicz et al. 1966; Zhu 1998).

$$\left. \begin{aligned} v_x &= -k_x \frac{\partial H}{\partial x} \\ v_y &= -k_y \frac{\partial H}{\partial y} \\ v_z &= -k_z \frac{\partial H}{\partial z} \end{aligned} \right\} \quad (4.24)$$

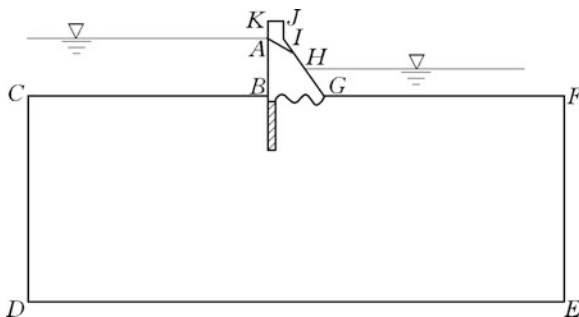
where v_x, v_y, v_z = components of velocity, m/s; k_x, k_y, k_z = permeability coefficient in the direction of $x, y,$ and $z,$ respectively, m/s.

Substituting Eq. (4.24) in the equation of continuity

$$\frac{\partial v_x}{\partial x} + \frac{\partial v_y}{\partial y} + \frac{\partial v_z}{\partial z} = 0 \quad (4.25)$$

The governing equation of the seepage flow in perfectly saturated materials under the assumptions that both material grains and pore water are incompressible is then obtained as:

Fig. 4.11 Boundaries of the seepage regime of gravity dam



$$\frac{\partial}{\partial x} \left(k_x \frac{\partial H}{\partial x} \right) + \frac{\partial}{\partial y} \left(k_y \frac{\partial H}{\partial y} \right) + \frac{\partial}{\partial z} \left(k_z \frac{\partial H}{\partial z} \right) = 0 \quad (4.26)$$

Restricted to the materials that are homogeneous and isotropic, i.e., $k_x = k_y = k_z$, Eq. (4.26) may be rewritten as the Laplace differential equation

$$\frac{\partial^2 H}{\partial x^2} + \frac{\partial^2 H}{\partial y^2} + \frac{\partial^2 H}{\partial z^2} = 0 \quad (4.27)$$

Equation (4.26) is subject to appropriate boundary conditions as follows (see Fig. 4.11):

- ① First type boundary. This is the boundary on which the hydraulic potential is specified. For instance, the upstream face (ABC), downstream exit surface (HI), and free discharge surface (FGH) are all the first type boundaries, on which

$$H = H_0(x, y, z) \quad (4.28)$$

where $H_0(x, y, z)$ = specified hydraulic potential, m.

- ② Second type boundary. This is the boundary on which the normal gradient of hydraulic potential (or flow rate) is specified. For instance, on the boundary (CDEF), the boundary condition is defined by

$$\left(k_x \frac{\partial H}{\partial x} l_x + k_y \frac{\partial H}{\partial y} l_y + k_z \frac{\partial H}{\partial z} l_z \right) = q(x, y, z) \quad (4.29)$$

or

$$k_n \frac{\partial H}{\partial n} = q(x, y, z) \quad (4.30)$$

where $l_x, l_y, l_z =$ normal direction cosines of the boundary surface; $q(x, y, z) =$ flow rate per unit area on the boundary surface; $q(x, y, z) = 0$ means the boundary is impervious.

Phreatic or free surface (or phreatic line in two-dimensional case) (AI) is a special boundary on which the following two conditions should be satisfied simultaneously:

$$\begin{cases} H = z \\ k_x \frac{\partial H}{\partial x} l_x + k_y \frac{\partial H}{\partial y} l_y + k_z \frac{\partial H}{\partial z} l_z = 0 \end{cases} \quad (4.31)$$

The solution of the governing Eq. (4.27) restricted by the boundary conditions specified in Eqs. (4.28)–(4.31) may provide the potential function $H = f(x, y, z)$ or conjugated stream function $q = \Psi(x, y, z)$ of major practical interest, which may further used to derive seepage gradient J and seepage velocity v . However, attributable to the complex boundaries, the exact analytical solution is very difficult, if not impossible, to obtain. The practical methods used for the solution are manual seepage flow net, physical model test, hydraulic method, numerical computation (e.g., FEM), and engineering analog.

2. Manual seepage flow net

It is a graphical method for the solution of the Laplace equation by drawing seepage flow net (Cedergren 1989), which is easy to exercise and has satisfied accuracy for not too complex problems (Figs. 4.12 and 4.13).

For steady seepage flow, the flow net consists of two sets of curves: isopotential lines and flow lines (streamlines)—that intersect each other at included angle of 90° where the material is isotropic. Along an isopotential line, the total head is constant, whereas a pair of adjacent flow lines defines a flow channel through which the rate of flow is constant.

The following rules may be helpful in the construction of seepage flow net:

- ① Flow (stream) lines cross the isopotential lines at right angles.
- ② For a flow net so constructed that each element is a curvilinear square with identical length–width ratio, the interval between two isopotential lines corresponds to identical head loss $\Delta H = \frac{H_1 - H_2}{m}$, where m is the

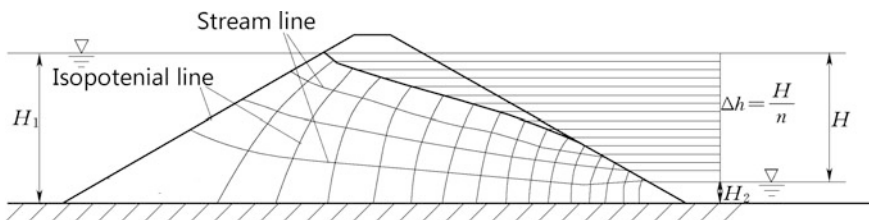


Fig. 4.12 Seepage flow net of an earth dam

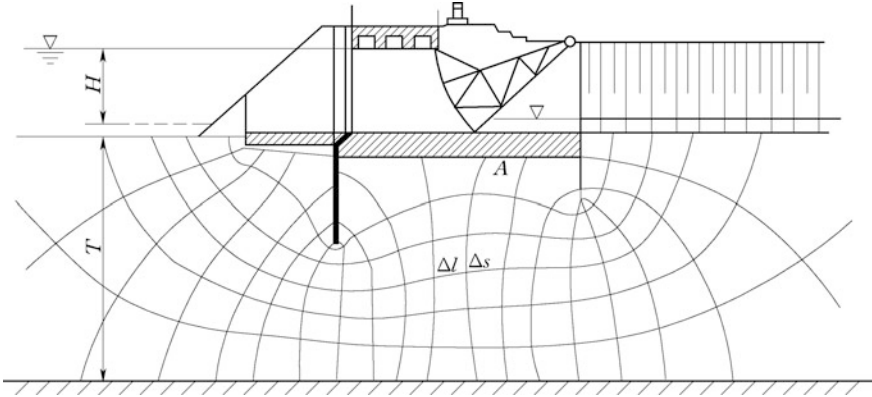
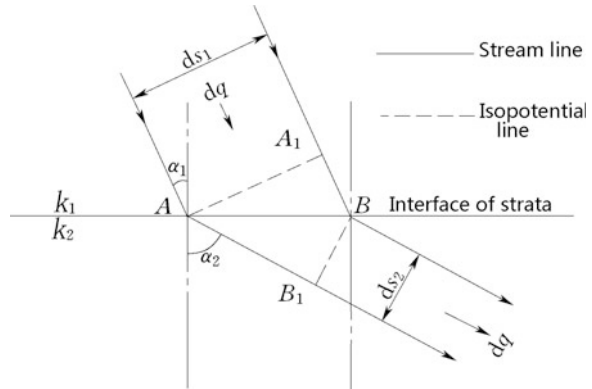


Fig. 4.13 Seepage flow net under the foundation of a sluice

total number of isopotential lines minus 1, whereas the interval between two flow lines corresponds to identical flow $q = -k\Delta H \frac{\Delta s}{\Delta l}$.

- ③ Bodies of water, such as reservoirs bottom and riverbed, up- and downstream dam slopes below the water level, are isopotential lines.
- ④ At a boundary between pervious and impervious materials, the velocity normal to the boundary must be zero; hence, it is a last flow line. The phreatic line is the first flow line marking the upmost boundary of the flow net.
- ⑤ The phreatic line and exit surface on the down slope of dam are flow lines of constant (zero) pore water pressure, i.e., $\Delta H = \Delta z$.
- ⑥ At a boundary between two pervious materials, isopotential lines and flow lines are deflected (Fig. 4.14). The continuity condition of flow should be ensured by the condition expressed as $dq = k_1 J_1 ds_1 = k_2 J_2 ds_2$. Since $A_1 A \perp A_1 B$ and $BB_1 \perp AB_1$, AA_1 and BB_1 are isopotential lines with head drop dh , therefore we have

Fig. 4.14 Streamline deflection between two pervious materials



$$J_1 = \frac{dh}{ds_1 \operatorname{tg} \alpha_1}, J_2 = \frac{dh}{ds_2 \operatorname{tg} \alpha_2}$$

The deflection angle of streamlines then observes the relation:

$$\frac{\operatorname{tg} \alpha_1}{\operatorname{tg} \alpha_2} = \frac{k_1}{k_2} \quad (4.32)$$

Suppose that the number of flow channels = n , and the number of isopotential drops = m . The flow net is so constructed using curvilinear squares with identical length–width ratio, to ensure identical head loss interval and flow through each element. For a curvilinear element i with average length of a_i and b_i , the quantities of design interesting from the flow net are calculated using Eq. (4.33)

$$\left. \begin{aligned} J_i &= \frac{H}{a_i m} \\ v_i &= k J_i = k \frac{H}{a_i m} \\ q &= k H \frac{b_i n}{a_i m} \end{aligned} \right\} \quad (4.33)$$

where J = average hydraulic potential gradient; v = average flow velocity, (m/s); q = average flow discharge per unit width, ($\text{m}^3/\text{s} \cdot \text{m}$).

3. Physical model test

Seepage problems also can be solved with the aid of physical model tests because the governing equation which describes the groundwater movement is, in many cases, analogous to the equations describing other physical phenomena, such as heat conductivity and conductivity of electric current.

Usually, the tests make use of electricity analogy, electrical net analogy, and sand box model. The most important one for the study on groundwater movement employs the method of the electrical analog, which is based on the similarity between the Darcy's law and the Ohm's law. For practical applications, a liquid or a solid substance, or a special kind of paper that is coated with a conductive carbon layer, can be used as an electrical conductor.

Nowadays, there is no much use of physical model tests due to their high expenditure and long period, in competing with the numerical computation.

4. Hydraulic method

The hydraulic method is approximate one based on the fluid dynamics applying assumptions to simply the problem, which is prevalent in the design of embankment dams and barrages (sluices) for determining the seepage characteristics such as the phreatic line, the seepage discharge, the seepage velocities, and the head gradient at any point of the seepage regime. The details of the computation will be addressed in the corresponding chapters of this book.

5. Finite element method

It will be introduced in Chap. 5 of this book.

6. Engineering analog method

The engineering analog method still widely exercised over the world employs large quantities of observation data as well as theoretic and experimental results, by which the uplift distribution patterns are recommended for different type of structures. The detailed computation of the uplift distribution pattern for a specific hydraulic structure will be discussed in the correspondent chapters of this book.

4.4.3 Computation of Seepage Force

As water seeps through porosity or fractured materials, it exerts a frictional drag on the material particles, which in turn results in head losses. The frictional drag is termed as seepage force in materials, which is calculated as force per unit volume (it has units similar to that of unit weight).

$$f = \gamma_w \bar{J} \quad (4.34)$$

where $\bar{J} = -\text{grad}(H)$, the gradient of hydraulic potential.

This is an important concept to bear in mind that the volumetric seepage force is transformed from the hydrodynamic pressure of the percolated water, which is in turn, transformed from the boundary actions related to the up- and downstream water. This concept may be helpful to prevent mistakes of neglecting or duplicate of the action of seepage flow.

Suppose the hydraulic potential $H(x, y, z) = z + \frac{p}{\gamma_w}$ has been solved in the regime, then the seepage force per unit volume may be computed by

$$\left. \begin{aligned} f_x &= -\frac{\partial p}{\partial x} = -\gamma_w \frac{\partial H}{\partial x} \\ f_y &= -\frac{\partial p}{\partial y} = -\gamma_w \frac{\partial H}{\partial y} \\ f_z &= -\frac{\partial p}{\partial z} = -\gamma_w \frac{\partial H}{\partial z} + \gamma_w \end{aligned} \right\} \quad (4.35)$$

where f_x, f_y, f_z = components of seepage force per unit volume, kN; γ_w = unit weight of water, kN/m³; p = seepage pressure, kN/m².

The total force may be integrated over the domain V_2 concerned as follows:

$$\bar{F} = \iiint_{V_2} \gamma_w \bar{J} \, dV \quad (4.36)$$

4.4.4 Remarks

- ① Permeability is a mechanism of the ease with which a fluid will flow through soil, concrete, and rock. Fluids do not flow easily through solid rock and concrete, so intact rock and concrete have low permeability. However, rock masses are commonly fractured where discontinuities (joints, fissures, faults, etc.) conduct fluids more readily, and they are easier for fluids to seep. Usually, joints appear in sets which are planar, persistent, and parallel. The width (aperture) of joint ranges from 0.000001 to 0.01 m, and the length of joint could be ranged from several meters to tens of meters. The joints of different sets intersected each other to form complicated seepage network. The real-world rock model of discrete fracture-porosity system is fairly difficult to be established due to the complex nature of fracture network. Considering the much larger dimension of dams, equivalent continuum model which smears the joints of high density into an equivalent porosity homogenous medium, is commonly thought to be a reasonable compromise between the real world and research level related to the investigations, experiments, and computations. Considering also that the aperture of joint is small, the laminar flow may be assumed on the safe side; hence, the Darcy's law may be true. On these basic simplifications, the beautiful differential Eqs. (4.26)–(4.31) may be employed and, nowadays, be easy to be solved using numerical methods. However, it should bear in mind that these assumptions are actually problematic. The successful applicability of the equivalent continuum theory relies on the following conditions: a REV (representative element volume) for the hydraulic behavior exists and its size is much smaller than the dimension of the structure concerned. Theoretically, the REV is defined as the size beyond which the rock hydraulic permeability tensor remains unchanged. Practically, the REV is identified when the permeability components only have small fluctuation when the size of the rock sample increases. Unfortunately, this is so far a not well-answered problem leaving a large room for the further study (Chen et al. 2008).
- ② By the solution of Eqs. (4.26)–(4.31) based on equivalent continuum model, the seepage characteristics including the phreatic line, the seepage discharge, the seepage velocities, and the head gradient at any point of the seepage regime may be obtained. The uplift on any of definite planar section is then further calculated easily. However, so far in the design of dams, the uplift distribution diagram by engineering analog is still prevailing over the solution aforementioned. The main reason lies in the complicated influencing factors (e.g., geological structures in foundation rock, characteristics of discontinuities, construction techniques, uplift relief measures, and boundary conditions), which are hard to be taken into account for precise computation.
- ③ Although we know that it is more reasonable to look at the reservoir water exerting on the hydraulic structure as volumetric forces, in the conventional design this action is usually simulated by surface hydrostatic pressure. In this

way, the calculation is highly simplified. One reason is that there is drain curtain formed as a hole array near the dam upstream face, the volumetric force in the vicinity of upstream dam face, accounting for a majority portion of the seepage force, and therefore, it may be equivalently replaced by a surface distributed water pressure.

- ④ For lower pervious membrane in embankment dams, such as thin central core and sloping core, concrete or asphalt concrete face slab, the hydrostatic surface pressure is also postulated in the design instead of the volumetric forces within the whole seepage regime.

4.5 Fluid Actions

4.5.1 Hydrostatic Pressure

Hydrostatic pressure is attributable to water standing against the surface of a hydraulic structure (e.g., dam). The hydrostatic pressure at a water depth h is simply expressed as follows:

$$p = \gamma_w h \quad (4.37)$$

where $\gamma_w = 9.8$, unit weight of water, kN/m^3 ; h = height of free water surface above the point concerned, m.

The hydrostatic pressure is a vector exerting on the surface of structure perpendicularly. For a curved surface, hydrostatic pressure is in the normal direction of the surface at the point concerned (Fig. 4.15).

The total pressure force on a section of a dam is calculated by the integral

$$\bar{P} = \int_A \bar{p} dA \quad (4.38)$$

It is customarily to determine the force of hydrostatic pressure by resolving it into horizontal and vertical components. The horizontal component is expressed in meters of water column. The resultant horizontal force is determined as $P_x = 0.5\gamma_w H^2$ and exerts at the height of $H/3$ above the base plane. The vertical component is equal to the weight of water mass confined by the head face of the structure and the vertical line drawn through its lower generatrix till it intersects with the free water surface. The portion of this body of pressure that is filled with water will exert force downward, while the unfilled portion will exert force upward. Take a gravity dam as example, the vertical force P_y is accounted for if the upstream face has a batter or is flared, i.e., $P_y = \gamma_w A$, and exerts through the centroid of the water mass confined.

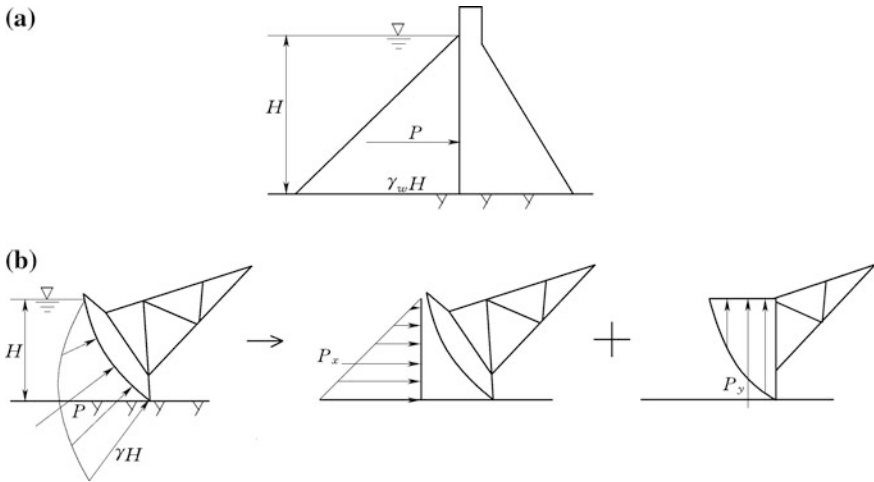


Fig. 4.15 Diagram to the computation of hydrostatic pressure

4.5.2 Hydrodynamic Force

Water is a kind of fluid, which flows under the action of pressure gradient or potential gradient (Featherstone and Nalluri 1995). Hydrodynamic action is attributable to water on the flowing elements of the structure, which comprises of the friction (drag) and hydrodynamic pressure on the surface of the structure, the reaction of discharged water on the structure during flood release, and the earthquake-induced water inertia on the structure surface.

1. Structure of water flow

Generally, water is a viscous and incompressible fluid. The flow of viscous water has patterns of laminar or turbulent. In hydraulic structures, the Reynolds number (ratio of inertia forces to viscous forces) is usually larger than 10^5 and the flow belongs turbulence (Featherstone and Nalluri 1995; Gatski and Bonnet 2009).

Turbulence produces eddies of different length scales. The production of eddies has related to the Reynolds number, velocity gradient, and boundary conditions. Most of the kinetic energy of the turbulent motion is carried in the large length scale eddy structures. The energy “cascades” from these large length scale eddies to smaller scale eddies by an inertial and essentially inviscid mechanism. This process continues creating smaller and smaller structures which forms a hierarchy of eddies. Eventually, this process creates eddies that are small enough where molecular diffusion becomes important and viscous dissipation of energy finally takes place.

It is well accepted to classify eddies into three categories based on their length scales.

(a) Integral length scale

This is the largest scale in the energy spectrum. Eddies obtain energy from the mean flow and also from each other. They have large velocity fluctuation and low frequency. Integral scales are highly anisotropic and are defined in terms of the normalized two-point velocity correlations. The maximum length of these scales is constrained by the characteristic length of the apparatus or works. For example, the largest integral length scale of a pipe flow is equal to the pipe diameter.

(b) Kolmogorov length scale

This is the smallest scale in the spectrum that forms the viscous sub-layer range. In this range, the energy input from nonlinear interactions and the energy drain from viscous dissipation are in exact balance. The small scales are in high frequency that is why turbulence is locally isotropic and homogeneous. Smallest Kolmogorov scales are around 1.0 mm in water.

(c) Taylor microscale

This is the intermediate scale between the largest and the smallest scales which make the inertial sub-range. Taylor microscales are not dissipative scales but passes down the energy from the largest to the smallest without dissipation. Some literatures do not consider Taylor microscale as a characteristic length scale. Nevertheless, the Taylor microscale is often used in describing the term “turbulence” more conveniently as it plays a dominant role in energy and momentum transfer in the wave number space.

So far, a complete description of turbulence remains one of the unsolved problems in physics. Although it is possible to find some particular solutions of the Navier–Stokes equations governing fluid motion, all such solutions are unstable at large Reynolds numbers. Sensitive dependence on the initial and boundary conditions makes fluid flow irregular in the spatial-time domain, so that a statistical description is ordinarily needed.

2. Hydrodynamic pressure

Hydrodynamic pressure is manifested by flowing water and exerts on the submerged surface of structure.

Uniform flow in long channel (or river) has a hydrodynamic pressure distribution identical to hydrostatic pressure. However, variation of flow sidewall or surface may deflect the pressure distribution considerably away from hydrostatic state. In gradually varied flow, the hydrodynamic pressure distribution may be still looked at as close to hydrostatic, this covers the cases of water convey channel, straight section of spillway chute, natural riverbed, etc. In rapid varied flow, due to the strong curve of streamlines, the hydrodynamic pressure distribution will be shifted significantly away from hydrostatic pressure; this covers the cases of weir surface, orifice transition section, curved section (of conduct, tunnel, chute), energy dissipation flip bucket, etc. Generally, if the overflowing bound is concave, the hydrodynamic pressure is larger than the hydrostatic pressure, and vice versa.

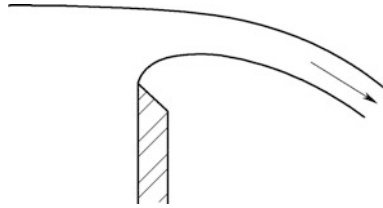


Fig. 4.16 Overflow through sharp-crested weir

A number of high weir profiles are available, of which the commonly used one in China nowadays is the WES profile standardized by USBR (Creager et al. 1966; Golzé 1977), in an attempted to fit the overflowing nappe through sharp-crested weir (Fig. 4.16). The curve equation for the weir profile downstream of the crest is as follows:

$$x^{1.85} = 2.0H_d^{0.85}y \tag{4.39}$$

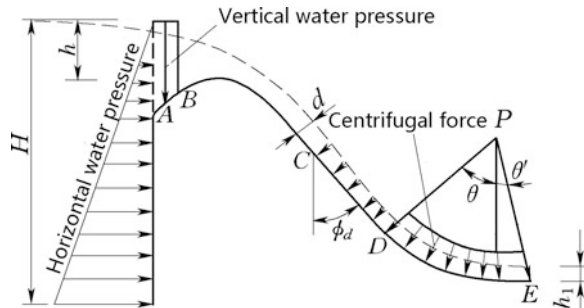
where H_d = design head over the crest.

Theoretically, dependent on whether the working head greater or smaller than or equal to the crest design head H_d , there is negative, positive, or zero pressure on the weir surface, respectively. Larger negative pressure increases the discharge ability but may raise the risk of cavitation damage. A compromise is to use frequently encountered flood head as design head. In China, for example, $H_d = (75\text{--}95\%) H_{\max}$ for the weir on overflow dams, and $H_d = (65\text{--}85\%) H_{\max}$ for the weir on river bank (shore) spillways, where H_{\max} is the maximum flood head.

Figure 4.17 illustrates the hydrodynamic pressure distribution on weir surface based on experimental results. In the design of overflow dams, very often, hydrodynamic pressure is computed proximately.

- ① The surface of weir is divided into section of (AB), (BC), (CD), and (DE) as shown in Fig. 4.17.
- ② For the upstream face section (AB), the pressure will be approximately represented by a trapezium identical to the hydrostatic pressure represented by Eq. (4.37).

Fig. 4.17 Distribution of hydrodynamic pressure on weir surface



- ③ For the crest curve section (BC), provided well-designed weir, the vacuum pressure or positive pressure exerting on this section is usually small and ignorable.
- ④ For the downstream straight line section (CD), a uniformly distributed normal pressure p may be taken into account as

$$p = \gamma_w d \sin \phi_d \tag{4.40}$$

where d = thickness of the water nappe, m; ϕ_d = included angle between (CD) and vertical line.

- ⑤ For the bucket section (DE), the hydrodynamic pressure force exerting on the bucket is mainly the dynamic force whose horizontal and vertical components may be, respectively, calculated by Eq. (4.41), which is established using momentum equation.

$$\begin{cases} P = \frac{\gamma_w}{g} qv(\cos \theta' - \cos \theta) & \text{Horizontal component, upstream wards} \\ V = \frac{\gamma_w}{g} qv(\sin \theta' + \sin \theta) & \text{Vertical component, down wards} \end{cases} \tag{4.41}$$

where q = unit discharge, $m^3/(s\ m)$; v = average velocity of the flow on bucket, which may be calculated approximately by means of energy equation, m/s; θ = central angle between the lowest point and the upmost endpoint of the bucket, ($^\circ$); θ' = central angle between the lowest point and the lip of the bucket ($^\circ$); g = acceleration of gravity, m/s^2 .

The dynamic forces calculated by Eq. (4.41) are the average portion of hydrodynamic pressure which may be assumed to exert at the middle point of the bucket. By experimental data, the fluctuation component of hydrodynamic pressure is approximately 2.5–5 % of the velocity head; hence, it is usually ignored in the stability and stress analysis of the weir. However, this fluctuation component of hydrodynamic pressure should be taken into account in the design of apron and riprap.

3. Wave pressure

Wind blowing over the reservoir area exerts a drag on the water surface, which in turn pulls the top surface along the direction of wind and thus ripples and waves are formed, which gives rise to additional transient pressure on dam faces. There are three essential parameters of wave as shown in Fig. 4.18: height of wave h (wave height h_p of cumulative frequency p , or average wave height h_m ,

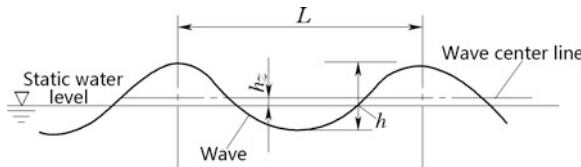


Fig. 4.18 Essential parameters of wave

in empirical formula), wave length L (average wave length L_m in empirical formula), and height h_z of wave center line above still water. In the design of embankment dams and barrages, a term named as average wave period T is also employed corresponding to the average wave length.

Three essential parameters of wave are related to the wind speed, the fetch length of reservoir and the depth of reservoir water: the higher of wind speed, the larger wave it may drag; the longer of the fetch length, the more waves may be superposed into larger wave.

Waves are influenced by water depth in terms of the restraint of reservoir bed: deep waves are not restrained by the reservoir bed when $H_1 > L_m/2$; shallow waves will be restrained by the reservoir bed when $H_k < H_1 < L_m/2$, where H_k is the critical water depth; when $H_1 < H_k$ breaking waves tend to tip over—they break out entirely and run up ashore.

Waves will be terminated on the faces of hydraulic structures such as dams, creating standing waves if the dam face is vertical, which doubles the wave height. Waves also may run up along an inclined dam face attributable to inertia. Both the standing wave and run-up wave will exert wave pressure on the surface, as shown in Figs. 4.19 and 4.21.

Wave pressures are of more importance in their effect upon gates and appurtenances (e.g., piers and parapet walls) as well as low barrages and sluices. However, they are of relatively small magnitude for medium to high dams and even may be neglected. Up to now, most of the wave essential parameters are calculated by using the empirical formulae illustrated hereinafter.

(a) Evaluation of wave essential parameters

- ① Formulae of Guanting Reservoir (China). These formulae are recommended by the SL319-2005 “Design specification for concrete gravity dams,” the SL282-2003 “Design specification for concrete arch dams,” the DL/T5395-2007 “Design specification for rolled earth-rock fill dams,” the SL274-2001 “Design code for rolled earth-rock fill dams,” and are applicable for the inland reservoirs in mountainous areas with fetch length $D < 20$ Km and wind speed $V < 20$ m/s.

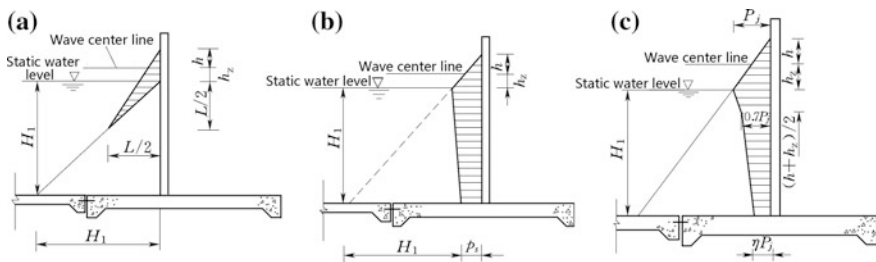


Fig. 4.19 Distribution of wave pressure. a Deep wave; b shallow wave; c breaking wave

$$\frac{gh_p}{V^2} = 0.0076V^{-\frac{1}{12}} \left(\frac{gD}{V^2} \right)^{\frac{1}{3}} \quad (4.42)$$

$$\frac{gL_m}{V^2} = 0.331V^{-\frac{7}{15}} \left(\frac{gD}{V^2} \right)^{\frac{4}{15}} \quad (4.43)$$

$$h_z = \frac{\pi h_p^2}{L_m} \operatorname{cth} \frac{2\pi H_1}{L_m} \quad (4.44)$$

where $h_p = h_{5\%}$ = wave height corresponding to cumulative frequency 5 % when $\frac{gD}{V^2} = 20-250$, m; $h_p = h_{10\%}$ = wave height corresponding to cumulative frequency 10 % when $\frac{gD}{V^2} = 250-1000$, m; L_m = average wave length, m; V = annual maximum wind speed 10 m above the reservoir surface and averaged in 10 min duration, m/s; D = fetch length of the reservoir, km; H_1 = reservoir depth in front of dam, m.

The relationship between the wave height h_p corresponding to cumulative frequency p (%) and the average wave height h_m is listed in Table 4.1, in which H_m is the average water depth along the wind direction, m.

The average wave length L_m and average wave period T_m can be conversed using Eq. (4.45).

$$L_m = \frac{gT_m^2}{2\pi} \operatorname{th} \frac{2\pi H_1}{L_m} \quad (4.45)$$

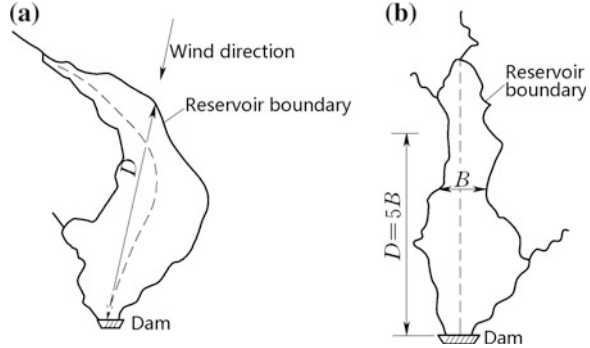
For deepwater wave, i.e., $H_1 \geq 0.5L_m$, Eq. (4.45) may be simplified as

$$L_m = \frac{gT_m^2}{2\pi} \quad (4.46)$$

Table 4.1 Ratio h_p/h_m

$\frac{h_m}{H_m}$	p (%)									
	0.1	1	2	3	4	5	10	13	20	50
0	2.97	2.42	2.23	2.11	2.02	1.95	1.71	1.61	1.43	0.94
0.1	2.70	2.26	2.09	2.00	1.92	1.87	1.65	1.56	1.41	0.96
0.2	2.46	2.09	1.96	1.88	1.81	1.76	1.59	1.51	1.37	0.98
0.3	2.23	1.93	1.82	1.76	1.70	1.66	1.52	1.45	1.34	1.00
0.4	2.01	1.78	1.68	1.64	1.60	1.56	1.44	1.39	1.30	1.01
0.5	1.8	1.63	1.56	1.52	1.49	1.46	1.37	1.33	1.25	1.01

Fig. 4.20 Definition of wind fetch D . **a** General case; **b** long and narrow reservoir



The critical water depth of wave breaking H_k is

$$H_k = \frac{L_m}{4\pi} \ln \frac{L_m + 2\pi h_p}{L_m - 2\pi h_p} \tag{4.47}$$

The wind fetch D is the maximum straight distance from the dam to the opposite reservoir bank (Fig. 4.20a). If the reservoir is very long and narrow, D is calculated as 5 times of the reservoir width (Fig. 4.20b).

- ② Formulae of Hedi Reservoir (China). These formulae are recommended by the SL319-2005 “Design specification for concrete gravity dams,” SL274-2001 “Design code for rolled earth-rock fill dams,” DL/T5395-2007 “Design specification for rolled earth-rock fill dams,” and are applicable for the deep reservoirs in hilly and plain regions with fetch length $D < 7.5$ km and wind speed $V < 26.5$ m/s.

$$\frac{gh_p}{V^2} = 0.00625V^{\frac{1}{6}} \left(\frac{gD}{V^2} \right)^{\frac{1}{3}} \tag{4.48}$$

$$\frac{gL_m}{V^2} = 0.0386 \left(\frac{gD}{V^2} \right)^{\frac{1}{2}} \tag{4.49}$$

where $h_p = h_{2\%}$ = wave height corresponding to cumulative frequency 2 %, m.

- ③ Formulae of Putian Experiment Station (China). These formulae are recommended by the SL274-2001 “Design code for rolled earth-rock fill dams,” the DL/T5395-2007 “Design specification for rolled earth-rock fill dams,” the SL319-2005 “Design specification for concrete gravity dams,” and SL265-2001 “Design specification for sluice” and are applicable for the reservoirs in plain and coastal areas.

$$\frac{gh_m}{V^2} = 0.13 \operatorname{th} \left[0.7 \left(\frac{gH_m}{V^2} \right)^{0.7} \right] \operatorname{th} \left\{ 0.0018 \left(\frac{gD}{V^2} \right)^{0.45} / 0.13 \operatorname{th} \left[0.7 \left(\frac{gH_m}{V^2} \right)^{0.7} \right] \right\} \quad (4.50)$$

$$\frac{gT_m}{V} = 13.9 \left(\frac{gh_m}{V^2} \right)^{1/2} \quad (4.51)$$

where h_m = average wave high, m; T_m = average wave period, s; and H_m = average water depth along the wind direction, m.

(b) Computation of wave pressure

- ① Arch dams. For deepwater wave ($H_1 > \frac{L_m}{2}$), the wave pressure can be determined as (Vide Fig. 4.19a)

$$P_L = \frac{\gamma_w \left(\frac{L_m}{2} + h_p + h_z \right) \frac{L_m}{2}}{2} - \frac{\gamma_w \left(\frac{L_m}{2} \right)^2}{2} \quad (4.52)$$

Equation (4.52) can be simplified as follows:

$$P_L = \frac{\gamma_w L_m}{4} (h_m + h_z) \quad (4.53)$$

where $h_p = h_{5-10\%}$ (for arch dam only).

For shallow wave ($H_k < H_1 < L_m/2$), the wave pressure can be determined as (Vide Fig. 4.19b)

$$P_L = \frac{\gamma_w (H_1 + h_p + h_z) \left(H_1 + \frac{p_s}{\gamma_w} \right)}{2} - \frac{\gamma_w H_1^2}{2} \quad (4.54)$$

Equation (4.54) can be simplified as follows:

$$P_L = \frac{1}{2} \left[(h_p + h_z) (\gamma_w H_1 + p_s) + H_1 p_s \right] \quad (4.55)$$

In which p_s is the intensity of residual wave pressure of the following:

$$p_s = \gamma_w h_p \operatorname{sech} \frac{2\pi H_1}{L_m} \quad (4.56)$$

Inclined dam face will weaken the reflection of wave. Generally, if the inclination angle of the face is greater than 45° , the wave are considered identical to that with vertical face; whereas the inclination angle of the face of is smaller than 45° , the pressure is calculated in terms of run-up wave similar to embankment dams, which will be presented later.

Table 4.2 Cumulative frequency p (%) of wave train for barrages or sluices

Grade of barrages or sluices	1	2	3	4	5
p (%)	1	2	5	10	20

- ② Gravity dams. The wave pressure is calculated using Eqs. (4.52)–(4.56), in which $h_p = h_1\%$.
- ③ Barrages and sluices. First, the cumulative frequency p (%) of wave train is selected using Table 4.2.

Then according to the average wave height h_m and cumulative frequency p (%), the corresponding wave height h_p is obtained using Table 4.1.

For deep wave ($H_1 \geq H_k, H_1 \geq L_m/2$), the wave pressure pattern is shown in Fig. 4.19a and the corresponding wave pressure is calculated using Eq. (4.53).

For shallow wave ($H_1 \geq H_k, H_1 > L_m/2$), wave pressure pattern is shown in Fig. 4.19b, and the corresponding wave pressure is calculated using Eq. (4.55).

For breaking wave ($H_1 < H_k$), wave pressure pattern is shown in Fig. 4.19c, and the corresponding wave pressure is calculated using Eqs. (4.57)–(4.58).

$$P_L = \frac{1}{2}P_j[(1.5 - 0.5\eta)(h_p + h_z) + (0.7 + \eta)H_1] \tag{4.57}$$

$$P_j = K_i\gamma_w(h_p + h_z) \tag{4.58}$$

where P_j = intensity of wave pressure, kN/m²; η = reduction coefficient of the wave pressure at the bottom of gate, $\eta = 0.5$ for $H_1 > 1.7(h_p + h_z)$, otherwise $\eta = 0.6$; K_i = influence coefficient of the riverbed sloping in front of gate which is listed in Table 4.3, where i is the average sloping of the riverbed in front of gate.

- ④ Embankment dam. The SL274-2001 “Design code for rolled earth-rock fill dams” and the DL/T5395-2007 “Design specification for rolled earth-rock fill dams” recommend Eq. (4.59) to evaluate the height h_z of the wave central line over the still water surface:

$$h_z = \frac{KV^2D}{2gH_m} \cos \beta \tag{4.59}$$

Table 4.3 Influence coefficient K_i of the riverbed sloping in front of gate

i	1/10	1/20	1/30	1/40	1/50	1/60	1/80	$\leq 1/100$
K_i	1.89	1.61	1.48	1.41	1.36	1.33	1.29	1.25

where $K = 3.6 \times 10^{-6}$ is a comprehensive friction and resistance coefficient; $\beta =$ included angle between wind direction and the normal of dam axis, ($^\circ$).

The cumulative frequency of the run-up height of design wave is selected according to the embankment grade: a run-up height $R_{1\%}$ corresponding to the cumulative frequency 1 % is stipulated for the dams of grade 1, 2, and 3; a run-up height $R_{5\%}$ corresponding to the cumulative frequency 5 % is stipulated for the dams of grade 4 and 5.

Denote m as the coefficient of slope, the average run-up height R_m is calculated by Eqs. (4.60) and (4.61).

When $m = 1.5-5.0$

$$R_m = \frac{K_\Delta K_w (h_m L_m)^{\frac{1}{2}}}{(1 + m^2)^{\frac{1}{2}}} \tag{4.60}$$

where $R_m =$ average wave run-up, m; $K_\Delta =$ coefficient related to the roughness and permeability of dam slope protection (see Table 4.4); $K_w =$ empirical coefficient (see Table 4.5).

When $m \leq 1.25$

$$R_m = K_\Delta K_w R_0 h_m \tag{4.61}$$

where $R_0 =$ unit wave run-up height for smooth and impervious slope ($K_\Delta = 1$) when $h_m = 1$ m, which is selected according to Table 4.6.

The run-up height R_p corresponding to the cumulative frequency p is calculated according to R_m using Table 4.7.

Table 4.4 Coefficient K_Δ versus dam slope revetment

Dam slope revetment type	K_Δ	Dam slope revetment type	K_Δ
Smooth and impervious (e.g., asphalt concrete)	1.0	Double-layered tipping stone rubble (on impervious base)	0.6-0.65
Concrete or concrete slab	0.9	Double-layered tipping stone rubble (on pervious base)	0.5-0.55
Stone pitching	0.75-0.8	Turf revetment	0.85-0.9

Table 4.5 Empirical coefficient K_w

$\frac{V}{\sqrt{gH_1}}$	≤ 1	1.5	2.0	2.5	3.0	3.5	4.0	≥ 5
K_w	1.0	1.02	1.08	1.16	1.22	1.25	1.28	1.30

Table 4.6 Unit wave run-up height R_0

m	0	0.5	1.0	1.25
R_0	1.24	1.45	2.20	2.50

N.B. In case of $1.25 < m < 1.5$, R_m is interpolated using the results of $m = 1.25$ and $m = 1.5$ in the table

Table 4.7 Distribution of statistical wave run-up height $\frac{R_p}{R_m}$

$p\%$	0.1	1	2	4	5	10	14	20	30	50
h_m/H_1										
<0.1	2.66	2.23	2.07	1.90	1.84	1.64	1.53	1.39	1.22	0.99
0.1–0.3	2.44	2.08	1.94	1.80	1.75	1.57	1.48	1.36	1.21	0.97
>0.3	2.13	1.86	1.76	1.65	1.61	1.48	1.39	1.31	1.19	0.96

Wave pressure exerting on embankment dam slope has a distribution pattern shown in Fig. 4.21. At point Z, the maximum intensity p_z (kN/m²) is computed by means of

$$p_z = K_p K_1 K_2 K_3 \gamma_w h_s \tag{4.62}$$

where h_s = effective wave height, where $h_{14\%}$ is customarily employed, m ; L_m = average wave length, m ; m = slope ratio, $m = \text{ctg}\alpha$, α = grading angle; $K_p = 1.35$, frequency scale factor; and coefficients K_1 , K_2 , and K_3 are calculated employing Eq. (4.63), Tables 4.8 and 4.9.

$$K_1 = 0.85 + \left(4.8 \frac{h_s}{L_m}\right) + m \left[0.028 - 1.15 \left(\frac{h_s}{L_m}\right)\right] \tag{4.63}$$

Fig. 4.21 Wave pressure exerting on embankment dam slope

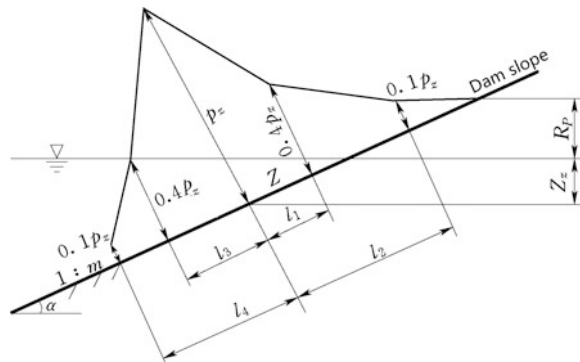


Table 4.8 Coefficient K_2

L_m/h_s	10	15	20	25	35
K_2	1.0	1.15	1.30	1.35	1.48

Table 4.9 Coefficient K_3

Effective wave height h_s (m)	0.5	1.0	1.5	2.0	2.5	3.0	3.5	>4
K_3	3.7	2.8	2.3	2.1	1.9	1.8	1.75	1.7

The vertical height Z_z of the point Z under water level, as well as the length l_1-l_4 in Fig. 4.21, are all calculated by Eqs. (4.64) and (4.65). Where the calculated Z_z is negative, $Z_z = 0$ is assumed.

$$\begin{cases} Z_z = A + \frac{1}{m^2} (1 - \sqrt{2m^2 + 1})(A + B) \\ A = h_s \left[0.47 + 0.023 \frac{L_m}{h_s} \right] \left(\frac{1+m^2}{m^2} \right) \\ B = h_s \left[0.95 - (0.84m - 0.25) \frac{h_c}{L_m} \right] \end{cases} \quad (4.64)$$

$$\begin{cases} l_1 = 0.0125S \\ l_2 = 0.0325S \\ l_3 = 0.0265S \\ l_4 = 0.0675S \\ S = \frac{mL_m}{\sqrt{4m^2 - 1}} \end{cases} \quad (4.65)$$

4. Ice pressure

The ice pressure may be static or dynamic.

It is well known that water on cooling below 4 °C expands in volume until it freezes at 0 °C. It shrinks on further cooling, as other solid materials do. During the night or any other low-temperature period, ice sheet cools and shrinks manifesting cracks that get immediately filled with water. This water solidifies and makes the ice sheet again continuous. As soon as temperature rises during the day, the ice expands and exerts pressure against dams and barrages, which is named as static ice pressure. The static ice pressure depends on the initial ice temperature, ice temperature mounting rate, and amount as well as duration, and the degree of restraint imposed around the perimeter of the ice sheet (e.g., reservoir banks).

The dynamic ice pressure is resulted from the impact of ice block or iceberg moving toward the dam and barrage in a nearly perpendicular direction. Its magnitude is related to the volume, the velocity and so on, of the ice block.

If a reservoir is located in the chilly area, ice pressure can be important under the circumstances where ice sheets form to appreciable thickness and persist for long periods. The design of hydraulic structures, especially of those like piers, parapet walls, gates, sluices, barrages, and slope revetments of embankment, should make allowance for the ice pressure.

(a) Static ice pressure

An acceptable initial provision for static ice pressure is for ice thickness in excess of 0.4 m. Where ice thickness is unlikely to exceed 0.4 m and/or will be subject to little restraint, and static ice pressure may be neglected. The DL5077-1997 “Specifications for load design of hydraulic structures,” the DL/T5082-1998 “Design specifications of hydraulic structures against ice and freezing action,” and the SL211-2006 “Code for design of hydraulic structures against ice and freezing action” stipulate standard values of static ice pressure exerting on the unit length of dam face, as listed in Table 4.10.

Table 4.10 Standard value of static ice pressure

Thickness of ice sheet (m)	0.4	0.6	0.8	1.0	1.2
Standard value of static ice pressure (kN/m)	85	180	215	245	280

NB. The thickness of ice sheet in Table 4.10 is a mean of annual maximum value. For small reservoirs, the static ice pressure in Table 4.10 is reduced by a fraction of 0.87; for the reservoirs in vast plain, the static ice pressure in Table 4.10 is amplified by 1.25

Researches on ice pressure commenced in the 1960s in China, and a series of methods had been proposed. However, it should be borne in mind that there are at least 10 % error between the calculation results using these existing methods and the field data.

Usually, the structures vulnerable to static ice pressure damage are protected by the countermeasures such as ventilating compressed air to the water in front of the structure concerned.

(b) Dynamic ice pressure

The DL5077-1997 “Specifications for load design of hydraulic structures,” the DL/T5082-1998 “Design specifications of hydraulic structures against ice and freezing action,” and the SL211-2006 “Code for design of hydraulic structures against ice and freezing action” stipulate that:

- ① Standard value of dynamic ice pressure exerting on a unit length of vertical and flat dam face is determined by Eq. (4.66)

$$F_{bk} = 0.07vd_i \cdot \sqrt{A \cdot f_{ic}} \quad (4.66)$$

where F_{bk} = standard value of dynamic ice pressure, MN; v = velocity of drift ice block, m/s; d_i = thickness of drift ice block, m; A = area of drift ice block, m^2 ; and f_{ic} = compressive strength of ice, MPa.

The parameters and quantities in Eq. (4.66) should be evaluated by field data. Where there are no such data available, they may be estimated as follows:

v —For rivers or canals, v may be identical to the velocity of flow; for reservoirs, v may be 3 % of the maximum wind speed during ice drift period, and less than 0.6 m/s; for ice pass works, v may be the approach velocity.

d_i —it is 0.7–0.8 times of the maximum ice sheet, of which the superior bound is for the initial period of ice drift.

f_{ic} —0.3 MPa for reservoir drift ice; 0.45 MPa for river drift ice at initial stage and 0.3 MPa at later stage.

These enumerated values are obtained by the comprehensive analysis using domestic field data of China solely, which are close to the design specifications of former USSR, but 1–3 times lower than the corresponding specifications of USA and Canada.

- ② Standard value of dynamic ice pressure exerting on vertical and independent triangular pier is calculated and selected as the minimum by Eqs. (4.67) and (4.68)

$$F_{p1} = m f_{ib} b d_i \quad (4.67)$$

$$F_{p2} = 0.04 v d_i \sqrt{m A f_{ib} t g \gamma} \quad (4.68)$$

where F_{p1} = standard value of dynamic ice pressure when ice is extruded through pier, MN; F_{p2} = standard value of dynamic ice pressure when ice strikes at pier, MN; $m = 0.54-1.0$, the cross-sectional coefficient of pier; f_{ib} = extrusion strength of ice, which is 0.75 Mpa for the initial stage of ice drift period and 0.45 Mpa for the later stage of ice drift period; b = front width of pier at the elevation where drift ice impacts, m; and γ = half of triangle interior angle.

5. Action of high-speed water flow

Generally, high-speed flow is roughly defined as $v > 16-18$ m/s, when phenomena such as cavitation, aeration, fluctuation, and shock wave might appear. The characteristics of high-speed flow are high Froude number and Reynolds number, strong turbulence, and sensitive to boundary condition (Gatski and Bonnet 2009).

As a very useful index for the high-speed flow in the design of hydraulic structures, the ratio of inertial and gravitational forces of streamlined kinetic flow in an open channel can be expressed by the Froude number as

$$F_r = \frac{v}{\sqrt{gh}} \quad (4.69)$$

where v = average velocity at the channel section, m/s; h = average depth at the channel section, m.

(a) Cavitation

It is well known that under normal air pressure (101.3 kN/m²), the vaporizing temperature of water is 100 °C. This vaporized temperature will decrease as the decrease of air pressure. Cavitation may manifest when the local static pressure in water reach a level below its vaporization pressure dependent on the actual temperature. The vaporization itself does not cause the damage—the damage only happens when the vapor almost immediately collapses after the evaporation, when the flow velocity is reduced and pressure is raised on the solid boundaries. Cavitation is a significant scenario of wear in some hydraulic structures. When entering high-pressure areas, cavitation bubbles that implode on a structure surface cause cyclic impaction. This results in surface fatigue of the material in a type of wear called “cavitation corrosion,” or “cavitation damage,” or briefly “cavitation.” Therefore, cavitation is a flow

phenomenon, whereas cavitation corrosion is a damage type of hydraulic structures (Brown 1963; Knapp et al. 1970).

The cavitation number or cavitation parameter is a “special edition” of the dimensionless Euler number, which is only dependent on the characteristics of flow and can be expressed as follows:

$$\sigma = \frac{(P_0 - P_v)/\gamma_w}{V_0^2/2g} \quad (4.70)$$

where σ = cavitation number; P_0 = reference pressure (Pa); P_v = vapor pressure of the water (Pa); γ_w = specific weight of the water (kg/m^3); and V_0 = velocity of water (m/s).

The critical cavitation number σ_i is dependent on both the flow characteristics and boundaries of the structure, which is usually obtained experimentally. Then the judgment may be made that where $\sigma > \sigma_i$, there is no cavitation and, if $\sigma < \sigma_i$, cavitation manifests.

The locally lower or even negative pressure is easily triggered at the portions where the boundary wall curves sharply, therefore the cavitation corrosion is very likely to emerge on the spillway face, the downstream straight portion of flip bucket, the side face of slotted roller bucket, the top face of deep outlet and tunnel intake, the tip of branch pipe, the downstream portion of gate slot, the downstream portion of slope variation and local protuberance. Countermeasures for prevention of cavitation damage are improving the surface finishes, protecting the surface by streamlining the boundaries, using cavitation resistant materials or coatings, installing aerators (or aeration devices) to introduce air in the water for damping the strong impaction pressure induced by the bubble collapse, etc.

(b) Aeration

High velocity water with a water/air interface eventually draws a part of the air into the water, forming a kind of water–air mixture as two-phase flow. This phenomenon often appears where water flowing in spillway chutes or overflows dam faces. The air concentration in water is dependent on the flow velocity, water depth, and surface roughness of the structure. Aeration can be distinguished as self-aeration and artificial aeration (Chanson 1989).

Self-aeration means the aeration without the triggering of boundary or sudden change in the flow. As the flow progresses, the surface becomes more and more rough, the transparency of the flow gradually and continuously diminishes till atmospheric air is insufflated, diffused, and dispersed into the flow. This type of air entrainment is of engineering interest in designing of chutes and stilling basins, where the entrained air influences on the velocity, flow depth, energy dissipation, turbulence, and other characteristics of the flow.

Artificial aeration is triggered by the gate slot, the pier, the drop sill and upgrade sill, the hydraulic jump vortex, or the two streams converge, where the broken of original flow state induces strong local fluctuation. For example,

the vortex could be sucked into flood discharge tunnel where the water depth is insufficient, which will give rise to an artificial aeration.

The physical characteristics on aerated water are changed when the air is entrained. It can mitigate the cavitation when aeration appears between the flow and solid boundary. It can also strength the energy dissipation as well as reduce the scouring on riverbed. Aerators are commonly installed at the spillway chute or tunnel and overflow dam, which supply air to cavitation ridden zones by means of artificial aeration. However, aeration gives rise to swelling of water flow which demands higher sidewall for an open channel spillway and higher sealing for closed outlets. Filling the outlet sectional area with water–air mixture reduces the discharge capacity and affects the flow stability.

The calculation on the clearance (headroom) margin or freeboard for tunnel spillway or open channel is given by the corresponding design specifications. The aerated water depth h_a for the sidewall of spillway chute should be based on the streamline calculation and/or be determined by the model test for a complex structure and may be approximately evaluated by:

$$h_a = h \left(1 + \frac{\xi v}{100} \right) \quad (4.71)$$

where v = average flow velocity of the cross section; $\xi = 1.0$ – 1.4 , the revision coefficient selected according to the velocity and the shrinkage of the cross section, and the upper bound is recommended for the flow with $v > 20$ m/s. It should be 15–20 % of headroom or clearance above the aerated flow in tunnel to ensure free flow inside. Sometimes, the intermediate air vents might be required for a long tunnel.

(c) Turbulent fluctuation

Fluctuation means that the velocity and pressure vary rapidly along the time, which is induced by external factors such as wave or internal factors such as turbulent (Kang et al. 2009). The pulsation pressure is an important parameter in the research on high velocity flow, whose dynamic force on the flow boundary of structures may result in following adverse effects:

- ① Vibration. When water flow passes through a stationary boundary wall at high velocity and the frequency of pulsation pressure approaching the natural frequency of thin and high structures such as the gate pier, the sidewall of spillway and stilling basin, and the power house roof, resonance vibration may occur which could be hazardous to the structures. Usually, the most dangerous pulsation frequency is the lowest basic frequency which contains larger fluctuation energy. One of the successful practices against the fluctuation-induced resonance vibration is the Wujiangdu power plant with a 5-m-thick roof as the bottom of spillway chute: field observations recorded that with the maximum vibration

displacement $8.99 \mu\text{m}$ in vertical direction on the powerhouse roof during flood releasing.

- ② Negative pressure. Pulsation pressure cyclic varies between positive to negative bounds. When such negative pressure exceeds the averaged pressure, instantaneous negative pressure manifests. Repeated negative pressure may result in cavitation damage to the structures. This often occurs at the portion with high speed, small pressure, and large fluctuation (e.g., the end of chute, the convex deflection portion of sidewall, and the upstream end of still basin floor).
- (d) Shock wave
- Shock waves are the interference waves (cross-waves and standing waves) of high-speed flow induced by the boundary changes in the section (Jan et al. 2009). Where the sidewall contraction, the water tends to pile up which is named as positive shock waves; on the contrary, the expansion sidewall creates negative shock waves. Their main consequence is that they require an increased freeboard and higher chute sidewall. The waves may also create additional flow fluctuation and unevenness in sectional velocity distribution, which in turn increase the difficulties associated with energy dissipation. Shock waves are stationary whose position depends on the discharge and whose height depends on the Fraude number, the deflection angle of sidewalls, the initial water depth, etc.
- (e) Atomization

As the main types of energy dissipation for high dams, the flow discharging by flip bucket or free fall often causes atomization, whose hazardous effects are increasingly becoming noticed (Liu et al. 2012).

Discharging atomization is a process that the jet flow traps the air and mixes with it during flying, dispersing, and splashing. The atomization affected area may be divided into three zones: the zone of atomization source by flow splashing, raining zone, and spray flying zone.

The normal operation and safety of hydraulic structures could be seriously affected by the atomization, if a heavy rain covers the river reach as well as the banks, which may give rise to problems on the communication, the electric device operation, and the stability of bank slopes. It could also cause ice problems on the transmission line and on the road transportation in the winter in chilly regions.

A typical example is provided by the Huanglongtan Project which employs differential flip buckets. During the period of flood releasing in 1980, a strong atomizing rain covered the whole power plant area. As a result, the 3.9 m deep water inundated the power plant, and the shock circuit occurred on high tension line, and the power generator units had to stop operating for 49 h.

The heavy rain by atomization can cause landslide in draught area in the northwestern China. For example, the landslide body in the Longyangxia Project moved fast after the flood releasing operating, and additional slope cutting and strengthening measures had to be taken. In another example, the

outdoor temporary switchyard was menaced by loose stones carried by splashing water in the Baishan Project.

Although the mathematical and physical models used in the study may be helpful to understand atomization mechanism, they usually provide poor quantified results for definite projects. Therefore insofar, field observation is the main manner in the study on atomization, and it is advisable to pay following provisions in the design of hydraulic project:

- Jet flow should be conducted to river reach and certain margin should be kept properly because of strong dispersing in prototype than that in the physical model.
- It is very difficult to establish the relationship between rainfall strength and flood discharge. Some experiences from sites are that it will have minor affection on the communication when rainfall strength is less than 100 mm/h except for landslide or unstable rock mass, whereas it will feel difficulties in walking or driving when the rainfall is 100–300 mm/h.
- Protecting measures and proper arrangements should be taken on access roads, buildings, and electric devices. The buildings and electric devices should be kept far away from the strong atomization area; the roads should be paved by concrete or asphalt and a good drainage system is demanded; the access entrances are not located where the rainfall is anticipated in excessive of 300–1000 mm/h; the banks must be protected by concrete lining or concrete shotcrete and a drainage system is also required with sufficient drainage capacity.
- The stilling basin for energy dissipation is recommended if some important buildings and electric devices are not able to be kept away from the strong atomization area.

6. Erosion and protection for hydraulic structures

The rise of head by dams accumulates huge energy in reservoir, which is desirably transferred into electric energy. However, in a flood season where the spare water should be released by spillways, the kinetic energy in the discharged flow would result in server damage to the downstream riverbed and banks, if there are no proper engineering countermeasures to dissipate the energy. The principle of energy dissipation is to kill the kinetic energy of discharged flow by vortex, turbulence, and friction, which transfer kinetic energy into heat and sound energy.

In a natural river channel, the flow velocity along the depth is logarithmically distributed; at the riverbed, the velocity is small and the velocity gradient is large. When the average velocity increases to some extend, the turbulence is stronger enough which on the one hand dissipates energy through the water–solid wall friction and on the other hand transfers vortex upward and dissipates energy through the Reynolds shear stress. These mechanisms of energy dissipation needs long distance to slow down the flow velocity for joining the downstream natural flow. Therefore, it is necessary to form a specified energy

dissipation regime using engineering structures, in which the strong vortex and blending may quickly dissipate the spare energy.

Energy dissipation structures fall into internal and external types (Elevatorsky 1959), depending on whether they dissipate energy within or on the structure surfaces. Internal energy dissipation may be implemented as stepped energy dissipation, energy dissipation of flaring pier, orifice/plate energy dissipation, and vortex flow energy dissipation through shaft inlet. External energy dissipation is commonly carried out at a portion downstream of the spillways, including bottom-flow dissipation through hydraulic jump, free fall into plunge pool, flip trajectory bucket, rolling or surface current energy dissipation through submerged bucket dissipator.

On the downstream riverbed behind the energy dissipation works where the outflow velocity is still fairly high enough, the erosion of soil or rock would give rise to river scouring. Different soil and rock has different scouring velocity. The most vulnerable portions are the end of apron, the starting of upstream blanket, the end of guide wall, etc. As the on going of scouring, riverbed depth increases and average flow velocity decreases, until a stable state of the riverbed is reached.

Concrete or steel-concrete lining should be installed to protect the portion of very high-flow speed with strong scouring force, such as the still basin and plunge pool. The cement-rubble masonry and dry-rubble masonry protection may be employed for the portion of relatively lower flow speed. The details in the consideration of the erosion and protection for hydraulic structures will be introduced in the corresponding chapters of this book.

4.6 Seismic Actions

Since earthquake generates undesirable dynamic actions to hydraulic structures, it must be considered in the design of hydraulic structures situated in high-risk seismic regions (ICOLD 1975). The seismic action comprises of seismic inertia force, seismic dynamic water pressure, and seismic dynamic earth pressure. The influences of earthquake on the uplift, the silt pressure, and the wave pressure are commonly ignored.

Seismic action is dependent on the intensity of ground shaking and the dynamic response of hydraulic structures (Severn 1976a, b; Chopra 1987; Chopra and Chakrabarti 1981; ICOLD 1989, 2013). The disastrousness of an earthquake is ordinarily indicated using Mercall scale intensity. The basic intensity is the maximum earthquake intensity likely encountered in the coming period, 50 years with exceedance probability 0.10 for example, in the work site. It is usually provided by the official document of the State Seismic Bureau in China, for example, the “Chinese seismic intensity zoning map (1990).” The design intensity is the earthquake intensity adopted in the practical aseismic design. Generally, the design

Table 4.11 Aseismic and fortifying design classification

Aseismic and fortifying design class	Importance grade of structures	Basic intensity of work site
1	1 (water retaining)	≥6
2	1 (non-water retaining), 2 (water retaining)	
3	2 (non-water retaining), 3	≥7
4	4, 5	

intensity is equal to the basic intensity. However, if a hydraulic structure is of particular importance or in a special situation, the design intensity can be raised adequately above the basic intensity. If the hydraulic structure is highly important and is located in an area where the earthquake intensity is higher than the 9, special researches should be carried out. On the contrary, the earthquake action may be overlooked when the basic intensity is lower than 6.

In China, the aseismic and fortifying design classification of hydraulic structures is stipulated according to their importance and base intensity, which is listed in Table 4.11.

The pseudo-static method, that conducts the static analysis by using the results of dynamic analysis indirectly, is customarily employed to calculate earthquake inertia forces in the design of hydraulic structures. The inertia forces are calculated in terms of the maximum acceleration selected for design and considered as equivalent to additional static loads. This approach, sometimes is referred to as the equivalent static load method, is generally conservative. It is therefore now applied only to small and less vulnerable concrete dams, or for the purposes of preliminary analysis. For high dams, or dams under situations where seismicity is considered critical, more sophisticated procedures, such as dynamic analysis method for example, are required (ICOLD 2001, 2002). According to the DL 5073-2000 “Specifications for seismic design of hydraulic structures”: For the hydraulic structures of aseismic and fortifying design class 1, seismic action should be calculated by the dynamic analysis method; for the hydraulic structures of aseismic and fortifying design classes 2 and 3, seismic action may be calculated by either the dynamic analysis method or the pseudo-static method; for the hydraulic structures of aseismic and fortifying design class 4, seismic action may be calculated by the pseudo-static method only. In the following, the pseudo-static method will be illustrated while the dynamic analysis method will be presented in Chap. 5 of this book.

4.6.1 Earthquake Inertia Force

Where a dam is situated in the region liable to moderate earthquake shake, it will be sufficient to take the acceleration in one direction either horizontally (upstream or/

Table 4.12 Standard value of horizontal earthquake acceleration a_h

Design intensity	7	8	9
a_h (g)	0.1	0.2	0.4

and downstream) or vertically (upward or/and downward). Where the region is liable to severe damage, both horizontal and vertical accelerations should be taken into account simultaneously.

Similar to the self weight, the effect of the earthquake inertia on a mass element i should be applied at its centroid. The inertia force in the horizontal direction can be determined as follows:

$$F_i = a_h \zeta G_{Ei} \alpha_i / g \quad (4.72)$$

where F_i = standard value of the horizontal earthquake inertia force of the mass element i , kN; $g = 9.81 \text{ m/s}^2$ (gravity acceleration); G_{Ei} = weight of the mass element i , kN; a_h = standard value of the horizontal earthquake acceleration, (Table 4.12); $\zeta = 0.25$ (comprehensive influencing coefficient); and α_i = dynamic distribution coefficient at the mass element i .

If the “slice method” is applied for the stability analysis (See Chap. 5), particularly in the cut slopes, the effect of inertia on the slice i is supposed to be applied at its centroid in horizontal direction and is determined by

$$F = K_c W \quad (4.73)$$

where W = weight of the i th slice mass, kN; K_c = earthquake coefficient calculated by

$$K_c = a_h \zeta \alpha_i / g \quad (4.74)$$

where α_i = dynamic distribution coefficient of the slice i , usually $\alpha_i = 1.0$, but for important high slopes α_i should be specially justified.

The comprehensive influencing coefficient ζ is installed to bridge the gap between the calculated results and the actual earthquake damages. This gap is mainly resulted from the fact that the model and parameters used in the calculation are based partly on the experiences. In addition, it is understandable that the pseudo-static method is not able to fully reflect the dynamic response and failure characteristics of the hydraulic structures.

If the vertical earthquake inertia force is wanted, the standard value of horizontal earthquake acceleration in Eq. (4.72) should be replaced by the vertical one, and $a_v = \frac{2}{3} a_h$. The vertical and horizontal earthquake inertia forces are postulated to exert either independently or simultaneously. In the later case, as the likelihood of the maximum earthquake inertia forces occurring simultaneously is small, a fraction coefficient of 0.5 should be multiplied to the vertical earthquake inertia force firstly, and then the combination of horizontal and vertical earthquake inertia forces is processed.

For a dam with reservoir full, the most disastrous earthquake effect is resulted when the earthquake is directed to upstream and perpendicular to the dam axis, whereas for empty reservoir the most dangerous earthquake direction is directed toward downstream. For any direction intermediate between the horizontal and vertical, the computation would be complicated. For the case of minor deviation from the horizontal, the earthquake effect is slightly greater than the horizontal acceleration. However, the difference is so small that it is not worth considering in view of the uncertainty involved in estimating the value of earthquake acceleration a .

The dynamic distribution coefficient α_i of the mass element i in Eq. (4.72) can be obtained by consulting the distribution diagram related to the height of the mass element i , which is based on a large quantity of dynamic analysis regarding various structure types and heights.

1. Gravity dams

$$\alpha_i = 1.4 \frac{1 + 4(h_i/H)^4}{1 + 4 \sum_{j=1}^n \frac{G_{Ej}}{G_E} (h_j/H)^4} \tag{4.75}$$

where n = number of mass elements representing blocks of dam monolith; H = dam height, m; h_i, h_j = height of the mass element i and j , m; G_E = standard value of total weight of dam, kN; G_{Ej} = standard value of the weight of the block represented by the mass element i , kN.

2. Arch dams

The horizontal earthquake inertia force for the mass element i representing a certain block of concrete is assumed to be in the radial direction and uniformly distributed along the arch ring. Linear variation along the dam height is assumed, which is $\alpha_i = 3.0$ at the dam crest and $\alpha_i = 1.0$ at the dam base.

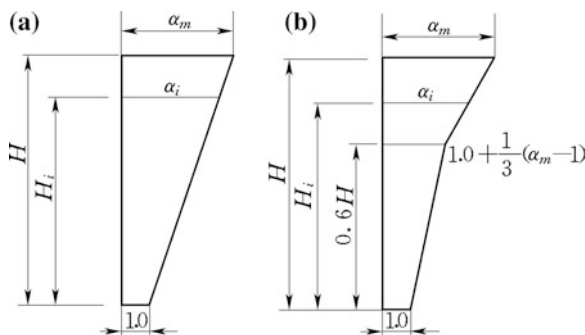
3. Embankment dams

The distribution of α_i is shown in Fig. 4.22, in which α_m is the dynamic distribution coefficient at dam crest. $\alpha_m = 3.0, 2.5,$ and 2.0 corresponding to the design earthquake intensity 7, 8, and 9, respectively.

4. Barrages and sluices

The distribution of α_i is shown in Fig. 4.23.

Fig. 4.22 Dynamic distribution coefficient α_i for embankment dams. **a** Dam height $H \leq 40$ m; **b** dam height $H > 40$ m



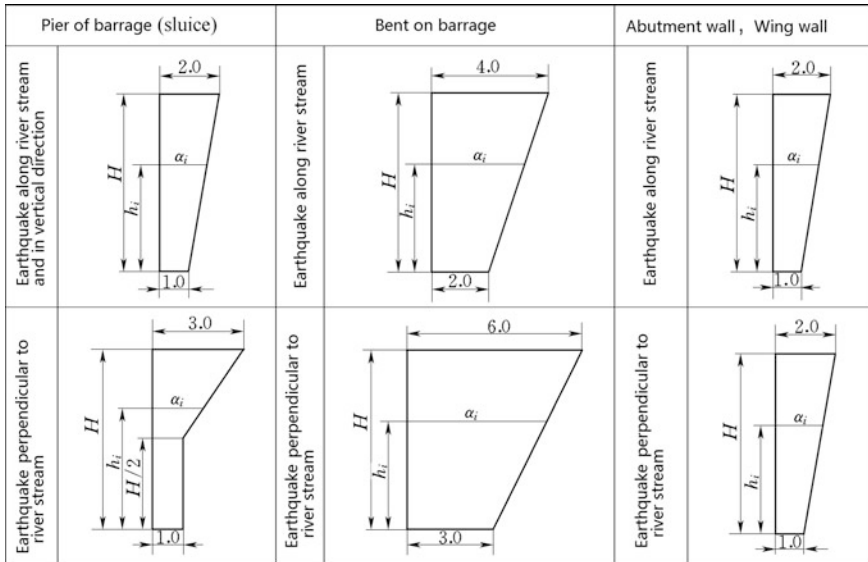


Fig. 4.23 Dynamic distribution coefficient α_i for barrages and sluices

5. Rock slopes

The DL 5073-2000 “Specifications for seismic design of hydraulic structures” does not stipulate the dynamic distribution coefficient α_i for rock slopes, although a dynamic distribution coefficient larger than one is often revealed by dynamic analysis. For example, the Xiaowan Project with an arch dam of 294.5 m high and installed generation capacity of 4200 MW is located at the up reach of the Lanchangjiang River (Yunnan Province, China). The intake slope of 106 m high and 300 m wide of the power tunnel is excavated in sound gneiss rock. Using El Centro earthquake (MC = 7.2, California, USA, 1940) N–S wave (duration = 10 s) and the Mercalli intensity of the earthquake 9 with the corresponding peak acceleration of $a = 0.4 g$ ($g = 9.81 \text{ m/s}^2$), the dynamic analysis provides the dynamic distribution coefficient α_i along the height of the slope which is listed in Table 4.13 (Chen et al. 2010).

It can be seen the amplification of earthquake inertia force along the height of rock slope, but not as appreciable as that of embankments. In addition, the distribution of α_i in slope is related to various factors such as the properties of rock and soil, and the sloping and the height as well as the shape of the slope concerned. Since insofar there are no convinced distribution patterns available,

Table 4.13 Distribution of α_i along the height of the intake slope in the Xiaowan Project

Elevation Z (m)	1100	1177	1226	1253
Dynamic distribution coefficient α_i	1.00	1.15	1.18	1.20

therefore $\alpha_i = 1.0$ is commonly assumed in the design practices. However, for important high rock slopes, appropriate amplification should be taken into account the subject to the justifications using reliable dynamic analysis.

4.6.2 Seismic Hydrodynamic Forces

While a dam is under motion due to earthquake, the body of water in front of it tends to remain in the place and causes seismic hydrodynamic pressure on the dam (Chakrabarti and Chopra 1974). Determination of this force is very complicated but, if the resistance to the vertical motion of water is neglected, the calculation of the horizontal pressure on the upstream face of the dam may be simplified greatly, as had been proposed by Westergaard (1933) using a parabolic approximation.

In Chinese design specifications, the seismic hydrodynamic pressure exerting on the vertical dam face distributes nonlinearly along the altitude. With respect to any elevation at the depth y below the water surface, the standard value of the hydrodynamic pressure p_y is determined by

$$p_y = a_h \zeta \psi(y) \rho_w H_1 \quad (4.76)$$

where p_y = standard value of hydrodynamic pressure at the depth y below the water surface, kN/m^2 ; $\psi(y)$ = distribution coefficient of hydrodynamic pressure at the depth y below the water surface (Table 4.14); ρ_w = standard value of water density, kg/m^3 ; H_1 = upstream water depth, m; a_h and ζ = identical to that in Eq. (4.72).

The total hydrodynamic force per unit width of dam monolith exerts at the depth $y = 0.54H_1$ below the water surface and is given by:

$$P_0 = 0.65 a_h \zeta \rho_w H_1^2 \quad (4.77)$$

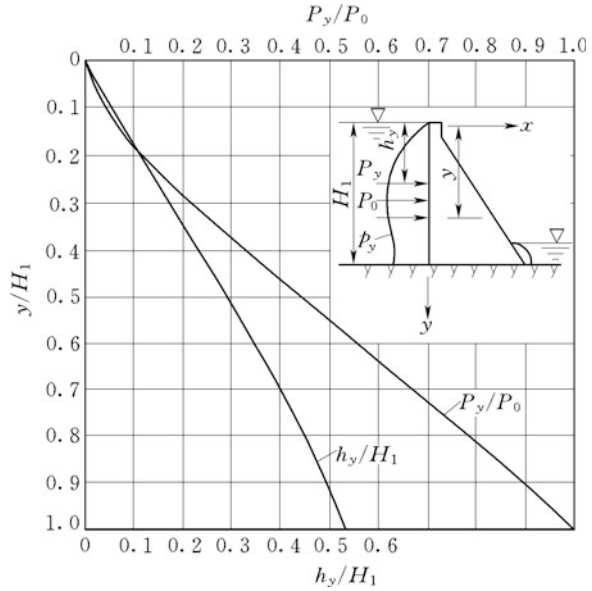
The resultant hydrodynamic force above any depth y per unit width of dam monolith inclusive resultant P_y and exerting depth h_y is referred to Fig. 4.24.

For an upstream dam face with inclination angle θ , a reduction factor $\eta_c = \frac{\theta}{90}$ should be multiplied in the calculation of hydrodynamic pressure. For a flared upstream dam face, if the vertical portion accounts for more than half of the pool water depth, the dam face may be looked at as totally vertical, otherwise the cut-short line from the dam heel to the dam crest gives an equivalent inclination angle θ in the reduction factor.

Table 4.14 Distribution coefficient $\psi(h)$ of hydrodynamic pressure

y/H_1	0.0	0.1	0.2	0.3	0.4	0.5	0.6	0.7	0.8	0.9	1.0
$\psi(y)$	0.00	0.43	0.58	0.68	0.74	0.76	0.76	0.75	0.71	0.68	0.67

Fig. 4.24 Distribution of hydrodynamic pressure



The above computation method is valid for all the other water retaining structures exclusive arch dam, whose standard value of hydrodynamic pressure p_w is determined by:

$$p_w(y) = \frac{7}{8} a_h \zeta a_i \rho_w \sqrt{H_1} y \tag{4.78}$$

Linear variation along the dam height is assumed, with $\alpha_i = 3.0$ at the dam crest and $\alpha_i = 1.0$ at the dam base.

The hydrodynamic pressure $p_w(y)$ can be assumed to be perpendicular to the arch dam face.

4.6.3 Seismic Dynamic Earth Pressure

The total seismic earth pressure is composed of static and dynamic components. The dynamic active earth pressure due to earthquake can be estimated by using the following formula:

$$F_E = \left[q_0 \frac{\cos \phi_1}{\cos(\phi_1 - \phi_2)} H + \frac{1}{2} \gamma H^2 \right] \left(1 \pm \frac{\zeta a_v}{g} \right) C_e \tag{4.79}$$

$$C_e = \frac{\cos^2(\varphi - \theta_e - \phi_1)}{\cos \theta_e \cos^2 \phi_1 \cos(\delta + \phi_1 + \theta_e)(1 + \sqrt{Z})^2} \quad (4.80)$$

$$Z = \frac{\sin(\delta + \varphi) \sin(\varphi - \theta_e - \phi_2)}{\cos(\delta + \phi_1 + \theta_e) \cos(\phi_2 - \phi_1)} \quad (4.81)$$

where F_E = representative value of earthquake excited earth dynamic pressure, kN, in which “+” and “-” are attempted, respectively, to get the maximum of F_E ; q_0 = unit length load on earth surface, kN/m; ϕ_1 = included angle of retaining wall face with vertical plane, ($^\circ$); ϕ_2 = included angle of earth surface with horizontal plane, ($^\circ$); H = height of retaining wall, m; γ = standard unit weight of soil, kN/m³; φ = internal friction angle of earth, ($^\circ$); δ = friction angle between retaining wall and earth, ($^\circ$); ξ = comprehensive influencing coefficient, 1.0 for the dynamic method, 0.25 for the pseudo-static method, 0.35 for reinforced concrete structures; and θ_e = coefficient angle of earthquake, $tg\theta_e = \xi a_h / (g - \xi a_v)$, in which a_h and a_v are the horizontal and vertical standard values of earthquake acceleration, m/s².

The dynamic passive earth pressure due to earthquake should be determined through special study.

4.7 Load (Action Effect) Combinations

All loads exerting on hydraulic structures have different and individually distinctive operating envelopes in terms of probability of occurrence, intensity, and duration. For example, the head- and tailwater levels are different in the period of normal service, reservoir drawing down, design flood or check (catastrophe) flood. The water pressure, wave pressure, uplift pressure, etc., are all changed correspondingly. The strongest wind and earthquake, and wave pressure and ice pressure have a negligible likelihood of occurrence at the highest reservoir level. In addition, the thermal action is important for arch dam while unappreciable for conventional solid gravity dam with permanent transverse joints. A hydraulic structure should be designed with regard to the most rigorous adverse groupings or combination of loads, which have a reasonable probability of simultaneous occurrence. For different load combinations, different allowable safety factors must be specified. Combinations of loads whose simultaneous occurrence is highly improbable should not be considered as reasonable.

There are two systems for the load combinations, corresponding to the limit-state-based partial coefficient design method and single safety factor method, respectively (Zhao et al. 2000).

In the earlier time, the safety documentation for a structure was commonly based on the ratio between a calculated carrying capacity (resistance) r (e.g., strength) and a corresponding load effect s (e.g., stress), which is called the safety factor. Although there are defects such as the arbitrary nature of the definition of the

resistance, the lack of theoretic clearness, and the deadlock for the development and application of improved or more universal theoretic models in the design, after a long period of practices the engineers become very familiar with the specifications employing the formulas for the resistance that correspond to the specified safety factor. Nowadays, a fairly number of the design codes or specifications for hydraulic structures in China are still based on the safety factor method, which are particularly adopted by the design institutes formerly belong to the State Electric Power Ministry, State Energy Ministry, or State Electric Cooperation. On the other hand, the design institutes belong to the State Water Resources Ministry are less conservative, in the popularization of the design codes or specifications based on partial safety factor and the limit-state reliability analysis.

4.7.1 Partial Coefficient Method

GB50199-94 “Unified design standard for reliability of hydraulic engineering structures” stipulates that: the design states of hydraulic structures are classified into permanent situations (e.g., normal operation), temporary situations (e.g., construction, repair), and accidental situations (e.g., check flood, design earthquake, drainage ineffectiveness), according to the probably occurred actions during the construction and operation as well as service periods, the structural system, and the environmental conditions.

The collapse limit states and serviceability limit states are considered, respectively, for above design situations. When the collapse limit states are calibrated for the works, the basic action combinations are employed for the permanent and temporary situations (i.e., combination for action effects considering permanent and alterable actions); the accident action combinations are used for the accidental situations (i.e., combination for action effects considering permanent and alterable actions plus one accident action). Since two accident actions occurring simultaneously within the design reference period have ignorable probability, an accident action combination comprises only of one accident action. For example, the check (catastrophe) flood and earthquake are not combined.

4.7.2 Safety Factor Method

The action effect combinations are specified through the load combinations, which are classified into basic combinations and special combinations.

A basic combination is composed of several kinds of basic loads that occur simultaneously, which covers the work states of normal storage, design flood, and freezing. A special combination is composed of several kinds of basic loads and one special load that occur simultaneously, which covers the work states of check flood or earthquake. The USBR categorizes load combinations as usual, unusual, and

extreme. The usual combination is equivalent to the basic combination, whereas the unusual combination is equivalent to the special combination considering check flood, and the extreme combination is equivalent to the special combination considering earthquake, in China.

References

- Brown FR (1963) Cavitation in hydraulic structures: problems created by cavitation phenomena. *J Hydraul Div ASCE* 89(HY1):99–115
- Casagrande A (1961) First rankine lecture—control of seepage through foundations and abutment of dam. *Géotechnique* 11(3):161–182
- Cedergren HR (1989) *Seepage, drainage and flownets*, 3rd edn. Wiley, New York
- Chakrabarti P, Chopra AK (1974) Hydro-dynamic effects in earthquake response of gravity dams. *J Structural Div ASCE* 106(ST6):1211–1225
- Chanson H (1989) Flow downstream of an aerator—aerator spacing. *J Hydraul Res* 27(4):519–536
- Chen SH, Chen ML (2014) *Hydraulic structures*, 2nd edn. China Water Power Press, Beijing (in Chinese)
- Chen SH, Feng XM, Shahrou I (2008) Numerical estimation of REV and permeability tensor for fractured rock masses by composite element method. *Int J Numer Anal Meth Geomech* 32(12):1459–1477
- Chen SH, Wang WM, Zheng HF, Shahrou I (2010) Block element method for the seismic stability of rock slopes. *ASCE Int J Geotech Geoenviron Eng* 136(12):1610–1617
- Chopra AK (1987) Simplified earthquake of concrete gravity dam. *J Struct Div ASCE* 113(ST8):1688–1708
- Chopra AK, Chakrabarti P (1981) Earthquake analysis of concrete gravity dams including dam-water-foundation rock interaction. *Earthquake Eng Struct Dynam* 9(4):363–383
- Craig RF (2004) *Craig's soil mechanics*, 7th edn. Spon Press, London
- Creager WP, Justin JD, Hinds J (1966) *Engineering for dams*, 9th edn. Wiley, New York
- Elevatorsky EA (1959) *Hydraulic energy dissipators*. McGraw-Hill, New York
- Featherstone RE, Nalluri C (1995) *Civil engineering hydraulics –essential theory with worked examples*, 3rd edn. Blackwell Science Ltd, Oxford
- Fanelli DIM, Giuseppetti G (1975) Techniques to evaluate effects of internal temperatures in mass concrete. *Water Power Dam Constr* 27(7):226–230
- Gatski TB, Bonnet JP (2009) *Compressibility, turbulence and high speed flow*. Elsevier, Oxford
- Golzé AR (1977) *Handbook of dam engineering*. Van Nostrand Reinhold Company, New York
- Grishin MM (ed) (1982) *Hydraulic structures*. Mir Publishers, Moscow
- Harza LF (1949) The significance of pore pressure in hydraulic structures. *Trans ASCE* 114(1):193–214
- ICOLD (1975) A review of earthquake resistant design of dams (Bulletin 27). ICOLD, Paris
- ICOLD (1989) Selecting seismic parameters for large dams—guidelines (Bulletin 72). ICOLD, Paris
- ICOLD (2001) Design features of dams to resist seismic ground motion (Bulletin 120). ICOLD, Paris
- ICOLD (2002) Seismic design and evaluation of structures appurtenant to dams (Bulletin 123). ICOLD, Paris
- ICOLD (2013) Selecting seismic parameters for large dams—guidelines (revision of Bulletin 72) (Bulletin 148). ICOLD, Paris
- Iqbal A (1993) *Irrigation and hydraulic structures—theory, design and practice*. Institute of Environmental Engineering & Research, NED University of Engineering & Technology, Karachi

- Ishikawa M (1991) Thermal stress analysis of concrete dam. *Comput Struct* 40(2):347–352
- Jan CD, Chang CJ, Lai JS, Guo WD (2009) Characteristics of hydraulic shock waves in an inclined chute contraction—numerical simulations. *J Mech* 25(1):75–84
- Kang A, Iaccarino G, Ham F, Moin P (2009) Prediction of wall-pressure fluctuation in turbulent flows with an immersed boundary method. *J Comput Phys* 228(18):6753–6772
- Keener KB (1950) Uplift pressures in concrete dams. *Trans ASCE* 116(1):1218–1237
- Knapp RT, Daily JW, Hammitt FG (1970) *Cavitation*. McGraw-Hill, New York
- Lin JY (2006) *Hydraulic structures*. China Water Power Press, Beijing (in Chinese)
- Liu SH, Tai W, Fan M, Luo QS (2012) Numerical simulation of atomization rainfall and the generated flow on a slope. *J Hydrodyn (Ser B)* 24(2):273–279
- Liu ZM, Wang DX, Wang DG (eds) (2013) *Handbook of hydraulic structure design, vol 1. In: Fundamental theories*. China Water Power Press, Beijing (in Chinese)
- Malkawi AIH, Mutasher SA, Qiu TJ (2003) Thermal-structural modeling and temperature control of roller compacted concrete gravity dam. *J Perform Constr Facil ASCE* 17(4):177–187
- Mehta PK, Monteiro PJM (2006) *Concrete: microstructure, properties, and materials*, 3rd edn. McGraw-Hill, New York (USA)
- Ministry of Electric Power of the People's Republic of China (1997) *Specifications for load design of hydraulic structures (DL5077-1997)*. China Electric Power Press, Beijing (in Chinese)
- Ministry of Electric Power of the People's Republic of China (1998) *Design specifications of hydraulic structures against ice and freezing action (DL/T5082-1998)*. China Electric Power Press, Beijing (in Chinese)
- Ministry of Water Resources of the People's Republic of China (2001a) *Design specification for sluice (SL265-2001)*. China Water Power Press, Beijing (in Chinese)
- Ministry of Water Resources of the People's Republic of China (2001b) *Design specification for rolled earth-rock fill dams (SL274-2001)*. China Water Power Press, Beijing (in Chinese)
- Ministry of Water Resources of the People's Republic of China (2003) *Design specification for concrete arch dams (SL282-2003)*. China Water Power Press, Beijing (in Chinese)
- Ministry of Water Resources of the People's Republic of China (2005) *Design specification for concrete gravity dams (SL319-2005)*. China Water Power Press, Beijing (in Chinese)
- Ministry of Water Resources of the People's Republic of China (2006) *Code for design of hydraulic structures against ice and freezing action (SL211-2006)*. China Water Power Press, Beijing (in Chinese)
- Novak P, Moffat AIB, Nalluri C, Narayanan R (1990) *Hydraulic structures*. The academic division of Unwin Hyman Ltd, London
- Price WH (1982) Control of cracking in mass concrete dams. *Concr Int* 4(10):36–44
- Severn RT (1976a) The aseismic design of concrete dams (part one). *Water Power Dam Constr* 28(1):37–38
- Severn RT (1976b) The aseismic design of concrete dams (part two). *Water Power Dam Constr* 28(2):41–46
- Singh M (1985) State-of-the-art finite element computer programs for thermal analysis of mass concrete structures. *Civil Eng Pract Des Eng* 4(1):129–136
- State Economy and Trade Commission of the People's Republic of China (2000) *Specifications for seismic design of hydraulic structures (DL 5073-2000)*. China Electric Power Press, Beijing (in Chinese)
- Tatro SB, Schrader EK (1985) Thermal considerations for roller-compacted concrete. *ACI J* 82(2):119–128
- USBR (1987) *Design of small dams*, 3rd edn. US Govt Printing Office, Denver
- Wang HS, Wueng QD (1990) *Hydraulic structures*. China Water Power Press, Beijing (in Chinese)
- Westergaard HM (1933) Water pressure on dams during earthquake. *Trans ASCE* 98(1):418–433
- Wu ML (1991) *Hydraulic structures*. Tsinghua University Press, Beijing (in Chinese)
- Zhang Z, Garga VK (1996) Temperature and temperature induced stresses for RCC dams. *Dam Eng* 7(4):336–350
- Zhao GF et al (2000) *Reliability theory of structures*. China Construction Industry Press, Beijing (in Chinese)

- Zhou JP, Dang LC (eds) (2011) Handbook of hydraulic structure design, vol 5. In: Concrete dams. China Water Power Press, Beijing (in Chinese)
- Zhu BF (1991) Equivalent equation of heat conduction in mass concrete considering the effect of pipe cooling. *J Hydraulic Eng* 25(3):28–34 (in Chinese)
- Zhu BF (1998) Thermal stresses and temperature control of mass concrete. China Electric Power Press, Beijing (in Chinese)
- Zhu BF (2006) Current situation and prospect of temperature control and cracking prevention technology for concrete dam. *J Hydraulic Eng* 37(12):1424–1432 (in Chinese)
- Zhu BF, Cai JB (1989) Finite element analysis of effect of pipe cooling in concrete dams. *J Construction Eng Manage ASCE* 115(4):487–498
- Zienkiewicz OC, Taylor RL (2005) The finite element method for solid and structural mechanics, 6th edn. Elsevier Butterworth-Heinemann, Oxford
- Zienkiewicz OC, Mayer P, Cheung YK (1966) Solution of anisotropic seepage by finite elements. *J Eng Mech Div ASCE* 92(1):111–120
- Zuo DQ, Gu ZX, Wang WX (eds) (1984) Embankment dams. In: Handbook of hydraulic structure design, vol 4. Water Resources and Electric Power Press of China, Beijing (in Chinese)
- Zuo DQ, Wang SX, Lin YC (1995) Hydraulic structures. Hohai University Press, Nanjing (in Chinese)

Chapter 5

Analysis of Action Effects for Hydraulic Structures

5.1 General

Under environmental actions or loads, action effects such as deformation (deflection) and stress will be developed within hydraulic structures. The failure will occur if the stress exceeds the bearing capacity of the structures.

Since the beginnings of human civilization, the engineering of hydraulic structures has increasingly evolved from primitive trial-and-error ventures to skillfully analytic approaches. Early hydraulic structure constructing was an uncertain art resting on cumulative experience. As the centuries unfolded, it was gradually merged with sciences. Mathematics and mechanics have been becoming increasingly effective in the seeking of safer designs. Nowadays, the analysis of action effects by means of physical modeling, mathematical modeling, and monitor modeling is indispensable in the design of important hydraulic structures.

Physical modeling is a fundamental tool in the effect analysis of actions because it may provide straight forward results and deep impression concerning the deformation and failure of hydraulic structures. Even with the great progress in mathematical modeling of recent decades, the physical modeling still plays an important role in the study of the problems with regard to cracking, sliding, and dynamic response, for important hydraulic structures. Physical modeling may be generally classified into three types according to the model materials used: brittle material modeling, geomechanical modeling, and emulation modeling (Fumagalli 1973).

Mathematical modeling is another paramount tool in the analysis of action effects for modern hydraulic structures (ICOLD 2001a, b, 2013). Mathematical modeling makes use of physical laws to build differential equations, which are solved under specified boundary and initial conditions. The most prevalent mathematical modeling employs analytic methods and numerical methods; the latter is a large family (Jing and Hudson 2002) including the finite difference method (FDM), finite element method (FEM), boundary element method (BEM), discontinuous deformation

analysis (DDA), discrete element method (DEM), numerical manifold method (MMM), and element free method (EFM). Great progress has been archived in mathematical modeling due to the advances in computer technology. Nowadays, a fairly large number of sophisticated commercial computer software implemented by numerical methods (e.g., ANSYS, FLAC, ADINA) is available in the design of hydraulic structures.

The performances of a hydraulic structure depend on many factors related to the materials, geologic conditions, construction, and operation situations. In the design phases, these factors are evaluated by the comprehensive study using field investigation, laboratory and field tests, and engineering analogue. However, the situation is not satisfactory because of high expenditure for large-scale field investigations and tests, difficulties with the control of field test conditions and poor representative of the laboratory samples. All these entail the possibility of detailed investigation during the design phases and in turn lead to the large performance differences between the designed and real-world status, of the works. However, starting from the construction and continuing throughout the whole operation period, new geologic features concerning discontinuities and weathering may be revealed, and monitored data concerning action effects (e.g., stress, displacement, temperature, uplift) can be collected, all these present invaluable messages with respect to the real status of the structure. Consequently, high attention should be called at the safety monitoring of hydraulic structures. Many countries such as Canada, USA, Australia, France, Russia, Italy, Austria, and China have enacted dam safety laws at the national level which are practiced in dam safety management covering inspecting and monitoring activities. Technically, monitoring of hydraulic structures is related to instrumentation science, computer science, and modern mathematics and is one of the most essential branches of the safety management. A successful safety monitoring system for hydraulic structures (e.g., dams) consists of four functional components, i.e., instrumentation, data collection, data evaluation and management, and response plan. Monitor modeling for the analysis and interpretation of observed data is intended to answer the questions such as what is the real status of the hydraulic structure and, how far is the real status shifted from the design stipulation and safety criteria? Bearing these questions in mind, it is apparent that the monitoring modeling plays a crucial role in the safety management of the modern hydraulic structures.

5.2 Physical Modeling

Rock and concrete are brittle materials. To similitude the performance of a prototype structure using physical models, a variety of materials have been exercised including gypsum class, gypsum diatomaceous mixture or concrete (pumice cement concrete and microconcrete). This kind of models may be employed to study the static and dynamic problems concerning the stress, deformation, and stability, of structures and foundations, and is named as brittle material structural models which

may be further classified into linear elastic model and destructive model. The former is employed for the study of normal working status; the latter is used for the study of ultimate bearing capacity and failure mechanism by the technique of overloading.

The geomechanical model expanding the research field of the physical modeling (Fumagalli 1973) was initiated in the 1960s. The major features of the geomechanical modeling are as follows:

- Adverse geologic structures in rock masses such as faults, fractured zones, weak seams, and major joint sets can be factually simulated. The mechanical characteristics of rock masses, such as heterogeneity, inelasticity, and discontinuity, can be reasonably described.
- It is a type of destructive tests focused on the deformation and failure mechanism covering the whole failure process of dam/foundation beyond the elastic range.
- Based on the current design codes or specifications as well as the engineering practices in China, the dam safety should be estimated in two aspects, i.e., the dam body strength and the stability of dam abutment and/or foundation against sliding. Using geomechanical modeling, the weakest portion in the structural system of dam body/foundation may be detected, and the potential failure mechanism may be identified. In this way, it may provide a reliable support for the improvement of design.

For the strength and cracking problems with respect to the structures such as penstocks, outlets, and spiral cases, microconcrete materials may be used, which is termed as emulating material modeling.

All kinds of physical modeling are systematic procedures in consequently comprising the model construction, the load application, the action effect measuring, and the control.

5.2.1 Principles of Modeling Similitude

Physical models must satisfy a series of similarity requirements in terms of geometry, physical and mechanical properties, actions, boundary conditions, and initial states. For a linear elastic model testing, according to the elasticity theory and dimensional analysis, these similarity requirements can be deduced from the force equilibrium equations, the geometry equations, the Hooke's law, and the boundary conditions (Chen et al. 1984).

Denoting the relative scale C (similarity or similitude constant) as a proportion of physical quantity between the prototype and the model, for a linear elastic modeling the relative scales should observe the following relationships named as similitude (or similarity) criteria

$$\frac{C_\sigma}{C_l C_x} = 1 \quad (5.1)$$

$$C_\mu = 1 \quad (5.2)$$

$$\frac{C_E C_\varepsilon}{C_\sigma} = 1 \quad (5.3)$$

$$\frac{C_\varepsilon C_l}{C_\delta} = 1 \quad (5.4)$$

$$\frac{C_{\bar{\sigma}}}{C_\sigma} = 1 \quad (5.5)$$

In which C_E , C_μ , C_γ , C_ρ , C_l , C_δ , C_σ , C_ε , $C_{\bar{\sigma}}$ and C_X represent the similarity constants for the Young's modulus, the Poisson's ratio, the volumetric weight, the density, the geometry dimension, the displacement, the stress, the strain, the boundary force, and the volumetric force, respectively. Equation (5.1) is derived from the equilibrium condition, Eqs. (5.2)–(5.3) are derived from the constitutive relation, Eq. (5.4) is derived from the geometry condition, and Eq. (5.5) is derived from the boundary condition.

For a destructive test using geomechanical modeling, in addition to the criteria formulated in Eqs. (5.1)–(5.5), the similarity criteria for C_c , C_f , C_{σ_T} representing the similarity constants for cohesive strength C_c , friction coefficient C_f , tensile strength C_{σ_T} , and compressive strength C_{R_c} are also necessarily established and observed.

Since all the mechanical parameters of a definite material are not tightly correlated, it is very difficult to build a model observes all the similitude criteria strictly, particularly for the destructive tests. As a compromise, it would be wise to satisfy several key similitude criteria only and to ignore the others (Chen et al. 1984).

5.2.2 Materials

The most commonly applied model material is the gypsum. With good and stable linear elastic characteristics, this is an ideal material for the construction of linear elastic model. With different water content, the physical and mechanical characteristics of the gypsum may be adjusted. Diatomite, sand, and cement may be added in the gypsum to further adjust its parameters.

In the stability study using destructive model, the self-weight is a key factor and should be well reproduced. Using of artificially distributed vertical forces interior the structure may be not sufficiently rational due to their restraints on the deformation and failure mechanism. The ideal solution for this difficulty is to reproduce materials with volumetric weight $C_\gamma \approx 1$, as in the geomechanical modeling.

5.2.3 Loads on the Model and Loading System

According to the similarity theory, similarity of load between the prototype and model must be satisfied. The loads exerting on hydraulic structures may be in the form of body (volumetric) force, surface force, and concentrated force. Application of body force frequently leads, in practice, to difficulties that are not easily solved and can frequently be a major factor in determining the fundamental scaling loads to the model.

For two-dimensional elastic models, the total volume of the model is usually subdivided into elementary volumes firstly, and then, their centers of gravity and the intensities of the equivalent concentrated forces are evaluated and applied. A common way to apply these equivalent concentrated forces is to drill a small hole in the gravity center of each elementary, through which a rod of high-tensile steel riveted by metal or plastic tube is passed. Placing of this steel rod in the tube effectively isolates it from the surrounding model material. The plastic tube has a modulus almost equal to that of the model material and has a sufficiently large diameter to avoid stress concentration and local failure in the model. At the two ends of rod, two vertical steel rods hanged with total weights corresponding to the equivalent force are linked (Chen et al. 1984; Fumagalli 1973).

For geomechanical models, the self-weight is applied mainly by adjusting the volumetric weight of model materials. Under this consideration, the similitude criteria require a model material possessing high volumetric weight and low strength. Since the materials found in the nature have limited volumetric weight, the model size has to be larger than that of conventional linear elastic models.

The other volumetric forces such as thermal and seepage forces are hard to simulate so far, attributable to their variation in direction and quantity within hydraulic structures. Actually, this is a critical factor which limits the extensive application of physical modeling.

Hydrostatic pressure is a typical and dominant surface load, which is linearly distributed along the height of the structure. Application of hydrostatic pressure by means of a liquid certainly provides a method which is both exact and easily exerted. The liquid is made to flow into and out of one or more rubber bags placed between the dam surface under load and a rigid surface to match that of the model and positioned 1–2 cm from it. The most suitable and economically available liquids are mercury in elastic modeling and water in geomechanical modeling. Due to its poisonous for human and environment, however, it should be very careful for the preservation and protection in the application of mercury, and it has very limited application nowadays. Hydraulic pressure also may be exerted by using jacking apparatus distributed in different elevations of the upstream surface of the dam, which are forced by an air- or oil-pressured instrument. Load-spreading boards are installed to eliminate the stress concentration. Actually, this method finds general application than the others, mainly because it is able to regulate the hydraulic pressure in the jacks easily.

Concentrated forces are normally applied by hydraulic jacks installed directly at the points concerned. It is preferable to apply these forces with loading rods to reduce restraint on the model.

5.2.4 Measuring System

The purpose of measuring system is to obtain the physical and mechanical responses of the model during the test. The measuring system comprises transducers and instruments for stress (via strain), load, displacement, crack, etc. The fundamental measuring instruments include those using the principles of mechanics, optics, and electricity. The optical fiber technique is now employed for the instrumentation in the physical modeling, too.

Mechanical measuring is an earlier way, which applies dial indicator, extension of leveraged instrument, and has limited application nowadays. Optical measuring employs laser holographic interferometer, speckle interferometer, and Moire method. Electrical measuring transforms strain and displacement into electric signal, which is then analyzed by corresponding facilities integrated with computers. Fundamental measuring instruments are extensometer, electric-resistance strain gauge, displacement sensor, and load transducer, etc. Since electrical measuring may be easily incorporated into computer to realize automation measurement and analysis, it is the most prevalent method.

5.2.5 Geomechanical Modeling

Geomechanical modeling is mainly exercised in the study of the interaction between hydraulic structure and rock foundation, for the purposes of quantitatively or semiquantitatively understanding concerning the deformation and stability status under normal loads, simulating the failure process, and revealing failure mechanism under over-load condition. The unique values of geomechanical modeling are as follows:

- It can trustfully reflect the failure process of a hydraulic structure with its foundation. The high self-weight of the model material enables to realize a good simulation of the volumetric gravity of the structure and rock mass, for avoiding the constraints imposed by complicated loading apparatus.
- It enables to view directly the deformation features and their development process as well as the failure mechanism, thereby obtaining valuable information for the design of the structure and its foundation.

- The yielding point, failure limit, and over-loading factor may be easily obtained which elucidate the safety margin of the structure and its foundation.
- It is flexible enough to simulate the excavating procedures of structure foundations, cut slopes, and underground openings.

Geomechanical modeling was commenced from the 1960s, when high dam projects were rapidly developing around the world. A group of experts headed by Fumagalli successfully performed a series of geomechanical model tests such as the Italian Vajont Arch Dam ($H = 216.6$ m), in the “Institute of Structure Model Experiment and Simulation (ISMES)” at Bergamo in Italy (Fumagalli 1973). The Itaipu Buttress Dam (Brazil and Paraguay, $H = 196$ m) was studied by the geomechanical modeling in ISMES to define the weakest position in the concrete dam and its foundation and, to identify the potential failure mechanism.

Large-size geomechanical modeling (2-D or 3-D) was for the first time practiced in the Chinese Gezhouba Barrage ($H = 47$ m) in the late 1970s. Since then, geomechanical models have been advocated in China. Comprehensive studies were carried out for the Longyangxia Arch Dam (abutment stability), the permanent ship lock (high slope excavation procedure and deformation) in the Three Gorges Project (TGP), the left bank powerhouse dam section (stability against deep-seated sliding in foundation) in the TGP, the Xiaolangdi Project (stability of fissured laminated rock mass in underground powerhouse), the Ertan Arch Dam and Xiaowan Arch Dam (overall stability and abutment stability), etc.

In order to achieve a better result, Chinese engineers and scholars had endeavored to the study and the improvement of analogue materials. In the earlier period with the experiences from the ISMES as main sources for reference, they comprehensively investigated the possibility of using dehydrated gypsum as cementing agent. After that, the material with epoxy as the cementing agent was studied. Then, the combinations of different types of analogue materials in one model were exercised in order to meet the requirement for 3-D model tests. For example, in the geomechanical modeling of the Longyangxia Arch Dam, the material was prepared using gypsum as cementing agent, barite powder as weight-simulation agent, starch and glycerin as admixture, in order to simulate hard rock and geologic features varying greatly in properties. The geomechanical model for the Gezhouba Barrage adopted barite mixed with sand, and barite mixed with limestone, to simulate the clayey sandstone and the sandstone. The geomechanical model for the TGP used viscous oil as cementing agent, and lead powder as reinforcement agent.

It would be reluctantly but should be admitted that large geomechanical modeling is both costly and time-consuming, and their application is increasingly challenged by the fast development of mathematical modeling with the help of numerical analysis methods. Nowadays, large geomechanical modeling remains to be a necessity only for a few of very significant and complicated projects in China.

5.3 Mathematical Modeling

The major advantages of mathematical modeling are as follows:

- It is relatively easier to build and can be employed for the simulation of construction and operation process;
- It may give prominence to the basic features of the hydraulic structures, to facilitate the analysis of their working principles and failure mechanism;
- It is easy to carry out the sensitive analysis by the adjustment of parameters and factors, to understand the tendency and extent of their influences on hydraulic structures, and to enlighten appropriate improvement measures in the design and construction.

As the development of computer industry and computational technique, “computation” based on mathematical modeling is parallel to the “theory” and “experiment,” to form three “pillars” in the attempt to understand the nature and of course, the hydraulic structures as well (Chen 2006; Jing and Hudson 2002; Morton and Mayers 2005; Zienkiewicz and Taylor 2005; Zhu 1998).

5.3.1 Typical Methods for Mathematical Modeling

1. Analytic method

A closed-form (analytic) solution of specific formula based on mathematical model may be used to calculate outputs directly after the plug of inputs into the formula. Closed-form solutions have an obvious advantage over other methods—accurate. Nevertheless, only under the simple boundary and initial conditions such solutions may be fortunately obtained. Nowadays, these precious closed-form solutions also play important roles in calibrating the validation and accuracy of computational solutions by numerical methods.

2. Limit equilibrium method (LEM)

There are two ways for determining the safety against loss of stability by means of LEM: the first one is based on the condition of stress equilibrium at every point of the structure, the highest load or lowest shear strength which does not lead to the loss of equilibrium of the structure is sought; the second one assuming the occurrence of a kinematically possible failure mechanism (e.g., a sliding soil/rock mass considered as a rigid body along the slip surface), the most unfavorable slip surface at which failure manifests, is sought (Meyerhof 1984).

In the first way, the state of stress must be determined for each point in the structure. Owing to the statically indeterminate of various hydraulic structures, deformations must also be taken into account. Thus, the stress–strain relations of the material must be established. Solutions can then be worked out by the application of numerical methods (e.g., FEM). The advantage of this approach is that the

analysis itself indicates the zones in which the potential surface of sliding is developing, while a relatively complete insight is obtained into the stresses and deformations in the material. Disadvantages lie in the complicated mathematical analysis with regard to the extensive and costly testing of samples, and the current impossibility of plugging the actual stress–strain behavior of the material concerned into the analysis. Therefore, this approach has to be used only in case of particular problems where deformations had to be considered.

The second way consists of analyzing equilibrium along various slip surfaces and is based on the strategy of finding a kinematically possible failure mode. This approach is generally employed in practice for a routine verification of the stability of existing or newly designed structural profiles. Normally, this approach leads to a sufficiently reliable result and is very attractive due to its simplicity, and it will be addressed in details in Sect. 5.3.2.

3. Finite difference method

The FDM was firstly developed by Thom in the 1920s under the title “the method of square” to solve nonlinear hydrodynamic equations. FDM is based upon the approximations that permit replacing partial differential equations by finite difference equations, which are algebraic in form, and whose solutions are related to grid points (Morton and Mayers 2005).

Compared to the FEM, the most attractive feature of the FDM is that it can be very easy to implement.

FDM is not so prevalent as FEM in the structural problems, although it is a major numerical method in the fluid mechanics and hydraulics.

4. Finite element method

The FEM [in its practical application often known as finite element analysis (FEA)] is a numerical technique for finding approximate solutions to partial differential equations and (less often) integral equations (Zienkiewicz and Taylor 2005). FEM is a special case of the more general Galerkin method with polynomial approximation functions. The FEM is originated from the need for solving complex elasticity and structural analysis problems in civil and aeronautical engineering. Its development can be traced back to the work by Hrennikoff (1941) and Courant (1943). Although the approaches used by these pioneers are different, they share one essential characteristics: mesh discretization of a continuous domain into a set of discrete sub-domains, usually called “elements.” Starting in the 1950s, Zienkiewicz gathered those methods together and built the pioneering mathematical formalism of the method.

Compared to the FDM, the most attractive feature of the FEM is its higher ability and flexibly to handle complicated geometries (and boundaries). While FDM in its basic form is restricted itself to rectangular grid and simple alterations thereof, the handling of geometries in FEM is theoretically straightforward.

The FEM has become prevailing analysis tool in hydraulic structures for nearly 40 years. Solutions to even very complicated stress problems, thermal problems, as

well as permeable problems can now be obtained routinely using the method. It will be addressed in details in Sects. 5.3.3–5.3.6.

5. Boundary element method

Boundary integral equations are a classical tool for the solution of boundary value problems based on the partial differential equations. The BEM is a numerical method of solving linear partial differential equations which have been reformulated as integral equations. The BEM is applicable to problems for which the Green's functions can be established (Brebbia et al. 1984).

The BEM have several advantages over other numerical methods (e.g., FEM or FDM):

- Only the boundary of the domain needs to be discretized. This allows for very simple data input and storage.
- Exterior problems with unbounded domains are handled as easily as interior problems.
- In some cases, the physically relevant data are given not by the solution in the interior of the domain but rather by the boundary values of the solution or its derivatives. These data can be obtained directly from the solution of boundary integral equations with high accuracy.
- The solution in the interior of the domain is approximated with a rather high convergence rate, and moreover, the same rate of convergence holds for all derivatives of any order of the solution in the domain.

Main difficulties with BEM are as follows:

- Boundary integral equations require the explicit knowledge of a fundamental solution, or the Green's functions, which are often problematic to obtain as they are based on a solution of the system equations subject to a singularity load.
- For a given boundary value problem, there exist different boundary integral equations and to each of them there are several numerical approximations. Thus, every BEM application requires that several choices be made.
- The classical theory of integral equations and their numerical solution concentrates on ordinary Fredholm integral equations of the second kind with regular kernel. However, boundary integral equations frequently encountered may be of the first kind, and the kernels are in general singular.
- If a boundary is not smooth but has corners and edges, then the solution of the boundary value problem has singularities at this boundary.

6. Block element method

The problem of the deformation and stability of rock foundations, abutments, and cut slopes are generally dominated by discontinuities which cut rock masses into blocks of various sizes, shapes, and positions.

The LEM is very useful in the conventional stability analysis due to its simplicity and the experiences accumulated in many applications. It has, however,

certain limitations: the deformation of the rock cannot be considered, and the safety factor will be over-estimated when the sliding surface is composed of multi-discontinuities, where postulations concerning the stress state on the sliding surface have to be employed to make the problem statically determinant (Chan and Einstein 1981; Chen 1993a, b).

The necessity of developing new analysis tool possessing mixed advantages of LEM and, for example FEM, has soon been understood by the researchers in the area of geotechnical engineering. Nowadays, methods such as DEM (Cundall 1971, 1988; Cundall and Hart 1992; Hart et al. 1988) and DDA (Shi 1992) are well acceptable. These methods are based on the discontinuous medium approach and able to deal more easily with the large and discontinuous deformation as well as the stability of the rock masses containing many discontinuities of various scales and orientations. There are, however, still enormous potentialities for the improvement if these methods are expected to play an essential role in the design of complicated hydraulic structures (e.g., arch dam abutment slopes). Among the possible improvements, the consideration of the special requirements from the engineering practices, for example, the preprocessing of complex structures with an irregular ground surface, the various loading conditions (seepage coupling, complex initial stress field, etc.), and construction processes (excavation, reinforcement and refilling step by step, etc.), would be particularly welcome.

Based on the systematic research on the discontinuous medium approach of rock masses (Chen 1993a, b; Chen et al. 1994), a methodology of block element analysis for the calibration of seepage, deformation and stability for rock masses containing many discontinuities of various scales and orientations, irregular ground surface, grout and drainage curtains, rock bolts and prestresses anchor cables is available (Chen 1993a, b; Chen et al. 1994; Xu et al. 2000). A more refined block element analysis can also be implemented by taking into account of the rock block deformations, the dam/foundation interaction, and seismic response (Chen et al. 2003, 2004a, b, c, 2010a, b).

Block element method has been recommended by the DL/T 5353-2006 (2006) “Design specification for engineering slopes in water resources and hydropower project,” and it will be formulated in details in Sect. 5.3.7.

7. Composite element method (CEM)

Nowadays in general, the FE models proposed to treat the discontinuities, bolts, and draining holes fall into two catalogues: one is the implicit (equivalent) model which takes the influences of them into the compliance tensor and permeability tensor but neglects their exact positions (Barenblatt et al. 1960; Chen and Egger 1999; Dershowitz et al. 1985; Long et al. 1985; Oda 1985; Pande and Gerrard 1983); another one is the explicit (distinct) model which uses special elements to simulate exactly their geologic and mechanical properties (Cacas et al. 1990; Chen and Egger 1997; Dershowitz and Einstein 1987; Swoboda and Marence 1991). Implicit model can be applied to very complex engineering problems with a large quantity of discontinuities and bolts as well as draining holes, whereas the explicit

model has the potentiality to describe them in much more detail and consequently gives more precise solution.

From the point view of practitioners, main disadvantage in the explicit simulation of fractures and bolts/drainage holes lies in the preprocess to discrete the calculation domain. This arises from two aspects: On the one hand, there are large quantity of discontinuities of different sizes, and large quantity of drainage holes and/or bolts of small diameter (e.g., 10 cm) deployed within a small width and largely stretched zone (e.g., 3 m in distance between holes); on the other hand, the special elements at hand have definite nodes deployed along them, and some of these nodes should be the common nodes of the nearby surrounding rock elements. This disadvantage combined with the complicated configuration of the structures such as dam foundation, cut slope, and underground cavern will lead to time-consuming and tedious preprocess work.

A CEM has been proposed to cover the disadvantage discussed above and has been implemented separately for rock fractures, rock bolts, and drainage holes (Chen and Feng 2006; Chen et al. (2004a, b, c, 2008a, b, 2010a, b, 2011, 2012; Chen and Qing 2004; Chen and Shahrour 2008). The most remarkable feature of this method is to locate the discontinuities and/or bolts and/or drainage holes, within the elements. In this way, less restraint is imposed on the mesh generation for complicated rock structures with considerable amount of discontinuities, bolts, and drainage holes. It may provide a detailed description of their performances as well as their interaction using simple mesh, which allows for a great simplification in the preprocess work in the engineering application.

5.3.2 Limit Equilibrium Method of Rigid Body

LEM of rigid body is a method which focuses on the safety factor concerning a definite failure mechanism (e.g., sliding, toppling, collapse, and buckling) while neglects the deformation characteristics and failure procedure, of hydraulic structures. It falls into two main categories: method that deals with structurally controlled planar or wedge slides and method that deals with curvilinear (circular or non-circular) failure surfaces in equivalent “homogeneous” materials. Many of these have been available for more than 40 years and can be considered reliable tools for the stability analysis of hydraulic structures and their foundations.

The factor of safety (or factor of stability) is generally employed to indicate if a structure is stable or not, which has two major definitions: The first one is termed as “over-load factor” defined as the ratio of the ultimate load to the actual load exerting on the structure, to bring it to a state of limiting equilibrium. The second one is termed as “strength reduction factor” defined as the ratio of the ultimate strength (resistance) divided by the mobilized stress (failure driving) to bring the structure to a state of limiting equilibrium at incipient failure. Dam foundation design commonly makes use of over-load factor, while the design for embankment and cut slope commonly makes use of strength reduction factor. For a definite

computation method, significant difference may be manifested with respect to the two definitions for the safety factor, although in particular simple cases they could be identical.

1. Consideration of groundwater in the LEM

There are two different ways for the consideration of the action effects of groundwater in undertaking stability analysis using LEM (Chen 2003; Chen et al. 2005). They all lead to identical results if applied appropriately. The first one is similar to the total stress approach for the sliding body of clay or saturated sandy soil under short-term loadings with the pore pressure not dissipated, which takes the mixture of material and water as the object of study. The second one is similar to the effective stress approach for the sliding body of residual soil in which drained conditions prevail, which takes the skeleton of material as the object of study.

(a) The mixture of material and water as object of study (Fig. 5.1)

The action between water and material skeleton is internal forces. In the formulation of static equilibrium equation of slip body, the following are considered:

- The weight above the phreatic surface should be computed using wet (natural) volumetric weight;
- The weight below the phreatic surface should be computed using saturated volumetric weight; and
- The water pressure on the slip body boundaries should be exerted. If a part of slip body is submerged in reservoir, the static pressure of reservoir water is taken into account.

Suppose that the slip body is partially saturated and the tension crack is partially filled with water, then the water is able to exit where the slip surface daylight on the slope face (Fig. 5.1). The water pressures generated in the tension crack and on the slip surface can be approximated by triangular force diagrams where the maximum pressure at both the base of the tension crack and the utmost upper end of

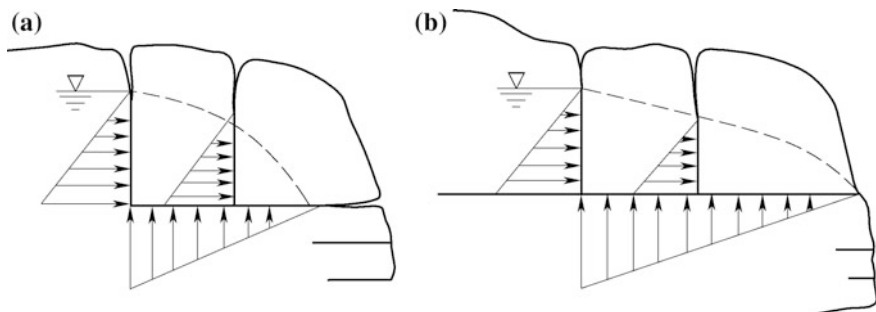


Fig. 5.1 Consideration of the action effects of water (mixture of rock and water as the object of study). **a** Open of fracture; **b** non-open of fracture

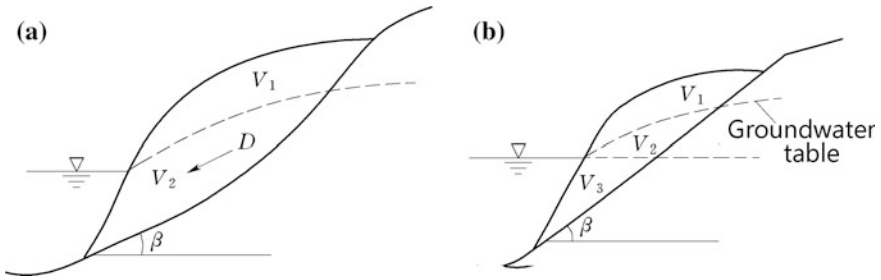


Fig. 5.2 Consideration of the action effects of water (skeleton of material as the object of study). **a** Conventional computation; **b** simplified computation

the slip surface is given by $\gamma_w Z_w$, in which Z_w is the head at the bottom of the tension crack, and γ_w is the unit weight of water.

(b) The skeleton of material as the object of study (Fig. 5.2)

The action between water and material skeleton is external forces, which is divided into buoyant pressure and seepage pressure. In the formulation of static equilibrium equation of slip body, that

- The weight above the phreatic surface (V_1) (Fig. 5.2a) should be computed using wet (natural) volumetric weight;
- The weight below the phreatic surface (V_2) (Fig. 5.2a) should be computed using buoyant volumetric weight;
- The hydrodynamic seepage force in the slip body below the phreatic surface (V_2) should be taken into account.

(c) Simplified method

Although the hydrodynamic seepage force is actually a volumetric force on the material skeleton and is related to the hydraulic gradient, by Eqs. (4.34)–(4.36), the influence of seepage force may be approximately calculated: In the calculation of sliding force, the weight below the phreatic surface (V_2) (Fig. 5.2b) is computed using saturated volumetric weight; while in the calculation of sliding resistance force, the weight below the phreatic surface (V_2) is computed using buoyant volumetric weight. It should be indicated that in the application of this simplified method, the following three restraints should be observed:

- The slip surface has small dip angle;
- The phreatic surface is nearly parallel to the slip surface; and
- The horizontal loads including seismic inertia force are not considered.

It also should be indicated that where the groundwater phreatic surface is steeper than the slip surface, the above-simplified method gives rise to higher safety factor

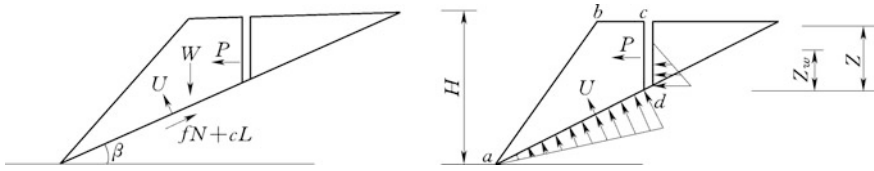


Fig. 5.3 Slope with single-planar slip surface

K , which results in an unsafe design; on the contrary, when the groundwater phreatic surface is gentler than the slip surface, the above-simplified method gives rise to lower safety factor K , which results in a conservative design.

2. Stability analysis with single-planar slip surface

This is the simplest case in the stability analysis. Figure 5.3 shows a slope embedded with a continuous joint dipping out of the slope face and forming a statically determinate sliding mass.

Calculation of the safety factor of the slip body shown in Fig. 5.3b involves the resolution of the force exerting on the slip surface into components, respectively, perpendicular and parallel to this surface. According to the principle of LEM, the stability of the block can be quantified by the ratio of the resisting to the driving forces, as

$$K = \frac{(W \cos \beta - U - P \sin \beta - F \sin \beta) \tan \phi + cL}{W \sin \beta + P \cos \beta + F \cos \beta} \quad (5.6)$$

where W = weight of the mass lying above the slip surface, kN; ϕ = friction angle of the slip surface ($^\circ$); c = cohesion of the slip surface, kN/m²; L = length of the slip surface, m; β = dip of the slip surface ($^\circ$); P = static water pressure in the vertical tension crack, kN; U = uplift on the slip surface, kN; F = horizontal earthquake inertia force, kN.

The values of U and P are dependent on the water-filling condition in the vertical tension crack. When the slope is partially saturated such that the tension crack is partially filled with water, and the water table exits where the slip surface daylights on the slope face (point a), the water pressures that are generated in the tension crack and on the slip surface can be approximated by triangular force diagram, as

$$\begin{cases} U = \frac{1}{2} \gamma_w Z_w (H - Z) \csc \beta \\ P = \frac{1}{2} \gamma_w Z_w^2 \end{cases} \quad (5.7)$$

where γ_w = unit weight of water; Z_w = height of water filling in the tension crack.

In order for this type of failure to occur, the following geometrical conditions must be satisfied that

- The plane on which sliding manifests must with a strike parallel or nearly parallel (within a deviation margin of approximately $\pm 10^\circ$) to the slope face;
- The slip plane must “daylight” on the slope face; this means that the dip of the slip plane must be gentler than the dip of the slope face;
- The dip of the slip plane must be greater than the friction angle of this plane;
- The upmost generatrix of the slip surface either intersects the upper slope face, or terminates at a tension crack; and
- Release surfaces that provide negligible resistance to sliding must be present in the structure and/or rock mass to define the lateral boundaries of the sliding.

A planar failure is a comparatively rare sight in dam foundations, embankments, and cut slopes because it is only occasionally that all the aforementioned geometric conditions to permit such a failure merging in an actual structure. However, it would not be right to ignore this case because there are many valuable lessons to be learned from a consideration of the mechanics of this simple failure mode. Planar failure analysis is particularly useful for demonstrating the sensitivity of the hydraulic structure to the changes in shear strength and groundwater conditions, attributable to its simplicity and lucidity in the computation.

3. Stability analysis with double-planar sliding surface

Figure (5.4a) presents the anatomy of a typical wedge (ABCD), which has the potentiality of slip along the intersecting line (CD) formed by the two slip surfaces. Wedge failures can occur over a much wider range of geologic and geometric conditions than single-planar failures.

It is well known to be a statically indeterminate problem (Hocking 1976; Hoek et al. 1973; Londe et al. 1969), and assumptions on the forces are required to render the problem statically determinate. However, since such assumptions have overlooked some important factors influencing the stability of rock wedge, its precision is not assured and sometimes it will lead to unsafe side design. Indeed, a higher allowable safety factor can be adopted to overcome this shortcoming, but engineers still feel no full confidence whether the stability safety is guaranteed. Let us have an investigation on this issue, by assuming that the load E forms an included angle γ_1 with the line (CD) and an included angle γ with the line (P) (Vide Figs. 5.4b, c). This load is resolved into the component S along the (CD) and the component N normal to the (CD), as

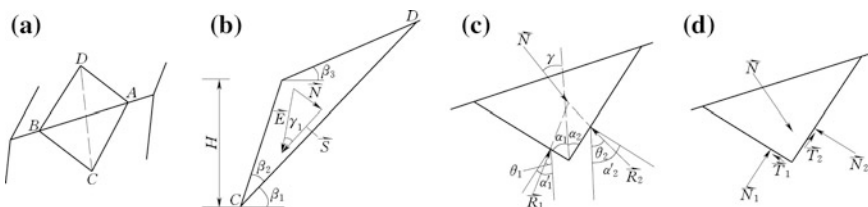


Fig. 5.4 Rock wedge in cut slope

$$\begin{cases} S = E \cos \gamma_1 \\ N = E \sin \gamma_1 \end{cases} \quad (5.8)$$

The component N and the reaction forces R_1 and R_2 on the two slip surfaces create an equilibrium system. Further, R_1 and R_2 can be resolved into the shear forces T_1 and T_2 and the normal forces N_1 and N_2 (Fig. 5.4d), as

$$\begin{cases} N_1 = N \sin(\theta_2 - \gamma) \cos(\alpha'_1 - \theta_1) / \sin(\theta_1 + \theta_2) \\ N_2 = N \sin(\theta_1 + \gamma) \cos(\alpha'_2 - \theta_2) / \sin(\theta_1 + \theta_2) \\ T_1 = N \sin(\theta_2 - \gamma) \sin(\alpha'_1 - \theta_1) / \sin(\theta_1 + \theta_2) \\ T_2 = N \sin(\theta_1 + \gamma) \sin(\alpha'_2 - \theta_2) / \sin(\theta_1 + \theta_2) \end{cases} \quad (5.9)$$

Denoting the areas of the slip planes 1 and 2 as A_1 and A_2 , the friction coefficients and cohesions as f_1 and f_2 , c_1 and c_2 , then the safety factor of strength reduction is

$$K = \frac{\sqrt{(N_1 f_1 + A_1 c_1)^2 - (K T_1)^2} + \sqrt{(N_2 f_2 + A_2 c_2)^2 - (K T_2)^2}}{S} \quad (5.10)$$

There are two basic problems in Eq. (5.10).

- (1) Since the angles θ_1 and θ_2 are unknown, the reaction forces T_1 , T_2 , and N_1 , N_2 , are statistically indeterminate, K is actually unsolved. By assuming $\theta_1 = \alpha'_1$, $\theta_2 = \alpha'_2$, then it turns out that

$$\begin{cases} N_1 = N \sin(\alpha'_2 - \gamma) / \sin(\alpha'_1 + \alpha'_2) \\ N_2 = N \sin(\alpha'_1 + \gamma) / \sin(\alpha'_1 + \alpha'_2) \\ T_1 = T_2 = 0 \end{cases} \quad (5.11)$$

$$K = \frac{(N_1 - U_1) f_1 + A_1 c_1 + (N_2 - U_2) f_2 + A_2 c_2}{S} \quad (5.12)$$

Equation (5.11) is the well-known “normal resolution assumption” (Londe 1965), which is equivalently to assume that T_1 and T_2 are zero; in this way, the calculated K by Eq. (5.12) is larger than that of by Eq. (5.10), i.e., there is a risk of over-estimation of the stability (Chen 1993a, b).

- (2) In the deduction of above equations, only the condition of force equilibrium has been taken into account. Overlooking of momentum will also lead to unsafe side analysis result (Chan and Einstein 1981).

Several methods for maximum or minimum safety factor such as “partition method” have been proposed for the improvement (Copen et al. 1977; Guzina and Tucovic 1969). Unfortunately, they are very likely too conservative; in some cases,

the difference between the calculated “minimum safety factor” and the safety factor calculated by Eq. (5.12) will be dramatically exaggerated.

4. Stability analysis with multi-planar slip surface

Stability analysis with multi-planar slip surface may be distinguished as those of single-dip angle and multi-dip angle. In the former case, the slip surface at the profile along the dip is a polygonal line, which may be calculated using “slice method”; the typical and simplest of the latter case is the wedge stability problem which may be analyzed by widely recognized method illustrated foregoing, while the other types of the latter are usually very irregular and have no widely recognized analysis methods insofar. The limit equilibrium system is also statically indeterminate confronting multi-planar slip surface problem, and assumptions on the inter-slice forces are demanded to render the problem statically determinate.

Normally, the slice method is two-dimensional, i.e., on the direction perpendicular to the cross section, the slip surface is assumed to extend infinitely to both sides or there are release surfaces providing negligible lateral resistance to the sliding. The slice method was initiated by the Swedish scholars and therefore named as “Sweden arc method.” It was anecdotally illuminated by evidence from the slope failures in Sweden in the early 1900s that suggested the failure surface was often cylindrical, especially in a homogeneous and isotropic soil mass (Fellenius 1927; Petterson 1916, 1955; Taylor 1937). The method was formally introduced by Fellenius (1936) when he divided the sliding soil mass contained within the circular arc into slices and analyzed their equilibrium by equating the moments to zero. The values of safety factor obtained by traditional Fellenius method are conservative and may lead to uneconomical design; this is especially marked in case of deep slip arcs and high pore pressure.

The early slice method assumed cylindrical failure surface only, and the inter-slice forces were greatly simplified or even ignored; therefore, computations could be carried out by simply using a calculator. Later on, with the assumption of non-cylindrical failure surface, and with the iterative nature of the solution process, it demands a computer for the solution.

As the development of geomechanics, the slice method has been improved by many scholars, of which the Bishop’s method largely enhances the accuracy of the analysis. The general principles of the method of slices extended by Nonveiller (1965) enable it to cover non-circular sliding surfaces. Today, the method has been further improved through better and more realistic assumptions, particularly with respect to the inter-slice forces, by Janbu (1954, 1973), Bishop (1955), Bishop and Morgenstern (1960), Morgenstern and Price (1965), Spencer (1967, 1973), Bell (1986), Sarma (1973), Sarma and Bhave (1974), and others.

Recommended by the DL/T 5353-2006 (2006) “Design specification for engineering slopes in water resources and hydropower project,” the “residual thrust method (RTM)” which is also named as “transfer coefficient method” or “thrust transmission method,” as well as the “Sarma method,” are typical and prevalent with the slice technique (Fig. 5.5a) . They will be envisaged in detail hereinafter.

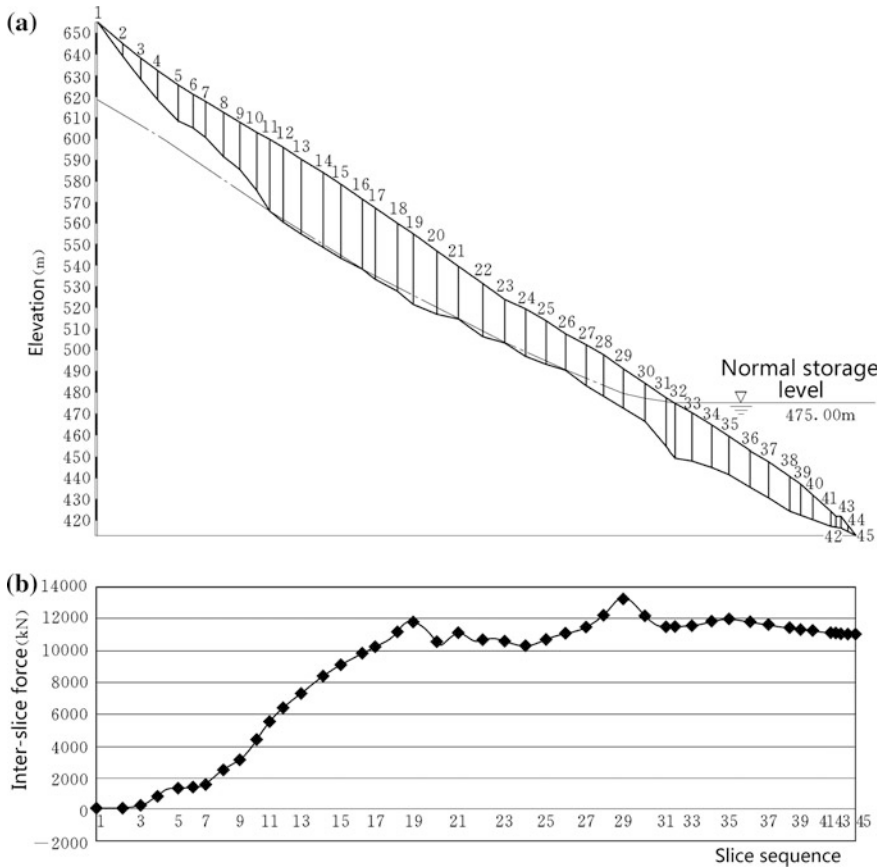


Fig. 5.5 Landslide on the power tunnel intake slope—the Sanbanxi Hydropower Project (China). **a** Slice model; **b** design inter-slice thrust force distribution ($K = 1.2$)

(a) Residual thrust method (RTM)

(1) Assumptions

- The potential sliding soil/rock mass is divided into a string of vertical slices and the slip surface is polygonal;
- The inter-slice force, i.e., the residual thrust from the back (passive) slice, is parallel to its slip surface. However, the tensile force on the inter-slice is not transferred and should be enforced as zero;
- The residual thrust of the whole slope is zero, i.e., the residual thrust of the final slice daylighting on slope surface is zero.

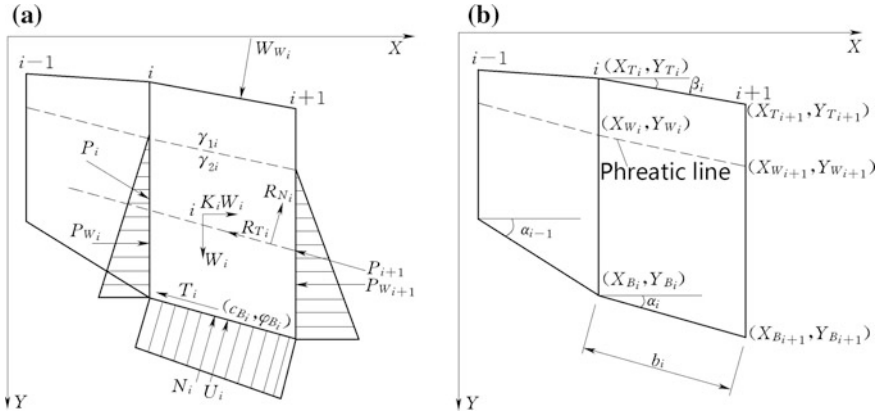


Fig. 5.6 Computation diagram of residual thrust method. **a** Mechanics model; **b** geometry model

(2) Algorithm

- i. The slip surface is simplified into polygonal line, which is further divided by vertical lines into slices that are numbered in a sequence along the sliding direction.
- ii. Take the i th slice as representative rigid body as shown in Fig. 5.6, in which: N_i = effective normal force on the base; T_i = shear force on the base; U_i = uplift on the sliding surface; P_i = inter-slice thrust force; P_{wi} = static water pressure on vertical slice face; W_i = weight of slice; γ_{1i} and γ_{2i} = unit weight of material above and under the underground water table, respectively; W_{wi} = static water pressure on the top surface of slice (in case there is water on the slope surface); K_c = horizontal earthquake coefficient; b_i = base length of the slice; α_i = base inclination angle, clockwise is taken as positive; β_i = ground slope angle, clockwise is taken as positive.
- iii. Taking the mixture of rock and water as object of study, the force equilibrium conditions for the slice i along and perpendicular to the slip surface are established. According to the definition of strength reduction safety factor, in the formulation of force equilibrium equations the shear strength parameters (friction coefficient and cohesion) on the slip surface are divided by K . The force equilibrium conditions for the slice i ($i = 1, \dots, n$) along and perpendicular to the slip surface $\sum R_{Ti} = 0$ and $\sum R_{Ni} = 0$ are given by:

$$\begin{aligned} P_{i+1} + T_i + (P_{W_{i+1}} - P_{W_i}) \cos \alpha_i - P_i \cos(\alpha_{i-1} - \alpha_i) \\ - W_i(\sin \alpha_i + K_c \cos \alpha_i) - W_{W_i} \sin(\alpha_i - \beta_i) = 0 \end{aligned} \quad (5.13)$$

$$\begin{aligned} N_i + U_i - (P_{W_{i+1}} - P_{W_i}) \sin \alpha_i - P_i \sin(\alpha_{i-1} - \alpha_i) \\ - W_i(\cos \alpha_i - K_c \sin \alpha_i) - W_{W_i} \cos(\alpha_i - \beta_i) = 0 \end{aligned} \quad (5.14)$$

The Mohr–Coulomb strength criterion is employed to obtain

$$T_i = \frac{c_{B_i}b_i + N_i tg \varphi_{B_i}}{K} \quad (5.15)$$

Using Eqs. (5.13)–(5.15) to eliminate N_i and T_i , the relationship of P_{i+1} and P_i is obtained as

$$P_{i+1} = P_i \psi_i - \Delta R_{T_i} - \Delta R_{N_i} tg \varphi_{B_i} / K \quad (\text{if } P_{i+1} < 0, \text{ let } P_{i+1} = 0) \quad (5.16)$$

in which

$$\begin{cases} \psi_i = \cos(\alpha_{i-1} - \alpha_i) - \sin(\alpha_{i-1} - \alpha_i) tg \varphi_{B_i} / K \\ \Delta R_{T_i} = (P_{W_{i+1}} - P_{W_i}) \cos \alpha_i - W_i (\sin \alpha_i + K_c \cos \alpha_i) - W_{W_i} \sin(\alpha_i - \beta_i) + c_{B_i} b_i / K \\ \Delta R_{N_i} = (P_{W_{i+1}} - P_{W_i}) \sin \alpha_i + W_i (\cos \alpha_i - K_c \sin \alpha_i) + W_{W_i} \cos(\alpha_i - \beta_i) - U_i \end{cases} \quad (5.17)$$

where ψ_i = thrust transmission coefficient.

- (iv) Attempting K , calculate the residual thrust force P_i (i.e., inter-slice force) of each slice in a sequence along the sliding direction, which is transferred to the next slice. If the thrust force of the last slice is equal to zero, the attempted K is exactly the required safety factor. Otherwise, K is adjusted according to definite rule, and the above algorithm is repeated until the correct solution of K is obtained.

In the stabilization design of cut slopes and dam foundations, the thrust curve is always useful, which may be calculated by replacing the K in Eq. (5.16) using the allowable safety factor $[K]$, the thrust P_i is then calculated and plotted into curve as shown in Fig. (5.5b). At the end of this curve, the residual thrust means the force should be provided by reinforcement measures if the overall safety factor $[K]$ against slide is required (per unit width). Figure 5.5 shows the slice model and thrust curve of the landslide on the power tunnel intake in the Sanbanxi Project (China), under $[K] = 1.2$.

(b) Sarma method

Sarma (1973) method allows for inclined inter-slice faces, which is mainly in view that the inter-slice faces are often not vertical in rock masses formed by discontinuities.

(1) Assumptions

- The potential slip soil/rock mass is divided into a string of slices, the slices may be not necessarily vertical and equally spaced;
- Simulation of dominate discontinuities is realized by incorporated them into oblique inter-slice faces and slip surface;
- At the limit state, the limit equilibrium conditions are reached simultaneously on the slip surface and inter-slice faces.

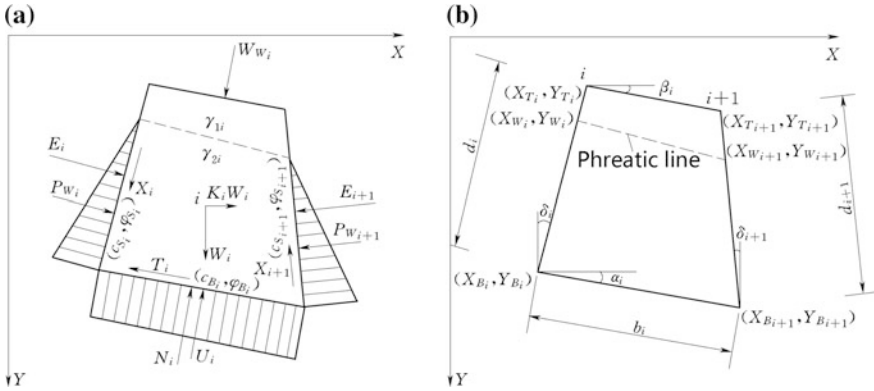


Fig. 5.7 Computation diagram of Sarma method. **a** Mechanics model; **b** geometry model

(2) Algorithm

- i. The important discontinuities are selected;
- ii. The occurrences of the selected discontinuities and slip surface are used to divide the slope into slices, several artificial slice faces also may be added, if necessary;
- iii. Take the slice i as representative rigid body as shown in Fig. 5.7, in which E_i = inter-slice effective normal force; X_i = inter-slice shear force; d_i = length of inter-slice face; δ_i = inter-slice inclination angle, clockwise is taken as positive; other nomenclatures are identical to the RTM shown in Fig. 5.6.
- iv. Taking the mixture of rock and water as object of study, the strength parameters on the slice bottom and side faces are all divided by K .

The horizontal and vertical equilibrium conditions $\sum X = 0$ and $\sum Y = 0$ for the slice i ($i = 1, \dots, n$) are expressed by

$$[(E_i + P_{W_i}) \cos \delta_i - X_i \sin \delta_i] - [(E_{i+1} + P_{W_{i+1}}) \cos \delta_{i+1} - X_{i+1} \sin \delta_{i+1}] + K_c W_i - W_{W_i} \sin \beta_i + (N_i + U_i) \sin \alpha_i - T_i \cos \alpha_i = 0 \tag{5.18}$$

$$[(E_i + P_{W_i}) \sin \delta_i - X_i \cos \delta_i] - [(E_{i+1} + P_{W_{i+1}}) \sin \delta_{i+1} - X_{i+1} \cos \delta_{i+1}] + W_i + W_{W_i} \cos \beta_i - (N_i + U_i) \cos \alpha_i - T_i \sin \alpha_i = 0 \tag{5.19}$$

in which

$$\begin{cases} X_i = \frac{c_{S_i} d_i + E_i t g \varphi_{S_i}}{K} \\ T_i = \frac{c_{B_i} b_i + N_i t g \varphi_{B_i}}{K} \end{cases} \tag{5.20}$$

- v. According to the above equations and boundary conditions, to deduce the expression of horizontal earthquake coefficient K_c as follows (Sarma and Bhawe 1974).

The relation of E_{i+1} and E_i is obtained by the elimination of X_i , X_{i+1} , T_i and N_i using Eqs. (5.18)–(5.20):

$$E_{i+1} = a_i - p_i K_c + e_i E_i \quad (5.21)$$

in which

$$\left\{ \begin{array}{l} a_i = -\frac{R_{X_i} + R_{Y_i} \zeta}{c e_{i+1}} \\ p_i = -\frac{W_i}{c e_{i+1}} \\ e_i = \frac{c e_i}{c e_{i+1}} \\ \zeta = \frac{t g \alpha_i - t g \varphi_{B_i} / K}{1 + t g \alpha_i t g \varphi_{B_i} / K} \\ c e_i = \cos \delta_i - \sin \delta_i t g \varphi_{S_i} / K + (\sin \delta_i + \cos \delta_i t g \varphi_{S_i} / K) \zeta \\ R_{X_i} = (P_{W_{i+1}} \cos \delta_{i+1} - P_{W_i} \cos \delta_i + W_{W_i} \sin \beta_i - U_i \sin \alpha_i - K_c W_i) \\ \quad + (c_{B_i} b_i \cos \alpha_i + c_{S_{i+1}} d_{i+1} \sin \delta_{i+1} - c_{S_i} d_i \sin \delta_i) / K \\ R_{Y_i} = (P_{W_{i+1}} \sin \delta_{i+1} - P_{W_i} \sin \delta_i - W_{W_i} \cos \beta_i + U_i \cos \alpha_i - W_i) \\ \quad + (c_{B_i} b_i \sin \alpha_i + c_{S_{i+1}} d_{i+1} \cos \delta_{i+1} - c_{S_i} d_i \cos \delta_{i+1}) / K \end{array} \right. \quad (5.22)$$

From Eq. (5.21) we have

$$\text{When } i = 1, E_2 = a_1 - p_1 K_c + e_1 E_1 = a_1 - p_1 K_c$$

$$\text{When } i = 2, E_3 = a_2 - p_2 K_c + e_2 E_2 = a_2 + a_1 e_2 - (p_2 + p_1 e_2) K_c$$

Taking into account of that at the boundary of exposure face $E_{n+1} = 0$, it leads to

$$K_c = \frac{a_n + a_{n-1} e_n + a_{n-2} e_{n-1} e_n + \cdots + a_1 e_2 e_3 \cdots e_{n-1} e_n}{p_n + p_{n-1} e_n + p_{n-2} e_{n-1} e_n + \cdots + p_1 e_2 e_3 \cdots e_{n-1} e_n} \quad (5.23)$$

- vi. Attempting a safety factor K , the corresponding earthquake coefficient K_c is calculated by Eq. (5.23). Revise the K according to definite rule and the algorithm is repeated until the K_c is equal to the specified earthquake coefficient, the corresponding K is the expected safety factor of the slope.

5. Stability analysis with curvilinear slip surface

When the materials may be regarded as equivalent continuum, such as the soil or highly fractured rock mass in which soil grains or rock blocks are very small compared to the dimension of the structure concerned, sliding failure may occur along a curved surface. The term ‘‘curvilinear slip’’ should be regarded as

synonymous with the more usual one “circular slip,” which is normally understood to include non-circular slips.

(1) Assumptions

- i. The potential slip mass is a rigid body;
- ii. The base normal force exerts at the middle of each slice base; and
- iii. The Mohr–Coulomb strength criterion is employed;

(2) Algorithm

- i. The sliding body over the slip surface is divided into a string of slices. The slices are usually cut vertically, but horizontal as well as inclined cuts also have been exercised by various researchers. However, the differences between different methods of cutting are not major, and the vertical cut is preferred by most engineers;
- ii. The strength of the slip surface is mobilized to the same degree to bring the sliding body into a limit state. That means there is only a single factor of safety which is applied throughout the whole slip mass;
- iii. Assumptions regarding inter-slice forces are employed to render the problem being statically determinate; and
- iv. The factor of safety is computed from force and/or moment equilibrium equations.

The 2D slice methods with curvilinear slip surface recommended by the DL/T 5353-2006 (2006) “Design specification for engineering slopes in water resources and hydropower project,” SL386-2007 (2007) “Design code for engineering slopes in water resources and hydropower projects,” SL274-2001 (2001) “Design specification for rolled earth–rockfill dams,” DL/T5395.2007 (2008) “Design specification for rolled earth–rockfill dams,” are summarized in Table 5.1. The algorithms based on the Sweden arc method, the simplified Bishop method, and the Morgenstern–Price method will be constructed in detail in the following.

(a) Sweden arc method

The Sweden arc method divides the sliding mass into a number of vertical slices, usually 6–12 being consistent with the general accuracy of the method. The width of the slices may be estimated by $b = \frac{R}{m}$, where R is the radius of arc and $m = 10$ –20, which need not be the same and is usually adjusted such that the entire base of any one slice is located in a single material. The body forces (e.g., weight) of the slice, the lateral inter-slice forces, and the pore pressures at both the base and sides of the slice are assumed to be composed into a resultant force on the slip surface. The condition of rotational stability about the center of the slip arc is enforced by the equality of the moments related to the sliding and resisting forces at the instant of limiting equilibrium state. The analysis itself does not directly indicate the potentially most dangerous slip surface. A slip surface, i.e., the surface with the lowest level of safety against sliding, can be sought only from the results through a set of analyses with regard to various slip surfaces.

Table 5.1 Summary of slice methods

Method	Shape of slip face	Assumptions on the inter-slice forces	Equilibrium conditions required				
			Overall			Slice	
			Moment	Vertical force	Horizontal force	Moment	
Sweden arc	Circular	$X_i = 0, E_i = 0$	✓				✓
Bishop	Curvilinear or multi-planar	$X_i = 0, E_i \neq 0$		✓			✓
Simplified bishop	Circular	$X_i = 0, E_i \neq 0$	✓				✓
Janbu	Curvilinear or multi-planar	E_i exerting at within the points of half and quarter of the slice face			✓		✓
RTM	Curvilinear or multi-planar	Resultant of X_i and E_i is parallel to the bottom slip surface of the upper slice					✓
Morgenstern-price	Curvilinear or multi-planar	$X_i = \lambda \cdot f(x) \cdot E_i$, λ is an arbitrary constant, $f(x)$ is a function	✓	✓	✓		✓
Spencer	Curvilinear or multi-planar	$X_i = \lambda \cdot E_i$, where λ is a constant	✓	✓	✓		✓
Sarma	Curvilinear or multi-planar	X_i and T_i satisfy the Mohr-Coulomb shear strength criterion					✓

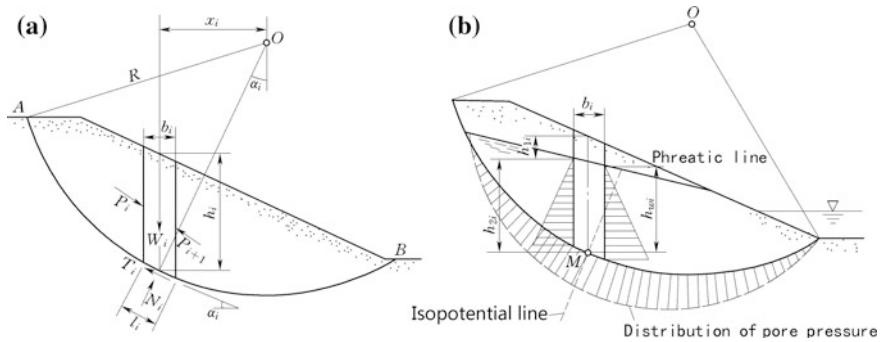


Fig. 5.8 Computation diagram of Swedish arc method. **a** Computation diagram; **b** consideration of pore pressure

The forces exerting on a slice with width b_i (Fig. 5.8) are weight W_i , thrust force P_i on the sides which may be resolved into shear force X_i , an normal force E_i , and shear force T_i , and normal force N_i on its base. The side (inter-slice) forces X_i and E_i depend on the deformation and stress–strain characteristics of the material and cannot be calculated by equilibrium conditions merely. They are usually assumed as zero in a simplified algorithm by conventional Swedish arc method, although it can be approximated with sufficient accuracy in more rigorous methods (e.g., method of Bishop).

Defining the factor of safety K as the ratio of the available anti-sliding moment mobilized by the shear strength of the material to the slip driving moment caused by loads as

$$K = \frac{\sum [c'_i l_i + (W'_i \cos \alpha_i - u_i l_i) \text{tg} \varphi'_i]}{\sum W_i \sin \alpha_i} \tag{5.24}$$

where W'_i = weight of the i th slice for the computation of sliding resistant moment, which is calculated using (1) natural unit weight above the phreatic line, and (2) saturated unit weight between the phreatic line and the water level of river/reservoir, and (3) buoyant unit weight below the water level of river/reservoir, kN; W_i = weight of the i th slice for the computation of sliding driving moment, which is calculated using (1) natural unit weight above the phreatic line, (2) saturated unit weight between the phreatic line and the water level of river/reservoir, and (3) buoyant unit weight below the water level of river/reservoir, kN; u_i = pore pressure on the bottom of the i th slice, which is equal to $u - \gamma_w Z$, in which u is the pore pressure due to the steady seepage flow, kPa; l_i = length of the base of the i th slice, m; α_i = inclination angle of the bottom of the i th slice; c' and φ' = effective shear strength parameters.

Equation (5.24) is implemented using effective stress taking the skeleton of material as the object of study. If the total stress is used where the mixture of material and water as object of study, the zero pore pressure is assumed in the Eq. (5.24), i.e., $u = 0$, and the shear strength parameters c' and φ' are replaced by the corresponding shear strength parameters related to total stress.

In case of the phreatic line is nearly parallel to the slip surface or the thickness of slip mass is small and horizontal loads including seismic inertia force are not considered, the influence of seepage pressure may be simply calculated using “volumetric weight replacement” assumption in a way of:

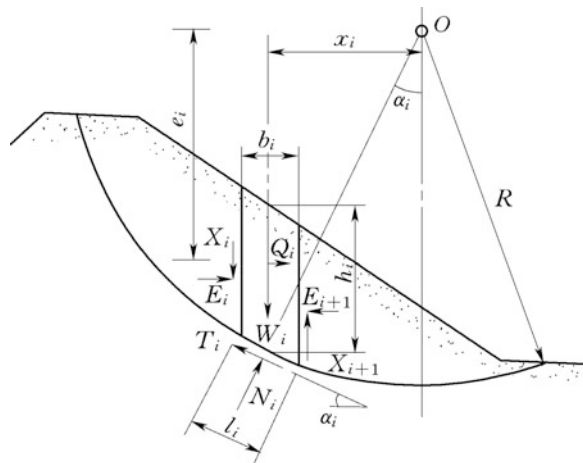
- The item $u_i l_i$ in Eq. (5.24) is neglected;
- The partial weight of the slice between the phreatic line and the pool water level is computed using buoyant or saturated volumetric weight for sliding resistance moment (W'_i) or sliding driving moment (W_i), respectively. The safety factor then may be expressed as

$$K = \frac{\sum [c'_i l_i + W'_i \cos \alpha_i \tan \phi'_i]}{\sum W_i \sin \alpha_i} \tag{5.25}$$

The minimum safety factor and the corresponding critical slip arc are tested by trial-and-error method. A series of potential slip surfaces (arcs) are drawn and the corresponding factors of safety are computed. The slip arc giving the minimum factor of safety is the critical one, because the failure, if it occurs, will take place along this arc. Usually, the larger of the cohesive, the deeper of the slip arc is situated, before the search of critical slip arc by trial-and-error entailed much loss of time. Nowadays, various optimal methods are available for the search with the help of computer programming.

The values of safety factor obtained by the Sweden arc method are conservative (around 10–20 %) and may lead to uneconomical design; this is especially aware where deep-seated slip arc rounds large variation in α , and where high pore pressure exists. Bishop method (Bishop 1955; Bishop and Morgenstern 1960) largely avoids these errors by taking into account of the side (inter-slice) forces in the algorithm (Fig. 5.9).

Fig. 5.9 Computation diagram of simplified Bishop method



(b) Simplified Bishop method

The simplified Bishop method assumes that $X_i = 0$. According to the Mohr–Coulumb strength criterion

$$T_i = \frac{1}{K} [c'_i l_i + (N_i - u_i l_i) \text{tg} \phi'_i] \quad (5.26)$$

By the vertical equilibrium condition of each slice, we have

$$N_i \text{con} \alpha_i = W_i - T_i \sin \alpha_i \quad N_i = \frac{1}{m_{ai}} \left[W_i - \frac{1}{K} (c'_i l_i \sin \alpha_i - u_i l_i \text{tg} \phi'_i \sin \alpha_i) \right] \quad (5.27)$$

where $m_{ai} = \text{con} \alpha_i \left(1 + \frac{\text{tg} \phi'_i \sin \alpha_i}{K} \right)$.

By the horizontal equilibrium condition of each slice, we further have

$$\sum W_i x_i - \sum T_i R + \sum Q_i e_i = 0 \quad (5.28)$$

where Q_i = external horizontal forces such as earthquake forces.

Defining safety factor K as the ratio of the available sliding resistance moment mobilized by shear strength of material to the slide driving moment caused by loads, from Eqs. (5.26)–(5.28) we obtain

$$K = \frac{\sum \frac{1}{m_{ai}} [c'_i l_i + (N_i - u_i l_i) \text{tg} \phi'_i]}{\sum W_i \sin \alpha_i + \sum Q_i \frac{e_i}{R}} \quad (5.29)$$

In which K and m_{ai} are solved by the iteration algorithm.

(c) Morgenstern–Price method

A general method of stability analysis based on the principle of limiting equilibrium, applicable to non-circular slip surface and in which the errors arising from approximate considerations are minimized, has been given by Morgenstern–Price (Morgenstern and Price 1965). The sliding mass is divided into slices, and the condition that there is no rotation of any slice is satisfied by equating the sum of the moments of all forces inclusive inter-slice forces about the base to zero. Since the side forces X and E can exert in several combinations, the problem of slice equilibrium is statically indeterminate and has no unique solution. To transform the statically indeterminate problem into determinate one, a function $f(x)$ is assumed which relates the side forces $E(x)$ and $X(x)$ as

$$\tan \alpha(x) = X(x)/E(x) = \lambda f(x) \quad (5.30)$$

The function $f(x)$ describes the pattern in which the angle $\alpha(x)$ varies from inter-slice to inter-slice. The practitioner has to make the judgment in assuming $f(x)$ or in other words must estimate how the angle $\alpha(x)$ will vary from slice to slice. The

actual magnitudes of these angles are computed as a part of the solution along with the values of forces E , X , N , and T . A computer programming is required to perform the complicated computations.

Having made a suitable assumption for $f(x)$, all the other computed quantities are examined for the reasonableness. For example, some values of $f(x)$ may lead to a distribution where the action line of side forces E falls outside the sliding mass, which is of course unreasonable. Also the values of X must not exceed the shearing strength of the material along the vertical boundary of the corresponding slice nor should any tensile stress manifest across a significant portion of any vertical boundary. By applying the criteria of the foregoing reasonableness, many of the solutions satisfying equilibrium conditions may be eliminated. All the remaining solutions and the values with regard to safety factor must be regarded equally correct. The accuracy of Morgenstern–Price method has not been fully accepted. However, Bishop has denoted that the range of equally correct values of safety factor is quite narrow. In other words, any assumptions leading to reasonable stress distribution will give practically the similar value of safety factor. Limited data indicate that the value of K obtained by this method is usually shifted by less than 6 % subject to various reasonable assumptions relating the function $f(x)$. Application of this method to arc slip surface gives results close to the Bishop’s simplified method.

The Morgenstern–price method involves a great deal of effort and sophisticated judgment; therefore, it is usually not adopted in the design directly. The use of this method has been valued as a “bench mark” for checking the accuracy of solutions obtained by other simpler methods.

5.3.3 Finite Element Method for Elastic Problems

In practice, a FEA commonly consists of three principal steps of preprocessing, structural response computation, and post-processing (Zienkiewicz and Taylor 2005; Zhu 1998).

1. Preprocessing

The user constructs a model to be analyzed in which the domain is divided into a number of discrete subregions, or “elements” connected at discrete points called “nodes” (Fig. 5.10). Certain of these nodes will have fixed displacements, and others will have prescribed loads. This model can be extremely time-consuming to prepare, and commercial codes vie with one another to have the most user-friendly graphical “preprocessor,” are indispensable to assist in this rather tedious work. Some of these preprocessors can overlay a mesh on a preexisting CAD file, so that FEA can be done conveniently as a part of the computerized drafting-and-design process.

The simplest type of two-dimensional solid (entity) element is triangular (Fig. 5.11). There are a variety of three-dimensional solid elements (Fig. 5.12 and

Fig. 5.10 Finite element mesh of a gravity dam

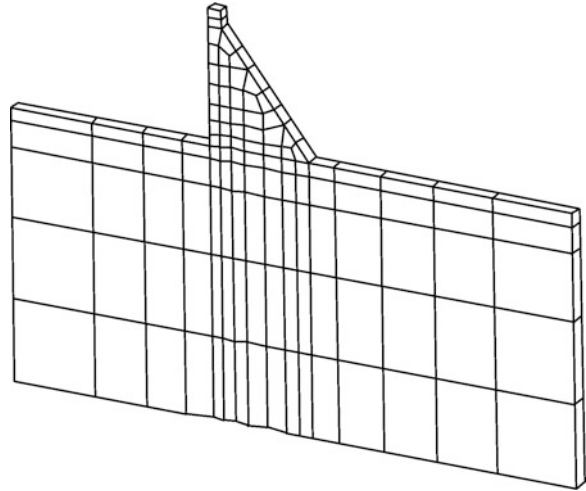


Fig. 5.11 Two-dimensional triangular element

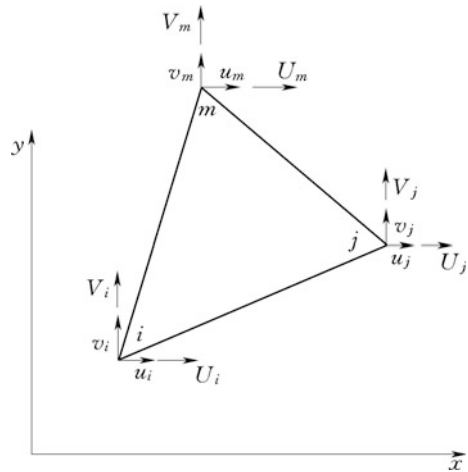


Table 5.2), of which the simplest one is tetrahedral. Usually, the curved edge elements are more adaptive to the structure configuration and have higher precision, but they need more computation capacity and time.

In the analysis of shell structures such as thin arch dams, shell elements are also useful (Fig. 5.13 and Table 5.3).

2. Displacement interpolation

The FEM discretizes the domain concerned into an assemblage of subregions, each of which has its own approximating functions. Take the triangular element ijm in Fig. 5.11 for instance, it has 6 nodal displacements, i.e.,

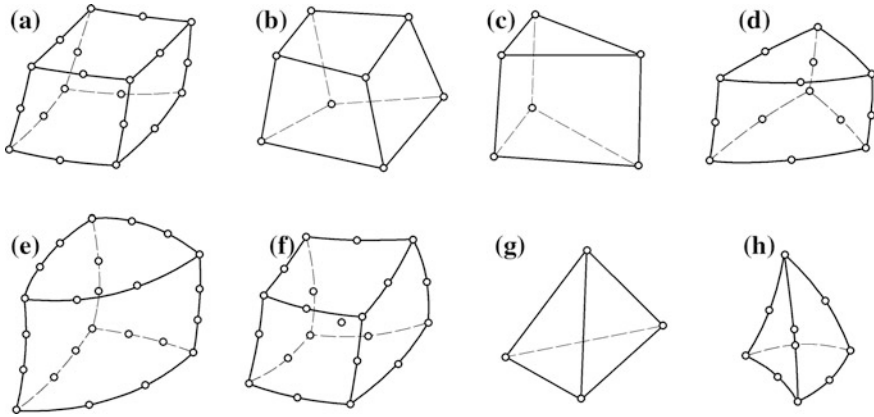


Fig. 5.12 Three-dimensional solid elements

$$\{\delta\}^e = [u_i \quad v_i \quad u_j \quad v_j \quad u_m \quad v_m]^T \tag{5.31}$$

There are also 6 nodal forces as

$$\{F\}^e = [U_i \quad V_i \quad U_j \quad V_j \quad U_m \quad V_m]^T \tag{5.32}$$

The approximation for the displacement within an element is expressed as a combination of the (as yet unknown) nodal displacements belonging to this element

$$\begin{Bmatrix} u \\ v \end{Bmatrix} = [N]\{\delta\}^e \tag{5.33}$$

where $\{\delta\}^e$ = nodal displacement vector; $[N]$ = interpolation function or shape function of the coordinates x and y .

For small deformation problems, we have

$$\left. \begin{aligned} \varepsilon_x &= \partial u / \partial x \\ \varepsilon_y &= \partial v / \partial y \\ \gamma_{xy} &= \partial v / \partial x + \partial u / \partial y \end{aligned} \right\} \tag{5.34}$$

Inserting Eq. (5.33) into Eq. (5.34) leads to

$$\{\varepsilon\} = [B]\{\delta\}^e \tag{5.35}$$

where $[B]$ = strain matrix.

Table 5.2 Three-dimensional solid elements

Type of element	Number of node	Freedom of element	Node number of edge	Remark		
Three-dimensional iso-parametric	Hexahedral	Quadratic curved edges	20	60	1	Figure 5.2a
		Straight edges	8	24	0	Figure 5.2b
		Variable nodes	8–21	24–63	0–1	Figure 5.2f
	Pentahedral	Straight edges	6	18	0	Figure 5.2c
		Curved edges	15	45	1	Figure 5.2d
Tetrahedral		Quadratic	24	72	2	Figure 5.2e
		Cubic	4	12	0	Figure 5.2g
		Straight edges Curved edges	10	30	1	Figure 5.2h

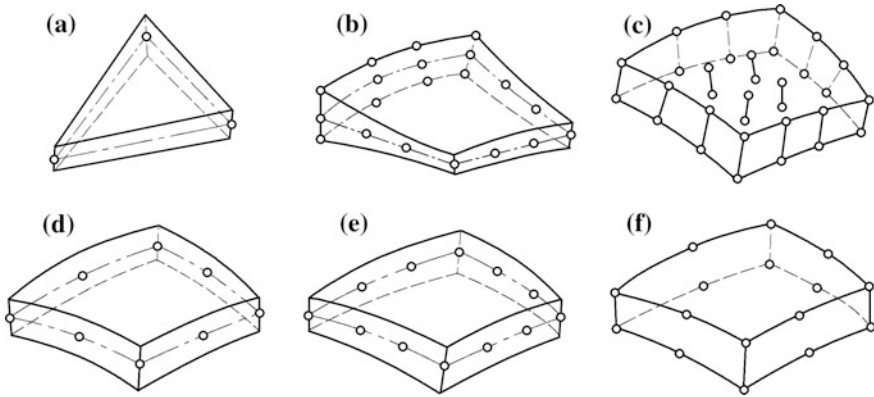


Fig. 5.13 Shell elements

Table 5.3 Shell elements

Type of element		Number of node	Freedom of element	Node number of edge	Remark
Thin shell		3	18	0	Figure 5.3a
Variable nodes	Thin shell	3–16	9–48	0–2	Figure 5.3b
	Thick shell	8–32	24–96	0–2	Figure 5.3c
Quadratic surface thick shell		8	40	1	Figure 5.3d
Cubic surface thick shell		12	60	2	Figure 5.3e
Iso-parametric thick shell		16	48	1	Figure 5.3f

3. Constitutive relation

According to the Hooke’s law,

$$\{\sigma\} = [D]\{\varepsilon\} \tag{5.36}$$

where $\{\sigma\} = [\sigma_x \sigma_y \tau_{xy}]^T$, the stress vector; $\{\varepsilon\} = [\varepsilon_x \varepsilon_y \gamma_{xy}]^T$, the strain vector; $[D]$ = elastic matrix.

Inserting Eq. (5.35) into Eq. (5.36) leads to

$$\{\sigma\} = [S]\{\delta\}^e \tag{5.37}$$

$$[S] = [D][B] \tag{5.38}$$

where $[S]$ = stress matrix.

4. Virtual work principle

If a small, virtual displacement $\{\delta^{*e}\}$ is superimposed on the element e , the corresponding virtual strain within the element is $\{\varepsilon^*\}$, then the virtual work principle is expressed as

$$\{\delta^{*e}\}^T \{F\}^e = \iint \{\varepsilon^*\}^T \{\sigma\} dx dy \quad (5.39)$$

Denoting

$$\{\varepsilon^*\} = [B]\{\delta^{*e}\},$$

the virtual work principle may be rewritten as

$$\{\delta^{*e}\}^T \{F\}^e = \iint \{\delta^{*e}\}^T [B]^T [D] [B] \{\delta\}^e dx dy \quad (5.40)$$

From Eq. (5.40), we have

$$\begin{cases} \{F\}^e = [K]^e \{\delta\}^e \\ [K]^e = \iint [B]^T [D] [B] dx dy \end{cases} \quad (5.41)$$

where $[K]^e$ = stiffness matrix of the element e .

Equation (5.41) is the governing equation for the element e . It is then carried out the algebraic procedure by looping over each element to form global stiffness matrix $[K]$ and force vector $\{F\}$ as is done in the assembly step of matrix truss method, to obtain the governing equation of the whole structure

$$[K]\{\delta\} = \{F\} \quad (5.42)$$

After the solution for the displacement vector $\{\delta\}$, the stress may be computed using Eq. (5.37).

5.3.4 Finite Element Method for Seepage Problems

Two-dimensional steady flow for isotropic permeability is described hereinafter. By the simplification of governing Eq. (3.26) and boundary conditions Eqs. (3.28)–(3.30), we have (Zienkiewicz et al. 1966; Duiguid and Lee 1977; Zhu 1998)

$$\begin{cases} \frac{\partial}{\partial x} \left(k_x \frac{\partial H}{\partial x} \right) + \frac{\partial}{\partial y} \left(k_y \frac{\partial H}{\partial y} \right) = 0 \\ H = H_0(x, y) \\ \left(k_x \frac{\partial H}{\partial x} l_x + k_y \frac{\partial H}{\partial y} l_y \right) = q(x, y) \end{cases} \quad (5.43)$$

The above-governing equation and boundary conditions lead to the following variational principle:

$$J(H) = \iint_D \left\{ \frac{1}{2} \left[k_x \left(\frac{\partial H}{\partial x} \right)^2 + k_y \left(\frac{\partial H}{\partial y} \right)^2 \right] \right\} dx dy + \int_C q H d\Gamma = \min \quad (5.44)$$

The variational function $J(H)$ in Eq. (5.44) is then discretized using the conventional finite element algorithm. Take the triangular element ijm similar to that of Fig. 5.11 as example, on which there are 3 nodal water heads H_i , H_j , and H_m grouped into the vector $\{H\}^e$. At any point within the element e , the hydraulic head may be interpolated as

$$H = [N]\{H\}^e \quad (5.45)$$

Introducing Eq. (5.45) into Eq. (5.44), the variational principle leads to the following:

$$\left\{ \frac{\partial J}{\partial H} \right\}^e = [K]^e \{H\}^e = 0 \quad (5.46)$$

where $[K]^e$ = conductivity matrix of the element e , which is the function of coordinates and permeability coefficient.

By looping over the elements around the node i using Eq. (5.46), we have

$$\frac{\partial J}{\partial H_i} = \sum_{e=1}^m \frac{\partial J^e}{\partial H_i} = 0 \quad i = 1, 2, \dots, n \quad (5.47)$$

The matrix form of Eq. (5.47) is

$$[K]\{H\} = \{Q\} \quad (5.48)$$

where $[K]$ = overall conductivity matrix of the structure; $\{H\}$ = overall water head vector; $\{Q\}$ = overall vector of discharge induced from boundary conditions.

By the solved nodal head $\{H\}$ using Eq. (5.48), the seepage flow velocity, discharge, head gradient, and seepage force are calculated (Vide Eqs. (4.24) and (4.34)–(4.36)). Based on which the flow net [Vide Figs. (4.12 and 4.13)] may be constructed and the velocity field may be drawn as in the Fig. 5.14.

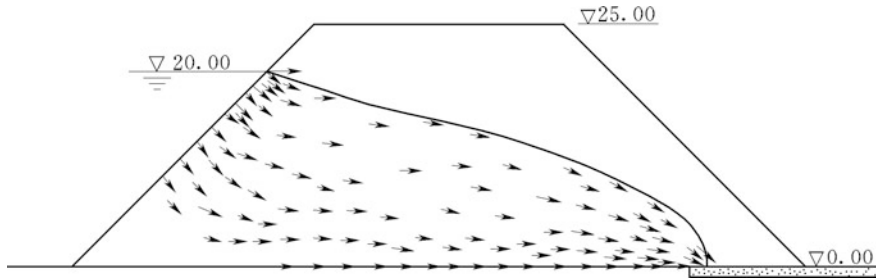


Fig. 5.14 Seepage velocity field in an embankment with horizontal drainage (by FEM)

5.3.5 Finite Element Method for Thermal and Thermal Stress Problems

The analysis is accomplished by two steps: Firstly, solve the thermal regime to obtain the temperature variation ΔT ; then, apply the temperature variation ΔT to induce initial strain or stress in the structures (Fanelli and Giuseppetti 1975; Leger and Leclerc 2007; Singh 1985; Tatro and Schrader 1985).

4. Steady thermal field

Compared to the partial differential equation for steady thermal problems [Eq. (4.22)] and the partial differential equation for steady permeable problems Eq. (4.27), as well as the boundary conditions of Eqs. (4.20)–(4.21) and Eqs. (4.28)–(4.29), the similarity is apparent between the two physical fields. Therefore, the FEM algorithm for the foregoing steady permeable problems may be applied to the steady thermal problems directly. Such similarity also exists between the partial differential equations for unsteady thermal problems and unsteady permeable problems.

2. Thermal stress

Take the triangular element ijm similar to that of Fig. 5.11 as example, on which there are 3 nodal temperature increments ΔT_i , ΔT_j , ΔT_m , and then, the averaged temperature increment is $\Delta T = \frac{1}{3}(\Delta T_i + \Delta T_j + \Delta T_m)$, which induces the initial strain $\{\varepsilon_0\}$ under the circumstance without any restraint

$$\{\varepsilon_0\} = \begin{Bmatrix} \varepsilon_{x0} \\ \varepsilon_{y0} \\ \gamma_{xy0} \end{Bmatrix} = \begin{Bmatrix} \alpha \Delta T \\ \alpha \Delta T \\ 0 \end{Bmatrix} \quad (5.49)$$

where α = coefficient of thermal expansion, which is around 1.0×10^{-5} for concrete, $1/^\circ\text{C}$.

Under certain restraint, the actual strain induced by ΔT is $\{\varepsilon\} = [\varepsilon_x \varepsilon_y \gamma_{xy}]^T$ (as yet unknown). The stress in the element is then calculated by

$$\{\sigma\} = [D](\{\varepsilon\} - \{\varepsilon_0\}) = [D][B]\{\delta\}^e - [D]\{\varepsilon_0\} \quad (5.50)$$

where $[D]$ = elastic matrix; $[B]$ = strain matrix; $\{\delta\}^e$ = nodal displacement vector.

According to the virtual work principle, the governing equation for the solution of nodal displacement vector is

$$[K]\{\delta\} = -\{F_t\} \quad (5.51)$$

in which the overall stiffness $[K]$ is identical to that of Eq. (5.42), and the overall equivalent force vector $\{F_t\}$ is formed by looping over each element using

$$\{F_t\}^e = \iint [B]^T [D] \{\varepsilon_0\} t A dx dy \quad (5.52)$$

where t = thickness of the element, m; A = area of the element, m².

After the solution for the displacement vector $\{\delta\}$, the thermal strain and stress may be computed using Eqs. (5.35) and (5.50).

5.3.6 Finite Element Method for Dynamic Problems

1. Governing equation

The structural analysis for earthquake effects consists of two categories: approximate sliding stability analysis using an appropriate seismic coefficient (see the pseudo-static method in the Chap. 4) and dynamic internal stress analysis (Clough and Penzien 2003; ICOLD 1975, 2001a, b, 2002; Severn 1976) using site-dependent earthquake ground motions. The latter is obligatory for the hydraulic structures whose aseismic and fortifying design class is 1 and is optional for those whose aseismic and fortifying design class is 2 or 3.

By the virtual work principle and the D'Alembert's principle, the governing equation of FEM for dynamic response under the exciting of earthquake is (Chopra 1987; Chopra and Chakrabarti 1981; Newmark 1965; Paulay and Priestley 1992) given as

$$[M]\{\ddot{u}(t)\} + [C]\{\dot{u}(t)\} + [K]\{u(t)\} = -[M]\{\ddot{u}_g(t)\} \quad (5.53)$$

where $[M]$ = mass matrix; $[C]$ = damping matrix; $[K]$ = stiffness matrix; $\{u(t)\}$, $\{\dot{u}(t)\}$, $\{\ddot{u}(t)\}$ = vectors of displacement, velocity, and acceleration, respectively; $\{\ddot{u}_g(t)\}$ = earthquake acceleration of ground motions.

Proportional damping (Rayleigh damping) is commonly stipulated as (Caughey and O'Kelly 1965).

$$[C] = \alpha_0[M] + \alpha_1[K] \quad (5.54)$$

In which α_0 and α_1 are found by the damping ratio as

$$\begin{cases} \zeta_1 = \frac{a_0}{2\omega_1} + \frac{a_1\omega_1}{2} \\ \zeta_2 = \frac{a_0}{2\omega_2} + \frac{a_1\omega_2}{2} \end{cases} \quad (5.55)$$

where ω_1, ω_2 = the 1st and 2nd natural frequencies.

2. Solution algorithm

Modal analysis and time-history analysis are generally employed for solving the Eq. (5.53). The modal analysis is based on the simplifying assumption that the response in each natural mode of vibration can be computed independently and these modal responses can be combined to form the overall response (Williams and Mustoe 1987). Modal analysis techniques applicable to elastic hydraulic structures fall into the simplified response spectrum method and the FEM using either a response spectrum or acceleration-time records for the dynamic input. The time-history analysis allows the designer to determine the number of cycles of nonlinear behavior, the magnitude of excursion into the nonlinear range, and the time the structure remains nonlinear.

Dynamic analysis should begin with the simpler response spectrum method and progress to more refined methods, if needed. The time-history analysis is only required when important yielding (cracking) of the structure is indicated by a response spectrum analysis.

In the following paragraphs, the modal analysis based on FEM using response spectrum is briefly introduced.

The FEM using response spectrum is able to simulate the linear dynamic response of structures by means of the natural (or characteristic) frequencies and corresponding normal modes (or natural modes, mode shapes). Since by the experiences the damping has minor influence on the natural frequencies and modes, it is ordinarily neglected in the modal computation.

Let $[C] = 0$ and $\{\ddot{u}_g(t)\} = 0$ in Eq. (5.53), the governing equation of free vibration without damping is

$$[M]\{\ddot{u}(t)\} + [K]\{u(t)\} = \{0\} \quad (5.56)$$

Assuming the displacements are harmonically related with time, that is

$$\{u(t)\} = \{\delta\} \sin(\omega t + \gamma) \quad (5.57)$$

where $\{\delta\}$ = vector of nodal displacement amplitudes; ω = natural frequencies; γ = initial phase angle.

Inserting $\{\ddot{u}(t)\}$ into Eq. (5.56) and dividing the transformed Eq. (5.56) by $\sin(\omega t + \gamma)$ at its two sides yield

$$\begin{cases} -[M]\omega^2\{\delta\} + [K]\{\delta\} = \{0\} \\ \text{or } ([K] - \omega^2[M])\{\delta\} = \{0\} \end{cases} \quad (5.58)$$

This is a generalized eigenvalue problem, from which non-virtual solution for $\{\delta\}$ does exist only if

$$|[K] - \omega^2[M]| = 0 \quad (5.59)$$

For a two-dimensional problem with n nodes, this is a $2n$ order polynomial equation regarding ω^2 , from which we can find $2n$ solutions (roots) of ω_i , of which ω_1 is the smallest called as the “fundamental frequency.” For each ω_i , Eq. (5.58) gives one solution of eigenvector $\{\delta\}_i$. The Jacobi method is normally applied to seek all the eigenvectors to form natural modes. Since only few frontal (less than 20) modes may be important in the response spectrum analysis, significant reduction in the size of system may be achieved. It is also worthwhile to indicate that for normal mode analysis, support (restraint) of the structure is unnecessary, and the magnitudes of eigenvectors and correspondent stresses have no physical meaning.

Supposing $s \leq 20$, natural frequencies $\omega_1, \omega_2, \dots, \omega_s$ and corresponding modes $\{\delta\}_1, \{\delta\}_2 \dots \{\delta\}_s$ have been found, the displacement of the structure is expressed as

$$\{u(t)\} = Y_1(t)\{\delta\}_1 + Y_2(t)\{\delta\}_2 + \dots + Y_s(t)\{\delta\}_s \quad (5.60)$$

in which $Y_1(t), Y_2(t), \dots, Y_s(t)$ are defined as principal coordinates.

Insert $\{\ddot{u}(t)\}$ and $\{\dot{u}(t)\}$ together with $\{u(t)\}$ by Eq. (5.60) into Eq. (5.53), and using the orthogonal conditions of natural modes, the coupled dynamic Eq. (5.53) may be transformed to the uncoupled equation set with respect to the principal coordinates $Y_i(t)$ as

$$\ddot{Y}_i(t) + 2\omega_i\zeta_i\dot{Y}_i(t) + \omega_i^2Y_i(t) = -(\eta_{x_i}\ddot{u}_{g_x}(t) + \eta_{y_i}\ddot{u}_{g_y}(t)) \quad (i = 1, 2 \dots s) \quad (5.61)$$

$$\begin{cases} \eta_{x_i} = \frac{\{\delta\}_i^T[M]\{I_x\}}{\{\delta\}_i^T[M]\{\delta\}_i} & \{I_x\} = [1 \ 0 \ 1 \ 0 \dots]^T \\ \eta_{y_i} = \frac{\{\delta\}_i^T[M]\{I_y\}}{\{\delta\}_i^T[M]\{\delta\}_i} & \{I_x\} = [0 \ 1 \ 0 \ 1 \dots]^T \end{cases} \quad (5.62)$$

$$\zeta_i = \frac{\alpha_0}{2\omega_i} + \frac{\alpha_1\omega_i}{2} \quad (5.63)$$

in which η_{x_i} and η_{y_i} are mode participation coefficients; ζ_i is damping ratio.

Equation (5.61) is called as modal equation, which are a set of uncoupled, second-order differential equation of $Y_i(t)$ and are much easier to be solved than the original Eq. (5.53).

3. Response spectrum method

$Y_i(t)$ represents the proportion of the i mode shape in the vibration. For a definite earthquake action and damping, the solution of $Y_i(t)$ from Eq. (5.61) depends on ω_i . Let ω as abscissa axis and $Y_i(t)$ as ordinate axis, a group of scattered points called as “displacement response spectrum,” may be plotted. Similarly, let $\dot{Y}_i(t)$ or $\ddot{Y}_i(t)$ as ordinate axis, and ω (or $T = \frac{2\pi}{\omega}$) as abscissa axis, “velocity response spectrum” or “acceleration response spectrum” also may be constructed. Because $Y_i(t)$, $\dot{Y}_i(t)$, and $\ddot{Y}_i(t)$ are time-dependent, such response spectra are time-dependent, too. Since in the practice the maximum earthquake response is the most concern, Y_{imax} , \dot{Y}_{imax} , \ddot{Y}_{imax} are customarily used instead of the time-dependent $Y_i(t)$, $\dot{Y}_i(t)$, and $\ddot{Y}_i(t)$ in the building of response spectra. With the help of such response spectra, it is no longer necessary to solve Eq. (5.61). Instead, Y_{imax} , \dot{Y}_{imax} , and \ddot{Y}_{imax} may be inserted into Eq. (5.60) to obtain an estimation of the maximum total responses (displacement, velocity, and acceleration).

The DL5073-2000 “Specifications for seismic design of hydraulic structures” provides a standard curve of acceleration response spectrum shown in Fig. 5.15, in which $\beta(T)$ is named as dynamic coefficient and defined as the ratio of horizontal maximum absolute acceleration of an elastic system with single degree of freedom (DOF) to the horizontal maximum acceleration of the ground.

Design acceleration response spectrum is dependent on the type of foundation rock and soil, and the distance from the earthquake epicenter to the work site. In Fig. 5.15, β_{max} is the maximum representative value of the design response spectrum, which is selected according to Table 4.4; T_g is the typical period of the design response spectrum related to the foundation character. For rock foundation $T_g = 0.2$ s, for general non-rock foundation $T_g = 0.3$ s, for soft foundation $T_g = 0.7$ s, in case of the design earthquake intensity is not in excessive of 8 and the fundamental period is larger than 1.0 s, the typical period T_g is to be elongated by 0.05 s; β_{min} is

Fig. 5.15 Design acceleration response spectrum

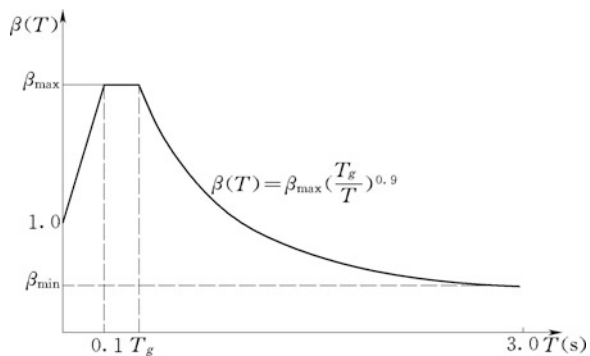


Table 5.4 Maximum representative value of the design response spectrum β_{\max}

Type of structure	Gravity dam	Arch dam	Other concrete structures (e.g., barrage, sluice, intake tower)
β_{\max}	2.00	2.50	2.25

the minimum representative value of the design response spectrum, which should be at least greater than 20 % β_{\max} (Table 5.4).

According to the design response spectrum, the displacement corresponding to the i mode shape is

$$\{u\}_i = \frac{\eta_i}{\omega_i^2} c a_h \beta_i \{\delta\}_i \tag{5.64}$$

where c = comprehensive influencing coefficient, which is similar to the parameter ζ in Eq. (3.70), usually $c = \frac{1}{4} \sim \frac{1}{3}$ but $c = \frac{1}{2} \sim \frac{2}{3}$ for important structure; a_h = standard value of horizontal earthquake acceleration (Table 3.12); β_i = may be found in Fig. 5.15 according to T_i .

The stress corresponding to the i mode shape is

$$\{\sigma\}_i = [D][B]\{u\}_i \tag{5.65}$$

To obtain the overall stress response, the “square root of the sum of squares (SRSS)” method for two-dimensional structures in which the frequencies are well separated may be employed as

$$\{\sigma\} = \left\{ \sqrt{\sum_j^s \sigma_j^2} \right\} \tag{5.66}$$

The SRSS method may dramatically over-estimate or significantly underestimate the dynamic response for three-dimensional structures; hence, the “complete quadratic combination (CQC)” method should be employed to combine the modal responses under such circumstances.

$$S_E = \sqrt{\sum_i^s \sum_j^s \rho_{ij} S_i S_j} \tag{5.67}$$

$$\rho_{ij} = \frac{8\sqrt{\zeta_i \zeta_j} (\zeta_i + \gamma_w \zeta_j) \gamma_w^{3/2}}{(1 - \gamma_w^2)^2 + 4\zeta_i \zeta_j \gamma_w (1 + \gamma_w^2) + 4(\zeta_i^2 + \zeta_j^2) \gamma_w^2} \tag{5.68}$$

where S_E = total effect of earthquake action; S_i, S_j = effects of earthquake action corresponding to the i th and j th mode shapes, respectively; s = number of mode shapes adopted in the computation; ρ_{ij} = correlation coefficient of the i th and j th

mode shapes; ζ_i, ζ_j = damping ratio of the i th and j th mode shapes, respectively; $\gamma_{\omega} = \omega_j/\omega_i$; ω_i, ω_j = natural frequencies of the i th and j th mode shapes, respectively.

For water retaining structure, the hydrodynamic effects are simulated as an added mass $[M_P]$ of water moving with the dam, the dynamic Eq. (5.53) may be rewritten as (Chakrabarti and Chopra 1974):

$$([M] + [M_P])\{\ddot{u}(t)\} + [C]\{\dot{u}(t)\} + [K]\{u(t)\} = -([M] + [M_P])\{\ddot{u}_g(t)\} \quad (5.69)$$

And the solution process is unchanged as has been discussed foregoing.

5.3.7 Block Element Method

The conventional block element method looks at the rock blocks delimited by discontinuities as rigid bodies, while the discontinuities possess elasto-plastic or elasto-viscoplastic characteristics (Chen 2006). The governing equation is formulated considering the force and moment equilibrium condition of blocks, the deformation compatibility condition, as well as the elasto-viscoplastic constitutive relation of discontinuities. After more than twenty years of development, this method may be applied in the nonlinear deformation analysis, stability analysis, seepage analysis, reinforcement analysis, dynamics analysis, and stochastic analysis (Chen 1993a, b; Chen et al. 1994, 2003, 2004a, b, 2010a, b).

In Fig. 5.16, the block r_l is taken as a representative block element, the boundary plane of the block is marked with j_{rlrm} , and the adjoining block contacting the block r_l through the plane j_{rlrm} is marked as r_m .

The total load increment (action) exerting at the centroid of the block r_l is expressed in the global coordinate system as $\{\Delta F\}_{rl} = [\Delta F_X \ \Delta F_Y \ \Delta F_Z \ \Delta M_X \ \Delta M_Y \ \Delta M_Z]^T$, in which $\Delta F_X, \Delta F_Y, \Delta F_Z$ and $\Delta M_X, \Delta M_Y, \Delta M_Z$ are the load

Fig. 5.16 Contact of block elements r_l and r_m

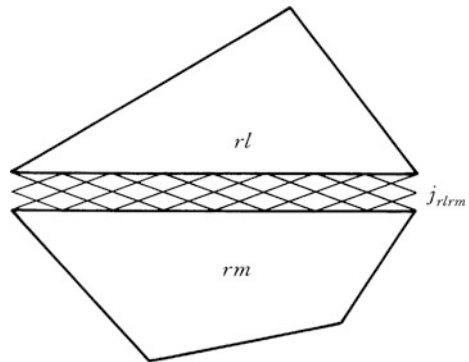
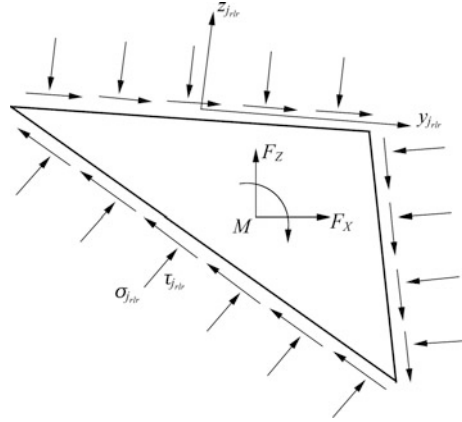


Fig. 5.17 Equilibrium of representative block r_l



and moment increments exerting at the centroid of the block r_l , respectively. The displacement increment of the block r_l is also expressed in the global coordinate system as $\{\Delta U\}_{rl} = [\Delta U_X \ \Delta U_Y \ \Delta U_Z \ \Delta W_X \ \Delta W_Y \ \Delta W_Z]^T$.

1. Force and moment equilibrium equation

Integrating stress increments on each boundary plane of the block r_l and summing them to the centroid, the equilibrium equation for the block r_l is (Fig. 5.17) given as follows:

$$\{\Delta F\}_{rl} - \sum_{j_{rlm}} J(j_{rlm}) \iint_{\Gamma_{j_{rlm}}} [P]_{j_{rlm}} \{\Delta \sigma\}_{j_{rlm}} dx_{j_{rlm}} dy_{j_{rlm}} = 0 \quad rl = 1, \dots, nr \quad (5.70)$$

in which function $J(j_{rlm})$ is defined as

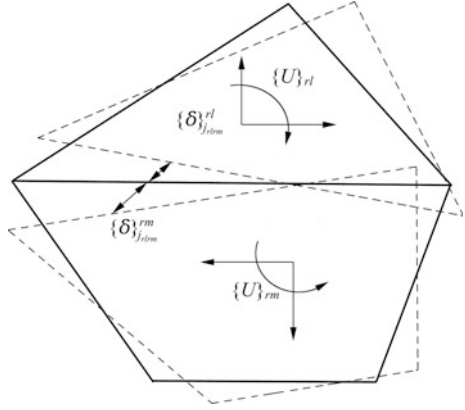
$$J(j_{rlm}) = \begin{cases} 1 & \text{if the block } r_l \text{ is about the plane } j_{rlm} \\ -1 & \text{if the block } r_l \text{ is under the plane } j_{rlm} \end{cases} \quad (5.71)$$

where $[P]_{j_{rlm}} = 6 \times 3$ matrix which is the function of the global coordinate of the discontinuity j_{rlm} on the block r_l , the global coordinate of the centroid of the block r_l , and the dip angle as well as the strike angle of the plane j_{rlm} .

2. Deformation compatibility equation

The displacement increments of the blocks r_l and r_m will give rise to deformation increment $\{\Delta \delta\}_{j_{rlm}}$ on the plane j_{rlm} . By kinematics, the relationship between them can be expressed as (Fig. 5.18) follows:

Fig. 5.18 Deformation of discontinuity j_{rlm} attributable to adjacent blocks r_l and r_m



$$\{\Delta\delta\}_{j_{rlm}} = J(j_{rlm})[L]_{j_{rlm}}([M]_{rl}\{\Delta U\}_{rl} - [M]_{rm}\{\Delta U\}_{rm}) \quad (5.72)$$

where $[L]_{j_{rlm}}$ = matrix function of the strike and dip angle of the plane j_{rlm} ; $[M]_{rl}$ = matrix which is the function of the strike and dip angle of the plane j_{rlm} , the global coordinate of the centroid of the block r_l , and the local coordinate of the discontinuity plane j_{rlm} on which the deformation is concerned.

3. Constitutive equation

Classical phenomenological theory for small strain elasto-viscoplasticity problems postulates that the total strain may be divided into components related to elasticity and viscoplasticity, where the viscoplastic component is usually established either by the Duvaut–Lions formulation (projection formulation) or by the Perzyna formulation (potential formulation) (Perzyna, 1963; Owen and Hinton 1980). According to the prevalent potential formulation, if an explicit time-stepping scheme is employed, the deformation and stress increments at any point $(x_{j_{rlm}}, y_{j_{rlm}})$ on the discontinuity plane j_{rlm} will have the following relationship:

$$\{\Delta\sigma\}_{j_{rlm}} = [D]_{j_{rlm}}\{\Delta\delta\}_{j_{rlm}} + \{\Delta\sigma^0\}_{j_{rlm}} \quad (5.73)$$

where $\{\Delta\sigma^0\}_{j_{rlm}}$ = viscoplastic stress increment; $[D]_{j_{rlm}}$ = elastic matrix expressed by the normal and tangential stiffness coefficients (k_n and k_s) of the plane j_{rlm} .

4. Equilibrium equation of the whole block system

Substituting Eqs. (5.72) and (5.73) into Eq. (5.70), the equilibrium equation of the block r_l becomes

$$[K]_{rl,rl}\{\Delta U\}_{rl} + \sum_{rm} [K]_{rl,rm}\{\Delta U\}_{rm} = \{\Delta F\}_{rl} + \{\Delta F^0\}_{rl} \quad (r_l = 1, 2, \dots, n_r) \quad (5.74)$$

where r_m over-loops all the neighbor blocks of the block r_l in corresponding to the plane j_{rlrm} , and

$$\left\{ \begin{array}{l} [K]_{rl,rl} = \sum_{j_{rlrm}} \iint_{\Gamma_{j_{rlrm}}} [P]_{j_{rlrm}} [D]_{j_{rlrm}} [L]_{j_{rlrm}} [M]_{rl} dx_{j_{rlrm}} dy_{j_{rlrm}} \\ [K]_{rl,rm} = - \iint_{\Gamma_{j_{rlrm}}} [P]_{j_{rlrm}} [D]_{j_{rlrm}} [L]_{j_{rlrm}} [M]_{rm} dx_{j_{rlrm}} dy_{j_{rlrm}} \\ \{\Delta F^0\}_{rl} = - \sum_{j_{rlrm}} J(j_{rlrm}) \iint [P]_{j_{rlrm}} \{\Delta \sigma^0\}_{j_{rlrm}} dx_{j_{rlrm}} dy_{j_{rlrm}} \end{array} \right. \quad (5.75)$$

For the other blocks there also exist similar equations as above, combining all of such equations in the system, the equilibrium equation set of the block system is finally constructed as

$$[K]\{\Delta U\} = \{\Delta F\} + \{\Delta F^0\} \quad (5.76)$$

in which $\{\Delta U\} = [\{\Delta U\}_1^T \dots \{\Delta U\}_{nr}^T]^T$, $\{\Delta F\} = [\{\Delta F\}_1^T \dots \{\Delta F\}_{nr}^T]^T$, and $\{\Delta F^0\} = [\{\Delta F^0\}_1^T \dots \{\Delta F^0\}_{nr}^T]^T$ are the vectors of the displacement increment, the load increment, and the viscoplastic equivalent force incremental, respectively, of the block system.

5.4 Monitoring Modeling

By instrumentation, key parameters concerning the ongoing performance of the hydraulic structures such as dams are monitored. These parameters could be the deformation, thermal, stress/strain, and permeability. Deformation parameters fall into horizontal and vertical displacements, apertures of joint and crack, flexivity and inclination, consolidation, etc.; thermal parameters are mainly temperature; stress/strain parameters comprise stress and strain, earth pressure, dynamic response, etc.; and permeability parameters are seepage discharge, uplift, phreatic line and pore pressure, etc. The instrumentation also provides loading conditions and background information such as reservoir level, seismic shaking, and climate conditions (i.e., rainfall, ambient temperature, and barometric pressure).

For a thorough understanding of the measured parameters and for the early warning where specific action items should be identified for the most likely outcomes from the monitoring, a detailed decision-making process should be prepared to evaluate what the monitoring results mean and whether a condition of concern is developing. For these purposes, a comprehensive study on the monitoring models is essential (Ardito et al. 2008; Gerald and Fritz 2003; Gu and Wu 2006). In the following, the deformation will be taken as an example, to illustrate the modeling principles for the safety monitoring of concrete dams.

5.4.1 Statistical Modeling

Being originated from regression analytic technique and accumulated abundant experiences, the statistical modeling is most prevalent (Ispas et al. 2000). It builds up mathematical relation between loading and deformation through analyzing the relevance between dependent variables and independent variables of monitoring. It has the property of “posterior.”

1. Construction of model

Generally speaking, the deformation of a concrete dam is mainly dominated by hydraulic pressure (up- and downstream water depth, or head difference), temperature, and time (Draper and Smith 1966; Heunecke and Welseh 2000). The statistical model is then conventionally expressed as

$$\hat{y}(t) = \hat{y}_H(t) + \hat{y}_T(t) + \hat{y}_\theta(t) \quad (5.77)$$

where $\hat{y}(t)$ = statistically estimated value of the monitored effect quantity; $\hat{y}_H(t)$ = hydraulic pressure component of $\hat{y}(t)$; $\hat{y}_T(t)$ = temperature component of $\hat{y}(t)$; $\hat{y}_\theta(t)$ = time-dependent component of $\hat{y}(t)$.

(a) Hydraulic pressure component

Hydraulic pressure component may be in a form of polynomial

$$\hat{y}_H(t) = \sum_{i=0}^w a_i H^i(t) \quad (5.78)$$

where $H(t)$ = headwater level or depth, or the head difference between up- and downstream, at time t , m ; a_0 = regression constant; a_i = regression coefficient; $w = 3-4$.

In case of wide variation of downstream level but small variation of up- and downstream head difference, the hydraulic pressure component should be expressed using up- and downstream levels separately

$$\hat{y}_H(t) = a_0 + \sum_{i=1}^w a_{1i} H_1^i(t) + \sum_{i=1}^w a_{2i} H_2^i(t) \quad (5.79)$$

where $H_1(t)$ = headwater level or depth at time t , m ; $H_2(t)$ = tailwater level or depth at time t , m .

(b) Temperature component

The construction of temperature component is tightly related to the manner of thermal regime description. When there are sufficient temperature observation points, the monitored temperatures may be used directly to construct temperature component as

$$\hat{y}_T(t) = b_0 + \sum_{i=1}^q b_i T_i(t) \quad (5.80)$$

where $T_i(t)$ = temperature observation value of the point i at time t , °C; b_0 = regression constant; b_i = regression coefficient; q = number of temperature observation points.

Too many of temperature observation points will give rise to excessive regression coefficients in Eq. (5.80), which will lead to the difficulties with the model solution. Under such circumstances, the means and gradients of the temperature at several horizontal sections may be employed to construct the temperature component as

$$\hat{y}_T(t) = b_0 + \sum_{i=1}^q b_{1i} \bar{T}_i(t) + \sum_{i=1}^q b_{2i} T_{ui}(t) \quad (5.81)$$

where $\bar{T}_i(t)$ = mean temperature of the horizontal section i at time t ; $T_{ui}(t)$ = temperature gradient of the horizontal section i at time t ; b_0 = regression constant; b_{1i} and b_{2i} = regression coefficients; q = number of horizontal observation sections.

Another extraordinary case is that there are only very few or even no temperature observation points. Under such circumstances, the boundary temperatures have to be used to construct the component, subject to the retarding effect of ambient temperature. The temperature component is then constructed as

$$\hat{y}_T(t) = b_0 + \sum_{i=1}^q b_i T_{i(s-e)}(t) \quad (5.82)$$

where $T_{i(s-e)}(t)$ = i th temperature factor, which is the average temperature over the s th day to the e th day from the observation date; q = number of temperature factors; b_0 = regression constant; b_i = regression coefficient.

If there are good temperature observations for the reservoir water, the water temperature factors are added in Eq. (5.82) using the similar form of the ambience temperature factors.

The cyclical form is also widely employed in the construction of temperature component.

(c) Time-dependent component

The origins that give rise to time-dependent deformation are complex, which synthetically reflect the creep of materials of the dam and the foundation, the compression/shear deformation of the geologic discontinuities within the dam foundation, and so on. Referring to the related literatures, time-dependent component may be commonly expressed by

$$\hat{y}_\theta(t) = c_0 + \sum_{i=1}^p c_i I_i(t) \quad (5.83)$$

in which $p = 1-8$; $I_i(t)$ = base functions selected from Eq. (8.84); c_0 = regression constant; c_i = regression coefficient.

$$\begin{cases} I_1 = \ln(t_1 + 1) \\ I_2 = 1 - e^{-t_1} \\ I_3 = t_1/(t_1 + 1) \\ I_4 = t_1 \\ I_5 = t_1^2 \\ I_6 = t_1^{0.5} \\ I_7 = t_1^{-0.5} \\ I_8 = 1/(1 + e^{-t_1}) \end{cases} \quad (5.84)$$

where t_1 = time parameter, which is equal to the days from the onset date to the observation date, divides by 365.

It should be indicated that the statistical model Eq. (5.77) is only for the effect value of displacement (and stress/strain as well). For the effect value of seepage, particularly if the hydraulic structure is near the riverbanks and is influenced by rainfall remarkably, and where the influence of temperature is not so important, three components of the hydraulic pressure, rainfall, and time-dependent are taken into account. The construction of rainfall and time-dependent components is similar to that of Eq. (5.83).

2. Regression of model

Traditional regression techniques include simple linear regression, multiple linear regression, principal component regression, and stepwise regression (Chattefuee and Hadi 2006). Each of them can be employed to analyze the relationship between dependent variables and independent variables. Among them, stepwise regression is the most prevalent one in the analysis of dam deformation.

(a) Multiple linear regression

The monitored effect value $y(t)$ may be looked at as a continuous random variable that observes normal distribution with mathematical expectation E and variance σ^2 . The data consist of m observations on a dependent or response variable $y(t)$ and $n - 1$ predictor (or explanatory) variables, i.e., $x_1(t), x_2(t), \dots, x_{n-1}(t)$. The relationship between $y(t)$ and $x_1(t), x_2(t), \dots, x_{n-1}(t)$ is formulated by linear model. The conditional mathematical expectation $E\{y(t)|x_1(t), x_2(t), \dots, x_{n-1}(t)\}$ of $y(t)$ observes the following regression equation

$$E\{y(t)|x_1(t), x_2(t), \dots, x_{n-1}(t)\} = \beta_0 + \sum_{i=1}^{n-1} \beta_i x_i(t) \quad (5.85)$$

where β_i = coefficient.

Suppose there are m observations for $x_1(t), x_2(t), \dots, x_{n-1}(t)$ (increment), the regression equation based on these observation is

$$\hat{y}(t) = b_0 + \sum_{i=1}^{n-1} b_i x_i(t) \quad (5.86)$$

where $\hat{y}(t)$ = regression of the monitored effect value $y(t)$, which is the unbiased estimation for E of the parent body $y(t)$ under the environmental factors; b_i ($i = 0, 1, \dots, n - 1$) = constants referred to as the model partial regression coefficients (or simply as the regression coefficients), which is the unbiased estimation for the parameters β_i ($i = 0, 1, \dots, n - 1$) of the parent body.

The variance σ^2 of the parent body $y(t)$ is estimated by Eq. (5.86) using the sum of squared residuals S^2 .

Where $m < n - 1$, Eq. (5.86) cannot be solved. On the contrary when $m > n - 1$, Eq. (5.86) has more than one solutions, under such circumstances the least square method may be employed to get the optimal solution of Eq. (5.86) by minimizing the sum of the squares of the errors, i.e.,

$$\frac{\partial Q}{\partial b_i} = \frac{\sum_{j=1}^m [y_j(t) - \hat{y}_j(t)]^2}{\partial b_i} = 0 \quad (i = 1, 2, \dots, n - 1) \quad (5.87)$$

By a direct application of calculus, it can be shown that the least square estimates b_i ($i = 0, 1, \dots, n - 1$) are given by the solution of a group of linear equations known as the normal equations.

Because the unit of $x_i(t)$ ($i = 1, 2, \dots, n - 1$) in Eq. (5.86) is not consistent, it is to be non-dimensionally normalized.

(b) Stepwise regression

Stepwise regression is a composite method using forward and backward multiple regressions, which removes and adds the predictive variables to the regression model through a sequence of tests, so that the best subset of the predictors can be identified. The regression model is very prevalent in China for the purpose of constructing the relationship between dam deformation and environmental variables.

The stepwise method is essentially a forward selection procedure, but with the added proviso that at each stage the possibility of deleting a variable, as in backward elimination, is considered (Chattefuee and Hadi 2006). In this procedure, a variable that entered in the earlier stages of selection may be eliminated at later stages. The calculations made for inclusion and exclusion of variables are the same

as forward selection (FS) and backward elimination (BE) procedures. The procedure is terminated, when dropping a variable does not lead to any further improvement in the accuracy. The final regression equation obtained by the step-wise regression is

$$\hat{y}(t) = b_0 + \sum_{i=1}^k b_i x_i(t) \quad (5.88)$$

where k = final number of predictor (or explanatory) variables, ($k \leq n - 1$).

3. Model tests and diagnostics

(a) Multiple correlation coefficient (R)

Multiple correlation coefficient R ($0 \leq R \leq 1$) is an important index to check the validation of the regression. It is used as a summary gauge to judge the fitness of the linear model $y(t)$ for a given body of data $x_i(t)$ ($i = 1, 2, \dots, k$)

$$R = \sqrt{\frac{\sum_{j=1}^m [\hat{y}_j(t) - \bar{y}]^2}{\sum_{j=1}^m [y_j(t) - \bar{y}]^2}} \quad (5.89)$$

where \bar{y} = mean of the effect value $y(t)$.

When the model fits the data well, i.e., the observed and predicted values closes to each other, the value of R is close to unity. On the other hand, if there is no linear relationship between $y(t)$ and the predictive variables $x_i(t)$ ($i = 1, 2, \dots, k$), i.e., the linear model gives a poor fitting, then R will approach to zero.

(b) Residual standard deviation (S)

$$S = \sqrt{\frac{\sum_{j=1}^m [y_j(t) - \hat{y}_j(t)]^2}{(m - k - 1)}} \quad (5.90)$$

The number $m - k - 1$ in the denominator of Eq. (5.90) is named as the degrees of freedom (DOF). It is equal to the number of observations minus the number of estimated regression coefficients. Residual standard deviation S is also an important index to check the quality of regression equation. The smaller of the S , the higher accuracy of the regression equation is.

(c) Fitting residual $\varepsilon(t)$

Theoretically, the residual $\varepsilon(t)$ ($j = 1, 2, \dots, m$) between the standard deviations of the regressed response variable $\hat{y}(t)$ and the observed one $y(t)$ is a stochastic series observes normal distribution $N(0, \sigma^2)$. If $\varepsilon(t)$ ($j = 1, 2, \dots, m$) does not observe normal distribution and in which there are the periodical or trend terms, the regression equation shall be improved by measures such as to revise original predictive variables.

Using statistical models, the relationship between input and output signals can be formulated only in the sense of regression and/or correlation analysis without physical significance. If an observation is in excess of history record (e.g., a reservoir level higher than the maximum history level), the statistical model may not be able to predict and explain the monitored data, i.e., the accuracy of extrapolated prediction cannot be guaranteed. This is why sometimes such a model is called as “black box” model.

5.4.2 Deterministic Modeling

The deterministic model is an a-priori model which bases on the hydraulic structure design theory according the environmental conditions including loads, structural characteristics, and mechanical properties. There are basically two steps in the modeling: the first step is to determine the displacement at discrete water elevations or discrete temperatures using analytic or numerical methods (e.g., FEM); the second step is to use the least square regression method to determine the best fitted polynomial for the discrete displacements calculated. The polynomial (displacement function) is then used to describe the general relationship between the action effects (displacements) and the actions (loads).

The deterministic model may be used to describe the relation between the environmental variables and the effect variables more profoundly because it is established partially through the simulation analysis of the loading conditions and the structural characteristics of dams. In this sense, only the deterministic model is able to analyze and to explain the mechanism attributable to effect variables.

1. Construction of model

The deterministic model is commonly expressed as

$$\hat{y}(t) = \tilde{y}_H(t) + \tilde{y}_T(t) + \hat{y}_\theta(t) \quad (5.91)$$

where $\hat{y}(t)$ = statistic estimated value of the monitored effect quantity; $\tilde{y}_H(t)$ = hydraulic pressure component of $\hat{y}(t)$; $\tilde{y}_T(t)$ = temperature component of $\hat{y}(t)$; $\hat{y}_\theta(t)$ = time-dependent component of $\hat{y}(t)$.

(a) Hydraulic pressure component

Using a series of representative hydraulic pressure (or headwater depth) H_1, H_2, \dots, H_m , the displacements $y_{H_1}, y_{H_2}, \dots, y_{H_m}$ at the monitoring point k can be obtained, for example, by the FEM calculation. In this way, the data group (H_j, y_{H_j}) ($j = 1, 2, \dots, m$) is collected.

The relation of the displacement and up- and downstream water levels can be gained by the following polynomial regression:

$$y_H = \sum_{i=0}^w a_i H^i \quad (5.92)$$

where y_H = computed displacement; H = hydraulic pressure (or water depth), m; a_0 = regression constant; a_i = regression coefficient; $w = 3-4$ is the maximum order of the polynomial.

The data group (H_j, y_{H_j}) ($j = 1, 2, \dots, m$) applied to Eq. (5.92) produces equation for the regression constant a_0 and regression coefficient a_i , which is solved by regression methods

$$\tilde{y}_H(t) = \sum_{i=0}^w a_i H^i(t) \quad (5.93)$$

where $H(t)$ = hydraulic pressure (or water depth) at time t , m.

(b) Temperature component

Suppose there are q monitoring points for temperature. Unit load method is generally used to calculate the effect values. The unit effect value y_{Ti} under 1 temperature variation at the node i while the rest nodes are unchanged may be calculated by the FEM. Based on the actual temperature increments $\Delta T_1, \Delta T_2, \dots, \Delta T_q$ of all the q temperature monitoring points, the temperature component of the effect value is

$$y_T = \sum_{i=1}^q y_{Ti} \Delta T_i \quad (5.94)$$

The temperature component in the deterministic model is then constructed as

$$\tilde{y}_T(t) = \sum_{i=1}^q y_{Ti} \Delta T_i(t) \quad (5.95)$$

where $\Delta T_i(t)$ = actual temperature increment on point i at time t .

(b) Time-dependent component

The theoretic relation of time-dependent component is difficult to formulate so far. Therefore, the statistical model of Eqs. (5.78)–(5.79) is adopted directly for the time-dependent component even in the study of deterministic modeling.

2. Regression of model

Equations (5.93)–(5.95) are formulated using numerical computation, in which the environmental conditions with respect to loads, structural characteristics, mechanical properties, etc., are not ascertained to be the real-world ones. Therefore, they are subject to adjustment.

Suppose the error of hydraulic pressure component is mainly induced by the inadequate Young's modulus of the dam concrete and foundation rock, then it may be adjusted by a coefficient Φ and the revised hydraulic pressure component is

$$\tilde{y}_H(t) = \Phi \sum_{i=0}^w a_i H^i(t) \quad (5.96)$$

Similarly, suppose the error of temperature component is mainly induced by the inadequate coefficient of thermal expansion of the dam concrete and foundation rock, then it may be adjusted by a coefficient Ψ and the revised temperature component is

$$\tilde{y}_T(t) = \Psi \sum_{i=1}^q y_{Ti} \Delta T_i(t) \quad (5.97)$$

Inserting Eqs. (5.83), (5.84), (5.96), and (5.97) into Eq. (5.91), we have

$$\begin{aligned} \hat{y}(t) &= \tilde{y}_H(t) + \tilde{y}_T(t) + \hat{y}_\theta(t) \\ &= \Phi \sum_{i=0}^w a_i H^i(t) + \Psi \sum_{i=1}^q y_{Ti} \Delta T_i(t) + \sum_{i=1}^p c_i I_i(t) \end{aligned} \quad (5.98)$$

The adjustment coefficients Φ and Ψ as well as regression coefficients c_i related to time in Eq. (5.98) are then regressed in the similar manner of the foregoing statistical modeling.

3. Model tests and diagnostics

Use is also made of multiple correlation coefficient R , residual standard deviation S , and fitting residual $\varepsilon(t)$, for the test and diagnostics of deterministic model.

In addition, the adjustment coefficients Φ and Ψ should be verified, too. The rational value of Φ and Ψ is around 1.0. If the regression produces too large or too small Φ and Ψ , it is necessary to find and to remove the error sources (e.g., wrong mechanical parameters in computation, poor computation algorithm, improper time-dependent component), and to re-establish the model.

5.4.3 Mixed Modeling

There are two kinds of mixed models. One is to use hydraulic component deterministically; meanwhile, to use temperature and time-dependent components statistically, which is in the form of

$$\hat{y}(t) = \tilde{y}_H(t) + \hat{y}_T(t) + \hat{y}_\theta(t) \quad (5.99)$$

Equation (5.99) may be further expressed as

$$\hat{y}(t) = \Phi \sum_{i=0}^w a_i H^i(t) + \hat{y}_T(t) + \sum_{i=1}^p c_i I_i(t) \quad (5.100)$$

Another is to use temperature component deterministically, while to use hydraulic and time-dependent components statistically, which is in the form of

$$\hat{y}(t) = \hat{y}_H(t) + \tilde{y}_T(t) + \hat{y}_\theta(t) \quad (5.101)$$

Equation (5.101) may be further expressed as

$$\hat{y}(t) = \sum_{i=0}^w a_i H^i(t) + \Psi \sum_{i=1}^q y_{Ti} \Delta T_i(t) + \sum_{i=1}^p c_i I_i(t) \quad (5.102)$$

The monitoring models elucidated above have following features:

- They are based on the functional relationship between independent variables (the environmental variables) and dependent variables (e.g., the displacements);
- The models are established for a single dependent variable at one monitor point only;
- In the selection of basic components, the hydraulic pressure, temperature (or rainfall), and time are traditionally taken into account;
- The differences of the foregoing three models lie mainly in the component construction. The solution of the models is identically based on the mathematical and statistical forecast algorithms using least square regression methods.

However, conventional regression approaches including stepwise regression cannot effectively address the difficulty brought about by correlation among the predictive variables. One has to acknowledge the existence of this type of correlation and its adverse influences on the regression modeling and to pay more attention to the selection of environmental variables. Additionally, disadvantage is that the regression appears incapable of analyzing data collected over a short time period, especially if the observation time steps are less than the number of predictor variables.

Presently, a wide range of research activities in the dam deformation analysis by monitoring data are directed to the elaboration of new models, which covers artificial neural network (ANN) model, time series (TS) model, gray system (GS) model, fuzzy mathematic model, and various combined models. They have been extensively exercised and shown good performance in the modeling and predicting of dam behaviors (Gu and Wu 2006).

References

- Ardito R, Maier G, Massaiongo G (2008) Diagnostic analysis of concrete dams based on seasonal hydrostatic loading. *Eng Struct* 30(11):3176–3185
- Barenblatt GI et al (1960) Basic concepts in the theory of seepage of homogenous liquids in fissured rocks. *J Appl Math Mech* 24(5):12–18
- Bell JM (1986) General slope stability analysis. *J Soil Mech and Found Div ASCE* 94 (SM6):1253–1270
- Bishop AW (1955) The use of slip circle in the stability analysis of slopes. *Geotechnique* 5(1):7–17
- Bishop AW, Morgenstern N (1960) Stability coefficients for earth slopes. *Geotechnique* 10(4):129–150
- Brebbia CA, Telles JCF, Wrobel LC (1984) *Boundary element techniques: theory and applications in engineering*. Springer, New York
- Cacas MC, Ledoux B, De Marsity G, Tillie B, Barbreau A, Durand E, Feuga B, Peaudecerf P (1990) Modeling fracture flow with a stochastic discrete fracture network: calibration and validation, 1. The flow model. *Water Resour Res* 26(3):479–489
- Caughey TK, O’Kelly MEJ (1965) Classical normal modes in damped linear dynamic systems. *J Appl Mech ASME* 32(3):583–588
- Chakrabarti P, Chopra AK (1974) Hydro-dynamic effects in earthquake response of gravity dams. *J Struct Div ASCE* 106(ST6):1211–1225
- Chan HC, Einstein HH (1981) Approach to complete limit equilibrium analysis for rock wedges the method of ‘artificial supports’. *Rock Mech* 14(2):59–66
- Chattefuee S, Hadi AS (2006) *Regression analysis by example*, 4th edn. Wiley, New Jersey
- Chen SH (1993a) Numerical analysis and model test of rock wedge in slope. In: *Proceedings of international symposium on assessment and prevention of failure phenomena in rock engineering*. Istanbul (Turkey). Balkema AA, Rotterdam, Netherlands, pp 425–429
- Chen SH (1993b) Analysis of reinforced rock foundation using elastic-viscoplastic block theory. In: *Proceedings of 1993 ISRM international symposium-EUROCK 93*, Lisbon (Portugal). Balkema AA, Rotterdam, Netherlands, pp 45–51
- Chen ZY (2003) *Soil slope stability analysis—theory, method and programs*. China WaterPower Press, Beijing (in Chinese)
- Chen SH (2006) *Computational rock mechanics and engineering*. China WaterPower Press, Beijing (in Chinese)
- Chen SH, Egger P (1997) Elasto-viscoplastic distinct modeling of bolt in jointed rock masses. In: Yuan JX (ed) *Proceedings of computer methods and advances in geomechanics*. Balkema AA, Wuhan, pp 1985–1990
- Chen SH, Egger P (1999) Three dimensional elasto-viscoplastic finite element analysis of reinforced rock masses and its application. *Int J for Num and Anal Meth in Geomech* 23(1):61–78
- Chen SH, Feng XM (2006) Composite element model for rock mass seepage flow. *J Hydrodyn (Series B)* 18(2):219–224
- Chen SH, Qing S (2004) Composite element model for discontinuous rock masses. *Int J Rock Mech Min Sci Geomech Abstr* 41(7):865–870
- Chen SH, Shahrour I (2008) Composite element method for the bolted discontinuous rock masses and its application. *Int J Rock Mech Min Sci* 45(3):384–396
- Chen XH et al (1984) *Structure model of brittle material*. China WaterPower Press, Beijing (in Chinese)
- Chen SH, Shen BK, Huang MH (1994) Stochastic elastic-viscoplastic analysis for discontinuous rock masses. *Int J Num Meth Eng* 37(14):2429–2444
- Chen SH, Xu MY, Shahrour I, Egger P (2003) Analysis of arch dams using coupled trial load and block element methods. *J Geotech Geoenviron Eng ASCE* 11:977–986
- Chen SH, Li YM, Wang WM, Shahrour I (2004a) Analysis of gravity dam on a complicated rock foundation using an adaptive block element method. *J Geotech Geoenviron Eng ASCE* 130 (7):759–763

- Chen SH, Qiang S, Chen SF, Egger P (2004b) Composite element model of the fully grouted rock bolt. *Rock Mech Rock Eng* 37(3):193–212
- Chen SH, Xu Q, Hu J (2004) Composite element method for seepage analysis of geo-technical structures with drainage hole array. *J Hydrodyn (Series B)* 16(3):260–266
- Chen ZY, Wang XG, Yang J et al (2005) *Rock slope stability analysis—theory, method and programs*. China WaterPower Press, Beijing (in Chinese)
- Chen SH, Feng X, Shahrour I (2008a) Numerical estimation of REV and permeability tensor for fractured rock masses by composite element method. *Int J Numer Anal Meth Geomech* 32(12):1459–1477
- Chen SH, Qiang S, Shahrour I, Egger P (2008b) Composite element analysis of gravity dam on a complicated rock foundation. *Int J Geomech ASCE* 8(5):275–284
- Chen SH, Wang WM, Zheng HF, Shahrour I (2010a) Block element method for the seismic stability of rock slopes. *Int J Geotech Geoenviron Eng ASCE* 136(12):1610–1617
- Chen SH, Xue LL, Xu GS, Shahrour I (2010b) Composite element method for the seepage analysis of rock masses containing fractures and drainage holes. *Int J Rock Mech Min Sci* 47(5):762–770
- Chen SH, Su PF, Shahrour I (2011) Composite element algorithm for the thermal analysis of mass concrete: simulation of lift joint. *Finite Elem Anal Des* 47(5):536–542
- Chen SH, He J, Shahrour I (2012) Estimation of elastic compliance matrix for fractured rock masses by composite element method. *Int J Rock Mech Min Sci* 49(1):156–164
- Chopra AK (1987) Simplified earthquake of concrete gravity dam. *J Struct Div ASCE* 113(ST8):1688–1708
- Chopra AK, Chakrabarti P (1981) Earthquake analysis of concrete gravity dams including dam-water-foundation rock interaction. *Earthq Eng Struct Dyn* 9(4):363–383
- Clough RW, Penzien J (2003) *Dynamics of structures*, 3rd edn. Computers & Structures Inc., Berkeley
- Copen MD, Lindholm EA, Tarbox GS (1977) Design of concrete dams. In: Golzé AR (ed) *Handbook of dam engineering*. Company Press VNR, New York, pp 385–498
- Courant R (1943) Variational methods for the solution of problems of equilibrium and vibrations. *Bull. Amer. Math. Soc.* 49(1):1–23
- Cundall PA (1971) A computer model for simulating progressive, large-scale movement in blocky rock system. In: *Proceedings of the international symposium on rock fracture*. ISRM, Nancy, 1 (paper no. II–8), pp 129–136
- Cundall PA (1988) Formulation of three-dimensional distinct element model. Part 1. A scheme to detect and represent contacts in system composed of many polyhedral blocks. *Int J Rock Mech Min Sci Geomech Abstr* 25(3):107–116
- Cundall PA, Hart DH (1992) Numerical modelling of discontinua. *Eng Comput* 9(2):101–113
- Dershowitz WS, Einstein HH (1987) Three dimensional flow modeling in jointed rock masses. In: Herget and Vongpaisal (eds) *Proceedings of 6th international congress on ISRM*, Balkema AA, Rotterdam, vol 1, pp 87–92
- Dershowitz WS, Gordon BM, Kafritsas JC (1985) A new three dimensional model for flow in fractured rock. In: *Proceedings of IAH conference, IAH, Arizona*, vol XVII, pp 449–462
- Draper NR, Smith H (1966) *Applied regression analysis*. Wiley, New York
- Duiguid JO, Lee PCY (1977) Flow in fractured porous media. *Water Resour Res* 13(3):25–28
- Fanelli DIM, Giuseppetti G (1975) Techniques to evaluate effects of internal temperatures in mass concrete. *Water Power Dam Constr* 27(7):226–230
- Fellenius W (1927) Erdstatische berechnungen mit reibung und kohae-sion und unter annahme kreiszylindrischer gleitflaechen [Statistical analysis of earth slopes and retaining walls considering both friction and cohesion and assuming cylindrical sliding surfaces] Berlin (Germany): W Ernst und Sohn (in German)
- Fellenius W (1936) Calculation of the stability of earth dams. In: *Proceedings of the second congress of large dams, ICOLD, Washington DC*, vol 4, pp 445–463
- Fumagalli E (1973) *Statical and geomechanical models*. Springer, Wien

- Gerald B, Fritz N (2003) Mining the data storing dam data to improve safety and management. *Int J Water Power Dam Constr* 55(7):38–43
- Gu CS, Wu ZR (2006) Safety monitoring of dams and dam foundations—theories and methods and their application. Hohai University Press, Nanjing (in Chinese)
- Guzina B, Tucovic I (1969) Determining the maximum three dimensional stability of a rock wedge. *Water Power* 21(10):381–385
- Hart R, Cundall PA, Lemos J (1988) Formulation of three-dimensional distinct element model. Part 2. Mechanical calculations for motion and interaction of a system composed of many polyhedral blocks. *Int J Rock Mech Min Sci Geomech Abstr* 25(3):117–125
- Heunecke O, Welseh W (2000) A contribution to terminology and classification of deformation models in engineering surveys. *J Geospatial Eng* 2(1):35–44
- Hocking G (1976) A method for distinguishing between single and double plane sliding of tetrahedral wedges. *Int J Rock Mech Min Sci Geomech Abstr* 13(9):225–226
- Hoek E, Bray J, Boyd J (1973) The stability of a rock slope containing a wedge resting on two intersecting discontinuities. *Quart J Engng Geol* 6(1):22–35
- Hrennikoff A (1941) Solution of problems of elasticity by the frame-work method. *ASME J Appl Mech* 8(1):A619–A715
- ICOLD (1975) A review of earthquake resistant design of dams (Bulletin 27). ICOLD, Paris
- ICOLD (2001a) Design features of dams to resist seismic ground motion (Bulletin 120). ICOLD, Paris
- ICOLD (2001b) Computational procedures for dam engineering—reliability and applicability (Bulletin 122). ICOLD, Paris
- ICOLD (2002) Seismic design and evaluation of structures appurtenant to dams (Bulletin 123). ICOLD, Paris
- ICOLD (2013) Guidelines for use of numerical models in dam engineering (Bulletin 155). ICOLD, Paris
- Ispas D, Scumpu C, Hulea D, Popescu TD (2000) Dams and their foundations monitoring by statistic methods. *Hidrotehnica* (Special issue edited by the Romanian Committee on Large Dams), vol 45, pp 37–44
- Janbu N (1973) Slope stability computations. In: Hirschfeld RC, Poulos SJ (eds) *Embankment dam engineering—casagrande volume*. Wiley, New York, pp 447–486
- Janbu N. Applications of composite slip surfaces for stability analysis. In: *Proc. of European Conf on the Stability of Earth Slopes*. Stockholm (Sweden): ISRM, 1954, 3:43–49
- Jing LR, Hudson JA (2002) Numerical methods in rock mechanics. *Int J Rock Mech Min Sci* 39(4):409–427
- Leger P, Leclerc M (2007) Hydrostatic, temperature, time-displacement model for concrete dams. *J Eng Mech ASCE* 133(3):267–277
- Londe P (1965) Une method d’analyse a’ trois dimensions de la stabilite d’une rive rocheuse. *Ann Ponts Chaussees* 1:37–60 (in French)
- Londe P, Vigier G, Vormeringer R (1969) Stability of rock slopes—a three-dimensional study. *J Soil Mech Fndn Engng, ASCE* 95 (SM1):235–262
- Long JCS, Gilmour P, Witherspoon PA (1985) A method for steady fluid flow in random three-dimensional networks of dice-shaped fractures. *Water Resour Res* 21(8):35–40
- Meyerhof GG (1984) Safety factors and limit states analysis in geotechnical engineering. *Can Geotech J* 21(1):1–7
- Ministry of Water Resources of the People’s Republic of China SL274-2001 (2001) Design specification for rolled earth-rock fill dams. China WaterPower Press, Beijing
- Ministry of Water Resources of the People’s Republic of China.SL386-2007 (2007) Design code for engineering slopes in water resources and hydropower projects. China WaterPower Press, Beijing (in Chinese)
- Morgenstern NR, Price VE (1965) The analysis of the stability of general slip surfaces. *Geotechnique* 15(1):79–93
- Morton KW, Mayers DF (2005) Numerical solution of partial differential equations, an introduction. Cambridge University Press, Cambridge

- National Reform and Development Commission of the People's Republic of China DL/T 5353-2006 (2006) Design specification for engineering slopes in water resources and hydropower projects. China Electric Power Press, Beijing (in Chinese)
- National Reform and Development Commission of the People's Republic of China DL/T5395.2007 (2008) Design specification for rolled earth-rock fill dams. China Electric Power Press, Beijing
- Newmark NM (1965) Effects of earthquakes on dams and embankments. *Geotechnique* 15(2):139–160
- Nonveiller E (1965) The stability analysis of slopes with a slip surface of general shape. In: Proceedings 6th international conference on soil mechanics and foundation engineering. Montreal, University of Toronto Press, pp 522–525
- Oda M (1985) Permeability tensor for discontinuous rock masses. *Geotechnique* 35(4):483–495
- Owen DRJ, Hinton E (1980) Finite elements in plasticity: theory and practice. Pineridge Press Ltd., Swansea
- Pande GN, Gerrard CM (1983) The behaviour of reinforced jointed rock masses under various simple loading states. In: Proceedings of 5th ISRM congress. Brown Prior Anderson Pty Ltd., Melbourne, pp F217–F223
- Paulay T, Priestley MJN (1992) Seismic design of reinforced concrete and masonry buildings. Wiley, New York
- Perzyna P (1963) The constitutive equations for rate sensitive plastic materials. *Quart Appl Math* 20:321–332
- Petterson KE (1916) Kajraset i Gotenborg des 5te Mars 1916 [Collapse of a quay wall at Gothenburg March 5th 1916]. *Tek Tidskr* (in Swedish)
- Petterson KE (1955) The early history of circular sliding surfaces. *Geotechnique* 5(4):275–296
- Sarma SK (1973) Stability analysis of embankments and slopes. *Geotechnique* 23(3):423–433
- Sarma SK, Bhavne MV (1974) Critical acceleration versus static factor of safety in stability analysis of earth dams and embankments. *Geotechnique* 24(4):661–665
- Severn RT (1976) The aseismic design of concrete dams (part one). *Int J Water Power Dam Constr* 28(1):37–38
- Shi GH (1992) Discontinuous deformation analysis: a new numerical model for the statics and dynamics of deformable block structures. *Eng Comput* 9(2):157–168
- Singh M (1985) State-of-the-art finite element computer programs for thermal analysis of mass concrete structures. *Civil Eng Practic Des Eng* 4(1):129–136
- Spencer E (1967) A method of analysis of the stability of embankments assuming parallel interslice forces. *Geotechnique* 17(1):11–26
- Spencer E (1973) Thrust line criterion in embankment stability analysis. *Geotechnique* 23(1):85–100
- Swoboda G, Marenc M (1991) FEM modelling of rockbolts. In: Beer G et al (ed) Proceedings of computer methods and advances in geomechanics, Balkema AA, Cairns (Australia), pp 1515–1520
- Tatro SB, Schrader EK (1985) Thermal considerations for roller-compacted concrete. *ACI J* 82(2):119–128
- Taylor DW (1937) Stability of earth slopes. *J Boston Soc Civ Eng* 24(3):197–246
- Williams JR, Mustoe GGW (1987) Modal methods for the analysis of discrete system. *Comp Geotech* 4(1):1–19
- Xu MY, Wang WM, Chen SH (2000) Research on the dangerous sliding-block combination of rock slopes. *Rock Soil Mech* 21(2):148–151 (in Chinese)
- Zhu BF (1998) Finite element method—principle and application, 2nd edn. China WaterPower Press, Beijing (in Chinese)
- Zienkiewicz OC, Taylor RL (2005) The finite element method for solid and structural mechanics, 6th edn. Elsevier Butterworth-Heinemann, Oxford
- Zienkiewicz OC, Mayer P, Cheung YK (1966) Solution of anisotropic seepage by finite elements. *J Eng Mech Div ASCE* 92(1):111–120

Chapter 6

Design Criteria and Methods for Hydraulic Structures

6.1 Safety and Reliability Calibration for Hydraulic Structures

6.1.1 Basic Concepts

The structural performance is usually assessed by means of calibration models based on physical understanding and empirical data. Due to idealized modeling, inherent physical uncertainties, and inadequate or insufficient data, these models themselves and the parameters entering the models (e.g., material parameters and load characteristics) are uncertain.

The limited ability of engineers to calibrate structural performance is bridged by a variety of design criteria. These may be broadly classified as safety factor and reliability, depending on the extent of the application of probability theory and statistics in the treatment of stochastic characteristics encountered in engineering (Ang and Tang 1984; Cornell 1969; Ellingwood et al. 1982; Hasofer and Lind 1974; Madsen et al. 1986).

Design using factor of safety belongs to the philosophy of deterministic design (Ministry of Electric Power of the People's Republic of China 1997). It documents the safety of a structure based on the ratio of the calculated bearing capacity R (resistance) to the corresponding load effect S (stress), which is called the safety factor K . It treats the stochastic parameters deterministically using empirical methods. For example, for the loads of extreme adverse, small probability-oriented values are used, whereas for the material strength, conservative and high dependability (assurance factor)-oriented values are adopted. When the safety factor evaluated by computations or experiments is equal to or larger than the specified value (i.e., allowable safety factor or design safety factor), the structure is considered as safe.

Structural reliability theory belongs to the philosophy of indeterministic design (Ministry of Construction of the People's Republic of China 1994). It uses probabilistic modeling for the uncertainties and provides methods for the quantification of

the probability that a structure does not fulfill the performance criteria. In this way, uncertainties can be related quantitatively to the design reliability of a structure. The development of structural reliability theory since the 1970s has provided a more rational basis for the design of structures in the sense that it formulates a consistent basis for the comparison between the reliability of well-tested structures and the reliability of new types of structures.

Nowadays, the theory of structural reliability has been exercised increasingly in connection with the new versions of design codes or specifications all over the world. By means of structural reliability theory and based on existing design codes, the safety formats, such as the design equations, characteristic values, and partial safety factors, may be so specified that the level of reliability of all designed structures is homogeneous and independent of the choice of material and the prevailing loading, as well as the operational and environmental conditions. The choice of the desired level of reliability, or “target reliability,” is commonly understood as “code calibration.”

Nowadays in China, a fairly large part of new version design codes or specifications for hydraulic structures are based on limit state reliability analysis using partial safety factors, which are exercised particularly by the design institutes that formerly belong to the State Electrical Ministry, Energy Ministry, or State Electrical Cooperation. On the other hand, the institutes that belong to the Water Resources Ministry are used to adhere the design codes or specifications mainly based on the traditional safety factor analysis.

6.1.2 Principles of Structural Reliability

1. Reliability

Structural reliability is defined as the probable ability of a structure to complete designed functions under definite period and working conditions.

In the engineering design, the so-called definite period is referred to as the design reference period of the structure. According to the GB50199-94 “Unified design standard for reliability of hydraulic engineering structures”: for the grade 1 water retaining works, the design reference period is equal to 100 year; for the other permanent hydraulic works, the design reference period is equal to 50 year; and for the temporary works, the design reference period is decided according to its anticipated service period subject to possible delay. It should be noted that the design reference period is only a time parameter in the design, which is not equal to the service life of the structure. A structure existing longer than the design reference period means a certain decrease of reliability, but not necessarily to be decommissioned.

The so-called “defined terms” means the working conditions under normal design, construction, and operation.

The so-called “intended function” means the structure should satisfy the following conditions:

- ① During the normal construction and operation period, the structure should be able to sustain possible actions.
- ② During the normal operation period, the structure should have good serviceability. For example, larger deformation or cracking should be well controlled.
- ③ Under normal maintenance, the structure should have no excessive deterioration, i.e., good durability should be assured.
- ④ Under accidental situation (e.g., catastrophe (check) flood, design earthquake), the overall stability of the structure should be maintained.

Items ① and ④ refer to the safety of structure, whereas ② and ③ refer to serviceability and durability.

2. Limit state and limit function

A limit state of a structure entails its loads at which the structure is just on the verge of not satisfying the intended function. The structural performance may be treated in probabilistic terms by means of limit state function, which is the function of the most important uncertainties—the basic random variables. Limit state function is the boundary between reliability and unreliability of the structure concerned.

The limit state is given by a set of values of the input random variables

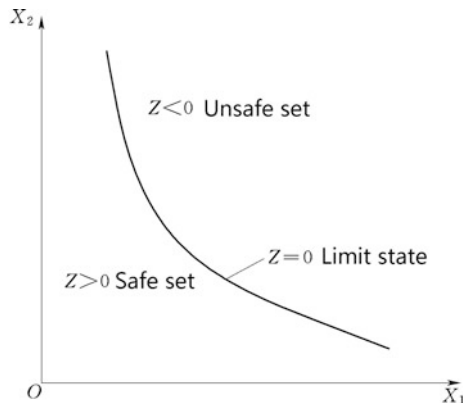
$$Z = g(x_1, x_2, \dots, x_n) = 0 \quad (6.1)$$

where Z and $g(\bullet)$ = function of structure (state function); $x_i (i = 1, 2, \dots, n)$ = variables that independently contribute to the mathematical model concerning geometry, strength properties, and actions.

A given limit state function divides the domain of the design model into three sets (Fig. 6.1):

- When $Z > 0$, the structure is within the safe set;
- When $Z = 0$, the structure is on the boundary of the safe set (also the boundary of the failure set), which is called the limit state;

Fig. 6.1 Working state of a hydraulic structure



- When $Z < 0$, the structure is within the unsafe set.

Limit state may be distinguished as failure events (collapse) and serviceability deterioration.

(a) Collapse limit state

A collapse limit state usually represents a situation where the structure is just at the critical point losing its integrity and passing into an irreversible procedure that may have a catastrophic nature, and from which the structure is only able to be recovered by repair or reconstruction. The following situations may be considered as the collapse limit states of structures:

- The whole structure or a part of the structure loses limit equilibrium (e.g., sliding along the base of a gravity dam).
- Appurtenant of the structure fails due to the excess stress with regard to its strength (including fatigue failure) or can no longer bear loads due to large plastic deformation.
- Loss of elastic stability (buckling).
- The whole structure or a part of the structure is transformed into geometrically unstable (kinematical) system.
- Seepage instability (erosion, piping, pop-off, and flow-off) failure occurs in embankment dams.

One of the collapse limit states for the gravity dam (Fig. 6.2) may be given by the consideration of stability against sliding (Vide Chap. 7):

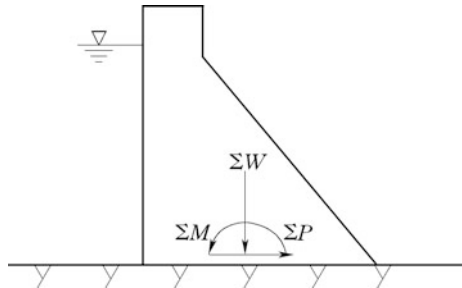
$$Z = f' \sum W + c'A - \sum P$$

where $\sum W$ and $\sum P$ = resultant of forces normal to and parallel to the assumed sliding plane at the dam base, respectively, kN; f' and c' = shear frictional coefficient and cohesion, of concrete–rock bond plane, kN/m²; and A = area of the contact or sliding plane, m².

(b) Serviceability limit state

A serviceability limit state corresponds to the boundary between an acceptable state and a not acceptable state under normal use. Such a state with respect to direct

Fig. 6.2 Loads on a gravity dam base



and catastrophic damage of the structure is often reversible in a sense that the structure by unloading will pass back to the safe set. The following situations may be considered as the serviceability limit states of structures:

- Large but elastic deformation which influences normal operation or external appearance.
- Strong vibration which influences badly on the operating staff, facilities, and instruments.
- Local failure which influences seriously on the structural profile, duration, and anti-seepage ability.
- Other situations which influence the normal operation.

Serviceability limit states permit local permanent damages in a structure such as the formation of cracks or other visible defects. Generally, these damages will not raise a fatal problem in the collapse limit state category provided the structure is subject to general running maintenance.

The requirement for non-tensile stress at the dam heel belongs to the category of serviceability limit states. Based on the gravity method (Vide Chap. 7), the state function Z can be constructed as:

$$Z = \frac{\sum W}{T} + \frac{6 \sum M}{T^2} = 0$$

where $\sum M$ = summation of moments determined with respect to the centroid of the plane, kN m; T = distance from upstream face to the downstream face, of the sectional plane concerned, m.

3. Probability of failure and reliability index

The structural reliability P_s with respect to a definite state function is defined as:

$$P_s = P\{Z \geq 0\} \quad (6.2)$$

Since the case $\{Z \geq 0\}$ and the case $\{Z < 0\}$ are complementary, therefore the failure probability P_f is

$$P_f = P\{Z < 0\} = 1 - P\{Z \geq 0\} = 1 - P_s \quad (6.3)$$

Equation (6.3) indicates a complementary relation between the failure probability P_f and the reliability P_s , i.e., larger P_f means smaller reliability P_s , and vice versa. Therefore, the failure probability P_f is customarily employed to gauge the reliability of structures.

Suppose the joint probability density function of the Z in respect to the random variables (x_1, x_2, \dots, x_n) in Eq. (6.1) is $f_{x_1, x_2, \dots, x_n}(x_1, x_2, \dots, x_n)$, then the probability of failure P_f may be determined by the following integral:

$$P_f = \iiint \dots \int f_{x_1 x_2 \dots x_n}(x_1, x_2, \dots, x_n) dx_1 dx_2 \dots dx_n \tag{6.4}$$

This integral is, however, non-trivial to solve except few cases (e.g., linear limit state functions and normal distributed variables). Therefore, numerical approximations are expedient.

For introducing another commonly employed quantification index—reliability index β , we will first consider the case where the limit state function is a linear function of the basic random variables (x_1, x_2, \dots, x_n) , and the limit state function is

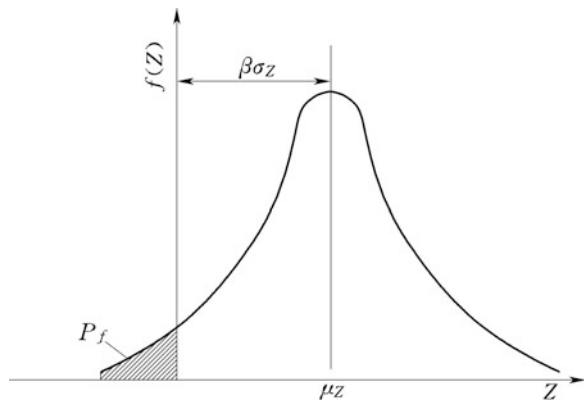
$$Z = R - S$$

in which R is the resistance of structure, S is the effect of actions, R and S are independent and normally distributed with mean value μ_R, μ_S and variance σ_R^2, σ_S^2 , respectively. Under such circumstances, $Z = R - S$ is also normally distributed with mean value μ_z , variance σ_z^2 , and probability density function $f_z(Z)$, as follows (Zhao et al. 2000).

$$\begin{aligned} \mu_z &= \mu_R - \mu_S \\ \sigma_z^2 &= \sigma_R^2 + \sigma_S^2 \\ f_z(Z) &= \frac{1}{\sqrt{2\pi}\sigma_z} \exp\left[-\frac{1}{2}\left(\frac{Z - \mu_z}{\sigma_z}\right)^2\right] \end{aligned}$$

The failure probability P_f (see the area of shadow portion in Fig. 6.3) is then

Fig. 6.3 Computation diagram for failure probability P_f



$$\begin{aligned}
 P_f = P\{Z < 0\} &= \int_{-\infty}^0 f_z(z) dz = \int_{-\infty}^0 \frac{1}{\sqrt{2\pi}\sigma_z} \exp\left[-\frac{1}{2}\left(\frac{Z - \mu_z}{\sigma_z}\right)^2\right] dz \\
 &= \int_{-\infty}^{-\frac{\mu_z}{\sigma_z}} \frac{1}{\sqrt{2\pi}} \exp\left(-\frac{t^2}{2}\right) dt = 1 - \Phi\left(\frac{\mu_z}{\sigma_z}\right) \\
 t &= \frac{Z - \mu_z}{\sigma_z}, dz = \sigma_z dt
 \end{aligned}
 \tag{6.5}$$

where $\Phi(\bullet)$ = standard normal distribution function.

Let $\beta = \frac{\mu_z}{\sigma_z}$ (i.e., $\mu_z = \beta\sigma_z$, see Fig. 6.3), then

$$P_f = 1 - \Phi(\beta) = \Phi(-\beta) \tag{6.6}$$

From Eq. (6.6) (also see Table 6.1), it may be found that smaller β leads to larger P_f , and vice versa; this is why β is named as “reliability index” (Tables 6.1 and 6.2).

It should be pointed out that the formula $\beta = \frac{\mu_z}{\sigma_z} = \frac{\mu_R - \mu_S}{\sigma_z}$ is only valid for the case of $Z = R - S$ with independently and normally distributed R and S , or Z is the linear function of the basic random variables (x_1, x_2, \dots, x_n) independently and normally distributed. Under such circumstances, the probability of failure in the simplest case described foregoing reduces to some simple evaluations in terms of mean values and standard deviations of the basic random variables, i.e., the first- and second-order information.

Table 6.1 Target reliability index β_T and corresponding probability of failure P_f for collapse limit states under permanent situations

Safety grade of structure		I	II	III	
Type of failure	Failure type 1	β_T	3.7	3.2	2.7
		P_f	1.08×10^{-4}	6.8×10^{-4}	3.47×10^{-3}
	Failure type 2	β_T	4.2	3.7	3.2
		P_f	0.13×10^{-4}	1.08×10^{-4}	6.8×10^{-4}

N.B. Failure type 1: non-sudden failure, obvious premonitory before failure, failure progresses slowly

Failure type 2: sudden failure, no obvious premonitory before failure, difficult to remedy or restore once the accident take places

Table 6.2 Safety grade of hydraulic structure versus grade of hydraulic structure

Safety grade of hydraulic structure	Grade of hydraulic structure
I	1
II	2.3
III	4.5

The reliability index β has a simple geometrical interpretation defined as the shortest distance from the origin to the line (or the hyper-plane) forming the boundary between the safe domain and the failure domain. It would be worthwhile to indicate that this more broad definition of the reliability index does not depend on the type of limit state function (linear or nonlinear). The point on the failure surface with the shortest distance to the origin is commonly denoted as the “design point” or “most likely failure point.”

Where the basic random variables (x_1, x_2, \dots, x_n) are not independent or not normally distributed, the function Z is no longer in linear form, β may only be calculated approximately as in the JC method (design point method) (Zhao et al. 2000).

4. Target reliability

A reliability-based design can address the issue of safety in a transparent and quantitative manner. An important element in this process is the specification of maximum permissible probabilities of failure (or non-compliance) in all modes that are relevant to the given kind of the structure.

The “target reliability” (or design reliability), which is the complement of the maximum permissible failure probability, should depend foremost on the consequences of failure in question, which are injury or loss of life, direct and indirect economic losses (including repair/replacement expenditures, loss of revenue, and compensation for damages), environmental pollution, and so on. Consequences should be measurable, and all relevant consequences should be included in the analysis. Target reliabilities also should depend on the algorithm of reliability analysis, on the types of uncertainties included in the analysis, and on future maintenance strategies. However, due to the difficulties with insufficient statistics and complicated analysis, the “code calibration” is normally employed to evaluate target reliability level, which is determined by the calibration for existing practices (i.e., on existing codes), assuming that the existing practices are optimal. Hydraulic structures such as dams, tunnels, spillways, and cut slopes, that have a history of successful service, can be deemed sufficiently safe, and their reliability levels may be used as the targets for new structures of the same kind. This, in principle, is customarily done when a new reliability-based code is developed for a given class of structures with a successful history of service. The objective of such new design code compiling is solely to produce more uniform safety levels, which may provide a more rational and solid platform for the next generation of design code in the future.

Table 6.1 lists the target reliability index β_T and corresponding probability of failure P_f for collapse limit states under permanent situations, which are stipulated in the GB50199-94 «Unified design standard for reliability of hydraulic engineering structures» using code calibration method.

6.1.3 Partial Safety Factor Method for Hydraulic Structures

Direct reliability design using the methods and criteria as illustrated above may comprehensively and sufficiently take into account the stochastic characteristics of the factors influencing the safety of hydraulic structures, but it is complex and inconvenient for implementation. To facilitate the applications and to attend the habits of engineers, many Chinese design codes or specifications recommend partial safety factor method based on limit state equation. In its mathematical principles, the partial safety factor method is a deterministic way to analyze limit state equation. However, it does consider the uncertainty by introducing a group of so-called partial safety factors larger than or equal to 1 (see later though).

The partial safety factor method is an extreme simplification by representing the random variables (x_1, x_2, \dots, x_n) completely rudimentary and replacing each of them by a single or some few “characteristic values” in a form of suitable fractile values. Then, these characteristic values are divided by or multiplied by partial safety factors meant to amplify the actions or to reduce the material strength, which are denoted as “design values.” This is to be interpreted such that a structure is just sufficiently safe where $Z = g(x_1, x_2, \dots, x_n) \geq 0$ for all possible choices of design values (Zhao et al. 2000).

The method in itself contains no possibilities for choosing partial safety factors; hence, their value assessments must be based on a calibration with the aid of a realistic probability model for having a safety margin. For a given structure type, there are, in general, several different choices of dimensions or material strength levels that give the same failure probability. After each choice (of which some are more convenient and economical than others), the characteristic values are uniquely fixed. Although there is still a certain freedom to choose the values of the partial safety factors, it is usually possible to calibrate them such that much more structures have the given failure probability.

1. General design requirements

The GB50199-94 《Unified design standard for reliability of hydraulic engineering structures》 stipulates 3 design situations during the periods of construction, operation, and service, as follows:

- Permanent situations: They are corresponding to long duration, usually same as the design reference period. An example is the normal operation situation.
- Temporary situations: They correspond to construction situation, service situation, or the other temporary situation during operation.
- Accidental situations: They correspond to situations with lower probability, but if happens, it will result in serious consequences. For example, the catastrophe (check) flood, the design earthquake, and the drainage ineffectiveness are distinguished as accidental situations.

According to the probabilities of occurred actions during the construction, operation and service periods, as well as the structure system and environmental

conditions, the collapse limit states and serviceability limit states are considered for different design situations. Collapse limit states are compulsory for all permanent, temporary, and accidental situations. Serviceability limit states are compulsory for permanent situations, but optional for temporary situations, and not necessary for accidental situations.

Different reliability levels should be targeted according to the probability and the effects of situations. Table 6.1 lists the reliability level for hydraulic structures under permanent situations considering collapse limit states. For temporary and accidental situations, the GB50199-94 “Unified design standard for reliability of hydraulic engineering structures” stipulates no specifications. However, it is bearing in mind that under temporary situations, the reliability levels could be lower than that of permanent situations, whereas under accidental situations, the reliability level could be further lower than that of temporary situations, but the reduction should be not too exaggerated.

For collapse limit states, the following two action effect combinations are considered:

- Basic combinations: For permanent situation and temporary situation, combination of action effects considering permanent and alterable actions.
- Accident combinations: Under accident situations, combinations of action effects considering permanent and alterable actions plus one accident action. Since two accident actions that occur within the design reference period have ignorable probability, the accident action combinations comprise merely one accident action, for example, the catastrophe (check) flood and earthquake are not combined.

The deformation and crack aperture depend on the duration of the actions. The longer duration under lower action level could give rise to increasing action effects (e.g., rheology); on the contrary, the shorter duration even with higher action level could only induce smaller action effects. Hence, for serviceability limit states, the following two action combinations are considered:

- Short-term combinations. Under permanent situations and temporary situations, combination for considering short-term effects of alterable actions plus effects of permanent actions.
- Long-term combinations. Under permanent situations, combination for considering long-term effects of alterable actions plus effects of permanent actions. The standard value of alterable action is multiplied by a long-term combination coefficient ρ .

2. Types and selection of partial safety factors

There are 5 types of partial safety factors.

- (a) Structure importance factor (γ_0)

It is employed to represent the reliability level for different safety grades of hydraulic structures. $\gamma_0 = 1.1, 1.0,$ and 0.9 is corresponding to the safety grade I, II, and III (Table 6.2), respectively.

(b) Design situation factor (ψ)

It is employed to reflect the reliability level corresponding to different design situations. According to the DL5108-1999 “Design specification for concrete gravity dams”, $\psi = 1.0, 0.95,$ and 0.85 (apart from earthquake) for permanent situations, temporary situations, and accidental situations, respectively.

(c) Load (action) factor (γ_f)

It is used to consider the adverse variation to the characteristic values of actions and is defined as:

$$\gamma_f = \frac{F_d}{F_k} \quad (6.7)$$

where F_k = characteristic value of action specified in the DL 5077-1997 “Specifications for load design of hydraulic structures” and F_d = design value defined at near the design point (check point) of the limit state equation. In case of difficulties, it also may be chosen by the code committee among the existing structures that represent good (optimal) and safe engineering practices.

For commonly encountered distribution models, the load factor is calculated as:

① Normal distribution

$$\gamma_f = \frac{1 + K_{f1} \delta_f}{K_{f2} \delta_f} \quad (6.8)$$

② Logarithmic normal distribution

$$\gamma_f = \exp \left[(K_{f1} - K_{f2}) \sqrt{\ln(1 + \delta_f^2)} \right] \quad (6.9)$$

③ I-shaped extreme value distribution

$$\begin{cases} \gamma_f = \frac{1 - 0.45005\delta_f - 0.77970\delta_f \ln\{-\ln[\Phi(K_{f1})]\}}{1 - 0.45005\delta_f - 0.77970\delta_f \ln\{-\ln[\Phi(K_{f2})]\}} \\ K_{f1} = \Phi^{-1}(P_{f1}) \\ K_{f2} = \Phi^{-1}(P_{f2}) \end{cases} \quad (6.10)$$

where δ_f = coefficient of variation of the action; P_{f1} = probability according to the normal distribution of the design value of the action F_d ; and P_{f2} = probability according to the normal distribution of the design value of the action F_k .

(d) Resistance (material property) factor (γ_m)

It is employed to consider the adverse variation to the characteristic values of material property and is defined as:

$$\gamma_m = \frac{f_k}{f_d} \quad (6.11)$$

where f_k = characteristic value of material property and f_d = design value of the material.

The characteristic value of the strength f_k for artificial materials (exclusive massive concrete) is equal to the 0.05 tantile on the probability distribution, whereas for massive concrete, foundation, and underground cavern surrounding rock masses, f_k is equal to the 0.2 tantile on the probability distribution, and for rock and earth (in embankment dams) and soil foundation, f_k is equal to 0.1 tantile on the probability distribution. The characteristic values of the Young's modulus, the Poisson's ratio, and the other parameters of artificial materials, foundation, and surrounding rock masses are equal to the 0.5 tantile on the probability distribution.

Usually, the material design value f_d should be adopted as to close to the design (check) point. However, it is also able to use a certain tantile on the probability distribution according to the design experiences. For example, the design strength value for steel bars may use $\mu_m - 2\sigma_m$, in which μ_m, σ_m are the mean and covariance of the steel bar.

For commonly encountered normal distribution and logarithmic normal distribution, resistance (material property) factors are computed as follows.

① Normal distribution

$$\gamma_m = \frac{1 - K_{m2}\delta_m}{1 - K_{m1}\delta_m} \quad (6.12)$$

② Logarithmic normal distribution

$$\begin{cases} \gamma_m = \frac{1}{\exp[(K_{m2} - K_{m1})\sqrt{\ln(1 + \delta_m^2)}]} \\ K_{m1} = \Phi^{-1}(P_{m1}) \\ K_{m2} = \Phi^{-1}(P_{m2}) \end{cases} \quad (6.13)$$

where δ_m = coefficient of variation of the materials characteristics; P_{m1} = probability according to the normal distribution of the design value of the material property f_d ; and P_{m2} = probability according to the normal distribution of the characteristic value of the material property f_k .

(e) Structural coefficient (γ_d)

It is employed to consider the uncertainties in action effect calculation and resistance calculation, as well as in others that can not be reflected in the heretofore four factors. γ_d should be decided according to the target reliability and the

corresponding factors γ_o , ψ , γ_f , and γ_m . Using limit state expression containing partial safety factors, a series of structural coefficient γ_d may be tentatively calculated corresponding to the different design situations, the optimal one is selected through the compromising comparison.

3. Limit state expression containing partial safety factors

For the basic combination and collapse limit state, we have the following:

$$\gamma_o \psi S(\gamma_G G_k, \gamma_Q Q_k, a_k) \leq \frac{1}{\gamma_{d1}} R\left(\frac{f_k}{\gamma_m}, a_k\right) \tag{6.14}$$

where $S(\bullet)$ = action effect function; $R(\bullet)$ = resistance function; γ_G = partial safety factor for permanent action (see Table 6.3); G_k = characteristic value of permanent action; γ_Q = partial safety factor for alterable actions (see Table 6.3); Q_k = characteristic value of alterable action; a_k = characteristic value of geometry parameter; γ_m = partial safety factor for material property (see Table 6.4); and γ_{d1} = structural coefficient for the basic combination and collapse limit state.

For the accident combination and collapse limit state, we have the following:

$$\gamma_o \psi S(\gamma_G G_k, \gamma_Q Q_k, A_k, a_k) \leq \frac{1}{\gamma_{d2}} R\left(\frac{f_k}{\gamma_m}, a_k\right) \tag{6.15}$$

where A_k = characteristic value of accident action; γ_{d2} = structural coefficient for the accident combinations and collapse limit state.

Table 6.3 Partial safety factors (γ_Q) for actions

Type of action		Partial safety factors
Self weight		1.0
Hydraulic pressure	Static pressure	1.0
	Dynamic pressure: time averaged pressure, centrifugal pressure, impact pressure, fluctuation pressure	1.05, 1.1, 1.1, 1.3
Uplift	Seepage pressure	1.2 (solid gravity dam), 1.1 (slotted or hollow gravity dam)
	Uplift pressure	1.0
	Uplift with pump drainages	1.1 (before the main drains)
	Residual uplift with pump drainages	1.2 (after the main drains)
Silt pressure		1.2
Wave pressure		1.2

NB. The other partial safety factors for actions may be found in the DL5077-1997 “Specifications for load design of hydraulic structures”

Table 6.4 Partial safety factors (γ_m) for material properties

Material property		Partial safety factors	Remarks		
Shear friction strength	Concrete/foundation rock	Friction coefficient f'_R	1.3		
		Cohesion c'_R	3.0		
	Concrete/concrete	Friction coefficient f'_c	1.3		Inclusive the lift joints of normal concrete and RCC
		Cohesion c'_c	3.0		
	Foundation rock/foundation rock	Friction coefficient f'_d	1.4		
		Cohesion c'_d	3.2		
Weak seam	Friction coefficient f'_d	1.5			
	Cohesion c'_d	3.4			
Strength of concrete		Compressive strength σ_c	1.5		

For accident combinations, the partial safety factors corresponding to accident actions are equal to 1.0, and for the alterable action that occurs simultaneously with accident actions, its characteristic value may be reduced appropriately according to engineering experiences. For example, in the consideration of catastrophe (check) flood, the wind speed in the calculation of wave height may be lower than that of normal storage level.

For the short-term combination and serviceability limit state, the partial safety factors for actions and material properties are all equal to 1.0, and the corresponding design expression is

$$\gamma_o S(G_k, Q_k, f_k, a_k) \leq \frac{c}{\gamma_{d3}} \tag{6.16}$$

where c = limit value of structural function; γ_{d3} = structural coefficient for the short-term combination and serviceability limit state.

For the long-term combination and serviceability limit state, the partial safety factors for actions and material properties are all equal to 1.0, and the corresponding design expression is

$$\gamma_o S(G_k, \rho Q_k, f_k, a_k) \leq \frac{c}{\gamma_{d4}} \tag{6.17}$$

where γ_{d4} = structural coefficient for the long-term combination and serviceability limit state; ρ = coefficient of alterable actions in long-term combination, $\rho \leq 1$.

Take the gravity dam (vide Chap. 7) for example, the stability against sliding along dam base and compressive strength at dam toe belong to collapse limit states, whereas the requirement for non-tensile stress at dam heel belongs to the category of serviceability limit state. According to the limit equilibrium method and the gravity method, the action effect function $S(\bullet)$ and resistance function $R(\bullet)$ corresponding to these limit states may be established as follows.

① Collapse limit state based on stability against sliding

$$\begin{aligned}
 S(\bullet) &= \sum P \\
 R(\bullet) &= f' \sum W + c'A
 \end{aligned}
 \tag{6.18}$$

where $\sum P$ = resultant of forces parallel to the assumed sliding plane, kN; $\sum W$ = resultant of forces normal to the assumed sliding plane, kN; f' = shear frictional coefficient of the concrete–rock bond plane; c' = cohesion representing the unit shearing strength of concrete–rock bond plane under conditions of zero normal stress, kN/m²; and A = area of contact or sliding plane on the dam base, m².

② Collapse limit state based on compressive strength at dam toe

$$\begin{aligned}
 S(\bullet) &= \left[\frac{\sum W}{T} - \frac{6 \sum M}{T^2} \right] (1 + m^2) \\
 R(\bullet) &= \sigma_C
 \end{aligned}
 \tag{6.19}$$

where $\sum W$ = resultant vertical load above the dam base, kN; $\sum M$ = summation of moments determined with respect to the centroid of the plane, kN m; T = distance from upstream face to the downstream face, of the plane concerned, m; m = slope of down-stream face; and σ_C = compressive strength of concrete, kN/m².

The structural coefficients for above two limit states are listed in Table 6.5.

③ Serviceability limit state based on tensile strength at dam heel

Table 6.5 Structural coefficients for gravity dams

Item	Combination	Structural coefficient	Remarks
Stability against sliding	Basic combination	1.2	Inclusive dam base, geologic construction interfaces within foundation
	Accident combination	1.2	
Compressive strength	Basic combination	1.8	
	Accident combination	1.8	

$$\begin{aligned}
 S(\bullet) &= \frac{\sum W}{T} + \frac{6 \sum M}{T^2} \geq 0 \\
 R(\bullet) &= 0
 \end{aligned}
 \tag{6.20}$$

In Eqs. (6.18)–(6.20), all the variables are design values calculated using the partial factors and the characteristic values by Eqs. (6.7)–(6.13).

6.2 Optimal Design for Hydraulic Structures

6.2.1 Basic Concepts

It is a fairly accepted fact that one of the most important human activities is decision-making, no matter what field of activity one belongs to. Optimization techniques play a key role in structural design; the very purpose of which is to find the best way so that a designer or a decision-maker can derive a maximum benefit from the available resources. To reach this goal, the traditional manner is to use the trial-and-error procedure repeatedly: According to the experiences and judgments of the designers, a preliminary scheme is contemplated; the scheme is repeatedly adjusted on the basis of permissible criteria with respect to stress, stiffness, and stability until a satisfied scheme is finally accepted.

This design procedure has two basic apparent shortcomings: On the one hand, it is long-winded and low-efficiency process; on the other hand, the final optimized scheme is much influenced by the selection of initial scheme, which is dependent on the experiences of the designers; this means the final scheme could not be exactly the real optimal one.

Such shortcomings can now be overcome by undertaking a direct or optimal design procedure with the help of powerful computers. The feature of such optimal design is that it consists of only logical decisions. The basic requirements for an efficient structural design is that the response of the structure should be acceptable as per various specifications, i.e., it should at least be a feasible design. There can exist a large number of feasible designs, but it is desirable to choose the best one from them. In making a logical decision, one sets out the constraints and then minimizes or maximizes the objective function, which could be either expenditure, weight, or merit function (Bogle and Zilinskas 2009; Wang et al. 1998).

There are various factors (constraint conditions) influencing the structural design, such as:

- Conditions for normal operation, including stresses, deflections, natural frequencies, and buckling loads.
- Conditions for normal construction, including placement or fill ability, and thermal control requirements.

- Other requirements from service, including limited deflections and facilitated operation.

Optimal design for hydraulic structures is commonly accomplished by the following three steps:

- Building of mathematical model, considering the major factors in the design, transforming the engineering problem into mathematical problem.
- Selection of effective optimal algorithm.
- Implement the algorithm, and solve it using computer.

6.2.2 *Mathematical Models for Structural Optimal Design*

A structural design problem can be represented by a mathematical model whose constituent elements are design parameters, constraints, and objective or merit function (Li, 1979; Wasserman, 1984; Yao and Choi 1989).

1. Design parameters (variables)

Design parameters specify the geometry and topology of a structure and the physical properties of its members. Some of these can be independent design parameters, and others can be dependent on the independent design variables. From the design parameters, a set of derived parameters are defined as behavior constraints, e.g., stresses, deflections, natural frequencies, and buckling loads. Design parameters are functionally related through laws of structural mechanics to the behavior constraints.

A group of design parameters $x_1, x_2, x_3, \dots, x_N$ may be represented by a design vector entailing a design scheme as $x = [x_1 \ x_2 \ x_3 \ \dots \ x_N]^T$.

A hyper surface in the design variable space, such that all designs represented by points on this surface are on the verge of failure in a particular failure mode for a particular load combination, is called the behavior-constrained surface. The eventual task of optimal design is to find a point in this design variable space which minimized or maximized objective function.

2. Fixed parameters

Some of the design parameters are fixed and chosen by the judgments and experiences of the designers so as to reduce the size of the problem. This results in large savings in computational time, which in turn reduces the cost of the design. For example, the Young's modulus, the Poison's ratio, and the volumetric weight may be fixed during the optimal procedure. The dam height, the available bedrock surface contour at the dam site, the design loads, as well as other similar parameters, also may be looked at as fixed parameters.

3. Objective function

The objective or the merit function $V(x)$ is formed by a proper choice of the design parameters. This function is either maximized or minimized. For example, if it is the cost or the weight, then the function is minimized. On the other hand, if it is some other function such as the safety or reliability, it is maximized.

4. Constraint conditions

Constraint conditions fall into geometry constraint conditions and characteristics constraint conditions, which are mainly specified by the corresponding design codes.

(a) Geometry constraint conditions

They are constraints to the design variables related to the shape of structure, to specify their permitted range of variation. For example, the crest width and the up- and down-stream slopes of gravity dams, and the central angle of arch dams are geometry constraint conditions, whose range is decided according to the engineering experiences, design codes or specifications, and operation requirements.

(b) Characteristics constraint conditions

They are constraints to the design variables related to the working states under different situations. For example, the deformation, strength, and stability requirements according to the design codes or specifications are characteristics constraint conditions. Take the displacement constraint for instance, the governing equation of the elastic FEM (Eq. (5.42)) may be rewritten as

$$\{\delta\} = [K]^{-1}\{F\} \quad (6.21)$$

where $[K]$ = stiffness matrix; $\{\delta\}$ = nodal displacement; and $\{F\}$ = nodal load.

Suppose there is a displacement constraint at a certain positions, then the displacement constraint may be expressed as $\delta(s) \leq u(s)$, in which $\delta(s)$ and $u(s)$ are the computed and allowable displacements at s , respectively.

Constraints may also be classified mathematically into equality constraints and inequality constraints, depending on the nature of the problem.

i. Equality constraints

$$h_j(x) = 0 \quad j = 1, 2, 3, \dots, n \quad (6.22)$$

ii. Inequality constraints

$$g_j(x) \leq 0 \quad j = n + 1, n + 2, \dots, n + m \quad (6.23)$$

where $h_j(x)$ and $g_j(x)$ = functions of the design vector x .

In general, the design variables are real (e.g., the orientation angle), but some times, they could be integers (e.g., the number of layers).

One equality constraint reduces one freedom in the objective function and therefore facilitates the solution of the optimal problem. However, too many of equality constraints means the problem approaches determinant problem or super-determinant problems, which lead to the invalidity of the definition of optimal problem.

Based upon the above discussion, the structural optimization problem can be posed as follows: under the deterministic parameters and all the constraint conditions, to obtain the optimal solution of the objective function (Bazarrá and Shetty 1979; Luenberger and Ye 2008; Li 1979; Spall 2003), i.e.,

$$\begin{aligned}
 &\text{Minimize or Maximize } V(x) \\
 &\text{Subject to } h_j(x) = 0 \quad j = 1, 2, 3, \dots, n \text{ equality constraints} \\
 &\quad \quad \quad g_j(x) \leq 0 \quad j = n + 1, n + 2, \dots, n + m \text{ inequality constraints}
 \end{aligned}
 \tag{6.24}$$

If the objective function and the constraints involving the design variables are all linear, then the optimization is termed as linear optimization problem. If even one of them is nonlinear, it is distinguished as nonlinear optimization problem.

6.2.3 Solution of Optimal Problems

A very simple problem with few design variables may be solved by analytical or graphical techniques. For the problems with fixed structure layout and shape, criterion method also may be feasible, in which the full stress criterion or energy criterion may be applied to solve the design variables using iterative algorithm. However, for a complicated structural optimal problem, advanced mathematical tools are indispensable to provide a best solution with certain degree of logical elegance that is hard to dispute (Bazarrá and Shetty 1979; Spall 2003; Luenberger and Ye 2008).

Methods of seeking the best design fall into simultaneous and sequential ones. The simultaneous search is characterized such that all trial designs are selected before the analysis of any design is started, whereas the sequential search is characterized that future trial designs may be generated by using the results of the previous generation of trial designs. Over the years, a large number of techniques have been proposed to solve the equations resulted from an optimal design, including traditional mathematical programming and relatively new artificial intelligent methods [e.g., genetic algorithms (GA) and artificial neural network (ANN)]. Nevertheless, these techniques do not always lead to a global optimum. If the constraint equations and the objective function are all convex, then it is possible to conclude that the local optimum will be a global one. However, in most of the structural optimal problems, it is practically impossible to check the convexity of

the functions. One of the simplest ways is to start with different feasible solutions, to avoid being trapped in local optimality.

6.2.4 Optimal Design of Concrete Gravity Dams

1. Parameters to be fixed

- ① Dam height H , which is decided by the flood regulation and planning for the river basin;
- ② Maximum storage level H_0 , which is decided by the flood regulation and planning for the river basin;
- ③ Reduction factor of seepage pressure α (vide Chap. 7), which depends on the characteristics of the foundation rock and treatment quality, the deployment of drainage and grouting curtains, the observation data of analogous projects, the importance of the dam, etc.;
- ④ Volumetric weight γ_c of the dam concrete;
- ⑤ Shear frictional coefficient f' of the concrete–rock bond plane;
- ⑥ Cohesion c' representing the unit shearing strength of concrete–rock bond plane under conditions of zero normal stress;
- ⑦ Friction coefficient f of the concrete–rock bond plane;

2. Design variables

The design variables may be grouped as (see Fig. 6.4):

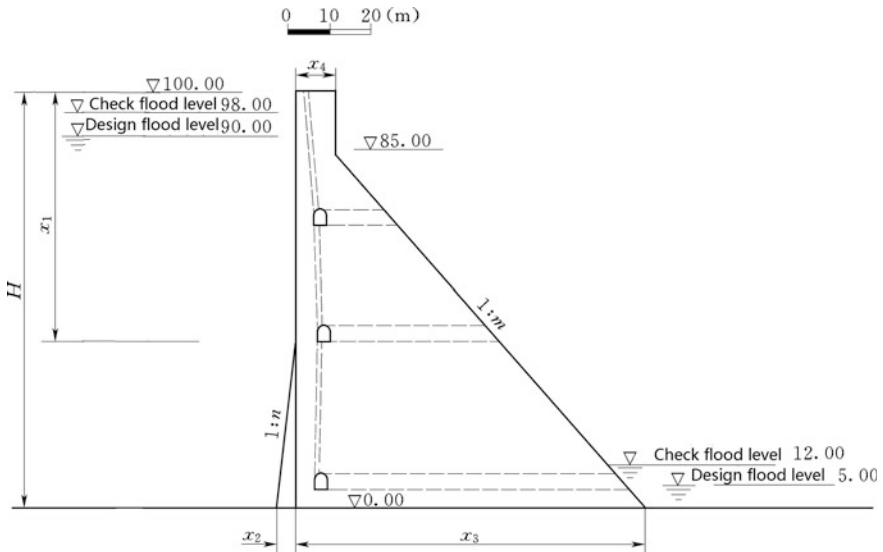


Fig. 6.4 Diagram to the optimal computation for a gravity dam

$$x = [x_1 \quad x_2 \quad x_3 \quad x_4]^T$$

where x_1 = height from the dam crest to the generatrix point of upstream batter; x_2 = horizontal distance from the dam heel to the upstream dam crest; x_3 = horizontal distance from the dam toe to the upstream dam crest; and x_4 = width of the dam crest.

3. Structural analysis methods

Gravity method (vide Chap. 7) or finite element method (vide Chap. 5) may be employed.

4. Constraint conditions

(a) Geometry constraints

$$\text{Upstream slope} \begin{cases} g_1(x) = -x_2 + 0.3(H - x_1) \leq 0 \\ 0 \leq n \leq 0.3 \end{cases} \quad (6.25)$$

$$\text{Downstream slope} \begin{cases} g_2(x) = -x_3 + 0.9H \leq 0 \\ g_3 = -x_3 + 0.6H \leq 0 \\ 0.6 \leq m \leq 0.9 \end{cases} \quad (6.26)$$

$$\text{Positive constraints} \begin{cases} g_4(x) = -x_1 \leq 0 \\ g_5(x) = -x_2 \leq 0 \\ g_6(x) = -x_3 \leq 0 \\ g_7(x) = -x_4 \leq 0 \end{cases} \quad (6.27)$$

$$\text{upper and inferior constraints} \begin{cases} g_8(x) = x_1^{\text{lower bound}} - x_1 \leq 0 \\ g_9(x) = x_1 - x_1^{\text{upper bound}} \leq 0 \\ x_1^{\text{lower bound}} \leq x_1 \leq x_1^{\text{upper bound}} \end{cases} \quad (6.28)$$

$$\begin{cases} g_{10}(x) = x_2^{\text{lower bound}} - x_2 \leq 0 \\ g_{11}(x) = x_2 - x_2^{\text{upper bound}} \leq 0 \\ x_2^{\text{lower bound}} \leq x_2 \leq x_2^{\text{upper bound}} \end{cases} \quad (6.29)$$

$$\begin{cases} g_{12}(x) = x_3^{\text{lower bound}} - x_3 \leq 0 \\ g_{13}(x) = x_3 - x_3^{\text{upper bound}} \leq 0 \\ x_3^{\text{lower bound}} \leq x_3 \leq x_3^{\text{upper bound}} \end{cases} \quad (6.30)$$

$$\begin{cases} g_{14}(x) = x_4^{\text{lower bound}} - x_4 \leq 0 \\ g_{15}(x) = x_4 - x_4^{\text{upper bound}} \leq 0 \\ x_4^{\text{lower bound}} \leq x_4 \leq x_4^{\text{upper bound}} \end{cases} \quad (6.31)$$

(b) Stress constraints

The stress at the dam heel should be lower than or equal to the allowable tensile stress of concrete:

$$g_{16}(x) = \sigma_{\text{dam heel}} - [\sigma_t] \leq 0 \quad (6.32)$$

where $[\sigma_t]$ = allowable tensile stress of concrete, which is usually zero in gravity method.

The stress at toe should be lower than or equal to the allowable compressive stress of concrete:

$$g_{17}(x) = \sigma_{\text{dam toe}} - [\sigma_c] \leq 0 \quad (6.33)$$

where $[\sigma_c]$ = allowable compressive stress of concrete.

(c) Stability constraints

$$g_{18}(x) = [K] - \frac{f \sum W}{\sum P} \leq 0 \quad (6.34)$$

or

$$g_{18}(x) = [K'] - \frac{f' \sum W + c'A}{\sum P} \leq 0 \quad (6.35)$$

where $\sum P$ = resultant of forces parallel to the assumed sliding plane, kN; $\sum W$ = resultant of forces normal to the assumed sliding plane, kN; f = friction coefficient of the concrete–rock bond plane; f' = shear frictional coefficient of the concrete–rock bond plane; c' = cohesion representing the unit shearing strength of concrete–rock bond plane under conditions of zero normal stress, kN/m²; A = area of plane of contact or sliding, m²; and $[K]$ and $[K']$ = allowable stability safety factor of dam base against sliding.

(d) Objective function

For a unit-thick slice of dam monolith, the sectional volume $V(x)$ may be expressed as the objective function of the design variables, then let

$$V(x) = V(x)_{\min} \quad (6.36)$$

6.2.5 Optimal Design of Concrete Arch Dams

Objective function $C(x)$ for the arch dam may be expressed as (Seyedpoor et al. 2010; Wasserman, 1984; Yao and Choi 1989; Zhu et al. 1992):

$$C(x) = C_1 V_1(x) + C_2 V_2(x) \tag{6.37}$$

where $V_1(x)$ = concrete volume of dam body, m^3 ; $V_2(x)$ = rock volume of foundation excavation, m^3 ; C_1 = unit price of concrete; and C_2 = unit price of rock excavation.

1. Geometry constraints

They comprise the position of dam axis, thickness of dam crest, overhang degree of upstream dam face, central angle, and distance of the arch ring i to the major faults.

2. Stress constraints

Under any specified load combinations, the maximum stress should be limited within the allowable stress. The stress of dam body may be computed by trial load method (vide Chap. 8) or by finite element method (vide Chap. 5).

3. Stability constraints

When there are potential sliding surfaces within dam foundation and/or abutments, the stability should be defined as constraints.

The first optimally designed arch dam in China is the Ruixiang Arch Dam (Zhejiang Province, $H = 54.5$ m) (Fig. 6.5). The dam is located in a V-shaped symmetrical valley, the width of the river bed is 35 m, and the foundation rock is breccia-alloyed tuff. The dam body is single centered and double curved, where quadratic curve is adopted to configure the geometrical profile of the cantilever along the dam height. The chore of dam crest is 140 m long, and the chord to height ratio is 2.6.

All together, 14 design variables were selected to describe the dam axis and the profile of cantilever section. The concrete volume of the dam body was employed as objective function. The constraint conditions are as follows:

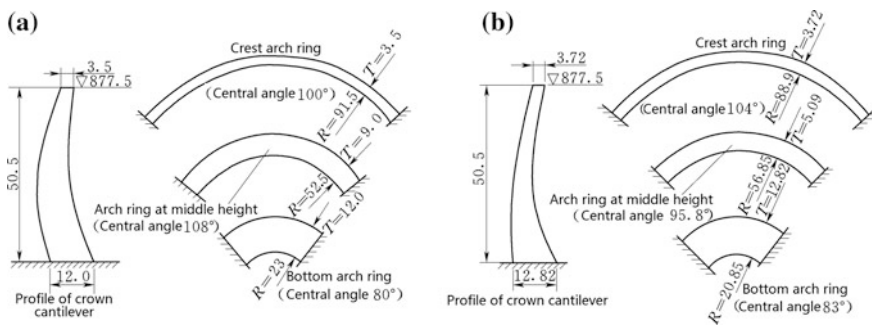


Fig. 6.5 Optimal design of the Ruixiang Arch Dam (China, $H = 54.5$ m). **a** Initial scheme; **b** optimal scheme

- ① Geometry: Minimum dam crest thickness = 3.5 m; maximum dam base thickness = 15 m; upstream face overhang ≤ 0.25 ; downstream face overhang ≤ 0.2 ; and maximum sloping of the downstream base of the crown cantilever = 45° .
- ② Stress: Allowable compressive stress for both the cantilever and arch ring = 5 MPa; allowable tensile stress = 1.65 MPa and 1.2 MPa for the cantilever and arch ring, respectively, during operative period; and = 0.3 MPa during the construction period.
- ③ Stability: The included angle between the normal of the arch abutment and the available bedrock surface contour $\geq 30^\circ$.

The penalty method was used in the optimization, and the dominate load combination is the following: normal storage reservoir level + silt pressure + self weight + uniform temperature drop.

The concrete volume of the initial design scheme was $3.82 \times 10^4 \text{ m}^3$, whereas the optimal scheme reduced it down to $2.65 \times 10^4 \text{ m}^3$, i.e., totally $1.17 \times 10^4 \text{ m}^3$ (31 %) had been saved.

6.3 Computer Aided Design for Hydraulic Structures

6.3.1 Basic Concepts

Computer-aided design (CAD) is a comprehensive application of computer system to assist in the creation, modification, analysis, or optimization, of a design. CAD may enhance the productivity of the designer, improve the quality of the design, accelerate the communications through documentation, and create a database for manufacturing and management.

CAD is an important industrial art extensively employed in many applications, such as automotive and ship building as well as aerospace industries, architectural design, and of course hydraulic project design. Attributable to its enormous economic importance, CAD has been a major impetus to the research in computational geometry, computer graphics (both hardware and software), and discrete differential geometry (Carlson 2003; Narayan 2008; Spall 2003).

6.3.2 Structure of CAD System

1. Hardware of CAD system

Initially, with 3-D in the 1970s, CAD was typically limited to producing drawings similar to hand-drafted ones. Advances in programming and computer

hardware, notably solid modeling in the 1980s, have allowed more versatile applications of CAD in the engineering design activities.

Medium-sized machines (e.g., VAX) and workstations (e.g., SUN, HP, IBM) were the prevalent hardware to support CAD/CAM system. The first commercial applications of CAD were in large companies of automotive and aerospace industries, as well as of electronics industry, since only these large corporations could afford the computers capable of performing the huge amount of calculations for CAD.

As computers became more and more affordable since the 1990s, the application areas have gradually expanded. The development of CAD software for personal desktop computers permits almost universal applications in all areas of construction including architectural and hydraulic engineering.

2. Software of CAD system

Basically, CAD software system is constructed by providing an integrating infrastructure of three levels distinguished as system software, supporting software, and application software for a particular engineering design.

(a) System software (first level software)

It is used for the management, operation, maintenance, and control, including:

- Operation System: DOS, WINDOWS, and UNIX are used to operate and control the resources of computer (hardware and software). Operation system is the interface between computer and users.
- Language and compile system: It comprises a large family including FORTRAN, C++, BASIC, programming and compile service software, mathematics library, error diagnosis, and error correction software.

(b) Supporting software (second level software)

It is the kernel software of CAD system and the base for the development of application software.

Supporting software comprises computer graphics, engineering database management system, network management system, customer interface. Of which, computer and database management have tight relation with the development of CAD. Computer graphics may be interactive or parametric. Interactive computer graphics and parameterized computer generated imagery can be categorized into several different types, such as 2-D, 3-D, and animated graphics (Carlson 2003; McConnell 2006; You 2006). Following the progress in the technology, 3-D computer graphics have become more and more common, but 2-D computer graphics are still widely exercised, particularly in hydraulic and hydropower engineering.

Nowadays, there are many influential computer graphics softwares of 3-D, including:

- Rendering: 3DMAX and MAYA.
- 3-D modeling: AutoCAD, Solid Works, ANSYS.
- Large-scale integrated system: Apart from the function of CAD/CAE (Computer Aided Engineering), they also have the function such as CAPP (Computer Aided Process Planning) and PDM (Product Data Management), for example, the CAD/CAM/CAE/PDM application system CATIA V5 (You 2006) by the French aircraft company Dassault and the USA company IBM, 3-D parametric software Unigraphics (UG) by the US company Unigraphics Solutions, and software Pro/E, Autodesk.

(c) Application software for engineering design (third-level software)

It is the interface between the designers and the CAD system, which is developed according the requirements and specifications of a particular engineering field.

6.3.3 Development and Application of CAD Technology in the Chinese Hydraulic Engineering

The development of CAD application software for Chinese hydraulic engineering had experienced three stages:

- Single-function CAD system;
- Multi-function CAD system based on file management; and
- Integrated CAD system based on engineering database.

The first two types of CAD software have disadvantages of inconvenient in application, difficult to guarantee data consistency and reliability, and lower efficiency. The integrated CAD system using engineering database as its kernel and having hierarchical structure enables it to meet the following two important requirements:

- The functionality of such CAD system is complete and robust and may be always effectively applied in every stage during the whole design procedure.
- A whole information flow is formulated from design data inputting, generating of design outcomes of every stage, until the construction and management.

According to the particular concerns of different design stages or phases of a hydraulic project, emphasis should be focused on the corresponding CAD software system as follows.

- Investigation in the early planning phase: The CAD software is systematically used to collect the data concerning engineering topography, geology, hydrology, and meteorology and to input them into the database of the system to establish digitized model, for the users of follow-up design.

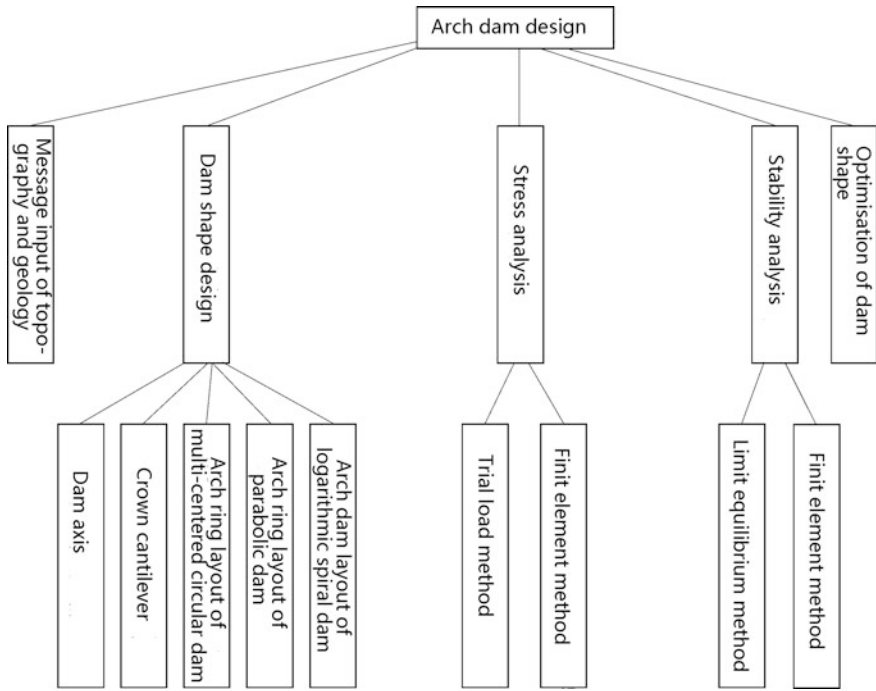


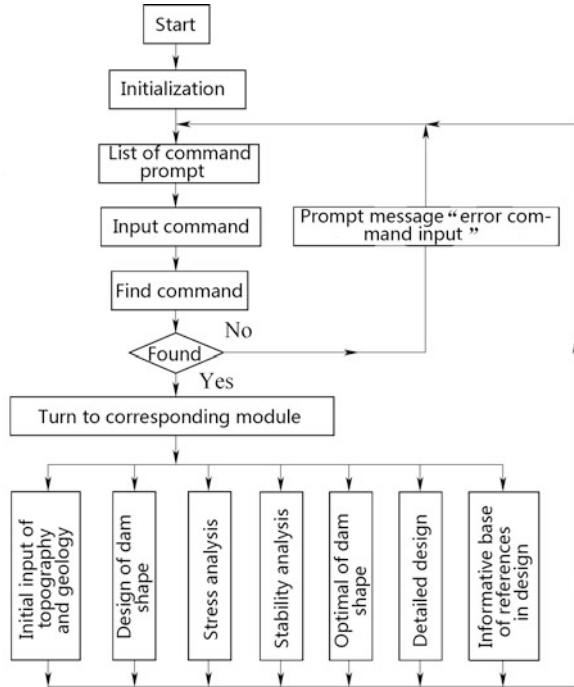
Fig. 6.6 Functional modules and feature segmentation map of the arch dam CAD

- Feasibility study phase: The CAD software system is mainly employed for the establishment and application of database. According to the national policies, laws, and regulations, planning requirements as well as other engineering design data, the feasibility study for the design schemes is accomplished.
- Preliminary design phase: The CAD software system is mainly intended for geometric modeling, techno-economic comparison of alternative design schemes to obtain optimal design scheme, structural analysis, and optimization.
- Construction documentary design phase: The CAD software system is mainly used for detailed analysis of structure, drawing, integrating, and coordinating the professional results, material statistics, compiling report, preliminary budgeting, and general estimating.

The CAD for the hydraulic project in China was initiated in the 1970s. One of the most influential events in the development was the founding of the CAD systems for arch dams (by the Mid-South China Hydroelectric Investigation, Design and Research Institute) and gravity dams (by the East China Hydroelectric Investigation, Design and Research Institute), on the platform of DDM (Calma company) installed in the Apollo work station, in the 1980s.

The CAD system for arch dams developed by the Mid-South China Hydroelectric Investigation, Design and Research Institute divided the design task

Fig. 6.7 Basic structure of the master-control program



into several functional modules; each of them was further fractionized. They had been related and centralized dispatchers by master-control program. According to the prompting of the master-control program, the designers may execute every functional module. Figure 6.6 explains the settings of these functional modules.

The interface of master-control program is an operation interface for users which employs traditional arch dam design process as the control flow. Applying the master-control program to realize the control of functional modules, every task in the arch dam design may be accomplished. The basic structure of the master-control program is illustrated in Fig. 6.7.

The developments of PC and internet since the 1990s provide ever greater times with the generalized use of customer/server structure computer environment for CAD applications. Nowadays, a series of new generation CAD systems for hydraulic structures are available, such as the CAD system for the hydraulic power house by the Tianjin Hydroelectric Investigation, Design and Research Institute, the CAD system for the Hydraulic Tunnel by the Mid-South China Hydroelectric Investigation, Design and Research Institute.

References

- Ang AH-S, Tang WH (1984) Probability concepts in engineering planning and design, vol I & II. Wiley, New York
- Bazarra MS, Shetty CM (1979) Nonlinear programming, theory and algorithms. Wiley, New York
- Bogle DJ, Zilinskas J (eds) (2009) Computer aided methods in optimal design and operations. World Scientific Publishing, Singapore
- Carlson W (2003) A critical history of computer graphics and animation. Ohio State University, Ohio
- Cornell CA (1969) A probability based structural code. *ACI J* 66(12):974–985
- Ellingwood B, MacGregor JG, Galambos TV, Cornell CA (1982) Probability based load criteria: load factors and load combinations. *J Struct Div ASCE* 108(ST5):978–997
- Hasofer AM, Lind NC (1974) An exact and invariant first order reliability format. *J Eng Mech Div ASCE* 100:111–121
- Li BW (1979) Optimal design for structures. Science Press, Beijing (in Chinese)
- Luenberger DG, Ye YY (2008) Stanford university linear and nonlinear programming. Springer, New York
- Madsen HO, Krenk S, Lind NC (1986) Methods of structural safety. Prentice Hall, Englewood Cliffs
- McConnell J (2006) Computer graphics: theory into practice. Jones & Bartlett Publishers, Massachusetts
- Ministry of Construction of the People's Republic of China (1994) GB50199-94 unified design standard for reliability of hydraulic engineering structures. Research Institute of standards and norms (MOC), Beijing (in Chinese)
- Ministry of Electric Power of the People's Republic of China (1997) DL5077-1997 specifications for load design of hydraulic structures. China Electric Power Press, Beijing (in Chinese)
- Narayan KL (2008) Computer aided design and manufacturing. Prentice Hall of India, New Delhi (India)
- Pan JZ, He J, Zhu WX, Shi RM (eds) (2000) Hydropower engineering in china—hydraulic structures. China Electric Power Press, Beijing (in Chinese)
- Seyedpoor SM, Salajegheh J, Salajegheh E (2010) Shape optimal design of arch dams including dam-water-foundation rock interaction using a grading strategy and approximation concepts. *Appl Math Modelling*. 34(5):1149–1163
- Spall JC (2003) Introduction to stochastic search and optimization: estimation, simulation and control. Wiley, New Jersey
- Wang SY, Liu GH et al (1998) Computer Aided Design. China Electric Power Press, Beijing (China) (in Chinese)
- Wasserman K (1984) Three dimensional shape optimization of arch dams with prescribed shape function. *J Struct Mech* 2(4):465–489
- Yao TM, Choi KK (1989) Shape optimal design of an arch dam. *J Struct Eng ASCE* 115(9): 2401–2405
- You CF (2006) Advanced application of CATIA V5. Tsinghua University Press, Beijing (in Chinese)
- Zhao GF et al (2000) Reliability theory of structures. China Construction Industry Press, Beijing (in Chinese)
- Zhu B, Rao B, Jia J, Li Y (1992) Shape optimization of arch dam for static and dynamic loads. *J Struct. Eng ASCE* 118(11):2996–3015

Chapter 7

Gravity Dams

7.1 General

Gravity dam may be the earliest water retaining structure in the human history. As early as around 2950–2750 BC, the Egyptians built a masonry gravity dam of 14 m high at the Nile River, called in Arabic “Sadd el-Kafara” meaning “Dam of the Pagans,” which was discovered over 100 years ago in Egypt (Jansen 1980; Schnitter 1994).

Gravity dams built before the 1800s were all stone masonry since the Roman era. By 1872, attributable to the widespread use of Portland cement, the application of concrete in the construction of gravity dams made an important breakthrough. The design theory developed step by step following the practice in gravity dam construction. From 1853 to 1890, French and British engineers and scholars (Delocre 1866; Lévy 1895; Rankine 1881; Sazilly 1853) published milestone papers on the gravity dam design, in which the gravity method and elastic theory were elaborated. At the end of the nineteenth century, the uplift was found through the study on several gravity dam accidents such as the Bouzey dam failure in 1895 (France, $H = 22$ m), which finally resulted in the arrangement of drainage system within dam body. Since the twentieth century, with a various innovations in concrete technique and construction machinery came the booming of modern gravity dams: arranging vertical drainage pipes near the upstream face within dam body; arranging grouting curtain and the drainage curtain in dam foundation; concrete cracking control by constructing the dam in a series of individually stable monoliths separated by transverse and longitudinal joints; and temperature control during and after the placement of mass concrete using pre-cooling and post-cooling techniques. At the beginning of the 1940s, systematic and sophisticated design and construction technique as “tool kits” were formulated based on the existed experiences, particularly the experiences from the recently erected giant, super gravity dams such as the Hoover and Shasta in USA. After the World War II, the economy recovery highly required cost saving in works, so arch dams and buttress dams became more

prevalent. However, the gravity dam technique continued its remarkable advances: the tallest concrete gravity dam—the Grande Dixence ($H = 285$ m) was built in the Swiss Alps from 1951 to 1962; the Alpa Gera Dam ($H = 174$ m) built in Italy employed a series of new techniques including low-heat Portland cement, self-discharging truck dump, elimination of individually monolith placement, and contraction joint cut using tractor-mounted vibratory blade; the Izvroul Muntelui Dam ($H = 127$ m) built in Romania developed a concrete placement technique using staggered longitudinal joints, which are not necessarily grouted after the post-cooling. Since the 1970s, with the development of Roller Compacted Concrete (RCC), the reduction in expenditure and construction schedule has further enhanced the competitiveness of gravity dams in the selection of dam types (ICOLD 1989; US Bureau of Reclamation 2005).

Since the 1950s, gravity dams have been developed greatly in China (Ru 1983; Pan 1987; Zhou and Dang 2011), too. The widespread practices stimulated the research on the issues with regard to the structural type, concrete material, layout of project, flood releasing and energy dissipation, foundation treatment, and construction technique and design theory. According to the incomplete statistics of 2000, among the completed China's hydropower projects with the installed capacity 15 MW or above, there were 149 gravity dams, of which 34 were higher than 70 m and 17 were higher than 100 m. Among the completed 50 China's hydropower projects with the installed capacity 250 MW or above, there were 34 gravity dams, of which 15 were higher than 100 m. The Three Gorges Project (TGP) initiated in 1993 is the world's largest hydraulic project with installed capacity of 18,200 MW (ground power plant) + 4200 MW (underground power plant)—the first turbine generator started service in 2003. The TGP gravity dam is of 175 m high and 2309.47 m long. China also records a large quantity of traditional masonry gravity dams, of which 416 are at least 15 m high and with gross storage capacity over 10×10^4 m³.

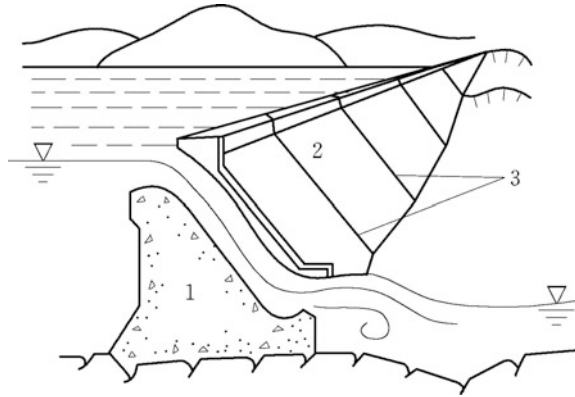
The modern gravity dams made of concrete are widely exercised throughout the world and well known for their simplicity in design and facilitation in construction, high reliability at any dam height and in any climatic conditions inclusive of harsh winter (ICOLD 2000).

7.1.1 Features and Working Conditions of Gravity Dams

Basically, gravity dam is a kind of solid concrete structure that resists horizontal water pressure of reservoir to maintain its stability against sliding by both the friction related to the concrete weight and the cohesion between the dam concrete and the foundation rock. The flared or inclined upstream dam face enables it to make use of a part of water weight to improve its stability against sliding (Golzé 1977; Grishin 1982; Iqbal 1993; Novak et al. 1990).

Gravity dams built in earlier time had almost trapezoidal or even rectangular profiles in cross section. Later, with the development of design theory, more

Fig. 7.1 A gravity dam on riverbed. 1 overflow dam monolith; 2 non-overflow dam monolith; 3 transverse joints



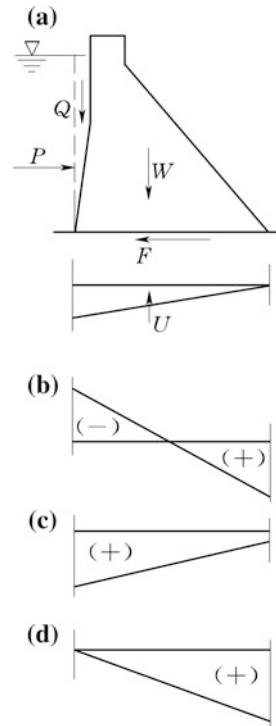
economical profiles of curvilinear or polygonal appeared. Nowadays, almost all modern concrete gravity dams are triangularly configured in cross section.

Generally, gravity dams are constructed on a straight axis, but may be slightly curved or angled to accommodate the specific site conditions. A gravity dam is conventionally divided into independent dam monoliths cut by transverse joints (Fig. 7.1), each of them can be looked at as a cantilever fixed on the foundation. At any horizontal section of dam monolith, there is a moment M attributable to the water pressure P , which leads to tensile stress at the upstream and compressive stress at the downstream (Fig. 7.2b). Since the tensile strengths of concrete and rock are very low, the tensile stresses within the dam body and at the dam/foundation interface are not permitted. Therefore, the compressive stress induced from the dam weight W and the water weight Q as well as the uplift U (Fig. 7.2c) should be larger enough to offset the tensile stress due to the water pressure P (Fig. 7.2d).

The modern solid gravity dam shown in Fig. 7.1 has been widely practiced attributable to the following advantages:

- With solid concrete structure, water may overflow the gravity dam or be bleed-off through the bottom outlets (permanent or temporary) during the service period and construction period.
- Compared to the arch dam and buttress dam, the sectional profile of the gravity dam is simpler, which facilitates the mechanized concrete placement and simplifies the formwork technique.
- The gravity dam possesses high degree of safety in any climatic conditions inclusive of harsh winter.
- Regarding the foundation rock quality requirement, the gravity dam has moderate adaptability, which is higher than the arch and buttress dams, but lower than the embankment dam.
- The engineers have plenty of experience and expertise in the design and construction of gravity dams, which guarantees higher reliability, longer service life, and lower maintenance cost.

Fig. 7.2 Working principle of gravity dam



The main disadvantages with gravity dams are cited as follows:

- Due to the huge bulk of dam concrete and relatively lower stress level, the strength of the concrete material is not fully exploited.
- Also due to the huge bulk of dam concrete, the dissipation of the heat from hydration process and thermal flow is difficult, which may give rise to cracking and in turn, deteriorate the monolithic and strength of the dam.
- Due to the larger surface of dam base compared to the arch and buttress dams, the gravity dam is exerted by larger uplift which offsets a portion of the dam weight and is not favorable to the dam stability.
- With respect to the unit construction cost, the gravity dam is more costly than the embankment dam, but less costly than the arch and buttress dams.

To make the most of the advantages and to remedy the weaknesses of gravity dam, the design and construction techniques have been developing in recent decades, by which the most important advances achieved are given as follows:

- Use of inclined or flared upstream dam face, to improve the stability;
- Use of different concrete grade in the zoned dam body, to save the cement;
- Use of roller compacted concrete (RCC) technique, to save the cement and to raise the construction speed; and

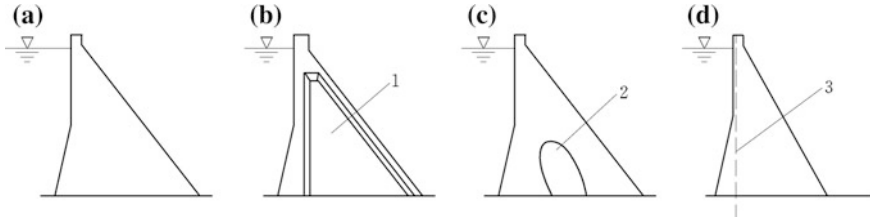


Fig. 7.3 Cross sections of gravity dam. **a** Solid gravity dam; **b** slotted gravity dam; **c** hollow gravity dam; **d** prestressed gravity dam. 1 slot; 2 hollow; 3 prestressed bolt

- Structural innovation. The slotted gravity dam (Fig. 7.3b), the hollow gravity dam (Fig. 7.3c), and the prestressed gravity dam (Fig. 7.3d) are good examples of such innovations. However, it should be pointed out that structural innovations also could undermine the merits of solid gravity dam.

1. Slotted gravity dams

Generally, the thickness of the transverse joint perpendicular to solid gravity dam axis is very small ($\leq 1-2$ cm). Slotted gravity dam means that the central portion of the transverse joint is enlarged to a wide slot. The slot enables the seepage pressure exerting on the dam base to be relieved by an appreciable extent; in this way, the dam concrete volume can be reduced approximately by 10 %. Slots also improve the thermal dissipation conditions during the concrete placement. However, slots complicate the construction technique and raise framework cost.

2. Hollow gravity dams

Hollow gravity dam means that there is a large longitudinal hollow installed along the dam axis. The deployment of hollow can cut a part of uplift; in this way, the dam concrete volume can be reduced. The hollow also can be used to accommodate power plant. However, the installation of hollow complicates the construction technique and raises the framework and steel costs.

3. Prestressed gravity dams

Prestressed gravity dam means that prestressed steel bars or stranded anchor cables are employed to improve the stability and strength conditions; in this way, the dam concrete volume can be reduced. This kind of dam also complicates the construction technique and increases the steel consumption and is merely exercised in small dam projects or in old dam rehabilitations. The prestressed gravity dam has been built successfully in the Lushui Project (Hubei province, China, $H = 49$ m).

Actually, the buttress dams (including massive-head buttress dam, slab buttress dam, and multiple-arch buttress dam) also may be looked at as the structural innovations intended to partially overcome the disadvantages of solid gravity dams.

7.1.2 Design Theory and Profile of Gravity Dams

In the mid of the nineteenth century, the cantilever theory was firstly proposed for the profile design of gravity dams by Sazilly—a French engineer. A bit of late, this design theory was improved by Delocre (French), Lévy (French), and Rankine (British). Nowadays, this theory becomes classical termed as “gravity method” and is still widely exercised in the gravity dam design, which includes following principles:

- ① That the resultant of all forces exerting above any horizontal plane through a dam intersects that plane inside the middle third kernel, to maintain compressive stresses.
- ② That it is safe against sliding on any horizontal or near-horizontal plane within the dam, at the base, or on any rock seam in the foundation.
- ③ That the allowable stresses in the dam concrete or in the foundation rock shall not be exceeded.

Generally, the principles of non-tensile stress and stability against sliding are the major two conditions to ensure the safety of the gravity dam. The analysis according to these principles leads to a theoretic (basic) profile of triangular cross section. Actually, the prevalent practical profile of modern gravity dam is revised by this triangular basic profile.

7.1.3 Layout of Gravity Dam Projects

Basically, a gravity dam project consists of overflow dam monoliths, non-overflow dam monoliths, abutment piers, guide walls, and crest works. Figure 7.4 shows the layout of a most typical and simple gravity dam project, which consists of the non-overflow dam monoliths on the right and left banks, the overflow spillway dam monoliths on the main river stream. The power station of dam toe type is located to the left riverbed.

The layout of gravity dam depends on the comprehensive consideration concerning the topographic and geographic conditions as well as the accommodation requirements for the other structures (e.g., hydropower plant and ship lock or lift). The layout also should pay attention to the shape harmoniousness of the dam monoliths. Where there are significant differences in the topographic and geographic conditions with different dam monoliths, it is advisable to use different downstream dam slopes while to keep a consistence upstream dam slope.

Overlapping layout could be a good solution for narrow crayon with large flood flow discharge, when the length of dam is not sufficient to accommodate spillway dam monoliths and power plant dam monoliths. For example, the overflow (ogee) spillway and deep outlet can be accommodated in a same dam monolith at different

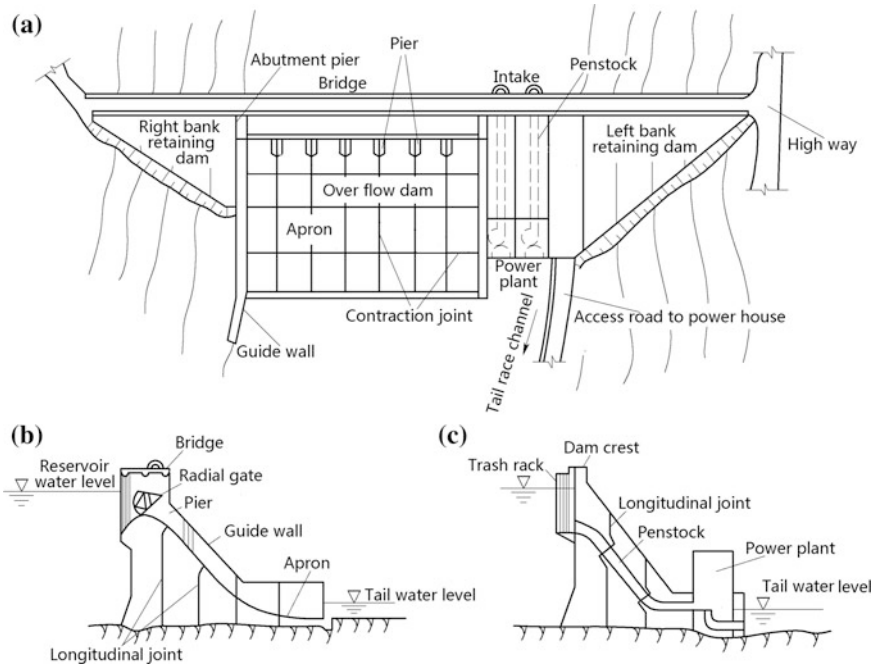


Fig. 7.4 Layout of a gravity dam project. **a** Plan; **b** profile of spillway dam monolith; **c** profile of non-overflow dam monolith

altitudes; the power plant can be located within the spillway dam monolith, or below the trajectory flip bucket of the overflow dam monolith.

In order to make the general layout of a project more economically rational, safe, and reliable, modern trends are to use solid gravity dams, particularly on deep gorge sites in mountainous areas, which are mainly guided by the following considerations:

- Dam safety is the paramount concern and the quick reservoir drawing down or emptying under emergent situations (e.g., accidents of the project and civil air defense) should not be neglected. In addition to crest spillway, intermediate and bottom outlets have to be installed for controlling the reservoir’s water level as flexibly as possible.
- It is necessary to provide sluices of certain-scale as bottom outlets for discharging flood water and flushing silt, to keep effective reservoir storage capacity and to get rid of sediments in front of power plant intakes.
- With respect to construction diversion and schedule, the solid gravity dam performs well by the flexible combination using open channels and bottom outlets of large diameter.

- With a solid gravity dam, penstocks and powerhouse can be flexibly arranged, powerhouse inside the dam or at the toe are all good alternatives, and power intakes even may be installed in the piers of surface outlets.

Similar to the artworks, layout of dam project is basically a creative activity relying on the engineer's talent. There are unlimited variants and no two exactly identical projects. However, where the flood-releasing and powerhouse works are taken as the key factors dominating the design, the layout of gravity dam project falls roughly into 6 typical types as illustrated hereinafter.

1. Abutment powerhouse at dam toe + flood release structures in riverbed

Since the 1970s, this type of project layout as shown in Fig. 7.4 has been widely exercised in China, especially for the gravity dam at a height around 100 m built in 1980–2000. The Ankang Hydropower Project (Shanxi Province, China) on the Hanjiang River completed in 1995 has a maximum dam height of 128 m, a gross reservoir storage capacity of 2.585 billion m^3 and a maximum flood discharge of 35,700 m^3/s . The unit discharge of 250 $\text{m}^3/(\text{s}\cdot\text{m})$ is the largest among the similar projects in China. The flared piers and stilling basin are jointly employed for energy dissipation. The angled dam axis consists of 5 straight segments to increase the front length for flood releasing and drawing water to the power plant. The powerhouse at dam toe by the right abutment is installed with 4×200 MW generator units.

2. Powerhouse at the mainstream dam toe + ski-jump spillway over powerhouse

This type of project layout may be called as “overlapping.” Due to the constraint of the gorge topography and in order to reduce the excavation on abutment slopes, the flip bucket on riverbed is generally employed and located over the roof of powerhouse. Since the 1960s, this type of project layout has been widely exercised for large- and medium-sized projects. One example is the Xin'anjiang Hydropower Project (Zhejiang Province, China) completed in 1957. With a 105-m-high slotted gravity dam and a gross reservoir storage capacity of 22 billion cubic meter, it is the first high dam project with large reservoir capacity completed in China. The overflow spillway of 9 bays (each bay is 13 m in width) is arranged in the middle portion of the river channel. The powerhouse is installed with 4×75 MW and 5×72.5 MW generating units, which were the largest ones made in China at the time. The penstock intakes with interior diameter of 5.2 m are installed in the piers of the surface (overflow) spillway dam monoliths. The overflow spillway has a maximum flood discharge capacity of 13,200 m^3/s , and the corresponding unit discharge flowing over the roof of the powerhouse is 76.0 $\text{m}^3/(\text{s}\cdot\text{m})$.

3. Composite powerhouses at dam toe and underground + releasing flood by shore spillway and deep outlets (tunnels)

The Liujiaxia Hydropower Project (Gansu Province, China) on the Yellow River is completed in the early 1970s. The 147-m-high gravity dam is located in a narrow river valley and flanked by concrete auxiliary dam and loess core embankment dam

on the both banks. Two powerhouses are installed at the dam toe on the main stream ($4 \times 225\text{--}250$ MW) and in the mountain near the dam abutment (1×300 MW), respectively, with total capacity of 1225 MW. The spillway is placed in a saddle on the right bank mountain, the bottom and deep outlets through the dam body are installed on the left and right abutment monoliths, respectively. Their maximum flood discharge capacity is $9220 \text{ m}^3/\text{s}$.

4. Riverbed powerhouse at dam toe + flood releasing on both banks

The typical example is the Baozhushi Hydropower Project (Sichuan Province, China) on the Bailongjiang River built in the 1990s. Its maximum dam height is 132 m, gross reservoir storage capacity is 2.55 billion cubic meter, and maximum flood discharge capacity is $16,060 \text{ m}^3/\text{s}$. Since the project is located in a U-shaped river valley, the powerhouse with 4×175 MW generator units is situated in the mainstream of the river channel. The bottom outlets are installed at the both sides of the powerhouse, respectively; their sill elevation is 15 m lower than that of the power intakes for effectively excluding silt. On the right abutment, the open diversion channel and overflow dam monoliths are located and the problem of energy dissipation is handled by hydraulic jump in the stilling basin. On the left abutment, the intermediate outlet is installed, and the ski-jump chute is employed for its energy dissipation.

5. Powerhouses at dam toe by both banks + flood-releasing structures in main river stream

The Three Gorges Project (Hubei Province, China) on the Yangtze River—with the largest hydropower station in the world at present—is an example of this project layout (Fig. 1.3).

6. Underground powerhouse + flood-releasing works in main river stream

The Dachaoshan Hydropower Project (Yunnan Province, China) on the Lancangjiang River completed in 2003 is an example of this project layout. The maximum height of the RCC gravity dam is 115 m, the gross reservoir storage capacity is 940 million cubic meter, and the maximum flood discharge capacity is $23,800 \text{ m}^3/\text{s}$. The layout of the project has following features:

- Since a large flood discharging capacity is demanded, the whole river stream gives way to the overflow spillway dam monoliths and silt flushing sluice outlets. The flared pier bucket basin and ski-jump energy dissipaters are, respectively, employed for energy dissipation. The underground powerhouse installed with 6×225 MW generator units is located in the right bank mountain and the power intakes are arranged along the right abutment monoliths which, together with the whole dam axis, forms a compact front for intakes and flood-releasing works.
- The RCC construction method is adopted, and the longitudinal joints are abolished; in this way, the construction is greatly simplified.

- The river flow is diverted by a 5 m × 17 m tunnel and the foundation pit is protected by a RCC arch cofferdam; in this way, the dam construction can be carried out throughout the whole year.
- The excavation of the underground works and the concrete placement of the dam are the two independent construction processes without any interference.

7.1.4 Main Design Tasks for Gravity Dams

1. Overall layout

Overall layout is accomplished by the selection of dam site and axis, the alignment of the dam monoliths, and the other works along the dam axis, in the whole project.

2. Flood-releasing design

Flood-releasing design comprises the study on the flood-releasing methods and their combination, the positioning and sizing of spillway, the flood routing, the computation of the design and the catastrophe (check) flood levels, the energy dissipation of high velocity flow as well as the downstream river protection against scouring, the discharge atomization and bank-slope protection, the gate operation and control scheme, etc.

3. Profile design

Profile design is tightly related to the study on the loads and load combinations. The optimization of dam profile is obtained mainly by means of stability and stress analyses (static and dynamic). The results of stability and stress analyses also provide guidelines for the dam foundation treatment and appurtenant design.

4. Appurtenant and miscellaneous design

The appurtenant and miscellaneous design comprises of concrete zoning with respect to corresponding concrete grades and performance indices (physical and mechanical property, thermal property, permeability property, freezing resistance property, abrasion resistance property, corrosion resistance property, cement–water ratio, cement type and consumption, aggregate, and cement admixture), transportation system, gallery system and lift, anti-seepage and drainage systems in dam body and foundation, lighting and ventilating systems within the dam body, piers and bridges on the dam, guide walls and handrails, etc.

5. Foundation treatment design

In the foundation treatment design, the major attentions are focused on the issues such as the requirements for the foundation excavation, anti-seepage, drainage, and grouting; the study on the seeping, deforming, piping, and argillizing of foundation rock under the action of water and dam; the treatment for the fractures, faults,

and seams in the foundation. The deformation and stability of the abutment slopes are also studied.

6. Design for the interests of the other national economy sectors

The possibility and necessity to accommodate high way, ship lock or ship lift, fish way, etc., within the dam project, are studied.

7. Instrumentation design

Instrumentation system is installed to monitor the structural integrity and to check the design assumptions, as well as to forecast the performance of the foundation and dam body during the construction and service periods.

8. Construction design

The design works conducted in this stage comprise the following: the selection of lift thickness, transverse and longitudinal joints, time interval between lifts, maximum allowable placing temperature of concrete, surface insulation, and post-cooling scheme; to put forward technical requirements for the construction and to specify the concrete placement method including construction equipment; to complete the design of main temporary structure for construction and general construction schedule; and the selection of construction diversion scheme and the design of diversion works (e.g., cofferdam and diversion bottom outlets). Care also should be called at the issues with regard to the traffic and downstream water supply during the construction period.

7.2 Loads and Load Combinations of Gravity Dams

The loads often encountered in the gravity dam design are given as follows:

- Self (dead) weights of the dam body and the permanent facilities;
- Static pressures from headwater and tailwater;
- Dynamic pressures on the overflow bucket;
- Uplift;
- Ice pressure;
- Earth and silt pressures;
- Wave pressure;
- Earthquake forces, including earthquake inertia, earthquake hydrodynamic pressure, earthquake dynamic earth, and silt pressures;
- Loads by the restrained or confined volumetric variation internally or externally (temperature drop, drying shrinkage, etc.), if necessary; and
- Other loads that in some cases or for appurtenant and miscellaneous works cannot be ignorable (e.g., wind pressure, snow pressure, mooring rope tension and berthing impact, temporary loads of vehicles and hoisting machinery, and concussion caused by explosion).

In the interests of safety and economy, the strength and stability calibration should be made for the most adverse combinations of loads which have a reasonable probability of simultaneous occurrence.

7.2.1 Load Computation—With Particular Emphasizing on the Uplift

The description and conventional evaluation of the foregoing loads that may exert on a gravity dam have been presented in Chap. 4.

The wind pressure, snow pressure, mooring rope tension and berthing impact, temporary loads of vehicles and hoisting machinery are commonly ignorable for gravity dams due to their very low proportion to the amount of loads. However, these loads could be important for the appurtenant and miscellaneous structures, e.g., the bridge over the spillway dam monoliths and the hoist frame on the dam crest.

Hereinafter, the details in the uplift calculation for gravity dams will be discussed.

Uplifts exert upward on the dam base and any horizontal planar sections within the dam body, so they are unfavorable for the stability of dam (Harza 1949). The uplift is composed of two partitions, namely buoyant pressure and seepage pressure. The former is attributable to the tailwater level and the latter is caused by the difference in the headwater and tailwater.

The main difficulties with an accurate and quantitative calculation of uplift lie in the facts that: the dam body and foundation materials do not exactly observe the Darcy's law; there exist complexly distributed joints and seams in rock foundation; grouting and draining systems are conventionally installed. Hence, the uplift pressure is usually evaluated using simplified pressure diagram derived from the prototype monitoring data of the existed dams. However, under the circumstances of complex dam structure or foundation geology structure, the simplified pressure diagram should be justified by the numerical computation (e.g., FEM) or laboratory test (Keener 1951).

1. Uplift along the dam base

Where there have no provisions provided for uplift reduction, the hydraulic head may be assumed to vary straightly from the headwater at dam heel to zero or the tailwater at dam toe, i.e., the intensity at the dam heel is $\gamma_w H_1$ and at the dam toe is $\gamma_w H_2$.

Figure 7.5 shows the uplift distribution on the base of solid gravity dam. In Fig. 7.5a, the rectangle (abcd) represents the buoyant pressure and the quadrilateral (cdef) is the seepage pressure. Grouting curtain (Fig. 7.5b) is usually emplaced near the dam heel to cut uplift pressure under the dam base, and drainage curtain is also often constructed to drain off seeping water. In practical projects, both the grouting

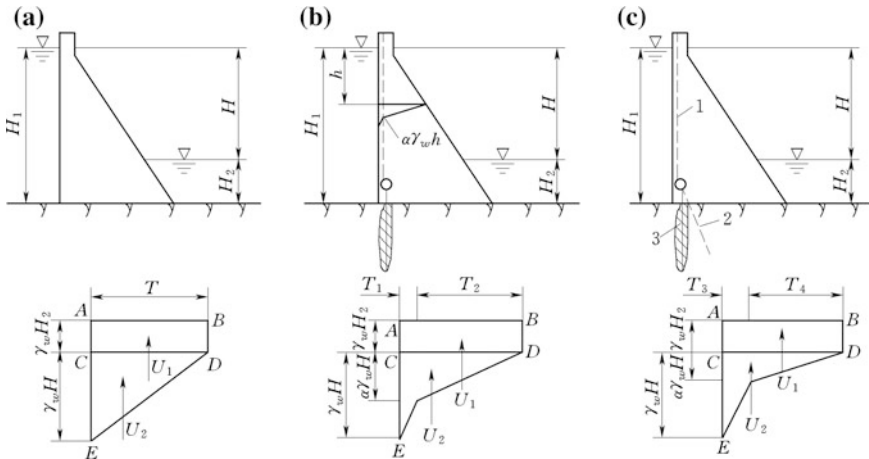


Fig. 7.5 Uplift distribution on the base of the solid gravity dam

curtain and drainage curtain are often employed simultaneously to strengthen the seepage prevention and pressure reduction (Fig. 7.5c), although it is widely recognized nowadays that the latter is more effective in the reduction of uplift.

Where both the grouting curtain and drainage curtain are installed simultaneously, the uplift pressure distribution will be in a form of broken line with two turning points. As the uplift pressure is reduced sharply and the effectiveness of grouting curtain is much less certain than that of drainage curtain, for simplification the uplift pressure diagram may be assumed to have only one turning point located at where the drainage hole intersects the dam bottom base. The intensity of seepage pressure is reduced to $\alpha\gamma_w(H_1 - H_2) = \alpha\gamma_w H$ after the seeping water flows through the drainage curtain, in which α is named as the “reduction factor of seepage pressure.” The factor α should be studied carefully taking into account the characteristics of foundation rock and foundation treatment quality, the depth and size as well as the spacing of drains, the depth of grouting curtain, the facility with which the drains can be maintained, the observation data of analogous projects, the importance of the dam concerned, etc.

The arrangement of auxiliary draining galleries (transverse and longitudinal) and corresponding draining holes may further reduce the uplift (Fig. 7.6a, b). However, their effects are usually looked at as a safety margin and not considered in the design.

Grouting curtain and drainage curtain can reduce the seepage pressure effectively but without help to reduce the buoyant pressure. The pumping drainage may be employed to reduce the buoyant any further, provided the depth of tailwater is relatively deep, and the foundation rock is not vulnerable to piping and chemistry erosion. This is realized by installing pumping sumps and automatic pumping facilities for the auxiliary draining system, together by emplacing auxiliary grouting curtain and drainage curtain near the dam toe. In this case, the intensity of uplift

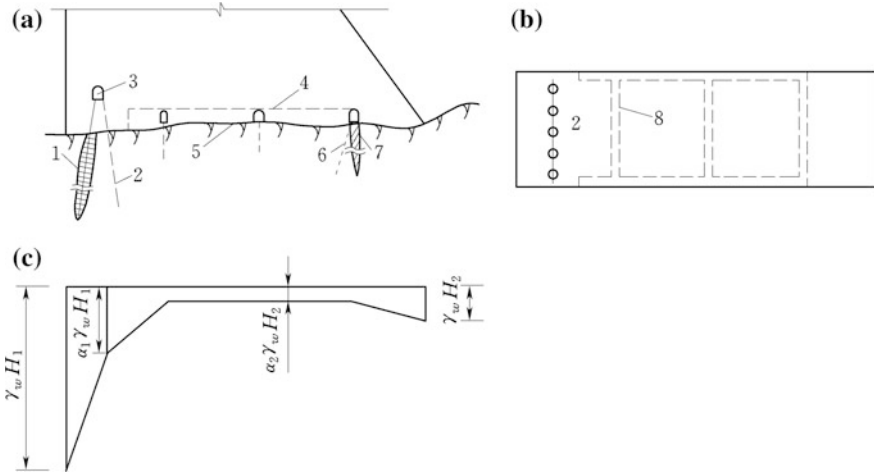


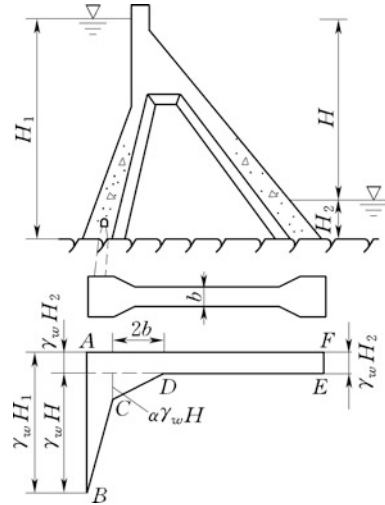
Fig. 7.6 Uplift distribution on the base of a solid gravity dam with pumping drainage. **a** Cross section; **b** plan; **c** uplift distribution. 1 upstream principal grouting curtain; 2 upstream principal drainage curtain; 3 grouting gallery; 4 longitudinal drainage gallery; 5 rock foundation surface; 6 downstream auxiliary drainage curtain; 7 downstream auxiliary grouting curtain; 8 transverse drainage gallery; and H_1 and H_2 are the upstream and downstream water depth

distribution may be assumed as in a pattern that (Fig. 7.6c) $\gamma_w H_1$ at the dam heel, $a_1 \gamma_w H_1$ at the line of main drains, $a_2 \gamma_w H_2$ at the auxiliary draining galleries, and $\gamma_w H_2$ at the dam toe, where a_1 and a_2 are the “reduction factor” and “residual factor” of uplift, respectively.

The Xiaokou Project (Zhejiang province, China) has dam height of 62 m and axis length of 286 m. In addition to the upstream grouting curtain and drainage curtain, there are 1–2 auxiliary drainage galleries on the dam base. The spacing and depth of the draining holes under these galleries are 2 and 4 m, respectively. The pumping drainage technique is exercised in this dam. According to the field observation data, twice pumping per day can guarantee dry galleries and ensure the design uplift diagram requirements. Other dams in China successfully achieved pumping draining design are the Gongzhui Gravity Dam (Sichuan Province, $H = 85.5$ m), the Hunanzhen Massive-head Buttress Dam (Zhejiang Province, $H = 129$ m), the Longtang RCC Gravity Dam (Guangxi Province, $H = 216.5$ m), etc.

Figure 7.7 shows the uplift distribution on the base of a slotted gravity dam. Due to the strengthened relief efficiency of slots, the uplift drops sharply. The intensity of uplift is then stipulated as follows: $\gamma_w H_1$ at the dam heel; $\gamma_w H_2 + a \gamma_w H$ at the line of foundation drains (C); zero at (D); between (BC) and (CD) the uplift varies straightly; from (D) until to the dam toe the uplift is constantly $\gamma_w H_2$; and (D) is at a distance of twice dam thickness b , from the starting point of the slot.

Fig. 7.7 Uplift distribution on the base of the slotted gravity dam



The SL319-2005 “Design specification for concrete gravity dams” stipulates the reduction factor of seepage pressure, and the reduction factor and residual factor of uplift, on the dam base, which are listed in Table 7.1.

2. Uplift within dam body

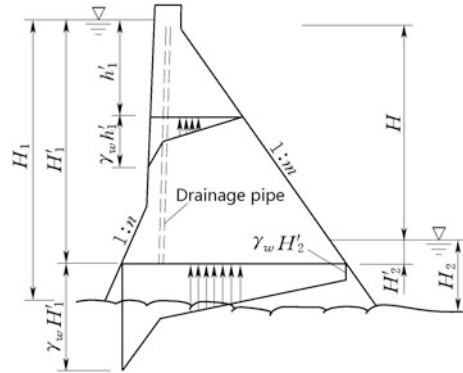
Similar to the seepage in dam foundation, the flow permeates into a dam body will also build up uplift. The construction joints are weak planes within the concrete monolith and are intended to be seepage pathways. In high dams, uplift may account for a major portion of the overturning forces leading to the tensile stress at

Table 7.1 Reduction factors of seepage pressure and uplift

Dam type and portion		Foundation treatment		
		(A)	(B)	
		Grouting curtain + drainage curtain	Grouting curtain + drainage curtain + pumping drainage	
Portion	Dam type	Reduction factor of seepage pressure α	Reduction factor of uplift α_1	Residual factor of uplift α_2
Dam monolith on riverbed	Solid gravity dam	0.25	0.20	0.50
	Slotted gravity dam	0.20	0.15	0.50
	Hollow gravity dam	0.25	–	–
Dam monolith on bank slope	Solid gravity dam	0.35	–	–
	Slotted gravity dam	0.30	–	–
	Hollow gravity dam	0.35	–	–

N.B.: If there is no grouting curtain in front of drainage curtain, the reduction factor of seepage pressure α in the column (A) is to be raised appropriately

Fig. 7.8 Uplift distribution on a horizontal plane within the gravity dam



the upstream edge. To reduce the uplift within dam body, low permeable concrete of 3–5 m thick is usually placed at the upstream dam face. In addition, drainage pipes are also often installed in the dam body to reduce the uplift in dam, as shown in Fig. 7.8. In the practical calculation, the uplift on a horizontal plane is assumed to vary bilinearly that has an intensity of $\gamma_w H'_1$ (or $\gamma_w h'_1$) on the upstream face and $\gamma_w (H'_2 + \alpha_3 H)$ (or $\alpha_3 \gamma_w h'_1$) at the drainage pipe inlet, and $\gamma_w H'_2$ (or 0) on the downstream face, dependent on whether the plane is below or above the tailwater. H'_1 and H'_2 are the head- and tailwater depths, respectively, at the plane concerned.

The uplift distribution on the horizontal plane within a slotted gravity dam body may be calculated similarly to that on its dam base.

α_3 is the intensity factor of the of uplift pressure within dam, generally $\alpha_3 = 0.2$ for solid gravity dams and $\alpha_3 = 0.15$ for slotted gravity dams.

7.2.2 Load (Action Effect) Combinations

The load (or action effect) combinations corresponding to the design methods using the conventional safety factor and the limit state-based partial safety factors have been discussed in Chap. 4 of this book, for more details, the SL319-2005 “Design specification for concrete gravity dams” (safety factor), and the DL5108-1999 “Design specification for concrete gravity dams” (limit state-based partial safety factors) may be consulted.

7.3 Stability Analysis for Gravity Dams

The purpose of this work is to check the stability safety for gravity dams under probable load combinations (Henny 1934; Stelle et al. 1983). Since conventional gravity dams are intersected by transverse joints into independent dam monoliths, the stability analysis are normally conducted on two-dimensional principles. A

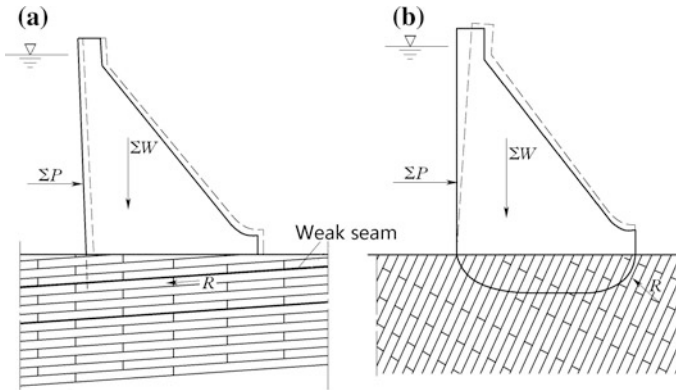


Fig. 7.9 Sketch of the failure mechanism of gravity dam. **a** Sliding failure; **b** overturning failure. 1 sliding surface; 2 tensile crack; 3 crush zone; R resistance

three-dimensional analysis (e.g., multiple-wedge analysis) may be required with respect to particular geometric and loading conditions (e.g., bank-slope dam monolith).

The stability of gravity dams generally falls into the overturning stability and the sliding stability (Fig. 7.9). However, according to the (SL319-2005) and (DL5108-1999) “Design specification for concrete gravity dams”: since no tensile stresses are allowable within the dam body, it implicates that the resultant of all forces exerting on any horizontal intersection plane within a dam is inside the middle third kernel, therefore the overturning stability is not calibrated obligatory.

The sliding failure process of the gravity dam on homogenous foundation revealed by theoretic and experimental studies is very complicated. The most countries in the world use design codes in which the sliding stability analysis is based on a mixed way of semi-theoretic and semi-empirical, presuming that failure surfaces can be any combinations of planes and curves. Very often in practices, failure surfaces are assumed to be planar for simplicity. It should be noted that for an analysis to be realistic, these assumed failure planes have to be kinematically possible.

Conventionally, sliding stability is expressed in terms of a safety factor against sliding (SL319-2005), by means of limit equilibrium method (Vide Chap. 5). A sliding failure will take place along the presumed slip surface when the applied shear force exceeds the shear strength.

7.3.1 Stability Analysis Along Dam Base

The dam base is often a critical plane due to its weak concrete-rock bond and larger horizontal resultant thrust force. The stability against sliding along the base is therefore calibrated obligatory in the design.

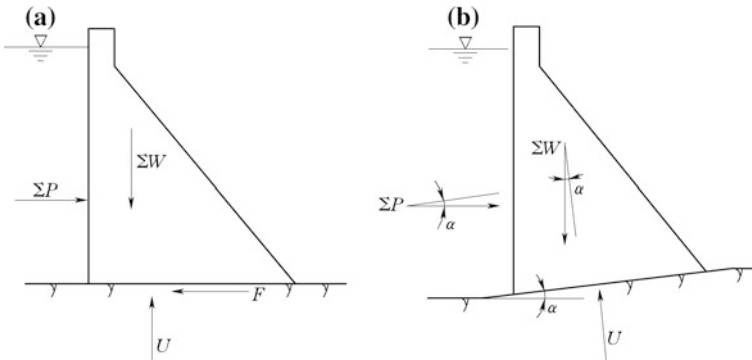


Fig. 7.10 Stability against sliding along dam base. **a** Sliding along horizontal dam base; **b** sliding along inclined dam base

1. Friction factor K

The friction factor K is simply expressed as a ratio of friction resistance to slip driving on the plane concerned. It is assumed that the resistance is purely frictional, and no shear strength or cohesion can be mobilized. The plane is horizontal or inclined at a small angle of α (Fig. 7.10).

For a horizontal slip plane, the friction factor K is the ratio of the maximum resistance friction to the applied shear force which can be calculated using Eq. (7.1)

$$K = \frac{\text{resisting friction}}{\text{shear}} = \frac{f(\sum W - U)}{\sum P} \quad (7.1)$$

where $\sum W$ = resultant of forces normal to the assumed slip plane, kN/m; $\sum P$ = resultant of forces parallel to the assumed slip plane, kN/m; U = resultant of uplift exerted perpendicular to the slip plane, kN/m; and f = friction coefficient of the assumed slip plane.

If the plane is inclined at a small angle of α , the foregoing expression is modified as follows:

$$K = \frac{f(\sum W \cos \alpha - U + \sum P \sin \alpha)}{\sum P \cos \alpha - \sum W \sin \alpha} \quad (7.2)$$

The uplift U is always perpendicular to the slip plane. The angle α is defined as positive where sliding operates in uphill sense. The gravity dam base is frequently so excavated to give a small positive inclination of α as to obtain higher K , enlightened by Eq. (7.2).

2. Shear factor K'

The shear factor K' is defined as the ratio of total shear resistance mobilized on a slip plane to total slip driving. With this approach, both the cohesion and frictional components of shear strength are accounted for, and

$$\begin{cases} K' = \frac{f'(\sum W - U) + c'A}{\sum P}, \text{ or} \\ K' = \frac{f'(\sum W \cos \alpha - U + \sum P \sin \alpha) + c'A}{\sum P \cos \alpha - \sum W \sin \alpha} \end{cases} \quad (7.3)$$

where f' = shear frictional coefficient of the concrete-rock bond plane; c' = cohesion representing the unit shearing strength of concrete-rock bond plane under zero normal stress, kN/m^2 ; A = area of contact or slip plane, m^2 ; and α = inclination angle of the slip plane defined as positive where the sliding operates in uphill sense.

Although the above formulae are far from perfect, yet seemingly correct and simple, they have been used in the design of gravity dam for many years, and since the 1980s, the shear factor K' has been prevailing among Chinese engineers. The allowable safety factors against sliding along dam bases are listed in Table 7.2.

It should be indicated that the forces $\sum W$ and $\sum P$ are directly proportional to the square of dam height, whereas the area of contact plane A is directly proportional to the dam height only. Therefore, the cohesion c' contributes less to the stability of higher dams, if the shear factor K' in Eq. (7.3) is employed.

It is widely recognized that the shear frictional coefficient f' or the corresponding friction angle φ' is a more stable parameter (Lo et al. 1991). By contrast, the cohesion c' is not so stable and is influenced by various factors such as the roughness of concrete-rock bond plane, and the type and integrity of foundation rock, as well as the geologic structures. Considerable variation in cohesion may emerge for one specific rock within the confines of the dam site in consequence of local weathering or alteration. Cohesion may also be diminished due to saturation for some vulnerable rocks (e.g., several shales).

In the planning phase, the parameters f' , c' , and f may be referred to Table 7.3 (GB50487-2008). However, started from the preliminary design, thorough investigation, extensive in situ and laboratory tests, are highly demanded to confirm these design parameters (Lo et al. 1991). Applied to the middle- and lower dams in the middle-class projects, when there is no possibility for in situ tests, the parameters listed in Table 7.3 may also be used in the design, subject to appropriate verification through laboratory tests.

Table 7.2 Allowable safety factors against sliding along dam base

Allowable safety factor	Load combination	Grade of dam		
		1	2	3
[K]	Basic	1.10	1.05	1.05
	Special ⁽¹⁾ (catastrophe flood)	1.05	1.00	1.00
	Specia ⁽²⁾ (earthquake)	1.00	1.00	1.00
[K']	Basic	3.0		
	Special ⁽¹⁾ (catastrophe flood)	2.5		
	Special ⁽²⁾ (earthquake)	2.3		

Table 7.3 Strength parameters of foundation rock mass and contact surface (GB50487-2008)

Classification of rock	Contact surface between concrete and rock			Rock mass		
	f'	c' (MPa)	f	f'	c' (MPa)	f
I	1.50–1.30	1.50–1.30	0.85–0.75	1.60–1.40	2.50–2.00	0.90–0.80
II	1.30–1.10	1.30–1.10	0.75–0.65	1.40–1.20	2.00–1.50	0.80–0.70
III	1.10–0.90	1.10–0.70	0.65–0.55	1.20–0.80	1.50–0.70	0.70–0.60
IV	0.90–0.70	0.70–0.30	0.55–0.40	0.80–0.55	0.70–0.30	0.60–0.45
V	0.70–0.40	0.30–0.05	0.40–0.30	0.55–0.40	0.30–0.05	0.45–0.35

N.B. 1: f' and c' are the parameters against shearing, and f is the friction coefficient

2: The parameters listed in the table are only applicable for hard rocks, and the reduction considering softening coefficient is demanded for soft rocks

7.3.2 Stability Analysis Along Deep-Seated Slip Planes

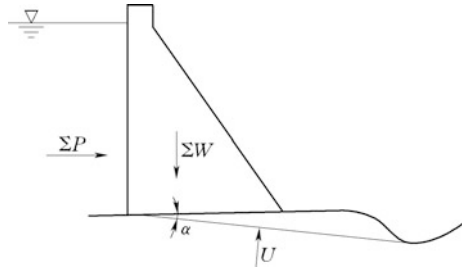
Founded on solid and integral rock foundation, a gravity dam designed and built using modern theory and technique is very reliable, and the stability against sliding along the dam base is merely necessary to be checked. However, weak geologic structure faces (discontinuities, including joints, seams, faults, etc.) are ubiquitous within rock masses which might dominate the dam stability in a manner of deep-seated sliding inside the dam foundation. The Austin Dam (USA, $H = 15$ m) is a typical lesson of failure due to the water softened shale within the foundation (Wise 2005).

The stability issue resulted from discontinuities in dam foundation has been widely studied throughout the world since the 1960s. According to the incomplete statistics data insofar, of nearly one hundred China's dams under construction or design, about one-third are affected by serious adverse geologic structure faces which lead to consequences such as construction delay or even shutdown, important design revisions or even change of dam site and reduction of dam height, limitation of operation reservoir level, or reinforcement after completion.

The study on the deep-seated sliding proceeds in the following steps:

- The defects within the foundation are investigated, and the slip surfaces (boundaries) are specified;
- The strength parameters of the slip surfaces are evaluated;
- The safety calibration method and corresponding allowable safety margin are chosen; and
- The countermeasures for improving the stability are selected and justified.

Fig. 7.11 Stability analysis along single slip plane



The safety against deep-seated sliding in dam foundation is calibrated mainly by means of limit equilibrium method (LEM) in China. For very important and complicated dam projects, the finite element method (FEM) and geo-mechanical model test are demanded for the purpose of comprehensive analysis and evaluation.

1. Stability analysis along single slip plane

For single slip plane problem shown in Fig. 7.11, the safety factor K' can be given by

$$K' = \frac{f'_B(\sum W \cos \alpha - U + \sum P \sin \alpha) + c'_B A}{\sum P \cos \alpha - \sum W \sin \alpha} \tag{7.4}$$

where f'_B = friction coefficient of the discontinuity; c'_B = cohesion of the discontinuity; and A = area of the discontinuity.

The angle α is defined as positive if the sliding operates in uphill sense.

2. Stability analysis along the multiple slip planes

The combination of discontinuity planes may delimits the dam foundation into a group of wedges (slices), which fall into driving wedges, structural wedges, and resisting wedges. In Fig. 7.12, the driving wedge is neglected by assuming a vertical crack (ab) from the dam heel, (abcd) forms structural wedge, (cdef) and (efg) form two resisting wedges. According to the general principles of slice

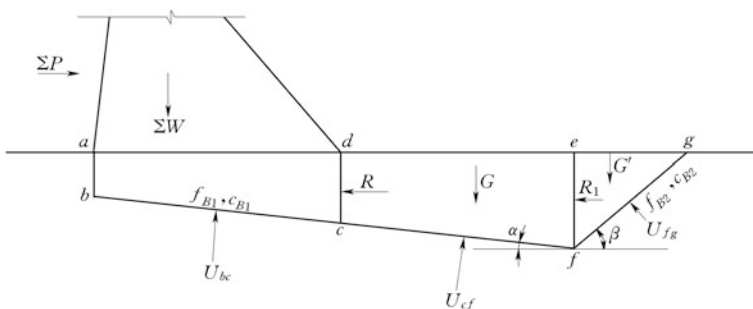


Fig. 7.12 Stability analysis along multiple slip planes

method (vide Chap. 5), the resistances R_1 and R (i.e., inter-slice forces) are inclined at an inclination angle within $0-\varphi$ to the normal of vertical inter-slice faces, and φ is the angle of internal friction. When the resistances R_1 and R are horizontal, the computed safety factor K' against sliding is the minimum; K' increases with the increase of the inclination angle of resistances until the maximum when the angle reaches φ . The assumption that the resistances R_1 and R are parallel to the slip planes of their preceding wedges (slices), i.e., they are inclined at an angle of α (Fig. 7.12), is customarily adopted. This assumption actually entails the computation as a kind of the residual thrust method (RTM) elaborated in Chap. 5 of this book.

There are three definitions and algorithms for the computation of safety factor of deep-seated sliding with multiple slip planes.

(a) Passive reaction

Let the wedge (efg) be at the state of limit equilibrium, i.e., its safety factor is equal to the allowable value $[K']$, the resistance R_1 is then deduced as

$$R_1 = \frac{f'_{B2}(G' \cos \beta - U_{fg}) + c'_{B2}A_{fg} + [K']G' \sin \beta}{[K'] \cos(\alpha + \beta) - f'_{B2} \sin(\alpha + \beta)} \quad (7.5)$$

Next, let the wedge (cdef) be at the state of limit equilibrium, the resistance R can be deduced as follows:

$$R = \frac{1}{[K']} [f'_{B1}(G \cos \alpha - U_{cf}) + c'_{B1}A_{cf} - [K']G \sin \alpha + [K']R_1] \quad (7.6)$$

Finally, the safety factor of the structural wedge (abcd) is derived and looked at as the representative stability safety factor of the whole foundation with deep-seated slip planes

$$K' = \frac{f'_{B1}(W \cos \alpha - U_{bc} - P \sin \alpha) + c'_{B1}A_{bc}}{P \cos \alpha + W \sin \alpha - R} \quad (7.7)$$

where $f'_{B1}, f'_{B2}, c'_{B1}, c'_{B2}$ = shear strength parameters of the slip planes; W = resultant vertical loads of the dam and wedge (abcd), kN; A_{fg}, A_{cf}, A_{bc} = areas of the slip planes (fg), (cf), (bc), respectively, m^2 ; and the other nomenclatures are indicated in Fig. 7.12.

(b) Active reaction

The procedure is just a retroaction to that of the passive reaction algorithm: Let the wedge (abcd) be at the state of limit equilibrium, the resistance R is obtained; exerting R at the wedge (cdef) and let this wedge be at the state of limit equilibrium, the resistance R_1 is obtained; finally exerting R_1 at the wedge (efg), the calculated safety factor K' of the wedge (efg) is looked at as the representative stability safety factor of the whole foundation with deep-seated failure planes.

(c) Equal safety factor

The algorithm of passive reaction or active reaction takes the first wedge (abcd) or the last wedge (efg) to represent the safety of the whole dam foundation, which might lead to unrational results in some cases. The equal safety algorithm is a seemly good compromise between them, by assigning an identical safety factor for each wedge. However, it also may be debated that the equal safety factor is not totally vindicated, attributable to the asynchronous mobilization of the shear strength at different slip planes related to their deformation.

In the equal safety factor algorithm, the equations for the unified safety factor of the wedges (efg), (cdef), and (abcd) are established taking into account their equilibrium conditions simultaneously

$$\left. \begin{aligned} K' &= \frac{f'_{B2} [G' \cos \beta - U_{fg} + R_1 \sin(\alpha + \beta)] + c'_{B2} A_{fg}}{R_1 \cos(\alpha + \beta) - G' \sin \beta} \\ K' &= \frac{f'_{B1} (G \cos \alpha - U_{cf}) + c'_{B1} A_{cf}}{R + G \sin \alpha - R_1} \\ K' &= \frac{f'_{B1} (W \cos \alpha - U_{bc} - P \sin \alpha) + c'_{B1} A_{bc}}{P \cos \alpha + W \sin \alpha - R} \end{aligned} \right\} \quad (7.8)$$

By the solution of above three equation set, K' , R , and R_1 are calculated. Where there are n wedges, n similar equations can be formulated to solve the safety factor and inter-wedge (slice) forces, similar to the RTM elaborated in Chap. 5 of this book.

Where there is only one discontinuity plane dipping downstream and there is no obvious second discontinuity plane within the resisting wedge, the potential uphill slip plane delimiting the resisting wedge is decided using trial and error process: From the intersection point (B) (Fig. 7.13), several slip planes with different angle β are presumed, to attempt the minimum safety factor.

Equations (7.5)–(7.8) are elaborated using the shear factor K' . The corresponding equations using the friction factor K may be obtained by replacing f' with f and letting $c' = 0$.

The Chinese engineering geology sector in charge of water resources and hydropower project recommends empirical strength parameters for the discontinuities, which are listed in Table 7.4 (GB50487-2008). These parameters are summarized from the in situ large-scale tests and laboratory middle-scale tests, which were carried out for more than 30 water resources and hydropower projects.

Fig. 7.13 Potential slip plane within the resisting wedge

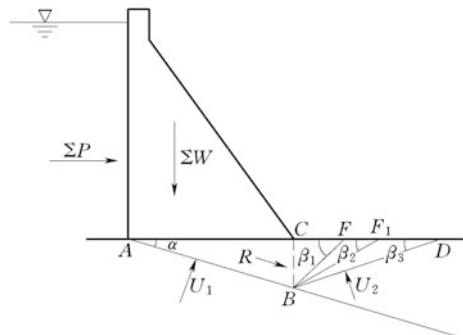


Table 7.4 Strength parameters of discontinuity (GB 50487-2008)

Type of discontinuity		f'	c' (MPa)	f
Well-cemented		0.90–0.70	0.30–0.20	0.70–0.55
Unfilled		0.70–0.55	0.20–0.10	0.55–0.45
Weak seam	Rock-laden debris filled	0.55–0.45	0.10–0.08	0.45–0.35
	Argillite-laden debris filled	0.45–0.35	0.08–0.05	0.35–0.28
	Debris-laden argillite filled	0.35–0.25	0.05–0.02	0.28–0.22
	Argillite filled	0.25–0.18	0.01–0.005	0.22–0.18

N.B. 1. f' and c' are shear parameters and f is the friction parameter

2. The parameters listed in the table are applicable only to the geologic structure faces within hard rock

3. For the geologic structure faces within soft rock, the parameters listed in the table are subject to reduction

4. For the well-cemented and unfilled structure faces, the strength parameters are selected among the upper and lower bounds according to the roughness of structure faces

Concerning the allowable safety factor for the deep-seated sliding stability, there are no detailed specifications in the corresponding Chinese design codes due to the complexity and uncertainty in the foundation rock properties. Currently, it is often selected in light of sliding along the base or even larger. The allowable safety factor adopted for the gravity dam design in the Three Gorges Project (Hubei, China, $H = 185$ m) is $[K'] = 3.0$ for basic load combinations, $[K'] = 2.3–2.5$ for special load combinations; the allowable safety factor for the gravity dam design in the Xiangjiaba Hydropower Project (Sichuan, China, $H = 161$ m) is $[K'] = 3.0–3.5$ for basic load combinations, $[K'] = 2.0–3.0$ for special load combination (1) (catastrophe flood), $[K'] = 2.3–2.5$ for special load combination (2) (earthquake).

For the lower-to-medium gravity dams or barrages affected seriously by seams daylighting at downstream, the aforementioned analysis methods and criteria are too conservative which will lead to huge engineering amount. Under such circumstances, the Chinese engineer usually employs the analysis methods and criteria for lower head hydraulic structures on soft foundation: the small cohesion c' is ignored and the friction factor K is applied for the stability calibration. The allowable safety factor $[K]$ is normally higher than that for the dam base (Table 7.2), for example: $[K] = 1.2$ for the Baishan Gravity Arch Dam (Jilin Province, China, $H = 149.5$ m); $[K] = 1.3$ for the Dahua gravity dam (Guangxi Province, China, $H = 78.5$ m); $[K] = 1.1–1.2$ for the Tongjiezi Gravity Dam (Sichuan, China, $H = 82$ m).

7.3.3 Stability Analysis of Bank-Slope Monoliths

The base of a bank-slope monolith comprises of one or more inclined planes. The sliding direction will have a component perpendicular to the river stream under the

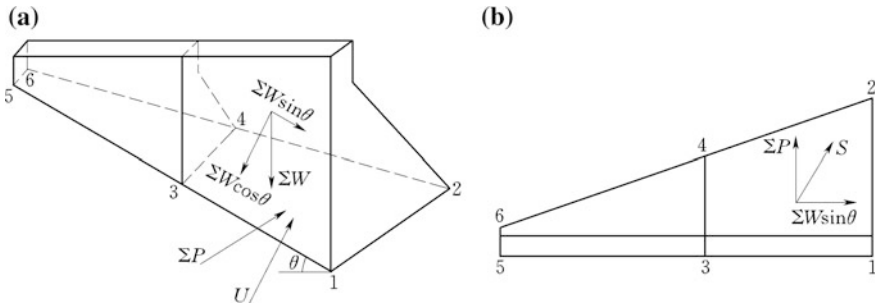


Fig. 7.14 Diagram to the stability analysis for bank-slope dam monolith. **a** Three-dimensional view; **b** plan

action of gravity as shown in Fig. 7.14, which leads to a lower stability safety, particularly during the phase of construction.

Denote: θ = included angle between the base of bank-slope monolith and horizontal plane; U = uplift; $\sum P$ = horizontal water pressure; $\sum W \cos \theta$ and $\sum W \sin \theta$ = components of resultant vertical loads perpendicular and parallel to the base, respectively; and S = resultant of $\sum W \sin \theta$ and P (Fig. 7.14), which is computed as $S = \sqrt{(\sum P)^2 + (\sum W \sin \theta)^2}$. Then the safety factor against sliding is calculated by

$$K = \frac{f(\sum W \cos \theta - U)}{\sqrt{(\sum P)^2 + (\sum W \sin \theta)^2}} \tag{7.9}$$

or

$$K' = \frac{f'(\sum W \cos \theta - U) + c'A}{\sqrt{(\sum P)^2 + (\sum W \sin \theta)^2}} \tag{7.10}$$

7.3.4 Engineering Countermeasures for the Improvement of Stability

The countermeasures can be categorized as those that reduce adverse loadings, in particular uplift, and those that add stabilizing forces to the structure, as well as those that raise shear resistance (ICOLD 2005).

- ① Flattening upstream dam slope uniformly or in variable batter, to make use of water weight for stability (Fig. 7.15a). However, since too flat slope may induce upstream tensile stress, it is advisable to limit the upstream slope within a range of 1:0.1–1:0.2.

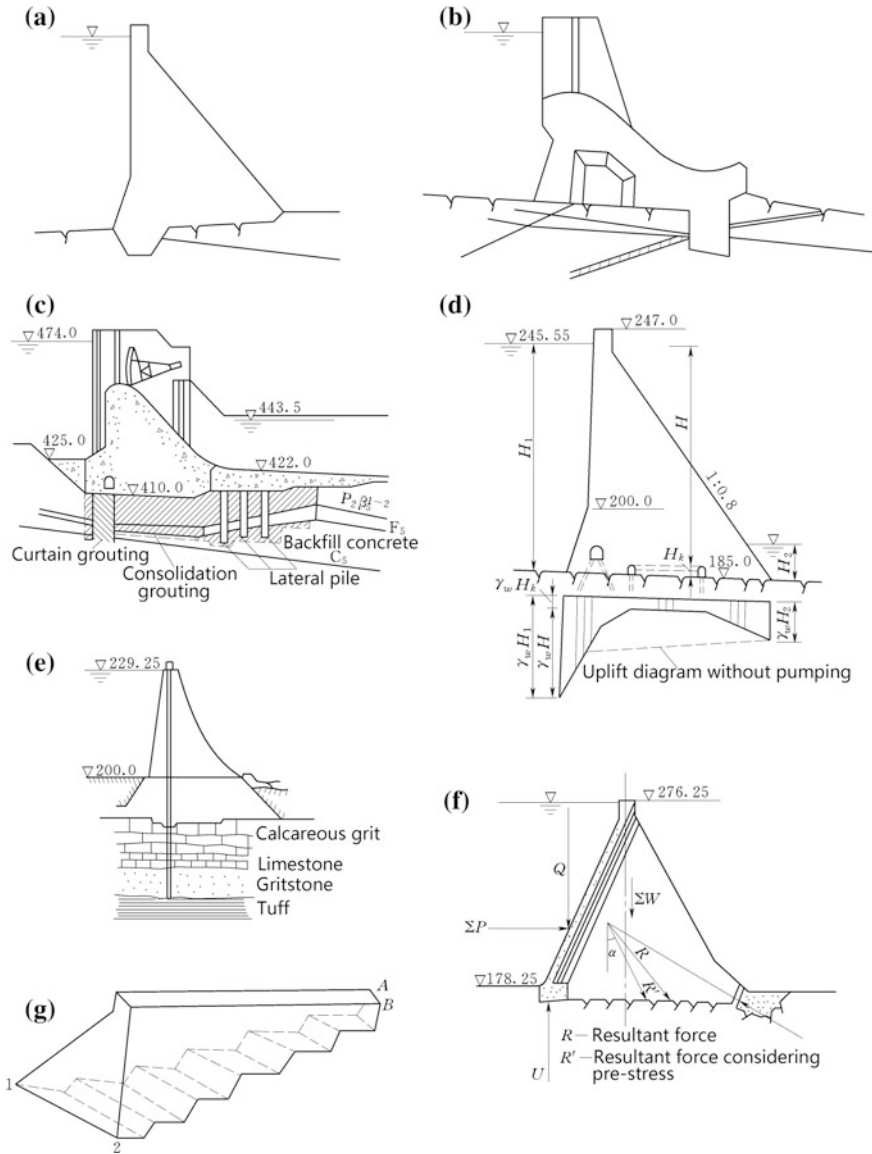


Fig. 7.15 Engineering countermeasures for improving foundation stability

- ② Excavating dam base inclined toward upstream (Fig. 7.15b). A zigzag inclined dam base is more practical and effective for hard rock foundation or horizontally stratified rock foundation. However, this measure may raise the amount of rock excavation and concrete placement.

- ③ Dental treatment in the foundation at the vicinity of dam toe or/and heel (Fig. 7.15a, b).
- ④ Installing large-scale reinforced concrete piles. It is particularly advisable for the foundation containing several weak structure planes nearly parallel (Fig. 7.15c).
- ⑤ Strengthening foundation grouting and drainage. It may effectively reduce the uplift. When the tailwater is deep and the foundation rock is not vulnerable to piping or chemistry erosion, the pump drainages can be employed to reduce the uplift any further (Fig. 7.15d).
- ⑥ Prestressing foundation with anchor system. It may be one of the most economical ways to increase rotating and sliding resistance along the dam base. Prestressing may improve dam heel stress condition, too. Usually, the prestressed steel-strand cables or tendons are introduced from the dam crest level to the foundation (Fig. 7.15e). One of the alternatives is to employ flat jack at the dam toe (Fig. 7.15f), which may shift the resultant force to more favorite direction and reduce the shear load.
- ⑦ Grouting the transverse joints of bank-slope monoliths. Permitted by the topographic and geologic conditions, it is also advisable to excavate bank slopes in the form of stepping platforms (Fig. 7.15g).

The applicability of the above-engineering countermeasures is studied taking into account the conditions of topography, geology, material, construction, importance, etc., for a specific dam project.

7.4 Stress Analysis for Gravity Dams

7.4.1 Purposes and Methods of Stress Analysis

Stress analysis for gravity dams is performed to determine the magnitude and distribution of stresses in the dam body under static and dynamic load conditions during service and construction period, as well as to investigate the structural adequacy of appurtenances and foundation. If the stresses are smaller than the corresponding allowable values, the dams are thought as in safe state.

Stress analysis is carried out for the following:

- Specified horizontal sections, including the sections located more or less uniformly along the dam height, the sections at the turning points of up and down dam slopes;
- Near the weakened portions (e.g., galleries, holes, and water pathways);
- appurtenances (e.g., dam crest, bridge, pier, and guide wall); and
- Other portions, if necessary.

Stresses are analyzed by either theoretic computations or physical model. Each method can test whether the other method is right. Physical modeling is only

suggested in the detailed design or verification of high dams. Theoretic computations comprise of simplified and approximate formulae, elastic theory, and numerical analysis (e.g., FEM), which are selective according to the refinement required for the particular level of design and the type of dam. Among all of these, with the basic hypothesis of linear distribution of vertical normal stress σ_y on horizontal plane sections, the gravity method based on the cantilever beam principles is prevalent in the design of many low dams. More rigorous analyses and physical modeling prove that with the gravity method, the dam stresses of the upper two-third portion can be calculated with sufficient accuracy, but the calculation results of the lower one-third portion are not correct. For low-to-medium high dams ($\leq 60\text{--}70\text{ m}$), the gravity method is stipulated as appropriate according to the (SL319-2005) and (DL5108-1999) “Design specification for concrete gravity dams” However, for the final design phase of high dam, it is demanded to additionally employ other methods including the physical modeling and numerical analysis.

7.4.2 Stress Analysis by Gravity Method

By gravity method, stress analysis is conducted for a dam slice of 1 m thick perpendicular to the dam axis, that is, a “planar problem.” Figure 7.16 is the stress calculation diagram of a non-overflow dam monolith, in which the positive directions of coordinate axes, loads, and stresses are indicated. The stresses of up- and downstream faces are indicated by the superscript “'” and “''”, respectively.

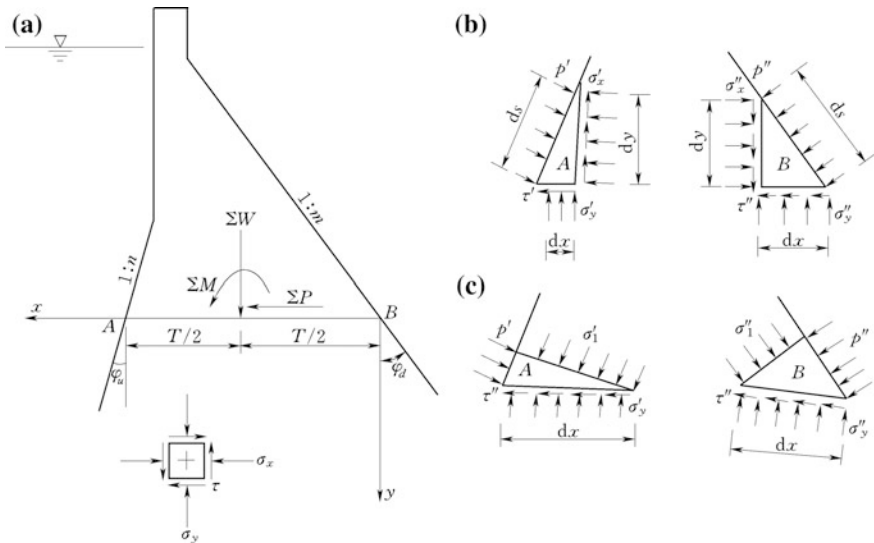


Fig. 7.16 Diagram to the stress calculation for a non-overflow dam monolith

The maximum and minimum principal stresses occur at the up- and downstream dam faces. The stresses within dam body are extrapolated using equilibrium conditions and face stresses. Hence, the face stress calculation is a basic mission in the stress analysis using gravity method.

1. Vertical normal stresses σ'_y and σ''_y on dam faces

The “trapezoidal law”—linear variation of vertical stress σ_y between up- and downstream faces on all horizontal section planes is postulated, i.e.,

$$\left. \begin{aligned} \sigma'_y &= \frac{\sum W}{T} + \frac{6 \sum M}{T^2} \\ \sigma''_y &= \frac{\sum W}{T} - \frac{6 \sum M}{T^2} \end{aligned} \right\} \quad (7.11)$$

where $\sum W$ = resultant vertical loads above the plane considered, exclusive of uplift, kN; $\sum M$ = summation of moments determined with respect to the centroid of the plane, kN m; and T = distance from upstream face to the downstream face of the sectional plane, m.

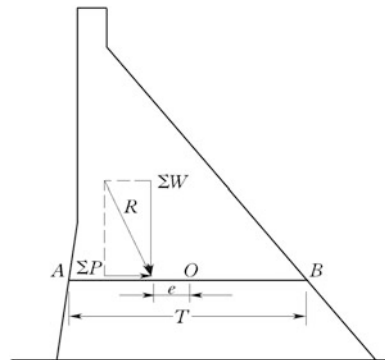
As it is evident from Fig. 7.17 that $\sum M = e \sum W$, Eq. (7.11) leads to

$$\left\{ \begin{aligned} \text{If } e > \frac{T}{6}, & \quad \sigma''_y < 0 \\ \text{If } e = \frac{T}{6}, & \quad \sigma''_y = 0 \\ \text{If } e < \frac{T}{6}, & \quad \sigma''_y > 0 \end{aligned} \right. \quad (7.12)$$

$$\left\{ \begin{aligned} \text{If } e < -\frac{T}{6}, & \quad \sigma'_y < 0 \\ \text{If } e = -\frac{T}{6}, & \quad \sigma'_y = 0 \\ \text{If } e > -\frac{T}{6}, & \quad \sigma'_y > 0 \end{aligned} \right. \quad (7.13)$$

Equations (7.12) and (7.13) define the “kernel” lying between the trisection-points with regard to the width T . Where the resultant R exerts at inside the kernel, the compressive stresses σ'_y and σ''_y at the up- and downstream faces are guaranteed, whereas a resultant R exerting at outside the kernel may result in vertical tensile

Fig. 7.17 Schematic drawing of the kernel of a horizontal section plane



stress at the face away from the intersection point. This is a very important concept in the design of gravity dams.

2. Shear stresses τ' and τ'' on dam faces

The shear stresses τ' and τ'' can be found with the equilibrium consideration of the elementary triangles singled out in the profile of dam on its faces (Fig. 7.16b).

For the elementary triangle on the upstream face around (A), the equilibrium condition of all forces along the y axis, i.e., $\sum F_y = 0$, leads to

$$p' \sin \varphi_u ds - \tau' dy - \sigma'_y dx = 0$$

or

$$\tau' = p' \frac{dx}{dy} - \sigma'_y \frac{dx}{dy} = (p' - \sigma'_y) n \quad (7.14)$$

In a similar manner, the equilibrium condition $\sum F_y = 0$ for the elementary triangle on the downstream face around (B) brings about

$$\tau'' = (\sigma''_y - p'') m \quad (7.15)$$

where p' and p'' = external hydrostatic pressures assumed to exert on the up- and downstream faces, respectively (if applicable, the silt pressure and seismic hydrodynamic pressure are included), kN/m^2 ; n and m = slopes of up- and downstream faces, $n = tg \varphi_u$, $m = tg \varphi_d$; φ_u and φ_d = inclination angles of up- and downstream faces, respectively.

3. Horizontal stresses σ'_x and σ''_x on dam faces

The horizontal stresses σ'_x and σ''_x on dam faces can be found by the equilibrium condition $\sum F_x = 0$ of the elementary triangles (Fig. 7.16b).

For the elementary triangle on the upstream face around (A), the equilibrium condition of all forces along the x axis can be written as

$$\sigma'_x dy + \tau' dx - p' ds \cos \varphi_u = 0$$

or

$$\sigma'_x = p' - \tau' \frac{dx}{dy} = p' - (p' - \sigma'_y) n^2 \quad (7.16)$$

The same equilibrium condition for the elementary triangle on the downstream face around (B) leads to

$$\sigma''_x = p'' + (\sigma''_y - p'')m^2 \tag{7.17}$$

4. Principal stresses σ' and σ'' on dam faces

Principal stresses σ' and σ'' may generally be determined from the knowledge of corresponding normal and shear stresses and construction of a Mohr's circle diagram to represent the stress conditions at a point. However, there is another much simpler way to calculate the principal stresses on the up- and downstream faces directly. Since the upstream and downstream faces are all the planes of zero shearing, therefore they are the directions of the principal stresses. The elementary triangles singled out in the profile of dam on its faces for determining principal stress are shown in Fig. 7.16c. The equilibrium condition $\sum F_y = 0$ for the elementary triangle on the upstream face around (A) is given as follows:

$$\sigma'_1 dx \cos \varphi_u \cos \varphi_u + p' dx \sin \varphi_u \sin \varphi_u - \sigma'_y dx = 0$$

Then, we have

$$\begin{aligned} \sigma'_1 &= \frac{\sigma'_y - p' \sin^2 \varphi_u}{\cos^2 \varphi_u} = (1 + tg^2 \varphi_u) \sigma'_y - p' tg \varphi_u \\ &= (1 + n^2) \sigma'_y - p' n^2 \end{aligned} \tag{7.18}$$

Similarly,

$$\sigma''_1 = (1 + m^2) \sigma''_y - p'' m^2 \tag{7.19}$$

Clearly, the second principal stresses on the dam faces are given as follows:

$$\sigma'_2 = p' \tag{7.20}$$

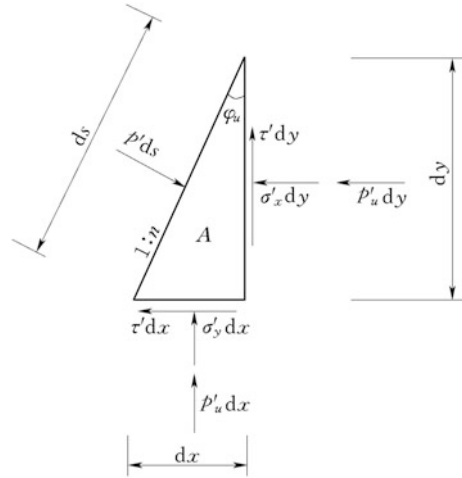
$$\sigma''_2 = p'' \tag{7.21}$$

It can be inferred from Eq. (7.18) that the tensile principal stress σ'_1 may occur at an inclined upstream face if $\sigma'_y < p' \sin^2 \varphi_u$, even when $n > 0$ and $\sigma'_y \geq 0$. To prevent such tensile principal stress, it is born in mind that the upstream slope n should be small, or better be zero.

5. Dam face stresses considering uplift

Where a gravity dam is just completed or impounded, the above formulae are adequate for the face stress calculation, because the steady seepage field has not been built up within the dam body. For dams of long term and continuous service exposed to all possible adverse load combinations, the uplift is not ignorable in the stress analysis. In this case, Eq. (7.11) holds for the vertical σ'_y and σ''_y subject to the

Fig. 7.18 Diagram to the calculation of dam face stress considering uplift



inclusion of uplift in $\sum W$ and $\sum M$; in this way, the stress σ_y obtained is an effective stress. The other face stresses are calculated using the stresses σ'_y and σ''_y and the equilibrium conditions taking into account the uplift. Taking the upstream face stresses as example (Fig. 7.18), the conditions $\sum F_y = 0$ and $\sum F_x = 0$ lead to

$$\begin{cases} \tau' = (p' - p'_u - \sigma'_y)n \\ \sigma'_x = (p' - p'_u) - (p' - p'_u - \sigma'_y)n^2 \end{cases} \quad (7.22)$$

where p'_u = uplift pressure strength on upstream face.

Similarly,

$$\begin{cases} \tau'' = (\sigma''_y + p''_u - p'')m \\ \sigma''_x = (p'' - p''_u) + (\sigma''_y + p''_u - p'')m^2 \end{cases} \quad (7.23)$$

where p''_u = uplift pressure strength on downstream face.

Principal stresses

$$\begin{cases} \sigma'_1 = (1 + n^2)\sigma'_y - (p' - p'_u)n^2 \\ \sigma'_2 = p' - p'_u \end{cases} \quad (7.24)$$

$$\begin{cases} \sigma''_1 = (1 + m^2)\sigma''_y - (p'' - p''_u)m^2 \\ \sigma''_2 = p'' - p''_u \end{cases} \quad (7.25)$$

If silt pressure and seismic hydrodynamic pressure are not applicable, p' and p'' are the external hydrostatic pressures exerted on the up- and downstream faces, and they are equal to the uplift pressure strength p''_u and p'_u . Under such circumstances, $(p' - p''_u)$ and $(p'' - p''_u) = 0$ in the Eqs. (7.22)–(7.25).

Generally, the surface stresses computed using gravity method are sufficient for the strength calibration in the dam profile configuration. If required, the stresses within dam can be interpolated using face stresses, by assuming that the stresses σ_y , σ_x , and τ are all linearly distributed. If necessary, a better distribution of parabolic for τ also can be adopted.

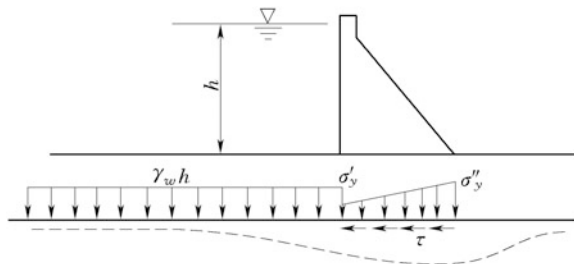
7.4.3 Influence of Non-load Factors on the Stress Distribution in Gravity Dams

1. Foundation deformation

The gravity method assumes the validity of the “trapezoidal law,” i.e., the linear variation of vertical stress between upstream and downstream faces on all horizontal planes. This assumption is based on the infinite wedge theory that any horizontal plane may keep untwisted after the deformation. However, if a wedge of finite height (e.g., dam of triangular profile) is placed on foundation as infinite semi-space, the stresses are redistributed due to the dam–foundation interaction (Fig. 7.19).

The solution of this contact problem for gravity dams has been studied in many countries by rigorous theoretic and experimental tools. These analyses indicate that the “trapezoidal law” assumption is not invalid in the area near the dam base (around 1/3–1/4 of the dam height) due to stress concentration at the heel and toe of the profile, which is attributable to the deformation adjustment for the consistence between the dam body and foundation. The stresses in this case depend largely on the elastic properties of the dam and foundation, on the Young’s moduli E_c and E_r , and also on the Poisson’s ratio μ_c and μ_r . Figure 7.20 shows the distribution of vertical stress σ_y at different levels when $E_c = E_r$. Figure 7.21 shows the distribution of vertical stress σ_y related to different E_c/E_r under the situations of reservoir empty and full. For empty reservoir, larger E_c/E_r gives rise to higher stress concentration of σ_y and τ . For full reservoir, if E_c/E_r is very small (i.e., very hard foundation), σ_y is tensile both at the dam toe and heel; when $E_c/E_r \approx 1$, σ_y will be strongly concentrated at dam toe only; if E_c/E_r is very large (i.e., soft foundation), σ_y is compressively concentrated both at the dam toe and heel. Comprehensive analysis suggests a favorable E_c/E_r within a range of 1–2.

Fig. 7.19 Dam foundation deformation



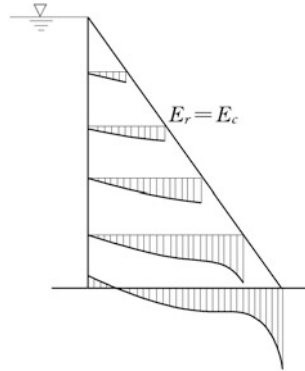


Fig. 7.20 Influence of foundation on dam body stresses

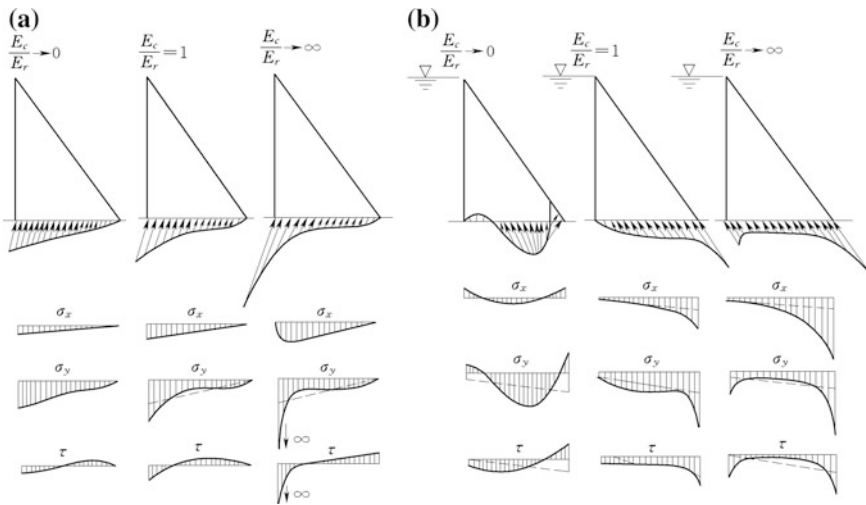


Fig. 7.21 Stress distribution on homogeneous dam base

2. Foundation heterogeneity

It often occurs but not always, the foundation comprises rock masses of different properties. This also influences the dam stress distribution in the portion near base around 1/3–1/4 of dam height, as illustrated in Fig. 7.22 obtained by physical experiments. It is indicated that a higher stiffness of upstream foundation rock will result in higher tensile stress concentration at dam heel; on the contrary, the higher stiffness of downstream foundation rock will reduce tensile stress concentration at dam heel as well as the compressive stress concentration at dam toe. This founding is useful in the selection of dam foundation and in the design of consolidation grouting for dam foundation.

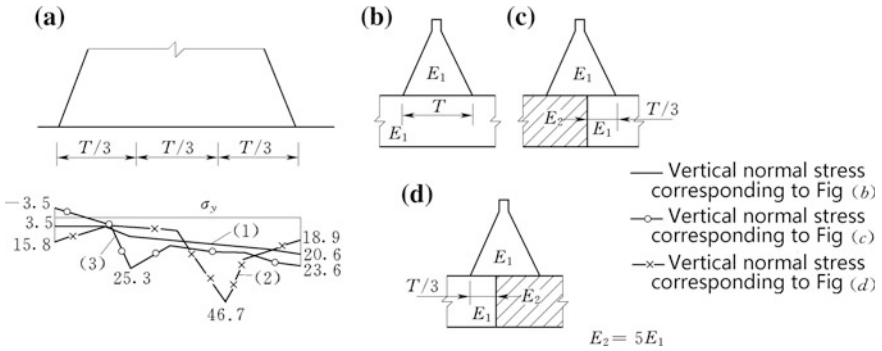
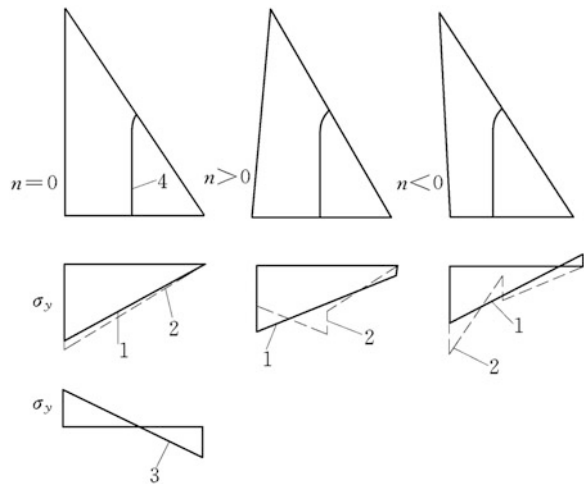


Fig. 7.22 Stress distribution on heterogeneous dam base (unit: kPa)

3. Construction longitudinal joint

Due to the massive volume of concrete in a dam monolith, the thermal tensile stress control and the concrete placement capacity during the construction phase require longitudinal construction joints parallel to the dam axis. They will be grouted to form the integral dam monolith at a suitable time after the cooling of concrete and before the reservoir impounding. This means that the self weight of a concrete block is borne independently by itself before the joint grouting. Figure 7.23 shows the stress distribution attributable to the self weight related to different upstream slopes ($n = 0, n > 0, n < 0$). It indicates that where $n = 0$, the stress distribution due to the self weight has no relation with longitudinal joints; where $n > 0$, the stress at dam heel induced by the self weight will be reduced due to the installation of longitudinal joints, which is disadvantageous for the stress state at dam heel after reservoir full; and where $n < 0$, the stress at the dam heel induced by the self weight is raised due to the installation of longitudinal joints, which is

Fig. 7.23 Influence of longitudinal joint on the stress distribution along dam base. 1 self weight without longitudinal joint; 2 self weight with longitudinal joint; 3 stress induced by water pressure; 4 longitudinal joint



advantageous for the stress state at dam heel after reservoir full. The Grand Dixence Dam (Switzerland, $H = 284$ m,) and the Shiquan Dam (China, $H = 65$ m) have profiles of $n < 0$. However, to prevent larger tensile stress at dam toe during the construction period, this advantage cannot be exaggeratedly exploited.

7.4.4 Stress Control Standard for Gravity Dams

The stress analysis is mainly intended for the strength calibration of dam body. If the material strength is not satisfied or not fully exploited, the dam profile is subject to revision. For this purpose, the stress control standard must be specified.

Stress control standard depends on the stress analysis method. The SL319-2005 “Design specification for concrete gravity dams” and the DL5108-1999 “Design specification for concrete gravity dams” stipulate the stress control criteria for both gravity method and finite element method.

1. Stress control standard related to the gravity method

(a) Dam base

- ① Service period. Under the actions inclusive or exclusive uplift, the maximum vertical compressive stress at dam toe should be smaller than or equal to the allowable stress of foundation rock for the basic load combinations and the special load combination considering check flood. For the special load combination considering earthquake, the allowable vertical compressive stress could be amplified by a fraction equal to or smaller than 1.33. Under the actions inclusive of uplift, the minimum vertical compressive stress at dam heel should be greater than or equal to zero for the provisions of tensile damage to seepage control devices (grouting curtain and drainage curtain).
- ② Construction period. The maximum vertical tensile stress at dam toe should be smaller than or equal to 0.1 MPa.
- ③ Allowable stress of foundation rock is defined as the ratio of the uniaxial compressive strength of rock to its strength safety factor. This safety factor is selected according to the following principles: 20–25 for hard and fractured rock; 10–20 for medium hard rock; and 5–10 for lower strength rock, or soft rock.

(b) Dam body

- ① Service period. Under the actions inclusive of uplift, the minimum compressive principal stress on upstream face should be greater than or equal to zero for the provisions of cracking, i.e., $\sigma_{\min} \geq 0$; However, a tensile stress smaller than the allowable tensile stress may be admitted at portions far away from upstream face for slotted

gravity dams; the steel bar reinforcement should be employed at the portions around the crest of weir, galleries, and holes within dam, to resist potential tensile stresses.

The maximum principal compressive stress on downstream face should be smaller than or equal to the allowable stress of concrete.

- ② Construction period. At any horizontal plane, the maximum principal compressive stress should be less than or equal to the allowable stress of concrete; the principal tensile stress on downstream face should be smaller than or equal to 0.2 MPa.
- ③ Allowable compressive stress of concrete is defined as the ratio of the uniaxial compressive strength of concrete to its strength safety factor. This safety factor is selected according to the following principles: higher than or equal to 4 for the basic load combinations; 3.5 for the special load combination considering check flood; and for the special load combination considering earthquake, the allowable compressive stress could be amplified by a fraction smaller than or equal to 1.33. Allowable tensile stress of concrete is defined as the ratio of uniaxial tensile strength of concrete to a safety factor equal to 4.0.

2. Stress control standard related to the finite element method

Compared to the gravity method, the main difference in the stress control standard related to the finite element method is the allowable tensile stress on the upstream face.

(a) Heel at dam base

Under the actions inclusive of uplift, the width of tensile regime should be shorter than or equal to that 0.07 of the dam base, or keep away from the axis of grouting curtain in the foundation.

(b) Upstream dam face

Under the actions inclusive of uplift, the width of tensile regime should be shorter than or equal to that 0.07 of the sectional width at the horizontal plane considered, or keep away from the axis of drainage curtain within dam body.

7.5 Profile Design for Gravity Dams

7.5.1 Design Principles

Design principles for the sectional profile of gravity dams are the following:

- That it be safe with respect to the overall stability against sliding and to the local strength;
- That it be economical with respect to the engineering expenditure;

- That it be feasible with respect to the construction; and
- That it be convenient with respect to operation.

The major factors influencing the sectional profile design comprise loads, foundation conditions, operation requirements, construction materials, and techniques (Iliev and Kalchev 1981; Joshi 1980). These are comprehensively considered in the comparison and selection of optimal scheme. In recent decades, these works have been greatly simplified with the help of optimal design and CAD techniques.

7.5.2 Basic Profile

The major loads of gravity dams are hydrostatic pressure, uplift, and self weight. With the assumption of infinite wedge, the basic profile may be proven as triangular entailed by the requirements for stability and stress.

7.5.3 Practical Profile

Practical profile is obtained by the revision of the basic profile to accommodate the crest spillway, deep outlets, and other appurtenance structures.

The profiles of non-overflow dam may be divided into three basic types (Fig. 7.24): vertical upstream face, inclined upstream face, and partially inclined upstream face (battered). For a competent foundation with larger shear strength on the dam base, since the profile is mainly controlled by the principal tensile stress, the upstream may be vertical; on the contrary, where the profile is mainly controlled by the sliding stability due to inferior foundation, an inclined or partially inclined upstream face may be beneficial from the additional sliding resistance due to the weight of reservoir water.

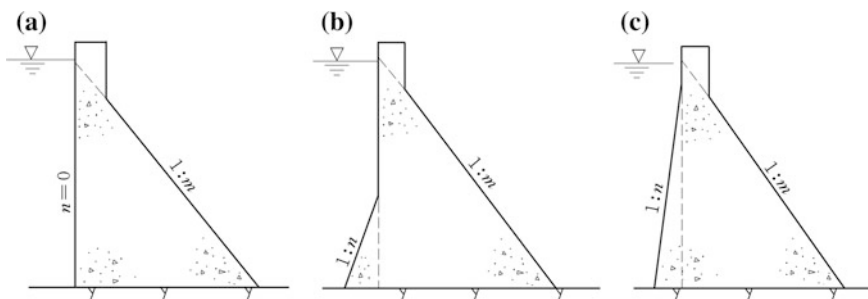


Fig. 7.24 Practical profiles of non-overflow dam

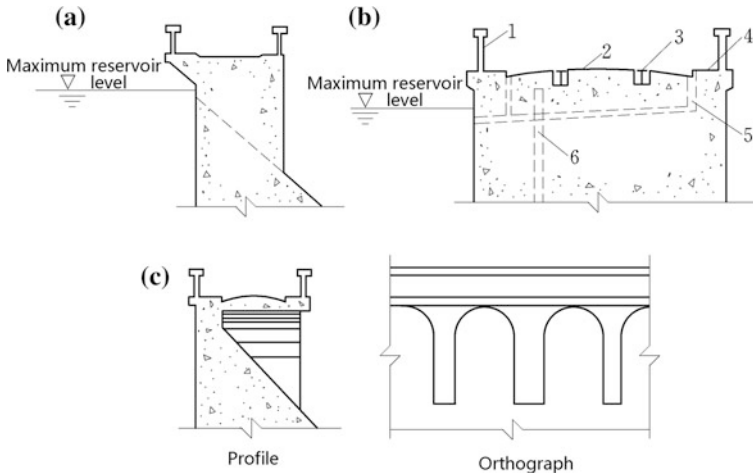


Fig. 7.25 Typical layouts of dam crest. 1 water tight parapet; 2 road way; 3 crane runway; 4 pedestrian passage; 5 drain pipe of dam crest; 6 drain pipe in dam body

Generally, the upstream slope is $n = 0-0.2$, the downstream slope is $m = 0.6-0.8$, and the width of dam base is 60–80 % of the dam height. These empirical data may be useful in the setting of preliminary profile for further optimal analysis.

Figure 7.25 is a typical layout of non-overflow dam crest. The width of dam crest is mainly decided taking into account the operation and transportation requirements, such as the installation and operation of crane runway, the accommodation of access road or even highway on the crest. If there are no special requirements, the width of dam crest may be 8–10 % of the dam height but not smaller than 2 m.

The height of dam crest over the still water level Δh is named as “freeboard” and is calculated by the following:

$$\Delta h = h_{1\%} + h_z + h_c \tag{7.26}$$

where $h_{1\%}$ = wave height, m; h_z = height of wave center line (height of wave induced surge), m; and h_c = safe addition, dependent on the dam grade (see Table 7.5), m.

In the calculation of $h_{1\%}$ and h_z , different wind speeds should be applied for the design and check floods, respectively. The elevation Z_{crest} of the dam crest (or top of the upstream watertight parapet, if any) should be the larger one of the following

Table 7.5 Safe addition h_c (unit: m)

Situations	Grade of dam		
	1	2	3
Basic combination	0.7	0.5	0.4
Special combination	0.5	0.4	0.3

$$Z_{\text{crest}} = \text{Maximum} \left(\begin{cases} \text{design flood level} + \Delta h_{\text{design}} \\ \text{check flood level} + \Delta h_{\text{check}} \end{cases} \right) \quad (7.27)$$

In Eq. (7.27), Δh_{design} and Δh_{check} are calculated using Eq. (7.26), respectively. Where a reliable watertight parapet is installed on the dam crest, the dam crest itself should be not lower than the still water level corresponding to the MPF for grade 1 and 2 dams. The height of watertight parapet is commonly 1.2 m, which should be linked with dam crest reliably with the help of steel bars. The parapet also should have contraction transverse joints corresponding to that of the dam body, in which the water stops are installed.

In the design of non-overflow dam, several typical dam monoliths along the dam axis are to be worked out according to the topographic and geologic conditions, then these monoliths are subject to be comprehensively analyzed and revised, to obtain harmonic overall function and external appearance.

7.6 Flood Release and Erosion Prevention of Gravity Dams

Outlet works such as spillways are basic project elements providing a safe passage for floods from the reservoir into the downstream river reach, to meet the requirements for flood regulation and reservoir drawdown.

Outlet works are ordinarily classified according to their most prominent features, either as they pertain to the control, to the discharge channel, or to some other components. Often, spillways are referred to as controlled (gated) or uncontrolled (ungated). Other types commonly referred to are the free overfall (straight drop), ogee (overflow), side channel, open channel or chute, conduit, tunnel, drop inlet (shaft or morning glory), baffled apron drop, culvert, and siphon.

For a concrete gravity dam, the outlet works are customarily accommodated within or on the dam. The flood flow is straightly discharged to the downstream river reach through surface spillways or inside outlets.

The overflow spillways of the concrete gravity dam are often built on the riverbed monoliths where rock foundations are permitted. In this arrangement, the spillways usually occupy the whole riverbed portion or either side of the dam. The main advantage of this layout is to convey the flow back to the river smoothly. If the outlet works and power plant are all attended to be layout in the central portion of the river stream, other types of arrangements may be considered, such as the spillway over the roof of power plant, the spillway in front of power plant, or the power plant inside of dam. Although these are the most compacted layout with minimum engineering amount, it must be fully verified taking into account the high velocity flow over the roof and the conflicts in the construction schedule and arrangement.

Often but not always, deep outlets are accommodated within the overflow spillway dam monoliths; in this manner, they share a common stilling basin to dissipate the kinetic energy. Where an outlet work conduit is installed in the non-overflow dam or where an outlet must empty into a canal, a separate dissipating device will, of course, be necessary. Instead of a large single conduit, multiple small conduits might be utilized to provide a less expensive as well as a more feasible arrangement for handling outlet releases. The conduits might be either placed at a single level, or be positioned at several levels for more flexibility in operation.

There are two ways to discharge flood through banks, i.e., chute spillway (or ski-jump spillway) and spillway tunnel, which are basic flood release schemes for earth and rockfill dam projects. However, they also may be employed for concrete dams (arch dams, too) when there is additional flood flow to be discharged and the geologic and topographic conditions on abutments are available. The advantage of this arrangement is to send the flow far away from the dam toe so as to avoid adverse geologic conditions near the dam.

The design of bank spillways will be discussed in Chap. 12 of this book; hereinafter, the dam outlet works for gravity dams will be elaborated.

7.6.1 Design of Dam Spillways

Spillway capacity is related to various factors including inflow discharge, frequency and standard of flood, shape of hydrograph; storage capacity of reservoir at various levels; and geologic and other site conditions (e.g., steepness of terrain, possibilities of downstream scour, and stability of bank slopes).

There are three major components of an overflow spillway or deep outlet:

- An entrance structure (intake) which admits reservoir water entering the spillway and control the discharge;
- A conduit which carries the spillway discharge from the entrance structure to low-level exit; and
- An exit structure to dissipate the kinetic energy of the high velocity flow and to convey the water to downstream river channel.

Dam spillway design begins with the configuration of flood-releasing layout schemes. Each scheme is a possible combination of overflow dam monoliths, outlet conduits, and tunnels. Then, the size (height and width of crest) and amount of intake are estimated. The design flood and check flood levels, and the corresponding releasing discharges, are obtained by routing computation using flood of specified frequency or recurrence interval. The optimal layout scheme is finally selected based on the techno-economic comparison using the indices such as the benefits, submerging losses, and the project expenditures.

Fig. 7.26 An overflow dam spillway (unit: m). 1 gantry crane; 2 service gate

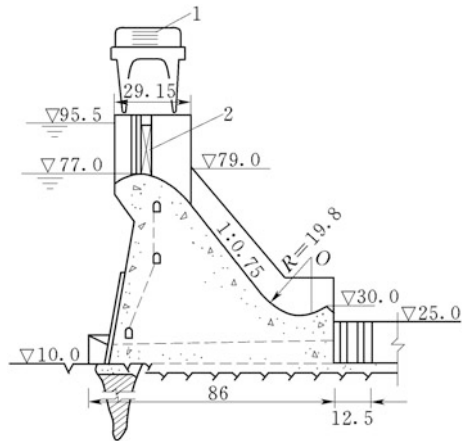
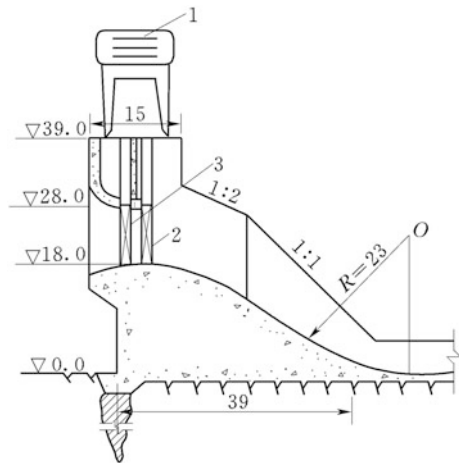


Fig. 7.27 An orifice dam spillway (unit: m). 1 gantry crane; 2 service gate; 3 bulkhead gate



1. Type of intakes

According to the location and the existence of parapet, the dam spillways may be divided into three types of overflow (open flow) (Fig. 7.26), orifice when there is parapet or controlled with gate (Fig. 7.27), deep or bottom outlet (Figs. 7.28 and 7.29).

Overflow spillways may be further distinguished as gate controlled and uncontrolled; the former may control the reservoir level within larger range, and when the gate is partially lifted, the outflow pattern is similar to orifice. The overflow spillway is able to release flood with high discharge efficiency: When the gate is fully lifted, the discharge is proportional to $H^{3/2}$ (H = water head over crest); therefore, as the rising of reservoir level, the discharge capacity increases quickly. The overflow spillway is also able to release floating ice and debris. Be located at high elevation, the intake size of overflow spillway may be larger attributable to

smaller hydrostatic pressure; the operation and reparation of gates are also facilitated.

Be located at lower elevation, orifice spillways and deep (or bottom) outlets enable to drawdown the reservoir level quickly; in this way, more flood control storage capacity may be mobilized to reduce the dam height and inundation losses. They also may be used as diversion openings in dam during construction period, particularly after the sealing of temporary diversion outlets.

Orifice spillways are usually referred to as large openings make use of parapets to lower down the crest level and to reduce the gate height (Fig. 7.27). When the reservoir level is lower, the parapet does not influence on the discharged water and the flow type is identical to the free overflow. However, when the reservoir level is higher, the parapet will obstacle floating ice and debris. As an improvement, the parapet may be constructed movable, which may be lifted to release floating ice and debris, or in case of extraordinary flood to obtain larger releasing ability so as to guarantee the safety of the dam.

Deep (or bottom) outlets are smaller openings compared to orifices, through which the water of pressure (with long pressurized conduit) (Fig. 7.28) or free flow (with short pressurized conduit) (Fig. 7.29) may be discharged for the purpose of reservoir drawdown, silt flushing, construction diversion, and auxiliary flood releasing. The discharge of deep outlets is proportional to $H^{1/2}$ (H = water head), which means smaller over releasing capacity. Exerted by high hydrostatic pressure, their gates are complex and expensive for manufacturing and operating.

2. Size of intakes

Sizing of intake is accomplished by the following three major steps:

Fig. 7.28 A pressure bottom outlet in dam (unit: m). 1 air vent pipe; 2 equalizing (bypass) pipe; 3 bulkhead gate; 4 transition section

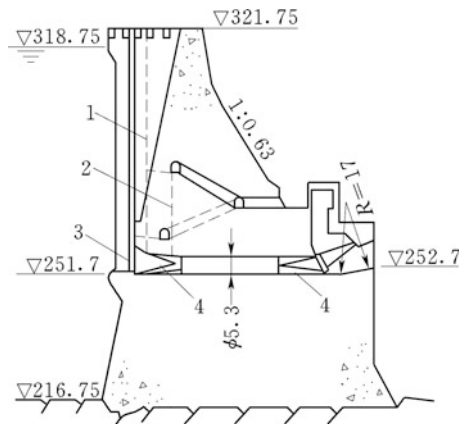
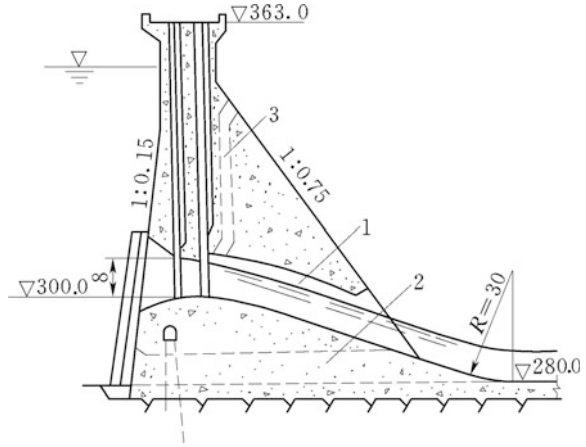


Fig. 7.29 A free-flowing bottom outlet in dam (unit: m). 1 free-flowing outlet; 2 diversion bottom outlet; 3 air vent



(a) Selecting of flood standard

Peak flood inflow discharge and total flood volume are the key hydrologic parameters in the selection of the crest level and intake size. The details may be referred to Chap. 2 of this book.

(b) Selecting of unit discharge

Unit discharge (specific discharge) is the discharge per unit width of the water way (spillway front), which is one of the key hydraulic parameters in the selection of the crest level and intake size.

Suppose the total flood outflow discharge through dam after the flood routing is Q_{total} , of which the flood flow through spillways is given as:

$$Q_{spillway} = Q_{total} - \alpha Q_0 \tag{7.28}$$

where Q_0 = released discharge through power plant and deep outlets, m^3/s ; $\alpha = 0.75-0.9$ for design flood and 1.0 for check flood.

Denote the water way width of overflow dam as L (i.e., the net front length of the overflow dam monoliths exclusive of the width of piers), then the unit discharge through the overflow spillway is as follows:

$$q = \frac{Q_{spillway}}{L} \tag{7.29}$$

Larger unit discharge may shorten the water way width of the spillway and facilitate the layout of the whole project, but it gives rise to highly concentrated energy carried by the released flow which could lead to difficulties with the downstream energy dissipation and scouring protection. Therefore, the unit discharge has tight relation to the project layout, crest level, size of intakes, downstream energy dissipation and scouring protection, and safety and expenditure of the project.

Unit discharge is normally selected by a comprehensive technoeconomic study taking into account above enumerated factors. The commonly used unit discharge on the conservative side is soft rock or well-fractured rock, $q = 20\text{--}50 \text{ m}^3/(\text{s m})$; medium quality rock, $q = 50\text{--}80 \text{ m}^3/(\text{s m})$; and high-quality rock, $q = 100\text{--}130 \text{ m}^3/(\text{s m})$. In recent decades, following the progress of energy dissipation technologies, the unit discharge has been raised considerably.

(c) Sizing of overflow spillway entrance

In the sizing of entrance, gates and their lift machines are also necessarily taken into account. Larger width of intake means larger size of gate which in turn requires larger headstock gear or gantry crane and stronger operating bridge. On the contrary, smaller width of intake increases the number of intake vents and piers, which makes spillway wider. The other considerations in the design of entrance size are to facilitate the manufacture of gates and to save the cost, the standard size recommended in the design specifications for hydraulic steel gates is preferable; to obtain good symmetric outflow pattern during the gate operation, the odd number of intake vents are desirable; for important project, a backup length of spillway may be demanded, otherwise emergency shore (bank) spillway should be installed provided adequate topographic and geologic conditions.

7.6.2 Crest Profile of Overflow Spillway Dams

1. Open overflow crest

Overflow spillway usually possesses a control weir of ogee reversely S-shaped, which is in a shape approximating the under nappe contour of a free jet flowing over a sharp-crested weir. To provide an ideal form for optimum discharges, the flow over the crest is so guided to adhere to its face by preventing access of air to the under side of the nappe. Because of its high discharge efficiency, the nappe-shaped ogee profile is exercised for most overflow spillway crest. The size of such a profile depends upon the crosshead, the inclination of upstream dam face, and the height of the overflow dam above the floor of entrance channel (which influences the velocity approaching to the crest).

An ogee crest and apron may comprise an entire spillway, such as the overflow monolith of a concrete gravity dam, or may only be the control structure for some other types of spillways. A number of ogee crest profiles are available (Grishin 1982; Novak et al. 1990), which are mostly based on experimental results, although some are designed as pure theoretic considerations. Out of the many, the profile type prevailing in the China's high dam design is the WES (Fig. 7.30) recommended by the US Army Corps of Engineers and the Bureau of Reclamation Hydraulic Laboratories (Golzé 1977; USBR 1987), attributable to its merits of keeping negative pressures within safe limits and facilitating construction setting-out (lofting).

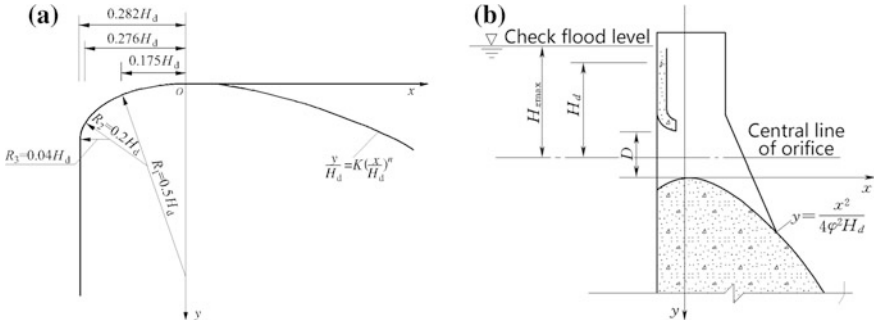


Fig. 7.30 Ogee spillway crests. a Crest of free overflow; b orbit of flow jet through orifice

The WES profile is configured as it relates to the axes at the apex of the crest. A discontinuity near the upstream face may give rise to an abrupt stimulation of the turbulent boundary layer, which is problematic to the discharge coefficient. It can be overcome partially by a well-shaped crest curve in the upstream quadrant using one, two, or three arcs, of which the three arcs quadrant are the most popular in China (Fig. 7.30a), although an ellipse could have a better link from the beginning to the end of the quadrant.

The upper curve at the crest following the upstream quadrant from the origin is defined by Eq. (7.30b) as (State Economy and Trade Commission of the People’s Republic of China 2008)

$$\frac{y}{H_d} = -K \left(\frac{x}{H_d}\right)^n \tag{7.30}$$

where H_d = design head over the crest, usually be equal to 75–95 % of the maximum flood head; K and n = constants whose values depend on the upstream inclination and on the approaching velocity, when the upstream dam face is vertical, $n = 1.85$ and $K = 0.5$.

The WES profile may be made either broader or sharper than the nappe contour, depending on the selected design head H_d . For the discharge at the designed head, the flow glides over the crest without interference from the crest surface and attains standard discharge efficiency. For the discharge at a head lower than the designed head, the outflow nappe will be supported by the crest surface and positive hydrostatic pressure will manifest. The supported nappe thus creates a backwater effect and reduces the efficiency of discharge. For the discharge at a head higher than the designed head, the nappe tends to pull away from the crest surface, in this way to produce sub-atmospheric pressure along the contact surface. This negative pressure increases the effective head, thereby increases the discharge. In the releasing of check flood, negative pressure may appear in the region immediately below the gate, which should be controlled within 30–60 kPa.

The discharge Q over an ogee crest of free overflow is given by

$$Q = n \cdot \sigma \cdot \varepsilon \cdot m \cdot b \sqrt{2gH_0^3}$$

$$H_0 = H + \frac{v_0^2}{2g} \quad (7.31)$$

where Q = discharge, m^3/s ; m = coefficient of discharge, for ogee type weir a set of curves for calculating m may be found in design codes or hydraulic handbooks; n = number of sluice vents; σ = discharge reduction coefficients with regard to the degree of submergence, $\sigma \leq 1.0$; ε = lateral contraction coefficient induced by pier or abutment, $\varepsilon < 1.0$; b = net width of sluice vent, m; H_0 = head over crest of weir, m; and v_0 = average velocity in front of spillway, m/s.

The total head on the crest H_0 does not include allowances for the losses due to approach channel friction, curvature of the upstream channel, entrance into the inlet section, and transition. Where these losses are appreciable, they must be deducted from H_0 .

The profile below the upper curve is continued tangent along a slope (usually but not always, identical to that of non-overflow dam monoliths), to support the nappe of the outflow on the dam face (Fig. 7.30a). A reverse curve at the bottom of the slope turns the flow onto either the apron of a stilling basin, or into the flip bucket, or into the spillway discharge channel, depending largely on the nature of the work site and on the tailwater conditions.

With high-quality rock foundation, the profile required by hydraulic conditions could be more “fat” than the basic profile, which is not reasonable from the point view of economy and external shape beauty. To slender spillway dam profile, it may offset the upstream face into the reservoir in order to gain sufficient width to configure the spillway crest (see Figs. 7.26, 7.27). The effect of such offset on the coefficient of discharge is negligible if $h_1 \geq H_{\max}/2$, in which H_{\max} is the maximum head over the crest and h_1 is the height of the offset.

2. Orifice

Flood release under partial gate openings for gated or parapeted crest will give rise to orifice flow following the orbit of a jet issued from the orifice.

For a vertical orifice when $H/D > 1.5$, in which H is the head above crest and D is the height of intake (Fig. 7.30b), the parabolic orbit of the jet expressed by Eq. (7.32) may be used as the upper crest curve connecting the upstream quadrant.

$$y = \frac{x^2}{4\varphi^2 H_d} \quad (7.32)$$

where H_d = design head, usually be equal to 75–90 % of the height from the maximum reservoir level to the center of the opening; φ = flow velocity coefficient of the opening, usually $\varphi = 0.96$, where there is bulkhead gate slot $\varphi = 0.95$.

For an orifice inclined at an angle of θ , the equation of the jet will be

$$-y = x \tan \theta + \frac{x^2}{4\phi^2 H_d \cos^2 \theta} \quad (7.33)$$

where $H/D = 1.2\text{--}1.5$, the upper crest curve of orifice should be decided through hydraulic experiment.

The discharge through an orifice is computed by

$$Q = mnA\sqrt{2gH_0} \quad (7.34)$$

$$A = e \cdot b$$

where m = coefficient of discharge; A = area of orifice vent, m^2 ; and e and b = net height and width of the orifice vent below the gate or parapet wall, m.

The coefficients σ , ϵ , and m in Eqs. (7.31) and (7.34) may be consulted in design codes or hydraulic handbooks.

7.6.3 High-Speed Flow Problems in the Spillway Dam Design

The velocity of discharged outflow may reach 30–40 m/s or even higher for high gravity dams during the flood releasing. The problems such as cavitation, aeration, fluctuation, and shock wave might manifest as have been described in Chap. 4 of this book.

7.6.4 Energy Dissipation and Scouring Protection

Attributable to the collected water head by damming, the discharged outflow attains tremendous kinetic energy. For instance, an outflow with specific discharge $q = 100 \text{ m}^3/(\text{s m})$ and head $H = 50 \text{ m}$, the kinetic energy delivered into riverbed per 1 m width is approximately 50 MW. If no adequate countermeasures are provided, the energy will cause serious scouring damage to the dam toe, the river bedrock, and the bank slopes at the vicinity of the dam. The shore spillway in the Ricobayo Arch Dam (Spain, $H = 99.4 \text{ m}$) eroded a scouring pit of 70 m deep, from which 10^6 m^3 rock was washed away.

Energy dissipation is intended to kill kinetic energy by converting it into heat energy through the friction and formation of eddies which are created by the internal resistance (diffusivity and viscous resistance) and external resistance (resistance from baffle pier, etc.) to the outflow (Elevatorsky 1959). Generally, the energy dissipation process of the outflow may be divided into five stages, some of them may be overlapped or absent for a particular type of dissipation device:

- On the spillway surface;
- In a free-falling jet;

- At the impact into the downstream pool;
- In the stilling basin; and
- At the outflow into the river.

The stepped spillway consisting of weir crest and steps on the tangent along the downstream slope (or spillway chute) is a typical application of energy dissipation on the spillway surface and has been exercised for over 3500 years since the first structures were built in Greece and Crete (Chanson 2001–2002). The steps increase the rate of kinetic energy dissipation taking place in the spillway, thus eliminating or greatly reducing the need for an energy dissipater at the exit of the spillway. However, unless aeration is provided at the protrusions, the increased energy dissipation rate may be achieved only by raising an opportunity for cavitation damage.

Another philosophy in the energy dissipation design is to deliver high-speed flow far away from the dam, in this way to keep the scour pit at a safe distance from the dam. The commonly employed energy dissipaters of this category are the jet trajectory (ski-jump) by flip bucket, the hydraulic jump by stilling basin, the surface current by submerged bucket, and the rolling current by submerged bucket basin.

In the design, the suitable energy dissipation layout is elaborated based on the comprehensive technoeconomic comparisons considering the factors related to topography, geology, project layout, crosshead, discharge volume, depth, and variation of tailwater. Hydraulic experiments are indispensable for the design of energy dissipation, except for small dams.

1. Energy dissipation on the spillway surface

The energy loss on the spillway surface can be expressed as follows:

$$e = \xi \alpha v'^2 / 2g \quad (7.35)$$

where v' = velocity at the end of the spillway; α = coriolis coefficient; and ξ = head loss coefficient.

Head loss coefficient is related to the velocity coefficient φ (the ratio of actual velocity to theoretic velocity) by

$$\frac{1}{\varphi^2} = 1 + \xi \quad (7.36)$$

The ratio of the energy loss e to the total energy E (i.e., the relative energy loss) is given as

$$\frac{e}{E} = \frac{\xi v'^2}{2g} / \left(\frac{v^2}{2g} + \frac{\xi v'^2}{2g} \right) = \frac{\xi}{1 + \xi} = 1 - \varphi^2 \quad (7.37)$$

Defining a ratio of the spillway crest height S to the overflow head H , then with $S/H < 30$ and for smooth spillways:

$$\varphi = 1 - 0.0155 S/H \quad (7.38)$$

Accordingly, for a given S , φ reduces following the decrease of H . For example, where $S/H = 5$, $\varphi = 0.92$, and the relative head loss is 15 %, whereas for $S/H = 25$, $\varphi = 0.61$, and the loss is 62 %.

The coefficient ζ can be raised (and φ decreased) by using a rough tangent (or spillway chute) or by placing baffles on the tangent surface. During the first half of the twentieth century, stepped spillway became out of fashion, partly due to the high maintenance costs and partly due to the development in hydraulic jump stilling basins. Yet, in recent years, it has become revival, particularly in the design of low- or medium-head RCC gravity dam (Fig. 7.64) and CFRD with crest spillways (Chanson 2001–2002).

2. Energy dissipation by jet trajectory through flip bucket

This is a kind of ski-jump energy dissipation which was successfully invented in France on the Dordogne Project as early as in the mid-1930s, with detailed prototype observations on the jet flow by Maitre and Obolensky in 1954. Jet trajectory absorbs larger quantity of air during the flow diverging, this process dissipates around 20 % of kinetic energy by friction, turbulence, and impact. Once entering of the jet trajectory into river stream, very strong swirl scours the rock to form deep pit; in this process, a majority of energy is dissipated by friction, formation of eddied, and erosion of bedrock. The deeper the scour pit is, the smaller of the erosion effects are, until a stable pit shape is formulated.

The flip bucket is usually employed whenever the geologic and topographic conditions are suitable. However, in the design, their adverse influences on the project should be taken into account:

- Slightly inclined weak seams under dam base, if exist, would be cut by scour pit. As a result, the seams would daylight on the walls of the scouring pit as the exposure faces, which in turn, could reduce the deep-seated stability of foundation;
- Downstream river bank stability would be affected by the scouring of high-speed current, particularly in the narrow valley; and
- Atomized flow by jet trajectory nappe may expand hundreds of meters. The transmissions and bridges are better to be kept away from this area, or reliable protections should be installed.

The commonly used flip buckets fall into continuous (plain) type (Fig. 7.31b) and slotted type (Fig. 7.31c, d).

(a) Plain flip bucket

The major merits of the plain flip bucket are simplicity in structure, facilitation in construction, and far jet trajectory distance; all these explain their popularity in engineering application. The shortcomings compared to the slotted flip bucket are the lower dissipation efficiency due to weaker divergent and less aeration of the jet

trajectory in air, which in turn will result in deeper scour pit and stronger tailwater fluctuation.

Key parameters for the flip bucket design are the approach flow velocity and depth, the radius R of the bucket, and the flip angle θ (Mason 1993). Flip buckets are usually “tailor-made” for a given project, and the designs are developed with the aid of physical model experiments. For the preliminary design, there are valuable experiences for reference accumulated from engineering practices and laboratory experiments.

The designer’s main concern is normally to have an impact zone as far as possible from the bucket to protect the structure against retrogressive erosion, which may be realized by larger flip angle (takeoff angle). However, in doing so the dip angle of the jet trajectory into streambed will also be larger, which will in turn result in deeper scouring pit. Therefore, a flip angle of $\theta = 15^\circ\text{--}35^\circ$ is often suggested to compromise between the requirements for jet trajectory throw distance and scouring pit depth.

A larger bucket with larger R guarantees better flow condition, but it will result in higher cost; on the contrary, smaller R may give rise to non-smooth jet stream over the bucket which in turn leads to a shorter jet trajectory throw distance. Therefore, it is customarily to adopt a bucket with $R = (6\text{--}10) h$, in which h is the water depth over the bucket.

The bucket lip may be 1–2 m higher than the maximum tailwater level, to obtain good aeration of the lower bound of the jet nappe.

The jet trajectory throw distance L is measured from the dam toe to the deepest point of the scour pit (Fig. 7.31a), which may be estimated by

$$L = \frac{1}{g} \left[v_1^2 \sin \theta \cos \theta + v_1 \cos \theta \cdot \sqrt{v_1^2 \sin^2 \theta + 2g(h_1 \cos \theta + h_2)} \right] \quad (7.39)$$

where g = gravity acceleration, m/s^2 ; v_1 = velocity at the top of bucket lip, m/s , which is nearly 1.1 times of the average velocity v ; θ = flip angle; h_1 = vertical

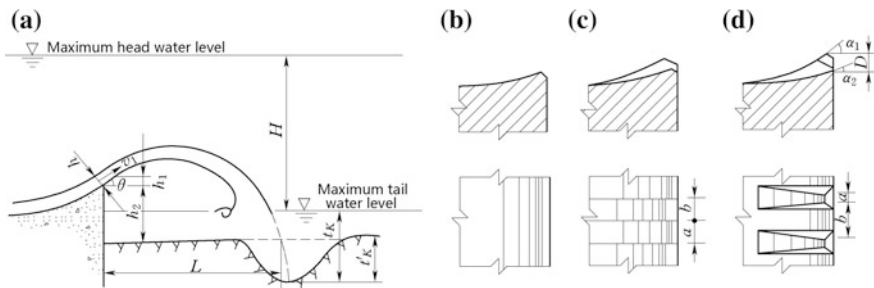


Fig. 7.31 Types of flip buckets

projection of the average water depth h at the bucket lip, $h_1 = h \cos \theta$; and $h_2 =$ height from bucket lip to riverbed, m.

The jet trajectory is hardly affected by air resistance in case the jet velocity is below 20 m/s, however where the jet velocity is over 40 m/s, the throw distance can be reduced by as much as 30 % due to air resistance.

There are several approximate formulae available for the estimation of scour pit depth; among them the computation error may be as high as 30–50 %. Equation (7.40) is the most widely exercised one in China

$$t_K = \alpha q^{0.5} H^{0.25} \quad (7.40)$$

where $t_K =$ thickness of the water cushion measured from the pit bottom to the tailwater surface, m; $q =$ unit discharge of jet trajectory, $\text{m}^3/(\text{s m})$; $H =$ difference in headwater level and tailwater level, m; and $\alpha =$ coefficient.

For hard and integrity rock, $\alpha = 0.9\text{--}1.2$; for hard but fractured rock $\alpha = 1.2\text{--}1.5$; and for soft and fractured rock $\alpha = 1.5\text{--}2.0$.

The allowable jet trajectory throw distance L is stipulated as 2.5 times of the scour pit depth, for the purpose of the bedrock stability near dam toe; the width of jet trajectory should be the allowance for the bank stability surrounding the scour pit.

(b) Slotted flip bucket

By slotted flip bucket (Fig. 7.31c, d), energy dissipation efficiency is higher due to stronger water dispersion, aeration, and collision of the jet trajectory in sky. In this way, the depth of scour pit may be reduced. However, the jet trajectory throw distance is also reduced, and cavitations are easier to be triggered due to the complex high-speed flow within the slotted bucket.

According to experiments, the suitable average take off angle of slotted buckets is $(\theta_1 + \theta_2)/2 = 20^\circ\text{--}30^\circ$, and the angle difference is $(\theta_1 - \theta_2) = 5^\circ\text{--}10^\circ$; the ratio of dental top width a to dental bottom width b should be larger than 1.0; the dental height difference D is around 1.5 m. Air vent holes are installed at the side of dentals, and rounded dental top is desirable.

3. Energy dissipation by bottom flow

Energy dissipation by bottom flow makes use of hydraulic jump within low-level apron; at its end, there is commonly an end sill (Bradley and Peterka 1957a, b). When the water jet flows over the apron, a hydraulic jump forms strong roller. Energy is dissipated most effectively by a submerged jump manifests under the tailwater depth t a little higher than the second conjugate depth h'' after the jump, i.e., $t = (1.05 - 1.1)h''$. It may be employed for overflow dams of any height and is particularly advantageous under the situations of poor geologic conditions with lower scour resistance of riverbed, and the typical examples are Bhakra Dam (India, $H = 226$ m) and Dworshak Dam (USA, $H = 213$ m). Since it is efficient and reliable, the residual kinetic energy of the outflow into the river stream is small. As a result,

the navigation and power generation are less disturbed. However, the construction of stilling basins requires larger amount of rock excavation and concrete placement.

(a) Flow conditions and energy dissipaters

During the flood period, the discharge rate Q increases upon the liftoff of gate. The depth h_c at contraction section ($=h'$, first conjugate depth) and the second conjugate depth after hydraulic jump h'' may be calculated with respect to different Q . Based on the results, the relationships of $Q-h''$ and $Q-t$ may be established in which t is the depth of tailwater. By the comparison of $Q-h''$ and $Q-t$, five cases may be identified as shown in Fig. 7.32.

- ① Curves of $Q-h''$ and $Q-t$ are overlapped within the whole discharge range Q (Fig. 7.32b). It means that critical hydraulic jump may occur under any discharge Q , and stilling basin is not necessary except proper revetment within the range of hydraulic jump. Actually, this is merely a theoretic possibility.
- ② $Q-h''$ curve is over the curve $Q-t$ within the whole discharge range Q (Fig. 7.32c). It means that driven off jump may occur under any Q , and a stilling basin is demanded in order to produce a submerged jump near the dam toe.

Under the circumstances of large unit flow q and low Froude number F_{r1} , which often happens in low dams, the energy dissipation efficient is low by hydraulic jump. For example, when $F_{r1} < 4.5$, the energy dissipation (head loss) ratio is smaller than 50 %, and the residual kinetic energy could result in serious scouring to riverbed and banks. The energy dissipation ratio may be improved by installing

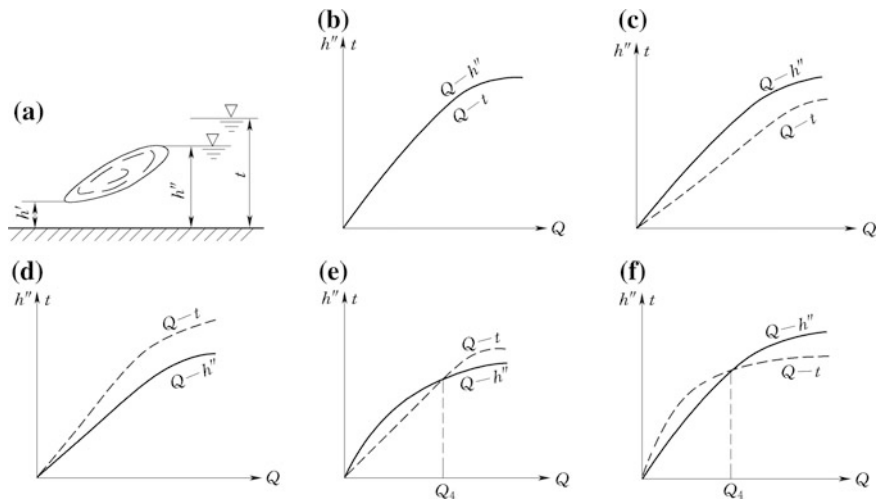


Fig. 7.32 $h''-Q$ and $t-Q$ relationships

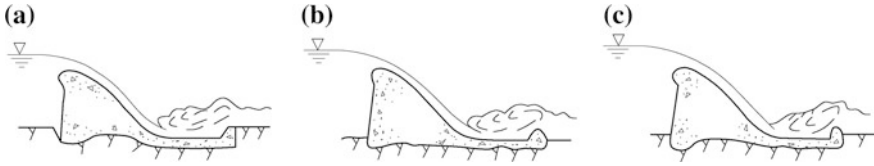


Fig. 7.33 Measures for procuring submerged hydraulic jump. **a** Stilling basin; **b** end sill; **c** compound stilling basin

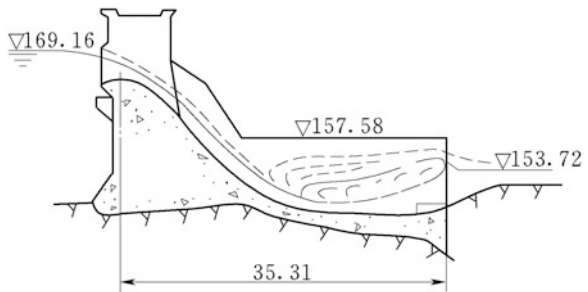
energy dissipaters (e.g., baffle piers or wall, dents) (Fig. 7.33) on the stilling basin, which are intended to reduce the next-to-jump depth, as well as the depth and length of stilling basin. However, when the flow velocity is over 15 m/s, the energy dissipaters are vulnerable to the cavitation damage.

- ③ $Q-h''$ curve is below the curve $Q-t$ within the whole discharge range Q (Fig. 7.32d). It means that submerged jump may be guaranteed under any Q and the stilling basin is not necessary, and only a horizontal apron protecting the downstream riverbed is demanded. However, with high submerging degree, the high-speed submerging current will result in long jump length and low energy dissipation efficient. In this case, use should be made of submerged bucket (Fig. 7.39) or inclined apron (Fig. 7.34).

It should be pointed out that insofar there are no reliable computation methods for the design of inclined apron. The sloping and length of the apron for critical hydraulic jump is commonly decided after the studies by laboratory physical experiments.

- ④ $t < h''$ happens only at low discharge (i.e., when $Q < Q_K$), whereas $t > h''$ happens at high discharge (i.e., when $Q > Q_K$); this means that driven off jump will occur under low discharge but submerged jump will occur under high discharge (Fig. 7.32e). Under such circumstances, the combination of inclined apron and stilling basin may be employed. When $Q < Q_K$, the jump is limited within the stilling basin but when $Q > Q_K$ the jump will take place at the inclined apron.

Fig. 7.34 Inclined apron (unit: m)



- ⑤ Contrary to the case ④ (Fig. 7.32f). In this case, the size and shape of stilling basin has to be designed according to the maximum discharge.

(b) Structure of apron

Apron is a concrete slab structure in the jump regime, which is usually horizontal but in some cases it has inclined portion. Steel bars are commonly layout on the surface of apron to resist thermal stress. To prevent the adverse effect of non-uniform settlement, the apron is normally separated from the dam body by contraction joints. However, for low dams of insufficient safety factor against sliding, a monolithic structure with thick apron linked to the dam may be helpful. Thermal contraction joints within the apron may be necessary to prevent thermal cracking in case of larger apron extension. The transverse joints are usually spaced 10–15 m apart identical to that of the dam body. To resist the scouring and abrasion actions of high-speed flow, the concrete strength grade should be not lower than C20. Use of drainage system in form of vertical holes and horizontal gutter network may be made to reduce the uplift beneath the apron.

The minimum thickness δ of apron is estimated by floating stability condition, which may be carried out with respect to the unit area of apron (Fig. 7.35)

$$\delta \geq [K] \frac{u + p_m - p}{\gamma_c} \tag{7.41}$$

where $[K] = 1.2-1.4$ is allowable safety factor against floating; $u =$ uplift on the base of apron, kN/m^2 ; $\gamma_c =$ saturated volumetric weight of concrete, kN/m^3 ; $p =$ static water pressure on the top surface of apron, kN/m^2 ; and $p_m =$ time-averaged fluctuation pressure, kN/m^2 .

$$p_m \approx \pm a_m \frac{\gamma_w v^2}{2g} \tag{7.42}$$

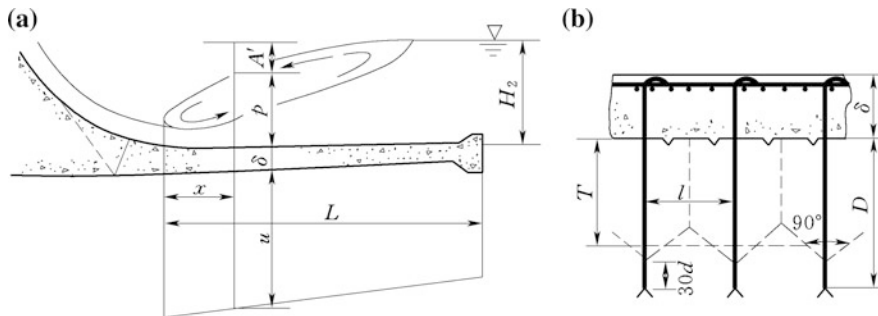


Fig. 7.35 Diagram to the stability analysis of apron

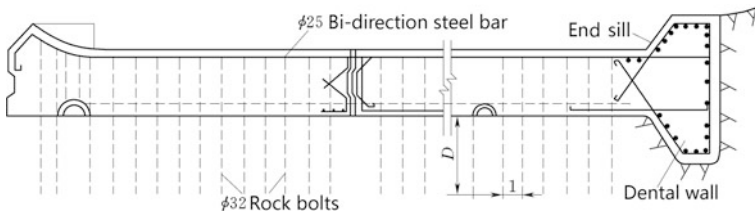


Fig. 7.36 Structure of an apron on rock foundation (unit: m)

where v = average velocity at the calculated section of apron, m/s; a_m = coefficient of fluctuation pressure, which is ranged between 0.05 and 0.20 and is related to the velocity of flow.

At the upstream generatrix of apron, the static water pressure p on the unit area may be calculated by $p = (1/3 - 1/2)\gamma_w H_2$, to take into account the effects of submerging degree and dynamic pressure of hydraulic jump; started from the distance $x = (1/3 - 1/2)L$ after the contraction section, p may be calculated by $p = \gamma_w H_2$.

The thickness of apron on rock foundation is normally 1–3 m, under particular circumstances a thicker apron may be employed. Depending on the forces exerted, the thickness may be varied from upstream to the downstream. Figure 7.36 shows a typical structure of apron.

The application of rock bolts may reduce the thickness of apron significantly. Instead of Eq. (7.41), the thickness of apron with bolting reinforcement may be estimated by

$$\delta \geq [K] \frac{(u + p_m - p) - (\gamma_r - 1)T}{\gamma_c} \quad (7.43)$$

where γ_r = volumetric weight of rock, kN/m^3 ; T = effective length of rock bolt, m.

The length D of bolt embedded within rock is commonly 1.5–2 m, which is related to the effective length T by

$$D = T + \frac{l}{4} + 30d \quad (7.44)$$

where l = spacing of bolts, $l = 1.5 - 2$ m; and d = diameter of bolts (steel bars of $\Phi = 25 - 36$ mm are customarily employed).

For low overflow dams (or barrages) on earth foundation, the riprap is necessary to protect the downstream riverbed after the apron (Fig. 7.37) by further dissipating the residual kinetic energy and adjusting the velocity distribution. The design of apron and riprap on earth foundation is referred to the Chap. 11 of this book.

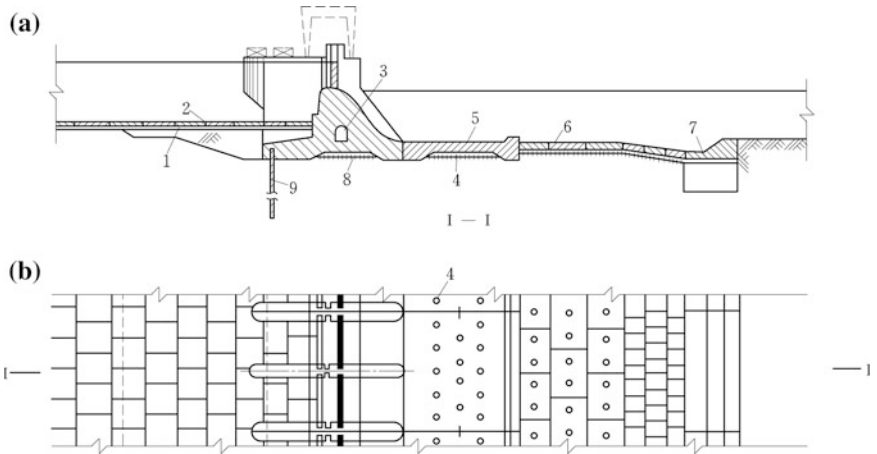


Fig. 7.37 Layout of dissipation and scour protection for an overflow dam on earth foundation. 1 clay blanket; 2 blanket mounting; 3 sump gallery for the drainage system under dam; 4 draining well under apron; 5 apron; 6 riprap; 7 reinforcement at the end of riprap; 8 drainage with filter; and 9 steel sheet pile

4. Energy dissipation by rolling surface current

By rolling surface current as shown in Fig. 7.38, surface or overflow regime under which the jet leaving off the bucket flows at the surface and only when fully flared it reaches the bed-bottom. A ground flow tends to form a clockwise retrogressive roller under the jet. Under certain conditions, the surface flow turns to a surface-bottom flow featured that, initially the jet, either free or with a roller on, rises and then lowers reaching the bed-bottom with a surface roller above it as the case of bottom flow. The roller and diffusion dissipate the kinetic energy of the discharge flood. The high-speed current roller is on the river surface for a certain distance from the bucket, which is favorable to alleviate riverbed scouring.

Energy dissipation by surface current may be a good choice for gravity dams on rock foundation with deep and stable tailwater, when the wood drift or ice releasing are required, and when the length of riverbed revetment can be reduced to a minimum or even eliminated. However, since the tailwater transition of surface

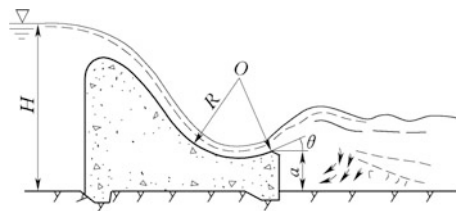


Fig. 7.38 Energy dissipation by surface current

stream produces wave trains slowly damping while propagating toward downstream, it is not welcome with handling of power generation and navigation. The wave trains also may increase evermore bank erosion.

The gravity dams of the Fuchunjian (China, $H = 47.7$ m), the Xijing (China, $H = 41$ m), and the Gongzhui (China, $H = 85.5$ m) adopt this kind of energy dissipation.

Although there are empirical formulae available for the design of energy dissipation by surface current, the radius R of the bucket, the flip angle θ , and the height of the bucket lip a are finally fixed by laboratory experiments.

5. Energy dissipation by submerged bucket basin

Submerged bucket basin is a kind of energy dissipation basically initiated by laboratory experiments. The large bucket with lip submerged under the water performs like a stilling basin. The surface regime with a submerged jump is formed with the bucket having a surface roller within its boundaries (Fig. 7.39). The foundation of the bucket has to be protected against erosion because the roller at the flow bottom after the lip may carry sands and gravels into the bucket.

The applicability and disadvantages of energy dissipation by the submerged bucket basin are similar to that of by surface current. This kind of energy dissipation was firstly used in the Grand Coulee Dam (USA, $H = 168$ m) completed in the 1930s. Since the 1960s, the Shiquan Dam (China, $H = 65$ m), the Daheiding Dam (China, $H = 52.8$ m), the Baojixia Dam (China, $H = 49.6$), and several other gravity dams employed this kind of energy dissipation. Where the unit flow discharge is large, a horizontal apron section may be added to elongate the bucket, for the purpose to raise the energy dissipation efficiency and to ensure the submerged bucket pattern, which has been exercised successfully in the Ankang Dam (China, $H = 128$ m).

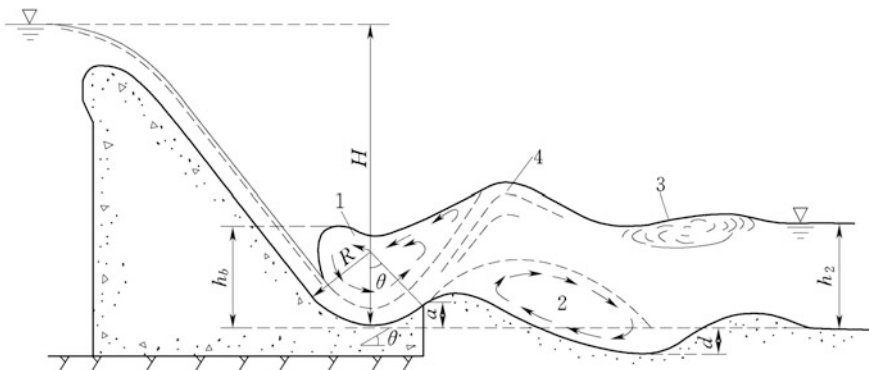


Fig. 7.39 Energy dissipation by submerged bucket basin. 1 roller within bucket; 2 roller at the flow bottom after bucket lip; 3 roller on downstream surface; 4 wave at the flow surface after bucket lip

Generally, where the bottom of bucket is at the same level of the riverbed and $H/R = 3-6$, and when the submerging degree $\sigma > 1.1$, the submerged bucket flow pattern may be maintained. The application scope of submerged bucket basin is $h_b/h_2 = 0.4-0.8$. H is the head measured from the bottom of the bucket, and R and h_b are the radius and depth of the bucket, and h_2 is the tailwater depth. Other useful data in the sizing of submerged bucket basin are explained in the following.

(a) Flip angle θ

Most existing dams make use of $\theta = 45^\circ$; some are as lower as 40° or even 37° . The larger of the flip angle, the easier to form submerged flow pattern in the bucket basin, but the higher of the surge wave and the deeper of scour pit. On the contrary, an excessive small flip angle may lead to the roller stretching outside of the bucket.

(b) Radius R

The larger of R , the better condition of the outflow and the larger volume of the roller within the bucket, hence the energy dissipation efficiency is higher. However, when the radius R reaches a certain limitation, the energy dissipation efficiency cannot be further perceivably improved meanwhile the bucket volume increases remarkably.

Figure 7.40 shows the statistical relation of $H/R-K$ ($K = \frac{q}{\sqrt{g}H^{1.5}}$, where q = unit discharge; H = head measured from the bottom of bucket) from 27 completed projects.

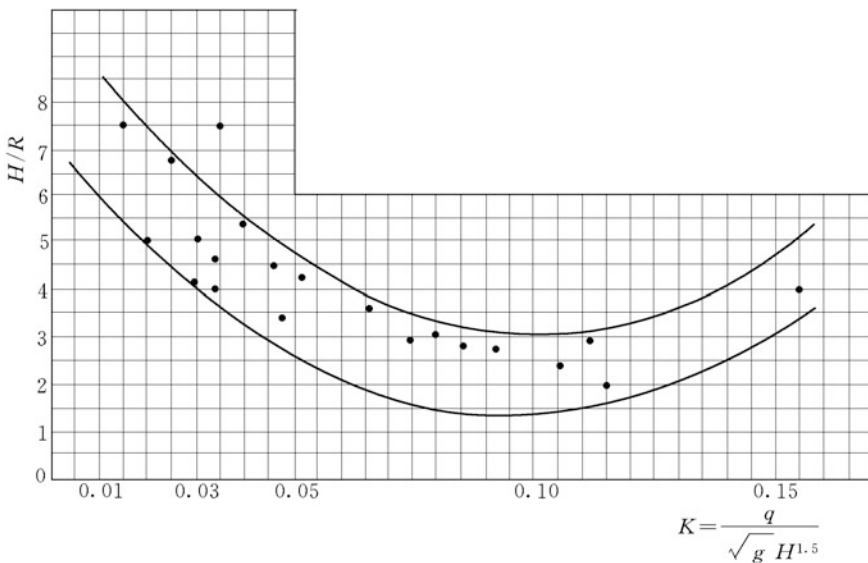


Fig. 7.40 Statistical relation of $H/R-K$

(c) Height a of bucket lip

To prevent too much of sand and gravel from entering the bucket, the height a of the bucket lip over riverbed is suggested to be $\frac{1}{6}$ or higher of the tailwater depth.

(d) Bottom elevation of bucket

Generally, it should keep identical level to the riverbed. The principal concern is that a stable submerged bucket basin pattern should be guaranteed. Higher elevation could result in jet trajectory flow pattern while lower elevation will raise the amount of rock excavation.

6. New types of energy dissipaters

Several new types of energy dissipaters have been applied in many large hydraulic projects with high head and large discharge since the 1970s (Khatsuria 2004; Panwar and Tiwari 2014). These new types of energy dissipaters can be divided into three categories of contracted (slit bucket and flaring gate pier), dispersed (large differential flip bucket, tilted and tongue shape bucket, dispersed bucket with short guide wall), and flow jet colliding or dropping (separately or combined with plunge pool).

(a) Slit bucket

It is suitable for projects with medium or high water heads, especially on narrow river valleys. It can be employed for chute spillways, spillway tunnels, surface spillways, or bottom outlets. The Froude number in front of slit bucket should be larger than 3.5. There is, in fact, no clear difference in the flaring gate pier and the slit bucket with regard to the contracting ratio.

(b) Flaring gate pier series

It is an invention by Chinese engineers started from the 1970s comprising two main variants: one is combined with flip buckets, such as the dams of the Panjiakou (China, $H = 107.5$ m) and the Geheyan (China, $H = 151$ m); another is combined with stilling basins, such as the dams of the Ankang (China, $H = 128$ m), the Yantan (China, $H = 110$ m), the Wuqiangxi (China, $H = 85.8$ m), the Shuidong (China, $H = 63$ m), and the Taolinkou (China, $H = 74.5$ m). The latter is prevalent in the China's projects with medium or high water head, large unit discharge flow, and low Froude number.

(c) Dispersed dissipaters

They are developed from the normal bucket and the differential bucket. The flow jets disperse and drop into the targeted zone on the river by adjusting the elevation, the position, and the shape of bucket. The three main sub-types are large differential buckets such as the dams of the Baishan (China, $H = 149.5$ m) and the Manwan (China, $H = 132$ m); tilted and tongue-shaped bucket such as the dams of the Lubuge (China, $H = 103.8$ m), the Dongjiang (China, $H = 157$ m), the Ertan (China,

$H = 240$ m), and the Tianshengqiao I (China, $H = 178$ m); dispersed bucket with short guide wall such as the Ankang Dam (China, $H = 128$ m).

(d) Jet flows colliding or dropping

Colliding jet flows can raise the efficiency of energy dissipation and reduce the downstream scouring. The flows are collided in the air by adjusting the elevations, positions, and the shapes of differential buckets, such as the Fengtan Dam (China, $H = 112.5$ m). The projects using jet flows colliding or dropping combined with plunge pool are the Ertan (China, $H = 240$ m), the Xiaowan (China, $H = 294.5$ m), the Goupitan (China, $H = 132.5$ m), and the Xiluodu (China, $H = 278$ m).

Laboratory and field prototype observations show that the length of plunge pool can be reduced significantly when overflow spillways and orifices are operated at the same time to exploit colliding jet flows.

7.7 Appurtenant Features of Gravity Dams

7.7.1 Materials for Gravity Dams

The materials used for modern gravity dam construction are concretes, steel bars (or rebars), and water stop materials, as well as various tubular products and steel materials. For medium- to small gravity dams, grouted rubble or stone masonry may also be used provided high-quality building stone and skillful labors, as was widely practiced in China from the 1950s to the 1970s.

The properties of concrete for gravity dams must be accurately determined include the mechanical properties, thermal properties, and the other properties with regard to the resistances against permeability, frozen, abrasion, and cavitation, which have been discussed in Chap. 3. These properties are closely related to the concrete grade. Since the properties of concrete develop with the age and therefore, the design age should be stipulated in the selection of concrete grade. In China, for example, the design age of compressive strength is stipulated as 90d, however, for the early age strength control, the 28d strength is additionally required; whereas for the design age of tensile strength, only 28d is specified.

“Zonal” concretes (e.g., seepage-resistant zone on the upstream face, frost-resistant zone on the open surface, and abrasion-resistant zone on the face of spillway) are usually placed at the different portions of gravity dam, for better response to the property requirements and for economically and rationally utilization of cement. The general zonal principles are shown in Fig. 7.41.

- Zone I. Surface concrete above the maximum head- or tailwater levels;
- Zone II. Surface concrete between the maximum and minimum head- or tailwater levels;
- Zone III. Surface concrete below the minimum head- or tailwater levels;
- Zone IV. Base concrete;

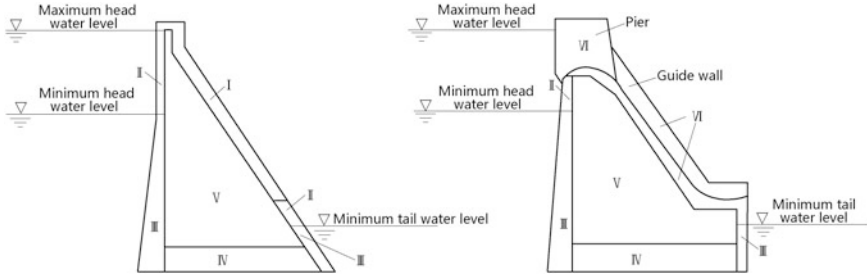


Fig. 7.41 Concrete zoning of gravity dams

- Zone V. Internal concrete; and
- Zone VI. Abrasion and cavitation resistance concrete (surfaces of spillways, conduits, guide walls, and piers).

Table 7.6 lists the requirements for the different concrete zones.

In the selection of zonal concrete strength grade, apart from the stress requirements, the grade difference between adjoining zones should not exceed two, to prevent cracking due to strong stress redistribution. The types of concrete are limited and the minimum thickness of any zonal concrete should be larger than 2–3 m.

7.7.2 Appurtenant Structures of Gravity Dams

Appurtenant design of gravity dams covers dam crest structure, dam joints, water stops, drainages, and galleries. A reasonable layout of these appurtenants may improve the working performance, increase the stability and strength, facilitate the construction and operation, and ensure the safety of the dam.

1. Dam crest

The selection of the width and the elevation of dam crest have been discussed in the foregoing Sect. 7.5.3. The solid structure for dam crest is commonly adopted (Fig. 7.25a, b), whose surface is designed as pavement, on which the draining and lighting systems are arranged. The light structure also may be employed, particularly for dams in seismic areas (Fig. 7.25c).

2. Joints

In the construction period, massive concrete in a dam monolith with strong fluctuation of temperature and long cooling period will give rise to adverse tensile stresses therein due to restricted thermal shrinkage and expansion. Similarly, the

Table 7.6 Requirements for the different concrete zones

Zone	Strength	Seepage resistance	Frozen resistance	Scour resistance	Erosion resistance	Low heat	Maximum W/C		Main factors influencing the width of zone
							Chilly and cold region	Mild region	
I	+	-	++	-	-	+	0.60	0.65	Frozen resistance, construction
II	+	+	++	-	+	+	0.50	0.55	Frozen resistance, seepage resistance, construction
III	++	++	+	-	+	+	0.55	0.60	Seepage resistance, crack resistance, construction
IV	++	+	+	-	+	++	0.55	0.60	Crack resistance
V	++	+	+	-	-	++	0.70	0.70	N/A
VI	++	-	++	++	++	+	0.50	0.50	Abrasion and cavitation resistances

NB: “+”, “++”, “-”, “-” indicate the main factor, general factor, and ignorable factor, respectively, in the zonal concrete design

shrinkage and swelling processes will take place due to non-uniform distribution of moisture (Carlson et al. 1979).

In the service period, temperature stresses emerge in a concrete dam attributable to the incapability of concrete mass to expand or shrink freely as it is keyed on or into the foundation, during seasonal or/and annual variations in the ambient temperature.

Where the tensile stresses exceed the tensile strength of concrete, vertical cracks or/and other dangerous cracks will manifest in the dam. To prevent the dam concrete from cracking, the dam is customarily divided into blocks using temperature joints (Price 1982).

Beside these and often in a combination therewith, shrinkage or expansion joints are provided to avoid the formation of cracks in dam due to different properties of rocks constituting the foundation.

(a) Transverse joints

For a gravity dam, transverse joints normal to the dam axis are ordinarily installed. The spacing between the joints is so selected as to prevent serious tensile stresses in the dam, which is usually 12–20 m; in particular case, it may be up to 24 m. The main factors influencing the joint spacing are the foundation geology, river valley topography, temperature variation, structure layout, and concrete placement capacity.

These joints are thus artificial cracks which allow the contraction of the concrete on the two sides to relieve thermal stresses or uneven settlements. The edges of the transverse joint at dam face are chamfered to give a pleasing appearance and to avoid squashed spalling. Usually such chamfers are 4×4 cm on the face of non-overflow dam monoliths and 2×2 cm on the downstream face of overflow dam monoliths.

Transverse joints may be either temporary or permanent. Often, permanent transverse joint is of flat without keys and grouting system, and no joint aperture is reserved. However, if the anticipated uneven settlements of adjoining dam monoliths are significant, the permanent joints may be filled with asphalt felt of 1–2 cm in thickness.

The water stops (seals) are provided in permanent transverse joints for preventing the water from entering the joints, as shown in Fig. 7.42. Usually copper water stop sheets (strips) of 1.0–1.5 mm thick are employed. Stainless steel stops

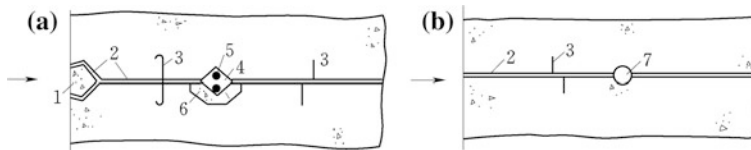


Fig. 7.42 Water stops in permanent transverse joints. 1 contour seal of concrete; 2 asphalt felt; 3 water stop strip (sheet); 4 asphalt well; 5 melting electrode; 6 pre-made block; 7 drainage well

are also applicable. Sometimes rubber (preferable in cold area) and polyvinyl chloride (preferable in mild climate area) water stops are applied. The common practice is to install two water stops of U- or M-type copper sheets with an asphalt seal in between for high dams (Fig. 7.42a). The distance of the first seal from the upstream face is about 0.5–2.0 m. The size of asphalt well is 20 cm × 20 cm–30 cm × 30 cm. Steel bars inside the asphalt well are installed for melting asphalt and adding more asphalt at a later period by passing electricity. Another metal seal placed downstream of the asphalt well is to limit the travel of asphalt along the joint in between the two seals and to make seal effective. Sometimes an inspecting shaft (or drainage well) of cross-sectional size 1.2 m × 1.2 m to 0.8 m × 0.8 m is arranged behind the second water stop, in which ladder and rest platforms are installed. This inspecting shaft is linked with observation or/and inspecting galleries.

For medium and lower dams, the water stops may be simplified, as shown in Fig. 7.42b.

Water stops must be extended continuously into dam foundation with a depth of 30–50 cm. Copper water stops must be extended above the maximum water level. The asphalt well must be extended until the crest of dam, pier, or overflow spillway surface, on which a cover board is laid. The water stops should be installed along all the dam faces contacted to water (e.g., upstream face, spillway surface, and downstream face below the maximum tailwater level) and the cavities within the dam (e.g., galleries and openings), where they are intersected with the transverse joints.

Temporary transverse joints are recommended in the following cases:

- ① For a gravity dam at narrow canyon, if the analysis indicates that a monolithic gravity dam is more economical by transfer a part of water thrust to the abutments;
- ② To ensure the stability of abutment dam monoliths by linking them using joint grouting; and
- ③ To reduce the uneven settlement and to improve the foundation bearing capacity for the dam monoliths on weak zones (faults).

Temporary transverse joints are typically battered (keyed or hinged) joints and equipped with grouting system. If the keys are intended to transmit horizontal and tangential forces between dam monoliths, the keys are vertically layout, as in the heretofore enumerated cases of ① and ②; whereas if the keys are intended to transmit vertical and tangential forces between dam monoliths, the keys are horizontally layout, as in the foregoing case ③. Grouting lift in a transverse joint consists of an area bounded by grouting stops (or seals) adjacent to the upstream and downstream faces of the dam, and by grouting seals spaced 15–20 m apart from the top to the bottom.

High-quality face contact between dam and base, particularly for abutment dam monoliths, should be guaranteed to prevent leakage and adverse uplift. Depending on the sloping of the contact face, the following principles are to be observed:

- In case the transverse slope is flatter than 1:2, the contact grouting is carried out through the curtain grouting holes after the placement of dam monoliths.
- In case the transverse slope is steeper than 1:2, water stops may be used to seal the contact face, which is preceded by digging ditches in the foundation in which water stop strips are installed.
- In case the transverse slope is steeper than 1:1, the contact face should be looked at as a temporary joint: Surrounding the contact face grouting seals are installed and grouting system is arranged, the grouting is carried out after the cooling of concrete monoliths.

The last two cases are usually inevitable for abutment dam monoliths located in the deep and narrow canyon.

(b) Longitudinal joints

As the height of dam increases, its base thickness approaches to a limiting dimension beyond which, conditions favorable for vertical cracking parallel to its axis, will manifest. To prevent such uncontrolled cracks, longitudinal joints parallel to the dam axis are provided, which divide a dam monolith into several blocks. Since these joints are intended for meeting the requirements of construction, therefore they are usually termed as construction longitudinal joints.

Spacing of these joints varies from 15 m (usually near the downstream dam face) to 30 m (near the upstream dam face). Where the longitudinal joint approaches the downstream face, it is turned normal to the face, to avoid squashed spalling of concrete. A gap is often provided at the inclined portion of joints which will be dry packed later.

The schemes of longitudinal sectionalizing fall into columnar division by vertical or inclined longitudinal joints, half overlapped by staggered longitudinal joints, and long sectional without longitudinal joints (Fig. 7.43). Mixed divisions are also occasionally exercised.

- ① Columnar division by vertical joints (Fig. 7.43a). Construction by columnar section using vertical joints enables the erection of dam to be proceeded at a fast rate of concrete placement. In addition, a large cooling surface is provided and a high rate of dispersion of hydration heat is achieved by columnar

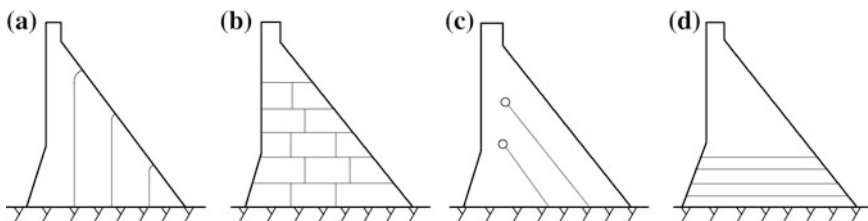


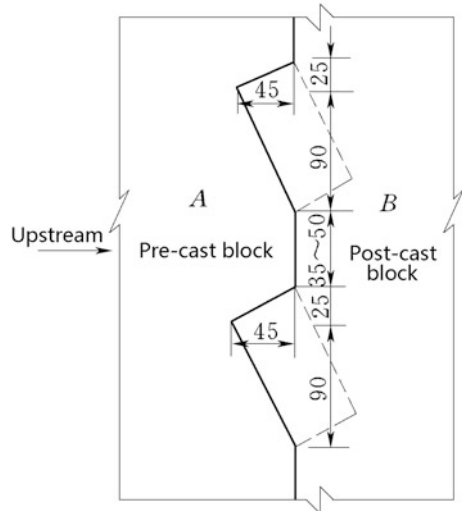
Fig. 7.43 Dam division into concrete blocks. **a** Columnar division by vertical joints; **b** half overlapped division by staggered joints; **c** columnar division by inclined joints; and **d** long sectional division

section. Vertical joints are widely exercised and the majority modern high gravity dams in the USA, European countries, Japan, India, and China are constructed with this type of joint. The joint spacing is 15–30 m, which is decided by placement capacity of concrete and requirement for temperature control. Provision of shear keys in joints enables to transfer shear stress from one block to the other. These shear keys are often triangular, whose short and long edges are perpendicular to the first and third principal stresses, respectively. Figure 7.44 shows a typical layout of longitudinal joint, of which (A) is the pre-cast block and (B) is the post-cast block. Where (B) should be pre-casted, the key should be layout according to the broken line.

The purpose of longitudinal joint grouting is to bind the blocks together so that the structure performs as a monolithic mass. Looped supply header-return pipes are embedded in the concrete adjacent to the lower boundary of the lift and connected to the vertical riser pipes. Grout outlets are connected to the risers to give better coverage of the longitudinal joint. The supply header-return pipes provide grout mixture to the riser pipes from one or both ends, as necessary, and assure that the grout will be admitted to all parts of the joint area. The top of each grout lift is vented to permit escape of the air and water, as the grouting proceeds upward. The location of the inlets and outlets of the supply header-return pipes and vents varies, and normally they terminate at the downstream dam face. However, where necessary, they can be so arranged to terminate in galleries.

In longitudinal joints, the only function of water stops or water seals is to retain the grout mixture. They are Z-type sheets termed as grouting seals. To ensure effective joint grouting and to prevent excessive pressure on the seals, the grouting area of a longitudinal joint consists of vertical seals placed close to the transverse joints on either side and horizontal seals placed at intervals of 15–20 m.

Fig. 7.44 Keying layout of a vertical longitudinal joint (unit: cm)



- ② Half overlapped (Fig. 7.43b) by staggered joints. They are short vertical joints in the given layer staggered by a $1/3$ – $1/2$ layer height with, respectively, the next overlying layer. These staggered joints are spaced 10–15 m apart. They are not necessary to be grouted and may be used in lower dam. The Dnieper Dam (Ukraine, $H = 60$ m) is constructed using half overlapped division with staggered joints.
- ③ Columnar division by inclined joints (Fig. 7.43c). Inclined joints are layout approximately along the principal stress, to reduce the tangential force on them and to cancel joint grouting. The inclined joints are terminated at a distance from upstream dam face, at which steel bars or galleries are installed. The erection of the vicinity blocks on the two sides of an inclined joint should be kept as uniformly as possible, to prevent the constraint stress between blocks during the cooling of concrete. The Ansha Dam (Fujian Province, China, $H = 92$ m) is constructed using inclined joints. Due to the complex with construction, inclined joints are seldom practiced nowadays.
- ④ Sectional or long sectional division (Fig. 7.43d). The whole portion of dam mass between transverse joints is made of concrete as one monolith, which may simplify and accelerate the construction process, and achieve high integrity of dam. However, the thermal cracking control will be more crucial. Following the progresses in the concrete material science as well as the thermal control and construction techniques, several high dams over one hundred meters had been constructed using long sectional division since the 1970s, including the Dworshak Dam (USA, $H = 219$ m) and the Libby Dam (USA, $H = 129$ m). The design codes of gravity dams require a particular study on the thermal stress problem in case of long sectional division. Since the 1980s, the fast development of roller compacted concrete (RCC) in dam engineering fully exploits the advantages of long sectional division.

(c) Horizontal construction joints

Generally, concrete is placed in lifts of 1.5–4.0 m thick. Each lift is continuously placed by 30–60 cm thick layers, and then 3–7 d will be rested before the placement of next upper lift. At dam base, the thickness of lifts reduced to 0.75–1.00 m, for better heat release and cut the temperature mounting. To develop proper bond between lifts, the lift surface is roughened and freed of all laitance, coatings, stains, and all foreign materials. Such a joint between the old and fresh concrete is known as horizontal construction joint or lift joint. Usually there is no water stops for construction joints. Sometimes, a water stop of Z-type and 0.5 m long is installed for the construction joint in front of openings (e.g., galleries) located close to the upstream face, to prevent potential seepage along the lift joint.

3. Dam body drainage

Drainage of seeping water from joints and cracks is essential to prevent the buildup of uplift in dams during operation period (Ma and Chang 2007). Dam body

is drained by an array of porous concrete pipes of 15–20 cm in diameter embedded within the dam, which run vertically the full dam height. The spacing of these porous concrete pipes is 2–3 m. They are installed as close as possible to the upstream dam face immediately after the impermeable concrete layer, if placed, for higher efficiency in uplift relief. However, the distance between the dam face and draining pipes should be not smaller than $1/10$ – $1/20$ of the water depth, to prevent the leaching deterioration of concrete due to excessive head gradient. The draining pipes discharge seeping water into the drainage gallery system first, and then the water is directed into sump wells and from therein further diverted into the downstream river by pumping or flowing automatically (Fig. 7.45).

It is important to design a drainage system such that draining pipes may be reamed out or redrilled in the event of blocking. The connecting of the draining pipes to the galleries is sketched in Fig. 7.45c, where the first type is the most prevalent for it facilitates reamed out or redrilled operation.

4. Galleries

Horizontal or inclined galleries and vertical chambers or shafts are installed in the body of gravity dam for inspecting its interior parts, observing the seepage process and appearance of cracks, locating various measuring instruments, and sometimes also for communication between the banks (Fig. 7.46).

(a) Foundation grouting gallery

Where there are several galleries in a dam, one of the lowest and the nearest galleries to the upstream face is commonly intended for curtain grouting.

The city-gate section is generally employed for the foundation grouting gallery (Fig. 7.47b). The height and width of the grouting gallery should not be smaller than 2.2–3.5 m and 2.0–2.5 m, respectively, to meet the requirement for drilling and grouting operation. Tracks on the floor and hanging hook at the top of the gallery are installed for moving machinery. Gutters are installed at the both sides of the gallery, to collect and to deliver the seeping water during grouting construction and reservoir service.

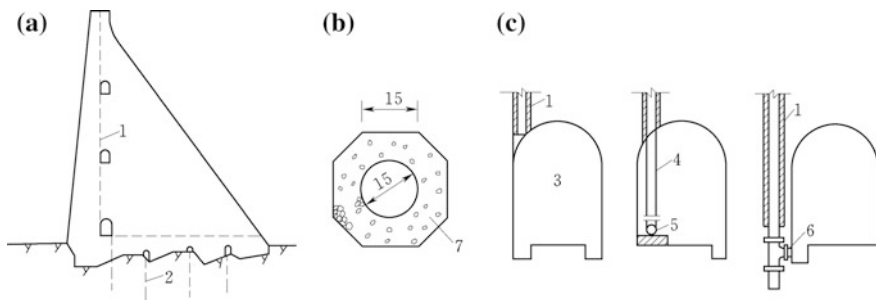


Fig. 7.45 Draining pipes in a gravity dam (unit: cm). 1 draining pipe; 2 draining hole; 3 gallery; 4 cast iron pipe; 5 collector pipe; 6 outlet; 7 porous concrete pipe

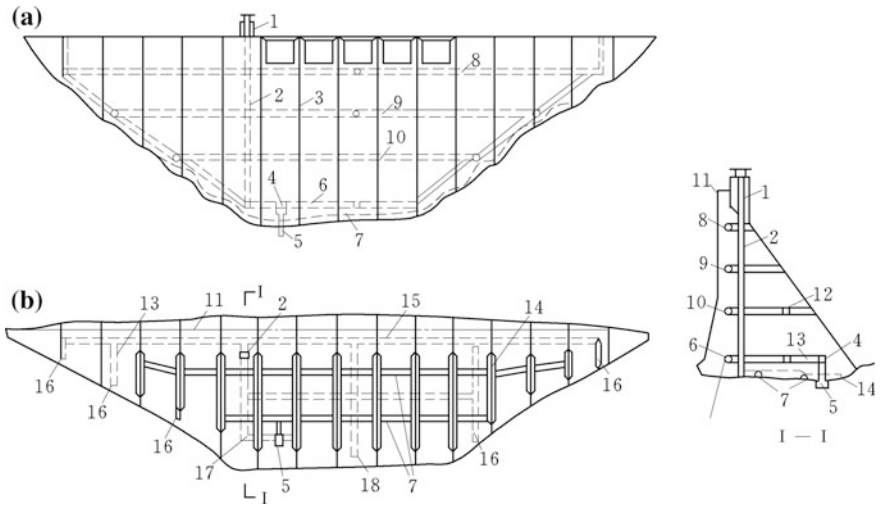


Fig. 7.46 Galleries within a gravity dam. **a** Elevation drawing; **b** plan. 1 lift tower; 2 lift shaft; 3 transverse joint; 4 pump chamber; 5 sump well; 6 foundation grouting gallery; 7 foundation drain gallery; 8 inspection gallery 1; 9 inspection gallery 2; 10 inspection gallery 3; 11 dam axis; 12 downstream inspection gallery; 13 access gallery; 14 drain gallery for transverse joint; 15 upstream inspection and grouting gallery; 16 gallery entrance; 17 main access gallery; 18 observation gallery

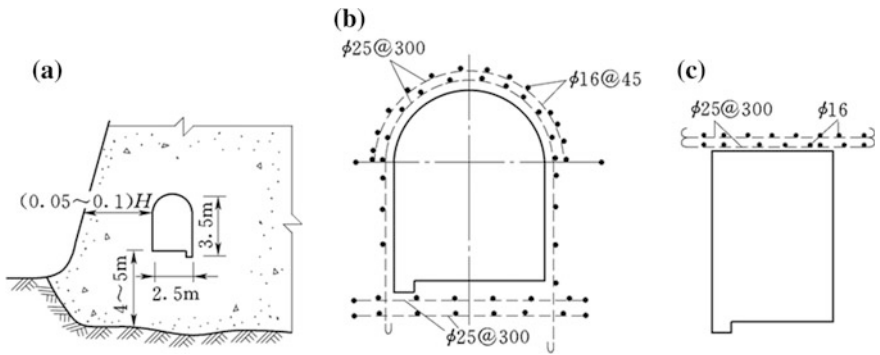


Fig. 7.47 Sectional types of gallery. **a** Position and size of grouting gallery; **b** city-gate gallery; **c** rectangular gallery

The minimum distance between the upstream dam face and gallery is ordinarily $1/10$ – $1/20$ of the water depth and not smaller than 4–5 m. The distance between the dam base and gallery floor should be larger than 1.5 times of the gallery width. At the downstream side of the gallery, foundation draining holes and uplift pressure observation holes are drilled.

The grouting gallery climbs up to the abutments following the valley topography, and the slope is desirable to be more flat than 40° – 45° , to facilitate the drilling and grouting operation, and machinery movement. If the abutment is too steep, the grouting tunnels are to be arranged within the abutments.

(b) Inspection and drain galleries and other types of galleries

The minimum width of an inspection gallery is 1.2 m. If necessary, this value may be increased to 2.5–3.0 m or even more. The height of an inspection gallery is 2.2 m or more. The city-gate section is also commonly exercised for these galleries. In recent 30 years, the rectangular section is more and more prevalent in many gravity dams, for obtaining smaller section (Fig. 7.47c) and facilitating construction.

At every 15–20 m elevation interval near the upstream face, inspection and drainage galleries are installed. The minimum distance between the upstream dam face and the galleries is usually $1/10$ – $1/20$ of the water depth but not smaller than 3 m. The exits from these horizontal galleries are provided either on the bank slopes or in the inclined and vertical chambers on the dam crest. If there are lift shafts, these galleries are connected to.

For high dams, other longitudinal galleries for the purposes of inspection and observation as well as communication, transverse galleries, gate operating galleries, and access galleries for entering penstocks may be installed.

For slotted gravity dams, along the slots, the inspection and access platforms are provided, and the galleries should pass through the slots by bridges.

Sometimes, cavities or chambers are arranged in the dam to locate, for example, the machine room of hydropower plant. Vertical shafts are usually installed for communication and observation.

The continuity of dam body is disturbed on making galleries and cavities/chambers in it, which results in redistribution of stresses. The local stresses surrounding galleries should be determined by experiments or numerical analyses. Depending on the value of stresses, sometimes steel bars are placed, particularly at the corners and the tops of the galleries, to counteract the concentrated stresses. For reducing locally concentrated stresses, the corners of galleries are rounded. A much better method of reducing stress concentrations is to make the gallery arch-shaped (closing to an ellipse) in cross section.

7.8 Foundation Treatment and Preparation for Gravity Dams

The purposes of foundation treatment for gravity dams are (ICOLD 1993) as follows:

- Improvement of deformation modulus to ensure the homogenous and integrity of the foundation;

- Improvement of strength to prevent sliding and uneven settlement of the foundation;
- Improvement of seepage resistance to reduce uplift and to prevent piping; and
- Improvement of life duration to prevent foundation from erosion and deterioration during the long period of service.

A variety of foundation treatment measures routinely available for gravity dams will be elucidated hereinafter.

7.8.1 Excavation and Clearance

Excavation and clearance consist of digging a construction pit down to the given elevation of the dam base, of treating and cleaning the rock surface, and of ensuring contact between the dam base and the bedrock. It has been accepted unanimously that the following must be done in the preparation for a gravity dam foundation:

- All alluvial and diluvium deposits present in foundation should be removed;
- Rocks, which can be removed without the use of explosives, should be removed; and
- The upper layer of removable rock, usually the weaker layer than the lower lying mass, as well as the pockets of weak material, should be removed.

The determination of the dam base elevation and the corresponding cutting depth in bedrock has high technical and economic significance. Theoretically, concrete dams should rest on conceptional “healthy” rock capable of bearing all stipulated load combinations.

According to the design codes in China, gravity dams higher than 100 m should be located on fresh rock, the slightly weathered rock, or near the bottom of weakly weathered rock; gravity dams at height of 100–50 m should be located on slightly weathered rock, or near the middle of weakly weathered rock; gravity dams lower than 50 m may be located on the middle or the upper portion of weakly weathered rock. These rock excavation requirements may be relaxed appropriately for lower abutment dam monoliths, or in case reliable consolidation grouting is provided.

The excavated slopes around the pit for a dam base should be stable. Along the river stream, an inclination of the excavated base in the direction of downstream should be avoided, whereas an inclined or stepping down excavation in the direct of upstream may be encouraged, if necessary. Abutment slopes are better to be excavated in steps down to the riverbed, to achieve reliable lateral stability for the abutment dam monoliths. If the foundation is composed of weathering vulnerable rocks (e.g., schists, argillites, and shales), the final layer of the excavated base should be stripped just before the concrete placement.

The rock surface at the design base elevations should remain safe during blasting and should have protrusions. To achieve this, the finally excavated rock layer at depth of 0.5–1 m is removed by rotary pneumatic drilling and small-intensity

explosion, or manually jack hammer and cotter and sledge hammer, depending on the hardness of the rock.

Before concrete placing, the rock foundation is cleaned and free of clay, soil, dust, rubbish, and oil trace, by water and sand blasting or metallic brushes.

7.8.2 Consolidation Grouting

The primary objective of consolidation grouting is to stiffen the rock in the contact zone immediately under the dam. It also assists to reduce seepage around this contact zone, where the rock may be more fissured or weathered than that at deeper overburden.

Consolidation grouting is sometimes employed as a means to solidify fractured but otherwise good rock and thereby to reduce the amount of rock excavation and concrete backfill. Deeper consolidation grouting is also sometimes required for specific geologic features, such as fault zones, or for subsurface materials around shafts and deep structures.

In situ tests show that the Young's modulus may be raised by 30–100 % for a well-fractured rock by competent consolidation grouting. However, the effectiveness of consolidation grouting is questionable under foundation conditions where the discontinuities in the rock are filled with clay unless the filling may be removed before grouting operation. Treatment of stratified or fractured rock may result in wasting a large quantity of grout mixture through joints and seams leading away from the foundation area. By grouting an array of holes on the periphery of the area at low pressure, substantial savings may sometimes be achieved.

More concentrated consolidation grouting is normally carried out at the vicinity of dam toe where the requirements for the Young's modulus are higher. Where the seepage control conditions permit, the consolidation grouting near the dam heel may be simplified or even omitted, to reduce the tensile stress concentration. Figure 7.48 shows the typical layout of the consolidation grouting on a dam base.

Consolidation grouting is generally carried out after the placement of base concrete, by grouting a shallow zone in a particular area utilizing holes arranged in a pattern of grid. The space of the first batch of holes should be sufficiently sparse (e.g., 10–20 m) so that connections between grout holes do not occur. The split-spacing method by reducing the grout hole interval is followed until the final spacing (e.g., 2–4 m), which should be determined during grouting operations on the basis of the results being monitored from these operations. The hole depth should be selected according to the geologic conditions and grouting tests, which is commonly 5–15 m or as deep as 20 m for high dam, and even reaches 20–30 m for well-fractured laminate bedrock.

Portland cements are the most common and best known as the basic ingredient for grouts. The water–cement ratio (W/C) in grouting mixtures should be carefully studied, because it not only influences strength and workability but also affects pumpability, viscosity, penetration, grout take, setting time, and pumping pressures.

Curtain grouting is commonly conducted subsequent to the consolidation grouting and after the placement of concrete to a considerable height or even after the whole dam has been completed. It is performed from the grouting gallery and tunnels driven into the abutments. The stage grouting method, by which progressively deeper holes are drilled and grouted, is customarily employed in dam engineering: previously emplaced grout in holes is removed prior to hardening, and then the holes are drilled to a deeper depth, followed by another stage of emplacement. This process is completed until either a predetermined depth of curtain is reached or a specified permeable condition is met (Fig. 7.49).

The main design task of curtain grouting is to decide the depth of curtain (or hole depth), the thickness of curtain (the rows of hole, spacing of rows, and spacing of holes), the position of curtain, the depth into abutments, and the grouting pressure.

1. Depth of curtain

Depth to which grout holes are drilled is governed by the permeable conditions of the foundation rock and by the hydrostatic head to which the foundation rock will be subjected. Grout curtain should be sufficient deep to minimize seepage discharge and to assist in the reduction of uplift pressure. Where conditions permit, grout holes should be drilled into sound, impervious stratum. Otherwise, the grout holes should be drilled 3–5 m deeper into relatively impervious stratum. The criterion of relatively impervious stratum and the standard of curtain grouting are listed in Table 7.7, in which the lower bound is for pumped storage power stations and reservoirs in shortage of water resources.

In case when the relatively impervious stratum is embedded very deeply, the depth of hole is selected among 0.3–0.7 times of the dam height.

2. Thickness of curtain

The thickness of curtain l_4 is dependent on the row number n of holes (Fig. 7.50) and may be estimated by

Fig. 7.49 Diagram to the design of curtain grouting

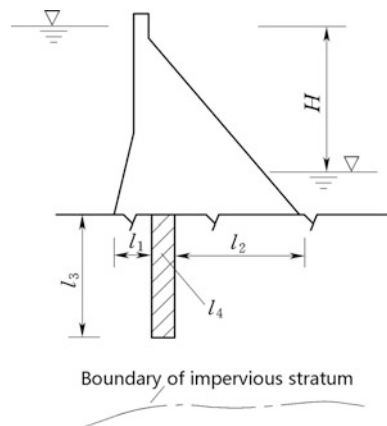
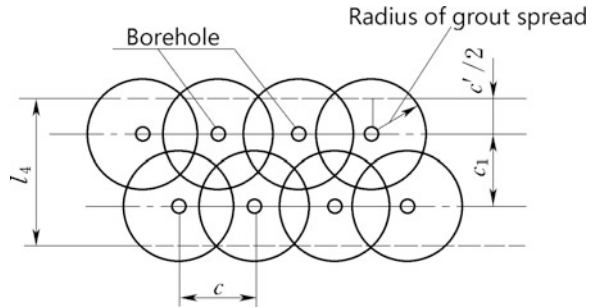


Table 7.7 Criterion of relatively impervious stratum and standard of grouting curtain

Dam height (m)	Water percolation rate of curtain q (Lu)	Permeability coefficient k (cm/s)	Allowable seepage gradient [J]
>100	1–3	2×10^{-5} – 6×10^{-5}	20–15
50–100	3–5	6×10^{-5} – 1×10^{-4}	15–10
<50	≤ 5	1×10^{-4}	≤ 10

Fig. 7.50 Thickness of grouting curtain



$$\begin{cases} l_4 = (0.7 - 0.8)c & \text{single-row} \\ l_4 = (n - 1)c_1 + c' & \text{n-rows} \\ c' = (0.6 - 0.7)c \end{cases} \quad (7.45)$$

where c = hole spacing in a row, which is usually 1.5–4 m and better to be selected by in situ tests; c_1 = row spacing, which is usually a bit of smaller than the hole spacing.

The thickness of curtain should be able to resist seepage failure. A majority completed gravity dams in China possesses grout curtains whose thickness is designed following the principle of the former USSR, which takes into account the actual hydraulic gradient and allowable hydraulic gradient of the curtain thickness. On the contrary, many countries such as Japan and USA do not consider the hydraulic gradient requirements in the curtain design; instead, the curtain thickness is designed directly according to the permeable characteristics of rock and the dam height. This design philosophy also has been accepted step by step in recent years by Chinese engineers.

The curtain grouting with a single row of holes will ordinarily provide a satisfactory curtain thickness for medium- to low gravity dams constructed on competent rocks, while for high dams double-rowed arrangement could be necessary. The grout curtain for dams on inferior rocks even requires triple-rows of grouting holes. For the grout curtain of multiple-rowed, the holes in adjoin rows should be staggered with respect to each other. For a triple-rows curtain, only one row reaches the design depth while the rest rows merely reach 1/2–2/3 of the design depth, and they should be drilled and injected in the following sequence: firstly, the upstream row then the downstream row, and vice versa, and the central row is always the last

one. However, if a soluble rock is encountered, or where the joints or fissures are fine and closely spaced and erratic, all the hole rows may need to be constructed to the full depth. It is necessary to emphasize that specifications should be flexible enough for additional rows of grout holes at any location or depth, as indicated necessary in the field test.

3. Position of curtain

The grout curtain is commonly located near dam heel, as possible. The exact location of a curtain is determined by the type of dam as well as by the foundation conditions peculiar to the work site.

Foundation grouting holes of gravity dam are commonly vertical. However, inclined holes may allow them to intersect perpendicularly or at larger included angles with fractures and joints, which is advantageous for higher grouting efficiency. Grout holes inclined in an upstream direction may also provide an adequate spacing between the grout curtain and drainage curtain. However, the inclination angle is ordinarily limited within 10° for the purposes of construction facilitation and quality control. Anyway, larger inclination or even horizontal grouting holes could be incorporated within the grouting tunnels in the dam abutments, where needed.

4. Grouting curtain driven into abutments

The depth and direction of the curtain driven into abutments are decided taking into account the geologic conditions. The continuity of curtain from riverbed to abutments is strictly demanded. Where conditions permit, grout holes should be driven into sound, impervious or relative impervious rock. In case when the relatively impervious rock is embedded far away from the abutments, the holes are bottomed at point (B) as indicated in Fig. 7.51 (right abutment), which is the intersection point of the highest reservoir level and the original groundwater table. Drainage may be installed above (BC) to control the rise of the phreatic line after the reservoir impounding. The curtain grouting in the abutments may be carried out on the ground or in the grouting adits, dependent on the ground topography.

5. Grouting pressure

The grouting pressure should be decided by in situ tests, which may meet best for any particular set of conditions encountered during the grouting operation. Factors influencing the determination are the size of fracture voids to be filled, the depth of zone and the lithology of area to be grouted, the grout mixture viscosity, and the resistance to the grouting pressure-induced fracturing. Usually it should be larger than 1–1.5 times of the head difference between upper and lower pools at the portion near the base, and not smaller than 2–3 times of the head difference at the portion of the lowermost curtain bottom.

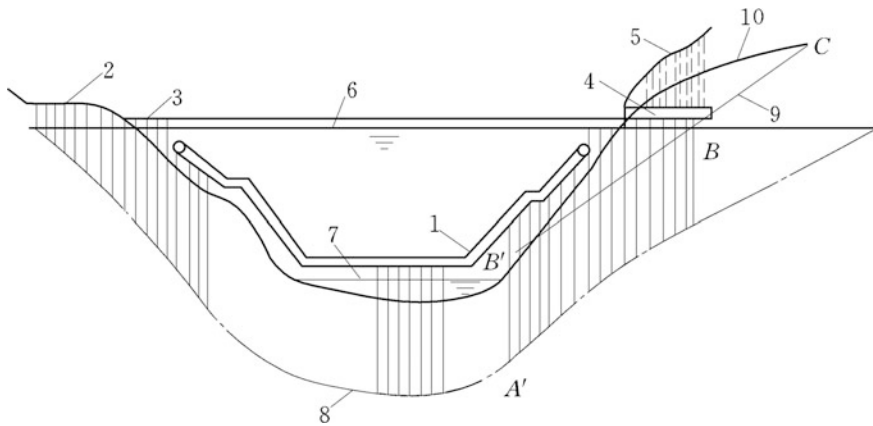


Fig. 7.51 Diagram to the design of grouting curtain in abutments. 1 grouting gallery; 2 drilling from abutment; 3 drilling from dam top; 4 grouting adit; 5 drain hole; 6 maximum reservoir level; 7 river level; 8 boundary of impervious rock; 9 original ground phreatic line; and 10 phreatic line after the reservoir impounding

7.8.4 Contact Grouting

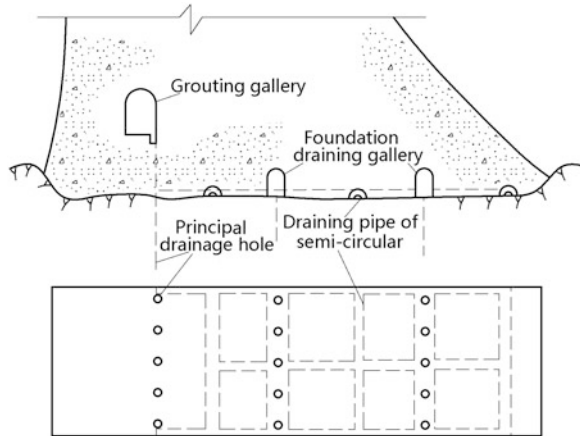
Shrinkage of concrete may give rise to seepage pathways along the contact face with rock. Contact grouting is advisable where such conditions are critical. Contact grouting is the injection of neat cement grout mixtures at the contact of a concrete structure with an adjacent rock surface, for filling the void at the contact that results from concrete shrinkage and bringing about a fully bonded contact. Contact grouting may be done through either header pipes installed for that purpose during construction, or post-drilled holes. The header pipes or drilled holes are thoroughly washed before the grouting operation. The contact grouting is employed most frequently where

- The abutment areas of concrete dams, where the transverse inclination angle of the dam base is steeper than 50° ;
- In the crown areas of lined tunnel in rock (see Chap. 13);
- The contact surfaces on the side of large concrete dental which are steeper than 45° ; and
- The side walls and top vault of the concrete replacement for deep-seated faults or intercalations.

7.8.5 Drainage

In addition to grouting, foundation drainage is conventionally installed to control seepage and to relieve uplift in foundation or abutments as well as to prevent

Fig. 7.52 Drainage system in/on dam foundation



seepage failure (e.g., piping). Foundation drainage devices for gravity dams include drainage curtain formed by draining holes, drainage adits, and drainage galleries (Fig. 7.52).

Drainage curtain is one of the most effective means for seepage control. Foundation draining holes are connected to the grouting gallery by pipes for releasing the seeping water to gutters, which is further gathered in sump wells. Apart from the main drainage curtain behind the grouting curtain, 2–3 or 1–2 rows of auxiliary drains may be installed for high- or medium dams, respectively. Foundation drainage curtain installed from grouting gallery is frequently inclined at 10° – 15° in downstream direction to keep sufficient distance between the draining holes and the grouting holes larger than or equal to 0.5–1.0 times of the grouting hole space.

The foundation draining holes should be 2–3 m in space and minimum 100–150 mm in diameter. The depth of holes is usually 40–60 % of the grout curtain and no smaller than 10 m for high-to-medium dams, which is related to the geologic and hydrogeologic conditions. Auxiliary drains are drilled from the longitudinal drainage galleries on the dam base (Fig. 7.52), and the hole spacing and depth are 3–5 m and 6–12 m, respectively.

Draining holes in abutments may be vertical or inclined at any angle. If draining holes are horizontal or inclined upward in shale or other sensitive materials, they should be provided with traps at the collar to prevent air circulation in holes and should be cased, if necessary.

Draining holes should not be drilled until after the curtain grouting has been completed. When grouting is necessary near existing drainage devices, care is called at avoidance of grouting the draining holes. Draining holes should be so designed as they are accessible and can be periodically inspected and cleaned.

Where the abutments are high and steep, the draining holes are drilled from the grouting adits.

7.8.6 Treatment of Weak Seams and Karst

Treatment of weak seams (intercalations, faults, etc.) of adverse trends, usually inevitable, consists of grouting and filling of weak portion with concrete, and strengthening fragment zones using different connection arrangements and structures.

1. Treatment of faults

A fault is a typical large weak seam containing rock fragments and clay, across which there has been significant differential displacement as a result of earth crust movement. Fractured zones on the two sides of a fault are also formed by the movement. The fault and fractured zones have poor characteristics in strength, deformation, and permeability. When the fault-fractured zone is located below the dam base, significant deflection or differential displacement may result in stress concentration and cracking in dam. If the fault links the reservoir headwater and tailwater, the uplift may be raised considerably, and the concentrated seepage flow will induce mechanical or chemical piping in the fault, which in turn may seriously threaten the safety of dam.

Where a fault-fractured zone is vertical or at large dip angle, a portion of the weak material may be removed and replaced by concrete (Fig. 7.53), to reduce differential settlement and stress concentration. There are two types of concrete replacements, i.e., concrete ground beam and arch, which are constructed monolithically with the dam body. In preliminary study, the simplified analysis diagram based on Fig. 7.53c, d may be employed. The finite element method allows precise

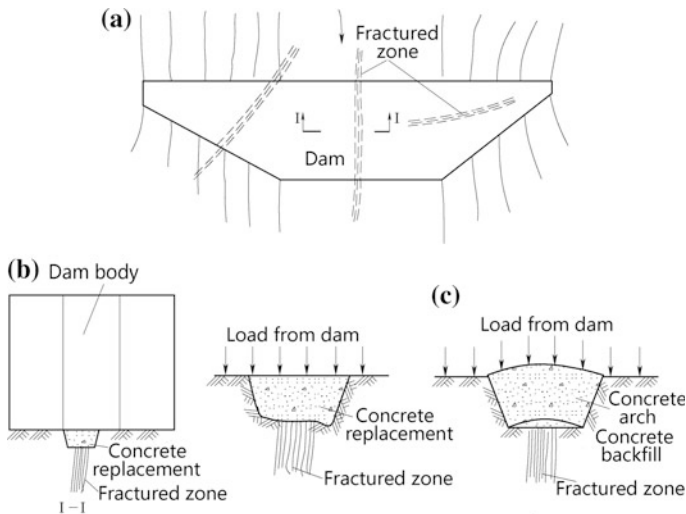


Fig. 7.53 Treatment of fault zone. **a** Plan; **b** concrete beam replacement; **c** concrete arch replacement

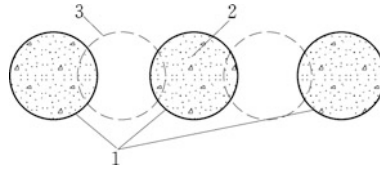


Fig. 7.54 Construction of concrete cutoff wall. 1 borehole drilling of the first phase; 2 refill by fine aggregate concrete; 3 borehole drilling of the second phase

analysis of the stresses in concrete ground beam (or arch), which looks at the dam body and beam (or arch) as a monolithic structure. According to the analysis, the depth, span, shape, and reinforcement of beam and arch are decided.

According to the engineering experiences, for a fault-fractured zone of medium width, the approximate size of replacement concrete beam may be estimated as: excavation depth = 1–1.5 times of the width of fault-fractured zone, and not smaller than 1 m; the slope of the excavated wall = 1:1–1:0.5; if the fault connects the headwater and tailwater, the concrete replacement beam should be elongated into up- and downstream 1.5–2.0 times of the excavation depth.

For a fault connects the headwater and tailwater, the remedial treatment for concentrated seepage must be carefully studied. The conventional countermeasure is deep area grouting (cement or chemical) using higher grouting pressures. Another countermeasure is using concrete cutoff wall constructed by borehole drilling of 30–50 cm in diameter and concrete backfilling; (Fig. 7.54). Concrete anti-seepage plugs (keys) along the larger scale faults combined with grouting curtain to form an enclosed anti-seepage system also may be a good choice (Fig. 7.55).

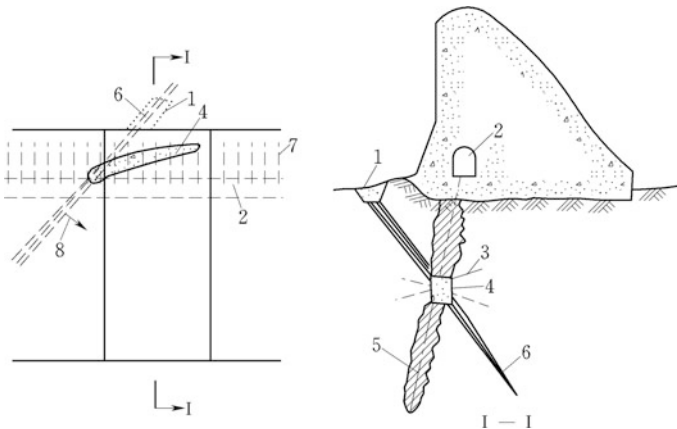


Fig. 7.55 Concrete anti-seepage plugs. 1 backfilled concrete; 2 grouting gallery; 3 consolidation grouting on shaft wall; 4 concrete anti-seepage plug; 5 grouting curtain; 6 fractured zone; 7 grouting hole; and 8 dip of fractured zone

For a fault-fractured zone of definite dip angle, apart from the ground beam by concrete replacement on the base surface, the adverse influences of its deeper portion on the dam are also controlled. Taking the fault-fractured zone in Fig. 7.56 as example, sloping shafts and adits are excavated along the fault, and then backfilled by steel reinforced concrete to form a high rigid frame composed of concrete keys. The frame may transfer the loads from the hanging wall to the footwall and may enclose the rock fragments tightly; in this way, the adverse deformation and seepage of the foundation rock may be restrained. For larger scale key construction, attention should be called at the thermal control measures, and the contact grouting should be carried out.

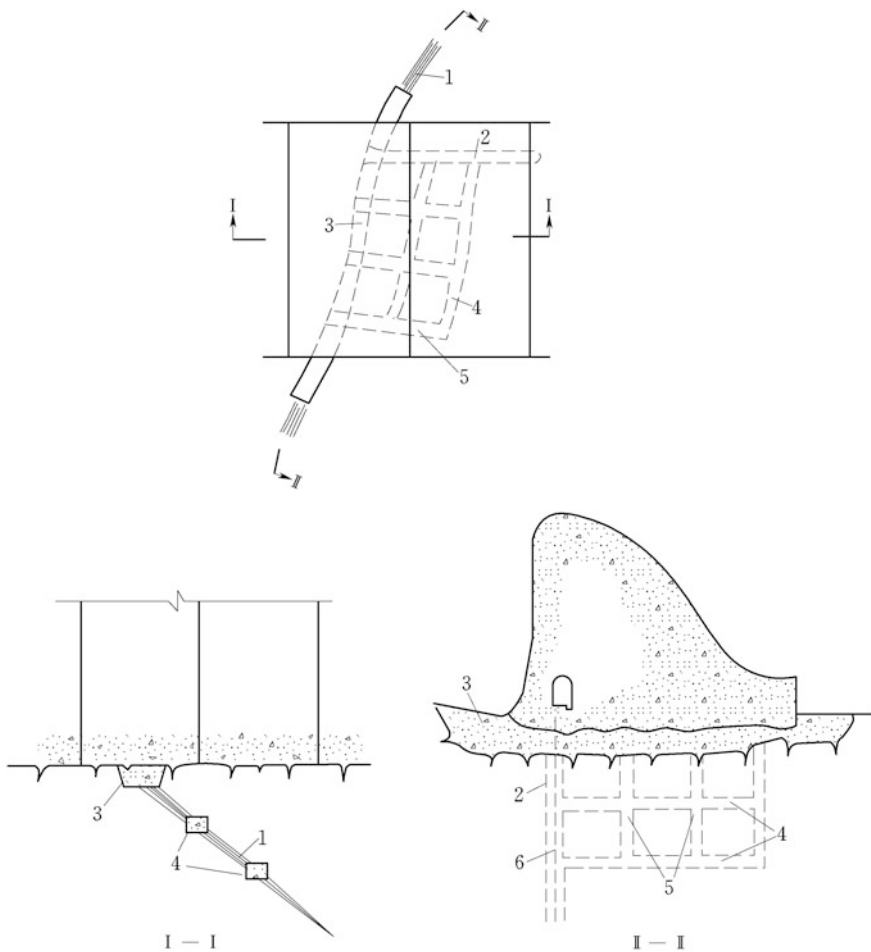


Fig. 7.56 Treatment of inclined fault zone. 1 fractured zone; 2 inclined impervious concrete key; 3 concrete replacement ground beam; 4 adit backfill; 5 inclined reinforcement concrete key; 6 curtain grouting hole

When there is a single dominant weak seam with very low shear resistance, concrete keys (plugs) against sliding (Fig. 7.57) may be installed by excavating tunnels and backfilling with reinforced concrete along the seam. Where there are more than two such weak seams, lateral shearing piles (Fig. 7.58) are probably more economic and technically efficient for improving the stability against sliding.

Rock bolt reinforcement (Post-Tensioning Institute 1985) also can be employed in dam foundation treatment, particularly during the foundation excavation stage when it is found that the geologic conditions are much more adverse than anticipated. If the study shows that the foundation grouting gives rise to only negligible

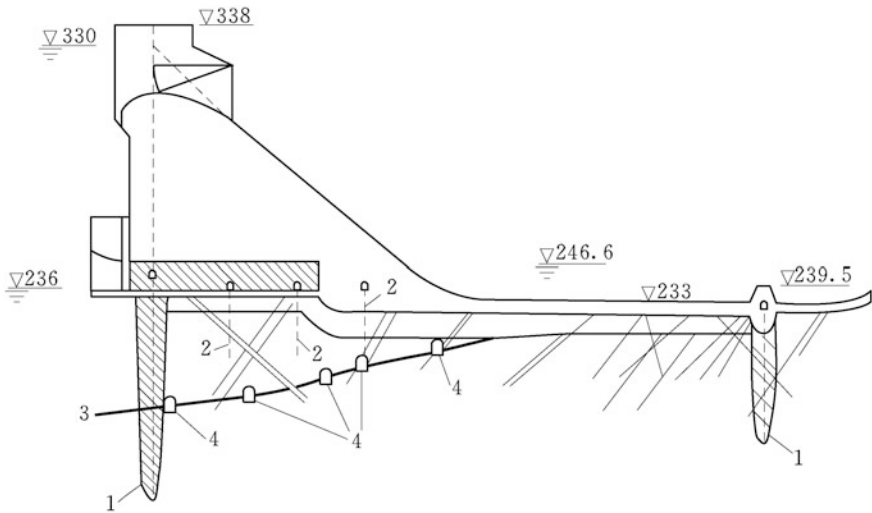


Fig. 7.57 Concrete keys (plugs) against sliding—the Ankang Dam (China, $H = 128$ m). 1 grouting curtain; 2 drainage of dam foundation; 3 fault f_1^p ; 4 concrete keys (plugs)

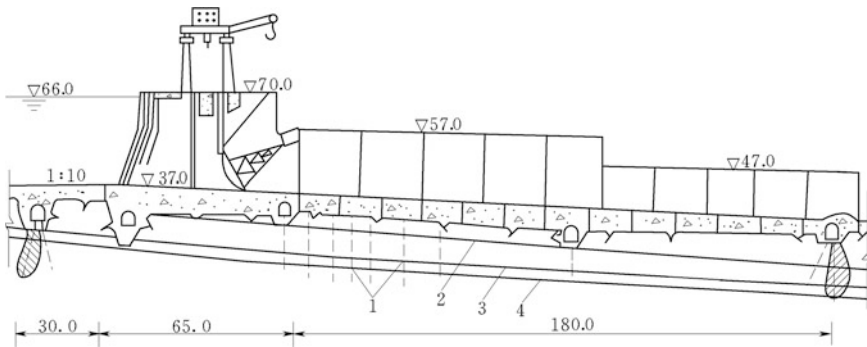


Fig. 7.58 Shearing piles (unit: m)—the Gezhouba Barrage Project (China, $H = 53.8$ m). 1 shearing pile; 2 No. 212 weak seam; 3 No. 202 weak seam; 4 No. 201 weak seam

improvements, the deeper excavation and the dam body enlargement are also limited by the completed cofferdams, and the countermeasure using rock bolts has remarkable advantages. Fully grouted, passive dowels comprising steel bars are installed in boreholes drilled across the potential slip surfaces or the whole base of the dam monolith, which are then encapsulated in cement or resin grout. These steel bars perform as rigid shear pins across any planes of discontinuities in the rock; in this way, to raise the shear resistance along discontinuities or any potential slip surfaces in the foundation in three different mechanisms: tension force in the bolt, friction as a consequence of the increase in the normal stress, and dowel effect.

The pioneering work of rock bolt reinforcement for dam foundation is the Tirso Dam (Italy, $H = 100$ m) whose foundation rocks are micaschist, gneiss, and granite (Egger 1992). After the excavation down to the designed dam base, it was found that the rock was strongly weathered and poor in quality; therefore, the rock bolt reinforcement on the whole foundation ($20,000 \text{ m}^2$) was arranged. This dam has been completed and been operating normally.

The Xiaoxi Project is located at the middle reach of the Zijiang River, Hunan, China. The rock masses are Cambrian system (€) and Devonian system (D). The regional fault F_1 passes through the center of the riverbed with a fractured zone of 180 m wide, which dips to the left bank in an steep angle of 67° – 78° . Nearly all the 8 spillway dam monoliths are located on F_1 . To improve the stability of the dam foundation, the designer proposed and implemented a series of stabilization measures such as to enlarge the dam section, to move the grouting curtain in the direction of upstream, to intensify drainage all over the dam foundation, and to excavate the dam foundation dipping in the direction of upstream; connect the dam body with the downstream stilling basin apron and approaching wall, etc. However, since the cofferdams had been completed when the geologic characteristics of the fault F_1 were fully revealed, all the above measures had insufficient effectiveness in the improvement of the dam stability due to a limited space within the cofferdams. As a result, the safety factor against sliding (K') of the spillway dam monoliths 1–7# are not satisfied taking into account the above countermeasures. Finally, the rock bolt reinforcement scheme had to be employed. The dam has been completed and started normal operation in January 2008 (Chen et al. 2012).

Figure 7.59 is the layout of the rock bolts at the overflow spillway dam foundation, each rock bolt ($3\Phi 32@2$ m) is made of three steel bars with 32 mm in diameter. The spacing between rock bolts is 2 m. The boreholes for the bolt installation are $\Phi 130$ in diameter, and whose inclinations are alternatively varied (15° or 25°).

2. Treatment of Karst

Karst is a geologic formation created by the dissolution of a layer or layers of soluble rocks, usually carbonate rocks such as limestone or dolomite. A Karst area displays distinctive features such as karrens, solution cavities, cenotes, sinkholes, dolines, and underground rivers. Although it may be a tourism attraction, the Karst is a geologic defect which poses difficulties for the sustainability and water tightening in dam engineering (Soderberg 1988).

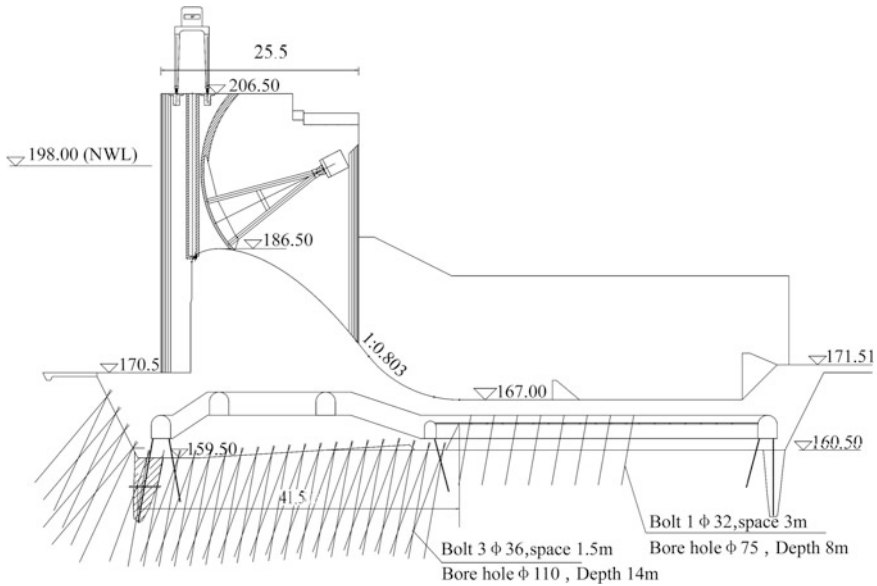


Fig. 7.59 Layout of the rock bolts at the overflow spillway dam foundation (unit: m)—the Xiaoxi Dam (China, $H = 44.5$ m)

The treatment of dam foundation in the Karst area comprises of excavation, backfill, and grouting. For the caves bear surface, the excavation, wash, and backfill are good choices. For the deeper but small size caves, the curtain grouting may be alternatively employed, and in the grouting operation lower W/C is required, and sometimes clay and/or fine sand are added in the grouting mixture. In case of server leakage, accelerators such as the calcium chloride may also be added in the mixture, and gravel as well as hot asphalt also may be applied to block the leakage path effectively. For the deeper but large size caves, the concrete backfill may be carried out by digging adits and shafts.

A very successful example of the Karst foundation treatment is provided by the Wujiangdu Arch Gravity Dam (China, $H = 165$ m).

7.9 Roller Compacted Concrete (RCC) Gravity Dams

7.9.1 Features of RCC Dams

In the absence of desirable progress toward an ideal cement, the problems with regard to optimizing concrete dam construction and reducing costs may be approached in several directions such as:

- Reappraisal of design criteria, particularly with respect to accepting modest tensile stresses;
- Improvement of concretes through the use of admixtures to enhance tensile strength and to modify stress–strain relation, and/or through the use of modified cements with reduced thermal activity; and
- Development of rapid continuous construction techniques based on the use of special concretes (Hansen 1996; Hansen and Reinhardt 1991).

The concept of dam construction using roller compacted concrete (RCC) developed since the 1970s is based primarily on the last one of the above approaches cited (Dunstan 2007). Nowadays, several variants of RCC have been available offering prospect of significantly faster and cheaper construction, particularly for large gravity dams (American Society of Civil Engineers, United States Army Corps of Engineers 1994; ICOLD 2003; Nagayama and Jikan 2003; United States Bureau of Reclamation 2005).

The main features of RCC dam may be summarized in the following:

- With a lower cost variant of concrete, i.e., dry lean concrete, the unit cement content is reduced;
- Upstream distorted concrete or high-quality concrete membrane is used as main anti-seepage devices;
- Transverse construction joints, if necessary, may be sawn through each successive layer (lift) of concrete after the lift placing;
- Construction in RCC permits an intensively mechanized construction process;
- RCC is delivered by conveyer belts and handled by standard earth moving and compaction facilities;
- Amount of framework consumption is reduced; and
- RCC offers the greatest potential through financial benefits associated with a shortening of construction period by up to 35 %.

Although RCC dams may possess remarkable economic benefits compared to conventional vibrated concrete (CVC) dams, yet under certain conditions, it may not be suitable for dam construction, for instance, where

- There are no sufficient proper aggregates near the dam site;
- Poor foundation rock quality or the overburden is very thick;
- Very narrow and steep valley allow for insufficient operation space for construction equipments; and
- Outlets, pipes, and galleries are complex but cannot be avoided.

7.9.2 History of RCC Dams

Research on RCC dams started from the 1960s. The first experiment of RCC was carried out in the cofferdam of the Shimen Dam (Taiwan, China, $H = 133$ m). A

high gravity dam—Alpe Gera ($H = 172$ m) in Italy tried to use the construction technology of embankment to construct concrete dam in 1963. Later on, this method was introduced to construct dams, cofferdams, and for dam rehabilitations in Canada, USA, UK, Pakistan, Japan, and Brazil. By these practices, engineering experiences and expertise were accumulated gradually. The Shimajigawa Dam in Japan ($H = 89$ m) and the Willow Creek Dam in USA ($H = 52$ m) belongs to the initial batch of RCC dams in the world, which are named as RCD by the Japanese engineers. Until the end of 1998, there were 29 and 32 RCC dams built in the USA and Japan, respectively.

The Chinese dam engineers learned RCC technology from Japan and USA in 1978, when some experimental RCC blocks were placed in the works such as the Shamen Airport Project, the longitudinal diversion wall and switchyard foundation of the Shaxikou Hydraulic Project, the lower diversion wall of the navigation lock in the Gezhouba Hydraulic Project, and the Niurixi No.1 Auxiliary Dam of the Tongjiezi Hydropower Project. The first water retaining structure of RCC is the Kengkou Dam (Fujian, China), and its construction was started from the November of 1985 and completed in the June of 1986. The dam height is 56.8 m, crest length is 122.5 m, and concrete amount is $60,600 \text{ m}^3$ (of which $42,000 \text{ m}^3$ is RCC). Until the end of 1998, 30 RCC dams had been erected in the country. The Longtan Gravity Dam (China) completed in 2009 (first phase) and the Guangzhao gravity dam (China) completed in 2009 are at heights of 192 m and 200.5 m, respectively. Table 7.8 lists the representative RCC gravity dams in China over 100 m.

Since the 1990s, the RCC had been applied in the construction of arch dams, too. The highest RCC arch dam then—Puding Arch Dam (China, $H = 75$ m)—was completed in 1994. With the Wenquanbao Arch Dam (China, $H = 48$ m) completed at the same period, they became the milestones of RCC arch dams in the Southern and Northern China. They are followed by a series of higher RCC arch dams such as the Shapai Arch Dam (China, $H = 132$ m), the Longshou Arch Dam (China, $H = 80$ m), and the Dahuashui Arch Dam (China, $H = 134.5$ m).

In the following paragraphs, the main design issues for RCC gravity dams is discussed, whereas the design principles of RCC arch dams will be elaborated in Chap. 8 of this book.

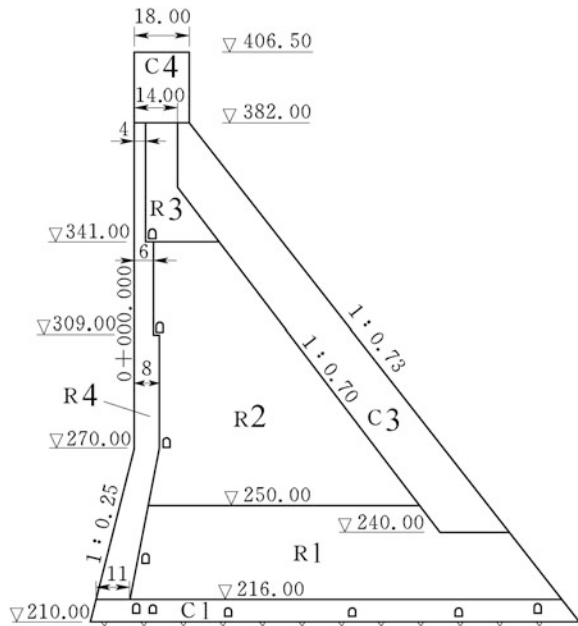
7.9.3 Design of RCC Dams

The main difference between RCC and CVC gravity dams lies in the construction material and method, while the principles of their profile configuration are nearly identical. According to the project requirements, they may be constructed as non-overflow dam monoliths (Fig. 7.60) or overflow dam monoliths (Fig. 7.61). To meet the machinery placing requirements, outlets and pipes at different levels are simplified; in this way, the profile of RCC gravity dams may be designed as simple as possible. There are a variant of profile types and construction methods for RCC gravity dams.

Table 7.8 Representative RCC gravity dams in China (over 100 m in height)

Project name	River	Height (m)	Gross storage capacity (10 ⁸ m ³)	Installed capacity (MW)	Year of completion
Longtan	Hongshuihe	192/216.5	162.10/272.70	4200/6300	2009
Guangzhao	Beipanjiang	200.5	32.45	1040	2009
Guandi	Yalongjiang	168	7.83	1800	Under construction
Jinanjiao	Jinshajiang	160	8.47	2400	Under construction
Jiangya	Loushui	131	17.41	300	2000
Baishe	Youjiang	130	56.60	540	2006
Hongkou	Huotongxi	130	4.51	200	Under construction
Wudu	Fujiang	119	5.72	150	Under construction
Suofengying	Liuguanghe	121.81	2.01	600	2006
Gelantan	Lixianjiang	113	4.09	450	2008
Mianhuatan	Dingjiang	113	20.35	600	2001
Dachaoshan	Lancangjiang	111	9.40	1350	2002
Jinghong	Langcangjiang	110	11.39	1500	2009
Yantan	Hongshuihe	110	33.80	121	1995
Silin	Wujiang	117	15.93	1000	Under construction

Fig. 7.60 Concrete zoning of the standard profile (unit: m) —the Longtan Dam (China, $H = 192$ m). $C1, C2, C3, C4$ CVC; $R1, R2, R3, R4$ RCC



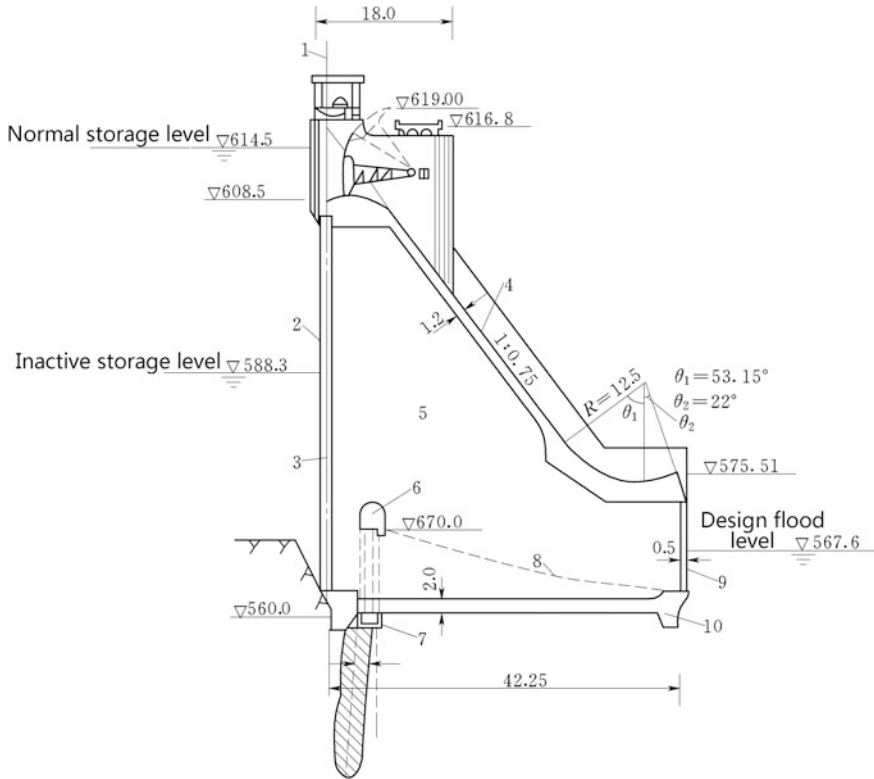


Fig. 7.61 Profile of overflow monolith (unit: m)—the Kengkou Dam (China, $H = 56.8$ m). 1 dam axis; 2 anti-seepage layer of bituminous mortar; 3 precast reinforced concrete slab; 4 anti-scouring layer of reinforced concrete; 5 RCC; 6 grouting and drainage gallery; 7 sump well; 8 natural ground; and 9 precast concrete slab; 10 CVC

1. Profile types

(a) Dry lean concretes of low cementitious material (binder)

The design philosophy of the US Army Corps of Engineers for the Willow Creek Dam was that:

- Be simple and fast in construction;
- Under the limitations of sufficient strength and durability as well as low hydration heat, use as less as possible of cement (American Society of Civil Engineers, United States Army Corps of Engineers 1994).

Hence, dry lean concretes of lower cementitious material (66 kg/m^3) and water content were invented. Transverse and longitudinal joints were not installed, and

the up- and downstream dam faces were protected by a cement-enriched concrete layer. This type of profile has larger section volume but lower unit cost of concrete. The major problem of this profile type is the poor performance in seepage resistance, particularly with the leakage through lift joints. Nowadays, apart from cofferdams and lower dams, this type is seldom practiced in China.

(b) Dry lean concretes of high cementitious material

The design philosophy of the USBR for the Upper Stillwater Dam (USA, $H = 87$ m) was using RCC of high strength and seepage resistances to reduce the dam section volume and concrete amount (United States Bureau of Reclamation 2005). Hence, dry lean concretes of high cementitious material ($240\text{--}250$ kg/m³), high fly ash content (account for 70 % of the cementitious material), and a bit higher water content were invented. The lift joints were not treated, and thin up- and downstream dam faces of CVC were installed for providing better seals and preventing seepage through lift joints. The downstream slope is 1:0.6, which means less amount of concrete consumption. However, the unit cost of such RCC is higher than that of the Willow Creek Dam, due to higher cementitious materials. Since there were no contraction joints, transverse thermal cracking manifested in this long structure, and several cracks were significantly serious and required extensive treatment due to heavy leakage.

(c) Dry lean concretes wrapped with thick- and high-quality CVC

In the Japanese RCD practices, the profile is divided into functional zones of external concrete employed at the surface of dams, foundation concrete adjoining the bedrocks, structural concrete in and around structural elements, and internal concrete inside the dam (Isao and Shigeharu 2003; Nagayama and Jikan 2003). The up- and downstream dam surfaces as well as the dam base should be covered by high-quality CVC of 2–3 m thick to ensure watertightness and durability against freeze-and-thaw attack or other aging scenarios. The RCD concrete is placed only in the internal zone. Transverse contraction joints are installed in order to prevent temperature cracking, which are made by vibratory joint cutters. Water stops and draining system are all installed within the CVC layer.

This type is recommended and widely employed in Japan and China as well. Figure 7.60 shows the standard profile of the Longtan Dam (China, $H = 192$ m). Such structures have high reliability in leakage resistance but are complicated in the mixing and transporting, due to the employment of two different kinds of concrete.

In more than 30 years of RCC dam practices, the first batch of RCC dams in China has adopted Japanese RCD design (Sun et al. 2004). Later on, various practices to improve the profile type have been attempted in the country, such as the installation of upstream asphalt mortar face and reinforced concrete wall. In the recent twenty years, the Chinese RCC gravity dams have been going to use all RCC structure with GEVRCC (Grouting Enriched Vibratable RCC) (Forbes 1999) on dam faces, and with an internal RCC formulation in between the two USA: dry lean concrete aforementioned—medium cementitious material (around 180 kg/m³), and high fly ash content (account for 50–70 % of the cementitious material).

2. Appurtenants

(a) Joints

High content of pozzolan (fly ash) and lower cement in the RCC mixture give rise to lower hydration (Tatro and Schrader 1985). For medium- to small RCC dams, if the concrete placing may be carried out and completed only in draught and cool seasons, the fluctuation of temperature will be so small to result in only minor or even without significant cracking, although some of these have had other problems with lift joint seepage. Under such circumstances, transverse joints may be omitted. But where the severe winter will attack the surface of RCC, the protection of RCC surface may be demanded by insulation blankets or other protective measures, to prevent surface fissures from developing into macro-cracks across the dam body. The Willow Creek Dam (USA) and the Kengkou Dam (China) are built of dry lean concrete with low cementitious material, and there were no hazardous cracks even without transverse joints.

However, transverse joints are required for the RCC dams of high cementitious material or for the control of uneven foundation settlement induced stress/strain concentration attributable to foundation terrain, particularly where significant changes in abutment slope exist. The Upper Stillwater Dam of USA is built of dry lean concrete with high cementitious material without transverse joints, and serious transverse thermal cracking was reported after its commission.

In the North China, transverse joints spaced 12–30 m apart are installed, such as in the Guanying Dam ($H = 82$ m), the Baishi Dam ($H = 49.3$ m), and the Taolinkou Dam ($H = 74.5$ m). In South China, the transverse joints can be spaced 40–60 m apart, such as in the Mianhuatan Dam ($H = 113$ m) and in the Dachaoshan Dam ($H = 111$ m). These joints are customarily made by joint cutters.

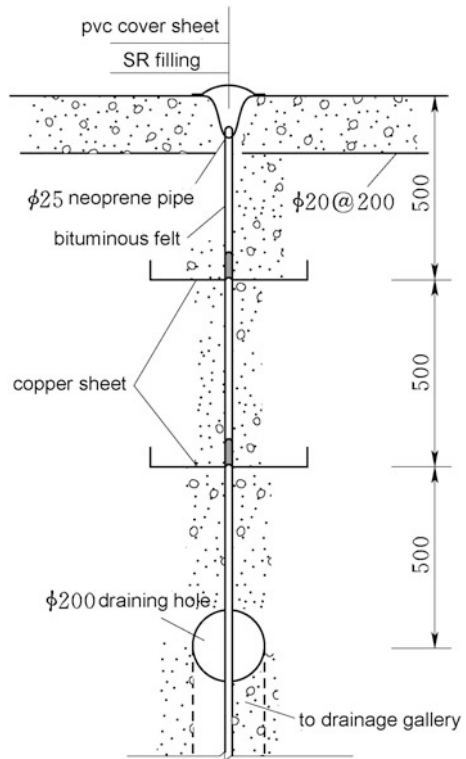
If a RCC dam uses CVC on its upstream and downstream faces, water stops for transverse joints are installed in the CVC similar to that of whole CVC gravity dams. Figure 7.62 shows the joint structure of the Longtan Dam (China, $H = 192$ m).

(b) Anti-seepage devices

Although the seepage resistance index of RCC may be designed higher than W_6 , the upstream anti-seepage devices are still demanded due to the lack of confidence of owners and designers with regard to lift joints as weak planes if their surface treatment cannot be guaranteed. Under such circumstances, segregation and cold joints in the RCC will appear, and heavy seepage/leakage through lift joints will be inevitable. Therefore, the treatment of surface layers is worthy of full care, and the following measures are widely exercised.

- ① Using CVC with a thickness of 2–3 m as an anti-leakage/leakage device is recommended by the Japanese RCD, and in CVC, the transverse joints with 2–3 water stops are installed. A much thinner CVC thickness around 0.3–1.0 m is adopted in USA, e.g., 45 cm for the Galesville Dam ($H = 50$ m) and 30 cm for the Middle Fork Dam ($H = 38$ m), and only one seal is installed in transverse

Fig. 7.62 Structure of the transverse joint (unit: cm)—the Longtan Dam (China, $H = 192$ m)



joints. As a result, higher leakage is reported for these dams. The first generation of RCC dams in China [e.g., the Tianshengqiao No. 2 Dam ($H = 58.7$ m), the Tongjiezi Dam ($H = 82$ m), the Daguangba Dam ($H = 57$ m), the Yantan Dam ($H = 110$ m), the Shuikou dam ($H = 100$ m), the Wan'an dam ($H = 58$ m), and the Guanying Dam ($H = 82$ m)] had adopted the Japanese RCD. Due to the complicity resulted from using two different kinds of concrete, nowadays this method is employed only under special circumstances in China.

- ② Various attempts to improve the profile type have been exercised in China, including the installation with asphalt mortar wall on the upstream faces (6 cm thick) in the Kengkou Dam ($H = 56.8$ m), with reinforced concrete (2.5–6 cm thick) in the Longmentan Dam ($H = 56.6$ m), with precast block in the Shuidong Dam ($H = 63$ m). However, all these measures did not perform so well according to the field observation after commissions.
- ③ Additional anti-seepage devices such as the PVC membrane may be employed for RCC dams. For a low dam, precast framework on the upstream may also be effective to control leakage, such as the Winchester Dam (USA, $H = 23$ m); between the framework and dam, a PVC cushion was filled. PVC membranes are used for many RCC dams in other countries, excluding Chinese RCC gravity dams.

- ④ The Chinese RCC gravity dam construction in recent twenty years have been shifting to use all RCC structure with GEVRCC of 2–3 m in thickness on the upstream face. They were successfully practiced in the Jiangya Dam, the Dachaoshan Dam, the Mianhuatan Dam, and the other RCC arch dams. The treatment of lift joints is accompanied by adding 1–1.5 cm thick cementitious and fly ash mortar in the region of 2-grade RCC. Although experiences had proved that such a kind of structure is suitable for high RCC dams, special researches are believed to be undertaken for RCC dams higher than 150 m. The RCC layer of high cementitious material and fine aggregate (2–3 m thick) also has been successfully applied to the upstream seepage protection, for instance, the Rongdi Dam ($H = 56.3$), the Wenquanbao Dam, the Changshun Dam ($H = 69$ m).

(c) Galleries

The number of galleries in dam body should be as few as possible, to simplify the construction of RCC dams. According to the statistics, for RCC dams lower than 50 m, galleries may be omitted; for RCC dams higher than 50 m, at least one gallery is required. In Japan, only one gallery of foundation grouting and drainage is installed for medium- to-high dams, and two rows of galleries are installed for dams up to 100 m. The Upper Stillwater Dam (USA, $H = 87$ m) and the Kengkou Dam (China, $H = 56.8$ m) installed one foundation grouting and drainage gallery only. There are several rows of galleries in China's high RCC dams; for example, the Dachaoshan RCC dams used 2 rows, the Jiangya Dam used 3 rows, and 6 rows are used for the Longtan dam.

The best location of galleries should be just behind the low permeable 2-grade RCC not far from the upstream face. The drainage galleries can be located in CVC cushion layers, if the thickness is enough.

The methods of gallery construction in RCC dams have varied widely, ranging from very rough RCC to smooth cast-in-place or precast conventional concrete. Generally, there are three types as shown in Fig. 7.63, in which the shadow portion is CVC.

(d) Dam body draining

The diameter and spacing of draining hole is 50–70 cm and 3 m, respectively. There are many manners to make draining holes in dam body, such as plastic tubes filled with sand and porous concrete pipes, but all these would fail due to the heavy roller compaction. Therefore, it is believed that more reliable draining holes would be formed by post-drilling.

Figure 7.64 shows the profile of the Suofengying Dam (China, $H = 121.81$ m), and on its up- and downstream faces, there are GEVRCC layers for the protection of internal RCC, and in the dam body, the drainage gallery and draining holes are installed.

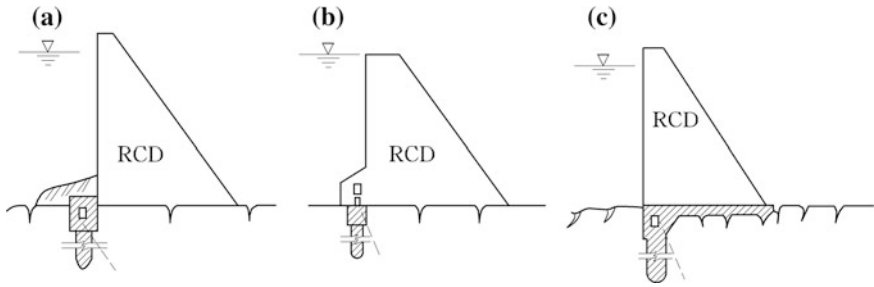


Fig. 7.63 Layout of foundation grouting and drainage gallery in RCC gravity dams

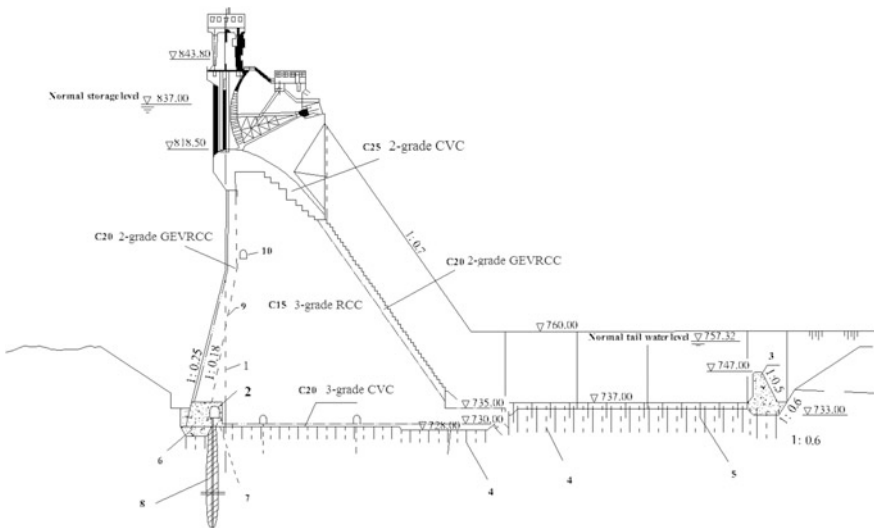


Fig. 7.64 Overflow spillway monolith—the Suofengying Dam (China, $H = 121.81$ m). 1 dam axis; 2 drainage and grouting gallery; 3 end sill; 4 rock bolt; 5 drainage hole; 6 C20 CVC dental; 7 drainage curtain; 8 grouting curtain; 9 draining pipe; and 10 drainage and inspection gallery

7.9.4 Construction of RCC Dams

There are two directions in transporting concrete to a dam site: horizontal and vertical. Using dump trucks to directly transport concrete onto placing plane is simple and fast for a wider valley, but the access road sometimes may be rather expensive. To avoid the pollution of placing surface, truck wheels must be thoroughly washed, and the cleaning water must be drained outside the placing plane. Measures should be taken to avoid segregation during the delivery from dump trucks. Another method is to use conveyer belts, which is more advanced

equipment to transport RCC mixtures but more expensive. The advantages of the conveyer belt are no segregation, easy moving, and continuous placement of concrete. Cable cars and port cranes may be used as additional means.

The thickness of RCC layers is in general 30 cm. The time lag between layers should not be too long. Sometimes, 25-cm thick layers are also applicable, where the area of placing plane is too large. The spreading should be along the direction of dam axis, generally using bulldozers.

To improve the impermeability for 2-grade RCC, a thin additional layer of cement–fly ash mortar may be spread on the surface of layers. At beginning, in the Rongdi Dam and the Puding Dam, for example, such spreading was done by manpower, which will influence the speed of construction and quality. Later on, a type of loaders was used in the Jiangya Dam. However, on the corners or sides, where the machine is not able to reach, manpower has to be used. The spreading surface should be inclined in the direction of upstream for a better stability against sliding.

Compaction is the main means to get high density of RCC. Vibrating rollers are selected according to the thickness of layers, the area of placing plane, the workability of RCC, and the maximum diameters and kinds (artificial or natural) of aggregates, by determining their exciting force, frequency, amplitude, speed, and other parameters.

Most completed China's RCC dams used German BW vibrating rollers, which were formerly designed for the compaction of rockfill, and lately were employed for the compaction of RCC after 1980. Special light rollers or other hand rollers should be available for the placement near forms or frameworks.

For the GEVRCC, the cementitious mortar is added in the upstream region of 0.3–0.5 m thick to produce high slump concrete which is compacted by ordinary vertical vibrators.

7.10 Other Types of Gravity Dams

7.10.1 Slotted Gravity Dams

1. Working features

Slotted gravity dam is basically a variant of the solid gravity dam by introducing intermediate space in the central portion of transverse joints. With a slotted gravity dam, the following features may be summarized:

- With free drainage of the foundation from the slots, uplift on the dam base is considerably reduced;
- The horizontal section is nearly I-shaped, which has larger geometric moment of inertia for better dam strength condition; and

- The loads and working conditions against a slotted dam are exactly the same as those that against a solid gravity dam except the vertical hydrostatic load presented by the water on a slotted gravity dam is larger;

Due to the above features, a slotted gravity dam requires 10–20 % less concrete amount than a solid gravity dam.

- The formwork and reinforced steel used in the building of slotted gravity dam account for higher unit cost than that of solid gravity dam and will ultimately offset a part of costs saved by the volume reduction;

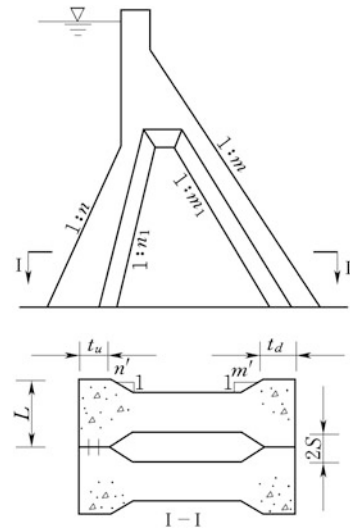
For example, the Xinganjiang Slotted Gravity Dam (China, $H = 105$ m) had an unit cost of concrete 8.4 % higher, and a total cost of concrete 10 % lower, than that of its solid dam alternatives.

- Slots within dam facilitate the inspection and observation works as well as the maintenance and repair works during the service period;
- Post-cooling is still indispensable, and the lateral exposure faces of slots may be more vulnerable to cracking damage during the construction period;
- Lateral stability is lower compared to solid gravity dams, under the action of seismic shaking; and
- Generally, slotted gravity dams are disadvantageous on aspects of project layout and construction conditions, compared to solid gravity dams (Fig. 7.65).

2. Profile

The profile of a slotted gravity dam is more complicated than solid gravity dams (Fig. 7.66), whose major profile sizes are as follows:

Fig. 7.65 Configuration of slotted gravity dam



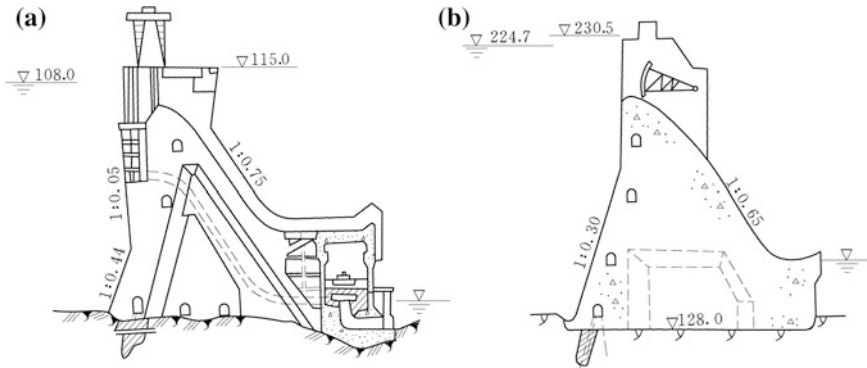


Fig. 7.66 Representative slotted gravity dams in China. **a** Xinganjiang Dam ($H = 105$ m); **b** Panjiakou Dam ($H = 107.5$ m)

- Thickness of the dam monolith L , which is usually ranged from 15 to 24 m;
- Ratio of slot width to dam monolith thickness $2 S/L$, which is commonly ranged from 0.2 to 0.4. A wider slot may save more concrete, but induce larger tensile stresses, particularly in the areas near upstream face and the central portion. When the ratio $2 s/L$ is over 0.5, slotted gravity dams are actually transformed into massive-head buttress dams, which will be discussed later in this Chapter;
- Up- and downstream slopes n and m , as well as the elevations of the knick points v_n and v_m . A majority of China’s slotted gravity dams adopt $n = 0.3\text{--}0.5$. The parameters m , v_n , and v_m are selected according to the requirements for strength, stability, and structure arrangement;
- Thicknesses of up- and downstream faces t_u and t_d . The thickness t_u should meet the requirements for strength, anti-seepage, foundation grouting and drainage gallery, and dam body-draining system. Usually $t_u \geq 0.1 h$ and is not smaller than 3.0 m, in which h is the headwater depth above the horizontal section concerned. The thickness t_d is decided according to the requirements for strength and construction and is usually selected within 3–5 m;
- The neck slopes n' and m' are commonly selected in the range of 1–2.

Table 7.9 lists several representative slotted gravity dams with their basic profile data.

7.10.2 Hollow Gravity Dams

A hollow gravity dam, also named as arch-abdomen dam, has large hollow space left within the dam body along the dam axis, for the purposes of reducing the weight and more effective use of concrete, or sometimes, to accommodate a power plant.

Table 7.9 Representative slotted gravity dams

Name	Country	Height H (m)	Upstream sloping n	Downstream sloping m	Thickness of dam monolith L (m)	Width of slot $2S$ (m)	Ratio of slot width and dam monolith thickness $2S/L$
Krasnoyarsk	Russia	124	0	0.72–0.75	10–15	3–5	0.30–0.333
Bratsk	Russia	127	0	0.8	22	3–7	0.136–0.318
Panjiakou	China	107.5	0.3	0.7	18	3	0.445
Xinganjiang	China	105	0.44	0.8	20	8	0.40
Danjiangkou	China	97	0.53	0.67–0.75	15–24	4–6	0.25–0.267
Jianxi	China	147	0.24	0.7	17–23	4–5	0.235–0.218
Qingshiling	China	143.5	0.45	0.65	18	7.4	0.40
Yantan	China	108	0.3	0.7	19	6	0.316

Table 7.10 Representative hollow gravity dams in China

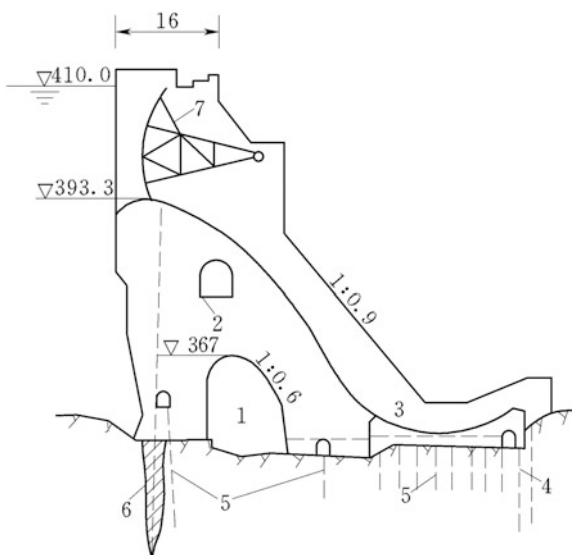
Technical index		Fengtang	Fengshuba	Niululing	Yanwutan	Shiquan	Gutian 4
Installation capacity (MW)		400	150	80	9	135	34
Type of power plant		Within dam	Within dam	Within dam	Diversion	Dam toe	Within dam
Maximum height (m)		112.5	91.5	90.5	66.0	65.0	31.0
Base width (m)		60.7	86.5	68.0	50.6	41.0	26.2
Size of hollow	Length (m)	255.8	57.0	81.3	59.0	102.5	4.2
	Width (m)	20.5	25.5	22.4	16.5	14.0	6.9
	Height (m)	40.1	31.25	28.5	24.0	15.0	9.7
Concrete amount (10^4 m^3)		107.5	73.1	40.7	9.7	37.0	0.19
Steel consumption per cubic meter of concrete (kg)		7.1	6.2	7.3	0.8		7.3

Since the 1970s, China had built six hollow gravity dams as listed in Table 7.10.

1. Profile

A typical arch-abdomen profile is shown in Fig. 7.67. The arch-abdomen is in the shape of ellipse whose axis is tilted in the direction of upstream with an angle of 60° – 70° , which is nearly coincident to the resultant force exerting on the arch-

Fig. 7.67 Profile of the hollow gravity dam (unit: m)
 —the Shiquan Project (China, $H = 65.0 \text{ m}$). 1 lower hollow; 2 upper hollow; 3 submerged bucket; 4 grouting hole; 5 draining hole; 6 grouting curtain; and 7 radial gate



abdomen. The height of arch-abdomen is about one-third of the dam height; the width of arch-abdomen, the front leg, and rear leg account, respectively, for nearly one-third of the dam base width of which the front leg can be a bit of wider.

2. Working features

- Arch-abdomen may improve the stress distribution in the profile and make better use of concrete strength;
- Vast hollow within the dam enables to accommodate hydropower plant; in this way, the conflict between plant layout and flood releasing may be better compromised;
- Hollow dams are adaptive to the uneven settlement of the foundation along the river stream;
- The lower portion of hollow dam has less concrete placement amount, which enables to use overtopping cofferdams of lower diversion flood standard, in this way to accelerate the construction schedule;
- The front and rear legs may be placed independently without longitudinal joints. The larger exposure faces are favorable for hydration heat dissipation during the construction period;
- The formwork and reinforced steel consumption of hollow gravity dams are higher and will ultimately offset rather portion of the costs saved by concrete reduction, particularly in the modern times.

The total costs of the Shiquan Dam, the Fengshu Dam, and the Fengtan Dam were saved by 24.73, 34.72, and 11.86 %, respectively. However, due to the complex in the design and construction, nowadays hollow gravity dams are rarely constructed.

7.10.3 Stone Masonry Gravity Dams

Dry-laid-stone dams are not considered here in this book.

Masonry dams are mainly made of stones and bricks. Stone masonry dams are normally constructed of closely placed large stones with the spaces in between filled with mortar. Stone masonry dams are distinguished from cyclopean concrete dams, in which large stone “plums” are embedded in concrete with the spaces in between filled with concrete. Masonry dams are either gravity type or arch type (Creager 1917). The largest masonry dam in the world is the Nagarjunasagar Dam in India, which is of 124.6 m high and 1450 m long.

Stone masonry dams are constructed without regular lifts or vertical contraction joints. The stone blocks are fit together as tightly as possible, but often have large gaps in between. Small rock chips or “spalls” are often placed with the mortar between the larger stone blocks. The mortar is composed of varying proportions of sand and cement and is either packed into place by hand or grouted in place. Roughly, 50 % of a stone masonry dam is stone blocks, 25 % is spalls, and 25 % is mortar.

The unit weight of stone masonry dams may vary considerably, depending on the type and percentage of stone blocks. Generally, the weakest material in a stone masonry dam is the mortar between stone blocks. In many old stone masonry dams, the deterioration of the mortar between stone blocks is responsible for leakage and abnormal deformation. Often, the thin layer of mortar is cracked due to the different properties of the stone and the mortar. Therefore, unless there is a preponderance of evidence otherwise, the mortar should be assumed to be cracked and have no cohesion in the design.

Stone masonry dams had long history in ancient China. The Lingqu Canal located in the Guangxi Province of China and completed in 214 BC connects the Xiangjiang River (which flows northward into the Yangtze River) to the Lijiang River (which flows southward into the Gui River and Xijiang River, the latter is a tributary of the Pearl River) by the installation of one large and one small masonry dams, respectively, and thus is a part of a historic waterway between the Yangtze River and the Pearl River Delta. It was the first contour canal in the world to connect two river basins, which enabled vessels to travel as far as 2000 km from the latitude of Beijing to Hong Kong. Another earliest masonry dam still in service for irrigation in China is believed to had been built in 833 whose name is Tuoshan Yan (Weir), and it was built on the Zhangxi River near the Ningbo city, Zhejiang Province. The weir is a gravity structure of 27 m high and 126 m long.

In the human history, due to the lower level of the productive forces and high population in the countries such as India and China, the gravity dams were all made of stone. Stone masonry dams were thrived in China particularly around the 1960s–1970s. Table 7.11 lists several representative China's masonry gravity dams. But

Table 7.11 Representative stone masonry dam in China

Name	Location	Dam type	Dam height (m)	Base wideness (m)	Storage capacity (10^4 m^3)	Masonry type	Year of completion
Zhuzhuang	Hebei	Gravity	95	111	43,600	Grouted rubble	1979
Baoquan	Henan	Gravity	107.5	102.9	6850	Grouted rubble	Heightened in 2007
Yudong	Yunan	Gravity	87	84.9	36,300	Grouted rubble	1998
Shimen	Henan	Gravity	90.5	79	3000	Grouted rubble	1974
Qunying	Henan	Gravity arch	101.3	52	1900	Grouted rubble	1971
Na'an	Guangxi	Massive head	56	43.90	2915	Concrete for massive head, stone masonry for buttress	1974
Yegoumen	Hebei	Multi-arch	45	5	5000	Grouted rubble	1976
Yanwutan	Hunan	Hollow gravity	66	50.6	1030	Grouted rubble, block stone, concrete	1979
Xiaolongtan	Hebei	Frame filled with ballast	39.6	34.6	700	Stone masonry	1972

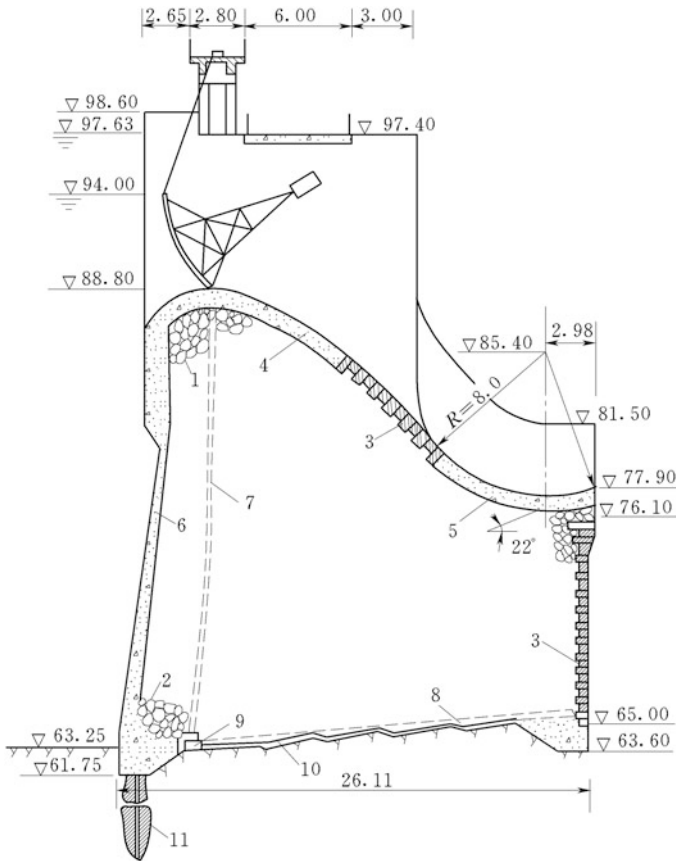


Fig. 7.68 Overflow spillway monolith (unit: m)—the Shuifumiao Project (China, $H = 35.8$ m). 1 M2.5 cement mortar grouted rubble; 2 M5 cement mortar grouted rubble; 3 M7.5 cement mortar - rubble masonry; 4 C15 concrete; 5 C20 concrete; 6 C15 concrete cutoff wall; 7 draining pipe ($\Phi 15@ 1.9$ m); 8 gutter of $30\text{ cm} \times 30\text{ cm}$; 9 sump channel ($30\text{ cm} \times 30\text{ cm}$); 10 C10 concrete cushion; and 11 grouting curtain

nowadays, the masonry dams are rarely constructed in China, except for very small heights or in remote mountainous villages.

Figures 7.68 and 7.69 show the profiles of the overflow dams in the Shuifumiao and Fengtuo projects, respectively.

7.11 Buttress Dams

Buttress dams are those in which the upstream face is held up by a series triangularly shaped buttresses. Buttress dams evolved from solid gravity dams, by eliminating the extra concrete and meanwhile eliminating most of the uplift

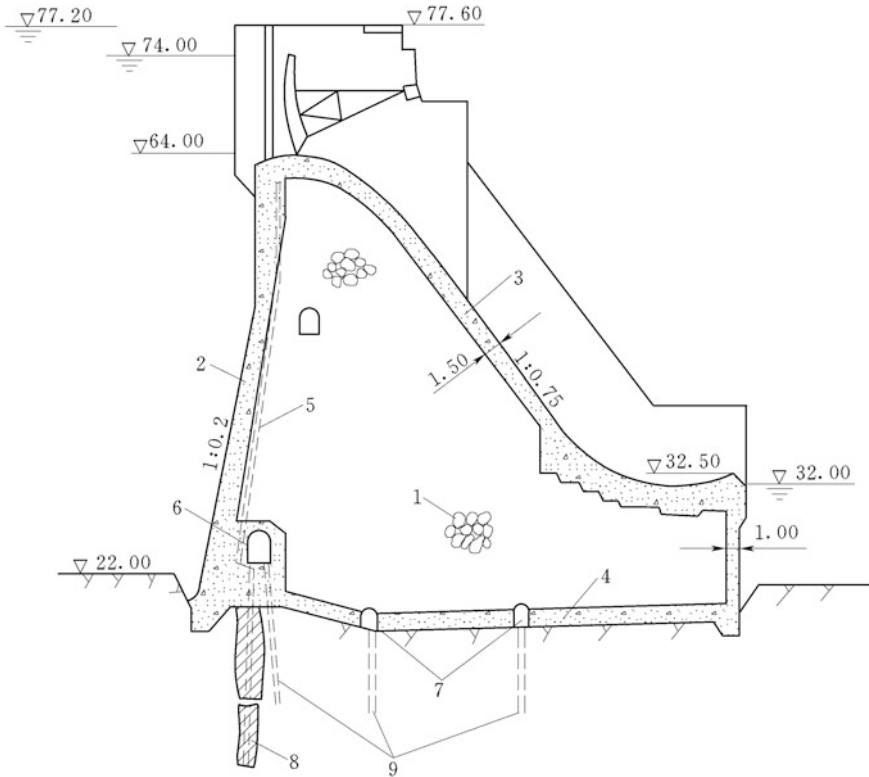


Fig. 7.69 Overflow spillway monolith (unit: m)—the Fengtou Project (China, $H = 60.1$ m). 1 M10 fine aggregate mortar-rubble masonry; 2 C15 concrete; 3 C20 concrete; 4 concrete cushion (1.5 m thick); 5 draining pipe; 6 grouting gallery; 7 foundation draining gallery; 8 grouting curtain; 9 foundation draining hole

pressures. Stability is further enhanced by flattening the upstream slope so that the weight of water performs as a major stabilizing load. Modern buttress dams are usually made of concrete or reinforced concrete. For small dams, masonry materials also may be applied, except for flat-slab type.

Buttress dams were originally developed to help conserve water in areas where materials were either in scarce supply or expensive. They were used mostly for irrigation and in mining operations. Some of very old buttress dams ever built actually dated back to the Roman Empire. Approximately one-third of all the dams built on the Iberian Peninsula (Spain) were buttress dams (Jansen 1980; Schnitter 1994). At the beginning of the twentieth century, there was a period of wide spreading of buttress dams due to the development of reinforcement concrete technique.

7.11.1 Classification of Buttress Dams

Buttress dams are distinguished as massive-head type, flat-slab (deck) type, and multi-arch type.

- ① In a massive-head buttress dam, there is no deck slab. Instead of the deck, the upstream edges of the buttresses are flared to form massive heads which span the space between the buttresses (Fig. 7.70a).
- ② A flat-slab buttress dam consists of a series of inclined decks supported by buttresses. Buttresses are triangular concrete walls which transmit the water pressure from the deck slab to the foundation. Buttresses are compression members. The deck is usually a reinforced concrete slab supported between the buttresses (Fig. 7.70b).
- ③ In a multiple-arch buttress dam, the deck slabs are replaced by horizontal arches supported by buttresses. The arches are usually of small span and made of reinforced concrete (Fig. 7.70c).

7.11.2 Features of Buttress Dams

Compared with solid gravity dams, buttress dams have the following features:

- Buttress dams require less concrete consumption than gravity dams. This is due to the uplift pressure being generally no longer a major factor influencing the stability of dam and the vertical component of the water pressure on deck preventing the dam from overturning and sliding failures. Compared to solid gravity dams, buttress dams may save up to 30–50 % of concrete consumption.
- Ice pressure is relatively less important, because it tends to slide over the inclined deck.
- Powerhouse and water treatment plant can be accommodated between buttresses. The back of the deck and the foundation between buttresses are accessible for inspection.
- It can be easily raised subsequently by extending buttresses and deck slabs.

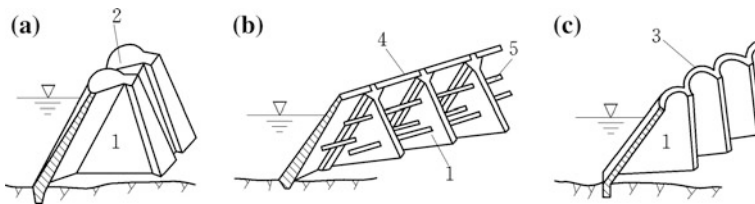


Fig. 7.70 Types of buttress dams. **a** Massive-head dam; **b** flat-slab dam; **c** multi-arch dam. 1 buttress; 2 massive head; 3 multi-arch; 4 flat-slab; 5 buttress brace (stiff girder)

- Massive-head type has similar overflow discharge ability to that of solid gravity dam, whereas flat-slab type only has lower ability of overflow discharge due to the potential strong vibration of the thin structures induced by flow, and multi-arch type is totally not suitable for overflow.
- Buttress dams have poor lateral stability. The buttresses are thin and independent walls, which have much lower stiffness in the lateral direction than that in the longitudinal (stream flow) direction. As a result, they call for special measures to ensure the lateral overturning and cracking safety against seismic actions. In addition, the buttresses are walls bearing compressive stress, and buckling failure may occur under the load excess of allowable critical value. Buttress bracing or trussing are customarily installed between adjacent buttresses, to prevent buckling failure under compressive loads.
- Buttress dams should be constructed on relatively stronger foundations. The buttresses exert higher pressure on their bases; hence, the quality of foundation rock should be competent. Particularly, the multi-arch dams are sensitive to the uneven settlement of buttresses due to the statistically indeterminate multi-arches. However, the flat-slab dams have better adaptability to the uneven settlement of foundation, attributable to the hinged connection between the flat-slabs and buttresses, and may even be built on soil foundation where the dam height is limited within 30–50 m.
- Buttress dams require larger amount of reinforcement. The steel consumption for flat-slab type and multi-arch type is around 30–40 kg per cubic meter of concrete, and for massive-head type it is around 2–3 kg per cubic meter of concrete which is similar to slotted gravity dams.
- Heat dissipation condition is good in buttress dams, and as a result, the speed of construction is higher. However, buttress dams require costlier formwork (particularly for multi-arch type), and more skillful labors.
- Buttress dams are more susceptible to aging deterioration. Because the upstream deck slab is thin, its deterioration may have very serious impact on the dam safety.
- Buttress dams are not suitable in chilly area.

7.11.3 Massive-Head Buttress Dams

Massive-head dams are buttresses having thick heads on the upstream side as barriers. The buttresses are separated by joints and may work independently of each other, to accommodate heterogeneous foundations and temperature fluctuations (Fig. 7.71). Among the buttress dams built in China, massive-head buttress type accounts for large percentage. In 1955, the 82-m-high Mozitan Massive-head Dam with double-walled buttresses was completed on the tributary of the Huaihe River. Later on, the buttress dams over 100 m such as the Zhexi in the Hunan Province and

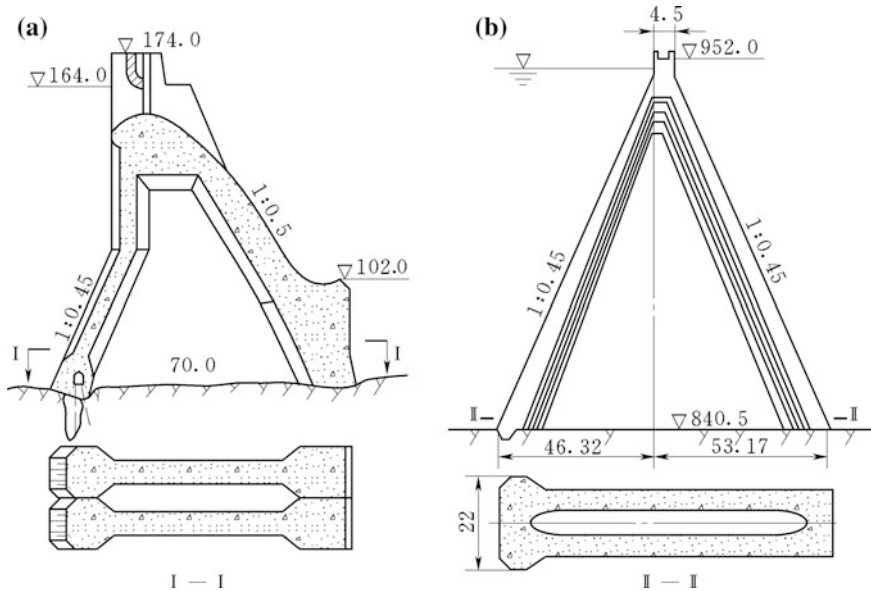


Fig. 7.71 Profiles of massive-head buttress dam (unit: m). **a** Massive-head dam with single-wall buttress; **b** massive-head dam with double-walls buttress

the Hengren in the Liaoning Province were erected. Many massive-head buttress dams were built in the medium-to-small hydraulic projects.

The highest massive-head buttress dam in the world is the Itaipu Dam (Brazil and Paraguay, $H = 196$ m).

Massive heads are so shaped to minimize tensile stresses within them, which in turn minimizes or eliminates the need for reinforcement. For a properly shaped head, tensile stress should appear only as a minor principal stress near the center of the head. There are basically three types of massive-head, namely the Tee-head, the diamond-head, and the round-head, as shown in Fig. 7.72. The Tee-head is the

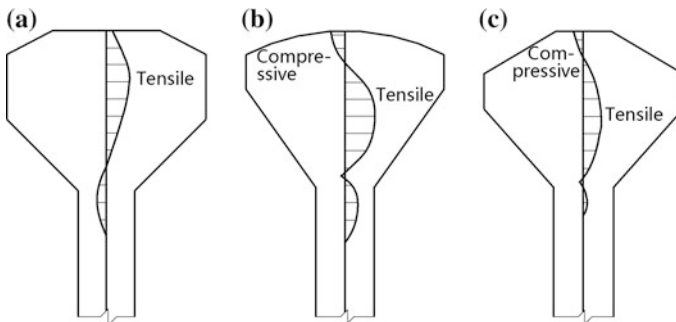


Fig. 7.72 Types of massive-head. **a** Round-head; **b** tee-head; **c** diamond-head

simplest in construction but tensile stress is almost inevitable on its upstream face; the round-head is the most perfect with regard to the distribution of water pressure-induced stresses, largely in compressive, but is complex in construction; the diamond-head makes good compromises between the Tee-head and the round-head, and therefore it is most prevalent.

Horizontally, the cross section of buttress can have four basic types as shown in Fig. 7.73.

1. Solid single-wall buttress

Solid single-wall buttresses of 3–8 m thick are spaced at not more than 15–18 m apart between their axes. They have advantages of simple in structure and convenient for construction and facilitating for observation and repairing, but they have lower lateral stiffness and poor concrete thermal insulation conditions in chilly areas. Solid single-wall buttresses are suitable for the medium-to-low dams.

2. Enclosed single-wall buttress

In modern usage, a buttress dam has the external appearance similar to the gravity dam, but which has large open areas inside. They are actually the buttress dams, in which the downstream portion is covered with a reinforced concrete slab or with flaring of the downstream end of buttresses. They are often employed for overflow spillway on buttress dams or housing power plant. This kind of buttress dam has higher lateral stiffness and good insulation condition, and therefore it is widely employed in seismic and chilly regions.

3. Open double-walls buttress

Spaced at 22–26 m, double-walls buttresses have much higher resistant to lateral forces than single ones, but are complicated for construction. The diversion bottom outlets and penstocks may be accommodated within the hollow in the buttress. Open double-walls buttresses are mainly used for high dams.

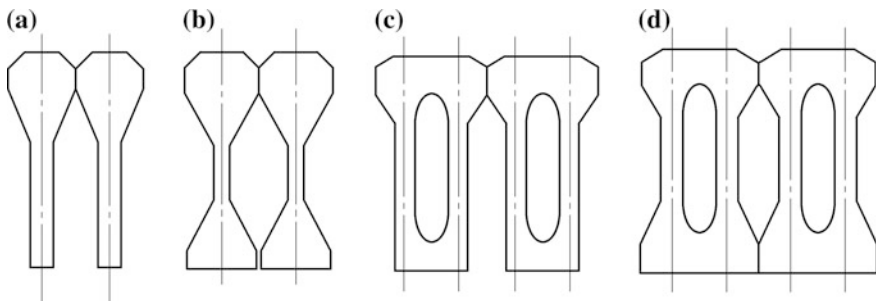


Fig. 7.73 Horizontal section of buttresses. **a** Open single-wall buttress; **b** enclosed single-wall buttress; **c** open double-walls buttress; **d** enclosed double-walls buttress

4. Enclosed double-walls buttress

This type has the highest lateral stiffness and the most complication in construction.

Transverse joints are installed between massive-heads to ensure the independent work of each dam monolith and to adapt the uneven settlement of foundations as well as the temperature fluctuations. Water stops in the joints are similar to that of gravity dams. The transverse joints also may be temporary which are grouted after the cooling of concrete to form a monolithic structure, for better resistance to the seismic actions.

Longitudinal joints are necessary for the purposes of preventing cracks due to temperature and dry shrinkage, whose types and grouting method are similar to that of solid gravity dams.

7.11.4 Flat-Slab and Multi-Arch Buttress Dams

1. Flat-slab buttress dams

The first flat-slab buttress dam was designed and patented by Nils F. Ambursen in 1903. As a result, this type of dam is also referred to as “Ambursen dam.” The flat-slab buttress dam is a buttress dam in which the upstream face is a series of thin flat-slabs made of reinforced concrete. Typically, the slabs are simply supported on the buttresses which make the structure more flexible. As a result, ordinary foundation movements have minor effect on the stress distributions in the dam. Compressible materials and water stops are normally provided between the slabs and the corbels of the buttresses to allow for movement yet remain watertight. However, the slabs can be continuous in some designs, making the structure more rigid. The top thickness of slab is dependent on the requirements for climate, structure, and construction, usually not smaller than 0.2–0.5 m. The bottom thickness of slab is decided by the structural strength.

Single buttresses are generally employed at space of 5–10 m, whose top thickness is 0.3–0.6 m and the bottom thickness is decided by the structural strength. The basic profile is decided by the safety of stability against sliding and tensile strength at upstream face. The commonly adopted upstream and downstream slope angles are 40°–60° and 60°–80°, respectively.

Flat-slab buttress dams may be either overflow or non-overflow and may be built on either rock foundation or soil foundation. Flat-slab buttress dams are suitable for medium- to low head project located in mild climate regions. Figure 7.74 shows the Longting Project (China, $H = 43.5$ m) completed in the 1970s. The highest flat-slab buttress dam in the world is the Escaba Dam (Argentina, $H = 83$ m) completed in 1948. Flat-slab buttress dams are seldom built in recent years for their shortcomings with large steel consumption, poor lateral stability, and durability, except for small dam projects.

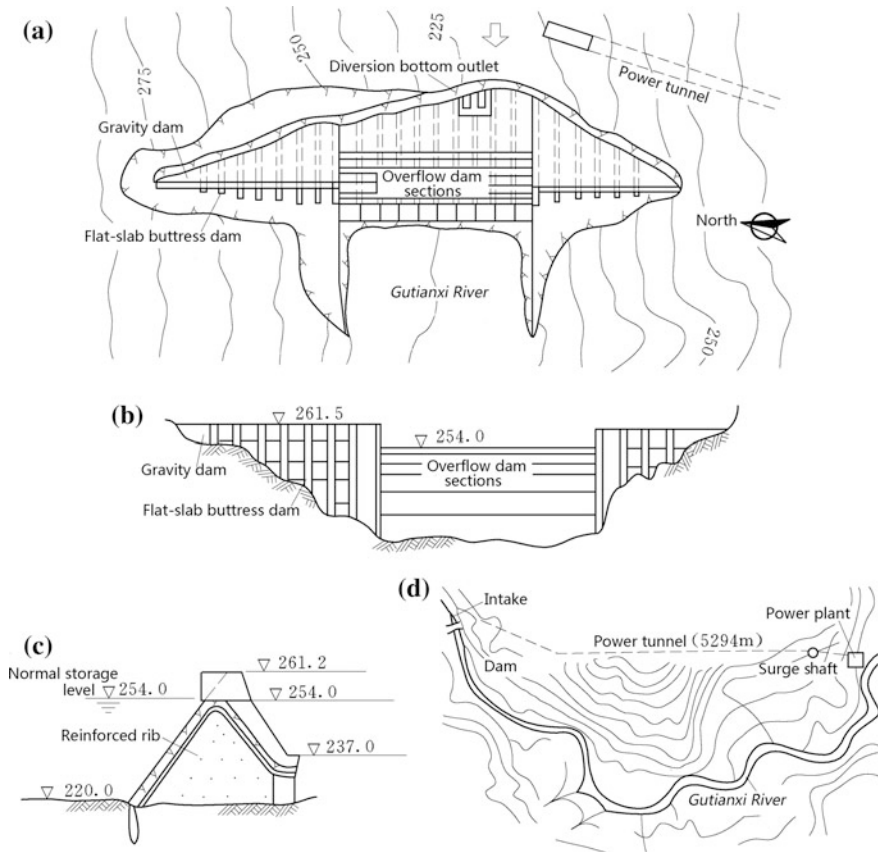


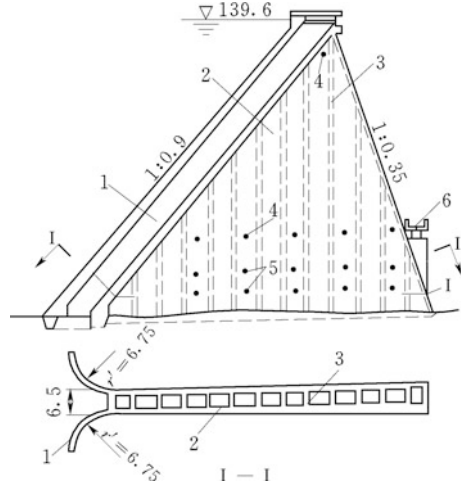
Fig. 7.74 The Longting Project (China, $H = 43.5$ m). **a** Plan of head works; **b** downstream elevations; **c** profile of overflow dam; **d** river morphology

2. Multi-arch buttress dams

Multi-arch buttress dams are those that the upstream face is a series of arches spanning between buttresses. The arches are generally semi-circular with central angles 100° – 180° , though non-circular arches may be used, too. The arches may be unreinforced or reinforced. The arches may be integral with the buttresses, making the structure rigid but susceptible to the damages due to uneven foundation settlements. Multi-arch buttress dams impose significant lateral load on buttresses. This load is resisted in part by adjoining arches. As a result, failure of one arch could cause catastrophic failure of the entire dam.

Multi-arch buttress dams were the first type of buttress dam ever built, such as the Roman buttress dam near the village of Esparragalejo (Spain, $H = 5.6$ m). One of their advantages is less reinforced steel consumption. The arch design also permits the spanning of greater distances between buttresses.

Fig. 7.75 Multi-arch Buttress Dam (unit: m)—the Meishan Project (China, $H = 88.24$ m). 1 arch; 2 bracing; 3 separating wall; 4 air vent hole; 5 draining hole; 6 access bridge



Multi-arch buttress dams are suitable on good rock foundation in mild climate areas, for their poor adaptability to the uneven foundation settlement and temperature fluctuation. Deterioration and cracking of the concrete can expose the reinforcing steel to air and water, being responsible for steel corrosion. Therefore, the concrete tensile strength and seepage resistance are more rigorously observed.

Figure 7.75 shows the Meishan Multi-arch Buttress Dam completed in 1956 (China, $H = 88.24$ m). The arches have central angle of 180° and intrados radius of 6.75 m, the thickness at crest is 0.60 m and at base is 2.30 m. The double-walls buttresses are uniformly spaced 20 m apart.

At 214 m high and 1312 m long, the Daniel-Johnson Dam in Canada completed in 1968, formerly known as Manic-5, is the highest multi-arch buttress dam in the world. The dam is composed of 14 buttresses and 13 arches. Of the dam's 14 buttresses, the principal two that support the center arch are spaced 160 m apart at their base while the others are spaced about 76 m apart.

7.11.5 Development of Buttress Dams in China

Due to their unique merits and structural elegance, buttress dams occupy an important position in the history of dam engineering. The typical buttress dams constructed in China since the 1950s are the Foziling Multi-arch Buttress Dam ($H = 74.4$ m), the Meishan Multi-arch Buttress Dam ($H = 88.24$ m), the Mozitan Massive-head Buttress Dam ($H = 82.4$ m), the Shuanpai Massive-head Buttress Dam ($H = 58.8$ m), the Zhexi Massive-head Buttress Dam ($H = 104.0$ m), the Hengren Massive-head Buttress Dam ($H = 78.5$ m), the Xinfengjiang Massive-head Buttress Dam ($H = 105.0$ m), the Jingjiang Flat-slab Buttress Dam ($H = 54.0$ m), and the Longting Flat-slab Buttress Dam ($H = 46.0$ m).

Due to the shortcomings of thin and weak in structure, complex in construction, sensitive to temperature variation, lower in aging resistance, the buttress dam construction is on the wane. In the whole 1980s, only two massive-head buttress dams of the Xizhijiang ($H = 66$ m) and the Hunanzhen ($H = 129$ m) were built in China. Since then until the end of the 1990s, except in small and low dam projects, buttress dams were seldom practiced.

References

- American Society of Civil Engineers, United States Army Corps of Engineers (1994) Roller-compacted concrete (Technical engineering and design guides as adapted from the US Army Corps of Engineers). ASCE Press, New York
- Bowen R (1981) Grouting in engineering practice, 2nd edn. Appl Sci, New York
- Bradley JN, Peterka AJ (1957a) The hydraulic design of stilling basins: hydraulic jumps on a horizontal apron (Basin I). *J Hydraulics Div ASCE* 83(HY5):paper1401-1-1401-24
- Bradley JN, Peterka AJ (1957b) The hydraulic design of stilling basins: high dams, earth dams, and large canal structures (Basin II). *J Hydraulics Div ASCE* 83(HY5):paper 1402-1-1402-14
- Carlson RW, Houghton DL, Polivka M (1979) Causes and control of cracking in unreinforced mass concrete. *ACI J* 76(7):831-837
- Chanson H (2001-2002) Historical development of stepped cascades for the dissipation of hydraulic energy. *Trans Newcomen Soc* 71(2):295-318
- Chen SH, Yang ZM, Wang WM, Shahrour I (2012) Study on the rock bolt reinforcement for the gravity dam foundation. *Rock Mech Rock Eng* 45(1):75-87
- Creager WP (1917) *Engineering for masonry dams*. Wiley, New York
- Delocre FE (1866) *Mémoire sur la Forme du Profil à Adopter pour les Grands Barrages en Maçonnerie des Réservoirs*. Mémoires et Documents, Annales des Ponts et Chaussées, 2nd Sem, pp 212-272
- Dunstan MRH (2007) Overview of RCC dams at the end of 2006. In: Jia J et al (eds) *New progress on roller compacted concrete dams*. China WaterPower Press, Beijing, pp 9-17
- Egger P (1992) Ground improvement by passive rock bolts, experimental and theoretical studies, example. *Memorie GEAM*. 29(1):5-10
- Elevatorsky EA (1959) *Hydraulic energy dissipators*. McGraw Hill, New York
- Forbes BA (1999) Grout enriched RCC: a history and future. *International water power & dam construction*. Wilmington Business Publishing, Kent, pp 34-38
- Golzé AR (1977) *Handbook of dam engineering*. Van Nostrand Reinhold Company, New York
- Grishin MM (ed) (1982) *Hydraulic structures*. Mir Publishers, Moscow
- Hansen KD (1996) Roller-compacted concrete: a civil engineering innovation. *Concr Int* 15(3):49-53
- Hansen KD, Reinhardt WG (1991) *Roller compacted concrete dams*. McGraw-Hill, New York (USA)
- Harza LF (1949) The significance of pore pressure in hydraulic structures. *Trans ASCE*. 114(1):193-214
- Henny DC (1934) Stability of straight concrete gravity dams. *Trans ASCE* 99(1):1041-1061
- ICOLD (1989) *Roller compacted concrete for gravity dams—State of the Art (Bulletin 75)*. ICOLD, Paris
- ICOLD (1993) *Rock foundations for dams (Bulletin 88)*. ICOLD, Paris
- ICOLD (2000) *The gravity dam: a dam for the future—review and recommendations (Bulletin 117)*. ICOLD, Paris

- ICOLD (2003) Roller-compacted concrete dams—state of the art and case histories (Bulletin 126). ICOLD, Paris
- ICOLD (2005) Dam foundations. Geologic considerations. Investigation methods. Treatment. Monitoring (Bulletin 129). ICOLD, Paris
- Iliev S, Kalchev L (1981) Selecting the optimum cross section of a concrete gravity dam. *Water Power Dam Constr* 33(12):23–27
- Iqbal A (1993) Irrigation and hydraulic structures—theory, design and practice. Institute of Environmental Engineering & Research, NED University of Engineering & Technology, Karachi
- Isao N, Shigeharu J (2003) 30 years' history of roller-compacted concrete dams in Japan. In: Berga L et al (eds) Proceedings of the 4th international symp on RCC dams. AA Balkema, Madrid, pp 27–38
- Jansen RB (1980) Dams and public safety, a water resources technical publication. CO (Water and Power Resources Service, Bureau of Reclamation, US Department of the Interior), Denver
- Joshi CS (1980) Designing the profile of gravity dams. *Int Water Power Dam Constr* 31(1):28–30
- Karol RH (1990) Chemical grouting, 2nd edn. Marcel Dekker, New York (USA)
- Keener KB (1951) Uplift pressures in concrete dams. *Trans ASCE* 116(1):1218–1237
- Khatsuria RM (2004) Hydraulics of spillways and energy dissipators. CRC Press, New York
- Lévy MM (1895) Quelques considérations sur la construction de grands barrages. *Comptes-Rendus de l'Académie des Sciences* 6:288–300
- Liu ZM, Wang DX, Wang DG (eds) (2013) Handbook of hydraulic structure design, vol 1—Fundamental theories. China WaterPower Press, Beijing (in Chinese)
- Lo KY, Ogawa T, Lukajic B, Dupak DD (1991) Measurement of strength parameters of concrete-rock contact at the dam-foundation interface. *Geotech Test J* 14(4):383–394
- Ma GY, Chang ZH (2007) Theory and practice of grouting drainage and anchorage of rock mass. China WaterPower Press, Beijing (in Chinese)
- Mason PJ (1993) Practical guidelines for the design of flip buckets and plunge pools. *Int Water Power Dam Constr* 45(9):40–45
- Ministry of Water Resources of the People's Republic of China (SL319-2005) (2005) Design specification for concrete gravity dams. China WaterPower Press, Beijing (in Chinese)
- Ministry of Water Resources of the People's Republic of China (GB 50487-2008) (2009) Code for engineering geological investigation of water resources and hydropower. China Planning Press, Beijing (China) (in Chinese)
- Nagayama I, Jikan S (2003) 30 years' history of roller-compacted concrete dams in Japan. In: Key note paper in: 4th international symposium on roller compacted concrete (RCC) Dams. Balkema AA, Lisse, pp 27–38
- Novak P, Moffat AIB, Nalluri C, Narayanan R (1990) Hydraulic structures. The Academic Division of Unwin Hyman Ltd, London
- Pan JZ (1987) Design of gravity dams. Water Resources and Electric Power Press of China, Beijing (in Chinese)
- Panwar A, Tiwari HL (2014) Hydraulic energy dissipators—a review. *Int J Sci Eng Technol* 3(4):400–402
- Post-Tensioning Institute (1985) Recommendations for prestressed rock and soil anchors. Post-Tensioning Institute, Phoenix
- Price WH (1982) Control of cracking in mass concrete dams. *Concr Int* 4(4):36–44
- Rankine WJM (1881) Miscellaneous scientific papers: Report on the design and construction of masonry dams. Charles Griffin and Company, London
- Ru RH (1983) Gravity dams. Water Resources and Electric Power Press of China, Beijing
- Sazilly J (1853) Note sur un type de profil d'égal résistance proposé pour les murs de réservoirs d'eau. *Annales des Ponts et Chaussées*. 6:191–222 (in French)
- Schnitter NJ (1994) A history of dams: the useful pyramids. Balkema AA, New York
- Soderberg AD (1988) Foundation treatment of karstic features under TVA dams. Geotechnical aspects of Karst Terrain. *ASTM Geotechnical* 14:149–165 (Special publication)

- State Economy and Trade Commission of the People's Republic of China (DL5108-1999) (1999) Design specification for concrete gravity dams. China Electric Power Press, Beijing (in Chinese)
- State Economy and Trade Commission of the People's Republic of China (DL 5073-2000) (2000) Specifications for seismic design of hydraulic structures. China Electric Power Press, Beijing (in Chinese)
- State Economy and Trade Commission of the People's Republic of China (DL/T 5166-2002) (2008) Design specification for river-bank spillway. China Electric Power Press, Beijing (in Chinese)
- Stelle WW, Rubin DI, Buhas HJ (1983) Stability of concrete dam: case history. *J Energy Eng ASCE* 109(3):165–180
- Sun GY, Wang SY, Feng SR (2004) High RCC gravity dams. China Electric Power Press, Beijing (in Chinese)
- Sun Z (2004) Grouting in dam's rock foundation. China WaterPower Press, Beijing (in Chinese)
- Tatro SB, Schrader EK (1985) Thermal considerations for roller-compacted concrete. *ACI J* 82 (2):119–128
- United States Bureau of Reclamation (2005) Roller-compacted concrete: design and construction considerations for hydraulic structures. US Department of the Interior, Bureau of Reclamation, Technical Service Center, Denver
- USBR (1976) Design of gravity dams. US Government Printing Office, Denver
- USBR (1987) Design of small dams, 3rd edn. US Govt Printing Office, Denver
- Weaver K, Bruce D (2007) Dam foundation grouting. ASCE Press, Resto, No. 0-7844-0764-9
- Wise EC (2005) The day Austin died. *Penn Lines* 40(9):8–11
- Zhou JP, Dang LC (eds) (2011) Handbook of hydraulic structure design, vol 5—concrete dams. China WaterPower Press, Beijing (in Chinese)

Chapter 8

Arch Dams

8.1 General

There is a long history of arch dam construction. As early as in Roman era, the high bearing capacity of arch structures was realized. Dated back to the first century BC, the first known arch dam, the Glanum Dam, also known as the Vallon de Baume Dam, was built by the Romans in France (Jansen 1980; Schnitter 1994; Stelle et al. 1983). Around 1350, the Iranian built the Kurit Arch Dam (Iran, $H = 60$ m). Added 4 m height in 1850, it became 64 m high and remained the highest dam in the world until the early twentieth century (Jansen 1980; Schnitter 1994). The dam is still erect, even though part of its lower downstream face fell off. In the nineteenth century, European countries, such as Britain, France, Spain, and Yugoslavia, started to build modern arch dams. At the beginning of the twentieth century, arch dam practices were initiated in South America and Oceania. In 1910, USA built the 108-m-high Buffalo Bill Dam. During the 1920s–1940s, USA built several modern arch dams including famous arched gravity dam of 221 m high—the Hoover Dam. The arch dam technique achieved significant advances and was boosted after the Second World War. Only in Italy, more than 90 arch dams were built during 1955–1960, including the famous 265-m-high Vajont Dam. Before 2010, the highest arch dam in the world is the Inguri Dam (Georgia, $H = 271.5$ m, $T = 86$ m, $T/H = 0.33$), whose record was broken in 2010 by the completion of Xiaowan Arch Dam (China, $H = 294.5$) (Fig. 8.1).

China has an ancient civilization with outstanding tradition in the construction of dams and arch bridges, but it is pity that the history of arch dam in the country lagged behind (Zhu 1995). In 1928, a 27.3-m-high masonry arch dam was built near the Xiamen city of the Fujian Province, which is still in service. Several small masonry arch dams were also built in the Sichuan Province before 1950. In the 1950s, China completed the Xianghongdian Arch Dam ($H = 87.5$ m) and the Liuxihe Arch Dam ($H = 78$ m), after that the arch dam construction in China started to be prospered. According to the statistic data of CHINCOLD (Chinese Committee of Large Dam),

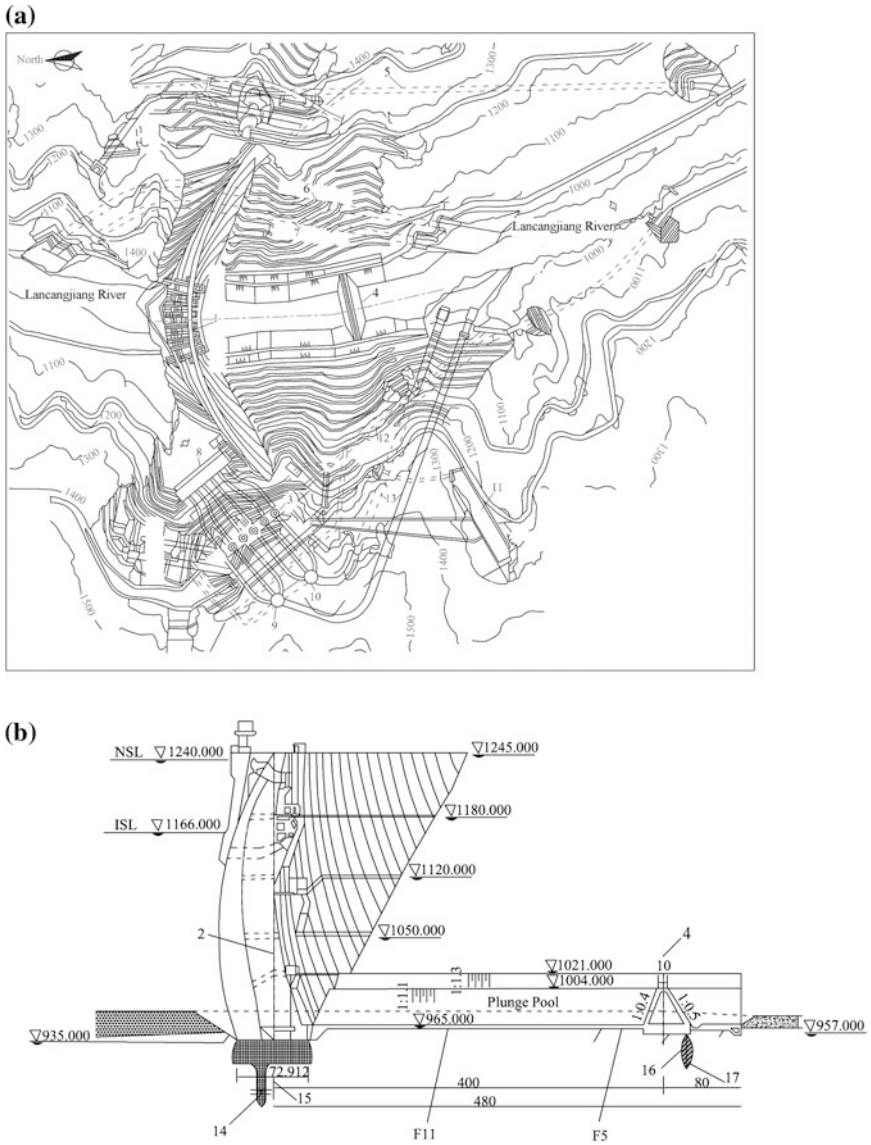


Fig. 8.1 The Xiaowan Arch Dam (unit: m) China, $H = 294.5$ m. **a** Plan; **b** profile of crown cantilever. 1 arch dam; 2 dam axis; 3 powerhouse; 4 auxiliary weir; 5 flood release tunnel; 6 diversion tunnel 2; 7 diversion tunnel 1; 8 intake of power tunnel; 9 tailrace surge chamber 1; 10 tailrace surge chamber 2; 11 switch yard; 12 access tunnel; 13 tailrace tunnels; 14 main grouting curtain; 15 main drainage curtain; 16 auxiliary drainage curtain; 17 auxiliary grouting curtain

at the end of 1998, China possessed 521 arch dams higher than 30 m including the Ertan Arch Dam ($H = 240$ m) and the Longyangxia Arch Dam ($H = 178$ m).

The “Development of the West Regions” policy of China since the new Millennium further accelerates the arch dam construction in the country. The Xiaowan Arch Dam (China, $H = 294.5$) completed in 2010 and the Jinping 1 arch Dam (China, $H = 305$ m) and the Xiluodu Arch Dam (China, $H = 278$ m) currently under the construction establish landmarks for the Chinese great achievement in the modern arch dam techniques.

8.1.1 Features of Arch Dams

An arch dam is a water retaining barrier curvilinear in plan, similar to a dome or shell, which resists horizontal loads mainly dependent on its support in the abutment banks of canyon. Providing a satisfactory valley shape and qualified foundation rock capable of supporting the load exerted on it, an arch dam offers significant advantages over other conventional dam types such as gravity and embankment (Creager 1917; Li 1982; USBR 1987a, b; National Reform and Development Commission of the People’s Republic of China 2006).

1. Load-bearing capacity

One of the remarkable differences between arch dams and gravity dams lies in the ways of transferring the load. The arch dam is usually designed initiatorily as a series of horizontal arch rings, and each is submitted to a constant radial hydrostatic pressure. These horizontally arch rings transfer the hydrostatic pressure to the abutments or in some instances to the gravity dam monoliths on the abutments, which in turn distribute the thrusts to the prepared rock surface. The proportion of load sharing between horizontal arch ring element and vertical cantilever element depends on their relative stiffness: For more narrow and deep valley, the arch rings have larger stiffness and share larger portion of loads, and the cantilevers have lower stiffness and share smaller portion of loads. Under the action of water pressure, the majority part of arch dam concrete is compressed. Since concrete in compression is much stronger than that in tension, the strength of arch dam body can be ensured more easily than the gravity dam. The overall stability of arch dams is provided by the reliable supports from the abutment rocks, i.e., it does not depend on the structure’s weight, as gravity dams. Therefore, the thickness of the arch dam (and hence the volume of concrete) is usually smaller than that of the gravity dam. For a most well-proportioned arch dam, the saving of concrete may be up to 1/3–2/3. However, in determining the expenditure, one must take into account the raised requirements for the concrete grade.

2. Safety

Arch dam is a kind of statically indeterminate structure which has strong stress-adjusting ability and load-bearing capacity. A well-designed arch dam transmits

fairly larger proportion of loads deep into the abutment bedrock. The overall failure is not easily occurred provided integral and sound foundation rock after proper treatments. Under overloading, local cracking may result in stress redistribution between arch rings and cantilevers, to prevent further failure of the entire dam. The two- or three-dimensionally stressed status may also raise the material strength. All these factors account for higher load-bearing capacity of arch dams. The structural experiments show that usually, the overload factor may be as high as 4–11. The structural experiment of the Fengle Arch Dam (Anhui Province, China, $H = 54$ m) provides a safety factor of 2.3 for cracking initiation and that of 11.0 for global collapse. A good prototype showing the outstanding overload capacity of arch dams was provided by the Vajont Dam (Italy, $H = 265$ m), and after three years of service, a landslide in 1963 has generated an immense water surge wave which overtopped the world's highest concrete arch dam at that time. This wave left its marks 238 m above the reservoir level (more than 100 m over the crest). 239 million m^3 of earth and rock from the landslide plunged and deposited in the reservoir, extending from the dam toe for a distance of about 1.61 km upstream (Kiersch 1964). Amazingly, except for local damage on the crest, the dam withstood the overpressures to which it was subjected.

Arch dams also perform well with regard to the earthquake action, and this is attributable to their integral and flexible structure. Many project prototypes verify their high earthquake resistance. The Ambiesta Dam (Italy, $H = 59$ m) was subjected to an $M = 9$ (Richter magnitude) earthquake in 1976, the observed maximum earthquake acceleration at the left abutment is 0.33 g, but no serious cracking damages were detected. The Deji Dam (Taiwan, $H = 181$ m) was subjected to an $M = 7.3$ earthquake in September 21, 1999, the estimated maximum earthquake acceleration on the dam foundation is 0.4–0.5 g, 2295 casualties and destruction of 20,815 houses were reported in the region, but the overall state of the dam is good after the disaster. In May 12, 2008, an $M = 8$ earthquake attacked Wenchuan, China. The Shapai RCC Arch Dam (China, $H = 132$ m) located 30 km from the epicenter, where the Mercalli intensity scale is 9, has suffered only minor damages by the fatal shaking.

3. Flood release

A traditional image was that the large flow discharge through arch dams is not permitted due to their thin structure. However, the practices in recent decades show that not only the large discharge may be released through the overflow spillways on dam crest, but also large-sized orifices may be applicable for arch dams, too. For example, in the Kariba Dam (Zambia and Zimbabwe, $H = 128$ m, $T = 24$ m), 6 orifices of $9.1 \text{ m} \times 9.46 \text{ m}$ are installed, the total discharge is $9500 \text{ m}^3/\text{s}$, and the unit flow rate is $176 \text{ m}^2/\text{s}$.

4. Effects of thermal action

Temperature variations that are usually not important for gravity dams will give rise to significant deflections and stresses in arch dams of statically indeterminate. The thermal stresses that result in internal forces push the arch dam moving in the

direction of upstream during the summer and downstream during the winter. Hence, it cannot be neglected in the course of design. According to the statistics, for a medium-to-low arch dam, of the total displacement induced by water pressure and temperature simultaneously, the temperature accounts for 1/3–1/2. The thermal action effects are more remarkable near the crest of the arch dams.

In conclusion, the arch dam is a kind of well-performed structure with regard to bearing capacity and duration, high overloading ability, reliable resistance for overtopping and earthquake, comparatively advantageous in economy and safety indices. Along with the technology development in the dam construction and foundation treatment, arch dams will be more and more prevalent in the dam engineering.

8.1.2 Topographic and Geologic Requirements for Arch Dams

Arch dams have rigorous requirements for the topographic and geologic conditions of the canyons where they are located on.

1. Topography

T/H , where T is the base thickness and H is the height of dam, is employed to describe the relative thickness of the arch dams. A thin arch dam is defined as with a T/H ratio of 0.2 or smaller, a medium-thick arch dam is defined as with a T/H ratio between 0.2 and 0.35, and a thick arch dam or gravity arch dam is defined as with a T/H ratio of 0.35 or more. The T/H ratio, suggested and adopted in the arch dam design practices, is usually determined by topographic conditions which are customarily indexed using the relative width of valley L/H , where L is the chord length (width at the crest elevation). In narrow sites with small relative width, the arch action can be brought into full play and most of the thrust forces can be transmitted to the abutment banks by arch action; as a result, only a small part of the forces are transmitted to the foundation by cantilever action. According to the engineering experiences, thin arch dams may be constructed in a narrow valley with $L/H < 2$, for medium-thick arch dams, $L/H = 2-3$ is demanded, whereas thick arch dams may be exercised in a wide valley of $L/H = 3-4$. When $L/H > 4.5$, it is generally believed that only gravity arch dam, arched gravity dam, and/or gravity dam can be constructed, due to the fact that the cantilever action will dominate the transmission of the forces, whereas the arch action may be even neglected. But nowadays, with the development of design and construction technology based on structural modeling and other sophisticated analytical methods, the applicable range of arch dams has been expanded. For instance, the Schlegeis Dam, built in Austria, is at a height of 131 m with ratios of $L/H = 5.5$ and $T/H = 0.25$. There are even a number of scientists and engineers who believe that arch dams may be built on valleys of $L/H = 7-11$.

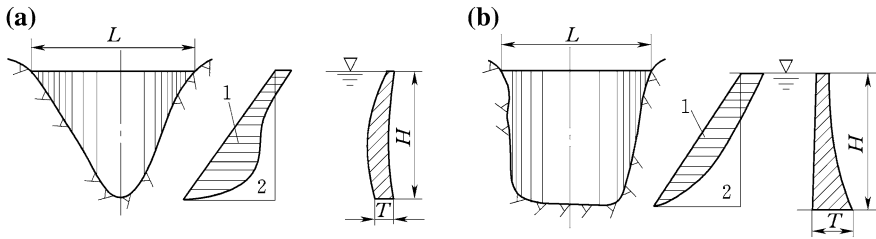


Fig. 8.2 Effects of valley shape on the load distribution and dam profile. **a** V-shaped valley; **b** U-shaped valley. 1 arch load component; 2 cantilever load component

Two dam sites having an identical relative width of valley L/H are likely to have different shapes as shown in Fig. 8.2.

In general, symmetric narrow valley of V-shape is considered as the best one: Although subjected to larger hydraulic pressure, the lower arch rings with rather shorter chord length can make a full use of arch action. Therefore, the base thickness of the arch dam can be kept rather thinner. In other words, the stress distribution in an arch dam at the V-shaped site is more acceptable because a greater percentage of loads are shared by arch action in the lower portion of the dam. On the contrary, in U-shaped sites, with rather larger chord length, the cantilever action is strong, which gives rise to thick cantilever base. Trapezoidal-shaped site, considering the same factors discussed above, is better than U-shaped site but worse than V-shaped site.

A dimensionless slenderness coefficient C for arch dams also may be defined to comprehensively describe the valley wideness and valley shape (Lombardi 1991).

$$C = \frac{F^2}{VH} \tag{8.1}$$

where F = area of arch dam mean surface, m^2 ; V = concrete volume of the dam, m^3 ; and H = maximum dam height, m.

Table 8.1 lists the slenderness coefficient C of several typical arch dams.

Concerning the planar topography, a valley with upstream entrance of morning-glory shape is desirable. At least, the dam site should be located at a valley of parallel topographic contours, to ensure sufficient rock masses at the abutments for stability. The downstream side of a morning-glory valley is to be avoided for its poor abutment stability.

With regard to the vertical valley profile perpendicular to the river stream, a totally or nearly symmetric canyon is desirable from the viewpoint of stress distribution. But very often the valley to be dammed is unsymmetrical. Even though the topography is symmetric, sometimes a dam site is asymmetrical in structure attributable to the spatial variation in the deformation and strength characteristics of the rocks on its abutments. Under such situation, engineering treatments are demanded to reduce their adverse effects on dam stress distribution.

Table 8.1 Slenderness coefficient of representative arch dams

Dam	Laxiwa (China)	Xiaowan (China)	Dongfeng (China)	Xiluodu (China)	Ertan (China)	Mauvoisin (Switzerland)	Vajont (Italy)	Contra (Switzerland)	Kolnbrein (Austria)
Length at crest elevation L(m)	475.80	922.74	254.00	681.51	770.00	535.00	190.50	380.00	626.00
Height H(m)	250	294.5	168	278	240	237	261.5	220	200
Base thickness of crown cantilever T(m)	40.00	69.49	25.00	60.00	55.74	55.00	22.10	27.00	36.00
T/H	0.196	0.238	0.163	0.216	0.232	0.232	0.085	0.122	0.18
L/H	1.9	3.16	1.66	2.451	3.21	2.26	0.73	1.727	3.13
Slenderness coefficient C	10.02	12.42	13.0	10.88	13.3	7.0	7.5	15.0	19.0

2. Geology

The foundations for arch dams are highly stressed than those for gravity dams: The compressive stress may be as high as 6–8 MPa and even higher than 10–12 MPa for particularly high arch dams. The geologic conditions of an arch dam should be able to transmit the major portion of the thrust forces to the abutments on which the dam is built. This demands uniform and sound bedrock of high strength, low deformability, low permeability, and good durability, in the foundation and abutments. Foundations of stone and claystone, although not being totally prohibited, are better to be avoided, for they may inevitably give rise to excessive dam volume enlargement and intensive foundation treatment.

It is customarily required that the Young's modulus of foundation rock be larger than that of concrete, namely $E_r/E_c > 1$. However, studies show that this requirement may be relaxed to a ratio of E_r/E_c as lower as 1/4. A cautious approach should be adopted to the foundation containing inhomogeneous rock of strong variation in Young's modulus, and special foundation treatments are normally indispensable for this kind of foundation.

Care must be exercised to pinpoint the bedding planes, joint sets, fracture systems, or other rock structures with adverse orientations that could result in abutment and foundation instability and large deformation. These may be paramount factors to be taken into account during the whole design process, covering the selection of dam axis, the layout of dam configuration, the analysis of stress and stability, and the foundation treatments.

In conclusion, arch dams impose higher requirements for the geologic conditions of foundation and abutments than that of gravity dams and embankment dams. A well-performed arch dam owes to perfect design and construction, which, in turn, should be based on the comprehensive investigation including all geologic aspects.

8.1.3 Classification of Arch Dams

1. Classification according to dam height

Arch dam may be classified into high, medium, and low types. The Chinese classification is listed in Table 8.2, in which H is the maximum dam height.

Arch dam with H equal to or higher than 200 m is named as super-high arch dam, while arch dam with H equal to or higher than 300 m is named as particular high arch dam.

2. Classification according to dam relative thickness

According to T/H , arch dams fall into

- Thin arch dam with a T/H ratio of 0.2 or less;
- Medium-thick arch dam with a T/H ratio between 0.2 and 0.35;
- Thick arch dam or gravity arch dam with a T/H ratio of 0.35 or more.

Table 8.2 Arch dam classification according to height

Classification	DL/T5346-2006 “Design specification for concrete arch dams”	SL282-2003 “Design specification for concrete arch dams”
High arch dams	$H > 100$ m	$H > 70$ m
Medium arch dams	$H = 50\text{--}100$ m	$H = 30\text{--}70$ m
Low arch dams	$H < 50$ m	$H < 30$ m

3. Classification according to arch radius and central angle

(a) Constant radius arch dams

An arch dam is termed as constant radius when the upstream face of the dam forms a part of vertical cylinder surface of constant radius. The trace line of the radius centers is straight and vertical; therefore, this type of dam is also known as the “constant center arch dam” or “cylindrical arch dam.” The vertical upstream face brings about convenience in construction and contributes to the convenience in the arrangement of control facilities for the outlet intakes.

Theoretically, the most economical (optimal) arch section is reached when its central angle is about 133° entailed by the strength condition of the dam body. However, the abutment stability against sliding demands a smaller central angle. The constant radius arch dam can be so laid out to have central angles for all arch rings around $75^\circ\text{--}110^\circ$ if the valley is U-shaped. But such a dam in a V-shaped valley gives very low central angle near the dam base. Therefore, this type of arch dam is most applicable for the U-shaped valley where the lower arch rings have approximately the same chord length as those near the crest, thus ensuring the uniform curvature all along the dam height.

The radius of intrados and/or the arch axis may be constant, too, and they may be concentric or non-concentric with respect to the extrados curves. In general, when the width of a valley is reduced from top to bottom greatly, the central angle of low arch rings tends to become very small, which results in the vanishing of arch actions. One of the traditional but uneconomic measures is to enlarge their thickness. Alternatively, one can improve this type of arch dam with constant extrados center and radii but with variable intrados center and radii, and this will give rise to triangular cantilever cross sections with increased thickness at the dam base.

(b) Constant angle arch dams

Such a dam usually possesses extrados or intrados curves of gradually reduced radii from crest to dam base. This is intended to keep the central angle as nearly constant as possible so as to secure maximum arch action at all elevations. The lower arch rings are relatively short; therefore, the greater part of the load is sustained by arch action. This type of dam is most economically suitable for the V-shaped canyon by using less concrete as compared with the constant radius arch

dam. However, a rigorous constant angle will generally lead to large overhang on the upstream face and is twisted on both upstream surface and downstream surface and in turn increases the difficulty with construction. The large twist and overhang can affect the tilt stability in the service period, too, when the reservoir water level is very low.

It should be noted that it is impossible in the practical engineering to retain the central angle absolutely constant along the whole dam height. In general, the central angles vary in a specific scope and decrease following the descending of arch ring altitude. For instance, the half central angles of the Quanshui arch dam ($H = 80$ m), built in the Guangdong Province, China, vary from 40° to 50° .

(c) Variable radius and central angle arch dams

A more commonly used design today is the variable radius and central angle that covers all classes of arch dams.

With this dam type, the radii and the centers of the extrados and intrados vary respect to the axis from the maximum at the top to the minimum at the base. The centers of the different radii of extrados or intrados fall on a smooth trace. The upstream dam face varies from vertical to overhanging both at the crown and at the abutments. The central angle of different arch ring is not constant, but usually ranges within 80° – 150° . Such dams are also known as “variable center arch dam.”

Variable center arch dams are flexibly applied on the valleys of narrow V-shaped, trapezoid, or other shaped and are adaptive to meet various foundation requirements.

4. Classification according to dam curvature

By the category of dam curvature, arch dams may be distinguished as single curvature and double curvature.

(a) Single-curvature arch dams

Single-curvature arch dams are curved only in plan (Fig. 8.3a). When the upstream face of the dam forms a part of the cylindrical surface of constant radius, and whose center forms a straight vertical line, it is also known as the “constant center arch dam,” or “cylindrical arch dam” (Fig. 8.3b). This type of arch dam is only applicable to U-shaped valleys.

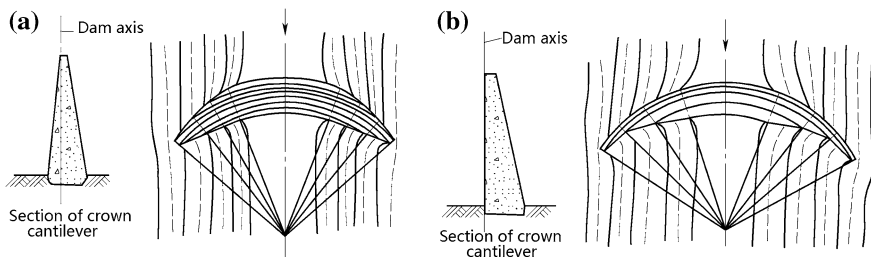


Fig. 8.3 Single-curvature arch dams. **a** Single-curvature arch dam; **b** constant center arch dam

(b) Double-curvature arch dams

Double-curvature arch dams are curved in plan as well as in elevation.

The best form of an arch dam intended to reduce bending deformation and rotation, meanwhile taking into account all loads and their effects, is a shell-like structure of double curvature. This type of dam utilizes concrete more efficiently due to well-distributed stresses and therefore gives rise to significant economy benefits.

The curvature radii of arch rings are reduced gradually on this count from crown to abutment, and tensile stresses induced by side cantilever overhang on the base can be compensated by means of self-weight.

By keying, the central angle of every arch ring may be kept fairly ideal. This type of dam is very suitable for V- or trapezoidal-shaped valleys. Another significant advantage brought about from double curvature is that the flow jet can be thrown rather far away from the dam toe when the dam releases flood through the orifices accommodated in the body.

Although a better stress distribution may be achieved in arch dams of double curvature, together with great flexibility and load-carrying capacity, such dams are less technically viable and require higher level of design skill. In addition, complication in the construction process may arise during their erection (Fig. 8.4).

(c) Gravity arch dams

A thick arch dam is usually called as gravity arch dam. It relies jointly on gravity and arch actions for its stability and is structurally an intermediate work in between the straight gravity and curved thin arch. A seeming compromise between simplicity in construction and lower unit cost is usually appreciated for the gravity arch dam, although there could have only slight expenditure saving over the gravity dam.

(d) Classification according to the shape of the arch rings (Fig. 8.5)

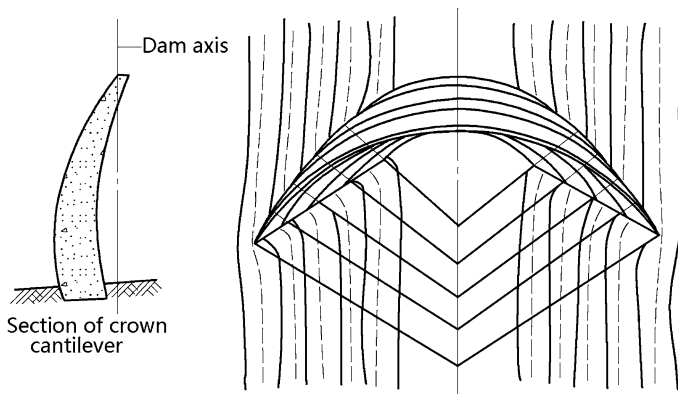


Fig. 8.4 A double-curvature arch dam

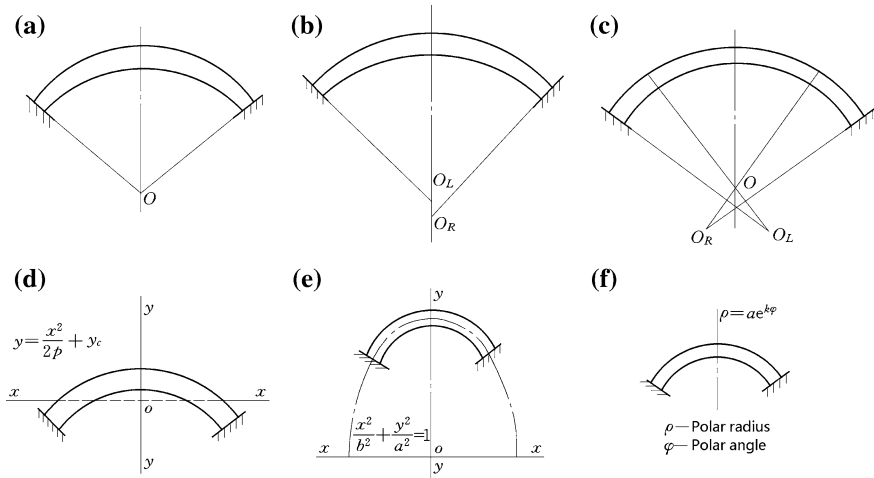


Fig. 8.5 Shapes of arch ring. **a** Circular arch; **b** double-central arch; **c** triple-central arch; **d** parabola arch; **e** ellipse arch; **f** logarithmic spiral arch

1. Circular arch dams

With horizontal arch rings in circular, the design and construction of dams are simple. However, the circular arch ring may deflect away considerably from the pressure line of the arch, and the included angle between the abutment thrust and topographic contour of bank could be small. All these are not advantageous for dam stress distribution and abutment stability. This kind of arch ring is ordinarily employed for medium-to-low arch dams.

2. Multi-central arch dams

Ranged from double-central to five-central, multi-central arch dams are adaptive to the valley shape by adjusting the curvature at the arch ring crown and the abutments, to improve the stress and/or stability conditions.

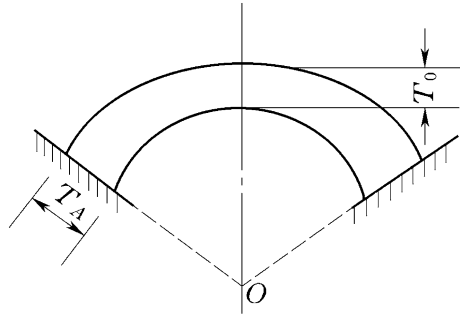
3. Variable curvature arch dams

This family of arch dam comprises types of ellipse, parabola, and logarithmic spiral. They have larger curvature near the crown to improve the stress conditions and smaller curvature near the abutments to secure the stability conditions against sliding. As a result, variable curvature arch dams are adaptive to various valley shapes, but they are complex in the design and construction and usually applied only for high-to-medium arch dams

4. Classification according to the thickness variation of arch rings

According to the variation in the thickness of the arch rings, arch dams may be further divided into two types which are called constant thickness arch dam and arch dam with variable thickness from crown to abutments. The latter has better

Fig. 8.6 An arch dam with variable thickness



stress conditions, but complicated in the design and construction, and is normally applied in the high-to-medium arch dams (Fig. 8.6).

5. Classification according to the dam structures

- (a) Arch abutments being keyed into sound bedrock

This is the prevailing arch dam structure.

- (b) Peripheral joint being installed

Often, such peripheral joint is provided between the dam and foundation and is intended to improve the stress conditions, to shape the dam body for best acceptance of loads, and to bridge the foundation rock zones of significant variations in mechanical properties due to seams, etc. A typical example is the Vajont Arch Dam (Italy, $H = 265$ m).

- (c) Bottom inducing joint being installed

For several dam monoliths, particularly for those that on the riverbed, the bottom inducing joints are anticipated to control the irregular dam heel cracking. The bottom inducing joint is a permanent short joint located at the based concrete and terminated at a gallery, to avoid the stress concentration at the joint tip. A careful water stop and draining system is installed for the joint. A typical example is the Xiaowan Arch Dam (China, $H = 294.5$).

- (d) Gravity pier being laid out

To improve the connection between arch dam body and abutments for better stress and stability conditions, as well as to improve the bearing capacity of the abutments, gravity pier (or thrust pier, wing dam, pad) is often employed. The examples are the Kurobe No IV Dam (Japan, $H = 186$ m), the Mratinje Dam (former Yugoslavia, $H = 220$ m), the Jinping No 1 Arch Dam (China, $H = 305$), the Lijixia Dam (China, $H = 165$ m), and the Longyangxia Dam (China, $H = 178$ m).

(e) Hollow being installed

Hollow may be installed within thick or gravity arch dams, to cut a part of uplift and to facilitate the thermal control. The hollow also can be used to accommodate power plants. Examples are the Fengtan Gravity Arch Dam (China, $H = 112.5$ m), the Fengshu Gravity Arch Dam (China, $H = 95.3$ m), and the Monteynard arch dam (France, $H = 155$ m).

8.2 Loads and Load Combinations

8.2.1 Loads

The various loads exerting on arch dams are basically the same as those on gravity dams, which have been discussed in Chap. 4 of this book.

However, the relative importance of the forces in arch dams is different (Chen and Chen 2014; Grishin 1982; Iqbal 1993; Lin 2006; Novak et al. 1990; Wang and Wueng 1990; Wu 1991; Zuo et al. 1995). For instance, temperature changes, which are usually not important for gravity dams, give rise to significant deflections and stresses in arch dams.

1. Thermal actions

The thermal action drives arch dams moving upstream during the summer and downstream during the winter, which cannot be ignored in the design. To avoid the appearance of strong expansion and shrinkage stress, in the period of construction, the whole arch dam is divided into monoliths with transverse construction joints, and in this way, the concrete poured within each monolith can be limited in both volume and height. They are artificially post-cooled and should be calked at a stable temperature named as “closure temperature,” for making the whole dam monolithic. This closure temperature is the reference level in the computation of temperature rise or drop, which is customarily selected as a bit of lower than the annually averaged temperature, for a better compromise between the control of the tensile stress within the dam body and the stability of dam abutment/foundation rock.

Computations of the thermal actions for arch dams have been discussed in Chaps. 4 and 5 of this book.

2. Uplift

An analysis of its effects on arch dams of moderate height shows that the additional stress in the dam body due to the uplift only accounts for approximately 5 percent of the allowable stress. As a rule, for thin arch dams, the uplift even can be neglected, while the effects of uplift are customarily taken into account during the design of medium-to-thick arch dams.

The effects of uplift must be taken into account during the stability analysis for dam foundation and abutments. The calculation of uplift is basically the same as for

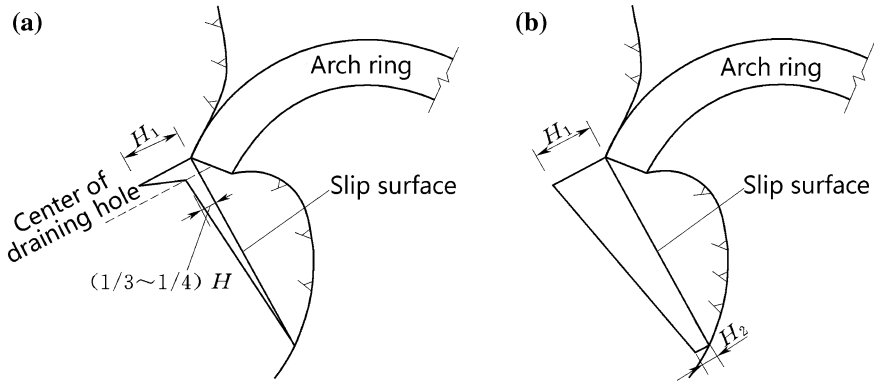


Fig. 8.7 Distribution of uplift in abutments. **a** Effective drainage; **b** ineffective drainage

gravity dams. The distribution of seepage pressure within the abutment rock depends on various factors related to the position and dimension of the grouting and drainage curtains (depth, spacing, hole diameter), as well as the characteristics of the faults and seams (distribution, dimension, aperture, filling material, etc.). Figure 8.7a shows a typical distribution diagram of the uplift in abutment, in which H_1 is the reservoir headwater depth, H_2 is the tailwater depth, and H is the head difference. The drainage ineffectiveness is also considered, if necessary, which is shown in Fig. 8.7b.

8.2.2 Combinations of Action Effects (Load Combinations)

According to the DL/T5346-2006 “Design specification for concrete arch dams,” in the design of arch dams, basic combinations and accident combinations are considered. Permanent situations and temporary situations use basic combinations, whereas accident combinations are used for accident situations which consider permanent and alterable actions plus one accident action.

According to the SL282-2003 “Design specification for concrete arch dams,” in the design of arch dams, load combinations are classified into basic combination and special combination. Basic combination consists of several basic loads that occur simultaneously. Special combination consists of several basic loads and one special load (check flood, earthquake) that occur simultaneously.

1. Basic combinations

- ① Normal storage reservoir level and corresponding tailwater level + design temperature drop + self-weight + uplift + silt pressure + wave pressure + ice pressure;

- ② Inactive reservoir level (or lowest operation reservoir level) and corresponding tailwater level + design temperature rise + self-weight + uplift + silt pressure + wave pressure.
- ③ Other adverse combinations frequently encountered.

2. Special combinations

- ① Check flood level and corresponding tailwater level + design temperature rise + self-weight + uplift + silt pressure + hydrodynamic pressure + wave pressure;
- ② Basic combination ① + earthquake loads;
- ③ Basic combination ① + one of other accident loads.
- ④ Load combination during construction period comprises the case of ungrouting and stage grouting of transverse construction joints:
 - (i) Ungrouting of transverse joints
 - Self-weight solely;
 - Self-weight + static water pressure corresponding to the flood level during construction period.
 - (ii) Stage grouting of transverse joints
 - Self-weight + thermal actions (rise or drop) of the grouted dam portion;
 - Self-weight + static water pressure corresponding to the flood level during construction period + thermal actions (rise only) of the grouted dam portion.

8.3 Stress Analysis for Arch Dams

8.3.1 Methods for Stress Analysis

The purpose of stress analysis is to examine whether the design is both economic and safe with respect to strength control criteria. One of the major factors, which affect the strength calibration for arch dams, is the selection of computational methods. Nowadays, there is a large family of frequently applied methods for computing the stress in arch dams such as the cylinder method, the method of independent arches, the trial load method, the method of elasticity shell, the finite element method, and the physical experiment method.

1. Cylinder method

This is the earliest and simplest of the method proposed for the design of arch dams, which looks at an arch dam as a part of vertical cylinder in the water.

Although it is only able to compute the tangential stress (i.e., normal stress) for the arch ring with uniform cross section, the effects of temperature, earthquake, and foundation deformation are all not taken into account, yet its fundamental equation may give important insight into the arch dam stress by

$$T = \frac{PR_u}{R\sigma} \quad (8.2)$$

where T = thickness of the arch ring; R = radius of the arch centerline; P = horizontal water pressure exerting on the arch ring; R_u = radius of the upstream face (i.e., extrados); and σ = average normal stress on the cross section of the arch ring. It can be easily seen that there is a geometrical relationship between R_u , R , and L , as

$$R_u = R + \frac{T}{2} \quad (8.3)$$

in which

$$R = \frac{L}{\sin \varphi_A} \quad (8.4)$$

where $2\varphi_A$ = central angle of the arch ring and L = length of the arch ring chord. Therefore, the cylinder formula in Eq. (8.2) can be rewritten as follows:

$$T = \frac{LP}{(2\sigma - P) \sin \varphi_A} \quad (8.5)$$

From Eqs. (8.2) and (8.5), it follows that the smaller the radius and the larger the central angle of arch, the smaller the stresses in the arch ring will be. However, with the increase of central angle, the length of arch increases, too. For the given allowable compressive stress σ_c and arch chord L , according to the mathematical deduction, a minimum volume of each arch ring is obtained with a central angle of $133^\circ 34'$. However, since too large central angle will bring about difficulty with the stability of dam abutments, in modern arch dams, the central angle of crest arch ring is normally selected within a range of 75° – 110° .

2. Method of independent arches

This method looks at an arch dam as made up of a series of independently horizontal arch rings which completely take up the load exerting on them. The critical stress calculated by this method, in general, is larger than the actual stress in the dam, especially for a thick or gravity arch dam. However, due to the availability of a large number of helpful tabulated coefficients, it is a convenient method in the design of thin arch dams in rather narrow canyon, where the dam efforts are transmitted to the abutment banks mainly through arch elements. By the way, it is also an essential integral part of the trial load method.

3. Method of elasticity shell

When the thickness is very small compared to the other dimension of an arch dam, the dam may be looked at as a three-dimensional elastic shell with variable curvature and thickness in the vertical and horizontal directions. Although as early as in the 1930s, Tolke had proposed an approximate calculation method based on the shell theory, a correct solution of the stress problem for such a structure is mathematically difficult. Nowadays, with the development of computers, it has become possible to use this theory for arch dams, by which the problem is solved based on the numerical method of finite difference or finite element.

4. Experimental method

Physical modeling studies on the stress state in the arch dam were booming in the 1960s mainly in European countries (e.g., Portugal and Italy). The models are made of materials similar to concrete and rock mass. This method enables the designers not only to study the stress state of the arch dam in view of the nonlinear stress distribution under loads and the actual structure of rock foundation, but also to determine the safety margin and the collapse mechanism of the structure. Experiments provide trials of the dam designed on the basis of analytical calculations. The problematic issues of experimental methods are the model materials, simulation techniques of self-weight, seepage, and temperature.

5. Trial load method

This is the routine and basic method for the stress analysis of arch dams in China for nearly 50 years, which was originally initiated in 1889, when Vischer and Wagoner (USA) described several horizontal arches and only one crown cantilever, in the stress calibration of the Bear Valley Dam ($H = 19.5$ m) and Sweetwater Dam ($H = 33$ m). The successive contributors to be remembered are Woodard, Wisner and Wheeler, Noetzli, Gryuner, Stucky and Gicot, Vogt, Howell and Jaquith, and their milestone works are summarized in Chap. 1 of this book.

The modern trial load method assumes that an arch dam may be discretized into n horizontal arch ring elements and $(2n - 1)$ vertical cantilever elements, where $n = 9, 7, \text{ or } 5$. The load applied to the arch dam is reciprocally divided and shared between the above-assumed elements in such a manner that identical movements are resulted in all directions at the intersection points (i.e., conjugate points) of these elements. With this method, the problem is largely confined to reciprocally dividing loads into shares for arch elements and cantilever elements. Furthermore, calculations are performed separately for the stresses in arch elements and cantilever elements.

There are two manners for dividing loads: One uses trial-and-error technique, which divides the load tentatively for arch rings and cantilevers and then calculates the deformation of arch rings and cantilevers separately, and the load dividing is adjusted if the deformation at conjugate points are not identical. This procedure

continues until the identity of deformation at all conjugate points is reached. In the early time, the trial-and-error technique was widely used, which led to the name of “trial load method.” With the development of computers, it has become possible to solve a set of algebraic expressions entailing the equality of deflections at all conjugate points, in this way to complete the load division in one go.

Within the framework of above complex method, some other simplified techniques for the analysis of crossed structure system may be employed, and by these, some alternatives of the method are invented. For example, the crown cantilever method is a simplified trial load method, which only considers one crown cantilever. The crown cantilever method is applicable for arch dams in approximately symmetric valley, or for the preliminary study of high arch dams and for the feasibility study of medium-to-low arch dams.

6. Finite element method

Today, the FEM is increasingly exercised in arch dam designs, and considerable efforts have been directed to the development of suitable software. It can be anticipated that with its further development, the conventional analytical methods will pass into secondary.

The principles and essential procedure in the analysis of hydraulic structures including arch dam using the FEM have been discussed in Chap. 5 of this book.

8.3.2 Analysis of Foundation Deformation

According to numerous theoretical and experimental studies, the deformation and stress states of an arch dam as a statically indeterminate structure depends on the foundation or abutment deformability to a greater extent. It is, therefore, essential that foundation deformability should be thoroughly investigated, studied, and taken into account.

The method suggested by Vogt (1925) has been prevalent for computing the deformation of foundation. According to this method, the displacement in the dam-to-foundation contact face is determined as the average displacement of an elastic half-space, on which forces transmitted from dam to foundation are exerted. Of course, such postulation cannot be accordant with the real world and it is fairly approximate instead of precise.

1. Basic formula of foundation deformation

To simplify calculation, there are several additional assumptions apart from that of elastic half-space, which are as follows:

- ① The surface of foundation rock is orthographic with the horizontal arch abutment. The ratio $m = b/a$ is assumed to be equal for all sections of the dam-to-foundation contact area, which is determined through the planar development of the contact surface substituted by a rectangle plane with equivalent

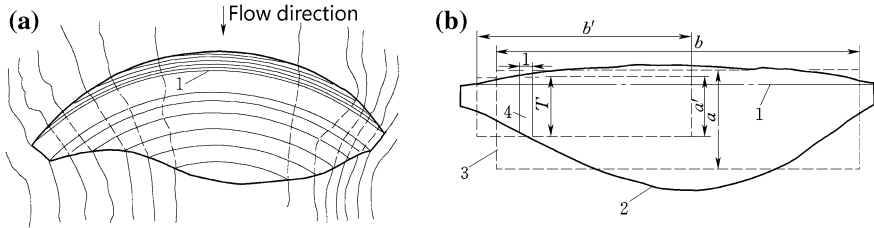


Fig. 8.8 Equivalent arch dam foundation (by Vogt). **a** Plan; **b** exploded view. 1 dam axis; 2 exploded foundation surface; 3 equivalent rectangle plane; 4 unit foundation plane

area (Fig. 8.8). This equivalent rectangle plane is looked at as a part of the surface of the elastic semi-space;

- ② The minor factors affecting the deformation such as the hydraulic pressure can be neglected;
- ③ The elastic modulus of the dam body material is equal to that of the foundation rock;
- ④ For calculating the foundation deformation at a certain elevation with element thickness T , a similar equivalent rectangle plane of width $a' = T$ and length b' , where $b'/a' = b/a = m$, is considered. It is postulated that under the action of uniformly distributed unit load along the b' direction, the average deformation of its central line is identical to that of the central line of the equivalent rectangle plane (ab), i.e., the deformation at any portion of foundation is the function of $m = b/a$, and the average deformation along the basic thickness is equal to that of the element area.

According to the above assumptions and using the solution of Boussinesq for elastic semi-space, six approximate rock deflection coefficients K_1 – K_6 illustrated in Fig. 8.9 (K_6 is used to be denoted as $\angle K_3$) are expressed in Eq. (8.6). They are termed as “Vogt coefficients” (USBR 1987a, b) representing the average normal, tangential, and torsion deflections under the unit loads and moments on the semi-infinite elastic space with deformation modulus of foundation rock $E_r = 1.0 \times 10^{-3}$ MPa.

$$\begin{cases} \alpha' = \frac{K_1}{E_r T^2} \\ \beta' = \frac{K_2}{E_r} \\ \gamma' = \frac{K_3}{E_r} \\ \delta' = \frac{K_4}{E_r T^2} \\ \alpha'' = \gamma'' = \frac{K_5}{E_r T} \\ \angle \gamma' = \frac{\angle K_3}{E_r} \end{cases} \quad (8.6)$$

where E_r = deformation modulus of foundation rock, kPa; T = base thickness of arch dam at the portion concerned, m; α' = angular deflection caused by unit moment, rad; β' = horizontal deflection caused by unit normal force, m; γ' = shearing deflection caused by unit shear force, m; δ' = torque deflection

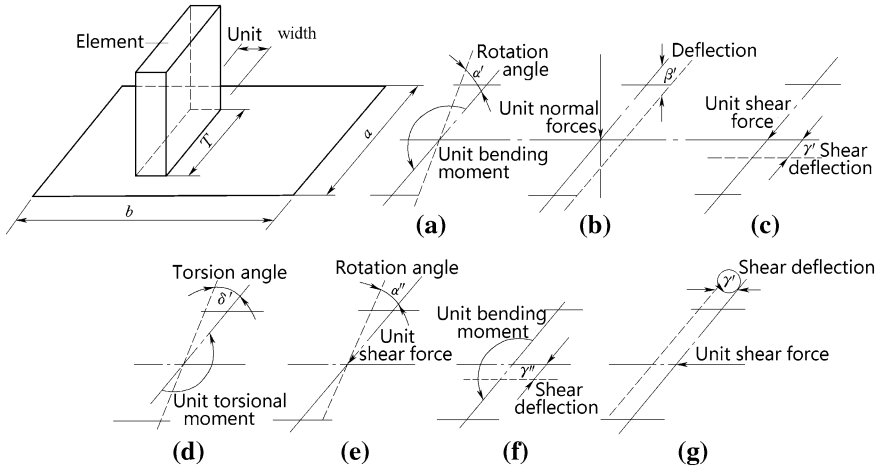


Fig. 8.9 Deflections of arch dam foundation (by Vogt). **a** unit bending moment vs rotation angle; **b** unit normal force vs normal deflection; **c** unit shear force vs shear deflection; **d** unit torsion moment vs torsion angle; **e** unit shear force vs rotation angle; **f** unit bending moment vs shear deflection; **g** unit shear force vs shear deflection

caused by unit twisting moment, rad; α'' = angular deflection caused by unit radial shear force, rad; γ'' = radial shearing deflection caused by unit moment, m; and $\angle\gamma'$ = radial shearing deflection caused by unit radial shear forces, m.

Vogt coefficients are the functions of the Poisson’s ratio μ and $m = b/a$ and may be computed in a diagrammatic manner using corresponding design handbook. In addition, it may be seen from Eq. (8.6) that they are dependent on both the base thickness T of the arch dam and the elastic modulus E_r of the foundation, too.

2. Deformation calculation of arch ring abutment

To compute the rock deformation induced by an arch or cantilever element, the forces exerting on the base of the element are transformed into the force system on the dam base, and the deformation obtained is then transformed and integrated into the arch–cantilever grid system. For this transforming operation, the only parameter that is related is the inclination angle of the abutment slope ψ (Fig. 8.10).

The abutment deformation coefficients after the transformation are as follows:

$$\begin{cases} \alpha = \alpha' \cos^3 \psi + \delta' \sin^2 \psi \cos \psi \\ \beta = \beta' \cos^3 \psi + \angle\gamma' \sin^2 \psi \cos \psi \\ \gamma = \gamma' \cos \psi \\ \alpha_2 = \alpha'' \cos^2 \psi \end{cases} \quad (8.7)$$

At the end of a unit arch ring, there are axial force H , radial shear force V , and bending moment M_z , and their positive directions are indicated in Fig. 8.10a (the left bank and right bank are defined by viewing from the downstream to the

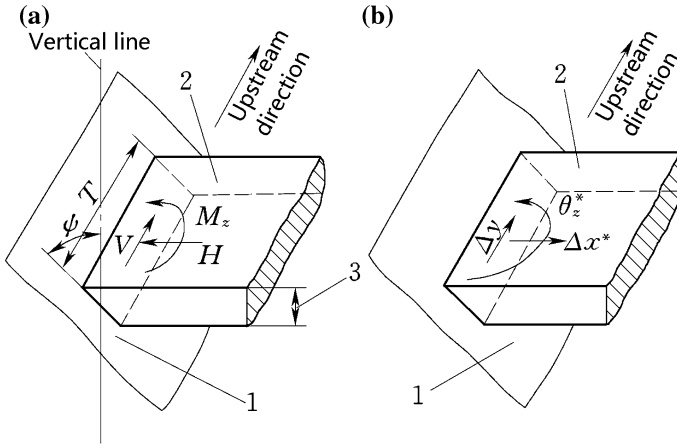


Fig. 8.10 Forces and displacements at the end of unit arch ring. **a** Forces and moments; **b** displacements. 1 foundation surface; 2 unit element; 3 unit width

upstream in the discussion of abutment deformation herein). Under their actions, the axial displacement Δx^* , radial displacement Δy , and horizontal angle deflection θ_z^* may be calculated using Eq. (8.8) whose positive directions are indicated in Fig. 8.10b.

$$\begin{cases} \theta_z^* = M_z\alpha + V\alpha_2 \\ \Delta x^* = -H\beta \\ \Delta y = V\gamma + M_z\alpha_2 \end{cases} \quad (8.8)$$

Equations (8.7) and (8.8) are applicable to the left abutment only. For the right abutment, the plus or minus sign of the quantities with star (*) should be reversed. The force system (H, V, M_z) at the abutment of a unit arch ring also induces deformation θ_z and Δz apart from $\Delta x, \Delta y$, and θ_z^* , which are usually neglected in the analysis.

3. Deformation calculation of a cantilever base

The deformation coefficients of a cantilever base after the transformation are as follows:

$$\begin{cases} \alpha = \alpha' \sin^3 \psi + \delta' \sin \psi \cos^2 \psi \\ \delta = \delta' \sin^3 \psi + \alpha' \sin \psi \cos^2 \psi \\ \gamma = \gamma' \sin \psi \\ \alpha_2 = \alpha'' \sin^2 \psi \\ \angle \gamma = \angle \gamma' \sin^3 \Psi + \beta' \sin \Psi \cos^2 \Psi \end{cases} \quad (8.9)$$

At the base of a unit cantilever, there are bending moment M_x , radial shear force V , twisting moment M_z , and tangential shear force H whose positive directions are

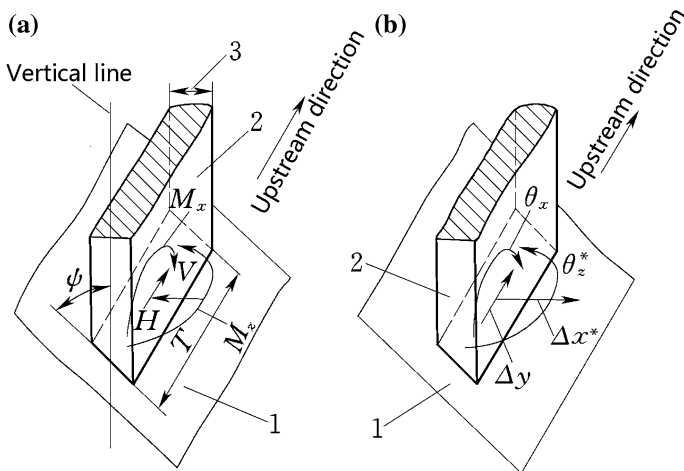


Fig. 8.11 Forces and displacements at the base of unit cantilever. **a** Forces and moments; **b** displacements. 1 foundation surface; 2 unit element; 3 unit width

indicated in Fig. 8.11a. Under their actions, the torque deflections θ_x and θ_z^* , radial displacement Δy , and horizontal angle deflection θ_z^* may be calculated using Eq. (8.10) whose positive directions at the left abutment are indicated in Fig. 8.11b.

$$\begin{cases} \theta_x = M_x \alpha + V \alpha_2 \\ \Delta y = V \gamma + M_x \alpha_2 \\ \theta_z^* = M_z \delta \\ \Delta x^* = -H \angle \gamma \end{cases} \quad (8.10)$$

Equation (8.10) is applicable to the cantilever on the left abutment only. For the cantilever on the right abutment, the plus or minus sign of the quantities with star (*) should be reversed.

The twisting moment M_z has effect on Δy , and both the bending moment M_x and the tangential shear force H have effects on θ_z , which are usually neglected in the analysis.

8.3.3 Independent Arch Method

The independent arch method is applicable for the initial design and for the study of simple arch dam of modest height, and it is also a fundamental technique in the formulation of the trial load method. The method looks at an arch dam as a series of horizontal and independent arch rings which bear the loads at the corresponding level.

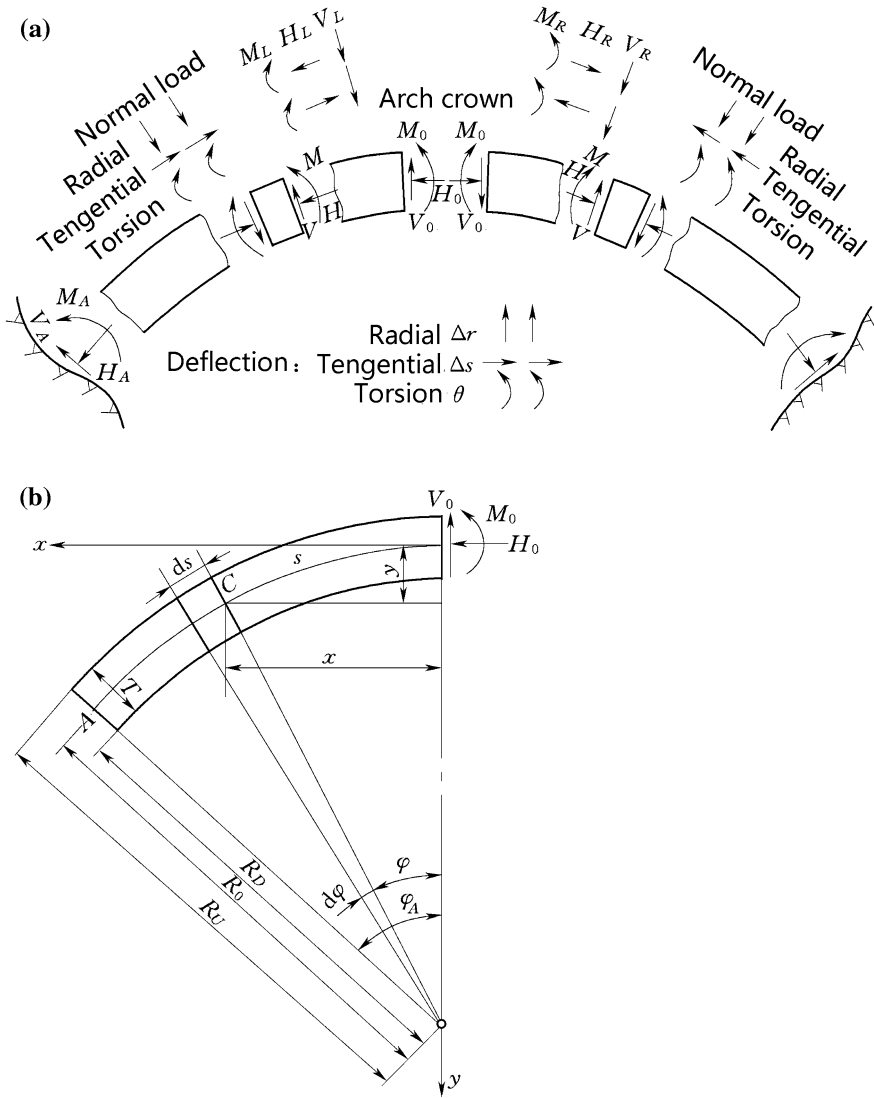


Fig. 8.12 Diagram to the stress analysis by independent arch method. **a** Loads and inner forces; **b** configuration of arch ring

Since elastic center is difficult to be pinpointed due to the foundation deformation, the redundant forces (M_0 , H_0 , and V_0) are ordinarily allocated on the arch crown section as shown in Fig. 8.12, and in this figure, the x -axis and y -axis, the positive directions of deflections (Δr , Δs , and θ), are all indicated. The left and right parts of the arch ring are analyzed as curved static cantilevers to obtain shape constants and load constants. Then, M_0 , H_0 , and V_0 are computed according to the

continuity condition at the section. The inner forces M , H , and V as well as the corresponding stress and deformation at any cross section are finally calculated. The detailed procedure of the computation may be referred to the corresponding design handbooks (Zuo et al. 1987).

8.3.4 Trial Load Method

The correct stress solution of an arch dam may be inferred from the Kirchhoff uniqueness theorem in the theory of elastic body, which implies the general requirements as follows:

- ① The elastic properties of the body must be completely expressible in terms of two constants—the Young's modulus and Poisson's ratio;
- ② If the volume of the body in the unstressed state is divided into small elements by passing through it a series of intersection surfaces, each of the elements so formed must be in equilibrium under the forces and stress which exerts upon it;
- ③ Each of the intersected elements described above must deform in such a way as the body passes into the stressed state that it will continue to fit with its neighbors on all side surfaces;
- ④ The stresses or displacements at the boundaries of the body must conform to the stresses or displacements imposed.

Under aforementioned conditions, Kirchhoff proved that it is impossible for more than one stress systems to exist. It follows, therefore, that if an actual structure conforms to the requirement ① and a stress system is obtained which meets the requirements ①, ③, and ④, this stress system is the one which must exist in the structure under the assumed conditions. A stress system of arch dam meeting the above requirements may be obtained by the trial load method apart from various numerical methods (e.g., FEM), whose illustration in more detail is referred to the corresponding design handbooks (Golzé 1977; Zhou and Dang 2011; Zuo et al. 1987).

The particular assumptions in the implementation of the trial load algorithm are as follows:

- The reservoir banks and bed have no deformation under the action of water pressure;
- On the horizontal section, the contact face between dam and foundation is perpendicular to the arch ring;
- The cross section of horizontal arch ring keeps planar after the deformation;
- Concrete and rock are homogenous, isotropic, and elastic;
- The axial stress of a horizontal arch ring is linearly distributed along its thickness;

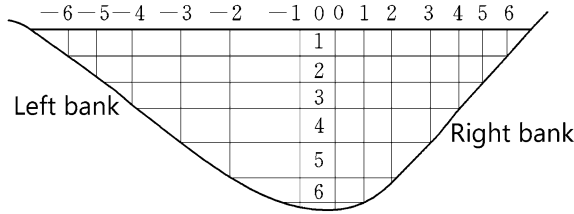


Fig. 8.13 Arch elements and cantilever elements for an arch dam

- The foundation deformation under the action of dam may be described by the Vogt coefficients.

1. Discretization of arch and cantilever systems

As a compromise between the computation accuracy and efficiency, usually 5–7 arch elements and 9–13 cantilever elements are discretized. The number of arch and cantilever elements should be compatible, and the conjugate nodes are as uniformly distributed as possible to cover the whole dam body. Suppose that the arch element number is n and the cantilever element number is m , very often the relation $m = 2n - 1$ is met to let any node at foundation to be a common node (conjugate point) of arch and cantilever. Figure 8.13 shows a system that comprises 7 arch elements and 13 cantilever elements.

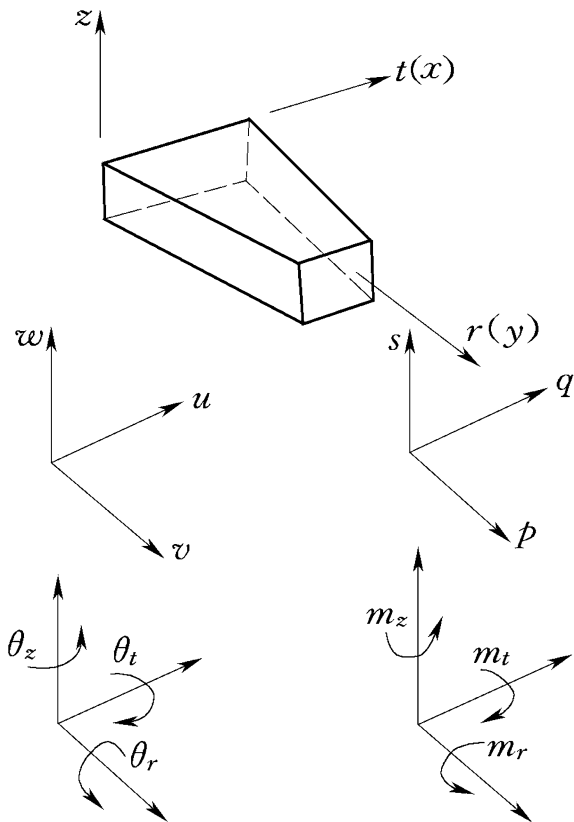
For a symmetric arch dam of not very important or in the stage of preliminary study, it happened but not very often, and only one crown cantilever element and several arch elements are employed in the computation, which is named as “crown cantilever method.”

2. Compatibility conditions

At each conjugate node, there are six deformation components (Fig. 8.14), i.e., three linear deflections and three angle deflections, which are arranged in sequence according to their importance: radial deflection v , tangential deflection u , angle deflection θ_z around axis z , angle deflection θ_t around tangential axis t , vertical deflection w , and angle deflection θ_r around radial axis r . The corresponding loads on arches or cantilevers are as follows: radial load p , tangential load q , vertical load s , horizontal moment m_z , and vertical moments m_t and m_r .

Generally, the six deflections and their compatibility are taken into account to obtain an exact load division between arches and cantilevers, which is named as six-directional whole adjustment. However, in practice, the first three deflections are usually adopted as independent variables, and the other three remaining deflections are expressed by these independent variables considering the relationship of six internal forces. The three key independent variables are solved by their deformation compatibility conditions at the conjugate nodes, which is named as three-directional adjustment. Similarly, four- or five-directional adjustment may be formulated.

Fig. 8.14 Deflections and loads



The strength control criteria of arch dams are based on the three- or four-directional adjustment in the Chinese design codes for concrete arch dams.

3. Load classification and division

(a) Load classification

The manner of load division for cantilever and arch elements is related to its type.

- ① External loads. An external load exerting before the transverse joint grouting (e.g., self-weight, a part of water pressure) is sustained by the cantilevers only, and the induced deflections will not be taken into account in the deformation compatibility adjustment between the cantilever and arch elements, too. On the contrary, the external load exerting after the transverse joint grouting is jointly sustained by the cantilevers and arches, and the induced deflections should be taken into account in the deformation compatibility adjustment.

The external loads exerting after the closure of arch may be further classified into three sub-types:

- (i) Those are divided between cantilever and arch elements according to the deformation compatibility equation. This type of loads comprises horizontal water pressure and silt pressure.
 - (ii) Those are sustained by the cantilever and arch elements simultaneously. However, their deflections induced will be taken into account in the deformation compatibility equation. This type of loads comprises temperature variation and dry shrinkage.
 - (iii) Those are sustained by the cantilevers solely; however, the induced deflections will be taken into account in the deformation compatibility equation as initial deformation between cantilever and arch elements. This type of loads comprises self-weight, loads on the dam top, vertical water pressure, and vertical silt pressure.
- ② Internal loads. They are also named as self-balancing loads, for they appear in pairs equal in value and opposite in direction: One exerts on the cantilever, and another exerts on the arch. Physically speaking, they are the interaction forces between arch and cantilever elements.

(b) Load division

Of the heretofore loads enumerated, only the type (i) is explicitly divided between the cantilever and arch elements. The types (ii) and (iii) are not divided. However, it should be pointed out that the latter two types are actually implicitly divided by influencing the deformation compatibility equation through their initial deflections induced.

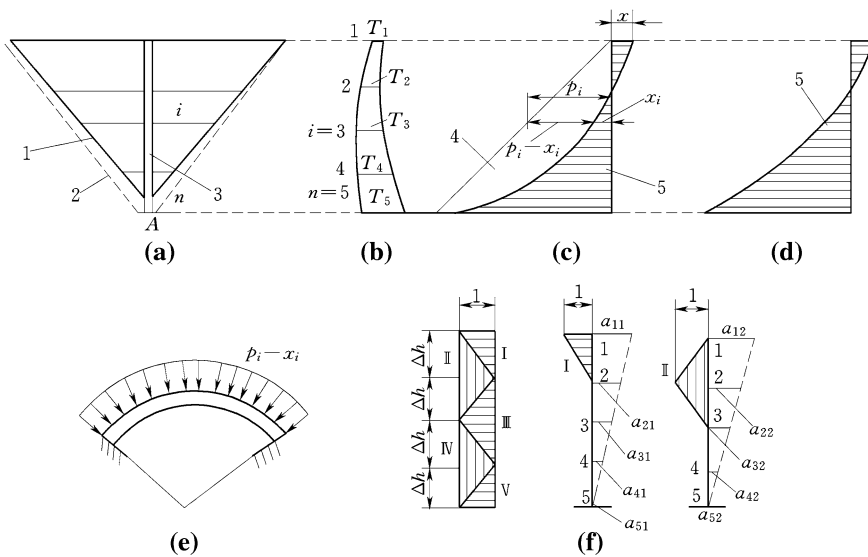


Fig. 8.15 Load division in crown cantilever method. **a** arch - crown cantilever grid; **b** crown cantilever; **c** load division **d** load shared by the crown cantilever. 1 ground surface; 2 bedrock surface as dam base; 3 crown cantilever; 4 arch load; 5 cantilever load

In the establishment of deformation compatibility equation, nodal unit loads exerted both on the arch and on the cantilever elements are very helpful: A nodal unit load has the intensity of 1 (or 1000) at the node concerned and extends linearly to zero at the adjacent nodes on either side as shown in Fig. 8.15. These unit loads may be amplified using the real load intensities and then be combined to approach any complicated load distribution pattern. It is obvious that the finer the nodal distribution, the more precise the approaching is.

(c) Crown cantilever method

Although it was proposed earlier, the crown cantilever method is actually a simplified version of the trial load method, which divides the radial loads based on the compatibility condition of several arch elements and one crown cantilever element. This division results in uniformly shared loads from one abutment to another abutment on each horizontal arch ring, whose deformation and stress may be computed by independent arch method. Therefore, the crown cantilever method also may be looked at as a compromise between the simple independent arch method and complicated trial load method, which may be used for symmetric arch dam of not very important or in the stage of preliminary study.

Taking the arch dam composed of n arch rings as example (Fig. 8.15, $n = 5$), the compatibility condition with respect to the radial deflection at the conjugate nodes of crown cantilever and arch rings is as follows:

$$\left. \begin{aligned} \delta_{11}x_1 + \delta_{12}x_2 + \dots + \delta_{1n}x_n + \delta_1^0 &= (p_1 - x_1)\Delta r_1 + \Delta r_1^0 \\ \delta_{21}x_1 + \delta_{22}x_2 + \dots + \delta_{2n}x_n + \delta_2^0 &= (p_2 - x_2)\Delta r_2 + \Delta r_2^0 \\ \dots & \\ \delta_{n1}x_1 + \delta_{n2}x_2 + \dots + \delta_{nn}x_n + \delta_n^0 &= (p_n - x_n)\Delta r_n + \Delta r_n^0 \end{aligned} \right\} \quad (8.11)$$

where p_j = intensity of resultant horizontal load at the j th arch ring including water pressure and silt pressure; x_j = divided load for the crown cantilever at the j th node; $p_j - x_j$ = divided load for the j th arch ring; δ_{ji} = unit cantilever radial deflection at the node j induced by the unit load at the node i , of the crown cantilever; Δr_j = unit arch radial deflection induced by the unit load of the j th arch ring; δ_j^0 = initial crown cantilever radial deflection at the node j induced by vertical water and vertical silt pressure, self-weight after the arch closure, as well as the temperature variation after the arch closure; and Δr_j^0 = initial arch radial deflection at the node j induced by the temperature variation after the arch closure.

Equation (8.11) is the linear equation set with respect to the shared load of the crown cantilever (x_1, x_2, \dots, x_n), which are further used to calculated divided load for the arch rings ($p_1 - x_1, p_2 - x_2, \dots, p_n - x_n$), and then, the stresses in the cantilever and horizontal arch rings may be computed using conventional beam and arch theory.

8.3.5 Strength Calibration for Dam Body

One of the major factors in the strength calibration for arch dams is the computational methods. According to the design specifications of concrete arch dams in China, engineer, in general, should regard the trial load method as the fundamental method in the course of stress analysis. For high or complex arch dams, finite element analysis is additionally demanded. The corresponding criteria for the control of principal compressive stress and tensile stress are illustrated hereinafter.

1. Safety factor of strength for trial load method

(a) Allowable compressive stress

$$[\sigma_c] = \sigma_c / K \quad (8.12)$$

where σ_c = ultimate compressive strength of concrete and K = factor of strength safety.

Under the basic load combinations, $K = 4.0$ for arch dams of grades 1 and 2, and $K = 3.5$ for arch dams of grade 3; under the special load combinations exclusive of earthquake, $K = 3.5$ for arch dams of grades 1 and 2, and $K = 3.0$ for arch dams of grade 3.

The allowable compressive stress entails the concrete grade, which should be studied with regard to the dam height. For medium-to-low arch dams, the dam dimension mainly depends on the construction condition and structural elastic stability condition, and a high allowable compressive stress is not helpful in the reduction of dam volume; therefore, the appropriate allowable compressive stress is around 2–4 MPa. For a super- or particular high arch dam with huge water thrust, too low allowable compressive stress may result in very thick dam body and undermines its technique and economy merits. A majority of China's super- or particular high arch dams have allowable compressive stress around 8.0–10.0 MPa.

(b) Allowable tensile stress

As a rule, the safety factor of compressive stress is larger, while that of tensile stress is rather lower. According to the SL282-2003 "Design specification for concrete arch dams," regardless of the dam grade, $[\sigma_t] = 1.2$ MPa for basic combinations and $[\sigma_t] = 1.5$ Mpa for special combinations exclusive of earthquake, $[\sigma_t]$ may be raised up to 30 % for special combinations inclusive of earthquake.

A majority of China's arch dams have allowable tensile stress around 0.5–1.5 Mpa.

2. Elastic finite element method

Numerous computations show that the results by FEM and trial load method are close at the portions considerably away from the dam/foundation contact face. The

Table 8.3 Allowable tensile stress and compressive stress (by FEM)

Allowable compressive stress		Identical to the trial load method (MPa)
Allowable tensile stress	Basic (permanent situation)	1.5
	Basic (temporary situation)	2.0
	Construction period for non-closed dam monoliths	0.5
	Special (check flood)	2.0

larger difference between these two methods near the contact face is mainly resulted from the stress concentration around the singularity by elastic assumption. Chinese engineers usually employ “equivalent stresses” in the calibration of dam strength: The stresses by FEM are integrated along the arch or cantilever section to get the inner forces (e.g., axial, shear, moment), and then, these inner forces are used to calculate the equivalent stresses according to arch or beam theory. The details of the equivalent computation may be referred to the corresponding design handbooks or codes (Ministry of Water Resources of the People’s Republic of China 2003; Zhou and Dang 2011).

The allowable compressive stress (equivalent) with FEM computation is identical to that with trial load method, whereas the allowable tensile stress (equivalent) with FEM computation is higher than that with trial load method, which are all listed in Table 8.3, according to the SL282-2003 “Design specification for concrete arch dams.”

Where there are a few points on the dam face at which the stresses are not satisfied referred to Table 8.3, the cracked zone should be studied to calibrate the cracking stability and its influence on the dam safety. Model experiments and nonlinear numerical computation have proved that when the arch dam surface is cracked partially, the structure is able to redistribute tensile stress by adjusting itself, until the crack ceases to propagate at definite depth. Therefore, the danger brought by the cracking in arch dams is not as serious as that in gravity dams. As a result, the tensile limited within a certain value is permitted in the process of arch dam design.

8.4 Stability Analysis for Dam Abutments

Resting on the banks of the valley, an arch dam transmits considerable loads to the abutment rocks. If the structure is not properly keyed into the banks, then the loads may give rise to abutment rock mass spalling or sliding along the discontinuities toward downstream. Therefore, the safety requirements on an arch dam include not only the stability of the dam structure itself but also the stability of its contiguity with banks. After the failure of the Malpasset Dam (France, $H = 66$ m) in 1959 due

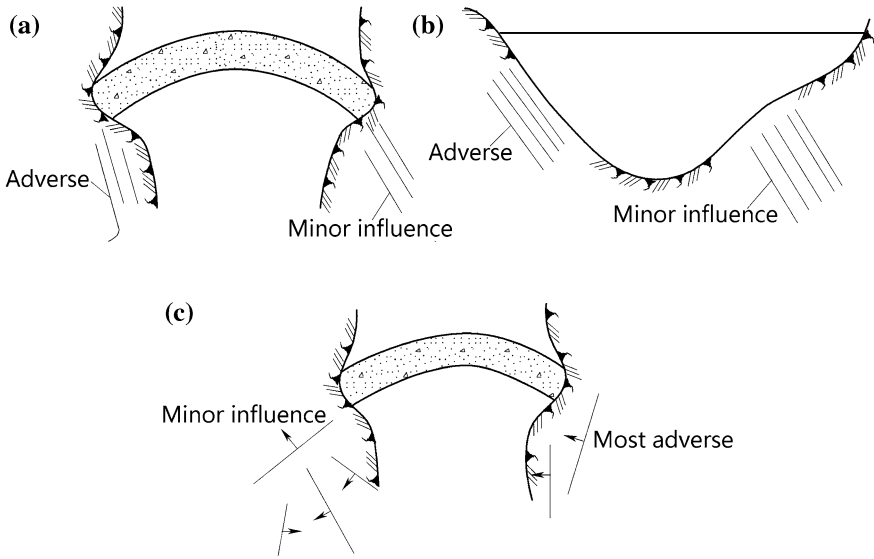


Fig. 8.16 Influence of the discontinuity tilting on the stability of arch dams

to the failure of its left bank rock mass (Londe 1987; Ru and Jiang 1995), the design codes of many countries have stipulated the abutment stability calibration as obligated step in the arch dam design process.

Before the stability analysis for the arch dam, geologist must firstly investigate the joints, fissures, and the forms of other structural planes or weak seams in the rock masses near the foundation and abutments. The discontinuities, which are parallel with the bank surface or tilted toward the river, may lead to potential sliding, and on the contrary, the discontinuities tilted into mountain have less influence on the abutment stability (Fig. 8.16).

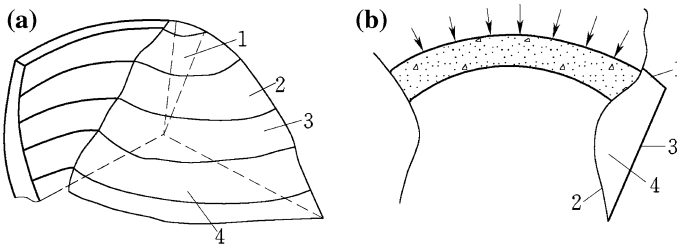


Fig. 8.17 Schematic boundary faces defining arch dam abutment stability. 1 upstream cracking face; 2 exposure face; 3 side slip surface; 4 bottom slip surface

8.4.1 Sliding Conditions of Abutment Rock Masses

Generally, abutment stability against sliding should be limited within the macroscopic slip boundaries with regard to upstream, downstream, side, and bottom (Fig. 8.17). In engineering practices, there are many discontinuities interacted with each other, which result in very complicated sliding patterns and analysis difficulties. For simplicity, engineer can anticipate several potential slip surfaces first and then calculate the corresponding safety factor against sliding.

1. Upstream boundary face

Since often, there is tensile stress in the foundation rock near the upstream heel which may trigger perpendicular cracking; therefore, the upstream boundary is normally supposed as from the vicinity of dam heel (Fig. 8.18) which stretches vertically deep down into the foundation.

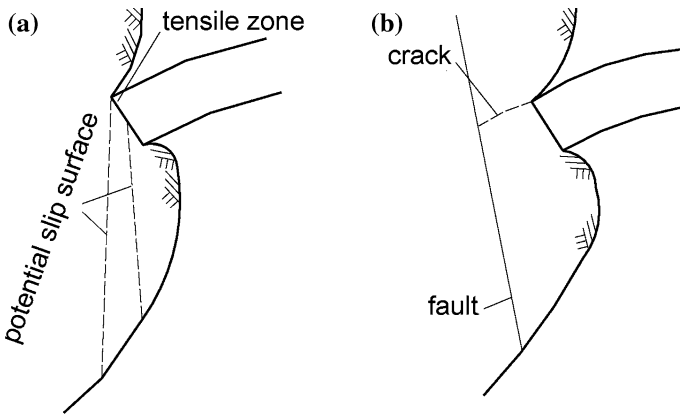


Fig. 8.18 Upstream boundary face

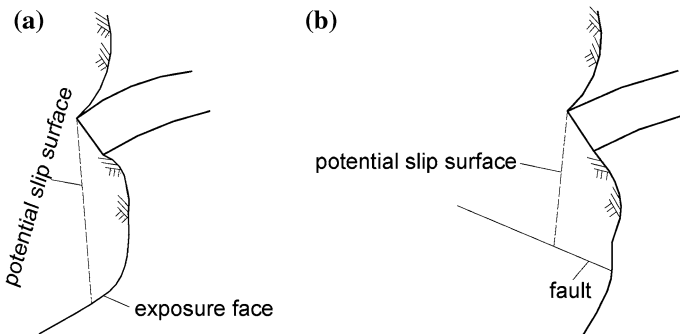


Fig. 8.19 Downstream boundary face

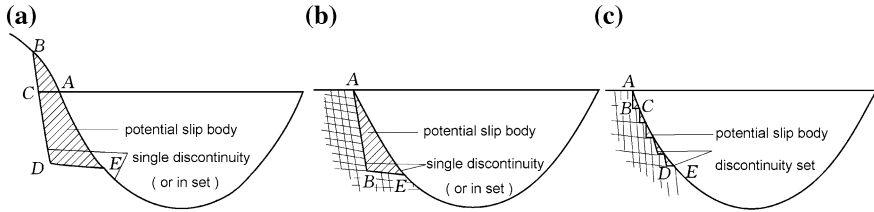


Fig. 8.20 Combination of side and bottom slip boundary faces

2. Downstream boundary face

Exposure face is customarily looked at as a downstream boundary, which may be the flair valley surface or the high deformable fault or seam (Fig. 8.19).

3. Side slip boundary face

This is usually formed by a fault, seam, or joint, of high dip angle (Fig. 8.20a, b); it also may be formed as a series of slab staggering by high-dip-angle joints in group (Fig. 8.20c).

4. Bottom slip boundary face

This is usually formed by a fault, seam, or joint, of small dip angle (Fig. 8.17). It also may be formed as a series of slab staggering by low-dip-angle joints in group (Fig. 8.20c).

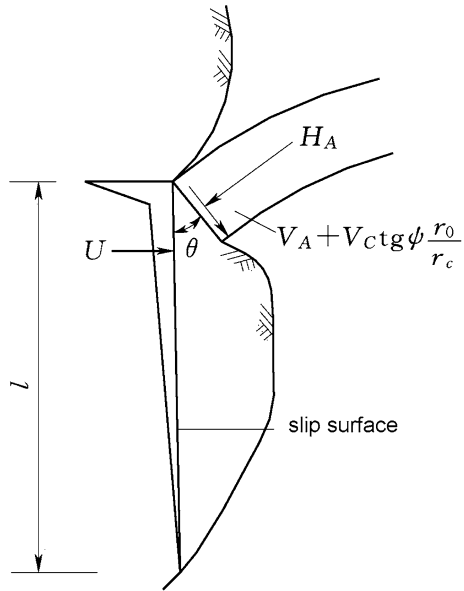
8.4.2 Analysis Methods

There are two basic methods to quantitatively evaluate the stability safety of arch abutments. One is the physical model experiment, and the other is the computation. The former, according to the features of the modeling, can be further classified into structural stress modeling, structural destructive modeling, geomechanical modeling, etc. The latter, on the basis of different assumptions with regard to the characteristics of rock mass, can be divided into two major methods:

- Numerical method. According to this method, both the dam and its foundation are considered as solid elastic or elastic–plastic bodies;
- Limit equilibrium method of rigid body. This method, on which emphasis is put on thereafter, regards the rock mass as a rigid body.

The arch dam design codes of China stipulate that the limit equilibrium method is the principal method for the stability analysis of arch dam foundation and abutments. For the large dams with complicated geologic conditions, numerical methods (e.g., finite element method) and geomechanical modeling are required to help the comprehensive study on the stability issues.

Fig. 8.21 Diagram to the local stability computation



8.4.3 Limit Equilibrium Method of Rigid Body

1. Assumptions and principles

The general assumptions and principles of the LEM have been elaborated in Chap. 5 of this book.

The procedure of stability analysis particularly for arch dam abutments can be started from the local stability (sectional stability) checking of arch rings with per unit height. If they are all stable, the whole structure will be stable without doubt. If not, check the overall safety (monolithic stability) of the whole structure.

2. Sectional stability analysis

Generally speaking, in this analysis, one can take several arch rings with unit height at ambitious elevations into account for simplicity (Fig. 8.21). There is also the assumption that the weight of dam and rock is not considered in the analysis.

Denote H_A and V_A as the projection of the axial and shear forces, respectively, exerting on the arch ring abutment, V_C as the shear force at the base from the cantilever of unit width, U as the uplift on the slip face, and θ as the included angle between the slip face and the axial direction at the arch ring abutment.

The normal force on the slip face is expressed as follows:

$$N = H_A \cos \theta - \left(V_A + V_C \frac{r_0}{r_c} \operatorname{tg} \psi \right) \sin \theta \tag{8.13}$$

where ψ = included angle between the bank slope and the vertical face; r_0 = radius of arch ring axis; and r_c = radius of the central line of arch ring.

The tangential force on the slip face is computed by

$$Q = H_A \sin \theta + \left(V_A + V_C \frac{r_o}{r_c} \operatorname{tg} \psi \right) \cos \theta \quad (8.14)$$

And the uplift is

$$U = \frac{1}{2} \gamma_w \beta h l \quad (8.15)$$

where β = action coefficient of uplift (computed by the uplift distribution diagram, usually $\beta = 0.3-0.5$); H = upstream head on the arch ring concerned; l = length of the slip face; and γ_w = unit weight of water, kN/m^3 .

The safety factor may be defined in the following:

$$K' = \frac{f'(N - U) + c'l}{Q} \quad (8.16)$$

$$K = \frac{f(N - U)}{Q} \quad (8.17)$$

where f' = shear frictional coefficient of the concrete–rock bond plane; c' = cohesion representing the unit shear strength of concrete–rock bond plane under zero normal stress, kN/m^2 ; f = friction coefficient of the assumed slip plane; and K' and K = shear factor and friction factor, respectively.

For an arch dam with variable central angle, the term $\frac{r_o}{r_c} \operatorname{tg} \psi$ in Eqs. (8.13) and (8.14) should be replaced by $\frac{\operatorname{tg} \psi}{B_A}$, where B_A is the average width at the bottom of the cantilever section.

According to Eq. (8.16), the minimum length of slip face against sliding is

$$l = \frac{K'Q - f'N}{c' - \frac{1}{2}f\beta h\gamma_w} \quad (8.18)$$

The envelope line of l_1, l_2, \dots encloses a zone in which the geologic defects should be well treated (Fig. 8.22).

3. Monolithic stability analysis

Figure 8.23 shows another important and frequently encountered local failure mode, for which the stability analysis is preceded in the following procedure:

- ① Planes enclosing the failure mode (slip body) are defined. In Fig. 8.23, (ABGF) is the base of dam with attitude $\varphi \angle \psi$, (AEJF) is the upstream boundary by cracking (P_1 , for short) with attitude $\varphi_1 \angle \theta_1$, (EDIJ) is the side

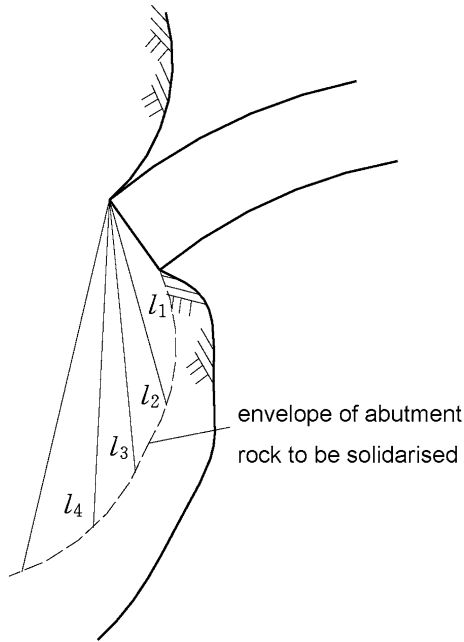


Fig. 8.22 Enveloped zone in which the geologic defects should be well treated

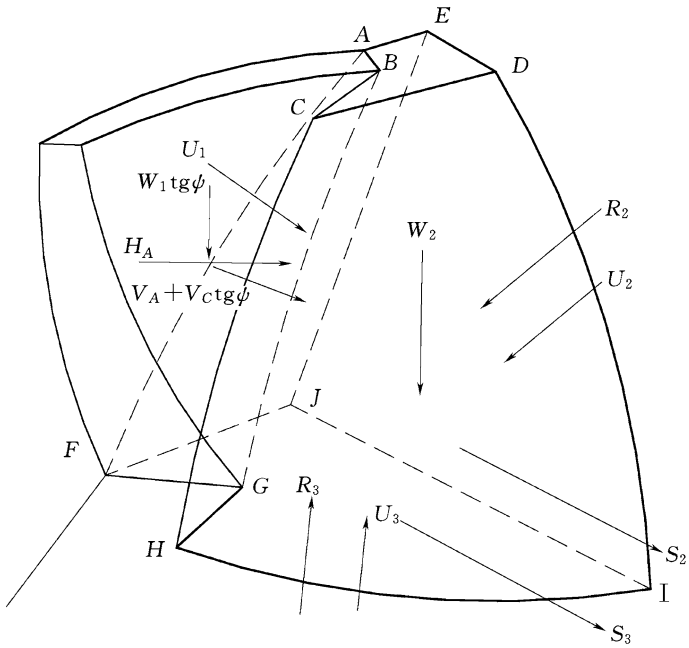


Fig. 8.23 Diagram to the monolithic stability analysis of arch dam abutment

boundary face (P_2 , for short) with attitude $\varphi_2 \angle \theta_2$, and (FGHIJ) is the bottom slip face (P_3 , for short) with attitude $\varphi_3 \angle \theta_3$;

- ② Areas A_1, A_2, A_3 of the foregoing faces P_1, P_2, P_3 are computed;
- ③ Uplifts U_1, U_2, U_3 exerting on the faces P_1, P_2, P_3 are computed, and the hydrostatic forces perpendicular to the faces, if any, are computed, too;
- ④ Forces exerting at the slip body are computed as H_A = horizontal axial force from the arch abutment, V_A = radial shear force exerting on the arch abutment, $V'_C = V_c \tan \psi$ = shear force at the horizontal bottom of cantilever, $W = W_1 \tan \psi + W_2$, $W_1 \tan \psi$ = weight of dam body and water, and W_2 = weight of rock;
- ⑤ Resultant of all forces is computed;
- ⑥ Resultant of all forces is resolved into the normal forces R_2 and R_3 , as well as the shear forces S_2 and S_3 , on the faces P_2 and P_3 . It is assumed that the directions of the shear forces S_2 and S_3 are parallel to the sliding direction under the limit equilibrium state;
- ⑦ Since the sliding on three planes simultaneously is impossible for a rigid body, only the possibility of sliding on one or two planes is checked. Tentative calculation is carried out with respect to each possible combination of resisting planes. If the resultant force associated with the sliding body has a component normal to a plane and cause compression, then the plane offers resistance to sliding. Depending on whether there is only one plane or two planes satisfying the above compressive criterion, the potential slip surface will be only one plane or be composed of two planes, respectively. With regard to Fig. 8.23, the above tentative calculation is specified as follows:
 - If the computed $R_2 - U_2$ and $R_3 - U_3$ by steps ①–⑥ are positive, the potential slip surface is composed of two planes (i.e., P_2 and P_3). The sliding failure may occur only in the direction parallel to their intersection line and toward the exposure face.
 - If the $R_2 - U_2$ on the side face is tensile, the potential slip surface is comprised of the plane P_3 only. Under such circumstances, the normal force R_3 and shear force S_3 on the face P_3 are recomputed by equilibrium condition, and during the computation, the uplift U_2 is looked at as a kind of hydrostatic pressure exerting on P_2 .
- ⑧ Factor of safety against sliding is computed for all cases where sliding is possible.

For a sliding on the two planes, the shear factor K' and friction factor K are computed by

$$K' = \frac{f'_2(R_2 - U_2) + f'_3(R_3 - U_3) + c'_2 A_2 + c'_3 A_3}{S} \quad (8.19)$$

$$K = \frac{f_2(R_2 - U_2) + f_3(R_3 - U_3)}{S} \tag{8.20}$$

where $S = S_2 + S_3$ and f_2', f_3' = shear frictional coefficients of the faces P_2 and P_3 , respectively; c_2', c_3' = cohesion representing the unit shear strength under zero normal stress of the faces P_2 and P_3 , respectively, kN/m²; and f_2, f_3 = friction coefficient of the faces P_2 and P_3 , respectively.

For the sliding on the plane P_3 only, the shear factor K' and friction factor K are computed simply by

$$K' = \frac{f_3'(R_3 - U_3) + c_3'A_3}{S} \tag{8.21}$$

$$K = \frac{f_3(R_3 - U_3)}{S} \tag{8.22}$$

4. Allowable safety factor against sliding

According to the summarization of 24 China’s arch dams completed, allowable safety factors against sliding are $[K'] = 2.5\text{--}3.5$ and $[K] = 1\text{--}1.3$. Table 8.4 lists the allowable safety factor against sliding stipulated by the SL282-2003 “Design specification for concrete arch dams.”

The fact that the parameter f had no united evaluation method for the completed arch dams in China leads to the difficulties with the selection of corresponding allowable friction factor. Therefore, the friction factor is merely recommended for grade 3 structures. On the contrary, a majority of arch dams in and outside of China had been designed using friction formula, and several European countries even employ friction formula solely in the stability analysis. Nowadays, for high arch dams, Chinese engineers are shifted to adopt the friction formula in parallel to the shear formula, as a part of the comprehensive calibration for the abutment stability.

USA, former USSR, and Japan all demand $K \geq 1.5$ for the arch dams. For example, USBR stipulates that regardless of the dam grade, $K \geq 1.5$ by friction formula for abutment stability. The Chirkey Dam (Georgia, $H = 235.0$ m) required a $K \geq 1.5$ in the analysis of abutment stability dominated by faults and seams; for the abutment stability of the Inguri Dam (Georgia, $H = 271.5$ m), $K \geq 1.8$; and the Kurobe No IV Dam (Japan, $H = 186$ m) specified a $K \geq 1.5$ in the analysis of abutment stability. The representative friction safety factor of arch dam abutment

Table 8.4 Allowable safety factor against sliding

Load combination		Grade of dam		
		1	2	3
Shear formula	Basic	3.50	3.25	3.00
	Special (exclusive earthquake)	3.00	2.75	2.50
Friction formula	Basic	–	–	1.30
	Special (exclusive earthquake)	–	–	1.10

stability in China is ranged between 1.0 and 1.3, which are listed in Table 8.5. They are 20–30 % lower compared to that outside of China, which might be resulted from the different evaluation process of friction coefficient f .

5. Countermeasures to improve the stability against sliding

If the sliding stability of dam abutments is not met according to the analysis, the following countermeasures may be selectively adopted:

- Intensify foundation treatment, by washing and consolidation grouting of fractures, replacing concrete for dominant faults and seams, and transmitting dam abutment thrust deeper into solid bedrock by keys and/or piles;
- Intensified grouting and draining within abutment rocks to reduce uplifts;
- Keying the dam deeper into abutment rocks, to enlarge the resistant rock mass downstream of the arch rings;
- Adjusting the abutment thrust at high angle to the dominant seams and bank surface, if possible. In this way to increase the normal forces and to decrease the shear forces on the potential slip surfaces;
- Flair abutments or installing thrust piers, at the upper elevations of the valley where the bearing capacity of rocks is not sufficient. They are often made as gravity walls whose thickness is increased toward banks.

The details of the above countermeasures will be discussed later in this chapter.

8.5 Design of Dam Body

8.5.1 Arch Dam Layout

The primary objective in the layout of an arch dam at a particular site is to determine the kind of arch dam that will fit the topographic and geologic conditions most advantageously and will distribute the load with the most economical use of materials. Meanwhile, attempt is made to achieve suitable conditions for both the service of the dam and its contiguity with the banks at the minimum volumes of concrete placement and rock excavation involved. The result, in general, is presented in the form of a plane, profile, and section along the referenced plane (Golzé 1977; Jansen 1988; Zhou and Dang 2011). The general procedure for arch dam body layout includes contemplate layout specifying the shape and size of arch dam according to engineering experiences and the dam site conditions; then, this scheme is hand over for the stress and stability analysis; based on the analysis results, the dam shape and size are revised to improve the strength, stability, and economic indices. This procedure is repeated until the following conditions are satisfied as perfect as possible:

Table 8.5 Allowable safety factor by friction formula of representative arch dams in China

Name	Dam type	Height (m)	Foundation rock	f	[K]
Xiaowan	Double curvature	294.5	Biotite granitic gneiss	0.48–0.95	1.3
Xiluodu	Double curvature	278	Basalt	0.3–1.31	1.3
Jinping 1	Double curvature	305	Marble, sand slate	0.33–0.97	1.3
Ertan	Double curvature	240	Simaite, basalt	0.6–1.1	1.3
Baishan	Gravity arch	149.5	Metamorphic migmatite, hornblende–plagioclase, leptynite amphibolite	0.55–0.6	1.3
Dongjiang	Double curvature	157	Granite	0.62–0.73	1.1
Longyangxia	Gravity arch	177	Granodiorite, metasandstone	0.25–0.6	1.1–1.3
Lijiaxia	Double curvature	155	Biotite migmatite, hornblende–plagioclase, leptynite amphibolite	0.4–0.45	1.3
Fengtian	Hollow arch	112.5	Quartz sandstone	0.25–0.6	1.05–1.3
Shimen	Double curvature	88	Mica–quartzose schist, quartz schist	1.0–1.18	1.2–1.5
Liuxihe	Double curvature	78	Granite	0.59	1.0
Quanshui	Double curvature	80	Granite	0.5–0.7	1.0
Yanxi 1	Double curvature	75	Tufflava	0.3–0.5	1.0
Lishimen	Double curvature	74.3	Tuff	0.5–0.6	1.0–1.05
Jinshuitan	Double curvature	102	Granite	0.25–0.79	1.1–1.15

- That the stresses are uniformly distributed;
- That the maximum compressive stress approaches allowable stress of the concrete;
- That the maximum tensile stress does not exceed the allowable tensile stress of the concrete;
- That the abutment stability is satisfied as required;
- That the concrete volume and rock excavation volume are minimum;
- That it is feasible and convenient in construction.

It is difficult to obtain an ideal arch dam configuration rigorously and simultaneously satisfying all of the foregoing requirements; therefore, it is up to the engineers to make compromising solution for a rather good design which yields a

dam that has some very low compressive stresses and zones of tensile cracking, provided that they are within the defined allowable limits.

The layout for an arch dam comprises the selection of parameters such as the axis equation of arch ring, the shape of crown cantilever, the thickness at arch crown and abutments, and the curvature radius. The restraint conditions are stress, stability, overhang degree, central angle, etc. The major factors considered in the layout of arch dam are as follows:

- The dam should be adaptive to the foundation uneven settlements and openings in the dam body.
- The thrust direction from arch abutment should be in favor of abutment rock stability. This is customarily achieved by reasonably adjusting central angles to let the thrust have high included angle with the bank surface and the dominant seams. The maximum central angle is ranged between 75° and 110° , which makes a good compromise between the requirement for the abutment stability and dam body strength;
- The overhang degree of the cantilever is controlled within 0.3, to facilitate the construction and to control the cracking on the dam surface;
- The earthquake resistance should be guaranteed.

The fineness of elaboration in the layout is different due to the design phase concerned:

- In the phase of planning, the arch dam shape may be configured only based on the dam height, valley topography, geology, and the other similar dams completed;
- In the phase of feasible study, the dam site should be fixed, the layout and the shape as well as the sizes of the dam should be studied based on the stress and stability analysis, and comparative schemes are provided for the selection preparatory. For important high arch dams, rather detailed analyses and computations are necessitated;
- In the phase of preliminary design, various basic and special load combinations are taken into account, the stress and stability are analyzed comprehensively, and the layout and the shape as well as the control sizes of the dam are fixed. The designed dam by this phase should meet all the requirements of design codes and is technically and economically viable. For important high arch dams, physical model experiment is carried out, and the research reports on the particular issues are also provided;
- In the phase of construction documentary, the working drawing for construction site is provided according to the results of feasible phase which are adjusted by the recently revealed geology and other conditions during the construction.

8.5.2 Procedure and Key Issues in the Design

The routinely recommended design procedure can be divided into following steps:

- According to the topography and geology documents, figure out the depth of foundation excavation that is based on the topographic maps and the geologic data at the proposed work sites. Then, draw out the contour map of the bedrock surface that is capable of being used as dam base;
- Considering the topographic and geologic conditions, the hydrologic data, as well as the construction conditions, select the competent type of arch dam;
- Draw a tentative axis of dam overlaid on the site topography, and adjust this axis to obtain optimum orientation;
- Assume a tentative thickness and shape of the crown cantilever;
- Build the plan of the dam developed along the chosen axis in the form of a series of arch rings at different altitudes. Generally, the central angles vary from 90° to 100° . However, on the valley with poor geologic conditions, they can be as lower as 75° . In order to ensure the stability of arch abutment, the angle of the intersection of the intrados and the abutment surface should be not smaller than 30° . After the selection of central angles, the arch rings at crest and bottom are firstly fixed, then the trace line of arch centers is fitted, and the representative arch rings from top to bottom are drawn;
- A number of cantilevers are selected from the plan of above tentative arch dam, to check their smoothness, twist, and overhang. The adjustment is carried out, if necessary;
- The engineering amount, stress, and stability are analyzed. Based on the analysis results, the dam shape is modified.

The above steps are repeated and terminated when a rather satisfied arch dam configuration is obtained. In the following, a circular arch dam with variable thickness will be taken as example, to illustrate the layout procedure of the arch dam.

1. Foundation surface

Dam height is the vertical distance from dam crest to the lowest foundation surface. The determination of the dam base and corresponding cutting depth in rock is technically and economically significant. The deeper the foundation excavation, the deeper the arch abutments keyed into the sound bedrock, to mobilize more rock masses for withstanding the applied loads, which is in favor of abutment stability safety.

However, too deeper abutment keying involves excessive excavation and high hydrostatic pressure attributable to longer arch span, and the other difficult issues such as the excavation rebound and relaxation and stability of excavated slope will manifest. Therefore, under the restriction of sufficient safety, shallow excavation for

the foundation surface may save the engineering amount and shorten the construction period.

The SD 145-1985 “Design specification for concrete arch dams” issued in 1985 stipulates that the base of arch dam should be on intact or slightly weathered rock masses. A number of arch dams of 100–150 m high in China were constructed according to this foundation requirement.

The SL282-2003 “Design specification for concrete arch dams” issued in 2003 stipulates that the arch dam foundation should satisfy the requirements for integrity, stability, anti-seepage, and durability. The dam base may be on intact, slightly weathered, medium-and-lower portion of weakly weathered rock masses, which is decided by the comprehensive study regarding the dam height, the loads, the stress distribution in foundation, the foundation geologic and mechanical conditions, the effect and period as well as the expenditure of foundation treatment.

The DL/T5346-2006 “Design specification for concrete arch dams” issued in 2006 stipulates that the foundation excavation depth should be selected on the economical and technical studies considering the rock mass type and quality (BQ), the physical and mechanical properties, the bear capacity requirements, the foundation treatment effect and period as well as cost. For a high arch dam, the excavation should be down to grade II rock masses, whereas grade III rock masses may be used locally in certain position only; for a medium-to-low arch dam, the requirements could be relaxed appropriately.

The above standards are applicable for arch dams lower than 200 m, and for arch dams higher than 200 m, the foundation surface should be studied with special care. The recent experiences of China’s particular high arch dams such as the Ertan ($H = 240$ m), the Laxiwa ($H = 250$), the Goupitan ($H = 232.5$ m), the Xiluodu ($H = 278$ m), and the Xiaowan ($H = 292$ m) show that provided the appropriate foundation treatment, the usage of weakly rock masses in the foundation for particular high arch dams may guarantee the safety and reduce rock excavation as well as concrete placement, which brings about remarkable economy benefits.

To provide stable abutments under all loading conditions, in making the layout, cares should be called at the trends of discontinuity system in the rock mass.

2. Dam axis

In China, the extrados of crest arch ring is customarily defined as the axis of arch dam, and its left or right half central angle φ_L or φ_R is measured from the corresponding abutment to the arch crown. The central angle is usually adjusted along the height. For a symmetric arch dam, φ_L is identical to φ_R at any elevations. The position, shape, and central angle of the dam axis dominate the configuration features of an arch dam, including its position, thrust forces (quantity and direction), and curvature.

The relationship between the central angle and the direction angle of arch abutment thrust is shown in Fig. 8.24, which is plotted according to the

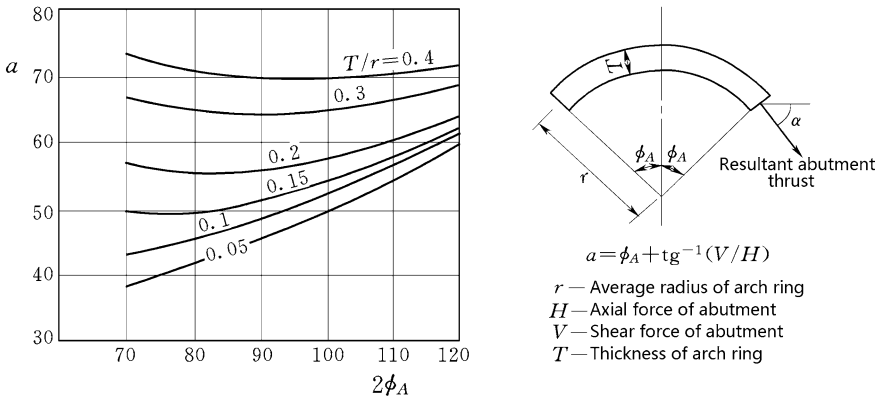


Fig. 8.24 Relationship between the central angle and the direction angle of abutment thrust

computation results for a symmetric circular arch dam with constant thickness and Young’s modulus ratio $E_c/E_r = 1$. For any other type of arch dams, similar performance may be expected. Generally, the larger the central angle, the smaller the axial inner force at arch ring section and the thinner its cross section, but the longer the arch ring length. The volume of a unit arch ring will be reduced before the central angle approaches approximate limitation of 130° . On the other hand, with the increase of central angle, the included angle between the arch abutment thrust and the abutment slope contour decreases, which is not in favor of abutment stability. This is why a central angle of 75° – 110° is desirable to adopt: In this range, the included angle between the arch abutment thrust and the abutment slope contour may be kept within 35° – 50° , and the included angle between the intrados at the abutment and the abutment slope contour may be larger than 30° .

For a single circular arch dam, the radius r_0 , the half central angle ϕ_A , and the length of chord L_1 are exactly related by

$$r_0 = L_1/2 \sin \phi_A \tag{8.23}$$

For a nearly symmetric valley, r_0 may be estimated by

$$r_0 = 0.61L_1 \tag{8.24}$$

where L_1 = chord length, m .

In the layout of dam axis, the bedrock topography and geology may be inaccurately mapped and the arch abutments may need to be extended to somewhat deeper than originally planned. Therefore, it is necessary to leave certain room for a further elongation in L_1 .

Where the contours of foundation face are parallel to the river, Eq. (8.24) is equal to state that $2\varphi_A = 110^\circ$. If the r_0 estimated by Eq. (8.24) cannot meet the abutment stability, the radius of dam axis should be raised to reduce the central angle.

To obtain the best position of a dam axis, which makes nearly uniform and sufficiently large central angles, the initial dam axis should be tentatively adjusted by moving and rotating, and during this procedure, the radius r_0 as well as chord L_1 will be correspondingly changed.

3. Shape and size of crown cantilever

(a) Crest thickness T_c

In general, the cantilever thickness T_c at crest basically stands for the stiffness of the crest arch ring. It can affect not only the stress at the upper portion of the dam, but also that at the cantilever base. For instance, in a fairly wide valley, an increase of crest thickness can reduce the tensile stress at the cantilever base near the dam toe.

There are several methods available for fixing T_c in the following:

- When the roadways and so on are not demanded at the top of dam, the thickness of crest arch ring may vary from 3 to 5 m, which is decided by the height of dam and the width of valley.
- The accommodation of roadway, curbside, and parapet often requires a greater thickness than it is necessary for satisfactory arch and cantilever stress only;
- If there is no criterion made to govern and the data on similar structures are not available, the crest thickness may be estimated by the following empirical formula:

$$T_c = 0.01[H + AL_1] \text{ (m)} \quad (8.25)$$

where H = structural height of dam, i.e., the vertical distance from the dam crest to the lowest point of the foundation and L_1 = chord length; $A = 1.2\text{--}2.4$.

(b) Base thickness T_B

The base thickness is another critical geometrical parameter in the design of an arch dam. It is determined by many factors such as the geologic and topographic conditions of the valley, loads and materials, and type of arch dam and its structural height.

In general, it can be estimated analogously using similar dams existed. Of course, loop calculation and adjustment of the base thickness are always necessary to obtain an ideal result.

After pooling the data for all types of canyons, the USBR gives an empirical formula, which may be used as an initial estimation only for primary layout (Golzé

difference between (A) and (C) to the dam height H , β_2 is the ratio of the horizontal difference between (B) and (D) to the dam thickness T_B , and β_3 is the ratio of the horizontal difference between (A) and (B) to the dam thickness T_B which sometimes is termed as the degree of convexity. β_1 , β_2 , and β_3 are selected empirically by designers within $\beta_1 = 0.55\text{--}0.66$, $\beta_2 = 0.3\text{--}0.6$, and $\beta_3 = 0.1\text{--}0.2$. The typical crown cantilever shape recommended by the USBR (1987a, b) has the value of β_1 , β_2 , and β_3 as 0.55, 0.67, and 0.177, respectively. The points (A), (B), and (C) (additional fourth point may be added, if necessary) are therefore employed to construct the upstream curve of the crown cantilever.

The upstream curve of crown cantilever may be single arc or multi-arc, quadratic, cubic, or other types of curve (suitable for double-curvature arch dams) and may be vertical or inclined straight line, or polyline (suitable for single-curvature arch dams). Suppose the upstream curve of the crown cantilever is composed of two arcs (CA) and (AB), whose centers are all located at the horizontal line passing point (A), the radii R_1 and R_2 of the arcs (CA) and (AB) are computed by Eqs. (8.27) and (8.28) as follows:

$$R_1 = \left[\frac{\beta_2 + \beta_3}{2} + \frac{\beta_1^2}{2(\beta_2 + \beta_3)} \left(\frac{H}{T_B} \right)^2 \right] T_B \quad (8.27)$$

$$R_2 = \left[\frac{\beta_3}{2} + \frac{(1 - \beta_1)^2}{2\beta_3} \left(\frac{H}{T_B} \right)^2 \right] T_B \quad (8.28)$$

The thickness at the point (A) may be estimated by

$$T_A = \frac{0.7L_A\beta_1H}{[\sigma_c]} \quad (8.29)$$

where H = height of crown cantilever, m; $[\sigma_c]$ = allowable compressive stress of concrete, kPa; and L_A = straight distance from right abutment to left abutment at the elevation of (A), m.

There are two ways to construct the downstream face of crown cantilever:

- According to the (A), (B), and (C) points and the thicknesses T_A , T_B , and T_C , the corresponding points (E), (F), and (G) are computed, and then, the downstream curve may be fitted similar to that of upstream;
- Assume that the thickness varies quadratically or cubically, then the thickness function $T(z)$ may be interpolated by T_A , T_B , and T_C , and the downstream curve is fitted by the upstream curve plus $T(z)$.

The above methods for the configuration of crown cantilever are for double-curvature arch dam only. For single-curvature arch dam, vertical or sloping straight line, or polyline, is commonly employed.

The crown cantilever contemplated foregoing should be adjusted repeatedly in the optimal design.

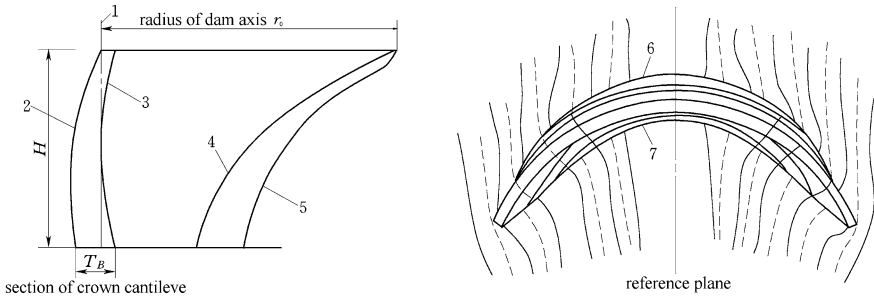


Fig. 8.26 Layout of single-centered arch dam with uniform thickness. 1 dam axis; 2 upstream face; 3 downstream face; 4 central line of intrados; 5 central line of extrados

(d) Layout of arch rings

Generally, 5–10 horizontal arch rings are uniformly laid out along altitudes, to configure the shape of dam body. The distance between adjoining arch rings is smaller than 30 m but larger than 6 m.

Referring the position and profile of the crown cantilever, the intrados and extrados curves (concentric or non-concentric) as well as the central angles of arches are drawn. These arches are drawn in plan for the purpose of stress analysis and to examine the smoothness, overhang, and continuity. To ensure that the dam is smooth, the centers of arch radii must lie along the reference plane in plan and be connected by smooth continuous curves in elevations, which is called trace lines of center, as shown in Fig. 8.26.

(e) Reshaping

The layout scheme of dam is analyzed with respect to stress and deflection as well as stability under stipulated load combinations. The amount of rock excavation and concrete placement are also computed, too. The results of analysis serve to evaluate the adequacy of the design, and to judge if any adjustments to meet the demand of safety and economy consistent with the technological and environmental considerations, are required. Reshaping is the key step to produce a complete and balanced arch dam design. The task of the designer is to determine where and to what degree the dam shape should be adjusted. Several issues of how a design can be improved by reshaping are explained as follows:

- When the lower portions of cantilevers have too large overhang degree, they are unstable and tend to overturn in the direction of upstream during construction due to self-weight. The cantilevers must be adjusted to redistribute the self-weight;
- If an arch ring exhibits excessive tensile stress on the downstream face at crown, one alternative would be to reduce the arch thickness by cutting concrete from the downstream face at the crown while keeping the same intrados near the

- abutments. Another possibility would be to strengthen the crown area of the arch by increasing its horizontal curvature, i.e., increasing the rise of the arching;
- Load and deflection distributions should be smooth from point to point. Very often, when an irregular distribution manifests, it is necessary to shift the load from vertical cantilever elements to the horizontal arches. Such a transfer can be realized by reducing the stiffness of the cantilever relative to the arch;
 - Whenever the overall stress level in the dam body is below the allowable limits and the stability of the dam abutments is above allowable limits, concrete volume should be cut, thereby utilizing the remaining concrete more efficiently and improving the economic indices.

8.5.3 *Optimal Design*

Through more than 30 years of endeavors, high level of the research and application of arch dam optimal design has been fully put into practice (see Chap. 6). So far, altogether more than one hundred arch dams have been designed and constructed in China using this technique.

8.5.4 *Factors Affecting the Layout*

1. Ratio of width to height of valley

The thickness T_B estimated by Eq. (8.26) is subject to the adjustment according to the valley shape. The ratio of T_B/H , suggested and adopted in dam design, is mainly dependent on the topographic conditions customarily represented by the relative width L/H of the valley.

2. Symmetry of valley

An exactly or nearly symmetric valley is desirable for good stress distribution in arch dams, because a region of strong stress concentration is likely to appear in an arch dam having an asymmetrical profile. However, dam sites are rarely regular, and most often the valley is topographically asymmetrical. In addition, structural asymmetry may be resulted from the variations in the deformation and strength properties of the abutment rocks, too.

For asymmetrical valley, there are five countermeasure solutions in the design, and they are as follows:

- To excavate the foundation/abutments deeper until appropriate bedrocks;
- To construct an artificial abutment or reorient the dam;
- To keep the dam asymmetrical in conforming with the shape of the valley and meanwhile to attain symmetry stress by the proper variation of structural thickness;

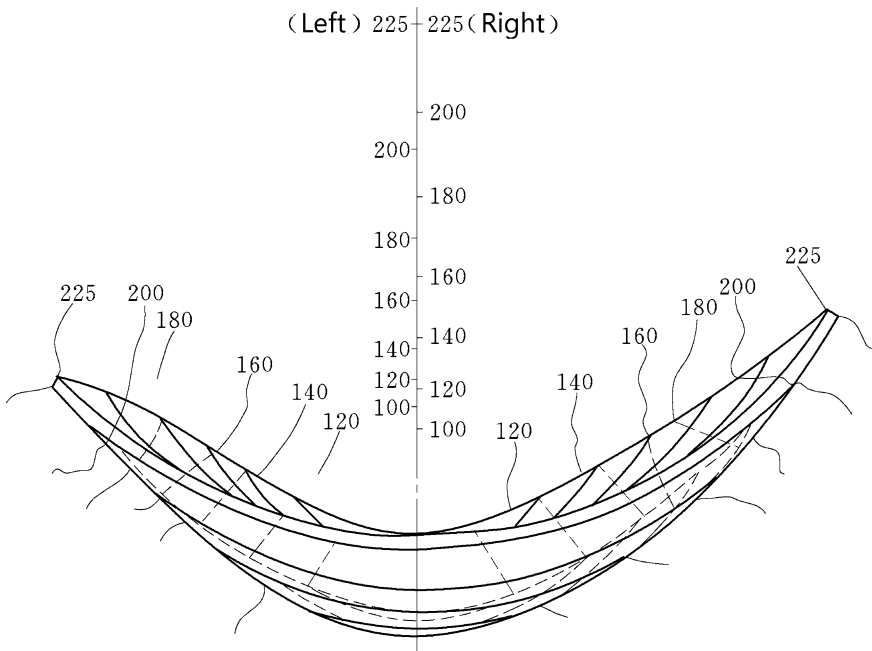


Fig. 8.27 A two-centered double-curvature dam with uniform thickness arches

- If a single-centered arch dam is not able to well fit the asymmetrical canyon, two-centered or multi-centered alternatives may be employed, as shown in Fig. 8.27;
- For an asymmetrical valley where abutment thickening is desirable, short radius fillets on the downstream face may be added.

3. Shape of valley

In U-shaped sites with fairly larger chord length, the cantilever action is strengthened, which gives rise to a thickened dam near base, hence constant radius and variable thickness arch rings may be employed. In V-shaped sites on the contrary, constant central angle and variable radius arch dams are more adaptive and flexible in the course of layout. Figure 8.28 shows a two-centered double-curvature dam with variable thickness arches.

In a wide valley, cantilevers bear larger portion of water pressure, and under such circumstances, the up- and downstream faces are to be curved forming double curvature, where the arches have variable thickness and multi-centers. Peripheral joint also may be installed between the dam body and the foundation pad, to cut the cantilever stiffness.

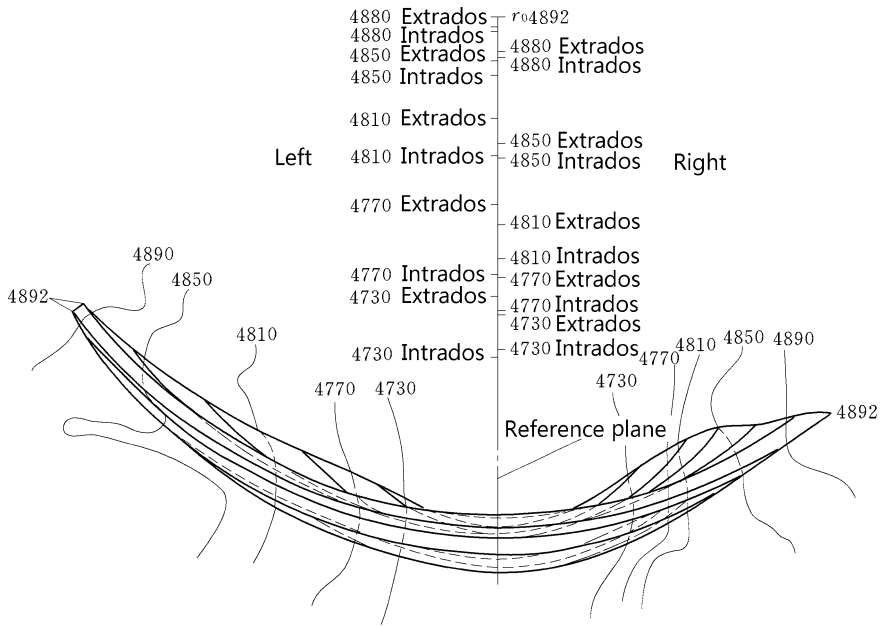


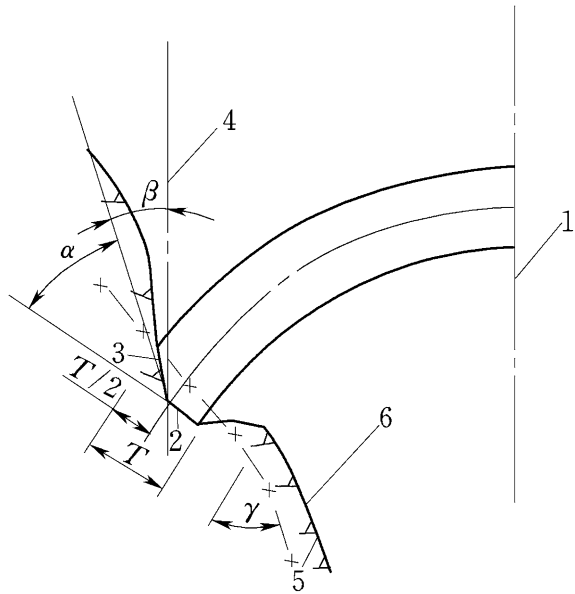
Fig. 8.28 A two-centered double-curvature dam with variable thickness arches

4. Arch shapes

Generally, an arch with constant thickness is advisable near the crest of dam, where it bears small loads. At medium-to-low elevations, the arch with variable thickness is in more favor of stress condition. For this purpose, short radius fillets may be added to the initially uniform thickness arches on their downstream face. In horizontal plan, the fillet centers at each side of the dam call smooth curves to avoid irregularly warped surfaces. The locus of the points of tangency between the arch intrados and the fillets—the trace of the beginning of fillets—also should fall on a smooth curve. The fillet radii should be sufficiently long to secure that the resultant of arch forces is directed safely to the abutment rock and that the curvatures on the downstream face of both the arch and cantilever elements are not too larger to produce excessive stresses parallel with the dam face. For this reason, the included angle between the fillet and the abutment should be greater than 45° . As a common rule, fillets should be so laid out that the up generatrix of their traces will intersect the crest arch exactly at its abutment and that the down generatrix will terminate approximately in the region with maximum arch abutment stress, which is at around $1/2$ – $3/4$ of the dam height above base. Figure 8.29 shows a constant thickness arch dam with fillets.

In wide valleys of all shapes (U, V, trapezoidal), triple-centered circular arch, parabola arch, elapse arch, or logarithmic spiral arch all may be selectively

Fig. 8.31 Arch abutment arrangement. 1 central line; 2 full-radial excavation face; 3 upstream half-radial excavation face; 4 line parallel with central line; 5 face of sound bedrock; 6 face of natural ground



The orifice within dam would induce strong stress concentration around the opening; therefore, they are better to be located in lower stressed zones.

8.6 Flood Release and Energy Dissipation of Arch Dams

8.6.1 Layout of Flood Release

There are five types of the spillway in arch dam projects, and they are basic arch dam appurtenance ensuring a safe flood passage from the reservoir into the downstream river reach.

1. Spillways in/on dam body

Flood may be released from the arch dam by overflow (open flow) weir, orifice, and deep and bottom outlets. The distinguishability of orifices and deep outlets is roughly based on the altitude and main purpose: The former is located above the half dam height and mainly for the purpose of flood discharge, while the latter is below the half dam height and mainly for the purpose of reservoir drawdown as well as for the late-stage river diversion. Very low level water passages mainly used for early-stage river diversion or water supply are customarily named as “bottom outlets.”

2. Spillways on dam abutments

They are ordinarily positioned at the two sides of the dam near abutments, with entrance structures (intakes) within the dam. When the elevation of the entrance is high, a chute-type trough is followed to form ski-jump spillway, such as in the Karaj Dam (Iran, $H = 180$ m); when the elevation of the entrance is low, an open channel may be followed to form open-channel spillway along the downstream riverbank, such as in the Lijiaxia Dam (China, $H = 147$ m) and in the Jinshuitan Dam (China, $H = 102$ m).

3. Spillways on riverbanks

This kind of spillway may be arranged at one bank or only on both banks of dam, with the entrance structure and chute or channel in the excavated rock. The chute or channel is usually longer than that of the abutment spillways, which may deliver the released flow jet far away from the dam toe.

The Amir-Kabir Dam (Iran, $H = 180$ m) and the Gokcekaya Dam (Turkey, $H = 158$ m) employ this kind of spillway.

4. Tunnel spillways

This kind of spillway is laid out in the mountain at one bank only or on both banks of the dam, with the entrance structure and water conduit totally within the excavated rock.

5. Combination of different spillways

To meet the need of large flood releasing, the underground powerhouse + combined spillways is a prevalent layout nowadays. According to the discharge as well as the topographic and geologic conditions, two, three, or even four types of spillways may be integrated in one arch dam project.

The Longyangxia Dam (China, $H = 178$ m) adopts the spillway layout scheme of dam abutment + riverbank; the Yellow Tail Dam (USA, $H = 160$ m), the EI Cajon Dam (Honduras, $H = 234$ m), the Ertan dam (China, $H = 240$ m), the Xiaowan Dam (China, $H = 294.5$), the Xiluodu Dam (China, $H = 278$ m), and the Dongjiang dam (China, $H = 157$ m) adopt the spillway layout scheme of dam body + tunnel; the Wujiangdu dam (China, $H = 165$ m) adopts the spillway layout scheme of dam body + dam abutment + riverbank; the Dongfeng Dam (China, $H = 168$ m) adopts the spillway layout scheme of dam body + riverbank + tunnel.

The details of tunnel spillway and riverbank spillway will be given in Chaps. 12 and 13 of this book. The spillways on/in arch dam body will be discussed hereinafter.

8.6.2 Types of Dam Body Spillways

Spillways on riverbanks were commonly exercised in the early period of arch dam construction due to the worries that large opening in dam would undermine its safety. As the progress in arch dam stress analysis methods, and in the manufacture

technology of larger steel gate, as well as in the energy dissipation, spillways on/in dam body are more and more prevalent. The practices in recent 40 years show that the flood discharge through arch dam body may be as high as 10,000 m³/s. The types of spillways on/in arch dam body may be selectively employed among free over-fall, jet trajectory, ski jump, and dam orifice or outlet (Mason 1993). These spillways are further referred to as controlled or uncontrolled, depending on whether they are gated or ungated.

1. Free over-fall

A free over-fall or straight drop is one by which the overflow drops from the roundhead (or bulkhead) weir crest (Fig. 8.32). This type is applicable to a thin arch dam on good foundation rock, and the allowable unit flow discharge is normally 20–30 m³/(s m). Flows may be free discharging, or they may be supported along a narrow crest. Occasionally, the crest is extended in the form of overhanging lip to direct small discharges away from the dam toe. In free over-fall spillways, the underside of the nappe is ventilated sufficiently to prevent a pulsation and fluctuation in the outflow jet.

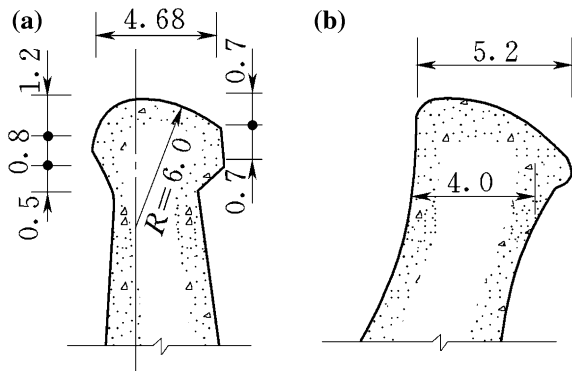
If the tailwater depth is sufficient, a hydraulic jump will occur when a free over-fall jet falls upon a flat apron. It has been demonstrated that the momentum equation may be applied to determine the parameters of the jump. Where no artificial protection is provided at the base of the over-fall, scouring will manifest in most streambeds giving rise to a deep plunge pool.

2. High-level jet trajectory

Weirs with high-level jet trajectory frequently employed for arch dams are shown in Fig. 8.33, which are actually bulkhead weirs revised by adding higher-level flip buckets. This enables outflow water to be plunged farther than free over-fall and is in favor of dam toe safety against scouring. The allowable unit discharge may be larger than that of free over-fall.

The commonly used flip bucket has continuous type, and the slotted bucket is seldom exercised in arch dams.

Fig. 8.32 Crests of free over-fall spillway (unit: m).
a The Banjiang Dam (Hunan Province, China, $H = 43.1$ m);
b the Sakamoto Dam (Japan, $H = 103$ m)



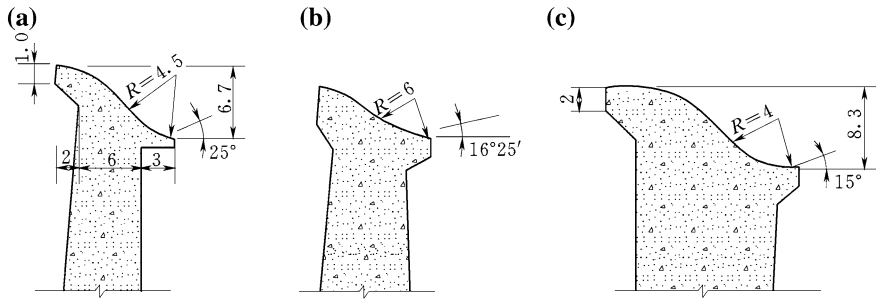


Fig. 8.33 Weir profiles with high jet trajectory (unit: m). **a** The Changshaba Dam (Sichuan Province, China, $H = 52.8$ m); **b** the Huamuqiao Dam (Hunan Province, China, $H = 38.7$ m); **c** the Shuichetian Dam (Guizhou Province, China, $H = 63.30$ m)

The key parameters for the flip bucket design are the height of lip, radius R of the bucket, and the flip angle θ , which are mainly decided by laboratory experiments. A lower lip may create higher velocity of water jet with farther throwing distance, but it results in larger profile of weir and correspondingly higher expenditure. Usually, the height difference from the crest to the bucket lip is smaller than 6–8 m (Fig. 8.33) and is approximately 1.5 times of the design head H_d . θ is smaller than 25° but larger than 10° , and R is nearly identical to H_d .

For the thick arch or gravity arch dam, sometimes an ogee profile of spillway may be configured, which may be named as low jet trajectory similar to that of

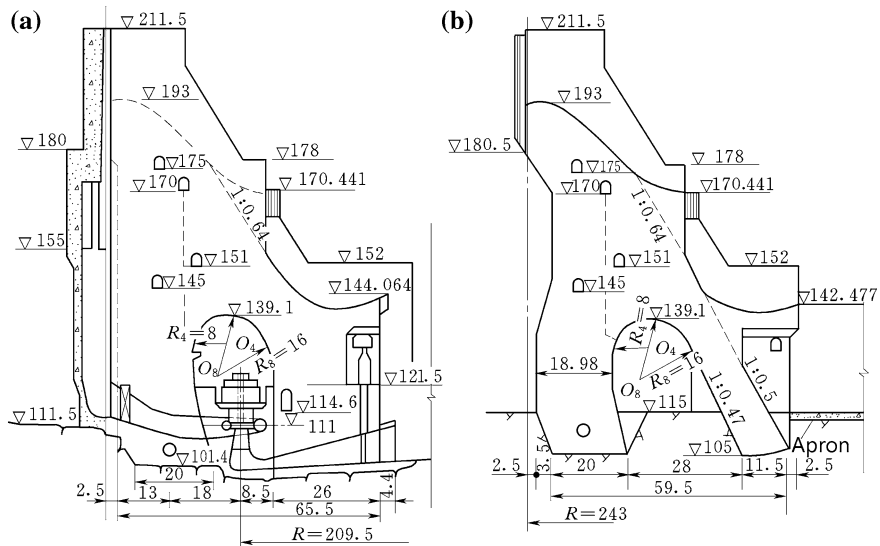


Fig. 8.34 Profile of the gravity arch dam (unit: m) the Fengtan Project (Hunan Province, China). **a** Profile 1; **b** profile 2

gravity dam. The Fengtan Gravity Arch Dam (Hunan Province, China, $H = 112.5$ m) (Fig. 8.34) employs this kind of spillway with unit discharge of $183.3 \text{ m}^3/(\text{s m})$. According to the studies mainly based on experiments, 6 high and 7 low jet trajectory buckets are installed. The impact angle of the water jets is 50° – 55° .

3. Ski jump

In many modern spillway designs, increased energy dissipation is achieved by using high-speed free-falling jets, either at the end of a “ski jump” or at the downstream of a flip bucket.

The Marèges Dam at a height of 90 m on the Dordogne River (France) was constructed between 1932 and 1935. The dam, designed by André Coyne, incorporated several innovative features to include a ski-jump spillway placed on the roof of the downstream riverbed power plant.

The dispersed and aerated jet stresses the downstream riverbed (plunge pool) much less than a compact unaerated jet. Its use brings substantial economic benefits where geologic and morphological conditions are favorable and particularly where the spillway can be placed over the power plant or at least over the bottom outlet works.

The head loss in the jet itself is not very substantial—it only accounts for about up to 12 %. If, on the other hand, the jet is split into several streams which collide, or if two spillways with colliding jets are installed, then the energy loss in the jet itself is dramatically enhanced. Here, most of the energy losses occur through the collision of water masses and through the compression of air bubbles. Therefore, one of the main benefits from energy dissipation by ski-jump spillways is the jet impact before plunging into the downstream pool.

The profile is mainly based on physical experiments focusing on the issues such as the relief of cavitation and vibration induced by high-speed flow.

Figure 8.35 shows the Xiuwen (Maotiaohe 3) Arch Dam (Guizhou Province, China, $H = 49$ m) whose spillway dam monolith is 36.3 m high, and the spillway with a design unit discharge of $61.8 \text{ m}^3/(\text{s m})$ is placed over the power plant. The altitude difference from the weir crest to the bucket lip is 10.3 m. The experiments and prototype observations all show that the vibration induced by outflow is not significant.

4. Outlets

Outlet, flowing under pressure, conveys flow from the openings placed below the dam crest and controlled by gates. The large opening with discharge capacity at higher level is termed as “orifice,” and the small opening at lower level is termed as “deep or bottom outlet.” The flow jets from outlets attain higher velocity compared to those from dam crest, which is in favor of the safety against downstream river scouring.

Figure 8.36 shows the orifice profile of the Shimen Arch Dam (Shanxi Province, China, $H = 88$ m). Orifices are usually laid out within the dam monoliths on river

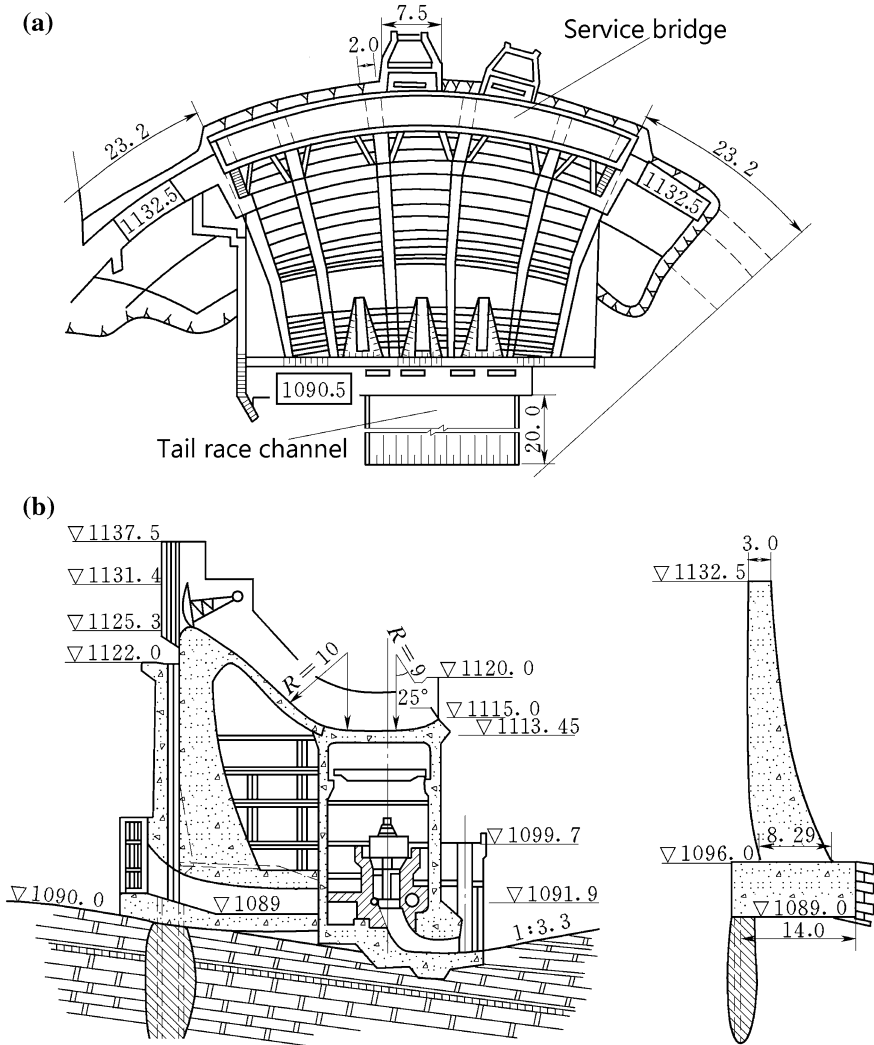


Fig. 8.35 The Xiuwen (Maotiaohe 3) Arch Dam (unit: m) China, $H = 49$ m. **a** Plan; **b** profile

stream, for facilitating the energy dissipation. Occasionally, they are also laid out at the abutment dam monoliths, to give way to the powerhouse on the riverbed.

The main (operation) gate is usually located at the downstream exit of orifice, and radial type is prevalent. The advantages of such arrangement are that it may facilitate the layout of gate hoist, and the piers and flip bucket at the downstream face may help to reinforce the opening. To prevent cracking around the orifice, steel reinforcement is demanded. If necessary, local thickening of the arch dam around the large opening is required.

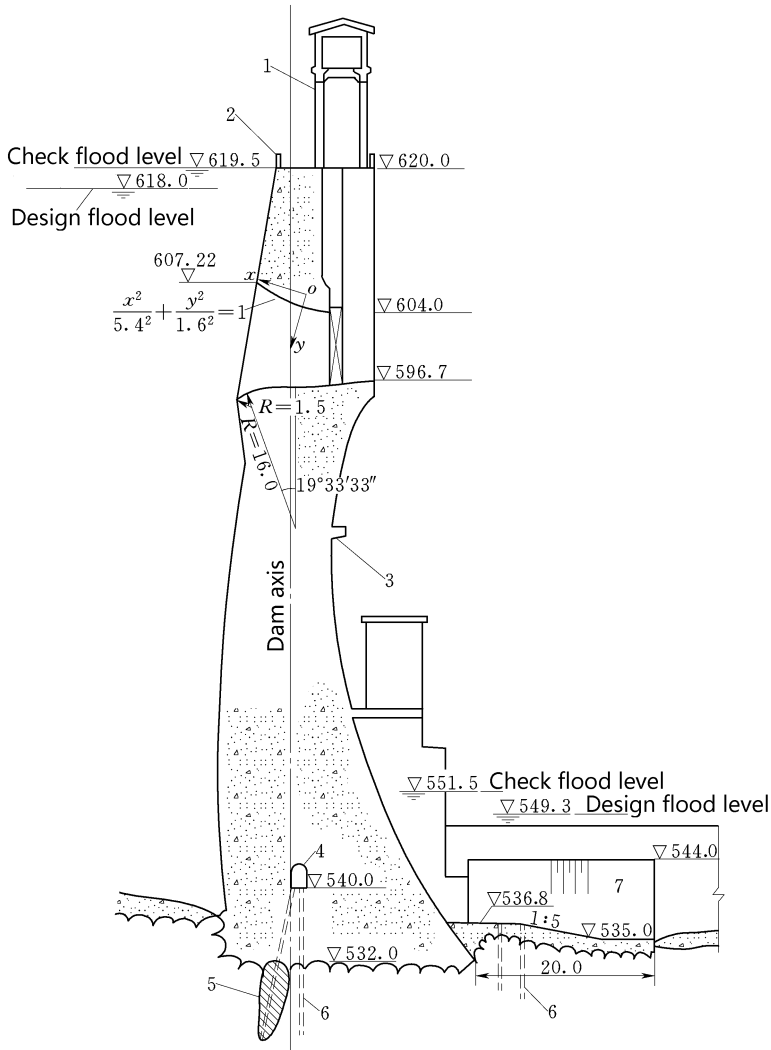


Fig. 8.36 Orifice of the arch dam (unit: m) the Shimen Project (China, $H = 88$ m). 1 bent frame for hoist; 2 parapet; 3 operating bridge; 4 grouting gallery; 5 grouting curtain; 6 draining hole; 7 concrete protection of bank slope

The section of orifice is usually rectangular in shape. To secure the smoothness of flow and get high discharge coefficient as well as to alleviate cavitation and vibration, the walls of orifice should be curved according to the hydraulic experiments.

Deep outlets are usually rectangular in thin arch dams, but may be circular for thick or gravity arch dams, and in the latter case, a transition is needed to connect the gate section and entrance section of rectangular to the circular conduit.

Fig. 8.37 Deep outlet of the arch dam (unit: m)
the Dongfeng Project (China,
 $H = 168$ m)

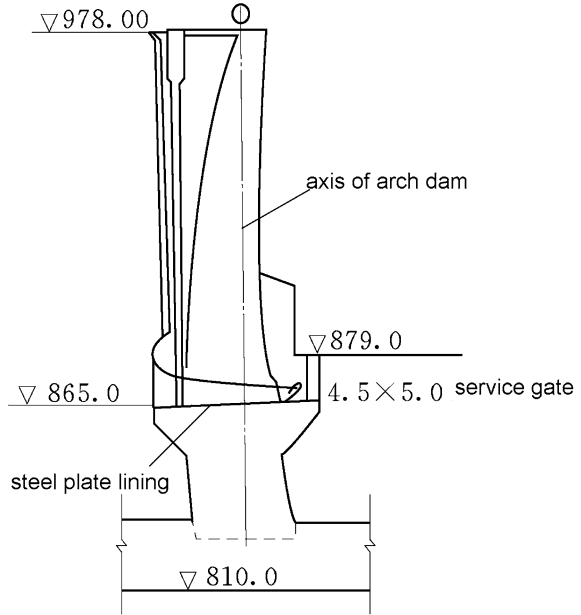


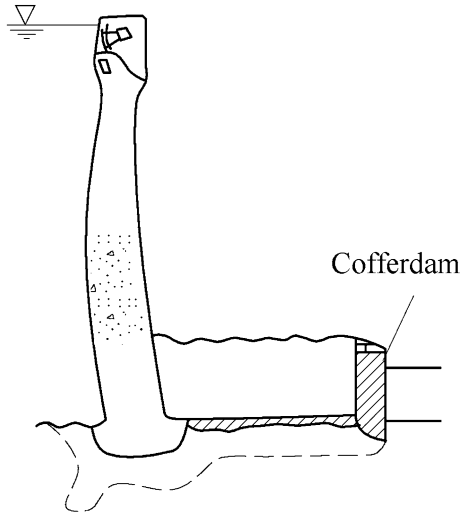
Figure 8.37 shows the profile of the deep outlet of the Dongfeng Arch Dam (China, $H = 168$ m).

The size of deep and bottom outlets is restrained by the gate manufacture and operation conditions. Nowadays, the maximum head of deep outlets has reached 150 m, and the deep outlets under the design or construction phase have a head over 200 m and a size over 10 m^2 . The aforementioned types of outlets are generally combined in one arch dam, to undertake the different tasks such as flood release, reservoir drawdown, and silt flushing.

8.6.3 Energy Dissipation and Scouring Protection of Arch Dams

Energy dissipation of arch dams is similar to that of gravity dams. If the jet trajectory or ski jump is applied, they may be laid out symmetrically, to exploit the advantages of flow jet colliding in the air attributable to the curved shape of arch, which may reduce the scouring of riverbed significantly. This design philosophy had been exercised successfully in many arch dam projects such as the Quanshui Arch Dam (Guangdong, China, $H = 80$ m) and the Cabora Bassa Dam

Fig. 8.38 Plunge pool the Vouglans Dam (France, $H = 130$ m)



(Mozambique, $H = 163.5$ m). However, problem of atomization should be reminded in the design of water jet collision. Since arch dams are usually located on narrow valleys, the scouring to the riverbed and banks will threaten their slope and abutment stability more seriously. The protection and reinforcement countermeasures should be comprehensively studied and implemented based on the detailed investigations on the geologic structures around downstream riverbanks.

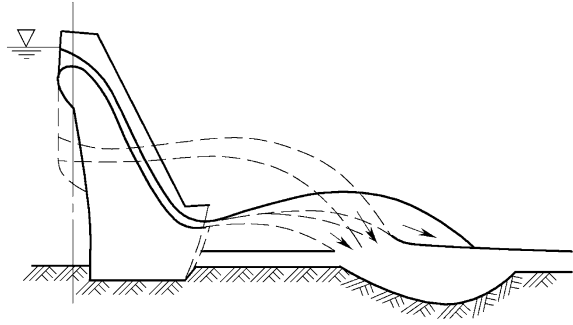
1. Plunge pool energy dissipation

Energy dissipation by the water cushion in plunge pool is the simplest arrangement for the energy dissipation of arch dam. The plunge pool is lined by reinforced concrete apron, and a downstream auxiliary dam or cushion dam may be installed to keep sufficient depth of water cushion. In case of low-quality bedrock and frequently operated flood release outlets, the plunge pool protection is obligated. In the Vouglans Dam (France, $H = 130$ m), downstream cofferdam was used to form plunge pool for energy dissipation (Fig. 8.38); in the Calderwood Dam (USA, $H = 71$ m), a 12-m gravity “cushion” dam is located at a distance of 110 m



Fig. 8.39 Plunge pool the Calderwood Dam (USA, $H = 71$ m)

Fig. 8.40 High- and low-level flip buckets the Baishan Dam (China, $H = 149.5$ m)



downstream from the main dam, creating a plunge pool that protects the riverbed. The pool's effectiveness is enhanced by a deflection unit at the base of the main dam (Fig. 8.39).

2. Energy dissipation by jet trajectory

Energy dissipation by jet trajectory may be applied in case of qualified downstream bedrock, and it is not necessary to install aprons.

The designer's main concern is naturally to have the impact zone as far as possible from the bucket to keep the structure from retrogressive erosion. Many designs with skew or disperse jets and various three-dimensional forms of flip buckets have been invented and exercised according to the topographic and geologic conditions. In recent years, the layout of multi-level flip buckets is widely practiced, which uses the impact of jets from different levels to dissipate a fair part of kinetic energy before plunging into the downstream pool (Fig. 8.40).

3. Slit bucket

The slit bucket is applicable for a project built in a narrow valley. It has been adopted on the bank-side spillways in several China's projects, such as the arch dams of the Dongjiang, the Longyangxia, and the Lijiaxia. It also may be employed for dam outlets, chute spillways, and spillway tunnels, such as in the Dongfeng Dam.

The design philosophy of slit bucket is to make its cross section contracting rapidly. The deflecting angle can be selected from -10° to -45° , so the whole jet flow is fully dispersed both longitudinally and vertically, which looks like a cocktail. A great amount of air is entrained, and the energy is dissipated in a high efficiency. The depth of scouring pit can thereby be reduced by $1/2$ – $2/3$, compared to a normal bucket with same hydraulic condition. The cross section of the bucket can be rectangular, Y-shaped, symmetric, or asymmetrical V-shaped.

The main consideration in applying slit bucket is to have sufficient large Froude number (e.g., larger than 4.0). However, if the Froude number is too large, serious shock wave may manifest in the bucket. An acceptable shock wave may be controlled by adjusting the width of channel within a certain distance. The contracting ratio is normally $1/6$ – $1/3$, and the trajectory angle is -10° – 10° . The slit bucket was

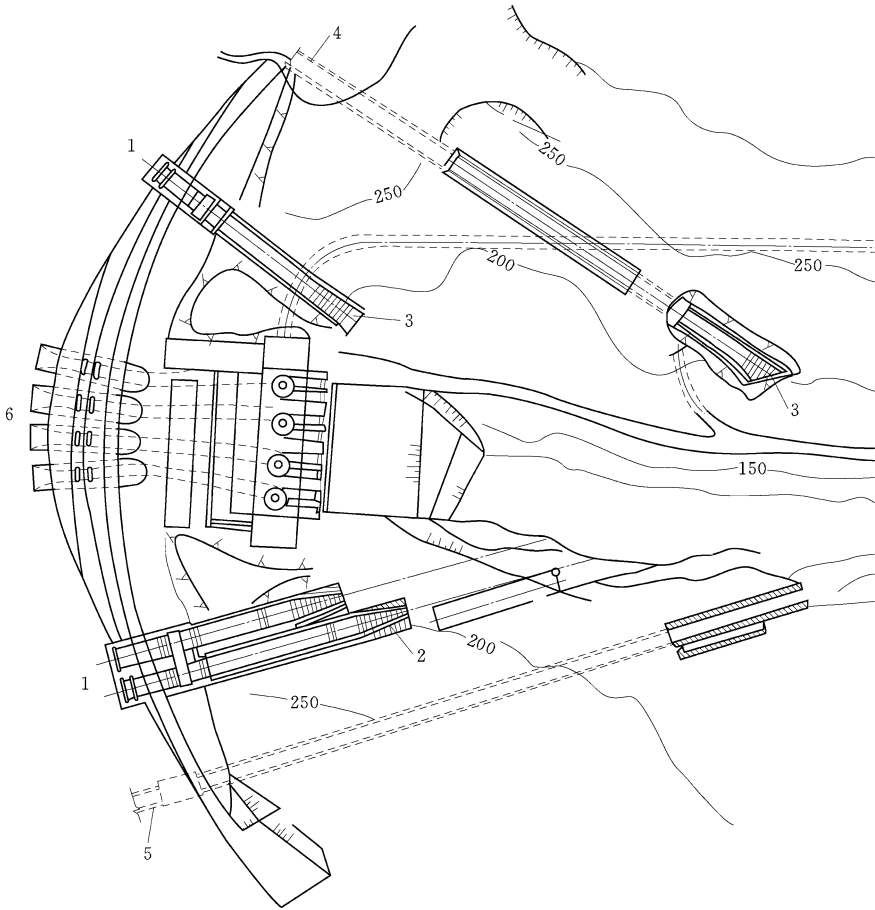


Fig. 8.41 The Dongjiang Arch Dam (China, $H = 157$ m). 1 ski-jump spillway (10 m (wide) \times 7.5 m (high)); 2 slit bucket; 3 dispersed flip bucket; 4 drawdown and flood release tunnel; 5 drawdown tunnel; 6 intake of power tunnel

firstly used in China for the Dongfeng Arch Dam Project. Figure 8.41 shows the flood discharge arrangement of this project including two ski-jump spillways located on the right bank, with channel slopes of 0.961 for the left one and 0.643 for the right one. The cross-head above the bucket is 91 m under normal storage level. The slit buckets are adopted in the both channels with the same elevation at 194 m and with the trajectory angle of 0° . The length of contraction section is 30 m which is divided into two segments, each 15 m long but with the contracting angles of $4^\circ 45' 49''$ for the first segment and $9^\circ 27' 44''$ for the second one. The contracting ratio is 0.25, and the width of the outlet is 2.5 m. The prototype observations indicate that the design is very successful.

4. Dispersed energy dissipater

(a) The single-dispersed dissipater

The flow nappe disperses and drops into a proper reach by mainly changing the shape of the deflector. The normal forms are dispersed, tilted, tongue shaped, and their combinations.

(b) The multi-dispersed dissipater

It is also named as larger differential deflector by selecting different sill elevations and positions to get desired flow patterns.

The Baishan Arch Gravity Dam (Fig. 8.40) is at a height of 149.5 m and with the maximum discharge rate of 11807 m³/s. The bucket sill elevations and deflector angles are all different with its four overflow spillways and three orifices. The horizontal dispersion is adopted for each flip bucket, to let the outflow covering the full downstream river surface. There were two large floods in 1986 and 1995, and satisfied operation results were recorded: good dispersion of jet flows, high efficiency in energy dissipation, and minor scouring on riverbed. The flood discharge did not influence the dam safety as well the power plant operation, too.

8.7 Materials and Structural Elements of Arch Dams

8.7.1 Materials

Concrete is the most prevalent material used for arch dams, and masonry arch dams are also constructed in ancient times or even occasionally in the modern times.

The concrete used for arch dams should meet the requirements for the strength, seepage resistance, freezing resistance, scouring/abrasion resistance, erosion resistance, and lower hydration heat. Since the stress level in arch dams is higher, the strength requirement is of the first concern. Actually, the satisfaction of strength requirement often guarantees the seepage resistance and freezing resistance. In chilly areas, the freezing resistance of the dam faces exposed in air and between the fluctuating water levels should be specified. For thin arch dams, the concrete zone with respect to freezing resistance and seepage resistance, as well as to the internal and external portions, is not necessary. If the dam is fairly high, which manifests much higher stress level at the dam abutments than at the mid-portion of the dam body, higher concrete grades may be used for the abutment portions. Around the holes and energy dissipation devices, the raise of concrete grade and requirements on seepage resistance and scouring resistance may be desirable.

8.7.2 Structural Elements

1. Dam crest and faces

The form and the arrangement of arch dam crest are basically identical to those of gravity dams. The thickness at crest should not only secure the adequate strength but also meet the requirements for operation and transportation. In general, the minimum thickness at crest is 3 m. Since the crest thickness of the arch dams is normally very small according to the structural requirements merely, a service road on dam may demand a special extension in its width, conventionally of beam/cantilever type. The balustrade on the upstream dam crest can be in the form of solid parapet that can keep the rain and wave out, whose height varies from 1.0 to 1.2 m. The balustrade on the downstream dam crest can be made up of metal pipe or reinforced concrete structure. The rainfall on the dam crest is drained off to the upstream reservoir or to the drainage pipes located in the dam body. The trans-figured lighting system should be designed at the dam crest. In high seismic areas, light structure is recommended for the crest design and heavy cantilever structure is to be avoided.

The upstream face is sometimes covered with gunite to strengthen watertightness and freezing resistance, but the downstream face lining is normally not required. However, in the area of harsh climate, a heat-insulating wall may be installed on the downstream face to protect the dam against adverse ambient temperature.

There are no steel reinforcements for dam crest except the following special cases: In severe chilly regions, the steel bars may be embedded to enhance cracking resistance against freezing of seeping water; in earthquake area, the steel bars passing transverse joints may improve the integrity of dam body and cracking resistance.

2. Joints of arch dams

To avoid the appearance of expansion and shrinkage-induced cracking in the period of construction, the arch dam is divided into monoliths with transverse construction joints, by which the concrete poured within each monolith can be limited in volume and in height. These joints should be calked at a possible low

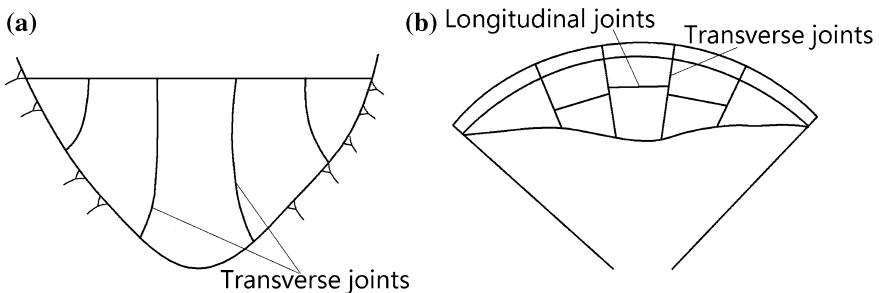


Fig. 8.42 Transverse and longitudinal joints in an arch dam. **a** Elevations; **b** plan

temperature for making the dam monolithic. For this purpose, the dam monoliths are sometimes artificially post-cooled, termed as “second-phase cooling.”

For a variable radius arch dam, transverse joints in radial direction tend to be twisted, because the radial directions of every arch ring are different. However, for the sake of simplicity in construction, the dam of not very high can be divided by a series of vertical joint, which is fixed along the radial direction of the arch ring at the middle of the dam height. At the dam base, the included angle between the joint and the ground should be not smaller than 60° and better to be perpendicular to the ground surface. Figure 8.42 shows the partially radial transverse joints of an arch dam.

Transverse joints are usually spaced 15–25 m apart, depending on the following considerations:

- That it should be adequate to prevent dam monolith from cracking induced by temperature variation and dry shrinkage;
- That it should be appropriate to accommodate appurtenant structures (outlets in dam, spillways in dam, powerhouse in or behind dam);
- That it should be suitable for qualified joint grouting, which is guaranteed by an aperture larger than 0.5 mm after second phase of cooling;
- That the casting area limited by joints should be compatible with the time of initial setting and placement capacity of concrete, to prevent cold joints within concrete;
- That the stress concentration should be controlled to prevent cracking induced by the span of faults and seams as well as by the significant change in foundation topography or rock quality;
- That smaller joint spacing should be adopted for dam monoliths on sloping abutments, to prevent cracking perpendicular to the foundation surface.

Transverse joints of arch dams generally have trapezoidal keys vertically laid out. In recent years, circular keys have been successfully employed in the Dongfeng Dam, the Ertan Dam, and the Xiaowan Dam, which proven their advantages of good stress condition, facilitation, and damage free during the construction.

For a considerably thick arch dam (e.g., thicker than 60 m), apart from transverse joints, longitudinal joints may have to be installed in its lower flared portion. They are usually formed at regular intervals of 20–40 m along the dam axis, which are selected regarding the similar factors for transverse joints. In recent years, the trend is shifted to strengthen thermal control measures in the construction to delete longitudinal joints. The Ertan Dam with a maximum thickness of 58.5 m at arch abutment, the Goupitan Dam with a maximum thickness of 58.4 m, the Laxiwa Dam with a maximum thickness of 54.7 m, the Xiluodu Dam with a maximum thickness of 64 m, and the Jinping 1 Dam with a maximum thickness of 66 m all have no longitudinal joints.

Construction joints in arch dams on the basis of the method of calking, if installed, may be wide joints and narrow joints.

Equipped with reinforced concrete plug on the upstream dam face, wide joints have a considerable width varying from 0.7 to 1.2 m, which are backfilled with very

dense concrete after the monoliths have been cooled down to the closure temperature. The advantage of wide joints lies in the good quality of heat emission, whereas the disadvantage of them is that ultimately, the backfilled concrete is possible to shrink which can result in cracking. Therefore, this kind of joints can only be applied in rather small project. The Merwin Arch Dam (USA, $H = 98$ m) is a typical example using wide joints. The Bort Gravity Arch Dam (France, $H = 121$ m) applied both longitudinal and transverse joints of 4 m wide, for the spanning over large-scale fault in the foundation. The Des Toules Arch Dam (Switzerland), erected its height from 25 m of the first phase to 86 m of the final phase, the wide longitudinal joint between old and new monoliths was employed.

The surface of narrow joints of small aperture, in general, is in a form of key. The embedded parts, grout pipes and grout boxes with free ends, are installed in the joints for injecting cement-based grout mixture, which are similar to those of gravity dams. The advantage of this kind of joints relies in the fact that by injecting cement-based grout mixture, the arch rings can be pre-compressed. This can reduce tensile stresses in the dam in the course of operation. This kind of joints is prevailing in the construction of large arch dam.

According to the data from field inspection and monitoring, grouting quality is often, although not always, not guaranteed for transverse construction joints. Bear in mind of this fact, it would be wise to let transverse joints of high-level portion up to crest to be permanent in the design, particularly for an arch dam on wide valley or with poor geologic condition. In this case, the stress analysis of the up portion should not taken into account arch action, such as the Geheyuan Arch Dam (China, $H = 151$ m). In addition, one of the modern trends is to use as few joints as possible, by strengthening pre- and post-cooling measures during construction.

3. Fillets, foundation pads, and peripheral joints

If the stresses at arch abutments are much greater than those at the crown, they may be reduced by providing fillets at the ends of the intrados curves, and in this way, the arch thickness near the abutment is locally increased and the resultant thrust is shifted closer to the centerline of the arch. However, where extensive and thick fillets are demanded, variable thickness arch dam would be a better alternative with respect to its more uniform stress distribution than the arch dam with fillets, attributable to its gradual variation in the thickness without any change in curvature.

Foundation pad, as a structural component between arch dam and its foundation indented to better meet the requirements for arch symmetry and abutment excavation, was advocated in China around 1960–1980. Its advantages are recognized as follows:

- It can be placed at any time prior to the construction of the dam body. This facilitates the foundation preparation and grouting and provides the protection for abutment rocks against weathering;
- It may be used to smooth out any irregularities in the foundation, and in this manner, the foundation may be accurately planned and defined prior to the cast of the dam body. Thus, the arch can be designed without the necessity of

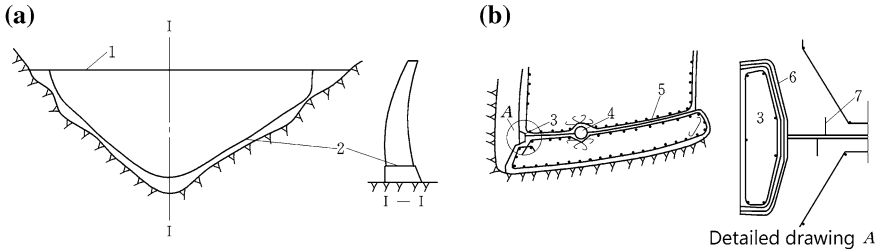


Fig. 8.43 Foundation pad and peripheral joint of an arch dam. **a** Elevations and profile; **b** peripheral joint. 1 crest; 2 peripheral joint; 3 concrete seal plate; 4 collector pipe; 5 steel; 6 impervious material; 7 copper sheet

revisions due to unexpected foundation conditions revealed during the excavation;

- The concrete properties in the pad may be so designed that it performs as a transition structure between the arch dam and the rock;
- It may be thickened, widened, and, if necessary, reinforced, to reduce and to distribute the stresses on the foundation rock or to bridge over the areas of weak rock.

Often, a joint is provided between the arch dam and the foundation pad, commonly known as peripheral joint (Fig. 8.43). Comparisons of models with and without peripheral joint are reportedly showing distinct advantages attributable to the peripheral joint—the stresses are claimed to be lower and better distributed. The peripheral joint serves the following purposes:

- There is a tendency of tension in the area around abutment extrados, which may be relieved by the peripheral joint. Should the tensile stress emerge, the joint will provide a zone of minimum tensile resistance and define the exact location of cracking where leakage proof is made by providing water stops;
- The installation of peripheral joint permits shaping the transverse section for better acceptance of the loads from arch rings;

The Osiglietta Dam (Italy, $H = 76$ m) constructed in 1939 is the first arch dam in the world with peripheral joint. The Vajont Dam (Italy, $H = 265$ m), the Inguri Dam (Georgia, $H = 271.5$ m), the Dez Dam (Iran, $H = 203$ m), the Kurobe No IV Dam (Japan, $H = 186$ m), the Deji Dam (Taiwan, $H = 181$ m), the Guangming dam (Zhejiang, China, $H = 20$ m), etc., are all installed with peripheral joint.

The dam concrete is placed directly on the foundation pad, and the contact face is not necessarily roughened. The transverse construction joints are perpendicular to the peripheral joint as possible. Large-scale pads are usually installed with water stops and draining pipes (Fig. 8.43b), which are complicated in construction. Provisions should be made that leakage may be resulted from the poor quality control in the construction.

The variants of peripheral joints are bottom joints, half peripheral joints, and base joints at dam heel.

1. Bottom joint. This is a peripheral joint installed at riverbed monoliths in the form of slipping bottom joint by placing asphalt or other low-friction materials on the surface of pad. For example, the Matilija Dam (USA, $H = 61$ m) put graphite frost on the pad surface, on which asbestos sheet coated with graphite was installed, and in this way, the dam may move more freely along the joint. The Guangming Dam's (Zhejiang, China, $H = 20$ m) pad surface was polished and coated with asphalt, and the joint was sealed with rubber water stops near the upstream dam face. Experiments and computations all show that the vertical stress can be released effectively by the installation of bottom joints. However, slipping bottom joints as well as conventional peripheral joints on abutments may weaken the stiffness of arch dams, and in this way, the horizontal stress along arch rings and the vertical stress on downstream low-level surfaces are raised, which may in turn result in lower safety factor against sliding along the joints. Therefore, the installation of peripheral joints, particularly with bottom joints, is called at comprehensively and carefully studies.
2. Half peripheral joint. Half peripheral joints are going between peripheral joints and bottom joints. The philosophy is that at the lower and mid-level of the dam with strong foundation restriction, a half peripheral joint is installed to eliminate such restriction, while at the upper portion of the dam, the peripheral joint is deleted to maintain restraint on the dam for preventing it from sliding and "lifting" failure.
3. Base joint at dam heel. The philosophy of installing a base joint at dam heel is that near the portion around dam heel, a short base joint terminated at a termination gallery is arranged to pinpointedly direct the cracking propagation along the dam base, if any. The termination gallery may make use of grouting gallery or may be specially designed whose best shape with respect to good stress distribution would be ellipse. The base joint is at the same level or a bit of higher than the dam base.

The base joint at dam heel may transfer compression stress but has no resistance to the tensile stress. After the joint opening by tension, the stress in dam will be redistributed, and the horizontal shear stress will be transferred into the portion downstream the termination gallery. Therefore, the thickness of the intact portion behind the termination gallery should be sufficient to ensure the shear resistance.

The water stops, draining and grouting system comprising seal sheets and draining holes, should be laid out for the base joint at dam heel. Near the surface of joint, steel reinforcement is installed, too.

The Hongrin Dam (Switzerland, $H = 123$ m), the Hendrik Verwoerd Dam (South Africa, $H = 88$ m), the Katse Dam (Lesotho, $H = 185$ m), and the Xiaowan Dam (China, $H = 294.5$ m) are all installed with base joints at dam heel.

The base joint at dam heel may transfer compression stress but has no resistance to the tensile stress. After the joint opening by tension, the stress in dam will be redistributed, and the horizontal shear stress will be transferred into the portion downstream the termination gallery. Therefore, the thickness of the intact portion behind the termination gallery should be sufficient to ensure the shear resistance.

The water stops, draining and grouting system comprising seal sheets and draining holes, should be layout for the base joint at dam heel. Near the surface of joint steel reinforcement is installed, too.

The Hongrin Dam (Switzerland, $H = 123$ m), the Hendrik Verwoerd Dam (South Africa, $H = 88$ m), the Katse Dam (Lesotho, $H = 185$ m), and the Xiaowan Dam (China, $H = 294.5$ m), are all installed with base joints at dam heel.

4. Galleries and draining pipes

Inspection galleries, shafts for instrumentation and lifts, and cantilever service bridges on the downstream face of dam are normally necessitated for normal operation. Often the way-outs to service bridges are provided in inspection galleries. In thin arch dams, however, only downstream service bridges are installed instead of galleries.

Inspection galleries are generally combined with drainage galleries. A low-level inspection gallery is always demanded to collect seeping inflow from the draining holes. The gallery also serves to give access to the instruments, internal discharge valves, and pipe works. Adequate provisions must be made for the access, ventilation, and lighting, of the gallery. The structural design of gallery is identical to that for gravity dams. Large arch dams may have one or more galleries at higher levels interconnected by vertical shafts. Since the arch dams are thin structures compared to gravity dams, the gallery layout is largely spaced along the altitude, to prevent excessively dam body weakening. For arch dams not very high or thinner than 10 m, only one foundation gallery for grouting and draining is installed, and the inspection, monitoring, transportation, and joint grouting works may be operated on the downstream service bridges. These bridges are 1.2–1.5 m in width and installed at every 20–40 m in altitude interval.

The uplift in the body of an arch dam has almost negligible effects on its stability and strength. Therefore, it is usually not necessary to provide drains in arch dams, particularly for thin arch dams located at mild climate areas. However, in some cases, particularly for thick dams, the dam body drainage system is demanded. This may be explained mainly by the climatic conditions, i.e., drains are intended to protect the dam body against possible concrete deterioration under the action of FT cycle. Uplift within the dam is relieved by formed holes running the full height of the structure. It is important that draining pipes may be reamed out or redrilled in the event of blocking. Relief drain efficiency is a function of drain geometry, i.e., diameter, spacing, and distance to the upstream face. The draining pipes of arch dams differ in no way from those used in gravity dams, except that the drainage holes are located very close to the dam surface and their diameter is smaller, e.g., 15–20 cm.

Fig. 8.44 The Xianghongdian Gravity Arch Dam (unit: m) China, $H = 87.5$ m

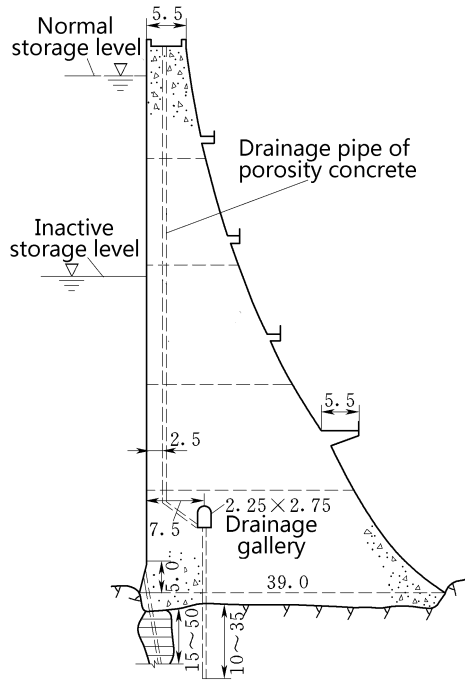


Figure 8.44 shows the profile of the Xianghongdian Gravity Arch Dam (China, $H = 87.5$ m) in which the galleries and drain pipes are shown.

5. Pipelines within dam

For the purpose of delivering water into a closed conduit system for power generation (i.e., penstock), irrigation, and flood release, outlet works consist of closed conduit waterway or as a pipe may be embedded in arch dams. Such outlet works may be classified according to its hydraulic feature, whether it is gated or ungated or, for a closed conduit, whether it flows under pressure or only as a freeflow waterway. The cross section of the penstock is circular, with a rectangular section near the upstream intake and a transition section in between, whereas the cross section of a flood release orifice or deep outlet is usually rectangular. If the flow velocity and/or pressure is high, the steel plate lining is commonly employed to secure high abrasion resistance and seepage resistance. This lining also may improve the stress conditions around the opening. Where the inner pressure is not large, the steel plate lining may be not necessary, but the roundoff and the steel bar reinforcement at the corner of rectangular opening should be undertaken to cut and to resist the stress concentration around the corner.

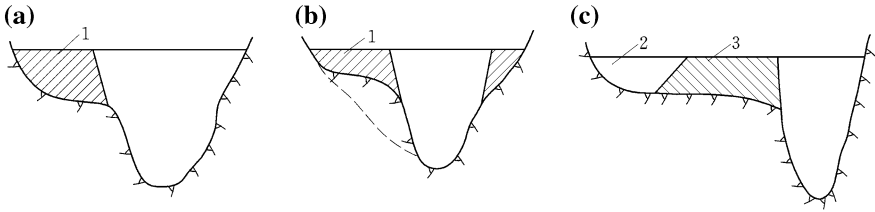


Fig. 8.45 Layout of gravity piers. 1 gravity pier; 2 spillway or the other dam monolith; 3 gravity dam

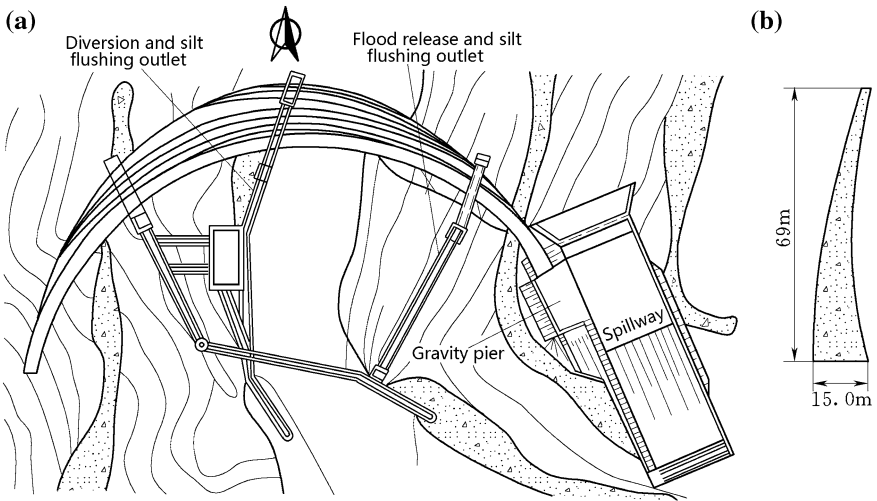


Fig. 8.46 The Hengshan Arch Dam (Shanxi, China, $H = 69$ m). **a** Plan; **b** profile

6. Gravity piers

Artificial abutments are sometimes built at the upper elevations on the valley where

- It expands at the upper altitude of valley (Fig. 8.45a);
- To prevent excessive excavation of complicated valley (Fig. 8.45b);
- A gravity or embankment dam is located at one wider side of the valley, which should be connected with the arch dam through artificial abutment (Figs. 8.45c and 8.46).

An artificial abutment is often made as massive gravity pier whose thickness is increased toward bank, and its stability and stress analysis are similar to those of gravity dams.

8.8 Foundation Treatment

More strict requirements are imposed on the foundation of arch dams than those of gravity dams because of high stress level transmitted from the arch dam to its foundation and large seepage gradients attributable to small dam thickness. Therefore, before casting the dam to its foundation, several measures intended to strengthen the foundation and to reduce the seepage are conventionally taken (ICOLD 1993, 2005).

The main purposes for foundation treatment are similar to gravity dams, i.e., to improve deformation modulus, to prevent the foundation from sliding and uneven settling as well as seepage failure (e.g., piping), and to reduce pore pressure as well as seeping discharge (Casagrande 1961; Harza 1949; Keener 1951; Ma and Chang 2007).

To obtain the required strength for foundation with unfavorable geologic conditions, treatments are selectively conducted similar to gravity dams. Hence, only the particular aspects on the foundation treatments for arch dams are discussed hereinafter.

8.8.1 Foundation Excavation

Foundation (inclusive abutments) excavation for an arch dam is so undertaken that weak areas should be removed to provide a firm base capable of withstanding the loads applied to it, and during this operation, blasting must not damage the base rock. All excavations should conform to the lines and dimensions shown on the construction drawings. Sharp breaks and surface irregularities such as ridges, depressions, or undulations should be avoided. The undulation degree of foundation surface should be controlled within 0.3–0.5 m.

Foundations containing seams of shale, siltstone, chalk, or mudstone that will be exposed for a period of time prior to concrete placement require protection against weathering. Final foundation surfaces should be protected by leaving a 0.3–0.5 m thick sacrificial layer in place, or by covering them with shotcrete that would be removed prior to concrete placement, or by immediately covering them with a minimum 30-cm-thick cushion concrete, etc.

Asymmetrical valleys frequently have to be employed as arch dam sites. Under such circumstances, it is not very wise to over-excavate for presenting a symmetric site. Because the abnormal stress problems resulted from the asymmetry, if not too exaggerated, may be overcome by proper design. For instance, abutment pad between the dam and foundation may be installed to overcome some of the detrimental effects of asymmetry or foundation irregularities. Thrust blocks or gravity piers are potential alternatives employed at asymmetrical sites, although the primary intension of a thrust block or gravity pier is not to provide symmetry valley but to establish an artificial abutment where a natural one does not exist.

Connection of arch dam with the rock in horizontal section is normally by excavating along radial planes in the form of flat abutment. However, where the arch dam is thick, particularly where the arch approaches the horizontals at a high acute angle, the arrangement of radial abutments involves too much excessive rock excavation. In this case, partial-radial abutments (Fig. 8.31) may be adopted for the upper level arch rings, while the lower level arch rings keep full-radial abutments. It should be emphasized that a smooth transition between the full-radial excavation and the partial-radial abutments is demanded.

The height difference of foundation surface from upstream to downstream should be controlled. If possible, it is preferred that the downstream base is a bit of high than upstream base.

The included angle between the topography contour and the intrados of arch abutment should be greater than 30° .

The defects within foundation such as intercalations, faults, strongly fractured zones, and weathered dikes are better to be removed totally if their bedding is not very deep.

The depth of foundation excavation down to competent bedrock has direct relation to the arch dam safety and engineering amount of placed concrete and excavated rock. In some countries such as France, Switzerland, and China, the amount of foundation excavation even accounts for nearly $1/3$ – $1/2$ of the concrete volume of dam body. Therefore, thorough studies should be carried out with respect to the depth of foundation excavation according to the safety and economy indices based on the stress and stability analysis.

8.8.2 Consolidation Grouting

Compared to gravity dams, particular attentions that should be called at in the consolidation grouting for arch dams are explained hereinafter.

1. Grouting arrangement

Grouting arrangement is related to the foundation geologic conditions, rock mass integrity, and loads from dams (Bowen 1981).

- For most arch dams, especially the high arch dams, the consolidation grouting should be carried out for the whole foundation. For medium-to-low arch dams with good geologic conditions, only the local consolidation grouting for faults, fault fractured zones, and concentrated fracture zones may be necessary. For gravity arch dams, if the stress level at the middle of the base is small, the local consolidation grouting solely for dam toe and heel may be indicated.
- At a fault fractured zone and its vicinity influenced zone, the medium or deep consolidation grouting with smaller hole space may be required, depending on the geologic conditions revealed after the excavation and the grouting absorb condition during the grouting operations.

- The medium or deep consolidation grouting with smaller hole space, or wide range of grouting, are customarily demanded for high arch dams at portions such as abutments, toe and heel, where the stress level is higher.
- Deep consolidation grouting sometimes is necessitated for fractured rock masses and large-scale discontinuity belts influencing the deformation and stability of arch dams, apart from the concrete replacement and reinforcement.
- Consolidation grouting is usually required around the foundation concrete replacement (beam or arch).

2. Depth of grouting

Grouting depth varies from 5 to 10 m (shallow hole) and 10 to 15 m (medium hole), depending on the local conditions. Generally, the depth of grout holes is 5–8 m, and the spacing between the holes is 2–4 m. In case of well-fractured rock masses and highly stressed foundation, the holes may be as deep as 10–15 m. For high arch dams with special treatment requirements, the deep hole grouting of 20–30 m or even deeper may be exercised.

A splits pacing process should be observed to assure that all groutable voids, fractured zones and cracks, have been filled.

3. Grouting pressure

Consolidation grouting may be termed as common pressure (lower than 2 MPa) and high pressure (as high as 2.0–5.0 MPa). The former is employed for loosen stratum layer due to foundation excavation within a depth of 5–10 m and a hole space of 1.5–5.5 m arranged in a pattern of grid.

The hole depth for high-pressure consolidation grouting may reach 20–30 m. This kind of grouting is employed under the following situations:

- Concrete replacement or reinforcement may be the first choice for large-scale fracture concentrated zones (belts), or discontinuity belts, which influence the deformation and stability of arch dams. However, if their thickness is not large (e.g., several cm) and not filled with clay, the high-pressure consolidation grouting could be one of the good alternatives instead of replacement or reinforcement;
- For fracture concentrated belts, fault fractured belts, weak seams, and discontinuity belts which influence the deformation and stability of arch dams, the high-pressure consolidation grouting is usually applied around the replacement concrete and the rest portions of weak rock masses.

High-pressure consolidation grouting had been successfully accomplished in the arch dam projects such as the Lijiaxia with the maximum pressure of 5.0 MPa and the Longyangxia with the maximum pressure of 3.0–6.0 MPa. However, it should be emphasized that it might result in uplift deformation of foundation rock and dam body; therefore, the grouting pressure should be carefully estimated according to grouting testing, particularly where small dip angle fractures are well developed in the rock masses.

High-pressure consolidation grouting may be carried out from either foundation surface, adits, or galleries.

8.8.3 Curtain Grouting

The purposes of curtain grouting for arch dams are as follows:

- To form a partial cutoff to bring down the downstream pressure regime and in this way to improve the stability of abutments and foundation against sliding;
- To prevent piping in foundation rock, particularly in faults, weak seams, and Karst zone;
- To protect rock from softening by lowering down the groundwater table and keep the rock in dry state, which is particularly important for arch dams located on sandstones and claystones;
- To reduce water loss due to seepage, which is particularly important for arch dams located in Karst areas.

The seepage resistance of curtain grouting is controlled by water percolation rate of curtain (q), which is identical to that of gravity dams (Table 7.7).

The layout of curtain grouting for arch dams should observe the following principles:

- That the grouting curtain should be positioned along the footprint of the dam in a region of zero or minimum tensile stress. It should extend into the foundation so that the base of the grouting curtain is located at near the vertical projection of the dam heel;
- That the depth of the grouting curtain will depend on the foundation characteristics, and usually, it should be stretched into the relatively impervious bedrock;
- That where there are no relatively impervious rock formations at banks, or they are embedded far away from abutments, the grouting curtain should be stretched

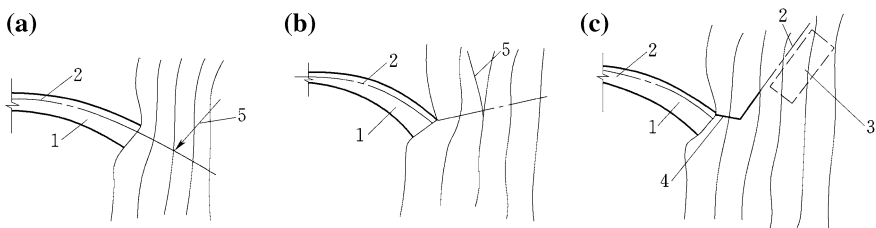


Fig. 8.47 Layout of grouting curtain within arch abutments. 1 arch ring; 2 central line of grouting curtain; 3 underground powerhouse; 4 retaining wall; 5 direction of seepage pressure

until the intersecting point of the normal storage level and the natural groundwater table (before impounding);

- That if the intersecting point of the normal storage level and the natural groundwater table is also far away from the abutments, the curtain depth is frequently comparable to the dam height, varying from 30 to 70 % of the maximum difference in headwater and tailwater.

The curtain grouting in abutments running in the direction of downstream gives rise to high groundwater table in a large portion of rock around abutments, which is disadvantageous for the stability of dam and abutment rock masses (Fig. 8.47a). Therefore, the curtain is desirable to run upstream within the abutments (Fig. 8.47b). However, caution should be exercised to ensure a sufficiently large obtuse angle between the curtain in riverbed and in abutment, to avoid curtain cracking at the turning point. Where there is underground powerhouse near the reservoir and a sharp acute included angle is inevitable, a water retaining wall may be installed to allow for the obtuse angle between the curtain in riverbed and abutment, as shown in Fig. 8.47c.

The curtain grouting in Karst areas could be extended as long as several kilometers, such as the Dongfeng Arch Dam (China, $H = 168$ m), the curtain length and area are 3650 m and 550,000 m², respectively. The curtain layout in Karst areas often encounters Karst rivers or caves, which should be treated by means of concrete replacement, high-pressure grouting, impervious cutoff wall, etc.

To permit a higher grouting pressure, grouting curtains are usually installed from the foundation gallery in the dam or from the top of concrete placements. The grouting should be proceeded, however, before any appreciable reservoir storage takes place to avoid grouting operations being performed against reservoir head or in an environment of high groundwater velocity. Grouting curtains can also be installed from adits or tunnels extended into abutments which are connected with dam galleries, and the altitude interval of adits is commonly 30–50 m. Curtain grouting from adits is prevalent in China.

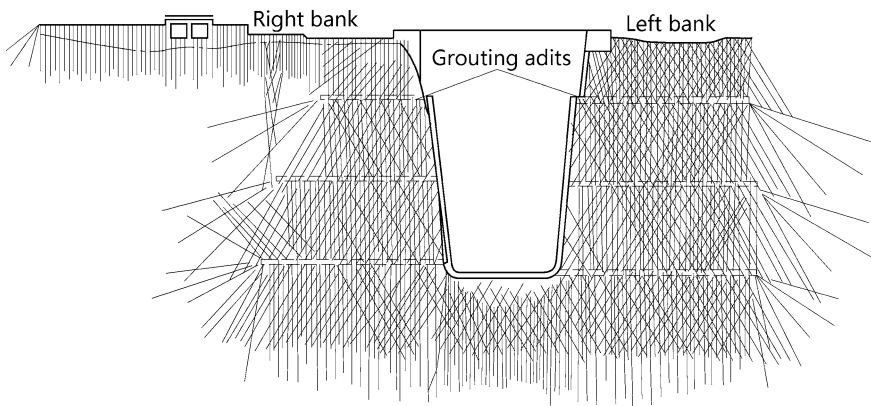


Fig. 8.48 Layout of the curtain grouting hole the Santa Giustina Dam (Italy, $H = 153$ m)

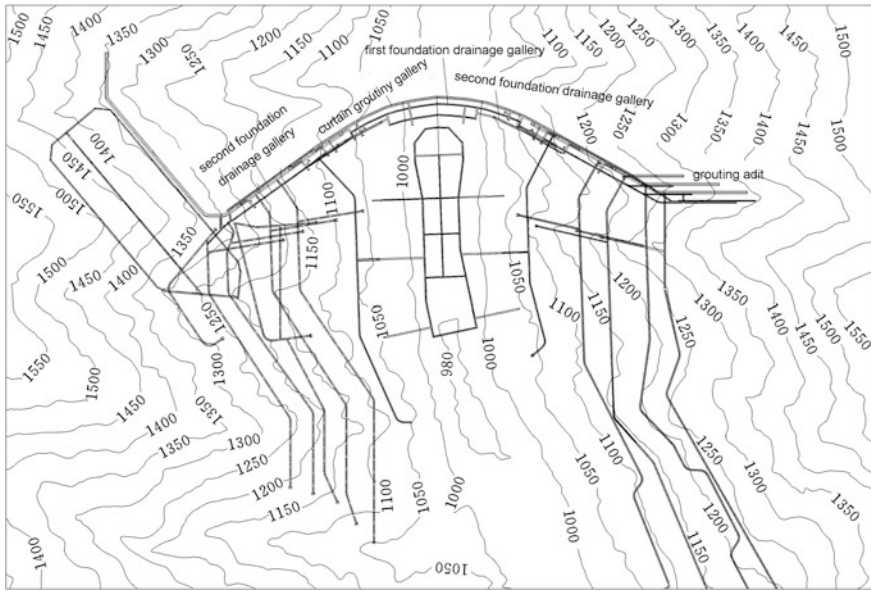


Fig. 8.49 Plan of the seepage control system the Xiaowan Project (China, $H = 294.5$ m)

Figure 8.48 shows the curtain grouting hole layout of the Santa Giustina Dam (Italy, $H = 153$ m).

The consideration with respect to the grouting techniques related to the grout mixtures, the rows of grouting holes, the sequence of grouting operation, the space and depth as well as the inclination of grouting holes, the grouting pressure, etc., is all identical to that of gravity dams (vide Chap. 7).

8.8.4 Foundation Drainage

The drainage for modern concrete arch dams is invariably formed by drainage curtains which can fall into three categories (Ma and Chang 2007): foundation drainage, mountain drainage for downstream resisting body, and other drainage if necessary. Figure 8.49 is the plan of the seepage control system in the Xiaowan Project.

A line of drainage holes, which is behind and close to the grouting curtain, reduces the foundation uplift significantly. These foundation drainages under dam base and in abutments are similar to those of gravity dams.

Mountain drainage for the downstream resisting body at the vicinity of dam abutment is intended to further release the seeping water through the grouting curtain and drainage curtain within abutments and foundation and to bring down the natural groundwater within mountains, as well as to release the seeping water due to

rainfall or atomization. For high-to-medium arch dams on steep canyon under complex geologic conditions, multi-layer draining adits are laid out longitudinally and transversely within the mountains at the vicinity downstream of the dam abutments, and from these adits, the draining holes are drilled which form a spatial drainage grid. Geologic exploration adits, access adits, and reinforcement adits may be incorporated into such mountain drainage system.

In addition, runoff and other surface water should be prevented from entering the mountain, by installing surface infiltration such as shotcrete to intercept the rainfall water, ditches and dikes to intercept runoff and other surface water and to direct it away from the dam abutment areas.

8.8.5 Treatment of Large-Scale Discontinuities

1. Treatment of large-scale discontinuities with high dip angle

Where a large-scale discontinuity such as fault (or weak intercalation) is composed of well-cemented and hard rock (breccia, schistoid, etc.) and it has no serious influence on the abutment stability and deformation, only its superficial fractured portion is cleared and replaced by concrete, supplemented by rigorous consolidation grouting. If the fault is composed of poorly cemented and weak rock (mylonite, fault gouge, etc.), which has important influence on the abutment stability and deformation, a deep excavation (dental treatment) and concrete replacement supplemented with rigorous consolidation grouting is required.

For a high dipping fault at and parallel to riverbed, the treatment in the form of removing a portion of the weak material and backfill the excavated pit with concrete is commonly employed for transferring the forces from dam base to the solid bedrock by the span over two sidewalls of the fault (Fig. 8.50a). The size estimation and strength calibration of the dental are similar to those of gravity dams (Fig. 8.50b).

For a high dipping weak seam at and transverse the riverbed, the dental should transfer not only the vertical pressure from dam, but also the shear forces, which demands a deeper and larger dental size (Fig. 8.50c). If the width of such seam is too large, the arch dam scheme is suspicious.

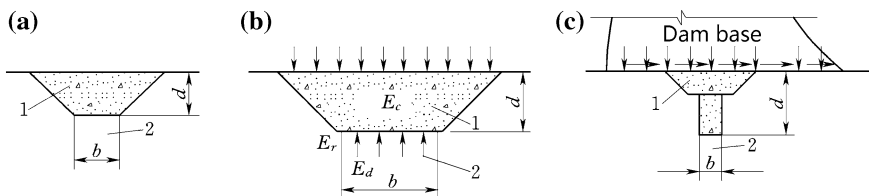


Fig. 8.50 Treatment for high dipping fault at riverbed. **a** Narrow fault parallel to river; **b** wide fault parallel to river; **c** narrow fault transverse to river. 1 concrete dental; 2 fault

Concerning the high dipping fault at abutments, if it is transverse to the riverbed, the treatment is similar to that at riverbed. If such a fault is parallel to the riverbed, apart from the force transferring problem, the stability against sliding would be a paramount concern in the treatment design. Based on the scale and properties of the fault and the construction conditions, the fault within the affected area may be mostly replaced by concrete using grided tunnels (including adits and shafts) excavating along the fault or using stress transferring concrete plugs through tunnels driven across the fault, so as to meet the requirements for the deformation and shear resistance. The rest portion of the fault within the influence of abutment thrust is treated by high-pressure grouting, for the purpose of improving its overall strength and the imperviousness.

Be located on a strong seismic area, the Nagawado Dam (Japan, $H = 155$) shown in Fig. 8.51 is a slender arch dam of 155 m high and 355.5 m in chord length. The

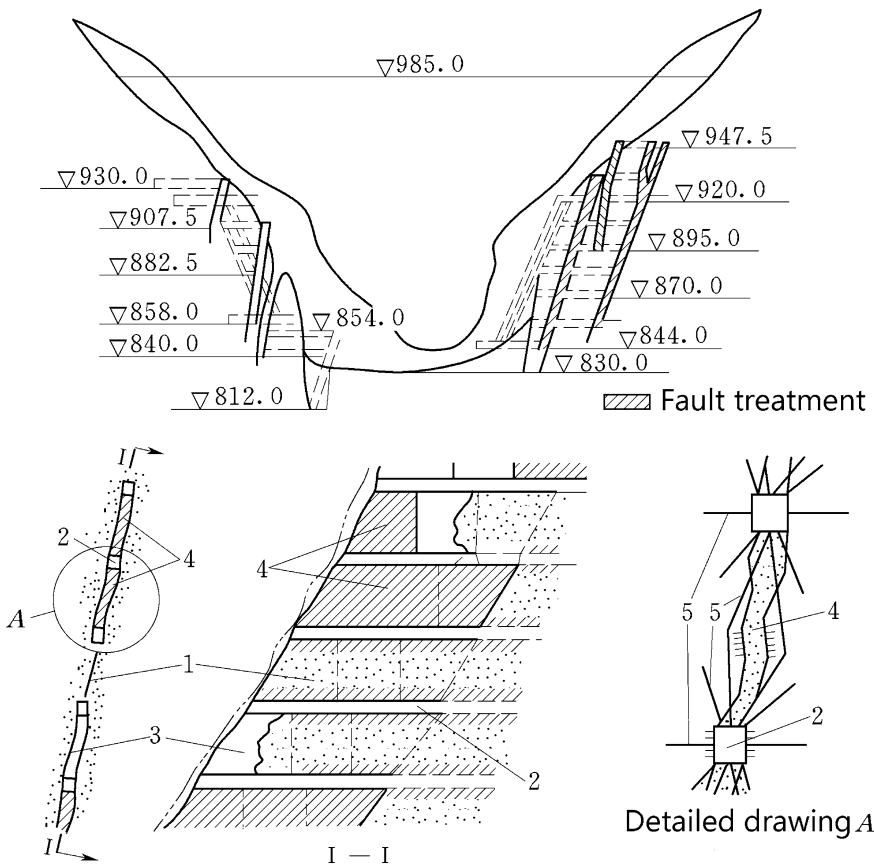


Fig. 8.51 Foundation treatment the Nagawado Dam (Japan, $H = 155$ m). 1 fault; 2 operation tunnel; 3 excavation; 4 replacement concrete; 5 grouting

recorded maximum accelerations were 193 and 242 gal at the crown and the 1/4 point of the crest arch, respectively, during the Naganoken Seibu earthquake (September 14, 1984) of magnitude 6.8. The maximum accelerations in the foundation rock were in the range of 21–31 gal. There are numerous faults of tens centimeters in width along the riverbed which influence both the stability and deformation of abutment rock. The faults in a depth equivalent to the dam base width were tunneling excavated and replaced using concrete. Consolidation grouting was also carried out from the excavation surface to the sidewalls of the faults. In addition, the abutments were reinforced by prestressed anchor cables from the downstream banks, the borehole number is 171, and the total prestress force is 400 MN. The steel consumption is 330 tons, and the concrete replacement volume is 30,000 m³ which accounts for 4.55 % of the dam concrete. The treatment expenditure accounts for 6.5 % of the whole dam body.

In the Longyangxia dam ($H = 178$, China), analyses were conducted with regard to the stability against sliding on both the left and right abutments, as well as to the compressive deformation and shear displacement of the major faults. The findings indicated that the safety margins of the rock mass on both the left and right abutments could not meet the safety requirement stipulated in the design codes. It was also found that the displacement of the faults at different elevations is accounted for 13–62 % and 75–92 % of the total foundation displacement, respectively, on the left and right banks. The excessive compressive and shear displacements of the faults would result in poor transfer of the dam's thrust forces and high stress concentration. The tensile stress in the dam body reached as high as 1.92 MPa. Accordingly, the fault zones within the affected areas were mostly

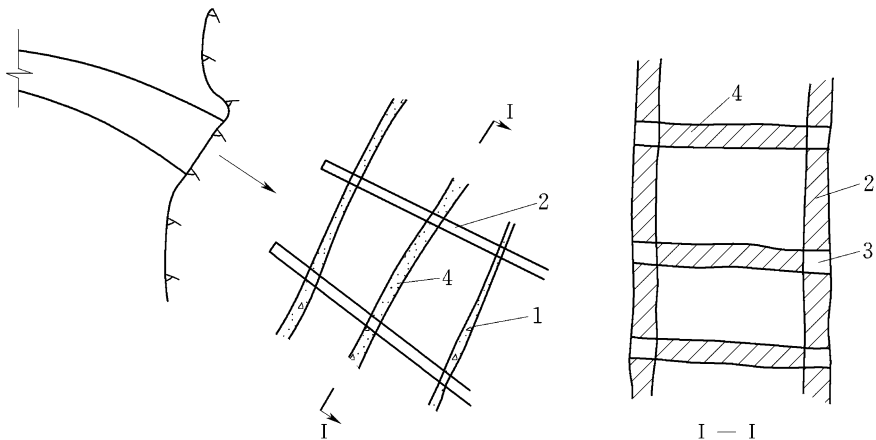


Fig. 8.52 Layout of the replacement treatment for the left abutment the Longyangxia Dam (China, $H = 178$ m). 1 fault; 2 vertical cutoff wall; 3 adit; 4 replacement concrete in fault

replaced by concrete through grided tunnels excavated along and across the faults. The rest portions of the fault zones within the influence of thrust forces were treated by high-pressure cement grouting or chemical grouting. The layout of the replacement treatment for its left abutment is shown in Fig. 8.52.

2. Treatment of large-scale discontinuities with low dip angle

For those who are shallow in bedding depth, the concrete replacement through the adits and inclined shaft along the fault is customarily employed. If their bedding is deep, the analysis concerning deformation and stability will give insight with respect to their performance, and then, the countermeasures such as deep consolidation grouting or adit concrete replacement may be implemented, if necessary.

3. Protection against seeping and piping in large-scale discontinuities

Faults and weak intercalations may be highly permeable and contain erodible materials. To protect them against leaking and piping, upstream and downstream cutoff shafts may be excavated in each seam or fault, which are backfilled with concrete, in addition to the strengthened curtain grouting by increase grout rows or using chemical mixture. The dimension of the shaft perpendicular to the fault should be equal to the width of the weak zone plus a minimum of 0.25 m on each end to key the backfilled concrete into sound rock. In any instance, a minimum shaft dimension of 1.6 m in each way should be kept to provide sufficient working space. The depth of cutoff shafts may be decided with regard to the requirements for the reduction of seepage and the elimination of piping failure.

8.8.6 Prestress Reinforcement

In recent years, prestress reinforcements installed in the abutment slopes at the downstream vicinity of the arch dam toe are widely practiced within China and the other countries (Ceng et al. 2003). The prestress reinforcement prevents or limits the deformation and dilation of the rock that might lead to collapse. The primary reason for the success in prestress reinforcement is the immediate restraint which reduces rock deformation and enhances early stabilization: The shear strength of discontinuities will always be decreased after a slippage or separation has taken place. Therefore, the prestress reinforcement should be installed as soon as possible after the foundation excavation is made.

The layout of reinforcements is dependent on the geologic conditions of the abutments and foundation as well as the thrusts from dam. As is the case in the design of any structure, the reinforcement parameters are determined not only by available design procedures but also by experience and appropriate empirical rules. For prestress reinforcement, these parameters are element spacing, size, prestress forces, and lengths. Prestress reinforcements are available as either deformed steel bars or strand cables (Post-Tensioning Institute 1985). The maximum length of the former is normally 15 m, while the latter may be as long as 50 m or even more.

Strand cables are widely exercised in the dam abutment reinforcement. The abutments of the Contra dam (Switzerland, $H = 220$ m) are reinforced by prestress anchor cables with design tension of 500 kN per cable, spaced 3–5 m apart and in a length of 30 m. The Aldeadavilla Dam (Spain, $H = 139.5$), whose foundation rock is schist, the steel reinforced concrete grid beams spaced 5 m apart are layout on the bank slope surface, at the nodes of these beams prestress anchor cables are installed, the depth of the borehole is 50 m, the design prestress tension force is 1000 kN per cable.

8.8.7 Karst Foundation Treatment

Carbonate rock is widely distributed in China, which accounts for 36 % areas of the country. Under definite conditions, Karst will manifest in these areas, which gives rise to engineering troubles related to the leakage, bearing capacity, abutment/foundation stability, and reservoir triggered earthquake, etc., for the arch dams.

The Karst treatment for the arch dam foundation is similar to that of gravity dams, which has been illustrated in Chap. 7 of this book.

8.9 Layout of Arch Dam Projects

The layout of an arch dam project depends on the comprehensive consideration concerning the topographic and geologic conditions as well as the arrangement of other hydraulic structures (e.g., hydropower plant, ship lock, or lift). The following factors should be taken into account in the layout of an arch dam project:

- That dam axis coordination and dam type selection always have priority in the layout of the project;
- That layout of flood release and energy dissipation is a paramount issue dominating the safety of the project;
- That rationally coordination of power plant and related structure elements (intake, tailrace, etc.) is other key issues in the project layout;
- That attention should also be called at to facilitating construction diversion and shortening construction schedule;
- That cautions are exercised for the stability problem of abutments and bank slopes;
- That studies concerning the atomization and its influence as well as counter-measures should be carried out;
- That sufficient silt flushing sluices in the form of bottom outlets are provided for discharging flood and flushing sand, to keep effective reservoir storage capacity and to exclude silt in front of power intakes;
- That requirements for drawing down or emptying reservoirs should be met.

Similar to the layout of gravity dam projects, where the flood releasing and powerhouse works are taken as the most important features dominating the design, the project layout style with arch dam roughly falls into the following eight types.

1. Flood releasing through arch dam body + power plant at dam toe

The powerhouse is immediately behind the dam toe and occupies the whole riverbed due to narrow valley. Consequently, the flood releasing structures are arranged to the left and right flanks of the power plant. Large-sized outlets (orifices) are installed to quickly draw down or empty the reservoir, if necessary. Capacity of generator unit is so selected as large as possible, to reduce the number of units and to control the size of powerhouse at dam toe. Penstocks are placed on the downstream dam surface. Tunnels for construction diversion, and large tonnage cableways for placing concrete, may be employed.

In spite of the disadvantages that the dam toe powerhouse interferes the project construction and that power intakes and penstocks penetrate the dam body, the project layout is compact and has a smaller overall construction amount. However, since the power plant and tailwater areas are near the plunge area of discharged outflow jets, the influence of jet on the operation conditions (e.g., stability of generator system, atomization damage to electric facilities) should be evaluated. The Sayano-Shushenskaya Arch Dam Project is the highest (Russia, $H = 245$ m) and largest one with this configuration. It is installed with a generator capacity of 6400 MW, the largest discharge is $24,400 \text{ m}^3/\text{s}$, and the length of arch chord and the width of the dam base are 1066 m and 114 m, respectively. The Dongjiang Project possesses a double-curvature arch dam at a height of 157 m and with a base width of 35 m. The maximum flood discharge is $7830 \text{ m}^3/\text{s}$, which is handled by the large orifice outlets in dam and emptying tunnels in both the left and right banks. All releasing structures adopt the ski-jump energy dissipation, and the energy dissipating area is located downstream of the tailrace canal. The powerhouse at dam toe is installed with 4×150 MW generator units. The penstocks of 5.2 m in diameter and about 70 m in vertical height are placed on the downstream dam surface. A large-diameter tunnel is excavated for construction diversion.

2. Flood releasing through arch dam body + bank-side power plant

It is also a commonly exercised layout scheme, particularly where the arch dam is located on or near the downstream exit of a canyon. The influence of discharged jets on the power plant working conditions should be carefully mitigated. The Geheyan Project has a gravity arch dam of 151 m high. Since the Qingjiang River valley at the dam site is asymmetrical and the bedrock level on the left bank is low, the dam adopts the gravity structure from above its upper 1/3 height whereas keeps arch structure for its rest lower 2/3 height. It is the first time in China to adopt a dam structure of "upper gravity + lower arch." The dam base is 62 m wide, and the slenderness ratio C is about 0.4. The maximum flood discharge is $23,460 \text{ m}^3/\text{s}$, which is handled by 7 large overflow spillways ($12 \text{ m} \times 18.2 \text{ m}$), 4 deep outlets ($4.5 \text{ m} \times 8.0 \text{ m}$), and 2 bottom outlets ($4.5 \text{ m} \times 7.5 \text{ m}$) in combination with the downstream plunge pool energy dissipation. These flood releasing structures

occupy the whole riverbed. The intakes of deep and bottom outlets are arranged in the spillway piers. The bottom outlets are also used for drawing down or emptying the reservoir. A tunnel is excavated for river diversion. The open-air powerhouse installed with 4×300 MW generator units is located at the downstream right bank, to exploit the advantages of the right bank topography: As sufficient site for the open-air powerhouse, the headrace penstocks are short and straight, and the tailrace canal may be located far away from the energy dissipating area.

3. Flood releasing through arch dam body + underground power plant

It is a very prevalent layout type of arch dam project in the south-western areas with narrow and steep valleys. The powerhouse and headrace penstock system are separated from the arch dam to reduce construction interference and to facilitate diversion, giving rise to a shorter construction schedule. The Cabora Bassa Dam (Mozambique, $H = 163.5$ m) and the Kariba Dam (Zambia and Zimbabwe, $H = 128$ m) are layout in this way. The Laxiwa Arch Dam is located on the main stream of the Upper Yellow River. The logarithmic spiral double-curvature arch dam, 254 m at dam height and 45 m in base width, has a slenderness ratio $C = 0.219$. The maximum flood discharge of $6000 \text{ m}^3/\text{s}$ is handled by two crest spillways ($13 \text{ m} \times 9 \text{ m}$) and two bottom outlets ($4 \text{ m} \times 4 \text{ m}$), and a downstream auxiliary dam is installed to create a plunge pool for energy dissipation. The power plant installed with 6×620 MW generator units, the headrace and power generation systems, are all arranged in the underground caverns within the right bank mountain. A large-diameter tunnel is provided in the left bank for river diversion.

4. Flood releasing through arch dam abutment + power plant at dam toe

It is a comparatively compact layout type of arch dam project if the flood discharge is very high. The Lijiaxia Dam and the Jingshuitan Dam in China are the typical projects using this kind of layout. The Jinshuitan Dam at a height of 102 m and with a chord length of 350.6 m, is 5 m and 24.5 m thick at dam crest and base, respectively. The maximum flood discharge $14,900 \text{ m}^3/\text{s}$ is handled by the symmetrically coordinated large intermediate orifices and bottom outlets with ski-jump energy dissipation. The powerhouse at dam toe is installed with 6×50 MW generator units. The ship lift and log/bamboo cableway are provided at the right bank. Diversion tunnel and upstream concrete arch cofferdam are adopted for river flow diversion.

5. Flood releasing through arch dam body + powerhouse within dam

The first hollow gravity arch dam built in China—the Fengtan ($H = 112.5$ m)—was completed by the end of the 1970s. The maximum flood discharge $23,300 \text{ m}^3/\text{s}$ after reservoir regulation is handled by the crest overflow spillway of 13 vents ($14 \text{ m wide} \times 12 \text{ m high}$ for each). One bottom outlet ($6 \text{ m} \times 7 \text{ m}$) for reservoir drawdown with a discharging capacity of $812 \text{ m}^3/\text{s}$ is installed in the right non-overflow dam monolith. The crest spillway employs staggered high and low flip buckets to dissipate nearly 50 % energy by colliding water jets in the air before plunging into the riverbed protected by apron. The dam body on the riverbed is

hollow, and its left 4 dam monoliths are installed with 4×100 MW generator units. The power intakes are located in the lower portion of the spillway piers.

6. Flood releasing through tunnels + power plant at dam toe

The Chirkey Dam (Georgia) and the Glen Canyon Dam (USA) are representatives of this kind of layout.

7. Combined flood releasing + power plant at dam toe

Nowadays, overflow spillways, large orifices, and bottom outlets for releasing flood in combination and/or supplemented with bank-side (shore) spillways and flood tunnels are prevalent in the construction of high arch dams in China. The gravity arch dam of Longyangxia on the upper reach of the Yellow River is 178 m in height, 394.34 m in chord length, 15 m in top thickness, and 80 m in bottom thickness. After regulation, the maximum flood discharge $6000 \text{ m}^3/\text{s}$ is released by one orifices at left ($8 \text{ m} \times 9 \text{ m}$), one deep and one bottom outlets ($5 \text{ m} \times 7 \text{ m}$ each) in dam and two right bank-side spillways ($12 \text{ m} \times 17 \text{ m}$). Since the bedrock elevation is not high enough on both banks, 35-m-high gravity thrust blocks are provided on both abutments which are connected to the left and right non-overflow gravity dams. The powerhouse at dam toe has installed capacity of 4×320 MW.

8. Combined flood releasing + underground power plant

The high arch dam projects completed or under construction since the 1990s in China such as the Dongfeng Dam ($H = 168$ m), the Ertan Dam ($H = 240$ m), the Xiaowan Dam (294.5 m), the Xiluodu Dam (273 m), the Laxiwa Dam (254 m), the Jingping I Dam (305 m), the Goupitan Dam (225 m), etc., all have distinctive features of large water pressure, narrow and steep valley as well as complex geologic condition, problematic large flood releasing and energy dissipation, huge power plant, complex in the layout of water diversion and construction. As a result, use is made of combined flood releasing + underground power plant in the layout of these arch dam projects.

The Dongfeng Arch Dam located at an asymmetrical U-shaped valley is typical (Fig. 8.53). The valley is very narrow and steep with a bank slope angle of 75° – 85° and a width of 50–60 m in dry seasons. It is a parabolic double-curvature thin arch dam of 162 m in height, 254.35 m in chord length, 6 m in top width, and 25 m in base width. The slenderness ratio is $C = 0.163$. The maximum flood discharged is $12,580 \text{ m}^3/\text{s}$ after the regulation, which is handled by three crest overflow spillways ($11 \text{ m} \times 7 \text{ m}$), two large deep outlets ($5 \text{ m} \times 6 \text{ m}$), one small deep outlets ($3.5 \text{ m} \times 4.5 \text{ m}$), one left bank spillway ($15 \text{ m} \times 21 \text{ m}$), and one left bank flood releasing tunnel of city-gate shape ($12 \text{ m} \times 17.5 \text{ m}$). The ski-jump energy dissipation is employed. The underground powerhouse and the short headrace system are laid out in the right bank mountain. The tailrace exits at the upstream side of the ski-jump energy dissipating area. The power plant is installed with 3×170 MW generator units. The river flow is diverted by the diversion tunnel in the right bank.

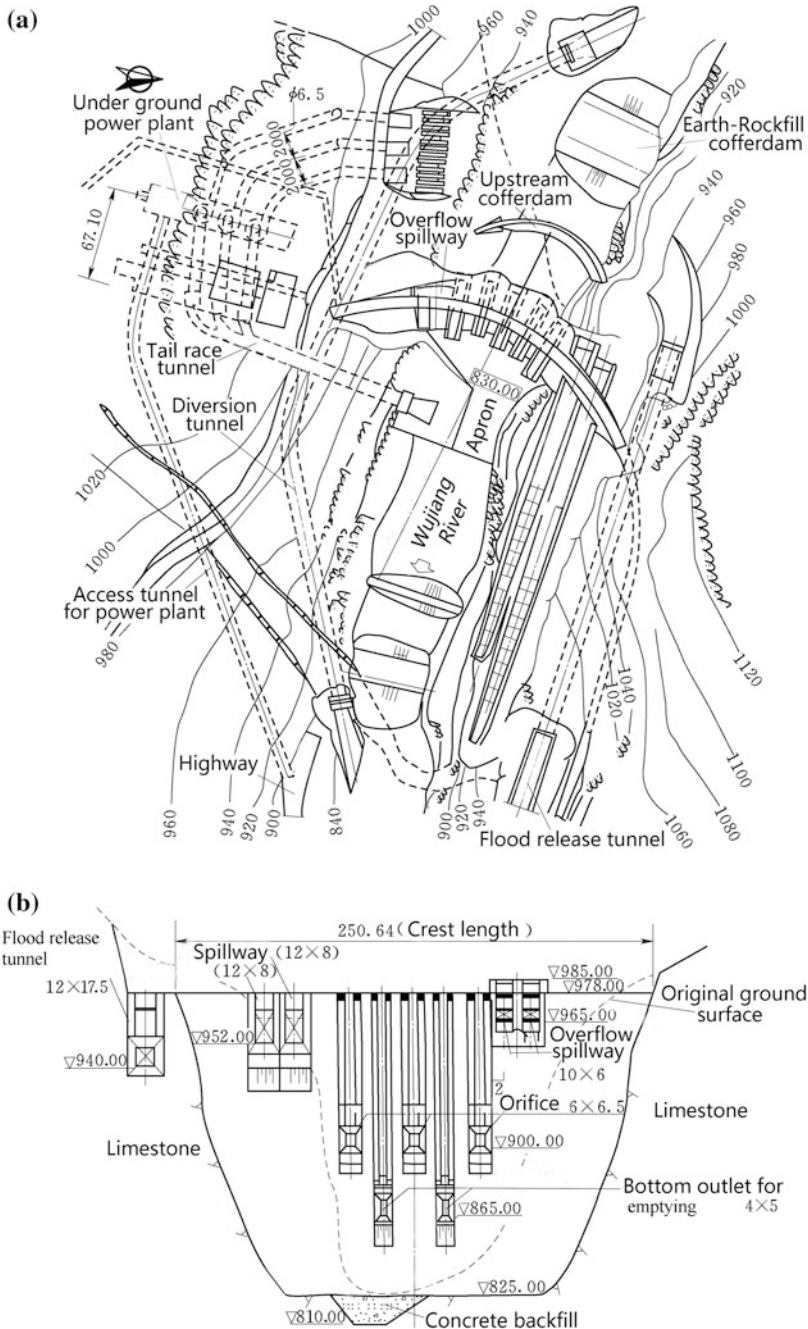


Fig. 8.53 The Dongfeng Project with arch dam (unit: m) China, $H = 162$ m. **a** Plan; **b** upstream elevations

8.10 Stone Masonry Arch Dams

8.10.1 Working Features of Stone Masonry Arch Dams

Stone masonry arch dams are advantageous for their simplicity in construction, low cost, and higher safety compared to embankment dams. Stone masonry arch dams are also convenient for flood releasing and construction diversion. With respect to the structural features, a stone masonry arch dam is similar to concrete arch dam. It was a prevalent dam type used in medium-to-small water hydraulic projects in China, particularly in the years from the 1950s to the 1990s.

Of all completed stone masonry dams, arch type accounts for 60 %, and of the four stone masonry dams higher than 100 m, three are arch dams. The major advances achieved by modern Chinese engineers in the stone masonry arch dam construction are as follows:

- Dam body configuration is developed from single curvature to double curvature, and arch ring type is developed from single circular to multi-circular, ellipse, and parabola;
- Trial load method and finite element method are normally practiced in the stress and stability analysis, based on which the optimal design is realized for fairly large number of stone masonry arch dams;
- Apart from the conventional cement-based mortar which is solely used in the dam surface protection, the fine aggregate concrete is mainly employed in the construction of stone masonry, in which fly ash and admixture are used to reduce the cement content and hydration heat and to improve the workability;
- To reduce the joint number and to increase the integrity of dams, the stones are vertically placed, and in this way, the height of each construction lift is over 1 m approximately. The stone content is around 50–55 %, the unit cement usage is around 100 kg/m³, and the volumetric weight of dam body can reach 23.5 kN/m³;
- Machinery replaces man power step by step. Trucks and conveyor belts in horizontal transportation, crane and gantry cranes in vertical transportation, vibratory units, are widely employed;
- Dam spillway is conventionally installed for flood releasing, of which the crest spillway is predominant with specific discharge exceeds 100 m³/(s m).

Stone masonry arch dams have particular features compared to concrete arch dams on the following aspects:

- If a double-curvature arch structure is employed, the overhang degree should be limited within 1/10–1/5. The crest thickness is commonly larger to prevent cracking at near the dam top and to improve the stress state of the whole dam body as well;
- The dam body is composed of concrete seepage sealing and stone masonry, and the latter comprises large quantity of joints. Therefore, the dam material is neither homogeneous nor isotropic. The stress and stability would be influenced by these characteristics significantly.

8.10.2 Structural Features of Stone Masonry Arch Dams

1. Dam body

The requirements for the stone masonry arch dams are basically similar to those of stone masonry gravity dams, except that the strength should be higher, which results in higher cement consumption up to 100–150 kg per cubic meter. In the portions of abutments and foundation as well as the other important position, local use of CVC is advisable.

2. Spillway

The crest spillway is generally equipped. The following three manners may be selective in the pavement of spillway surface:

- (a) Pure concrete or reinforced concrete (by steel rods)

The thickness should be not smaller than 0.6–1.0 m, as the Qunying Stone Arch Dam (China, $H = 101.3$ m), as shown in Fig. 8.54.

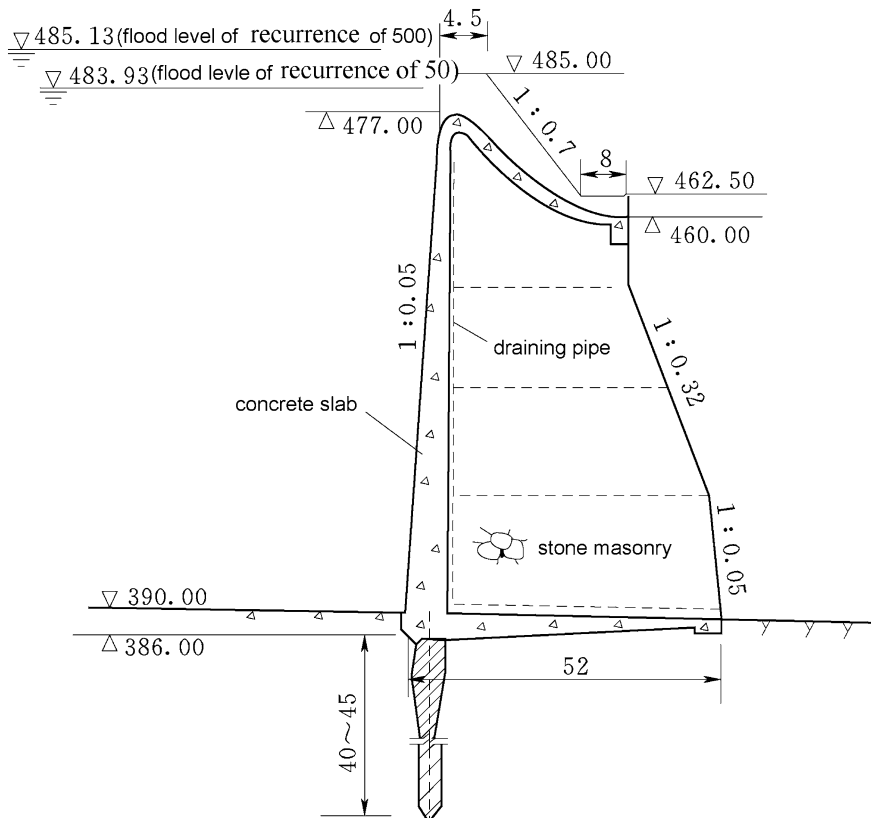


Fig. 8.54 The Qunying Stone Arch Dam (unit: m) China, $H = 101.3$ m

(b) Mixture of concrete and boulder strip

To save steel and cement, several projects installed reinforced concrete only at the portions of spillway crest and flip bucket, while at the straight slope section, the boulder strip was used with higher cement mortar grade.

(c) Pure rock boulder or block strip

This is only exercised under the circumstances of small specific discharge.

3. Joints

The stone masonry arch dams built in early time ordinarily had no transverse contraction joints, which often resulted in cracking later during the operation period. To prevent cracking, it is advisable that

- When the ambient temperature is approaching the annually maximum, the stone placement construction is suspended; when the ambient temperature is approaching the annually average, the stone placement may be resumed for the monoliths with joints; when the ambient temperature is lower than the annually average, the stone placement may be carried out for the monoliths without joints.
- The stone placement is carried out continuously in all seasons for the monoliths with joints; the joints are grouted when the ambient temperature is at the lowest of year.

8.11 RCC Arch Dams

Just a bit of later after the construction of the RCC arch dams in South Africa (Wolwedans and Knellpoort), the first two RCC arch dams of China were completed in 1993: One is the Puding RCC Arch Dam in the Guizhou Province at a height of 75 m, and another one is the Wenquanpu RCC Arch Dam in the Hebei Province at a height of 49 m (Dunstan 2007; Hansen and Reinhardt 1991; ICOLD 1989, 2003; Zhang 2002). More valuable experiences were collected followed by two RCC arch dams higher than 100 m completed in 2001: One is the Shapai RCC arch dam at a height of 129 m, and another one is the Shimenzi at a height of 109 m. Until the end of 2008, there were 9 China's RCC arch dams higher than 100 m completed or under construction, and their parameters are listed in Table 8.6.

As one of the world's first batch of RCC arch dams—Puding, creates a reservoir of partial regulation. The design flood level is 1145 m, and the normal tailwater level is 1087.5 m. The installed generator capacity in the underground powerhouse within the right bank mountain is 3×25 MW. This arch dam consists of non-overflow dam monoliths, 4 open spillways, gravity pier, an excluder sluice acting also as emptying bottom outlet, apron, and bank protection structures. The layout of this dam is shown in Fig. 8.55.

Table 8.6 Representative China’s RCC arch dams higher than 100 m (until the end of 2008)

Project name	Dam height (m)	Chord length (m)	Thickness of crest (m)	Thickness of base (m)	T/H	L/H	Situation
Cascade 3 of Yunlong River	135.0	119.23	5.5	18.0	0.134	0.88	Under construction
Dahuashui	134.5	198.43	7.0	23.0	0.171	2.14	Completed in 2007
Shapai	132.0	250.25	9.5	28.0	0.238	1.80	Completed in 2003
Luopo	114.0	191.72	6.0	20.0	0.175	1.68	Under construction
Tianhuaban	113.0	159.87	6.0	24.2	0.215	1.42	Under construction
Shemenzi	109.0	176.50	5.0	30.0	0.275	1.30	Completed in 2003
Zhaolaihe	105.0	198.05	6.0	18.5	0.176	1.89	Completed in 2005
Bailianya	104.6	421.86	8.0	25.0	0.287	4.05	Under construction
Linhekou	100.0	311.00	6.0	27.0	0.282	3.11	Completed in 2004

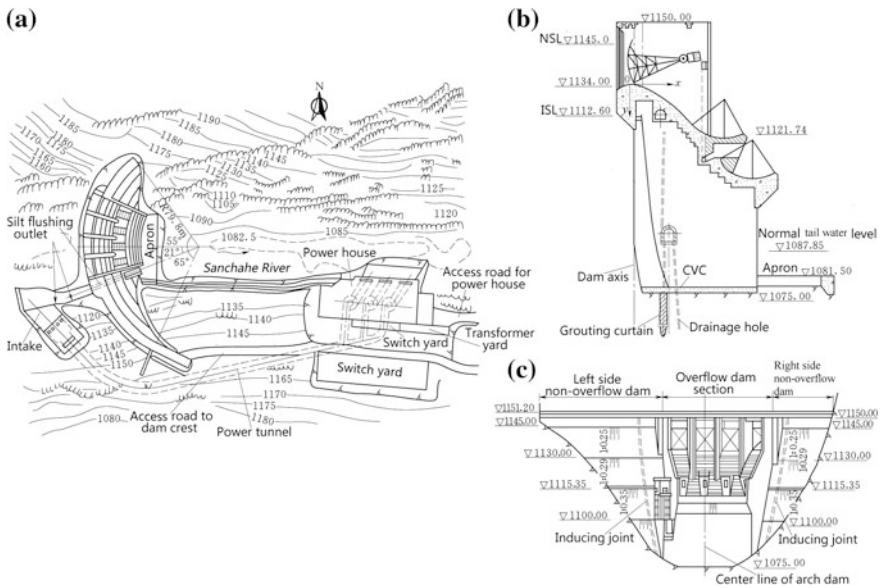


Fig. 8.55 The Puding RCC Arch Dam (China, $H = 75$ m). **a** Plan; **b** profile of spillway; **c** downstream development

On December 15, 1989, the cofferdam closure was commenced, followed by abutment and foundation excavation. On December 10, 1991, the pouring of CVC cushion layer initiated, whose top elevation is 1078.6 m. From January 23, 1992, the dam started to be rolled, and by April 21, 1992, the dam had reached 1099.3-m elevation. Then, the flood period came, and the construction had to be suspended. During this period, the flood had overtopped the dam for seven times, and the concrete age is 23 days when the first flood came. The second stage of construction was resumed on November 17 in the same year and was completed on May 30, 1993. In March of 1993, the gate in the diversion tunnel was shut down, which claimed the stage of reservoir impounding. However, due to some reasons, the regular storage period was postponed to November 30, 1993, and the first generating unit was put into operation on June 1, 1994.

The dam is located in an asymmetrical limestone U-shaped valley of $L/H = 2.0$ and is designed as an arch dam with constant thickness of $T/H = 0.376$ but with variable radius and central angle. The minimum central angle is 30.6° , and the maximum central angle is 120° . The maximum extrados radius is 79.8 m. The total volume of concrete is 137 km^3 , of which 103 km^3 is RCC. The other parameters concerning this dam are listed in Table 8.6.

8.11.1 Layout of RCC Arch Dam Projects

There is no much difference in the design of CVC and RCC arch dams. The requirements for the topographic and geologic conditions are almost identical. The treatment of foundation and abutments also must be observed as a routine design. However, several particular requirements may be imposed in the layout of RCC arch dam projects, for example,

- Spillways may be located on the crest, such as the Puding Dam, the Wenquanpu Dam, and the Xibinxi Dam. Use of dam outlets is also made, such as the Bailianya Dam and the Hongpo Dam. A special spillway tunnel on the right bank in the Shapai dam enables it to release flood with discharge of $280 \text{ m}^3/\text{s}$. To simplify the construction of RCC dams and to speed up the placement of concrete, dam type spillways are better to be located on the same elevation, if possible;
- To simplify the construction of RCC dams, all hydropower stations are layout on the downstream, and the intakes of long power tunnels are located independently in dam monoliths or on banks;
- Use tunnels for river diversion, if possible;
- The volume of CVC should be reduced as small as possible. For instance, use of pre-cast form for galleries and elevator chambers, etc., is advisable;
- The width of crest should be not smaller than 4–6 m for the convenience in the construction of RCC.

8.11.2 Design of RCC Arch Dams

1. Temperature and thermal stress control

One of the main differences in RCC gravity dams and RCC arch dams is the temperature control and design of joints (Tatro and Schrader 1985). Monoliths of gravity dams are stable on their own, so transverse joints without grouting may be permitted. On the other hand, transverse joints without grouting are not permitted in arch dams.

There are no transverse joints but only several cracking inducers in the first batch of RCC arch dams constructed in the world (e.g., the Knellpoort Dam and the Wolwedans Dam in South Africa and the Puding dam in China). After a period of practices, engineers were aware of that grouted transverse joints and relevant temperature control measures are generally necessary for RCC arch dams, except the small ones constructed in winter seasons. It is also suggested that transverse joints may be made by pre-cast concrete and the dam may be artificially cooled by water flowing in embedded pipes. Thereafter, transverse joints grouted after post-cooling are generally exercised in the China's RCC arch dam construction. However, where the closure temperature in dam body is higher than the stable temperature field, the grouting joints could open again in winter. Therefore, a special repeated grouting system was invented in recent years.

There are different standpoints with regard to the pre- and post-cooling in summer construction. Actually, this is mainly an economical issue: The expenditure of cooling system and other measures should be lower than the benefits obtained by the earlier operation of RCC dams.

2. Design of dam body

The profile of RCC arch dams is dependent on various conditions related to valley topography, geology, flood discharge, stress and stability control, and construction. The RCC arch dam in a valley of small L/H ratio has nearly identical profile as that of CVC. The overhang is also permissible such as the Puding RCC Arch Dam which is an asymmetric arch dam with fixed center, variable radius, and central angles. The Wenquanpu Dam has fixed center, variable radius, and vertical upstream face. The Xibinxi Dam uses single-centered circular arches with upstream slope of 1:0.082. The Hongpo Dam is laid out with fixed center and variable radius arches. The Shapai Dam is a single-curvature arch dam of three centers.

3. Joints

Since RCC arch dams are ordinarily not very thick, longitudinal joints are customarily not installed. Although there may be no transverse joints for a RCC arch dam on narrow canyon, it is necessary to cut transverse joints where the valley is wider.

In general, there are two classes of transverse joints in the RCC arch dam: The first one is normal grouting joint, with two sets of water stop sheets on the upstream side and one set on the downstream side. Grouting operation should be carried out

when the temperature of RCC drops to the stable state; another one is so-called inducing joint (crack inducer), within which wooden or steel sheets covered by asphalt or pre-cast form with keys are commonly installed, to reduce the effective section by 75–60 %. These joints are ordinarily spaced 20–80 m apart dependent on the stress status in dam body and the adverse influences of these joints. In narrow canyons or mild climate areas, only crack inducers or peripheral short joints are to be installed for RCC arch dams.

(a) Inducing joints

The inducing joints would not open, where the tensile stress is not excessive. For instance, the Puding Dam has two inducing joints, and the Wenquanpu Dam has two grouting joints and one inducing joint. In the Shapai Dam, there are two normal joints and two inducing joints, accompanied with a special grouting system allowing regrouting operation.

The inducing joints are composed of pre-split areas made of many small artificial fractures that do not coalesce each other (Fig. 8.56). Every fracture is defined by a rectangle whose long axis and short axis are around 1 and 0.3 m, respectively.

A special kind of short inducing joints for the purpose of relieving tensile stress in RCC arch dams was installed in the Xibinxi Dam and the Shimenzi Dam (Figs. 8.57 and 8.58). They are on the upstream faces near abutments and on the downstream faces at crown, respectively. The former is termed as “peripheral short joint,” and the latter is “stress release joint.” The depth of such joints should not exceed one-third of the dam thickness where it is located. Stop holes and steel bars are laid out at the end of these short joints, and water stops are installed on their upstream sides.

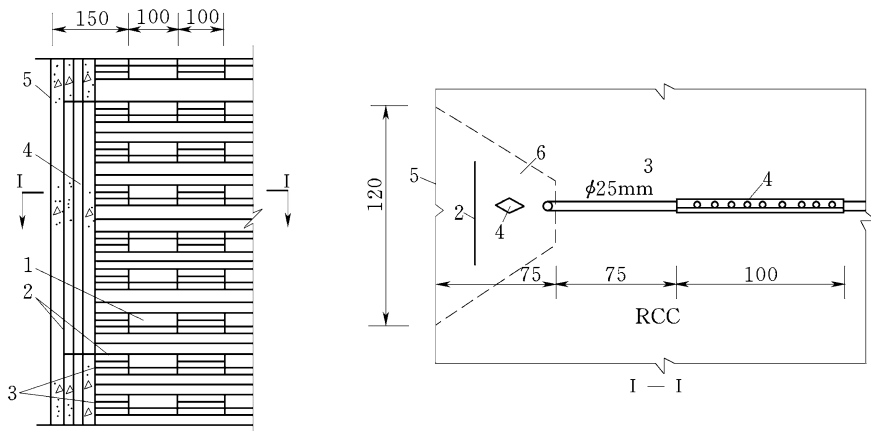


Fig. 8.56 Schematic drawing of inducing joint (unit: cm). 1 inducer plate; 2 plastic sealing sheet; 3 grouting hole; 4 crack inducing hole; 5 upstream dam face; 6 plug of GEVRCC

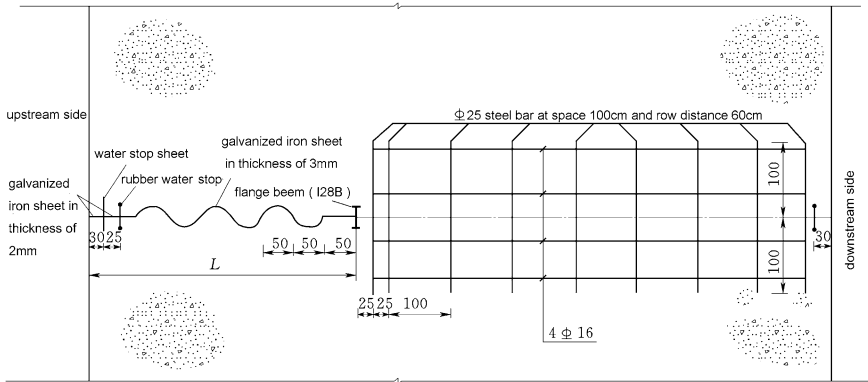
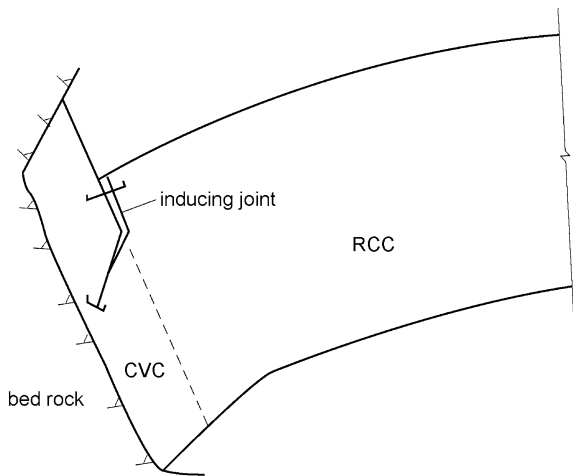


Fig. 8.57 Detailed drawing of a peripheral short joint (unit: cm)

Fig. 8.58 Position of the stress release joint at the arch abutment



(b) Grouting joints

The problem in grouting is that the temperature of RCC is still rather high and far from being stable, but the impounding of water should be started. Sometimes the inducing joints could not open under the action of water pressure and could not be grouted. The joints in the Wenquanpu RCC Dam (Fig. 8.59) all opened due to cold weather, with the maximum aperture of 0.5–4.0 mm on surface and 0.16–0.468 mm in interior. Altogether, three times of grouting were carried out for these joints: in March of 1994, March and June of 1995, and April of 1996. In the second grouting operation, the volume of cement mixture reached 16 kg/m² for induced joints and 41 kg/m² for normal joints.

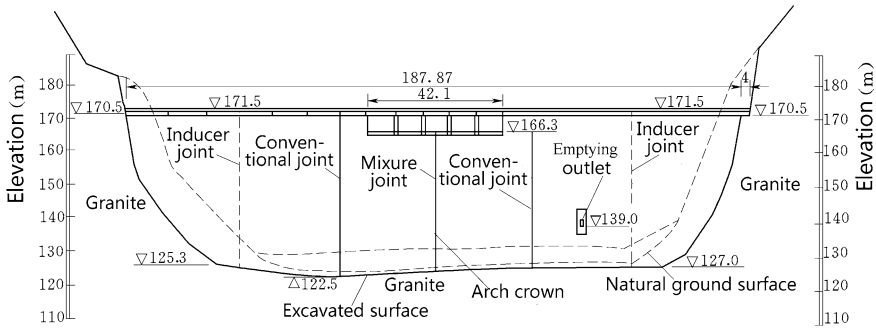


Fig. 8.59 Joint system of RCC arch dam (unit: m)—The Wenquanpu Project (China, $H = 48$ m)

8.11.3 Upstream Waterproof and Construction Joints

The requirements for watertightness of RCC arch dams are higher than those for RCC gravity dams, but the measures available for RCC gravity dams (e.g., CVC of thickness 2–3.0 m as an anti-leakage structure) are not very applicable for RCC arch dams due to their thin dam body.

Grout-enriched vibratable RCC (GEVRCC) for upstream face of all RCC dams has been developed and exercised worldwide (Forbes 1999), in which the cementitious mortar is added in the upstream region of 2–8 m thick to produce high slump concrete and compacted by ordinary vertical vibrators. The seepage resistance index of GEVRCC may be as high as W_8-W_{10} . The mortar amount added is approximately 6–10 % by weight, with lower VC value. Near the GEVRCC, drainage holes are installed.

The bonding strength between RCC layers depends on the content of cementitious, segregation resistance, VC value, and setting process. The experiments by the Gezhouba Technology Research Institute in 1994 showed that the VC value should be controlled within a range of 6–15 s, and the interval between two layers should be as short as possible. It would be better to place the next layer before initial setting of old layer and compact it immediately.

In general, there are two types of layer surfaces (lift joints) in the RCC similar to the horizontal construction joints in the CVC:

- Normal lift surface. The height of lift depends on the climatic condition and technology of construction. The lift surface should be roughened after the removal of laitance and covered with 1.0–1.5-cm thin layer of cement fly ash mortar, before the placement of the RCC mixture continues;
- Temporary construction layer surface. It is not necessary to treat, if the interval between two successive layers is shorter than the setting time. However, on the surface of the 2-grade RCC layer, normally a thin layer of mortar is placed.

Experiments by the Gezhouba Technology Research Institute showed that the tensile strength and shear strength of the lift joints covered with mortar in the RCC will be raised by 21 and 47 %, respectively.

In all joints, water stops or slurry stop sheets and repeated grouting system are installed. In cold areas, or if a dam is very thin, supplementary seepage protections such as PVC geomembrane on the upstream dam surface are advisable.

References

- Bowen R (1981) Grouting in engineering practice, 2nd edn. Applied Science, New York
- Casagrande A (1961) First rankine lecture—control of seepage through foundations and abutment of dam. *Géotechnique* 11(3):161–182
- Ceng LK, Fan JL, Han J, Xu JP (2003) Rock and soil reinforcement. China Building Industry Press, Beijing (in Chinese)
- Chen SH, Chen ML (2014) Hydraulic Structures, 2nd edn. China WaterPower Press, Beijing (in Chinese)
- Creager WP (1917) Engineering for masonry dams. Wiley, New York
- Dunstan MRH (2007) Overview of RCC dams at the end of 2006. In: Jia J et al (eds) New progress on roller compacted concrete dams. China WaterPower Press, Beijing, pp 9–17
- Forbes BA (1999) Grout enriched RCC: a history and future. International water power & dam construction. Wilmington Business Publishing, Dartford, pp 34–38
- Golzé AR (1977) Handbook of dam engineering. Van Nostrand Reinhold Company, New York
- Grishin MM (ed) (1982) Hydraulic structures. Mir Publishers, Moscow
- Hansen KD, Reinhardt WG (1991) Roller compacted concrete dams. McGraw-Hill, New York
- Harza LF (1949) The significance of pore pressure in hydraulic structures. *Trans ASCE* 114 (1):193–214
- ICOLD (1989) Roller compacted concrete for gravity dams—state of the art (Bulletin 75). ICOLD, Paris
- ICOLD (1993) Rock foundations for dams (Bulletin 88). ICOLD, Paris
- ICOLD (2003) Roller-compacted concrete dams—state of the art and case histories (Bulletin 126). ICOLD, Paris
- ICOLD (2005) Dam foundations. geologic considerations. Investigation methods. Treatment. Monitoring (Bulletin 129). ICOLD, Paris
- Iqbal A (1993) Irrigation and hydraulic structures – theory, design and practice. Institute of Environmental Engineering & Research, NED University of Engineering & Technology, Karachi
- Jansen RB (1980) Dams and public safety, a water resources technical publication. CO (Water and Power Resources Service, Bureau of Reclamation, US Department of the Interior), Denver
- Jansen RB (1988) Advanced dam engineering for design, construction, and rehabilitation. Van Nostrand Reinhold, New York
- Keener KB (1951) Uplift pressures in concrete dams. *Trans ASCE* 116(1):1218–1237
- Kiersch GA (1964) Vajoint reservoir disaster. *Civ Eng* 34(3):32–39
- Li ZM (1982) Arch dams. Water Resources and Electric Power Press of China, Beijing (in Chinese)
- Lin JY (2006) Hydraulic structures. China WaterPower Press, Beijing (in Chinese)
- Lombardi G (1991) Kölnbrein dam: an unusual solution for an unusual problem. *Water Power Dam Constr* 43(6):31–34
- Londe P (1987) The malpasset dam failure. *Eng Geol* 24(1–4):295–329

- Ma GY, Chang ZH (2007) Theory and practice of grouting drainage and anchorage of rock mass. China WaterPower Press, Beijing (in Chinese)
- Mason PJ (1993) Practical guidelines for the design of flip buckets and plunge pools. *Water Power Dam Constr* 45(9):40–45
- Ministry of Water Resources of the People's Republic of China (2003) (SL282-2003) "Design specification for concrete arch dams". China WaterPower Press, Beijing (in Chinese)
- National Reform and Development Commission of the People's Republic of China (2006) (DL/T5346-2006) "Design specification for concrete arch dams". China Electric Power Press, Beijing (in Chinese)
- Novak P, Moffat AIB, Nalluri C, Narayanan R (1990) Hydraulic structures. The academic division of Unwin Hyman Ltd, London
- Post-Tensioning Institute (1985) Recommendations for prestressed rock and soil anchors. Post-Tensioning Institute, Phoenix
- Ru NH, Jiang ZS (1995) Arch dams. Accident and safety of large dams. China Water Power Press, Beijing (in Chinese)
- Schnitter NJ (1994) A history of dams: the useful pyramids. AA Balkema, New York
- Stelle WW, Rubin DI, Buhas HJ (1983) Stability of concrete dam: case history. *J Energy Eng ASCE* 109(3):165–180
- Sun Z (2004) Grouting in dam's rock foundation. China WaterPower Press, Beijing (in Chinese)
- Tatro SB, Schrader EK (1985) Thermal considerations for roller-compacted concrete. *ACI J* 82(2):119–128
- USB (1987a) Design of small dams, 3rd edn. US Govt Printing Office, Denver
- USB (1987b) Design of small dams, 3rd edn. US Govt Printing Office, Denver
- Vogt F (1925) Über die berechnung der Fundament Deformation. *Avhandlingar utgitt av Det Norske Videnskaps Akademi Oslo* (Norway) (in German)
- Wang HS, Wueng QD (1990) Hydraulic structures. China WaterPower Press, Beijing (in Chinese)
- Wu ML (1991) Hydraulic structures. Tsinghua University Press, Beijing (in Chinese)
- Zhang ZQ (2002) RCC arch dams. China WaterPower Press, Beijing (in Chinese)
- Zhou JP, Dang LC (eds) (2011) Concrete Dams. In: Handbook of hydraulic structure design, vol 5. China Water Power Press, Beijing (in Chinese)
- Zhu SA (1995) Technical history of dam engineering. Water Resources and Electric Power Press of China, Beijing (in Chinese)
- Zuo DQ, Gu ZX, Wang WX (eds) (1987) Concrete dams. In: Handbook of hydraulic structure design, vol 5. Water Resources and Electric Power Press of China, Beijing (in Chinese)
- Zuo DQ, Wang SX, Lin YC (1995) Hydraulic structures. Houhai University Press, Nanjing (in Chinese)

Chapter 9

Embankment Dams

9.1 General

Dams constructed of earth and rock materials are generally referred to as embankment dams or fill-type dams (Golzé 1977; Guo and Chen 1992; Sherard et al. 1963; USBR 1987; Zuo et al. 1984).

The history of embankment dams is much earlier than that of concrete dams. It is evident that some simplest embankment dams were constructed about 3000 years ago in the cradles of ancient cultures such as Egypt, Indian, Sri Lanka, Peru, China, and other countries (Hill 1996; Jansen 1980, 1988; Schnitter 1994; Zhu 1995). According to the statistic data in “Dams and public safety (ICOLD 1986),” from 1963 to 1983 altogether 33 dams higher than 200 m had been built, among them 5 were embankment dams, as listed in Table 9.1.

Until 1949, there was only one modern embankment dam in China located at the Gansu Province. After extension works during the 1950s, its final height is 37.5 m and its gross reservoir storage is 1.1×10^9 m³. During 1949–1986, China constructed 18820 dams higher than 15 m, of which embankments accounted for 16,853 (90 %). Among the 2668 dams higher than 30 m, 2174 were embankments (81.5 %). However, there were only 3 embankment dams higher than 100 m: the Shitouhe Earthfill Dam with clay central core (Shanxi, China, $H = 114$ m), the Bikou Earth- and Rockfill Dam with loam central core (Gansu, China, $H = 101.8$ m), and the Lubuge Rockfill Dam with soil central core (Yunan and Guizhou, China, $H = 103.8$ m). Since the 1990s, as the accumulation of experiences and the advancement in technology of embankment dam design and construction, the materials for dam construction were expanded to a wider class: More and more weathered rock, soft rock, gravelly soil, and excavation residues were applicable. For materials do not fully meet the requirements, the water content and grade adjustment enable them to be placed within dams. As a result, the number of high embankment dams, particularly high earth-core rockfill dams and concrete-faced rockfill dams (CFRDs), soared. The representative projects of this period were the

Table 9.1 Embankment dams higher than 200 m built from 1963 to 1983

Name of dam	Country	Height (m)	Completion year
Rogun	Tadzhikistan	325	Under construction
Nurek	Tadzhikistan	300	1980
Mihoesiti	Rumania	242	1983
Oroville	USA	235	1968
San Rogue	Philippine	210	1968

Tianshengqiao 1 CFRDs (Guizhou, China, $H = 178$ m) and the Xiaolangdi Rockfill Dam with inclined central core (Henan, China, $H = 160$ m).

The prevailing of embankments in the modern dam construction is mainly attributable to

- Rigorous conditions concerning climate, topography, and geology are relaxed. Particularly, while hard and sound rock foundation is required for concrete dams, embankment dams may be constructed even on alluvial deposit and pervious foundation after adequate treatments;
- Construction materials are principally supplied near the dam site. The advancement in design methods, construction techniques, and soil mechanics, enable a wide applicable range of materials for embankment dam construction. The materials previously regarded as “inferior materials,” such as weathered gravel soil, dynamic earth, middle-fine-sand, and excavation residues, are employed nowadays in zoned dams. In this way, advantageous conditions are also created for the large-scale excavation in diversion and flood discharge works;
- Construction of embankment dams has a potential economical advantage because the consumption of cement, steel, wood, transportation, etc are reduced. As a result, the construction period and cost could be saved. For a similar-scale project, although the volume of embankment dam is 4–6 times larger than the concrete dam, yet its unit price is only 1/15–1/20, in some countries even as low as 1/30–1/70, of the concrete dam;
- As the development of rock and soil mechanics, computation methods, test and monitoring equipments, the design theory and method have achieved great progress;
- The advanced construction equipments, such as heavy vibrating roller, hydraulic vibrating plate, laser-oriented gradall, on-site processing of long copper water stop, non-railed slip form, etc., have been widely applied to improve the construction quality and speed. The technology of nondestructive test for filled density has been developed and used as auxiliary measure in the construction quality control;
- With respect to diversion works during construction, many practical alternatives are available. For example, using high cofferdam to retain the whole year flood, retaining flood with temporary section of dam, or discharging construction flood with both overtopping the protected embankment and diversion tunnel, using high cofferdam as a part of permanent dam body, all enable embankment dams

to be applicable for various natural conditions of dam site and improve the comprehensive benefits. The typical examples are the Jinpen Rockfill Dam with clay central core (China, $H = 133$ m) (Fig. 9.18), the Lubuge Rockfill Dam with central core (China, $H = 103.8$ m), and the Nuozhadu Rockfill Dam with central core (China, $H = 261.5$ m), they all incorporated the upstream cofferdam into the main dam body; and

- It has been verified by studies and practices that the seismic resistance of embankment dams is higher than concrete dams. The Rogun Dam (Tadzhikistan, $H = 335$ m) located in a seismic area of 9° , the embankment dam with inclined central core replaced the concrete dam scheme in the final phase of design; the Chicoasen Dam (Mexico, $H = 261$ m) also replaced the concrete dam scheme by the rockfill dam with central core due to the worries over strong seismic actions.

9.1.1 Design Requirements for Embankment Dams

According to an investigation conducted by the ICOLD in the 1990s, the failure of embankment dams accounted for 70 % of the total dam failure accidents, of which 70 % were lower than 30 m. The major scenarios of embankment failure accidents are (Foster et al. 2000; Ru and Niu 2001; Ministry of Water Resources of the People's Republic of China 2001; National Reform and Development Commission of the People's Republic of China 2008) as follows:

- Overtopping. Most of catastrophic accidents of embankment dams are resulted from overtopping by reservoir water attributable to flood or loss of freeboard. Case histories reveal that the inadequate capacity of spillway, that is, the insufficient estimation of the amount of flood, has often led to the failure of embankments due to overtopping;
- Construction quality problems. Other main factor in embankment failures is the poor-quality control in construction, which lead to hydraulic erosion or slope sliding in the dam body and/or foundation, leakage through the spillway and/or embedded culverts (pipes) within the dam; and
- Inadequate management.

Accordingly, the following requirements should be met in the design of embankment dams:

- (i) Since more than one-quarter of embankment failure accidents are resulted from slope sliding according to the statistic data, stability of slope is the basic requirement for the dam safety. The slopes, foundation, and abutments must be stable during construction and reservoir operation, including rapid reservoir drawdown, if applicable. No unacceptable deformations take place under earthquake actions, too.
- (ii) Since seepage through the foundation or embankment has been responsible for more than one-third of embankment dam failure accidents, they must be collected and controlled to prevent excessive uplift, piping, sloughing,

removal of material by solution, and erosion of material into cracks (joints) and cavities (sink holes). Sometimes the discharge rate of seeping water should be controlled, too.

- (iii) The embankment must be safe against excessive overtopping. Freeboard must be sufficient to prevent overtopping by wave actions including an allowance for the post-construction settlement of the dam and foundation, and the deformation due to earthquake. In addition, freeboard must be sufficient to retain the maximum design flood often chosen as the probable maximum flood (PMF). Spillways and outlets must be designed with sufficient discharge capacity such that overtopping of the dam does not occur.
- (iv) Protections on both the upstream and downstream slopes must be reliable to prevent erosion due to the actions of wave, rainfall, and wind. Materials of slope protection must be durable and resistant to the actions of wetting/frying and freeze/thaw.

9.1.2 Classification of Embankment Dams

According to construction methods, embankment dams can be roller compacted, hydraulically filled, water dumped, pin point blasting filled. Hydraulically filling dams use hydraulic jet to wash and transport soil to the construction surface, the embankments are erected by natural deposit and consolidation of the soil. Water dumping dams are erected by filling soil in water without mechanical compaction. Roller compacted dams are distinguished as the embankment constructed with subsequence mechanical compaction of the filling layers, which is the most prevalent type. Several generalized sectional profile of roller compacted embankment dams showing typical zoning and devices for controlling seepage is illustrated in Fig. 9.1.

When practically only one impervious material is available and the dam height is relatively low, the homogeneous dam with internal drain (Fig. 9.1a) may be employed. The drain serves to prevent the downstream slope from becoming saturated and susceptible to piping and/or slope failure.

Embankment dams with impervious cores, as shown in Fig. 9.1b, c, are constructed when locally borrowed materials do not provide adequate quantities of impervious materials. The philosophy for cored embankment dams is to surround the impervious core by strong shells providing stability. A vertical core located near the embankment center is preferred over a sloping upstream core because the former provides higher contact pressure between the core and foundation to prevent leakage, and greater stability under earthquake actions, as well as better access for remedial seepage control. Nevertheless, a sloping upstream core allows the downstream portion of the embankment to be placed in advance and reduces the risk of hydraulic fracturing.

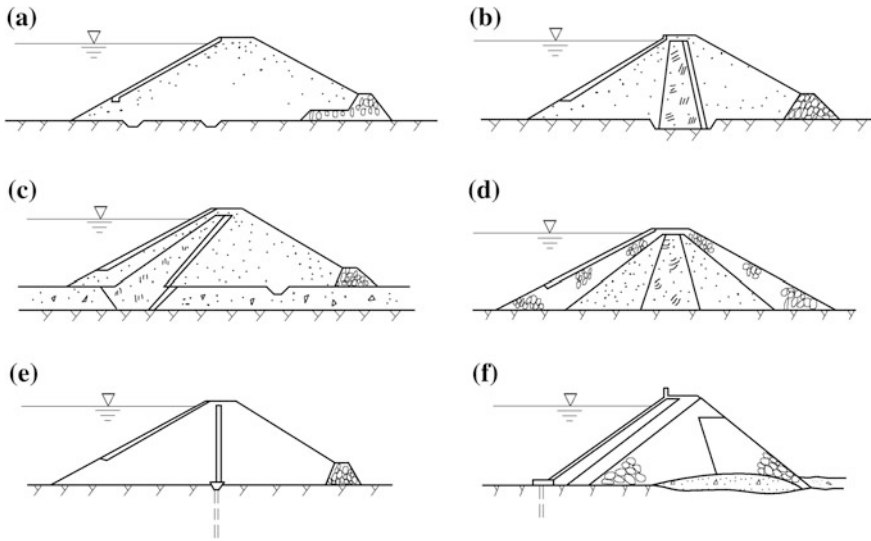


Fig. 9.1 Types of roller compacted embankment dams. **a** Homogeneous dam; **b** central core dam; **c** sloping core dam; **d** multi-zonal dam; **e** impervious membrane centered dam; **f** impervious membrane decked dam

For dams on pervious foundations, as shown in Fig. 9.1d–f, under seepage control devices are installed to prevent excessive uplift pressure and piping through the foundation, apart from the seepage control devices within the embankment. The devices for the control of under seepage in foundations are horizontal drains, cutoffs (compacted backfill trenches, slurry walls, and concrete walls), upstream impervious blankets, downstream seepage berms, toe drains, and relief wells.

For the purposes to facilitate the construction, to improve the stress state and cracking resistance, inclined central cores are more and more prevalent in modern high embankment dams.

Figure 9.2 is the profile of the Xiaolangdi Dam inclined central core (China, $H = 160$ m). It is the largest hydraulic project on the Yellow River completed in 2001, mainly purposed for the flood control while simultaneously with comprehensive benefits of power generation, and irrigation. The rockfill dam with loam-inclined central core, 1320 m in crest length and 49 million m^3 in dam volume, is the largest embankment dam in China. The dam foundation is covered by sand–gravel overburden of averagely 30–40 m thick and maximum 80 m thick. A concrete cutoff of 1.2 m wide and 81.9 m deep, inserting 12 m into the loam-inclined central core, is installed for under seepage control.

Conventionally, depending on the dominant content of earth or rock in the maximum cross section, to say, accounting for half of the materials or more, an embankment dam may be distinguished as earthfill or rockfill (Snethlage et al. 1960).

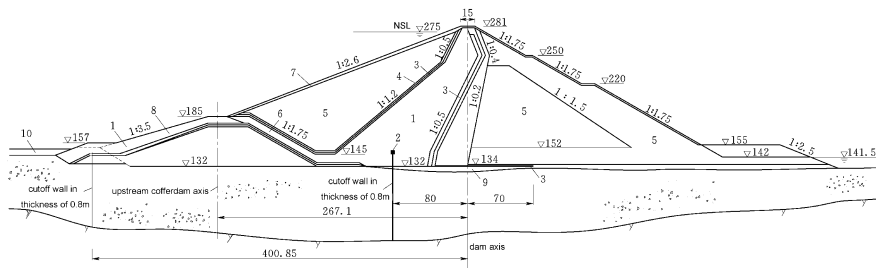


Fig. 9.2 The Xiaolangdi Rockfill Dam with inclined central core (unit: m) China, $H = 160$ m. 1 clay; 2 high-plastic clay; 3 filter layer; 4 transition layer; 5 rockfill; 6 mixture material; 7 crushed rock revetment; 8 rockfill riprap; 9 backfilled gravel; 10 upstream blanket

1. Earthfill dams

An earthfill dam is mainly composed of suitable soils such as earth, sand, and sand–gravel obtained from borrow or excavation areas. Following the preparation of a foundation, soils are transported to the site, dumped, and spread in layers of required depth, and compacted by mechanical means such as tamping rollers, sheep’s foot rollers, heavy pneumatic-tired rollers, vibratory rollers, tractors, or earth-hauling equipment. The gravel content in the earthfill dam is normally lower than 60–70 %; therefore, it does not form skeleton and the permeability of dam body is low. Earthfill is the most common type of embankment dams, attributable mainly to its advantage that the foundation requirements are less stringent than for other types of embankment dams. The earthfill dams can be further subdivided as follows:

- Homogeneous, constructed entirely from a more or less uniform natural earth material. The dam must be sufficiently impervious to provide an adequate water barrier and the slopes must be sufficiently flat to maintain stability against sliding. When practically only one impervious earth material is available and the height of the dam is relatively low, a homogeneous dam with or without internal drain may be employed;
- Modified homogeneous, in which small amount of carefully placed impervious materials control the adverse seepage so as to permit much steeper embankment slopes; and
- Zoned, containing materials of distinctly different properties in the different portions of the dam.

Where a variety of soils are readily available, the choice of earthfill dam types should always be zoned due to the consideration over a less cost in construction.

2. Rockfill dams

A rockfill dam is comprised of three structural components: rockfill compacted using fragmented rocks such as pebbles, block stones, and weathered rocks of all sizes, to provide stability; impervious membrane in the form of impervious core or upstream face (Fig. 9.1e, f), to provide watertightness; and transition layers separate

the impervious core or upstream face from the rock shell by a series of zones built of properly graded materials. A membrane of concrete, asphalt, or steel plate on the upstream face should be considered in lieu of an impervious earth core when sufficient impervious material is not available. The gravel content in sand–gravel material is normally higher than 70 %, the gravel does form skeleton, and the permeability of the dam body is high.

The rockfill dam with steeper slopes demands a foundation with more rigorous conditions compared to earthfill dams, although its requirements may be relaxed with respect to concrete dams.

The impervious membrane placed either within the embankment or on the upstream slope performs as water barrier. Various materials have been exercised in the building of membranes, including clayey earth, concrete, asphaltic concrete, steel, and wood. Depending on the material and position of the impervious membrane, rockfill dams may be further subdivided into types of central core, sloping core, diaphragm, and concrete faced (decked).

Rockfill zones are compacted by heavy rubber-tired or steel-wheel vibratory rollers. It is often desirable to determine the best methods of compaction works on the results from testing quarry and testing fill. Dumping rockfill and sluicing with water, or dumping in water, is generally acceptable only in constructing cofferdams that are not to be incorporated in the dam embankment. Free-draining, well-compacted rockfill can be placed with steep slopes if the dam is on a rock foundation. If it is necessary to place rockfill on an earth or strongly weathered rock foundation, the embankment slopes must, of course, be much more flat, and transition zones are installed between the foundation and the rockfill. Materials available for rockfill dams are ranged from sound free-draining rocks to the more friable materials such as sands, stones, and silt shales that are crushed down under handling and compacting. The last class of materials, due to their insufficient free-draining and shear strength compared to sound rockfill, is often termed as “random rock” and can be merely used for the particular zone in the rockfill embankment.

Rockfill dams may be economically attributable to large quantities of rocks available from excavation (pits, slopes, tunnels, etc.) or nearby borrow sources, adaptive to wet and freezing climates, and ability to conduct foundation grouting with simultaneous placement of rockfill (for sloping core and decked dams).

The general design theory for embankment dams (inclusive earth- and rockfills) will be addressed in this chapter. The particular considerations on the rockfill dam, which has been developing fast in recent years, will be discussed in Chap. 10 of this book.

9.1.3 Layout of Embankment Dam Projects

Project site selection should take into account of the topographic and geologic conditions simultaneously for the dam and other structures, particularly the spillways. Axis of a long embankment with respect to its height is desirably straight or,

sometimes curvilinear fitting the topographic and foundation conditions. Sharp changes in the axis should be avoided by curving transition sections, to prevent downstream deformation at these locations from tending to manifest tension zones. The axes of high dams on narrow and steep-walled valleys could be curved upstream so that the downstream deflection under water loads will tend to compress the impervious zones longitudinally, aiding to resistance against transverse cracking. Shore chute spillways (or ski-jump spillways) and tunnels are demanded, to obtain sufficient discharge ability and operation reliability. The protections should be carefully designed in order to prevent the dam toe and river banks from scouring due to the released outflow. For a chute spillway with high head, a curved approaching channel is customarily designed and various kinds of flip bucket can be employed to adjust outflow direction. Spillways are advisable to be located on rock foundation. For dams of high to medium in strong seismic regions, the embedded pipes or culverts below embankments on soft foundations are not allowed. By the accumulated experiences of high earth- and rockfill construction since the 1990s, embankment project layout has the tendency of following distinctive features in recent years:

- In order to obtain high adaptability to topographic and geologic conditions, the central core rockfill dam and the CFRD are prevailing. CFRD is commonly exercised where the dam height is 100–150 m, although a number of this type of dams at height of 150–200 m are erected. Rockfill dam is often significantly advantageous where the dam is higher than 200 m and perhaps even more, with very deep riverbed overburden;
- Based on the principle of overall balance between the excavation and filling, excavated spillways as well as approach and tailrace channels of power and flood tunnels are extensively employed in the project layout, because over 80 % of the excavated slag may be utilized for the dam filling;
- Underground powerhouses or bankside powerhouses near dam toe are widely adopted to obtain a power headrace system as short as possible and eliminate surge shaft (chamber). For power stations over 1000 MW in capacity, large-capacity units are often desirable for reducing the number of units and the construction amount of underground caverns;
- Floods are mainly released by shore spillways in combination with ski-jump energy dissipation; and
- Tunnels are generally used for construction diversion and as deep (bottom) outlets for supplementary flood releasing.

Figure 9.3 shows the Bikou Hydropower Project, which is mainly purposed for power generation and with simultaneous comprehensive benefits of flood control, log passing, irrigation, etc. The reservoir storage capacity is 521 million m³ and the installed generator capacity is 3 × 100 MW. The loam core dam at a height of 101.8 m is the first embankment dam higher than 100 m completed in China. The foundation overburden is 25–34 m in depth, in which two concrete cutoff walls are installed for the control of under seepage. The first wall is 42.5 m deep and 1.3 m

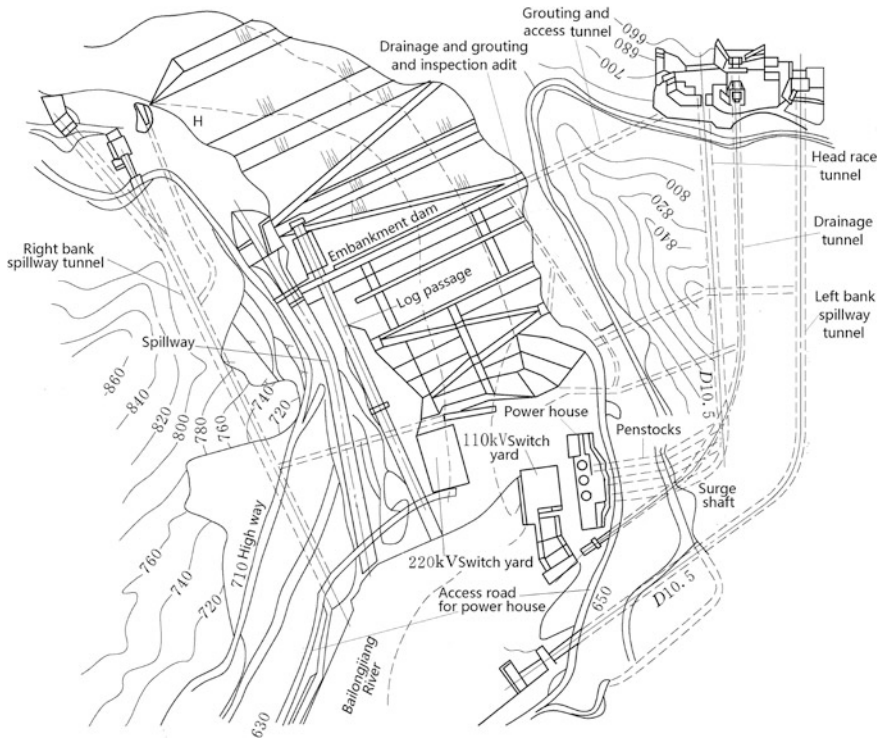


Fig. 9.3 The Bikou Hydropower Project (unit: m) China, $H = 101.8$ m

thick, the second wall of 68.5 m deep and 0.8–1.0 m thick is installed 13 m behind of the first one. The spillway is layout on the right bank, the headrace and power generation system is on the left bank. The maximum flood discharge of $9550 \text{ m}^3/\text{s}$ is handled by the spillway and flood tunnel with ski-jump energy dissipation. The flood tunnel of $13 \text{ m} \times 11.5 \text{ m}$ in cross section with a raised intake is rebuilt from the diversion tunnel.

9.2 Loads and Load Combinations

9.2.1 Loads

The loads on embankment dams are basically identical to those on concrete dams. However, the concept of pore pressure and its computation is special and attention should be called at.

9.2.2 Load Combinations

1. Basic (usual)
 - Normal storage level or design flood level or other level above dead (inactive) level + corresponding steady-state seepage;
 - Frequent routine variation of reservoir level between foregoing levels + corresponding steady-state seepage; and
 - Frequent variation of reservoir levels in pumping power stations + corresponding unsteady-state seepage.
2. Special I (unusual)
 - Construction period;
 - Maximum reservoir elevation + corresponding steady-state seepage; and
 - Reservoir drawdown from maximum reservoir level, or from normal level, to inactive level + corresponding unsteady-state seepage.
3. Special II (extreme)
 - Basic load combination + maximum credible earthquake.

9.3 Seepage Analysis for Embankment Dams

The seepage analysis is carried out for the purposes

- To determine the location of seepage line (phreatic line or phreatic surface in three-dimensional case) and the downstream exit point, based on which the stability of up- and downstream slopes may be calibrated, and the sectional profile may be revised;
- To determine the seepage head gradient, (J), based on which the seepage stability (piping and pop-off) is calibrated, the anti-seepage devices and materials are designed;
- To determine the seepage velocities (v) and discharge (q), based on which the capacity and size of draining system are designed; and
- To determine the line of seepage and pore pressure during reservoir drawdown.

9.3.1 Permeable Characteristics of Embankment Materials

The term “isotropic permeability” is often employed in the embankment dam design when the permeability of soils is independent of direction. However, as a result of the genesis of the ground, mainly by sedimentation of layers, lateral moraines, and formation of the soil structure, directional differences in soil

permeability normally appear and the soil exhibits the permeability of anisotropy as well as heterogeneity.

Solution of the seepage problem for grade 1 and 2 embankment dams should make use of numerical approach, whereas for the other dams hydraulic method is conventionally employed.

9.3.2 Hydraulic Method

The hydraulic method being widely exercised in the design of embankment dams is intended for approximate seepage calculation, to determine the location of phreatic line, the seepage discharge, the seepage velocities, and the head gradient, at any point of a seeping regime (Chen and Chen 2014; Grishin 1982; Novak et al. 1990; USBR 1987).

1. Basic assumptions of hydraulic method

- The materials are homogenous and isotropic; and
- The seepage flow is gradually varied (equipotential lines and streamlines vary gradually), i.e., at all points on a vertical section, the velocities and head are identical.

Suppose an embankment profile with up- and downstream slopes be vertical, i.e., the shape of the section is rectangular (Fig. 9.4), the Dupuit–Forchheimer assumption (Dupuit 1863; Forchheimer 1886) for the seepage discharge will be

$$\begin{cases} v = k \frac{H_1 - H_2}{L} \\ q = k \frac{H_1 - H_2}{L} \frac{H_1 + H_2}{2} \end{cases} \quad (9.1)$$

where H_1 and H_2 = head- and tailwater depths, respectively, m; L = horizontal distance from upstream to downstream, m; k = permeability coefficient, m/days.

2. Seepage in a homogeneous dam without drain on impervious foundation

A dam foundation may be ordinarily looked at as impervious if $k_f \leq \frac{k_d}{100}$. Under this assumption, Pavlovskiy–Dachler (Dachler 1936; Pavlovsky 1956) established a hydraulic method based on cutting dam profile into three parts. By the revision using an imaged rectangle to replace the upstream wedge, a simplified “two parts”

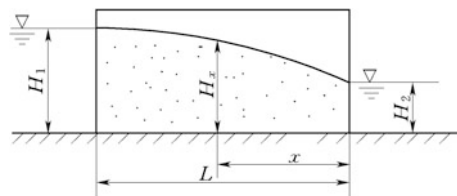


Fig. 9.4 Diagram to the seepage computation by hydraulic method

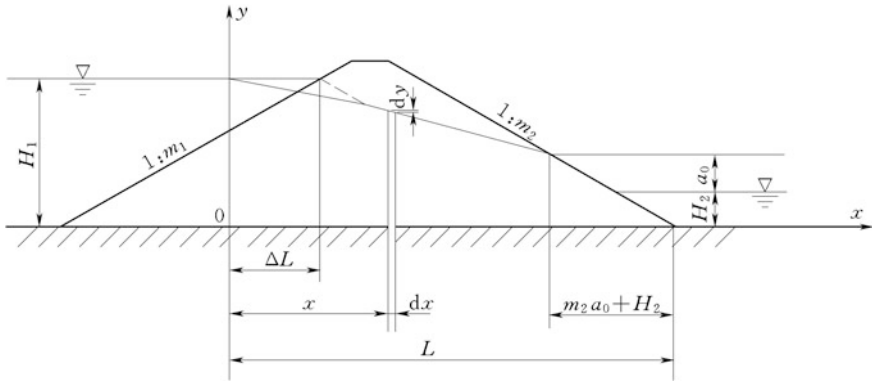


Fig. 9.5 Seepage computation for homogeneous dams without drain on impervious foundation

algorithm is now widely employed (Fig. 9.5), in which the wedge of the dam with upstream slope can be replaced by a profile bounded from the headwater side with vertical surface, whose width is generally $\Delta L = 0.4H_1$. In case of steep upstream slope, ($m_1 < 2$), $\Delta L = \frac{m_1 H_1}{1+2m_1}$.

(a) Analysis of upstream portion

At any point in the seepage regime, the head gradient is

$$J = -\frac{dy}{dx}$$

According to the Darcy's formula,

$$v = k \cdot J = -k \cdot \frac{dy}{dx}$$

The seepage discharge through any vertical section of the regime is calculated by

$$q_1 = v \cdot y \cdot 1 = -k \cdot y \cdot \frac{dy}{dx}$$

or

$$q_1 dx = -k \cdot y \cdot dy \tag{9.2}$$

Integral Eq. (9.2) from the starting to the ending of the upstream part gives

$$q_1 \int_0^{L-m_2(a_0+H_2)} dx = -k \int_{H_1}^{a_0+H_2} y dy$$

It leads to

$$q_1 [L - m_2(\alpha_0 + H_2)] = \frac{k}{2} [H_1^2 - (\alpha_0 - H_2)^2]$$

Therefore,

$$q_1 = \frac{k [H_1^2 - (\alpha_0 + H_2)^2]}{2[L - m_2(\alpha_0 + H_2)]} \tag{9.3}$$

where a_0 = required value; the other nomenclatures are shown in Fig. 9.5.

Integral of Eq. (9.2) from the upstream starting to a specified section

$$q_1 \int_0^x dx = -k \int_{H_1}^y y dy$$

It gives rise to

$$q_1 x = -k \frac{1}{2} (y^2 - H_1^2)$$

The equation of phreatic line is then obtained as a parabola

$$y^2 = H_1^2 - \frac{2q_1 x}{k} \tag{9.4}$$

(b) Analysis of downstream portion

Presumably the streamlines in the downstream part and above the tailwater level are horizontal. With regard to a flow tube above the tailwater level of $dz \times 1$ in height, $m_2 z$ in length, and Z in exerting head (the origin of local coordinate system is at the downstream exit point), the head gradients will be $J = \frac{z}{m_2 z} = \frac{1}{m_2}$ and the corresponding seepage flow discharge through the tube is $dq = k \cdot \frac{1}{m_2} \cdot dz$, so the whole discharge above the tailwater level is

$$q' = \int_0^{a_0} dq = \int_0^{a_0} \frac{k}{m_2} dz = \frac{k \alpha_o}{m_2} \tag{9.5a}$$

For a flow tube under the tailwater level, the exerting head is constant as $z - H_2 = a_0$, then the head gradient will be $J = \frac{\alpha_o}{m_2 z}$ and the corresponding seepage flow discharge through the tube is $dq'' = k \cdot \frac{\alpha_o}{m_2 z} dz$, so the whole flow discharge under the tailwater level is

$$q'' = \int_{a_0}^{a_0+H_2} k \frac{\alpha_o}{m_2 z} dz = k \cdot \frac{\alpha_o}{m_2} \ln \frac{\alpha_o + H_2}{\alpha_o} \tag{9.5b}$$

The total flow discharge through the downstream part is therefore summed as

$$q_2 = q' + q'' \tag{9.6}$$

According to the principle of continuous flow $q_1 = q_2$, Eqs. (9.3) and (9.6) may be simultaneously solved to get the required value a_0 .

The phreatic line of Eq. (9.4) is to be revised locally at the vicinity of the starting point near the upstream slope. In case of zero tailwater, $H_2 = 0$.

3. Seepage in the homogeneous dam with drain on impervious foundation

(a) Surface drainage

Since it is situated outside of the dam slope and does not cut-short the paths of percolation, it has no effect on the position of phreatic line.

(b) Horizontal blanket drainage (Fig. 9.6a)

Horizontal blanket drainage is only effective when there is no tailwater (i.e., $H_2 = 0$).

Assume the phreatic line is a parabola with its focus at the generatrix of the drainage where the height of the phreatic line is α_0 , the origin of the parabola is located to the right of the generatrix of the drainage at a distance of $a_0/2$. The Dupuit–Forchheimer formula gives

$$q = k \cdot \frac{H_1^2 - \alpha_0^2}{2L'} \tag{9.7}$$

And

$$q = k \frac{a_0^2 - y^2}{2x'} \tag{9.8}$$

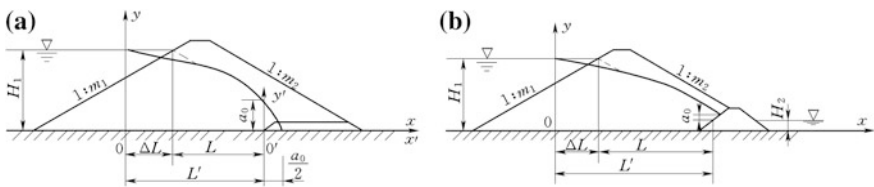


Fig. 9.6 Diagram to the seepage computation for homogeneous dams with drain on impervious foundation. **a** Horizontal blanket drainage; **b** drainage prism

Substitutes the coordinate of the parabola origin into Eq. (9.8), it gives rise to

$$q = k \frac{a_0^2}{2 \frac{a_0}{2}} = ka_0$$

Which is then introduced into Eq. (9.7) to produce

$$\alpha_0 = \sqrt{H_1^2 + L^2} - L' \tag{9.9}$$

The phreatic line is represented either in the coordinate system $x - y$ by Eq. (9.4) where $q_1 = q = ka_0$ or in the coordinate system $x' - y'$ as

$$y' = \sqrt{a_0^2 - \frac{2qx'}{k}} \tag{9.10}$$

(c) Drainage prism (Fig. 9.6b)

Drainage prism is exercised widely for embankment dams. Where there is no downstream tailwater, the seepage analysis is similar to that for horizontal blanket drainage. Where the downstream tailwater level is H_2 , with respect to the joint point of the water level and the upstream prism face, the prism is divided into two portions by the horizontal water surface, and the portion above the tailwater level is looked at as identical to that with the horizontal blanket drainage, that is,

$$\alpha_0 = \sqrt{(H_1 - H_2)^2 + L^2} - L' \tag{9.11}$$

$$q = k \cdot \frac{H_1^2 - (H_2 + \alpha_0)^2}{2L'} \tag{9.12}$$

The phreatic line is represented by Eq. (9.4) where $q_1 = q$.

4. Seepage in the central core dam on impervious foundation

The trapezoidal central core is replaced by an equivalent rectangle with thickness δ , and its upstream water depth H_1 is identical to that at the upstream surface of dam shell; the diagram to the computation is shown in Fig. 9.7.

Suppose the water depth at the downstream of the central core is H , then the flow discharge through the central core will be

$$q = k \frac{H_1^2 - H^2}{2\delta} \tag{9.13}$$

Denote the downstream tailwater depth as H_2 , the flow discharge through the downstream dam shell behind the central core is

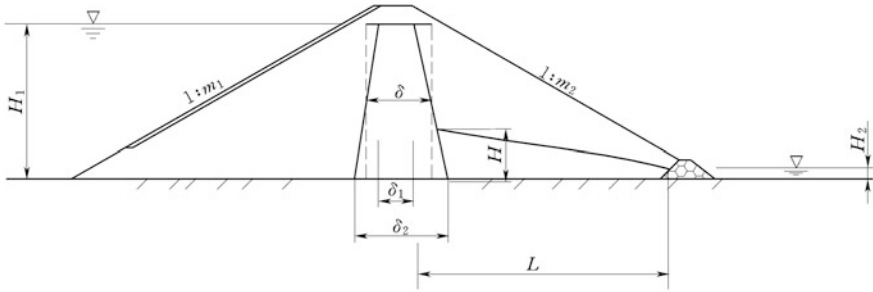


Fig. 9.7 Seepage computation for central core dams on impervious foundation

$$q = k \frac{H^2 - H_2^2}{2L} \tag{9.14}$$

According to the principle of the continuity of flow, Eqs. (9.13) and (9.14) may be simultaneously solved to obtain q and H .

5. Seepage in sloping core dams on impervious foundation (Fig. 9.8)

Denote the upstream and downstream water depths of the sloping core are H_1 and H , respectively, and the tailwater depth is H_2 . The flow discharge through the sloping core is divided into two portions:

- ① The lower portion below the depth H . The head difference is constant as $H_1 - H$, and the thickness of the core wall is $t = t_1 - \frac{t_1 - t_2}{L_1 + L_2} x$, and then, the flow discharge through this part is

$$q_1 = k_1 \int_0^{L_1} \frac{H_1 - H}{t_1 - (t_1 - t_2)x / (L_1 + L_2) \cos \theta} dx \tag{9.15}$$

- ② The upper portion higher than H . The head difference is $H_1 - y$, and then, the flow discharge through this part is

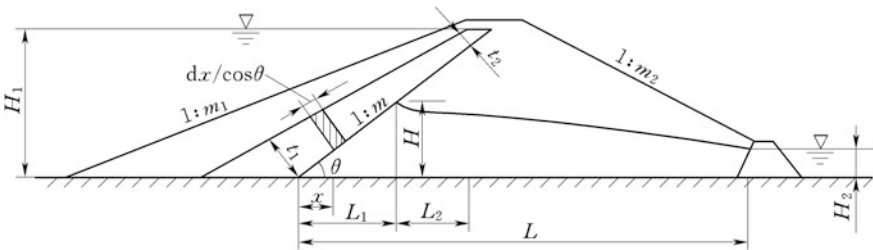


Fig. 9.8 Seepage computation for sloping core dams on impervious foundation

$$q_2 = k_1 \int_{L_1}^{L_2} \frac{H_1 - y}{t_1 - (t_1 - t_2)x / (L_1 + L_2)} \frac{dx}{\cos \theta} \tag{9.16}$$

The flow discharge through the downstream dam shell is

$$q = k_2 \frac{H^2 - H_2^2}{2(L - mH)} \tag{9.17}$$

According to the principle of continuity of flow, we have

$$q = q_1 + q_2 \tag{9.18}$$

Equations (9.15)–(9.18) may be simultaneously solved for q and H .

6. Seepage in homogeneous dams on pervious foundation (Fig. 9.9)

Assuming that the foundation is impervious, the discharge q_d through the dam body may be calculated by Eqs. (9.4)–(9.6); meanwhile, the discharge q_f through the foundation is calculated by the assumption that the dam body is impervious, and then the total flow discharge is summed as $q = q_d + q_f$.

Since the streamlines will be deflected at the entrance of seepage into foundation, they are longer than the width of dam base. According to the analysis using more accurate fluid dynamics, the average length of the streamlines in dam foundation is $L' + 0.44T$, and the width of the equivalent rectangle foundation is

$$\Delta L = \frac{\beta_1 \beta_2 + \beta_3 \frac{k_f}{k_d}}{\beta_1 + \frac{k_f}{k_d}} \tag{9.19}$$

where $\beta_1 = \frac{2m_1 H_1}{T} + \frac{0.44}{m_1} - 0.12$; $\beta_2 = \frac{m_1 H_1}{2m_1 + 1}$; $\beta_3 = m_1 H_1 + 0.44T$.

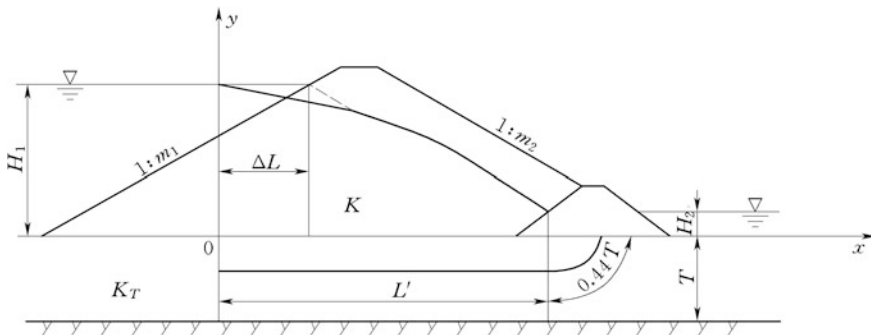


Fig. 9.9 Seepage computation for homogeneous dams on pervious foundation

Where there is no tailwater,

$$q = k_d \frac{H_1^2}{2L'} + k_f \frac{H_1}{L' + 0.44T} \cdot T \tag{9.20}$$

Where there is tailwater,

$$q = k_d \frac{H_1^2 - H_2^2}{2L'} + k_f \frac{H_1 - H_2}{L' + 0.44T} \cdot T \tag{9.21}$$

Transforming the base thickness T into an equivalent thickness $\frac{k_f T}{k_d}$, which has the same permeability coefficient of the dam body, the phreatic line may be obtained from Eq. (9.4) as follows:

$$y = \sqrt{\left(H_1 + \frac{k_f T}{k_d}\right)^2 - 2\frac{qx}{k_d} - \frac{k_f T}{k_d}} \tag{9.22}$$

7. Computation of total seepage discharge

The dam is firstly divided into several segments along its axis according to the topographic and geologic conditions (Fig. 9.10), then the average seepage flow discharge of each segment is calculated, and the total seepage discharge will given by

$$Q = \frac{1}{2} [q_1 L_1 + (q_1 + q_2)L_2 + \dots + (q_{n-1} + q_n)L_n + q_n L_n] \tag{9.23}$$

where q_i = average seepage flow discharge of the segment i , $m^3/(sm)$; L_i = length of the segment i , m.

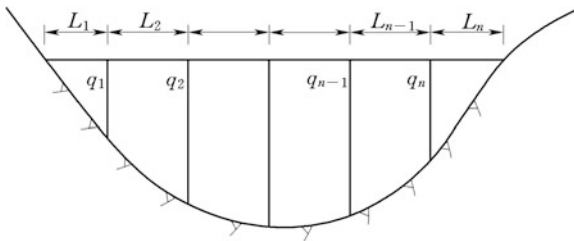


Fig. 9.10 Diagram to the computation of total seepage discharge

9.3.3 Seepage Failures and Countermeasures

1. Seepage failures

Seepage is inevitable in all embankment dams and ordinarily it does no harm. However, uncontrolled seepage may result in erosion within the embankment and foundation which will further lead to seepage failures (Grishin 1982; Novak et al. 1990; USBR 1987).

When seeping water flows through soils in an embankment and foundation, seepage forces will exert on soil particles due to water viscosity. If the seepage forces are large enough as compared to the resisting forces, erosion will take place by washing soil particles away, and seepage failure will successively develop as the erosion gradually progresses. The Teton Dam (USA, $H = 126$ m) was one of the eight dams authorized by federal agencies, which suffered a catastrophic failure on June 5, 1976, when it was being impounded for the first time. The collapse of the dam resulted in the deaths of 11 people and 13,000 heads of cattle. Study of the dam's environment and structure placed blame for its collapse majorly on the permeable loess soil compacted in the core and, on the fissured (cracked) rhyolite in the foundation that allowed water to seep under the dam (Smalley 1992).

(a) Mechanical piping

Mechanical piping is a progressive erosion which develops through or under the dam. It begins at a point of concentrated seepage where the gradients are sufficiently high to produce erosive velocities and corresponding drags. If forces resisting erosion comprising cohesion, interlocking effect, weight of soil particles, action of downstream filter, etc., are smaller than those which tend to manifest, the soil particles are washed away. Piping failure occurs only in non-cohesive soils.

(b) Pop-off

It is the simultaneous transfer of a large volume of sandy or clayey soil by the rising seepage flow, which often takes place at the exit portion on downstream dam slope or foundation.

(c) Contact scour (washout)

It is the loss of soil contact by seeping water parallel to and along the contact face that differs by size of particulars.

(d) Contact pop-off (flow-off)

It is the loss of soil contact by seeping water perpendicular to the contact face that differs by size of particulars.

(e) Chemistry piping

This is the phenomenon of soil salts being dissolved and washed away by seeping water.

2. Calibration of seepage failures

According to the SL274-2001 “Design specification for rolled earth–rockfill dams” and DL/T5395-2007 “Design specification for rolled earth–rockfill dams,” calibration of seepage failures comprises the sequent steps including failure-type judgment, critical seepage gradient computation, and allowable seepage gradient criterion.

(a) Type judgment

① Mechanical piping and pop-off

Several criteria developed by many years of experiences are available to judge the type of seepage failures.

The content of fine-grained particles P_c and porosity n are ordinarily employed in the judgment

$$\begin{cases} P_c \geq \frac{1}{4(1-n)} \times 100 & \text{Pop-off} \\ P_c < \frac{1}{4(1-n)} \times 100 & \text{Mechanical piping} \end{cases} \quad (9.24)$$

where P_c = content of fine-grained particles, %; n = porosity, %.

Content of fine-grained particles may be determined from the gradation curve (grain-size distribution) of the soil material.

For continuously gradated soils, the size of fine-grained particles d_f is evaluated by

$$d_f = \sqrt{d_{70}d_{10}} \quad (9.25)$$

where d_f = size to classify fine- and coarse-grained particles, mm; d_{70} = size of grain particles below which the content account 70 % of the total soil weight, mm; d_{10} = size of grain particles below which the content account 10 % of the total soil weight, mm.

For discontinuously gradated soils with coefficient of uniformity $C_U > 5$, P_c may be used for the type judgment solely with neglecting of the porosity n , i.e., instead of Eq. (9.24), Eq. (9.26) should be applied

$$\begin{cases} P_c \geq 35\% & \text{Pop-off} \\ 25\% \leq P_c < 35\% & \text{Transition} \\ P_c < 25\% & \text{Mechanical piping} \end{cases} \quad (9.26)$$

② Contact scour and contact pop-off

For two-layered soils, where their coefficients of uniformity C_U are all smaller than or equal to 10, contact scour will not occur if Eq. (9.27) is met

$$\frac{D_{10}}{d_{10}} \leq 10 \quad (9.27)$$

where D_{10} and d_{10} = the grain sizes (mm) of the filter material and the protected (or base) material, respectively, and the weight content percentage is 10 % below these sizes.

Suppose the seeping flow is upright, the contact pop-off will not occur if the following conditions are met:

- Coefficient of uniformity C_U is smaller than or equal to 5, and

$$\frac{D_{15}}{d_{85}} \leq 5 \quad (9.28a)$$

where D_{15} = grain size for the filter material (mm), the weight content percentage is 15 % below this size; d_{85} = grain size for the protected (or base) material (mm), the weight content percentage is 85 % below this size.

- Coefficient of uniformity C_U is smaller than or equal to 10, and

$$\frac{D_{20}}{d_{70}} \leq 7 \quad (9.28b)$$

where D_{20} = grain size for the filter material (mm), the weight content percentage is 20 % below this size; d_{70} = grain size for the protected (or base) material (mm), the weight content percentage is 70 % below this size.

(b) Critical seepage gradient

For pop-off failure,

$$J_{cr} = (G_s - 1)(1 - n) \quad (9.29)$$

where J_{cr} = critical seepage gradient; G_s = density ratio of soil grain to water; n = porosity, %.

For mechanical piping or transition,

$$J_{cr} = 2.2(G_s - 1)(1 - n)^2 \frac{d_5}{d_{20}} \quad (9.30)$$

where d_5 , d_{20} = the grain sizes of the soil, respectively, and the weight content percentage is 5 and 20 % below these sizes, mm.

Critical seepage gradient for mechanical piping also may be computed by

$$J_{cr} = \frac{42d_3}{\sqrt{\frac{k}{n^3}}} \quad (9.31)$$

where k = permeability coefficient, cm/s; d_3 = grain sizes for the soil, and the weight content percentage is 3 % below this size, mm.

(c) Allowable seepage gradient for non-cohesive soil

Allowable seepage gradient for non-cohesive soil is obtained by $[J] = \frac{J_{cr}}{K}$ where J_{cr} is the critical seepage gradient and $K = 1.5-2.0$ is the safety factor.

If there are no adequate experimental data concerning J_{cr} , the allowable seepage gradient may be referred to the corresponding design codes or handbooks. The allowable seepage gradient for soils is usually ranged between 3–4 for light loam, 4–6 for loam, and 6–8 for clay.

3. Engineering countermeasures for seepage failures

Pertain the dam safety, the following countermeasures may be employed to reduce seepage gradient, and/or to raise seepage failure resistance.

- Protective measures. Grouting, cut-off trenches, impervious blankets, drainage blankets and horizontal drains, chimney drains, relief wells and toe drains, weighted and graded filters are selectively installed to control and to safely discharge seeping flow as well as to reduce seepage forces from endangering the stability of the downstream slope;
- Filters and transition zones. They are obligately installed to prevent soil particles from moving and clogging drains or resulting in piping (Sherard and Dunnigan 1984, 1985, 1989);
- Contacts of seepage control devices with the foundation, abutments, embedded structures, etc., are carefully designed to prevent the occurrence of contact piping and scouring; and
- Compaction requirements, seepage collars, placement of special materials, etc., for preventing the internal erosion at the contact interface with concrete structures, are clearly specified.

If seepage collars are installed, special attention should be called at compaction requirements around them. The use of seepage collars is generally not recommended in new construction.

For existing embankments, all records concerning foundation configuration, treatment and grouting at the contact between the impervious core and foundation, seepage inspection during the existence of the structure should be reviewed with regard to significant trends or abnormal changes. The causes of any abnormalities should be investigated comprehensively and thoroughly.

9.4 Stability Analysis for Embankment Dams

Stability analysis for embankment dams is compulsorily conducted for the purposes of profile design and safety calibration, in which the following four typical situations are normally concerned for:

- ① Analysis of the up- and downstream slopes immediately after the end of the construction;
- ② Analysis of the upstream slope at the first filling of the reservoir, when the water level is at about half of the normal storage level;
- ③ Analysis of the upstream slope during a rapid drawdown of the reservoir water; and
- ④ Analysis of the up- and downstream slopes when earthquake takes place under the action of full or intermediate reservoir water level.

In general, two categories of stability analyses are performed with respect to the situations under consideration. One is the total stress analysis which is applicable to the situations ① and ②; another is the effective stress analysis which is applicable to the situations ③ and ④.

9.4.1 Strength Properties of Soil

The strength and stiffness properties of soils can be derived from the relationship between normal and shear stresses as well as strains including changes in volume and distortion, as have been elucidated in the Chap. 3 of this book.

The strength of soils is customarily determined by the maximum deviator stress that the soil can carry at the point when progressively increasing deformations onset. The stiffness of soils is defined by the ratio of stress to strain.

This stress–strain relation of soils is generally nonlinear, non-elastic, and time-dependent. As a three-phase system comprising solid (i.e., particles), water, and air, the following properties may be characterized (Craig 2004):

- Tensile stresses cannot exist;
- The stiffness and strength continuously increase when subjected to isotropic compression;
- The stiffness decreases with increasing distortion and this finally becomes zero;
- Dilatancy may occur especially in sandy soils, this means that distortion leads to changes in volume, i.e., loose sand may become denser, and dense sand may become looser;
- Settlements are often time-dependent. Clays and peats, in particular, show creep phenomena mostly referred to the secular or secondary effect. The water present in saturated soils is often the main cause of the time-dependent behavior (consolidation); and

- The behavior of soils is irreversible. In a stress cycle of loading–unloading–reloading, permanent deformation manifests as a result of changes in their granular structure. When reloaded, the soil will exhibit a higher stiffness than during the first loading phase.

The aforementioned soil properties are expressed in the dam design, either separately or in combination, by the shearing strength and the compressibility. In accordance with the principle that the shear stress in a soil can be resisted only by the skeleton of solid particles, shear strength is usually expressed as a function of effective normal stress at failure (σ')

$$\tau_f = c' + \sigma' \tan \phi' \quad (9.32)$$

where c' and ϕ' = shear strength parameters corresponding to effective stress.

9.4.2 Stability Analysis Methods and Allowable Safety Factor

For the embankment dams of cohesive soils, the limit equilibrium analysis is ordinarily implemented using the “slice method” initiated by the Swedish scholars (Bell 1968; Bishop 1955; Bishop and Morgenstern 1960; Fellenius 1927, 1936; Janbu 1954, 1973; Morgenstern and Price 1965; Nonveiller 1965; Petterson 1916, 1955; Spencer 1967, 1973; Sarma 1973; Sarma and Bhawe 1974; Taylor 1937). The mostly prevalent algorithms with regard to arc or general curvilinear slip surface belong to the class of LEM have been discussed in the Chap. 5 of this book.

Sliding along linear or bilinear slip surface occurs frequently in non-cohesive dam slopes such as the up- and downstream slopes of central core embankments, the downstream slope, the protective layer of inclined core, and the inclined core itself. Figure 9.11 shows one of such slip mode, in which (ADC) is a bi-linear slip surface, an artificial inter-slice surface (DE) divides the sliding body into two slices (wedges) (BCED) and (ABD). The direction of inter-slice force P should be stipulated before the analysis. SL274-2001 “Design code for rolled earth–rockfill dams” gives two selective assumptions with respect to the direction of P :

- ① P is horizontal; and
- ② P is at the averaged direction of the upstream slope and the slip surface.

The passive reaction or active reaction (residual thrust) algorithm takes the first (ABCD) or the last (EFG) slice (wedge) to represent the safety of the whole dam slope, which would lead to unreasonable results in some cases. Under such circumstances, the equal safety factor algorithm may be alternatively employed to calculate the force P and corresponding safety factor K , which has been discussed in the deep-seated stability issues with regard to gravity dam foundation in Chap. 7 of this book.

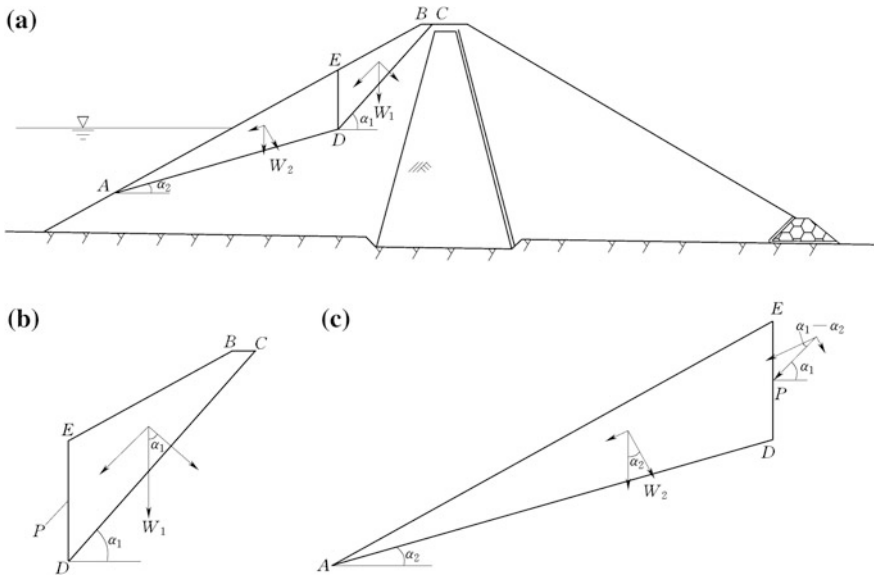


Fig. 9.11 Diagram to the stability analysis for bilinear slip surface problem

Where the foundation contains weak layers, it is necessary to find the most possible portion of the slip surface which would cut through the foundation (Fig. 9.12). For such composite slip surface, the general slice method (Vide Chap. 5) is usually employed.

1. Loads and load combinations

(a) Loads

The load computation for self-weight, steady seepage pressure, earthquake inertia force, etc., has been addressed in Chap. 5. In the following, the issue of excess pore water pressure is particularly discussed.

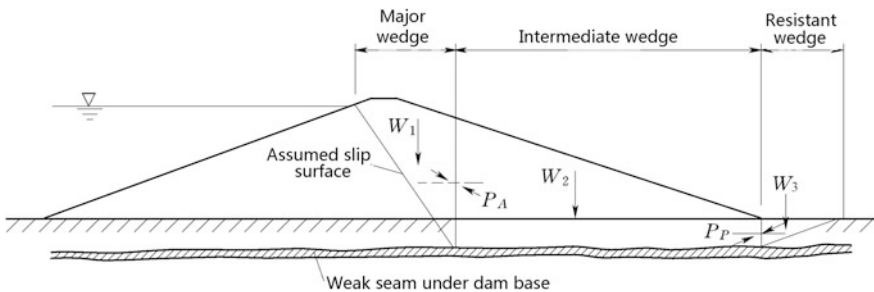


Fig. 9.12 Diagram to the stability analysis for composite slip surface problem

The importance of the forces transmitted through the soil skeleton from particle to particle was recognized in 1923 when Terzaghi presented the principle of effective stress, an intuitive relationship based on experimental data. The principle applies only to fully saturated soils and relates the following three stresses:

- The total normal stress (σ) on a plane within the soil mass, being the force per unit area transmitted in a normal direction across the plane, imagining the soil to be a solid (single-phase) material;
- The pore water pressure (u), being the pressure of the water filling the void space between the solid particles; and
- The effective stress (σ'), representing the stress transmitted through the soil skeleton only, is a force that keeps a collection of particles.

Pore water pressures are resulted from the seepage flow in below the phreatic level (say also groundwater). Usually, the vertical pore water pressure distribution in aquifers can be assumed to be close to hydrostatic. However, consider the case of a fully saturated soil subject to an increase in normal stress by earthfill construction or external loading such as earthquake shaking, volume change will give rise to excess pore pressure. When the total normal stress is increased, the solid particles immediately try to take up new positions closer together. However, if water is incompressible and the soil is laterally confined, no such particle rearrangement, and therefore no increase in the inter-particle forces, is possible unless some of the pore water can escape. Since the pore water is resisting the particle rearrangement, the excess pore water pressure is built up above the static value immediately the increase in total stress takes place. The increase in pore water pressure will be equal to the increase in total normal stress, i.e., the increase in total normal stress is carried entirely by the excess pore water. It creates a pressure gradient, resulting in a transient flow of pore water toward a free-draining boundary of the soil stratum. This flow or drainage will continue until the pore water pressure again becomes equal to the value governed by the position of the groundwater table.

Apart from the actions of earthfill construction and earthquake shaking, fast reservoir drawdown may also give rise to excess pore water pressure. If an embankment dam has been subjected to a prolonged high pool, the soil below the phreatic surface is in a completely saturated state and is fully consolidated under the weight of the overlying soil. Subsequently, when the reservoir pool is drawn down faster leaving no sufficient escaping time for pore water, excess pore water pressures develop.

Pore water pressure reduces the effective stress that keeps a collection of particles rigid to produce friction strength component in the Mohr–Coulomb strength criterion; therefore, it is adverse for dam stability. If effective stress principle is applied in the dam stability analysis, the pore water pressure distribution should be computed, which are related to the soil characteristics, water content, filling speed, and draining condition within the dam. Particularly, the excess pore pressure has complicated spatio-temporal distribution, which is usually only estimated by approximate methods.

Under the circumstances of fast earthfill construction, earthquake shaking, and reservoir pool drawdown, if the permeability coefficient of clay is fairly small, e.g., $k \leq 10^{-6}$ cm/s, it is reasonable to assume that the excess pressure u will be dispersed slowly, which may be estimated as identical to the initial value u_0 . Otherwise, the evolution of u_0 should be studied. The initial pore water pressure u_0 is the function of the volumetric weight and the height of the filled earth above the point concerned

$$u_0 = B\gamma_s h \quad (9.33)$$

where γ_s = volumetric weight of the earth- or rockfilling; h = height of the earth- or rockfilling; B = coefficient of initial pore water pressure tested by triaxial facilities, usually $B \leq 30\text{--}40\%$ where the water content approaching the plastic limit.

The pore pressure dispersion process, if necessarily required in the deformation or stability analysis, may be evaluated by numerical analysis based on unsteady seepage theory (Ouria et al. 2007).

After a reservoir pool has been maintained at a particular level (e.g., normal storage level) for a sufficient duration of time, steady seepage develops by establishing a steady phreatic line through the embankment. The seepage forces related to the steady-state condition exert in the direction of downstream, which may be critical for downstream slope stability. The seepage forces due to steady seepage can be computed by the method described in Chaps. 4 and 5.

(b) Load combinations

See Sect. 9.2.

2. Allowable safety factor

The factor of safety provides a margin to safeguard ultimate stability, to avoid unacceptable deformations, and to bridge over the uncertainties associated with the soil properties or the computation methods. In selecting the allowable safety factor which is a minimum acceptable value dependent upon the degree of confidence in the engineering data available, an evaluation should be carried out for both the degree of conservatism with which assumptions were made in choosing soil strength parameters and pore water pressures, and the influence of the assumptions postulated in the analysis method. It should be emphasized that in selecting the allowable safety factor, the consequences of a failure with respect to human life, property damage, and impairment of project functions are all important considerations.

Factors influencing the selection of minimum factor of safety are specified as follows:

- Reliability of laboratory testing data with regard to shear strength;
- Embankment height;
- Storage capacity;
- Thoroughness of investigations;
- Construction quality;

Table 9.2 Allowable stability safety factor of dam slope (Sweden arc method, without inter-slice force)

Load combination	Grade of embankment dam			
	1	2	3	4, 5
Basic (usual)	1.3	1.25	1.2	1.15
Special I(unusual)	1.2	1.15	1.1	1.05
Special II(extreme)	1.1	1.05	1.05	1.05

- Judgment based on past experience;
- Design conditions being analyzed; and
- Predictions of pore water pressures used in effective stress analysis.

There are two design specification systems available in China, each has stipulated minimum factor of safety for the slope stability of embankment dam.

(a) DL/T5395-2007 “Design specification for rolled earth–rockfill dams”

For Sweden arc method neglects the side (inter-slice) forces, the allowable safety factor is listed in Table 9.2.

For embankment dams of grade 1 and 2, high dams, and dams under complex conditions, it is stipulated that the simplified Bishop’s method or the other more rigorous methods should be employed, and the corresponding allowable safety factor for the slope stability of embankment dam is listed in Table 9.3.

In addition, the DL/T5395-2007 also recommended partial coefficient design method and corresponding coefficients.

(b) SL274-2001 “Design specification for rolled earth–rockfill dams”

For homogenous dams, thick sloping core and central core dams, the simplified Bishop’s method is recommended; for any type of embankment dams with weak seams in foundation, as well as thin sloping core and central core dams, the Morgenstern–Price method is recommended. The corresponding allowable safety factor for the slope stability of embankment dam is identical to that of Table 9.3.

For the stability analysis of dam slopes with non-cohesive soil, linear, bilinear, or multi-linear slip surfaces are usually postulated. If the direction of inter-slice forces between wedges are assumed parallel to the averaged sloping of the slope face and slip surface, the corresponding allowable safety factor is identical to in Table 9.3; if the direction of inter-slice forces between wedges are assumed horizontal, the corresponding allowable safety factor for grade 1 dam is 1.30 under the basic load combinations and is reduced by 8 % of that in Table 9.3 or observes Table 9.2 directly under other load combinations.

Table 9.3 Allowable stability safety factor of dam slope (simplified Bishop’s method or the other more rigorous method, with inter-slice force)

Load combination	Grade of embankment dam			
	1	2	3	4, 5
Basic (usual)	1.5	1.35	1.3	1.25
Special I (unusual)	1.3	1.25	1.2	1.15
Special II (extreme)	1.2	1.15	1.15	1.10

9.4.3 Test and Selection of Shear Strength Parameters

Generally, the shear strength parameters used in stability analysis are determined from laboratory or in situ testing procedures on the specimens which are compacted to the density in the attempt to duplicate the various loading conditions to which the embankment is expected to be subjected (Brinkgreve 2005; Duncan and Wright 2005; Leps 1970; Terzaghi et al. 1996). Since the shear tests are expensive and time-consuming, testing programs are generally limited to representative foundation and borrow materials. Samples to be tested should be selected only after careful analysis of boring logs, including index property determinations. Tests corresponding to the drainage conditions are stipulated in the SL274-2001 “Design code for rolled earth–rockfill dams” and the DL/T5395-2007 “Design specification for rolled earth–rockfill dams.”

1. Shear strength of cohesive soil

The following three representative triaxial tests may be conducted to obtain the shear strength parameters.

- ① Unconsolidated–undrained (UU) or Q tests in which no initial consolidation is allowed under the confining pressure and the water content is kept constant during shear. The Q (UU) test is performed on the specimens of impervious materials under the simulated loading conditions expected to occur during the construction of embankments. Usually, the test is directed to obtain the total stress parameters c_u and ϕ_u for the unsaturated soil in an approximation of at end of the construction.
- ② Consolidated–undrained (CU) or R tests in which consolidation is allowed under initial stress conditions, but the water content is kept constant in the following application of stress increments. The R (CU) tests apply to conditions in which impervious or semi-pervious soils that have been fully consolidated under one set of stresses are subjected to a stress change without time for consolidation to take place (soil is sheared without allowing dissipation of pore pressures). Pore water pressure measurements are made during R test. This test may be used to obtain total stress parameters c_{cu} and ϕ_{cu} , as well as effective stress parameters c' and ϕ' .
- ③ Consolidated–drained (CD) or S tests in which consolidation is permitted under the initial stress and each subsequent increment of stress. The shear strength resulting from a S (CD) test is obtained by fully consolidating the soil specimen under the applied confining stress and, when drainage is complete, applying incremental shear stresses slowly enough to allow full drainage to take place during each loading increment. In practices, S parameters c_d and ϕ_d may be looked at as identical to the effective stress parameters c' and ϕ' .

Direct shear facilities also may be applied to perform S tests, R tests, and Q tests.

2. Shear strength of non-cohesive soil

Permeability of non-cohesive soil is normally much higher, and its strength depends mainly on the effective normal stress together with friction angle, and the latter is customarily obtained from drained test (S). For the soil under and above phreatic line, the shear strength parameters are selected with respect to saturated and wet situations, respectively. Attention should be drawn to the case of sudden reservoir drawdown, for the soil between long-term steady and temporary varied phreatic line, the shear strength parameters with regard to saturated situation are adopted conservatively.

3. Selection of shear strength for analysis

An embankment may be subjected to various loading conditions during its life circle, ranging from construction to full pool operation until decommission. Apart from the soil characteristics and test sampling process, the strength parameters c and ϕ are also related to the loading conditions for which an embankment must be analyzed. Engineering experiences show that the difference among different tested parameters may be as large as 50 % for an embankment dam using a specific analysis method. This indicates that the reliability of stability analysis is mainly dependent on the correct selection of shear strength parameters related to the loading conditions.

In general, there are two types of stress analysis employed in the evaluation of existing and proposed embankments, i.e., the total stress analysis and the effective stress analysis. The former is used in the design of embankments for loading conditions during construction, rapid drawdown, and earthquake. The latter is applicable only in cases where the soils behave drained and piezometer data are available. The cases that may be handled using the effective stress method are partial pool and steady seepage.

(a) Loading conditions during and at the end of the construction

For homogeneous dams or for dam zones constructed by impervious materials, pore water pressures will be built up during the construction under its own weight and due to the inability to drain rapidly, and at the end of the construction when they would be still undergoing consolidation.

The shear strength applicable to the impervious dam or the zones within the dam under the construction loading conditions is determined by the Q test conducted at field moisture contents and at field confining stresses. The type of stress analysis that applies to these loading conditions is the total stress analysis using c_u and ϕ_u . Because of the difficulty with estimating pore water pressures within the embankment during this stage of loading, an effective stress analysis using c' and ϕ' or c_d and ϕ_d is generally not feasible. The effective stress analysis may, however, be conducted using the pore pressure responses from analysis, field monitoring, or engineering analogue in previously constructed dams with similar materials, construction methods and schedules. The analysis with respect to the end of the construction using Q shear strengths in the impervious zone represents a lower limit of

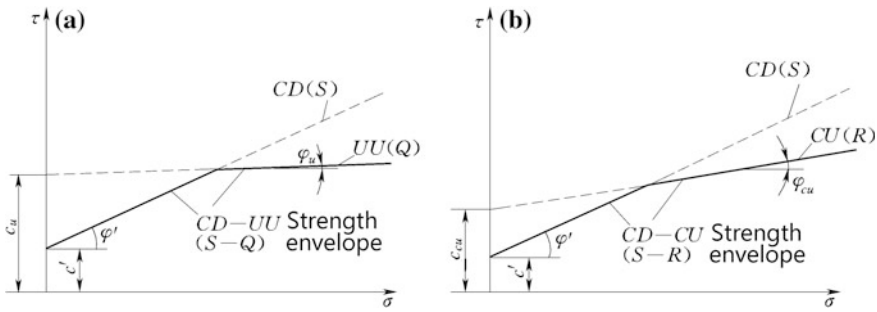


Fig. 9.13 Strength envelope of cohesive soil. **a** CD-UU strength envelope; **b** CD-CU strength envelope

stability since consolidation is progressing during the course of construction. To be on the safe side, when conducting a construction period analysis, the shear strength based on the minimum envelope of the combined CD(S) and UU(Q) may be employed (Fig. 9.13a).

For pervious zones of non-cohesive soil in the embankment where drainage can occur rapidly, S strengths should be used in the analysis.

If there are any serious problems concerning stability during the construction, installation of piezometers is highly advisable for a reliable evaluation of the stability status during the construction.

(b) Sudden drawdown loading condition

The shear strength parameters needed for the analysis under this loading condition are obtained from the R test. An expression is determined for relating consolidation pressure to the R shear strength. Laboratory tests are performed under consolidated–undrained conditions, in which the samples are consolidated under stresses corresponding to the conditions immediately preceding the drawdown. This type of computation belongs to the class of total stress analysis.

If an effective stress analysis is conducted, one method of measuring the effective stress parameters is to perform R tests on the soil samples with the measurement of pore pressure. The accuracy of this type of analysis rests on how well the pore water pressures may be estimated. If tests are conducted on undisturbed samples retrieved from an existing embankment, data of pore pressure observations in the field may be employed in determining pore pressure coefficients to be used in the testing procedure. To be on the safe side, when conducting a sudden drawdown analysis the shear strength based on the minimum envelope of the combined CU(R) and CD(S) may be adopted (Fig. 9.13b). The unit weight of the soil to be introduced in analyzing the “before drawdown” condition will be the moist weight above and buoyant weight below the phreatic line, respectively. In analyzing the “after drawdown” condition, moist unit weight will be used for the zone above the original phreatic line, whereas saturated unit weight will be used

within the drawdown zone, and buoyant weight will be used below the level after the drawdown.

Shear strengths of free-draining materials where dissipation of pore water pressure can proceed instantaneously as the reservoir pool is drawn down will be based on the *S* test.

(c) Steady seepage loading condition

The stability condition under full reservoir is always analyzed using the effective stress method and the pore water pressures are assumed to be those governed by gravity flow through the embankment, which can be well estimated by the steady-state seepage theory as described in Chaps. 4 and 5 of this book. Where sufficient instrumentation is available, piezometer levels in both the embankment and foundation can be reviewed and phreatic line can be developed accordingly.

The same information applies to the partial pool loading condition, where the upstream slope is analyzed for various pool elevations to determine which pool elevation creates the lowest safety factor of stability against sliding.

The Chinese design codes stipulate that:

- For impervious and high-plasticity soils, for the purpose of safety, the shear strength corresponding to a midway strength envelope between the *R* and *S* strength envelopes is employed where the *S* strength is greater than the *R* strength. On the contrary, the *S* envelope is used when the *S* strength is smaller than the *R* strength; and
- The shear strength of freely draining non-cohesive soils should be represented by the *S* test. Unit weights to be used in the analysis will be the moist weight above the phreatic line and buoyant weight below this line.

9.5 Stress and Deformation Analysis for Embankment Dams

9.5.1 Consolidation and Settlement Analysis

It is well known that a soil under loading does not assume an instantaneous deflection, instead, it settles gradually at a variable rate. Such settlement is particularly apparent in saturated clays, which is due to commonly known excess pore water pressure-related soil consolidation.

Factors related to the excess pore water pressures in embankments and their foundation during construction comprise soil water content, weight of overlying fill, length of drainage path, rate of construction (including stoppages), characteristics of the core and other fill materials, drainage features such as inclined and horizontal drainage layers and pervious shells.

The shear strength of a soil is affected by its consolidation characteristics. If a foundation consolidates slowly, a substantial portion of the applied load will be carried by the pore water which has no shear strength, and the available shearing resistance is limited to the in situ shear strength as determined by undrained Q tests. Where the foundation shearing resistance is low, it may be necessary to flatten slopes, to slow down the speed of construction, or to accelerate consolidation by installing drainage layers or wick drains.

Since excess pore water pressure developed in pervious materials dissipates much more rapidly than those in impervious soils, normally their effect on the stability is not apparent. However, excess pore pressures may temporarily build up, especially under earthquake shaking, and effective stresses contributing to shearing resistance may be reduced to very low levels. In the liquefaction of sand masses, the shearing resistance may even temporarily drop down to a small fraction of its normal value.

Dam and foundation settlements should take into account of consolidation behavior of soils. For example, overfilling of the embankment and core is required to ensure a dependable freeboard.

1. Consolidation analysis

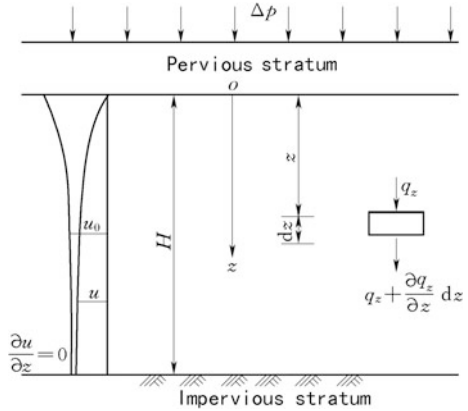
Consolidation tests are performed in the laboratory on undisturbed samples of the embankment and foundation materials. The test consists of loading a laterally confined sample compressed between two porous plates. The loads exerted on the sample should approximate the stresses that will be imposed by the embankment/foundation. The test results are plotted to show the degree of consolidation after the application of the load.

A simple mechanism to explain consolidation phenomenon was first proposed by Terzaghi et al. (1996). The assumptions made in the Terzaghi's theory of one-dimensional consolidation are as follows:

- The soil is homogeneous and elastic;
- Strains are small;
- The soil is fully saturated, and the Darcy's law is valid at all hydraulic gradients, and the coefficient of permeability and the coefficient of volume compressibility remain constant throughout the consolidation process;
- The solid particles and pore water are incompressible; and
- Both the compression and flow are one-dimensional (vertical); the load and stress are sustained along the ongoing of time (Fig. 9.14).

By the above assumptions, any change in the volume $\frac{\partial \varepsilon_v}{\partial t} dz$ is equal to the flow rate through the element's surface $\frac{\partial q_z}{\partial z} dz$, i.e., $\frac{\partial \varepsilon_v}{\partial t} = \frac{\partial q_z}{\partial z}$, in which ε_v = volume change and q_z = unit surface flow discharge.

Fig. 9.14 One-dimensional consolidation problem



According to the Darcy’s law,

$$q_z = - \frac{k}{\gamma_w} \frac{\partial u}{\partial z} \tag{9.34}$$

where k = coefficient of permeability, m/s; γ_w = volumetric weight of water, kN/m³; u = pore pressure, kN/m².

We have

$$\begin{cases} \frac{\partial \varepsilon_v}{\partial t} = \frac{\partial \varepsilon_z}{\partial t} = -m_v \frac{\partial u}{\partial t} \\ m_v = \frac{a_v}{1+e} \\ a_v = \frac{\partial u}{\partial \sigma} \approx \frac{e_1 - e_2}{\sigma_2 - \sigma_1} \end{cases} \tag{9.35}$$

where ε_z = vertical normal strain; m_v = coefficient of volume compressibility, m²/MN; a_v = coefficient of compressibility (its value for a particular soil is actually not constant but depends on the stress range over which it is calculated); e = void ratio.

Let $C_v = \frac{k}{\gamma_w m_v}$, the differential equation of consolidation is expressed as follows:

$$\frac{\partial u}{\partial t} = C_v \frac{\partial^2 u}{\partial z^2} \tag{9.36}$$

$$C_v = \frac{k(1+e)}{a_v \gamma_w} \tag{9.37}$$

where C_v = coefficient of consolidation, m²/year.

Since k and m_v are assumed as constants, C_v is constant during the consolidation.

The total stress increment is assumed to be applied instantaneously. Therefore, at $t = 0$ the load increment $\Delta\sigma$ will be carried entirely by the pore water pressure u_0 . Since the permeability of the soil adjacent to each boundary being very high

compared to that of the clay, the upper and lower boundaries of the clay layer are assumed to be free-draining. Thus, the initial condition and boundary conditions at any time after the application of load increment are

$$\begin{cases} u|_{t=0} = u_0 \\ u|_{z=0} = 0 \\ \frac{\partial u}{\partial z}|_{z=H} = 0 \end{cases} \tag{9.38}$$

where u_0 = initial pore water pressure, kN/m^2 ; and H = longest depth of the drainage path, m.

By the method of variable separation, the solution of Eq. (9.36) gives

$$u(z, t) = \sum_{m=1}^{\infty} \left(\frac{2}{H} \int_0^H u_0 \sin \frac{Mz}{H} dz \right) \sin \frac{Mz}{H} e^{-M^2 T_u} \tag{9.39}$$

where $M = \frac{(2m_v - 1)\pi}{2}$; $T_u = \frac{C_v t}{H^2}$, the dimensionless time factor.

The value of C_v has dominant influence on the accuracy of consolidation computation. For a particular pressure increment in the oedometer test, it can be determined by comparing the characteristics of the experimental and theoretic consolidation curves, i.e., the procedure being referred to as curve fitting. The characteristics of the curves are brought out clearly if time is plotted to a square root or a logarithmic scale. It should be noted that once the value of C_v has been determined, the coefficient of permeability k can be calculated from Eq. (9.37). Therefore, the oedometer test is a useful method for obtaining the permeability k of clay, too.

The Terzaghi's theory is retrained to the one-dimensional problem of a soil column under a constant load. From the viewpoint of mathematical physics, Biot (1941) made the extension to the three-dimensional problem, which valid for any arbitrary loads variable with time. The Biot's theory leads to more rigorous results, which may be used to evaluate the process of coupled elastic deformation/seepage and to obtain the consolidation process along with the dispersion of excess pore water pressure. However, its computation requires larger computer capacity and time.

For cohesive soils such as clays, rheologic characteristics of the soil skeleton also should be considered in the consolidation computation.

2. Settlement analysis

Only a very small fraction of the embankment settlement may be attributable to the elastic deformation of soil grains. The principal components of the vertical settlement are due to particle rolling and sliding, which produce a change in the void ratio and grain crushing. As a consequence, if the applied stress is removed, merely little part of the settlement may be recovered.

Settlements of embankment may be divided into three phases as initial settlement, consolidation settlement, and secondary compression settlement. Initial settlement occurs as soon as the self-weight exerts. Consolidation settlement is a change in void ratio entirely due to a change in effective stress brought about by the dissipation of excess pore water pressure, with permeability alone governing the time dependency of the process. Secondary compression settlement is thought to be a phenomenon related to the gradual re-adjustment of the clay particles into a more stable configuration following the structural disturbance caused by the decrease in void ratio, especially if the clay is laterally confined.

Settlement analysis may provide the final settlement, the settlement at just the completion of construction, and the settlement during construction, and normally takes into account of consolidation factor solely. These results are important in the evaluation of the overfill height for the freeboard calculation of embankment (Schmertmann 1970).

Although the settlement comprises only a very small elastic component, it is convenient to look at the soil as a pseudo-elastic material with “equivalent elastic” parameters to estimate the whole settlement. This is named as the “method of one directional and stratified compression,” which would appear reasonable because a stress change causes a corresponding settlement, and larger stress changes produce larger settlements. In addition, experience indicates that this manner provides satisfactory solution with larger biased result, which is at safe side.

Tasks of settlement computation comprise the following:

- The final settlement using compaction curve under saturation state;
- The settlement just after the completion of construction using compaction curve under unsaturated state; and
- Process of settlement, this is usually only for cohesive soil.

Settlement computation ordinarily employ methods of theoretic (e.g., Terzaghi’s theory and Biot’s theory), numerical (e.g., FEM), or table (chart) look-up.

For sandy soils, settlement manifests immediately after loading, and there are so far no perfectly methods available for the settlement computation. The commonly used Schmertmann method (1970) is based on layer stiffness data or cone tip bearing resistances obtained from a cone penetration test (CPT). The method postulates a simplified triangular strain distribution and calculates the settlement accordingly. A time factor also can be taken into account concerning time-dependent (creep) effects.

9.5.2 Stress and Strain Analysis

Soil is a complicated material with the following features:

- Nonlinearly and non-elasticity. It exhibits nonlinear behavior well below the failure criterion with stress-dependent stiffness;

- Stress–strain curve varies with the confine pressure;
- It undergoes plastic deformation and is inconsistent in dilatancy. For normal consolidated cohesive soil and loosen sand, triaxial tests show that at the loading state, the volume is shrinking. For over-consolidated cohesive soil and tight sand, triaxial tests show that at the initial stage of loading, the volume is shrinking a bit, then expanding quickly as the increase of loading, which presents dilation behavior;
- Generally, soil behaves differently in primary loading, unloading, and reloading, which is called as stress history and route-dependent;
- It often shows time-dependent characteristics when subjected to stress, such as consolidation and creep; and
- It often shows anisotropic characteristics when subjected to stresses.

The computation methods proposed before the 1960s for the stress and deformation of embankment dams were very simple and crude. After the 1960s, the development of numerical methods (e.g., FEM) has changed the situation greatly.

Nowadays, there are various constitutive models for soils (Brinkgreve 2005; Duncan and Chang 1970; Gens and Potts 1988; Mestat et al. 2004; Qian and Yin 2000; Roscoe 1970; Schofield and Wroth 1968; Ter-Stepanian 1975). The DL/T5395-2007 “Design specification for rolled earth–rockfill dams” and the SL274-2001 “Design code for rolled earth–rockfill dams” stipulate that:

- For embankment dams of grade 1 and 2 or on complex foundation, the finite element method should be used in their stress and strain analysis; and
- Nonlinear elastic constitutive models are recommended, elasto-plastic constitutive models also may also be exercised;

With respect to the coupled analysis between seepage and stress/strain, two methods are recommended in the aforementioned design codes:

- Iterative solution between two independent fields concerning seepage and stress/strain, which is actually an approximate algorithm of decoupling; and
- Simultaneous solution of seepage and stress/strain fields based on the Biot consolidation theory.

9.5.3 Cracking Provisions

Cracking manifests within zones of tensile due to differential settlement, filling of reservoir, and seismic action (Lo and Kaniaru 1990). Since cracking cannot be totally prevented, the design must include provisions to minimize its adverse effects. With regard to their spatial distribution, cracks are of four general types: transverse, horizontal, longitudinal, and shrinkage. Shrinkage cracks are generally shallow and can be easily treated from the surface by removing the cracked material and backfilling.

1. Transverse cracks

Transverse cracking in the impervious core is of primary concern because it creates pathways for concentrated seepage flow through the embankment.

Transverse cracking is resulted from tensile stresses related to differential embankment and/or foundation settlements. Differential settlements may occur at steep abutments, at the junction of closure sections, at the adjoining structures where compaction is difficult, and at the old stream channel or meander filled with compressible soils.

2. Horizontal cracks

Horizontal cracking in the impervious core may occur when the core material is much more compressible than the adjacent transition or shell materials so that the core material tends to arch across the less compressible adjacent zones. Such “arch effect” is responsible for the reduction of the vertical stress in the core and a separation out of the lower portion of the core, which in turn, give rise to horizontal cracking in the core. Arching also may take place if the core rests on highly compressible foundation materials. Horizontal cracking is not visible from the outside and may damage the dam seriously before it is detected.

3. Longitudinal cracks

Longitudinal cracking may be resulted from the settlement of upstream transition zones or shell due to the initial saturation by the reservoir impounding or due to the rapid drawdown of reservoir. It also may be resulted from the differential settlement between adjacent materials or due to seismic actions. Longitudinal cracks do not provide continuous seepage pathways across the dam core, as transverse and horizontal cracks do, and therefore pose no direct threat with regard to piping through the embankment. However, longitudinal cracks may reduce the overall embankment stability leading to slope failure, particularly if the cracks are filled with water.

4. Countermeasures

- Since the prevention of cracks cannot be secured, an adequate downstream filter must be provided as the primary defense frontier against the concentrated seepage flow through the dam core;
- The susceptibility to cracking can be reduced by adequately shaping the foundation and structural interfaces to reduce differential settlements;
- Densely compacting the upstream shell to reduce the settlement attributable to saturation collapse;
- Compacting core materials at water contents sufficiently high so that stress-strain behavior is at plastic side, i.e., low deformation modulus and shear strength, so that cracks cannot remain opening. However, in doing so the adverse side effects of higher pore pressure and lower stability against sliding must be avoided; and
- Staged construction to control the settlement effects of the foundation and the lower embankment portions.

9.6 Basic Profile of Embankment Dams

The basic profile of embankment dams may be designed preliminary according to engineering experiences related to the height, grade, material characteristics available, foundation characteristics, construction, and operation conditions of the dam. The seepage and stability analyses are then carried out to check and to revise the profile until an optimal design is achieved.

9.6.1 Crest of Dam

The elevation of dam crest must be sufficient to prevent overtopping due to wind setup, wave actions, or earthquake effects. The height of dam crest over the design static water level is named as freeboard and determined by formula (Fig. 9.15):

$$d = R + h_z + A \tag{9.40}$$

where R = wave run-up (See Chap. 4), m; h_z = height of wave center line, m; A = safe addition (Table 9.4), m.

The crest height should be the maximum considering basic (normal storage level, design flood level) and special (check flood level, normal storage level + earthquake) conditions. Where there is a reliable parapet wall on the dam crest, the crest height calculated by Eq. (9.40) may look at as to the top of the

Table 9.4 Safe addition A (m) (SL274-2001 “Design code for rolled earth-rockfill dams”)

Dam grade		1	2	3	4, 5
Basic combination		1.5	1.0	0.7	0.5
Special combination	Mountainous and hilly region	0.7	0.5	0.4	0.3
	Plain and coastal region	1.0	0.7	0.5	0.3

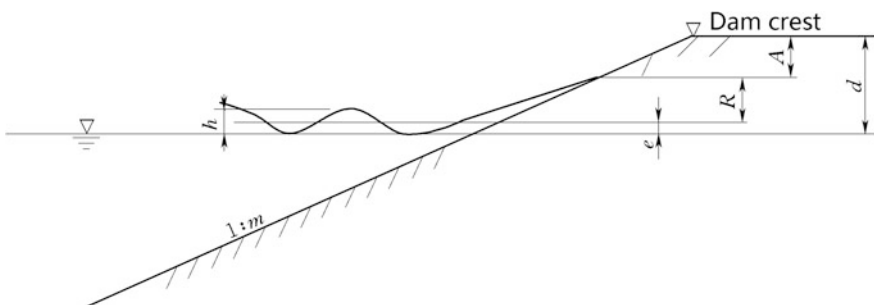


Fig. 9.15 Diagram to the computation of dam crest freeboard

parapet wall. Under such circumstances, however, the minimum freeboard with respect to the dam crest should be not smaller than 0.5 m under the basic conditions and be higher than the maximum static level under the special conditions.

The crest of dam should generally additionally be overfilled to allow for subsequent loss in height due to the consolidation of the embankment and/or foundation, which is around 0.2–0.4 % of the dam height for well-constructed dam.

The crest of dam should also additionally be overfilled to allow for subsequent wave run-up due to earthquake. The DL5073-2000 “Specifications for seismic design of hydraulic structures” stipulates that such additional seismic wave run-up is 0.5–1.5 m, depending on the intensity of design earthquake. In case the intensity is equal to or over 8, the subsequent loss in height due to the additional consolidation of embankment and/or foundation should be studied particularly.

9.6.2 Width of Crest

The crest width of an embankment dam within conventional limits has little effect on the dam stability and is governed by whatever functional purposes the dam crest must serve. Depending upon the height of the dam, the minimum crest width should be 10–15 m for high dams and 5–10 m for medium to low dams. According to the SL274-2001 “Design code for rolled earth–rockfill dams” and the DL/T5395-2007 “Design specification for rolled earth–rockfill dams,” the minimum crest width also may be estimated by

$$B = \sqrt{H} \quad (9.41)$$

where H = dam height, m.

The width of crest should meet the requirements for the layout of central core or sloping core and the filters. If the dam is compacted of clayed soil and located at chilly area, the crest is covered with protective layers of sandy or gravel materials.

The embankment zoning near the top is sometimes simplified to meet the requirements for the accommodation of hauling and compaction equipments.

Where the dam crest is to accommodate a public highway, road and shoulder width should conform to the corresponding requirements.

9.6.3 Slope of Dam

The slope of dam may vary widely, depending on the factors such as the soil, dam type, dam height, dam grade, construction, and operation and is mainly dictated by the stability against sliding.

Generally, roller compacted embankment dams have steeper slopes than that of hydraulically filled and water dumping, for the latter two have lower shear strengths

and high pore water pressures during construction. Following rules are conventionally observed in the preliminary design of compacted dam slopes:

- Since the upstream slope is saturated under reservoir level and reservoir sudden drawdown may be proceeded, the stability requirements demand an upstream slope more flat than the downstream slope, if the same soil is compacted in up- and downstream dam shells;
- The slopes of homogeneous dam with cohesive soil, or of cohesive dam shell, are more flat than that with non-cohesive soil;
- The upstream slope of sloping core dams is controlled by the lower soil strength of core; therefore, it is more flat than that of central core dam. On the contrary, if an identical soil material is used, the downstream slope of the central core dam is more flat than that of sloping core dam;
- Dam slopes with cohesive soils usually vary from steep to flat at an interval of 0.25 or 0.5 from high altitude to low altitude, by dividing the height into several benches of 10–30 m in elevation, with or without berms; and
- Homogeneous dams made of silt, sand, and light loam have larger permeability and higher phreatic line, therefore their downstream slopes are usually more flat.

For the preliminary estimation of dam slopes, the following data from engineering experiences may be referred to

- Clayey homogeneous dams or dam shells. The upstream slope is varied according to 1(V):2.0(H), 2.5, 3.25, and 3.5. The downstream slope is varied according to 1:2.0, 2.75, and 3.25;
- Soil central core dam. If the downstream dam shell is compacted by gravel, the slope is commonly 1:1.5–1:2.5. It will be 1:2.0–1:3.0 where the downstream shell is filled with soil. If the upstream dam shell is compacted by gravel, the slope is ordinarily 1:1.7–1:2.7. It will be 1:2.5–1:3.5 where the downstream shell is filled with soil;
- Soil-sloping core dams. The downstream dam shell slope is similar to that of central core dams but may be a bit of steeper, whereas the upstream dam shell slope is about 0.5 more flat than that of central core dams; and
- Surface diaphragm dams. If the dam shell is well roller compacted, the upstream slope may vary within 1:1.4–1:1.7. The downstream slope is 1:1.3–1:1.4 for high-quality rockfill shells. More flat downstream slopes such as 1:1.5–1:1.6 are sometimes adopted, if the dam shell is composed of gravel sediment or the dam high is over 100 m. Slope of central diaphragm dams may be estimated similarly as foregoing, and the identical up- and downstream slopes may be employed;

Berms spaced at 10–30 m apart along altitude are installed on the downstream slope to house ditches necessary for removing rainfall water. The minimum width of berms is 1.5–2.0 m. Berms on the downstream slope can also be used for the installation of service roads, railroads, pipelines, sometimes even for monitoring, and canals. Berms on upstream slope are provided to make a stop at the end of the revetment.

Berms are usually located at the deflection point of sloping. The arrangement of berms may improve the stability of dam slopes.

Where required excavation or borrow area stripping produces slag materials unsuitable for use in the embankment, slag berms can be installed for upstream slope protection, or to contribute to the stability of upstream and downstream embankment slopes. Care must be taken, however, not to block drainage in the downstream area by placing such slag berms.

9.7 Soil Available and Compaction Standard

9.7.1 General Principles in the Selection of Embankment Materials

The design of embankment materials is intended to determine, on the basis of obtained data, the future properties of these materials after filling them to compose various elements of the dam: volumetric weight, strength and deformation properties, permeability characteristics, etc.

The term “soil” as used herein includes such materials as sands, stones, or other rocks that break down into soil during handling and compaction. Most soils can be used for embankment construction as long as they are insoluble and substantially inorganic.

The use of fine-grained soils with high water contents may give rise to high pore water pressures in the embankment under its own weight. Typical rock flours and clays with liquid limits above 80 should generally be avoided. Some slow-drying impervious soils may be unusable in some climatic areas under anticipated rainfall during construction, where the artificial reduction of moisture content would be impracticable. However, if a fine-grained soil can be brought readily within the range of water contents suitable for compaction and for operation of construction equipment, it may be useful. In other cases of lower water contents, soils may require additional water to approach optimum water content for compaction, by pounding or sprinkling over borrow areas.

As it is generally difficult and expensive to substantially reduce the water content of impervious soils, borrow areas containing impervious soils more than about 2–5 % wet of optimum water content (depending upon their plasticity characteristics) may be impractical to be used in an embankment. However, it depends upon local climatic conditions and the size and layout of the work, and must be assessed for each specific project on an individual basis. The expenditure of using drier materials but requiring a longer haul should be compared with the expenditure of using wetter materials but flatter slopes. Other factors being equal, and a choice being possible, soils having a wide range of grain sizes (well-graded) are preferable to those having relatively uniform particle sizes, since the former ordinarily are stronger, less susceptible to the failures of piping, erosion, and liquefaction, and less

compressible. Cobbles and boulders in soils may add to the cost of construction since stones with maximum dimensions greater than the thickness of the compacted layer must be removed to permit proper compaction. Embankment soils that undergo considerable shrinkage upon drying should be protected by adequate thickness of non-shrinking fine-grained soils to reduce evaporation. Clayey soils should not be backfilled in contact with concrete or masonry structures, except in the impervious zone of an embankment.

Most earth materials suitable for the impervious zone of earthfill dams are also applicable for the impervious zone of rockfill dams. When water loss through seepage must be kept to a minimum (i.e., the reservoir is used mainly for long-term storage), and fine-grained materials are in short supply, the material used in the core should have a low permeability. Where seepage loss is less important, such as in some flood control projects not mainly intended for storage, less impervious materials may be used.

9.7.2 Requirements for Material Design

1. Requirements for materials

- **Impervious.** The permeability coefficient of sloping or central cores should be lower than 1×10^{-5} cm/s, in case of homogeneous dams or lower dams, the limit may be relaxed to 1×10^{-4} m/s;
- **Shear strength.** Stability of a dam is predominant by the shear strength of the dam shell. Since the strength of the sloping core significantly affects the upstream dam slope, higher requirement for its strength is emphasized than that for the central core;
- **Compressibility.** The compressibility should be not too large, to prevent the dam from excessive settlement after the impounding of reservoir;
- **Seepage failure resistance.** The gradation is adequate to keep high seepage failure resistance. The plasticity is adequate, too, to keep high scouring resistance for the unexpected cracks in dam, if any;
- **Moisture content.** To facilitate the soil compaction, the water content is better to near optimum moisture content. Customarily, the moisture content is controlled 0.5–1 % around the optimum moisture content, which makes good compromise between construction requirements on reducing excess pore pressure and on facilitating compaction. The core may be compacted at or a bit of wet of optimum water content, while the outer zones are compacted a bit of dry of optimum content;
- **Particle gradation.** Good and continuous gradation is always desirable. Inhomogeneity coefficient should not be smaller than 5. Since a high clay particle content will lead to poor compaction characteristics and sensitive in moisture content, the content of particles smaller than 0.005 mm should be

lower than 40 % and be better lower than 30 %. The maximum particle should not be in excess 2/3 of the compaction lift (layer);

- Swell and shrinkage. A swelling soil has characteristics of swelling due to additional water being adsorbed and shrinking as it dries out, which will give rise to sliding, cracking, and spalling of the dam. Therefore, it should be limitedly used only for lower dams. The laterite soil has characteristics of high natural moisture content and lower compacted dry volumetric weight, but it has good characteristics of high strength, low permeability, and compressibility. These enable it to be used in the dam construction. However, use of laterites will lead to inconvenience in construction due to their high clay particle content and high natural moisture (usually much higher than the optimum moisture content); and
- Content of soluble salt and organic content. According to the design codes, content of soluble salt should be limited within 3 %. Organic content should be lower than 5 and 2 % for homogeneous dams and core dams, respectively.

2. Requirements for compaction

In order to obtain designed strength and permeability in the field, compaction requirements should be specified in the design phases and placement process is severely controlled in the construction phase. In general, the strength and permeability of compacted soils are related in advance with the dry density using laboratory test data.

Field compaction tests of fill materials is customarily carried out by using compaction rollers such as the tamping (sheep's foot) roller, the rubber-tired roller and the vibration roller. The usefulness of each roller depends on its compaction characteristics and soil types. In general, either a sheep's foot roller or a rubber-tired roller is employed for impervious or semi-impervious materials. For pervious materials such as sand, gravel and rock, rubber-tired or vibration rollers are ordinarily employed.

The surface of the filling lift under compaction likely becomes smooth when a rubber-tired or a vibration roller is employed, particularly where soft rock materials are compacted by a vibration roller or when impervious materials are compacted by a rubber-tired roller. It is readily well known that the formation of such smooth surface is undesirable in the stability of embankment slopes, for it reduces the shear resistance along the surface. For narrow areas adjacent to the abutment valley walls and concrete structures, small compactors such as hand and air tamper are advisable instead of heavy equipment.

Selection of water contents and densities demanded the judgments and experiences to balance the interaction of the many factors involved, such as

- Type and height of dam;
- Borrow area water contents and the extent of artificial drying or wetting that may be practicable;
- Climatic conditions;

- Need to prevent tensile and cracking in the upper portion of the embankment, especially in impervious zones;
- Settlement of compacted materials on reservoir impounding saturation;
- Relative significance on embankment design of Q versus R strengths (i.e., construction versus operating conditions);
- Relative significance on foundation design; and
- Significance on the construction cost of design water contents and densities.

9.7.3 Materials for Anti-seepage Devices

Impervious materials comprise clays, clayey sands, and silty clays. Since the 1960s, more pervious materials such as silts and silty sands or gravels had been exercised in the impervious zone compaction.

1. Cohesive soils

Clay and loam usually exhibit high natural moisture content and poor compaction characteristics, which give rise to difficulties with construction and high expenditure, particular in the southern China. On the other hand, clays have high compressibility and are vulnerable to forming arch effect in central cores. Therefore, pure clays are not suitable for anti-seepage devices.

Apart from clays, laterite soils, swelling soils, dispersive clays, loess, etc., may also be encountered in the embankment construction.

There exists laterite soil of high liquid limit abundantly over the south west area of China, which is weathered from carbonate rocks due to humid and rainy climatic and geologic conditions. The laterite soil possesses unique features such as high natural moisture, inherent large void ratio, and strong structural pattern; therefore, it is difficult to meet the higher requirement for compaction. The dry density of laterite soil is usually ranged within 1.4–1.5 g/cm³. However, the compacted laterite soil has medium to lower compressibility and higher shear strength than common clays, and its permeability coefficient has a magnitude 1–2 orders higher than common clays. In addition, laterite soils will not collapse in water and have high scour resistance. All these advantages make the laterite soil a good material for homogeneous dam and anti-seepage device of zoned dams. Anyway, the high fine cohesive grain content, as well as the higher natural moisture content than the optimum content, will bring about construction inconvenience. Majority of laterite soils are sensitive to dry process, and the property variation due to drying is irreversible. Therefore, cautions should be exercised in the soil sample preparation (“from wet to dry” or “from dry to wet”) for the tests of optimum moisture content, maximum dry density, and shear strength. So far, a large number of embankment dams have been constructed using laterite soils in China, such as the Maojiaping dam (Yunnan province, China, $H = 80.5$ m) completed in 1971.

Expansive soil, also called shrink-swell soil, is a very common cause of dam and foundation problems. Soils with smectite clay minerals, including montmorillonite, have the most dramatic swelling properties. Expansive soils typically contain one or more of these clay minerals: montmorillonite, smectite, bentonite, and illite. Depending upon the supply of moisture in the ground, expansive soils will experience changes in volume of up to 30 % or even more, which will “heave” and can cause lifting of a dam during periods of high moisture. Conversely during periods of falling soil moisture, expansive soils will “collapse” and can result in dam settlement. In either foregoing scenarios, damages can be extensive. In order to determine the potential expansion property, the commonly used expansion indices are free swell index, Atterberg limits (the plastic and liquid limits), swelling pressure, or free swell volume. Mitigation of the adverse effects due to clay expansion and/or shrinkage on structures is one of the major challenges in geotechnical engineering, which comprises:

- In order for expansive soils to cause dam and foundation damages, there must be fluctuations in the moisture contained in the soils. If the moisture content of the soils can be stabilized, expansive problems can often be avoided;
- Tests also show that the confine pressure may restrict the expansion even the soil is watered. As the overburden depth increases, the weight of the overburden soil creates increasing confining pressure. For any particular uniform mass of expansive soil, the expansion resistance is generally greater at a deep place than it is near the surface. Therefore, it is possible to use expansive soils in the central core or the internal portion of homogeneous dams, where the high confine pressure may prevent them from swelling; and
- There are also chemical treatments available for expansive soils which are designed to alter the clay mineralogy and to reduce the expansion potential, of which the treatment with “lime” or calcium oxide are the most traditional. Together with cement and fly ash, lime is referred to as a “calcium-based treatment.”

China have built several homogeneous dams and zoned dams using expansive soils after the treatment. They are all operated normally insofar, except only a few of them manifesting local slip or creep in dam slopes.

Dispersive clays have remarkable physicochemical characteristics that make them potentially highly erodible under even low hydraulic gradients, which attracted the attention of dam engineers after the 1970s. The tendency for dispersive erosion hinges on clay mineralogy and soil water chemistry. The principal difference between dispersive clays and ordinary erosion-resistant clays lies in that dispersive clays have a high percentage of sodium cations adsorbed on the clay particle surfaces, relative to other common soil cations such as calcium, magnesium, and potassium. When these clays come in contact with water of low dissolved salts, the particles tend to disperse or to deflocculate and can then be easily carried away by seeping water. The possible existence of dispersive soils always should be considered in the geology investigation, especially where borrow areas are derived from alluvial, loessial, or marine deposits, or where there is surface evidence of

these soils such as unusual erosion patterns with tunnels and deep gullies, together with excessively turbid water in impoundments.

When dispersive soils are identified, and economic considerations demand to use them in an embankment, special provisions must be exercised in the design of which the most important one is the design of proper filters. Many failures attributable to dispersive clays take place in homogeneous dams without filters, and all dispersive piping failures are caused by the occurrence of an initial concentrated seepage pathway through the embankment. Compaction and moisture control are critical, too. Special care should be called at to secure proper compaction around conduits and other structures, as well as at steep abutments and foundation contacts. ICOLD (1990) provides a detailed review of dispersive soils in embankment dams, including countermeasures which can be used to prevent problems associated with these materials.

Loess is a type of soil whose name is originated from a German word meaning "loose." It is an Aeolian sediment formed by the accumulation of wind-blown silt, typically in the size of 20–50 μm , 20 % or less clay and the balance equal parts sand and silt that are loosely cemented by calcium carbonate. Loess can be described as a rich, dust-like soil, and it can be found in a wide area from north central Europe to eastern China and in the Midwestern America as well. Loess grains are angular with little polishing or rounding and composed of crystals of quartz, feldspar, mica, and other minerals. Due to the differences in the conditions of accumulation environment, geology, and climate, the properties of loess in different areas may have large variation. It is usually homogeneous and highly porous and is traversed by vertical capillaries that permit the sediment to fracture-forming vertical bluffs. Once soaked by water, the softening or solution of dissolvable salt in the loess damages the loess structure, the significant strength reduction and large settlement will emerge. This type of loess is named as collapsible loess. Loess may be used as materials for homogeneous dams and anti-seepage devices provided adequate compaction under suitable moisture content to prevent collapse after reservoir impounding. Due to its lower scouring resistance, the filter should be carefully designed.

2. Gravelly soil materials

Gravelly soil is a kind of clayey coarse-grained soils, or soil–rock mixtures, formed by coarse grains (larger than 5 mm) with content higher than 20 % and a quantity of fine grain (smaller than 0.1 mm). According to the content of coarse grains and properties of fine grains, it may perform as a fine cohesive soil or a sandy soil. It is often distinguished as fine material and coarse material by the sieve of 5 mm, and the granulometric composition affects its characteristics directly. Generally when the coarse grain content is around 30 %, the gap among coarse grain skeleton may be filled completely by fine grains; when the coarse grain content is around 65–80 %, the gap among coarse grain skeleton cannot be filled completely by fine grains, being responsible for a dramatic increase in permeability. Therefore, the gravelly soil used for anti-seepage devices should control the coarse grain content below 50 %.

The modern soil mechanics shows that the gravelly soil is a better material than pure clay for anti-seepage devices, attributable to:

- A well-graded gravelly soil has features of good compaction degree, high shear strength, low compressibility, easy for construction;
- The settlement of the gravelly soil core is small, which may reduce its arch effect and prevent it from hydraulic fracturing;
- The coarse grains may fix the walls of crack, which is advantageous to seal the crack for seepage stability; and
- Attributable to its high bearing capacity, the large-capacity construction facilities may be employed in construction.

The successful application of gravelly soil, or cohesive soil mixed with gravels, for anti-seepage devices contributed greatly to the high embankment dam construction since the 1960s. For example, the zoned embankment dams built in Japan earlier of the 1950s were restrained by the construction difficulties associated with humid and raining climate since they adopted fine-grained clays only, as a result the dam height generally did not exceed 40 m. Since the 1960s, the application of gravelly soil enabled the boom up of zoned embankment construction including the milestone projects such as the Miboro Dam (Japan, $H = 131$ m) with sloping core of gravelly soil and the Makio Dam (Japan, $H = 104.5$ m) with central core of gravelly soil. In the Nurek Dam (Tajikistan, $H = 300$ m), loess was firstly considered as the material for anti-seepage devices. The later studies indicated a larger settlement, and the loess is poor in scouring resistance in case of core cracking. As a result, the sand–gravel material was finally used for the anti-seepage devices in this giant project. The other famous embankment dams using gravelly soils for anti-seepage devices are the Oroville (USA, $H = 235$ m), the Mica (Canada, $H = 245$ m), the Takase (Japan, $H = 176$ m), and the Goachenen (Switzerland, $H = 155$ m). Weathered or soft rocks that are mechanically broken by roller into small pieces as artificial gravelly soils may also used for anti-seepage devices, such as in the New Melones Dam (USA, $H = 190.0$ m) and the Lubuge Dam (China, $H = 103$ m).

(a) Seepage resistance

Natural gravelly soils may be pervious, but it can be transformed into relative impervious after compaction. The gravelly soil used for anti-seepage devices should control the coarse grain content below 50 %, in this way the gap among coarse grain skeleton may be filled completely by fine grains and the permeability characteristics for anti-seepage devices can be met.

From the standpoint of resistance against seepage failure, the gravelly soil is lower than fine-grained clay. However, a well-graded gravelly soil has sufficient scouring resistance: once cracking appears in the core, the coarse grains are not easy to be transported by seeping flow, the crack is therefore stabilized. On the other hand, the wide gradation of gravelly soils may lock the small grains in the void among soil skeleton, to form a “natural filter” and to seal the crack finally.

Figure 9.16 shows the Lubuge rockfill dam with central core at maximum height of 103.8 m, which is the first rockfill dam using weathered materials for

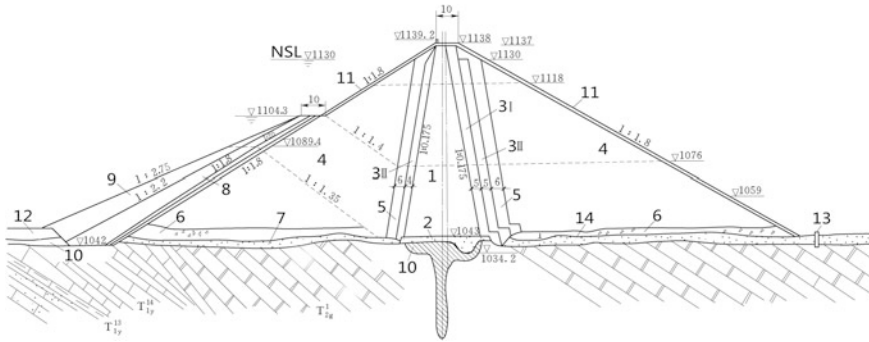


Fig. 9.16 Maximum profile of the Lubuge Dam (*unit: m*) China, $H = 103.8$ m. 1 central core of weathered material; 2 pure clay; 3 filter; 4 coarse grain dam shell; 5 transition layer; 6 settled material; 7 riverbed alluvium; 8 sloping core of weathered material for cofferdam; 9 protection layer of rock ballast; 10 concrete cushion; 11 rock revetment; 12 slag layer; 13 cutoff wall and measuring weir; 14 original ground surface

anti-seepage devices in China. The coarse grain content of 5 mm or larger was 50–60 %, after the compaction, it is reduced to 20–40 %, and the grain content smaller than 0.1 mm is 30 %. Tests show that when the coarse grain content of 5 mm or larger is 40–70 %, the permeability coefficient is 10^{-4} to 10^{-7} cm/s, the critical head gradient of seepage failure is above 40, which is higher than pure fine-grained soils.

(b) Compressibility, plasticity, and shear strength

The gravelly soil with high deformation modulus, low plasticity and tensile strength, is responsible for the poor adaptability to embankment settlement. On the other hand, it has low compressibility, low settlement, and high shear strength. The Shuibuya Dam (China, $H = 233$ m) is implemented as CFRD. However, during its preliminary design phase the rockfill dam with gravelly soil central core was considered as one of alternatives. The standard and heavy compaction tests were conducted for the natural gravelly soil materials. After standard compaction, the content of grains smaller than 5 mm was increased up to 41 %, which was further increased up to 48 % after heavy compaction. The corresponding maximum dry density was $1.91\text{--}2.00$ g/cm³ and $2.04\text{--}2.19$ g/cm³, respectively.

Where the requirements for gradation, permeability, and moisture are difficult to meet, artificial blending method may be employed to solve the issue. Take the Nurek Dam (Tajikistan, $H = 300$ m), for example, the gravelly soil had natural coarse grain content ranged among 0–80 %, which was out the design upper and inferior bounds of 50–20 %. During the construction, the cohesive materials and granular materials were rolled out by layers firstly and then the vertical excavation was carried out for the stockpiled materials by digging machinery, which were delivered to the dam after mixing. In the Miboro Dam (Japan, $H = 131$ m), the sandy clay had moisture content 40 % higher than the optimum content, after the

mixing of 20 % granite gravels smaller than 150 mm the optimum moisture content was obtained, and the friction angle was increased up to 40°.

To control the tensile cracking induced by high deformation modulus and low plasticity, the high-plasticity clay may replace the gravelly soil at the portions of the abutments near the dam crest elevation, and at the contact face between the dam and the rock foundation/abutments. The moisture of this high-plasticity clay could be a bit of higher than the optimum content.

3. Compaction requirements

The density and permeability, as well as the compressibility and strength of the impervious and semi-impervious fill materials are dependent upon water content under a definite compaction work. The relationship among the dry volumetric weight of compacted soils and the water content as well as the compaction work (i.e., compaction curves) of cohesive soils is shown in Fig. 3.6.

The design of an embankment is strongly affected by the natural water content of borrow materials and by drying or wetting that may be practicable either before or after delivery to the fill. In general, placement water contents for most projects will fall within the range of 2 % dry to 3 % wet of the optimum water content as determined by the standard compaction test. A narrower range will be required for soils having compaction curves with sharp peaks. It should be borne in mind that although natural water contents can be reduced to some extent, yet some borrowed soils are so wet that they cannot be reasonably used in an embankment unless dam slopes are flattened.

Where use of water contents practically obtainable is a principal construction requirement, the effect of water content on the properties of a compacted fill is of paramount design interest. Soils that are compacted wet of optimum water content exhibit a somewhat plastic stress–strain behavior (in the sense that their deformation moduli are relatively low and stress–strain curves are rounded) and may develop low Q strengths and high pore water pressures during construction. Alternatively, soils that are compacted dry of optimum water content exhibit a more rigid stress–strain behavior (in the sense that their deformation moduli are relatively high and stress–strain curves are sharpened) and may develop high Q strengths and low pore water pressures during construction. Soils compacted substantially dry of optimum water content may undergo undesirable settlements upon saturation due to reservoir impounding (collapse). Cracks in an embankment would tend to be shallower and more easily self-healing if the compaction is on the wet side of optimum water content.

The SL274-2001 “Design code for rolled earth–rockfill dams” stipulates the compaction requirements as follows.

- ① For cohesive pure clays or clays mixed with few amount of gravel. Dry density is used as the design index. Placement water content will fall within the small range of optimum water content, and is usually a bit higher than that of plastic limit, which may be estimated by Eq. (9.42)

$$W_{0p} = W_p + I_L I_p \quad (9.42)$$

where W_{0p} = design water content; W_p = plasticity number; I_L = liquid limit (0.07–0.1 for high dams, 0.1–0.2 for lower dams); I_p = plastic limit.

Where the dam is compacted under ambient temperature 0 °C, for preventing freezing, placement water contents may be a bit lower than plastic limit.

In addition, the limited water content on the wet side of optimum must be so selected as to obtain better plasticity, and on dry side of optimum must be selected to obtain higher compacted density, depending on the requirements for the portions in the dam. In the latter case, excessive settlements due to saturation should be avoided.

The maximum dry density is selected according to the capacity of compaction facilities and the mechanical parameters of the earthfill. The DL/T5355-2006 “Code for soil tests for hydropower and water conservancy engineering” categorizes soil compaction tests into light compaction test and heavy compaction test, the former is suitable for cohesive and fine soils of grain size smaller than 5 mm whose hitting work per unit is 592.2 kJ/m³, the latter is suitable for cohesive and coarse soils of grain size smaller than 20 mm whose hitting work per unit is 2687.9 kJ/m³. This is, however, a bit of general. For any specific project, the reasonable compaction work and compaction criterion should be studied based on the dam height and soil properties. Take the Xiaolangdi Dam (China, $H = 160$ m), for example, compaction experiments were firstly carried out under 967, 607.5, and 591.6 kJ/m³ according to the domestic and international standards, and then compaction experiments of 1104, 832.5, and 828.2 kJ/m³ were supplemented. Although the average value of the first group of compaction tests was adopted in the final design, the experimental results of the supplemented group showed that the dry density might be significantly raised as the increase of compaction work.

Densities obtained from field compaction tests by conventional tamping or pneumatic rollers and standard pass number are about equal to or slightly lower than the maximum densities by standard compaction tests. Although it has been well established the practical using of densities for initial design phases by performing laboratory tests, the final selection of design densities, while a matter of judgment, should be based on the results by test fills or past experiences with similar soils and field compaction equipments. The common postulation is that field densities will not exceed the maximum densities obtained from the standard compaction test nor get below 96 % of the maximum densities derived from the standard compaction test, that is,

$$\gamma_d = m \bar{\gamma}_{d,max} \quad (9.43)$$

where γ_d = design dry density, kN/m³; m = compaction coefficient, for dams of grade 1 and 2, m should not be lower than 98–100 %, whereas for dams of 3 grade or below, m should not be lower than 96–98 %; $\bar{\gamma}_{d,max}$ = averaged maximum dry density, kN/m³.

- ② The maximum dry density and optimum water content for cohesive soils mixed with gravels is customarily decided by large-scale compaction tests.
- ③ If the borrow areas for cohesive soils mixed with gravels are widely distributed and their properties have large variation, the relation of maximum dry density versus gravel content is difficult to obtain. Under such circumstances, the compaction degree of fine grains should be used as control index.
- ④ Since the water content of total gradation gravelly soils has linear relation with the water content of fine-grained material, it is practically obtainable to use water contents of fine-grained material to control the water content of the total gradation gravelly soil.

9.7.4 Materials for Dam Shell

Materials for dam shell should possess high strength to maintain the stability of dam slopes. The submerged portion of downstream shell and the water level fluctuation portion also should possess appropriate permeable properties. Zoned dams provide an opportunity to specify the use of excavated material, sand, gravel, pebble, boulder, etc., in the different portions of the dam shell. However, uniform medium to fine sands and silts may only be placed above seepage regime or wet areas, to avoid seepage failure or liquefaction.

1. Application of weathered and soft rock materials

As the advancement in construction techniques and equipments, weathered and soft rock materials may be filled in the dam shell nowadays (ICOLD 1993).

In China, rocks with a saturated compressive strength lower than 30 MPa are ordinarily categorized as soft rocks, their lowest strength practically permitted is 10 MPa. Soft rocks cannot be tested in a large volume due to the difficulties associated with the preparation of test specimen. Sometimes point loading tests of rock blocks are carried out; based on the point loading capacity, the compressive strength is calculated by empirical formula.

(a) Properties of weathered and soft rocks

Weathered and soft rocks have following characteristics: moderate deformation modulus and high strength, small size, and high fine grain content, good gradation, high density of low porosity after compaction. The DL/T5395-2007 “Design specification for rolled earth–rockfill dams” requires that the content of grain smaller than 5 mm should not exceed 30 %, for free draining and low pore pressure during construction.

Soft rock materials can be compacted into high density due to grain crushing; therefore, the design should be based on the mechanical characteristics according to the material gradation after compaction. One of the instance is the downstream rockfill zone of the Tainshenqiao No. 1 CFRD (China, $H = 178$ m): the designed

dry density and porosity were 2150 kg/m^3 and 22 %, but the average dry density and porosity in the tested during the construction were 2220 kg/m^3 and 20 %, respectively.

Laboratory tests show a moderate compressibility modulus of soft rockfilled embankment, such as 31–44 MPa for the Zhushuqiao CFRD (China, $H = 78 \text{ m}$) and 30–43 MPa for the Tianshenqiao No. 1 CFRD. The weathered and soft rockfills exhibit a friction angle of $\varphi = 49^\circ\text{--}37^\circ$, if proper compaction may be processed.

(b) Problems in the application of weathered and soft rocks

The zoning from the internal portion of lower quality to the external portion of higher quality for a dam shell is advisable, to make fully exploitation of materials existed near the dam site and from excavation. The main concern about these materials is the tendency of weathering and softening with time when exposed to air and water. A layer of intact rock pitch of 1–1.5 m thick installed on the surface of the rockfill may prevent it from further weathering. The content of fine grain should be controlled to permit free draining and compaction density. If the fine-grained content is too high and free draining is difficult, such material is only placed at “random zones” located at the dry portion of downstream shell or the portion near central core. The draining transition layer should be installed around the random zones. If the softening coefficient is lower, the collapse issue after reservoir impounding should be carefully addressed.

In China, soft rocks are ordinarily placed in the downstream rockfill zones above the tailwater level. Take the Zhushuqiao CFRD as an example, according to the initial design, the rockfill materials would be borrowed from a limestone quarry with a hauling distance of 8–9 km. In the later design consideration, the weathered slates with saturated compressive strength not lower than 10–25 MPa had been employed within a hauling distance of 0.5–1.5 km from the dam site, and a flattened downstream slope of 1:1.7 was adopted due to its relative lower shear strength. Although the embankment volume becomes larger, it is more economy than using particular limestone quarry due to much lower unit cost.

The CFRD of Tianshenqiao No. 1 at height of 178 m uses a large amount of mixtures of thin-layered limestone, mudstone, and sandstone in the zone downstream to the dam axis and above the tailwater level.

The Zhushuqiao and Tianshenqiao No. 1 Dams had been completed for many years. The performance is generally satisfactory except for the appearance of on large side settlement.

2. Compaction requirements

Although it is generally impracticable to consider exact differences between the field and laboratory compactions when selecting design densities, such differences do exist and are responsible for the shifted performance. This must be verified as early as possible during construction, which can often be done by incorporating a test section within the embankment.

Proper compaction at the contact between the embankment shell and the abutments is important. Inclining the fill surface up on a 10 % grade toward a steep

abutment facilitates compaction where heavy equipment is employed. Where compaction equipment cannot be operated against an abutment under overhangs, thin lifts tamped with hand-operated and powered tampers should be employed.

(a) Non-cohesive soil

The compaction standard for non-cohesive soils is related to the compaction work but has no relation with water content, and is specified using coefficient of relative density D_r defined in Eq. (3.18).

According to the SL274-2001 “Design code for rolled earth–rockfill dams” and the DL/T5395-2007 “Design specification for rolled earth–rockfill dams,” coefficient of relative density D_r should not be lower than 0.75, 0.7 and 0.7 for sandy gravels, sands, and filter materials, respectively. In seismic areas, D_r should meet the requirements stipulated in DL5073-1997 “Specifications for seismic design of hydraulic structures,” too.

(b) Rockfill

The modern vibratory roller may meet the requirement for a compacted porosity of 20–28 %. Compaction of rockfill depends on rock properties, maximum grain, gradation, etc. Since the grain size is large, laboratory tests using full-graded rockfill samples are difficult. Therefore, during the construction, the compaction parameters (rolling equipment, frequencies and weight, lift thickness, water sluice, and roller passes) and the dry density are both controlled simultaneously, to ensure the compaction quality. The dry density requirement for the downstream dam shell may be relaxed to some extent. In the preliminary selection of compaction parameters, the engineering experiences from completed projects are valuable.

It is often desirable, especially where rocks are soft, that procedures used in compacting rockfill materials are selected on the basis of test fills, in which lift thicknesses, numbers of passes, and types of compaction equipments (i.e., different vibratory rollers) are investigated. The rockfill should not be placed in layers thicker than 1.0 m unless the results of test fills show that competent compaction can be obtained using thicker lifts. The number of roller passes is normally 4–8. If necessary, for soft rocks the lift thickness should be reduced and the number of roller passes may be increased, and the water should be sufficiently sluiced. In no case should the maximum particle size exceed 0.9 of the lift thickness. Smooth-wheeled vibrator rollers with static weights of 10–15 t are effective in achieving high densities for hard rocks if the speed, cycles per minute, amplitude, and number of passes are correct.

Soft rocks, such as some sandstones and shales, often break down to fine materials on the surface of the lift. Scarifying has to be proceeded on soft sandstone layers to move fines down into the fill.

9.7.5 Materials for Filter, Transition, and Draining

The in situ average relative density of non-cohesive soil should be at least 85 %, and no portion of the pervious fill should tolerate a relative density lower than 80 %. This requirement applies to the drainage and filter layers as well as to the larger zones of pervious materials, but not applies to the bedding layers beneath the dumped riprap slope protection. The requirement also applies to the filter layers and the pervious backfill beneath and/or behind spillway structures.

It is possible to place pervious fills such as free-draining gravels or fine-to coarse sands, into a lift of 0.9–1.3 m thick in shallow water. In general, sands containing more than 8–10 % finer than the No. 200 sieve cannot be placed satisfactorily under water, and well-graded sand–gravel mixtures must contain even fewer fines. The technique to place pervious soils in shallow water after stripping simplifies construction and makes it possible to construct cofferdams using pervious materials by adding a temporary impervious blanket on the outer face. The cofferdam subsequently becomes a part of the pervious shells of the embankment.

9.8 Structural Elements of Embankment Dams

9.8.1 Anti-seepage Devices

Considerable volume of soils of a random nature or intermediate permeability may be available from the open air and underground excavations. It is generally economical to design the embankment in a way that these materials can be utilized, preferably without stockpiling. Where random zones are large, vertical (or inclined), and horizontal drainage layers within the downstream portion of the embankment can be installed to control seepage and to prevent the downstream zone from adverse effects of through seepage. Random zones need to be separated from pervious or impervious zones by suitable transition zones.

Homogeneous embankments are customarily considered satisfactory when internal vertical (or inclined) and horizontal drainage layers are installed to control through seepage. Such embankments are appropriate where available fill materials are predominantly of one type or where available materials are so variable that it is not feasible to separate them into specific soil types for placing them in specific zones and, when the height of the dam is relatively low.

In a common type of earthfill embankments using multi-materials, a less pervious thick central core may be installed which is flanked by more pervious shells that support the core, such as the Trinity Dam (USA, $H = 164$ m) (Fig. 9.17). The up- and downstream slopes of such thick core are steeper than 1.0. An upstream portion less pervious may also be employed which is supported by more pervious downstream shells using non-cohesive soils and gravels. The interfaces between different material zones may be tilted either upstream or downstream.

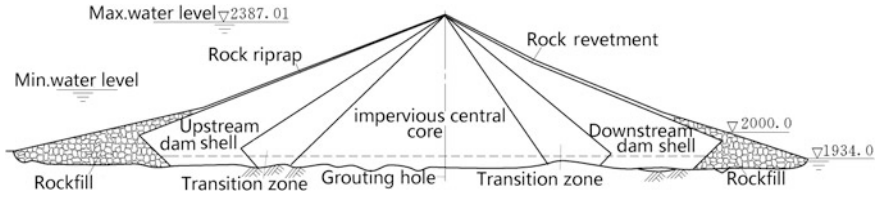


Fig. 9.17 The Trinity Dam (USA, $H = 164$ m)

1. Soil anti-seepage devices

Sloping or central soil core (Fig. 9.18) is exercised widely as impervious elements in embankment dams. Generally, the core is a thin or narrow zone compacted by the earth of plasticity number higher than 8–10, which contains a bit of higher amount of clay particles apart from lower amount of cohesive soils or gravelly soils. Soils of too high amount of clay particles is not suitable for impervious elements, for they are difficult to be well compacted. Previously, it was accepted that cohesive soils are the best material for impervious elements attributable to their good plasticity, good deformation adaptability, and strong impact resistance. However, engineering practices show that cores of cohesive soils have higher “arch effect” and will give rise to horizontal cracking.

Compared to sloping core dams, the upstream shell of central core dams affords more stability under the circumstances of construction, rapid drawdown, uniform settlement, earthquake, and other loading conditions. The downstream shell performs as a drain that brings down the phreatic line and provides stability. For the most effective controls of the through seepage and unsteady seepage during the reservoir drawdown, the permeability should be raised progressively from the core outward to outer slopes. The upstream slope could be steeper than that of sloping core dams depending on the characteristics of dam shell soils. Attributable to above advantages, a larger percentage of previous high embankment dams employs central cores. The disadvantages with central cores are the inconvenience in the construction during raining seasons, and the interference between the compaction of dam shell and core.

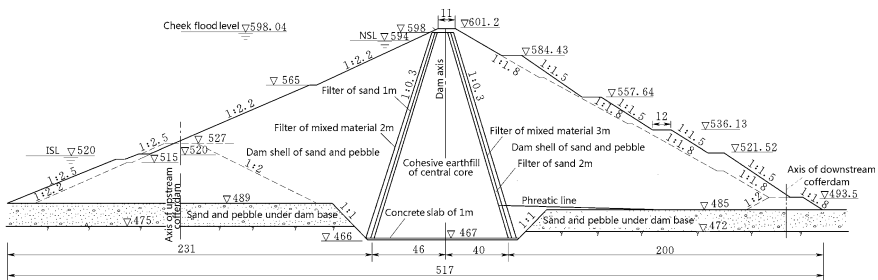


Fig. 9.18 The Jinpen Rockfill Dam with clay central core (unit: m) China, $H = 130$ m

Sloping soil core dams have remarkable advantage of minor interference between the compaction of dam shell and core, but the sloping core is sensitive to the dam shell settlement and easy to be cracked, which is adverse in seismic areas.

In recent years, there is a tendency of using inclined central cores for high embankment dams (Fig. 9.2). As a compromise between sloping core and central cores, the inclined central core has advantages of less arch effect in the core to prevent horizontal cracking, higher resistance to seismic action, and higher slope stability.

The core width for a sloping- or central core embankment should be established on the consideration concerning seepage and seepage failure (piping), types of materials available, the filter design, and seismicity. The maximum core width is normally controlled by the stability and availability of impervious materials. In general, the width of the central or sloping core at the dam base or cutoff should be at least equal to $1/5$ – $1/4$ of the head difference between the maximum reservoir headwater and the minimum tailwater. The greater width of contact area between the impervious core and the rock surface, the less likely a leakage will develop along this contact surface. Therefore, where a thin embankment core is selected, it is advisable to increase the width of the core at the rock juncture, to provide a wider contact area. Where the contact between the impervious core and rock is relatively narrow, the downstream filter zone becomes more important. A width of 3 m is considered as be the minimum entailed by construction equipments.

Anti-seepage devices should possess freeboard above the reservoir level. Under the normal situations, the freeboard is 0.3–0.6 m for central cores and 0.6–0.8 m for sloping cores. Under unusual situations, the crest of cores should not be lower than the corresponding static water level. If the parapet has tight and reliable connection with the anti-seepage devices, the restriction on the elevation of the core crest may be relaxed. However, in no case the crest should be lower than the static water level under normal operation situations.

The up- and downstream slopes of central core are normally 1:0.15–1:0.25. The up- and downstream slopes of sloping core are normally 1:2.0–1:2.5 and 1:1.5–1:2.0, respectively. The up- and downstream slopes of inclined central core are normally 1:0.6–1:0.7 and 1:0.4–1:0.5, respectively.

Where severe freezing takes place and soils are susceptible to frozen action, it is desirable to terminate the core at or slightly (1.5–2.5 m) below the bottom of the frozen zone, to avoid the freezing/thawing damage. Transition zones at the upstream contact face of core with shell are demanded to relief the settlement difference and to cut the seepage failure driving force. Filters also should be installed at the downstream contact face to prevent the core from seepage failure.

2. Asphalt concrete or concrete anti-seepage devices (ICOLD 1992, 1999)

Bitumen is a product from the refinery process of crude oil, while asphalt is the mixture of bitumen and aggregates. The asphalt used on roads and airfields, where deterioration becomes evident, has a different composition to the asphalt used in

dams. Inside a dam, the asphalt is kept under virtually ideal conditions. Fairly constant temperatures without exposure to the sun and the rich, dense asphalt mix mean that oxidation or hardening does occur very slowly over time. Asphalt concrete has been documented to be virtually impervious ($k \leq 10^{-7}$ to 10^{-10} cm/s) when compacted to a void content of lower than 3 %. The reservoir can be impounded during construction, which is not feasible for an upstream facing alternative. Furthermore, overtopping of an asphalt core during construction will not result in the catastrophic consequences as for a clay core or an upstream facing solution. However, the asphalt concrete core wall has disadvantage of difficult with repairing.

Asphalt concrete may be employed as central cores or inclined central cores in embankment dams. It is able to adjust with regard to the deformations in the embankment and to the differential settlements in the dam foundation. The asphalt concrete core is also specially adequate for seismically active areas. By adjusting the bitumen content or the viscosity penetration, the properties of the core can be tailor-made corresponding to local conditions and the core will remain flexible and impervious. For medium to lower dams, the thickness of core wall at base is 1/60–1/40 of the dam height but not smaller than 40 cm, while the thickness of core wall top is not smaller than 30 cm. The transition layers are layout on the two sides of core wall. Inspection gallery is installed at the base where the core wall adjoins the foundation, to monitor the seepage through the core.

If sloping core is installed, a cushion layer of 1–3 m in gravel is demanded as the base to adapt the deformation of the dam shell. The thickness of asphalt concrete sloping core is around 20 cm. At the upstream faces a bitumen layer is coated for the purpose of weathering and freezing/thawing protection. Required by construction conditions, the maximum upstream slope is 1:1.6–1:1.7.

Modern embankment construction using asphaltic concrete for central core was firstly introduced by the contractor Strabag in 1962, and nowadays, more than 200 of such dams were built in the world. The Finstertal Rockfill Dam with inclined central core of asphaltic concrete built in Austria reached height of 150 m. The Chinese engineers built the first asphalt core dams in the 1970s. Today, more than 20 dams of this type have been erected in China, inclusive the Shifayu Rockfill Dam with asphalt concrete sloping core (China, $H = 82.5$ m), the Gaodaoxi Dam with asphalt concrete central core (China, $H = 102.5$ m). The Yele Dam (China, $H = 140$ m) is the highest asphalt core embankment dam in the Sichuan Province, China, where there are extremely wet climate conditions, high altitude and high compressible foundation. Figure 9.19 is the Maopingxi Dam with asphalt concrete central core (China, $H = 104$ m), which is an auxiliary dam for the protection in the Three Gorges Reservoir.

Triaxial tests and finite element analysis may be performed to justify the suitability of using asphalt concrete in embankment dams. All dams with built-in asphalt cores are reported to have excellent field performance. Seepage through the core is claimed to be negligible. It seems quite probable that embankment dams with asphalt concrete cores are likely to find a more prominent place in the future dam construction.

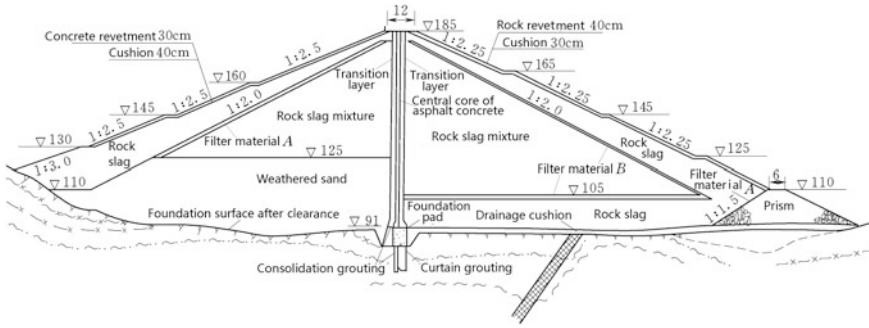


Fig. 9.19 The Maopingxi Dam with asphalt concrete central core (unit: m) China, $H = 104$ m

9.8.2 Draining of Dam Body

Drainage in embankment dams is primarily intended to bring down the phreatic line. The drainage system may reduce the pore water pressure in the downstream portion of dam, and thus, the stability of the downstream slope is improved. A proper drainage system with a combined filter system also helps to avoid pop-off and piping by arresting soil particles. In chilly areas, the freezing/thawing damage to the downstream slope is prevented by adequately designed drainage system, too.

Drainage arrangement is mainly governed by the height of dam, availability of pervious materials, and the permeability of foundation, as well as the facilitation for inspection and repair.

1. Drainage prism

Prism (Fig. 9.20) is generally installed on the fluvial foundation when the dam is raised without cofferdams and the river is closed by filling rock into water. With large amount of cheap rocks available, it can also be used for other sections of dam. The drainage prism is reliable and widely exercised, due to its advantages of truncating phreatic line, protecting the dam from freezing/thawing damage and tailwater scouring, enhancing the slope stability by downstream supporting, facilitating the

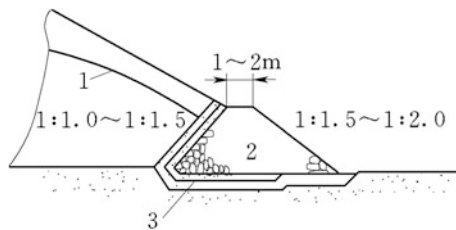


Fig. 9.20 Anatomy of a drainage prism. 1 phreatic line; 2 drainage prism; 3 filter

inspection and repairing operation. Transition filter is demanded between the dam body fill and the prism. The filter usually comprises 30 cm thick layer of fine sand ($d_{15} = 0.09$ mm), 45 cm thick layer of coarse sand ($d_{15} = 0.81$ mm), and 60 cm thick layer of gravel ($d_{15} = 7.3$ mm). As a rule the discharge capacity of the filter should be twice the seeping discharge documented by calculation.

The minimum height of prism is governed by the minimum allowable overburden depth over the phreatic line to prevent freezing/thawing damage and by the freeboard over the downstream water level. The top of the prism must be sufficiently higher than the tailwater level to prevent any wave splashes on the downstream face, which is at least 1.0 m for dams of grade 1 and 2, 0.5 m for dams of grade 3, 4, and 5. Generally, the discharge face (inward face) of the prism has a slope of 1:1.0–1:1.5, the outer face has a slope of 1:1.5–1:2.0 or, of the continuation with respect to the downstream embankment slope. The width of prism is selected according to the requirements of construction and access. However, it is avoided to use prism as traffic purpose, to prevent it from damage and blockage.

2. Surface drainage at dam toe

In short of rock materials, a surface drainage at the dam toe is usually installed as an alternative scheme (Fig. 9.21) instead of prism, which is one to two layers of rockfill or masonry plus a filter layout directly on the downstream dam shell surface. Surface drainage has advantages of control seepage failure near downstream toe, simplicity in structure, material saving and easy for repair. Since the surface drainage is situated outside of the dam shell and does not cut-short the paths of seepage, it is not able to bring down the phreatic line. Surface drainage is often employed in the medium to lower embankment dams of homogeneous loam, to protect the periodically inundated flood plain, or dams with low phreatic line.

The utmost elevation of surface drainage is selected with respect to:

- The highest position of seepage exit, by taking into account of capillary rise which is at least 2.0 m for the dams of grade 1 and 2, and at least 1.5 m for the dams of grade of 3, 4, and 5; and
- The highest tailwater level with allowance for the surge and run-up of waves.

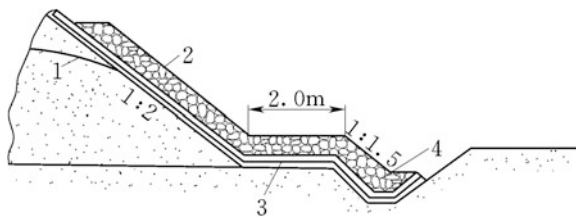


Fig. 9.21 Anatomy of a surface drainage at dam toe. 1 phreatic line; 2 surface drainage; 3 filter; 4 draining ditch

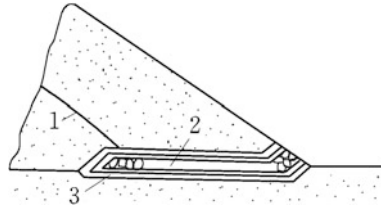


Fig. 9.22 Anatomy of a horizontal drainage blanket. 1 phreatic line; 2 horizontal drainage blanket; 3 filter

The thickness of surface drainage should be able to keep the freezing depth away from the dam body.

3. Internal drainage devices

Internal drainage devices cut the shortest seepage pathways, and they fall into horizontal drainage blanket, chimney drains, etc.

The horizontal drainage blanket is installed over that portion of the downstream foundation from the impervious zone where high upward seepage forces exist. The blanket must be pervious to drain off effectively and its design should fulfill the usual filter criteria, in order to prevent the movement of particles of the foundation or embankment due to seepage forces (Fig. 9.22). The blanket may be installed on homogeneous pervious foundations overlain by thin impervious layers, in order to stabilize the foundation and to relieve the pressure that may break through the impervious layer.

The length of blanket may be determined theoretically by means of flow net and/or FEM, provided the horizontal and vertical permeability of the foundation are known. Generally, a length of half dam base width is sufficient for homogeneous dams of clayey soil. This length could be reduced to 1/3 of the dam base width for homogeneous dams of gravelly clay. For central core dams, the horizontal drainage blanket may be extended until the downstream toe of the core.

Disadvantages of horizontal drainage blanket are inconvenient for inspection and repairing, and making the embankment be stratified and consequently be more pervious in the horizontal direction.

Usually, the horizontal blanket is combined with a rock prism and/or chimney drain (Figs. 9.23 and 9.24), to form combined drainage system in the dam body. Inclined or vertical chimney drains are provided in many homogeneous dams to intercept seeping water before it reaches the downstream slope. The chimney drain must be sufficiently pervious to drain off effectively and its design should fulfill the filter criteria. Transition filter is installed between the dam body fill and the chimney drain. The seeping water is released through the horizontal drainage blanket.

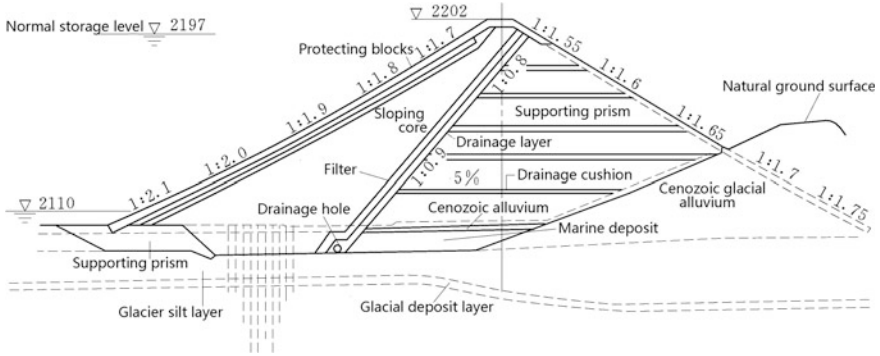


Fig. 9.23 The Mattmark Dam (Switzerland, $H = 117$ m)

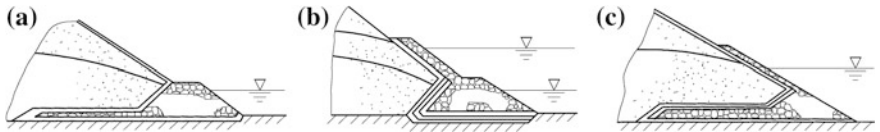


Fig. 9.24 Combined drainage devices

9.8.3 Dam Crest and Slope Pitch

1. Dam crest

To prevent it from scouring by rain fall, dam crest should be paved by gravel, masonry, asphalt, or concrete. If there is consideration of traffic, the requirements for the traffic road pavement should be met.

A solid and impervious parapet is usually installed on the upstream side of dam crest, which may be simply in vertical shape (Fig. 9.25b), or in circular shape (Fig. 9.25c), the latter is advantageous in reducing the energy of wave impaction. The parapet may be built using rubber masonry or reinforced concrete. The reliable connection of the parapet to the anti-seepage device should be guaranteed. On the downstream side of dam crest, the stone curb or hand roll is installed. To drain the rain fall flow, the crest is inclined to either both sides or only one side with a slope of 2–3 %.

2. Slope protection

The possibility of damage to a dam slope varies with the steepness of the slope, the nature of the embankment materials, the wind speed and fetch and exposure time to the wave attack, the rain fall flow, ice impact, freezing/thawing actions, etc. All these demand an adequate protection of embankment slope.

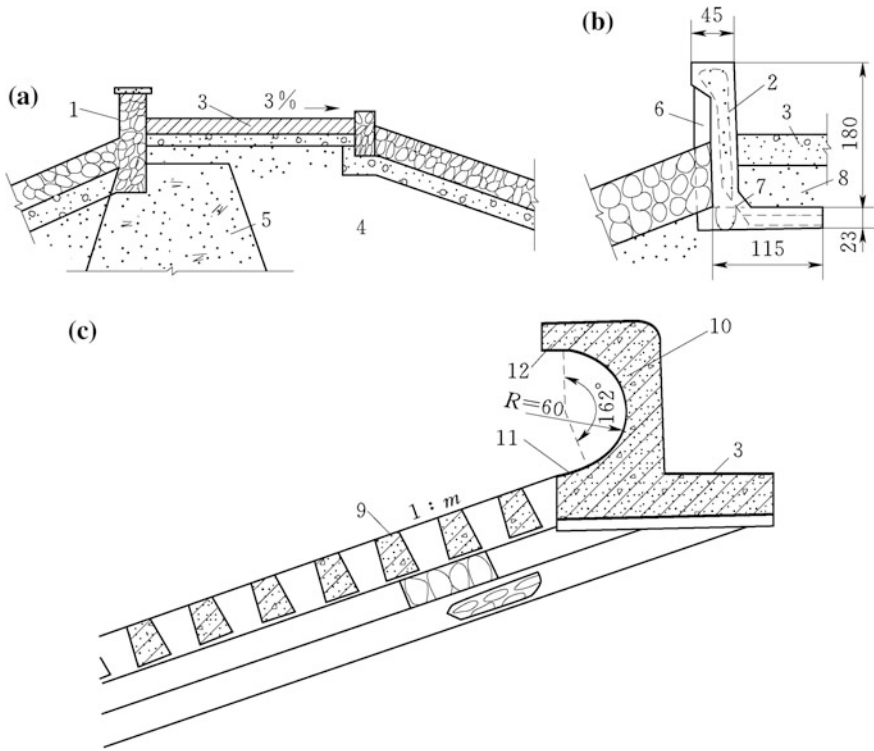


Fig. 9.25 Structural elements of the embankment dam crest (*unit: cm*). **a** Crest road and rubber masonry parapet; **b** reinforced concrete parapet; **c** circular parapet. 1 rubber masonry parapet; 2 reinforced concrete parapet; 3 road pavement; 4 sand and gravel dam shell; 5 central core; 6 square pillar; 7 draining pipe; 8 backfill soil; 9 grid plate revetment; 10 deep circular parapet

The upstream embankment slope with maximum exposure to the reservoir pool levels during normal project operation, which is usually 2.5 m below the dead level (1.5–2.0 m for grade 5 dams) and up to the crest elevation, should be well protected. Stone revetment in the form of riprap or in the form of concrete slab pavement placed in situ is ordinarily installed on an invert filter of subgrade. One alternative is to use riprap-quality, quarry-run stone dumped in a designated zone within the outer slope of the embankment. Another alternative is to use a well designed and properly controlled plant-mix, soil-cement layer placed with established and acceptable techniques. The slope protection placed at the near-crest elevations may vary for different reaches but must be stable under the design wave.

The whole downstream slope is customarily protected by stone pitching or dumped riprap of around 0.3 m thick. Where an adequate growth of grass can be maintained, vegetative cover of 0.05–0.10 m thick would be the most desirable type of downstream slope protection. A slope of approximately 1:3 is about the steepest on which mowing and fertilizing equipment can operate efficiently. In arid or

semiarid regions where adequate turf protection cannot be maintained, outer embankment zones composed of soils (silt and sand) susceptible to erosion may be protected with gravel or rock spill blankets of at least 3 cm thick, on which berms with collector ditches are installed (Fig. 9.26). The downstream slope below the maximum tailwater level should be well protected similar to that of the upstream slope. In many projects, the spatial relationship between the embankment and spillway precludes the necessity for extensive tailwater protection. For a project with large outflow discharge from spillway near the embankment toe, hydraulic model test is undertaken to recognize the flow velocities and wave heights, based on which the slope protection is designed.

The elevation of dam crest is usually selected much earlier in the design process than the consideration on slope protection. When the slope protection design has been processed, the elevation of dam crest should be reviewed to ensure that wave run-up computed is consistent with the type of protection to be placed.

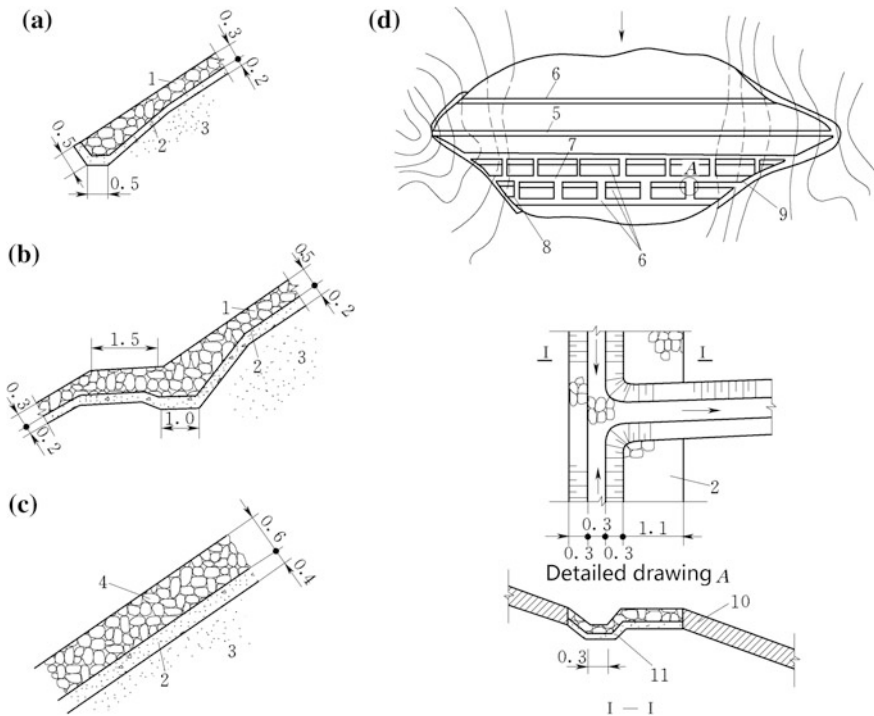


Fig. 9.26 Slope protection and drain (*unit: m*). **a, b** Stone pitching; **c** rockfill riprap; **d** slope drain. 1 dry-laid stone; 2 cushion; 3 dam body; 4 rockfill; 5 crest; 6 berm; 7 longitudinal draining ditch; 8 transverse draining ditch; 9 abutment draining ditch; 10 vegetative cover; 11 stone masonry ditch

9.8.4 Filters

In a zoned embankment, intermediate or transition zones meeting the requirements for filter are installed between the fine and coarse zones (Sherard and Dunnigan 1984, 1985).

All drainage or pervious zones should be well compacted. Where a large discharge capacity is required, a multilayer drain should be provided. The filter design for the drainage layers and internal zones is a paramount task in the embankment design. This is accomplished by “filter criteria,” which include following requirements:

- Retain the protected materials. The individual particles in the foundation and embankment are held in place and do not move in the form of piping and scouring as a result of seepage forces;
- Have sufficient discharge capacity to drain the protected materials. On the one hand, the filter material must be more open and have a larger grain size than the protected soil; on the other hand, clogging of the filter causing loss of the filter’s ability to remove seeping water from the protected soil should be prevented; and
- Filter materials are well gradated and allow for free movement of water. The content of particles smaller than 0.075 mm should be not excess 5 %, that is, $D_5 > 0.075$ mm.

For design, above three requirements are termed as piping or stability requirement, permeability requirement, and discharge capacity requirement, respectively.

The terms of filter and drain are sometimes employed interchangeably. Some definitions classify filters and drains by function. In this case, filters must retain the protected soil and have permeability greater than the protected soil but do not need to have a particular flow or drainage capacity, since flow will be perpendicular to the interface between the protected soil and filter. Drains, however, while meeting the requirements of filters, must have an adequate discharge capacity since they collect seeping water and conduct it to a discharge point or area. In practice, the critical issue is not definition, but recognition, by the designer, when a drain must collect and conduct water.

A filter (Fig. 9.27) is conventionally composed of 1–3 layers of uniformly gradated and weathering resistant sand, peddle, gravel, etc. The grain size is increased along the seeping direction. The minimum thickness is 0.3 m for horizontal filter layer and 0.5 m for vertical or inclined filter layer. If bulldozer is used in the construction of filter, the minimum horizontal width of filter is 3.0 m. Prevention of drains and filters should be made from contamination by runoff containing sediment, dust, construction traffic, and mixing with nearby fine-grained materials during placement and compaction. Caution of segregation, particularly well-graded filters, during handling and placement, is also called at. In situ relative density should be equal to or higher than 85 %, and in no case be lower than 80 %. Gradation should be monitored closely so that the filter criteria are met. Thickness

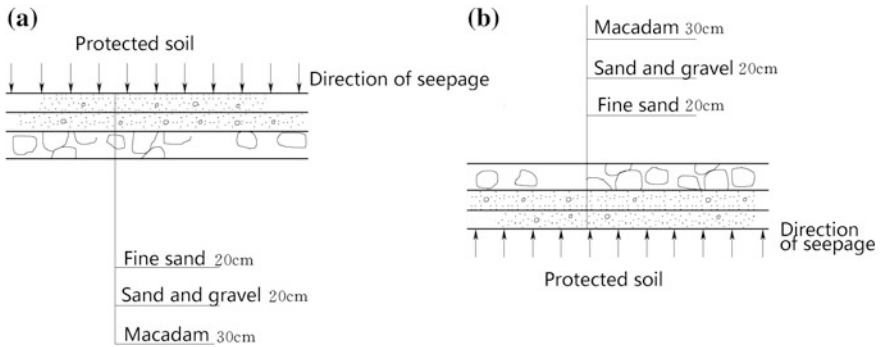


Fig. 9.27 Anatomy of filter

of layer should be monitored to secure the designed discharge capacity and the continuity of the filter.

Several criteria developed by the experiences are available for design filters which will prevent the movement of protected soil into the filter. These criteria, called “piping or stability criteria,” are based on the grain-size relationship between the protected soil and the filter soil. For the first layer of a filter contacting the protected soil, the following criteria should be observed

$$\begin{cases} D_{15}/d_{85} \leq 4-5 \\ D_{15}/d_{15} \geq 5 \end{cases} \quad (9.44)$$

where D_{15} = grain size showing that there are 15 % particles (by weight) of smaller size in the filter material, mm; d_{85} and d_{15} = grain size showing that there are 85 and 15 %, respectively, particles of smaller size in the protected material, mm.

For the second layer of the filter contacting the first filter layer, the above criteria may also be used, and reason out the rest by analogy. For a protected soil of larger inhomogeneity coefficient, d_{85} and d_{15} of the fine-grained particles within $C_u \leq 5-8$ may be used as the calculated particle sizes.

For a cohesive soil to be protected, requirements in Eq. (9.44) may be relaxed up to 10, but this is not a safe choice for pebbly clay. Several engineering experiences recommended that for the cohesive soil, $D_{20} \leq 1.0-1.5$ mm may be a reliable standard in the selection of filter materials.

In the recent 30 years, several remarkable advances in the filter design for modern embankment dams have been achieved, which are briefly introduced in the following.

1. Shift from uniform grading soils to non-uniform grading soils

In recent years, it has been gradually shifted from uniform grading soils without fine particles of $C_u \leq 5$ to non-uniform grading materials with high content of <5 mm particles and semi-pervious characteristics. Nowadays, the ideal gradation

for cushion zone suggested by Sherard is widely accepted, i.e., a continuous gradation with maximum diameter of 80 mm, 60 % content of <5 mm particles, 2–12 % content of <0.1 mm particles. It meets the semi-pervious and filter requirement for silt soils. It also has been recognized worldwide that all materials with continuous gradation and stable internal structure and without segregation during placement are utilizable.

It should be emphasized that a gap-graded filter material must never be allowed for since it will consist of either the coarse particles floating in the finer material or the fine particles having no stable position within the voids formed by the coarse grains. In the former case, the material may not be sufficiently permeable to provide sufficient drainage capacity, whereas in the latter case it is particularly dangerous since piping of the protected material can easily manifest through the large, loosely filled voids.

2. Protection of gap- or broadly graded soils

One of the fairly common soils placed in embankment dams is broadly graded material with particles ranging from clays to coarse gravels and containing all intermediate sizes. These soils may be of glacial, alluvial–colluvial, or weathered rock origin. As noted by Sherard, since 85 % of the soil is commonly on the order of 20–30 mm in grain size, a direct application of the stability criteria Eq. (9.44) would give rise to very coarse and uniform gravel without sands as a downstream filter.

For gap- or skip-graded soils, calculation of particle sizes d_{85} and d_{15} should be based on the grains below the horizontal section of grade curve (generally below 1–5 mm). If the soil of sand and gravel with $C_u = 5–8$ is employed as the first layer of filter, D_{15} should be based on the grains smaller than 5 mm, and it is required that the gravel content larger than 5 mm should be lower than 60 %. This is intended to ensure that the fine grains will be well protected.

3. Filter material for cohesive soil protection

In an embankment dam, the elements most vulnerable to seepage erosion are the anti-seepage devices such as the impervious core, usually of cohesive soil. This poses special problems because using traditional criteria Eq. (9.44) leads to a filter itself likely to be cohesive and offers no effective protection to the vulnerable cohesive soil core. Therefore, it is generally accepted that different design principles should be applied, which address the issue of the actual size of the clayey particles that a filter must retain. For example, Sherard proposed that the filter material should be selected according to the principle that the cracks in anti-seepage devices will not be propagated and can be self-healed.

The filter on the upstream side of anti-seepage devices may be relaxed to some extent.

4. Layer of filter

Most modern embankment dams utilize filters of one layer, occasionally two layers, and seldom three layers. For example, the Sarsang Aam (Azerbaijan,

$H = 130$ m), the Chivor Dam (Coulombia, $H = 237$ m), the Shimen Dam (Taiwan, China, $H = 133.1$ m), the Makio Dam (Japan, $H = 104.5$ m), the Miboro Dam (Japan, $H = 131$ m), the Yanase Dam (Japan, $H = 115$ m), all installed one-layered filter between the anti-seepage devices and the dam shells. Two-layered filters were employed in the Rogun Dam (Tadzhikistan, $H = 335$ m), the Nurek Dam (Tajikistan, $H = 300$ m), the Oroville Dam (USA, $H = 235$ m), the Shitouhe Dam (China, $H = 114$ m), etc.

The first layer is made of natural sand and gravel or by once screened, its non-homogeneity is entailed as $C_u \leq 50$. The third layer, if installed, is actually a transition layer to the rockfill shell which is made directly of natural sand and gravel material without limitation in C_u . The one-layered filter is always installed as the upstream filter for anti-seepage devices. Made directly of natural sand and gravel material, its thickness is larger than 3 m.

5. Application of geosynthetic filters

Consisting of synthetic fibers rather than natural ones (e.g., cotton, wool, or silk) geosynthetic filters are placed in soils that allow for water to flow through, but prevent the soil particles from passing (Giroud 1989, 1992a, b). Drainage applications include pavement edge drains, trench drains, prefabricated drainage panels, and leachate collection/leak detection systems. In China, the downstream surface drainage of the Maizihe Dam (Yunan, China, $H = 21.3$ m), the downstream toe trench of the Hongshan Dam (Inner Monolia, China, $H = 31$ m), the upstream protection cushion of the Daguangba Dam (Hainan, China, $H = 57$ m), etc., have been accomplished successfully using geosynthetic filters.

9.9 Treatment of Dam Foundation

The importance of adequate foundation treatment is evident due to the fact that approximately 40 % of all embankment dam failures are attributed to the deficits in foundation. Although the requirements for the foundation of embankment dam are not so rigorous as concrete dams, certain provisions through treatment should be made in the design to assure that the essential requirements concerning its bearing capacity, strength, deformation and seepage should be met (ICOLD 2005). As the development of foundation treatment techniques, many high embankment dams were erected on foundations with adverse geologic conditions. Concrete trench on the 120-m-deep overburden foundation enabled the Manic III Dam (Canada, $H = 107$ m) to be successfully completed; the Aswan High Dam (Egypt, $H = 111$ m) is built on a 225-m-thick riverbed alluvium, in which a grouting curtain of 150 m down to impervious stratum of Tertiary period is installed from the gallery within central core. China also achieved great progress in the treatment of deep overburden foundation for embankment dams: until 2002, of all 36 dams with trench walls deep than 40 m, China accounted for 17. The Xiaolangdi Dam is built

on the sand–gravel alluvium foundation, in which a concrete cutoff wall is installed, its maximum excavation depth reaches 81.9 m and the thickness of wall is 1.2 m.

Treatment methods are dependent on foundation types which may be grouped into three main classes according to their predominant characteristics: foundation of rock, foundation of coarse-grained material (sand and gravel), and foundation of fine-grained material (silt and clay) (Acker and Jones 1972; Day 2006; Fang 1991; Xanthakos et al. 1994).

9.9.1 Rock Foundation

Rock foundations should be cleaned off all loose fragments and projecting knobs of rock to facilitate operation of compaction equipment and to avoid differential settlement.

Anti-seepage devices should have tight contact with bedrock. Usually if the overburden layer is thin, only a shallow trench is necessary to be excavated down to solid bedrock for accommodating anti-seepage devices (e.g., core wall). However, for high embankment dams, to ensure the watertight and stability, larger area of overburden should be excavated down to solid bedrock to accommodate anti-seepage devices and dam shells. For example, in the Nurek Dam (Tajikistan, $H = 300$ m), a 20-m-thick overburden under the central core was removed; in the Oroville Dam (USA, $H = 235$ m), a 18-m-thick overburden of the whole dam foundation was removed, the sloping core and pervious dam shells are all located on the bedrock.

The excavation of shallow exploration or core trench by blasting may damage the bedrock. Where this may occur, exploration trenches are not recommended, unless they can be excavated without blasting. Where the core trench discloses cavities, large cracks, and joints, it should be backfilled with concrete cap to prevent possible erosion of core material by water seeping through the joints or other openings in the bedrock.

Where an embankment dam is constructed on a jointed rock foundation, it is essential to prevent embankment fill from entering joints or other openings in the rock. This can be done in the core zone by extending the zone into sound bedrock and by treating the rock (e.g., consolidation grouting). Where movement of shell materials into openings in the rock foundation is possible, joints and other openings should be filled. An alternative is to provide filter layers between the foundation and the dam shells. Such treatment will generally not be necessary beneath the shells of rockfill dams.

Grouting of rock foundations is customarily undertaken to control under seepage (Cambefort 1977) through cracks and joints. Cement, asphalt, clay, and various chemicals may be used as grouting materials of which cement grouting is prevalent. The choice of grouting material, pattern, depth and sequence of grouting are related to the foundation conditions, type, and height of the dam and objective desired. The curtain grouting for embankment dams are mainly justified by economic technology

study. In recent years, apart from indispensable grouting for faults and Karst strata, the grouting requirements are simplified or even eliminated, particularly for lower embankment dams.

For faults, the bearing capacity and settlement are usually not predominant, whereas seepage failure is the major concern. Careful study of grouting requirements is demanded where the foundation is crossed by faults, particularly when the shear zone of a fault consists of strongly crushed and fractured rocks. It is desirable to seal off such zones by consolidation grouting. Where such a fault crosses the proposed dam axis, it may be advisable to excavate trench along the fault that is backfilled by a concrete cap in which grout pipes are placed, so that the fault zone can be grouted at certain depth between the upstream heel and downstream toe of the dam. The direction of grout holes should be so oriented to optimize their intersection with fractures and other defects.

Many limestone deposits contain solution cavities. Piping may develop or the roofs of undetected cavities may collapse. Where there is suspicion, investigation by one row or more of closely spaced exploration holes is demanded. All solution cavities below the base of the embankment should be grouted with multiple rows of grouting holes.

Shale foundations do not permit drying out and swelling prior to fill compaction. Consequently, it is desirable to defer removal of the last layer of shale until just before the embankment fill placement begins.

9.9.2 Sand and Gravel Foundation

If the overburden is fairly deep and mainly composed of cobble and gravel, and the dam is high than 100 m, dynamic compaction and rolling technique may be undertaken to improve the bearing capacity of the foundation. For example, the Miaojiaba Dam (China, $H = 111$ m) with an overburden thickness of 44–48 m, round ramming hammer of 40 t lifted by crawling crane is used to treat the foundation. After the treatment, the foundation elevation is compressed by 55 cm. As a result of significant improvement in the foundation bearing capacity, the preliminary settlement of the dam is completed ahead of schedule.

One of the key issues in the construction of embankment dams on sand and gravel foundation is under seepage control (Bussey 1961; Cabanius and Margre 1958; Casagrande 1961) that is intended

- To reduce seepage gradient and to prevent excessive uplift pressure and piping through the foundation;
- To control seepage discharge within allowable value; and
- To prevent downstream from immersion.

The devices available to control the under seepage in sand and gravel foundations are distinguished as horizontal drains, vertical cutoffs (compacted backfill trench, slurry wall, and concrete wall), upstream impervious blankets, downstream

berms, relief wells, and trench drains. To select an appropriate anti-seepage device for a particular dam and foundation, the relative merits and efficiency of different devices should be evaluated by means of flow net or other manners (e.g., FEM). The changes in the quantity of under seepage, factor of safety against uplift, and uplift pressures at various locations should be documented to cover the possible range of anticipated field conditions. Safety must be the governing factor in the selection of anti-seepage devices. When the dam foundation consists of a relatively thick deposit of pervious alluvium, the designer must decide whether to make a complete cutoff or to allow for a certain amount of under seepage.

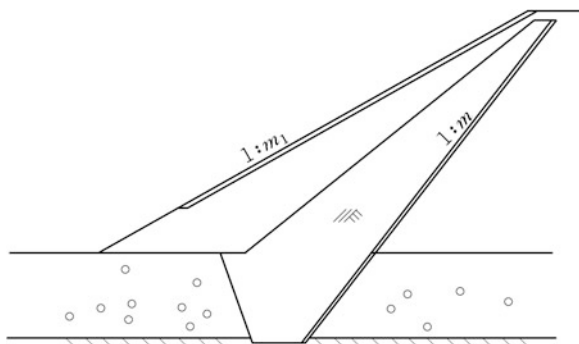
1. Vertical anti-seepage devices

Analysis shows that it is necessary for a cutoff to penetrate a homogeneous isotropic foundation at least 95 % of the full depth before there is any appreciable reduction in seepage beneath a dam. Therefore, when constructing a complete cutoff, the trench is desirable to fully penetrate the pervious strata and is carried a short distance deeper into unweathered and relatively impervious soil or rock. Partial cutoffs are effective only when they extend down into an intermediate stratum of lower permeability.

(a) Cohesive soil cutoff trenches

Vertically compacted backfill trench is an effective and reliable anti-seepage device and is customarily adopted for embankments on sand and gravel foundations of depth within 20 m. The cutoff trench is connected on its top to the anti-seepage device in the dam body and at its bottom to the bedrock; in this manner, a complete cutoff system is formed (Fig. 9.28). The compacted backfill trench is the only way for the control of under seepage which simultaneously provides a full-scale exploration trench that allows the designer to see the real geologic conditions and to adjust the design accordingly, permits the treatment of exposed bedrock as necessary, provides the access for the installation of filters to prevent the piping of soil at interfaces, and carries out high-quality backfilling operations. Cohesive soil cutoff trench was widely employed in China’s embankment construction before the 1960s, which falls into two general types as sloping-side trench and vertical-side

Fig. 9.28 Clay trench cutoff



trench. Sloping-side cutoff trenches are excavated by shovels, draglines, or scrapers and are backfilled with impervious materials which are compacted in the same manner as the impervious zone of the embankment. Vertical-side trenches may be open cut by bands or trenching machines, where it is necessary to remove and replace breccia or debris in fault zones.

Whenever economically possible, under seepage through a pervious foundation should be cut off by a trench extending to bedrock or other impervious stratum deeper into 0.5–1.0 m. If the gradation of the impervious backfill is such that the pervious foundation material does not provide protection against piping, an intervening filter layer between the impervious trench backfill and the foundation material is required on the downstream side of the cutoff trench. The bottom width L of the trench should meet the requirements for allowable gradient $L \geq \frac{\Delta H}{[J]}$, in which ΔH is the maximum head difference exerting at the cutoff, $[J]$ is the allowable gradient of the backfill, which is usually ranged between 3–4 for light loam, 4–6 for loam, and 5–10 for clay. The bottom width L of the trench also should meet the requirements for the allowable gradient of anti-contact scour $L \geq \frac{\Delta H}{[J_c]}$, and a minimum width of 3–5 m is stipulated with respect to construction operation. $[J_c]$ is the allowable gradient of the contact face between backfill and bedrock, which is usually ranged between 1.5–2 for light loam, 2–3 for loam, and 3–5 for clay.

In recent years, as the progress in excavation machines and the necessity of high embankment construction, if the groundwater table is not high, trench cutoff has a tendency of increasingly deeper. For example, the Mammoth Pool Dam (USA, $H = 142.8$ m) and the Keban Dam (Turkey, $H = 207$ m) are installed with trench cutoffs deeper than 40 m.

Dewatering system of well points or deep wells is ordinarily demanded during the excavation and backfill operation. Because the construction of open cutoff trenches with dewatering is a costly procedure, the trend has been shifted toward the use of slurry trench cutoffs (D'Appolonia 1980; Jones 1967; Stoetzer et al. 2006) in recent years.

(b) Slurry cutoff trenches

Slurry trenches are conventionally adopted for temporary structures on sand and gravel foundations of depth within 20 m. Where the dewatering and/or the depth of the pervious strata render the compacted backfill trench too costly and/or impractical, slurry trench cutoff may be a viable method for the under seepage control of permanent structures.

The slurry trench is excavated through the pervious foundation using a sodium bentonite clay (or attapulgite clay in saline water) and water slurry to support the side walls. The slurry-filled trench is backfilled by displacing the slurry with a backfill material that contains enough fines (passing the No. 200 sieve) and sufficient coarse particles to make the cutoff relatively impervious; meanwhile, to minimize the settlement of trench, this forms a soil-bentonite cutoff. Alternatively, cement may be introduced into the slurry-filled trench which is left to set or harden,

this forms a cement-bentonite cutoff. The slurry trench cutoff is not recommended when boulders, talus blocks on buried slopes, or open joints exist in the foundation due to difficulties associated with excavating through the rock and heavy slurry loss through the open joints. When a slurry trench is relied upon for under seepage control, the initial filling of the reservoir must be controlled and piezometers located at both the upstream and downstream of the cutoff must be documented to verify if the slurry trench is performing as anticipated. If the cutoff is ineffective for under seepage control, remedial actions must be taken prior to further raising of the reservoir pool.

Normally, the slurry trench should be located under or near the upstream toe of the dam, for the purposes to provide access for future treatment (provided that the reservoir could be drawn down) and to facilitate staged construction.

(c) Concrete wall

Where the depth of pervious foundation is not in excessive of 80 m and/or the foundation contains cobbles, boulders, or cavernous limestones, the concrete cutoff wall (Figs. 9.29 and 9.30) may be an effective and feasible device for the control of under seepage (Xanthakos et al. 1994). Using this method, a cast-in-place continuous concrete wall is constructed by tremie placement of concrete in a bentonite slurry-supported trench. Two general types of concrete cutoff walls, the panel wall and the element wall, are distinguished. Since the wall in its simpler structural form is a rigid diaphragm, rupture could occur due to earthquake. Therefore, concrete cutoff walls should not be used at a site where strong seismic shocks are anticipated.

The cutoff wall is excavated from the existing surface to a maximum depth using special excavator or cutter, and bentonite slurry is maintained in the trench to stabilize the trench walls. In addition, when working with the trench cutter, the slurry is used to convey excavated slag out of the trench. Concreting a slurry-filled trench is carried out using a “tremie pipe” that introduces fresh concrete down to the trench bottom and allows it to rise upwards displacing the slurry in the trench.

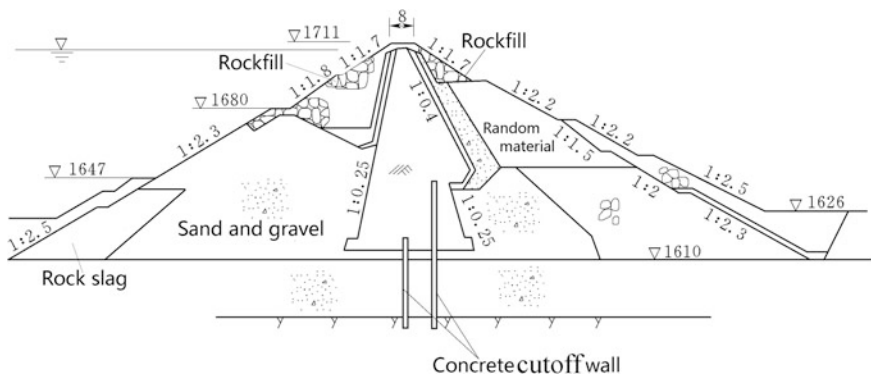


Fig. 9.29 Concrete cutoff wall in an embankment dam (unit: m)

The bottom of the cutoff wall should be keyed into weakly weathered bedrock at least 0.5–1.0 m, while the top of the wall should be keyed into anti-seepage device of the embankment at least 1/10 of the dam height and not smaller than 2 m. The thickness is selected with the range of 0.6–1.3 m depending on construction equipments, and the average thickness is 0.8 m. The Bikou Dam (China, $H = 101.8$ m) has a concrete cutoff wall of thickness 1.3 m, which was limited by the capacity of thrust borer. The modern trend is to use thin wall for economical purpose. If the anti-seepage requirement cannot be met, double cutoff walls may be installed.

From the 1960s, concrete cutoff walls are widely exercised in the treatment of embankment dam foundation, their maximum depth had reached 80 m. The Manic 3 Dam (Canada, $H = 107$ m) commissioned in 1975 is built on alluvial deposits of 126 m deep. The presence of a pervious granular and compressible foundation required special techniques to reduce under seepage, and to avoid cracking in the sloping core due to the differential settlement of the foundation. The double cast-in-place cutoff walls spaced 3 m apart are constructed, which consist of 0.6-m-thick interlocking piles and panels. The walls are keyed minimum 0.6 m into the bedrock. Until 1985, China had constructed more than 60 embankment dams with concrete cutoff walls, their minimum thickness is 20 cm. These cutoff walls continue to perform well for over 40 years until now. The recently completed double cutoff walls in the Xiaolangdi Dam (China, $H = 160$ m) reaches the maximum depth of 80 m, for each wall the thickness is 1.2 m. The cutoff wall in the Luding Dam (China, $H = 84$ m) has the maximum and average depth of 154 m and 80–100 m, respectively.

Concrete cutoff walls may be stiff or flexible (plastic). The former is made of high-strength concrete with steel bar reinforcement, if necessary, intended to resist high stress induced from high dams, architectures, or retain walls. The latter made of plastic concrete with deformation modulus similar to that of foundation soil for the purpose to reduce the wall stress is prevalent for dams or levees.

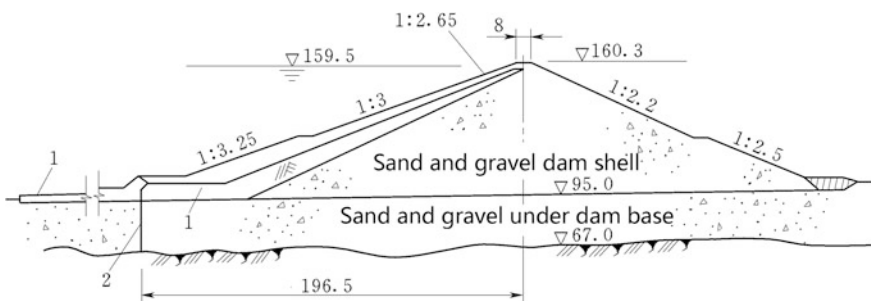


Fig. 9.30 The Baihe Dam (unit: m) the Miyun Project (China, $H = 66$ m). 1 cohesive sloping core and horizontal blanket; 2 concrete cutoff wall

(d) Grouting curtain

Grouting curtain is not so prevalent as cutoff wall in the treatment of sand and gravel alluvial deposits. However, when the depth of the pervious foundation is in excessive of 80 m and/or the foundation contains cobbles, boulders, or cavernous limestones, the combination of upper concrete cutoff wall and lower grouting curtain below the wall may be an effective and feasible way for the control of under seepage (Bowen 1981; Nonveiller 1989; Sun 2004).

The Serre Poncon Dam (France, $H = 129$ m) completed in 1957 is on the sand and gravel alluvial deposits. Cement, colloidal clay, and few chemical additions were mixed for constructing the grouting curtain of 110 m in depth, 35 m in top width, and 15 m in bottom width. All together 19 rows of boreholes were drilled (Cabanius and Margre 1958). Figure 9.31 shows the Pubugou Dam in the Daduhe River (China, $H = 186$ m) completed in 2010, whose closure cofferdam is a part of dam shell. The Pubugou Dam is a central core rockfill dam and constructed on the alluvium of maximum 75 m deep. Two concrete cutoff walls of 1.2 m thick are installed to control the under seepage in the dam foundation, and a concrete gallery is installed on the top of the cutoff walls for facilitating the curtain grouting below the wall and also for monitoring and maintenance during operation period.

The thickness T of grouting curtain is dependent on the allowable gradient $[J]$ to prevent the curtain from mechanical piping. The SL274-2001 “Design code for rolled earth-rockfill dams” stipulates that for general clay grouting $[J] = 3-4$. The curtain should be keyed deeper into impervious soil stratum at least 3–5 m or into bedrock at least 2 m, respectively. For deep multi-rows curtain, the thickness may be reduced from the maximum thickness T at the top to the minimum at the bottom. The hole and row centers should be decided by in situ tests, which are generally ranged within 1.5–3 m. The optimum mixture ratio of cement and clay in grout material should be tested, too. Usually the content of cement accounts for 20–50 % of the cement and clay by weight. The grouting pressure is also selected according to in situ tests.

Curtain grouting may be employed for deep treatment and locally particular treatment as well as strengthening remedy in addition to other treatments. However, curtain grouting is complex in construction technique, high in expenditure,

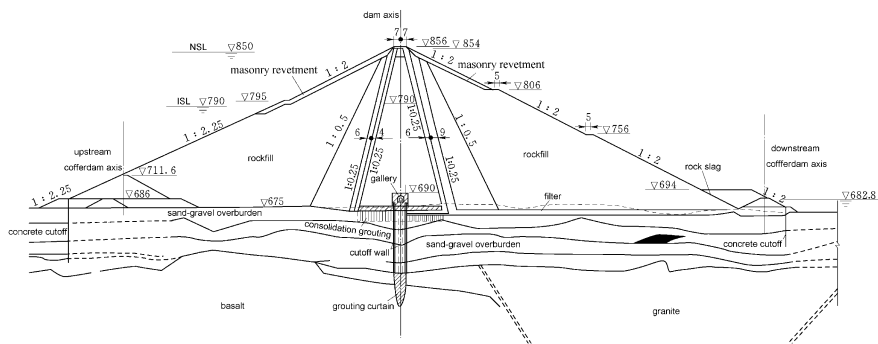


Fig. 9.31 The Pubugou Dam in the Daduhe River (unit: m) China, $H = 186$ m

necessity in overburden weight on surface. The applicability of curtain grouting for sand and gravel stratum is dependent on the gradation and permeability coefficient as well as the groundwater velocity and all these factors influence the injection and condense and control the grouting quality as well as cost. The SL274-2001 “Design code for rolled earth–rockfill dams” suggests a groutability ratio M for sand and gravel foundation as

$$M = \frac{D_{15}}{d_{85}} \quad (9.45)$$

where D_{15} = 15 % finer grain size of the grouted soil, mm; and d_{85} = 85 % finer grain size of the grout material, mm.

Generally, M should be greater than 15, but in some cases, it may be as low as 15, depending upon the physical properties of grouting materials. According to the filter principle, it also may be generally judged as: $M < 5$, no groutability; $M = 5-10$, poor groutability; $M > 10$, cement clay grouting; $M > 15$, cement grouting. After grouting, the permeability coefficient could be reduced down to $10^{-4}-10^{-5}$ cm/s.

Chemical grouting is applicable for all types of sand and gravel stratum (Karol 1990).

(e) Jet grouting

Jet grouting has a number of construction-related applications apart from groundwater control or cutoff, including structural underpinning, utility support, excavation support, temporary or permanent soft soil stabilization, slope stabilization, and hazardous waste containment control.

High-pressure spray grouting (Fig. 9.32) is a jet grouting technology invented by the Japanese engineers in the 1960s (Covil and Skinner 1992). After the 1980s, the technology has been widely exercised in China, particularly in the anti-seepage treatment for hydraulic structures. High-pressure spray grouting uses jets (2–3 mm in diameter) of high pressure (30–50 MPa), high velocity (100–200 m/s) to hydraulically erode, mix, and partially replace the in situ soil or weak rock with cementitious grout slurry. In this way, an engineered soil–cement product of high strength (compressive strength = 6.0–20.0 MPa) and low permeability ($10^{-5}-10^{-7}$ cm/s) is created. Jet grouting can be performed above or below the water table and in most strata ranging from non-cohesive soils to highly plastic clays.

The procedure that is common to all jet grouting involves first drilling to the planned depth using small diameter drill rods. Next, a large and powerful pump is connected to the drill rod, which pumps the high-pressure jet grout through the drill rods and horizontally into the soil. The drill rods are slowly rotated and raised creating columns of soil–cement material (Fig. 9.33). The shape of the grouted zone can be changed by directing the grout in the manners that create panels, floors, or other shapes. Jet grouting has three basic types according to the movement during the raising of drill rods: rotary spray, pendulum spray, and directional pray (Fig. 9.32b).

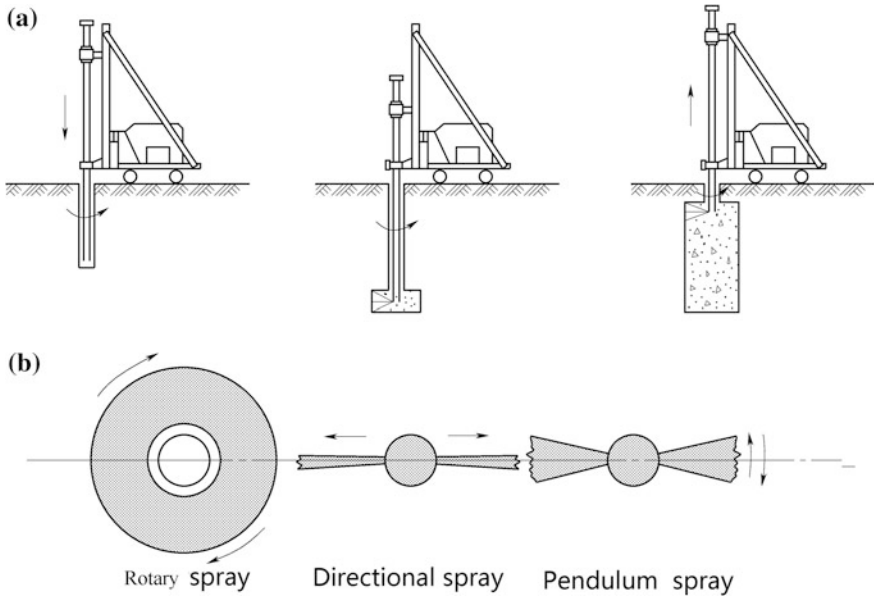


Fig. 9.32 High-pressure spray grouting. **a** Diagram of high-pressure spray grouting; **b** types of jet grouting

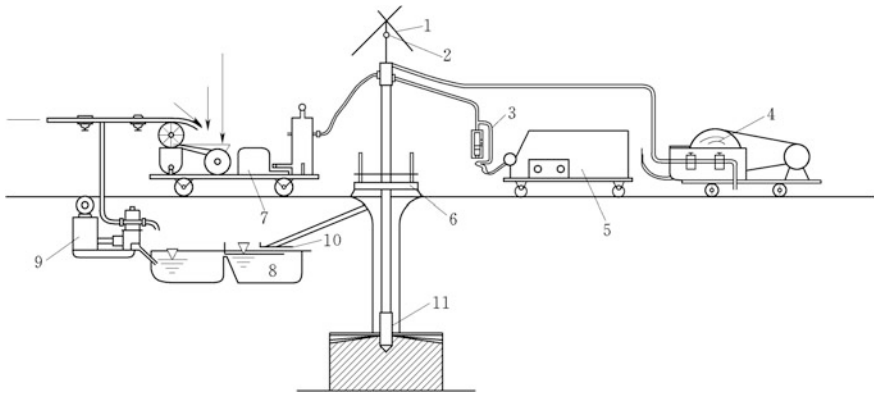


Fig. 9.33 Equipments for high-pressure spray grouting. 1 tripod mounting; 2 hoisting machine; 3 rotometer; 4 high-pressure jet pump; 5 air compressor; 6 device in the top of the drilled hole; 7 grout mixer; 8 stuff chest; 9 return pump; 10 sieve; 11 nozzle

2. Horizontal anti-seepage devices

Where a complete cutoff is not required or is too costly, an upstream impervious blanket tied into the impervious core of the dam may be employed to minimize the under seepage, as shown in Fig. 9.34.

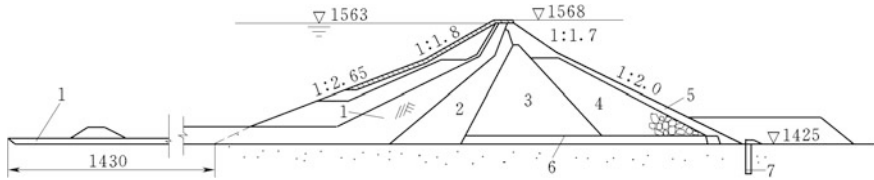


Fig. 9.34 An embankment dam with upstream blanket and downstream drainage. 1 blanket and sloping core; 2 transition zone; 3 major dam body; 4 rockfill; 5 slope protection; 6 drainage; 7 relief well

Impervious blanket may sometimes provide adequate control of under seepage for low-head structures. For high-head structures, it is usually necessary to incorporate downstream drainage system as a part of the overall seepage control design. The benefits derived from the impervious blanket are attributable to the dissipation of a part of the reservoir head through the blanket. The proportion of head dissipated is dependent upon the thickness, length, and effective permeability of the blanket in relation to the permeability of the foundation stratum. A filter is normally installed between the blanket and foundation.

The absolute permeability of the blanket soil should be lower than 10^{-5} cm/s, and the relative permeability of the blanket to the foundation material should be below 0.01–0.001. Since the material of the blanket is so tight in relation to the pervious stratum, it is not necessary to consider the flow through the blanket in determining the blanket length. The discharge of under seepage is somewhat less than inversely proportional to the total length of the impervious blanket. The thickness of blanket should vary linearly from 0.5–1.0 m at its upstream edge to the maximum where it adjoins the impervious core of the embankment. At any section the blank thickness may be determined by the allowable gradient of the blanket material. Where the length of the blanket exceeds 6–8 times of head, the additional reduction of seepage is not significant by further elongating the blanket. Therefore, the blanket length ordinarily does not exceed 10 times of the pounded water head. However, in case of fine sand or silty foundation strata, the length of blanket may be stretched as long as 15 times of the head.

Downstream control measures (relief wells or toe trench drains) are generally demanded for a combined use with upstream blanket to control the under seepage and/or to prevent excessive uplift pressure and piping through the foundation.

Upstream impervious blanket should be cautiously employed when the reservoir head exceeds 50 m because the high hydraulic gradient exerting across the blanket may result in piping and serious leakage.

To strengthen the seepage reduction effective, many embankment dams use additional composite geomembrane on the upstream face and reservoir surface (ICOLD 2010). This has been exercised for over 20 years in the embankment dam construction of China.

3. Draining measures

Drains are intended to relieve the seeping water through the embankment and to prevent excessive uplift pressure in the foundation. Embankment drains may be distinguished as horizontal drain, trench drain, relief well, and seepage berm, etc.

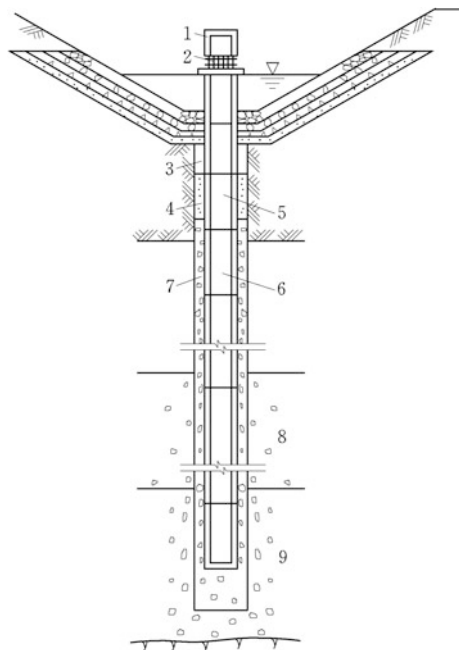
The use of horizontal drain may significantly reduce the uplift pressure in the downstream portion of the dam foundation. However, the use of the horizontal drain also increases the seepage discharge through the dam.

Where it is not feasible to construct a complete cutoff or an upstream impervious blanket is installed, a downstream seepage berm may be used to reduce uplift pressure. Relief wells or toe trench drains are often employed in combination with the downstream seepage berm.

A trench drain generally contains a perforated collector pipe and backfilled with filter material. The trench drain is applicable where the top impervious stratum is thin and the pervious foundation is shallow so that the trench can penetrate into the underneath aquifer. A trench drain also provides a means of measuring seepage discharge and of detecting the location of any excessive seepage.

Where the underlying pervious stratum is too deep, a trench drain of practical depth would only attract a small portion of under seepage. The detrimental under seepage would bypass the drain and emerge downstream of the drain, thereby undermine its function. Under such circumstances, relief wells are better than trench drains, which are installed along the downstream dam toe (Fig. 9.35). However, relief wells may increase under seepage discharge by 20–40 %, depending upon the

Fig. 9.35 Structure of a relief well. 1 well cover; 2 outlet; 3 backfill concrete; 4 backfill sand; 5 ascending tube; 6 porosity pipe; 7 filter; 8 sandy gravel; 9 sand and cobble



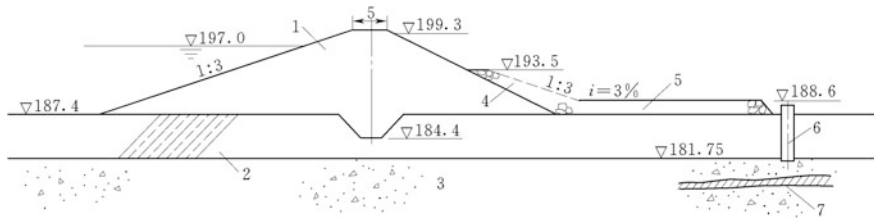


Fig. 9.36 Weighted filter cover + relief well + berm the Taipingghu Dam (China, $H = 12.3$ m). 1 silty clay; 2 heavy silt loam; 3 sandy gravel layer; 4 gravel; 5 seepage berm; 6 relief well; 7 weak seam

foundation conditions. Relief wells may be used in combination with other control measures such as upstream impervious blanket or downstream seepage berm. The relief wells surrounded by filter, if necessary, should penetrate into the principal pervious stratum at least its 50–100 % thickness for obtaining effective pressure relief, especially where the foundation is stratified. The wells, including screen and riser pipes, should possess a diameter which will permit the maximum design flow without excessive head losses, in no instance should the well's diameter be smaller than 15 cm.

Relief wells should be so located that their tops are accessible for cleaning, sounding for sand, and pumping to determine discharge capacity. Seeping water from relief wells should be delivered into open ditches or into collector system outside of the dam base which are independent of toe drains or surface drainage system. Experience with relief wells indicates that with the ongoing of time, the discharge of the wells will be gradually reduced due to clogging of the well screen and/or reservoir siltation. Therefore, the amount of well screen area should be oversized and a piezometer system should be installed between the wells to monitor the seepage pressure, and if necessary, additional relief wells should be driven.

To protect weak pervious soil at the downstream toe, if the relief wells are not installed, weighted filter cover may be placed to counterbalance the uplift beneath the stratum, whose length is customarily decided by the residual head at the end of the filter cover, which should be lower than the allowable gradient.

The combined utilization of the weighted filter cover and relief wells in the Taipingghu Dam (China, $H = 12.3$ m) is shown in Fig. 9.36.

9.9.3 Earth Foundation

The design of dams on fine-grained soil or earth foundation is tightly related to the shear strength of the foundation soil. For a weak foundation, use of stage construction, foundation strengthening, or removal of undesirable materials by excavation may be more economical than the use of flattened embankment slopes or stability berms.

After clearing and stripping, the foundation surface will be in a loose condition and should be compacted. However, if the silty or clayey foundation soil has a high water content and high degree of saturation, attempts to compact the surface with heavy sheep's foot or rubber-tired rollers will only remold and disturb the soil. Therefore, only light weighted compaction equipment could be used.

For dams on impervious earth foundation without necessity of a cutoff, an inspection trench at a minimum depth of 1.5 m is desirable. This will permit inspection for soft pockets, tile fields, pervious zones, or other undesirable features not discovered by earlier exploration.

Significant differential settlement of embankment may lead to tension zones along the upper portion of the dam and possible transverse cracking along the longitudinal axis in the vicinity of steep abutment slopes. To minimize this risk, steep abutment slopes and foundation excavation slopes should be avoided, if feasible, particularly beneath the impervious zone of the embankment.

The treatment of earth foundation under a rockfill dam should be substantially the same as that for an earthfill dam. The surface layer of the foundation beneath the downstream rockfill shell must meet the filter gradation criteria, or a filter layer must be installed, so that seepage from the foundation does not carry foundation material into the rockfill.

1. Liquefiable fine sand materials and their treatments

Dam sites over active faults should be avoided. For the project located near or over the faults in earthquake areas, special geologic and seismologic studies should be performed, the embankment and critical appurtenant structures should be evaluated with regard to the seismic stability (Newmark 1965).

China is situated between the two large active seismic belts in the earth crust and is a country with high seismicity risk. Since the beginning of the twentieth century to the end of 1996, there had been more than 3000 destructive earthquakes with magnitude greater than 5 occurred in China, 792 with magnitude greater than 6, 117 with magnitude greater than 7, 9 with magnitude greater than 8.

A majority of dams of medium and small size erected in China up to date are embankment dams, which are widely distributed over the country and more likely susceptible to earthquake damage. According to the incomplete statistic data during the Tangshan earthquake in 1976, among 412 reservoirs located in this region, almost 81 % of them were damaged, of which embankment dams accounted for 94 %.

(a) Baihe Dam of the Miyun Reservoir

The Miyun Reservoir is situated at the confluence of the Chaohe River and the Baihe River in the suburb of the Beijing City, China. The main dam, 66 m high and 960 m long at crest, consists of sand-gravel dam shell and sloping core. The core with an outer slope of 1:2.35 is composed of medium to heavy silty loam and covered with a thin surface layer of sand and gravel, forming an upstream face with a slope of 1:3. Foundation is on an alluvium of sand and gravel with the overburden depth of 44 m. A combination of concrete cutoff wall and grouting curtain is used to

controlling the under seepage. Shaking intensity in the vicinity of the dam was VI during the Tangshan earthquake; horizontal peak accelerations of 0.05 and 0.14 g were recorded on the downstream toe and on the dam crest, respectively. During the earthquake, a large slope sliding took place at the upstream face of sand and gravel, which had been compacted to a relative density of about 55 %. The slope sliding covered a wide area of about 60,000 m² with the volume of about 150,000 m³.

Just after the earthquake, settlements and displacements of the dam were measured. The maximum settlement was 59 mm and the maximum displacement in the downstream direction was 28 mm. No other damages such as cracks and abnormal seepage were found.

After comprehensive study, it is concluded that the slip movement was resulted from liquefaction of the protection layer with sand and gravel. This layer, even with a gravel content of 60 % and compacted moderately, is vulnerable to the loss of strength at relatively low acceleration levels for a duration of about 2 min.

(b) Douhe Dam

The dam of Douhe Reservoir, about 160 km northeast of Tangshan (Hebei Province, China), is a homogeneous embankment at maximum height of 22 m and with a crest length of 6115 m. The materials used for dam embankment are silt and clay with plasticity index 7–10. The average dry density of the compacted embankment is 1.88 t/m³. The dam was completed in 1956, and in 1970, it was raised additional 2 m. The materials added on the top portion of the dam were debris from spillway excavation, silt, and clay, which were poorly compacted. Beneath the dam, the upper portion of the foundation within a depth of 5–7 m is composed mostly of soft silt and clay with some pockets of medium to fine sand, below which are thick inter-bedded strata of dense sand, silt, and clay. The maximum horizontal acceleration was about 0.4 g during the earthquake. The main damages manifested during the earthquake were extensive longitudinal cracking, crest settling, and heaving at the embankment toe. The blame was placed for these damages primarily on the liquefaction of the saturated silt and soft clay in the dam foundation. Fortunately, in spite of aforementioned damages to the embankment, there was no serious loss of water due to a very low reservoir water level (only 8 m deep) when the earthquake occurred.

One lesson learned from the foregoing and other earthquake damages to embankment dams is that the upstream surface layer composed of sand and gravel materials is more liable to liquefaction, if:

- The material is discontinuously graded and deficient in intermediate particles;
- The gravel content is lower than 70 %;
- The coefficient of permeability is lower than 10⁻² cm/s; and
- The relative density is lower than 0.6.

Another lesson learned is that due attention should be paid to the earthquake resistant properties of the foundation material. The saturated silt layer of particular thickness beneath dam is more vulnerable to liquefaction failure and is more probable to develop large differential settlements and transversal cracks in the dam.

The GB50287-2006 “Code for water resources and hydropower engineering geological investigation” recommends following guiding indices for the liquefaction potential:

- Geological age. For example, there is no liquefaction case reported in the Late Quaternary Pleistocene or earlier strata;
- Particle gradation. When the content of sand and gravel is over 70 %, the gravel skeleton has predominant role in the soil, which indicates the possibility of liquefaction;
- Relative density. According to the SL203-1997 “Specifications for seismic design of hydraulic structures,” if the relative density is over 75 %, liquefaction probability is lower under the earthquake action of 8 grade;
- Effective stress resulted from overburden weight. The larger of the effective stress is resulted, the higher of the liquefaction resistance will have; and
- Blow count of SPT. According to the SDJ10-1978 “Specifications for seismic design of hydraulic structures,” under the earthquake action of grade 8 or above, for the stratum under overburden depth 5, 10, and 15 m, the liquefaction will not occur if the blow count of SPT reaches 11, 20, and 26, respectively.

Available defensive measures with respect to material properties for the liquefiable soil foundations may be selectively employed as follows:

- Dewater the saturated soil. Try to bring down groundwater table and phreatic line within dam and abutments, in this way to transform a portion of saturated soil into unsaturated soil;
- Core materials should have a high resistance to erosion;
- Ensure the adequate densities for foundation sands (at least 70 % relative density). The measures include blasting, vibratory probe, vibro-compaction, heavy-tamping (dynamic compaction), of which the vibro-compaction is the most effective;
- Additional compaction of outer zones or shells will increase permeability and shear strength, respectively;
- Drain and pressure relieve. This is to create good conditions for quick dispersion of excessive pore pressure during seismic vibration. Vibro-replacement stone and sand columns are useful in this aspect;
- Ballast and enclosure using mix-in-place piles and walls. This is to strengthen the restraint on the liquefiable soil;
- Make the impervious zone more plastic. This is to prevent it from the failure due to the large deformation resulted from earthquake;
- Use pile foundation. It may transfer loads to reliable non-liquefiable soil stratum;
- Use grout to fill the voids of soil and to stabilize the soil skeleton;
- Removal of liquefiable soil; and

- Compact embankment shell to higher densities. For non-cohesive soils, at least 75 % relative density above the phreatic line and at least 75–85 % relative density below the phreatic line are demanded.

Available defensive measures with respect to structure elements which can enhance seepage control and liquefaction safety may be selectively employed as follows:

- Geometric considerations may be directed to use a vertical instead of inclined core, to wider dam crest, to increase freeboard, to flatten embankment slopes, and to flare the embankment at the abutments;
- Relatively wider transition and filter zones adjacent to the core and extending the full height of the dam are advisable; and
- It is demanded to locate the spillway and outlet works on rock rather than in the embankment or foundation overburden.

Based on the case studies of earthquake damage to dams in the world and in China, the specifications (DL5073-1997) puts forward following major recommendations and general suggestions for the aseismic design:

- For embankment dams in earthquake regions, straight axis or upstream curved axis should be adopted, whereas downstream curved, broken-line, or S-shaped axes should be avoided;
- When the design earthquake intensity is 8 or 9, rockfill embankment type should be selected, and rigid core wall should not be employed as impervious element. When a homogeneous dam is to construct, the internal drainage system should be installed to bring down phreatic line;
- When the design earthquake intensity is 8 or 9, the additional settlement of the dam and foundation soils under seismic action should be incorporated in determining the freeboard;
- The surge height due to earthquake should be incorporated in determining the freeboard of embankment dams. It may be ranged within 0.5–1.5 m, according to the design intensity and water depth in front of dams;
- The surge wave resulted from massive bank caving and slope failure, which is probably triggered by earthquakes, should be investigated specially;
- When the design earthquake intensity is 8 or 9, a widened dam crest and flattened slope at upper portion should be adopted;
- The watertight elements should be strengthened, especially at the dam crest and the adjoining of dam with rigid structures (e.g., bank slope and concrete dam), where cracks are liable to occur. On the upstream and downstream sides of these elements, filters and transition zones should be widened properly;
- Well-graded soil materials with satisfactory earthquake resistant and relatively strong seepage stability are desired. Uniform medium sand, fine sand, silty sand, and silt should not be served as embankment materials;
- Filling density of cohesive soil, as well as its compacting function and design porosity, should be determined in accordance with the relevant provisions,

specified in the SDJ218-84 “Specifications for design of rolled embankment dams” and its supplementary stipulations;

- In the compaction of non-cohesive soil, the relative density of material above the phreatic line should not be lower than 0.75, and that below the phreatic line should be 0.75–0.85. For a sand and gravel material, if the content of coarse grains greater than 5 mm is lower than 50 %, the relative density of fine grains shall meet the compaction requirements for non-cohesive soils as mentioned foregoing; and
- For the embankment dams of grade 1 and 2, buffed conduit below the dam should not be installed. If it is inevitable, reinforced concrete conduit or cast iron pipe should be employed and placed in the bedrock trench. Anti-seepage and sealing for the joints in the conduit should be reliable, and the control valve of the conduit should be installed at the upstream intake.

2. Treatment for soft clay and collapsible loess foundation

There are no consistent understanding and standard for the definition of soft soil. The “Manual of engineering geology” (China) defines the soft soil as a plastic clay in the state of soft plastic to flow, high natural water content, high compressibility, low bearing capacity. The “Technical code for railway engineering design” (China) proposes the indices for soft soil as large natural water content, or approaching liquid limit; porosity ratio $e > 1.0$; compressive modulus $E_s < 4000$ kPa; SPT blow count $N_{63.5} < 2$; static sounding penetration resistance $P_s < 700$ kPa; undrained strength $c_u < 25$ kPa. The JTJ0170-96 “Technical code for design and construction of highway embankment on soft ground” stipulates the indices for soft soil as natural water content $\omega \geq 35$ %, or $\omega \geq$ liquid limit; natural porosity $e > 1.0$; vane-shear strength $S_u < 35$ kPa; static sounding penetration resistance $P_S \approx 750$ kPa. In addition, Table 9.5 also may be referred to in the definition of soft soil for hydraulic structures.

Cohesive soft clay and collapsible loess are usually not qualified as embankment dam foundation, except the dam being low and the foundation being treated properly. However, a homogeneous dam may be constructed on the soft foundation, the moisture content of earthfill should be a bit higher of optimum moisture content, to have sufficient plasticity for better adaptability to the foundation settlement. Only low dams may be constructed on collapsible loess foundation subject to good

Table 9.5 Definition of soft soil

Stratum	Cumulosol and lutaceous foundation		Chiltern foundation
Thickness (m)	<10	>10	<10
Blow count of SPT (N)	<4	<5	N/A
Unconfined compressive strength (kPa)	<60	<100	N/A

treatments including excavation removal, turned over and suppression, dynamic compaction, presoak, etc., to eliminate or to reduce its collapsibility.

Large difference in the stress–strain characteristics of the embankment and foundation may lead to progressive failure. Therefore, where a dam has to be constructed on weak and compressible foundation, the embankment and foundation materials should have stress–strain relations as similar as possible.

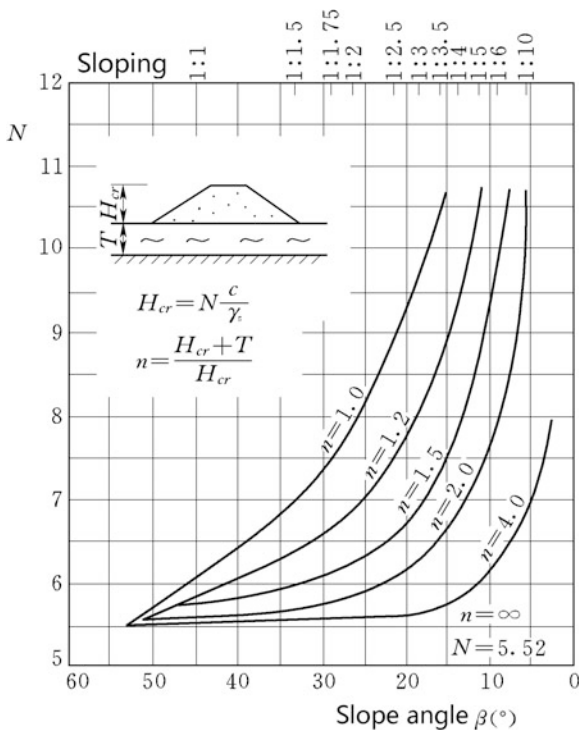
For a lower embankment dam on weak and compressible foundation, the blow count of SPT should be used to justify its limited height, and effective treatments should be carried out before the embankment compaction.

The limit height of embankment dam may be evaluated using plastic flow or analysis of stability against sliding. In case of soft soil foundation with $\varphi = 0^\circ$, the limit height of embankment dam may be evaluated by

$$H_{cr} = N \frac{c}{\gamma_s} \tag{9.46}$$

where H_{cr} = limit height of embankment dams; N = stability parameter selected from Fig. 9.37, which is from the computations using the Swedish arc method; c = cohesion of soil from direct shear (Q) or triaxial (UU) test; and γ_s = volumetric weight of the earthfill.

Fig. 9.37 Diagram to the computation of limit height of embankment dam on soft soil foundation



The parameter n at the curve in Fig. 9.37 is defined as

$$n = \frac{H_{cr} + T}{H_{cr}} \tag{9.47}$$

where T = overburden depth of soft stratum.

Since n is in turn the function of H_{cr} and T , trial-and-error iteration is conducted to get H_{cr} .

If a dam higher than the limitation indicated by Eqs. (9.46) and (9.47) is constructed on the soft foundation, reinforcement measurements are required, including:

- ① Earth cushion;
- ② Sand drain preloading;
- ③ Vibro-flotation or vibration and substitution;
- ④ Heavy-tamping;
- ⑤ Shallow or deep mixing;
- ⑥ Geosynthetics reinforcement; and
- ⑦ Mounting stress platform.

Methods ①–⑤ are generally exercised in the foundation treatment of building, retaining wall, barrage, and sluice. For long-axis structures such as levee and road, since the methods ①–⑤ could be costly and elongate the construction period, the mounting stress platform could be a good choice, and the geosynthetics reinforcement is another good alternative, too, to achieve low cost and short construction schedule.

The sand wells used in soft foundation treatment (Fig. 9.38) are usually 30–40 cm in diameter and arranged in grid pattern, the wells are spaced 2–3 m apart. Coarse gravel is filled in the wells below the dam toe drainage prism, if any, and on their top, a rough sand cushion of about 1 m thick is installed.

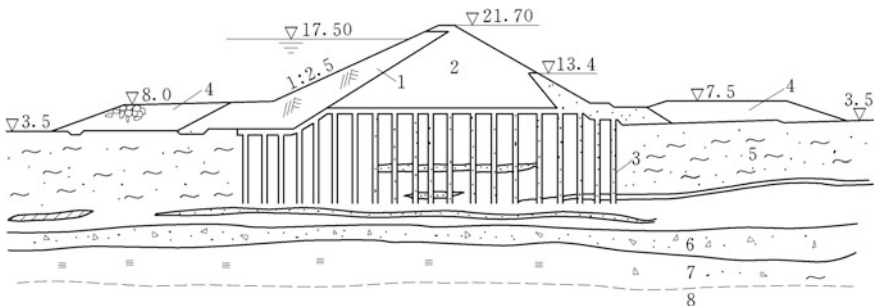


Fig. 9.38 Sand well treated soft foundation of an earth dam. 1 clay sloping core; 2 loam dam body; 3 sand well; 4 suppression layer; 5 mucky clay; 6 coarse sand mixed with a small amount of crushed stone; 7 silty soil; 8 gravel mixed with a small amount of sand

9.10 Connection of Embankment Dam with the Other Structures

9.10.1 Connection of Embankment Dam with Foundation and Abutments

1. Foundation

Cleaned areas of the foundation provide the surfaces beneath the dam with particular care called at the connecting of core and filters. It is a good practice to carry out both a preliminary and a final cleanup of these areas. The purpose of the preliminary cleanup is to facilitate the inspection and identification of the locality that require additional preparation and treatment. Within these local areas, all irregularities should be removed or trimmed during the final clean up.

Earth- and rockfill dams, particularly those that in glaciated regions, may have to be founded on the preglacial valley with pervious alluvial or morainal deposits. Under seepage control, such earth foundation is actualized by extending the upstream impervious blanket in the lateral direction to wrap the abutments up to the maximum water surface elevation, by placing a filter layer between the pervious abutments and the dam shell downstream of the impervious core, and, if necessary, by installing relief wells at the downstream toe of the pervious abutments.

2. Abutments

Connection should avoid to tie into narrow ridges formed by hairpin bends in the river or to tie into abutments that diverge in the downstream direction. Grouting may be demanded to reduce bypass seepage through the abutments. Zones of weak materials in abutments such as weathered overburden and talus deposits are frequently encountered. It may be more economical to flatten embankment slopes for attaining the desired stability than to excavate these weak materials deep down to bedrock. Adequate surface drainage should be installed at the juncture between the dam slope and the abutment.

Flat abutments are desirable to avoid possible tension zones and resultant transverse cracking in the embankment, but this may not be economically feasible where the abutment slopes are too steep and high. Under such circumstances, the core and filter as well as transition zones should be widened at locations of possible tension zones attributable to differential settlements. Widening of the core may not be directly effective unless cracks developing in the core tend to close. Since materials in the filter and transition zones are more self-healing, an increased width of these zones is significantly beneficial. Whenever possible, construction of the top portion of the embankment adjacent to steep abutments should be delayed until significant embankment and foundation settlements have completed.

Where an abutment slope is steep or change abruptly (e.g., benches or vertical faces), it may be advisable to compact soils on the wetter side of optimum water

content in the upper portion of the embankment, to eliminate cracking risk due to large differential settlements.

Several successful examples do exist with regard to steep dam abutments: the Baihe Dam in the Miyun Reservoir (China, $H = 66$ m) (Fig. 9.30), the rock abutment slope is 1:0.3; the Blue Mesa Dam (USA, $H = 120$ m), the rock abutment slope is 1:0.1–1:0.2. Their successes are mainly contributed to:

- Advancement of modern roller facilities and construction techniques, which provides high construction quality, high compaction density, and tight dam/abutment contact;
- Use of higher placement water contents combined with flared core sections to fit large differential settlements near abutments; and
- High-quality design and construction of filter.

In some cases, however, it may be more economically feasible to flatten abutments. A steepest slope of 1:0.5–1:0.75 for rock abutment or 1:1.5 for soil abutment may be acceptable. The additional cost of abutment flattening due to excavation and refilling may be offset partially by the reduction in abutment grouting.

9.10.2 Connection of Embankment Dam with Adjacent Concrete Structures

1. Outlet works (towers and conduits)

Where the dam foundation consists of high compressible soil, the outlet works should be founded upon or in a stronger abutment soil or rock. When a conduit is laid in the excavated trench in soil foundation, concrete anti-seepage collars should not be installed for the purpose of strengthening seepage resistance, since their presence often results in poor compacted backfill around the conduit. Collars should be considered only as necessary to couple pipe sections or to accommodate differential movement on yielding foundations. Excavation for an outlet conduit in soil foundation should be wide enough to allow for backfill compaction parallel to the conduit using heavy rolling compaction equipment.

Excavated trench slopes in soil for conduits should be not steeper than 1:2, to facilitate adequate compaction and to secure reliable bonding of backfill with the sides of the trench. Drains should be provided around the conduit in the downstream zones of embankment without pervious shell. A concrete cap should be used as backfill for cut-and-cover conduit within the core zone to ensure a watertight bond between the conduit and vertical rock surfaces.

For the embankment having a random or an impervious downstream shell, horizontal draining layers should be placed along the sides and over the top of the conduit downstream of the core.

2. Concrete dams

The contact face of embankment and concrete dam is vulnerable to the settlement difference and concentrated seepage. Basically, the connection of embankment and concrete dam may make use of keys and wing walls.

(a) Keys

Keying is a simple way as shown in Fig. 9.39. The concrete dam monolith contracts from the contact face and keys into the embankment and eventually becomes a stiff concrete core wall for the embankment. The Shasta Dam (USA, $H = 183$ m) starts the contact of its concrete monolith with embankment at the height of 48 m, whose cross section finally contracts into a concrete core wall of 1.5 m wide at top and 3.0 m wide at base. The Miyagawa Dam (Japan, $H = 42$ m) keys concrete monolith into embankment in a form of three segments with downstream slope 1:0.5, 1:0.3, and 1:0.1, respectively. It finally becomes a concrete core wall of 1.5 m wide at top, and with up- and downstream slopes of 1:0.1, keying into the central core of the embankment.

Since this kind of connection gives rise to a long-stretched embankment to wrap concrete dam monoliths, it is normally not suitable for medium to high dams, particularly in case where there are wide spillway dam monoliths on the riverbed. The anti-seismic resistance is often suspicious for such structure, too. The Sandaoling Dam (China, $H = 24$ m) connects the concrete monoliths to the embankment at height of 17.0 m using key structure. This dam is 18 km from the epicenter of the Haicheng earthquake with intensity of 8, when the reservoir level was 7 m below the dam crest. After the earthquake, a long stretch of crack with width of 3–15 cm was found on the dam crest. The earthfill shell outside of the concrete key had a settlement of 60–70 cm. The clay on the two sides of the concrete key had a settlement of 8 cm, which gave rise to a visible crack of 1 m deep along the contact face.

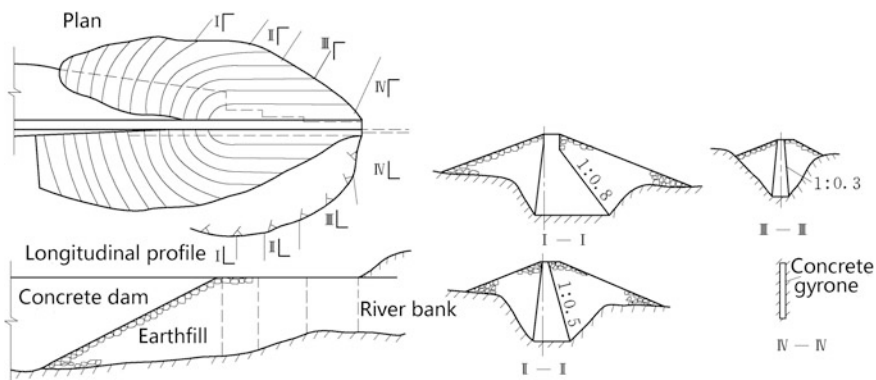


Fig. 9.39 Keying structure

(b) Wing walls

At the conjugate place, a retaining wall may be installed which stretches up- and downstream in a form of wing wall, this is the common type of embankment dam connection with ship lock or spillway dam monoliths. To obtain tight contact with high seismic resistance, such wing walls may be designed according to the following guidelines:

- That the wall possesses gentle rear slope around 1:0.5. In this way, the embankment height may be gradually varied, to prevent settlement induced cracking;
- That the anti-seepage devices are enlarged for larger contact surfaces. For example, the Shijushida Dam (Japan, $H = 50$ m) has a central core with up- and downstream slope of 1:0.5.
- That the filter is installed within several meters at the conjugate. Along the downstream portion of the wing wall of the Shijushida Dam (Japan, $H = 50$ m), a filter of 2.0 m wide and 1.0 m in deep is installed, which is connected with the filter of the central core; and
- That the conjugate surface is inclined. The Gosho Dam (Japan, $H = 60.7$ m) has a wedged type of conjugate surface (Fig. 9.40a) whose slope is 1:0.65. Under the pressure from reservoir water, the contact face is pressed tightly. The Eigenji Dam (Japan, $H = 68$ m) uses curved contact surface (Fig. 9.40b), the soil may be settled down along the curved surface while maintaining the contact in case of large shear deformation.

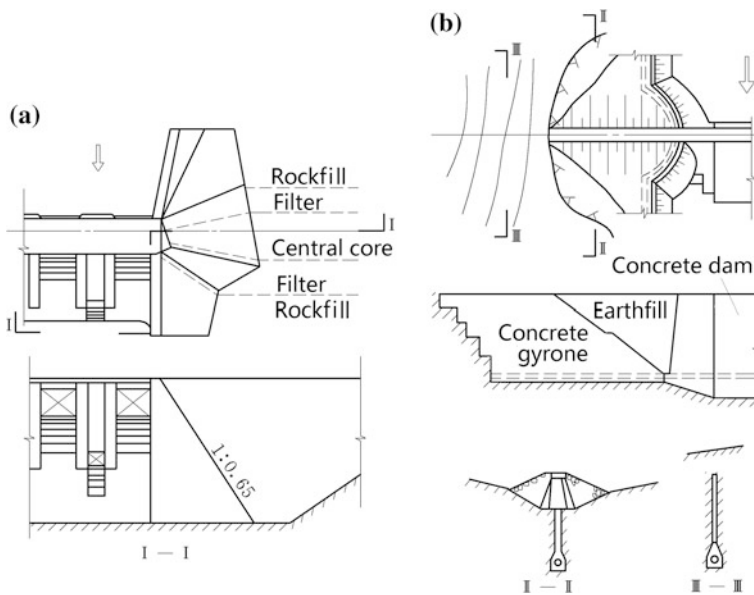


Fig. 9.40 Wing wall structures. a The Gosho Dam; b the Eigenji Dam

9.11 Selection of Embankment Types

Site conditions that may lead to the earth- or rockfill dam rather than a concrete dam include a wide stream valley, lack of solid rock abutments, considerable depths of soil overlying bedrock, poor-quality bedrock from a structural standpoint, availability of sufficient amount of suitable soils or rocks, and existence of a good site for a spillway of sufficient capacity. In China, although the proportion of embankment is low in all completed high dams, yet embankments account for predominant ratio of all dams in the country, and in the near future, there will be an apparent tendency to construct more and higher embankment dams. This is mainly attributable to the advancement in the design theory and construction technology for high embankment dams, and suitable dam sites for high concrete dams become more and more scarce.

The homogeneous type is remarkably advantageous in its simplicity for design and construction and is recommended where the lack of free-draining materials make the construction of a zoned embankment uneconomical. The soils for homogeneous dams usually have lower permeability coefficient, which will give rise to excessive pore pressure during construction. In addition, the shear strength of the homogeneous abutment soil is also relatively lower. All these result in its fat profile, and correspondingly, a larger amount of material should be placed. Homogeneous type is prevalent in lower or small embankment construction. A homogeneous dam may have seepage control devices such as chimney and blanket drains, accompanied with transition zones between the main embankment fill and the drains. Even if a homogeneous embankment has no specific seepage control devices, it must have adequate internal drainage capability against seepage outbreak on the downstream slope or abutments.

A high embankment dam needs large quantity of soil materials. Where several distinctively different materials are available from excavation and borrow areas, more complex embankment zoning may be employed, and the most economical type of dam will often be the one for which materials can be found within a reasonable hauling distance from the site, including materials which must be excavated for the dam foundation, spillway, outlet works, powerhouses, and other appurtenant structures. If suitable soils for an earthfill dam can be found in the nearby borrow pits, it may prove to be more economical. On the contrary, the availability of suitable rocks may in favor of a rockfill dam.

Sloping core and central core of soil are the most prevalent zoned embankment dams. The sloping core may be linked easily to the horizontal anti-seepage devices such as horizontal impervious blanket, while the central core may be linked easily to the vertical anti-seepage devices such as cutoff wall. Near the upstream face, the sloping core has advantage of less construction interference because it permits construction of pervious downstream shells during wet seasons with later placement of the sloping impervious zone during dry seasons. However, lower permeability and strength materials near upstream give rise to more flat upstream slope and larger

sectional profile. Sloping core is also sensitive to the settlement of the dam, which make it difficult to be connected with steep abutments.

Very often, but not always, topography influences the first choice of dam type. The possibility of tensile cracking resulted from arching in narrow valleys and shear cracking in the vicinity of steep abutments must be investigated and may play a role in the selection of the dam type. As a general rule, a relatively narrow valley would suggest a central core dam. Embankment dams higher than 200–300 m are nearly all equipped with central core, such as the Nurek Dam (Tajikistan, $H = 300$ m), the Jinpen Dam (China, $H = 133$ m), the Nuozhadu Dam (China, $H = 261.5$ m), and the Pubugou Dam (China, $H = 186$ m). To improve the stress state and to eliminate the arch effect in core, inclined central core is more and more prevailing, such as the Rogun Dam (Tadzhikistan, $H = 335$ m) and the Xiaolangdi Dam (China, $H = 160$ m).

The geologic features at the dam site may dictate a suitable type of embankment dam, too. Gravel foundations, if well compacted, are suitable for earth- or rockfill dams, on conditions that special precautions must be taken to provide adequate and effective under seepage cutoffs or seals and that the liquefaction potential and corresponding countermeasures, if any, should be fully investigated. Silt or fine sand foundations can be dammed using earthfill type but are not suitable for rockfill type. The main problems arising from these foundations are significant settlements, excessive percolation losses, risks of piping, and erosion. Earthfill dams may be founded on clay foundations, too, but flattened embankment slopes are necessitated due to the lower shear strength of the foundation materials. Because of too excessive flat slopes and the tendency of much larger settlements, clay foundations are generally not applicable to rockfill dams.

Climatic conditions dominate in many aspects the selection of embankment type. In regions where there are a lot of rainy days, preference is given to dams with pervious dam shell, and sloping core is advantageous over central core, for the former enables the pervious dam shell to be constructed in rainy seasons while the sloping core in dry seasons. Asphalt concrete face, concrete face, or geomembrane is also suitable in the areas of long raining season.

The purposes and operation conditions also may have influence on the selection of embankment type. For example, if the reservoir level varies frequently and in large extent, soil-sloping core is not suitable due to the upstream dam slope stability problem induced by sudden drawing down of the reservoir.

Recently, environmental considerations have become very important in the selection of embankment type. The principal environmental concerns on the embankment selection can affect the type of dam, its dimensions, and location of the anti-seepage devices. For example, the worries over the detrimental environment impact due to the borrowing of impervious soils on steep limestone valleys had considerable influence on the final decision to use CFRD in lieu of central core rockfill dam, for the Shuibuya Project (China, $H = 233$ m).

In conclusion, the final selection of the type of an embankment dam project should be made only after the careful analysis and comparison of possible alternatives, and after thorough economic analysis that consists of the costs of spillway, power and control structures, as well as foundation treatment.

References

- Acker RC, Jones JC (1972) Foundation and abutment treatment for rockfill dams. *J Soil Mech Found Div* 98(SM 10):995–1015
- Bell JM (1968) General slope stability analysis. *J Soil Mech Found Div* 94(SM6):1253–1270
- Biot MA (1941) General theory of three dimensional consolidation. *J Appl Phys* 12(2):155–164
- Bishop AW (1955) The use of slip circle in the stability analysis of slopes. *Geotechnique* 5(1):7–17
- Bishop AW, Morgenstern N (1960) Stability coefficients for earth slopes. *Geotechnique* 10(4):129–150
- Bowen R (1981) *Grouting in engineering practice* (2nd edn). Applied Science, New York
- Brinkgreve RBJ (2005) Selection of soil models and parameters for geotechnical engineering application. In: Yamamuro JA, Kaliakin VN (eds) *Geotechnical special publication*, No. 128. ACSE, pp 69–98
- Bussey WH (1961) Control of seepage through foundation and abutments of dams. *Foundation evaluation and treatment. Casagrande Geotechnique* 11(3):161–182
- Cabanius J, Margre R (1958) The Durance development—the Serre-Ponçon dam. *Travaux* 286:43–60
- Cambefort H (1977) The principle and applications of grouting. *Q J Eng Geol* 10(2):57–95
- Casagrande A (1961) First rankine lecture—control of seepage through foundations and abutment of dam. *Géotechnique* 11(3):161–182
- Chen SH, Chen ML (2014) *Hydraulic structures* (2nd edn). China WaterPower Press, Beijing (in Chinese)
- Covil CS, Skinner AE (1992) Jet grouting—a review of some of operating parameters that form the basis of the jet grouting process. *Grouting in the ground*. In: Bell AL (ed) *Proceedings of conference ICE*. Thomas Telford, London, pp 525–538
- Craig RF (2004) *Craig’s soil mechanics*, 7th edn. Spon Press, London
- D’Appolonia DJ (1980) Soil-bentonite slurry trench cutoffs. *J Geotech Eng Div* 106(4):399–417
- Dachler R (1936) *Grundwasserströmung*. Springer, Wien (in German)
- Day RW (2006) *Foundation engineering handbook*. McGraw-Hill, New York
- Duncan JM, Chang CY (1970) Nonlinear analysis of stress and strain in soils. *J Soil Mech Found Div* 96(SM5):1629–1653
- Duncan JM, Wright SG (2005) *Soil strength and slope stability*. Wiley, Hoboken
- Dupuit J (1863) *Estudes Théoriques et Pratiques sur le mouvement des Eaux dans les canaux découverts et à travers les terrains perméables*, 2nd edn. Dunod, Paris (in French)
- Fang HY (ed) (1991) *Foundation engineering handbook*. Van Nostrand Reinhold, New York
- Fellenius W (1927) *Erdstatische berechnungen mit reibung und kohäsion und unter annahme kreiszylindrischer gleitflächen* (Statistical analysis of earth slopes and retaining walls considering both friction and cohesion and assuming cylindrical sliding surfaces). W Ernst und Sohn, Berlin (in German)
- Fellenius W (1936) Calculation of the stability of earth dams. In: *Proceedings of the second congress of large dams*, vol 4. ICOLD, Washington DC, pp 445–463
- Forchheimer P (1886) Über die Ergiebigkeit von Brunnen-Anlagen und Sickerschlitzten. *Z. Architekt. Ing.-Ver. (Hannover)* 32:539–563 (in Germany)
- Foster M, Fell R, Spannagle M (2000) The statistics of embankment dam failures and accidents. *Can Geotech J* 37(5):1000–1024
- Gens A, Potts DM (1988) Critical state models in computational geomechanics. *Eng Comput* 5(3):178–197
- Giroud JP (1989) Are geosynthetics durable enough to be used in dams? *Water Power Dam Constr* 41(2):12–13
- Giroud JP (1992a) Geosynthetics in dams: two decades of experience. *Geotech Fabrics Rep* 10(5):6–9
- Giroud JP (1992b) Geosynthetics in dams: two decades of experience. *Geotech Fabrics Rep* 10(6):22–28

- Golzé AR (1977) Handbook of dam engineering. Van Nostrand Reinhold Company, New York
- Grishin MM (ed) (1982) Hydraulic structures. Mir Publishers, Moscow
- Guo CQ, Chen HY (1992) Embankment dams. Water Resources and Electric Power Press of China, Beijing (in Chinese)
- Hill D (1996) A history of engineering in classical and medieval times. Routledge, New York
- ICOLD (1986) Geotextiles as filters and transitions in fill dams (Bulletin 55). ICOLD, Paris
- ICOLD (1990) Dispersive soils in embankment dams—review (Bulletin No. 77). ICOLD, Paris
- ICOLD (1992) Bituminous cores for fill dams—state of the art (Bulletin 84). ICOLD, Paris
- ICOLD (1993) Rock materials for rockfill dams—review and recommendations (Bulletin 92). ICOLD, Paris
- ICOLD (1999) Embankment dams with bituminous concrete facing (Bulletin No. 114). ICOLD, Paris
- ICOLD (2005) Dam foundations. Geologic considerations. Investigation methods, treatment, monitoring (Bulletin 129). ICOLD, Paris
- ICOLD (2010) Geomembrane sealings systems for dams (Bulletin 135). ICOLD, Paris
- Janbu N (1954) Applications of composite slip surfaces for stability analysis. In: Proceedings of European conference on the stability of earth slopes, vol 3. ISRM, Stockholm, pp 43–49
- Janbu N (1973) Slope stability computations. In: Hirschfeld RC, Poulos SJ (eds) Embankment dam engineering—casagrande volume. Wiley, New York, pp 447–486
- Jansen RB (1980) Dams and public safety, a water resources technical publication. CO (Water and Power Resources Service, Bureau of Reclamation, US Department of the Interior), Denver
- Jansen RB (1988) Advanced dam engineering for design, construction, and rehabilitation. Van Nostrand Reinhold, New York
- Jones JC (1967) Deep cut-offs in pervious alluvium, combining slurry trenches and grouting. In: Transactions, ninth international congress on large dams, vol I. ICOLD, Istanbul, pp 509–524
- Karol RH (1990) Chemical grouting, 2nd edn. Marcel Dekker, New York
- Leps TM (1970) Review of shearing strength of rockfill. *J Soil Mech Found Div* 96(SM4):1159–1170
- Lo KY, Kaniaru K (1990) Hydraulic fracture in earth and rock-fill dams. *Can Geotech J* 27(4): 496–506
- Mestat PH, Bourgeois E, Riou Y (2004) Numerical modelling of embankments and underground works. *Comput Geotech* 31(3):227–236
- Ministry of Water Resources of the People's Republic of China (2001) SL274-2001 “Design specification for rolled earth-rock fill dams”. China WaterPower Press, Beijing (in Chinese)
- Morgenstern NR, Price VE (1965) The analysis of the stability of general slip surfaces. *Geotechnique* 15(1):79–93
- National Reform and Development Commission of the People's Republic of China (2008) DL/T5395-2007 “Design specification for rolled earth-rock fill dams”. China Electric Power Press, Beijing (in Chinese)
- Newmark NM (1965) Effects of earthquakes on dams and embankments. *Geotechnique* 15(2): 139–160
- Nonveiller E (1965) The stability analysis of slopes with a slip surface of general shape. In: Proceedings of 6th international conference on soil mechanics and foundation engineering. University of Toronto Press, Montreal, pp 522–525
- Nonveiller E (1989) Grouting theory and practice. In: Developments in geotechnical engineering, vol 57. Elsevier Science Publisher, Netherland
- Novak P, Moffat AIB, Nalluri C, Narayanan R (1990) Hydraulic structures. The Academic Division of Unwin Hyman Ltd, London
- Ouria A, Toufigh MM, Nakhai A (2007) An investigation on the effect of the coupled and uncoupled formulation on transient seepage by the finite element method. *Am J Appl Sci* 4(12): 950–956
- Pavlovsky NN (1956) Collected works. Akad Nauk USSR, Leningrad
- Petterson KE (1916) Kajrasat i Gotenborg des 5te Mars 1916 (Collapse of a quay wall at Gothenburg March 5th 1916). *Tek Tidskr* (in Swedish)
- Petterson KE (1955) The early history of circular sliding surfaces. *Geotechnique* 5(4):275–296

- Qian JH, Yin ZZ (2000) Principle and computation of geotechnical engineering, 2nd edn. China WaterPower Press, Beijing (in Chinese)
- Roscoe KH (1970) The influence of strains in soil mechanics. 10th Rankine lecture. *Geotechnique* 20(2):129–170
- Ru NH, Niu YG (2001) Embankment dams. In: Accident and safety of large dams. China WaterPower Press, Beijing (in Chinese)
- Sarma SK (1973) Stability analysis of embankments and slopes. *Geotechnique* 23(3):423–433
- Sarma SK, Bhavé MV (1974) Critical acceleration versus static factor of safety in stability analysis of earth dams and embankments. *Geotechnique* 24(4):661–665
- Schmertmann JH (1970) Static cone to compute static settlement over sand. *J Soil Mech Found Div* 96(3):1011–1043
- Schnitter NJ (1994) A history of dams: the useful pyramids. Balkema AA, New York
- Schofield AN, Wroth CP (1968) Critical state soil mechanics. McGraw-Hill, New York
- Sherard JL, Dunnigan LP (1984) Filters for silts and clays. *J Geotech Eng* 110(6):927–718
- Sherard JL, Dunnigan LP (1985) Filters and leakage control in embankment dams. In: Volpe RL, Kelly WE (eds) Seepage and leakage from dams and impoundments. ASCE, New York, pp 1–30
- Sherard JL, Dunnigan LP (1989) Critical filters for impervious soils. *J Geotech Eng* 115 (GT7):927–947
- Sherard JL et al (1963) Earth and rockfill dams. Wiley, New York
- Smalley I (1992) The Teton dam: rhyolite foundation + loess core = disaster. *Geol Today* 8(1):19–22
- Snethlage JB, Scheidenhelm FW, Vanderlip AN (1960) Rockfill dams: review and statistics. *Transactions* 125(2):678–699
- Spencer E (1967) A method of analysis of the stability of embankments assuming parallel interslice forces. *Geotechnique* 17(1):11–26
- Spencer E (1973) Thrust line criterion in embankment stability analysis. *Geotechnique* 23(1):85–100
- Stoetzer E, Brunner WG, Fiorotto R, Gerressen FW, Schoepf M (2006) CSM cutter soil mixing—a new technique for the construction of subterranean walls, initial experiences gained on completed projects. In: 10th international conference on piling and deep foundations. Deep Foundations Institute, Amsterdam, pp 534–541
- Sun Z (2004) Grouting in dam's rock foundation. China WaterPower Press, Beijing (China) (in Chinese)
- Taylor DW (1937) Stability of earth slopes. *J Boston Soc Civ Eng* 24(3):197–246
- Ter-Stepanian G (1975) Creep of clays during shear and its rheological model. *Geotechnique* 25(2):299–320
- Terzaghi K, Peck RB, Mesri G (1996) Soil mechanics in engineering practice. Wiley, New York
- USBR (1987) Design of small dams, 3rd edn. US Govt Printing Office, Denver
- Xanthakos PP, Abramson LW, Bruce DA (1994) Ground control and improvement. Wiley, New York
- Zhu SA (1995) Technical history of dam engineering. Water Resources and Electric Power Press of China, Beijing (in Chinese)
- Zuo DQ, Gu ZX, Wang WX (eds) (1984) Embankment dams. In: Handbook of hydraulic structure design, vol 4. Water Resources and Electric Power Press of China, Beijing (in Chinese)
- Zuo DQ, Wang SX, Lin YC (1995) Hydraulic structures. Houhai University Press, Nanjing (in Chinese)

Chapter 10

Rockfill Dams

10.1 General

Rockfill dam, a kind of embankment or so called earth–rock dams, is a water retaining barrier composed of three major parts: fill of loose rock by dumping or roller compaction; impervious membrane made of masonry, concrete, asphaltic concrete, steel sheet piles, timber, or other materials; and transition layer. The impervious membrane is employed as the waterproof and can be placed either within the embankment or on the upstream slope. Although the history is short compared to that of other ancient dam types, the development of rockfill dams during the last several decades was booming around the world (Chen et al. 1982; Galloway 1939; Golzé 1977; Guo and Chen 1992; Hill 1996; ICOLD 1991; Jansen 1980; Schnitter 1994; Sherard et al. 1963; Sherard and Cooke 1987; USBR 1987; Zhu 1995).

Rockfill dams could prove economical when any of the following conditions exist:

- Large quantities of rock are readily available or will be excavated in the vicinity of the dam site (e.g., from a spillway or tunnel);
- Only a short construction season for cohesive soil core is available;
- Borrow of earthfill material without necessity of extensive processing is difficult or even will result in serious environmental impact;
- Excessively wet and/or chilly climatic conditions restrain the large-scale compaction of earthfill materials;
- The dam will be additionally raised at later date.

Other factors that favor the use of a rockfill dam are the possibility of grouting the foundation while simultaneously placing the embankment. In addition, uplift pressure due to the seepage through the rockfill material generally does not result in significant erosion problems.

Rockfill materials have been used in dam construction since ancient times. However, modern rockfill dam construction was essentially originated in California

(USA) about 160 years ago as a result of the need to impound water for mining operations during the gold rush era. Drill and blast mining techniques provided an abundant supply of rock materials for using in dam construction. Gold mining also required a large and steady supply of water for sluicing and extracting the heavier gold nuggets from alluvial placer deposits. The gold miners used the rock quarry materials to construct water storage dams in remote areas by hand or with available mine haul and dump equipment. The early rockfill dams were small and generally consisted of a single lift of loosely dumped rockfill with an upstream timber facing as anti-seepage device. The downstream slope was typically at the natural angle of repose approaching 1:1.2. The upstream slope was sometimes hand shaped as steep as 1:0.75. One of the highest dumped rockfill dams constructed during this early period was the Meadow Lake Dam at a height of 23 m.

During the period of 1910–1940, the “dry rock dump” technique developed into the placement of single or multiple rockfill lifts in combination with relatively low permeability upstream facing materials (timber, steel, concrete, or asphaltic concrete). One of the highest dry rock dump dams in this period was the Salt Springs Dam in California (USA) of 100 m high. An important feature of larger dams constructed in this period was excessive post-construction settlement and deflection of the upstream facing materials during their first reservoir impounding, although they remained stable without slope failure. The post-construction settlement appeared to be directly attributable to the hydraulic loading on the upstream facing, which gave rise to differential movement of the rigid facing materials and leakage through face slab joints. The wetting action by leaked water, on the one hand, increased the total moist unit weight of the rock dump mass and softened the rockfill. As a result, additional settlement took place due to such subsequent wetting of the dry rockfill (i.e., saturation collapse). Remedy of facing leakage during reservoir operations was expensive, requiring underwater repair or reservoir drawing down.

Through wetting or flooding dry rock dump lifts during the placement from the 1940s to the 1950s, as well as reducing loose lift thickness in the mid-to-late 1950s, such post-construction settlement in larger dams had been minimized considerably. The 1940s also included the first use of earthfill core and filter materials in the interior of rockfill dams. Rockfill dam heights began to exceed 100 m in the 1940s to more than 152 m in the 1950s. Contrast with a previous larger settlement of 5–7 %, wetting during construction brought the post-construction settlement of rockfill dam down to only about 1 %. Prior to 1955, the loose rock dump lift thickness for in-place wetting or flooding was typically ranged from 11 to 50 m, with the maximum known rock dump lift placed at the height of 61 m. After 1955, the lift thickness was reduced for the purpose to use weaker rock materials in dam construction and this also reduced rock segregation where larger sized rocks tend to roll to the bottom of the lift during dumping and dozing operations. By the late 1950s, the rock dump lift thickness on several large dams was reduced to 3–4 m with the top surface leveled and tracked by dozer passes and loaded haul truck traffic. This also provided a limited amount of compaction effort in the upper half of the lift, but the lower half remained relatively loose.

Although no rockfill dam failures were recorded for both the earlier “dry” and subsequent “wet” rockfill dumps, there was growing worries over the stability of large rockfill dams in more populated areas, taking into account the limited amount of engineering knowledge with respect to rockfill strengths and the lack of established rockfill placement and test control procedures. This led to a rapid change in rockfill dam construction by the late 1950s, after 110 years of successful rock dump practice.

From the 1960s, the widely accepted practices for modern rockfill dam construction are moisture conditioning with wetting of rock materials in the borrowing or on the fill and the compaction in lifts of controlled thickness using roller compactors. Large-scale tests on rockfill by the Corps of Engineers and Bureau of Reclamation (USA) in the early 1960s confirmed a better compaction by heavy steel drum vibratory rollers compared to non-vibrating heavy pneumatic rubber-tired or steel drum rollers. These new techniques further reduced post-construction settlement, efficiently controlled material segregation, significantly increased the rockfill density and related strength, and facilitated the lateral and vertical placement of transitional zones and the internal earthfill core as well as drain filter systems within the embankment (Cooke 1984). In 1958, the Quoich Dam (UK, $H = 38$ m) became the first rockfill dam using these new techniques. The wet rock dump technique was essentially terminated by 1965 on large rockfill dams around the world, and the New Exchequer Dam (USA, $H = 150$ m) completed in 1966 became the last rockfill dam by the mixed methods of “dry rock dump” technique of thick lifts and “wet” roller compacted of thin lifts. The tractor-pulled rollers began to be replaced by self-propelled rollers in the 1970s because the latter are more efficient, particularly at dam abutments. In 1989, the compacted rockfill mounted at the height of 243 m by the completion of the Alberto Lleras Dam, also known as the Guavio Dam, was constructed in Columbia. Until now, the highest central core rockfill dam is the Nurek Dam (Tajikistan, $H = 300$ m) completed in 1980. Several other compacted earthfill and rockfill dams under construction will climb greater heights, including the Rogun Dam in Tadjikistan at 335 m high.

A remarkable event in the modern rockfill dam construction is the boost of concrete-faced rockfill dams (CFRD) (Cooke 1984, 2000; Cooke and Sherard 1987; Fu and Feng 1993; ICOLD 1989, 2011). The Cethana dam (Australia, $H = 110$ m) completed in 1971 establishes preliminary technique guidelines for the modern CFRD. From the Foz do Areia dam (Brazil, $H = 160$ m) completed in 1980, to the Salvajina dam (Colombia, $H = 148$ m) completed in 1985, until the Aguamilpa Dam (Mexico, $H = 187$ m) completed in 1993, the design and construction techniques for the CFRD achieved amazing progress. Nowadays in China, in parallel to concrete arch dam and RCC dam, CFRD is often, although not always, strongly competent in the selection of dam types.

The first China’s rockfill dam is the 52 m-high Shizitan Dam in the Sichuan Province constructed in 1957, which is a dumped rockfill dam with reinforced concrete face in a form of concrete gravity wall. The earliest CFRD in China is the 48.7 m-high Baihua Dam built in 1966 with an upstream slope of 1:0.6. There is a large size of dry-laid stone in the upstream side of the dam section, together with

the reinforced concrete face slab for anti-seepage. Later on, other similar types of dams such as the Nanshan Dam and the Sanduxi Dam were completed in China with dam height lower than 50 m. The construction of CFRD dams using modern techniques in China was actually started in 1985—by the milestone dam of the Xibeikou, at the height of 95 m and completed in 1990.

Until now, the highest compacted rockfill dam with central core in China is the Nuozadu Dam ($H = 261.5$ m). The other important rockfill dams in China include the Xiaolangdi Dam with sloping core ($H = 154$ m) completed in 2001, the Pubugou Dam with central core ($H = 186$ m) completed in 2010, the Shuibuya CFRD ($H = 233$ m) completed in 2008, and the Lianghekou Dam with central core ($H = 295$ m) under the construction.

10.1.1 Classification of Rockfill Dams

According to construction methods, rockfill dams may be classified into three groups as follows:

- Dumped rockfill dams;
- Compacted rockfill dams; and
- Directional (pin-pointed) blasting rockfill dams.

Nowadays, the most prevalent rockfill dams are roller compacted, which will be mainly addressed in this chapter.

According to the materials of anti-seepage membrane, compacted rockfill dams may be further distinguished as (Fig. 10.1) follows:

- Earth–rockfill dams;
- Asphaltic concrete rockfill dams;
- Reinforced concrete rockfill dams; and
- Wood rockfill dams.

According to the location of anti-seepage membrane, rockfill dams also may be categorized into:

- Central core dams;
- Sloping core dams; and
- Upstream membrane or “decked” dams.

Each membrane type (material and location) has its advantages and disadvantages and is dictated in many ways by the materials available and foundation conditions at a specific work site. Central and sloping cores are referred to as “internal membranes,” and they are generally made of impervious earth materials. Economic analysis should be undertaken for determining the type of material used in constructing the membrane, either internal or external. If an internal membrane is to be considered, it is recommended that a central vertical core of impervious earth

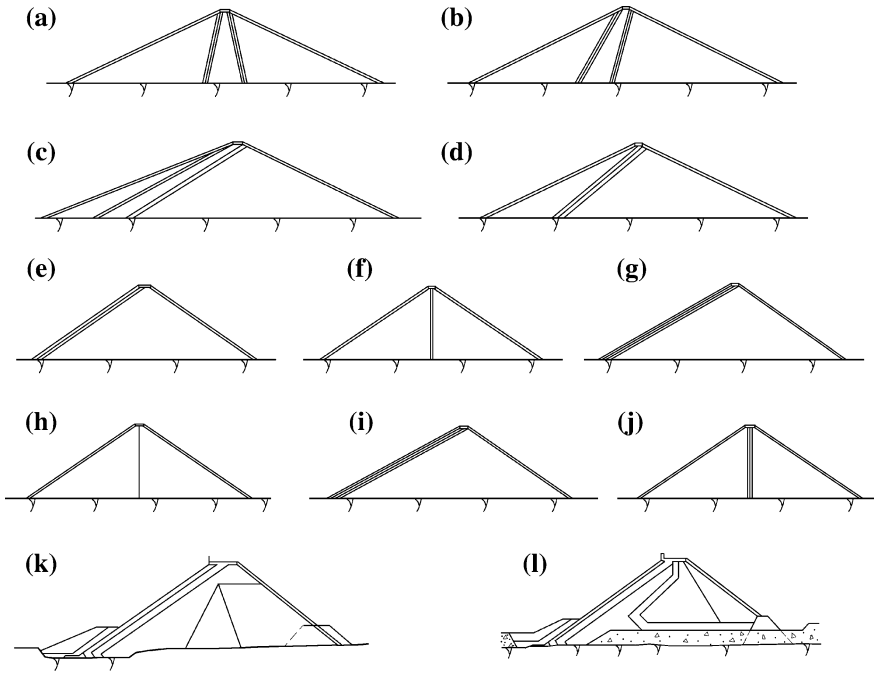


Fig. 10.1 Types of rockfill dams. **a** Central clay core; **b** inclined central clay core; **c** sloping clay core; **d** soil faced; **e** sloping concrete core; **f** central concrete core; **g** sloping asphalt concrete core; **h** central asphalt concrete core; **i** sloping geomembrane core; **j** central geomembrane core; **k** and **l** concrete-faced

be the first choice, attributable to its maximum contact pressure with the foundation and less rigorous requirement for the construction. If an external membrane is considered, it is desirable to be constructed of concrete or asphalt.

10.1.2 Requirements for Rockfill Dams

(a) Prevention of overtopping

The crest of dam must be high enough to allow for rockfill embankment and foundation settlements, as well as to provide sufficient freeboard to prevent waves from overtopping the dam at maximum pool level.

In the history, there were a number of cases of rockfill dam failure due to the under estimation of flood, the insufficient elevation of dam crest, or the insufficient flood release capacity and improper management of reservoir. The Hell Hole Rockfill Dam (USA, $H = 125$ m) with sloping core was built in California in 1964. The dam failed during construction when partially completed embankment was

overtopped by a flood that was twice as great as the maximum flood of record and the total volume of rockfill washed away was $53.5 \times 10^4 \text{ m}^3$.

Exceptionally, concrete-faced rockfill dams can keep stable when subjected to through seeping flow or overtopping flow at the initial construction stage when the dam is not high, which is clearly an important advantage over earthfill structures. However, the velocity of flow on dam face should be controlled within 5–7 m/s, and reliable protection measures against scouring should be adopted (Chanson 2009; Olivier 1967).

(b) Seepage control

Seepage through the rockfill embankment, foundation, and abutments must not exert excessive forces in the structure nor piping of material be permitted. Excessive seepage forces will lead to sliding of dam or abutment slope, while piping, if not controlled, will eventually give rise to the break of dam.

The site of the Teton Dam of 93 m high in Idaho (USA) is composed of basalt and rhyolite, both of which are considered unsuitable for dam construction attributable to their high permeability. Test cores, drilled by engineers and geologists, showed that the rock at the dam site is highly fissured and unstable, particularly on the right side of the canyon. The USBR planned to seal these fissures by injecting grout into the rock under high pressure to create a grouting curtain of triple rows and 100 m deep in the rock. The thick central core was built using eolian silt. The dam was completed in November 1975 and collapsed on Saturday, June 5, 1976. Study on the dam's environment and structure placed blame for the collapse on the permeable loess soil used in the core and on the fissured (cracked) rhyolite in the foundations of the dam that allowed for water to seep under the dam. It is postulated that the combination of these flaws led to internal erosion (piping) that eventually resulted in the collapse of the dam.

The Gouhou CFRD (China, $H = 71 \text{ m}$) was completed in 1989. The actual vertical settlement of the dam body was much larger than anticipated because of poor construction quality. As a result, the base slab of the L-shaped parapet at the dam crest was pulled apart from the face slab and a cavity was formed. The water stop in the horizontal joint between the face slab and parapet was also damaged. When the reservoir pool level had raised over this joint, the water commenced to leak into the dam body. To make the matter worse, the cushion layer was not well functioned as an effective seepage barrier due to the segregation of fill materials and the coarse cobble layer was placed around the top of the dam body. Leaked water through the dam body formed erosion channels in the main rockfill, which finally brought about the failure catastrophe of the dam on the August 27, 1993.

(c) Stability

The foundation, abutments, and embankment must be stable under all situations during construction and operation.

For a CFRD using hard rocks, the empirical slope of 1:1.3–1:1.4 is customarily adopted, which could be slightly more flat if soft rocks or gravels are placed. These slopes secure dam stability under conventional situations, and the stability analysis

is usually not necessary. However, if the dam is located on weak seamed or fine silt foundation, the stability analysis is demanded.

(d) Rational utilization of rock and soil materials

From the point view of the balance for earth–rock haulage, when determining the project layout for a rockfill dam, it might not be economical that the volume of earth and rock excavation is minimum. If the excavated materials can be used for the dam construction, additional borrow areas are usually not necessary or can be reduced. Under such circumstances, the scheme of heavier excavation might be more favorable.

(e) Ensure the reliability and durability

Systematic researches on the raw materials and mixing ratios of face slab concrete should be carried out with regard to additive and admixture for improving anti-cracking resistance and anti-seepage resistance and durability. The downstream slope should attain good resistance to the scouring of rainfall. The anti-seepage devices also should be well protected to prevent them from cracking induced by summer sunshine and winter freezing/thawing. For high CFRD, the excess leakage through perimetric jointing and face slab cracking resulted from the settlements of embankment and foundation should be controlled by appropriate countermeasures.

10.1.3 Design Theory of Rockfill Dams

Rockfill dams belong to embankment dams, their load computation, seepage analysis, stability analysis, deformation analysis, etc., are all identical as have been illustrated in Chap. 9 of this book. Hereinafter in this chapter, only the special considerations on the design for rockfill dams are addressed, including compaction criteria and quality control, structural elements, and foundation treatments.

10.2 Profile of Rockfill Dams

Profile design is mainly accomplished by the selection of rock materials and the designing of embankment sections.

10.2.1 Elevation of Dam Crest

Elevation of dam crest is decided according to the requirements specified in Chap. 9, where the freeboard is calculated using Eq. (9.40).

Freeboard requirements will depend on the maximum wind velocity, fetch, reservoir operating conditions, spillway capacity, and whether or not a parapet wall is installed. The bottom of parapet wall should be higher than the normal storage reservoir level.

10.2.2 Crest Width and Structural Requirements

The width of dam crest is dependent on the requirements of structure elements such as type of anti-seepage membrane, dam height, traffic, construction, and operation. The emergency flood fighting may also impose requirements for the dam crest width. A minimum width of 4–5 m is recommended, and generally, the crest width may be 10–15 m for high dams and 5–10 m for medium to low dams.

The layout of central core or sloping core as well as filters should be taken into account in the design of dam crest width. In chilly areas, sufficient protecting thickness on the crest for soil anti-seepage devices is demanded. The traffic requirements, if any, should be considered in the design of dam crest, too.

10.2.3 Slope

The up- and downstream slopes depend upon the type of impervious membrane and its location and have predominant influence on the dam safety and investment.

Slopes adopted for rockfill dams have evolved from very steep (e.g., 1:0.5–0.75) for early rockfill dams, to more flat (e.g., 1:1.3–1.7) for current practices. Early rockfill dams used upstream membranes exclusively and were constructed with steep upstream and downstream slopes to minimize the volume of rockfill mass. Since their slopes were considerably steeper than the natural repose angle of dumped rock, they were stabilized by thick zones of crane-planed, dry rubble masonry with protection. Later on, designers eliminated the rubble masonry on the downstream slope by flattening it to the repose angle of the rock, but the very steep upstream slope was retained. Since most of the upstream zones were constructed by the crane placement of large rocks, the expenditure was increased significantly. Gradually, designers found that it would be more economical to use an upstream slope approximating the repose angle of the rock material and eliminate crane placement in favor of compacted rockfill.

The upstream and downstream slopes for rockfill dams with central or sloping earth core will be dependent on the size and soil properties of the earth core, the width of filter zones, type of foundation materials, drawing down requirements, construction sequence, etc. Governed by the lower strength of earth, the upstream slope of sloping core dam is more flat than that of central core dam, while the downstream slope of sloping core dam is steeper than that of central core dam. Since the upstream portion of rockfill embankment is saturated in reservoir, and the

reservoir level may also be drawn down quickly, the stability requirements dictate more flat slope of upstream than that of downstream. However, this difference is not so significant as in the case of earthfill dams. Generally, upstream and downstream slopes of a typical high central earth-core rockfill dam will be ranged between 1:1.8 and 1:2.0. A few of high dams have steeper upstream slopes; for example, the Gepatsch Dam (Austria, $H = 153$ m) has an upstream slope of 1:1.5 and the Charvak Dam (Uzbekistan, $H = 168$ m) has an upstream slope of 1:1.3. High rockfill dams with sloping earth core will have upstream slope ranged from 1:2.5 to 1:2.75 and downstream slope ranged from 1:1.6 to 1:1.2.

Most CFRDs compacted by hard rocks have slopes of 1:1.3–1:1.4, and very few stability problems have been reported for these slopes according to the review of available literatures. The slope could be as flat as 1:1.5–1:1.7 for a CFRD using soft rocks and gravels.

Most asphaltic concrete-faced dams are constructed with upstream slopes of 1:1.6–1:1.7, to facilitate the construction of the asphaltic concrete membrane with respect to its rheologic characteristics. A slope ranged between 1:1.3 and 1:1.4 may be exercised for the downstream rockfill shell of this dam type.

10.2.4 Zoning of CFRD

1. Composition of CFRD

Concrete-faced rockfill dam (CFRD) is a kind of rockfill structure composed of rockfill mass as a stability supporter and a concrete membrane on its surface forming impervious barrier (ICOLD 1993a, b; Marulanda and Pinto 2000; Materon and Mori 2000; Sherard 1985). It was originated during the California Gold Rush in the 1860s where gold miners constructed rockfill timber faced dams for sluice operations. Later on, the face slab of timber was replaced by that of asphaltic concrete or reinforced concrete as the design interesting was directed to irrigation and electric power generation.

The impervious structure is composed of concrete slab, toe slab (plinth), grouting curtain under toe slab, joints and water stops within joints, parapet, upstream blanket (strengthening zone for anti-seepage), etc. The stability supporter is composed of semi-pervious cushion layer (Zone II) and main rockfill (Zone III). Figure 10.2 is the profile of the Shuibuya Dam showing a typical zoning of CFRD.

2. Rockfill embankment zoning

The zoning of CFRD has been nearly finalized in the modern design (Sherard 1985). As shown in Fig. 10.2, the interior section of the CFRD can be divided into three zones: Zone I is the anti-seepage strengthening zone, Zone II is the cushion zone playing the role of second anti-seepage defense frontier intended to limit the infiltration discharge and drain out along the transition zone, and Zone III is the main embankment rockfill mass. For each zone, the requirements with respect to the

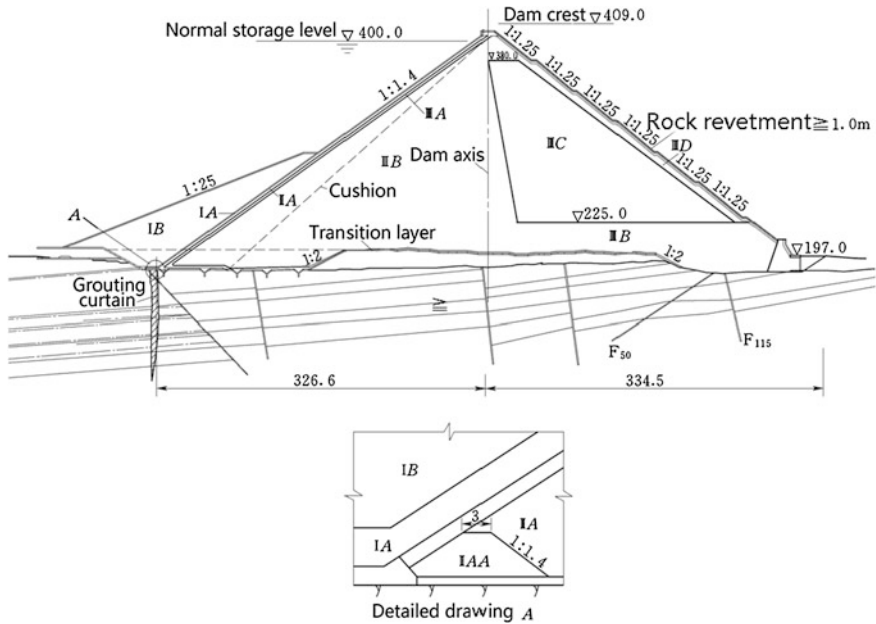


Fig. 10.2 Zoning of the Shuibuya CFRD (unit: m)—China, $H = 233\text{ m}$

material properties including maximum grain, gradation, compaction density, deformation modulus, permeability, and construction techniques are specified.

(a) Zone I

This zone is composed of impervious blanket and weighting. The impervious blanket makes use of cohesive soil or non-cohesive silt, which is installed on the perimetric joint and the face slab at lower elevation. To protect the blanket, random materials, i.e., weighting of non-cohesive fine materials such as fly ash and silty fine sand, are put into use for coverage. Fine particles brought by the seeping water will enter the opened joints and deposit there attributable to the filter at the joint bottom; in this way, the joints are able to “self-heal”. The top of this zone may be as high as the inactive storage level. Where the inactive level is too high, the top may be lower than the inactive level but in no case would it be lower than the working depth of urinator, to avoid potential repairing operation under excessive water depth.

(b) Zone II

This is a cushion zone of well-graded and smaller sized rocks and gravels, intended to provide uniform, flat, and reliable bedding for the upstream concrete slabs and to retard extreme water losses should the face slab crack and the joint open. When the slabs have not completed in construction period, this zone also performs as a temporary barrier for retaining water in flood season. This will minimize the construction difficulty by raising the embankment up to the water

retaining elevation before flood season. The cushion materials should have properties of high shear strength, lower compressibility, and semi-perviousness. The cushion is customarily made of intact, hard, and weathering resistance rocks, which may be artificial or natural sands and gravels, or the mixture of both.

(c) Zone III

This is the largest downstream zone of the embankment mass, consisting of compacted rockfill of good quality and larger grain size. It provides high stability, high shear strength, low compressive, good permeability and duration, to the embankment. To make appropriate use of materials, the Zone III is further divided into sub-zones of IIIA (transition zone), IIIB (main rockfill zone), and IIIC (secondary rockfill zone or random zone), according to their deformation characteristics. In general, materials in these sub-zones should be graded from upstream fine rocks to downstream coarse rocks, with the largest and strongest material be placed in the lower downstream portions. Located faraway from the face slab, the zone IIIC may be placed by rocks of certain inferior quality, such as the excavated materials from spillways, for minimizing the expenditure.

10.3 Selection of Rockfill Materials and Compaction Standard

In recent 30 years, the requirements for the rockfill grains and strengths are relaxed gradually. In addition to hard rocks, applications of soft rocks and sand-gravel materials have been world widely exercised. The applicability of such materials is supported by lots of scientific tests, theoretic analyses, and prototype observations.

10.3.1 *Quality Requirements for Rockfill Materials*

For rockfill placement, the igneous rock of high strength and density is the best parent rock, whereas the shale and marlstone rocks are the worst ones (ICOLD 1993a, b). From the standpoint of material properties, the hard rock possesses high weathering resistance, high shear strength, and high free drainage ability, which allows for a steeper dam slope with sufficient safety, and enables to reduce the expenditure.

Selection of rocks for each zone should be made according to the dam type.

- For decked rockfill dams which are sensitive to the settlement of dam shell, the downstream zone of the embankment requires the largest and best quality rocks available. Large shabby rocks should not be placed in the fill since they tend to bridge, causing large voids which may in turn lead to excessive settlement due to their breaking.

- For central earth-core rockfill dams, the larger and stronger rock should be placed in the downstream rockfill shell and be graded from fine rock adjacent the filter to coarse rock near the downstream toe. Oppositely, the upstream rockfill shell should be graded from fine rock adjacent the filter to coarse rock on the upstream face. The rockfill on the upstream slope has the highest requirements for the quality, for it is subject to the erosion of wave and climatic changes.

Generally, the compressive strength of rocks is demanded to be higher than 20 Mpa. Where a stiff upstream membrane is installed on the rockfill surface such as the CFRD does, compressive strength of rock should be higher than 30 Mpa. The softening coefficient of rock should be higher than 0.7.

It should be pointed out that the SL274-2001 “Design specification for rolled earth–rockfill dams” has no specific requirements for the quality of rockfill materials, and it indicates that “materials from borrow sites and excavated from structure foundation, such as non-cohesive soils (including sand, gravel, pebble, and erratic boulder), stones, gravelly soils, and other weathered materials, may all be employed for the dam shell in different portions according to their properties.”

10.3.2 Compaction Requirements for Rockfill Materials

The SL274-2001 “Design specification for rolled earth–rockfill dams” stipulates that porosity is employed as design index for the compaction standard of rockfill, which satisfies

- The porosity should be 20–28 % for the rockfill shell of central or sloping earth-core dams and asphaltic concrete central core dams;
- The porosity for the rockfill shell of asphaltic concrete-faced dams should be selected between the concrete-faced rockfill dams and earth-core rockfill dams.
- If soft and weathered rocks are used, the porosity should be selected according to the deformation, stress, and shear strength conditions of the specific dam.
- For the dam on a seismic area with intensity of 8–9, the lower bound of the above standard should be adopted.

According to the present levels of Chinese construction management, the quality of rockfill placement is controlled mainly by the placement parameters and is checked by dry density tests in situ, which is the so-called double control measure. The placement parameters are determined in advance by the roller compaction tests or engineering analogy with regard to vibrating roller type, lift thickness, volume of watering, passes of roller compaction, etc.

The placement parameters should be often checked dynamically. Before, it was accepted that 4 passes of lot-vibrating roller can meet the compaction requirement. But along with the increase of the dam height, a rockfill mass with high density and less deformability is desirable for reducing the damage risks to perimetric joint and

face slab; therefore, it is customarily demanded that the compacting effort should be raised as far as possible to get high density, if the additional cost attributable to higher compaction parameters is not too significant. Nowadays, 18t articulated vibrating roller and 25t self-propelled vibrating roller are ordinarily available; therefore, it is fairly realistic to select heavy vibrating roller to proceed the compaction operation more effectively.

It has been proved that the over-thickness of filling lift is an important factor for reducing the rockfill dry density. Therefore, the lift thickness should be controlled during the process of material dumping, spreading, and leveling. During the construction of the Tianshengqiao No.1 CFRD from 1996 to 1998, according to the statistics of 1197 sets, the average lift thickness was 82 cm, which was close to the design thickness 80 cm, among them the lift thickness smaller than 90 cm accounted for about 86.8 %.

Pass of compaction is easy to control if operated conscientiously, but it is liable to missing if the control is not rigorous.

It is shown that the quantity of watering must be well guaranteed by relevant technical measures. Ordinarily in China, a high-level pool is built, and the rubber tube is used to watering the lift surface manually. This is suitable solely to the location nearby the pool. Recently, a high-level pool cooperated with a watering car remade from a 32t dumping track was employed in the construction of the Baixi CFRD to watering the rockfill surface, which yielded a favorable effect.

10.4 Structural Elements of Rockfill Dam

After the design of basic dam profile satisfying seepage and sliding stability, the design for structural elements is carried out, which comprise the anti-seepage device, slope protection, dam crest, etc.

10.4.1 *Anti-Seepage Devices*

1. Soil anti-seepage devices

Earth core is a kind of soil anti-seepage devices most prevalent in rockfill dams and is distinguished as central core and sloping core. The permeability of soil anti-seepage devices is usually in a magnitude of 3–4 orders lower than that of rockfill shell and smaller than 10^{-6} cm/s. Figures 10.3 and 10.4 show the structural elements of the Nuozadu Dam with central core (China, $H = 261.5$ m) and the Brownlee dam with sloping core (USA, $H = 128$ m), respectively.

Earth-core rockfill dams are economical where site conditions recommend the use of rockfill but reject the use of a decked structure. This can be the case where the upstream abutments show highly weathered rock to great depths and thus

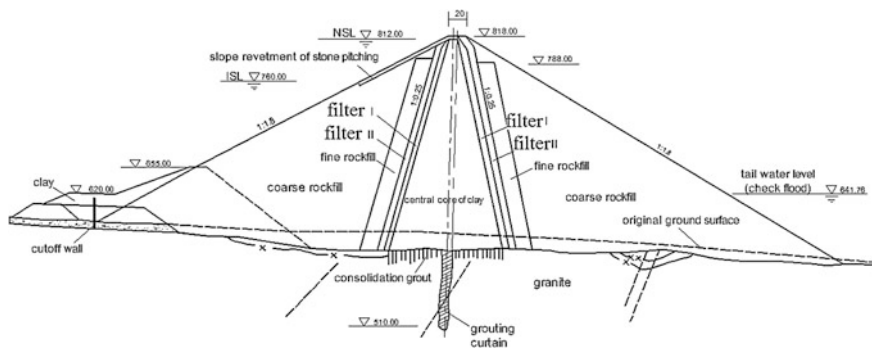


Fig. 10.3 The Nuozadu Dam with central core (China, $H = 261.5$ m)

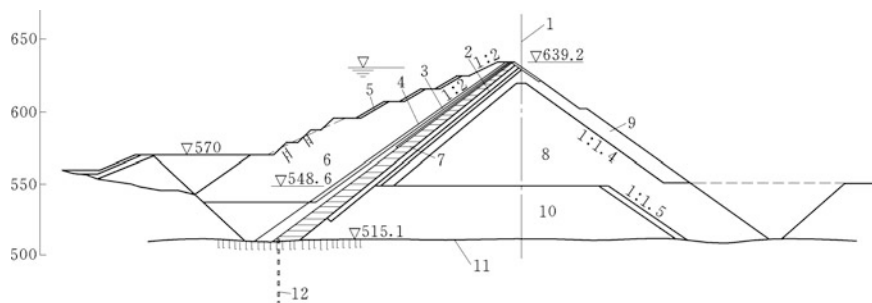


Fig. 10.4 The Brownlee Dam with sloping core (USA, $H = 128$ m). 1 dam axis; 2 fine-grained filter; 3 coarse-grained filter; 4 finger stone filter; 5 stone pitching; 6 upstream rockfill; 7 sloping core; 8 roller compacted rockfill; 9 riprap; 10 sandy gravel stratum; 11 bedrock; 12 grouting curtain (at the depth of 51 m)

present questionable cutoff conditions for an upstream membrane, or where the higher elevations of the abutments are covered with deep layers of overburden and impede an economical installation of trench-type cutoff linked with the decked membrane.

The impervious material used in the core should be similar to that used for the earthfill dams (see Chap. 9). The material should be placed at or near optimum moisture content and compacted by tamping roller. The plasticity index of the material should be sufficient to allow for the core to deform without cracking.

Filter zones should be adequate to prevent impervious material from any piping. Multiple filters may be required if gradation differences between the impervious core material and rockfill material are large.

The core width for a sloping or central core rockfill embankment should be established with respect to the seepage and piping considerations, the types of materials available for the core and shells, the filter design, and the seismic actions. The soil anti-seepage devices should have freeboard above the maximum reservoir level. All these details are referred to Chap. 9.

2. Artificial material anti-seepage devices

Artificial material membranes of concrete, asphalt, geotextile, and steel may be employed as either internal or external anti-seepage devices (Giroud 1992; ICOLD 1992, 1999, 2010).

(a) Flexible artificial material anti-seepage devices

As a kind of viscoelastic–plastic material, asphalt concrete has good anti-seepage properties with permeability coefficient = 10^{-7} – 10^{-10} cm/s and is highly compatible to the movements and settlements of the rockfill and foundation. The flexible properties of the asphalt make such dams especially acclimatizable to earthquake regions and are less influenced by climatic condition during the construction.

Asphalt concrete membrane may be in the form of sloping wall (Fig. 10.5) or central core (Fig. 9.20). The details of the structural features may be referred to Chap. 9.

(b) Stiff artificial material anti-seepage devices

Internal membranes of concrete and steel are usually not recommended for modern high rockfill dams due to the difficult with achieving compatible deformation between the membranes and dam shells, and with inspecting or repairing. A larger number of rockfill dams with stiff anti-seepage devices have been decked using conventionally placed reinforced concrete. In most cases, they have performed well, with acceptable limits of leakage and minor repairs. Slab thickness and reinforcing requirements are ordinarily determined by experience or precedent taking into account the following:

- Low permeability;
- Sufficient strength to bridge subsided areas of the face;
- High resistance to weathering action; and
- Sufficient flexibility to tolerate embankment and foundation settlements.

A well-compacted rockfill dam has acceptable embankment settlement, and the use of a well-compacted transition zone performing as a continuous, firm, and bedding surface may help to meet the bridging requirements on the face slab.

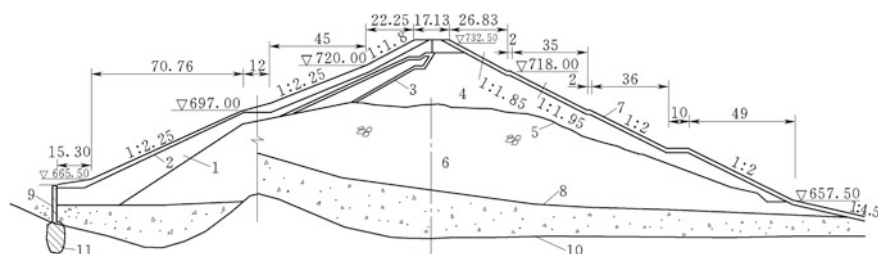


Fig. 10.5 The Shifayu Dam (by pinpoint explosion) with asphalt concrete sloping core (unit: m)—China, $H = 82.5$ m). 1 asphalt concrete sloping core; 2 dry-laid stone cushion; 3 filter; 4 artificial rockfill; 5 contour of explosion heap; 6 pinpoint blasting rockfill; 7 dry-laid stone pitch; 8 original ground surface; 9 concrete cutoff wall; 10 top of bedrock; 11 grouting curtain

The concrete should be dense, durable, weather resistant and of low permeability. If significant foundation settlement is anticipated or if other factors such as earthquake actions exist, it would be wise to increase the membrane thickness. The amount of steel reinforcement should meet the customarily accepted requirement, i.e., 0.5 % of the sectional area, and should be placed both horizontally and vertically. If the single-layered reinforcement is employed, it should be placed in the neutral plane of the slab.

Vertical joints may be demanded to compensate for horizontal expansion on the dam of considerable length and are often used to facilitate the construction of slabs. Polyvinyl chloride or rubber water stops should be installed to secure the watertightness along the joints. Because of the low reservoir head and the small amount of settlement, horizontal or vertical expansion joints are normally not required in the reinforced concrete face slab for low dams.

The type of cutoff between the concrete facing and the foundation will depend on the quality of bedrock encountered. For sound rock, the doweled cutoff has demonstrated its adequacy and economy, whereas in highly jointed and weathered rock, or in rock of questionable quality, the cutoff wall should be installed. Water stops should be provided between the cutoff and the face slab. Rigid cutoff is not recommended since it restrains the allowable settlement of the face slab.

Since smooth concrete face slab provides less resistance to wave run-up, an increased freeboard is needed to control the wave run-up and over-splash. Parapet wall can be employed to reduce the height of embankment, which should be constructed as integral continuation of the concrete face slab and reinforced accordingly. When a parapet wall is installed, the requirements for it should be similar to that for earthfill dams. Height of the parapet wall can be determined either by precedent or the designer's experience and is normally 1.0–1.2 m.

Slab concrete placement generally employs the slip-forming process identically exercised in road construction, but in some cases, shotcrete has been used effectively. Placement of the concrete membrane should not begin until the entire embankment has been compacted; this allows for the maximum construction settlement and reduces the risk of cracking and excess leaking.

10.4.2 Slope Protections

There is no slope protection problem for the CFRD. However, the surface protection of upstream slope is required for the other kind of rockfill dams, which is meant to prevent the destructive wave action. Usual types of surface protection for the upstream slope are stone riprap either dry dumped or hand placed, concrete slabs or wedged blocks, from crest down to 2.5–3.0 m lower than the wave trough at the lowest reservoir level. Since the dumped riprap is stronger in dissipate wave actions and resist impaction of floating objects, it is the most economical and efficient. The downstream protection is usually not necessary if the rockfill grains

are large. However, where the downstream slope is vulnerable to tailwater scouring, protection might be installed.

When a thin protection layer is employed, hand-placed riprap may be more economical than dumped riprap. The rocks for riprap should be solid and durable against weathering and dry/saturation circling. Some kinds of sandstones may be used, but the sandstone intercalated by shale should be avoided. There are several empirical methods available to find out the thickness of riprap, which take into account the wave height, embankment slope, rock weight of average size, and its specific weight. The details may be referred to the corresponding design codes or handbooks.

10.4.3 Toe Slabs, Face Slabs, and Water Stops of CFRD

Water sealing system of CFRD consists of concrete toe slab, foundation grouting curtain or other anti-seepage installation, and concrete face slab (Gratwick et al. 1999). The function of the toe slab is to connect anti-seepage installation with concrete face slab. Perimetric joint exists at the adjoining of toe slab and face slab. Since both the toe slab and face slab are poured by panels, joints also exist between these panels. Water stops at these joints are therefore important structural elements in the anti-seepage system of CFRD.

1. Toe slab (plinth, toe plate)

(a) Toe slab on rocks

Classically, toe slab should be placed on sound, non-erodible, and groutable rock foundation. Nowadays, practical experiences have over-crossed this traditional restraint, by the utilization of weathered rock in different degrees as the base of the toe slab (Gratwick et al. 1999). Under such circumstances, the main concern is to assure the seepage stability of foundation, since the strength and stability of the rock foundation are commonly not the predominant issues.

The details of the toe slab is shown in Fig. 10.6.

The width of toe slab is determined according to the allowable hydraulic gradient of the foundation rock, i.e.,

$$B = H/[J]$$

where B = width of the toe slab, m; H = design head, m; and $[J]$ = allowable hydraulic gradient of foundation rock, which may be selected according to Table 10.1.

Cutoff wall or hinge plate (Fig. 10.7) can be installed for lengthening the seepage path, if necessary. It is often employed in the rock foundations with fractures or mud seams, to seal the leakage of strongly weathered rock. In addition to extend seepage path, it also serves to prevent the mud seams from seepage failure. In the Zhushuqiao Dam (China, $H = 78$ m) where a part of riverbed stratum is composed

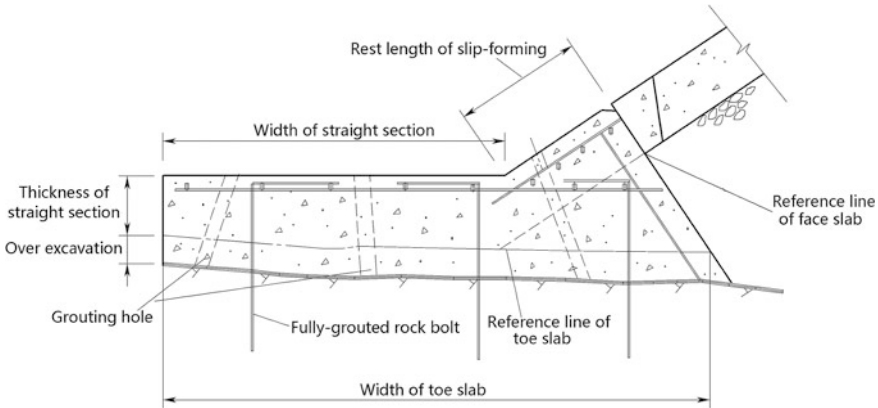


Fig. 10.6 Details of a toe slab

Table 10.1 Allowable hydraulic gradient $[J]$ of toe slab foundation rock

Classification of foundation rock	$[J]$
Fresh/slightly weathered	≥ 20
Weakly weathered	10–15
Strongly weathered	5–10
Totally weathered	3–5
Native soil or riverbed alluvium	2–3

of strongly weathered slate, the concrete cutoff wall with a width of 1–2 m and a depth of 2–5 m was installed. In the Chaishitan Project (China, $H = 101.8$ m), concrete cutoff wall was also employed for the strongly weathered rock foundation at the mid-upper part of the left abutment. Cooke (2000) proposed a new concept in the design of toe slab that the basic width of toe slab be 3–4 m in order to facilitate the grouting works and the shortage in the width of toe slab be compensated by installing a blanket of normal concrete or shotcrete in the up- or downstream side of the toe slab. A joint is set between the toe slab and the concrete blanket and covered with filter layer to avoid erosion of fine particles. The Reece Dam (Australia, $H = 122$ m), the Shuibuya Dam, the Babagon Dam (Malaysia, $H = 70$ m), and the Ita Dam (Brazil, $H = 125$ m) all have succeeded in the installation of the downstream concrete or shotcrete blanket connecting the toe slab. This kind of installation has been realized in the Xiaoxikou Dam ($H = 67.3$ m) in China, too.

The thickness of toe slab is identical to the adjacent face slab, which is usually 30–100 cm. Commonly, C20 concrete or an identical grade to the face slabs is preferable for the toe slab, whose indices of permeability, freezing resistance, and durability may also be the same as the face slab or even lower.

Reinforcement for toe slab is intended to limit the propagation of crack which usually occurs only at its top where slight tensile zone may emerge. Reinforcement also serves to prevent cracking attributable to temperature variation and dry shrinkage. Two-way reinforcement ratio of 0.3–0.4 % is currently exercised; for the

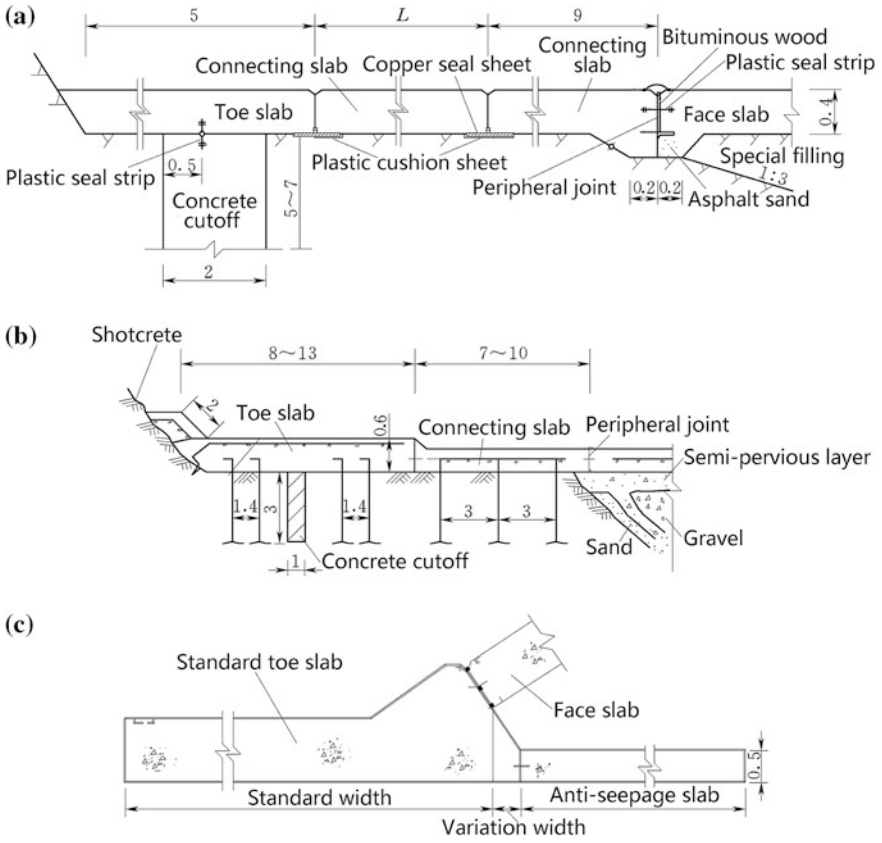


Fig. 10.7 Methods to elongate seepage path (unit: m). **a** Vertical cutoff wall + connecting plate (the Zhushuqiao Dam); **b** upstream anti-seepage plate (the Salvajina Dam); **c** downstream anti-seepage plate (the Shuibuya Dam)

toe slab on soft foundation, the upper bound is suggested. Rock bolts are installed to tie the toe slab and foundation, whose spacing and depth are 1.2–2.0 m and 3–5 m, respectively. These bolts should be connected with the steel bars on the top of toe slab.

Except for high toe slab, there normally has no necessity to conduct stability analysis. The stability analysis, if necessary, is accomplished using limit equilibrium method with design loads including vertical water pressure, horizontal water pressure, self weight, uplift, pressure from rockfill, and friction resistance. In the computation, the pressure from rockfill is looked at as active soil pressure, and the action of face slab and rock bolts are not taken into account.

All faults, joints, and weak seams crossing the toe slab should be treated according to the technical requirements. In addition, a filter layer should be installed at the downstream side to avoid erosion damage. Sometimes this filter layer is extended to the downstream exit face, which is an effective measure and has already

received increasing application, such as in the Chaishitan Dam (China, $H = 101.8$ m).

The rock foundation treatments for toe slab include surface treatment, consolidation grouting, and curtain grouting. Consolidation grouting of depth 5–10 m is customarily employed. Careful observation should be made during the process of grouting to avoid the heaving or cracking of the toe slab.

(b) Toe slab on sand–gravel alluvium

Until 2001, there are nine completed China's CFRDs with toe slabs being located on sand–gravel alluvium. Concrete cutoff wall was commonly employed as anti-seepage device for such foundation. The face slab is connected to the cutoff wall by using toe slab and hinge plate for forming a closed anti-seepage system. Usually, only one cutoff wall is sufficient for water sealing purpose. An exception is the auxiliary dam of the Tongjjezi Project on the left bank (China, $H = 48$ m), where two rows of cutoff walls were served as a bearing structure apart from anti-seepage devices.

When special topographic or geologic conditions are encountered, and difficulties arise associated with the project layout, lengthening of the seepage path on horizontal or inclined surface can be implemented either at upstream or downstream side of the toe slab by connecting plate (hinge plate) linking the toe slab and face slab, such as the Salvajina Dam (Columbia, $H = 148$ m). For several China's CFRD erected on alluvium with moderate dam height and project scale, the direct connection of cutoff wall and the face slab by the toe slab performs well. However, for higher dam or deeper alluvium, it is preferable to arrange the cutoff wall a certain distance away from the upstream dam toe and then link the wall to the toe slab by a hinge plate, such as the Kekeya Dam (China, $H = 41.5$ m). The benefits brought about by this arrangement are as follows:

- The space left between rockfill mass and cutoff wall reduces the interferences in stress and deformation. In addition, the hinge plate is poured after the completion of cutoff wall and a part of embankment when the deformation has partly finished, which provides a more favorable stress condition for the cutoff wall;
- Embankment and cutoff wall may be constructed separately without interferes in construction;
- There are at least three expansion joints available for adjusting the differential deformation between the dam and the cutoff wall, which are favorable for the working condition of water stops; and
- The length of hinge plate can be determined independently.

In the Xinjiang Autonomous Region, China, the Wuluwati CFRD is erected on the deep sand–gravel deposit at its right abutment and is designed with connecting plate to avoid excessive excavation.

2. Concrete face slab

Nowadays, with the application of non-railed slip form, the most concrete face slabs are divided into individual bays by a series of vertical joints to adapt the deformation of embankment and to meet the requirement for concrete pouring.

Long face slab of high dam may be poured by several stages to reduce the construction difficulties and to prevent the face slab from cracking. Stage pouring is also desirable from the standpoint of staged water storage for high dams and early beneficial payback. For medium to low dams, it may either be poured at one operation or in stages, under the consideration of flood protection and water storage requirements. Horizontal joints due to staged pouring are treated as construction joints with reinforcing bars passing through. Deformation of embankment during continuous placing can induce gaps between the previously poured face slab and the adjacent cushion zone, which is not rare in the CFRD dam construction, such as the CFRD of Tianshengqiao No.1: Because the considerable deformation took place during the embankment compaction, gaps were manifested at the top of the first-stage face slab with a width of 15 cm and a maximum depth of 7 m. The second-stage face slab was continuously poured after the treatment of these gaps by cleaning up and grouting with mixture of low-grade cement and fly ash.

Stress analysis showed that there is no strong relation between the thickness and the stress/deformation of face slab. A thin face slab is of more beneficial for its higher flexibility. Therefore, determination of the thickness of face slab mainly depends on the requirements for the durability and the installation of reinforcing bars and water stops. For medium to low dams, equal thick face slabs of 30–40 cm may be employed; while for high dams, increased thickness from top to bottom may be adopted. Thickness at the top should be not smaller than 30 cm, and it is gradually increased downward according to the formula

$$t = 0.3 + \alpha H \quad (10.1)$$

where H = height from the top of face slab to the calculating section, $\alpha = 0.002$ – 0.0035 , coefficient by current experience.

A value of $\alpha = 0.003$ is frequently adopted for the high CFRD in China, but exceptions also may be found such as the CFRDs of the Baiyun and the Daqiao with $\alpha = 0.002$. $\alpha = 0.001$ were individually adopted such as the Reece Dam (Australia, $H = 122$ m). Since the modern design theory and construction techniques of concrete mix proportion may improve the concrete quality of face slab and its durability without essential difficulties, thin face slab will be more and more prevalent.

3. Joint sealing

Joints are distinguished as the perimetric joint at the connection of face slab and toe slab, the vertical joint between bays of face slab, and the horizontal joint attributable to staged pouring of face slab (Fig. 10.8). The vertical joint may be tensile near the abutments and compressive at the mainstream portion. All these joints are weak but important elements in the anti-seepage system of CFRD. Opening and water stop failure of these joints are the main scenarios of infiltration through dam which may lead to the occurrence of dangerous accident.

Typical design of water stops is shown in Fig. 10.9.

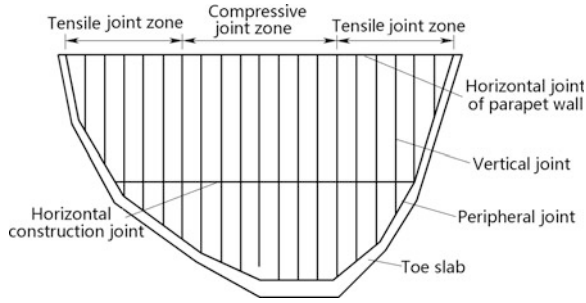


Fig. 10.8 Jointing system in face slab

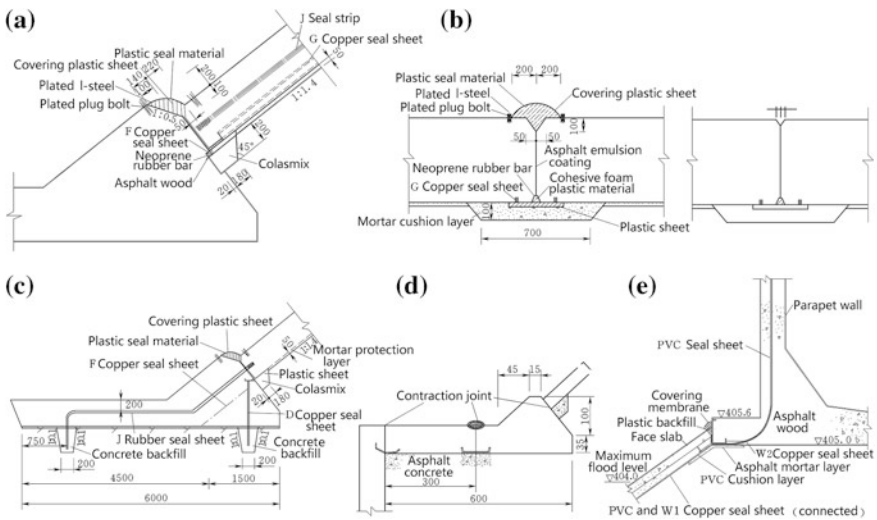


Fig. 10.9 Typical design of water stops (unit of size: cm; unit of elevation: m). **a** Perimetric joint; **b** vertical joint of face slab; **c** contraction joint of toe slab; **d** joint of toe slab on sand–gravel alluvium; **e** horizontal joint of face slab and parapet wall

(a) Perimetric joint

On the one side of perimetric joint, there is toe slab founded on bedrock or alluvium and on the other side, there is face slab on compressive rockfill. Differential deformation in the perimetric joint may occur and can reach to a magnificent value, in the ways of opening, offsetting, or shearing. Initiated from the construction of the Xibeikou CFRD in China, according to the experiences from domestic and abroad, three lines of water stop are commonly set for perimetric joints, namely copper water stop at bottom, plastic water stop at middle, and plastic filler at surface.

Non-cohesive fine materials such as fly ash and silty fine sand are put into use to cover the joint surface. Special cushion serving as filter zone is placed at the joint

bottom for the purpose of the joint self-healing. On the lower portion of the face slab where repairing can not be made by urimators, cohesive earth blanket is customarily installed as an auxiliary seepage prevention backup, and its upstream surface is protected by ballast. This kind of self-healing structure had been exercised successfully in the project of the Tianshengqiao No.1 and has been accepted as a routine procedure nowadays.

In some dams, it was stated that the effectiveness of middle water stop is not so certain. In addition, the use of middle water stop will hinder the concrete pouring and vibrating nearby, particularly for middle to low dams, and the space for three lines of water stop is very limited particularly for equal thick plate of 30–50 cm. Therefore, there was suggestion to cancel the middle water stop, remaining only the water stops at bottom and surface. For instance, the Longxi CFRD (Zhejiang, China, $H = 58.9$ m) uses equal thick face slab of 40 cm, and only two water stops at bottom and surface were installed.

(b) Vertical joint

Vertical joint is categorized into tensile joint near abutments and compressive joint at mainstream embankment. Water stops at tensile joints are treated identical to the perimetric joint, which may be simplified into two lines at surface and bottom. For compressive joints, only bottom water stop of copper sheet is required. Generally, no compressive materials are used to fill the vertical joints, except for a thin layer of asphalt painted at joint interface to separate face slabs. The steel bars for the reinforcement of face slab should not penetrate through the joints.

Generally, the space between vertical joints lies within a range of 12–18 m upon practical experiences, which is dependent on the topographic and geologic conditions, the temperature variation, the settlement anticipated, and the construction conditions. Previously, some additional vertical joints midway between the main joints were introduced in the areas close to abutments where horizontal tensile strains were expected to occur. However, this kind of arrangement is no longer exercised nowadays.

(c) Horizontal joint

Horizontal joint in face slab is handled as construction joint. Reinforcement bars are installed through the joint interface. Roughening, cleaning, and placing cement mortar are demanded before the successive pouring of the next bay.

(d) Joint of toe slab

Previously, the toe slab concrete is poured by segment bays of 12–15 m long. Water stop is installed at the joint to seal temperature and dry shrinkage induced cracks. Currently, more and more projects do not set expansion joints, except for unfavorable topographic or geologic conditions. Such construction joints with reinforcing steel bars across through and without water stop are arranged during concrete pouring according to the requirement for construction. Before pouring the next segment, the joint face should be cleaned, roughened, and covered with cement mortar. This kind of practices was carried out in the CFRD of the Tianshengqiao

No.1 and the Tianhuangping Lower Reservoir. At the Wanaxi CFRD additives, UEA with slight expansion property had been blended into the toe slab concrete. No cracks were founded in the 30-m-long toe slab segments. However, the toe slab in the project of the Tianshengqiao No.1 poured by slip form with long segment manifested serious cracking. Therefore, concrete mix proportion design, pouring technology, and curing preservation should be emphasized for minimizing toe slab cracking.

(e) Joint of toe slab located on sand–gravel alluvium

Concrete cutoff wall is usually used as under seepage prevention device for modern CFRD projects where the toe slab has to be located on sand–gravel alluvium. The face slab is connected to the concrete cutoff wall by using the toe slab and hinge plate for forming a closed anti-seepage system.

Width of toe slab is determined according to the construction condition. Generally, it is 4.0–4.5 m wide and 0.7–1.0 m thick. Water stop for the joint is handled identical to the perimetric joint.

(f) Horizontal joint between face slab and parapet wall

For a horizontal joint between the face slab and the parapet wall, two lines of water stop at surface and bottom should be installed. According to the lesson learnt from the Gouhou Dam, the DL/T5016-1999 “Design specifications for concrete face rockfill dams” stipulates that the horizontal joint between the face slab and the parapet wall should be located higher than the maximum static pool level.

(g) Contraction joint of parapet wall

The joints in parapet wall are usually arranged identical to that of the vertical joints in face slabs. Since the water pressure is small on the parapet wall, the water stop could be simplified into one line of plastic sheet.

10.5 Foundation Treatments

The foundation requirements for rockfill dams are less rigorous than that for concrete gravity dams, but more rigorous than that for earthfill dams (Acker and Jones 1972; ICOLD 2005).

Foundation treatments for rockfill dams must meet the following demands:

- Minimum leakage;
- Prevention of piping;
- Limited settlement; and
- Sufficient strength to maintain stability against sliding.

Of critical importance in a rockfill dam is the prevention of under seepage and the watertight seal between membrane and foundation. To prevent seepage beneath rockfill dams, foundations are conventionally grouted. The determination of

whether grout is necessary and its extent should be based on the careful study with respect to the site geology by visual examination and borehole packer test.

Cutoff wall excavated down to bedrock is generally installed to prevent leakage in foundation, to facilitate grouting operation, to provide a watertight seal together with membrane, and to sustain the downward thrust of the membrane. Drainage gallery is sometimes installed in conjunction with the cutoff wall to facilitate later phase grouting and to determine seepage locations and quantities, but it is not recommended for small dams.

For rockfill dams located on sand and gravel foundation, the necessity and extent of excavation should be studied. If there is no inter-layer of poor quality with detrimental influences on the stability against sliding and piping, and the properties of foundation sand and gravel are similar to the rockfill embankment, the excavation may be avoided. If the sand and gravel alluvium is thick and the bearing capacity should be strengthened, measures such as dynamic compaction, vibro-flotation, and impact rolling may be carried out. However, their effective depth is usually limited within 3–8 m.

For CFRDs on sand and gravel foundation of river alluvium, the early practice was to place toe slabs on excavated bedrock, and the river alluvium was left as the foundation for main rockfill mass, provided that there are no weak seams of clay and silt. Nowadays, many CFRDs locate their toe slabs on river alluvium. One typical example is the Santa Juana Dam (Chile, $H = 106$ m) (Fig. 10.10a) completed

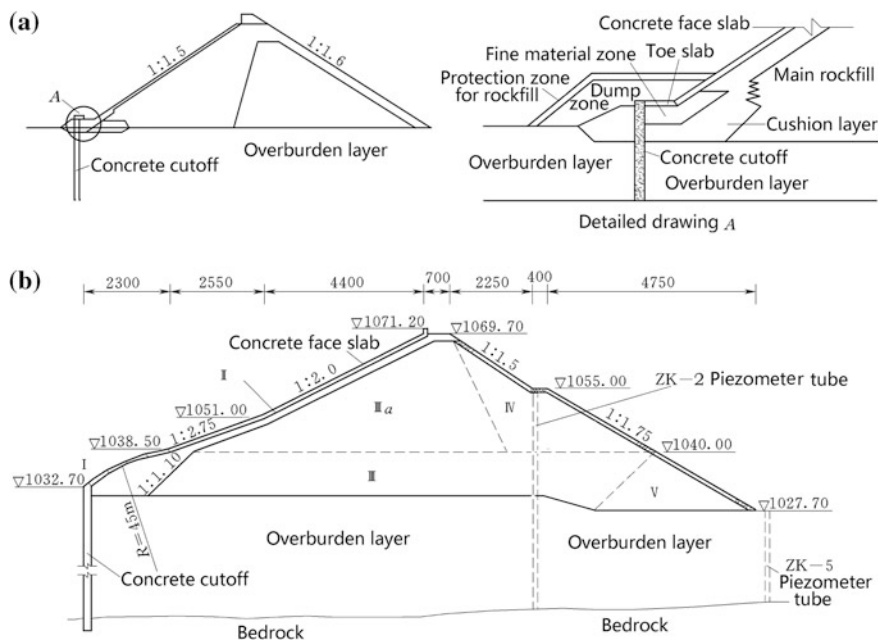


Fig. 10.10 Under seepage prevention of CFRD on river alluvium (unit for dimension: cm, unit for elevation: m). **a** The Santa Juana Dam; **b** the Kekeya Dam

in 1995 with river alluvium at a depth of 30 m. Another example is the Puc Laro Dam (Chile, $H = 80$ m) with river alluvium over 100 m in depth. These two dams use hinge plate to connect their toe slabs and concrete cutoff walls; in this manner the concrete cutoff walls and the main embankments can be constructed at the same time without interference. An additional joint due to the installation of hinge plate is also beneficial to tolerate larger differential settlement.

Until 2001, there are 7 CFRDs completed in China situated on sand and gravel alluvium foundations with concrete cutoff walls, of which the precedent the Kekeya CFRD was completed in 1986 (Fig.10.10b). The operation of these dams is successful which provides valuable experiences for flexible dam site selection and project layout. The Kekeya Dam ($H = 41.5$ m) is located on the 37.5 m deep sand and gravel alluvium; the concrete cutoff wall is built at a distance of 23 m from the upstream dam toe and is connected to the face slab by using an arched connecting (hinge) plate.

The auxiliary dam at the left abutment of the Tongjiezi Project in the Sichuan Province is a CFRD at a height of 48 m. Part of the dam is located on a 30.0–73.5 m deep sand and gravel trough. Two parallel concrete cutoff walls were installed in the foundation; between them, there are cross-walls to form a frame that works not only as an anti-seepage device, but also as the bearing walls. The project was completed in 1992 and is operated normally so far. In the raised work of the Hengshan CFRD (China, $H = 48.6$) to the new height of 70.2 m, concrete cutoff wall was installed in the earth core of the existing dam, which extended down to the bedrock with a maximum depth of 72.3 m. A toe slab was installed on the crest of the old dam connecting the cutoff wall and the face slab.

10.6 Type Selection of Rockfill Dams

Rockfill dam type should be determined by the technoeconomic appraisal according to the local natural conditions at the dam site and the purposes of the project.

10.6.1 *Materials Available*

The principle of rockfill material design is to make full exploitation of local practicable materials (e.g., effective excavated material, sand and gravel from river alluvium, and riverbank moraine soil), and only the insufficient part for dam filling is borrowed from quarry under the promises of engineering safety, economy, and environment. The embankment should be zoned based on the material sources as well as the requirements for the strength/permeability/compressibility of filling material (Leps 1970), expedient construction, and economical efficiency.

10.6.2 Topographic and Geologic Conditions

Topography, of course, dictates the maximum possible dam height and the length. The topographic details are important in locating dam axis, spillway, diversion works, outlet control, and power facilities. Generally speaking, a rockfill dam has strong compatibility to each kind of river valley terrain. However, the configuration of the valley walls should be taken into account in coordinating dam axis to avoid a large vertical or overhang area where the core adjoins abutment.

A majority of rockfill dams are founded on rock stratum. However, this is not a requirement for utilization of rockfill construction as, for example, at the Kekeya Dam, which is founded on a deep alluvium, or at the Gepatsch Dam on moraine and alluvial materials.

10.6.3 Climatic Conditions

Climatic conditions could be a predominant factor in the type selection of rockfill dams. Rockfill can be placed in areas where heavy rainfall would make the construction of an earthfill difficult or virtually impossible. Some types of rockfill construction can be accomplished at below-freezing temperatures which would preclude earthfill placement. Thus, the construction season is much less restricted with respect to rockfill rather than earthfill.

10.7 Further Developments and Other Key Issues of CFRD

Attributable to its safety, economy, and good adaptability, the CFRD is practiced world widely in recent years. There are over 200 CFRDs higher than 100 m around the world, and a fairly large number of particular high CFRDs (>200 m) are under the construction or design. The CFRD design is undergoing a period transmitting from experience-based judgment to experiment- and computation-based analyses (State Economy & Trade Commission of the People's Republic of China, 1999). The scientific test and prototype observation are playing an increasingly important role for high CFRD design and construction. The CFRD can be constructed on a dense gravel layer, provided there are no weak inter-layers of fine silt sand or clayey soil influencing the deformation and stability of the dam body.

It has been nearly 30 years since China employed the modern technology to construct CFRDs, and during this period, significant progresses have been achieved. Nowadays, the CFRD becomes an important alternative during dam-type selection competitive to the concrete arch dam and the RCC dam.

10.7.1 Advantageous of CFRD

1. Safety

CFRD has good anti-sliding stability. The slope of CFRD is nearly identical to the natural repose angle of dumped rockfill (e.g., 1:1.3), which secures the dam slope stability against sliding. The dam has high scouring resistance against through seepage, too. Because that the most area of rockfill embankment is dry, which can effectively reduce or even eliminate the additional pore water pressure caused by earthquake, and the structure has high earthquake resistance. As the CFRD is mainly composed of compacted rockfill of high density, the deformation induced by self weight is small (usually within 1 % of the dam height), of which the majority will be completed fast during the construction period. The deformation due to reservoir pool water reaches stable state quickly in a few years after the initiation of impounding, which is favorable for the safe operation.

2. Economical efficiency

The quick advocating of CFRD is also attributable to its economical efficiency when comparing with other kind of dams:

- Compared with the concrete dam, the unit price of the raw material is significantly reduced. Furthermore, the construction machinery and processes of CFRD are obviously simpler than the concrete dam;
- Compared with the earth-core rockfill dam, the CFRD filling amount can be reduced by about 40–50 %. Actually, the profile of CFRD is the smallest one of all earth–rockfill dams. In addition, the slope of CFRD is steep and the bottom width is small; therefore, the length of discharge and conveyance structures (e.g., spillways, tunnels) is short, too. As a consequence, the project layout may be more compacted.

3. Adaptability

- CFRD has good compatibility to each kind of river valley terrain;
- CFRD performs well under various geologic conditions;
- CFRD may be constructed under various climatic conditions;
- CFRD is particularly advantageous for dams that should be stage constructed with dam height to be raised later.
- CFRD is advantageous for damming the upper and lower reservoirs in the pumped-storage power station with regard to its good performance during fast reservoir level fluctuation.

10.7.2 Layout of Flood Releasing Works and Balance Between Excavation and Placement

When selecting the location or determining the project layout for a CFRD, if the excavated materials can be used for dam construction, special borrow areas are usually unnecessary or the quantity of borrowing can be reduced.

The layout of three Brazilian high CFRDs such as the Foz Do Areia (Brazil, $H = 160$ m), the Segredo (Brazil, $H = 145$ m), and the Singo (Brazil, $H = 151$ m) is very compact with large excavation of spillways and tailrace channels. The Foz Do Areia dam has volume of 14 million m^3 , of which 12.5 million m^3 is from the effective excavation for appurtenance structures, and the average hauling distance is smaller than 1.5 km. The Segredo Dam has volume of 7.2 million m^3 , of which 6.9 million m^3 is from the effective excavation for appurtenance structures.

The volume of the CFRD of Tianshengqiao No.1 (China, $H = 178$ m) is 17.8 million m^3 . At the initial design phase, the spillway was positioned at near the right abutment for shortest approach channel and chute. However, the geological condition in the right abutment area is so adverse which might give rise to slope instability problems. Later on, the spillway was moved to a Karst valley faraway from the dam abutment. The length of its approach channel is 1122 m with a width of 120 m. The volume of the spillway excavation is 17.64 million m^3 , of which 15.2 million m^3 was used for dam construction and as concrete aggregate. The other rock materials needed were supplied by an additional borrow area at the right of the spillway.

The CFRD of Shisanling Upper Reservoir (Beijing, China) is 75 m high. The volume of the dam is 2.25 million m^3 , which is all filled with excavated materials including large quantity of weathered andesite rock. No special borrow is necessary for the dam construction.

It can be shown, at least theoretically, that under certain conditions pertaining to the embankment configuration and the developed pore pressures as well as the characteristics of rockfill, a deep-seated slide failure could occur in a rockfill embankment subjected to overtopping or through flow. Laboratory tests and prototype observations have indicated that the failure of an unreinforced rockfill subjected to through seepage flow would be initiated by raveling and minor sliding at the downstream toe, and then, the successive retrogression of larger slides progresses and the hydraulic gradient is steepened. The slides could finally cut through the crest of the dam and cause complete breaching of the structure. However, if the initial erosion is prevented by securely anchoring the larger rocks, the rockfill mass will remain stable under flow gradients far greater than those which would otherwise cause failure. Based on these understanding, rockfill may be designed to be stable when subjected to through flow or overflow (Olivier 1967), clearly an important advantage of rockfill dams over earthfill structures subject to overtopping during construction.

The susceptibility to failure by through seepage flow of an unreinforced rockfill slope is dependent upon the inclination of slope, the maximum hydraulic gradient,

the rate of discharge, and the characteristics of rockfill with respect to the size, shape, gradation, and specific weight of the rock particles. The evaluation of these factors can be approached logically, but the design of an anchorage system to prevent the dislodgment of larger key rocks at the embankment toe is largely empirical. Weiss (1951) pioneered the concept of stabilizing the downstream rockfill slope to permit it to be safely overtopped, by reinforcing the rocks with a grid of steel bars anchored in place, which are back-tied extending horizontally into the rockfill mass. Other designers have utilized and further developed this method. Slope stabilization by means of concrete slabs, asphaltic concrete membranes, or long flat beams of heavy rock also has been exercised (ICOLD 1993a, b; Chanson 2001–2002, 2009; Manso and Schleiss 2002; Olivier 1967).

The Crotty Dam (Australia, $H = 83$ m) is the first CFRD with a spillway laid on the dam crest whose total and specific discharges are 245 and 20 m³/s, respectively. Similarly, the Batubesi Dam (Indonesia, $H = 30$ m) installed emergence spillway on the dam crest in a form of fuse-plug dam; the discharge is 800 m³/s. China had designed three CFRDs with crest spillways, of which the Tongbai CFRD (Zhejiang Province, China, $H = 70.6$ m) and the Yushugou CFRD (Xingjiang, China, $H = 67.5$ m) (Fig. 10.11) have been completed.

10.7.3 Layout of DrawDown Tunnels

Before, being in short of experience, and in view of the case that some reservoirs had to be emptied for maintenance when serious leakage/seepage manifested, drawdown tunnels were customarily installed at the lower elevation, which were transformed from diversion tunnels. For example, the Xibeikou Project was emptied for treatment due to heavy leaking water loss at the high water level. Nowadays, along with the accumulation of engineering experiences and the advancement of techniques, with the less deformation of rockfill compacted by vibration roller, as well as with the improvement of concrete materials and the advances of joint sealing structures and materials, it is rare to find serious leakage through face slab and joints. Even though the leakage appears through joints, it can be self-healed by the fine particles with the effects of cushion layer under the slab. That is why the special empty tunnel is no more highly required for maintenance. The CFRD of the Wan'anxi in the Fujian Province is 93.5 m high and has 2.28×10^8 m³ in storage capacity. This project had a drawdown tunnel at the initial designing. After the detailed research and study, the drawdown tunnel was considered unnecessary and canceled. Other examples of drawdown tunnels being eliminated and the diversion tunnels being blocked after the project completion are the Foz Do Areia Dam, the Segrado Dam, and the Xingo Dam. However, the drawdown tunnel of the Tianshengqiao No.1 is installed because of its comprehensive functions of water diversion, water supply, and flood discharge.

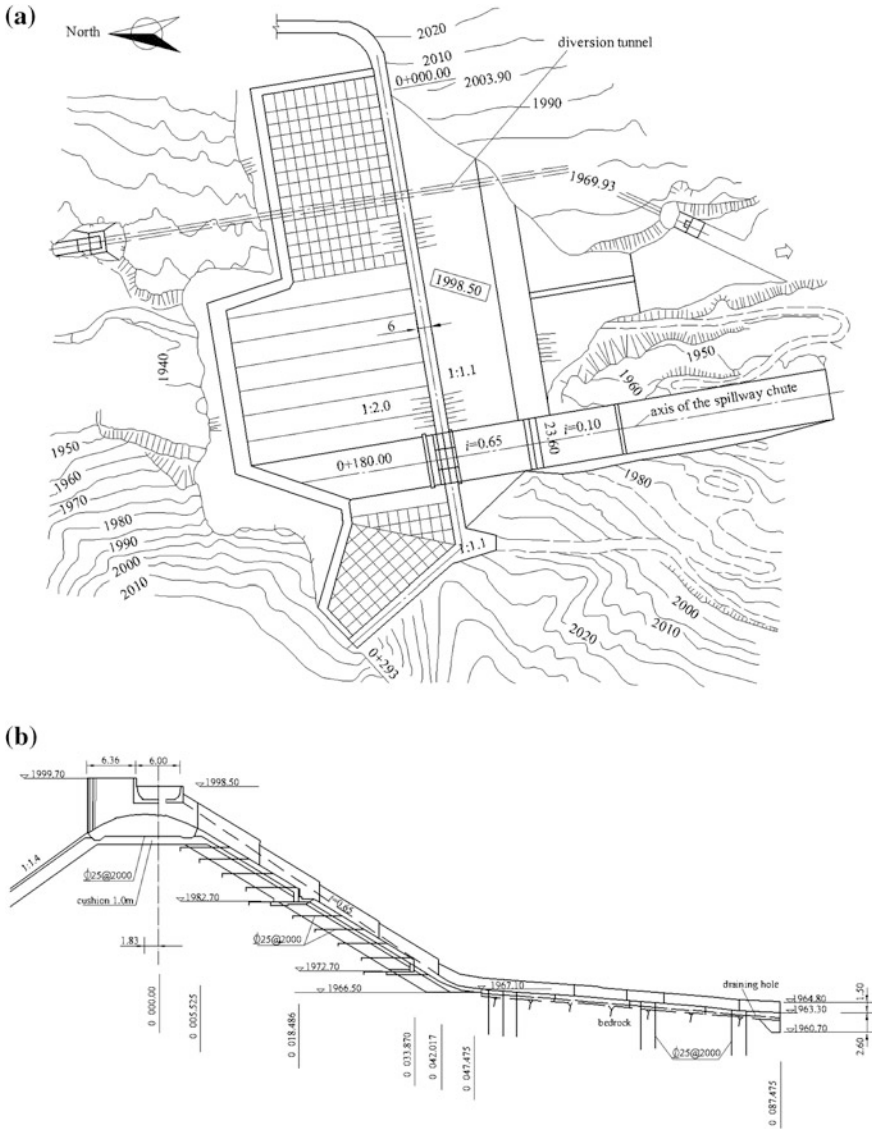


Fig. 10.11 Crest spillway (unit: m)—the Yushugou Dam (China, $H = 67.5$ m). **a** Plan; **b** profile

10.7.4 Materials for Dam Body

Usually, saturated compressive strength 30 MPa is looked at as a dividing boundary of soft rock and hard rock. The lowest strength practically exercised is 10 MPa. Engineering practices show that the medium strength rock of 60–80 MPa has the

best characteristics compromising among different design and construction requirements (ICOLD 1993a, b).

1. Soft rocks

Soft rocks are ordinarily compacted in the downstream rockfill zones above tailwater level. The Zhushuqiao CFRD can serve as an example. According to the initial design, the rockfill materials are borrowed from a special limestone quarry with a hauling distance of 8–9 km. In view of a large amount of weathered slate was reserved in a hauling range of 0.5–1.5 km from the dam site, and because the deformation of the downstream rockfill zone had minor influence on the face slab, weathered slate with a saturated compressive strength not lower than 10–25 MPa had been used. Correspondingly, a more flat downstream slope of 1:1.7 was adopted due to the lower shear strength. It has been finally proved that the new design is more economic, although the volume of the embankment is larger.

The CFRD of the up reservoir of the Shisanling Pumped-Storage Power Station (China, $H = 70$ m) is filled by excavated weathered andesite with a minimum saturated compressive strength of 11 MPa.

The CFRD of the Tianshenqiao No.1 Project at a height of 178 m had used a large amount of mixture of thin-layered limestone, mudstone, and sandstone in the downstream zone above the tailwater level.

The rockfill dam of the Bailey (USA, $H = 94$ m) is constructed totally using thin-layered sandy shale. The upstream slope is flattened to 1:2.0 and is covered by the hard rock protection.

The Tianshenqiao No.1 Dam, the Zhushuqiao Dam, and the Shisanling Upper Reservoir Dam all have been completed. Their performances are satisfactory except some larger side deformation of the embankments.

Laboratory tests show a moderate compressibility modulus of soft rockfill embankment, such as 31–44 MPa for the Zhushuqiao CFRD and 30–43 MPa for the Tianshenqiao No.1 CFRD.

Soft rock materials will be crushed and become finer during compaction; therefore, the design should be based on the mechanical properties according to the gradation after compaction.

Tests using weathered shale of grain size smaller than 60 mm show that, after testing under confined pressure of 1.0 MPa, the content of <5 mm particles is increased from 25 to 47 % and that of medium diameter particles is decreased from 18.5 to 5.8 mm. Due to grain crushing, soft rock materials can be compacted into high density. Taking the Tianshenqiao No.1 CFRD for example, the design dry density and porosity are 2150 kg/m³ and 22 %, respectively, for its downstream rockfill zone, while the average dry density measured during the construction is 2220 kg/m³, which is equivalent to an actual porosity of 20 %.

2. Sand and gravel materials

Compacted sand and gravel materials behave similar to the rockfill materials with high shear strength, whereas their deformation moduli are several times higher than those of the rockfill materials. Therefore, they are favorable materials for

CFRD and are now widely used in the CFRD construction. Among the 70 CFRDs completed or under construction in China, there are 15 dams using sand and gravel materials, of which 4 are at height over 100 m. The highest one is the Wuluwati Dam (China, $H = 138$ m), and the other 3 dams are the Shanxi dam (China, $H = 130.8$ m), the Heiquan Dam (China, $H = 123.5$ m), and the Gudongkou Dam (China, $H = 120$ m).

With regard to the embankment zoning, there are three fundamental types:

- Entirely built with sand and gravel materials, such as the Kekeya Dam (41.5 m) and the Gouhuo Dam (70 m);
- Sand and gravel materials are put in the upstream main rockfill zone for the high deformation moduli, while the downstream rockfill zone is set to prevent the rolling of gravel along the downstream slope and the shallow sliding, in this way to maintain a steeper downstream slope, such as the Wuluwati Dam and the Heiquan Dam;
- A rockfill zone is just located at the downstream side of transition zone to serve as a drain for possible leakage; then, a sand and gravel zone and probably a downstream rockfill zone are arranged. The sand and gravel zone is located at the central portion of dam body, such as the Shanxi Dam (China, $H = 132.5$ m) and the Gudongkou Dam.

The difference of CFRD using sand and gravel materials in comparison with rockfill one rests on the seepage control and surface erosion. Cautions should be exercised to prevent the depression surface in dam body, piping at the downstream exit and surface erosion in case of possible leakage.

- The cushion zone should play the role of second anti-seepage defense line. Its permeability coefficient is desirable to lie within the range of 10^{-3} – 10^{-4} cm/s, i.e., 1–2 orders of magnitude lower than that of transition zone in order to limit the infiltration discharge;
- If the sand and gravel materials cannot satisfy the requirement for free drainage, vertical and horizontal internal drains should be installed for discharging the seeping water and maintaining the downstream dam shell dry. Where there is a large downstream rockfill zone which can be served as the drainage zone, a transition zone between the upstream sand and gravel materials and the downstream rockfill is demanded;
- Restraint should be provided at the downstream slope to avoid the rolling of gravel and the shallow sliding. A slightly more flat downstream slope of 1:1.5–1:1.6 is ordinarily acceptable; and
- Sand and gravel materials are erodible and sensitive to surface erosion. Therefore, it is important to emphasize the water sealing system in the joint between face slab and parapet wall. Two lines of water stops should be provided, and the quality of installation should be guaranteed. The elevation of this horizontal joint should be above the normal storage water level.

3. Extremely hard rocks

In some projects, troubles had encountered during the construction with rocks of saturated compressive strength around 200 MPa.

During the heightening of the Hengshan Dam, rocks of tuff lava with compressive strength of 160 MPa were used. The flanges and corners of rock blocks were so sharp as to cause many troubles during the placement process, including the damages to truck tyres and bulldozer tracks, and the abnormal operations of vibrating rollers. In addition, the gradation is in lack of fine particles smaller than 10 cm. The situation was improved by proper blasting design and by placing a thin layer (about 10 cm thick) of sand and gravel materials on the each lift of rockfill.

Another problem would be brought about by using of extremely hard rocks is the large softening coefficient and low maximum dry density. A lesson comes from the Foz do Areia Dam (Brazil, $H = 160$ m), the compressive strength of basalt rock reaches 250 MPa, and the porosity of rockfill is 25 %. The settlement during the construction was 358 cm (2.24 % of the dam height) and the deflection of face slab after impounding reached 77 cm.

4. Cushion zone materials

The function of cushion (transition) zone has been progressively understood from providing a uniform face slab support only, to additionally providing second defense frontier of anti-seepage satisfying the requirements for semi-perviousness and filter. The gradation requirement also has been gradually shifted from uniform grading without fine particles to grading materials with high content of <5 mm particles and semi-pervious characteristics. Nowadays, the gradation for the cushion zone suggested by Sherard et al. (Sherard and Dunnigan 1984, Sherard 1985, 1989) is widely accepted, i.e., a continuous gradation with maximum diameter of 100–80 mm, content of <5 mm particles is 35–55 %, and content of <0.1 mm particles is 2–12 % (Table 10.2). For CFRDs located in chilly areas or high-intensity earthquake areas, well-permeable coarser gradation may be exercised to avoid freezing/thawing action and dynamic pore pressure. The Guanmenshan CFRD located in chilly area; a coarser gradation with the maximum particle grain of 150 mm and an average content 17 % of particle grain <5 mm was employed.

The opening of perimetric joint followed by serious leakage is the “Achilles heel” of CFRD. Recently, a special cushion zone with <40 mm fine materials under perimetric joint becomes a prevalent practice. It can be compacted to a denser state for reducing its deformation on one hand and can limit the leakage and perform as a filter in case of possible leakage on the other hand.

Table 10.2 Gradation of cushion layer suggested by Sherard

Grain (mm)	0.074	0.6	5	19	37	75
Percentage smaller than the grain size (%)	2–12	8–30	35–55	55–80	70–95	90–100

The cushion zone is ordinary installed with equal width depending on the type of construction machines and methods. Its horizontal width is not smaller than 3 m when the dump truck and bulldozer are used. It can be greatly reduced down to 1.0–1.5 m where the cushion materials are placed using backhoe, scraper, and manpower. Some CFRDs in China at height lower than 100 m have been equipped with cushion zones of 1 m in horizontal width and accompanied with wider transition zone, such as the Tainhuangping Lower Dam (China, $H = 96$ m), and the Longxi Dam (China, $H = 58.9$ m). Near abutments, the cushion zones should be widened and extended downstream to a certain distance.

Because of the rigorous grading requirement for the cushion zone to which the natural materials are difficult to meet, they need to be processed. The resources of materials and processing methods employed in engineering practices can be summarized in the following:

- Processing from natural sand and gravel materials, such as the CFRD of the upper reservoir in the Guangzhou Pumped-Storage Power Station, the screened riverbed sand and gravel materials of particle size <100 mm are used in the cushion zone.
- Mixing of manufactured sands and aggregates by predetermined ratio, such as at the Xibeikou CFRD, or directly manufactured using stone crusher with adjustable gradation of finished product, such as the Tianshenquao No.1 CFRD.
- Quarry-run materials by special explosion design, such as the Guanmenshan CFRD; cushion materials were directly borrowed from a quarry of andesite by blasting.
- Mixing of artificially crushed stones and natural sands and gravels, such as the use of crushed stones and riverbed sands at the Chengping CFRD, the use of crushed stones and weathered granite coarse sands at the Wan'anxi CFRD, and the use of crushed gravels and sands at the Baixi CFRD.

In some CFRDs, sand and gravel materials were placed for main rockfill, where the gradation coefficient between the cushion zone and the main rockfill already satisfied filter criteria. Therefore, special cushion zone is not needed, such as the Gouhuo CFRD, and the Xiaogangoudam CFRD.

10.7.5 Cracking of Face Slab

Cracking is frequently encountered in concrete face slab due to its large length and small thickness. Serious cracking occurred in the earliest batch of CFRDs in China due to lack of experience. In the Xibeikou Dam (China, $H = 95$ m), the concrete face slab was placed at one stage in 1989. Altogether, 262 cracks were reported in the 23 of total 24 face slabs, of which 128 cracks were wider than 0.3 mm, 95 cracks were wider than 0.3–0.49 mm, and 36 cracks were wider than 0.5–0.99 mm. The maximum crack width was 1.2 mm.

Cracks in face slab have following features that

- They are almost horizontal;
- Most of them are distributed at the middle and lower portions of the longer slab;
- Their width is usually smaller than 0.3 mm, the majorities are smaller than 0.1 mm, and a few reach 0.5 mm;
- They penetrate the whole depth of the slab, narrowed slightly at the location of reinforcement bars; and
- Most of them are manifested soon after pouring and developed after winter season.

Possible driving forces of cracks are rockfill deformation, temperature variation, and drying shrinkage. Since the embankments are filled of high density and deformation modulus, cracking due to differential deformation is very seldom, whereas the factors of temperature variation and drying shrinkage are considered as predominant. Face slab cracking can be prevented by enhancing the concrete crack resistance, as well as by reducing the driving force related to the variations of temperature and humidity, which comprise the following aspects:

- To optimize the concrete ingredient materials and its mix proportion;
- To enhance its tensile strength and ultimate tensile strain, by the utilization of high grade Portland cement, sand, and aggregate with small water absorption and mud content.
- Reducing cement and water consumption and water/cement ratio by blending high effective water-reducing agent, air-entraining agent, and fly ash;
- Limiting the crack development by reinforcement bars;
- Employing appropriate construction technology to ensure the concrete quality;
- Using slightly expanding agent to compensate contraction; and
- Selecting coarse aggregates with small thermal expansion coefficient (e.g., limestone).

Recent researches recommend the employment of reinforcing materials (e.g., steel fiber, polypropylene fiber, and geosynthetic material fiber) (Giroud 1989, 1992) to raise the tensile strength and ultimate tensile strain, the use of admixture of every kind of additives to enhance crack resistance, and the improvement of concrete with high strength and low elastic modulus.

For high CFRDs, the long face slab may be poured by two or three stages to reduce the pouring length in each stage, and in this way, the restraint of cushion to the face slab could be relaxed. Proper pouring season also may be scheduled to avoid high temperature, freezing, strong wind, and dry climates, so as to alleviate the damage due to temperature variation and dry contraction. Preserving and curing of face slab are meaningful measures to prevent cracking, too. Humid and thermal conservation measures should be employed, which would be better to be maintained until reservoir impounding.

Since the leaking discharge through face slab cracks is usually not large and the main rockfill zone is pervious, flow through cracks will not result in the rising of phreatic line, nor produce excess pore pressure. Nevertheless, the durability of face

slab could be considerably affected by cracking. Currently, according to the SDJ20-78 “Specifications of design standard of reinforced concrete structure in hydraulic engineering,” DL/T5016-1999 “Design specifications for Concrete face rockfill dams,” and the SL191-2008 “Design code for hydraulic concrete structures,” cracks of width over 0.15–0.20 mm should be treated. Methods of crack treatment are grouting, surface coverage with sealing material for the purpose of seepage prevention, as well as restoration of concrete integrity. It should be mentioned that the cracks of width below 0.3 mm were not treated in the Xibeikou Dam and the cracks of width below 0.25 mm were not be treated in the Zhushuqiao Dam. However, in the Longxi CFRD and Guangxu CFRD, the cracks of width smaller than 0.2 mm were all treated.

Reinforcement for the face slab serves the purposes to prevent cracking caused by temperature variation and dry contraction in construction period and to restrain the propagation of cracks once they occur. Reinforcement ratio has been gradually reduced from early 0.5 % to currently two-way reinforcement ratio of 0.3–0.4 %, and a single-layer reinforcement may be placed in the neural plane of the face slab for higher slab flexibility.

10.7.6 Resistance Against Earthquake

Theoretic analysis and experimental study have indicated high earthquake resistance of CFRD. However, whether the excellent safety record is due to the fact that very few major CFRDs have been subjected to violent earthquake shaking is not very clear. The 85-m-high Cogoti CFRD in Chile, constructed in 1938, is a dumped rockfill embankment with an upstream slope of 1:1.4 and a downstream slope of 1:1.5, which has been shaken by several earthquakes. The 1943 Illapel earthquake with a magnitude of 7.9 and an epicentral distance about 90 km from the dam site produced a peak ground acceleration (PGA) of 0.19 g. Although there was no significant damages to the face slab which had a thickness varying from 80 cm at the base to 20 cm at the top, following hazardous phenomena were documented:

- Rock stagger and fall occurred;
- Longitudinal cracking on the face slab crest of the mainstream embankment appeared;
- An instantaneous crest settlement of 38.1 cm took place;
- The joints of face slab above water level were not damaged, but the slab near the crest had been separated from the rockfill;
- There were crushing at the two sides of joint, the asphalt filler in the joints was squashed out;
- The leakage increased with the rise of the reservoir level; in May 1985, the leaking discharge was gauged as 2400 L/s.

China has a number of CFRDs built in the regions with strong earthquake, such as the Daqiao (China, $H = 93$ m), the Xiaogangou, the Heiquan, the Kekeya, and the Wuluwati. However, they all have not tested out by strong earthquake except for the Zipingpu (China, $H = 156$ m) located at the Dujiangyan City on the up reach of the Minjiang River, 60 km northwest of the Chengdu City (the capital of Sichuan Province). The main purposes of the project are water supply and electric power generation. The total storage of the reservoir is 1080×10^6 m³ and the installed generator capacity is 760 MW. The upstream slope of the dam is 1:1.4, whereas the downstream is designed with two slopes to secure the stability of dam crest during earthquake. The upper portion of the downstream slope is 1:1.5, and the lower portion of the downstream slope is 1:1.4. According to the original earthquake intensity map, the basic earthquake intensity at the work site is 7 and the designed earthquake intensity is 8, with the corresponding PGA of 0.26 g.

The project was completed at the end of 2006. On May 12, 2008, a strong earthquake hit the Wenchuan County in the Sichuan Province of China at 2:28 pm. The quake measured 8.0 on Richter scale with the epicenter located at 31.0° north latitude and 103.4° east longitude, according to the State Seismological Bureau (SSB) of China. The distance from the Zipingpu CFRD to the epicenter is 17 km. During the earthquake, the accelerometer recorded that the acceleration at dam crest had reached 2 g. Considering the normal amplification factor, the ground acceleration should be larger than 0.5 g, which is much higher than the intensity anticipated in the design. The reservoir level when the earthquake occurred was 830.0 m.

After careful inspections immediately after the earthquake, the Zipingpu CFRD is considered structurally stable and safe. However, the dam did suffer from a range of damages during the quake.

1. Deformation

By the earthquake, significant settlement was induced. Immediately after the earthquake, an obvious settlement of dam crest in the mainstream rockfill could be identified even by eye view. By the measuring of the benchmark points on the dam crest, the maximum settlement was 683.9 mm. After the main earthquake, the observed settlement of dam crest still continued. But the rate of settlement dropped rapidly. On May 12, the maximum settlement of dam crest reached 744.3 mm. On May 22, the settlement of dam crest was basically stable. The maximum displacement of dam crest in the direction of river flow was 199.9 mm. With regard to the displacement parallel to the dam axis, the rockfill at abutment areas was trended to move toward the river stream. The maximum horizontal displacement toward right abutment was 226.1 mm and that toward left abutment was 106.8 mm.

2. Dam crest

As the maximum dynamic response appeared at dam crest, the quake gave rise to cracks and ruptures in the parapet wall. Near the abutments, the originally closed joints were opened with the maximum aperture of 30 mm. In the mainstream rockfill, the parapet wall was ruptured by large compression stress. The limestone

handrails at the downstream side of the crest were all damaged. The cracking and slab staggering took place at the contact of the crest and abutment slopes: At the right abutment, the height difference of slab staggering is 150–200 mm, and at the left abutment, it is 60 mm.

3. Concrete face slab

The strong earthquake had produced certain damages on the concrete face slab in the form of cracking and rupturing. On El. 845 m, where there is a construction joint between the second-stage face slab and the third-stage face slab, the face slab is overlapped. The height difference of overlapping is 150–170 mm, and the reinforcement bars across the joint were bended into “Z” shape.

The face slab number 5 and 6 (near left abutment) and the face slab number 23 and 24 (at riverbed) were ruptured by the action of large compression stress parallel to the dam axis.

By drilling detection, large upper portion of concrete face slabs was separated from the rockfill. The maximum gap between the rockfill and the third-stage face slab is 230 mm, whereas the maximum gap below the second-stage face slab is 70 mm.

4. Perimetric joint

The perimetric joint had manifested large displacement, and some of the installed instruments were damaged. In some positions, the displacements were beyond the gauging range of the instrument. According to the available data, the measured displacements of the perimetric joint at left abutment (El. 833) were 92.85 mm (settlement), 57.85 mm (opening), and 13.42 mm (shearing), respectively. For comparison, the displacements at the same position before the earthquake were 1.59 mm (settlement), 11.99 mm (opening), and 4.67 mm (shearing).

5. Leakage

The dam leakage has a close relationship with the reservoir water level. Before the earthquake, the leaking discharge of the dam was 10.38 L/s (May 10) corresponding to the reservoir level 830.0 m. After the earthquake (July 8), it was increased up to 19.3 L/s corresponding to the reservoir level 818.0 m. In the first two days after the earthquake, the leaking water was turbid; thereafter, the water became clearer and clearer.

The Wenchuan earthquake has a very strong scale and very high intensity. As a high CFRD near the epicenter, the Zipingpu Dam had successfully survived from such a strong shaking. Although the quake has produced severe damages on the dam, it is still structurally stable and safe. This proves that the design of the dam is rational and the construction quality is good.

The performance of the Zipingpu CFRD during the strong earthquake may be looked at as an important demonstration of the safety features of the CFRD against earthquake.

10.7.7 Protection of Cushion Zone

The cushion zone must be protected; otherwise, it might be washed out by heavy rains or damaged by man-made factors during construction and be engraved by wave during water retaining period. Several protective measures have been exercised in the construction of CFRDs in China, including shotcrete or guniting, emulsified asphalt spraying, and rolled mortar. The method of manually rolled mortar pavement of low strength was firstly employed in the Guanmenshan CFRD, whose mortar grade was M5. After trimming the upstream slope, two passes of roller compaction without vibration were executed at first, followed by two passes of roller compactions with vibration. Then, the mortar was manually placed and spread out along the upstream slope in blocks of 4–6 m wide and 4–8 cm thick. After spreading and leveling, the roller compaction along the slope was carried out with one pass without vibration at first and four passes with vibration. Finally, one pass of overall roller compaction without vibration was executed. The time interval between spreading and compaction should be about 4 h at daytime and 12 h at night in summer, and it could be extended properly in spring or autumn. Cure with watering should be started one day and night after the placement and should be lasted at least half a month. If it is necessary to retain flood when the age of mortar has not been reached, an impervious cement paste layer of 2–3 mm thickness might be painted on the surface of mortar.

The rolled mortar protection also can be placed together with the slope roller compaction. In this way, a mixture layer of mortar and the cushion material can be formed on the surface of cushion zone, which makes the protective layer tightly combined with the cushion zone. Due to fast construction and low cost, nowadays it is widely exercised in the most of China's CFRDs, especially in the medium to small projects. The grade of the mortar for protecting slope should be lower (e.g., M5) to reduce the restraint from the cushion on the face slab.

The other protective methods with actual applications are, for example, shotcrete for the Xibeikou CFRD, grouting for the Daqiao CFRD, and emulsified asphalt spraying for the Tianshengqiao No.1 CFRD. All these have shown positive results and are selectively determined by the experience of the constructor taking into account the local conditions.

In recent years, a number of CFRDs in South American countries apply extruding wall which enable

- To construct the sidewall and cushion at the same time;
- To omit dam slope trimming, slope compaction, and slope protection;
- To avoid extra-fill of cushion materials;
- To speed up the placement; and
- To improve the compactness and to reduce the scouring risk of cushion materials during the construction, as well as to facilitate dam slope protection and to realize water retaining during flood season.

The Gongboxia Dam (China, $H = 132.2$ m) employed the extruding wall successfully. From the existed engineering experiences, the concrete extruding wall should have cement content of around 70 kg/m^3 and meet the following criteria:

- Not exceeding 5 MPa in compression strength at 28d, the 2–4 h compression strength is such that the wall will not collapse when the cushion materials are compacted;
- Controlling its elastic modulus within the range of 5000–7000 MPa, and the lower, the better;
- Controlling its density within the range of $2.0\text{--}2.25 \text{ t/m}^3$ and approaching to the compactness degree as closely as possible;
- Controlling its permeability coefficient within 10^{-3} cm/s , to be consistent with the cushion layer (semi-permeable body);
- Painting a thin coat of asphalt emulsion on the surface of extruding wall, to reduce the constraints on concrete face slabs and prevent the face slab from cracking.

10.7.8 Inverse Filtration

It happened from time to time in China that the cushion zone, protective layer, and even concrete face slab were damaged by the filtrated water from downstream side when the tailwater level is higher than the headwater level. This is commonly termed as “inverse filtration” blamed by two scenarios.

The first scenario is that there is no downstream cofferdam in some projects, and the upstream construction pit was much lower than the downstream riverbed due to the excavation of toe slab foundation. Water pressure from the downstream side exerting on the cushion zone and protective layer gives rise to cracking and piping. In 1989, the Xibeikou CFRD after the flood season conducted pumping operation to resume the work in construction pit, while the downstream water level did not drop. As a result, an inverse water head of 7 m was exerted on the cushion zone and responsible for more than 20 concentrated seepage exits, and 6 local cavities of which the most serious one was 6 m (long) \times 3 m (wide) \times 0.5 m (deep). The pumping was suspended immediately after the situation had been revealed; then, the seepage flow was stopped by equalizing water pressure. The damaged cushion zone was carefully restored according to the original design.

Another scenario is related to the topography of dam foundation, where a profile perpendicular to the dam axis indicates that the bedrock is higher in the middle and lower on both sides, or the bedrock is inclined upstream. Seeping water would flow in the direction of upstream, producing certain water pressure on the cushion zone and protective layer. The Dongjin CFRD (China, $H = 85.5$ m) has a foundation bedrock higher in the middle and lower at both sides. The excavation for the toe slab further brought down the construction pit. The water from rain, construction operation, and others had to discharge toward upstream; as a result, the reverse

water pressure was built up. When the preliminary face slab concrete will be placed, it was discovered that water was seeping out from the cushion zone close to the bedrock face, which would affect the construction quality of the toe slab. Seven draining holes were drilled through the concrete toe slab to relieve the seeping water, which were blocked after the completion of concrete placement.

In several projects, cracks were discovered on the first-stage face slabs due to the reverse filtration when pumping water from upstream construction pit for the preparation of the clay blanket placement.

The prevention and treatment of reverse filtration have aroused general concerns and have been stipulated in construction specifications. It is required that the excavated depth at upstream toe slab should be appropriate. Where there is free drainage condition, generally draining holes may be drilled through the concrete toe slab to discharge reverse filtration toward upstream and to pump it away. Where there is no free drainage condition, steel pipes with holes may be installed in advance in the upstream rockfill to collect seeping water. After the rockfill reaches a certain elevation, the holes would be blocked at the time when the face slab is placed.

10.7.9 Quality Control of Rockfill Placement

With regard to the concern that whether the constructor would be able to control the placement parameters strictly, several methods for density measuring, such as compactometer, surface wave instrument, and settlement observation have been exercised, by which positive effects have been obtained (Materon and Mori 2000).

Compactometer is installed on the vibrating roller with the sensor on its tamping drum and the indicator in its driver's cabin. The readings on the indicator reflect the extent of compaction. This is an easy manner for a roller driver to examine himself.

The surface wave technique uses sensing apparatus in a certain distance to accept the vibrating signal produced by shock apparatus. The dry density could be calculated in accordance with the relationship between the surface wave and the dry density.

Compactometer and surface wave instrument were both employed in several China's projects, such as the CFRDs of the Shisanling Upper Reservoir, the Xibeikou, and the Guanmenshan.

Watering test pit is often adopted in the in situ density evaluation for coarse rockfill materials. Although the plastic membrane might not be closely contact the irregular pit wall, it is fairly objective and reliable. The gradation test can be carried out simultaneously. Present Chinese design codes for the CFRD stipulate that the average dry density should not be lower than the design value and the standard deviation and coefficient of deviation should not exceed the allowable range. According to the statistical data of the CFRDs in China, the standard deviation is often lower than 0.08 t/m^3 and the coefficient of deviation is below 5 %.

According to the observation data concerning the settlement during construction, the quality of rockfill embankment also could be evaluated with the deformation modulus conversed from the measured settlement (back analysis). For example, the vertical deformation modulus of Tianshengqiao No.1 CFRD is about 42–70 MPa, the vertical deformation moduli of the CFRDs of the Xibeikou, Chengping, and Guanmenshan all reach 100 MPa, by the back analysis based on the field readings of settlement.

10.8 Hardfill Dams

10.8.1 Anatomy and History

Hardfill dam is a kind of symmetrically and trapezoidally shaped embankment using low-cost-cemented sand and gravel material known as hardfill and having a concrete impervious face on its upstream face. The hardfill dam has advantages such as high safety, high earthquake resistance, low demand for foundation, simple and quick construction, low cost, and small detrimental impacts on environment. The first proposal for hardfill dam as “optimistic gravity dam” was made by Raphael (1971), and later on, Londe and Lino (1992) named it as “Faced Symmetrical Hardfill Dam (FSHD).” Nowadays, the European countries commonly term it as “Hardfill Dam,” and Japan calls it as “Cemented Sand and Gravel Dam (CSG dam)” (Toshio et al. 2003). Actually, hardfill or CSG dam may be looked at as an “intermediate dam” between the concrete gravity type and rockfill embankment type. Figure 10.12 shows the typical profile of a hardfill dam.

Since the beginning of the 1990s, with the first application to the cofferdam ($H = 15$ m) in the construction of the Nagashima Dam (Japan), this type of dam has

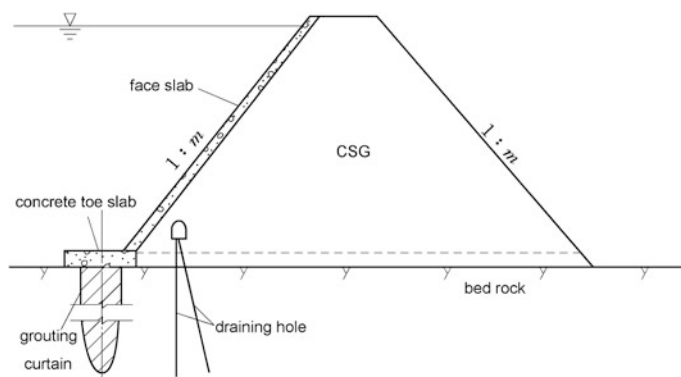


Fig. 10.12 Typical profile of a hardfill dam

been developed in the engineering practice (Batmaz 2003). The Cindere dam (Turkey, $H = 107$ m) completed in 2005 is the tallest hardfill dam in the world at present.

There have been five engineering practices in China of hardfill dams until 2010, including the upstream cofferdam ($H = 7$ m) of the Daotang Dam completed in 2004 and the upstream cofferdam ($H = 35.5$ m) of the Hongkou Hydropower Project completed in 2006. The profile of the latter is shown in Fig. 10.13, whose total volume poured in 50 days was up to $32,000 \text{ m}^3$ and maximum daily height rise was 1.2 m. In April 2006, the cofferdam was completed and withstood severe test against a 50-year recurrence flood with a peak discharge of $5500 \text{ m}^3/\text{s}$ and a maximum head of 8 m above the crest, which was 1.45 m higher than the design level. The overtopping duration was 44 h. The examination after the flood showed that there were no cracks in the cofferdam. This is the first successful application of hardfill technology in the construction of dam higher than 30 m in China.

The material properties of hardfill or CSG lie in between those of concrete and rockfill; therefore, the dam body configuration and construction technique are also featured between them (Mason et al. 2008).

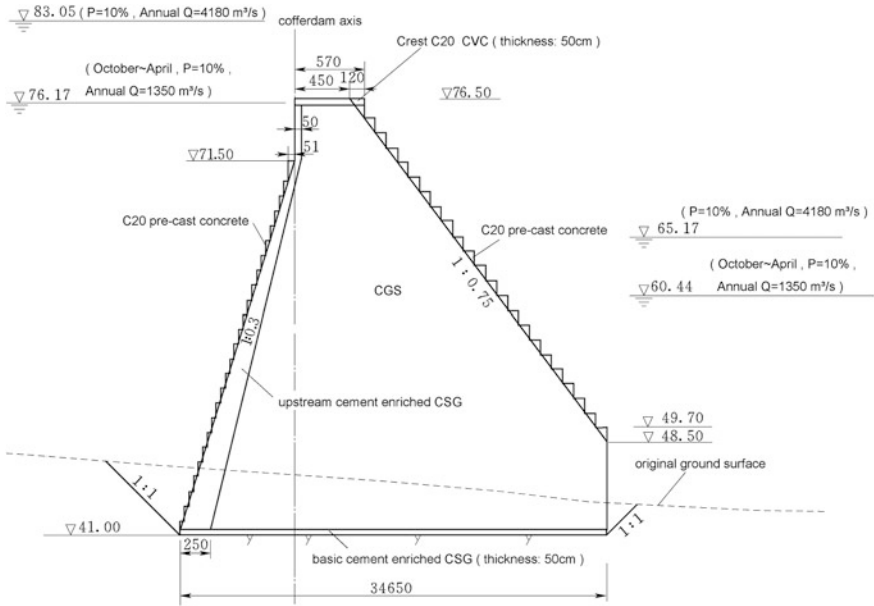


Fig. 10.13 Profile of the upstream hardfill cofferdam (unit: cm)—the Hongkou Project (China, $H = 35.5$ m)

1. Shape

The profile of hardfill dam is trapezoidal with a dam slope ranged within 1:0.5–1:0.7.

2. Material

Hardfill is a material made by adding cement about half content of RCC (approximately $50\text{--}60\text{ kg/m}^3$) to rock like materials such as gravels or excavated rocks that can be obtained easily near work sites. It is mixed and compacted with vibration rollers, which also can be considered as a kind of extreme lean RCC (Toshio et al. 2003).

3. Seepage control

The hardfill has strong seepage erosion resistance compared to earthfill and rockfill dams. It is sufficient using a seepage-proof face slab or membrane on the dam surfaces. In addition, because the deformation modulus of the hardfill is greater than the rockfill, the deformation and settlement of the hardfill dam are much smaller; therefore, the face slab safety may be easily secured.

4. Construction diversion

Since the hardfill dam has higher scouring resistance and higher strength compared to the earthfill and rockfill dams, the crest may be overtopped during construction period provided appropriate protection. It is also able to install outlet works within dam body, which is advantageous for project layout and construction arrangement.

5. Construction technique

A trapezoidally shaped hardfill dam has much greater weight and longer base width for shear resistance than a gravity dam. As a result, the requirement for the treatment of lift joints is not very strict. Since the hydration heat of the hardfill material is very low, the contraction joints and thermal control measures may be neglected, too. The construction technique is similar to that of RCC or embankment dams: simple, cheap, and short schedule.

6. Earthquake resistance

From the viewpoint of structural dynamics, the hardfill dam with a symmetrical and trapezoidal cross section possesses a better dynamic stability than the conventional concrete gravity dam with an almost vertical upstream surface.

7. Foundation

A trapezoidally shaped hardfill dam can be constructed even on poor foundations.

10.8.2 Major Features in the Design of Hardfill Dams

Hardfill dam normally employs panel (face slab) as anti-seepage device on the upstream face and utilizes low-intensity cementation gravels in the dam body for meeting the stress and stability requirements (Mason et al. 2008).

1. Profile design for hardfill dams

The stability against sliding along base and strength at the up- and downstream edges similar to gravity dams, as well as the slope stability similar to embankment dams, is calibrated for hardfill dams. To verify the susceptibility on strength and stability, which is connected with cohesion, internal friction angle, and Young's modulus of the material, FEM also may be applied. For the hardfill dam located in a seismic area with intensity over 8, the dynamic calculation should be undertaken apart from pseudo-static method, to estimate the earthquake action and the response of the dam to the shaking. If there are weak seams beneath the foundation, the deep-seated sliding stability also should be studied.

2. Anti-seepage

The hardfill dam uses reinforced concrete slab, concrete slab, asphalt concrete slab, or the other impervious materials for seepage control on its upstream face. Concrete cutoff wall or curtain grouting may be installed for the under seepage control in the foundation, depending on the geologic conditions. Face slab is linked to abutments and riverbed by pads and toe slab, respectively. The thickness t of face slab usually varies from dam crest to toe according to Eq. (10.1), and it is customarily to stipulate that $\alpha = 0.00235$.

The draining devices may be the embedded pipes under the porosity concrete slab, the pre-cast hollow slabs as framework, etc.

3. Diversion and flood releasing works

During the construction period, the dam allows excess of flood so that the construction diversion standard could be lowered and the overtopping could be permitted. In the operation period, the dam has certain resistance to seepage erosion and flooding overtopping so that the spillway might be located on the dam crest.

4. Face slab and toe slab

The design of face slab and toe slab is similar to that of CFRD, and the DL/T 5016-1999 "Design specifications for concrete face rockfill dams" is the major guidelines to be observed.

5. Compaction standard

Different requirements may be put forward for the different portions in the hardfill dam, which should be experimented at the first stage of construction. The compaction standard is controlled using placement parameters determined in

advance by roller compaction tests or engineering analogy with respect to vibrating roller type, lift thickness, passes of roller compaction, etc.

6. Materials

The mechanical properties of hardfill material are similar to that of rockfill material before being hardened; however, its strength and deformation modulus after hardening are much greater. Generally, they fall in an intermediate area of RCC material and rockfill material. They are governed, on the one hand, by the friction between the grains, and on the other hand, by the bonds between the grains due to cementation. Therefore, one can look at the hardfill material as a cohesive-frictional material. Usually, there is no requirement for the tensile strength, and the shear strength is not predominant due to the low shear stress level in the dam; therefore, the compressive strength is the principal requirement for the hardfill material.

10.8.3 Mixing Proportion Design and Functional Parameters

More relaxed requirements for aggregates enable engineer to make an utmost use of local materials such as the weathered rock and the excavation slag, so as to avoid land vegetation destruction due to quarrying and borrowing, this is why the hardfill dam is called “zero emission dam” (dam without pollution). Figure 10.14 shows the sand–gravel gradation curves of the CSG in the Haizuka Dam (Japan, $H = 50$ m) and the cofferdam dam in the Daotang Project (China, $H = 7$ m).

The Oyuk Dam (Turkey, $H = 100$ m) is the first hardfill dam of Turkey (Batmaz et al. 2003). All together, eight mixing proportion tests were carried out, and the No 4 mixing proportion was recommended (Table 10.3).

Fig. 10.14 Sand–gravel gradation curves of CSG

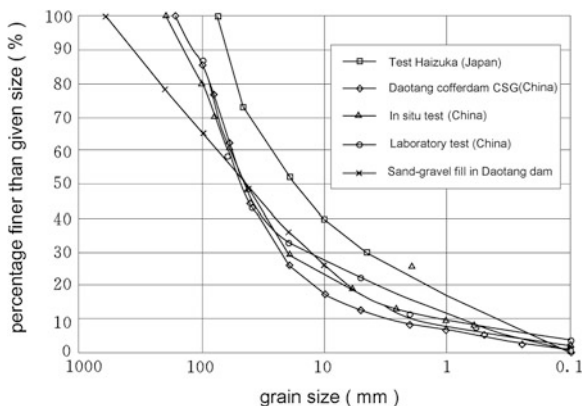


Table 10.3 Mixing proportion of the hardfill for the Oyuk Dam

Hardfill sequence no.	Cement (kg/m ³)	Fly ash (kg/m ³)	Sand-gravel material with grain size <75 mm (kg/m ³)	Water (kg/m ³)	Water/binder ratio	Compressive strength of 90d (MPa)
1	45.0	34.84	2296.0	135	1.69	38.3
2	49.5	31.35	2296.0	135	1.67	35.8
3	50.4	53.88	2270.0	140	1.34	46.3
4	50.4	100.34	2218.0	140	0.93	60.5
5	60.3	22.99	2296.0	135	1.62	34.2
6	40.0	0	2317.0	135	3.38	18.8
7	50.0	0	2308.0	135	2.70	23.1
8	60.0	0	2300.0	135	2.25	38.4

Table 10.4 Recommended mixing proportion of the hardfill in the upstream cofferdam of the Hongkou Project

Cement (kg/m ³)	Fly ash (kg/m ³)	Sand and gravel (kg/m ³)	Water (kg/m ³)	Water/binder ratio	Sand ratio (%)
35	35	2243	70	1.0	31

Table 10.5 Functional parameters of the hardfill in the upstream cofferdam of the Hongkou Project

Volumetric weight (kg/m ³)	VC (s)	Compressive strength of 90d (MPa)	Young's modulus of 90d (GPa)	Limit tensile strain of 90d ($\times 10^{-6}$)	Permeability coefficient (10^{-5} cm/s)	Dry shrinkage deformation of 60d ($\times 10^{-6}$)	Adiabatic temperature rise of 28d (°C)
2350	5	4.2	7.47	52	2.18	183	5.2

Based on experiments, the recommended mixing proportion and corresponding functional parameters for the hardfill in the upstream cofferdam of the Hongkou Project are listed in Tables 10.4 and 10.5, respectively.

References

- Acker RC, Jones JC (1972) Foundation and abutment treatment for rockfill dams. *J Soil Mech Found Div ASCE* 98(SM 10):995–1015
- Batmaz S (2003) Cindere dam-107 m high roller compacted hard-fill dam. In: Berga L et al. (eds.) *Proceedings of the 4th international symposium on RCC dams*. Balkema AA, Madrid, pp 121–126
- Batmaz S, Köksal A, Erganeman I, Dogan P (2003) Design of the 100 m-high Oyuk Hardfill dam. *Int J Hydropower Dams* 10(5):138–142

- Chanson H (2001–2002) Historical development of stepped cascades for the dissipation of hydraulic energy. *Trans Newcomen Soc* 71(2): 295–318
- Chanson H (2009) Embankment overflow protection systems and earth dam spillways. In: Walter PH, Michael CB (eds) *Dams: impacts, stability and design*. Nova Science Publishers, New York
- Chen MZ et al (1982) Design of rockfill dams. Water Conservancy Press, Beijing (in Chinese)
- Cooke JB (1984) Progress in rockfill dams (18th Terzaghi lecture). *ASCE J Geotech Eng* 110 (10):1383–1414
- Cooke JB (2000) The high CFRD. In: Mori RT, Sobrinho JA, Dijkstra HH, Guocheng J, Borgatti L (eds.) *Concrete face rockfill dams*, J Barry Cooke volume. 20th ICOLD Congress. ICOLD, Beijing, pp 1–4
- Cooke JB, Sherard JL (1987) Concrete-face rockfill dams: II design. *ASCE J Geotech Eng* 113 (10):1113–1133
- Fu ZA, Feng JJ (1993) *Concrete faced rockfill dams*. HUST Press, Wuhan (in Chinese)
- Galloway JD (1939) The design of rock-fill dams. *Trans ASCE* 104(1):1–24
- Giroud JP (1989) Are geosynthetics durable enough to be used in dams? *Water Power Dam Constr* 41(2):12–13
- Giroud JP (1992) Geosynthetics in dams: two decades of experience. *Geotech Fabr Rep* 10(6):22–28
- Golzé AR (1977) *Handbook of dam engineering*. Van Nostrand Reinhold Company, New York
- Gratwick C, Erwee A, Tente T (1999) Geometrical design of the plinth for CFRDs. *Int J Hydropower Dams* 6(6):74–78
- Guo CQ, Chen HY (1992) *Embankment Dams*. Water Resources and Electric Power Press of China, Beijing (in Chinese)
- Hill D (1996) *A history of engineering in classical and medieval times*. Routledge, New York
- ICOLD (1989) Rockfill dams with concrete facing—state of the art (Bulletin 70). ICOLD, Paris
- ICOLD (1991) Watertight geomembranes for dams—state of the art (Bulletin 78). ICOLD, Paris
- ICOLD (1992) Bituminous cores for fill dams—state of the art (Bulletin 84). ICOLD, Paris
- ICOLD (1993a) Rock materials for rockfill dams—review and recommendations (Bulletin 92). ICOLD, Paris
- ICOLD (1993b) Reinforced rockfill and reinforced fill for dams—state of the art (Bulletin 89). ICOLD, Paris
- ICOLD (1999) Embankment dams with bituminous concrete facing (Bulletin 114). ICOLD, Paris
- ICOLD (2005) Dam foundations. geologic considerations. Investigation methods. Treatment. Monitoring (Bulletin 129). ICOLD, Paris (ICOLD)
- ICOLD (2010) Geomembrane sealings systems for dams (Bulletin 135). ICOLD, Paris
- ICOLD (2011) Concrete face rockfill dams—concepts for design and construction (Bulletin 141). ICOLD, Paris
- Jansen RB (1980) *Dams and public safety, a water resources technical publication*. CO (Water and Power Resources Service, Bureau of Reclamation, US Department of the Interior), Denver
- Leps TM (1970) Review of shearing strength of rockfill. *J Soil Mech Found Div ASCE* 96 (SM4):1159–1170
- Londe P, Lino M (1992) The faced symmetrical hardfill dam: a new concrete for RCC. *Int J Water Power Dam Constr* 44(2):19–24
- Manso PA, Schleiss AJ (2002) Stability of concrete macro-roughness linings for overflow protection of earth embankment dams. *Can J Civil Eng* 29(5):762–776
- Marulanda A, Pinto NL (2000) Recent experience on design, construction, and performance of CFRD dams. In: Mori RT, Sobrinho JA, Dijkstra HH, Guocheng J, Borgatti L (eds.) *Concrete face rockfill dams*, J Barry Cooke volume. 20th ICOLD Congress. ICOLD, Beijing, pp 279–315
- Mason PJ, Hughes RAN, Molyneux JD (2008) The design and construction of a faced symmetrical hardfill dam. *Int J on Hydropower Dams* 15(3):90–94
- Materon B, Mori RT (2000) Concrete face rockfill dams. Construction features. In: Mori RT, Sobrinho JA, Dijkstra HH, Guocheng J, Borgatti L (eds.) *Concrete face rockfill dams*, J Barry Cooke volume. 20th ICOLD congress. ICOLD, Beijing, pp 177–219

- Olivier H (1967) Through and overflow rockfill dams—new design techniques. *Proc Inst Civil Eng* 36(3):433–471
- Raphael JM (1971) The optimum gravity dam. In: *Rapid construction of concrete dams, proceedings of the engineering foundation Conference*. ASCE, New York, pp 221–247
- Schnitter NJ (1994) *A history of dams: the useful pyramids*. AA Balkema, New York
- Sherard JL (1985) The upstream zone in concrete faced rockfill dams. In: Cooke JB, Sherard JL (eds) *Concrete face rockfill dams—design, construction and performance*. ASCE Geotech Eng Div, New York, pp 618–641
- Sherard JL, Cooke JB (1987) Concrete-face rockfill dam: I. Assessment. *J Geotech Eng ASCE* 113(10):1096–1112
- Sherard JL et al (1963) *Earth and rockfill dams*. Wiley, New York
- Sherard JL, Dunnigan LP (1984) Filters for silts and clays. *J Geotech Eng* 110(6):927–718
- Sherard JL, Dunnigan LP (1989) Critical filters for impervious soils. *J Geotech Eng* 115(GT7): 927–947
- State Economy & Trade Commission of the People’s Republic of China (1999) DL/T5016-1999 “Design specifications for concrete face rockfill dams”. China Electric Power Press, Beijing (in Chinese)
- Toshio H, Tadahiko F, Hitoshi Y, et al (2003) Concept of CSG and its material properties. In: Berga BL et al. (eds.) *Proceedings of the 4th international symposium on roller compacted concrete dams*. Balkema AA, Madrid, pp 465–473
- USBR (1987) *Design of small dams*, 3rd edn. US Govt Printing Office, Denver
- Weiss A (1951) Construction technique of passing floods over earth dams. *Trans ASCE* 116(1): 1158–1178
- Zhu SA (1995) *Technical history of dam engineering*. Water Resources and Electric Power Press of China, Beijing (in Chinese)

Chapter 11

Sluices and Barrages

11.1 General

11.1.1 Definitions

Sluice or regulator is a water channel consisting of an array of large gates that can be opened or closed to control the amount of water passing a barrage or entering a canal. The gates are set between flanking piers responsible for resisting water actions.

Barrage is a kind of low-head dam in the regulating project which is often used to control and to stabilize water flow for irrigation system, navigation system, stagnant water draining system, or hydropower station. Barrages are also built at the mouth of rivers or lagoons to prevent tidal incursion or to utilize the tidal flow for electric power generating (Chen and Chen 2014; Garg 1976; Iqbal 1993; Grishin 1982; Lin 2006; Novak et al. 1990; Varshney et al. 1982).

A barrage (regulating) project constructed across river mainly comprises of mainly diversion works (e.g., sluices) to raise the water level and control its flow, but there are other components serving the whole project, which are equally important, such as:

- Canal head regulator. It is a structure that regulates the water inflow into a canal;
- Sediment excluder device. It is a structure that attempts to remove sediment carried by river flow and helps in reducing or preventing sediment from entering into the canal;
- Gates and stoplogs. Gates are used to control flow through the main diversion structure as well as through the head regulator. Stoplogs are used for the emergency closure of the flow through the bays of barrage or head regulator;
- River training works. They are installed to guide the water toward the barrage or head regulator; and

- Navigation and fish passing facilities. The obstruction of river by the construction of barrage requires special structures for free passage of vessels and boats or migratory fishes up and down the river.

Though all the above appurtenant structures are important, only the first two, that is, canal head regulator and sediment excluder device, will be discussed in this chapter in detail, whereas the others (e.g., gates, navigation, and fish passing facilities) will be presented in Chaps. 15–17.

11.1.2 Working Features of Barrages and Sluices

Barrages and sluices may be built on various foundations, but the majority of them in China are founded on earth stratum, and their design principles will be discussed in this chapter. The barrages and sluices founded on rock stratum have similar design principles to the gravity dams on rock foundation with respect to water flow, foundation treatment, and structural type, which may be referred to Chap. 7 of this book.

As a low-head water retaining and flood release structure, the barrage/sluice has following working features.

1. Water flow

The structure built on earth foundation is more vulnerable to the scouring and seepage failure than that on rock foundation, and the following two issues impose strong restraint on its safety.

(a) When gates are closed

Head difference forms thrust on the work giving rise to the stability issue of sluice chamber and abutment structures. The seepage resulted from head difference may also lead to reservoir leakage and seepage failure at the downstream percolation exit.

(b) When gates are opened

The energy should be dissipated efficiently within the downstream stilling basin, to prevent the riverbed and banks from scouring due to high-speed flow. It should bear in mind that the most dangerous working situation does seldom emerge under the maximum flow discharge. At the initiation of gate operation when the opening of gates is small, or the gates are partially opened for maintaining flow discharge, driven-off hydraulic jump may be formed due to the shallow tailwater level. This driven-off hydraulic jump may be responsible for serious scouring and endanger the safety of structure if the riverbed is not well protected. As the gate opening increases, the tailwater level increases which triggering critical hydraulic jump and further submerged hydraulic jump. When the gates are all fully opened, the small head difference (afflux) and low Froude number may also result in difficulties with energy dissipation and erosion protection.

In addition, chopping jump or reflection and scour flow often manifest at the downstream of barrages and sluices due to low Froude number or improper project layout, which will intensify the erosion to the riverbed and banks.

2. Foundation

The design of barrage and sluice on earth foundation involves the problems concerning the erosion of foundation material, settlement, and under seepage. The complexity of these problems varies greatly and depends on the type, stratification, permeability, homogeneity, and other properties of the foundation materials, as well as the size and physical requirements for the structure itself (Craig 2004; Terzaghi et al. 1996).

3. Structure

Unlike massive structures such as gravity dams and embankment dams, the sluice chamber is a typical spatial thin-walled structure composed of piers, bottom floor slab, parapet, etc., and is subjected to water pressure, self weight, foundation reaction force, and uplift. Apart from the advanced numerical methods such as FEM, the structural mechanics or material mechanics methods may be conventionally employed for the structural analysis of sluice chamber that it is looked at as a system of independent components of plate (slab), beam, and pillar. Rational diagram of structure free-body is an important base for obtaining a safe and economic design.

11.1.3 Types of Sluices (Fig. 11.1)

1. Classification according to the purposes of sluice

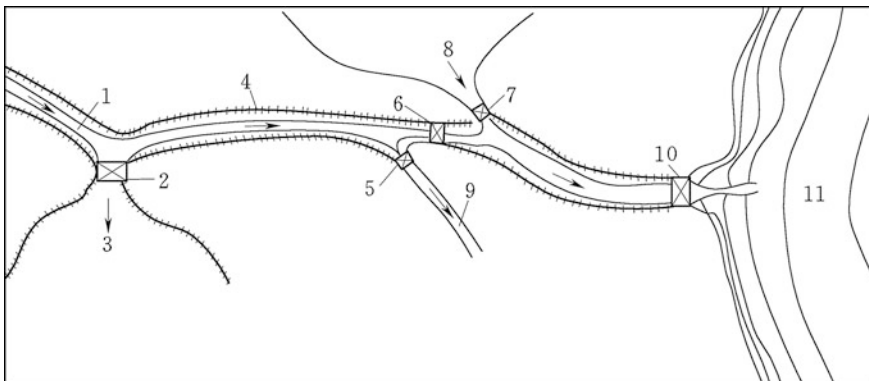


Fig. 11.1 Types and positions of sluices. 1 river; 2 flood diversion sluice; 3 flood diversion area; 4 levee; 5 head sluice; 6 regulating sluice; 7 drainage sluice; 8 accumulated water area; 9 diversion canal; 10 tidal retaining sluice; 11 sea

(a) Head sluices (or regulators)

Head sluices are built on the shore of river, lake, reservoir, or diversion channel. They control diversion water into a supply canal for irrigation, electric power generation, domestic and industrial uses, etc.

(b) Regulating sluices (or under-sluices)

Regulating sluices are important components of a barrage, whose axis is nearly perpendicular to the river or canal. In the inland navigation project, regulating sluices provide adequate and stable upstream headwater level, and they also may be employed to maintain stable downstream tailwater depth by keeping suitable discharge flow. In the water diversion project, they raise the river level sufficiently to divert the flow in full, or in partial, toward the regulator.

(c) Water release (or escape) sluices

Water release sluices are used to release the excessive water of reservoirs and lakes. In a barrage project, the task of water release (or escape) sluices is implemented by regulating sluices and sand excluders (or silt flushing sluices). In an embankment dam project, water release sluices play the role of control structure for shore spillway.

(d) Drainage sluices

Drainage sluices are usually built on the shore of river, to drain the accumulated water from rainfall or sanitary wastewater. They have features of lower bottom floor and high sluice chamber as well as of being subjected to bidirectional head: Where the river level is higher, the sluices are closed to prevent water intrusion; where the river level is lower, the sluices are opened to drain stagnant water.

(e) Tidal retaining sluices

Tidal retaining sluices are installed to allow water moving out of a bay or river and to keep salty seawater from intrusion into the inland river. This is done by measuring the tidal flow and controlling the sluice gates at key times of the tidal cycle. Structurally, tidal retaining sluices are similar to drainage sluices: lower bottom floor and high sluice chamber as well as of being subjected to bidirectional head. However, their operative frequency is very high.

(f) Flood diversion sluices

Flood diversion sluices are usually built on the shore of river, to divert a part of the peak floodwater into flood diversion area or natural lake and to cut the flood peak discharge at downstream river reach for its safety. After passing of flood, the accumulated floodwater will be drained back to the river through drainage sluices.

(g) Silt flushing sluices (or sand excluders)

With a lower bottom floor, silt flushing sluices reduce or prevent silt from entering canal. In a water diversion project, the position of silt flushing sluice is

close to the head sluice (or regulator), for cut the silt accumulation height in front of the head sluice. Silt flushing sluices also play the concurrent role of regulating sluices in a barrage project.

There are also other types of sluices such as ice release sluices and trash (debris) release sluices.

2. Classification according to the structures of sluice chamber

(a) Open flow sluices

An open flow sluice (Fig. 11.2a) possesses large discharge capacity and is generally employed in ice (debris) release sluices and regulating sluices.

(b) Parapet (breast) wall sluices

In case of large variation of pool level and restriction on downstream discharge flow, parapet wall may be installed to reduce the height of gates (Fig. 11.2b). At low pool level, the parapet wall imposes no restraint and the flow is free, while at high pool level, the orifice flow takes place. Parapet (breast) wall type is often employed in the head regulators, escape sluices, and tidal retaining sluices.

(c) Culvert sluices

A culvert sluice is usually placed on either vertical or inclined upstream face of levee (Fig. 11.2c). If a free flow for all discharge is desirable which is usually applied in small diversion sluices, special precautions are taken to prevent the conduit from flowing full. If a full flow is desirable which is often applied in silt flushing or escape sluices, a bell mouth or streamlined inlet is provided. Special hooded inlets are sometimes added to facilitate the flow pattern transferring from partly full to totally full as well as to prevent the formation of vortices which would interfere with the full flow pattern.

Culvert sluices should not be utilized for high-head installations where large negative pressure may develop. In addition, the transition flow phenomenon, when the flow pattern changes from free to full, is accompanied by rather severe pulsations and vibrations. For cross-head not exceeding 6 m, culvert sluices offer advantages over other types attributable to their adaptability for either partially full or totally full flow operation as well as their simplicity and economy for construction. As is the case of spillway with a drop inlet or siphon, a principal

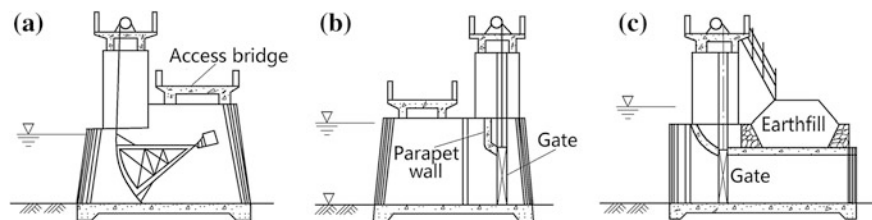


Fig. 11.2 Structural types of sluice chamber. **a** Open type; **b** parapet type; **c** culvert type

disadvantage of the culvert sluice is that its discharge capacity does not substantially increase with the increase of head.

3. Classification according to the construction methods

(a) Cast in situ

This is the most common method for the construction of barrage and sluice.

(b) Assembled

The bottom floor slab is cast in situ, whereas the other components using precast concrete sheets and piles are assembled in the work site. Advantages of assembled sluice are convenient inland water transportation, rapid constructing progress, low expenditure, and minor hydrologic and climatic influence. However, the linkage of components is weak and the stiffness whole structure would be lower. Design of the components for an assembled sluice should take into account of transportation and lift capacities, as well as its stress states during transportation and lift process, to prevent it from damage and rupture. The joints and linkages of the components should satisfy the requirements for strength and anti-seepage.

(c) Float-towed

It is suitable for tidal retaining sluices or escape sluices near the shore of sea or lake. The sluice chamber is constructed at a position near the waterway; then, it is transported to the sluice axis during high tide period (or by open-channel flow). After the positioning, the water flows into the chamber until it is sunk down to the foundation. Float-towing method may reduce cost and shorten the construction schedule.

4. Other classifications

According to the design experiences of completed barrage and sluice projects, the classification of barrage and sluice can be based on the passing discharge of design (or check) flood. For example, the barrage or sluice of large class is defined as with discharge over $1000 \text{ m}^3/\text{s}$ and of medium class is defined as with discharge between 100 and $1000 \text{ m}^3/\text{s}$. Structure height or design afflux may also be used as the index for barrage and sluice classification. For example, the barrage or sluice of large class is defined as with height over $8\text{--}10 \text{ m}$. The Erjiang regulating sluice in the Gezhouba Project (China, $H = 47 \text{ m}$), whose flood discharge is $83,900 \text{ m}^3/\text{s}$, belongs to the class of particular large sluice, or giant sluice.

11.2 Composition of Sluice and Project Layout

A sluice is mainly composed of sluice chamber, upstream transition, and downstream transition, as shown in Fig. 11.3.

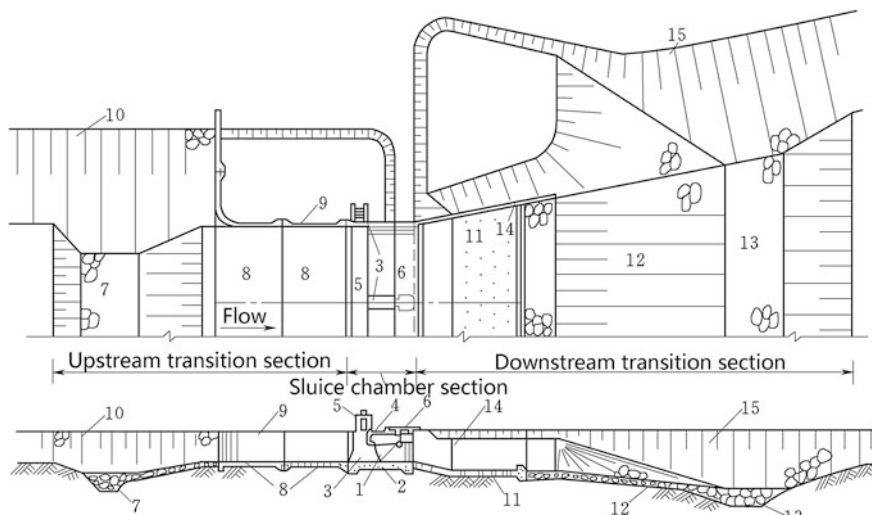


Fig. 11.3 Composition of a sluice. 1 gate; 2 bottom floor; 3 pier; 4 parapet wall; 5 operative bridge; 6 access bridge; 7 upstream anti-scouring ditch; 8 upstream anti-scouring section and blanket; 9 upstream wing wall; 10 upstream bank protection; 11 apron; 12 rear apron; 13 downstream anti-scouring ditch; 14 downstream wing wall; 15 downstream bank protection

11.2.1 Sluice Chamber

Sluice chamber is a major portion of sluice used to control flow, which consists of gates, piers, bottom floor slab, bridges, parapet wall, and hoist.

Gates installed on the weir crest or sluice bottom floor slab and supported by piers are intended to provide a moveable damming surface, in this way to allow for the crest or bottom floor slab being located below a given operation water level. The top of gate is connected to the hoist. There are usually both the working (service, operation) gate and the bulkhead gate. The former is for water retaining and discharge controlling, whereas the latter is for the inspection and repair of the sluice chamber. Stoplogs usually are employed as bulkhead gate which are smaller beam or girder structures that span the desired opening and are stacked to a desired damming height.

Piers installed at an interval of 10–20 m along the axis of barrage or sluice are intended to separate sluice vents and to support the gates, bridge decks, and hoists. Piers should be separated from foundation in case of pucca floor. When raft floor is employed, piers may be constructed monolithically with the floor.

Breast (parapet) walls are installed over the working gates, for helping the water retaining. Installation of parapet wall may reduce the gate height where the upstream water level has large variation. Parapet walls may be movable steel structure, which are vertically lifted in case of particular large flood, to archive larger discharge by forming free flow.

Bottom floor forms the base of sluice chamber, which transfers the loads from piers, the self weight of floor slab, and the water pressure on the floor, to the foundation. The stability of the sluice chamber on soft foundation is mainly maintained by the friction between the bottom floor and the foundation soil. The bottom floor also has function of scouring and under seepage prevention.

Operative bridge is used for installing hoists and gate operation, whereas access bridge links the riverbanks for transportation.

Bottom floors, piers, and parapet walls are usually made of concrete or reinforcement concrete, but masonry structure also may be used for small projects.

11.2.2 Upstream Transition

Upstream transition is near to flow approaching area, whose function is to introduce flow entering sluice chamber smoothly, as well as to resist scouring and under seepage. It usually comprises upstream wing walls, impervious blanket, riverbed, and bank protections (Hinds 1928; USBR 1987).

Upstream wing wall introduces flow entering sluice chamber smoothly. It also resists the earth pressure from bank abutments, the river scouring, and bypass seepage. The wing wall should be normally kept vertical up to the end of the impervious floor beyond which it should be flared from vertical to the actual slope of the canal (or river) banks.

An upstream impervious blanket will frequently be advantageous for soil- and pile-founded barrages or sluices, as it increases the length of under seepage path and thereby reduces the uplift pressure under the structure. The blanket will usually be of clay material for the purpose of economy. An impervious membrane, in lieu of a clay blanket, is ordinarily not recommended due to a high risk of puncture and tear. The surface of clay blanket should be protected from scouring. An upstream anti-scour ditch may be installed at the upstream end (generatrix) of the blanket, for scouring protection.

When geologic investigations and studies indicate that the upstream riverbanks at the work site will not be stable under operating conditions, they should be protected and stabilized.

11.2.3 Downstream Transition

The outflow from a sluice chamber carries fairly amount of kinetic energy, which should be dissipated in the downstream transition section to avoid serious scouring. Downstream transition customarily comprises apron (inclusive stilling basin), rear apron, downstream anti-scour ditch (or anti-scour wall), downstream wing wall, riverbed, and bank protections (Hinds 1928; USBR 1987).

Downstream wing wall guides an even dispersion of discharged flow and resists earth pressure as well as scouring. Stilling basin as an external energy dissipation device is placed at the exit of sluice chamber, which is characterized by some combination of chute blocks, baffle blocks, and end sill designed to trigger a hydraulic jump dependent on tailwater condition. Apron is the bottom floor of stilling basin for riverbed protection. Rear apron after the stilling basin is intended to further dissipate residual kinetic energy. Downstream anti-scour ditch is used to protect the end of rear apron, to prevent river from retrogressive scouring. Riverbed and bank protections of downstream are similar to that of upstream.

11.2.4 Layout of Barrage Project

Barrage is usually layout in the main stream with narrow river section, to save the engineering expenditure.

The length of overflow front (waterway) (L) is worked out according to the specific and total flood discharges. If the length of waterway is wider than the natural river channel, the crest level should be so adjusted as to keep (L) equal to or a bit smaller to the width of the natural river channel. A good project layout changes river morphology as less as possible and reduces engineering amount including the upstream and downstream transition structures. In most case, it is advisable to adopt shorter waterway to reduce the number of sluice vents whose expenditure is relatively higher, although this will require longer upstream and downstream transitions to ensure a smooth flow passing the sluice or barrage.

Where the shape of crest piers and abutments gives rise to side contractions of the overflow, the effective length of waterway L will be shorter than the net length of the crest, which may be computed according to Eq. (7.29).

In a wide river, the under-sluice width is much shorter than the natural river channel, and in this case, the remaining section of the river is dammed by barrage or power station. Divide wall (gyrone) is erected between the barrage weir and the under-sluice, stretching a little far upstream to the canal regulator and downstream to the end rear apron. It is a concrete or masonry structure aligned at right angle to the barrage and sluice axis. Another function of the divide wall is to separate the floor of under-sluice which is at the lower level than the barrage weir, if any, to prevent the formation of crosscurrents. Divide walls are expensive structures and are likely subjected to maximum differential pressure when the full discharge of the river is passing through the barrage or sluice.

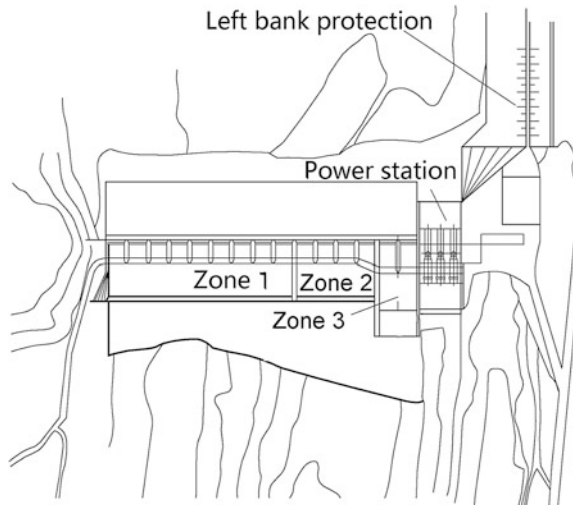
In a wide river channel, barrage and sluice also may be constructed on the flood land near the main stream, which enables the construction during dry season and facilitates diversion. However, a definite length of approach channel and exit channel for smooth transition of inflow and outflow through the sluice will be demanded. The estimation of river morphologic changes also should be fully studied for the calibration and mitigation of detrimental silting and scouring.

The location of canal head regulator is interlinked with the location of diversion work. The head regulator is preferably located at the end of the outer curve (convex bend) of the main stream, if possible, to minimize the sediment from entry into the off-taking canal. The axis of canal forms commonly an included angle of 30° – 45° with the axis of main river stream.

In a barrage project, silt flushing sluice should be located as close to the head regulator as possible. Bed load deflecting sill is installed in front of the head regulator to block silt from entry and to enable effective silt flushing through the silt flushing sluice.

Figure 11.4 shows the layout of the Miaozitou Project (China, $H = 19$ m) with 15 sluice vents separated by gyrones into 3 bays of 9 vents, 4 vents, and 2 vents, respectively. The weir is hump type with crest elevation of 110.0 m. The service gates for the 1 and 2 bays are vertical lift, the two sluice vents in the bay 3 concurrent as silt flushing sluices on which the radial gates are installed as service gates. The maximum discharge flow is 13, 200 m^3/s . The power station is located near the regulating sluice with 3 generator units.

Fig. 11.4 The Miaozitou Barrage Project (China, $H = 19$ m)



11.3 Size of Intake

Size of intake is mainly dependent on the hydraulic design through following procedures (Garg 1976; Golzé 1977; Tan 1986; USBR 1987; Varshney et al. 1982; Zhang et al. 1988; Zuo et al. 1987):

- Fixation of headwater level of the pool upstream the barrage;
- Fixation of crest level, width, and shape of sill or weir;

- Fixation of waterway length, number and span width of sluice vents, height of gate openings, requirement for parapet wall, etc.;
- Shape of approaches and other component parts;
- Safety of structure regarding surface flow conditions;
- Safety of structure regarding under seepage conditions; and
- Energy dissipation arrangements.

The design of intake size should take into account of sluice type and its structure feature. The waterway should be adequate to release flood of anticipated discharge without difficulty, which is dependent on the number and span width of sluice vent, thickness of pier, weir type and crest elevation, and afflux during the releasing of flood. For passing a discharge Q , the required head H_0 over the sill on bottom floor or the weir crest, together with a net waterway $L = nb$, has to be worked out using Eqs. (7.28)–(7.31).

Generally, the intake size of barrage (or regulating sluice) is dominated by the discharge capacity for releasing maximum flood. The reservoir pool upstream barrage ordinarily has no storage capacity for regulation; therefore, the outflow discharge is identical to the peak inflow discharge corresponding to the flood recurrence. However, where the river barrage project has regulating ability, the discharge should be computed by flood routing.

To reduce the waterway length and the number of sluice vents, free outflow, or small submerged outflow, is desirable. In dry seasons with small inflow, the outflow discharge is controlled by the partially opening of gates to maintain the minimum pool level and water amount demanded by the head regulator from the diverted river or reservoir; the downstream level is lower; and the orifice or free outflow pattern is commonly considered. When releasing of check flood with high downstream water level, river barrage is generally in submerged outflow pattern, which is a control working situation in the computation of discharge capacity. Both the aforementioned two situations should be taken into account in the computation of discharge capacity.

Hereinafter, the intake size of the regulating sluice in river barrage project will be mainly discussed, whereas the head sluice and drainage sluice will be generally addressed.

11.3.1 Regulating Sluices

In sizing intakes for regulating sluices, the following conditions (limitations) should be taken into account.

1. Inflow of flood

The design inflow of flood is decided according to the hydrologic analysis with respect to the project grade (Table 1.3). Since the regulation ability is small due to

the small storage of reservoir, the discharge outflow through a regulating sluice is usually equal to the flood inflow.

2. Unit (specific) discharge

Selection of discharge per meter is a predominant factor influencing the total waterway length of regulating sluice: The larger the unit discharge, the shorter the waterway length; as a result, the cost of sluice chamber is reduced. However, larger unit discharge has stronger scouring potential to the riverbed, which increases the cost in energy dissipation and protection works. Therefore, the scouring resistance of riverbed, in turn, is one of important factor in the selection of unit discharge.

Apart from the soil properties of riverbed, the scouring resistance is also dependent on the outflow pattern: Deeper water and smaller afflux and smooth dispersion of outflow may allow for larger unit discharge with respect to the same foundation soil properties.

In China, the unit discharge for barrages and sluices is usually selected within 5–30 m³/(s m), and Table 11.1 lists empirical data of scouring resistant unit discharge exercised in the Jiangsu Province, China.

3. Upstream and downstream water levels

In some rivers, the construction of barrage project may result in a progressive downstream riverbed degradation toward upstream, a phenomenon that is termed as “retrogression,” which has been found to be more pronounced in alluvial rivers carrying abundant silt of finer bed material and having steep slope. The retrogression depth is generally between 1 and 2 m, depending upon the amount of silt in the river, type of bed material, and slope. As a result of retrogression, low water levels are generally affected more significantly compared to the maximum flood levels. It implies that for the same flood discharge, a non-retrogressed river may exhibit submerged flow pattern instead of a free flow condition under retrogressed situation. In the design of medium to small barrage project, the natural tailwater rating curve may be applied directly in the preliminary design. However, for larger or important barrage projects, tailwater rating curve should be established through the analysis of gauge discharge data first, and then, the proposed tailwater rating curve for new designs is revised by subtracting the anticipated retrogression depth from the existing average tailwater levels.

The normal storage level is dependent on the tasks and submerging loss of the project. Under the normal operation situations, it should meet the water diversion and navigation requirements.

Table 11.1 Scouring-resistant unit discharge [m³/(s m)]

Foundation soil	Silt, mealy sand	Silty soil	Fine sandy soil	Silty loam	Clay
Non-scouring unit discharge	5–16	9	4–9	9–12	12–24

The rise in the maximum flood level of upstream pool as a result of barrage construction is defined as “afflux” which extends gradually toward upstream till the new river slope is finally established. The upstream maximum level is dependent on the check flood release capacity, when the gates are all opened and the upstream level is equal to the tailwater levels plus afflux. The amount of afflux will determine the top altitude of guide walls and their lengths, as well as the top altitude and sectional size of flood protection bunds. It also will govern the hydrodynamic performance, such as the depth and location of the standing wave. By providing a high afflux, the length of waterway can be narrowed, but the cost of training works will go up and the risk of failure by outflanking will increase. Selection of a realistic afflux value is imperative, which is commonly limited within 1 m. More strict limitation on afflux is demanded in the plain areas, which is ordinarily 0.1–0.3 m.

4. Type of weir

Open broad crested weir is commonly employed for barrage projects on soil foundation, attributable to the advantages such as the simplicity in structure, convenience in construction, uniformity in foundation stress distribution, larger discharge capacity and small afflux, easy for silt flushing, etc. The discharge coefficient m of broad crested weir is 0.36–0.385. For better foundation, hump weir may be employed, while for rock foundation, ogee weir may be a good alternative. Hump- and ogee-type weirs have larger coefficient of discharge compared to broad crested weirs, which allow for shorter waterway. Since the discharge coefficient of the ogee weir drops sharply following the increase of submerging degree, the broad crested or hump weirs are more suitable for barrage projects mainly controlled by submerged outflow.

For barrage projects with large upstream-level variation, parapet walls may be installed to reduce the height of gates.

5. Crest level and shape of sill

By crest level, it means the altitude of crest, which is decided through comprehensive comparison aimed at optimal safety and economy taking into account of task, unit discharge, topographic and geologic conditions, scouring resistance of riverbed, construction condition, and expenditure. The crest level of broad crested weirs is also named as bottom floor (or sill) level.

For a regulating sluice with flat bottom floor (broad crested weir), its surface elevation is usually equal to or a bit lower than the natural riverbed, to reduce the silting in front of barrage. The sill level is fixed by subtracting the head over the sill for passing the full discharge into the river (or canal) from a specified pool level. The width of sill has to meet the requirements for gates, trash racks, and stoplogs. The sill should be placed on hard soil, if possible. For this requirement, the sill elevation could be deepened, if necessary. The sill crest level and waterway length are interrelated. Generally, lower sill elevation may give rise to a larger discharge capacity and shorter waterway, but the project should bear larger afflux and unit discharge. The full opening of all gates during check flood is commonly a dominant design situation in the sill-level selection. For small barrage projects, the sill level

may be so adjusted to let the waterway length be nearly identical to the width of natural riverbed, to reduce the engineering amount of abutment transition structures.

11.3.2 Head Regulators

The waterway length of head regulator should be selected according to the diversion discharge, the reservoir pool level and tailwater level, unit discharge, weir type, and sill level.

The upstream pool level of canal head regulator may be obtained by adding the working head for passing the design diverting discharge with the downstream full supply water level in the canal plus the head loss through the regulator.

Downstream level in the canal is decided by the canal system planning, and the diversion discharge is decided by the project tasks. According to the canal system planning, the annual hydrograph curve ($Q-T$) at the canal head may be obtained, and the downstream rating curve also may be computed.

Based on the upstream and downstream hydrograph curves, the control situation for sluice vent (waterway) size can be selected where afflux is small, but the diversion discharge is large. The control situation for stability calibration can also be selected where afflux is large. Similar to the barrage design, parapet wall may be considered in case of large pool-level variation. However, it is desirable that the parapet is so designed to permit an open flow in the normal diversion situation.

To prevent sands from entering into canals, it is desirable that the sill of a head regulator be higher than the sill of the under-sluices of river barrage, at least by a height of 1.2–1.5 m. If silt excluders are installed, then the crest level of the head regulator sill should be located about 0.5 m higher than the top of the silt excluders.

Where the foundation soil condition is competent and the pool level is high, the sill level of head regulator may be further raised, or the ogee weir with high discharge capacity may be employed.

11.3.3 Drainage Sluices

They are usually designed for free drainage. During and after the raining in lower lake districts, the water level of outer river or lake will be raised correspondingly. Therefore, the fast drainage of accumulated water from the lower lake districts to the outer river or lake is demanded. The factors influencing the waterway length are as follows: accumulated water level in lower lake districts (as headwater level), water level of the outer river or lake (as tailwater level), rain intensity and duration, speed requirement for drainage from lower lake districts, etc.

Conditions are permitted, the sill level of drainage sluice should be as lower as possible, and open flow with broad crested sill is desired, to meet the fast drainage requirement. Where the river or lake level has large variation, parapet walls may be

installed to reduce the height of gates. In the city area, culvert type is commonly exercised for drainage sluices.

The rainfall standard (duration and intensity) is selected according to the importance of drained areas. Based on the rainfall standard and runoff confluence characteristics, the draining discharge is obtained by hydrologic computation. Since the water level of outer river or lake also rises during the drainage period, the water release capacity varies correspondingly. Therefore, piecewise algorithm should be carried out to calculate the demanded drainage time. In practices, the “method of average flow discharge” is customarily exercised: The total runoff during a heavy rain is divided by drainage time to obtain the average discharge through the sluice with an prescribed afflux of 0.1–0.3 m, and the sluice waterway (total width of vents) may be calculated.

Where the water level of outer river or lake is high and the free drainage is difficult to implement, auxiliary draining pump station is installed for helping the drainage.

11.4 Energy Dissipation and Scouring Protection

11.4.1 Features of Energy Dissipation and Scouring Protection

Compared to high-head flood release structures, the energy dissipation and scouring protection of barrage projects have following remarkable features:

- Low afflux. Since the most barrages are built in plain areas with small afflux and large variation of tailwater level as well as with low scour resistance of soil, energy dissipation of flip bucket trajectory and surface current generally cannot be applied. The widely exercised manner for energy dissipation is the bottom flow by hydraulic jump;
- Low scouring resistance of foundation soil;
- Low Froude number. This occurs when releasing large discharge and results in uncompleted jump or even chopping jump, which in turn results in insufficient energy dissipation and strong scouring to the downstream riverbed and banks;

The most dangerous situation is not definitely the largest discharge of flood when the afflux is small; instead, it often takes place at the initial opening of gate when the tailwater level is low.

11.4.2 Layout of Energy Dissipation and Scouring Protection

For barrages or sluices located on non-erodible riverbeds, precautions for scouring may not be necessary. However, if they are located on non-cohesive and erodible foundations, the unlined portion of floor has to be protected against scouring.

On the upstream edge of bottom floor, a cutoff (or sheet pile) has to be installed, and on the downstream side of sill, proper energy dissipating arrangement should be provided, which is usually accomplished through the formation of a hydraulic jump under different discharge conditions. For various gate openings, the discharge through barrages or sluices have to be worked out, based on which the level and length of the stilling basin are calculated. Additional energy dissipating devices such as chute blocks, baffle piers, and end sill or dentated sill could be helpful. Figure 11.5 shows the typical layout of energy dissipation and scouring protection downstream of a barrage (sluice).

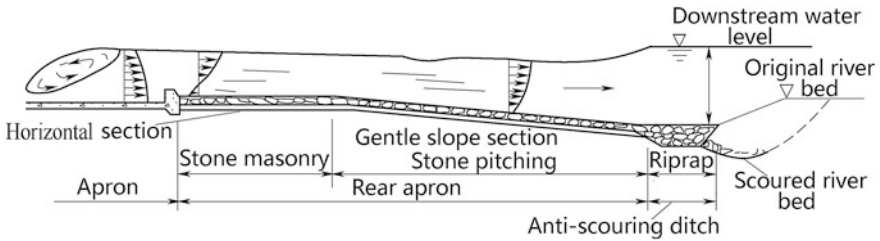


Fig. 11.5 Typical layout of energy dissipation and scouring protection downstream of a sluice

11.4.3 Stilling Basins

Denote h' and h'' as the conjugate depths at the beginning and the end of hydraulic jump. The former may be looked at as identical to the contraction depth h_c . Under a certain inflow situation, the starting of hydraulic jump is dependent upon the initial tailwater depth. If it is below the second conjugate depth h'' , then a long driven-off jump manifests; otherwise, submerged jump will appear. There are transition states as undulating waves in between aforementioned two extreme cases (Chow 1959; French 1985; Ippen 1951; Sylvester 1964). In engineering practice, the inflow situation and tailwater-level condition are changeable, which in turn shift the positions of hydraulic jump. The design of stilling basin is therefore aimed at the phase match issue of tailwater level and second conjugate depth h'' , for the purpose of maintaining steady jump within the anticipated range for reliable energy dissipation and scouring protection.

1. Conjugating conditions of hydraulic jump (Fig. 11.6)

According to the Bélanger equation, the hydraulic jump occurs in the stilling basin only if the tailwater is deeper than h'' calculated by

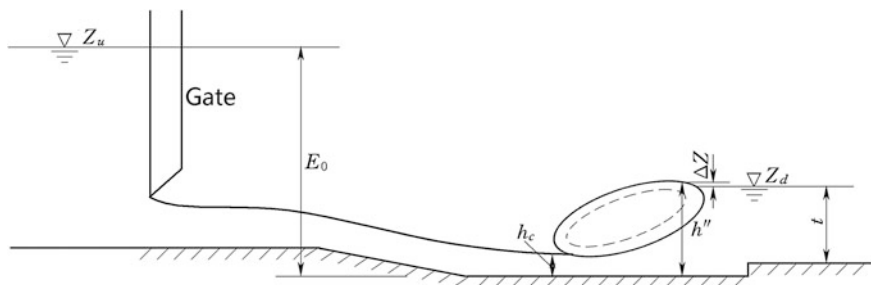


Fig. 11.6 Conjugating relationship of hydraulic jump

$$h'' = \frac{h_c}{2} \left(\sqrt{8F_r^2 + 1} - 1 \right) \tag{11.1}$$

where h'' = second conjugate depth of jump, m; F_r = Froude number before jump at the contraction section, $F_r = \frac{v_c}{\sqrt{gh_c}}$; and h_c and v_c = contraction depth and velocity before jump, respectively (h_c is also looked at as the first conjugate depth of jump and denoted by h').

Under free flow situation (open-channel flow), the contraction depth h_c before jump depends on the head difference E_0 between the upstream pool level Z_u and the stilling basin bottom floor, according to Eq. (11.2)

$$h_c^3 - E_0 h_c^2 + \frac{\alpha q^2}{2g\varphi^2} = 0 \tag{11.2}$$

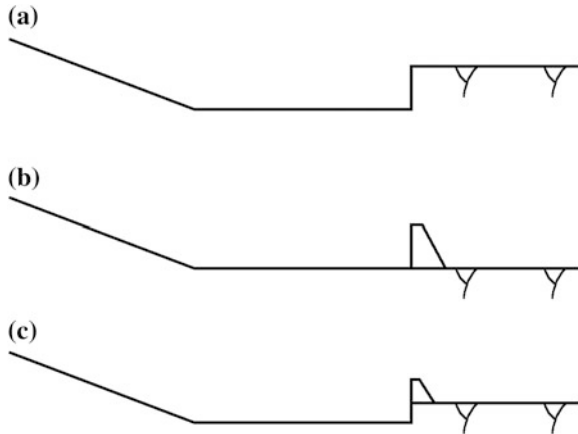
where α = revision coefficient for kinetic energy, $\alpha = 1.00-1.05$; φ = coefficient of velocity (for sluice vent, $\varphi = 0.95-1.00$); q = unit discharge at contraction section, $m^3/(s\ m)$; and E_0 = head difference, m.

2. Structure of stilling basin (Fig. 11.7)

If hydraulic jump is employed for energy dissipation, it should be confined within a heavily armored apron using solid materials (e.g., concrete) to resist scouring. Since the cost of concrete structure is relatively high, the length of hydraulic jump is generally controlled by accessories (energy dissipaters) that not only stabilize the jump action, but also reduce the length of apron structure.

Since there are different crest levels in a barrage project, the discharge passing through each of them will have to be estimated separately and then summed up. Where silt excluder tunnels are provided in the under-sluice bays, the discharge through these tunnels and over them needs to be calculated separately and summed up, too.

Fig. 11.7 Stilling basin structure. **a** Normal stilling basin; **b** end sill; **c** combined stilling basin



Considerations that should be taken into account in the design of stilling basin are as follows:

- Jump position. Positions that allow for a hydraulic jump to manifest downstream of transition are controlled by tailwater level;
- Tailwater condition. Tailwater fluctuation due to the change in discharge complicates the design procedure. It should be handled by distinguishing conditions according to the rating curves of tailwater and hydraulic jump;
- Jump type. Oscillating jumps in a range of $F_r = 2.5-4.5$ are avoided unless specially designed wave suppressers are installed. The greater of the Froude number, the higher is the effect of tailwater on the jump. Therefore, for a Froude number as lower as $F_r = 8$, the tailwater depth should be greater than the second conjugate depth of the jump so that the jump will stay on the apron. When the F_r is greater than 10, the common stilling basin may not be as cost-effective as special bucket-type dissipation.

Rectangular stilling basin is the most preferable, whose width is customarily equal to the waterway of the sluice. However, in order to meet the topographic condition of downstream riverbed, expansive stilling basin also may be employed to reduce unit exit discharge, which is usually done at the sloping apron section with expansive angle smaller than 7° .

Where the tailwater depth is low, the sloping apron is usually installed extending from the crest level to the horizontal floor (Bradley and Peterka 1957a, b, c, d, e, f). Thus, the worst case due to low tailwater level which governs the formation of hydraulic jump decides the location of the end elevation of sloping apron as well as that of horizontal floor (Fig. 11.7a). The sloping apron usually has a slope of 1:3–1:6, the higher of the flow velocity and head difference, the more flat is the sloping apron. For very high velocity, parabolic curve may be applied to link the bottom floor and the horizontal stilling basin apron. The composition stilling basin also may be exercised using both the end sill and the sloping apron, as shown in Fig. 11.7c.

3. Appurtenance works for energy dissipation

Jump may be controlled by several appurtenance works (dissipaters) such as end sill, chute blocks, and floor blocks (baffle piers) (Fig. 11.8) (Ippen 1951; Forster and Skrinde 1950; Sylvester 1964).

According to the SL265-2001 “Design specification for sluice”, there is a wide choice in the energy dissipaters concerning their type, shape, and size by laboratory studies or by analogy on the basis of existing full-scale data. It is not necessarily to provide simultaneously all types of dissipaters in one project.

(a) End sill

The purpose of an end sill located at the end of stilling basin is to trigger jump and to control its position under most probable operation conditions.

- The reactive action of end sill may shorten the hydraulic jump and alleviate the cavitation risk of baffle piers (floor blocks) by the backpressure created by the sill. This is most significant in case of small flow discharge at the initial opening of gate;
- The water level in stilling basin may be raised by the end sill, to meet the requirement for the second conjugate depth of hydraulic jump;
- Anticlockwise tumbling flow downstream of end sill can be attained by local flow separating, which may prevent the base of stilling basin from scouring;
- End sill may be continuous or dentated, and the latter is advantageous in splitting and dispersing the outflow from the stilling basin.

(b) Baffle piers (floor blocks)

Baffle piers are blocks in the intermediate positions across the basin floor. They produce reactive, dissipative, and splitting actions on the flow; in this way, it is possible to submerge the jump at a depth lower than the conventional second

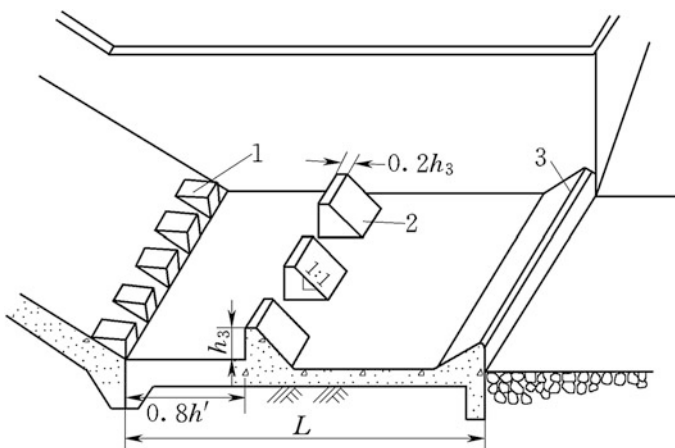


Fig. 11.8 Typical layout of energy dissipaters. 1 chute block; 2 floor block; 3 end sill

conjugate depth, which in turn may bring down the depth and length of stilling basin.

The baffle piers installed on the front portion of hydraulic jump which have large velocity is named as front piers, for the purpose of using reactive action to create dissipative effects. The baffle piers installed on the rear portion of hydraulic jump which has relative lower velocity are used to split flow for improving the flow pattern. In practice, front piers are mainly applied for medium to small project with medium to low head or low flow velocity. This is due to the fact that high velocity may result in cavitation damage on the piers and the downstream portion of the basin floor.

To prevent cavitation damage of baffle piers, the following principles shall be observed:

- The velocity at the front piers should not exceed 15 m/s;
- The shape of front piers is improved using streamline. However, this reduces the energy dissipation efficient, and the cavitation cannot be eliminated for very high velocity (e.g., 20–30 m/s); and
- Methods such as air aeration for the front piers are proved to be effective. However, there are few such practices in China because of economical or technical reasons.

(c) Chute blocks

Chute blocks are used at the entrance to stilling basin, in the shape of triangular dent. Their function is to furrow the flow jet, lift a portion of it from the floor, and cut Froude number. In this way, they trigger a shorter length and lower depth of jump than would occur without them. They are employed under the circumstances of very high tailwater level where undular jumps or oscillating waves take place with a Froude number between 2.5 and 4.

(d) Platform of small threshold

Platform of small threshold is installed at the end of bottom floor and the starting of sloping (inclined) apron, whose cross section is generally trapezoidal (Fig. 11.9).

The purpose of platform of small threshold is similar to chute piers. It is used where $F_r < 1.7$, to prevent undular jump.

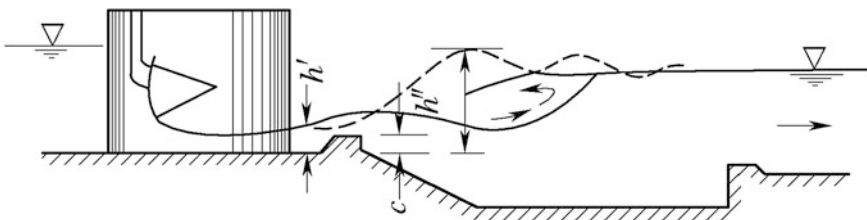


Fig. 11.9 Platform of small threshold

4. Height of end sill and depth of stilling basin

Having fixed the number of sluice bays and their crest levels, it is necessary to work out the excavation depth and the height of end sill of the stilling basin. Sharp crest or broad crest or even curved crest weirs at a height of 0.8–1.5 m are ordinarily employed as end sill to stabilize and to control hydraulic jump. Too high end sill may indicate the problems of second-stage energy dissipation after the sill and the stability of itself.

The excavation depth d of stilling basin should be able to control jump position within the basin at any discharge conditions, which may be estimated by

$$d = \sigma_0 h'' - t - \Delta Z \quad (11.3)$$

$$\Delta Z = \frac{\alpha q^2}{2g\varphi^2 t^2} - \frac{\alpha q^2}{2gh''} \quad (11.4)$$

where σ_0 = coefficient for submerged jump (usually $\sigma_0 = 1.05-1.10$); t = tailwater depth, m; h'' = second conjugate depth of hydraulic jump, m; and ΔZ = afflux by end sill, m.

Where $d \leq 0$, it means that the stilling basin excavation may be not necessary.

The determination of the stilling basin level is proceeded as follows:

- (a) For any given hydraulic conditions, calculate the total energy corresponding to unit discharge q ;
- (b) Assume a stilling basin level, e.g., by Eq. (11.3);
- (c) The energy above the crest level on the upstream is determined;
- (d) The depth of water before jump (first conjugate depth) is calculated;
- (e) Calculate the pre-jump Froude number F_{r1} ;
- (f) The post-jump depth (second conjugate depth) h'' is calculated;
- (g) The required stilling basin level under the considered hydraulic condition is calculated.
- (h) In the first trial, the initially assumed stilling basin level by step (b) and the calculated stilling basin level in step (g) may not be the same, which indicates that the stilling basin level assumed initially has to be revised. A few cyclic trials may be demanded to arrive at a final solution of the stilling basin level.

5. Length of stilling basin

The length of stilling basin comprises that of sloping and horizontal aprons, i.e.,

$$L_{sj} = L_s + \beta L_j \quad (11.5)$$

where L_s = length of sloping apron, m; L_j = length of free hydraulic jump, m; and β = adjustment coefficient of hydraulic jump length (usually $\beta = 0.7-0.8$).

Hydraulic jump is supposed to occur in the horizontal apron. Due to the afflux action of end sill, the actual hydraulic length may be shortened to 0.7–0.8 fraction

of free jump L_j , and the latter may be well predicted by the Elevatorski formula (1959) as

$$L_j = 6.9(h'' - h') \quad (11.6)$$

6. Sidewall of stilling basin

Since there is large vertical velocity component in a hydraulic jump, the vertical sidewall of stilling basin is most preferable for the stability of hydraulic jump as well as the stability of wall itself. Inclined sidewall can be only considered under the circumstances of small flow discharge and poor foundation stratum.

7. Apron protection of stilling basin

Protection of stilling basin is demanded for the provisions of strong scouring potential. The type and thickness of concrete apron should be adequate to counterbalance the hydraulic jump impaction, pressure fluctuation, and uplift pressure and to maintain sliding stability and floating stability.

According to the momentum equation, the reaction provided by the apron should be sufficient to resist the kinetic energy of the flow. The thickness of apron may be preliminarily estimated as

$$t = k_1 \sqrt{q \sqrt{\Delta H'}} \quad (11.7)$$

where t = thickness of apron at the starting point, m; $\Delta H'$ = afflux, m; and k_1 = thickness coefficient for apron floor (usually $k_1 = 0.15-0.20$).

The thickness of apron estimated by floating resistance is similar to Eqs. (7.41)–(7.42), i.e.,

$$t = k_2 \frac{u - p + p_m}{\gamma_c} \quad (11.8)$$

where k_2 = safety factor against floating (usually $k_2 = 1.1-1.3$); u = uplift pressure beneath the apron floor, kN/m^2 ; p = water column weight over the apron floor, kN/m^2 ; p_m = fluctuation pressure on the apron floor, kN/m^2 ; and γ_c = saturated volumetric weight of the apron materials, kN/m^3 .

In the design, the maximum value from Eqs. (11.7), (11.8) is adopted.

Since the loads such as water impaction, uplift, and fluctuation are all decreased from upstream to downstream, it is desirable to reduce the thickness of apron floor correspondently.

8. Rear apron

Although a majority part of energy has been dissipated within stilling basin, yet the outflow from the basin carries certain residual energy and has uneven velocity distribution with maximum value at the riverbed, which may lead to river scouring.

Rear apron is therefore installed for the purpose of residual energy dissipating, velocity distribution adjusting, good transiting to the downstream natural river stream, and preventing riverbed from scouring. Rear apron should be flexible to some extent, for the provisions of uneven foundation settlement. Rear apron also should be pervious, for draining under seepage flow and reducing uplift. The surface of rear apron should be rough enough to exert drag to the flow, for better residual energy dissipation and velocity adjustment. The rear apron may be inclined with a slope smaller than 1:10, beneath which a cushion layer is installed.

(a) Length of rear apron

It may be estimated by

$$L_p = K_s \sqrt{q_s \sqrt{\Delta H'}} \tag{11.9}$$

where L_p = length of rear apron, m; q_s = unit discharge at the end of stilling basin, $m^3/(s\ m)$; and K_s = coefficient for rear apron length is stipulated in Table 11.2.

(b) Structure of rear apron

Structure of rear apron should be competent with the flow velocity by selectively using:

- Dry stone pitching. It is made of rock blocks larger than 30 cm in a layer with a thickness of 0.3–0.7 m. The larger the rock block is, the higher scouring resistance it has. Cushion of gravel is commonly installed beneath the pitching. To further strengthen the scouring resistance, masonry embankments (stone ridges) may be installed at a space of 6–10 m.
- Masonry. Rear apron made of masonry has larger scouring resistance than that of dry stone pitching, but it has lower flexibility and permeability. This kind of rear apron is normally installed at the first-third portion of the rear apron just adjacent to the stilling basin. Draining holes within and filter beneath the apron are demanded.
- Riprap. As a material that has long been used to protect soils against the forces of water, riprap with good flexibility and permeability characteristics is most commonly exercised for rear apron (Maynard et al. 1989). Use of riprap rear apron facilitates construction, too. The material can be pit-run (as provided by the supplier) or specified (standard or special). Riprap is preferably a layer of large and durable rock fragments or blocks. A layer of sand and gravel is ordinarily placed under the riprap to prevent the material under the riprap from erosion.

Table 11.2 Coefficient of K_s

Soil type	Silty sand, fine sand	Medium sand, rough sand, silty loam	Silty clay	Hard clay
K_s	14–13	12–11	10–9	8–7

Equation (11.10) may be used in the selection of rock block size

$$v = (4.2-6.5)\sqrt{d} \quad (11.10)$$

where d = rock block size of riprap, m; and v = flow velocity, m/s.

- Concrete. Concrete rear apron may be applied in the areas in short of rock materials or where the outflow velocity from stilling basin is high (e.g., 6–8 m/s), which is in a form of square concrete slabs of 2–5 m in length and 0.1–0.2 m in thickness. Gaps between slabs are laid of 70–100 mm width and packed with gravel, for the relief of uplift. The concrete slab should be installed on a graded filter (Sherard and Dunnigan 1984, 1989).

Reinforcement gabion, fascine, reinforcement concrete, etc., also may be employed to build rear apron, too, depending on the project requirements.

It is also encouraged to combine different types of rear apron in one design, to let the rear apron vary from hard to soft along the river stream direction: The upstream portion is hard to obtain higher scouring resistance, and the downstream portion is flexible to achieve good settlement adaptability and economy.

9. Anti-scouring ditch and wall

Beyond the end of rear apron located on alluvial foundation, anti-scouring ditch with loose stones and boulders commonly have to be laid. The minimum boulder size is 0.3 m and should weigh heavier than 40 kg. These stones and boulders are expected to fall below at an angle, or launch, when the riverbed starts getting scoured at the commencement of a heavy flood. The size of anti-scouring ditch shall be selected according to the size of potential scour pit. In China, wide shallow ditch is generally arranged whose top width and depth are 10–17 m and 1.5–2.0 m, respectively.

It may be mentioned that the loose stone protection shall be installed not only at the downstream brink of the rear apron, but also at the positions along the base of guide bunds, wing walls, abutment walls, divide walls, etc.

Anti-scouring wall at the end of rear apron also may be installed to prevent rear apron from scouring damage. The wall should be deeper than the depth of scouring pit d_m evaluated by

$$d_m = 1.1 \frac{q_m}{[v_0]} - h_m \quad (11.11)$$

where q_m = unit discharge at the exit of rear apron, $\text{m}^3/(\text{s m})$; $[v_0]$ = allowable non-scouring velocity of alluvial foundation, m/s; and h_m = tailwater depth at the exit of rear apron, m.

10. Wing wall and bank slope protection

Wing walls are intended to protect riverbanks adjacent to the sluice from scouring and to help outflow being dispersed uniformly. The wing wall normally should be kept vertical up to the end of the impervious bottom floor beyond which

it should be flared from vertical to the actual slope of the river or canal. A certain length of riverbank after the wing wall should be protected by rubble masonry, dry pitch, or concrete slab. Reliable linkage of the foot of slope protection with the rear apron and the anti-scouring ditch should be provided.

11.4.4 Other Issues in the Energy Dissipation and Anti-scouring Design

1. Downstream water level

Generally, there are 5 types of relationship regarding tailwater depth and second conjugate depth after jump, which have been illustrated in Fig. 7.32. The energy dissipation and anti-scouring measures should be designed according to the different situations with respect to the upstream and downstream levels.

The stilling basin level and its length have to be determined for various combinations of flow and tailwater level that may be physically possible on the basis of the gate operation corresponding to the river inflow. The most severe condition would entail the lowest stilling basin level when the maximum length required. The hydraulic conditions that have to be checked are

- Flow at pool level, with a few gates opened;
- Case with discharge concentration enhanced by 20 % and a retrogressed downstream riverbed level; and
- Flow at high flood level, with all gates opened;

The length of horizontal apron by Eq. (11.5) can be reduced with a considerable saving in cost by the installation of some appurtenant structures. The most common is either one or a combination of end sill, baffle piers, etc.

2. Situation of low Froude number

When the Froude number $F_r = 1.0$, the flow is at critical and a jump cannot be triggered.

With $F_r = 1.0-1.7$, the flow is only slightly below critical depth and the change from supercritical to subcritical flow will lead to only a slight disturbance of the water surface. On the high end of this range (i.e., F_r approaching 1.7), standing or undulating waves manifest—the downstream depth will be about twice the incoming depth. Only <5 % fraction of energy being dissipated, the wave can propagate in the direction of downstream for long distance, which is commonly named as wave jump. The auxiliary countermeasures for reducing this wave jump are chute blocks and platform of small threshold.

When $F_r = 1.7-2.5$, weak jump or a series of small rollers begins to appear and becomes more intensive as F_r increases. The water surface is quite smooth, the velocity throughout the cross section is nearly uniform, and the energy loss is around 20 %.

An oscillating form of jump resulting in objectionable surface waves occurs under $F_r = 2.5-4.5$, where the incoming jet alternately flows near the bottom and then along the surface. Only 15–45 % fraction of energy is dissipated by the jump, which results in problems of very unevenly distributed velocity in post-jump flow, intensive surface fluctuation, and strong turbulence. This often manifests at lower afflux with deep tailwater, particularly when the gates are all opened and the outflow is submerged. The design principle for this case is focused on the smooth transition of flow from upstream to downstream and on the riverbed protection. The auxiliary countermeasures for improving the energy dissipation effect are end sill or baffle piers.

A well-balanced and stable jump is maintained where F_r of the incoming flow is greater than 4.5. Fluid turbulence is mostly confined within the jump, and for a F_r up to 9.0, the downstream water surface is comparatively smooth. Jump energy loss of 45–70 % can be expected. With $F_r > 9.0$, a high efficient jump may be produced, but its rough water surface may lead to serious downstream erosion problems.

3. Multi-bay sluices and their operation guidelines

A barrage is such a structure being equipped with gates across almost the whole river section and its crest levels being very close to the riverbed indicated by maximum flood inflow. The arrangement of multi-bay sluices provides many possibility of gate operation schemes in flood seasons, which allow for flexible and convenient running to achieve the structural safety taking into account of project purpose as well as the requirements for downstream and upstream reaches.

Operation of a gate or a group of gates affects not only the flow pattern in the upstream, but also the riverbed-level changes associated with the inflow velocity. In order to prevent any adverse flowing patterns and river morphologic changes and to prevent sediments from entering into diversion canals, a set of general guidelines for gate operation have to be observed. Some of the important ones among these are enumerated as follows:

- The dry season flows remain as near the under-sluice bays as possible so that feeding of the canal through a head regulator is less affected. It is only the under-sluice bays that operate and pass most of the river discharge which, in turn, creates a deep channel in the riverbed toward the bank where the diversion canal is off-taking.
- The gate operation should be such that the risk of deep scouring or shoaling in the vicinity of the barrage is minimized. In order to achieve this, it is essential that the gate openings of adjacent bays should not be abruptly changed.
- If a shoal has been formed on either upstream or downstream, it has to be washed out by an appropriate gate opening sequence.
- A gate opening sequence has to be evolved such that deposition of silt and debris is avoided as far as possible on the upstream pool.
- High intensity of flow is to be avoided in the regions of deep scouring, if any.

Generally, opening of one or few gates is a critical situation in the energy dissipation and scouring protection, when the tailwater level is low. Cross-flows and vertex formations dangerously lead to deep scouring both on the upstream and downstream of barrage. Good planar layout, rational expansion angle, etc., are all crucial for controlling such detrimental flow pattern. Apart from the countermeasures by design, rational gate operative scheme is also demanded to control current and vortex formation during small and medium floods, by judiciously selecting the correct operation using symmetrical opening and compartment opening. For this purpose, it is advisable to divide under-slucices into several independent portions along the barrage axis using divide walls (gyrones).

The Erjiang under-slucice in the Gezhouba Project (China, $H = 47$ m) comprises 27 sluice vents, which are divided by gyrones into three portions comprising 6 vents, 9 vents, and 12 vents, respectively. The under-slucice in the Miaozitou Barrage Project (Fig. 11.4) includes 15 vents, which are divided by gyrones into three portions comprising 2 vents, 4 vents, and 9 vents, respectively. The two vents of the first portion near the left abutment equipped with radial gates also play the role of silt excluders, whose stilling basin with end sill is longer than that of the remaining vents in the other portions. It is demanded that the open sequence is from left to right, and only if the flood inflow exceeds the release capacity of the two vents in the first portion, the gates of the portion two will be opened, followed by the portion three when encountering larger flood. As a result, the stilling basins are shorter in the second and third portions.

11.5 Under Seepage Control for Barrages and Slucices

Under seepage below a barrage or sluice gives rise to two detrimental effects:

- Uplift tends to lift up the barrage raft floor; and
- Upward rising seepage force just downstream of solid apron drags soil particles to erupt upward in a form of piping failure or pop-off failure.

Seepage also results in water loss. However, in a barrage project, water loss is commonly not very important concern in the design of under seepage control.

For a safe design with regard to under seepage, it is stipulated specially that

- The exit gradient of upward seepage flow just downstream of solid apron has to be determined and controlled, which should be safe against seepage failures;
- The total length of solid floor and the depth of cutoffs (or sheet piles) have to be determined, according to the conditions enumerated for under seepage.

To prevent riverbanks from failure due to bypassing seepage, treatment of barrage abutments is also demanded by the installation of cutoff wall, competent bank tie-in structure, and bank slope protection.

11.5.1 Creep Line Layout

The bottom floor of barrage (or sluice) has to be checked for critical subsurface flow conditions, if the barrage or sluice is located on a permeable foundation. The primary purpose of controlling the under seepage is to prevent the foundation material from piping and pop-off failures, which could lead to the structural collapse due to the loss of support. A secondary purpose of controlling under seepage is to reduce foundation uplift pressures that undermine the stability by offsetting a portion of self weight of the structure. From upstream to downstream, such seepage control is generally accomplished in sequence by impervious (clay) blanket, sheet pile (or cutoff wall), impervious bottom floor (foundation slab), apron of stilling basin, etc., which form the first streamline in seepage flow net and are termed as “creep line.”

Strategy in the design of the creep line is “upstream prevention and downstream drainage,” i.e., the foundation upstream of sluice/barrage is mainly used for seepage prevention with horizontal or vertical anti-seepage devices, to block seepage and to dissipate seepage head, whereas the foundation downstream the sluice/barrage is mainly used for dewatering with draining and pressure relief devices.

It must bear in mind that the floor length can be reduced by increasing the depth of cutoff and vice versa.

The draining layout has remarkable influence on both the uplift pressure distribution and exit gradient, which is illustrated in Fig. 11.10. Where there is no

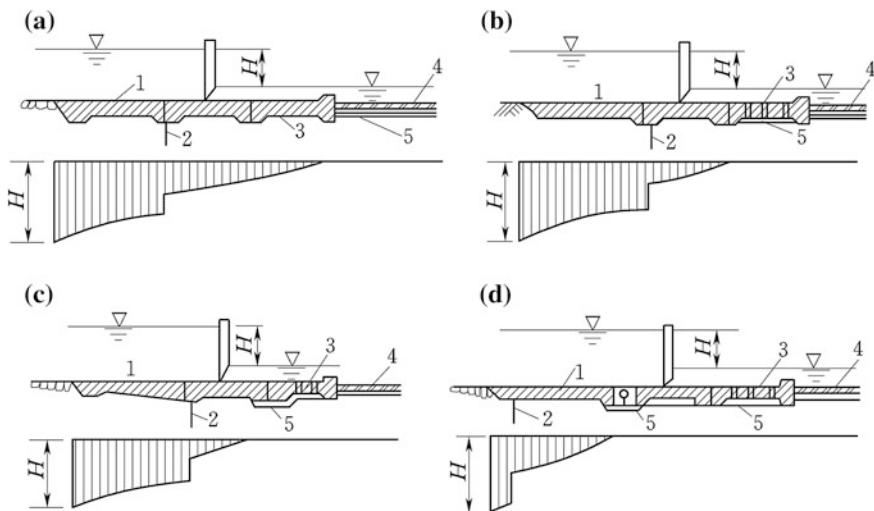


Fig. 11.10 Influence of creep line on the uplift. **a** Upstream sheet pile under floor + draining under rear apron; **b** upstream sheet pile under floor + draining under apron; **c** upstream sheet pile under floor + draining under downstream portion of floor; **d** upstream sheet pile under blanket + draining under whole floor. 1 impervious blanket; 2 sheet pile; 3 apron; 4 rear apron; 5 draining and filter

draining under floor and apron (Fig. 11.10a), although there are impervious blanket and sheet pile, yet the uplift pressure on the floor and apron is high. In Fig. 11.10b, horizontal draining is installed under the apron; as a result, there is no uplift pressure under apron and the uplift under floor is reduced significantly, too. Suppose the draining is further extended into under the downstream portion of the bottom floor as shown in Fig. 11.10c, further reduction of the uplift under the floor may be achieved. In Fig. 11.10d, a sheet pile is installed near the upstream brink of blanket; from there, the draining is extended until the rear apron; and the uplift under the floor is totally relieved. Therefore, it is clear that, for the purposes of cutting uplift pressure and improving the stability against sliding and floating, the seepage head should be dissipated by upstream blanket and sheet pile or should be relieved by extending drain in the direction of upstream, as far as possible.

However, if the upstream anti-seepage devices are kept unchanged and only the draining extends in the direction of upstream, the average seepage gradient will be raised as the shortening of the creep line, which is adverse for seepage failure protection. This means that the cut of uplift and the prevention of seepage failure are often inconsistent, and a compromise for meeting the requirements for economy and safety should be made mainly taking into account of the foundation soil properties.

Clayey soil foundation possesses low permeability and friction coefficient, but has high seepage failure resistance. For example, the consolidated silt and clay have permeability coefficient as low as 10^{-6} cm/s. In the layout of creep line, the major attention and caution are called at cutting the uplift under the floor so as to obtain sufficient stability against sliding and floating. This may be achieved by the extension of draining toward upstream meanwhile to keep shorter length of creep line. Sheet pile is usually not employed for its potential damage to the natural structure of clay which, in turn, would create concentrated seepage pathway. The upstream protection is mainly intended for scouring resistance; therefore, concrete slabs are customarily employed. The draining may be extended, even until to the whole bottom floor (Fig. 11.10d). The draining and filter layer under the bottom floor also help to accelerate foundation consolidation.

Sandy soil foundation has high permeability and friction coefficient, but low seepage failure resistance. In the layout of creep line, the main interesting is directed to prevent seepage failure and to reduce seepage discharge. Where the sandy layer is thick, continuous cutoffs of sheet piling upstream of the bottom floor are conventionally installed in combination with an upstream impervious blanket. The sheet pile should be embedded 0.25–0.5 m into the floor concrete and should be driven down to a depth that meets the seepage cutoff requirements indicated by analysis. The draining is only installed under stilling basin apron (Fig. 11.10b) and is not necessarily further extended in the direction of upstream. If the foundation is of fine sand, short sheet pile may be installed at the upstream of the blanket to elongate creep line and to cut seepage gradient. If the sandy layer is thin (less than 1–1.5 times of the head), it is desirable to cut sandy layer by dentated cutoff walls or sheet piles (Fig. 11.10c), to totally block the under seepage. In the latter case, draining should be installed under the stilling basin.

Silt sand foundation is vulnerable to liquefaction under the actions of earthquake; therefore, it is desirable to seal the foundation by sheet piles around the foundation. Since there is sheet pile at the downstream side of bottom floor, the uplift pressure under the floor will be raised; therefore, the upstream seepage prevention should be strengthened.

For multilayered foundation with a deep layer of strong permeability, the high water pressure in this deeper layer should be taken into account, the seepage resistance and floating stability of the top layers should be calibrated, and the relief wells under the stilling basin would be installed, if necessary.

11.5.2 Anti-seepage and Draining Devices

1. Horizontal anti-seepage devices

An upstream impervious blanket will frequently be advantageous for the soil- and pile-founded barrage or sluice, as it increases the horizontal length of creep line and thereby reduces seepage pressure under the structure. The blanket will usually be of clay material (Fig. 11.11), concrete or reinforced concrete (Fig. 11.12), impervious membrane (Giroud 1992), etc.

Normally, the permeability coefficient of blanket clay is $k = 10^{-5} - 10^{-7}$ cm/s and should be lower than 1/100 of the foundation soil. The blanket and the bottom floor should be linked tightly. Typically, the blanket will be of minimum 0.5–0.75 m thick at its upstream end and extended downstream until the floor where the thickness is dependent on the seepage gradient and is conventionally 1/4 of the maximum head difference between the headwater and tailwater. The blanket should

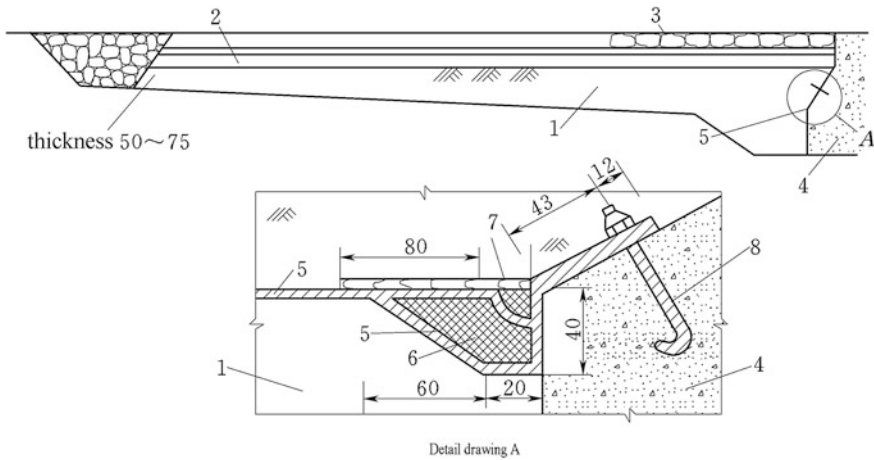


Fig. 11.11 Structure of clay blanket (unit: cm). 1 clay; 2 cushion; 3 masonry protection; 4 raft floor; 5 asphalt felt; 6 asphalt filler; 7 cover slab; 8 steel bar

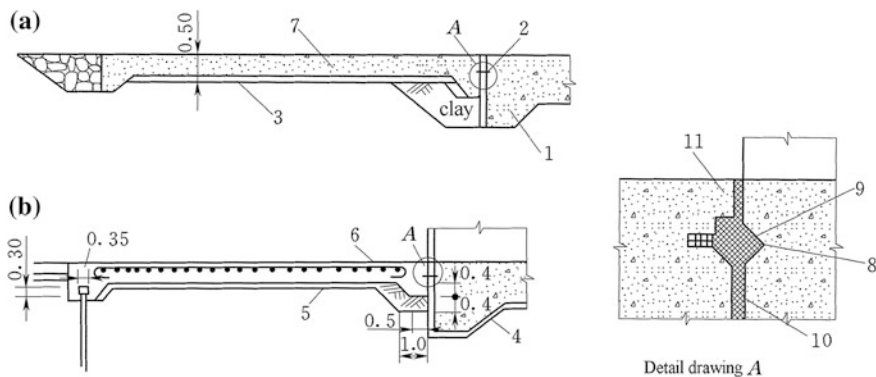


Fig. 11.12 Structure of concrete and reinforced concrete blankets (unit: cm). **a** Concrete blanket; **b** reinforced concrete blanket. 1 raft floor; 2 water stop; 3 concrete cushion; 4 cushion; 5 clay cushion; 6 reinforced concrete blanket; 7 concrete blanket; 8 metal sealing sheet; 9 asphalt; 10 asphalt felt; 11 cement mortar

be extended laterally to the adjacent riverbank (channel) slopes. To prevent potential separation between the blanket and the bottom floor, an impervious membrane, with laps to allow for lateral movement without tearing the membrane, is attached to the face of floor and embedded into the blanket. The surface of the impervious blanket should be protected, for preventing it from scouring damage.

The length of blanket is approximately equal to 3–5 times of the maximum upstream and downstream head difference. A too long blanket has negligible additional effect on further cut of uplift while increasing the cost significantly. Where the blanket of reasonable long cannot meet the requirement for seepage control, the vertical seepage prevention, or the adjustment of draining, may be considered.

Water stops of copper and plastic sealing sheet should be installed between the concrete blanket and bottom floor raft. The minimum thickness of concrete blanket is 0.4 m. Permanent joints are installed at a space of 8–20 m along the stream direction, in provision of temperature variation and uneven settlement.

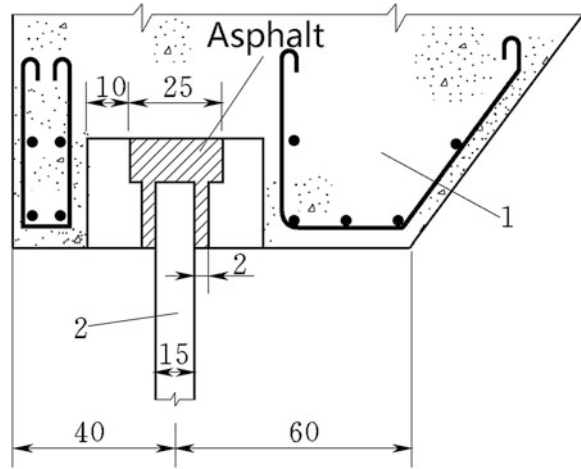
An impervious membrane, in lieu of a clay or concrete blanket, may be employed with careful protection on its surface, to prevent the high risk of punctures and tears by stones and tree branches. The thickness is dependent on the factors such as head difference, soil crack width under membrane, strain and strength of membrane, etc. Usually, it is not thinner than 0.5 mm.

2. Vertical anti-seepage devices

Vertical anti-seepage devices comprise steel sheet piles, reinforced concrete sheet piles, timber sheet piles, concrete cutoff walls, and curtains of high-pressure jet grouting. Figure 11.13 shows the connection of sheet pile with bottom floor.

Timber sheet piles are rarely exercised nowadays.

Fig. 11.13 Connection of sheet pile with bottom floor (unit: cm). 1 bottom raft floor; 2 sheet pile



Cutoff walls made of 12–25 m long plate or trough-shaped sheet piles may be driven using vibrator down to a maximum depth of 50 m. The design depth should meet the seepage cutoff requirements indicated by the analysis.

Reinforced concrete cutoff wall can be employed even in soil materials containing crushed stones. They are preferred to steel cutoff walls attributable to the possibility of making them at site. The minimum thickness and width are 0.2 and 0.4 m, respectively. The end of the reinforced concrete cutoff wall is in a shape of wedge, and the dynamic compaction is applied to drive the piles into the foundation.

To account for the potential settlement of barrage or sluice, a stiff link between the sheet piles and the bottom floor raft is not recommended.

Shallow depth cutoffs may be constructed where shallow trenches are excavated and backfilled with concrete. An intermediate depth (up to about 20 m) cutoff can be achieved by the slurry trench method. As the trench is excavated by conventional equipments—backhoe, dragline, etc., the bentonite slurry is introduced to support the trench sidewalls during the excavation, which is displaced when the concrete is placed by the tremie method (D'Appolonia 1980). When concrete cutoffs need to be extended to a great depth (e.g., 30 m), a 60 m to 80 cm wide excavation is accomplished by special equipments.

Curtains of high-pressure jet grouting have been illustrated in Chap. 9 of this book.

3. Draining devices

Reduction of uplift pressure may be accomplished by pipe drains. However, the draining pipes in stilling basin should not be provided near the beginning of stilling basin, nor in front of energy dissipaters, to avoid the transmission of a larger part of pulsating pressure through these pipes into the apron.

Adequate draining blanket (horizontal draining) should be installed under the floor slabs and/or stilling basin apron on clayey foundation, for delivering the seeping water quickly and effectively to the transverse collector drains.

The draining blanket is designed as a graded reverse filter of cobbles, pebbles, gravels, sands, and finer materials, with transversely embedded perforated sewer pipes of 5–8 cm in diameter and 1.0–1.5 m in spacing, adjacent to the concrete floor slab. It is important that the gradation of filter materials used in conjugation with the draining holes should be carefully selected with respect to the gradation of foundation soil materials, to prevent piping failure. Exits of these transverse drains discharge the seeping water through the walls or floor slabs at an elevation as practically low as possible, to achieve the maximum pressure reduction. Exits should be provided with flat-type check valves, to prevent surging and the entrance of foreign matter in the drainage system. For stilling basin apron, it may be preferable to place a connecting header along each wall and discharge all seeping water into the stilling basin just upstream the hydraulic jump at the practically lowest elevation, in order to secure the maximum reduction of uplift for the downstream portion of the floor slab.

11.5.3 Seepage Analysis for Barrage and Sluice Foundation

The main task in seepage analysis is to document the uplift pressure distributed under the raft floor and the exit gradient just downstream of the solid apron, while the amount of under seepage is only sometimes important. Of the seepage analysis methods illustrated in Chap. 4 of this book, the hydraulic method is prevalent attributable to its simplicity and effective, which mainly falls into the creep or weighted-creep method and the drag coefficient method.

1. Creep method

The method was firstly proposed by Bligh in 1910 (Bligh 1912) who assumed that the head loss along the creep line L is uniformly distributed. Accordingly, the average head gradient on the creep line is

$$\bar{J} = \frac{H}{L} \quad (11.12)$$

In Fig. 11.14, the uplift pressure at a distance x from exit is $h_x = \frac{H}{L}x$, and the loss of the element i along the creep line is $h_i = l_i \frac{H}{L} = (x_i - x_{i-1}) \frac{H}{L}$.

In 1934, Lane made an improvement for the Bligh theory (Lane 1935). After the analysis of more than 200 dams on pervious foundation, both failed and safe, he postulated that

- The weighted-creep distance is the sum of the vertical creep distance (steeper than 45°) plus one-third of the horizontal creep distance (gentler than 45°);
- The weighted-creep head ratio is the weighted-creep distance divided by the effective head;

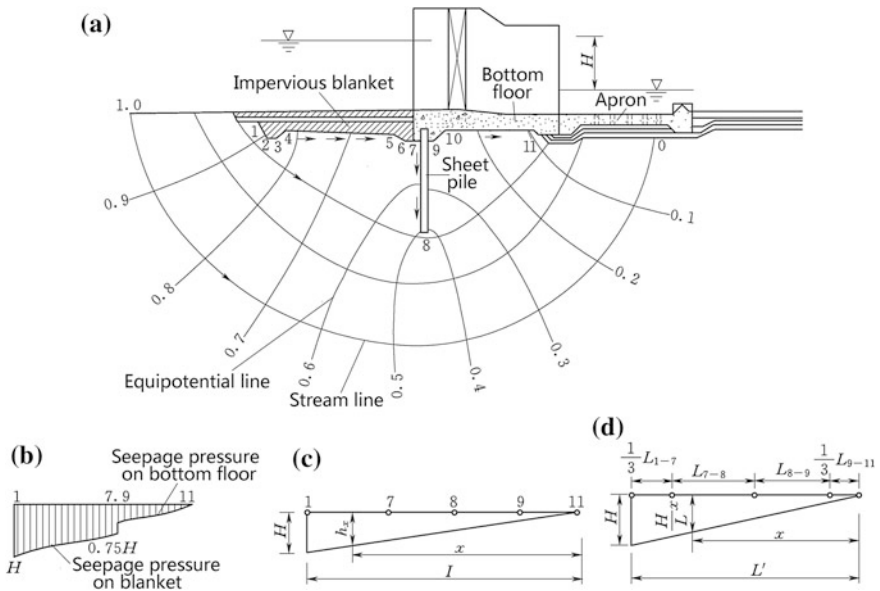


Fig. 11.14 Diagram to the uplift calculation by creep and weighted-creep methods. **a** Flow net; **b** uplift pressure distribution by flow net; **c** uplift pressure distribution by Bligh method; **d** uplift pressure distribution by Lane method

- Reverse filter drains, weep holes, and draining pipes aid to the security with regard to under seepage, and the safe weighted-creep head ratio recommended may be reduced as much as 10 % if they are installed;
- Care must be exercised to secure that cutoff is properly tied in at the ends so that the water will not outflank them; and
- The upward pressure to be used in design may be estimated by assuming that the drop in pressure from headwater to tailwater along the creep line is proportional to the weighted-creep distance.

According to the assumption of Lane, the equivalent length of creep line is $L' = L_1 + L_2/3$, in which L_1 and L_2 are vertical and horizontal length of creep line. According to Eq. (11.12), the length of creep line necessitated to prevent seepage failure should satisfy $L > CH$ or $L' > C'H$, in which C and C' are the ratios corresponding to the Bligh and Lane methods, respectively (see Table 11.3).

Creep method is convenient and normally employed in the preliminary design phase to evaluate the length of creep line, and it also may be employed for small barrages and sluices in any design phases.

2. Improved drag coefficient method

Drag coefficient method is suggested by Chugaev (1971), and its improved version is recommended by the SL265-2001 “Design specification for sluice”.

Table 11.3 Ratios C and C' corresponding to the creep method

Drain condition	Material									
	Very fine sand or silt	Fine sand	Medium sand	Coarse sand	Medium gravel	Coarse gravel including cobbles	Soft clay	Medium clay	Hard clay or loam	Very hard clay or hardpan
C	13-9	9-7	7-5	5-4	4-3	3-2.5	9-7	7-5	5-3	3-2
Without filter	-	-	-	-	-	-	-	-	7-4	4-3
C'	8.5	7.0	6.0	5.0	3.5	3.0	3.0	2.0	1.8	1.6

(a) Principles

In the presence of a water confining layer in the foundation, the deeper of this layer, the less of its influence on the pressure distribution along the creep line, the outlet (exit) head gradient, and the seepage discharge.

The seepage regime confined between the creep line and the water confining layer is assumed to be a tube and divided into several elements (Fig. 11.15), and the head loss at each element of the creep line with a laminar seepage flow is expressed by the principle of Darcy as

$$q = kJ_i T = k \frac{h_i}{l_i} T = k \frac{h_i}{\zeta_i} \tag{11.13}$$

where k = permeability coefficient of soil, m/s; J_i = hydraulic gradient in the element i ; T = thickness of the pervious layer, m; h_i = head loss in the element i , m; l_i = length of the element i , m; and ζ_i = drag coefficient of the element i .

It can be found from Eq. (11.13) that the drag coefficient $\zeta_i = \frac{l_i}{T}$ depends on the geometry feature of the element i , and through this element, the head loss is $h_i = \zeta_i \frac{q}{k}$. The total head losses are then summed by

$$H = \sum h_i = \frac{q}{k} \sum \zeta_i \tag{11.14}$$

And the loss in the element i may be expressed as

$$h_i = \zeta_i \frac{H}{\sum_{i=1}^n \zeta_i} \tag{11.15}$$

By Eq. (11.15), the head loss h_i through the creep line element i can be determined provided ζ_i and H are known.

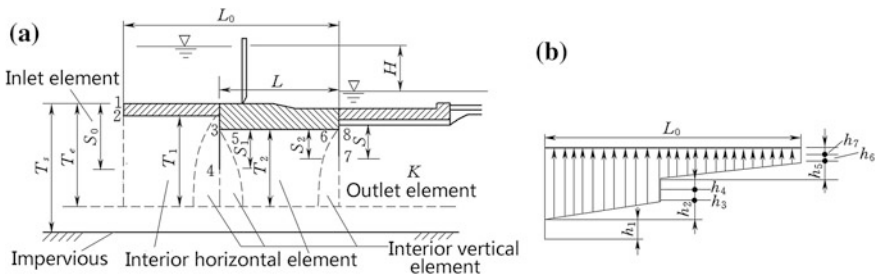


Fig. 11.15 Diagram to the seepage calculation by the improved drag coefficient method. **a** Element dividing of creep line; **b** uplift distribution

(b) Drag coefficients of typical seepage elements of creep line

According to the rigorous analysis based on fluid dynamics, the seepage elements of creep line may be summarized into three types as shown in Fig. 11.16.

(i) Inlet and outlet elements

$$\zeta_0 = 1.5 \left(\frac{S}{T} \right)^{\frac{3}{2}} + 0.441 \tag{11.16}$$

where ζ_0 = drag coefficients of the inlet and outlet elements; S = depth of the sheet pile or the cutoff wall, m; and T = depth of the pervious stratum, m.

(ii) Interior vertical element

$$\zeta_y = \frac{2}{\pi} \ln \operatorname{ctg} \left[\frac{\pi}{4} \left(1 - \frac{S}{T} \right) \right] \tag{11.17}$$

where ζ_y = drag coefficients of the interior vertical element.

(iii) Horizontal element

$$\zeta_x = \frac{L_x - 0.7(S_1 + S_2)}{T} \tag{11.18}$$

where ζ_x = drag coefficients of the interior horizontal element; L_x = length of the horizontal element, m; and S_1 and S_2 = depth of the sheet pile or the cutoff wall at inlet and outlet, m, respectively.

(c) Effective depth of seepage tube

Where the water confining stratum layer is not deep, the seepage analysis is based on its actual depth; otherwise, the actual depth in the analysis is substituted by an effective design depth T_e calculated by Eq. (11.19):

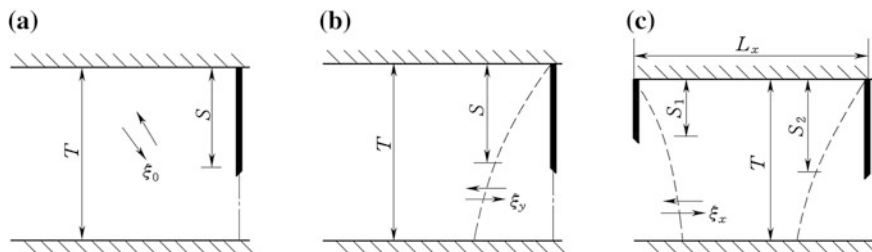


Fig. 11.16 Typical seepage elements of creep line

$$\begin{cases} T_e = 0.5L_0 & \frac{L_0}{S_0} \geq 5 \\ T_e = \frac{5L_0}{1.6\frac{L_0}{S_0}+2} & \frac{L_0}{S_0} < 5 \end{cases} \quad (11.19)$$

where L_0 = total length of the horizontal portions of the creep line, m; and S_0 = depth of the lowest point of the creep line, m.

Where the actual depth of the water confining layer T_0 is larger than the effective depth T_e , use of $T = T_e$ should be made in the seepage analysis. Otherwise, $T = T_0$.

(d) Local revision for the inlet and outlet elements of creep line

The hydraulic gradient has sharp variation at the inlet and outlet elements. Where the sheet piles or the cutoff wall is short or even absent, the head losses computed by Eq. (11.15) have low accuracy and therefore subject to revision, which may be preceded according to the SL265-2001 “Design specification for sluice”.

11.5.4 Control of Seepage Failure

The seepage gradients at horizontal and outlet elements should be controlled within the allowable gradient $[J]$ by the proper design of creep line.

The allowable gradient for clayey soil with regard to pop-off failure is listed in Table 11.4.

For sandy soil, firstly, the type of seepage failure should be judged as

- Where $4P_f(1 - n) > 1.0$, pop-off is indicated, whose allowable gradient is controlled according to Table 11.4.

Table 11.4 Allowable gradient $[J]$ with regard to pop-off failure

Material	$[J]$	
	Horizontal element	Outlet element
Very fine sand or silt	0.05–0.07	0.25–0.30
Fine sand	0.07–0.10	0.30–0.35
Medium sand	0.10–0.13	0.35–0.40
Coarse sand	0.13–0.17	0.40–0.45
Medium and fine gravel	0.17–0.22	0.45–0.50
Coarse gravel including cobbles	0.22–0.28	0.50–0.55
Sandy loam	0.15–0.25	0.40–0.50
Loam	0.25–0.35	0.50–0.60
Soft clay	0.30–0.40	0.60–0.70
Hard clay	0.40–0.50	0.70–0.80
Very hard clay or hardpan	0.50–0.60	0.80–0.90

- Where $4P_f(1 - n) < 1.0$, piping is indicated, and the allowable gradient is calculated by

$$[J] = \frac{7d_5}{Kd_f} [4P_f(1 - n)]^2 \quad (11.20)$$

where $d_f = 1.3\sqrt{d_{13}d_{85}}$, the boundary grain of coarse and fine particles, %; P_f = percentage content of soil particles smaller than d_f , %; n = porosity of soil; d_5, d_{15}, d_{85} = grain sizes of particle percentage content smaller than 5, 15, and 85 %, respectively (at the foundation soil grading curve), mm; and K = safety factor against piping failure (usually $K = 1.5-2.0$).

11.5.5 Bypass Seepage and Its Control

Bypass seepage takes place in the zone where the abutment pier or wing wall adjoins the permeable riverbank or earthfill dam. Behind the abutment pier or wing wall on the side of earthfill dam (or riverbank), a free seepage regime is created under the action of pool water. As the soil material beneath this seepage regime is saturated, the wing wall is exposed to hydrostatic pressure which has to be pre-determined for its stability and strength analysis. Bypass is actually a three-dimensional free seepage problem, whose computation has been illustrated in Chap. 5 of this book. However, it is worthwhile to note that a bypass creep line behind the abutment pier or wing wall can be ordinarily evaluated, by the analogy with the under seepage creep line beneath the barrage (sluice).

The countermeasures for preventing bypass seepage-induced failure are to elongate the creep line by the installation of side pier, upstream and downstream wing walls, and gyrone perpendicular to the wing walls.

The layout of bypass seepage creep line should conform with the anti-seepage devices of barrage and under-sluice. It is generally demanded that the upstream wing wall should not be shorter than that of impervious blanket. Otherwise, the blanket should be extended laterally to the banks, for keeping sufficient bypass creep line. Vertical anti-seepage devices below and along abutment piers may be installed, too, to separate the pressure seepage regime under the barrage and the free seepage regime behind abutment piers (or wing walls). The concentrated seepage at the contact surface of abutment pier and soil should be prevented, by means of gyrone, for example, which is an impervious wall behind and perpendicular to the abutment pier, for increasing the length of creep line.

For relieving seepage pressure in transition structure, drains are generally provided behind the downstream wing walls, which also should conform to the anti-seepage devices under the barrage and the stilling basin.

11.6 Layout and Structural Design for Sluice Chambers

The type, layout, and structure of sluice chamber should be as light and integral as possible under the restriction of operation requirements, with sufficient stiff and clear distribution of bearing force. The layout also should facilitate the management. The elements of the upper portion of sluice chamber are so located that the load of upper structural elements together with other forces would give rise to evenly distributed and acceptable stresses on the base, to reduce uneven settlement in foundation.

The regulation of water through a head regulator is customarily provided by vertical lift gates. Nowadays, however, radial gates are also prevalent, though they are preferred for head works having a relatively large difference between pool level and canal level to secure non-submergence of trunnion pin. Normally, an access bridge is provided across a head regulator for vehicular traffic or for inspection purposes. For the operation of gates, a working platform or operation bridge across the head regulator has to be accommodated, too.

A sluice chamber monolith typically consists of a series of three-dimensional (3-D) concrete structural elements founded either on rock, soil, or piles and subjected to a variety of external and internal loads. 3-D computation might be desirable to analyze the monolith in high precision. However, for simplicity, the analysis of 2-D slices through a monolith may reliably indicate the behavior of the monolith when the cross section geometry of structure, the soil and water conditions, the support conditions, and the other loading effects are constant throughout an extended length of the monolith. The 2-D slice is obtained by passing parallel planes perpendicular to the longitudinal axis of the sluice (barrage) typifying adjacent slices and is sufficiently remote from any discontinuities in geometry and loading.

11.6.1 Bottom Floors

A bottom floor supports upper portion structures, protects riverbed from scouring, and provides certain length of creep line. Bottom floors normally utilized with barrage projects fall into concrete flat slab (i.e., broad crested weir), low weir, concrete-capped or concrete-filled cellular, invert arch, and bored pile.

Generally, there are two sub-types of concrete flat slab floor, the first being called the gravity (or separated) type and the second as the raft (or monolithic) type. In the former, the uplift pressure is balanced by the self weight of the floor slab only, whereas in the latter, the uplift pressure is balanced by the floor itself and the piers as well as the other superimposed dead loads considering a span as a unit, which is the contemporary design style of barrage bottom floors.

1. Types of bottom floor slab
 - (a) Raft flat slab (monolithic)

By raft flat slab, a sluice unit of 1–3 vents can be made monolithic and the whole structure can be designed as a trough section, which is usually exercised for the sluice on soil foundations.

In order to avoid excessive stresses in the concrete structure due to uneven foundation settlements and temperature variations, the whole barrage (sluice) is divided into monoliths with permanent joints, and each of them comprises 1–3 spans (vents). The spacing of transverse joints is smaller than 20 m on rock foundation and smaller than 35 m on earth foundation. The joints are often installed through the axis of piers to avoid uneven settlement of adjoining piers, which may lead to jamming of gates (Fig. 11.17a). The piers with joint are thicker than that without joint. On hard soil or rock foundation, joints also may be located at the middle of foundation slab (Fig. 11.17b), to reduce the thickness of pier as well as the length of overflow front (waterway). The maximum net width of a sluice vent with joint at the middle of bottom floor slab is smaller than 8 m.

Raft flat slab is most commonly employed due to its advantages of simplicity in structure, convenience in construction, and even stress distribution in the foundation.

The length of flat slab is dependent on the requirements for the stability against sliding, the stress distribution in foundation, and the layout of upper portion of structure. The higher of the head H or the worse of the foundation, the longer is the foundation slab. The slab length may be $(1.5\text{--}2.5) H$ for gravel and cobble foundations, $(2.0\text{--}3.5) H$ for sand and sandy loam foundations, $(2.0\text{--}4.0) H$ for silt loam and loam foundations, and $(2.5\text{--}4.5) H$ for clay foundation.

Uniform thickness is normally adopted for flat foundation slab, which should be adequate to counterbalance the loads under consideration, and is decided by structural analysis considering the foundation conditions, the loads, and the width

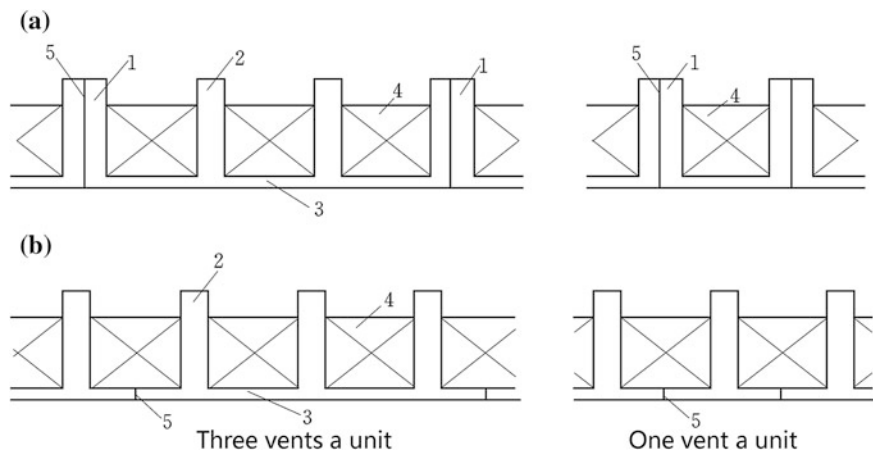


Fig. 11.17 Monolithic structure of flat foundation slab. **a** Joint in pier; **b** joint in slab. 1 jointed pier; 2 monolithic pier; 3 foundation slab; 4 gate; 5 permanent joint

of sluice vent. For large to medium projects, the thickness of flat slab is $1/6$ – $1/8$ of the net width of sluice vent, which is approximately 1.0–2.0 m and should not be smaller than 0.7 m.

Dentated walls (short cutoff walls) are usually provided for better conjugation of the slab with the foundation and to avert contact seepage as well as to increase the stability against sliding. The dents are commonly at a depth of 0.5–1.0 m.

Where the bearing capacity of foundation is very low, hollow slab of large stiff and lightweight may be employed, but it would be more congested with reinforcement steel bars.

(b) Separated flat slab

Transverse joints may be installed to separated foundation slab from piers; in this manner, the loads from piers are transferred to the foundation directly, and the slab plays only the role of anti-seepage and scouring protection. The separated slab is thinner than that of raft and is exercised where the sluice vent is wider than 8 m on hard soil or rock foundation.

(c) Bored pile foundation slab

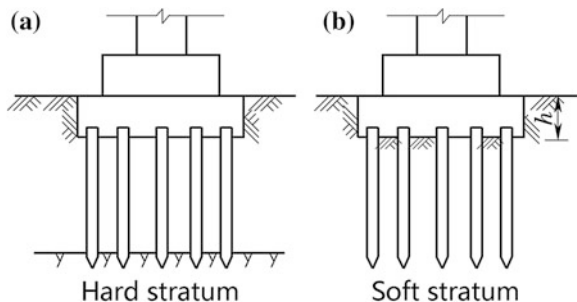
Piles are used when the bearing stratum is at a greater depth to which the load has to be transferred. Piling capacity comes mainly from end bearing (Fig. 11.18a) and skin friction (Fig. 11.18b). End-bearing piles, as the name indicates, obtain their capacity mainly by the end supporting from bearing stratum soil, while friction piles obtain their capacity from skin friction. Piles cannot be placed in soft clay, but they can be placed in medium-stiff clay. Under the latter circumstances, piles need to be designed as friction piles.

A pile cap is formulated on concrete piles, to support the loads from piers. The pile cap is separated from the foundation slab by permanent joints (sealed by water stops).

(d) Inverted arch foundation slab

The foundation consisting of inverted arches between the piers is known as inverted arch foundation. The rise of the inverted arches is about $1/5$ – $1/10$ of the span. In this type of foundation, the loads from the piers are transferred to the soil

Fig. 11.18 Bored piling foundation slabs. **a** End-bearing pile; **b** skin friction pile



by constructing arches in inverted position at their base, which is advantageous for the soil of low bearing capacity and when the depth of foundation should be kept low. The loads transmitted to the foundation soil through these arches are distributed over a wider area; hence, the soil may bear the structure more safely. Compared to the flat slab foundation, the slab thickness could be reduced by 40–50 %, and the steel consumption also may be reduced. However, the disadvantages of inverted arch foundation are also remarkable such as complication in construction, uneven distribution of flow in sluice chamber, and poor hydraulic conditions for energy dissipation and scouring prevention.

One of the difficulties with the design of inverted arch foundation is the computation of foundation reaction (foundation pressure), which is usually linearly distributed along the flow direction (Fig. 11.19a) but is changeable dependent on the construction sequence perpendicular to the flow direction:

- Inverted arches and pier foundation are placed firstly and then followed by the placement of piers, and the foundation reaction could be looked at as linearly distributed along the direction perpendicular to the flow (Fig. 11.19b);
- Pier foundation and lower portion of pier are placed firstly and then followed by the placement of inverted arches, the rest of the upper portion of piers is placed finally, and the foundation reaction could be nonlinearly distributed along the direction perpendicular to flow (Fig. 11.19c).

2. Computation for raft foundation slab

Since raft floor slab is a structure of biaxial bending, the computation is therefore proceeded to simplify it into two independent uniaxial bending structures transverse

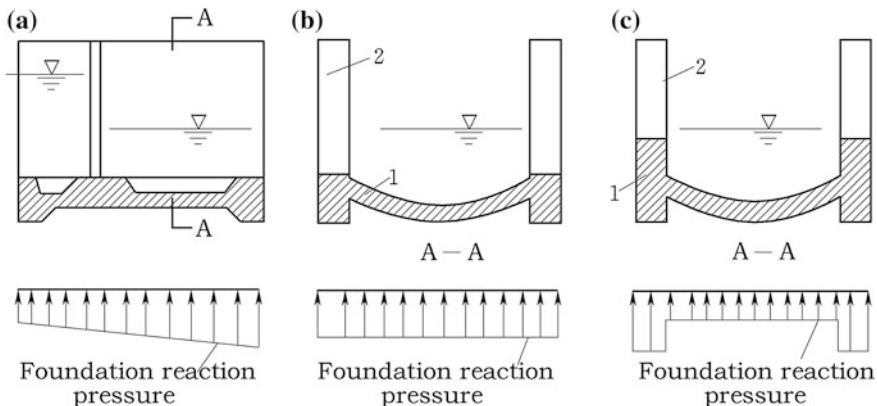


Fig. 11.19 Reaction distribution on inverted arch foundation. **a** Reaction distribution along the flow direction; **b** reaction distribution perpendicular to the flow direction (first placement of inverted arch and pier foundation); **c** reaction distribution perpendicular to the flow direction (first placement of inverted arch and lower portion of pier). 1 first placement zone; 2 last placement zone

and longitudinal to the flow direction. Apart from static pressure of water, self weight of slab, weight of piers, and the other loads of upper portion facilities, a foundation slab also subjects to the action of foundation (base) pressure, which depends on the type of foundation material, the nature of the loading, and the size and shape of the unit monolith.

Along the flow direction, the slab and piers form a structure similar to an inverted T-shaped beam with larger stiffness; hence, a linear distribution of base pressure can be assumed; and the eccentric compression formula may be applied for the pressure calculation.

Transverse to the flow direction, the span is considered as a monolithic and corrugated (ribbed) slab structure with flexible base whose ribs are provided by piers. The foundation pressure and inner forces in the slab are distributed in curvilinear due to soil/structure interaction. Usually, at least, two transverse strips of 1 m thick, respectively, in front of and behind the gate slot are cut as representative sections for the inner force and stress analyses, based on which the reinforcement design is carried out.

(a) Linear reaction method

This method assumes that the structure is sufficiently rigid in the direction transverse to the stream flow; hence, the normal contact stress (foundation pressure) is constant all along the slice identical to the value at the corresponding longitudinal foundation pressure diagram with linear distribution.

It is simple and suitable for sand foundation of relative density $D_r \geq 0.5$.

(b) Inverted beam method

Similar to the linear reaction method, inverted beam method also assumes that the normal contact stress (i.e., foundation pressure) transverse to flow is uniform along the slice identical to the value at the corresponding longitudinal foundation pressure diagram with linear distribution, and the slab is looked at as an inverted beam supported by piers.

The distributed loads q on the beam is computed as (Fig. 11.20)

$$q = q_3 + q_4 - q_1 - q_2 \quad (11.21)$$

where q_1 = self weight of slab; q_2 = weight of water; q_3 = uplift pressure; and q_4 = average foundation pressure on the transverse slice.

The inverted beam method may be applied in small projects with good foundation.

(c) Method of beam on elastic foundation

If the foundation is elastic and heterogeneous, the normal contact stress (foundation pressure) transverse to the flow direction has a changeable curvilinear pattern. The method of beam on elastic foundation looks at the slice section as a beam compatibly deforms with the foundation soil under the action of loads from upper portion.

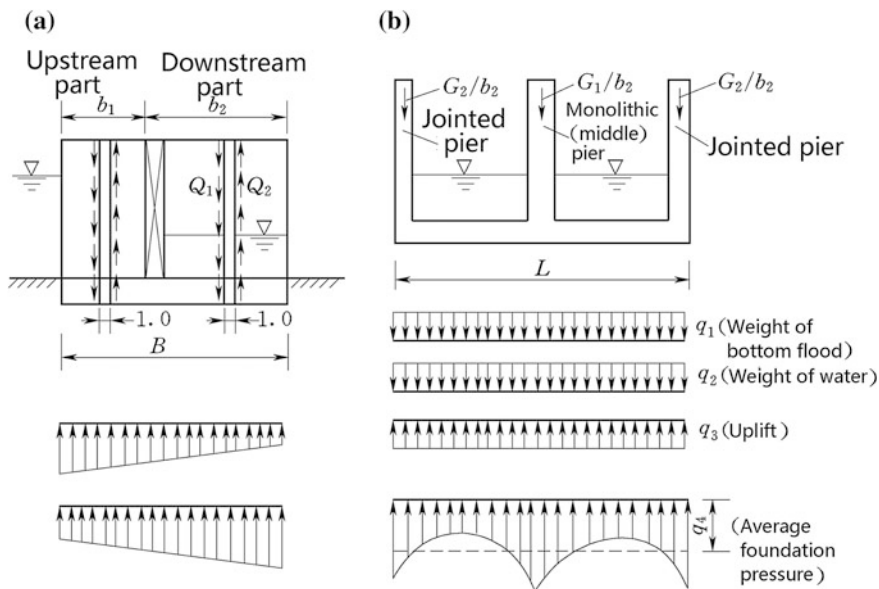


Fig. 11.20 Diagram to the calculation of foundation pressure. **a** Longitudinal distribution; **b** transverse distribution

By equilibrium condition (shear force distributing) and deformation compatibility condition (slab has identical deformation to the foundation settlement), the foundation pressure and inner forces in the slab may be solved (Hetenyi 1946; Winterkorn and Fang 1975).

The basic computation steps are proceeded in the following:

- ① Computation of forces exerting on foundation slab. As shown in Fig. 11.20, the concentrated forces on the foundation slab are the unbalanced force of piers and the weight of piers W inclusive permanent fixed facilities. The distributed forces on the slab slice are the water weight q_2 , the weight of slab q_1 , the uplift pressure q_3 , and the average foundation pressure q_4 on the slice, as well as the distributed unbalance shear force.

The SL265-2001 “Design specification for sluice” stipulates that the self weight of slab may be neglected in the method of beam on elastic foundation. This is attributable to the fact that the foundation slab is usually placed on an excavated foundation, and the slab weight gives rise to smaller foundation pressure than the initial stress. The settlement by the self weight of slab is a kind of recompression after the excavation rebound, which will completed in a short period. However, if a negative value of resultant distributed force is manifested under the slab by the computation, the self weight of the slab should be taken into account partially to maintain the zero value of the resultant distributed force under the slab.

Water weight is a distributed force with the strength of $q'_2 = q_2(L - 2d_2 - d_1)/L$.

- ② Computation of average pressure exerting on foundation slab. The average pressure on the slab is decided from the longitudinal foundation pressure diagram at the position of the slice concerned. This longitudinal pressure diagram is computed by the eccentric compression, as has been described foregoing.
- ③ Computation of unbalanced shear force exerting on the slice. This force is attributable to, on the one hand the assumption that the longitudinal foundation pressure varies linearly, on the other hand the fact that the loads such as water weight changes suddenly across the gate slot. Therefore, there is unbalanced shear on the slice to maintain its balance, which is provided by the difference of shear forces $Q_1 - Q_2$ on the two sides of the slice (Fig. 11.20a).

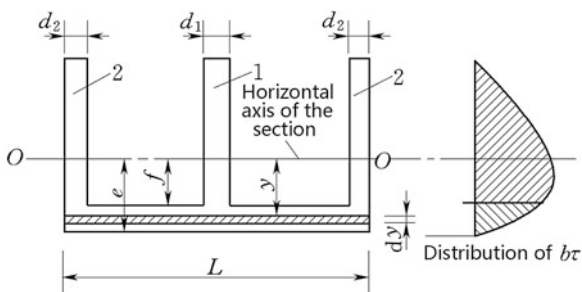
Taking the downstream portion of pier as example (Fig. 11.20a), according to the equilibrium condition $\sum Y = 0$, we have

$$\frac{W_1}{b_2} + 2\frac{W_2}{b_2} + \Delta Q + (q_1 + q'_2 - q_3 - q_4)L = 0 \tag{11.22}$$

where W_1 and $W_2 =$ weights of the monolithic pier and the jointed pier, respectively, kN ; and $\Delta Q =$ unbalanced shear force.

- ④ Redistribution of the unbalanced shear force. The unbalanced shear force is shared by the slab and the piers using the parabolic distribution assumption of shear stress on the whole slice (Fig. 11.21). The shear force shared by slab is a distributed force, while that shared by piers is a concentrated force.
- ⑤ Computation of foundation pressure and beam inner forces. The foundation pressure pattern is dependent on the thickness T of the compressive stratum. Denote that the length of beam is L , then:
 - Where $T/L < 0.5$, the Winkler assumption may be adopted in the computation;
 - Where $T/L > 4.0$, the foundation should be looked at as elastic half space, and the М.И.Горбунов-ПоСадов method may be applied;
 - Where $T/L = 0.5-4.0$, methods based on finite depth foundation should be applied.

Fig. 11.21 Diagram to the distribution of unbalanced shear force. 1 monolithic pier; 2 jointed pier



- ⑥ Analysis of side load effects on the foundation settlement and inner forces. Side load effects are resulted from the backfill earth adjoining to the abutment unit or from the adjoining barrage (sluice) units constructed in sequence. On the safe side, the side load is taken into account as follows:
- Where the computed barrage unit is constructed after the adjoining units. If the side load reduces the inner forces of the slab, its effects are neglected. If the side load increases the inner forces of the slab, 50 % of its effects may be considered in sand foundation and 100 % of its effects should be considered in clay foundation.
 - Where the computed barrage unit is constructed before the adjoining units. Since the side load increases the inner forces of the slab, 100 % of its effects should be considered in all kinds of foundation (Fig. 11.22).

11.6.2 Piers

The width, length, and height of pier are designed primarily related to the following operational features: shape requirements for the pier nose, height of gate in closed position, travel of gate to fully open position, trunnion girder location and trunnion anchorage requirements (for Tainter/radial gate only), support requirements for gate operation machinery (e.g., gantry), elevation of service bridge and service bridge supports, recesses (slots) for upstream and downstream maintenance bulkheads, dogging devices for bulkheads, and access stairwell.

Chinese barrages and sluices in existence usually possess piers of identical length to that of foundation slab in the flow direction. However, a bit extension of foundation slab in the direction of upstream or downstream may be advantageous, for adjusting the position of resultant load or for utilizing upstream water weight on the slab to raise the stability of barrage (sluice) unit.

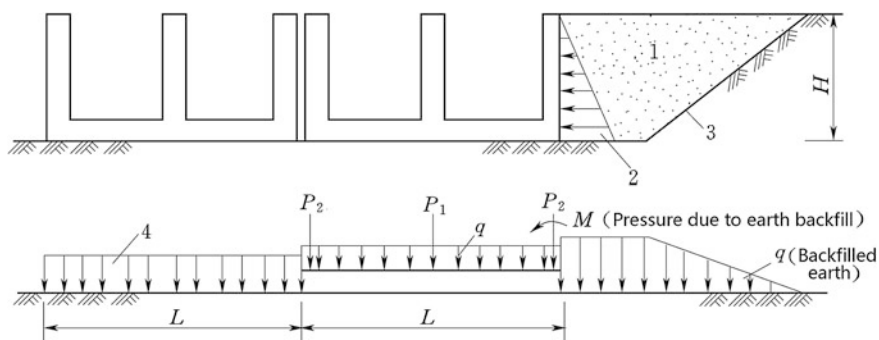


Fig. 11.22 Diagram to the calculation of side load effects. 1 backfill earth; 2 lateral earth pressure; 3 excavation boundary; 4 contact stress on the base of adjoining barrage unit

Pier thickness is ordinarily 2–3.5 m. Piers for supporting radial (Tainter) gates possess no gate slots; therefore, they may be thinner, whereas piers for supporting vertical lift (plate) gates possess gate slot with wideness/depth ratio of 1.6–1.8 and with minimum pier thickness 0.4 m at the gate slot. Jointed piers are thicker than monolithic piers.

Planar shape of pier affects the hydraulic performance and discharge capacity of sluice. The most common design is with a semicircular pier nose and a streamline tail for better dispersion of outflow. To facilitate the installation of bridge and machinery, the upper portion of pier above water level is commonly in rectangular shape.

1. Computation of pier stress

Piers and semi-piers (containing joint) work in bending to resist the pressure from gates and side loads, and the latter appears when an unbalanced load exerts on the side of pier.

Generally, the maximum stress manifests at the bottom of pier, which may be calculated as a cantilever plate fixed on the foundation slab, followed by the reinforcement design. Two work situations with respect to operation and repair should be taken into account in the computation of piers.

(a) Operation situation

The gates are all closed. The loads comprise static water pressure, self weight of pier and upper portion structure, weight of facilities, and earthquake action.

(b) Repair situation

One vent is closed for repair, while the adjoining vent is open. The bidirectional bending stresses at the pier bottom should be calibrated.

The stress computation for the semi-pier in a jointed pier belongs to this situation, too.

2. Computation for vertical gate slot

Several methods are available for the vertical gate slot computation.

- (a) Water pressure from gates is overtaken totally by reinforced steel bars, which is obviously conservative and steel congestion.
- (b) To obtain a rational reinforcement design, it is usually to cut the piers into several horizontal strips of 1 m thick, then to compute the stress and to reinforce the pier by layered scheme (Fig. 11.23).
 - The loads are shear forces Q_u and Q_d of upper and lower surfaces, water pressure $P = B\gamma_w(h - y)m$ from gates (in which B is the width of sluice vent, γ_w is the unit weight of water, h is the upstream water depth, and y is the water depth at the strip).

- According to the equilibrium condition, $P = Q_d - Q_u$.
 - P is shared among the upstream and downstream segments of pier in proportion to their moment of inertia, of which the upstream part is assumed to be transferred through slot. In this way, the slot stress is obtained which may be used for reinforcement design.
- (c) A more precise method is to consider the moment M and shear Q in pier and the deformation compatibility, and this method may reduce the reinforcement amount by 15–50 %. The computation diagram for the pier under normal retaining situation is shown in Fig. 11.23.

- According to the virtual work principle, the horizontal deflection at the height of Y above the foundation slab is

$$\Delta x_i = \frac{\alpha_i \gamma_w (B + b)}{120EI} \left[(h - y)^5 + 5h^4 y - h^5 \right] + \frac{\alpha_i \gamma_w (B + b) \beta}{6GA} \left[h^3 - (h - y)^3 \right] \quad (11.23)$$

where α_i = distribution coefficient of water pressure; E = Young's modulus of pier concrete, kN/m^2 ; β = distribution coefficient of shear force; A = horizontal section area of pier, m^2 ; and I = moment of inertia, m^4 .

- Denote the horizontal deflections of the upstream and downstream parts with respect to pier slot as Δx_1 and Δx_2 , the corresponding distribution coefficients of water pressure as α_1 and α_2 , and the consistence requirement for deflection leads to:

$$\Delta x_1 = \Delta x_2 \quad (11.24)$$

$$\alpha_1 + \alpha_2 = 1 \quad (11.25)$$

After the solution of α_1 and α_2 , curve of $y - \alpha_i$ may be drawn to facilitate the computation.

The water pressure shared by upstream and downstream parts of pier is expressed as

$$P_u = \alpha_1 (B + b) \gamma_w (h - y) \quad (11.26)$$

$$P_d = \alpha_2 (B + b) \gamma_w (h - y) \quad (11.27)$$

And the tensile force of the slot is

$$P_1 = \alpha_1 (B + b) \gamma_w (h - y) + b \gamma_w (h - y) \quad (11.28)$$

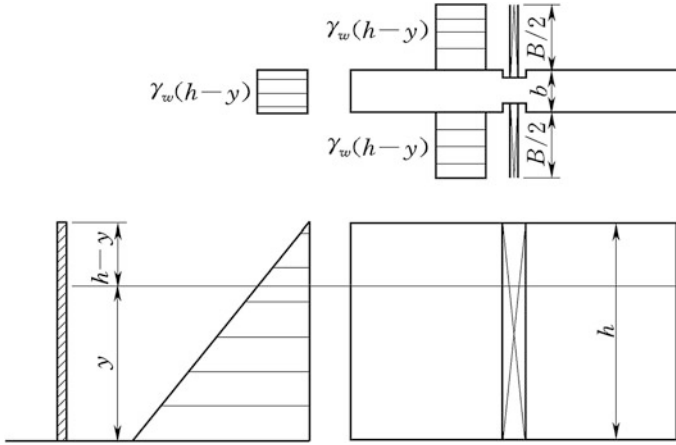


Fig. 11.23 Computation diagram for the pier slot under operation situation

3. Stress and reinforcement for the supporter of radial gate

Supporters of radial gates may be corbels, beams, and prestressed concrete trunnion girders.

Corbel is a short cantilever of simple hexahedral or girder structure placed monolithically with pier. The axis of corbel has commonly a slope of 1:2.5–1:3.5, in an attempt to conform the direction of thrust force from the radial gate trunnion when the gate closes. The minimum width b and the minimum height h of the corbel are normally 50–70 cm and 80–100 cm, respectively. At the end, a slope of 1:1 is customarily formed.

Corbel transfers the thrust load R from the gate trunnion to the pier, which is the half of total water pressure on the radial gate and gives rise to internal forces in the corbel merging as shear, moment, and torsion.

Under the concentrated force action, the corbel may induce large tensile stress in the pier. However, according to the three-dimensional photo-elastic model tests and FEM analyses, the excess tensile stress larger than the permissible value of concrete only appears within a limited regime in front of the corbel at a width of 2 times and at a height of 1.5–2.5 times that of corbel (see the broken line in Fig. 11.24b), respectively. The area should be reinforced according to Eq. (11.29).

$$A_g = \frac{KN'}{f_y} \tag{11.29}$$

where A_g = total area of bearing steel bars within the pier connected with the corbel, m^2 ; K = safety factor of strength; f_y = tensile strength of steel bar, kN/m^2 ; $N' \approx (0.7-0.8)N$, total surplus tension force of the corbel with regard to the concrete allowable stress, kN ; and N = component of R along the axis of corbel, kN .

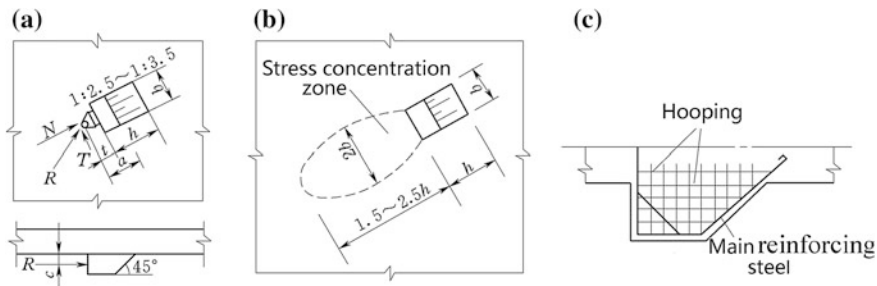


Fig. 11.24 Corbel structure and reinforcement. **a** Corbel structure; **b** pier stress; **c** corbel reinforcement

Larger piers are ordinarily equipped with prestressed concrete trunnion girders which bear against the downstream face of the pier and provide operational and stationary support for radial (Tainter) gates. Usually, these girders are of posttensioned design. The larger girders are generally cast-in-place, whereas the smaller ones can be precast and then lifted into place by crane. The girder should be located above most frequent flood elevations. However, submergence is sometimes allowed for in a limited range of time.

11.6.3 Gates

See Chap. 15 of this book.

11.6.4 Parapet Walls

Parapet wall may be plate type or deck-girder type, whose lower edge is in a shape of circular or ellipse favorable for the smooth passing through of flow.

The loads exert on the parapet are self weight, static water pressure, wave pressure, and floating debris impaction.

Deck-girder-type parapet wall consists of deck plate, up girder, and lower girder. Deck plate takes up and transfers water pressure to the girders, which are supported by piers. For high parapet wall, a middle stand girder may be added. Deck plate and stand girders are placed monolithically. If the edge ratio of deck plate is smaller than 2, the plate is looked at as a bidirectional plate supported along four sides; otherwise, the plate is looked at as a unidirectional plate supported solely by the stand girders.

The minimum thickness of the deck-girder-type parapet wall is 20 cm, the minimum height of the upper girder is 1/12–1/15 of the vent span, and the minimum height of the lower girder is 1/8–1/9 of the vent span.

Plate type is suitable for small sluice vent, and its thickness normally varies from the minimum 20 cm at the top. It may be placed monolithically with piers, or precast and supported in the slots.

11.6.5 Joints and Water Stops

Either metallic or nonmetallic sealing is designed to stop the water from migrating through open joints. Metallic water stops are rigid, made from steel, copper, bronze, or lead, which may be used in large barrage projects where strength rather than flexibility is emphasized. Nonmetallic water stops are usually made of natural rubber, synthetic rubbers (e.g., butyl rubber, neoprene, styrene butadiene rubber, nitrile butadiene rubber), and polyvinyl chloride, which may provide flexibility rather than strength and must possess high extensibility, recovery, chemical resistance, and fatigue resistance.

Water stops in a barrage project are distinguished as vertical type and horizontal type, and the former is installed in the vertical joints of piers, abutment retaining walls, and wing walls, while the latter is installed in the horizontal joints in blanket, bottom floor slab, stilling basin apron, as well as abutment wall and wing walls (Fig. 11.25). Water stops for vertical and horizontal joints should be linked together to form a closed sealing system. Expansive joints without anti-seepage requirements are sealed with materials such as asphalt felt.

A single line of plastic or rubble water stop is the common installation, whereas the double-lined water stops should be provided at all joints for important or large-scale barrages, of which the first line uses copper sheet. The introduction of joints may create openings which must be filled. Typical joint filler materials consist of a variety of substances and configurations, depending on the purpose of the filling.

Fig. 11.25 Layout of joints.
 1 abutment pier; 2 concrete blanket;
 3 stilling basin;
 4 upstream wing wall;
 5 downstream wing wall;
 6 monolithic pier;
 7 jointed pier;
 8 joint for thermal and settlement

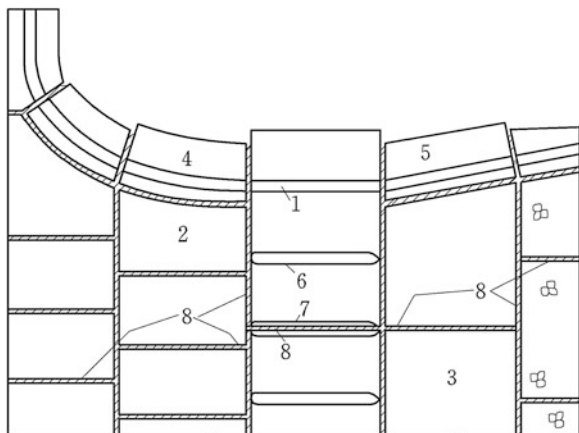


Figure 11.26 shows the structures of water stops for vertical joints. The water stops in Fig. 11.26a, b are water stops for piers installed at the upstream side of gate to reduce the lateral pressure, the water stop in Fig. 11.26a is simple and convenient for construction while in Fig. 11.26b may adapt large settlement but difficult for construction. The water stop in Fig. 11.26c is simple and convenient for construction, and is suitable for the joints in abutment walls and wing walls of small settlement and low anti-seepage requirements.

Figure 11.27 shows the structures of water stops for horizontal joints. The water stops in Fig. 11.27a, b are applied to the joints of large settlement with high anti-seepage requirements, whereas in Fig. 11.27c may be employed for the joints of small settlement with low anti-seepage requirements. On the bottom where the joints contact foundation stratum, two or three tiered sacks or asphalt saturated felt may be placed to strengthen anti-seepage.

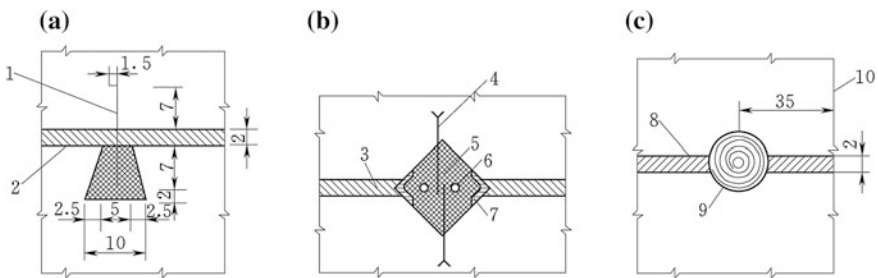


Fig. 11.26 Structures of water stops for vertical joints (unit: cm). 1 copper sheet and galvanized iron sheet; 2 0.25-cm asphalt shingles on both sides + asphalt; 3 asphalt felt; 4 metal water stop strip; 5 asphalt filler; 6 heating facilities; 7 angle iron; 8 asphalt shingles; 9 $\phi 10$ asphalt shingles; 10 waterside

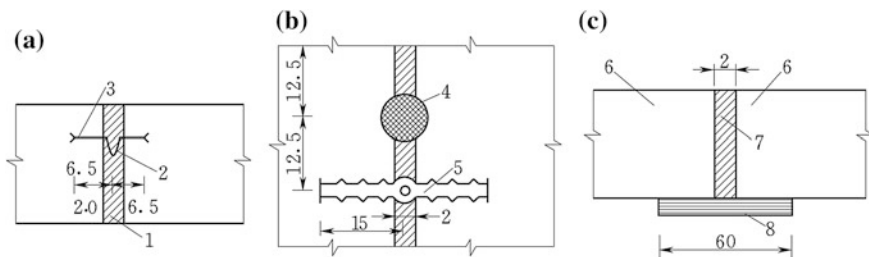


Fig. 11.27 Structures of water stops for horizontal joints (unit: cm). 1 asphalt shingles; 2 rosin tar; 3 cooper sheet; 4 tarred rope; 5 plastic sheet; 6 apron; 7 asphalt shingles; 8 three tiered sacks + two tiered asphalt saturated felt

11.6.6 Service and Access Bridges

A service bridge provides support for overhead cranes and/or provides access to the equipments located on the barrage or sluice. Typically, traveling hoist cars or gantry cranes may transport emergency bulkheads or vertical lift gates to each gate bay over the bridge. The service bridge usually consists of a concrete deck and up to three girders simply supported by piers. The crane rail is centered on the middle girder. The bottom elevation of the girders should be allowance for specified clearance above maximum operating upper pool with respect to possible navigation requirements.

An access bridge provides transportation between banks, which is usually installed on the downstream portion of piers for the purpose of bringing down the elevation of the bridge deck. However, where the gate operation facilities are the layout on the downstream, and the access bridge has to be installed on the upstream portion of the piers, such as the barrage projects of Gezhouba (China, $H = 47$ m) and Wangpuzhou (China, $H = 33.9$ m). The design of the access bridge connected to the public highway should meet the requirements specified in corresponding design codes. A minimum width of 3 m is normally demanded on the access bridge for local habitants and cattle as well as small vehicles.

11.7 Stability Analysis and Foundation Treatment

At the completion of a sluice unit, the self weight and the weight of its upper portion facilities ordinarily lead to the maximum contact stress on foundation. Under the action of such stress, large and/or uneven settlements may lead to insufficient top elevation, large inclination influencing the normal operation, and foundation slab cracking. This is particularly serious at the abutment sluice unit where the abutment pier is exerted by the backfill earth pressure.

If the contact stress exceeds allowable stress of foundation, the foundation stability may be lost. After the impounding, sliding failure along the base by the horizontal thrust and deep-seated sliding within foundation may occur. Under the repair situation, floating failure may also be possible due to insufficient weight and large uplift. Therefore, stability should be met taking into account of all situations including construction, completion, operation, and service (repair), which covers overall stability against sliding, foundation strength calibration, and floating stability. Stability analysis is normally carried out for a unit which comprises one or several monolithic sluice vents.

11.7.1 Loads and Load Combinations

Loads that can normally be expected to be imparted to a sluice unit are those resulted from construction and operation activities including lateral earth pressures,

hydrostatic pressure, uplift, dynamic forces from debris impact or earthquake, wind force, wave pressure, ice pressure, forces from gates and bridges, and thermal actions (Garg 1976; Golzé 1977; Tan 1986; USBR 1987; Varshney et al. 1982; Zhang et al. 1988; Zuo et al. 1987). Figure 11.30 shows the diagram to the load computation under normal water retaining situation. The description and computation of all these loads may be referred to Chap. 4 of this book, and only the particular features of several loads are explained hereinafter (Fig. 11.28).

1. Self weight

Self weight should include piers, slabs, and fixed facilities.

Movable facilities such as cranes and bulkhead gates have non-negligible influences on the barrage and sluice and should be selected according to the design situations. For example, loads due to movable cranes and other machinery can be significant and must not be taken into account in the stability analysis of the structure under usual situation and situation of repair, while they should be included in the bearing capacity analysis of the structure under situation of completion. They should be exerted as point loads at the appropriate positions.

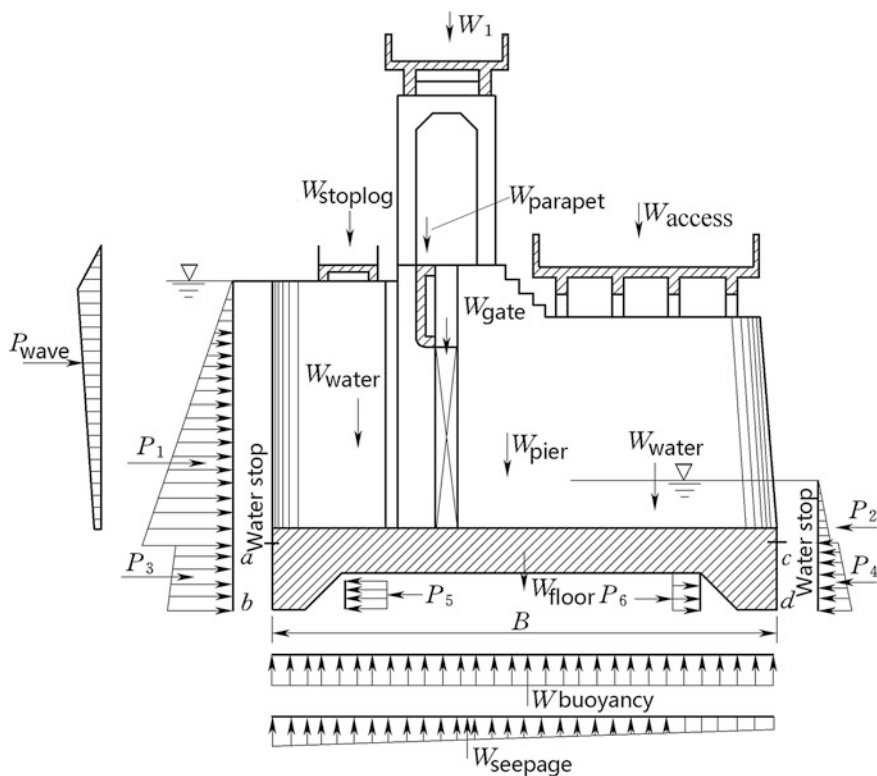


Fig. 11.28 Diagram to the load computation under normal water retaining situation

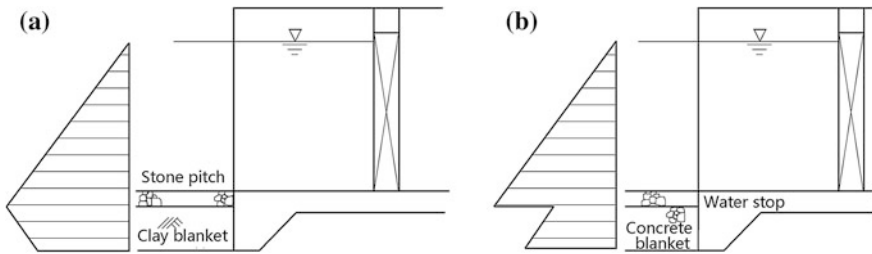


Fig. 11.29 Distribution of horizontal hydrostatic pressure. **a** Clay blanket; **b** concrete blanket

2. Hydrostatic pressure

Hydrostatic pressure may be resolved into horizontal and vertical components.

Where there is an upstream clay blanket, the horizontal pressure above blanket is hydrostatic pressure, and at the bottom where the blanket intimately contact with foundation slab, the horizontal pressure is reduced to the uplift pressure, which is illustrated in Fig. 11.29a.

Where there is an upstream concrete blanket, the horizontal pressure above the sealing sheet of water stop is hydrostatic pressure, and below the sealing sheet, the horizontal pressure is identical to the uplift pressure, which is illustrated in Fig. 11.29b.

On the interior side of dental wall, the hydrostatic pressure is identical to the uplift pressure.

3. Uplift

The uplift pressure at any point under the structure will be dependent on the presence, location, and effectiveness of foundation drains. Effective downstream drains will generally bring the uplift down to tailwater pressure at the toe of barrage. Since uplift may have a counterbalance effect on foundation loads, the stability of barrage or sluice unit (monolith) should be investigated with respect to both the maximum and minimum probable uplift pressures. The stability design should be checked with full uplift forces for sliding and overturning and without uplift forces for maximum foundation pressures.

11.7.2 Contact Stress and Bearing Capacity

The bearing capacity of foundation is dominated by the base contact stress or foundation pressure. The average base stress is calculated by

$$\bar{\sigma} = \frac{\sum W}{BL} \quad (11.30)$$

where $\sum W$ = resultant vertical load above the plane concerned, kN; B = length of the foundation bottom slab along the flow direction, m; and L = width of the foundation bottom slab perpendicular to the flow direction, m.

Base pressure computation should be undertaken by distributing the normal component of the resultant forces on the structure, to calculate the reaction on the base by means of general flexure formula.

Where the loads are symmetrical with respect to the perpendicular direction of the flow, the maximum and minimum stresses appear at upstream heel and downstream toe, which are computed by Eq. (11.31)

$$\sigma_{\begin{matrix} \text{max} \\ \text{min} \end{matrix}} = \frac{\sum W}{BL} \pm \frac{6 \sum M}{B^2L} \tag{11.31}$$

where $\sum M$ = summation of moments determined with respect to the centroid of the plane, kN m; $\sum W$ = resultant vertical load above the plane concerned, kN; B = width of the barrage or sluice unit, m; and L = length of the barrage or sluice unit, m.

Where the loads are asymmetrical with respect to the perpendicular direction of the flow, maximum and minimum stress are computed by

$$\sigma_{\begin{matrix} \text{max} \\ \text{min} \end{matrix}} = \frac{\sum W}{BL} \pm \frac{\sum M_x}{W_x} \pm \frac{\sum M_y}{W_y} \tag{11.32}$$

where $\sum M_x$ and $\sum M_y$ = summations of moments determined with respect to the along and perpendicular to the flow directions, respectively, kN m; and W_x and W_y = sectional moduli determined with respect to the along and perpendicular to the flow directions, respectively, m³.

In general, allowable foundation pressure should not be exceeded under any loading conditions. The SL265-2001 “Design specification for sluice” stipulates that:

- Under any situations, the average stress $\bar{\sigma}$ should be lower than the allowable bearing capacity $[\sigma]$ of the foundation, i.e., $\bar{\sigma} \leq [\sigma]$. The maximum contact stress should be lower than 1.2 times of the allowable bearing capacity of the foundation, i.e., $\sigma_{\text{max}} \leq 1.2[\sigma]$;
- Uneven distribution coefficient of contact stress $\eta = \frac{\sigma_{\text{max}}}{\sigma_{\text{min}}}$ should be lower than that of allowable value $[\eta]$ listed in Table 11.5, i.e., $\eta \leq [\eta]$.

Table 11.5 Allowable uneven distribution coefficient of contact stress $[\eta]$

Property of foundation soil	Load combination	
	Basic	Special
Soft	1.50	2.00
Medium hard	2.00	2.50
Hard	2.50	3.00

11.7.3 Stability Analysis Against Sliding

1. Computation method

Limit equilibrium analysis is customarily carried out to assess the stability safety against sliding. Because the in situ strength parameters of rock and soil are never known exactly, the factor of safety K with respect to strength reduction is employed to compensate for the uncertainty that exists in assigning determinate values to these crucial parameters.

The factor of safety K against sliding for a barrage or sluice monolithic unit along the base surface or the soil enclosed by upstream and downstream dents is calculated by:

$$K = \frac{f \sum W}{\sum H} \tag{11.33}$$

where $\sum W$ = resultant of vertical forces exerting on the monolithic sluice or barrage unit, kN; $\sum H$ = resultant of horizontal forces exerting on the monolithic sluice or barrage unit, kN; and f = friction coefficient of the concrete/soil contact face.

It is demanded that $K \geq [K]$, where $[K]$ is the allowable safety factor (or the design safety factor), which is listed in Table 11.6.

If there are adequate dental walls, the computed slip plane may be assumed as the straight line between the bottom edges of dents; in this case, the Eq. (11.31) is employed to calculate K

$$K = \frac{tg\varphi \sum W + cA}{\sum H} \tag{11.34}$$

where φ = friction angle of the foundation soil, ($^\circ$); c = cohesion of the foundation soil, kN/m²; and A = area of the foundation of the monolithic unit, m².

Basically, deep-seated sliding problem of foundation is equivalent to bearing capacity problem. However, since the foundation is generally heterogeneous and exerted by seepage pressure apart from horizontal loads, additional stability calibration concerning deep-seated sliding should be carried out. To do so, the allowable bearing capacity is firstly employed to estimate tentative size of foundation slab; then, the Swedish arc method or the other methods (slice, wedge) are applied to calibrate the deep-seated sliding stability; and the latter has been illustrated in Chap. 5 of this book.

Table 11.6 Allowable safety factor $[K]$ against sliding along the barrage/sluice base

Load combination		Grade of barrage and sluice			
		1	2	3	4, 5
Basic		1.35	1.30	1.25	1.20
Special	I	1.20	1.15	1.10	1.05
	II	1.10	1.05	1.05	1.00

For the barrages and sluices on rock foundation, the stability analysis is identical to the gravity dams illustrated in Chap. 7 of this book.

2. Countermeasures to improve the stability against sliding

Where the sliding stability is not sufficient, countermeasures for the improvement are selectively exercised as follows:

- Install the gates closer to the downstream edge of the foundation slab or lengthen the upstream portion of the foundation slab adequately, to profit from more vertical water weight;
- Change the structure size of barrage or sluice unit to increase the self weight. Increase the length of foundation slab which is effective, for this simultaneously increases self weight, water weight, and the contact area on the foundation. On the contrary, increase the thickness of foundation slab which has less effects and higher expenditure, due to the simultaneously raised buoyant action. The thickening of pier also has negative effects because it gives rise to wider flow front and larger water retaining surface, which in turn increase the horizontal thrust;
- Deepen the dental walls. It is effective by mobilizing more soil for slip resisting. However, restricted by the stiffness and strength, the depth of denting is limited;
- Adjust draining measures to cut the uplift;
- Install concrete blanket in front of and connected to the foundation slab, which will perform as an monolithic anti-slip slab;
- Install lateral piles or employ other prestressed reinforcements.

11.7.4 Floatation Computation

The stability analysis with regard to floatation should be carried out under repair situation, particularly where the upstream and downstream both have bulkhead gates and when the tailwater level is high.

The repair of barrage and sluice is usually carried out in dry seasons when the reservoir is at normal pool level. The downstream level is selected according to the repair circle by certain recurrence dry season flood. The self weights of movable facilities and plate steel gates are not taken into account.

The safety factor against floatation is defined as

$$K_f = \frac{\sum V}{\sum U} \quad (11.35)$$

where $\sum V$ = resultant of downward vertical forces apart from uplift, kN; $\sum U$ = uplift exerting on the bottom floor slab, kN; and K_f = safety factor against floating.

It is demanded that $K_f \geq 1.10$ under basic load combinations and $K_f \geq 1.05$ under special load combinations.

11.7.5 Settlement Computation

Foundation pressure should not produce significant differential settlements that lead to operational difficulties (e.g., improper operation of gates and rupture of water stops). By engineering experiences, if the contact stress satisfies the requirement for the allowable bearing capacity, the settlement will be able to meet, too. In locations where detrimental settlement of barrage and sluice foundation might occur, or the structures are of large scale, a settlement analysis should be carried out additionally. The final settlement of foundation may be calculated by Eq. (11.36).

$$S = m \sum_{i=1}^n \frac{e_{1i} - e_{2i}}{1 + e_{1i}} h_i \quad (11.36)$$

where n = layers of compressive stratum within the depth of consideration; e_{1i} = porosity ratio of the i th layer under the action of average stress due to self weight (using an $e - \log p$ curve); e_{2i} = porosity ratio of the i th layer under the action of average stress due to self weight + average subsidiary stress (using an $e - \log p$ curve); h_i = thickness of the i th layer, m; and m = modification coefficient of foundation settlement, which is usually ranged within 1.0–1.6 (lower bound for hard foundation, whereas upper bound for soft foundation).

Generally, the allowable settlement and differential settlement are 15 and 5 cm, respectively. If the settlement analysis indicates a possible concern, the settlement could be adjusted by the engineering countermeasures as follows:

- Using an alternative work site, if possible;
- Extending the foundation to reduce base pressure or deepen the foundation;
- Designing alternative foundation slab by foundation treatments (e.g., piling);
- Using light and stiff structures; and
- Changing of construction sequence (e.g., to reduce the effects of side loads).

11.7.6 Foundation Treatment

A prime consideration in the design of an earth foundation is the differential settlement, sliding stability, and bearing capacity. They must be within acceptable limits for the serviceability of the gates and other operating equipments. Adequate stability is attained by specific limitations on the magnitude of the foundation pressure (bearing capacity) and the resistance to sliding, and on the location of the

resultant force within the structure base. There are a variety of foundation treatment methods available for different earth foundations encountered (Bussey 1961; Day 2006; D'Appolonia 1980; USBR 1987; Winterkorn and Fang 1975; Xanthakos et al. 1994).

1. Earth cushion

By placing soil of high strength and density as well as low compressibility on the soft soil after the foundation surface clearance, earth cushion may improve the foundation pressure distribution and stability. It is suitable for the case where the soft soil stratum on the foundation surface is thin (Fig. 11.30).

The thickness of earth cushion is conventionally 1.5–3.0 m depending on the soil condition, structure type, and magnitude of load. Too thin earth cushion has very limited effects in the foundation improvement, whereas too thick earth cushion will result in draining difficulties with foundation pit. The wideness of earth cushion is designed by its diffused angle under pressure.

Medium loam and clay including sand are preferable cushion materials, because their good compaction characteristics enable to obtain high dry unit weight. Well-graded medium sand, rough sand, and gravel are also applicable and attributable to their workability to be vibrating compacted. Silt sand, light sand, or silty loam are not adequate as cushion materials.

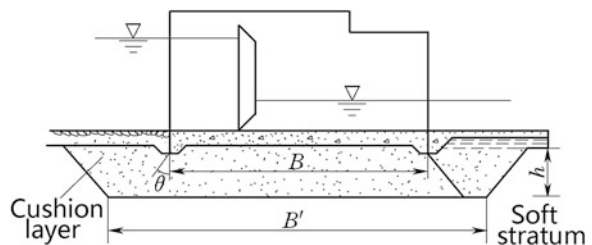
2. Drop shaft sinking (caisson)

Caisson is a prefabricated concrete box with sides but without bottom (HKIE 1981; Siu 1992). It is used under the circumstances of soft ground or high water table on surface and embedded with hard soil or rock stratum beneath, where open trench excavation is impractical. Caissons are sunk by their self-weight, concrete or water ballast placed on top, or by hydraulic jacks. The leading edge (or cutting shoe) of the caisson is inclined out at a sharp angle to aid sinking in a vertical manner and is usually made of steel. Once in place, it is filled with concrete to become part of the permanent works, such as the foundation of barrage and sluice, which improves the bearing capacity and stability as well as reduces the settlement.

3. Sand drain preloading

The purposes of vertical drain installation together with preloading by surcharge embankment or vacuum pressure are to accelerate the consolidation process and to

Fig. 11.30 Schematic drawing of earth cushion



gain rapid strength increase for improving the stability of structures on weak clay foundation. In this method, pore water squeezed out during the consolidation of the clay due to the hydraulic gradients created by the preloading can flow a much faster in the horizontal direction toward the drain and then flow freely along the drains vertically toward the permeable drainage layers. Sand drain preloading method is applicable where the soft or flow sand stratum is near ground surface or shallowly embedded.

Sand drains are formed by infilling sand into holes in the soft ground. There are two categories of installation, namely with displacement and non-displacement. In the displacement installation, a closed end mandrel is driven or pushed into the soft ground with resulting displacements in both vertical and lateral directions. The non-displacement installation requires drilling the hole by means of power auger or water jets and is considered to have less disturbing effects on the soft clay. It is noted that driven sand drains are harmful in soft and sensitive clays, because the disturbance will induce a significant reduction in shear strength and horizontal permeability. The planar layout of drains is in a pattern of square or triangle. The diameter of sand drains is ordinarily 20–30 cm, and the spacing of drains is 4–12 times of the diameter, which is commonly ranged within 2–4 m. They are preferable to penetrate the whole thickness of soft stratum.

4. Piling

Piling is particularly appropriate when a structure is to be erected on deep soil foundation that is not stable. In many cases, it may substantially reduce the required earthwork and the expenditure of concrete.

By construction method, piles may be classified into driven piles and cast in situ piles (Poulos and Davis 1980).

Driven piles are pushed into the ground using a pile driver and made of wood, steel, or reinforced concrete, of which the latter is widely applied in barrage and sluice projects. Concrete piles are available in the cross section of square, octagonal, and round. They are reinforced with steel bars and are often prestressed. Driving piles are advantageous because the pile driving operation compresses the surrounding soil, giving rise to greater friction on the sides of the piles, thus increasing their load-bearing capacity. The diameter of driven piles is $d = 0.25$ – 0.55 m, and the maximum length is 25–30 m.

Rotary boring techniques offer larger diameter cast in situ piles than any other piling methods and permit piling through particularly dense or hard strata. For end-bearing piles, drilling continues until the borehole has extended a sufficient depth into strong stratum. Depending on site geology, this can be a rock layer, or hardpan, or other dense and strong layers. Both the diameter and the depth of pile are highly specific to the ground conditions, load conditions, and nature of project. Rotary auger piles are available in diameters of $d = 0.3$ – 2.4 m or even larger, and using these techniques, pile length beyond 50 m can be achieved.

According to the properties of the soil at the lower end of pile, piles are distinguished as end-bearing piles supported by practically incompressible soil, and floating (friction) piles sunk in soil of uniform consistency and transmit their load to

the soil through both their lower and lateral surfaces. Most piles in barrage project are floating piles.

The spacing of piles depends on the kind and magnitude of loads that exert upon the foundation. Single pile is used under independent footings, while rows of piles are placed under continuous foot, and the latter is commonly employed in barrage projects. The design length of piles is chosen with regard to soil properties at the construction site.

A correct determination of the load-bearing capacity is essential for the design of a reliable and economical piling foundation. The load-bearing capacity of the piles can be calibrated through engineering and geological surveys, the data obtained by static probing of soil, and the results of testing the piles by static and dynamic loading, of which the last one is the most reliable.

5. Heavy tamping

Heavy tamping (dynamic consolidation or compaction) using free fall weight dropped from a height of 10–15 m is an effective means for improving the foundation of silt and clay. It is one of the oldest forms of ground improvements in existence (a variation of this technique reportedly utilized by the Romans). The time required for treatment is shorter than that for sand drain preloading

Dynamic compaction is applied in a systematically controlled pattern of drops on a coordinate grid layout. The initial impacts are spaced at a distance dictated by the depth of the compressible layer, depth to groundwater, and grain size gradation, which generally approximate the thickness of compressible layer. Typically, 5–15 blows per one grid point are conducted.

On the surface, 1–2 m thick pervious cushion is the layout. Several blows are applied at each location followed by 1–4 weeks of rest period, and then, the process is repeated for several cycles. In each cycle, the settlement is immediate, followed by draining of pore water. Draining is accelerated by the radial fissures formed around impact points and by the use of horizontal and peripheral drains.

Because of the necessity for a time lapse between successive cycles of heavy tamping when treating silts and clays, a minimum treatment area of 15,000–30,000 m² is necessitated for economical reason.

6. Vibro-replacement stone columns

Cohesive, mixed, and layered soils generally are not compacted easily when subjected to vibration alone due to their inability to properly respond to vibration. Vibro-replacement stone column (Hughes and Withers 1974) which is derived by further developing the vibro-compaction process extends the range of soil that can be improved by vibratory techniques to cover cohesive soils. Densification and/or reinforcement of soil with compacted granular columns or “stone columns” is accomplished by either a top-feed method or a bottom-feed method. With vibro-replacement stone columns, crushed stone with high friction angle is designed, to increase bearing capacity, reduce settlement, mitigate the potential for liquefaction, and improve strength and stiffness.

There are two different approaches that may be employed to construct the stone columns, depending on the ground conditions. In the top-feed system, the poker is completely withdrawn after initial penetration to the design depth. Stone of 40–75 mm in size is then tipped into the hole in controlled volumes from the ground surface. The stone column is compacted in layers through the continued penetration and withdrawal of the poker. The top-feed system is suitable where the hole formed by the poker will remain open during the construction of the column.

Alternatively, the stone may be fed from a rig-mounted hopper through a permanent delivery tube along the side of the poker, which bends inward and allows for the stone to leave from the poker tip. This bottom-feed process demands a smaller grade of stone (15–45 mm in size). By remaining in the ground during column construction, the poker cases its own hole and hence is suited to ground with a high water table or running sand conditions. The process of the bottom-feed system is schematically illustrated in Fig. 11.31.

Diameter of stone column is generally 0.6–0.8 m, arranged in the pattern of square or quincunx spaced 1.5–2.5 m apart. The depth is decided according to the requirements for design and construction. Where the soft stratum is not too thick, it is preferable to let the column penetrate the whole soft stratum.

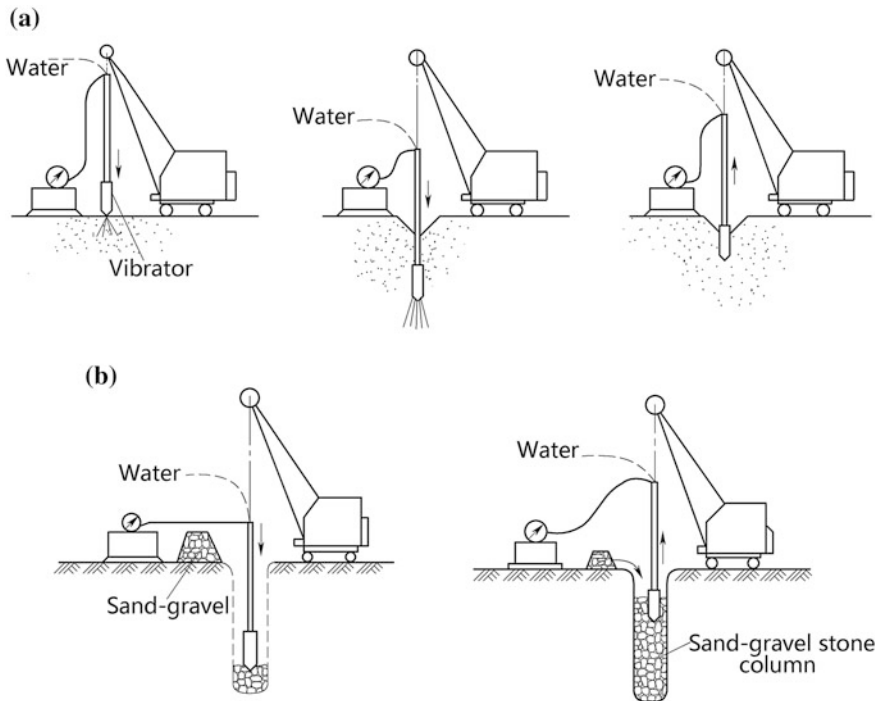


Fig. 11.31 Schematic drawing of vibro-replacement stone columns. **a** For loosen sand; **b** for soft clay

7. High-pressure spray grouting

See Chap. 9 of this book.

11.8 Abutment Transition Structures

11.8.1 Type of Abutment Transition Structures

Abutment transition structures are installed to adjoin riverbanks or various contiguous structures, for example, the hydropower station buildings and the earthfill or rockfill dams, for the purpose of bank slope stability and smooth passing of flow through the barrage (sluice). Abutment transition structures consist of side piers (or abutment piers), wing walls, gyrones (guide walls), quay walls, etc.

11.8.2 Wing Walls

The upstream wing walls are purposed for the smooth inflowing into the sluice, retaining the backfill earth, controlling bypass seepage, and preventing bank from scouring. All these requirements dictate the length of upstream wing wall.

The downstream wing walls should be conformed to the apron of stilling basin or even a bit far extended from the end of stilling basin, for smooth contiguous outflow.

1. Straight wing walls (Fig. 11.32)

They are vertical walls ordinarily employed in small barrages and sluices with low banks. Straight wing wall is composed of two perpendicular retaining walls, and at their conjugate point, a round off of small radius is installed for transition. The length of upstream and downstream sections inserting into bank perpendicular to the flow should meet the requirements for the seepage and scouring prevention.

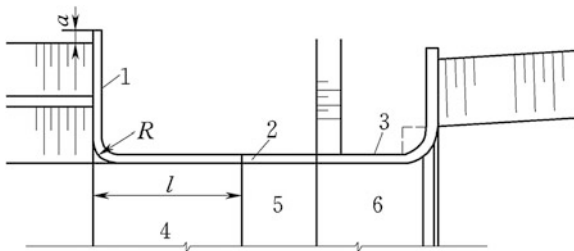


Fig. 11.32 Schematic drawing of a straight wing wall. 1 upstream wing wall; 2 abutment pier; 3 downstream wing wall; 4 blanket; 5 sluice chamber; 6 apron

Straight wing walls have good performance in bypass seepage prevention, but they are poor in the inflow contraction and high in engineering amount.

2. Splayed wing walls (Fig. 11.33)

They are vertical walls providing smooth entry and exit to the water. The downstream splay is usually at an angle of $\beta = 7^\circ\text{--}12^\circ$, to prevent the separation of outflow. The upstream splay angle may be large (even up to $\beta = 45^\circ$).

3. Return wing walls (Fig. 11.34)

They are vertical walls and used where banks are high and hard with large afflux and flow discharge. The radii of upstream and downstream wing walls are normally 15–30 m and 30–40 m, respectively.

4. Double-curvature wing walls (Fig. 11.35)

Double-curvature wing walls have vertical intersection with sluice bay, they vary gradually toward upstream or downstream until the identical sloping to conjugate bank. Double-curvature wing walls provide good inflow and outflow conditions but



Fig. 11.33 Schematic drawing of a splayed wing walls

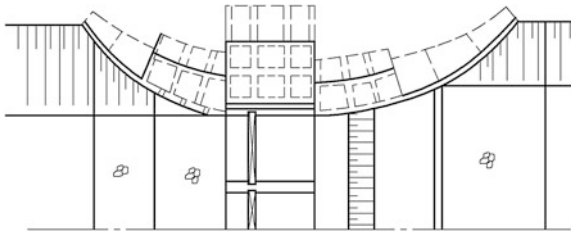


Fig. 11.34 Schematic drawing of a return wing wall

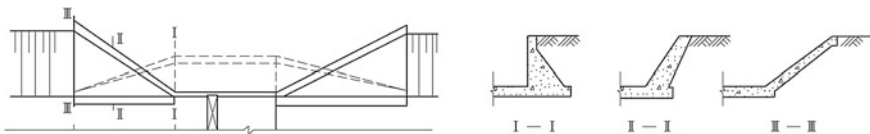


Fig. 11.35 Schematic drawing of a double-curvature wing wall

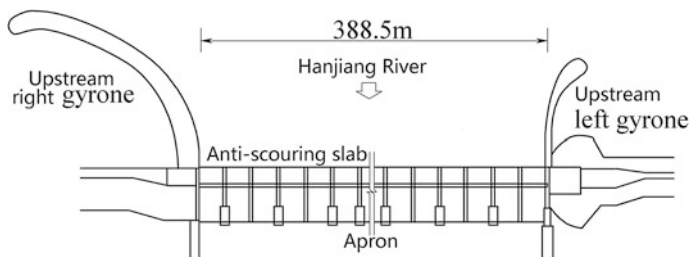


Fig. 11.36 The Wangpuzhou Barrage Project (China, $H = 33.9$ m)

are complicated in construction. They are used where banks are high and hard with large afflux and flow discharge.

5. Gyrones and training dikes

Gyrones and training dikes are walls located between weirs and under-sluices and other water retaining structures (e.g., embankment dams) extending toward upstream a little far beyond the horizontal blanket, and toward downstream at least to the end of stilling basin apron, or even to the end of the rear apron of under-sluices. Gyrone is a concrete or masonry structure, with top width of 1.5–3 m, and aligned at a right included angle to the weir axis. Training dike is easy to be constructed and has good stability condition, but should have double-curvature surface as it transits to the sluice bay.

Figure 11.36 shows the barrage of the Wangpuzhou Project whose flow front width is 388.5 m, which accounts for about 1/4 of the river width. There are two independent gyrones, of which the left one is 70 m long and composed of quarter ellipse (long axis = 50 m, short axis = 20 m) + 20 m long straight section; the right one approaching the main stream is 180 m long and is composed of double parabolic curve.

11.8.3 Structure of Retaining Walls

Wing wall is actually a kind of retaining walls designed and constructed to resist the lateral pressure of soil, where there is a desired change in ground elevation that exceeds the repose angle of soil. Retaining walls may be designed as gravity, cantilevered, buttressed, and cellular (Huntington 1957; Wei and Zhou 2004).

Vertical joints should be installed along the retaining wall. The spacing of such joints depends on the anticipated temperature variation and on the type of wall. Suitable locations for joints are where the foundation level, the top of the wall, or the properties of foundation soil change abruptly.

Where the retaining wall is impervious, drainage holes (weep holes) should be installed through the wall to prevent the built-up of hydrostatic pressure behind it.

1. Gravity walls

Gravity walls depend on their mass to resist pressure from backfill and may have a better setback to improve stability by leaning back toward the backfill soil.

Gravity walls are simple in configuration and convenient for construction and are customarily used as side pier or wing wall lower than 4–6 m.

Earlier in the twentieth century, taller retaining walls were often gravity walls made from large masses of concrete or stone. Today, taller retaining walls are increasingly built as composite gravity walls such as geosynthetic or with precast facing; gabions (stacked steel wire baskets filled with rocks); crib walls (cells built up log cabin style from precast concrete or timber and filled with soil); or soil-nailed walls (soil reinforced in place with steel and concrete rods).

Anti-sliding and anti-overturning as well as bearing capacity should be met in the design of gravity retaining walls. Sliding failure involves outward translation of retaining wall due to shearing failure along its base or along a deep-seated slip surface, and the allowable safety factor is identical to that of barrage unit (Table 11.6). Overturning failure involves rotation of wall about its toe, whose allowable safety factor is 1.50 under basic combinations and 1.30 under special combinations. The average stress on the base should be lower than allowable bearing capacity of the foundation, the maximum stress on the base should be lower than 1.2 times of the allowable bearing capacity of the foundation, and the unevenness coefficient of the base stress should meet the requirements listed in Table 11.5.

2. Cantilevered/buttressed walls

Cantilevered walls are made from an internal stem of steel-reinforced, cast in situ concrete or mortared masonry. These walls cantilever loads (like a beam) to a large structural footing and convert horizontal pressures from behind the wall to vertical pressures on the ground below. Therefore, this type of wall consumes much less material than a traditional gravity type. However, rigid concrete footings are demanded for these walls.

Cantilevered retaining walls are often separated by joints from apron slab, in a shape of an inverted T beam. Their sliding stability, bearing capacity, and strength requirements should be met in the design.

Cantilevered retaining walls are convenient for construction and generally economical for retaining heights of up to 6–10 m.

Where the wing walls are higher than 9–10 m, sometimes cantilevered walls are buttressed in the front at a space of 3–4.5 m or counterforted on the back. Buttresses are short wing walls at right angles to the main trend of the wall. The wall stem and base slab should be so designed to resist the bending moments and shear forces due to loads inclusive earth pressure, static water pressure, bypass seepage pressure, and self weight, etc., exerting on the wall. In the structural design, at-rest and compaction-induced (active) earth pressures should be taken into account.

3. Empty box walls

Empty box walls are intended for high retaining on poor foundation. It also may be advantageous in reducing the side load effects. T-shaped empty box wall is complicated in structure and high in expenditure. It may be unfilled or filled by soil, with regard to the stability against sliding and base pressure. Continuous arc empty box may save steel consumption.

4. Other types

Sheet pile walls are usually exercised in soft soils and tight spaces. They are made of steel, vinyl, or wood planks which are driven into the ground. For a quick estimation of the pile length, $2/3$ length is ordinarily driven below ground, while the rest $1/3$ length is erected above ground to form the retaining wall. However, this may be altered depending on the environment. Taller sheet pile walls will need a tieback anchor penetrating the potential slip surface in the soil behind the wall.

Anchor (tieback) can be employed in any of the aforementioned styles. Usually driven into the soil/rock with boring, anchors are then expanded at the end of the cable, either by mechanical means or often by injecting pressurized concrete/mortar grout, which expands to form a bulb in the soil/rock. Although technically complex, yet anchoring method is very useful where large loads are anticipated or where the wall itself has to be slender.

Soil nailing is a technique in which soil slopes, excavations, or retaining walls are reinforced by the insertion of relatively slender elements—steel bars. The bars are installed into a pre-drilled hole and then grouted into place or drilled and grouted simultaneously. They are usually untensioned and installed at a slightly downward inclination.

References

- Bligh WG (1912) *The practical design of irrigation works*. Constable, London
- Bradley JN, Peterka AJ (1957a) The hydraulic design of stilling basins: hydraulic jumps on a horizontal apron (Basin I). *J Hydraulics Div, ASCE* 1957, 83(HY5), paper 1401-1-24
- Bradley JN, Peterka AJ (1957b) The hydraulic design of stilling basins: high dams, earth dams, and large canal structures (Basin II). *J Hydraulics Div, ASCE* 1957, 83(HY5), paper 1402-1-14
- Bradley JN, Peterka AJ (1957c) The hydraulic design of stilling basins: short stilling basin for canal structures, small outlet works, and small spillways (Basin III). *J Hydraulics Div, ASCE* 1957, 83(HY5), paper 1403-1-22
- Bradley JN, Peterka AJ (1957d) The hydraulic design of stilling basins: stilling basin and wave suppressors for canal structures, outlet works, and diversion dams (Basin IV). *J Hydraulics Div, ASCE* 1957, 83(HY5), paper 1404-1-20
- Bradley JN, Peterka AJ (1957e) The hydraulic design of stilling basins: stilling basin with sloping apron (Basin V). *J Hydraulics Div, ASCE* 1957, 83(HY5), paper 1405-1-32
- Bradley JN, Peterka AJ (1957f) The hydraulic design of stilling basins: small basins for pipe or open channel outlets—no tail water required (Basin VI). *J Hydraulics Div, ASCE* 1957, 83(HY5), paper 1406-1-17

- Bussey WH (1961) Control of seepage through foundation and abutments of dams. *Foundation evaluation and treatment*. *Casagrande Geotechnique* 11(3):161–182
- Chen SH, Chen ML (2014) *Hydraulic structures*, 2nd edn. China WaterPower Press, Beijing (in Chinese)
- Chow VT (1959) *Open-channel hydraulics*. McGraw-Hill, New York
- Chugaev RR (1971) *Hydraulics*. Energiya, Leningrad (USSR) (in Russian)
- Craig RF (2004) *Craig's soil mechanics*, 7th edn. Spon Press, London (UK)
- Day RW (2006) *Foundation engineering handbook*. McGraw-Hill, New York
- D'Appolonia DJ (1980) Soil-bentonite slurry trench cutoffs. *J Geotech Eng Div* 106(4):399–417
- Elevatorski EA (1959) *Hydraulic energy dissipators*. McGraw Hill, New York
- French RH (1985) *Open-channel hydraulics*. McGraw Hill, New York
- Forster JW, Skrinde RA (1950) Control of hydraulic jump by sills. *Trans ASCE* 115(1):973–987
- Garg SK (1976) *Irrigation engineering and hydraulic structures*. Khanna Publishers, Delhi
- Giroud JP (1992) Geosynthetics in dams: two decades of experience. *Geotech Fabr Rep* 10(6):22–28
- Golzé AR (1977) *Handbook of dam engineering*. Van Nostrand Reinhold Company, New York
- Grishin MM (ed) (1982) *Hydraulic structures*. Mir Publishers, Moscow
- Hinds J (1928) The Hydraulic design of flume and siphon transitions. *Trans ASCE* 92(1): 1433–1459
- Hetenyi M (1946) *Beams on elastic foundation*. University of Michigan Press, Baltimore
- HKIE (1981) *Guidance notes on hand-dug caissons*. Hong Kong Institution of Engineers, Hong Kong
- Hughes JMO, Withers NJ (1974) Reinforcing of soft cohesive soils with stone columns. *Ground Eng* 7(3):42–49
- Huntington WC (1957) *Earth pressures and retaining walls*. Wiley, New York
- Iqbal A (1993) *Irrigation and hydraulic structures—theory, design and practice*. Institute of Environmental Engineering & Research, NED University of Engineering & Technology, Karachi
- Ippen AT (1951) Mechanics of supercritical flow. *Trans ASCE* 116(1):268–295
- Lane EW (1935) Security from under—seepages—Masonry dams on earth foundations. *Trans ASCE* 100(1):1235–1272
- Lin JY (2006) *Hydraulic structures*. China WaterPower Press, Beijing (in Chinese)
- Maynard ST, Ruff JF, Abt SR (1989) Riprap design. *J Hydraulics Div ASCE* 115(7):937–949
- Ministry of Water Resources of the People's Republic of China (2001) SL265-2001 “Design Specification for Sluice”. China WaterPower Press, Beijing (in Chinese)
- Novak P, Moffat AIB, Nalluri C, Narayanan R (1990) *Hydraulic structures*. The Academic Division of Unwin Hyman Ltd, London
- Poulos HG, Davis EH (1980) *Pile foundation analysis and design*. Wiley, New York
- Sherard JL, Dunnigan LP (1984) Filters for silts and clays. *J Geotech Eng ASCE* 110(6):701–718
- Sherard JL, Dunnigan LP (1989) Critical filters for impervious soils. *J Geotech Eng ASCE* 115 (GT7):927–947
- Siu KL (1992) Review of design approaches for laterally-loaded caissons for building structures on soil slopes. In: *Proceedings of seminar on lateral ground support systems*. Hong Kong Institution of Engineers, Hong Kong, pp 67–89
- Sylvester R (1964) Hydraulic jump in all shapes of horizontal channels. *J Hydraulics Div ASCE* 90(HY1):23–55
- Tan SX (1986) *Design of barrages*. Water Resources and Electric Power Press of China, Beijing (in Chinese)
- Terzaghi K, Peck RB, Mesri G (1996) *Soil mechanics in engineering practice*. Wiley, New York
- USBR (1987) *Design of small dams*, 3rd edn. US Govt Printing Office, Denver
- Varshney RS, Gupta SC, Gupta RL (1982) *Theory and design of irrigation structure*. Roorkee Press, Roorkee
- Wei XC, Zhou ML (2004) *Handbook of retaining structure design*, 2nd edn. China Building Industry Press, Beijing (in Chinese)

- Winterkorn HF, Fang HY (1975) Foundation engineering handbook. Van Nostrand Reinhold, New York
- Xanthakos PP, Abramson LW, Bruce DA (1994) Ground control and improvement. Wiley, New York
- Zhang SR et al (1988) Barrages, 2nd edn. Water Resources and Electric Power Press of China, Beijing (in Chinese)
- Zuo DQ, Gu ZX, Wang WX (eds) (1987) Barrages, spillways and control works. In: Handbook of hydraulic structure design, vol 6. Water Resources and Electric Power Press of China, Beijing (in Chinese)

Chapter 12

Shore Spillways

12.1 General

A spillway is designed to conduct flood flows safely passing the dam, which plays an important role similar to a safety valve in hydraulic projects (Chen and Chen 2014; Golzé 1977; Grishin 1982; ICOLD 1987; Lin 2006; Novak et al. 1990). Improperly designed spillways or spillways of insufficient capacity are responsible for many fatal accidents (e.g., failure) of dams. Therefore, spillways are, or should be, designed to accommodate flows during maximum flood period so as to prevent damage to the dam and appurtenant structures. Their size and location are determined by the size and type of dam, local topography, geology, and careful review of the stream flow history at the work site.

Spillways may be built integrally with dam located within or on the downstream face of dam, which have been described in the Chaps. 7 and 8 of this book, or separately outside of dam and termed as shore (or river bank) spillways (State Economy and Trade Commission of the People's Republic of China 2002; Ministry of Water Resources of the People's Republic of China 2000), which will be presented in this chapter.

12.1.1 Types of Separate Spillways

Shore or river bank spillways may be on one side or both sides to the dam abutments (Fig. 12.1), or within the bank of reservoir where adequate topographic condition is available.

Shore spillways may be categorized by the purposes into normal and emergence spillways. The former is employed to release the flood stipulated by the design standard, while the latter is used to release the extreme flood of lower frequency.

Shore spillways may also be classified by the flow pattern into the types of chute, side channel, drop inlet, siphon, etc. (Golzé 1977; Zuo et al. 1987; USBR 1987).

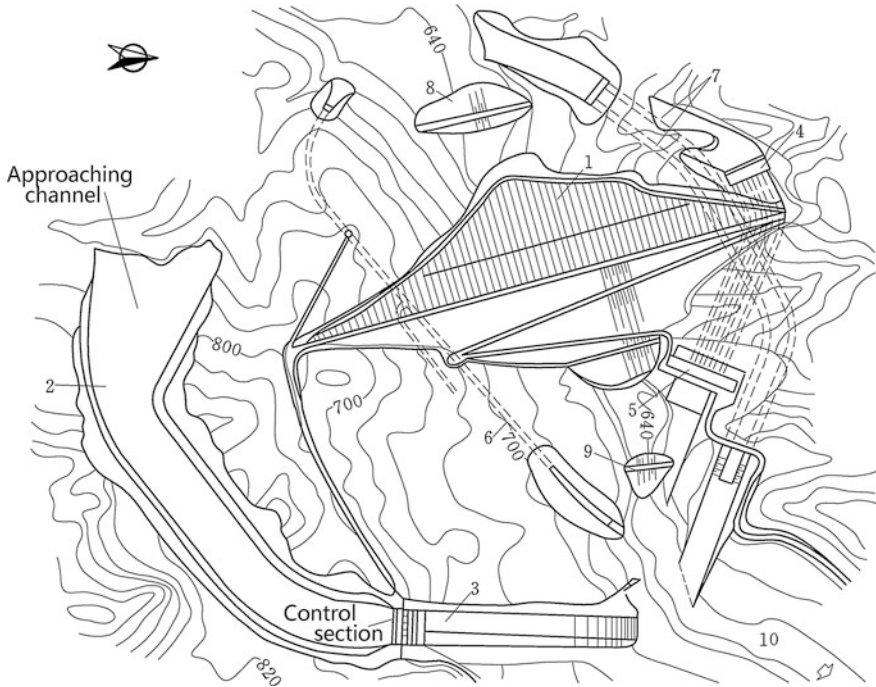


Fig. 12.1 The Tianshengqiao No. 1 Project (China, $H = 178$ m). 1 CFRD; 2 spillway; 3 chute; 4 intake of power tunnel; 5 power station; 6 flood release tunnel; 7 diversion tunnel; 8 upstream cofferdam; 9 downstream cofferdam; 10 the Nanpanjiang River

1. Chute (proper open channel or trough) spillways

Proper open-channel spillway is one of the most prevalent type in which control weir is placed approximately perpendicular to the adjoining spillway discharge channel.

2. Side-channel spillways

Side-channel spillway is one in which control weir is placed along the side of and approximately parallel to the adjoining spillway discharge channel. Flow over the weir crest falls into a narrow trough along the weir, turns an approximate right angle, and then continues into the main discharge channel, inclined shaft, or tunnel.

3. Drop inlet (shaft or morning glory) spillways

Drop inlet or shaft spillway, as the name implies, is one in which the water enters over a horizontally positioned weir lip, drops through a vertical or sloping shaft, and then flows to the downstream river channel through a horizontal or near-horizontal conduit or tunnel. The spillway may be considered as being made up of three elements, namely an overflow control weir, a vertical transition, and a closed

discharge conduit. Where the inlet is funnel-shaped, it is often termed as “morning-glory” or “glory hole” spillway (Bradley 1956; Peterkaon 1956).

4. Siphon spillways

A siphon spillway is a closed conduit system formed in an inverted shape, so that the interior of the bend of the upper pathway is at normal reservoir storage level. The initial discharges of the spillway, as the reservoir level rises above normal, are similar to that flow over a weir. Siphonic action takes place after the air in the bend over the crest has been exhausted. Continuous flow is maintained by the suction effect due to the gravity pull of the water in the lower leg of siphon (McBirney 1958).

12.1.2 Applicability of Separate Spillways

Shore spillways are usually employed with regard to the following situations:

- Flow over the dam is not permitted, e.g., where the embankment dam is erected as water-retaining structure in a hydraulic project (Fig. 12.1);
- Concrete arch dam is built in a narrow valley with large discharge requirement (Fig. 8.46);
- The space downstream of the dam is too limited to locate a dam-type spillway.

However, it should be emphasized that only expenditure and engineering function of all possible alternative designs can provide a basis for the consideration of shore spillway. For example, a natural saddle located near abutment with adequate elevation and competent rock is favorable to accommodate shore spillway.

12.2 Chute (Proper Open Channel or Trough) Spillways

Among all types of shore spillways, chute spillways have been exercised in embankment dam projects more often than any others. By the chute spillway, the flood discharge is conveyed from the reservoir to the downstream river reach through an open channel, placed either along a dam abutment or through a reservoir bank saddle, which might be called as chute-, open-channel-, or trough-type spillway. These designations can apply regardless of the control device used to regulate the flow. Thus, a spillway having a chute-type discharge channel, either controlled by an overflow crest, gated orifice, side-channel crest, or by some other control devices, might still be called as chute spillway. However, the name is most often employed when the spillway control is placed normal or nearly normal to the axis of an open channel, and where the streamlines of flow both above and below the control crest follow in the direction of the channel axis.

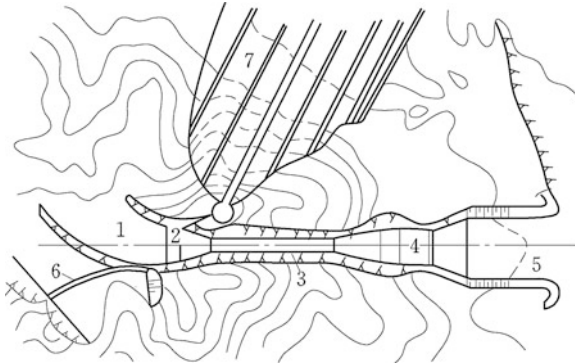


Fig. 12.2 Layout of the chute spillway in an embankment dam project. 1 entrance channel; 2 control structure; 3 discharge channel (chute, trough); 4 terminal structure; 5 outlet channel; 6 emergency spillway; 7 embankment dam

Factors in favor of the selection of chute spillways are the simplicity in their design and construction, their adaptability to almost any foundation condition, and their overall economy often attributable to the use of large amounts of spillway excavation in the embankment rockfill. Chute spillways have been constructed successfully on all types of foundation materials, ranging from hard rock to soft clay.

A chute spillway normally consists of an entrance (approaching) channel, a control structure, a discharge channel, a terminal structure, and an outlet channel (tail race channel) (Fig. 12.2).

The configuration of a chute spillway is usually dictated by the site topography and by the subsurface foundation conditions. The simplest form of chute spillway has a straight centerline and is of uniform width. Often, either the axis of entrance channel or that of discharge channel must be curved to fit the alignment entailed by the topography. Under such circumstances, the curvature segment is confined to the entrance channel with low approach velocities, if possible. Where the discharge channel must be curved, its floor is sometimes superelevated to guide the high-velocity flow around the bend, thus avoiding a piling up of flow toward the concave side of chute.

The control structure is generally placed in line with or upstream of the dam axis. Normally, the upper portion of the discharge channel is carried at minimum grade until it “daylights” along the downstream hillside to minimize excavation. The steep portion of the discharge channel then follows the slope along the abutment.

12.2.1 Entrance (Access or Approach) Channels

An entrance channel serves to draw water from the reservoir and convey it to the control structure. Where a spillway draws water immediately from the reservoir and

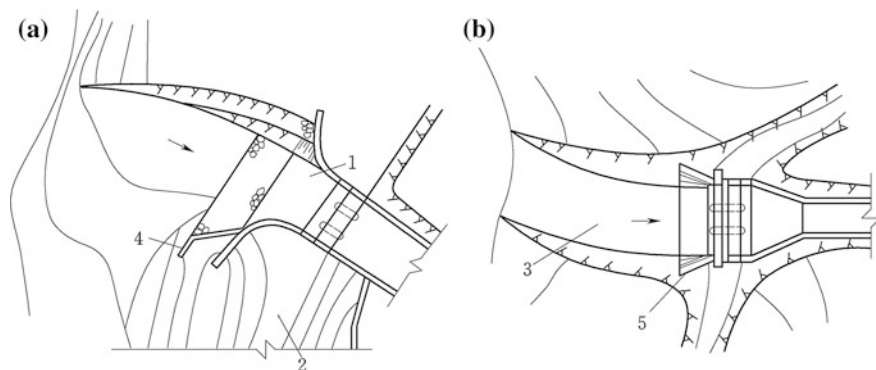


Fig. 12.3 Entrance channels to open-channel spillways

diverts it directly back into river, as in the case with an overflow spillway on a concrete dam, entrance and outlet channels are not needed. However, in the case where the shore spillway is placed through abutment, saddle, or ridge, the entrance channel leading to the spillway control structure and away from the spillway terminal structure may be required. Where the entrance faces the reservoir directly or contacts with dam, a guide wall should be installed at the side of dam in a planar shape of morning-glory mouth, to avoid transverse current or vortex flow (Fig. 12.3).

Entrance velocity is generally $v \leq 4$ m/s and head drop is smaller than 0.8 m, which should be greater than the non-deposit velocity of suspension load but smaller than scouring velocity. The channel curvatures and transitions should be made gradual. All these requirements are for the purposes to minimize head loss through the entrance channel and to obtain uniformity of flow passing the spillway crest. Effects of an uneven distribution of flow in the entrance channel might persist through the whole spillway structure to an extent that undesirable erosion could take place in the downstream river channel. Non-uniformity of head on the crest may also lead to a reduction in the discharge capacity. The longer of the channel, the larger of the head loss will be. Where the spillway is excavated in a steep mountain, larger velocity might be preferable to considerably reduce the excavation amount, such as the shore spillway in the Bikou Project (Fig. 9.3), whose velocity in entrance channel is 5.58 m/s for releasing design flood.

The approach velocity and the water depth below crest level have important influence on the discharge capacity through the overflow crest. The minimum depth below the crest level is $0.5H_d$ (H_d = design head of weir shape). For a given head over the crest, a greater approach depth with the accompanying reduction in approach velocity will result in a larger discharge coefficient. Thus, a deeper approach depth will permit a shorter crest length for a given discharge. Therefore, a small reverse gradient for the channel bottom floor may be employed.

Within the limits demanded to secure satisfactory flow conditions and non-scouring velocities, the determination of the relationship of entrance channel depth

to channel width is a matter of economics. The glory mouth transition section is usually installed to connect the entrance channel and control weir (Fig. 12.3), the length of guide wall along the flow direction should be greater than 2 times of the depth in front of crest, and the elevation of wall should be higher than the maximum reservoir level. The bottom of transition section should be lined using concrete of 0.2–0.3 m thick. The necessity of lining for the bottom and slope of entrance channel is dependent on the safety consideration with respect to stability, scouring resistance, and weathering resistance. The entrance channel is better to be layout in straight on plane to obtain good flow pattern. If bending is inevitable, the curvature radius should be larger than 4–6 times of the channel width in bottom.

Trapezoidal cross section is commonly adopted for entrance channel with a slope of 1:0–1:0.3 for fresh rock, 1:0.5–1:1.0 for weathered rock, and 1:1.5–1:3.0 for soil.

The water surface in the entrance channel may be solved using segmentation seeking algorithm by establish energy equation from the starting of the entrance channel until the section in front of crest at a distance 3–5 times of the head over crest.

Where restrained by the conditions of topography and geology, long entrance channel is inevitable (Fig. 12.1). Under such circumstances, the head loss in the channel should be taken into account in the computation of discharge capacity.

12.2.2 Control Structures

Consisting of weir, gates, piers, operative, and access bridges, etc., a control structure regulates and controls the outflows from the reservoir, which is a major component of the spillway. The control structure should be as close to the reservoir as possible to reduce head loss and should be built on competent foundation to bear large loads. The elevation of weir crest has very tight relation with the engineering amount; therefore, it should be determined by comprehensive studies taking into account of factors such as topographic condition in addition to rational specific flow discharge (Abecasis 1970). Usually, deep excavation leads to high and short weir, while shallow excavation gives rise to low and long weir.

Water should be prevented from seeping and leaking through the foundation in the spillway area. Generally, watertightness is provided by extending the grouting curtain of the dam adjacent to the spillway. Where the foundation rock under weir cannot be grouted, watertightness may be achieved by impervious blanketing.

1. Broad crested weir

With flat top and very small height, broad crested weir (Fig. 12.4a) has advantages of simplicity in structure and convenience in construction, but disadvantageous in lower discharge coefficient (approximately $m = 0.32–0.385$). It is suitable for low-headwater projects with a small crosshead (head difference of head- and tailwaters), or with soil foundation of low bearing capacity.

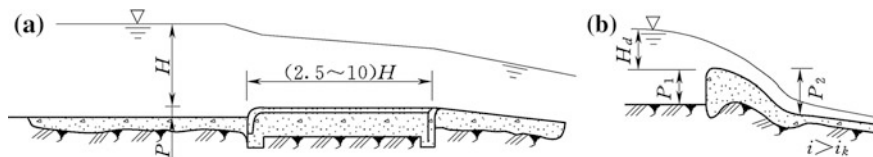


Fig. 12.4 Weirs of control structure. **a** Broad crested weir; **b** practical weir

2. Practical weir

Practical weir in a shape of ogee (e.g., WES) (Fig. 12.4b) may provide larger discharge coefficient than that of broad crested weir, which is advantageous in shortening the weir length, as a result the engineering expenditure could be saved and the layout of project may be facilitated. However, the construction of practical weir is more complicated. For large to medium projects, particularly where the bank slopes are steep, the practical weir is widely employed.

The most prevalent type of practical weir in the shape of ogee has a crest approximating the profile of the under nappe of a jet flowing over a sharp crested weir and provides the ideal form for obtaining optimum discharges. The design of ogee weir has been discussed in the Chap. 7 of this book. However, there are two main particularities in the ogee weir design for shore spillways:

- Since the ogee weir in spillways is often a low weir with high tailwater depth at downstream adjoined chute, large negative pressure and cavitation as well as vibration are unlikely occurred on the surface of weir; therefore, the smaller design head H_d than that of high-gravity dams is preferable to obtain higher discharge coefficient, e.g., H_d may be (0.65–0.85) times of the maximum head above the weir;
- The radius of bucket is larger than that of high dams, for the purpose of more smooth flow transition from weir to chute.

In the design of ogee weir for shore spillways, high attention should be called at that up- and downstream weir heights P_1 and P_2 (Fig. 12.4b) have great influence on the discharge coefficient. The definition of high and low weirs is based on the facts that:

- For sharp crested weirs with heights not lower than about one-fifth of the head, the coefficient of discharge remains fairly constant;
- For sharp crested weirs with heights lower than about one-fifth of the head, the contraction of the flow becomes increasingly suppressed, the velocity of approach is not negligible, and the discharge coefficient decreases significantly;
- When the weir height becomes zero, the contraction is entirely suppressed and the overflow weir becomes actually a channel or a broad crested weir.

With a relative height $P_1/H_d > 3$, the WES weir belongs to high weir placed in a channel, the velocity of approach is small and the under side of nappe flowing over the weir attains maximum vertical contraction. As a result, the discharge coefficient

Table 12.1 Variation of discharge coefficient m versus P_1/H_d for WES weirs

P_1/H_d	0.1	0.2	0.3	0.4	0.5	0.6	0.7	0.8	3.0
m	0.422	0.445	0.458	0.467	0.473	0.477	0.480	0.483	0.492

is nearly a constant. Nevertheless, many weirs on spillways are low weir entailed as $0.3 \leq P_1/H_d \leq 1$, whose discharge coefficient may be checked by Table 12.1.

When the water depth downstream a WES weir is high enough to affect the discharge, the weir is said to be submerged. The altitude difference P_2 from the weir crest to the downstream apron and the depth of flow in the downstream channel, as they are related to the headwater level, are major factors altering the coefficient of discharge. Generally, five distinct flow types can occur below an overflow weir crest, depending on the relative positions of the apron and the downstream water surface:

- Flow will continue as supercritical flow;
- A partial or incomplete hydraulic jump will occur immediately downstream from the crest;
- A true hydraulic jump will occur;
- A drowned (submerged) jump will occur; and
- The jet will break away from the face of the overflow and ride along the surface for a short distance, and then, it erratically intermingles with the slow moving water underneath.

Where the downstream flow is of supercritical or where the hydraulic jump takes place, the reduction in the coefficient of discharge is due principally to the back-pressure effect from the downstream apron and is independent on the submergence effect attributable to tailwater.

Based on the above considerations, $P_1 > 0.3H_d$ and $P_2 > 0.5H_{\max}$ are both desirable for the low WES weir. In medium to small spillways, $P_1 \geq (0.5-0.8)H_d$ and $P_2 \geq (0.6-0.7)H_{\max}$ may be demanded, where H_{\max} is the maximum head above the weir crest.

The low WES crest is continued tangent along a slope with a sufficient length; otherwise, the discharge coefficient m will be reduced with the mechanism similar to the downstream water depth submergence. According to the data from physical model tests, the minimum slope where the crest tangent the straight line is 1:1.4. Therefore, a direct tangent linkage of the crest to the chute is very often impossible. Instead, a bucket tangentially connecting the chute to the straight weir slope steeper than or equal to 1:1.4 is ordinarily employed (Fig. 12.5).

3. Hump weir

Configured in a shape of multi-circular (Fig. 12.6), hump weir is a kind of low weirs developed in China with discharge coefficient above $m = 0.42$. However, there is insofar no modular profile and the hydraulic experiments are indispensable to obtain discharge coefficient corresponding to a specific design. Table 12.2 lists the parameters of two typical hump weir profiles.

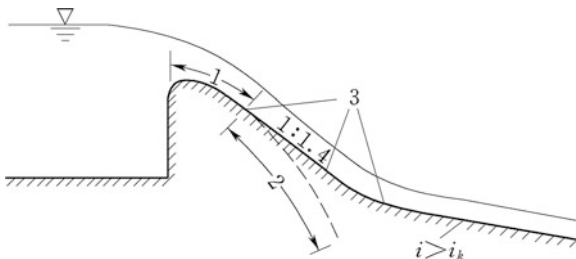


Fig. 12.5 Connection of chute and low WES crest through a bucket. 1 curvilinear length of low WES crest; 2 rest portion of normal WES crest; 3 tangent points

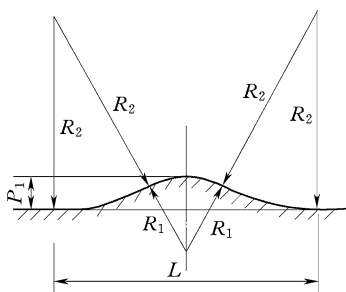


Fig. 12.6 Profile of a typical hump weir

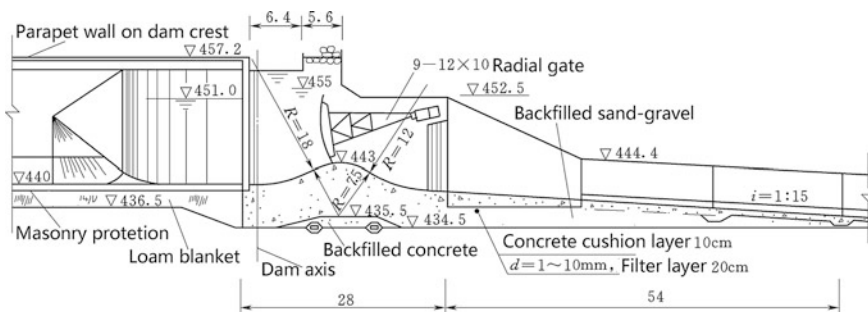


Fig. 12.7 Longitudinal profile of the spillway (unit: m)—the Yuecheng Project (China, $H = 55.5$ m)

Table 12.2 Parameters of typical hump weir profiles

Profile type	Upstream weir height P_1	Radius R_1 of middle circus	Radius R_2 of upper and lower circuses	Total length L
Type a	$0.24H_d$	$2.5P_1$	$6P_1$	$8P_1$
Type b	$0.34H_d$	$1.05P_1$	$4P_1$	$6P_1$

Hump weir has advantages of facilitation in construction, high discharge coefficient, and adaptability to weak foundation. The spillway in the Yuecheng Project (China) (Fig. 12.7) is one of the first batch using hump weir, the laboratory experiment showed that the discharge coefficient is around $m = 0.46$. The prototype investigation carried out in 1971 showed that $m = 0.47$ when $H = 5.30$ m, and $m = 0.458$ when $H = 5.57$ m.

4. Gate-controlled ogee crests

Water releasing from ogee crest with parapet, or from partial gate opening of gated crest, will exhibit orifice flow. If the ogee profile drops below the trajectory jet, gate operated with small opening under high-head manifests negative pressure along the crest in the region immediately below the gate. Experimental data show that for the ogee shaped to the ideal nappe profile with respect to maximum head H_{\max} , such subatmospheric pressures would be equal to around one-fifth of the design head. Consequently, if subatmospheric pressures are to be avoided along the ogee crest, the profile downstream the gate sill must conform to the trajectory jet issuing from an orifice (Fig. 7.30). For a vertical orifice, the path of the jet can be expressed by Eq. (7.32).

However, the adoption of a trajectory jet rather than a nappe in the weir design will lead to a fatter ogee profile and reduced discharge efficiency under full gate opening. Where the discharge efficiency is not prime important and where a fat ogee shape is demanded for structural stability, the trajectory jet profile may be ideal for avoiding subatmospheric pressure. Otherwise, by placing the gate sill, a bit of lower at the downstream side of the crest apex, a slimmer orifice profile may be obtained which is inclined downstream for small gate opening and thus will produce a steeper trajectory jet more closely conforming to the nappe-shaped profile.

12.2.3 Chutes

The chute is that portion of the spillway which connects the weir to the terminal structure. Chutes installed in conjunction with embankment dams often must have a slope slightly steeper than critical. With critical velocity occurring, flows in the chute are ordinarily maintained at supercritical state over the weir, either at constant or accelerating rates, until the terminal structure is arrived.

1. Layout of chute

Figure 12.2 shows a conventional layout of chute, i.e., weir \rightarrow convergence \rightarrow chute \rightarrow divergence. The purpose of convergence is to save the excavation and lining amount of chute, and the purpose of divergence is to reduce unit discharge for the energy dissipation and scouring protection of downstream river channel.

When the Froude number F_r in chute is larger than 2, aeration and fluctuation start to manifest; when the average velocity reaches 15 m/s, cavitation and erosion are easy to take place; when the chute turns in plan, the high velocity will give rise

to shock waves (ICOLD 1992). To obtain good hydraulic performance, abrupt vertical changes, sharp convex or concave curves in the vertical chute profile, should be avoided. Similarly, the convergence or divergence in plan should be gradual in order to avoid cross-waves, “ride-up” on the walls, excessive turbulence, or uneven distribution of flow at the terminal structure.

To avoid hydraulic jump, the discharged flow must remain in the supercritical state throughout the length of the chute. The flow in the chute may be uniform, accelerated, or decelerated, depending on the slopes and dimensions of the chute and on the total head drop. Where it is desired to minimize the slope to reduce excavation at the upstream portion of a chute, the flow might be uniform or decelerating in this portion, followed by accelerating flow in the steep drop leading to the downstream river channel. Flow along the chute will depend upon the specific energy available at the point concerned. This energy will be equal to the total drop from the reservoir water level to the floor of the chute at the point under consideration, subtracted by the intervening head losses (Bernoulli’s theorem concerning the conservation of energy). The velocities and depths of flow along the chute can be fixed by selecting its grade and the cross-sectional dimensions. The grade for chute ordinarily used is $i^0 = 1\text{--}5\%$ but sometimes may be $10\text{--}30\%$; in practices, the steepest slope even may be reached up to 1:1 for the chute on high-quality rock.

The longitudinal profile of a chute in the form of open channel is usually so selected to conform to the site conditions related to topography and geology. It is generally configured as straight segments joined by transition curves. Sharp convex and concave curves should be avoided to prevent adverse flows in the channel. Where it is inevitable, convex curves should be flat enough with regard to the trajectory of a free-discharging jet as it enters the curve, to maintain positive pressures and thus avoid the tendency for separation and spring away of the flow from the floor. Concave curves should have a sufficient radius of curvature to minimize the dynamic actions on the floor brought about by the centrifugal force attributable to the change in the direction of flow. The pressure will drive the water penetrating into and under the lined floor to build up high uplift if the drain condition does not work well, which may result in the damage to floor lining. The conventionally used radius may be selected among $5 < R/h < 10$.

The spillway chute of the Liujiaxia Project (China) is composed of six segments of different grades. In 1969, the accumulated flood releasing time was 324 h during flood season, the maximum discharge and velocity were $2350\text{ m}^3/\text{s}$ and 30 m/s , respectively. The examination after the flood season revealed three serious damage portions in the chute, which all happened at the concave portions: The lining was flushed away, and the deepest scouring pit was 13 m.

Convex and concave transition curves in the longitudinal profile should be avoided where the chute varies in plan. Sometimes, restricted by the conditions of topography, geology and layout requirements, longitudinal convex and concave curves and planar bending may not be avoided to be configured simultaneously, such as the spillway of the Yunlong Project (Yunnan, China) shown in Fig. 12.8. In this case, comprehensive studies should be carried out to mitigate the detrimental hydraulic phenomena for the safety of the project.

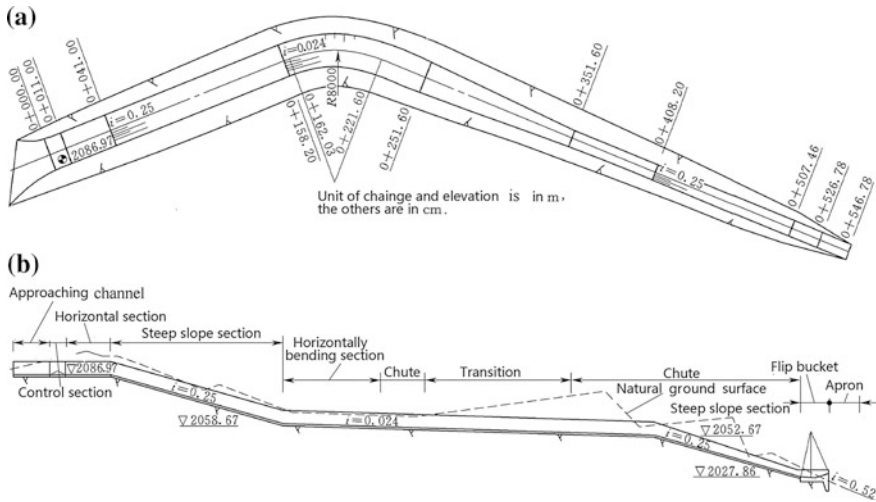


Fig. 12.8 Spillway layout—the Yunlong Project (China, $H = 77$ m). a Plan. b longitudinal profile

The type of cross section of chute (open channel or trough) is dependent on the geologic conditions and lining. For the trough excavated in bedrock and with lining, rectangular or steep trapezoidal cross section is commonly adopted (1:0.1–1:0.3); for the trough excavated in soil, flat trapezoidal cross section is commonly employed (1:1–1:2).

The height of side walls should be sufficient to retain the water, which is estimated by adding freeboard to the aerated and fluctuated water depth, the former is normally 0.5–1.5 m according to the SL253-2000 “Design code for spillway”.

The water surface in the chute may be solved using segmentation seeking method by establishing energy equation as follows:

$$\Delta l_{1-2} = \frac{\left(h_2 \cos \theta + \frac{\alpha_2 v_2^2}{2g} \right) - \left(h_1 \cos \theta + \frac{\alpha_1 v_1^2}{2g} \right)}{i - \bar{J}} \quad (12.1)$$

$$\bar{J} = \frac{n^2 \bar{v}^2}{R^{4/3}} \quad (12.2)$$

where Δl_{1-2} = length of the segment, m; h_1, h_2 = depth at the starting and ending of the segment, m; v_1, v_2 = average velocity at the starting and ending of the segment, m/s; α_1, α_2 = non-uniform velocity distribution coefficient at the starting and ending of the segment (usually 1.05); θ = inclining angle of the trough bottom, ($^\circ$); i = grade of the trough bottom; \bar{J} = average hydraulic gradient in the segment; n = roughness coefficient of the trough selected according to design code; $\bar{v} = (v_1 + v_2)/2$ = average velocity, m/s; $\bar{R} = (R_1 + R_2)/2$ = average hydraulic radius of the segment, m.

2. Design of convergence and divergence

The best hydraulic performance in a discharge chute is obtained by uniform flow. However, economy may dictate a chute section narrower or wider than either the crest or the terminal structure, thus requiring converging or diverging transitions in plan to fit the various components together.

The paramount phenomenon attributable to transitions and to be aware of is shock waves (cross-waves) of positive and/or negative. On the outer side of an angular bend, a positive shock wave (piling up) will take place leading to a rise of the water surface. The wave is stationary and across to the inside of the chute, continues to reflect back and forth repeatedly. Where the flow passes the inner side of an angular bend, a separation will take place which results in negative shock wave (drop in the water surface). This stationary negative shock wave will cross to the outside of the chute. Both the aforementioned positive and negative shock waves will continue to reflect off the walls, forming a very disturbed flow pattern.

(a) Convergent transition

Laboratory and field tests help to stipulate design criteria and guidance applicable to spillway chutes with convergence, by which an optimum flow conditions will prevail in the chute.

The commonly used symmetric sidewall convergence is shown in Fig. 12.9. It must be made gradual to avoid cross-waves, “ride ups” on the walls, and uneven distribution of flow across the chute trough. The maximum height of cross-wave is dependent on the deflection angle θ but has no relation with the curvature radii of the sidewalls. Since the deflection angle θ_1 of a curved side wall is always larger than that θ_2 of a straight side wall, straight side walls for convergence transition section are customarily employed subject to local round off.

(b) Divergent transition

When site or economic conditions indicate that a short crest length and a widened terminal structure are desirable, diverging chute walls may be employed. Similarly, the rate of divergence of the sidewalls must be limited or else the flow will not spread to occupy the entire width of the chute uniformly, which will lead to undesirable flow conditions in the terminal structure.

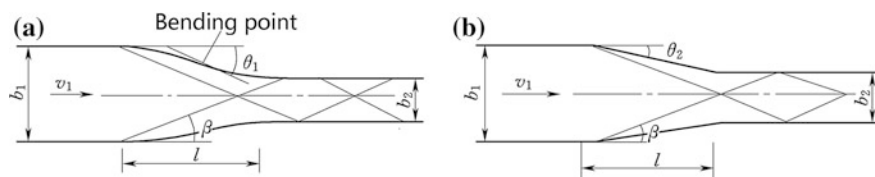


Fig. 12.9 Convergent transitions and cross-waves. **a** Curved; **b** straight

Experiments have shown that an angular deflection θ of the flow boundaries with respect to the trough centerline not exceeding that entailed by Eq. (12.3) will provide an acceptable transition for a divergent chute.

$$\operatorname{tg}\theta \leq \frac{1}{KF_r} \quad (12.3)$$

where F_r = Froude number at the initiation or end of the divergence; $K = 1.5\text{--}3.0$, revision coefficient (inferior bound for horizontal trough bottom, whereas upper bound for steeply inclined trough bottom).

In divergent transition, F_r varies along the flow; therefore, the angle θ theoretically varies according to Eq. (12.3). In practice, however, a uniform θ smaller than $6^\circ\text{--}8^\circ$ is commonly adopted for simplicity.

3. Design of curved transition

Curved transition may be desirable in case with limitation of topographic and geologic conditions, which should be located at the portion of lower velocity. To eliminate or to reduce the interference of shock waves, the requirements for curved transition are explained hereinafter.

(a) Curvature radii

Usually 6–10 times of the width of rectangular trough is adopted as the curvature radii of transition.

(b) Complex curve

Using of transition curve segments at the two ends of circular transition.

(c) Over height of trough bottom

Influenced by the centrifugal force, the flow pattern in a curved transition is complex: The water will be piled up at outside and dropped down inside, which in turn, results in non-uniform distribution of velocity in the transition (Fig. 12.10a). Over height ΔZ of trough bottom at outside may create a transverse slope as shown in Fig. 12.10b, to counter balance the centrifugal force. However, such an over height of trough bottom may only be applied to the trough with rectangular cross section.

ΔZ may be estimated using the formula of centrifugal force as follows:

$$\Delta Z = C \frac{v^2 b}{gr_c} \quad (12.4)$$

where v = average velocity at the starting section of curved transition, m/s; b = surface width of water in trough, m; g = gravity acceleration, m/s^2 ; r_c = curvature radius of the axis of transition curve, m; C = coefficient depending on the Froude number, geometry of the cross section and transition curve (rectangular cross section and simple circular transition: $C = 2.0$ for supercritical flow, $C = 1.0$ for subcritical flow).

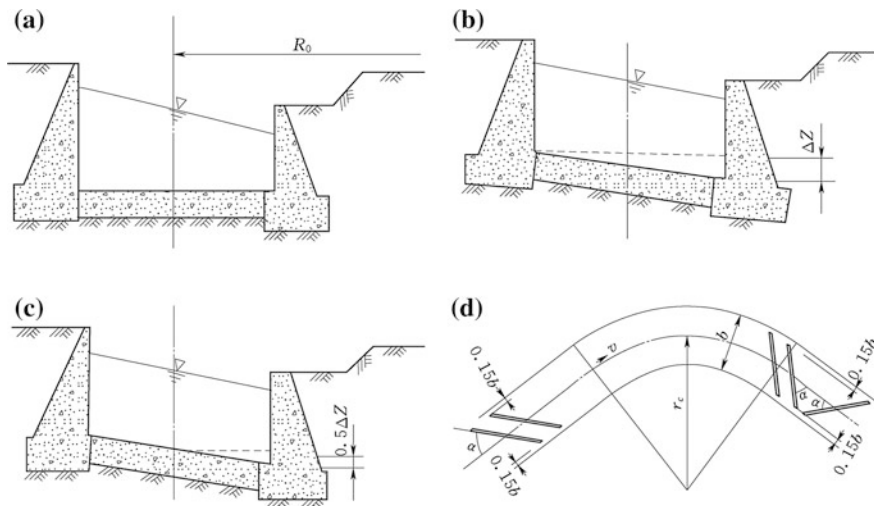


Fig. 12.10 Curved transitions of trough. **a** No measures; **b** over height of trough bottom at outside only; **c** over height of trough bottom at both sides; **d** sloping sill

Customarily, to facilitate the construction by keeping the elevation of chute axis unchanged, the inside of chute is brought down by $0.5\Delta Z$ and the outside is raised up by $0.5\Delta Z$, with respect to the axis, as shown in Fig. 12.10c.

It also should be emphasized that the over height of trough bottom should be varied gradually, as the spillway in the Bikou Project (China) shown in Fig. 12.11.

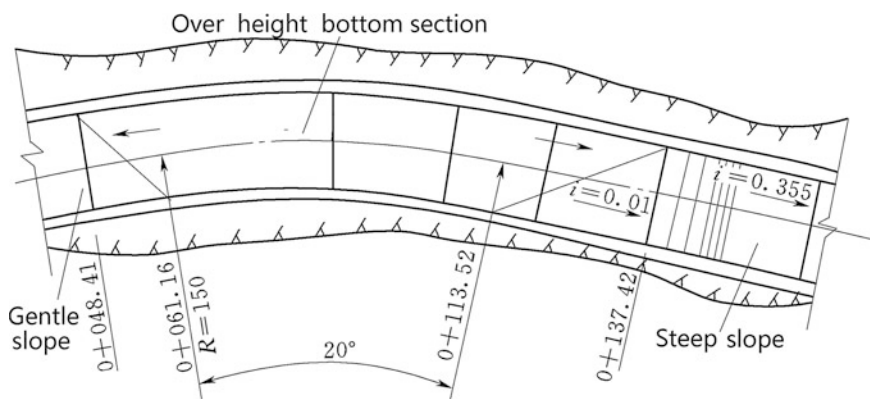


Fig. 12.11 Trough with over height bottom of the spillway (unit: m)—the Bikou Project (China, $H = 80$ m)

(d) Guide plate

The whole transition is divided into narrower subsections by circular guide plates of overlapped center, within which the water surface piling up and flow fluctuation is reduced.

(e) Sloping sill

This is customarily employed as a remedy measure for the constructed spillways, as shown in Fig. 12.10d.

4. Prevention of cavitation-induced damage to concrete trough

The damage potentiality resulted from cavitation is dependent upon the boundary configuration, the damage resistance of the concrete, the flow velocity and depth, the elevation of the structure above mean sea level, and the time duration of cavitation actions. Cavitation damage or erosion to the trough could happen where the pressure is lower or irregularity is too large, which might be derived from inaccurate construction setting-out and frame distortion, poor concrete quality, abrasion by sand to the flow boundary, and even the outcrops of reinforcing steel bar (Vide Chap. 4). The commonly encountered unevenness of concrete surfaces are illustrated in Fig. 12.12, and the corresponding cavitation and damage zones are shown in Fig. 12.13.

Damage to concrete surfaces can take place at velocities significantly lower than 25 m/s provided the adverse combination of cavitation parameters exists. As a rule of thumb, cavitation should be investigated whenever flow velocities are in excess of 9 m/s. The spillway tunnel in the Liujiaxia Project (China) is converted from the diversion tunnel by reuse it as the downstream leg conduit. In 1972, it was operated for flood releasing with a duration of about 315 h. The crosshead of the reservoir water level and the elevation on elbow part was 104.64 m with corresponding velocity about 40 m/s and discharge of 260–287 m³/s. Serious damages were found on the elbow part and adjacent downstream floor. There were three main damaged zones: two scouring pits were found in the first zone with depth of 0.3–0.5 m; a larger scouring pit with depth of 3.5 m was found in the second zone; the third zone was damaged very serious—a 190-m-long floor of concrete line was nearly all washed away. The construction irregularity was mainly blamed for these damages.

Cavitation-induced damage can be prevented by a number of methods, such as by increasing the cavitation index to ensure $\sigma > \sigma_i$, by providing a smoother boundary configuration, by improving the damage resistance of the boundary materials. A relatively new and very effective method is to disperse a quantity of air along the flow boundary. This is achieved by passing the water over aeration devices (e.g., aeration slot) specially designed to entrain air along the boundary (DeFazio and Wei 1983; ICOLD 1992), which may be particularly demanded when flow velocity is higher than 20 m/s and must be installed when velocity is over 35 m/s. An air duct or slot is the most prevalent form on steep chute or tunnel and easy to trap air, whose variants are

- Deflector ramp (Fig. 12.14a);
- Slot (Fig. 12.14b);
- Sill (Fig. 12.14c).

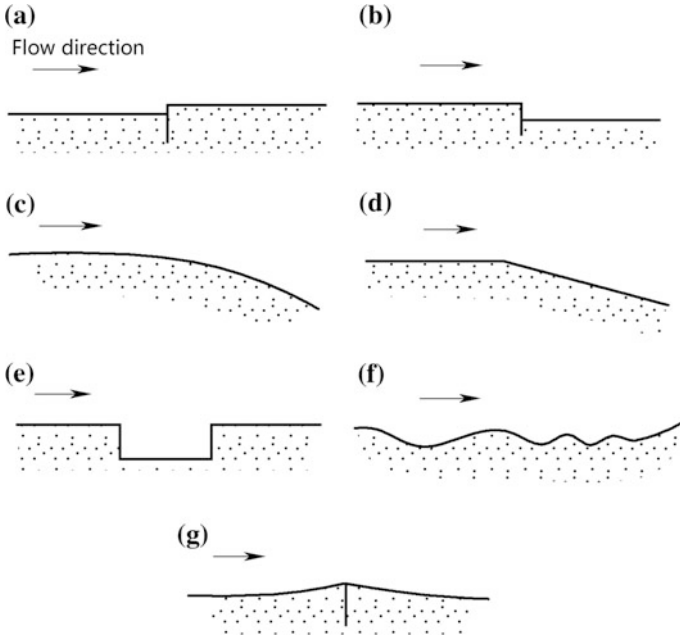


Fig. 12.12 Commonly encountered unevenness on concrete surface

Fig. 12.13 Flow states and cavitation damage zones on uneven surfaces

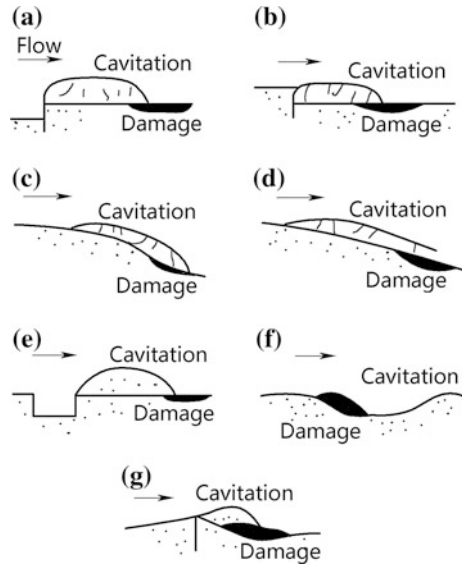
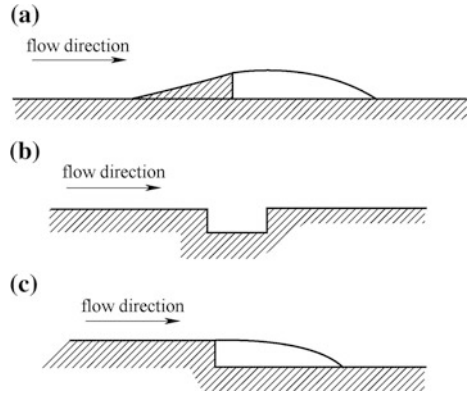


Fig. 12.14 Artificial aeration devices. **a** Deflector ramp; **b** slot; **c** sill



The configuration and location of aeration slot must be tailor-designed for the specific application. Until further experiences, data, and design guidelines, are significantly accumulated and developed, physical experimental studies for aeration slot design are strongly recommended insofar.

5. Lining structure of trough

When a spillway is working, the trough floor is subjected to the hydrostatic forces due to the weight of the water in the chute, to the boundary drag forces due to the frictional resistance along the surface, to the dynamic forces due to the flow impingement, and to the uplift forces due to the leakage through joints or cracks. When there are no spills, the trough floor is subject to the actions including thermal expansion and contraction, freezing/thawing, weathering and chemical deterioration, settlement and buckling, as well as uplift pressures brought about by under seepage or high groundwater table.

Purposes for lining chutes are to create a reasonable watertight surface over the channel to protect the trough structure from abrasion, erosion, and weathering (Bauer and Beck 1969). Whether, or not, the spillway has to be lined is one of the first questions in the design related to geologic conditions and velocity of the spillway discharge. For example, earths and soft sedimentary rocks that may be easily eroded need to be lined unquestionably. However, the decision on the need for lining is more difficult in hard sedimentary rocks and in crystalline rocks where rock structures are the important consideration. If the rock exhibits laminate structures with unfavorable trends (e.g., volcanic flow or thinly bedded sandstone), it will be susceptible to eroding by the rush of water. Scouring also can manifest in closely jointed or fractured rock where the rock blocks are small. Massive, hard crystalline rock generally does not have to be lined, but, unfortunately, this kind of rock is seldom encountered in the spillway construction.

Since it is not always possible to exactly evaluate the various forces which might occur nor to make the lining heavy enough to resist them, the thickness of the lining is most often established on the conditions of specific work site with regard to flow

and construction. Based on which type of lining is selected, countermeasures such as under drains, anchors, cutoffs are utilized to stabilize the floor.

(a) Lining on rock foundation

When a spillway trough is excavated in rock, the lining may be accomplished by concrete cast, cement–rubble masonry, or lime mortar–rubble masonry, etc., if necessary.

Lime mortar–rubble masonry lining may be applicable to the spillways in small reservoirs with flow velocity below 10 m/s.

Cement–rubble masonry lining may be employed for the spillways in small to medium reservoirs with flow velocity below 15 m/s. If the smoothness and joint seals as well as the under drains may be secured, the higher velocity up to 20 m/s may be allowable, such as the spillway of the Shibi Reservoir (China, $H = 48.19$ m). The thickness of cement–rubble masonry lining is generally 0.3–0.6 m. Composite lining with dry rubble masonry at bottom and cement–rubble masonry or concrete paving on surface also may be employed.

For medium to large projects, cast-in-place concrete lining around 0.3 m in thickness is customarily necessitated. The transverse and longitudinal joints are installed for thermal cracking control. The planar joint is conventionally used (Fig. 12.15a), whereas semi-overlapped (Fig. 12.15c), overlapped (Fig. 12.15d), or keyed joints (Fig. 12.15b) might be adopted where significant differential settlement is anticipated. Contraction joints are generally spaced 10–15 m apart in both the floor and walls, depending on the lining thickness and temperature variation. Reinforcement must be provided in both the transverse and longitudinal directions, with reinforcement ratio of 0.2 % in bidirections. These steel bars should not penetrate the contraction joints. Transverse joints over which flow velocities are high are arranged by lowering the upstream edge of downstream lower slab a certain depth, to prevent it from the building up of dynamic head beneath lining through the joints (Fig. 12.15c, d). Metal or rubber water stops are installed to seal the joints and to prevent high-pressured exterior water from penetrating into the foundation.

A grid work of under drains laid beneath transverse and longitudinal joints is demanded, by which seeping water is gathered into longitudinal drains and delivered into downstream. The longitudinal drains is usually formed by excavating ditches, in which earthenware pipes of 0.1–0.2 m in diameter depending on the seepage discharge are installed. Gravel envelope is used to cover the pipes; on the top of gravel envelope, it is covered by concrete plate or bituminous felt, to prevent the block from cementing during the lining placement. Where the seepage discharge

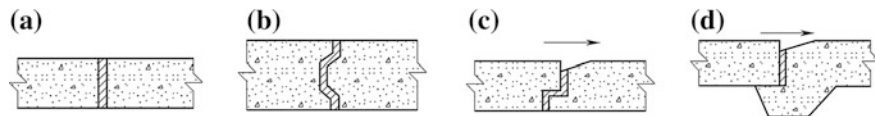


Fig. 12.15 Types of slab joints. **a** Planar; **b** keyed; **c**, **d** overlapped

is small, the ditch may be filled only by gravels which is covered by concrete plate or bituminous felt. Transverse drains are also formed by excavated ditches on rock foundation whose size is ordinarily $0.3 \text{ m} \times 0.3 \text{ m}$ depending on the seepage discharge. To be on the safe side, at least two rows of longitudinal drains should be installed.

Lining pavement also may be employed for side walls if the rock quality is competent. To facilitate the construction, the thickness of side wall lining is not smaller than 0.3 m , which should be back tied to the rock by bolts. The transverse joints of side walls are identical to that of floor lining slab, and a longitudinal joint is installed between the side wall and the floor. Where the rock is weak, the gravity-type retaining wall may be adopted. Drains also should be installed behind side walls, which link with the transverse drains under the floor lining slab. To ensure the draining, air vent is installed on the top of the side wall drain, which is located at near the top of the wall and above the maximum water surface. Berms should be installed on the top of the side wall to provide access pathway.

Fractured and weathered rocks should be cleared. In case with large uplift and pressure fluctuation from flow, anchorage using rock bolts may raise the effective weight of the slab against the displacement by a certain volume of foundation rock to which the bolts are tied. Depth and spacing of bolts depend on the nature of the bedrock such as stratification, jointing, and weathering. Conventionally, 1 cm^2 in cross-sectional area of bolt would be expected for 1 m^2 of slab, the diameter d and spacing are usually 25 mm or more and $1.5\text{--}3.0 \text{ m}$, respectively, the bolting depth into bedrock is $40\text{--}60d$.

(b) Floor paving on earth foundation

Figure 12.16 shows typical structures of floor paving on earth foundation. When a spillway chute channel is excavated through earth, the paving slab might be cast directly on the excavated surface. An intervening pervious blanket of approximately 30 cm thick may be laid, depending on the nature of the foundation soil as related to its permeability, susceptibility to the damage due to freezing/thawing action, and heterogeneity as it may give rise to differential settlement. A thicker slab of at least $0.3\text{--}0.5 \text{ m}$ should be provided, to forestall slab from moving, cracking or buckling due to expansion and contraction.

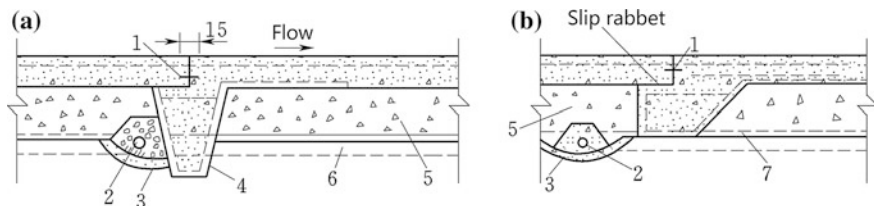


Fig. 12.16 Typical structures of floor paving on earth foundation. **a** Transverse joint; **b** longitudinal joint. 1 water stop; 2 draining pipe; 3 mortar pad; 4 cutoff wall; 5 pervious blanket; 6 longitudinal draining pipe; 7 transverse draining pipe

For a better bonding of the floor slab to the foundation, it is advisable to install reinforced concrete cutoff wall at the upstream end of each slab. Bulb anchors are sometimes employed for very important project.

Attributable to the fact that the slab is not strongly restrained by the foundation, the spacing of thermal contraction joints of the slab on earth foundation may be larger than 15 m. However, a reinforcement ratio 0.2 % in bidirections is still demanded to prevent thermal cracking.

A pervious gravel blanket is often provided between the slab and the foundation where the foundation soil is sufficiently impervious. The blanket serves not only as a free-draining layer but also aids to insulate the foundation from freezing/thawing action. The thickness of the blanket thus depends on the climate at the site and on the susceptibility of the foundation to FT heaving. A grid work of under drains is provided as a collecting system for seeping water. It is laid with open joints within gravel and embedded on a mortar pad to prevent the foundation material from being leached into draining pipes. The network of draining pipes links one or more trunk drains which carry the seepage flows to the outlets through the floor or side walls. For gravel pervious foundation, only network draining system is necessary. Filter should be installed around draining pipes.

12.2.4 Terminal Structures and Outlet Channels

When released outflow falls from reservoir pool level to downstream river level, the static head is converted into kinetic energy. The energy manifests itself in the form of high velocities which, if impeded, give rise to large pressure. Terminal structure provides means of returning the flow to the river without serious scouring to the dam toe or damage to the adjacent structures. The design principles of terminal structures with energy dissipation are similar to that of overflow gravity dams (Vide Chap. 7).

In case with good bedrock, the upturned deflectors, cantilevered extensions, or flip buckets can be employed to deliver high-velocity flow directly to the main river stream where the energy is absorbed along the streambed by impact, turbulence, and friction. Often, scouring in the streambed at the plunge point can be minimized by fanning the jet horizontally by the use of a flaring deflector or vertically by slit bucket into a thin sheet. The stability and strength of the flip bucket should be calibrated taking into account of its self-weight, the weight of water in bucket, the centrifugal force of flow, the fluctuation pressure, and uplift. In such arrangements, an adequate cutoff or other protection must be installed at the end of the bucket to prevent it from being undermined retrogressively (Fig. 12.17). The depth of the cutoff wall is ordinarily 5–8 m which depending on the depth, distance, and shape of the scouring pit. Rock bolts are commonly employed to back tie the bucket with the bedrock. To prevent scouring near the bucket at lower flow discharge, a short bottom lining of riprap or concrete is usually installed downstream the flip bucket. The measures such as air vent or expansion excavation of outlet channel are demanded to forestall the vacuum under the jet nappe, to ensure the jet impingement distance (Fig. 12.17c).

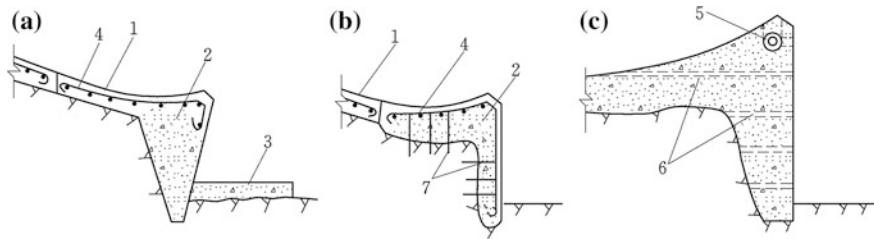


Fig. 12.17 Types and structures of flip bucket. **a** Gravity type; **b** reinforced thin lining type; **c** draining and air vent. 1 face slab; 2 cutoff wall; 3 concrete apron; 4 steel bar; 5 air vent; 6 drainage hole ($\Phi 15$); 7 rock bolt

Where serious streambed scouring is anticipated to endanger the dam or other important appurtenance structures, the alternatives of energy dissipation devices such as stilling basin and roller bucket should be taken into account (Bradley and Peterka 1957a, b).

Outlet channel conveys the flow from the terminal structure to the river stream. In some instance, only a pilot channel is provided, on the assumption that scouring action will enlarge the channel during major flood releasing. However, where the channel is in a relatively non-erodible material, it should be excavated to an adequate size to pass the anticipated flow without affecting the tailwater.

Although energy dissipation devices are provided, yet it might be impossible to reduce the outflow velocity below the natural velocity in the original stream, and certain scouring of the riverbed, therefore, cannot be avoided.

Under natural conditions, the beds of many streams are scoured during the rise stage of a flood and silted during the falling stage by the deposition of material carried in the flow. After the creation of a reservoir, the spillway will normally release clear water, and the materials scoured by the clear current of high velocity will not be replaced by deposition. Consequently, there will be a gradual retrogression of the downstream riverbed, which will bring down the tailwater level. On the contrary where only a pilot channel is installed, scouring may build up islands downstream, thereby effecting a degradation of the downstream river channel which will raise the tailwater level. The outlet channel dimensions and its need for protection by lining or riprap should be decided by all these considerations.

12.3 Spillways of Other Types

12.3.1 Side-Channel Spillways

Where a long overflow crest is desired in order to limit the surcharge head, and the abutment are steep and precipitous, or where the control structure must be connected to a narrow discharge channel or tunnel, side-channel spillway (Fig. 12.18)

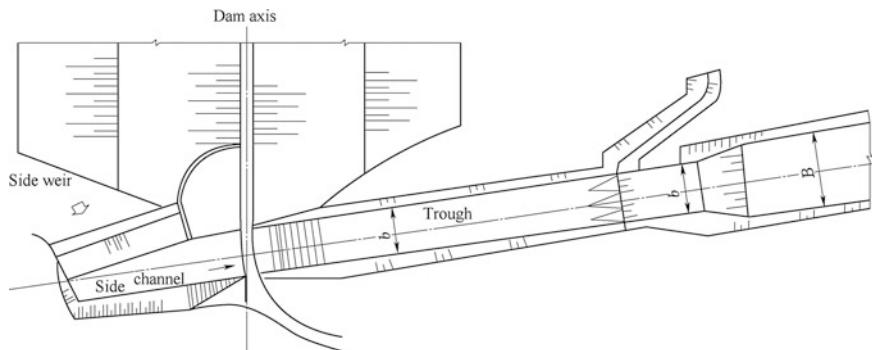


Fig. 12.18 An embankment project with side-channel spillway

is often a good choice. Flow from the side channel can be directed into an open discharge channel (chute) or into a closed conduit or inclined tunnel.

The design of side-channel spillway is concerned particularly with the hydraulic action in the upstream reach of the discharge channel and is more or less independent of the details selected for the other spillway components (Farney and Markus 1962; Hinds 1926).

1. Layout and work conditions of side-channel spillways

Side-channel spillway possesses control weir placed alongside and approximately parallel to the upper portion of the discharge channel. Flow into the side channel might enter on only one side of the trough in the case of a steep hillside location, or on both sides and over the end of the trough if it is located on a knoll or gently sloping abutment (Fig. 12.19).

Although side-channel spillways are generally ungated, there is no reason why gates cannot be installed.

Modifications to the conventional side-channel spillway include the addition of a short crest length perpendicular to the channel at the upstream end forming an L-shaped crest as illustrated in Fig. 12.19g. The labyrinth spillway (Darvas 1971; Hay and Taylor 1970) is also may be looked at as a modification of side-channel spillway characterized by a broken axis of crest in plan in order to create a greater crest length compared to a conventional spillway crest occupying the same lateral space (Fig. 12.19e, f). The broken axis forms a series of interconnected V-shaped weirs. Each of the V-shapes is termed as a cycle. The labyrinth spillway is particularly well-suited for rehabilitation of existing spillways and for providing a large capacity spillway in a site with restricted width, whose hydraulic characteristics are extremely sensitive to approach flow conditions. This requires sitting the crest configuration in the direction of upstream as far as possible into the reservoir, in order to achieve approach flow nearly perpendicular to the axis. Serious consideration of this type of spillway will require verification of the design by a physical model study. The other modifications of side-channel spillways are also shown in Fig. 12.19.

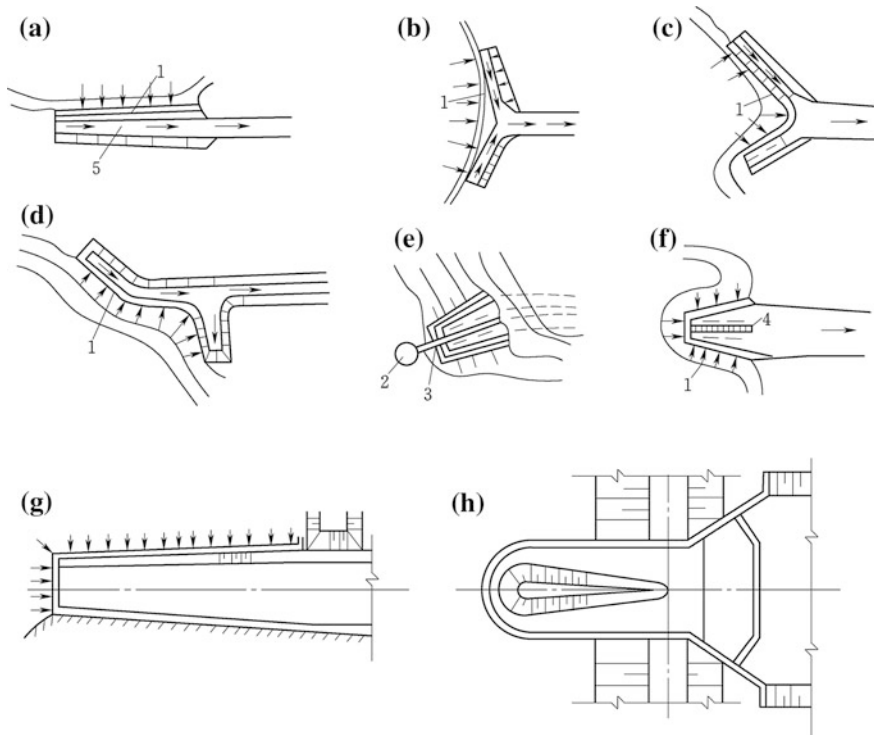


Fig. 12.19 Intake types of side-channel spillway. **a** Standard; **b** T-type; **c** Y-type; **d** contour-type; **e, f** labyrinth-type; **g** L-type; **h** circular type. 1 weir crest; 2 intake tower; 3 management bridge; 4 partition wall; 5 side channel

Because of turbulence and vibration inherent in side-channel flow, a side-channel design is ordinarily not considered except where a competent foundation (e.g., rock) exists.

2. Design features of side-channel spillways

A side-channel spillway is composed of control weir, side channel, chute (trough or tunnel), terminal structure, and outlet. Preliminary design of a side-channel spillway can be accomplished with respect to discharge ability, flow pattern, and water surface. In view of the complex nature of flow, physical hydraulic modeling is normally undertaken to ensure adequate and economical details for the final design.

Discharge characteristics of a side-channel spillway are similar to those of an ordinary overflow and are dependent on the selected profile of the weir crest (Fig. 12.20). However, for maximum discharges the side-channel flow may differ from that of the proper open-channel spillway in that the flow in the trough may be restrained and the flow over the crest may be partially submerged. Under such circumstances, the flow will be controlled by the downstream trough. The constriction may be resulted from a point of critical flow in the channel, an orifice

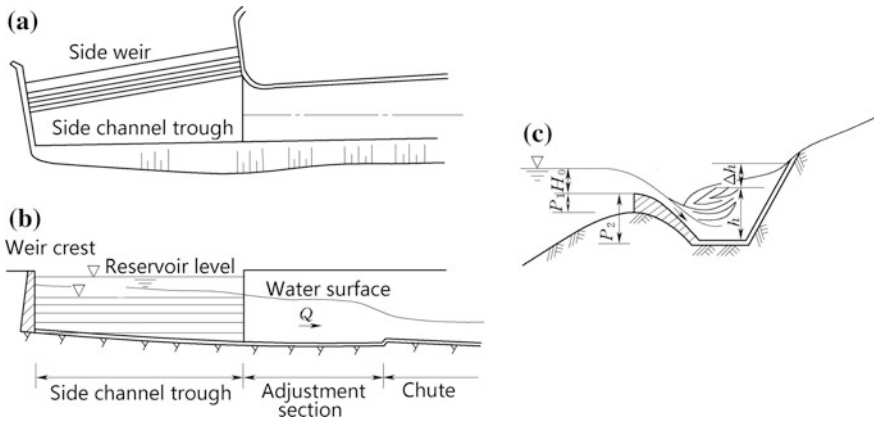


Fig. 12.20 Overflow weir and cross section of side channel. **a** Plan; **b** longitudinal section; **c** transverse section

control, or a conduit or tunnel flowing full. In the design of weir crest, its position and size are selected together with the side channel.

The water in side channel is spatially varied flow with strong lateral inflow whose flow pattern is restrained by both the weir and side-channel trough, which dictates the hydraulic design requirements as follows:

- ① The water level in the side-channel trough should not influence the flow discharge passing the weir, i.e., the flow is free over the weir. According to experiences $h_s = 0.5H_d$ may be used as the minimum value, in which h_s is the water depth over the weir at the starting of side-channel trough (m) (Fig. 12.21); H_d is the design head over weir corresponding to the design flow discharge Q_d , usually being equal to the maximum discharge Q_{max} .
- ② The assumption is made that the energy of flow over the crest is totally dissipated by turbulence as it turns and mixes with the side-channel flow and that the only force driving longitudinal motion in the side channel is attributable to the gravity. It is also assumed that the frictional resistance of the side channel is sufficiently small and may be neglected without seriously affecting the accuracy of the computations. A longitudinal grade smaller than 0.1 and usually varies between 0.01 and 0.05 is necessary for the channel floor to keep the movement of the flow along the side-channel trough.
- ③ The downstream end of side-channel trough should not be influenced by the connected open channel; therefore, it is demanded that:
 - The floor grade $i > i_k$, i_k is critical slope.
 - No hydraulic jump should occur in the side-channel trough. If the channel floor grade is small, i.e., the water depth all over the side-channel trough is larger than critical depth h_k , and at the end of trough $h_l > h_k$, a horizontal

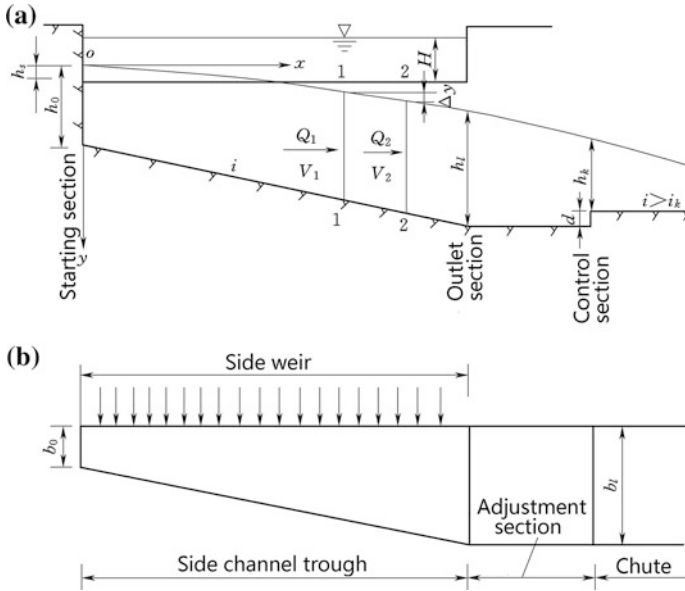


Fig. 12.21 Diagram to the water surface computation of side-channel trough. **a** Longitudinal; **b** plan

adjustment segment is installed between the end of the side-channel trough and the starting of open-channel chute (Fig. 12.21), whose length is $l \approx (2-3) h_k$. This enables the end of adjustment segment to be a control section with critical depth.

- Usually, divergence or bending transition is avoided near the end of side-channel trough.
- A trapezoidal cross section is prevalent for the side-channel trough. The sectional width ratio b_0/b_1 may be 0.25–1.0. The slope of the trapezoid side may be selected around 1:0.5–1:0.9 on the weir side and 1:0.3–1:0.5 on the hillside, depending on the rock properties (Fig. 12.20).
- The lateral difference of water in the side-channel trough should be limited. Usually, the raising of water level on the hillside Δh (Fig. 12.20c) is 10–25 % of the average depth (h), which is subject to hydraulic model verification.
- The crest length by the conventional computation must be corrected with regard to the loss in effective crest length caused by angularity of flow at the junction of the crest sections.

3. Open-channel chute, terminal structure, and outlet channel

Their design is identical to open-channel spillways.

4. Hydraulic computation of side-channel trough

The purpose of hydraulic computation of side-channel trough is to decide the water surface and corresponding floor elevation of side-channel through, according to the conjunction relationship among weir, side-channel trough, and open-channel chute.

The starting section for computation is usually located at the downstream end of the side-channel trough (Fig. 12.21), at which the water depth h_l termed as “economical depth” is commonly 1.20–1.35 time of the critical depth h_k of the starting section of the adjoining open-channel section (control section). The flow in the side-channel trough is a gradually varied flow whose surface may be computed using differential Eq. (12.5) based on the momentum principle, in which the item $\bar{J}\Delta s$ may be neglected if the flow segment is short.

$$\Delta y = \frac{Q_1}{g} \frac{(v_1 + v_2)}{(Q_1 + Q_2)} \left[(v_2 - v_1) + \frac{v_2(Q_2 - Q_1)}{Q_1} \right] + \bar{J}\Delta s \quad (12.5)$$

where Δy = water-level difference of up- and downstream computation sections, m; Δs = length of the segment; Q_1 and Q_2 = the flow discharges of the up- and downstream computation sections of the segment concerned, respectively, m³/s; v_1 and v_2 = the averaged flow velocities of the up- and downstream computation sections of the segment concerned, respectively, m/s; \bar{J} = averaged hydraulic gradient of the computed segment [Eq. (12.2)]; \bar{R} = averaged hydraulic radius of the computed segment, m.

5. Design procedure for side-channel spillways

- ① According to the outflow discharge related to the design flood, topographic and geologic conditions, and construction conditions, several layout schemes are contemplated. The schemes are specified as combinations concerning the length of weir L , side-channel trough width b_0 and b_l , as well as the floor grade i .
 - ② For each scheme, the critical depth h_k at the control section and the exit depth h_l of the side-channel trough are computed, which are subject to comparison with the design criteria. Unqualified schemes are abandoned.
 - ③ For the selected weir and side-channel scheme, the water surface in relation to outflow discharge is calculated.
- Where the floor slope i is small, the depth in side trough is higher than critical depth. The latter may be regarded as occurring at the conjunction of the horizontal adjustment section with the open-channel chute. A rising deflector may be added to the end of the horizontal adjustment section (Fig. 12.21a). Make use of the energy equation between the end section of side trough and control section, the height d of the deflector at control section floor may be obtained:

$$d = \left(h_l + \frac{v_l^2}{2g} \right) - \left[h_k + \frac{v_k^2}{2g} + \xi \left(\frac{v_k^2 - v_l^2}{2g} \right) \right] \quad (12.6)$$

where h_k, v_k = the critical depth and velocity at the control section, respectively; h_l, v_l = the depth and velocity at the exit end of side-channel trough, respectively; $\xi = 0.2$, the local drag coefficient.

Height of deflector sill d also may be estimated by 0.1–0.2 times of critical depth h_k at the control section.

- Use the exit end of side-channel trough as the first computation section, the water surface and corresponding depth of the side-channel trough is calculated retrogressively section by section according to Eq. (12.5). By parity of reasoning, until the whole water surface and depth are obtained.
- ④ The hydraulic design for the open-channel trough is carried out, which is identical to that of the proper open-channel chute.

12.3.2 Drop Inlet (Shaft or Morning Glory) Spillways

A drop inlet spillway, as the name implies, is one in which the water enters over a horizontally positioned lip, drops through a vertical or inclined shaft, and then flows to the downstream river stream through a horizontal or near-horizontal conduit (e.g., tunnel).

A drop inlet spillway can be used advantageously at the dam site in narrow valley where the abutments rise steeply or where a diversion tunnel/conduit is available for reuse as the downstream leg (Fig. 12.22). Another advantage of drop inlet spillway is that near maximum release capacity may be achieved at an early flood period with low surcharge heads, which makes the spillway ideal for use

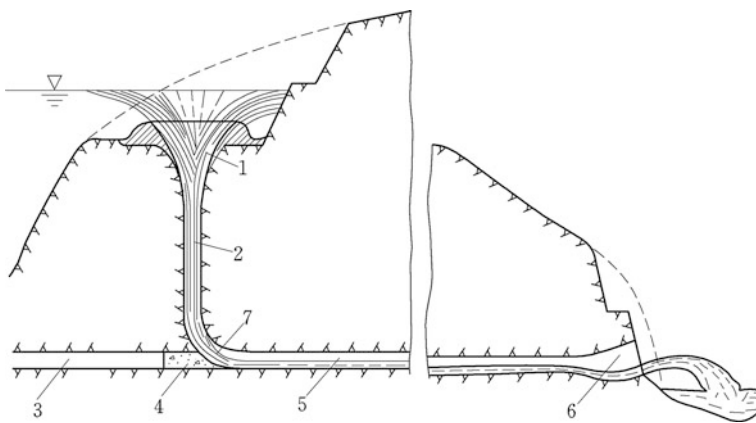


Fig. 12.22 A drop inlet spillway. 1 crest of morning glory; 2 shaft; 3 diversion tunnel; 4 concrete plug; 5 flood release tunnel; 6 outlet; 7 bending transition

where the maximum outflow is rigorously limited. However, the accompanied disadvantage is that there is little increase in capacity beyond the designed surcharge heads, should a flood larger than the design flood occur. Anyway, this disadvantage may be compensated for if the spillway is used as a main service spillway in conjunction with an auxiliary or emergency spillway.

1. Layout of drop inlet spillways

The spillway may be considered as consisting of four elements, namely diversion and anti-swirl facilities, an overflow control weir, a vertical transition, and a closed discharge channel in form of vertical or inclined shaft, which is often linked with diversion tunnel. Where the inlet is funnel-shaped, this type of structure is often termed as “morning-glory” or “glory hole” spillway.

2. Hydraulics and structure of drop inlet spillways

As the heads increase on a drop inlet spillway, the control will shift from the weir flow over the crest to the tube flow in the transition and then to the full pipe flow in the downstream portion. Full pipe flow design for drop inlet spillways except those with extremely low drops is not recommended.

The inflow discharge is dependent on the head over crest, type, and circular length of the morning glory. The capacity of inflow being diverted through tunnel is depending on the section size and effective head within tunnel.

There are two common profile types for the weir section: the ogee profile using parabolic curve, and the board crested profile with flat cone-shape (Fig. 12.23), of

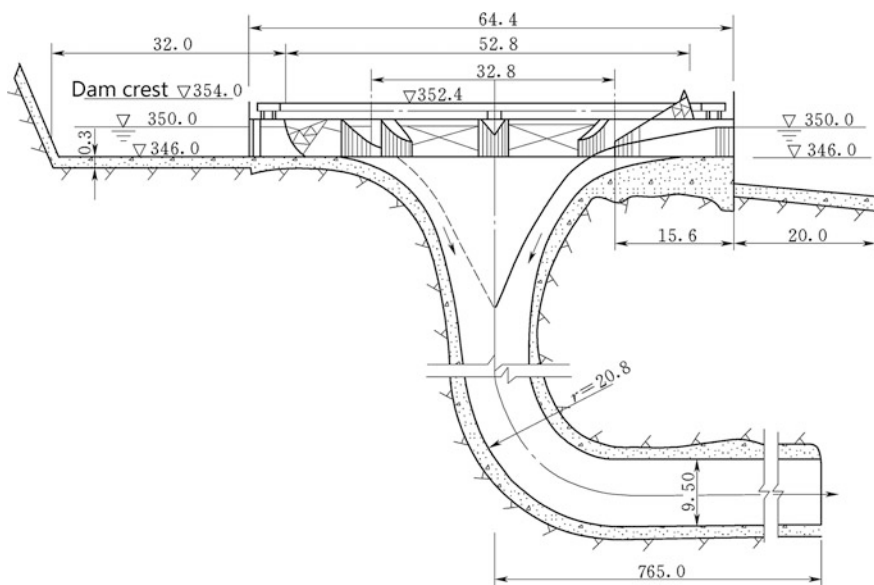


Fig. 12.23 A drop inlet spillway with board crested weir and radial gates (unit: m)

which the former is more prevalent. Gate may be installed on the crest of morning-glory entrance. Problems frequently encountered in this type of structure involve vortex action, unstable flow, and cavitation. Local topography may initiate vortex trends in the adjoining approach flow to the spillway, resulting in reduced capacity, flow instability, and surges in the shaft and tunnel. Laboratory studies indicate that the vortex over a submerged circular orifice may reduce the discharge by as much as 75 %. Piers, fins, vanes, and curtain walls may be installed to suppress vortex actions. However, physical model studies are imperative to verify their effectiveness. When the flow control shifts from the crest to the conduit and vice versa, violent surging originating in the shaft can induce severe pressure and flow pulsations throughout the structure. Deflectors and vents in the shaft have been exercised to prevent these surges and pulsations. The need for deflectors and vents and verification of their design must be established by hydraulic physical models. The likelihood of cavitation near the tangency of the curve connecting shaft to horizontal conduit should be explored.

3. Hydraulic design

The discharge ability of morning-glory entrance is computed by

$$Q = \varepsilon m(2\pi R - n_0 s) \sqrt{2g} H^{3/2} \quad (12.7)$$

where m = discharge coefficient ($m = 0.48$ for ogee crest, $m = 0.32$ – 0.38 for broad crested weir); ε = contraction coefficient (usually $\varepsilon = 0.9$); R = radius of morning-glory entrance, m; H = head over the crest, m; n_0 = number of piers; s = width of pier, m.

Usually, $R = (2-5)H$ for the ogee crest and $R = (5-7)H$ for the broad crest.

Beneath the morning glory, the inflow becomes full. A transition section is necessary to compress the flow gradually into a smaller section of pressure shaft or tunnel. In the transition section, the free drop of flow increases its velocity, but keeps its pressure identical to atmospheric pressure. Pressure flow is started in the shaft section, from there until the exit of the tunnel, the diameter d_r of the whole flow conduit and velocity is kept unchanged. The head difference h is used to overcome the friction drag and local drag of this pressure conduit; therefore, the suitable diameter d_r is selected in the design to secure a good balance between head difference h and the head loss resulted from the friction drag and local drag.

4. Countermeasures for improving the flow pattern in drop inlet spillways

Unstable flow in the transition from the crest control to the conduit control, which would take place over an extended period of time, is blamed for unacceptable noise, rapid pressure fluctuations, and strong vibrations. To improve the flow condition, air vent is installed around the shaft whose total cross-sectional area is around (10–15) % that of shaft (Fig. 12.24). In small to medium projects, guide piers or still walls may be employed for the same purpose.

Drop inlet spillways are more commonly exercised in France and Italy than the other counties. It was rarely used in China in the past time by the reason of large

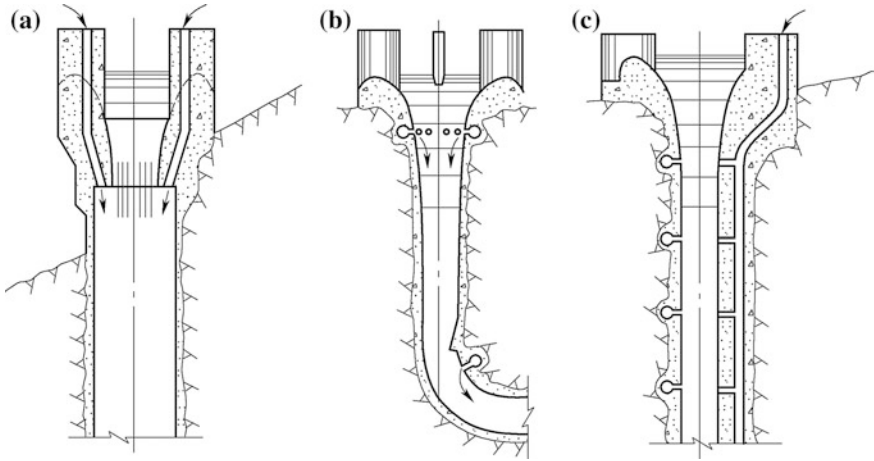


Fig. 12.24 Aerator installations for shaft spillways

inlet structure of morning glory, complex flow state, tiny increase in capacity beyond the design heads, rapid pressure fluctuations, and strong vibrations under small overflow discharge. However, a new version of drop inlet spillway has been studied and placed in the Shapai Project (China, $H = 132$ m) successfully that consists of a short length of pressure intake, approaching tunnel, vortex chamber, vertical shaft, and original diversion tunnel. The maximum head is 88 m and maximum flow discharge is $248 \text{ m}^3/\text{s}$.

12.3.3 Siphon Spillways

A siphon spillway is a closed conduit system in the shape of an inverted U tube and so positioned that the interior of the bending upper conduit (Fig. 12.25a) is at the normal storage level. The siphon spillway may be integrated into the dam or located at bank (Fig. 12.25b).

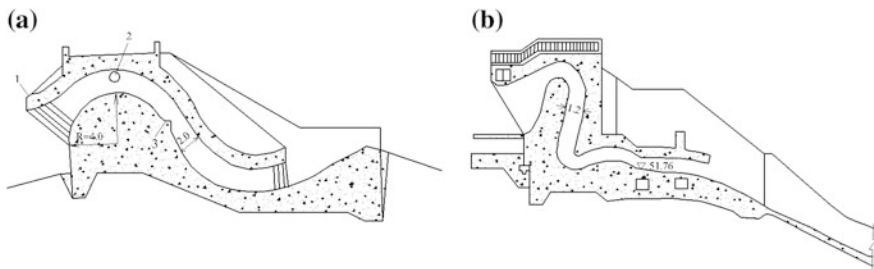


Fig. 12.25 Siphon spillways. 1 top cover; 2 siphon-breaker air vent; 3 deflector sill

Most siphon spillways consist of five elements including an inlet, an upper leg, a throat or control section, a lower leg, and an outlet. A siphon-breaker air vent is also provided to control the siphonic action of the spillway so that it will cease operation when the reservoir water surface is drawn down to the normal level. The inlet is generally placed below the normal reservoir water surface to prevent entrance of ice and debris. The upper leg is formed as a bending convergent transition adjoining the inlet to a vertical throat section. The throat or control section is generally rectangular in cross section and is located at the crest of the upper bend of the siphon. The upper bend then continues to join a vertical or inclined tube which forms the lower leg of the siphon. Often the lower leg is placed on an adverse slope, to provide a more positive priming action by forming a flow curtain which seals across the leg. The lower leg can be so terminated as to discharge vertically or along the face of a concrete dam, or it may be provided with a lower bend and diverging outlet tube to release the flow in a horizontal direction. The outlet flow can be free discharging or submerged, depending on the arrangement of the lower leg and on the tailwater conditions.

Due to the negative pressure prevailing in the siphon, the conduit should be sufficiently rigid to withstand the collapsing forces. Joints must be made watertight, and countermeasures must be taken to avoid cracking of the conduit.

The principal advantage of a siphon spillway is its ability to pass full-capacity discharges with narrow limits of headwater rise. A further advantage is its automatic operation without mechanical devices or moving parts.

In addition to its higher cost, as compared to other types, the siphon spillway has a number of disadvantages as follows:

- The inability of passing ice and debris;
- The possibility of clogging the siphon conduits and siphon-breaker air vents with debris or leaves;
- The possibility of water freezing in the inlet legs and air vents before the reservoir rises to the crest level of the spillway, thus preventing flow through the siphon;
- The occurrence of sudden surges and stoppages of outflow as a result of the erratic make-and-break action of the siphon, thus giving rise to radical fluctuations in the downstream river flow;
- Vibration disturbance is more pronounced than in other types of control structures.

As is the case with other types of closed conduit structures, a principal disadvantage of the siphon spillway is its inability to release flows greater than designed capacity although the reservoir head exceeds the design level. Consequently, the siphon spillway is best suited as a main service spillway in conjunction with an auxiliary or emergency spillway.

12.3.4 Baffled Apron Drop Spillways

Baffled aprons or chutes are used in spillways where it is desirable to avoid a stilling basin. The baffle piers partially obstruct the flow, dissipating energy as the water flows down the chute so that the flow velocities entering the downstream channel are relatively low. Advantages of baffled aprons are low expenditure, low terminal velocity of the flows regardless of the height of the drop, downstream degradation does not affect the spillway operation, and there are no requirements for initial tailwater depth in order for the stilling basin to be effective.

The chute is normally constructed on a slope of 2:1 or more flat, extending below the outlet channel floor. Chutes with slopes steeper than 2:1 should be model-tested and their structural stability should be checked. The lower end of the chute should be constructed far enough below the channel floor to prevent damage from degradation or scour.

12.3.5 Culvert Spillways

Culvert spillway is a special adaptation of the conduit or tunnel spillway. It is distinguished from the drop inlet and other conduit types in that its upstream or downstream inlet is placed either vertically or inclined, and its profile grade is made uniform or near uniform of any slope. The spillway inlet might be sharp edged or rounded, and the approach to the conduit might have flared or tapered sidewalls with a horizontal or sloping floor. If it is desired that the conduit flow partially full for all conditions of discharge, special precautions are taken to prevent the conduit from flowing full; if full flow is desired, bell mouth or streamlined inlet are provided.

Culvert spillways operating with the inlet unsubmerged will perform similarly to an open-channel spillway. Those who operate with the inlet submerged, but with the inlet orifice arranged so that full conduit flow is prevented, will perform similarly to an orifice-controlled drop inlet spillway, or to an orifice-controlled chute spillway. Where priming action is induced and the conduit flows full, the operation will be similar to that of a siphon spillway. When the culvert spillway is arranged to operate as a siphon, recognition must be taken of the disadvantages of siphon flow.

As is the case with a drop inlet or siphon spillway, a principal disadvantage of culvert spillway is that because its capacity does not substantially raised with the increase in head, it does not provide high safety margin against the emergencies due to the improper or varying hydrologic data with regard to the design flood. This disadvantage would be compensated for where the culvert type is used as a main service spillway in conjunction with an auxiliary or emergency spillway.

When culvert spillways placed on steep slopes flow full, reduced or negative pressures manifest along the boundaries of the conduit. Where negative pressures are large, there is a danger of conduit collapse or cavitation to the conduit surfaces.

Where cracks or joints appear along the low-pressure regions, there is the potentiality of drawing in soil surrounding the conduit. Culvert spillways, therefore, should not be used for high-head installations where large negative pressures are very likely manifested. Further, the transition flow phenomenon, when the flow pattern changes from partially full to full, is attended by rather severe pulsations and vibrations. With regard to these reasons, culvert spillways should not be employed where the head drops exceed 6 m.

For head drops not exceeding 6 m, culvert spillways offer advantages over similar types due to their adaptability for either partially full or full flow operation and due to their simplicity and economy in construction. They might be placed on a bench excavation along the abutment of steep side hill location, or they can be placed through the dam to discharge directly into the downstream river channel.

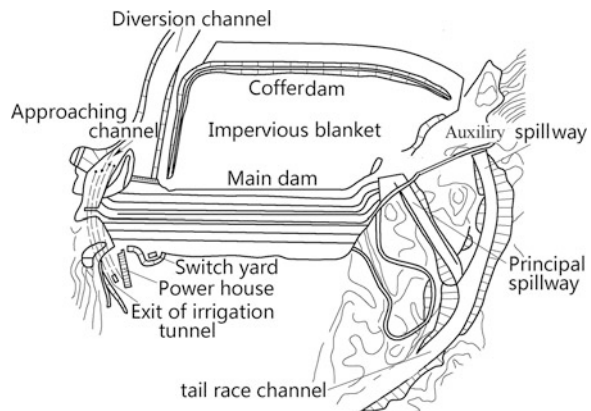
12.4 Emergency Spillways

Emergency spillway is a kind of auxiliary spillways performing as fuse plugs for additional safety, should emergencies not contemplated by normal design assumption, arise. Figure 12.26 shows the layout of the Tarbela Project (Pakistan, $H = 105$ m), at its right bank there is an auxiliary spillway.

Where conditions occur that have not been anticipated and considered in the design of the main spillway, they may lead to following emergency situations:

- The actual flood exceeds the design flood;
- There is an enforced shutdown of the outlets;
- There is a malfunctioning of spillway gates;
- There is damage or failure of the main spillway;
- A high flood occurs before the previous flood has been evacuated by the main spillway.

Fig. 12.26 The Tarbela Project with auxiliary spillway—Pakistan, $H = 143$ m



An emergency spillway is usually positioned in a saddle or depression along the reservoir rim or by excavating a channel through abutment/ridge. Because an emergency spillway is not needed to function under normal reservoir operations, its crest is placed at or slightly above the design maximum reservoir level. Thus, an encroachment on the minimum free board is usually permitted for the design of an emergency spillway. The emergency spillway is washed out as soon as the water level in the reservoir reaches a predetermined elevation. The breaching section is sometimes called as “fuse plug.” Although it may take many months to restore the fuse plug and channel after an emergency operation, the total damage and cost to repair is less than if the main water-retaining structures had been overtopped.

The following requirements in the design of emergency spillways should be observed:

- The structural safety standard could be suitably lower, for its lower operation chance;
- The total discharge of spillways in a project should not be excess the maximum inflow discharge;
- Fully preparation for the released flow passage and downstream area should be made;
- If there are two or more emergency spillways, they are applied in sequence, for control the downstream flood;
- Emergency spillways should be located on the stratum with good geologic conditions, to prevent unexpected scouring to the foundation and unexpected downstream flood;
- The foundation of control section should be protected, to avoid scouring of saddle into deep groove, which in turn, leads to large reservoir draw down and difficulties associated with rehabilitation.

The fuse plug may be sparked by manner of overtopping, natural washout (or flushing), and blast washout.

12.4.1 Overtopping Emergency Spillways

With a crest near the water level at which the emergence operation is anticipated, overtopping emergency spillway is similar to the open-channel spillway. Where the water level is higher than the crest, a free flow commences. Since the initial outflow depth is shallow, it usually possesses long crest located at a wide saddle, for the reduction of excavation amount. The Dahuofang Project added a 150-m-long emergence spillway of this type in 1977, to help release MPF only.

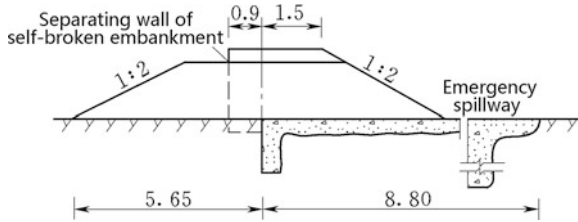


Fig. 12.27 An emergency spillway with natural wash out flushing embankment (unit: m)

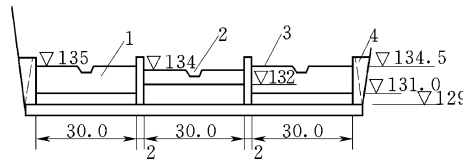


Fig. 12.28 Upstream elevations of a natural wash out flushing embankment with fuse ditches (unit: m)

12.4.2 Flushing Embankment Emergency Spillways

Flushing embankment emergency spillway consists of flushing dyke, concrete weir (or bottom sill), and chute. The flushing dyke may be either natural washout (or flushing) or blast washout.

An conventional emergency spillway with natural washout is shown in Fig. 12.27. The embankment and foundation should meet the requirements for the stability and seepage of permanent structures. Figure 12.28 shows another emergency spillway with natural washout flushing, at its middle portion fuse ditches are installed, as a result the washout of the whole dyke may be expedited.

Where the emergence spillway is long, separation walls may be installed to divide it into several segments with small difference in their crest elevations, this may stagger the operative time between segments, in this manner to prevent a sudden increase of discharge flood for downstream reaches. This design is implemented in the Dahuofang Project (China, $H = 49.2$ m).

12.4.3 Blast Washout Emergency Spillways

A blast washout emergency spillway also comprises the embankment and foundation satisfying the requirements for the stability and seepage of permanent structures, but it uses dynamite to form blasting cone as fuse ditches, as shown in Fig. 12.29.

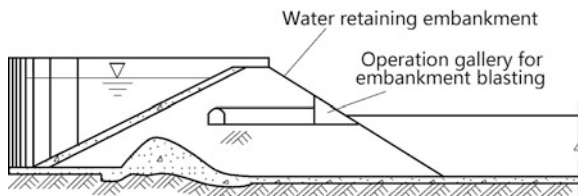


Fig. 12.29 A blast wash out emergency spillway

12.5 Type Selection and Layout of Spillways

There are two basic ways to release flood through bank: chute spillway (or ski jump spillway) and spillway tunnel. Large flood flow can only be discharged through bank structures for earth- and rockfill dams. This arrangement also can be exercised for concrete dams where there is additional flood flow to be discharged and geologic and topographic conditions on abutments are available.

The bank-side or shore spillways can send the flow far away from dam and will not affect dam safety and power plant operation. Where an angle will be formed between the chute spillway (or spillway tunnel) and the river, it should be as small as possible in order to reduce the erosion to the opposite bank and the strength of return current. For a chute spillway with high crosshead, a curved channel is normally designed in approach channel and various kinds of flip bucket can be used to adjust flow direction.

Topographic condition influences the excavation amount of spillway greatly. Open-channel spillway would be the first choice where there is a saddle whose elevation is near the reservoir level, and whose downstream gully enables the released flood back to the mainstream easily. For a dam site of steep valley, two open-channel spillways may be layout on both river sides, or the side-channel spillway may be employed. Under very steep topographic condition, tunnel spillways using side-channel entrance or morning-glory entrance may be indicated.

Geologic condition also significantly influences on the spillway design. The excavated slopes should be stable. The unstable bank slopes after the reservoir impounding, the large faults, and potential land sliding are to be shunned. Deep excavation is avoided as far as possible, to facilitate the treatment of cut slopes. Stable bedrock is desirable for accommodating the spillway. The open-channel spillway may be constructed on non-rock foundation, if the slope is quite steep along the trough, step energy dissipation of multi-level head drop could be contemplated.

The composite design of spillway can be prepared by properly considering the various factors related to the other structures (e.g., dam, hydropower station, and ship lock) which influence the spillway size and type, location, and correlating alternatively selected components. In this way to achieve competent design of technically reasonable, the entrance of spillway is so located to obtain a stream flow as smooth as possible and to keep the embankment dam at a safe distance, for

preventing the lateral current scouring the upstream dam slope; otherwise, the guide wall should be installed to separate the spillway and dam. The control weir of the spillway would be better near the reservoir, to shorten the entrance channel and corresponding head loss. The released water fluctuation should have minor influence on the normal operation of power plant and ship lock.

Regarding the flood discharge ability, open-channel spillway performs well in the increase of discharge along with the rise of head over crest (since $Q \propto H^{3/2}$); the side channel in front of the chute or non-pressure tunnel has similar advantage. On the contrary, the drop inlet and siphon inlet spillways have slow increase of the discharge ability governed by $Q \propto H^{1/2}$.

In the engineering practice, auxiliary spillway may be provided which should be separately layout with the main spillway. In suspicious of larger flood than that of the design and check ones, it is wise to provide an emergence spillway.

For the spillway located far away from the other main structures in the project, the construction is less interfered, but the operation management is inconvenient. On the contrary, for the spillway tightly combined with the other main structures in the project, the construction interference could be magnificent, but the excavated materials from spillway may be easily hauled for the embankment fill. Therefore, the slag line and slag dump should be carefully designed in the construction organization and layout, to obtain better inter-coordination and less interference in the project construction.

References

- Abecasis FM (1970) Designing spillway crests for high-head operation. *J Hydraulics Div ASCE* 96(HY12):2655–2658
- Bauer WJ, Beck EJ (1969) Spillways and stream-bed protection works (Sect. 20). In: Davis CV, Sorensen KE (eds) *Handbook of applied hydraulics*, 3rd edn. McGraw-Hill, New York
- Bradley JN (1956) Morning-glory shaft spillways: a symposium: prototype behavior. *Trans ASCE* 121(1):312–333
- Bradley JN, Peterka AJ (1957) The hydraulic design of stilling basins: stilling basin and wave suppressors for canal structures, outlet works, and diversion dams (Basin IV). *J Hydraulics Div ASCE* 83(HY5) (paper 1404-1-20)
- Bradley JN, Peterka J (1957) The hydraulic design of stilling basins: small basins for pipe or open channel outlets—no tail water required (Basin VI). *J Hydraulics Div ASCE* 83(HY5) (paper 1406-1-17)
- Chen SH, Chen ML (2014) *Hydraulic structures*, 2nd edn. China WaterPower Press, Beijing (in Chinese)
- Darvas LA (1971) Performance and design of labyrinth weirs—discussion by Hay and Taylor. *J Hydraulics Div ASCE* 97(80):1246–1251
- DeFazio FG, Wei CY (1983) Design of aeration devices on hydraulic structures. In: Shen HT (ed) *Frontiers in hydraulic engineering*. ASCE, New York, pp 426–431
- Farney HS, Markus A (1962) Side channel spillway design. *J Hydraulics Div ASCE* 88(HY3): 131–154
- Golzé AR (1977) *Handbook of dam engineering*. Van Nostrand Reinhold, New York
- Grishin MM (ed) (1982) *Hydraulic structures*. Mir Publishers, Moscow

- Hay N, Taylor G (1970) Performance and design of labyrinth weirs. *J. Hydraulics Div ASCE* 96(HY11):2337–2357
- Hinds J (1926) Side channel spillways: hydraulic theory, economic factors, and experimental determination of losses. *Trans ASCE* 89(1):881–929
- ICOLD (1987) Spillways for dams (Bulletin 58). ICOLD, Paris
- ICOLD (1992) Spillways: shockwaves and air entrainment - review and recommendations (Bulletin 81). ICOLD, Paris
- Lin JY (2006) Hydraulic structures. China WaterPower Press, Beijing (in Chinese)
- McBirney WB (1958) Some experiments with emergency siphon spillways. *J Hydraulics Div ASCE* 84(5):1–24
- Ministry of Water Resources of the People's Republic of China (2000) SL253-2000 "Design Code for Spillway". China Waterpower Press, Beijing (in Chinese)
- Novak P, Moffat AIB, Nalluri C, Narayanan R (1990) Hydraulic structures. The academic division of Unwin Hyman Ltd, London
- Peterkaon AJ (1956) Morning-glory shaft spillways: a symposium: performance tests on prototype and model. *Trans ASCE* 121(1):385–405
- State Economy and Trade Commission of the People's Republic of China (2002) DL/T 5166-2002 "Design Specification for River—Bank Spillway". China Electric Power Press, Beijing (in Chinese)
- USBR (1987) Design of small dams, 3rd edn. US Govt Printing Office, Denver
- Zuo DQ, Gu ZX, Wang WX (eds) (1987) Barrages, spillways and control works. In: Handbook of hydraulic structure design, vol 6. Water Resources and Electric Power Press of China, Beijing (in Chinese)

Chapter 13

Hydraulic Tunnels

13.1 General

Hydraulic tunnel is a water conduit formed by excavating abutment mountain or hill without removing the overlaying rock (Chen and Chen 2014; Grishin 1982; Lin 2006; National Reform and Development Commission of the People's Republic of China 2004).

Bored through competent abutment rock, the tunnel is not directly in contact with the dam embankment, and therefore, it provides a much safer and more durable layout that can be achieved with either a cut-and-cover conduit passed under or through the dam or an open-channel chute. A minimum of foundation settlement and differential movement as well as structural displacement will be experienced. In addition, the seepage along the outer surface of tunnel lining or the leakage into the rock surrounding the tunnel will be less serious. Furthermore, there is less likelihood that failure of some portion of tunnel would lead to the failure. Attributable to aforementioned inherent advantages, tunnel outlet works are preferred where abutment and foundation conditions will permit their utilization and it is economical compared with other types of outlet works.

In China, water and hydropower resources are mainly concentrated in the mountainous areas of her southwest territory with abundant rainfall, narrow and deep river valleys, sparse population, etc. In order to collect concentrated head drop, construction arrangement of long diversion tunnels and high dams are usually demanded. According to the statistics, more than 40 hydraulic tunnels with length over 5 km have been constructed nowadays, and a number of power tunnels with the length of 20–100 km will be constructed in the near future. The diameter of the spillway tunnels of the Xiaolangdi Project reaches 14.5 m. The cross section of the diversion tunnel of the Ertan Project is 17.5 m × 23 m. The maximum flow velocity in the spillway tunnel exceeds 30–50 m/s. The total installed capacity of the Jinping II Hydropower Project on the Yalongjiang River is 4 × 4 00 MW, and the diameter and length of its two power tunnels are 9.5 m and 18.7 km, respectively, with the

maximum overburden depth up to 2400 m, which raise a series of challenging problems such as high groundwater table and high tectonic stress.

China is a country with a vast territory of unevenly distributed water resources, too. In order to meet the water demand for industrial and agricultural uses in dry areas, inter-basin water transfer is highly desired. The trunk lines of some inter-basin water transfer projects have to pass through drainage divide lines and mountainous areas, which are mainly by means of hydraulic tunnels. For instance, the water diversion project from the Datong River (Qinghai Province) to the Qinwangchuan River (Gansu Province) constructed in 1994 has a main line of 86.9 km long, including 33 tunnels with total length of 75.11 km, the longest one being 15.72 km. The Yellow River Diversion Project (YRDP) diverting water from the Wanjiashai Reservoir through the Haihe River Basin to supply the Taiyuan City involves the construction of tunnels with total length over 200 km, and among them, the tunnel No. 7 of the south main canal is the longest one with a length of 42.9 km. The west line for the water diversion project from the Upper Yalongjiang River to the tributary of the Yangtze River, then continued to the Yellow River, will pass through the Bayankala Mountain. The length of any single tunnel for different alternatives will be more than 100 km and the longest one will be 243.8 km. These long tunnels are located on the altitude of above 4000 m with difficult working conditions. In addition to unfavorable conditions such as high groundwater table, high underground temperature, and high tectonic stress, there are intensive earthquakes (basic intensity over 8°) and large fault zones, which will seriously affect the design and construction.

13.1.1 Types and Functions of Hydraulic Tunnels

As one of the most important element structures in hydraulic project, the hydraulic tunnel is more and more widely applied under the following circumstances:

- When the water passage has to be carried deep underground rather than in an open cut for the reasons of economics and safety;
- Where the open water passage is inevitably subject to damages attributable to landslides, rock falls, etc.;
- Where the water passage is carried across a densely populated area.

By purposes, hydraulic tunnels may exist in following forms:

- Interconnection tunnel of reservoirs;
- Diversion tunnel during construction;
- Spillway tunnel;
- Power tunnel;
- Tailrace tunnel;
- Navigation tunnel;

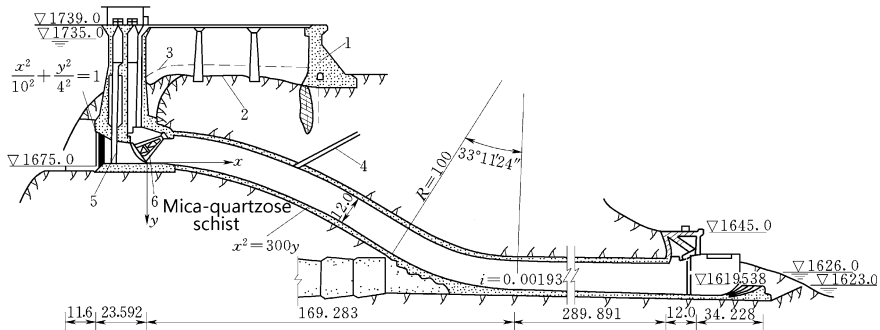


Fig. 13.1 Free-flowing tunnel for flood release (unit: m)—the Liujiaxia Project (China). 1 concrete auxiliary dam; 2 bedrock surface; 3 natural ground surface; 4 air vent; 5 bulkhead gate slot; 6 radial gate

- Surge shaft forestalling the sudden pressure changes in power tunnel due to sudden changes related to turbine operations;
- Silt flushing (excluding) tunnel for release silt piled in front of the dam;
- Drainage tunnel for release seepage water;
- Importing water tunnel for irrigation and daily life.

Apart from headrace and tailrace channels, tunnels are normally composed of intake structure, tunnel body (conduit), and outlet structure. Figure 13.1 shows the spillway tunnel in the Liujiaxia Project with arch dam (China, $H = 147$ m).

By pattern of flow, hydraulic tunnels are classified as pressure tunnel and free-flowing tunnel (non-pressure). More often but not always, the inlet tunnel flows freely. When the water level of downstream changes greatly and regularly, the tailrace tunnel may flow under pressure for the sake of reducing the height of cross section.

By position along water passage, hydraulic tunnels are distinguished as intake tunnel, transition tunnel, headrace tunnel, and tailrace tunnel.

By elevation of intakes, hydraulic tunnels fall into skin-deep non-pressure tunnel, deep non-pressure tunnel, deep pressure tunnel, and combination of deep non-pressure tunnel and pressure tunnel.

For selecting the types of hydraulic tunnels, much attention should be called at the differences between pressure tunnels and non-pressure tunnels.

- ① With regard to tunnel layout, pressure tunnel is advantageous over non-pressure tunnel.

Flow in non-pressure tunnel should be fluent and symmetric; otherwise, vortex occurs and the flow pattern in the tunnel is disturbed. However, these limitations do not exist in the pressure tunnel.

Non-pressure tunnel should be laid out as straight as possible; otherwise, transverse gradient and shock wave may demand a larger cross section. Nevertheless, the layout of pressure tunnel is more flexible.

- ② With regard to flowing condition, pressure tunnel is advantageous over non-pressure tunnel, too.

For non-pressure tunnel, many problems such as high flow velocity, complicated flow pattern, cavitation, and vibration manifest which require more net space and more smooth lining. Under the same water head and discharge capacity, these phenomena usually do not occur in pressure tunnel.

- ③ With regard to structure condition, non-pressure tunnel and pressure tunnel each has its strong and weak points.

Where surrounding rock is very strong, only a part of cross section needs lining for non-pressure tunnel, whereas the whole cross section needs lining for pressure tunnel. The pressure tunnel needs sufficient embedding depth, while the embedding depth of non-pressure tunnel is flexible. If surrounding rock is competent, the pressure tunnel possesses an advantage of utilizing surrounding rock resistance to counterbalance internal water pressure. Otherwise, the non-pressure tunnel is more advantageous.

- ④ With regard to installment and operation, non-pressure tunnel is advantageous over pressure tunnel.

Non-pressure tunnel is simple to operate and easy to maintain when accident occurs. For pressure tunnel, service gate bears huge water thrust, which needs more complicated structure to sustain.

- ⑤ With regard to engineering amount and construction conditions, non-pressure tunnel and pressure tunnel each has its strong and weak points.

Unless water head is high or surrounding rock is not competent, amount of rock excavation and concrete backfill as well as reinforcing steel for pressure tunnel is lower than that for non-pressure tunnel. On the contrary, the rock excavation, framework installation, and concrete placement for non-pressure tunnel are more convenient than that for pressure tunnel.

It is customarily recognized that non-pressure tunnel is preferable under a good layout condition, low water head, and low velocity of flow. Otherwise, use of pressure tunnel would be indicated.

13.1.2 Working Features of Hydraulic Tunnels

When designing a hydraulic tunnel, much attention should be called at its working features in the following (Bickel et al. 1996; Brekke and Ripley 1993; Golzé 1977; Hoek and Brown 1980; Szechy 1973; Xiong and Gao 1983; Wang 1987; Zuo et al. 1989):

- ① As a kind of underground works, hydraulic tunnels are tightly related to surrounding rocks. Tunneling will disturb the stress equilibrium of surrounding rock and result in stress redistribution around the tunnel, which will

bring forth considerable deformation. Temporary supporting and permanent lining should be employed for the safe construction and operation of the tunnel.

- ② Deeply located below the water, hydraulic tunnels, especially the power tunnel, diversion tunnel, and spillway tunnel, run under high internal water pressure and high-velocity flow. Therefore, the tunnel body and the lining should be strong enough to avoid vibration and cavitation damages, and the sectional shape of tunnel should be preferable for good flow pattern.
- ③ Compared with ground works, hydraulic tunnels possess many disadvantages, such as narrow construction space, heavy hauling traffic, mutual disturbance, high risk of accident, difficulty in reinforcement, complicated construction process, and requirement for high construction quality and speed. Therefore, improving construction conditions to avoid accident, and reasonably organizing construction to improve quality and speed, are very important to the design and construction of hydraulic tunnels.

13.2 Layout of Hydraulic Tunnels

It is very important to elaborate a reasonable layout scheme for the hydraulic tunnel, which can accelerate the process of construction, ensure the safety during excavation and operation, and acquire significant economic benefits. An unreasonable layout may result in fatal accident, overmuch disposing cost, and even delay of construction schedule (Ministry of Water Conservancy and Electric Power of the People's Republic of China 1984; Ministry of Water Resources of the People's Republic of China 2002).

13.2.1 Procedure of Layout

Layout of hydraulic tunnel is accomplished through the selection of tunnel route, elevation, and longitudinal grading. These three steps influence on each other and are all related to the conditions of topography, geology, construction, operation, etc. Therefore, layout of the hydraulic tunnel must be determined after thorough technical and economical studies, which comprises

- The function of the tunnel (single-purposed or multi-purposed) is firstly considered according to the tasks of the project, and then, the position, elevation, and intake of the tunnel are decided;
- The route of the tunnel is studied and accompanied by the selection of the structural type of intake and the position of control gate, taking into account of the topographic and geologic conditions;
- Longitudinal grading, type and dimension of cross section, temporary supporting, and permanent lining of representative sections are selected;

- The outlet position and its bottom elevation as well as energy dissipation devices are selected according to the conditions concerning topography, geology, tailwater level, construction, etc.; and
- Based on the comparative technical and economical studies of the alternatives, the optimum design scheme is recommended.

The optimum solution usually offers tunneling under most preferable conditions through competent rocks without considerable rock pressure and tectonic disturbances, slumps, karsts, and groundwater afflux. The recommended tunnel route also should be acceptable with regard to the sanitary hygiene, expenditure, and job management.

13.2.2 Longitudinal Profile

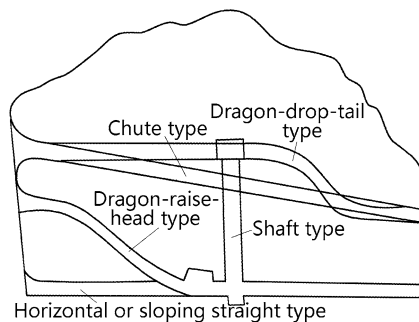
The minimum thickness of vertical and lateral overburden layers is determined by various factors such as geologic condition, shape of cross section, construction technique, internal water pressure, and type of lining. In general, for the pressure tunnel, the minimum thickness of vertical overburden is determined in accordance with the fact that it should be greater than the internal pressure head. For the intake and outlet of pressure tunnel, and the whole non-pressure tunnel, the minimum thickness of overburden is not specifically stipulated, provided that reasonable construction process and method are adopted to secure the stability during construction and operation period.

The thickness of rock wall between two tunnels is determined by the layout requirements, stress and strain state of surrounding rocks, dimensions of controlling sections, construction method, operation conditions, and other factors. Generally, two times of the diameter (or the width) of the tunnel is demanded. If the rock mass is competent, the thickness may be further reduced a bit, but not smaller than the diameter (or the width) of the tunnel.

For the hydraulic tunnel located near mountain slope, the lateral cover rather than the vertical overburden may be predominant. Under such circumstances, the efficient lateral cover should be found out by drawing a transverse profile inclusive ground surface. In case of strong fracture and stratification, special analysis to determine the stability of the rock mass should be carried out. When crossing the foundation or abutments of dam or other structures, the thickness of rock between the structure and tunnel should be secured, too.

Intake structure may take many forms, depending on the functions it must serve, on the fluctuation range in reservoir level under which it must operate, on the discharge it must handle, on the frequency of reservoir drawdown, on the floating debris conditions in the reservoir which will determine the need for or the frequency of cleaning for the trash racks, on the reservoir ice or wave actions which could affect the intake stability, etc. The entrance of free-flow tunnel should have symmetrical sidewalls, to avoid vortex detrimental for the flow pattern in the tunnel (Gordon 1970). Where the structure serves only as an entrance to the outlet conduit and where trash cleaning will not be necessary, a submerged intake structure can be employed.

Fig. 13.2 Typical longitudinal profiles of flood release tunnel



There are no special requirements for the entrance of pressure tunnel. The elevation of intake is decided by the operative requirements and flood routing computation.

The longitudinal profile of flood release tunnel may take a variety of forms as shown in Fig. 13.2:

- Horizontal or sloping straight line;
- Chute;
- Dragon-raise-head;
- Dragon-drop-tail; and
- Shaft.

For the flood release or the reservoir drawdown tunnel, the elevation of intake is usually lower than the lowest operative level added by a submerged depth, to prevent sucking-induced vortex.

In order to save expenditure, to speed up the construction schedule and to handle the difficulties associated with the layout of projects, diversion tunnels may be reconstructed into spillway tunnels with a short and high-level tunnel segment connecting to a inclined shaft (lifted head type, or dragon-raise head type, Fig. 13.1) when the river diversion has been completed. This type has been successfully exercised in many China's hydraulic projects.

Where there is silt flushing requirement, the possibility of combining silt flushing and flood releasing may be considered. Since the elevation of the intake of silt flushing tunnel is lower, this tunnel may be further used as construction diversion tunnel. Such multi-purposed tunnel has particularity of small longitudinal grading between entrance and exit, which may be longitudinally laid out in a form of straight line.

For deep flood release tunnel, the intake should be carefully designed using streamlined profile, to avoid excessive head loss and partial vacuum resulted from separation of flow from the tunnel walls. Such intake also should possess a definite submerged depth, to avoid the suck of air into tunnel giving rise to vibration. For the tunnel without task of silt excluding, the bottom of intake should be located above the silt elevation.

Longitudinal (slope) grading of hydraulic tunnels, except for vertical shaft and/or inclined shaft, is decided by the intake and outlet elevations and should be settled

for good flow condition and convenient in construction and operation. In terms of flow condition, inverse or changeable slopes should be avoided as far as possible for non-pressure tunnel. If necessary, a curved segment should be introduced to keep the flow fluent, to ensure the capacity of discharge, and to avoid the damage due to cavitation. For pressure tunnel, inverse slope should also be avoided for the consideration of convenience in draining. In terms of construction requirements, the slope should not be too steep for the convenience of excavation and slag hauling as well as material transportation. According to the engineering experience, adequate slope gradient by construction requirements is lower than $3/1000$ – $5/1000$ for railway transportation and lower than $3/1000$ – $15/1000$ for non-railway transportation. Also, according to the engineering experience, the slope gradient by draining requirements should be larger than $2/1000$. Therefore, compromise should be made between the construction requirements and draining requirements.

For a tunnel with its upstream portion be underneath the reservoir, precautions must be taken to ensure that the tunnel does not become a conduit or a pathway of leakage, particularly along the exterior wall of the tunnel lining. In hard and fractured crystalline rocks, this can be handled appropriately by installing grouting curtains around the tunnel in several locations indicated by geological investigation. In soft, fine-grained sedimentary rocks that are relatively non-fractured, grout penetration is difficult to secure. Under such circumstances, the impervious barrier can be achieved by building cutoff collars.

13.2.3 Gates in the Tunnel

In flood release tunnel, there are generally two gates: service (main) gate for routine operations and bulkhead gate for maintenance.

Bulkhead gates are usually installed at near the entrance of intake. Depending on the downstream water level, stoplogs may be used near the outlet. In medium to large flood release tunnel, the bulkhead gates are usually demanded to be shut in flowing water in case of accident fraught with dangerous consequences, but only opened in tranquil water, which are also termed as “emergency-guard gates.”

Service gates may be installed at the entrance, exit, or a proper position intermediate the tunnel body.

The tunnel with service gate at its entrance is usually non-pressure (Fig. 13.1). To ensure the free-flowing pattern in tunnel, the top of the tunnel after gate should be higher than the flow surface, and sufficient air vent is demanded. The advantages of such layout are as follows: facilitation in management with integrated service gate and bulkhead gate be in the intake and convenience in inspection and repair of non-pressure tunnel body. The disadvantages of such layout are as follows: If the profile of intake is inadequate or construction quality is poor, cavitation damage could be induced by high-speed flow (Knapp et al. 1970). The tunnel with service gate at intake also might be pressure; however, such layout ordinarily should be avoided except for low-speed diversion tunnels, due to the worry over the possible

cavitation and vibration resulted from unstable and complex flow during the operation of gate.

The tunnel with service gate at outlet is ordinarily pressure (Fig. 13.3). The advantages of such layout are as follows: good flow pattern in tunnel, good air vent condition behind gate, high flexible operation (e.g., partial opening), and convenient management. The disadvantages of such layout are as follows: High pressure is often exerted in tunnel; and if cracking gives rise to lining, seeping water will menace the stability of adjacent structures and tunnel itself. To overcome the disadvantages of such layout, emergency-guard gate may be installed at the intake to shut the tunnel and keep the tunnel in non-pressure state during the period without flood release operation.

Under certain circumstances, the service gate may be laid out in a proper position intermediate of tunnel; in this way, the tunnel segment in front of the gate is pressure, while that behind the gate is non-pressure (Fig. 13.4). This layout is mainly attributable to the considerations in the following:

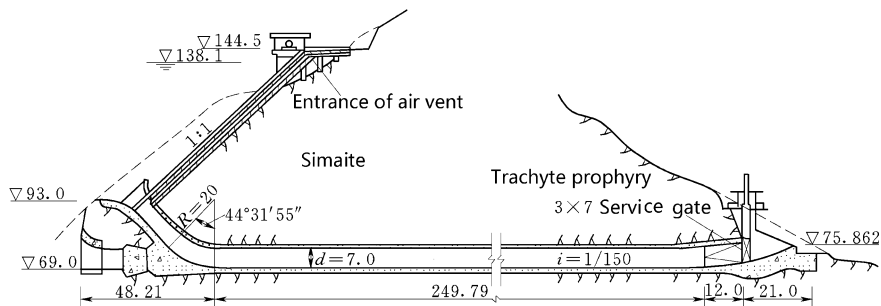


Fig. 13.3 Gate layout and longitudinal profile of the flood release tunnel (unit: m)—the Xianghongdian Project (China)

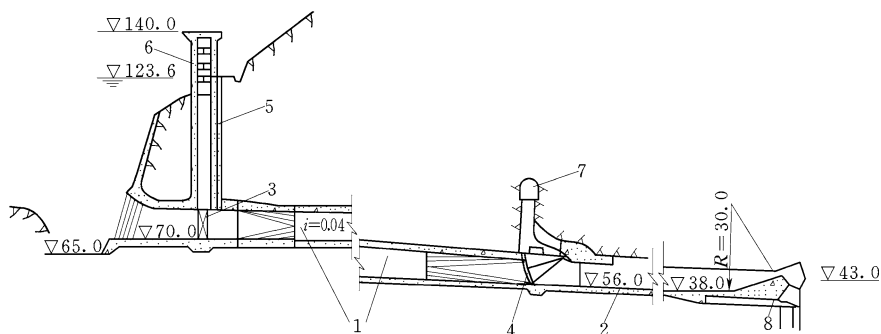


Fig. 13.4 Combination of pressure and non-pressure flood release tunnel (unit: m)—the Xingfengjiang Project (China). 1 pressure segment; 2 non-pressure segment; 3 bulkhead gate; 4 service gate; 5 air vent; 6 hoist tower; 7 operation chamber of service gate; 8 flip bucket

- Restrained by the factors related to topography, geology, construction, and project layout, the tunnel should be curved. To meet the requirements for good flow pattern, the gate should be installed at the straight segment after the bending transition;
- With a geology condition much better than that of exit, the intermediate gate may transfer the water thrust to rock mass reliably.

13.2.4 Route of Tunnels

Generally speaking, hydraulic tunnel should be located in the intact, strong, and stable rock masses, where tectonization is simple, overlying rock is thick, and hydrologic and geologic conditions are excellent. The tunnel should be as short and straight as possible, for the sake of saving excavation amount, obtaining good flow pattern, reducing head losses, enhancing economic benefits and construction conditions, and meeting the requirements for the overall project layout.

- ① The most favorable tunnel layout is straight with shortest length. In terms of topography, if the river is bending, hydraulic tunnel should be located on the convex bank to shorten the tunnel length and to improve flow condition by connecting intake and outlet flow with river fluently. When a tunnel swerving in the plane is inevitable, bending angle and curvature radius should be chosen properly. In general, with regard to the tunnel of lower flow velocity ($v \leq 10$ m/s), swerving angle should be smaller than 60° , and curvature radius should be not smaller than 5.0 times of the diameter (or the width) of tunnel. The length of each straight tunnel segments on the both sides of the bending should not be smaller than 5.0 times of the diameter (or the width) of tunnel. Whereas with regard to the tunnel of higher flow velocity, angle and curvature radius are determined by hydraulic modeling tests.

For non-pressure tunnel with high flow velocity, swerving in the plane should be avoided.

- ② In terms of geology, the weak rock strata with abundant groundwater should be shunned. Strong, intact, dry, and stable rock masses are desirable, for reducing surrounding rock pressure and external water pressure exerting on the lining and for facilitating construction. Although such requirements will probably lengthen the tunnel, it may be reasonable taking into account of overall expenditure. When hydraulic tunnel crosses stratification rock stratum, tunnel axis should keep an sufficient included angle with the orientation of stratification. In case of stratification with steep obliquity, for the purpose of sustaining the pressure from surrounding rock mass and external water, it is demanded that:

- The included angle should be not smaller than 30° in massive blocky rock masses;
- The included angle should be not smaller than 45° in laminar rock masses.

Temporary supporting is required when detrimental faults, joints, and groundwater are inevitable. In high tectonic stress areas, the tunnel is better to be parallel with the direction of the maximum principal stress.

- ③ The position of intake should keep away from steep slopes and narrow valley (gully); otherwise, asymmetric inflow pattern will appear, which will influence the capacity of discharge, the state of flow, and the distribution of pressure. Too flat topography of tunnel portal will raise engineering amount of intake structure by lengthening intake channel.
- ④ The outlet should adjoin the downstream river channel smoothly and keep sufficient distance from the toe of embankment dam or other structures, to avoid the erosion and scouring of rapid current to the dam toe and the normal operation of the other structures.
- ⑤ For the intake and outlet near ground surface where the rock masses are fractured and weathered to some extent, proper reinforcement for the cut slopes, if necessary, is installed.
- ⑥ Hydraulic tunnel should cross intact ridge and avoid passing over gullies and valleys as far as possible, to ensure the sufficient strength and thickness of overlaying rock. The rock around a gully or valley is usually very weak and will give rise to extra treatment expenditure, difficulty with construction, and other adverse situations. The possibility for a tunnel passing dam foundation or abutments should be carefully studied to secure the sufficient thickness between the tunnel and the influenced structures, with regard to the requirements for stress, strain, and seepage.
- ⑦ When the hydraulic tunnel is very long, several fork tunnels may be installed in advance, for adding work faces of excavation, accelerating construction speed, and assuring ventilation as well as material transportation. Fork tunnels may be horizontal, inclined, or vertical, according to geology and other factors. As for the fork angle with main tunnel, an included angle from 30° to 60° may be feasible. In the Diversion Project from the Luanhe River to the Tianjin City (China), 15 inclined fork tunnels and 6 vertical fork tunnels were laid out in a 9.68-km-long diversion tunnel.

13.3 Intakes

Intake structure is located at the entrance of tunnel meeting the needs of overall layout, flowing condition, and rock stability. The design of overflow intake has been discussed in Chaps. 11, and 12; therefore, only the design of pressure tunnel intake will be addressed herein.

The pressure tunnel entrance can be placed vertically, inclined, or horizontally, depending on the intake requirements. Where a sill level higher than the tunnel level is desired, the intake can be in a form of drop inlet. A vertical entrance is usually provided for an intake at the tunnel level. In certain instances, at small installations where the gate is placed and operated on the upstream slope of a low dam, an inclined entrance can be employed. In most cases, tunnel entrances should be rounded or bell mouthed to reduce hydraulic losses.

13.3.1 Types of Tunnel Intakes

According to the form and layout of structure, intakes of tunnel can be grouped into the four basic types as shaft intake, tower intake, bank-tower intake, and inclined intake.

1. Shaft intake

Figure 13.4 shows this type of intake, in which the trash rack is provided at the entrance, while the gate coordinated at a certain distance downstream of the entrance is operated through a vertical shaft approachable from hilltop. The advantages of this type over the other types are as follows:

- Compared to the inclined intake, the trash rack size is the same, but the size of gate is considerably reduced, and hence, it can resist much higher heads;
- Compared to the tower intake, vertical shaft is a stiff and low structure, which might be preferable in highly seismic zone.

The operation of trash racks for cleaning purposes and the reparation of the entrance before the gate are only possible when the reservoir level draws down. The trash rack may then be approached either by road at that level or through a barge.

Since the gate is located at a place quite downstream of the entrance, its size is considerably reduced equal to that of conduit size. As a result, vertical lift plate gates can be substituted by radial gates.

The shaft-type intake will be suitable where the head is very high, hillslopes are not stable, and the abutment rock is competent for constructing shaft.

Shaft may be wet or dry, depending on the tunnel type and working condition. For non-pressure tunnel behind bulkhead gate, the radial gate or plate gate with front seal element may be installed in the shaft, to keep the shaft dry. If the plate gate with rear seal element installed in the shaft as bulkhead gate, the shaft is always wet. The structural analysis for the shaft is normally controlled by the construction situation or the repairing situation when there is no water in the shaft. After the estimation of surrounding rock mass pressure according to the geologic and construction conditions, several horizontal representative sections of unit height may be analyzed as closed frame structures.

2. Tower intake

In the tower intake, the entry of water is through a tower (Fig. 13.1) connected to the tunnel. Sometimes, a tower-type intake is also installed in the masonry dam and it may be treated as a type of dam intake.

Gates generally installed in this kind of intake are of the cylinder type (vide Chap. 15).

The advantages of tower intake are as follows:

- The whole tunnel may be inspected and repaired by shutting gates in the tower;
- The closed tower structure may resist very high head; and
- The multilayered inlets may be installed at different altitudes, which enable to convey water from different reservoir levels, and this is important for the reservoir with very large-level variation or with different water-importing purposes of different temperatures.

The disadvantages of the tower intake are as follows:

- The top of the tower for operating the gates and trash rack can only be accessible by means of an approach bridge connecting the hilltop to the tower;
- Due to the worry over that the tower is a tall and slender structure, it might not be applicable in a highly seismic zone; and
- The tall and slender structure is also vulnerable to the actions of wave, wind, freeze, etc.

To lighten the structure and to raise the resistance to the actions attributable to earthquake, wave, and wind, frame-type tower intake may be employed. However, it permits repair only when the reservoir elevation is low, and the poor flow pattern of gate sill would give rise to cavitation. Therefore, this variant type of tower intake is seldom used in large project.

3. Bank-tower intake

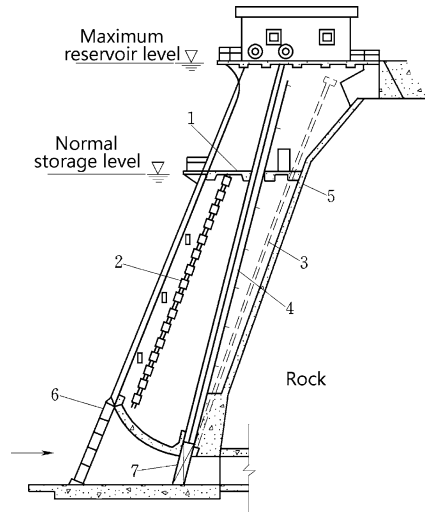
In this intake of hydraulic tunnel, a closed or framed tower is built on the hilltop, the underside of which is laid on the bank slope with reliable stability. The intake also provides inverse support for the rock slope (Fig. 13.5). The construction and installment of bank-tower intake are very convenient, and the access bridge may be very short or even be ignored. Bank-tower intake is suitable for the work site where the bank slope is very steep and the rock is very strong and integrity.

4. Inclined intake

In the inclined intake, the gate is operated on the guides placed parallel to the inclined hillslope, as shown in Fig. 13.3. Trash racks are placed upstream of gates, and they are operated from the operating platform seated on the hilltop. The inclined intake is one of the cheapest arrangements for operating tunnel since it employs natural hillslope with minor excavation. The selection of this type of intake would depend upon the stability of hillslope and a suitable platform being available at the hilltop for operation purposes. It is evident that the size of trash rack and gate

Fig. 13.5 Bank-tower intake.

1 operation platform for trash rack cleaning; 2 fixed trash rack; 3 air vent; 4 gate track; 5 rock bolt; 6 movable rash rack; 7 emergency gate



as well as the hoisting capacity will be larger related to the inclination of the slope. Hence generally, it is not preferable for very high heads although its popularity is increasing.

The aforementioned four basic types may be combined according to the conditions of topography, geology, tunnel layout, operation, and construction. For example, the No. 1 silt flushing tunnel of the Sanmenxia Project with gravity dam (China, $H = 106$ m) uses the combined intake of shaft and tower (Fig. 13.6).

13.3.2 Components of Tunnel Intakes

1. Transition

Transitions from one sectional shape to another are required either due to practical or structural considerations such as at the gate shaft and intake, or geological considerations such as at the place where poor ground might necessitate circular steel lining (Singh 1969).

From either entry into or exit from the tunnel, transitions are also needed to reduce head losses and to avoid cavitation. The converging transitions, in general, cause less head losses than the diverging ones.

The length and shape of transition depend upon the velocity and flow conditions in the tunnel, economic, and construction restraints, etc. Studies by hydraulic modeling should be conducted to determine an efficient and economical design of the transition.

To obtain best inlet efficiency, the shape of the entrance should simulate a jet discharging into air and should guide and support the jet with minimum interference until it is contracted to the tunnel dimension. If the entrance curve is too sharp or

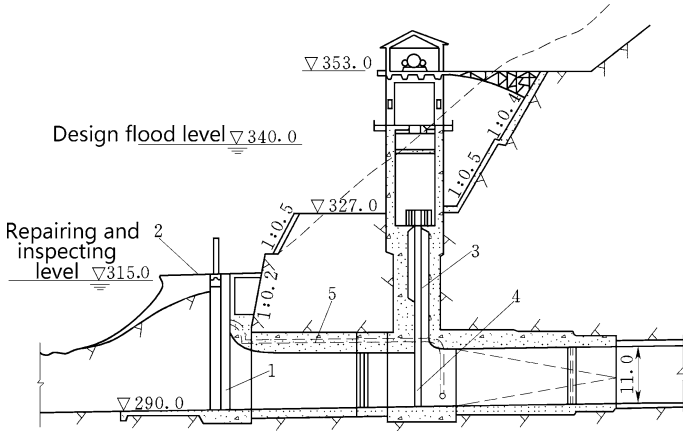


Fig. 13.6 No. 1 silt flushing tunnel (unit: m)—the Sanmenxia Project (China, $H = 106$ m). 1 stoplog slot; 2 deposit platform of stoplogs; 3 gate shaft; 4 emergency-guard (bulkhead) gate; 5 equalizing (bypass) pipe

too short, subatmospheric pressure may be induced and cavitation will manifest. A bell mouth entrance conforming to or slightly encroaching upon free jet profile will provide the best entrance shape, which is customarily configured using a quarter of elliptical curve (vide Figs. 13.1 and 13.5):

$$\frac{x^2}{a^2} + \frac{y^2}{b^2} = 1 \tag{13.1}$$

where a = long half-axis, which is the height of tunnel at the gate for the vault curve and the width of tunnel at the gate for the sidewall curve; b = short half-axis, which is 1/3 of the height of tunnel at the gate for the vault curve and 1/3–1/5 of the width of tunnel at the gate for the sidewall curve.

The contraction rate should be smaller than 0.5–0.55. In practical application, the length of transition may be a little shorter than one-quarter of ellipse, but usually not shorter than a half of the tunnel height at the gate. For very important project, hydraulic modeling should be conducted to finally determine the shape of bell mouth. For non-pressure tunnel, the vault between bulkhead gate and service gate should have a slope with a gradient of 1:4–1:6 toward downstream, to raise the pressure in the intake and to avoid cavitation.

The length of transition from behind the gate with rectangular shape to the tunnel body with circular shape should not be shorter than 2–3 times the diameter (or the width) of tunnel, to secure a fluent flow.

2. Air vent

An air vent of sufficient capacity located downstream of the control gate is demanded for the following purposes:

- To admit air entry when the gate is closed and the water in the tunnel recedes down;
- To exhaust air when the pressure tunnel is being filled through bypass pipes to balance the water pressure on the two sides of the bulkhead gate prior to its being lifted up; and
- To control sub-pressures downstream of gate at its partial opening.

The air vent is usually embedded within concrete as shown in Figs. 13.3 and 13.5, and its top should be above the maximum reservoir level. The cross section of air vent is conventionally circular with a size dependent on the air discharge and the rate of air. Air discharge Q_a is related to the water discharge and flow state in the tunnel. The empirical Eq. (13.2) may be used to estimate the cross sectional area of the air vent a

$$a \geq 0.09 \frac{V_w A}{[V_a]} \quad (13.2)$$

where $[V_a]$ = allowable air velocity in air vent (selective within 40–50 m/s); A = area of the tunnel cross section after gate, m^2 ; and V_w = water flow velocity in the tunnel.

3. Equalizing (bypass) pipe

Between the operation (service) gate and bulkhead gate, bypass pipe is installed in frusta or gate (Fig. 13.6). After the inspection and/or reparation of tunnel, the operation gate is shut down; the water is filled through the bypass pipe to obtain water pressure balance on the both sides of the bulkhead gate; and in this way, the raising effort for the bulkhead gate is reduced efficiently. The size of bypass pipe is determined by the time needed for filling up the space between the bulkhead gate and service gate (usually shorter than 8 h).

4. Trash rack

The trash rack is generally of a coarse type, which means that the clearance between bars forming the rack is large, so that only large drifts such as cakes of ice, roots, trees, and timbers are prevented from entering into the tunnel (Fig. 13.5). The trash rack for the intake is an important element requiring proper design and protection against trash by cleaning operation, as the drag due to trash rack in flow path will significantly lead to a loss of head and consequently the loss of energy. This head loss will be dramatically raised if the racks are clogged.

The necessity for the trash rack on a tunnel depends on the tunnel size, the type of control device used, the nature of the trash burden in the reservoir, the utilization of the water, the need for excluding small floating debris from the outflow, and other factors. These factors will determine the type and size of trash racks. The trash rack layout will also depend on the accessibility for removing accumulated trash.

13.4 Body of Tunnels

13.4.1 Shape of Cross Section

Various sectional shapes of tunnel such as horseshoe shape, city wall gate shape, and circular shape are widely exercised according to the usage, hydraulic requirement, geology setting, lining or bracing type, and construction condition (Ministry of Water Conservancy and Electric Power of the People’s Republic of China 1984; Ministry of Water Resources of the People’s Republic of China 2002). Figure 13.7 shows commonly used sections of lined tunnels.

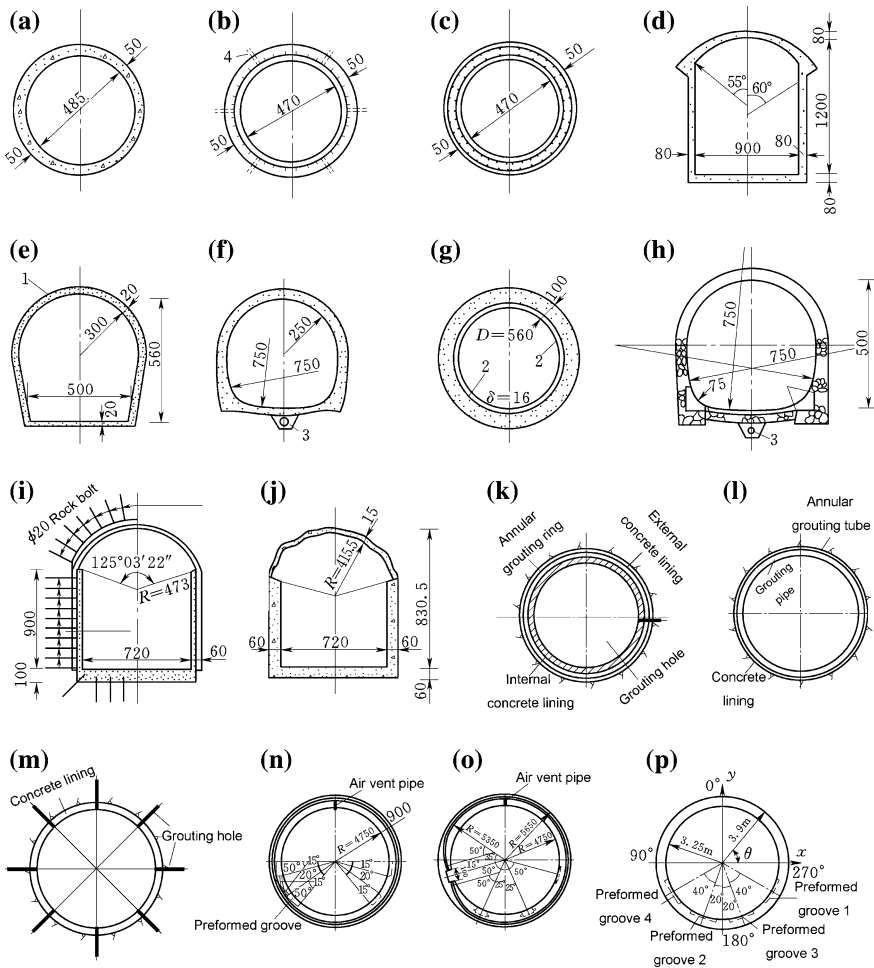


Fig. 13.7 Typical sections of lined tunnel (unit: cm). **a–f** Single shell lining; **g–j** combined lining; **k–p** prestressed lining. *1* shotcrete; *2* steel sheet; *3* draining pipe; *4* draining hole

Circular shape (Fig. 13.7a–c, g, k–p) is hydraulically and structurally desirable for pressure tunnel attributable to its most efficient. If the diameter and inner or external water pressure are not very high, the other shapes also may be employed to facilitate the construction. In case of poor geology condition, circular or horseshoe shape (Fig. 13.7f, g) is strongly recommended.

Horseshoe section (Fig. 13.7f, g) possesses a semicircular roof together with arched sides and invert. A horseshoe tunnel would be advantageous where a partial full channel providing better hydraulic flow is required, but it is not as efficient as the circular shape for carrying external loads. However, if a tunnel of this shape is lined, it may provide strong resistance against external loads on its sidewalls. For small pressure tunnels under only moderate heads, the horseshoe tunnel may be permissible, depending upon foundation conditions.

City wall gate section is commonly employed for free-flowing tunnels (Fig. 13.7d, e, i, j). The central angle of the vault arch is usually 90° – 180° . However, a central angle smaller than 90° is also possible for the purpose to obtain larger thrust of arch abutments. The height to width ratio of the section is normally ranged between 1 and 1.5, which is dependent on the hydraulic and geology conditions, particularly on the tectonic stress state: Larger water-level variation or larger vertical tectonic stress (compared to the horizontal one) indicates larger ratio; on the contrary, small ratio is recommended.

For a long tunnel with changeable geology conditions, composite shape comprising different sections can be or have to be adopted, particularly for tunnels of free flowing where only partial lining is required. Smooth transition between different sections and linings is demanded.

13.4.2 Cross-sectional Dimension

The maximum practicable size of a tunnel will be governed by the structural considerations related to supporting the roof during and after construction and thus will be dependent upon the nature of rock. The minimum practicable size of a tunnel depends upon the method of construction employed, permissible flow velocity, as well as the design discharge. It has been a common engineering experience that the greater number of tunnels, the greater cost will be, while the operation might be more flexible. Hence, the criteria for finding the economic diameter and lane number will be different related to the specific type of tunnel.

Where a tunnel interconnecting two reservoirs serves to divert a particular discharge Q from one reservoir to the other, the discharge, the length of the tunnel, and the receiving reservoir level are all fixed, and the variables are the dam height at the diverted reservoir and the tunnel diameter. If the tunnel diameter is kept low, then there will be greater drag loss in the tunnel requiring greater water head at the diverted stream and consequently higher dam. Therefore, smaller tunnel diameter would mean less tunnel cost but more dam cost. Thus, the economics of the system can be worked out by considering the minimum overall cost comprising dam and

the tunnel. Since the algorithm connecting the dam height with the tunnel diameter will be quite complicated, it would be expedient to find out the total cost with a number of tunnel diameters by drawing a curve with tunnel diameter as abscissa and total cost as ordinate and then reading off the diameter with the minimum cost from curve.

Where a purely diversion tunnel is contemplated along with the construction of temporary cofferdam, height of the cofferdam and its cost will be interrelated with the tunnel diameter. The same aforementioned criteria can be followed for determining the tunnel diameter and cofferdam height. The overall minimum cost will entail the optimal tunnel diameter and cofferdam height.

The minimum diameter of a headrace tunnel is subject to the constraints of workability during construction and based on relative economics. Larger diameter would mean smaller drag energy losses, which in turn means greater capital cost and less revenue loss. On the other hand, smaller diameter would mean smaller capital cost but larger revenue loss.

The diameter of spillway tunnel is also restrained by the maximum permissible velocity.

The discharge capacity of pressure tunnel is calculated by

$$Q = m\omega\sqrt{2gH} \quad (13.3)$$

where m = discharge coefficient taking into account of the friction (drag) losses and the local losses (e.g., trash rack interferences, entrance contractions, contractions and expansions at gate installations, bends, gate, and valve constrictions) of the tunnel; ω = sectional area of the tunnel outlet, m^2 ; and H = surcharge head, m .

Hydraulic grade line is worked out using the energy equation. To ensure the pressure state, the pressure margin on the tunnel vault should be larger than 2 m. The higher the flow velocity, the larger the pressure margin should be. For high-speed pressure tunnel, the pressure margin could be higher than 10 m.

The discharge capacity of free-flowing tunnel is decided by the pressure segment of the intake, which is also calculated by Eq. (13.3). For the section behind service gate, the surface of free flow is obtained by energy equation. To ensure the free-flowing state, freeboard above flow surface is needed: For low velocity and well air vented tunnel, the freeboard should be higher than 40 cm and the corresponding free area should be larger than 15 % of the whole tunnel sectional area; for high-velocity tunnel, the free area should be greater than 15–25 % of the whole tunnel sectional area after considering the aeration and shock wave. For city-gate tunnel, the peak of shock wave should be restrained below the vertical sidewalls.

In the design of tunnel sectional dimension, requirements for construction and inspection are also taken into account. Usually, the area of non-circular tunnel is not smaller than 1.5×1.8 m and the interior diameter of circular tunnel is not smaller than 1.8 m.

13.4.3 Lining of Tunnel Body

1. Purposes of lining

Lining is provided in the tunnel for both the hydraulic and structural reasons. The smooth boundary surfaces reduce frictional resistance and permit a smaller tunnel diameter for a specific discharge capacity. Lining is used to prevent the surrounding rock mass from the detrimental seepage, too. Structural lining is installed to support the tunnel against raveling or yielding surrounding rocks.

2. Types of linings

The first step in the lining design is to select appropriate lining type based on the functional requirements, geologic and hydrologic conditions, construction, and economic considerations.

(a) Protection (pavement) lining

Pavement lining is usually furnished with concrete, shotcrete, or masonry to reduce seepage and Manning's number related to surface roughness. But pavement lining is unable to bear loads. Pavement lining is also named as smooth lining, which is ordinarily employed for low-head tunnels in solid and hard rocks. The thickness of pavement lining may be determined by the requirements for shrinkage, temperature change, and concrete placement.

(b) Single-layered lining

Single-layered lining is usually accomplished with concrete (Fig. 13.7a), reinforced concrete (Fig. 13.7b–d), steel, and masonry.

A concrete lining is primarily placed to protect the rock from exposure and to provide a smooth hydraulic surface. Most shafts that are not subject to internal pressure are lined with concrete. This type of lining is advisable where the rock is in equilibrium prior to the concrete placement, the loads on the lining are expected to be uniform and radial, and leakage through minor shrinkage as well as temperature cracking is acceptable. The concrete lining is generally not acceptable for tunnels through soil overburden or in badly squeezing rock exerted by non-uniform actions.

The concrete grade should be higher than or equal to C15, generally based on 28d of age. If longer age (e.g., 90d in the Three Gorges Project) is exploited, studies and verifications should be undertaken.

The reinforcement bars of single layer should be placed close to the inner face of the lining to resist temperature and shrinkage stresses. This lining will remain basically undamaged for a deflection up to 0.5 %, defined as relative diameter change.

Where the internal tunnel pressure exceeds the external surrounding rock pressure and groundwater pressure, a steel lining might be required to prevent hydro-jacking (hydraulic fracturing) of the rock.

Single-layered lining is preferable for large cross section and high-head tunnels of moderate geologic condition. The thickness of concrete lining is ordinarily 1/8–1/12

of the width or the diameter of tunnel and not smaller than 25 cm, which is estimated by engineering experiences and finally decided by the structural analysis.

(c) Combined lining

Multilayered lining may be necessitated under the circumstances of large internal pressures, or squeezing/swelling ground, to resist potential non-uniform ground displacements with a minimum of lining deflection. There are various types of such lining, e.g., steel plate or shotcreted steel mesh internally + concrete or reinforced concrete externally (Fig. 13.7g); concrete at tunnel crest + masonry at sidewalls (Fig. 13.7h); and bolt and shotcrete at crest + concrete or reinforced concrete at sidewalls and bottom (Fig. 13.7i).

The Diversion Project from the Luanhe River to the Tianjin City, a 5 km segment of the 9.68 km-long diversion tunnel adopted bolting and shotcrete supporting, of which 1.7 km segment is equipped with shotcrete + concrete lining. The power tunnel for the underground power house in the Three Gorges Project has large cross section and high interior pressure, and the steel plate + reinforced concrete lining was installed. Figure 13.7g shows the outlet of the flood release tunnel with double-layered lining using steel plate + reinforced concrete in the Fengjiashan Project, whose inner pressure head is 70 m. In the design related to steel lining, care should be exercised for the buckling failure, under the circumstances of particularly high external water pressure.

(d) Prestress lining

Construction practice has shown that cracking of different scales will always manifest in tunnel linings due to the actions of concrete contraction and thermal stress. Where the seepage of internal water may lead to serious consequences such as the instability of hillslope and the softening of surrounding rock, the prestress should be applied for the concrete lining to secure a compressive state or to limit tensile stress within the allowable value, and in this way, the concrete cracking is avoided.

The construction of prestress lining may be implemented in two manners:

- High-pressure grouting for surrounding rock is conducted to make lining in a pre-compressive state. After the hardening of cement slurry, concrete lining still maintains a certain compressive stress. This is named as the grout prestressing. The grout prestressed lining is further subdivided as inner ring grouting (Fig. 13.7k), annular-tube grouting (Fig. 13.7l), and drill grouting under high pressure (Fig. 13.7m).
- Pipes or holes are buried or left inside the concrete firstly, and then, the bars or stranded cables are put through the pipes or holes. Reinforcing bars in lining are stretched using mechanical apparatus to produce pre-compressive stress in lining. Presently, only posttension method is employed to prestress lining. According to whether the pipes being filled by cement slurry after the stretching, the posttensioning is further subdivided as binding (Fig. 13.7n, o) and non-binding (Fig. 13.7p) types.

The grout prestress lining was exercised in the power tunnel of the Huangce Project (Hunan Province, China, diameter $D = 1.8$ m, interior head $H = 310$ m) and in the power tunnel of the Baishan Hydropower Project (Jilin Province, China, diameter $D = 3$ m, interior head $H = 150$ m). The posttension prestress lining was exercised in the power tunnel of the Geheyan Project (Hubei Province, China, diameter $D = 9.5$ m, interior head $H = 121.5$ m) and the power tunnel of the Xiaolangdi Project (Henan Province, China, diameter $D = 6.5$ m, interior head $H = 123$ m).

It may be necessary to select different lining types for different segments of a specific tunnel. For example, a steel lining may be demanded for a segment of pressure tunnel with low overburden or poor rock, while other segments may require a concrete lining solely or even without lining at all. A watertight lining may be installed through permeable zones or through strata with gypsum or anhydrite, but may be omitted for the remainder of the tunnel. Sometimes, however, concerns of construction will make it appropriate to select identical lining type throughout the whole tunnel.

The provision of reinforcement in the tunnel lining complicates the construction sequence. For free-flowing tunnels, reinforcement is not provided to merely resist external loads. However, the tunnel should ordinarily be reinforced wherever the overburden depth is less than the internal pressure head. An adequate amount of both longitudinal and circumferential reinforcement may be installed, if necessary, near the portals of both pressure and free-flowing tunnels, to resist loads resulting from loosened rock headings or from sloughing of the portals.

3. Selection of lining type

Ordinarily, pressure tunnels in competent rock do not demand lining reinforcement for withstanding full internal hydrostatic pressure, where the rock overburden has sufficient weight and lateral resistance is reliable to prevent blowouts. Concrete lining is only intended to provide watertightness in seamy rock and to smooth surface for better hydraulic flow pattern.

Where pressure tunnels are placed through less competent rocks (jointed or soft), the tunnel lining must be designed to withstand external pressure and rock loadings in addition to internal hydrostatic pressure. Near the entrance where external pressures may be nearly counterbalanced by the internal pressures, the lining may be reinforced to withstand rock loads only. However, if bulkhead gate is used for emptying the tunnel, an unbalanced hydrostatic condition will occur. At the outlet where external water pressures diminish, the design of the tunnel lining will need to consider both the external loads from the surrounding rock and internal water pressures.

For free-flowing tunnels in competent rock, particularly for flood release, city-gate type with single-layered lining (Fig. 13.7d) is conventionally practiced. Lining might be provided only along the sidewalls and bottom floor to form a smooth waterway. In less competent rock, lining of the complete cross section may be necessary to prevent caving. It is also practically possible to use bolts and shotcrete lining at the crown, while the sidewalls and bottom floor are lined using shotcrete,

reinforced concrete, or precast blocks, which may be back-tied to surrounding rock by rock bolts, if necessary. For a free-flowing tunnel segment immediately adjacent to the reservoir or just downstream of a pressure tunnel segment, cognizance must be taken of the possibility of hydrostatic pressure buildup behind the lining due to the leakage through the walls of the pressure tunnel or due to the seepage from the reservoir. Ordinarily, such external water pressure can be relieved by grouting and by providing draining holes through the lining.

The need for lining a tunnel in which an independent pressure pipe is installed depends entirely on the competency of surrounding rock. Since such a tunnel is used to accommodate the pressure pipe and provide access to an upstream gate, sufficient lining to avoid rock falls might be installed for the protection of pipe and operating staff personnel.

Initial ground supports (e.g., bolt and shotcrete support, steel ribs, and lattice girders) are installed shortly after the excavation in order to maintain the underground opening safe until permanent support is implemented. The initial ground support also functions as the permanent ground support or as a part of the permanent ground support system. Therefore, the initial ground support must be selected in view of both its temporary and permanent functions. If strong initial support has been implemented due to geologic features, permanent support may be reduced.

Generally, unlined tunnels may be employed only for construction diversion under the circumstances of good geologic condition and occasionally may be used for water feed of power plant, such as the Yuzixi 1 Project. In the unlined tunnel, water has direct access to the rock, and leakage into or out of the tunnel will occur. Changes in pressure may give rise to water pulsation in rock fractures, which in the long term can wash away fines and result in rock instability. In addition, metal ground support components (e.g., bolts) can be corroded, and certain rock types may be suffered from deterioration in water, given enough time. The rough surface of an unlined tunnel gives rise to a higher Manning's number; as a result, a larger cross section may be demanded. For an unlined tunnel to be feasible, the rock must be inert to water, be free of significant filled joints or faults, be able to withstand the pressures in the tunnel without hydraulic jacking or other deleterious effects, and be sufficiently tight that leakage rates are acceptable. Poor surrounding rocks in an otherwise acceptable formation can be locally supported and sealed. Occasional rock falls can be expected, and rock traps to prevent debris from entering valve chambers or turbines should be installed in front of the hydropower plant. Unlined tunnels are ordinarily furnished with an invert pavement consisting of 100–300 mm thick unreinforced or nominally reinforced concrete, to provide a smooth surface for maintenance traffic and to reduce erosion.

According to the influence of water seeping from the tunnel on the stability of surrounding rock, cut slopes on the tunnel portals as well as adjacent buildings, the lining design of concrete and reinforced concrete can be performed based on the standards either of crack prevention or of crack aperture limitation. In the design using crack aperture limitation, the maximum calculated aperture of cracks should be confined within the range of 0.15–0.4 mm. However, it should be indicated that

the crack prevention or crack aperture limitation has only a relative sense, and engineering practices and a lot of in situ observations performed in pressure tunnels show that cracking cannot be prevented in lining even if the tunnels have been designed according to the standard of crack prevention. There also exists a great difference between the real aperture of lining cracks and the calculated one. Where there is suspiciously unacceptable seeping water through lining cracks, some special engineering measures such as combined lining or prestress lining should be taken to control the occurrence and propagation of cracks.

4. Joints in lining

Depending on tunnel size and other factors, hydraulic tunnel is customarily lined in segments of certain length. The entire cross section may be placed at one time, or the invert may be placed first or last. Sometimes, precast segments are placed in the invert to protect a sensitive rock from the detrimental effects of tunnel traffic, followed by the placement of crown concrete. All these will leave transverse and longitudinal temporary joints in the lining. The spacing of transverse joints is selected according to the placement capacity. The longitudinal joints are, if necessary, installed either at the top, or at the intersection of sidewall and bottom floor, or at other portions where inner forces are small.

To prevent cracking damages due to dry shrinkage and thermal actions, permanent transverse contraction joints sealed by water stops are also demanded as shown in Fig. 13.8. The joint is ordinarily spaced 6–12 m apart, and the harder the surrounding rock masses, the smaller the joint spacing will be. The water conveying tunnel of the ship lock in the Three Gorges Project (Hubei Province, China) had permanent contraction joints spaced 12 m apart by the preliminary design. During the initial construction phase, fairly large number of cracks emerged at its middle portion. After comprehensive studies, the joint spacing was reduced to 8 m, and thermal control measures were strengthened. As a result, future cracking did not appear anymore.

When the tunnel passes through faults or weak seams, lining should be thickened (Fig. 13.8). Under the circumstances, permanent expansion and settlement joints should be installed at where the sudden change of lining thickness takes place.

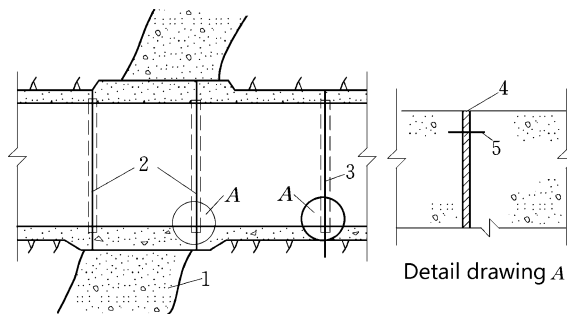


Fig. 13.8 Transverse permanent joints in the lining at a fractured zone of fault. 1 fractured zone of fault; 2 expansion and settlement joints; 3 expansion joints; 4 asphaltic felt; 5 sealing sheet

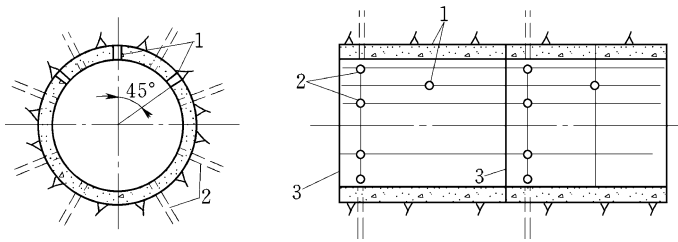


Fig. 13.9 Layout of grouting holes. 1 backpack grouting hole; 2 consolidation grouting hole; 3 expansion and contraction joint

Expansion joints also should be installed at the portions with anticipated large deflection, such as the conjunctions of intake, outlet, and transition.

5. Grouting

Grouting is routine in the construction of hydraulic tunnels nowadays, which is distinguished as backpack (backfill) grouting and consolidation grouting (Bowen 1981).

Holes for backpack grouting and consolidation grouting are normally arranged along the tunnel axis of certain intervals, as shown in Fig. 13.9.

(a) Backfill grouting

When a tunnel lining has to withstand appreciable loads, either external or internal, it is essential that the lining works uniformly with the surrounding rock mass. Hence, significant voids which are often the result of imperfect concrete placement behind the arch crown above vault cannot be tolerated. Since voids are virtually inevitable in blasted tunnels with irregular overbreak, it is therefore backpacked through standard grout holes that have been either preplaced or drilled through the finished lining.

Grouting is normally undertaken following the placement of tunnel or shaft linings (Fig. 13.9). This grouting usually employs Portland cement mixtures injected from the vault with a central angle ranging 90° – 120° . Backpack grouting at the tunnel crown contact area demands that the grouting pressure be maintained until the hardening of the grout mixture, to secure intimate contact of the grout with the crown. For shaft lining, a series of radial holes is drilled and grouted from the inside of the shaft. Hole spacing and sequence will vary within 2–6 m, and usually, split-spaced secondary holes will be drilled and grouted. The hole is deep into rock at least 5 cm. The pressure of backfill grouting is commonly 0.2–0.3 MPa.

(b) Consolidation grouting

Where the excavation of a tunnel or shaft has loosened the surrounding rock, it may be necessary to stiffen the rock by filling open joints and fractures using consolidation grouting to reduce rock pressure and external water pressure as well as seepage discharge and to raise elastic resistance. It would be carried out after the

completion of backfilling and contact grouting. Consolidation grouting is not undertaken in sequence among lines and holes, but from low position holes to high ones. For each hole, two or more grouting stages are needed. During the first stage, the grouting of internal portion close to the lining is performed. With continuing hole drilling deeper to the designed depth, the grouting of external turn in the second stage is undertaken.

Consolidation grouting is ordinarily proceeded in a form that the holes drilled 2–5 m, sometimes 6–10 m, deep into surrounding rock, are arranged in star pattern; the hole depth is 0.5–1.0 times of the radius of tunnel; the spacing of hole row is 2–4 m; each row contains at least six holes layout symmetrically; and the grouting pressure is 1.5–2.0 times of the internal pressure of tunnel. To avoid damages to the lining due to high-pressure consolidation grouting, observation and monitoring are demanded during the grouting operation.

If it is not prestressed, concrete lining will crack under the action of internal water head which exceeds 100 m. Under such circumstances, it is therefore necessary to provide high-pressure consolidation grouting for surrounding rock to reduce water seepage. The maximum static internal water head of the diversion tunnels in the Guangzhou and Tianhuangping Pumped Storage Hydropower Projects is 512 and 680 m, respectively. Successful performances are documented by the high-pressure consolidation grouting of 6.5 and 9.0 MPa for these two projects. The length of pressure tunnel in the Guangzhou pumped storage hydropower project is 1292.6 m, partially attributable to the high-pressure consolidation grouting, and the total seepage discharge through the outlet of steel-lined drainage system, the drainage gallery, the lower horizontal tunnel and manifold is only 0.84 L/s.

6. Anti-seepage and drainage devices

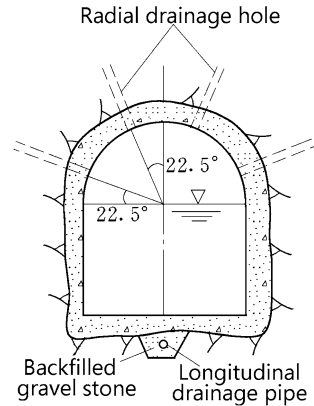
It must be recognized that seepage through permeable geologic discontinuities will manifest despite adequate confinement. Seepage around or through concrete linings into gypsum, porous limestone, and discontinuity fillings containing porous or flaky calcite can lead to rock erosion and collapse. Seepage from pressured waterways is also responsible for surface springs, mud slides, and landslides.

Drainage can be accomplished by drilling draining holes into the rock or by installing filter strips around the exterior face of the lining leading to the draining holes. It is necessary for the designer to have a good understanding of the geology, seepage regime, and the presence or absence of groundwater under pressure likely to be encountered with. Where heavy seepage is anticipated, provisions by grouting with cement and/or chemicals (Karol 1990) or extra drainage holes should be made.

For free-flowing tunnels with external water pressure attributable to higher groundwater table, draining hole system (Fig. 13.10) in the lining is very effective to cut the external pressure. For pressure tunnels or if the groundwater table fluctuates greatly, a special drainage tunnel may be installed to drain seeping or leaking water from the major tunnel, apart from consolidation grouting.

Permanent draining holes should always be drilled after the completion of all grout injections conducted in a particular area. Draining holes 2–4 m in spacing and 2–4 m in depth will be adequate for most conditions. For high or wide tunnel with

Fig. 13.10 Layout of draining for a free-flowing tunnel



high external water pressure, drainage hole system is allowable to be set below the flow surface, to reduce the external pressure during the emptying of tunnel. One of such examples is the diversion tunnel of the Liujiaxia Project, China.

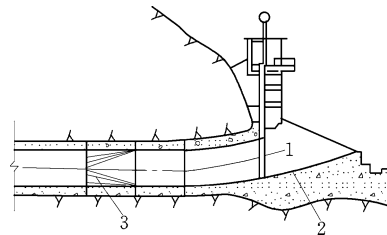
13.5 Outlets and Energy Dissipation

The discharge from the tunnel outlet will emerge at a high velocity, usually in a nearly horizontal direction. The overall size of an outlet work is determined by its head and the required discharge capacity.

Where a tunnel outlet is terminated as a submerged pressure pipe, operation gates and hoist chamber are normally installed. Before the gate, there is transition, and after the gate, there is energy dissipation device to kill the flow energy, as shown in Fig. 13.11.

For free-flowing tunnels in competent rock, the tunnel outlet is simpler. Usually, lining might be provided only along the sidewalls and bottom to form a smooth waterway, and at the top, a door-frame wall is installed for preventing the rock from falling, as shown in Fig. 13.12. Deflector devices might be employed to direct the high-velocity flow away from the outlet structure. Where soft foundations exist, a dissipating device might be provided to kill the kinetic energy of flow before it is returned to the river or canal (Bradley and Peterka 1957a, b, c).

Fig. 13.11 Outlet of pressure tunnel—the Xianghongdian Project (China, $H = 87.5$ m).
1 bulkhead gate; 2 flip bucket; 3 transition section



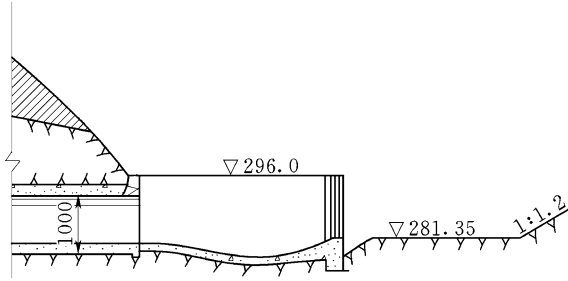


Fig. 13.12 Outlet of free-flowing tunnel (unit: m)—the Luhun Project (China, $H = 55$ m)

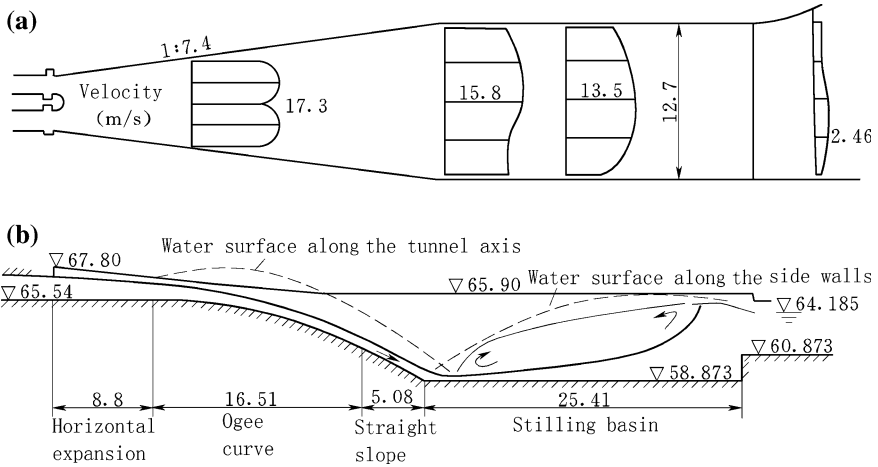


Fig. 13.13 Energy dissipating layout of a tunnel using stilling basin (unit: m)

When the tailwater is a bit of lower than the bottom floor of outlet, planar diffusion (divergence) and dissipation are commonly needed both for the pressure tunnel and for the free-flowing tunnel. It consists of horizontal expansion section, transition section, and stilling basin. The expansion section serves to reduce the unit discharge and the corresponding stilling basin length and depth. However, the expansion angle should be adequate to avoid unstable flow induced by the separation of high-speed flow from the sidewalls. Parabolic curve or straight line with slope grading smaller than 1:3 may be employed for the transition bottom (Fig. 13.13). Protection is generally required after the stilling basin to prevent the river or canal from scouring.

When the tailwater is sufficiently deep but is lower than the bottom floor of the outlet, and the riverbed rock is above moderate quality, the outflow from the outlet is in the form of a jet, which can be discharged directly into a downstream plunge pool, as shown in Fig. 13.14. The flip bucket may be expanded, or contracted, dependent on the topographic, geologic, and operative conditions.

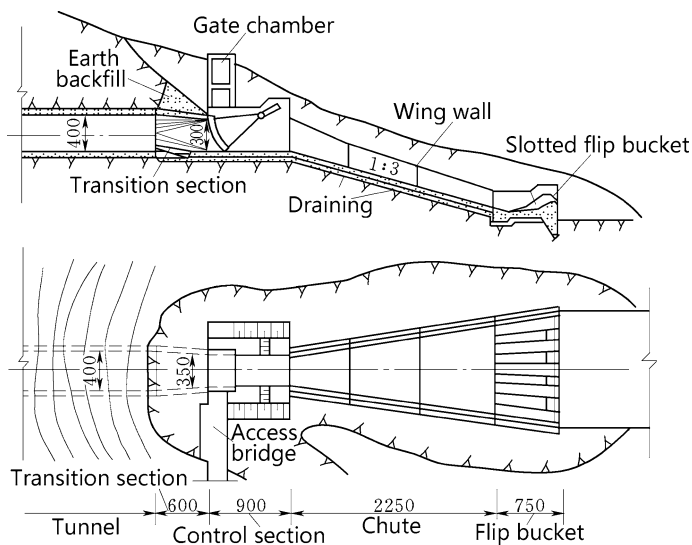


Fig. 13.14 Energy dissipation layout of a tunnel using flip bucket (unit: cm)

13.6 Countermeasures Against Cavitation to Hydraulic Tunnels

With the development of hydraulic engineering, more and more hydraulic tunnels with high head and high flow velocity are built. The examples are the spillway tunnels in the projects of the Liujiaxia, the Bikou, and the Wujiangdu, whose flowing velocity approaches or even exceeds 40 m/s. The maximum flow velocity reaches 50 m/s in the spillway tunnel of the Ertan Project. Under the actions of water flow at high velocity, hydraulic tunnels are vulnerable to cavitation and abrasion damages. For instance, the spillway tunnel of the Border Dam in USA had been operated for 4 months under the action of 46 m/s flow in 1941. A large pit of 35 m (long) \times 9.2 m (wide) \times 13.7 m (deep) was scoured on the bottom of bending segment connecting the sloping and horizontal tunnel segments. In 1974, after over 300-h flood release operation of outflow discharge 560–587 m³/s, the spillway tunnel on the right bank of the Liujiaxia Project in China was seriously damaged. A large pit of 32 m (length) \times 3.5 m (depth) on the bottom of the ogee transition segment was scoured. These incidents/accidents clearly indicate that cavitation and abrasion protection for hydraulic tunnels with high-velocity flow is crucial in the tunnel design.

The countermeasures against cavitation and abrasion of hydraulic tunnels with high flow velocity are similar to that of spillways in gravity dam and bank side spillways, including:

- Rational profile design;
- Strict control of offset on the flow surface;
- Using materials with high resistance to cavitation/abrasion damages;
- Correct arrangement of aeration devices; and
- Dissipating a part of energy inside tunnels.

13.6.1 Profile Design

Profile design for high-speed tunnel is basic and paramount to prevent it from cavitation. The lining surface should be sufficiently smooth, and any abrupt variation in curvature should be avoided. When the tunnel bending in the plane is inevitable, angle and curvature radius should be chosen properly. In general, with regard to tunnel of slow velocity flow, bending angle should be smaller than 60° , and curvature radius should not be smaller than 5.0 times the diameter (or width) of tunnel. The length of each straight segment adjoining the bending segment should not be smaller than 5 times the diameter (or width) of tunnel. If it is necessary to have transition segment from high elevation to low elevation, parabolic curve is preferable.

For pressure tunnel, contraction of outlet sectional area, or reduce the opening degree of the service gate located at outlet, are effective measures to raise tunnel pressure and to reduce cavitation. In doing so, however, the discharge ability is reduced, too. The outlet contraction ratio η is customarily 0.7–0.85.

Diversion tunnel may be reconstructed into spillway tunnel by building a new intake diverting water into a shaft connecting the downstream diversion tunnel leg, which has been widely exercised in the China's hydraulic projects. Where the surcharge head is high, the flow pattern of inflow may be unstable and easily gives rise to cavitation damages to the lining. A preferable change of water intake type can make water into the shaft to produce gyrating flow, whose centrifugal action will increase the pressure on lining wall and improve the resistance against cavitation damage. Friction and aeration by stream rotation have an effect of energy dissipation, to reduce flow velocity inside the tunnel, to improve cavitation resistance of lining, and also to reduce the risk of scouring at the downstream outlet. Therefore, nowadays, more and more attention has been called at the possibility of energy dissipation by gyrating flow in tunnel.

Aforementioned scheme has been successfully exercised in the Shapai Project. At the height of 132 m, the Shapai possesses the highest RCC arch dam in the world. The shaft spillway is composed of a short pressure inlet, open canal, spiral chamber, shaft, tunnel leg (original diversion tunnel), and outlet flip bucket. With a crosshead of 88 m and the maximum discharge of $240 \text{ m}^3/\text{s}$, it is the biggest one of this type in the world. The main testing data under the design flood level (1866 m) are as follows: The maximum pressure head at the perimeter of shaft bottom is 38–40 m, the ventilation discharge through air vents at the top of the spiral chamber is $34 \text{ m}^3/\text{s}$, and the maximum flow velocity in the tunnel is 21.3 m/s with a total energy

dissipation ratio of 73 %. Encouraged by the achievement in the gyrating flow shaft spillway of the Shapai Project, the possibility to reconstruct the diversion tunnel into gyrating flow shaft spillway in the Xiluodu Project with installed generator capacity of 14400 MW has been studied, too.

The Xiaolangdi Project is located on the Yellow River (China, $H = 160$ m). There are 3 spillway tunnels reconstructed from the original diversion tunnels on the left bank, each with a length of 1.1–1.2 km and a diameter of 14.5 m. If they were reconstructed to be free-flowing tunnels, the maximum velocity of high sediment-laden flow would reach 48 m/s, which would result in difficulties with the prevention of the concrete lining from cavitation and abrasion. If they were reconstructed to be pressure tunnels, it would lead to difficulties with the structural stability due to poor surrounding rock quality and large internal water pressure (about 140 m). After a detailed study, the intermediate gate chamber scheme was employed. Upstream of the chamber, the tunnel is pressure, and downstream of the chamber, the tunnel is free flowing. Three orifice plates for the dissipation of energy are provided in the upstream pressure tunnel (Fig. 13.15). The interval between the orifice plates is 43.5 m. The ratio of the internal diameter of the round orifice plate to the tunnel diameter d/D is determined as 0.690, 0.724, and 0.724, respectively (corresponding cavitation number is 5.85, 5.50, and 4.90). The hydraulic model tests showed that in the flood releasing, dissipation of energy by the three orifice plates helps to cut 59 m of the water head, so the risk of abrasion on lining is greatly reduced. It is the first attempt in China and in the world that the diversion tunnels are reconstructed for flood release using orifice plate for energy dissipation.

It is worthwhile to mention that before the construction of the Xiaolangdi Project, a prototype test was carried out for the sediment excluding tunnel with a length of 685 m and diameter of 4.4 m, in the Bikou Project. According to the test

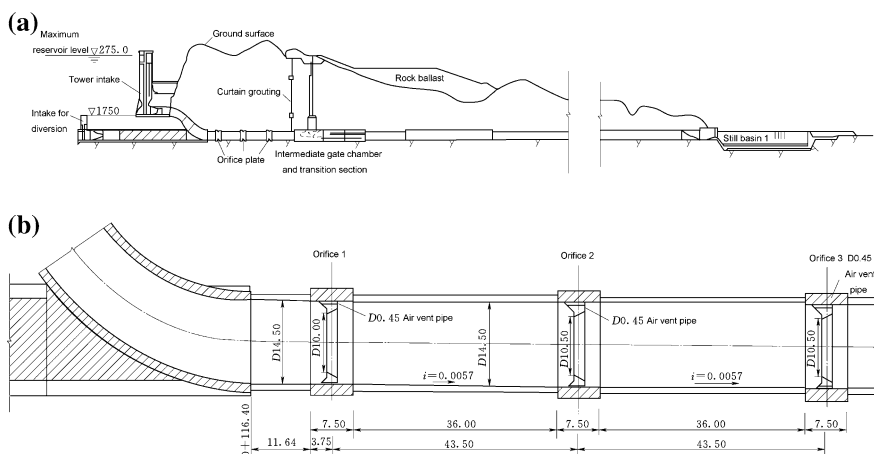


Fig. 13.15 Orifice plates for the energy dissipation (unit: m)—the Xiaolangdi Project (China, $H = 160$ m). **a** Longitudinal profile of the No. 1 spillway tunnel; **b** detailed drawing of the orifice plate section

requirements, a tunnel segment of 31.5 m long was made with a reduced diameter of 3.8 m. Two orifice plates spaced 11.4 m apart and with a ratio of the internal diameter of the round orifice plate to the tunnel diameter $d/D = 0.69$ were installed. Under the surcharge water head of 70.73 m, the test lasted 8.5 h with flow discharge of 78.5 m³/s and flow velocity 14.6 m/s at the orifice opening. This prototype test played a key role in the orifice plate designed for the Xiaolangdi Project.

13.6.2 Aeration Slots

Aeration into water flow may help to prevent cavitation damages on the tunnel lining surface. Aerator devices may be that with ramp, vertical drop, ramp and vertical drop, sudden enlargement, as well as their combination with slot aerator (Fig. 13.16).

Aerator devices with ramp and/or drop are widely exercised in China’s flood release tunnels such as the projects of Wujangdu, Lubuge, and Ertan. Aerator devices with sudden enlargement also have been employed in several China’s projects, such as the Xiaolangdi flood release tunnels. Some have been operated so far in good performance, but the others are not very successful.

The conventional aerator devices with ramp and/or drop will be not applicable when the tunnel has very gentle grading, due to the accumulation of water in this area. In the design of deep release tunnel of the Longyangxia Project, an improved aerator device is proposed based on hydraulic modeling, as shown in Fig. 13.17. It retains the backwater by the sill and uses pipe to release the accumulation of water in slot to maintain the aeration vacuum.

Figure 13.18 shows a strengthened differential ramp and drop aerator device, whose prototype inspection after operation indicated that the good aeration and effective cavitation damage protection under a variety of head may be secured.

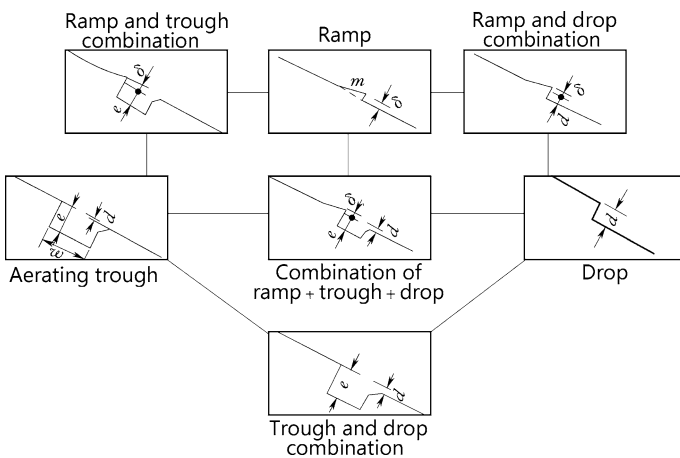


Fig. 13.16 Aerator devices with ramp and drop

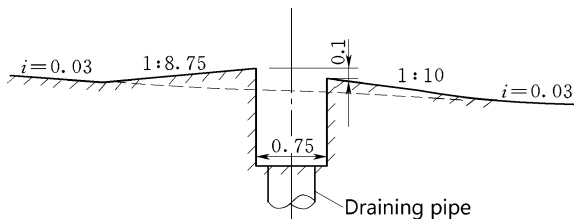


Fig. 13.17 Special aerator device (unit: m)—the Longyangxia Project (China, $H = 178$ m)

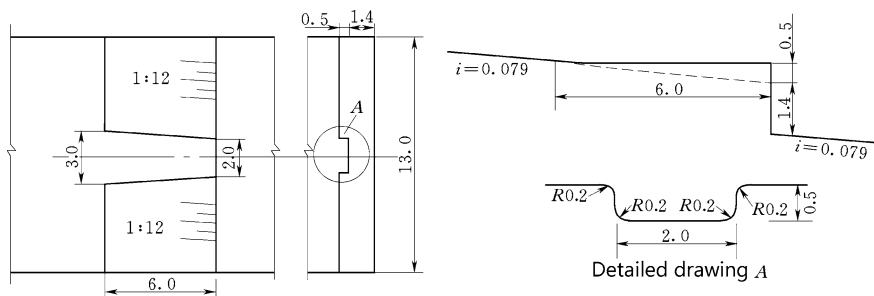


Fig. 13.18 A strengthened differential ramp and drop aerator device (unit: m)

The spillway tunnel located on the left bank of the Wujiangdu Project with the internal dimension of $9 \text{ m} \times 13 \text{ m}$ and the length of 184.5 m consists of a pressure inlet, an inclined tunnel, an ogee section, and a flip bucket. The inclined tunnel in turn consists of parabolic and straight segments. The maximum discharge is $2160 \text{ m}^3/\text{s}$, and the flow velocity reaches 43.1 m/s at the ogee section. To reduce cavitation damage, a mixing aeration with slots and grooves is equipped at the starting point of the ogee section. Four aeration pipes with a diameter of 1.2 m are embedded in each side of the abutment walls. The project has been operated satisfactorily for more than 30 years. In 1982 and 1985, the prototype observations were carried out, which showed that aeration slots played an important role in the cavitation damage prevention.

13.7 Stability of Surrounding Rock Mass During Tunneling

13.7.1 Stress Concentration in Surrounding Rock Mass

Prior to tunneling, the in situ stress of the rock mass is in equilibrium. Once the excavation is made, the stress in the vicinity of the opening is redistributed and stress concentration manifests (Herget 1988). The redistributed stress can overstress parts of the rock mass and makes it ruptured. The phenomena such as numerous

disk cores in boreholes and rock burst attracted attention of tunnel engineer with respect to the existence of high in situ stress. Apart from the initial stress, the geologic structure and strength of rock, the method of tunneling, the method of support, and the shape of the section are the other main factors that govern stress redistribution around the tunnel.

Although the properties of rock mass are complex, and no single theory is available to explain rock mass behavior perfectly, the stress analysis based on the theories of elasticity and plasticity may provide deep insight into the disturbance to the preexisting stress equilibrium due to tunneling. It interprets the performance of a tunnel in terms of stress concentrations and associated deformations and serves as the first step to quantitatively and rationally establish the requirements for design.

13.7.2 Deformation of Surrounding Rock Mass

Advances in continuum mechanics together with fast and low-cost computers have led to the proliferation of continuum analysis programs aimed at the solution of a wide range of geomechanical problems including tunnel and shaft excavation and construction. Continuum analysis refers to those methods or techniques that assume the rock mass to be a continuum and require the solution of a large set of simultaneous equations to calculate the states of stress and displacement throughout the rock. The available techniques include the FDM, FEM, and BEM (vide Chap. 5).

The behavior of a tunnel opening is most drastically manifested in the displacements of the tunnel walls and the rock mass surrounding the tunnel. Convergence of the tunnel walls is by far the most important indicator of tunnel performance and is also relatively easy to be observed. On the contrary, loads, strains, and stresses are generally more difficult to measure and interpret.

The absolute value of tunnel convergence can sometimes be predicted, and exceeding this value could become a concern. However, the rate of convergence is a more important parameter to watch. Fig. 13.19 shows the displacement and convergence of the Fenggang Tunnel 5 in the Shenzhen City which show convergence and indicate eventual stability of the structure, in which A is at the vault arch top of the tunnel, B and C are at the vault arch abutments, and D and E are at the mid-height of the sidewalls. Figure 13.20 shows the rate of convergence at different depth from the tunnel surface (points A, B, and C), and it may be found that the rock deformation fades away along the depth from the excavation surface.

13.7.3 Stability of Surrounding Rock Mass

Stability analysis of surrounding rock and supporting design may be performed by a number of available methods (Goodman and Shi 1985; Hudson 1992; Stagg and Zienkiewicz 1968) and will be briefly discussed therein.

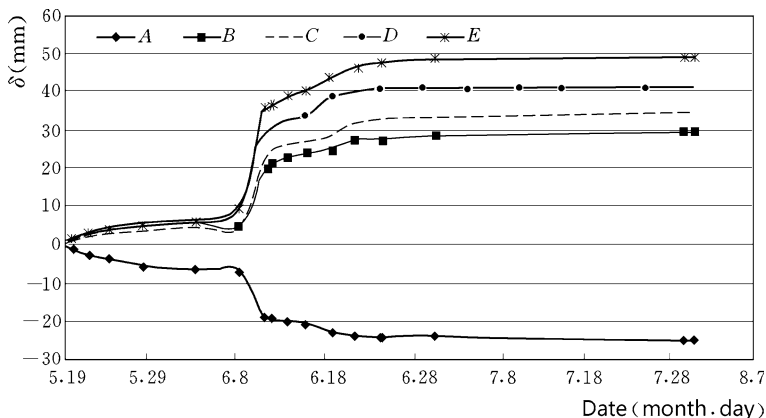


Fig. 13.19 Convergence curve—the Fenggang Tunnel 5 (China)

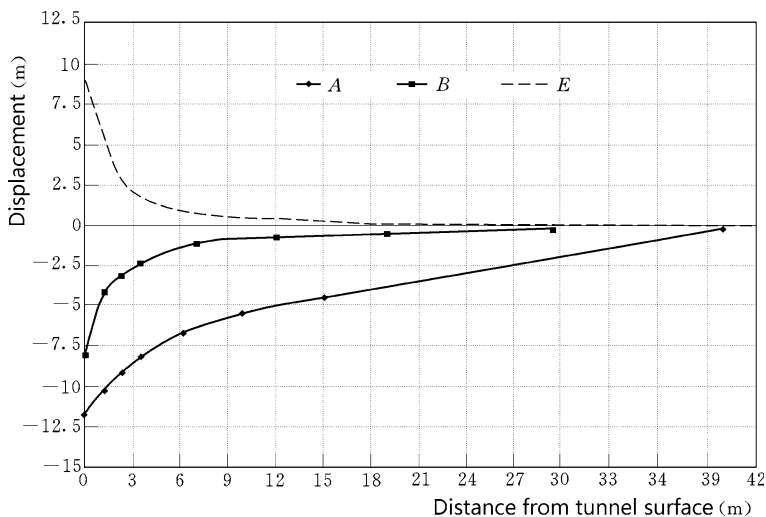


Fig. 13.20 Deformation versus rock depth—the Fenggang Tunnel 5 (China)

1. Rock mass classification

Stability assessment of surrounding rock mass may be preliminarily based on the rock mass classification, and the corresponding support types may be determined accordingly (Barton et al. 1974; Bieniawski 1979). Classification of surrounding rock masses follows the available methods such as “RMR method,” “Q system method,” (Deere and Deere 1988) and GB50218-94 “Standard for engineering classification of rock masses” (Ministry of Construction of the People’s Republic of China 1994) using the basic quality index (BQ). These methods are calibrated against and supplemented with each other, based on which the basic support types and structural

design are preliminarily worked out. However, they are only applicable to general conditions. When abnormal geological conditions appear, it is far from enough to make structure design and support design and construction organization exclusively using rock mass classification. For instance, the argillized intercalations above the arch crown, though far from the tunnel surface, have substantial influences on the crown deformation and stress redistribution around the tunnel, and special cautions should be called at; the strata of alluvial–lacustrine are very variable in lithology and facies, and thus, support measures should be adjusted timely according to the varied strata.

2. Numerical analysis

Computer programs may be employed to analyze the excavation-induced stress redistribution and its impact on the different portions of the tunnel, to identify the locations and the magnitudes of stress concentrated zone as well as the tensile zone and yielding zone and to estimate the maximum horizontal and vertical displacement around the tunnel in the process or after the completion of tunneling.

3. Geomechanical model test

Geomechanical model may be established for simulating the tunneling process and for observing the stress magnitude and its variation, the deflection and failure, as well as the margin of stability safety and the effectiveness of supporting measures of hydraulic tunnels.

4. Wedge analysis method

Limit equilibrium program may be performed, with the combination of macro-geological judgment, to determine the shape and scale of potentially unstable rock blocks formed by discontinuities and to analyze the effectiveness of supporting measures.

Each of the aforementioned four methods has its strong points and can be mutual complementation, to provide a reliable basis from various aspects for the rock supporting design.

13.8 Structural Analysis of Lining

Although the principal function of concrete lining is to reduce the friction losses, very often, a concrete lining also should be capable of standing external pressure from surrounding rock masses and groundwater in addition to the internal water pressure. Therefore, a rational analysis of concrete lining can provide great economic benefits by indicating its reasonable thickness and reinforcement (Deere et al. 1970; Kuesel 1987; Muir Wood 1975; Pender 1980; Sulem et al. 1987; Wang 1982).

There are two classes of limit states in the design of hydraulic concrete structures: limit states of bearing capacity (collapse related to rupture, sliding, etc.) and limit states of normal usage (serviceability with respect to deformation, crack,

seepage quantity, etc.). However, because of the combined working mechanism of the lining with the surrounding rock mass, the design of concrete and reinforced concrete lining for pressure hydraulic tunnels is different from the design of other hydraulic concrete structures. Under the circumstances that the quality of rock and backfill grouting is competent and overburden is thicker than 0.4 times of the internal water head, strength of lining is not critical in the design, whereas large seepage/leakage of water should be prevented to ensure the normal operation of tunnel. Thus, the limitation of crack apertures becomes one principal requirement for the lining design.

In 1962, a model study under the action of internal pressure was undertaken by the former USSR for the Inguri Project. The internal diameter of the model ring was 2.2 m with a lining of 15 cm thick and maximum internal pressure of 1.2 MPa. Double cylinder method for loading the internal pressure was employed in the test. The water did not contact with the lining, and the internal pressure was transferred to the lining through a robber film. The results showed that the number and aperture of lining cracks increased with the raising of internal pressure. The first crack occurred when the pressure reached 0.45 MPa, and 9 new cracks manifested while the pressure was raised up to 1.2 MPa.

In the 1970s, six direct water pressure tests on the lining for large-scale tunnel were carried out in China. High-pressure water penetrated into cracks and concrete so that the tensile stress decreased in the region away from the cracks. The results indicated that cracks appeared at a certain pressure in the test process. However, with the pressure being raised again, only the aperture of original cracks was considerably increased and no new cracks appeared.

The foregoing performances of hydraulic tunnel lining under internal water pressure are quite different with regard to the tests conducted in China and in the former USSR, which is attributable to the difference in the test methods. It is actually indicated that flowing of high-pressure water in cracks and concrete would play an important role in the propagation of lining cracks: When water pressure in the tunnel is larger than the critical value, the lining will crack on the weak section; along with high-pressure water flowing into the crack and concrete, the tensile stress of the lining will be released in the region near the crack. Beyond the region of stress releasing, the stress basically remains in the original tensile state, where the second batch of cracks may emerge; along the radial cracked section, additional tensile stress will occur in surrounding rock at certain depth, and additional shear stress will manifest on the contact surface of lining/surrounding rock.

Where the tunnel lining is reinforced, it must be made sufficiently thick both to accommodate the reinforcement mat and to provide sufficient room for placing the concrete in the confined space behind the forms. The portions of a tunnel that must be reinforced and the amount of reinforcement depend on the tunnel shape, external and internal loadings, requirements for watertightness, and various geological factors. The general guidelines for identifying reinforcement requirements for hydraulic tunnels are suggested as follows:

- ① Provision of reinforcement in the tunnel lining complicates the construction sequence in addition to requiring a thicker lining. For free-flowing tunnels, it is recommended that lining reinforcement should not be provided to resist external loads, if possible.
- ② Pressure tunnels should ordinarily be reinforced whenever the depth of overburden is adequate to withstand the unbalanced internal pressure or whenever leakage control is important. The reinforcement should be sufficient to provide structural strength and leakage control with respect to the maximum internal hydrostatic pressure partially balanced by a conservative estimated external hydrostatic pressure. Confinement from the surrounding rock mass should only be considered when the properties of rock are well known and a complete analysis is made. However, where there are provisions for dewatering in case of repair, the external pressure head should be the maximum that can be anticipated.
- ③ Transition from a pressure tunnel segment to a free-flowing tunnel segment should be specially reinforced to prevent serious cracking, in this way to prevent the leakage from the pressure portion to the free-flowing portion. Reinforcement of the pressure portion for a length equal to several times the tunnel diameter from the junction should be based on the full internal hydrostatic head without allowance for confinement from the surrounding rock. The free-flowing portion also should be reinforced for a length equal to several times the tunnel diameter from the junction, under an external static head equal to the internal head in the pressure tunnel segment just upstream of the junction.
- ④ Nominal amount of both longitudinal and circumferential reinforcement should be provided near the portals of both pressure and non-pressure tunnels, to resist loads due to loosened rock. This reinforcement should extend behind the portals for a length equal to at least twice of the tunnel diameter.
- ⑤ In competent rock, the tunnel body, other than at the portals and at the transition from pressure to free flowing, may be not reinforced where the rock overburden is adequate to withstand the unbalanced internal pressure head.

According to the SL279-2002 "Specification for design of hydraulic tunnel," the available methods for the structural analysis of tunnel lining are as follows:

- ① Finite element method may be employed for the interaction problem of lining and surrounding rock mass, i.e., the tunnel with lining is looked at as a kind of monolithic bearing structure;
- ② When the diameter of tunnel is smaller than 6.0 m and the surrounding rock mass belongs to type I or II, the thickness of lining is mainly controlled by internal water pressure, and closed-form solution based on the elastic theory may be applied;
- ③ For the tunnel in the surrounding rock mass belongs to type IV or V, and for the tunnel of free flowing, structure mechanics method may be employed.

13.8.1 Design Loads and Their Combinations

Depending on the function of the tunnel and service conditions, one or more of the following loads could exert on the lining:

- Self weight of lining;
- Surrounding rock pressure;
- Internal water pressure;
- External water pressure;
- Grout pressure;
- Seismic and thermal loads; and
- Other loads such as foundation counterforce, friction force, elastic resistance, and live loads.

The worst likely combination of loads under different operation situations has to be considered (e.g., normal operation, tunnel empty, transient).

1. Self weight of lining

One-meter slice of lining along the tunnel axis is taken for the calculation, under the assumption that the self weight uniformly exerts on the average line of lining thickness (Fig. 13.21).

Self weight intensity on the unit area, g , is defined by

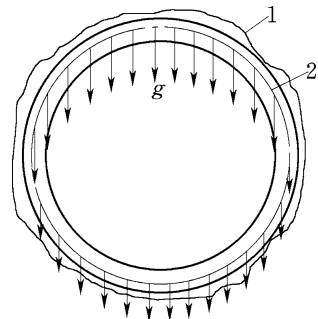
$$g = \gamma_c h \quad (13.4)$$

where γ_c = unit weight of concrete, kN/m^3 ; and h = lining thickness including an over-excavation of 0.1–0.3 m.

2. Surrounding rock pressure

For the design of supports, it is necessary to know the surrounding rock pressure due to the weight of surrounding rock. Surrounding rock pressure is difficult to be exactly computed because it is influenced by various factors such as geological structure, mechanical properties of rock, initial tectonic stress, groundwater,

Fig. 13.21 Self weight of lining. 1 excavation boundary; 2 average line of lining thickness



overburden depth of tunnel, shape and size of tunnel, construction method, and scheme and schedule of supporting and lining. The computation methods based on the loose grain theory, design code specification, and elastic-plastic theory will be introduced below.

(a) Loose grain theory

The surrounding rock mass is assumed as a body of loose grains. Tunneling disturbs the equilibrium of forces in these loosen grains; as a result, the entire rock mass or some portions thereof above the tunnel heading set to deform, which in turn imposes pressure on the lining. This standpoint had been postulated in early time and was prevalent since then. The typical formulae implemented are that of Protodyakonov and Terzaghi.

In the Protodyakonov's formula, a quasi-friction coefficient is employed to define the actual friction coefficient of rock grains as

$$f_k = \frac{\tau}{\sigma} = tg\varphi + \frac{c}{\sigma} \quad (13.5)$$

where τ = shear strength of rock, kN/m^2 ; σ = normal stress, kN/m^2 ; φ = internal friction angle of rock; and c = cohesion, kN/m^2 .

Therefore, quasi-friction coefficient contains not only friction coefficient but also, to some extent, unit shear resistance, which may range from a value of 20 for strong rocks to 0.3 for weak rocks.

When tunneling goes on, a parabola-shaped slip arch, also named as "equilibrium arch," is formed on the vault of tunnel, whose height is calculated as follows

- Slip faces do not exist on the both sidewalls

$$h = \frac{B}{2f_k} \quad (13.6)$$

- Slip faces do exist on the both sidewalls

$$h = \frac{L}{2f_k} = \frac{B + 2Htg(45^\circ - \frac{\varphi}{2})}{2f_k} \quad (13.7)$$

The heading of tunnel is exposed to the thrust of rock mass being on the verge of falling that (Fig. 13.22):

- On the roof, as the weight of slip arch, that in fact is a vertical rock pressure;
- On the walls is a horizontal rock pressure formed by the weight of rock within triangular zone.

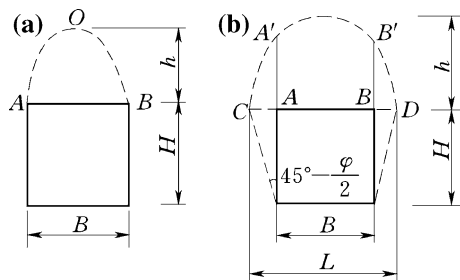


Fig. 13.22 Slip arch of flattop tunnel. **a** Without sideslip faces; **b** with sideslip faces

Vertical rock pressure is considered as a load uniformly distributed on the tunnel vault, whose value is the weight of rock related to a height of h , i.e.,

$$q = \gamma_r h \tag{13.8}$$

where γ_r = volumetric weight of rock, kN/m^3 .

For curved heading, vertical rock pressure should be reduced by 30 %, i.e., $q = 0.7\gamma h$.

By position, lateral horizontal rock pressure is distributed in a form of

- At crown

$$p_1 = 0.7\gamma_r h t g^2(45^\circ - \frac{\varphi}{2}) \tag{13.9}$$

- At bottom

$$p_2 = (0.7h + H)\gamma_r t g^2(45^\circ - \frac{\varphi}{2}) \tag{13.10}$$

For convenience, uniform lateral horizontal rock pressure may be adopted in design, which is averaged by p_1 and p_2 , i.e., $p = (p_1 + p_2)/2$ and is exerted on the both sidewalls of tunnel. If the rock is moderately strong or stronger enough to ensure a f_k larger than 2.0, lateral horizontal rock pressure may be ignored.

The Protodyakonov’s formula is now seldom exercised in large to medium tunnel engineering, for its crudeness in theory and inaccuracy verified by practices. However, for small tunnels, particularly that in poor-quality rock, the formula may be used in preliminary design phase.

(b) SL279-2002 “Specification for design of hydraulic tunnel”

Surrounding rock should be classified into five types according to the GB50287-1999 “Code for water resources and hydropower engineering geological investigation” and the GB50218-94 “Standard for engineering classification of rock masses”

using the BQ, which is mainly decided by the hardness and intactness and revised taking into account of groundwater, predominant weak structural plane, and initial tectonic stress. Type I and II surrounding rock masses are self-stable—basically stable, the lining is not demanded and only local bolting-shotcrete supporting is considered—type III surrounding rock mass has no sufficient stability, and therefore, the systematic bolting-shotcrete supporting or concrete lining bracing may be necessary; and type IV–V surrounding rock masses are not stable, and systematic bolting-shotcrete supporting and concrete lining bracing are always necessitated.

For self-stable surrounding rock masses, rock pressure may be ignored, i.e., $q = 0$, but attention should be called at the tectonic stress problem. For the surrounding rock mass of laminate, cataclastic texture, and grain structure, the vertical and horizontal rock pressures q_v and q_h exerting on the tunnel lining are computed by

$$\begin{cases} q_v = (0.2 - 0.3)\gamma_r B \\ q_h = (0.05 - 0.1)\gamma_r H \end{cases} \quad (13.11)$$

where B = excavation width of tunnel, m; and H = excavation height of tunnel, m.

For shallow embedded tunnels, surrounding rock pressure is calculated according to the overburden rock weight subject to the revision with regard to the supporting measures installed during the tunneling.

(c) Elasto-plastic theory

After the outreach of yield strength, plastic zone will be developed around the tunnel (Fig. 13.23). For a circular tunnel in the surrounding rock mass with initial tectonic stress p_0 , elasto-plastic theory gives the radial and tangential stresses σ_r and σ_θ as

$$\left. \begin{aligned} \sigma_r &= -c \operatorname{ctg} \varphi + (p_i + c \operatorname{ctg} \varphi) \left(\frac{r}{r_0} \right)^{\frac{2 \sin \varphi}{1 - \sin \varphi}} \\ \sigma_\theta &= -c \operatorname{ctg} \varphi + (p_i + c \operatorname{ctg} \varphi) \left(\frac{r}{r_0} \right)^{\frac{2 \sin \varphi}{1 - \sin \varphi}} \left(\frac{1 + \sin \varphi}{1 - \sin \varphi} \right) \end{aligned} \right\} \quad (13.12)$$

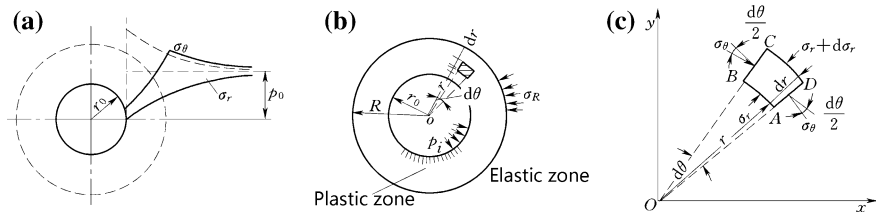


Fig. 13.23 Zoning of surrounding rock of circular tunnel and stress calculation in plastic zone

The reaction p_i of lining to rock (i.e., surrounding rock pressure) has relation with the radius of plastic zone R as follows:

$$p_i = -c \operatorname{ctg} \varphi + p_0 [c \operatorname{ctg} \varphi + (1 - \sin \varphi)] \left(\frac{r_0}{R} \right)^{\frac{2 \sin \varphi}{1 - \sin \varphi}} \quad (13.13)$$

or

$$R = r_0 \left[(1 - \sin \varphi) \frac{p_0 + c \operatorname{ctg} \varphi}{p_i + c \operatorname{ctg} \varphi} \right]^{\frac{1 - \sin \varphi}{2 \sin \varphi}} \quad (13.14)$$

where p_0 = initial tectonic stress, kN/m^2 ; r_0 = radius of tunnel, m; r = radius of the point concerned within plastic zone, m; and φ and c = shear strength parameters of rock.

Elasto-plastic theory is a progress compared to the loose grain theory, but it is only so far available for simple geology conditions and tunnel shapes.

3. Internal water pressure

Internal water pressure is the most important load in pressure tunnel, which often dominates the lining design. On the contrary, it is nearly ignorable for free-flowing tunnel. Internal water pressure varies along the tunnel, determined by the pressure slope line of pressure tunnel or by the water surface of free-flowing tunnel.

For convenience, internal water pressure in pressure tunnel may be divided into two parts: uniform internal water pressure and non-uniform full water pressure without water head (Fig. 13.24). The first part is attributable to the water over the top of tunnel and calculated by $\gamma_w h_n$, whereas the second part is attributable to the water just filling the tunnel with a value of zero on the top and $\gamma_w d$ on the bottom, where γ_w is the unit weight of water and d is the diameter of tunnel. Internal water pressure in free-flowing tunnel, if necessary, is so calculated as zero on the water surface and $\gamma_w h$ on interior periphery of the tunnel, where h is the water depth.

4. External water pressure

External water pressure is an important action in free-flowing tunnels, which is determined by groundwater table after the impounding of reservoir; therefore, it is

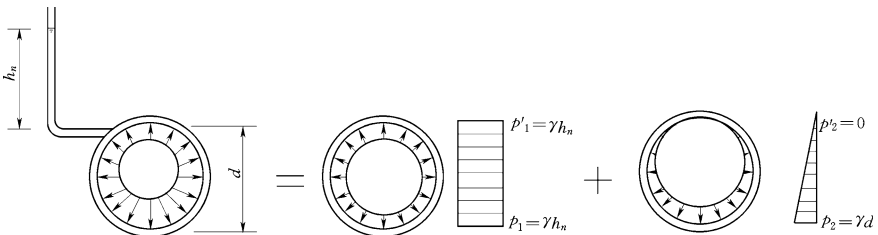


Fig. 13.24 Division of internal water pressure in pressure tunnel

Table 13.1 Reduction coefficient β with respect to groundwater level

Activity grade of groundwater	Influence of groundwater on the surrounding rock mass stability	β
1	No	0–0.2
2	Slightly and weakly	0.1–0.4
3	Remarkably	0.25–0.60
4	Strongly	0.40–0.8
5	Severely	0.65–1.0

also named as groundwater pressure (Femandez and Alvarez 1994). Up to now, there is not yet a conform viewpoint on how to describe the property of external water pressure and the related computation methods. Therefore, it is necessary for a designer to have a good understanding of the geology and the presence or absence of groundwater under pressure likely to be met with. Where heavy seepage of water is anticipated, provisions by grouting with cement and/or chemicals or extra drainage holes should be made.

The SL279-2002 “Specification for design of hydraulic tunnel” looks at the external pressure exerting on the external periphery of lining as boundary distributed force which may be estimated by $p = \gamma_w \beta h_0$, i.e., water head below groundwater table reduced by a corresponding coefficient β , which is classified into five grades as listed in Table 13.1.

Obviously, this method overlooks a variety of factors such as drainage facilities adopted for reducing groundwater pressure in free-flowing tunnel and therefore is not very convincing.

Nowadays, it is widely accepted that groundwater pressure is actually a seepage pressure exerting on surrounding rock and lining simultaneously (vide Eqs. (4.35 and 4.36)). On the basis of hydrologic and geologic conditions and layout of project, and bearing in mind the possible variation of groundwater after operation of project, the groundwater table and corresponding volumetric load by seepage analysis using FEM may be determined, as has been described in Chap. 4 of this book.

5. Elastic resistance

Under the pressure of internal water, concrete lining tends to deform toward surrounding rock which restricts the lining. This restrained force exerting on lining is named as elastic resistance, which is a kind of passive force.

Geology condition is the predominant factor influencing the elastic resistance. The stronger the surrounding rock mass, the greater the elastic resistance and the higher the benefits will be by counterbalancing internal water pressure. However, emphasis should be paid on the analysis and estimation of elastic resistance for the consideration of economy and reasonability. To profit reliable elastic resistance, tight contact between rock and lining should be secured by filling the gap around contact face using backfill grouting and consolidation grouting.

Suppose the surrounding rock is an ideal elastic space, then the elastic resistance p_0 is in the proportion to the deflection of lining δ , i.e., $p_0 = k\delta$, where k is the elastic resistance coefficient of surrounding rock in N/cm^3 , which means the force needed to prevent lining of 1 cm^2 to develop a deformation of 1 cm toward rock.

Since elastic resistance is not a constant, which is inversely proportion to the radius of tunnel, an unit elastic resistance coefficient is defined as k_0 supposing that the radius of tunnel is one meter

$$k = \frac{k_0}{r_0} \quad (13.15)$$

where r_0 = radius of circular tunnel or a half of width of tunnel for non-circular tunnel, m.

Unit elastic resistance coefficient k_0 may be obtained from design specifications with respect to rock properties, it also may be decided through engineering analogy or closed-form formulae. For important tunnels of complex geology condition, in situ experiments are demanded.

Apart from the properties of surrounding rock mass, elastic resistance coefficient is also dependent on the overburden depth of rock. For pressure tunnel, when the thickness of surrounding rock is smaller than 3.0 times the diameter of tunnel, further analysis must be made to decide whether elastic resistance is taken into account. When the thickness of surrounding rock is smaller than 1.5–2.0 times the diameter of tunnel, or the rock layer tends to slip due to internal water pressure, elastic resistance should be neglected. Under such circumstances, only foundation reaction of invert is taken into account, which exerts on the lower semicircle and is distributed either in cosine curve or uniformly.

6. Thermal action

Stress resulted from concrete shrinkage and swelling can be eliminated by construction and constitution measures including selecting appropriate cement, controlling ratio of water and cement, careful curing, shortening the length of pour, and collocating proper thermal reinforcing steel. Hence, thermal action is usually neglected in designing, but some special studies should be done when thermal stress is very large due to a great variation in temperature after the completion of tunnel. For example, in situ monitoring and 3-D FEM simulation had been conducted for the water conveying tunnel of the ship lock in the Three Gorges Project in China; based on the studies, high-quality temperature control and thermal cracking prevention were achieved.

7. Seismic action

According to the prevalent practice, the tunnel lining is not designed for resisting seismic actions, especially for deep tunnel with good geological conditions, unless the tunnel crosses an active fault. Under such circumstances, some flexibility is

provided at that segment to cater for some movement in case of an earthquake. However, for the intake and outlet of tunnel, seismic actions should be taken into account in the lining design.

8. Grouting pressure

For a tunnel in jointed rock mass or where seepage is to be minimized, the areas surrounding the tunnel are usually grouted both to stiffen the rock and to fill the voids between the lining and the rock.

Generally speaking, backfill grouting pressure varies in a range of 0.2 MPa–0.3 MPa and is distributed on the vault within a central angle ranging 90°–120°. Grouting pressure exerts against the vault of lining as a kind of temporary bracing action.

Consolidation grouting pressure exerts in a similar way of external water pressure, which presses the lining. Usually, it occurs before water filling, so it is not advisable to consider it in the design of lining unless this pressure is rather great.

9. Load combinations

Loads in tunnel fall into that of basic and special. Basic loads include long-term or often-acting loads, such as the self weight of lining (including backfilled weight due to over-excavation), surrounding rock pressure, internal water pressure at normal water level, and underground water pressure in case of steady seepage. Special loads include seldom-acting loads, such as internal water pressure at check water level, and corresponding groundwater pressure, construction loads, thermal loads, grouting loads, and seismic loads.

The following load combinations are recommended in the lining calculation.

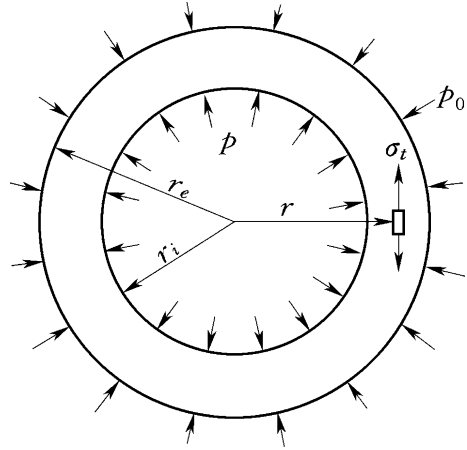
- Normal operation case: self weight of lining + surrounding rock pressure + internal and external water pressures at normal water level;
- Construction or inspection and reparation case: self weight of lining + surrounding rock pressure + possible maximum external water pressure;
- Extreme operation case: self weight of lining + surrounding rock pressure + internal and external water pressures at check water level.

Normal operation case indicates the basic combination, which is used to design the size of lining and amount of reinforcement, while the other cases are used for checking only.

13.8.2 Elasticity Theory for Lining Calculation

The stress of the single-layered lining on a circular tunnel may be computed using the elasticity theory, where such a tunnel is located within type I or II homogeneous surrounding rock masses and whose diameter is smaller than or equal to 6 m.

Fig. 13.25 Lining calculation under uniform internal pressure—circular tunnel



1. Lining calculation under uniform internal water pressure

When the thickness of surrounding rock mass is greater than 3 times the diameter of tunnel, elastic resistance of surrounding rock mass could be taken into account, and the lining can be looked at as a thick-walled cylinder (Fig. 13.25) in an infinite elastic space. In accordance with the compatible condition with respect to radial deformation on the interface between lining and surrounding rock mass, elastic resistance p_0 can be expressed by internal water pressure p under planar strain condition as

$$p_0 = \frac{1 - A}{t^2 - A} p \tag{13.16}$$

where A = elastic characteristic factor; t = ratio of external radius to internal radius.

$$A = \frac{E - k_0(1 + \mu)}{E + k_0(1 + \mu)(1 - 2\mu)} \tag{13.17}$$

$$t = \frac{r_e}{r_i} \tag{13.18}$$

where E and μ = respectively, Young's modulus and Poisson's ratio of lining concrete.

At any position with radius r , circular normal stress σ_t can be expressed as

$$\sigma_t = \frac{1 + (\frac{r_e}{r})^2}{t^2 - 1} p - \frac{t^2 + (\frac{r_e}{r})^2}{t^2 - 1} p_0 \tag{13.19}$$

Introduce Eq. (13.16) into Eq. (13.19), then let $r = r_i$ and $r = r_e$, respectively, the internal and external circumferential stresses at lining are obtained as

$$\sigma_i = \frac{t^2 + A}{t^2 - A} p \tag{13.20}$$

$$\sigma_e = \frac{1 + A}{t^2 - A} p \tag{13.21}$$

where surrounding rock mass is too weak, or construction quality is difficult to ensure, elastic resistance of surrounding rock should not be taken into account, under such circumstances, $k_0 = 0$, $A = 1$.

Replace σ_i by allowable tensile stress of concrete $[\sigma_{hl}]$ in Eq. (13.20), and let $t = \frac{r_e}{r_i} = 1 + \frac{h}{r_i}$, we have

$$h = r_i \left[\sqrt{A \frac{[\sigma_{hl}] + p}{[\sigma_{hl}] - p}} - 1 \right] \tag{13.22}$$

From Eq. (13.22), it may be found that as the internal water pressure p approaching $[\sigma_{hl}]$, h will become irrational large. To limit the lining thickness, the pressure should be lower than 20 m; otherwise, the reinforced concrete lining should be employed.

2. Double-layered reinforced concrete lining

Reinforced concrete lining falls into double-layered (internal and external layer) or single-layered (internal layer only). In the following, the double-layered reinforced concrete lining (Fig. 13.26) is taken as an example, to explain the basic steps of the computation.

If the seepage through lining cracks may give rise to instability of rock or be hazardous to the vicinity structures (e.g., earthfill dam), the cracking resistance

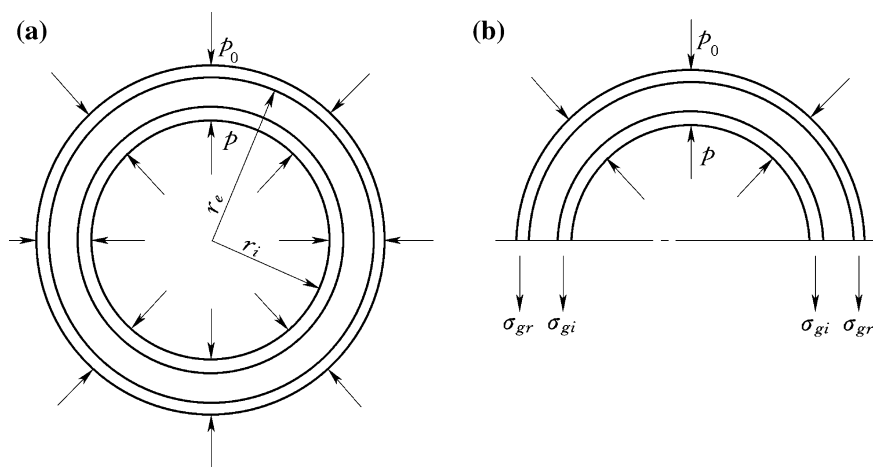


Fig. 13.26 Computation diagram for double-layered reinforced concrete lining—circular tunnel

requirement should be met; otherwise, the cracks can be permitted if their aperture is acceptable and they are not hazardous to the duration of concrete and steel bar due to corrosion. Permission by limitation aperture of crack enables to considerably save concrete and steel and is nowadays widely exercised in the design of hydraulic tunnels. The SL 191-2008 “Design code for hydraulic concrete structures” stipulates that the allowable aperture of crack for lining is 0.15–0.40 mm, which may be observed in the design, taking into account of environmental factors.

The lining computation is therefore should be conducted for two cases: concrete with or without cracks.

(a) Concrete lining does not crack

The thickness of reinforced concrete is determined by Eq. (13.22), in which the allowable tensile stress of concrete $[\sigma_{hl}]$ is replaced by the allowable tensile stress of reinforced concrete $[\sigma_{gh}]$. If the computed h is negative or less than the minimum thickness of the structure requirement, a minimum thickness (around 25 cm) should be adopted.

The steel bars are laid out symmetric, and the minimum reinforcement ratio is tentatively used, and then, the stress in the reinforced concrete lining may be computed by

$$\sigma_i = \frac{F}{F_0} \cdot \frac{t^2 + A}{t^2 - A} p \leq [\sigma_{gh}] \quad (13.23)$$

$$\sigma_e = \frac{F}{F_0} \cdot \frac{1 + A}{t^2 - A} p \leq [\sigma_{gh}] \quad (13.24)$$

where F = longitudinal sectional area of one-meter lining slice, m^2 ; F_0 = equivalent concrete area taking into account of steel bars, m^2 ; $[\sigma_{gh}]$ = allowable tensile stress of reinforced concrete, kPa.

(b) Concrete lining does crack

The thickness of lining is determined by the structural requirements, and the required area of steel bars is

$$f_i = f_e = \frac{pr_i + k_0 \left(m - \frac{r_i [\sigma_g]}{E_g} \right)}{\left(1 + \frac{r_i}{r_e} \right) [\sigma_g] - E_g \frac{m}{r_e}} \quad (13.25)$$

In which

$$m = \frac{pr_i}{0.85E_h} \ln(r_e/r_i) \quad (13.26)$$

where $[\sigma_g]$ = allowable stress of steel bar, kN/m^2 ; E_g = Young's modulus of steel bar, kN/m^2 ; f_i = required area of steel bars at the interior ring of the unit length (i.e., 1 m), m^2 ; and f_e = required area of steel bars at the external ring of the unit length (i.e., 1 m), m^2 .

13.8.3 Structural Mechanics Method for Lining Calculation

Structural mechanics method is employed in the case beyond the limitation of the elasticity theory. The detailed computation procedure is referred to SD134-84 "Specification for design of hydraulic tunnel" or corresponding design handbooks.

13.9 Bolt and Shotcrete Supports

Bolt and shotcrete support is a general term commonly referred to a flexible combination of ground supporting with steel bars, steel wire mesh, shotcrete, etc. (Lang 1961; Schmuck 1957; Stillborg 1986; Thomas 1948; Xu et al. 2002). These may be employed independently or conjunctively. There are six conventional types of the bolt and shotcrete supporting inclusive: rock bolt, shotcrete, bolt + shotcrete, mesh reinforced shotcrete, bolt + steel frame + shotcrete, and bolt + mesh reinforced shotcrete.

Bolt and shotcrete supporting was invented between 1957 and 1965 in Austria with the development of the "New Austrian Tunneling Method (NATM)". In hydraulic projects, bolt and shotcrete supports are commonly exercised for the initial or temporary supporting of permanent works or for the temporary works such as diversion tunnels. The first temporary supporting practice using rock bolt in China was the tunnel constructed in the Lahun Project in the 1950s, followed by the temporary support using bolt and shotcrete in the excavation of the 80-m-high surge shaft in the Bikou Project. Thereafter, that bolt and shotcrete supporting has been widely and successfully applied as permanent support in the underground caverns, free-flowing tunnels, as well as the pressure tunnels of medium to low head, such as the projects of Huilongshan, Jingpohu, Yuzixi, and Fengjiashan.

13.9.1 Principles of Bolt and Shotcrete Supporting

NATM is actually an approach or philosophy to tunneling rather than a set of excavation and supporting techniques (Hagenhofer 1990; Kovári 1994; Müller 1990; Rabcewicz 1964a, b, 1965). The basic principle of the NATM is to mobilize the strength of rock mass, namely the method relies on the inherent strength of the

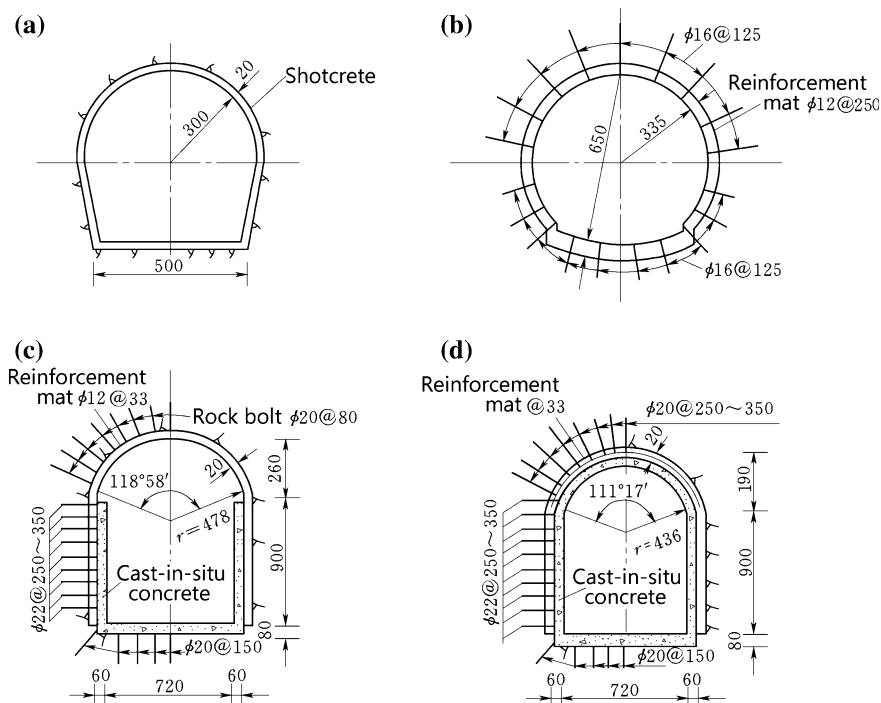


Fig. 13.27 Types of bolt and shotcrete supporting (unit: cm)

surrounding rock mass being conserved as the main component of tunnel support. To achieve this goal, sophisticated instrumentation is necessitated (Dunnicliff 1988). The monitored data combined with rock mass classification determine flexible supporting scheme and time. The flexible supporting permits the surrounding rock masses which have a compatible deformation, in this way to achieve both the rock stability and the lower pressure on the supporting.

Applying immediately after face advance, shotcrete protection of a thin layer (5–20 cm) is intended to limit rock loosening and excessive rock deformation, which works together in time with the surrounding rock mass (Fig. 13.27a). A part of shotcrete penetrated into rock fractures may also contribute multilaterally to the bonding of loosen rock, the protecting of rock weathering, the blocking of seepage passage, the filling of deficit, and the smoothing of surface.

In tunneling, rock bolts are installed to reinforce the rock mass by back-tying the rock blocks that is likely to fail around the excavation, to reduce the deformability, and to maintain the strength of the rock mass (Fig. 13.27b–d).

There are various types of rock bolts, which fall into two basic categories of active and passive ones.

- Active rock bolts exert a positive force to the rock mass and are made of steel bars that are anchored in the rock on one extremity with a plate and fixed by a

nut on the other extremity. Active rock bolts are always tensioned after installation and may be sealed by grout or resin for long-term applications. The anchorage may either be punctual at the end of the borehole at which they are installed or distributed along the entire length of the bolt, either through a sealing grout product or through rock/bolt friction.

- Passive rock bolts can be punctually anchored to the rock mass (either through mechanical anchorage or through localized grouting) or fully bonded to the rock mass along their entire length (either through friction or through a sealing grout product). Passive rock bolts only react to the deformation of the rock mass; therefore, they must be installed before significant movement of the rock mass has taken place.

For low strength or poor integrity rock strata, combination of rock bolts and shotcrete is widely exercised. For even worse situation of weak or strongly fractured rock, steel mesh may be installed before the spray of shotcrete, which may increase the integrity and strength of shotcrete and reduce the thermal induced cracks (Fig. 13.27b–d).

13.9.2 Design of Bolting and Shotcrete Support

1. Supporting parameters

Most theoretical methods for the design of rock bolts or shotcrete are based on certain assumptions with respect to the configuration of discontinuities.

The simplest method of rock bolting analysis is the wedge theory, where the stability of a wedge is analyzed using two- or three-dimensional equilibrium equations. This type of analysis is useful when the positions and orientations of discontinuities are known and the potential failure of wedge can be identified.

For a flat heading roof in a horizontally laminate rock, if the rock bolts are tensioned, either by active tensioning or by passive round movements, a horizontal compressive stress develops within the zone around the bolts. This forms the beam consisting of rock layers tied together to carry moment and shear loads. Thus, the reinforced rock stays suspended. In similar manner, bolts installed around a vault arch will increase the level of confinement in the zone around the bolts, in this way to raise the effective compressive strength of the rock in the arch.

The function of shotcrete is to create a semi-stiff and immediate lining on the excavated rock surface. The shotcrete must have a high initial strength for good bonding to the rock surface and a high degree of ductility and toughness to absorb and to block ground movement. The shotcrete, by its capacity to accept shear and bending, and its bonding to the rock surface, prevents the rock wedges from falling. It also can act as a shell accepting radial loads. It is possible to analyze all of these modes of failure only if the loads and boundary conditions are clear. The self weight of a rock wedge is assumed to exert on the skin of shotcrete, which may lead to the failure by shear, diagonal tension, bonding loss, or bending of the shotcrete. Given

the dimension of falling wedge and the properties of shotcrete, it is possible to determine the required thickness of shotcrete, using standard structural calculations. Near the vault arch crown of a tunnel, shotcrete also may be looked at as an arched shell under bending and compression. Where the shotcrete is held by bolts, it may be analyzed either as a curvilinear slab held by the bolts or as a one-way slab between rows of bolts.

It is important to bear in mind that neither analysis theories can be expected to provide anything more than crude approximations, attributable to the dynamic environment of bolt grout and fresh shotcrete. Hence for the moment, the support parameters (e.g., thickness of shotcrete, spacing, and depth of bolts) are mainly selected according to the empirical methods based on engineering analogy with regard to the type of surrounding rock masses, shape and dimension of tunnel, and working conditions.

In Chinese practices, the diameter and length of rock bolt are 16–25 mm and 2–4 m, respectively, and the spacing of rock bolts is smaller than a half of the bolt's length and smaller than 1.25 m under the circumstances of poor rock masses. The bolts are installed perpendicular to dominant joints as far as possible. Where the joints are randomly distributed, the bolts may be installed perpendicular to the tunnel surface.

Also based on the Chinese engineering practices, the basic requirements for shotcrete are as follows:

- Thickness is 5–20 cm;
- Grade of shotcrete should not be lower than C20;
- Tensile strength should be higher than 1.5 MPa;
- Seepage resistance index should be higher than W_8 ; and
- Bond strength of shotcrete and medium- to high-grade surrounding rock masses should be higher than 0.5 MPa.

Steel mesh is usually made of steel bar of $\Phi 6$ –12, and the grid size is 20 cm \times 20 cm–30 cm \times 30 cm, which should be connected to rock bolts by welding at a distance from the excavated surface of 3–5 cm. The shotcrete protection layer outside should be thicker than 5 cm.

When bolts and shotcrete are employed in the sequential excavating and supporting, it is possible to reproduce the construction sequence by computer simulation, including the effects of the variation in cement grout and shotcrete modulus and strength with respect to time, the local effects of bolts, and shotcrete at rock joints. In this fashion, it is possible to estimate the load buildup in the bolts and shotcrete lining.

2. Adequate time for supporting

NATM requires timely supporting. Deformation is allowable after the excavation provided, and it should be limited timely by supporting to prevent its hazardous effects. In this way, the minimum support cost and high safety could be simultaneously achieved.

Fig. 13.28 Convergence–confinement relation of a circular tunnel

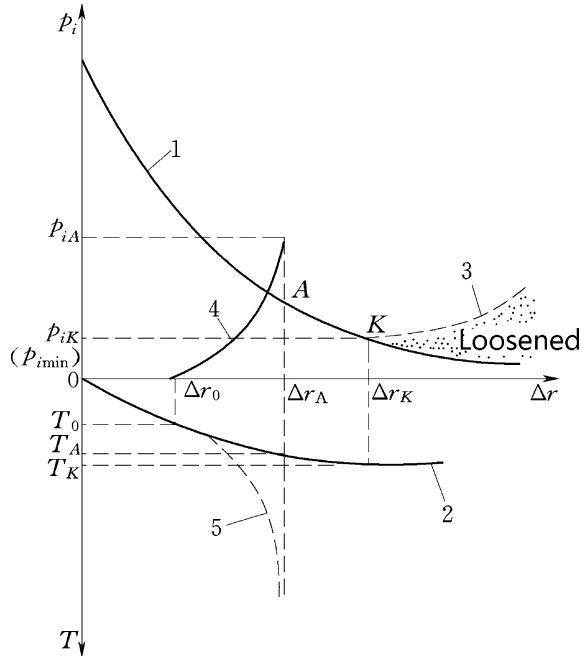


Figure 13.28 illustrates the concept of rock–support interaction in a circular tunnel excavated by the TBM. The ground relaxation curve represents rock that demands supporting to prevent collapse. The load p_i exerting on the support is proportional to the radius of plastic zone, which is in turn related to the radial displacement Δr on the tunnel surface. Therefore, p_i is the function of Δr , i.e., $p_i = f(\Delta r)$.

There are several notable features in Fig. 13.28. The curve 1 is the relation of supporting load p_i versus tunnel deformation Δr , and the curve 2 is the relation of tunnel deformation Δr versus time T after excavation. An early installation of support leads to excessive buildup of load leading to the support yield (without collapsing) to reach equilibrium state. A delayed installation of support leads to excessive tunnel deformation and support collapse, as represented by the curve 3. The designer can optimize supporting installation to allow for acceptable displacements around the tunnel and load on the support at Δr_K (or T_K), where the load p_{ik} on the support reaches the minimum.

Since the effective work of the support needs time, and a certain safety margin should be observed, therefore, the supporting should start at time T_0 ahead of T_K , and T_0 is termed as the “adequate time of supporting” and is commonly selected at the initiation of sharp mount in the Δr – T curve.

After the construction of support at T_0 (Δr_0), the supporting reaction p_i raises as the tunnel deformation increases (see curve 4). Meanwhile, the deformation of the tunnel is restrained by the support, which is developed along the curve 5.

The tunnel deformation will be convergent at Δr_A when the design strength of supporting system (or design p_{iA}) is reached.

The convergence–confinement relation is a powerful analysis tool that provides designer with a framework for understanding the support behavior in tunnels and shafts, as it entails the rock–structure interaction. Theoretically, the closed-form solutions or continuum analyses may be employed to identify the point K . However, attributable to the difficulties with obtaining these solutions due to the complicated tunnel shape and geology conditions, it is usually replaced by in situ monitoring.

For strongly fractured or weak rocks with poor stability, the shotcrete should be carried out immediately after the excavation, to ensure the safety during the tunneling operation.

13.9.3 Several Notes on the Bolt and Shotcrete Supporting

- ① Employ smooth surface blasting method as far as possible. This may be favorable due to the minor disturbance to surrounding rock masses and small roughness coefficient on rock surface.
- ② Shotcrete thickness is only approximately one-third of conventional concrete lining, which is lower in bearing capacity and seepage resistance. Therefore, at the portals of intake and outlet near ground surface as well as in the gate chamber where the rock masses are subject to weathering and fissuring, the conventional concrete or reinforced concrete lining should be installed, according to the design specifications. The lining length is dependent on the topographic and geologic conditions and normally no shorter than the 2–3 times of tunnel width or diameter.
- ③ Allowable flow velocity in a bolt- and shotcrete-supported hydraulic tunnel is usually below 8 m/s according to the design specifications, and this value may be raised a bit after verifications and studies.
- ④ In China, there are lots of hydraulic tunnels using bolt and shotcrete as permanent support. The surface of shotcrete is rough, and the roughness coefficient plays an important role in the assessment of tunnel discharge capacity (or head loss) and cavitation resistance (Huval 1969).

Among the existed tunnels using rock bolt and shotcrete support in China, the roughness coefficient adopted in the design are as follows: the Yuzixi I, $n = 0.0286$; the Jingpohui, $n = 0.03$; the Chaershen, $n = 0.026$; and the Huilongshan, $n = 0.023$. Prototype observation for the Huilongshan Tunnel in 1975 provided an actual roughness of $n = 0.327$, which is much larger than that postulated in the design phases.

Summarizing the in situ observations available in China, the empirical values of roughness coefficient for the rock bolt- and shotcrete-supported tunnels are suggested in the following:

- On smooth rock surface, $n = 0.016\text{--}0.018$;
- On fairly smooth rock surface, $n = 0.02\text{--}0.025$; and
- On uneven rock surface, $n = 0.03\text{--}0.35$.

These values are much higher than that of conventional concrete lining.

References

- Barton N, Lien R, Lunde J (1974) Engineering classification of rock masses for the design of tunnel support. *Rock Mech* 6(4):189–236
- Bickel JO, Kuesel TR, King EH (1996) *Tunnel engineering handbook*. Chapman & Hall, New York
- Bieniawski ZT (1979) The geomechanics classification in rock engineering applications. In: *Proceedings 4th ISRM congress (vol 2)*. AA Balkema, Rotterdam, pp 41–48
- Bowen R (1981) *Grouting in engineering practice*, 2nd edn. Applied Science, New York
- Bradley JN, Peterka AJ (1957a) The hydraulic design of stilling basins: short stilling basin for canal structures, small outlet works, and small spillways (Basin III). *J Hydraulics Div ASCE* 83 (HY5):1403-1–1403-22
- Bradley JN, Peterka AJ (1957b) The hydraulic design of stilling basins: stilling basin with sloping apron (Basin V). *J Hydraulics Div ASCE* 83(HY5):1405-1–1405-32
- Bradley JN, Peterka AJ (1957c) The hydraulic design of stilling basins: small basins for pipe or open channel outlets—no tail water required (Basin VI). *J Hydraulics Div ASCE* 83 (HY5):1406-1–1406-17
- Brekke TL, Ripley BD (1993) Design of pressure tunnels and shafts (chapter 14). In: Hudson JA (ed) *Comprehensive rock engineering (vol 2)*. Pergamon Press, Oxford, pp 349–369
- Chen SH, Chen ML (2014) *Hydraulic structures*, 2nd edn. China Water Power Press, Beijing (in Chinese)
- Deere DU, Deere DW (1988) The rock quality designation (RQD) index in practice. In: Kirkaldie L (ed) *Rock classification systems for engineering purposes*. ASTM Special Publication, Philadelphia 984, pp 91–101 (Am Soc Test Mat)
- Deere DU, Peck RB, Parker HW, Monsees JE, Schmidt B (1970) Design of tunnel support systems. *Highway Res Rec* 339:26–33
- Dunncliff J (1988) *Geotechnical instrumentation for monitoring field performance*. Wiley, New York
- Fernandez G, Alvarez TA (1994) Seepage induced effective stresses and water pressures around pressure tunnels. *J Geotech Eng ASCE* 120(1):108–128
- Golzé AR (1977) *Handbook of dam engineering*. Van Nostrand Reinhold Company, New York
- Goodman RE, Shi GH (1985) *Block theory and its application to rock engineering*. Prentice-Hall, New Jersey
- Gordon JL (1970) Vortices at intakes. *Int J Water Power Dam Constr* 22(4):137–138

- Grishin MM (ed) (1982) Hydraulic structures. Mir Publishers, Moscow
- Hagenhofer F (1990) NATM for tunnels with high overburden. *Tunnels Tunn* 22(5):51–52
- Herget G (1988) Stresses in rock. AA Balkema, Rotterdam
- Hoek E, Brown ET (1980) Underground excavation in rock. Institute of Mining and Metallurgy, London
- Hudson JA (1992) Rock engineering systems: theory and practice. Ellis Horwood Limited, Sussex
- Huval CJ (1969) Hydraulic design of unlined rock tunnels. *J Hydraulics Div ASCE* 95(HY4):1235–1246
- Karol RH (1990) Chemical grouting (2nd edn). Marcel Dekker, New York
- Knapp RT, Daily JW, Hammit FG (1970) Cavitation. McGraw-Hill, New York
- Kovári K (1994) Erroneous concepts behind the New Austrian tunnelling method. *Tunnels Tunn* 26(11):38–42
- Kuesel TR (1987) Principles of tunnel lining design. *Tunnels Tunn* 19(4):25–28
- Lang TA (1961) Theory and practice of rock bolting. *Trans AIME* 220:333–348
- Lin JY (2006) Hydraulic structures. China WaterPower Press, Beijing (in Chinese)
- Ministry of Construction of the People's Republic of China (1994) GB50218-94 "Standard for Engineering Classification of Rock Masses". Research Institute of standards and norms (MOC), Beijing (in Chinese)
- Ministry of Water Conservancy and Electric Power of the People's Republic of China (1984) SD134-84 "Specification for Design of Hydraulic Tunnel". Water Resources and Electric Power Press of China, Beijing (in Chinese)
- Ministry of Water Resources of the People's Republic of China (2002) SL279-2002 "Specification for Design Of Hydraulic Tunnel". China Water Power Press, Beijing (in Chinese)
- Muir Wood AM (1975) The circular tunnel in elastic ground. *Geotechnique* 25(1):115–127
- Müller L (1990) Removing the misconceptions on the New Austrian tunnelling method. *Tunnels Tunn* 22 (special issue):15–18
- National Reform and Development Commission of the People's Republic of China (2004) DL/T 5195-2004 "Specification for Design of Hydraulic Tunnel". China Electric Power Press, Beijing (in Chinese)
- Pender MJ (1980) Elastic solutions for a deep circular tunnel. *Geotechnique* 30(2):216–222
- Rabcewicz L (1964a) The New Austrian tunnelling method (part one). *Water Power* 16(11):453–457
- Rabcewicz L (1964b) The New Austrian tunnelling method (part two). *Water Power* 16(12):511–515
- Rabcewicz L (1965) The New Austrian tunnelling method (part three). *Water Power* 17(1):19–24
- Schmuck HK (1957) Theory and practice of rock bolting. *Colorado Sch Mines Quart* 52(3):233–263
- Singh A (1969) Transition from circular to rectangular section. *J Hydraulics Div ASCE* 95 (HY3):893–906
- Stagg HG, Zienkiewicz OC (1968) Rock mechanics in engineering practice. Wiley, New York
- Stillborg B (1986) Professional users handbook for rock bolting. Trans Tech Publications, London
- Sulem J, Panet M, Guenet A (1987) An analytical solution for time-dependent displacements in a circular tunnel. *Int J Rock Mech Min Sci Geomech Abstr* 24(3):155–164
- Szechy K (1973) The art of tunneling. Hungarian Academy of Sciences, Budapest
- Thomas E (1948) Suspension roof support. *Coal Age* 53(7):86–88
- Wang HZ (1982) Structural computation for underground caverns. China Electric Power Press, Beijing (in Chinese)

- Wang YC (1987) Tunnel engineering. People's Transportation Press, Beijing (in Chinese)
- Xiong QJ, Gao CX (1983) Tunnels. Water Resources and Electric Power Press of China, Beijing (in Chinese)
- Xu GC et al (2002) Supporting structures in underground engineering. Water Resources and Electric Power Press of China, Beijing
- Zuo DQ, Gu ZX, Wang WX (eds) (1989) Water power projects. In: Handbook of hydraulic structure design (vol 7). Water Resources and Electric Power Press of China, Beijing (in Chinese)

Chapter 14

Rock Slopes in Hydraulic Projects

14.1 General

Rock slope is a kind of geologic body located on the surface of the earth crust, which consists of sloping surfaces, top of slope, slope shoulder, foot of slope, and slope body of definite depth (Yan et al. 2000; Zaruba and Mencl 1969). A rock slope in the hydraulic project is a part of or at the vicinity to hydraulic structures, which if fails, will give rise to important impact on the safety and normal operation of the project (Ministry of Water Resources of the People's Republic of China 2007; National Reform and Development Commission of the People's Republic of China, 2006).

The failure of rock slopes may manifest as loose tension crack, slide, collapse, buckle, topple, creep, spall, and flow. The phenomenon of sliding failure of a slope body along a slip surface is usually named as "landslide." According to the statistical data from China's hydraulic projects, the landslides are accounted for above 70 % of all the slope failure accidents. Therefore, in this book, the sliding stability issues related to rock slopes will be mainly addressed.

Landslide hazard causes loss of human life, extension of construction schedule, and increase of budget due to large amount of stabilization work; hence, it has been an important concern in the construction and operation of hydraulic projects (ICOLD 2002). On October 9, 1963, an overtopping was resulted from the landslide of Monte Toc on the southern bank into the Vajont Reservoir (Italy), which created a 200-m-tall wave (ten times higher than anticipated) bringing massive flood and destruction to the Piave valley below the reservoir, and wiping out several villages completely (Kiersch 1963). On March 6, 1961, nearly one year earlier than the well-known Vajont landslide in Italy, a 1.65×10^6 m³ rock mass plunged into the reservoir of the Zhexi Project, creating a 21 m-high surge wave that overtopped the dam crest and killed more than 40 people who were working on the spillway. This is perhaps the first documented catastrophic reservoir landslide in the world.

Construction of large dams often involves high slope cutting at the abutments, spillways, intake and outlet structures, powerhouses, etc. The consequences due to

the collapse of these slopes can be very serious. Accidents of cut slopes took place in many China's hydraulic projects such as the Manwan, the Tianshengqiao, the Longyangxia, the Tianhuangping, and the Lijiaxia.

Figure 14.1 is a typical section of the double-laned and five-stepped continuous ship lock located on the left bank of the Yangtze River and constructed by deeply cutting into the Tanziling Mountain of granite, which constitutes one of the most essential structures in the Three Gorges Project. The ship lock comprises of up- and downstream approach channels, the ship lock chambers, the water conveyance system, and the drainage system located in the mountain around. The total length of the ship lock from the entrance of the upstream approach channel to the exit of the downstream approach channel is 6442 m. The main structure of the ship lock (inclusive six lock chambers) is 1621 m in length. The highest slope cutting is 170 m, and altogether 41.96 million m³ open cut and 980,000 m³ tunnel cut were undertaken. A 54–57 m wide rock pillar wall is left between the two lock lanes serving as the middle-isolated pier wall. The side walls of the ship lock chambers are of thin concrete lining back-tied on the vertical slopes; in this way, the rock mass also forms an integrity part of the ship lock structure.

The rock mass in the ship lock area consists of amphibole granite (Pre-Sinian Period), occasionally of schists, with 4 dominating sets of joints dipping at 50°–75°. Pegmatitic dikes are commonly encountered, which may potentially induce local wedge failures. The maximum principal initial tectonic stress is nearly horizontal in the ship lock area forming a small included angle (about 30°) with the main slope. The horizontal initial tectonic stress within the excavation channels is at a relatively lower level of 4–11 MPa.

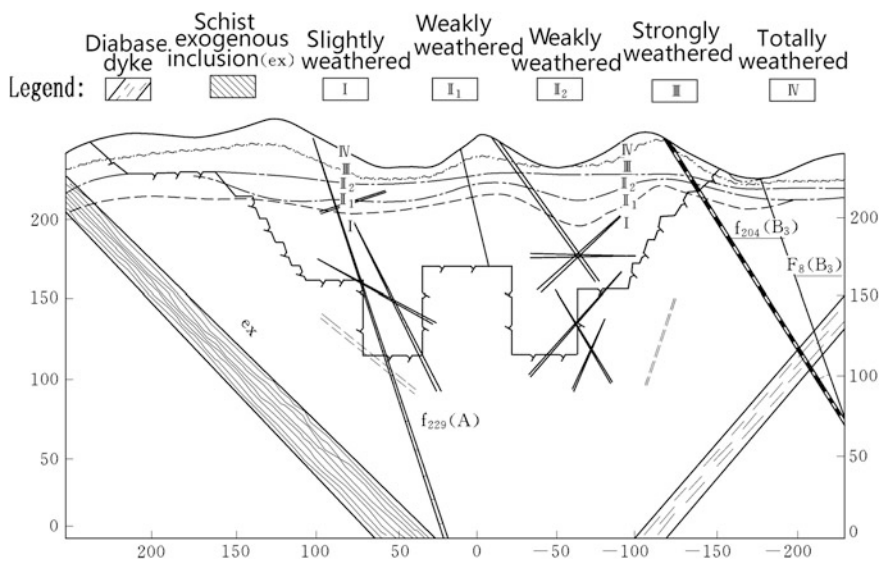


Fig. 14.1 Typical section of the double-laned and five-stepped continuous ship lock (unit: m)—the Three Gorges Project (blocky structure), China

The Yangtze River is the China's golden waterway. Therefore, the overall and local stability of the ship lock must to be guaranteed. In addition, the rheologic deformation of the ship lock slopes has to be strictly controlled within 5 mm, in order to meet the requirements for the normal operation of the lock gates (Chen et al. 2001).

Figure 14.2 is a typical section of the intake slope of the Longtan Project. The intake of the power tunnel for the underground power house is located on the left bank near a slope where bending and tilting deformation manifest in a vertical depth of 30–76 m and a volume of 12,880,000 m³. The slope rock is composed of Banana Group strata (T_{2b}) of Triassic system sandstone alternated with mud-slate rock strata, in which bedding faults are well developed (representative faults are F63, F69, F109, F1, F5, F8, F28, and F32). There are six sets of joints and fractures, of which the predominant one is steeply dipped. Affected by the topographic detachment, the maximum initial tectonic stress is nearly horizontal at the level of 6–9 MPa, with a lateral pressure coefficient of 1.3–1.6. The tilting and creeping rock mass exhibit a typical antithetic lamellar structure rock slope with a cut height of 435 m and cut surface of 270,000 m². Nine power tunnels with diameter of 12–13.35 m are installed through the toe of the slope. The deformation and stability of the rock mass will directly bring effects on the normal operation of the intake structures.

The Xiaowan Project, with an arch dam of 294.5 m high and generator installation capacity of 4200 MW, is situated at the Lancang River, Yunnan Province, China. The dam site is in a V-shaped valley with steep natural slopes at the height over 1000 m, and full of deeply cut gullies just connecting to ridges. The bedrocks distributed in the work site are of medium-deep metamorphic rock system, which

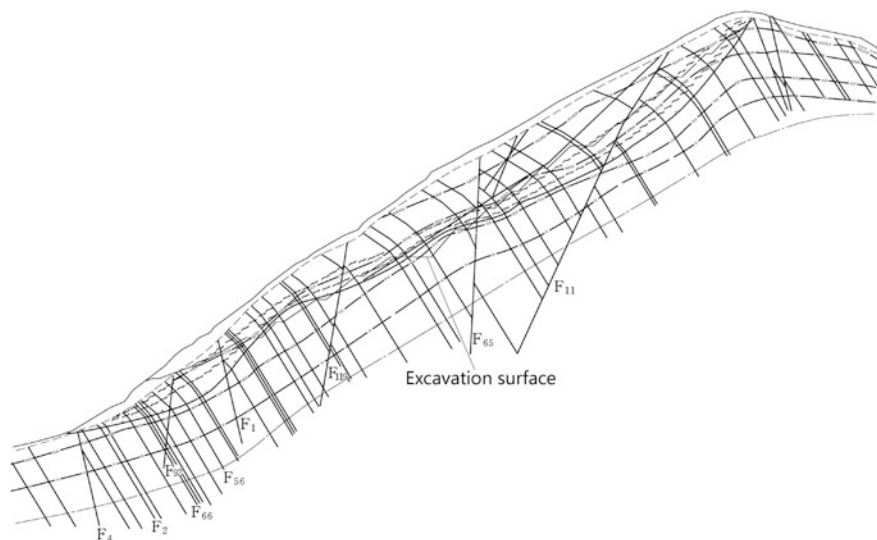


Fig. 14.2 Typical section of the intake slope—the Longtan Project (antithetic lamellar structure), China

consists mainly of granite, gneiss, and hornblende plagioclase gneiss, intercalated with discontinuous thin-layered schist. The base boundary of the moderate weathering rock under the dam foundation is at an overburden depth of 30–50 m. The superficial rocks on both bank slopes are strongly relaxed due to the valley trenching induced stress releasing. Altogether, 15 high and steep slopes have to be cut for the layout of permanent and temporary structures and construction sites in an area of 3 km^2 , with open cut amount more than $2000 \times 10^4 \text{ m}^3$, of which the largest one at the left dam abutment is 700 m high and 500 m wide, whereas the largest one at the right dam abutment is 600 m high and 550 m wide. Figure 14.3 shows the cut slopes located on the right abutment of the Xiaowan Project, where several important structures are located, including the headrace and intake, the tracks of the high and low cable ways, and the right dam abutment.

The aforementioned rock slopes show the basic features of high rock slopes encountered in the modern China's hydraulic engineering: tremendous scale and height; complex in topographic and geologic conditions; apart from the overall and local stability requirements, the deformation of slope has to be strictly controlled in order to meet the requirements for the normal operation of the related hydraulic structures. So far, these issues have been well handled through comprehensive studies, which contribute to the successful construction of the projects. These

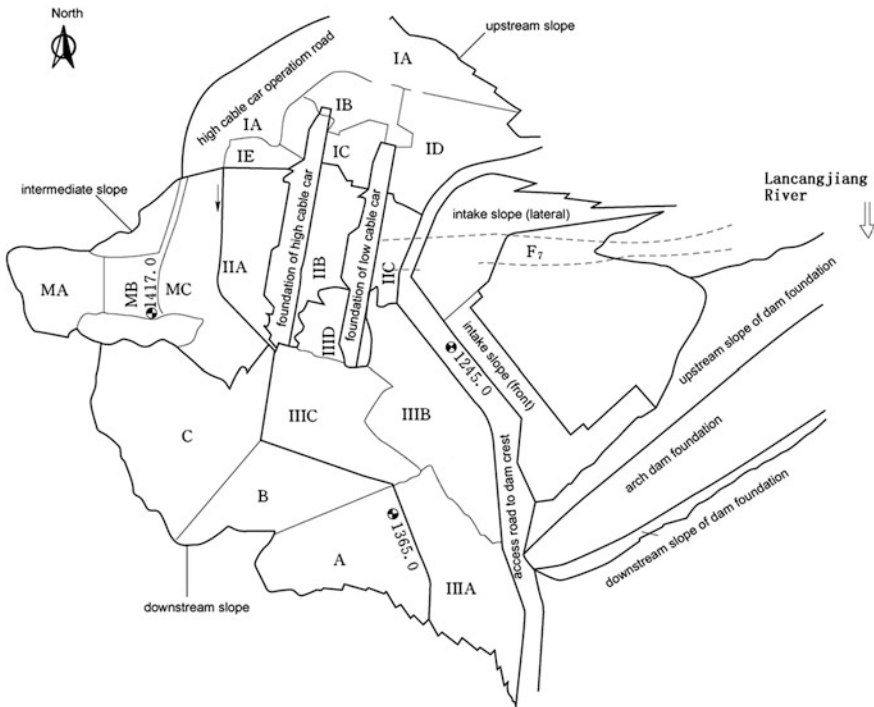


Fig. 14.3 Slopes located on the right abutment—the Xiaowan Project, China

achievements erected a milestone in the technique advancement of rock slope engineering including investigation, experiment, research, design, and construction, as well as monitoring.

14.1.1 Classification of Rock Slopes

Rock slopes may be ordinarily termed according to their height as particular high slope (>300 m), super high slope (100–300 m), high slope (30–100 m), medium slope (10–30 m), and low slope (<10 m); according to their origin as abrasion slope, erosion slope, collapse and slip slope, and cut slope; according to their degree of human influence as natural slope (on natural valley or reservoir bank) and artificial slope (dam foundation, dam abutment, tunnel portal, etc.); and according to their relationship with hydraulic engineering as engineering slope and non-engineering slope.

The Chinese community of engineering geology has proposed a systematic and prevailing classification for slopes as elaborated in Tables 14.1, 14.2, and 14.3.

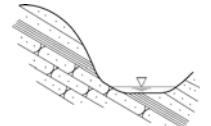
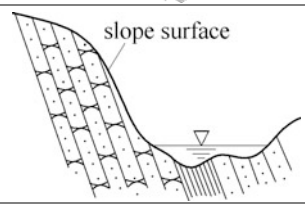
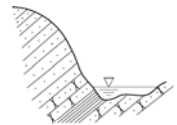
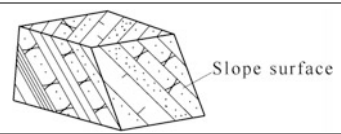
According to Table 14.1, rock masses are distinguished as igneous, sedimentary, and metamorphic in terms of their formation, which is the first important grade index in the classification of slopes.

According to Table 14.2, the variation in geologic structures is the secondary important factor affecting the stability of slope. The rock masses are divided into four types, namely the blocky, layered (laminated), fractured, and granular. For rock mass with layered structure, it is further required to identify whether the discontinuities dip into, away, or laterally crossing the slope. This peculiar feature in the classification system emphasizes the importance to understand the relationship between the rock structure characteristics and the cut surface geometry.

Table 14.1 Engineering geology classification of rock slopes (according to the first grade index—rock formation)

Rock type		Typical rock
Igneous rocks	Intrusives	Granite, Diorite, Porphyry
	Extrusives	Basalt, Rhyolite, Andesite, Tuff
Sedimentary rocks	Clastic sedimentary	Conglomerate, Sandstone, Shale
	Carbonatite	Limestone, Dolomite
	Weak bed intercalated sedimentary	Silted broken laminated sand stone and limestone
	Weak and soft	Claystone, Red sand stone
	Particular	Rocks containing soluble salts (gypsum and halite)
Metamorphic rocks	Ortho-rock	Serpentinite, Greisen, Gneiss, Hornblende schist
	Para-rock	Quartzite, Marble, Slate, Phyllite, Chlorite schist

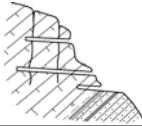
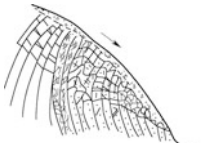
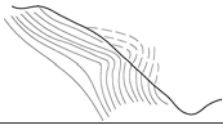
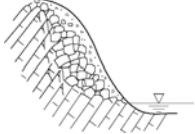
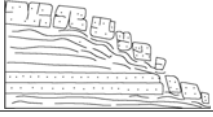
Table 14.2 Engineering geology classification of rock slopes (according to the secondary grade index—geologic structure)

Geologic structure		Typical profile
Blocky structure		
Layered (Laminate) structure	Horizontal	
	Slightly dipping away	
	Deeply dipping away	
	Dipping into	
	Dipping transversely	
Fractured (fragmented) structure		
Granular structure		

If deformation emerges in for a slope, then the slope will be further subdivided according to the deformation pattern which means different influence to the hydraulic structures (Table 14.3). For example, the sedimentary rock consists of bedding planes which may trigger either planar sliding or toppling failure dependent on the orientations and dip angles of the geologic discontinuities, while in igneous rock, large-scale toppling failures are rarely encountered.

The types of rock slope are then nominated in the order of: rock formation + geologic structure + deformation pattern. For example, the left abutment slope of the power intake in the Longtan Project (Fig. 14.2) may be named as sandstone slope of antithetic lamellar structure with toppling deformation.

Table 14.3 Engineering geology classification of rock slopes (according to the third grade index—deformation pattern)

Deformation pattern		Typical profile
Sliding		
Cracking		
Collapse toppling		
Creep deformation	Flexural toppling	
	Buckling	
	Loosening	
	Plastic flowing	

14.1.2 Main Tasks in the Rock Slope Design

1. Geologic exploration and investigation

General requirements for the geologic exploration and investigation are by means of geologic investigation and plotting using geologic drilling and excavating as well as geophysical prospecting, the features, scale, spatial distribution, origin, characteristics, type, stability state, and hazardous degree of the slopes are revealed and documented. The details may be referred to the Chap. 2 of this book, or the other literatures (Chang 2006; Chen et al. 2000; Price 2009).

2. Stability analysis

Stability analysis methods for rock slopes fall into four groups which are geologic history mechanism analysis, engineering geologic analogism, limit equilibrium analysis, and numerical analysis. The former two methods belong to the qualitative analytical methodology, whereas the latter two methods belong to the quantitative analytical methodology (Duncan 1996).

(a) Qualitative analysis

The points made in the employed qualitative analysis are as follows: on the one hand, the evolutive history of slope is analyzed, by which the current state and the future evolution of the slope are predicted taking into account of the changes such as the possible cuts at the slope toe, deforestation, surcharges, and excessive infiltration; on the other hand, according to the influencing factors to the stability of the slope concerned, similar slopes are used for analogy comparison by which the current state and the future evolution of the slope are estimated.

It is philosophically a truth that engineering is both a science and an art. Engineers cannot afford to defer making decisions until everything is clarified and understood as they need to make provisional decisions in order that progress can be made on site. Therefore, qualitative analytical methodology is extremely important in helping engineers to preliminarily estimate the slope stability, particularly in the phases of renaissance and planning when the comprehensive factors may be taken into account, whereas the experiments as well as the computations are not necessarily demanded in these phases. A fast judgment on the stability tendency for the slope provides good base for further research organization concerning investigation, exploration, quantitative calibration, and mitigation.

(b) Quantitative analysis

Limit equilibrium method is a most prevalent approach in slope stability analysis (Chen 2003; Chen et al. 2005) which looks at the sliding rock mass as a rigid body passing forces without deformation. Based on the equilibrium conditions with respect to forces and/or moments, the reaction forces on the slip surfaces and the corresponding safety factor may be computed. The major advantages with the limit equilibrium method are simplicity in computation algorithm; full of experiences in the parametric evaluation; and the selection of allowable safety factor. One of the major disadvantages with the limit equilibrium method is that the deformation that in some situations could be important (e.g., arch dam abutment slopes and ship lock slopes) cannot be obtained. This method will lead to statically indeterminate difficulty when the slip surfaces are more than two; hence, assumptions on the direction and exerting position of the forces on slip surfaces or inter-slice surfaces are needed to render the problem, which will in turn introduce fairly large error in the computation. This method may be employed for the calibration of sliding and toppling failure, but there are so far no well-recognized algorithms for the calibration of collapse and creep failure (Duncan and Wright 1980; Fredlund and Khran 1977; Krahn 2003; Ching and Fredlund 1983).

Numerical simulation of complex geologic phenomena is to reconstruct their formation and deformation process under the changing environments and engineering disturbance. With numerical approach, the intrinsic role of such phenomena is revealed, by which the stresses and strains developed in the slope may be examined. The stability is assessed by comparing the stresses in the slope with the rock strength. It can, to some extent, simulate the heterogeneity and anisotropy of the rock mass and is able to evaluate the present state of stability and predict future changes. Hence, numerical simulation may be employed to study the deformation and failure mechanism, process, and evolution trend, of the slope concerned. The most prevalent numerical methods are 2D and 3D linear or nonlinear FEM, Discrete Element Method, DDA Method, Block Element Method, Numerical Manifold Method, etc. (Jing and Hudson 2002), which have been generally addressed in the Chap. 5 of this book. Since each of them has respective advantages and different applicable conditions, therefore selection of one or more competent methods shall be based on the nature of the slope concerned and the requirements for the solution.

Engineering geologists, through nearly 40 years of practices, are thoroughly aware that it is not advisable to work out a design without computation. But it is not advisable, too, to rely solely or predominantly on numerical analysis because of the particularity and complexity of rock masses, hence computation can never replace the judgment of experienced geologists (Barton 1990; Barton et al. 1985; Bieniawski 1989; Chen 2006; Hencher and Richards 1989; Louis and Maini 1970). Bear this in mind, it is widely accepted that the following principles should be well observed in conducting numerical analysis:

- Giving high priority to the first-hand data collection. This means to utilize every possible exploration approach to derive as much raw data as possible, paving the way for undertaking numerical analysis;
- Establishing rationally generalized geologic model and mechanical model. Any numerical analysis must reproduce the geologic conditions of the prototype. By doing so, not only the prominence is given to major elements of engineering geologic problems, but also the possibility is rendered to numerical analysis;
- Timely optimizing computational conditions and parameters. The implementation of any rock slopes, especially those with complex geologic settings, is without exception a dynamic process in which understanding continues to be deepened and design is optimized, by modifying and perfecting the generalized geologic model and mechanical model as well as computational method;
- Properly employing in situ test and deformation monitoring technology. Increasingly extensive application of in situ test and deformation monitoring during design, construction, and operation of various slopes constitutes an important component of the emerging engineering informatics. Numerous practices prove that, if not validated by monitoring, the results of numerical analyses are hardly applicable. Parameters derived from back analysis, though their physical meaning could be ambiguous, can be helpful in optimal design.

3. Stabilization

Stabilization works must be undertaken on existing landslides and cut slopes of clearly unstable, or on slopes shown by calculation to have a factor of safety lower than that deemed satisfactory (Ceng et al. 2003).

In selecting and designing stabilization measures, the appropriate for issues related to the site, geotechnique, construction, and environment, etc., must be taken into account. Methods of slope stabilization fall into three general categories:

- Eliminate or ease the actions of water (e.g., by dewatering using horizontal or vertical wells or drainage galleries);
- Improve the equilibrium conditions (e.g., reinforcement by prestress anchor cable, changing the geometry of the slope by rock removal); and
- Improve the strength of discontinuities (e.g., reinforcement by passive rock bolts).

4. Monitoring

Attributable to the unpredictability of slope behavior related to various indeterminate factors, and that the remedial stabilization measures are mostly concealed works, the slope engineering has higher risk compared to the other hydraulic works. Monitoring programs are of high value in mitigating slope hazards, because they provide information that is useful for the design of remedial works (Hanna 1985; Dunncliff 1988; Peck 1969). Slope monitoring is both implemented during the construction and the operation periods.

The main purposes for construction period monitoring are given as follows:

- To ensure the safety in construction;
- According to the monitoring data and feedback analysis, if necessary, the design may be revised in time to obtain optimal scheme.

The main purposes for operation period monitoring are given as follows:

- To ensure the safety in operation;
- To check the design assumptions by answering questions such as what is the real status of the slope? How far is the status differing from the design to the reality? This is important for accumulating experiences in slope design.

14.2 Factors Influencing the Stability of Rock Slope

Rock slopes are formulated under internal and external geologic agents in a long geologic history, and they will evolve in future under various geologic and engineering factors, during this process the hazardous deformation and failure phenomena may occur. “Deformation” is featured by no penetrating slip/crack surface, while “failure” means appearance of penetrating slip/crack surface accompanied with large displacement of certain speed. Deformation and failure are the two

successive stages of slope evolution which are linked tightly. For hydraulic projects, the slope failure is always the paramount concern.

The factors influencing the slope deformation and failure are complex and difficult to be completely at command. Therefore, the study of factors influencing the slope stability is a very important task in the stability analysis and stabilization of slopes.

14.2.1 Stratum and Rock Characteristics

Stratum and rock characteristics are the main factors influencing the slope stability (Goodman 1989; Hudson and Harrison 1997; Jaeger et al. 2007; Stagg and Zienkiewicz 1968).

Several types of strata have high occurrence of slope failure. In some strata, landslides are well developed, which is attributable to special mineral materials of easily weathered. Marine clay and fissured clay of high sensitive, red shale of Tertiary system, and Cretaceous System as well as Jurassic system, mudstone strata, dyas coal strata, and ancient silt metamorphic series (phyllite, schist, etc.), are well-known “strata of easy slip.”

Rock characteristics also have direct influence on the slope stability. Hard and intact rock of blocky or thick-bedded may formulate steep slope of hundreds meters in height, as is often encountered in the limestone crayon of the Three Gorges; while in mud silting or mucky soft soil strata, the slope excavation is difficult due to its plastic flowing, as was encountered in the Bailianhe River channel excavation of the Xishui County (Hubei Province, China); slopes formed by several rock types may be stable in dry or natural conditions, but when soaked by water, the dramatic reduction in strength gives rise to the slope failure.

Because of the dominant role of the stratum and rock characteristics on the slope forming, evolving, and stability, the failure modes of slopes possess strong regional features. For example, in loess areas, the slope failure is normally in a form of slip, while in granite and massive limestone areas, the slope usually fails in collapse.

14.2.2 Geologic Structure

Factors of geologic structure comprise the characteristics of regional tectonic structure, fold morphology, attitude of bed, characteristics of fracture, and fault development, as well as the characteristics of new tectonic movement, which have significant influence on the rock slope stability (Goodman 1989; Hudson and Harrison 1997; Jaeger et al. 2007; Stagg and Zienkiewicz 1968).

In the areas of complex tectonic structure with strong folding and active tectonic movement, the stability of rock slope is commonly poor. Good examples may be the deep cut valley areas of the Hengduanshan Mountain and the Jinshajiang River

Basin, where landslides, collapses, mud, and stone flows are well developed. At the lower reaches of the Jinshajiang River, massive deposits of rock debris accumulated by slope failure may be found everywhere, some possess volume up to hundreds of million cubic meters. In November 1965, two sequence landslides occurred in the Fulu River of the Quanlu County (Yunnan Province), the landslide volume was 250–300 million m³, the sliding distance was 5–6 km, and a 3.7° earthquake was triggered by the landsliding.

Rock fold morphology and attitude of bed in the slope directly control the failure mode and scale. As for the faults and fractures, their influences on the slope stability are apparent—some of them are exactly the slip sources or sliding boundaries.

14.2.3 Rock Mass Structure

The stability of rock slope is often significantly influenced by the geologic structure in the hard rock or semi-hard rock. Rock structure refers to naturally occurring breaks in the rock such as bedding planes, joints, and faults, which are generally termed as discontinuities (or structure faces) (Barton 1986). The key parameters of rock structure are dip direction and dip angle, strike, sets and quantity, persistence, roughness, and infilling.

1. Dip direction and dip angle

Generally, the dipping away consequent bedding rock slope, with an included angle between the slope face and the beddings smaller than 30°, and with a dip angle lower than that of slope face, has a lower stability than that of dipping in bedding rock slope. In the dipping away consequent bedding rock slope, the steeper of the dip angle of bedding planes, the lower the stability is. The steepest unsupported cut slope that can be made is equal to the dip of the beddings. The nearly horizontal bedding planes present better stability.

2. Strike

The relation of slope and discontinuity strikes dominates the degree of freedom of potential instable slip body. Where the adverse discontinuities have strikes parallel to that of slope, the whole slope face has free sliding condition, which is the most unfavorable situation. The larger the included angle between the slope face and discontinuities, the higher stability of the slope will be, and a steeper slope face can be maintained.

3. Sets and quantity

The overall purpose of a geologic mapping program is to define a set or sets of discontinuities, or a single feature such as a fault, which will control the stability on a particular slope. For example, the bedding may dip out of the face and form a planar failure, or a pair of joint sets may intersect to form a series of wedges. It is common that the discontinuities will appear in three nearly orthogonal sets

(mutually at right angles), with possibly one additional set. It is conventionally suggested that four sets are the maximum that should be incorporated into a slope design, and that any additional sets that may appear are more likely to represent scatter in the orientation of the sets. Discontinuities that appear infrequently in the rock mass are not likely to have a significant influence on the overall stability of slope and therefore can be discounted in design. However, it is important to identify a single feature of large scale such as a through-going and adversely orientated fault that may be predominant in the overall stability of rock slope.

4. Persistence

In conventional stability analysis, a fully persistent discontinuity model is ordinarily assumed, which overlooks the effects of rock bridge. However, discontinuity persistence is one of the most important parameters because it defines, together with spacing, the size of rock blocks that can slip from the face (Einstein et al. 1983). Furthermore, a small bridge of intact rock between low persistence discontinuities can have a remarkable positive influence on stability because the strength of rock bridge will often be much higher than that of the discontinuities. Evidences are often found in high cliffs with deeply dipping away beddings or joints: if judged only by the strength parameters of discontinuity, sliding should definitely take place, but the reality is that these cliffs are very stable, this phenomenon is mainly, if not all, contributed by the discontinuity persistence. Unfortunately, persistence is one of the most difficult parameters to measure due to the fact that only a small part of the discontinuity is visible on the slope surface and, in the case of drill core, no information on persistence is available. However, it is encouraging that a number of procedures have been developed to estimate the approximate average persistence for a discontinuity set by measuring the exposed trace lengths on a specified area of sampling window (Pahl 1981).

5. Roughness and infilling

All natural discontinuity surfaces exhibit some degree of roughness, varying from sheared joints with very low roughness, to uneven and irregular tension joints with considerable roughness. These surface irregularities are assigned to a general term as “asperities.” The actual shear performance of discontinuity surfaces in rock slopes depends on the combined effects of the surface roughness, the rock strength at the surface, the applied normal stress, and the amount of shear displacement. For rough and clean discontinuity surfaces with rock-to-rock contact and no infilling, the shear strength is derived solely from the friction angle of the rock material. However, if the discontinuity contains an infilling, the shear strength properties are often modified, with both the cohesion and friction angle of the surface being influenced by the thickness and properties of the infilling. Take a clay-filled fault zone in granite, for example, it is customarily assumed that its shear strength would be that of the clay instead of the granite. Because the roughness and infilling can have a significant effect on the shear strength of a discontinuity, they should be

taken into account appropriately in design. In the case of a healed and calcite-filled discontinuity, a high cohesion could be adopted in the design, provided that it would remain intact after any disturbance due to blasting operation for slope excavation.

14.2.4 Action of Water

Slope stability is very sensitive to the groundwater attributable to natural rainfall or atomization rainfall of flood discharging flow (Kaiser and Hewitt 1982; Serafim 1968). On June 12, 1985, induced by the groundwater variation due to rainfall, a 20 million m³ landslide occurred at the Xintan Town, which is located at the Xilingxia Gorge (the last one of the Three Gorges, China). The ancient town was destroyed totally. Fortunately, the in time evacuation prevents any casualties. On April 9, 2000, the warmer climate gave rise to the melting of snow, the melted water seeped into mountain and induced a 280–300 million m³ high-speed landslide plunging into the Yaluzhangbujiang River, the Bomi County, Tibet, China. On July 13, 2003, after a continuous ten days of heavy rain, a landslide of 20 million m³ in volume occurred in the Qianjiangping area of the Three Gorges Reservoir, 24 were died or missing, the Qiangganhe River which is a tributary of the Yangzte River, was blocked.

There are a lot of examples of the slope catastrophes attributable to groundwater action in the hydraulic projects within China and over the world. In 1963, the reservoir landslide at the Vajont Project (Italy) induced by heavy rain and reservoir level rise generated an immense landslide more than 239 million m³ in volume, which caused approximately 2500 fatalities. The Longyangxia Project was put into operation in 1986 when the arch dam did not reach its maximum height. The limited storage of the reservoir was kept by a 40 continuous days of water releasing through the bottom outlets, during this period atomization rainfall was poured to the downstream right abutment hill. As the project is located in an extremely dry area of China, this unprecedented “rainfall” of long duration eventually led to a 200×10^3 m³ landslide at a distance 250 m from the power plant. The left bank ship lock of the Wuqianxi Project started excavation in 1991 and completed in 1994, during this period considerable deformation appeared in the rain seasons. Dangerous deformation also occurred during the slope excavation of the powerhouse in the Tianshengqiao 2 Project, after the examination the sewage from the living area located at the top of slope, was blamed for, and the stability was finally maintained by the countermeasures inclusive the removal of the living area from the slope top, the installation of draining tunnel, etc.

1. Mechanical action of groundwater

Water pressure undermines the stability of slope by diminishing the shear strength on the potential slip surfaces. Water pressure in tension cracks or nearly vertical fissures also reduces the stability of slope by additional slip driving forces. For a slope approaching limit stability state and kept by the rock weight on its foot,

the indulgent of slope foot during reservoir impounding process will lead to the instability or large deformation—some sensitive slopes have obvious relation between the deformation and reservoir level. This relation even may be employed to forecast the final deformation of slope after the completion of reservoir impounding. The Gepatsch Rockfill Dam (Austria, $H = 153$ m), a deep-seated rockslide system named as the “Hochmais–Atemkopf,” is situated above the reservoir bank near the dam. Data from surface and subsurface geologic investigations and deformation monitoring indicate that this landslide system involves several overlapped slip masses, one on the top of the other. During the initial impounding phases, uplift forces beneath the slope foot led to the activation of shallower slip bodies, which moved more than 10 m in 2 years. By continuous deceleration countermeasures for the slip mass including the restriction of water impounding speed, the deformation rates were reduced to about 2–4 cm per year, showing seasonal fluctuations that correlated with reservoir levels and drawdown conditions.

Groundwater table varies continuously depending on precipitation and drainage conditions. If a reliable estimation of stability is to be obtained or if the stability of a slope is to be controlled by drainage, it is essential that water pressures within the slope should be documented, which is conveniently carried out by piezometers sealed within the ground, generally in boreholes. The design of groundwater table is comprehensively analyzed according to the measured data combined with the analyses concerning hydro-geologic environment factors (type of groundwater, infiltration, runoff, permeability characteristics, relation of groundwater with precipitation and reservoir level, etc).

Where a substantial portion of slope is dry or partially saturated due to large permeability and good drainage condition, the effects of groundwater may be neglected, provided that appropriate seepage control measurements such as surface infiltration and drainage, are properly installed.

Basically, there are two different ways for considering the action effects of groundwater; all of them lead to identical results if applied appropriately. The first one takes the mixture of material and water as the object of study, whereas the second one takes the skeleton of material as the object of study. The details in the implementation have been discussed in Sect. 5.3.2 of this book.

2. Softening action of water

Changes in moisture content of some rocks, particularly shale, accelerate weathering and reduce shear strength. Freezing of ground water gives rise to wedging in water filled fissures due to temperature-dependent volumetric changes of ice.

3. Erosion action of water

Erosion of weathered rock with low strength infilling, by surface water groundwater, can result in local instability where the toe of slope is undermined, or a block of rock is loosened. Erosion potential of rock is specified by the criterion of “allowable erosion speed.”

4. Sudden reservoir drawdown

Stability analysis with regard to sudden drawdown is performed when the water level adjacent to the slope is brought down rapidly (Duncan et al. 1990; Morgenstern 1963). During the sudden drawdown, the phreatic surface may be nearly kept unchanged below which the slope body is totally saturated, which is often one of the most adverse situations for reservoir bank slopes.

A criterion for the judgment of sudden drawdown is necessarily set prior to the stability analysis, which customarily makes use of the index $k/S_y v$, where k is the permeability coefficient (Unit: m/d), v is the reservoir drawdown speed (Unit: m/d), S_y is the specific yield, also known as the drainable porosity, which is a ratio less than or equal to the effective porosity, indicating the volumetric fraction of the bulk aquifer volume that a given aquifer will yield when all the water is allowed to drain out under the action of gravity.

- When $k/S_y v < 0.1$, the reservoir's sudden drawdown should be considered. The phreatic surface is nearly kept unchanged, which may be employed to evaluate the water pressure in the stability analysis;
- When $k/S_y v > 60$, the reservoir drawdown is very slow. During the process, the phreatic surface is brought down nearly simultaneously along the reservoir level; the reservoir sudden drawdown may be neglected in the stability analysis;
- When $0.1 < k/S_y v < 60$, the reservoir drawdown is moderate. The unsteady seepage analysis should be carried out in the evaluation of the phreatic surface during the drawdown of the reservoir level.

14.2.5 Action of Vibration (Shaking)

Earthquake-, blast-, and machinery-induced vibrations may have important influence on the slope stability by stress cycling and material fatigue. The groundwater pressure also may be changed considerably due to the vibration (Ling and Cheng 1997; Oriard 1971). Rock falls and landslides will even continue for years attributable to the loosening of slope rocks and soils induced by earthquake shaking.

There are numerous records of rock falls and landslides induced by earthquakes in the world. For example, in 1980, a magnitude 6.0–6.1 earthquake at the Mammoth Lakes, California (USA), dislodged a boulder of 21.4 tons that bounced and rolled a horizontal distance of 421 m from its source. The Northridge earthquake of magnitude 6.7 in Los Angeles (USA) induced about 11,000 landslides in an area of approximately 10,000 km². These landslides occurred primarily in the Santa Susana Mountains where the slopes comprise Late Miocene through Pleistocene clastic sediments that have little or no cementation, and that have been folded and uplifted by rapid tectonic deformation. The largest earthquake-triggered landsliding disaster

happened in the Andes Mountain, Peru, 1970. Two cities and several villages were buried and at least 18,000 casualties were estimated.

In China, there are also many earthquake-triggered landslides, particularly in the mountainous area of her southwestern territory. According to the statistics data of 47 strong earthquakes from 1950 to 1969, 30 earthquakes above magnitude 8, each triggered landsliding; 17 earthquakes of magnitude 6–7, four triggered landsliding. The Diexi earthquake occurred on August 25, 1933, triggered landslides destroying the town of Diexi and surrounding villages and killed about 2500 people. The old town of Diexi sank into the Diexi Lake created by a landslide dam of approximate 100 m high on the Minjiang River. The dam broken on the October 9, 1933, induced a flood destroying more than half of the towns and villages along the 200 km river section. On May 11, 1974, the earthquake in Zhaotong City (Yunan Province, China) triggered 28 landslides and 39 mountain collapses. At 14:28 p.m. on May 12, 2008, a magnitude 8.0 earthquake struck the Wenchuan County (Sichuan Province, China). The earthquake triggered approximately 15,000 landslides and collapses resulting more than 20 thousands casualties, which account for 1/4 of the total casualties (88 thousands) brought about by the whole earthquake. Only by the Wangjiayan landslide in the Beichuan City, more than 1600 people were buried. The Daguangbao landslide in the Quanshui village of the An County is so far the largest recorded, with a volume of 742 million m³.

In the design of rock slope, the key issues should be carefully handled are the aseismatic design standard and the computation method of seismic action effects.

1. Aseismatic design standard

According to the statistic data, the earthquake-triggered landslides have following features:

- They are usually occurred at the areas with earthquake intensity of 7 or higher;
- They are usually occurred in thin and loosen soil and rock slopes;
- They are mainly the revival of ancient landslides; and
- They are easily triggered by even weak shaking when wetted or saturated by water, while in the dry season the earthquakes have less influencing on the slope stability.

In view of aforementioned features, the following two principles should be observed in the selection of aseismatic design standard for the slopes in hydraulic projects:

- With design seismic intensity 7 or higher, the aseismatic design is demanded; with design seismic intensity 6 or lower, the aseismatic design may be neglected; however, if the slope has potential influence on important structures, or the slope is loosen or saturated, the aseismatic design is necessary even the design seismic intensity is only 6.

- Design intensity is ordinarily equal to the basic degree. However, for important slopes (e.g., slope failure will menace the safety of grade 1 water retaining structures), the design intensity may be 1° higher than the basic degree.
2. Computation method of seismic action effects

The limit equilibrium method for determining the safety factor can be modified to incorporate the influence of seismic ground motion into the slope stability. The analysis procedure, known as the pseudo-static method, involves simulating the ground motions as static horizontal force exerting in a direction out of the slope face. The magnitude of this force is the product of a seismic coefficient K_c (dimensionless) and the weight of the sliding body W [Eq. (4.73)]. It is common that K_c is a fraction of the PGA (peak ground acceleration) with regard to the gravity acceleration (i.e., $K_c = 0.1$ means that the PGA is 10 % of the gravity). In addition, Chinese design code suggests that it is reasonable to carry out further fraction for K_c by the comprehensive influencing coefficient ξ [Eq. (4.74)].

14.2.6 Slope Shape

Slope shape refers to the height, length, profile configuration, planar feature, and exposed surface pattern, which have direct influence on the slope stability. Generally, the steeper and higher of a slope, the lower stability will it be. When a slope is controlled by gentle dip away discontinuities, the stability of the slope has little relation with the slope grading, but mainly dependent on the slope height. Exposure surface pattern of slope influences the stability of slope, too. It is well known that slopes convex in plan are less stable than concave ones (Piteau and Jennings 1970). This is generally attributable to lateral stresses in the rock in which slopes are excavated. According to the statistic data from mining engineering, for horizontally concaved slopes, when the curvature radius of slope surface is 60 m, the critical slope angle for stability is $39.5^\circ \pm 9^\circ$, while the curvature radius is raised up to 300 m, the critical sloping angle for stability is $27.3^\circ \pm 5^\circ$. For horizontally concaved slopes, when the curvature radius of the slope surface is smaller than the height of slope, the critical slope angle for stability may be 10° steeper than that calculated by two-dimensional model and vice versa.

14.2.7 Geostress

Geostress (in situ stress, initial tectonic stress) field could manifest as an important parameter influencing the deformation and fracturing of slopes, through the indirect influence on the deformation-dependent strength parameters. Measuring of the in situ stress field in the vicinity of large slope is seldom carried out, in spite of the fact that such measurements are entirely feasible. This is mainly because the

conventional standpoint that the in situ stress field is generally assumed to be of minor significance for slope stability. For example, Lorig (1999), based on the results of numerical analysis, concluded that in situ stress has no significant effect on the safety factor. Although this conclusion may be adequate for small and shallow slopes, yet it needs to be questioned for the design of very large and deeply cut slopes where in situ stress does have a significant influence on their deformation. If the slope is composed of rocks that become weaker as a result of such deformation, then the in situ stress can have a very important effect in reducing strength and thereby undermining slope stability.

Stress redistribution and blasting impact during the excavation of tunnel, slope, and dam foundation trigger relaxation in the surrounding rock masses. As a result, excavation disturbed (damage) zone (EDZ) due to relaxation will be formed along the excavation surface. The spatial-time distribution of such relaxation is influenced by a variety of factors including the mechanical parameters of the rock, the characteristics of the fracture, the tectonic stress, the excavation procedure, and the blasting method. Usually, the EDZ is further divided into the stress redistribution zone (SRZ) and the blasting impact zone (BIZ). The relaxation in SRZ is mainly induced by the tension and shear on the existing fractures. The depth of this zone may range from 5 m to 20 m. The relaxation in BIZ shows new cracking and fissuring over a depth in the range of 0.5–2 m. Rock relaxation demonstrates the reduction of the Young's modulus (E), friction angle (φ), cohesion (c), and the augment of Poisson's ratio (μ). The deterioration of the mechanical parameters is less pronounced in the SRZ than in the BIZ. Beyond the EDZ, the mechanical parameters of the rock mass undergo but a slight variation. When the relaxation develops to certain degree, the spalling from the excavation surface will be triggered. Under definite geologic condition, the surface instability such as rock burst, or larger extensive cracking along the excavation surface, will appear. These phenomena have been mostly recognized and studied in the tunneling engineering. The recent engineering practices also indicate that under certain circumstances such relaxation will strongly affect the deformation and stability of the cut rock slope, rock foundation, and the adjacent structures (e.g., dam), too.

The highest cut of the Three Gorges ship lock is 170 m (Fig. 14.1). Although by flexibly adopting the blast technologies (e.g., multi-mini second delay bench, smooth surface, pre-splitting, buffer, and other controlled blasts), the shock impact from the blast operations were minimized, yet after the excavation of the slope, the stress in the rock masses was inevitably redistributed and the corresponding band of EDZ was manifested. The stability of the excavated slope was influenced greatly by the EDZ band, which mainly contributed to numerous wedge failures. Over the six years of the slope excavation for the ship lock, more than 1000 wedge blocks of various types were detected, of which 52 were larger than 1000 m³ in volume, 107 were larger than 500 m³ in volume, and 360 were larger than 100 m³ in volume. Systematic bolting were employed, and about 400 forecast alerts were sent out, all these measures helped to avoid engineering accidents and casualties effectively.

At near the completion of the abutment and foundation excavation (2005) of the Xiaowan Arch Dam project, it was found that the high initial tectonic stress near

riverbed exceeds 30 MPa (20 MPa at the stage of preliminary study, Vide Fig. 2.1), and there was a set of blind joint parallel to the valley's surface. These factors gave rise to serious excavation rebound and relaxation EDZ in the foundation and abutment. According to the investigations (by ultrasonic, borehole camera, etc.) along the dam axis, the foundation relaxation mainly occurred below the elevation 975 m where the deformation and strength parameters were reduced by 55–25 %. Through the foundation rock grouting, the installation of rock bolts in the grouting holes, the backpressure by quick placement of dam body concrete, the dam foundation relaxation was controlled well and the construction was accomplished. Similar dam foundation excavation rebound and relaxation EDZ also manifested in the Laxiwa Arch Dam Project (China, $H = 250$ m).

14.2.8 Action Due to Other Engineering Structures

The possible loads exerting on hydraulic slopes are arch dam thrusts from abutments, seepage forces from pressure tunnels, reinforcement loads, etc.

14.3 Design Criteria for Slopes

In China, the strength reduction factor is widely employed in the slope design for hydraulic projects, because

- The loads of slope are relatively more clear and easier to be evaluated. On the contrary, the strength parameters of rocks have larger variation and more difficult to be evaluated. Therefore, it would be wise to use strength reduction factor to have a good understanding of the safety margin with regard to the parameter uncertainty.
- Self weight is a predominant load on slopes. Since self weight gives rise to both the driving force and the resistance force, therefore overload factor is not appropriate in the definition of the safety margin for slopes.

Although a slope is customarily considered as unstable if $K \leq 1.0$, yet it is common that many natural stable slopes have factors of safety lower than 1.0 according to the conventionally adopted design criteria. This phenomenon could be attributable to:

- Underlying of additional margin of safety on the strength parameters is quite common (e.g., neglecting of fracture persistence);
- The use of a heavy rainfall with a long recurrence period in the analysis;
- Three-dimensional effects are not considered in the analysis; and
- Additional stabilization due to the presence of vegetation or soil suction is not taken into account.

Allowable (or design) safety factor $[K]$ has direct relation with the safety, cost, and rationality of the slope engineering (Meyerhof 1984). An acceptable factor of safety should be based on the considerations concerning the project grade, service life, and even the state economy development level. For example, with respect to slopes on reservoir banks far away from hydraulic structures and villages, it is acceptable that creep movement of slope or/and possibly some partial failures will be admitted during the service life of the reservoir, therefore a design with factor of safety in the lower bound is acceptable. On the contrary, for the slopes at the vicinity of important structures or condensed villages, or the slopes are very high and steep, or there is a lack of previous experience as well as the long-term behavior of the geologic materials, an upper bound factor of safety is hence desirable for the design. In conclusion, an acceptable factor of safety should fulfill the basic requirements related to the mechanical principles as well as the other important factors such as:

- The depth and extensity of the understanding to the geologic conditions of the slope;
- The knowledge about the long-term behavior of the geologic materials, particularly the representativeness and reliability of the test and analysis in the selection of shear strength of slip surface;
- The load variation, particularly the groundwater, should be carefully justified considering recurrence period of heavy rainfall;
- The rationality and accuracy of the design model, analysis method, and load combination;
- The type and importance of project, as well as the consequence of the slope failure;
- The quality and reliability of blasting operation during construction, and of the installation of stabilization measures such as rock anchors;
- The difficulties with the remedy treatment in case of new slope problem manifested in the future;
- The experience of the designer, particularly in case of lack of geologic exploration and mechanical experiment; and
- The other indeterminate factors which cannot be taken into account in the computation solely.

Nowadays, there are great advancements in the selection of allowable safety factor corresponding to specific slip failure mode, which are solely based on the shear strength criteria. For the selection of allowable safety factor corresponding to other failure modes, there is still a long way to go.

In the selection of allowable safety factor for slopes, the countries such as UK, USA, and Canada pay more attention to the evaluation of strength parameters, environmental settings, and hazardous risks. The former USSR mainly considered the service life, rock type, and slope grading. The life and economy loss under different rainfall situations are the premier concern in Hong Kong. In the mainland of China, partial safety factor method based on limit state is exercised in the design specifications for port engineering and architecture engineering, while for traffic engineering and hydraulic engineering, the safety factor with respect to sliding

failure by limit equilibrium method is mainly employed, in which the allowable safety factor stipulated should observe the following principles:

- That new designed slopes are higher than existed ones;
- That important slopes are higher than less important ones;
- That slopes with higher strength parameters are lower than with lower parameter ones; and
- That circular slip slopes are lower than planar and multi-planar slip ones.

Absolute design standard and relative design standards may be employed independently or simultaneously in the slope design.

14.3.1 Absolute Design Standard–Design Code Specifications

According to the DL/T 5353-2006 “Design specification for engineering slopes in water resources and hydropower projects,” the slopes are divided into three grades and two types (Table 14.4).

The lower bound solution using limit equilibrium methods should satisfy the allowable safety factors listed in Table 14.5.

Table 14.4 Classification of slopes (DL/T 5353-2006)

Type of slope	Type A	Type B
Grade of slope	Slope at project area	Slope at reservoir area
I	Slope influencing the safety of grade 1 hydraulic structures	Landslide-induced hazard and surge wave may jeopardize grade 1 hydraulic structures
II	Slope influencing the safety of grade 2 and 3 hydraulic structures	Landslide-induced hazard and surge wave may jeopardize grade 2 and 3 hydraulic structures
III	Slope influencing the safety of grade 4 and 5 hydraulic structures	The overall stability is required, but slow movement of the slope and possibly some partial slope failures are allowable

Table 14.5 Allowable (design) safety factor (DL/T 5353-2006)

Type and work	Type A			Type B		
Slope state grade	Slope at project area			Slope at reservoir area		
	Permanent situation	Temporary situation	Accidental situation	Permanent situation	Temporary situation	Accidental situation
I	1.3–1.25	1.20–1.15	1.10–1.05	1.25–1.15	1.15–1.05	1.05
II	1.25–1.15	1.15–1.05	1.05	1.15–1.05	1.10–1.05	1.05–1.00
III	1.15–1.05	1.10–1.05	1.00	1.05–1.00	1.05–1.00	≤1.00

The DL/T 5353-2006 also stipulates that for slopes of high importance or with requirements for deformation, in parallel to limit equilibrium methods, the slope safety should be calibrated by numerical analysis methods, to meet an allowable safety factor higher than that stipulated in Table 14.5.

SL 386-2007 《Design code for engineering slopes in water resources and hydropower projects》 divided slopes into five grades (Table 14.6).

The lower bound solution using limit equilibrium methods should meet the allowable safety factors listed in Table 14.7.

For the references in the design, Table 14.8 lists the design safety factors adopted in several representative China’s hydraulic projects.

14.3.2 Relative Design Standard

For slopes satisfying current stability requirements, but the anticipated environment and engineering disturbances (e.g., reservoir impounding and human activities) will definitely undermine its stability, or the important structures are to be built on these slopes whose stability should be further enhanced, the relative design standard may be employed as follows:

Table 14.6 Classification of slopes (SL 386-2007)

Grade of hydraulic structure	Hazardous degree to the hydraulic structure			
	Serious	Fairly serious	Not serious	Mild
	Grade of slope			
1	1	2	3	4, 5
2	2	3	4	5
3	3	4	5	5
4	4	5	5	5

- Note 1 Serious—the safety and function of the related structure are totally lost
- 2 Fairly serious—the safety and function of the related structure are heavily lost or influenced, normal service is resumed only after special reinforcement
- 3 Not serious—the safety and function of the related structure are partially influenced, normal service may be resumed quickly after minor repair
- 4 Mild—the safety and function of the related structure are slightly or indirectly influenced

Table 14.7 Allowable (design) safety factor (SL 386-2007)

Work situation	Slope grade				
	1	2	3	4	5
Normal operation (basic)	1.3–1.25	1.25–1.20	1.20–1.15	1.15–1.10	1.10–1.05
Extreme operation I (special)	1.25–1.20	1.20–1.15	1.15–1.10	1.10–1.05	1.10–1.05
Extreme operation II (special)	1.15–1.10	1.10–1.05	1.10–1.05	1.05–1.00	1.05–1.00

Table 14.8 Design safety factors adopted in representative China's hydraulic projects

Name of landslide or cut slope	Slope type	Rock type	Height of slope (m)	Allowable safety factor	
				Construction period	Service period
Dahuangya landslide/Wujiangu Project	Reservoir bank slope/dipping in bedding structure	Limestone, shale	300	-	1.20-1.3
Chana landslide/Longjiangxia project	Reservoir bank slope/dipping transversely bedding structure	Half diagenetic clay intercalated by sand	420	1.00	1.10
I# Landslide/Lijiaxia Project	River bank slope/dipping away bedding structure	Mixtite intercalated with schist	210	1.05	1.15
Left abutment slope/Manwan project	Cut slope/blocky structure	Rhyolite	170-340	1.05	1.2, 1.05 (Earthquake)
Powerhouse slope/Nanyi Project	Cut slope/blocky structure	Granite	64	-	1.1
Tailrace outlet slope/Manwan Project	Cut slope/blocky structure	Rhyolite	180	1.05	1.2, 1.05 (Earthquake)
West side slope of powerhouse/Tianshengqiao 2 Project	Cut slope/blocky structure	Arenaceous shale	164	1.05	1.30
Ship lock slope/Wuqiangxi Project	Excavated slope/dipping in blocky structure	Phyllitic slate, sandstone	70	-	1.2-1.4
I# Landslide/Lijiaxia Project	Cut slope/dipping transversely bedding structure	Mixtite, metamorphic shale	255	1.05	1.10
Intake slope of diversion tunnel/Lijiaxia Project	Cut slope/dipping transversely bedding structure	Mixtite, schist	250	1.05	1.15

(continued)

Table 14.8 (continued)

Name of landsliding or cut slope	Slope type	Rock type	Height of slope (m)	Allowable safety factor	
				Construction period	Service period
Surge shaft slope/Tianshengqiao 2 Project	Cut slope/dipping transversely bedding structure	Arenaceous shale, gravelly soil	120	-	1.20
West side steep cliff of powerhouse/Tianshengqiao 2 Project	Cut slope/dipping transversely bedding structure	Sandstone, arenaceous shale	110	-	1.20
II# Deformation body of powerhouse/Laxiwa Project	Cut slope/fragmented structure	Igneous	250	1.30	1.5, 1.20 (Earthquake)
Bajiaolin slope/Tianshengqiao 2 project	Cut slope/granular structure	Gravelly soil	180	1.05	≥1.20
I# Landslide/Tianshengqiao 2 Project	Cut slope/granular structure	Gravelly soil	40	1.00	1.20
Huanglashi Landslide/Gezouba Project	Reservoir bank slope/granular structure	Carbonaceous shale, marlstone rock intercalated by mudstone, dolostone, sandstone	-	-	1.20, 1.05 (Extreme)
Yangjiachao Landslide/Shuibuya Project	rock-cut landslide	Block stone, gravel, clay	-	-	1.15, 1.0-1.05 (Extreme)
Permanent ship lock slope/Three Gorges Project	Cut slope/blocky structure	Granite	120-170	1.3, 1.1 (Earthquake)	1.5, 1.1 (Earthquake)
Intake of underground power plant/Xiaowan Project	Cut slope/blocky structure	Granitic gneiss	40-695	1.15-1.10	1.15-1.25, 1.01-1.05 (Earthquake)

- Firstly, with regard to the current status, the reduction in the safety factor due to the detrimental environment and engineering factors, or the requirement for the safety factor promotion, should be proposed.
- Secondly, the engineering countermeasures are studied to obtain the sensitivity of safety factor response.
- Then the compensation of the safety factor reduction due to adverse environment/engineering disturbances, or the promotion extent for the hydraulic structure construction, are elaborated. In this way, an engineering slope design with unchanged or even improved safety factor may be achieved.

Ordinarily, it is not necessary to consider all complex load combinations in the application of relative design standard.

14.4 Limit Equilibrium Method for Slope Stability Analysis

14.4.1 Specifications for Hydraulic Slopes

Limit equilibrium methods fall into two main categories: methods that deal with structurally controlled planar or wedge slides and methods that deal with circular or nearly circular failure surfaces in “homogeneous” materials. Many of these models (Vide Table 5.1) have been practiced for more than 40 years and can be convinced as reliable.

The variants of LEM listed in Table 5.1 may be selectively employed with regard to the following considerations:

- For nearly homogenous slopes, the theoretic and experimental studies show that the most dangerous slip surface is nearly circular, and the safety factor is not sensitive when the failure surface has small deviation from the arc. Therefore, the arc slip surface may be assumed and the classical Swedish arc method or the Bishop method may be employed.
- For slopes dominated by discontinuities, the slip surface is usually multi-planar or curvilinear; the RTM, the Sarma method, the Bishop method, and the Janbu method may be exercised.
- Methods should be matched with the allowable safety factor. For the homogenous slopes, the design tool kits (computation method and allowable safety factor) are mainly specified according to the long-term experiences using Swedish arc method (design specifications for hydraulic structure + strength reduction factor); for building foundation slopes, the design tool kits are mainly specified according to the long-term experiences using residual thrust method (design specifications for building foundation + overload factor). Therefore, if the other methods are performed to analyze the slope stability, the adjustment for allowable safety factor in the design specifications should be exercised.

14.4.2 Engineering Application—The Right Reservoir Bank Landslide (the Pubugou Project)

The Pubugou Project is located at the middle reach of the Daduhe River, Sichuan Province, China. The normal storage capacity is 53,900 million m³ corresponding to the normal storage level of 850 m, the central core rockfill dam is 186 m high and the underground power plant is installed with generator capacity of 3300 MW.

The landslide concerned is located at the right reservoir bank 780 m upstream the dam axis (Fig. 14.4), the altitudes of its toe and crest are 730 m and 1187 m, respectively, and the landslide width is approximately 360 m. The slope grading angle below the elevation of 980 m is nearly 50° and above 980 m is nearly 40°. The outcropped rocks on the landslide surface are mainly Pre-Sinian system and Sinian system meta-basalts. The landslide is near the intakes of the power tunnels and diversion tunnels, which could cause large impact on the safety of the construction and operation for these structures, if failed.

Altogether 9 major sections are used for the stability calibration (See Fig. 14.4). Figure 14.5 shows the principal Section 1–1 of the landslide, in which 601 and 602 belong to strongly weathered zone, 603 belongs strongly loosen zone, and 604 and 605 belong weakly loosen zone. The limit equilibrium analysis indicates that the slope is instable in the operation period, and the reinforcement measures should be carried out.

The prestress strand anchor cables are employed in the stabilization. Seven situations were considered in the design of the cables, of which the normal storage

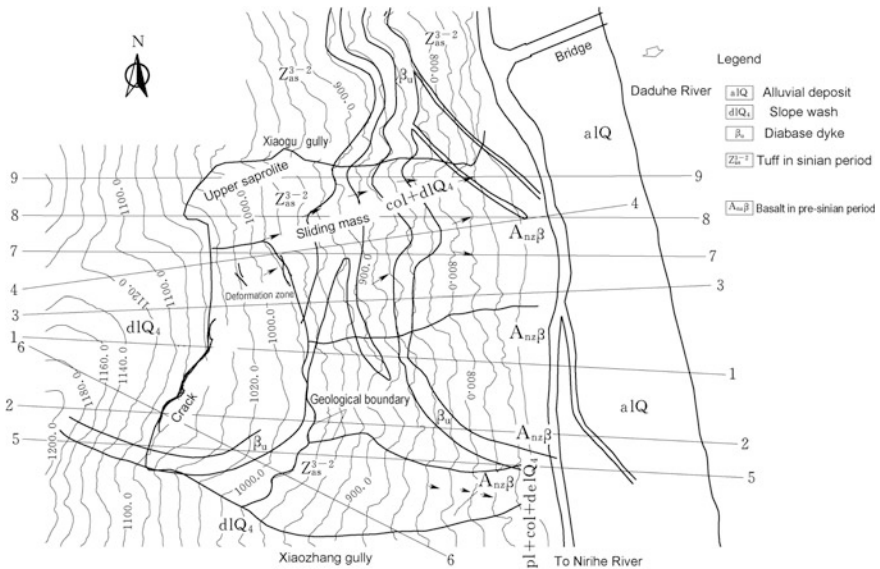


Fig. 14.4 Geologic plan of the right reservoir bank (unit: m)—the Pubugou Project, China

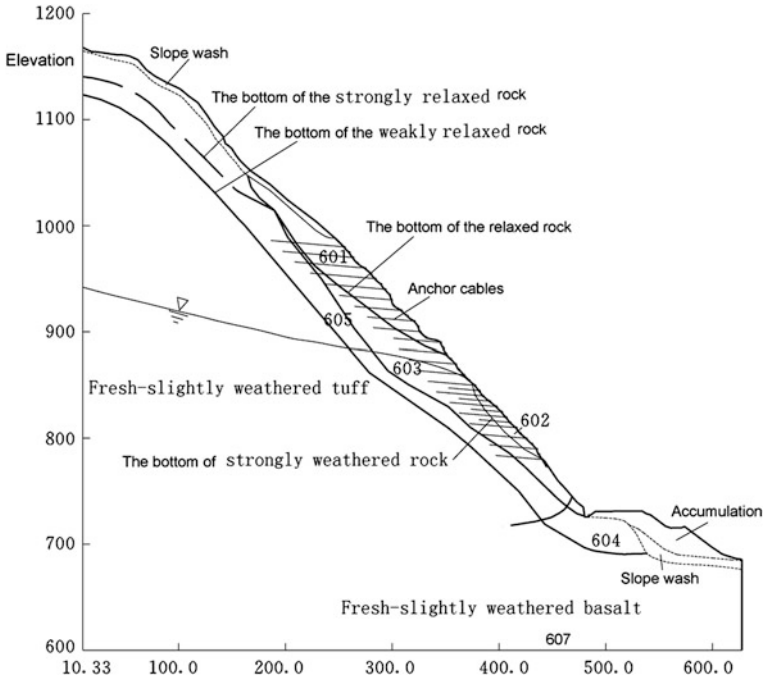


Fig. 14.5 Principal Section 1-1 of the landslide (unit: m)—the Pubugou Project, China

(NL = 850 m) + earthquake is the critical situation controlling the reinforcement amount under the corresponding target allowable safety factor $[K] = 1.05$. By a comprehensive analysis using limit equilibrium method and finite element method for all 9 major sections, the final layout scheme of cables are implemented as: 1891 cables of 1500 kN are installed with the borehole depth ranged 30–70 m and the hole spaced 5 m apart.

14.5 Numerical Method for Slope Stability Analysis

The design of any slope must involve analyses in which the disturbing forces are compared to the available strength of the rock mass. Traditionally, these analyses have been carried out by means of limit equilibrium methods but, more recently, numerical methods have been prevailing.

Numerical modeling for slope behavior is now a routine activity on many important slopes in hydraulic engineering. Methods such as FEM, BEM, DEM, and DDA are customarily used for such modeling. The advantage of numerical modeling over the limit equilibrium modeling is that it can be used to simulate progressive failure and ongoing displacement in addition to simple factor of safety

(Chen 2006; Zhou et al. 2007). Numerical modeling also can be used to determine the factor of safety of a complex slope in which a number of failure mechanisms (modes) can exist simultaneously or where the mechanism of failure may change as progressive failure occurs. However, realistic input information for numerical model and correct interpreting the output results are paramount for the successful computation in the context of large-scale slopes, which require well-trained skills and full understanding of the slopes concerned.

In practice, both methods of limit equilibrium and numerical are exercised together to generate a range of possible solutions for the input parameters that exist for a particular work site. While this may be frustrating for designers in that it does not appear to be capable of producing a single definitive design, it is far more realistic to look at the results of a parametric study than to rely on a single analysis. Therefore, the DL/T 5353-2006 stipulates that for grade I and II slopes, at least two methods should be applied for slope stability analysis, which include one lower bound limit equilibrium method, and at least one numerical analysis method. SL 386-2007 stipulates that for grade 1 slopes, when the deformation has significant influence on the hydraulic structures, or the slope excavation will induce the progressive deformation failure, the numerical methods such as FEM should be employed in the stability study apart from limit equilibrium methods.

In the following, the application of the finite element method and the block element method to the slope stability analysis will be particularly elucidated.

14.5.1 Finite Element Method

1. Simulation of excavation loads

Initial stress is an important geologic parameter influencing cut slopes. To determine the magnitude and orientation of initial stress by the field test at several points, much manpower and material resources should be invested. Based on these field readings, the algorithm is designed to determine the initial stress field $\{\sigma\}_0$ by means of regression method, least-squares method, and other mathematic methods (Vide Chap. 2).

The simulation of excavation involves determination of the nodal forces $\{\Delta F\}_0$ corresponding to initial stress field which are equivalent to the tractions from the excavated elements adjacent to the excavation boundary using (Naylor and Pande 1981):

$$\{\Delta F\}_0 = \int_v [B]^T \{\sigma\}_0 dv - \int_v [N]^T \gamma_r dv \quad (14.1)$$

where γ_r = unit weight of rock; $\{\sigma\}_0$ = initial stress; $[B]$ = strain matrix; and $[N]$ = shape function matrix.

The integral of Eq. (14.1) covers the excavated elements only and the forces appropriate to the nodes on the excavated surface are placed in $\{\Delta F\}_0$.

2. Simulation of discontinuities and stabilization

Fluid permeability and solid deformation of fractured rock masses can be simulated using either implicit (equivalent continuum) approach or explicit (discrete) approach. The former takes into account the influences of fractures by means of the permeability or elastic (compliance) matrix but neglects their exact positions, and is able to simulate fractures of large quantity; the latter considers the geologic and mechanical properties of each fracture deterministically and is often exercised for large-scaled fractures (e.g., faults). The need to use, for a particular problem, implicit or explicit approach depends on the size (or scale) of the fractures with respect to the scale of the structure that needs to be solved, and there are no universal quantitative guidelines to determine when one approach should be used in lieu of the other one.

The applicability of implicit approach for the deformation problem of the fractured rock masses is linked with the existence of elastic compliance matrix and representative element volume (REV). The quantitative solution on this issue normally should be obtained through large-scale laboratory or/and field physical tests (Hoek 1983). In recent years, the numerical techniques are also developed for the evaluation of the permeability tensor and elastic compliance matrix of the fractured rock masses. The algorithm is actually a kind of numerical test system (NTS) and is generally formulated as follows (Chen et al. 2008, 2012; Min and Jing 2003; Min et al. 2004; Wei et al. 1995; Zhang et al. 1996).

- First, a discrete fracture network in a sampling window is generated which will be used as the parent stochastic discrete fracture network (DFN);
- Next, a series of fractured rock blocks with different sizes and orientations are defined as test samples for each stochastic DFN;
- Then, the numerical methods (e.g., FEM, DEM, BEM, and CEM) are applied to the fractured rock samples to evaluate their fluid flow fields or deformation fields; and
- Finally, the permeability matrices or elastic compliance matrices of the samples are obtained and the existence of REV is identified.

It is obvious that the numerical estimation of the permeability tensor or elastic compliance matrix requires a large quantity of computation concerning different sample sizes and orientations. The situation becomes more rigorous if the stochastic characteristics of the rock fractures are considered, when many different discrete fracture networks in a sampling window are generated as the parent stochastic discrete fracture networks (DFNs), and the numerical tests are conducted on all these DFN. Therefore, from the standpoint of practice, it is important to find an algorithm facilitated in the preprocess of fractured rock samples containing fracture system with complex distributions (Chen et al. 2008, 2012).

3. Safety factor

The numerical model, in this case the FEM, is set up to incorporate all of the rock types, predominant faults, and joint systems as well as groundwater conditions within the slope. The strength of all the stratum units, faults and joint systems, is then reduced progressively by dividing them using a “strength reduction factor” (Dawson et al. 1999). The factor of safety is equivalent to the strength reduction factor at which failure initiates. However, in doing so one problem unsolved is, how to make the judgment if a slope is at the limit state? The problem is conventionally answered by the following criteria.

1. Divergent criterion

In the nonlinear iterative algorithm, when the incremental displacement curve or load curve of the system reaches extremity point, the computation will onset the divergence. Therefore, during the strength reduction computation, if a divergence is detected, then it may be judged that the limit equilibrium state is reached.

2. Energy criterion

The inner energy of a stable system should be equal to the work by external loads. After the strength reduction factor reaches extremity point, it may be detected that the external load work is larger than the internal energy, then it may be regarded that the system is entering limit equilibrium state.

3. Mutationism criterion

Status variables such as the displacement of a target on the slope, yield zone within the slope, and connectivity of yield zone which outcrops on the slope face are numerically monitored during the strength reduction process, and a sudden increase in one or more of above variables indicates that the failure of the slope commences.

4. Stress summation criterion

Since the strength reduction factor should be only obtained by trial and error computations, which is rather tedious because each tentative computation is based on one nonlinear FE analysis. Under certain circumstances, slope engineers may employ an approximate but simple way to estimate the safety factor based on FEM by defining a potential slip surface in the slope, after the completion of FEM computation, the safety factor K is computed as the ratio of shear resistance to the driving force, on the attempted slip surface:

$$K = \frac{\sum_{i=1}^n (f_i \sigma_i + c_i) l_i}{\sum_{i=1}^n \tau_i l_i} \quad (14.2)$$

where σ_i , τ_i , f_i , and c_i are the normal stress, shear stress, friction coefficient, and cohesive of the i th element on the slip surface, respectively; l_i is the length of the slip surface segment in the i th element.

The most dangerous slip surface should be sought by optimal algorithm. The method so carried out may be named as “FEM + LEM.” The advantages of this approximation are that only one nonlinear FEM is demanded, and the optimal search of the dangerous slip surface is relatively easy using the safety factor K defined in Eq. (14.2) as object function. If a more rigorous safety factor is to be further evaluated, the safety factor estimated by “FEM + LEM” gives good initial value in the trial and error algorithm.

4. Engineering application—deformation and stability of the ship lock slope (the Three Gorges Project)

The 20–20 section located at the gate chamber of the third step of the ship lock is chosen for the study, and the excavation bench and the corresponding completion time are shown in Fig. 14.6. The rock masses in the area of the ship lock can be recognized as 5 types according to the weathering degree: totally weathered, strongly weathered, weakly weathered, slightly weathered, and fresh. In addition, there are two main faults, one diabase dyke and one schist exogenous inclusion band (ex), and four sets of joints.

From the starting of excavation until the completion in the March of 1999, 17 benches for the 20–20 section were carried out (Fig. 14.6). Figure 14.7 is the FE mesh used in the computation.

The displacements at one of typical monitoring points predicted by the analysis are shown in Fig. 14.8. Compared with the observed displacements, it can be concluded that the analysis gives good prediction of the displacements for the ship lock slope during the excavation. The excavation of the section was completed in April 1999, at that time the maximum accumulated displacement is 71.63 mm, which taken place at the south slope. The elasto-viscoplastic analysis further forecasts that there is maximum 1.42 mm time-dependent displacement, which will be converged within 7–8 months after the completion of the excavation. Therefore, the conclusion could be made that if the miter gates are installed after the end of

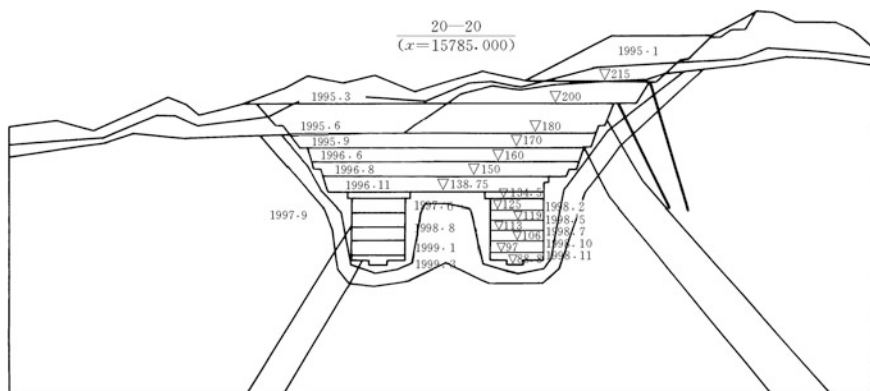


Fig. 14.6 Excavation bench and the corresponding time of the 20–20 section

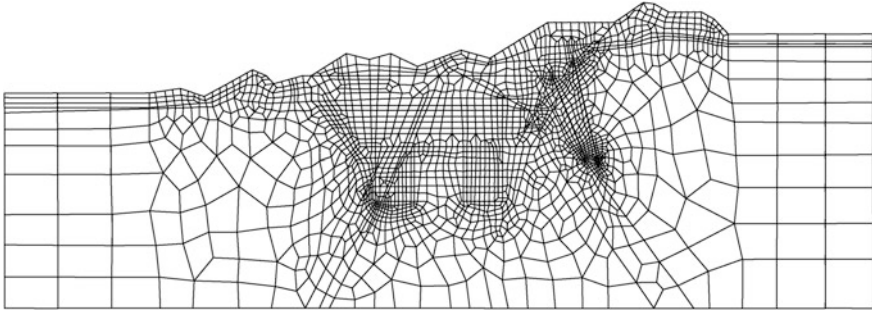


Fig. 14.7 FE mesh used in the calculation

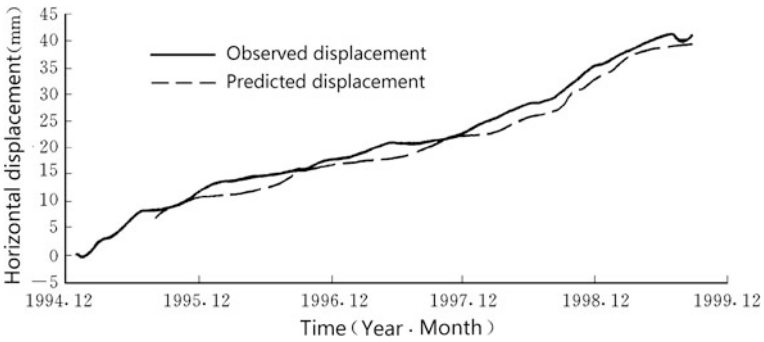


Fig. 14.8 Horizontal displacement at the monitoring point TP/BM36GP02

1999, there is no risk of hazardous displacement influencing the normal operation of the gates. It is worthwhile to indicate that the field readings so far have verified the above predictions.

Figure 14.9 presents the stress distribution after the completion of excavation. According to the prediction when the excavation of the ship lock was completed, the maximum stress at the toe of the south slope is 24.7 MPa, and the maximum

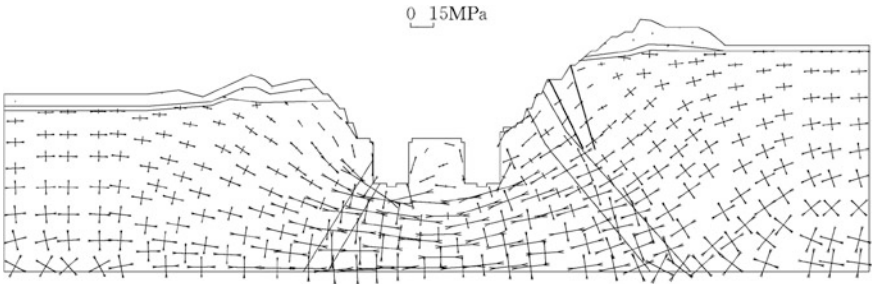


Fig. 14.9 Stress distribution after the completion of excavation

stress at the toe of the north slope is 24.1 MPa. Since the long-term creep strength of the granite is approximately 50 MPa, there is no danger of long-term creep deformation which could jeopardize the long-term operation of the miter gates. The analysis also shows that there are tensile stresses in the separation pier wall of the double-lane ship lock with maximum value of 0.817 MPa and maximum depth of 28 m from the pier wall top. It means that cracking and local failure could manifest frequently during the excavation construction. Therefore, care should be called at the intensive reinforcement of this area in the pier wall.

14.5.2 Block Element Method

The conventional block element method (BEM) considers the rock blocks delimited by the discontinuities as rigid bodies, while discontinuities exhibit elasto-plastic or elasto-viscoplastic behavior (Chen et al. 2002, 2003). The governing equation is then formulated considering the force and moment equilibrium condition of rock blocks, the deformation compatibility condition, and the elasto-viscoplastic constitutive relation at discontinuities. After more than twenty years of development, this method has covered a wide range of analysis with respect to nonlinear deformation, stability, seepage, reinforcement, and reliability. This method has been recommended by the DL/T 5353-2006 “Design specification for engineering slopes in water resources and hydropower project.”

1. Identification of complicated multi-block system

Geometrical description and preprocessing is fundamental for the analysis using BEM. A complete identification and preprocessing algorithm for the seepage and deformation as well as stability analyses of the complicated rock block system may be formulated on the direct body concept introduced by Ikegawa and Hudson (1992), which can deal with both convex and concave blocks in a unified algorithm.

2. Stability analysis

A failure case (mode) is defined as a potential partial failure in the slope formed by one block or by the combination of several blocks. If the slope contains m blocks, theoretically there will be $C_m^1 + \dots + C_m^{50} + \dots + C_m^m$ possible failure cases, and the calculation of the safety factor for each case will demand huge computing time. Fortunately, most of the failure cases are not important because their safety factors are much higher than the allowable value. Therefore, the interestingness may be merely directed to some dangerous failure cases which have comparatively lower safety factors. The search of dangerous failure cases is accomplished by the following two basic steps.

- First, the conventional LEM is applied to find a group of dangerous failure cases which have lower safety factors. To minimize the calculation time due to a huge number of possible block combinations in the slope, an intelligent search

methodology called “enlightening search by the information with deep treelike structure” can be performed.

- The second step considers each dangerous failure case indicated by the conventional LEM for which the “strength reduction” calculation is conducted using the BEM; in this procedure, the strength parameters of the discontinuities around the block combination corresponding to the specific failure case are reduced using the same fraction until the block combination fails, e.g., when the displacement vector of the slope is divergent. The safety factor is then calculated as the proportion of the normal strength parameters to the reduced strength parameters at failure.

3. Engineering application—the arch dam abutment slope (the Xiaowan Project)

The rock masses of the Xiaowan Dam foundation and the abutment are intersected by more than 100 faults, 4 geologic alteration zones, 10 loosen fissure bands, and three major joint sets (Fig. 14.10). The natural groundwater table is about 40–60 m below the ground surface.

The detailed study of the position, orientation, and mechanical parameters of the discontinuities, of the valley topography, and of the thrust forces exerted by the arch dam, allowed the definition of those discontinuities which should be included in the analysis:

- 3 joint sets;
- 10 alteration zones, caused by the heat of the magma during the geologic movement;

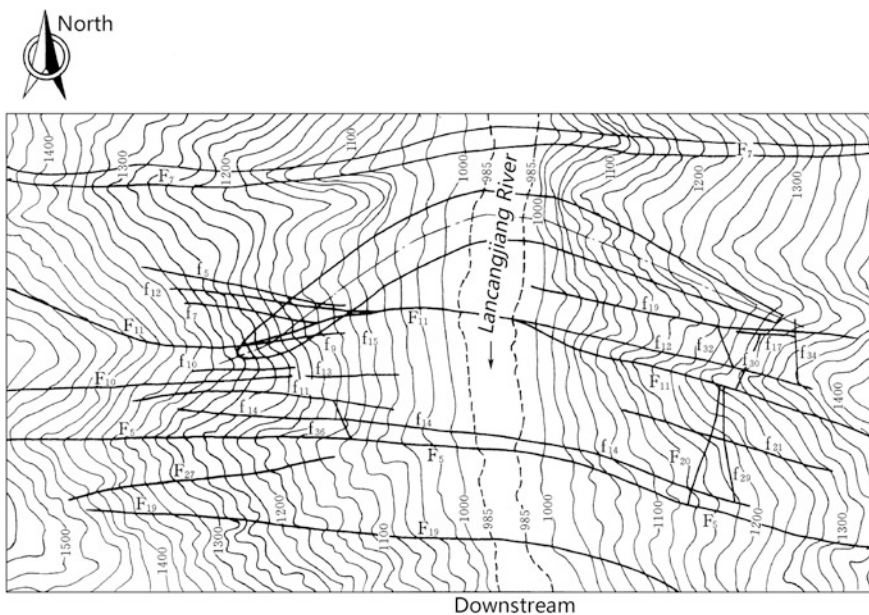


Fig. 14.10 Geologic plan of the Xiaowan Project

- 22 faults; and
- 10 loosened fissure bands, caused by the erosion of the corradng river.

The block system worked out for the calculations is shown in Fig. 14.11. The whole foundation of the dam is discretized into 2231 block elements, while the arch

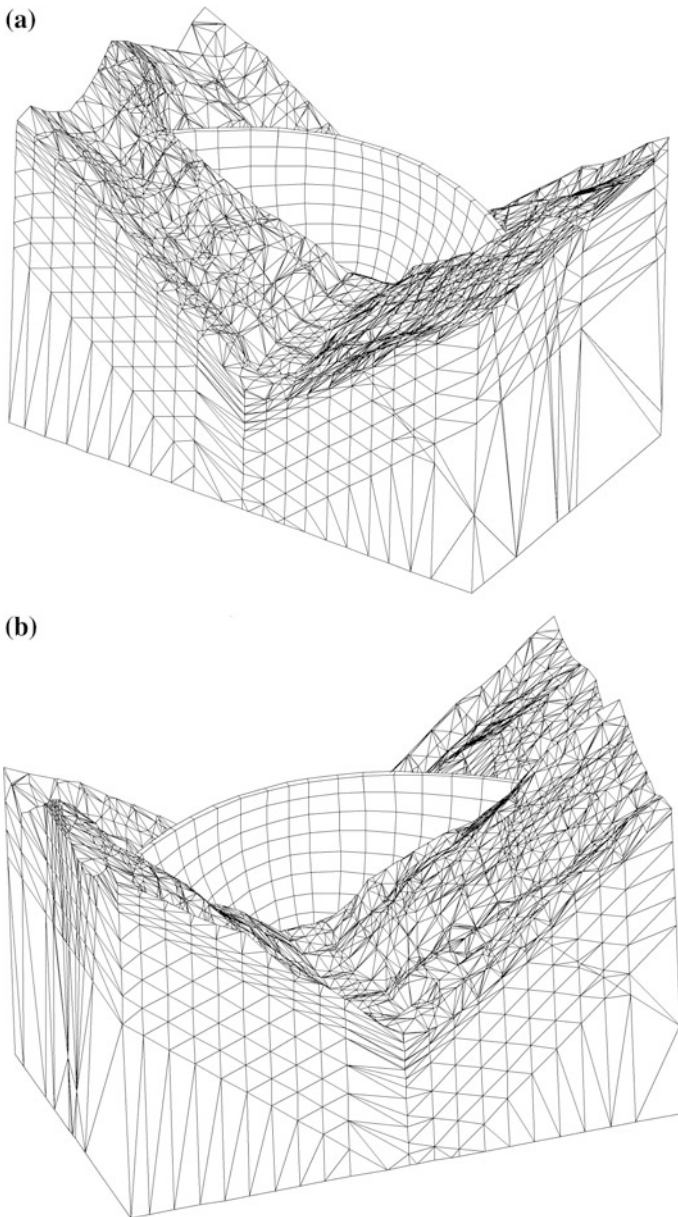


Fig. 14.11 Block system of the arch dam foundation and abutments—the Xiaowan Project

dam body is discretized into 88 arch-cantilever elements (9 arch rings and 17 cantilevers).

Calculation is carried out for the load combination of self-weight + water pressure of the normal storage water level (1240 m) + water pressure of the downstream tail water level (1004 m) + silt pressure of the inactive storage level (1097 m) + temperature drop + seepage pressure. Figure 14.12 shows the displacement and movement of the abutment slope induced by the impounding at the cross-sectional levels of 1090 m, when the reservoir is at the normal storage level (1240 m). Other cross sections present similar displacement patterns. It is indicated that the maximum displacements of the abutment slope manifest at the elevation of 1090–1010 m, which are about 0.027 m at the left abutment slope and about 0.020 m at the right abutment slope. The maximum downstream displacement of the arch dam appears on the crest of the crown cantilever, which is equal to 0.154 m. The phenomenon that the displacement at the left bank abutment slope is greater is attributable to the two deeper gullies at the upstream and downstream of the left abutment, their presence makes the rock mass to be moved more easily. It is, therefore, suggested that more attention should be called at the left bank in the design of the foundation and abutment treatment.

Seventeen main potential failure cases are found whose safety factors are lower. All of them are not situated directly under the dam; this means that the global stability of the dam abutments is secured, but local failure could emerge in the vicinity of the abutments indicated by these potential failure cases. Analysis shows

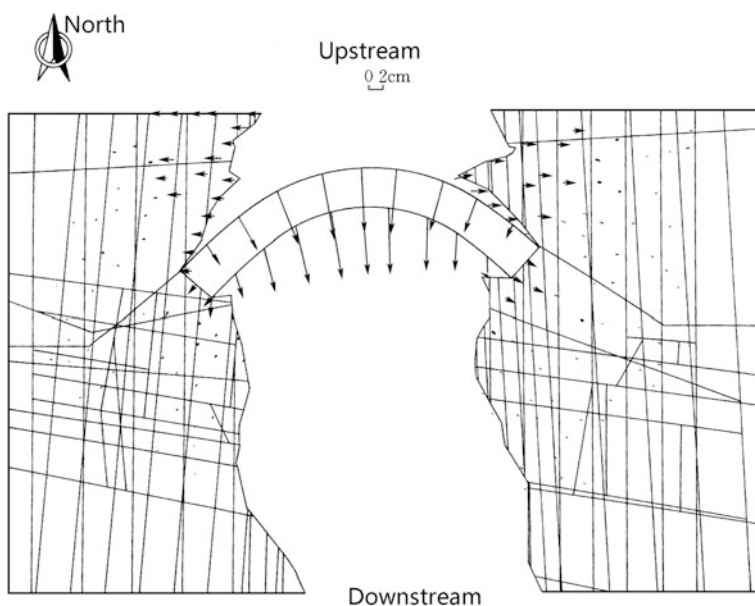


Fig. 14.12 Displacement at the elevation of 1090 m

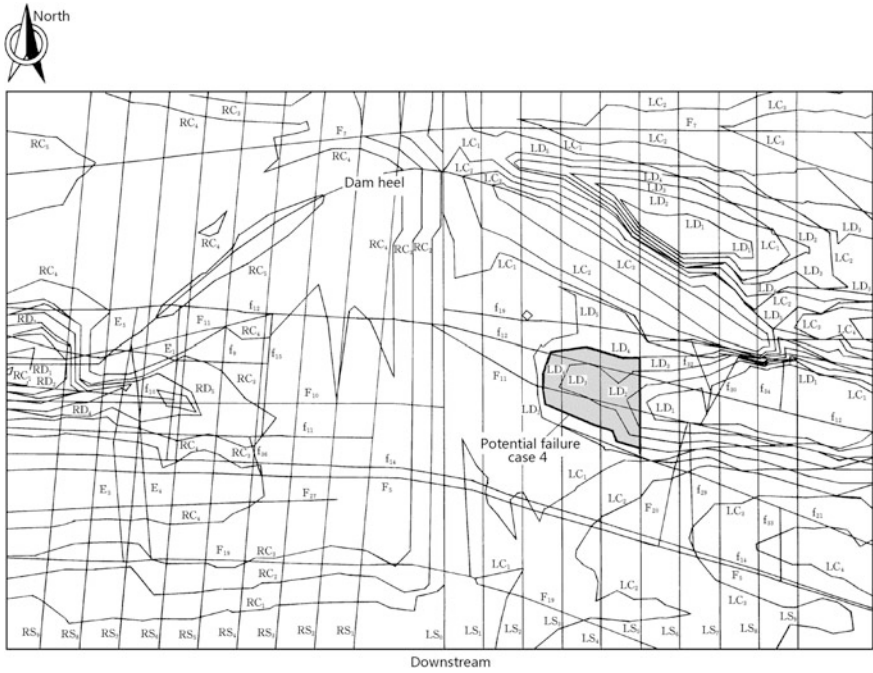


Fig. 14.13 Potential failure case 4 ($K = 2.1$)

that the left abutment slope includes more potential failure cases (12 cases) than at the right abutment slope (5 cases), due to the existence of deeper gullies at the left abutment slope. Figure 14.13 shows the location and size of the potential failure case 4 (in shadow) which possess a stability safety factor $K = 2.1$.

14.6 Slope Stabilization

14.6.1 Principles in the Slope Stabilization

“An ounce of prevention is worth a pound of cure,” this is to bear in mind the slope engineers. Large-scale landslides of poor stability are nearly impossible to be stabilized, or the treatment cost and time are intolerable. Therefore, such landslides are advisable to be shunned in the layout of hydraulic and hydropower projects. When it has been established that a slope is potentially unstable and cannot be shunned, the stabilization treatments should be carried out in time (Abramson et al. 2002; Baker and Marshall 1958; Hoek and Bray 1981). In the stabilization works, the following principles are to be observed:

- The construction in rainy season is not advisable, if has to, the temporary surface infiltration is demanded;
- The wide foot cut or trench at the slope toe is avoided;
- The controlled blast and in time reinforcement are highly preferable;
- The high attention for the monitoring in the construction period is called at.

Figures 14.14 and 14.15 show the layouts of two typical comprehensive stabilization treatments for slopes.

14.6.2 Stabilization Countermeasures

The countermeasures that are most commonly practiced fall within two categories:

- Reduce the sliding driven forces;
- Raise the sliding resistances.

Specifically, the selective measures in the stabilization of slope are as follows:

- Rock removal;
- Drainage;
- Reshape;
- Pressing foot;
- Retaining wall;
- Shear pile;

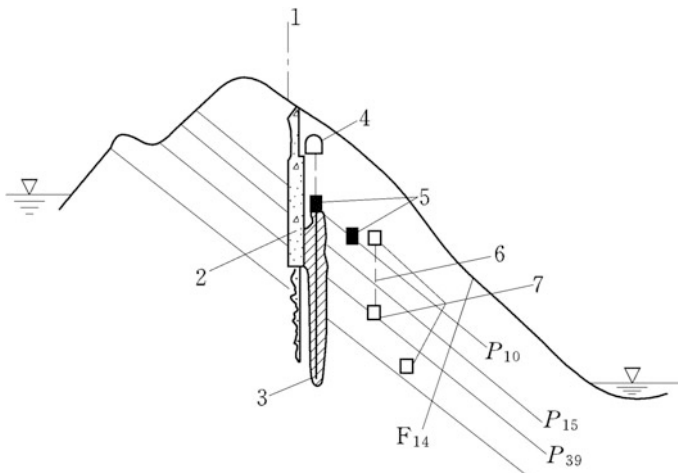
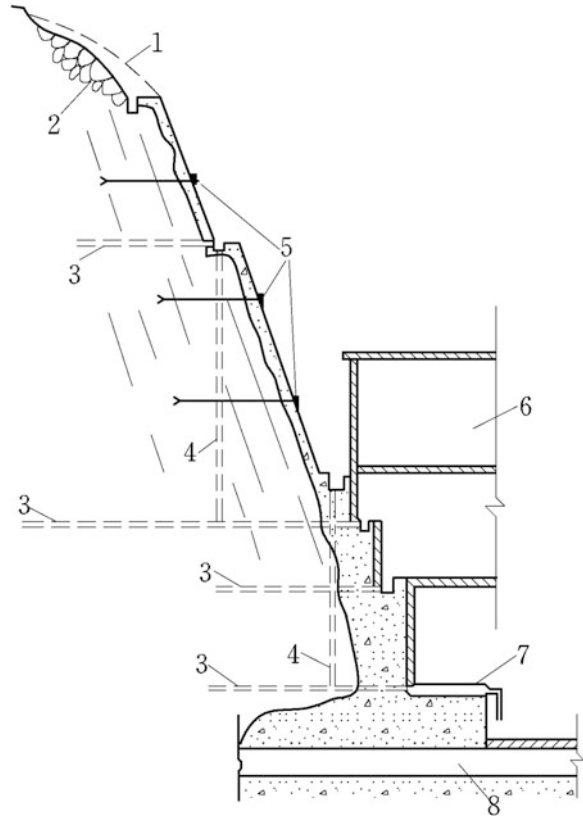


Fig. 14.14 Stabilization layout of the dam abutment slope—the Fengtan Project, China. 1 dam axis; 2 concrete replacement in shaft; 3 grouting curtain; 4 grouting adit at dam crest; 5 concrete replacement in adit; 6 draining hole; 7 drainage adit; 8 weak intercalation

Fig. 14.15 Stabilization layout of the tunnel intake slope—the Ouyanghai Project, China. 1 slope cut; 2 stone masonry revetment; 3 horizontal draining hole; 4 vertical draining hole; 5 rock bolt; 6 auxiliary room; 7 draining pipe; 8 penstock



- Shear key;
- Bolt reinforcement; and
- Changing the material properties.

1. Rock removal

By rock removal, it comprises cutting of unstable rock blocks, trim blasting overhangs, and scaling individual rock blocks off slope. In general, rock removal is a preferred method of surface stabilization because the work will eliminate the hazardous sources, and no future maintenance will be required. However, removal should only be used where it is certain that the new face will be stable, and there is no risk of undermining the upper portion of the slope. It would be safe to remove the outermost loose rock, provided that the fracturing was caused by blasting and only extended to a shallow depth. However, if the rock mass is deeply fractured, continued scaling will soon develop a cavity that will undermine the upper portion of the slope. Removal of loose rock on the slope face is not effective where the rock is highly degradable, such as shale—exposure of a new face will just start a new cycle of weathering and instability. Under such circumstances, more appropriate

stabilization methods would be the protection of the face with shotcrete and rock bolts, or the installation of back-tied retaining wall.

2. Drainage

Groundwater in rock is often a primary or contributory driving of slope instability, and a reduction in water pressures may improve the stability considerably (Freeze and Cherry 1979; Haar 1962; Cedergren 1973). Methods of depressurization include surface infiltration and subsurface draining, and the latter comprises of drilling horizontal drain holes or excavating drain adits at the slope toe to create outlets for the seeping water. The selection of the most appropriate manner for the specific work site will depend on such factors as the intensity of the rainfall or snow melt, the permeability of the rock, and the dimensions of the slope.

(a) Surface infiltration

In climates with intense rainfall which may rapidly saturate the slope and give rise to surface erosion, it is advisable to construct drains both behind the crest and on surface benches to intercept the water. These drains are lined with masonry or concrete to prevent the collected water from infiltrating the slope and are dimensioned to carry the anticipated peak design flows. The drains are interconnected so that the water is discharged to the storm drain system or nearby water courses. Where the drains are on steep gradients, it is sometimes necessary to incorporate energy dissipation protrusions or steps in the base of the drains, to cut flow velocities. In climates that experience high rainfall, there is usually rapid vegetation growth and therefore periodic maintenance will be demanded to keep the drains clear. Figure 14.16 shows the surface infiltration layout of the Yangjiachao Landslide in the Shuibuya Project (Hubei, China).

(b) Draining holes

An effective means of depressurization in many rock slopes is to drill a series of nearly horizontal draining holes (inclined upwards at about 5°) from the face. The holes should be long enough—conventionally about one-half to one-third of the slope height—to depressurize the rock mass in the vicinity of potential failure surfaces. In large rock slopes, holes of 200–300 m in length may be needed to achieve ideal effects. There are no widely accepted formulae for the calculation of the required spacing of drill holes, but as a common guideline, holes are normally drilled at a spacing of about 3–10 m. The holes are often lined with perforated casing or with the perforations, sized to minimize infiltration of fines that are washed from fracture infillings. Another aspect in the design of draining holes is the disposal of seeping water. If the drained water may result in degradation of material properties near the slope toe, or produce additional stability problems downstream of the drains, it may be necessary to collect all the seeping water in a manifold and dispose of it at safe distance from the slope.

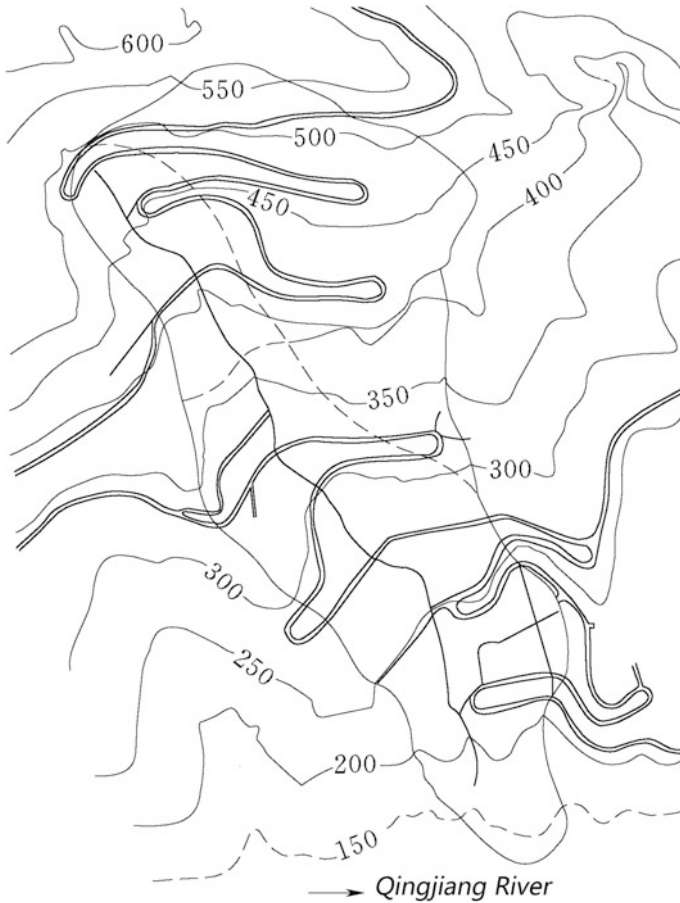


Fig. 14.16 Surface infiltration layout for the Yangjiachao Landslide—the Shuibuya Project, China

(c) Subsurface draining adits and holes

For large and deep landslides, it may not be possible to significantly reduce the water pressure in the slope with relatively small draining holes. Under such circumstances, drainage adits or tunnels may be driven into the slope from which a series of draining holes are drilled up into the saturated rock. In addition to the depressurization that can result from their construction, drainage adits also play an important role to collect valuable geologic information that is not normally accessible. For example, the Downie landslide in British Columbia has an area of about 7 km² and a thickness of about 250 m. Stability of the slope was of concern when the toe was flooded by the construction of a dam. A series of drainage tunnels with a total length of 2.5 km were driven at an elevation just above the high water level of the reservoir. From these tunnels, a total length of 13,500 m of draining

holes was drilled to reduce the groundwater pressures within the slope. These draining measures are effective in bringing down the water table in the landslide by as much as 120 m, and reducing the rate of movement from 10 mm/year to about 2 mm/year.

Another important role of subsurface draining is to install piezometers for monitoring the effect of depressurization in the slope.

Figure 14.17 shows a sub-surface draining layout of the Yangjiachao Landslide.

3. Reshape of slope

The main driving force for a landslide is the self-weight of the rock mass above any potential slip surface, and it is thus clear that a reduction in the angle of the slope or the removal of material from the top of the slope will improve the factor of safety.

Where a slide has developed, it may be necessary to unload the crest to reduce its height and diminish the driving force. For a common slope with curvilinear slip surface as shown in Fig. 14.19, reducing height is usually an effective solution to the problem by cutting the upper portion of slope since most of the volume of rock is contained in this upper portion. On the contrary, the improper excavation shown in Fig. 14.18 reduces both the driving force and resistance force, which is not effective in the improvement of safety factor. For the slope with straight slip surface as shown in Fig. 14.19, reducing the angle of the cut face would be a very effective stabilization measure. Since

$$K = \frac{W \cos \alpha \tan \varphi + cL}{W \sin \alpha} \quad (14.3)$$

Insert $W = \gamma_r \cdot \frac{1}{2} \cdot L \cdot h \cos \alpha$ into above Eq. (14.3), we have

$$K = \frac{\tan \varphi}{\tan \alpha} + \frac{4c}{\gamma_r \cdot h \cdot \sin 2\alpha} \quad (14.4)$$

where γ_r = unit weight of rock, kN/m².

When the inclination angle of slip face α and parameters c , φ , and γ_r are all fixed, the safety factor has relation only with the slope height h or the slope surface angle β but has nothing to do with the length of slip surface L . Therefore, the reduction of slope surface angle β may be effective in the improvement of the safety factor, whereas the cutting on the upper portion has minor meanings.

Larger scale support can be provided by placing a waste rockfill buttress at the toe of the slope, its supporting efficiency depends on the buttress weight, and the shear resistance generated along the base of the buttress. This can only be applicable, of course, if there is sufficient space at the toe to accommodate the required volume of rockfill. It is also important that the filled rock slag should be free draining so that water pressures will not build up in the slope behind the buttress.

The design procedure for re-sloping, unloading, and backfilling may start with the back analysis. By setting the target safety factor for the slope, it is possible to

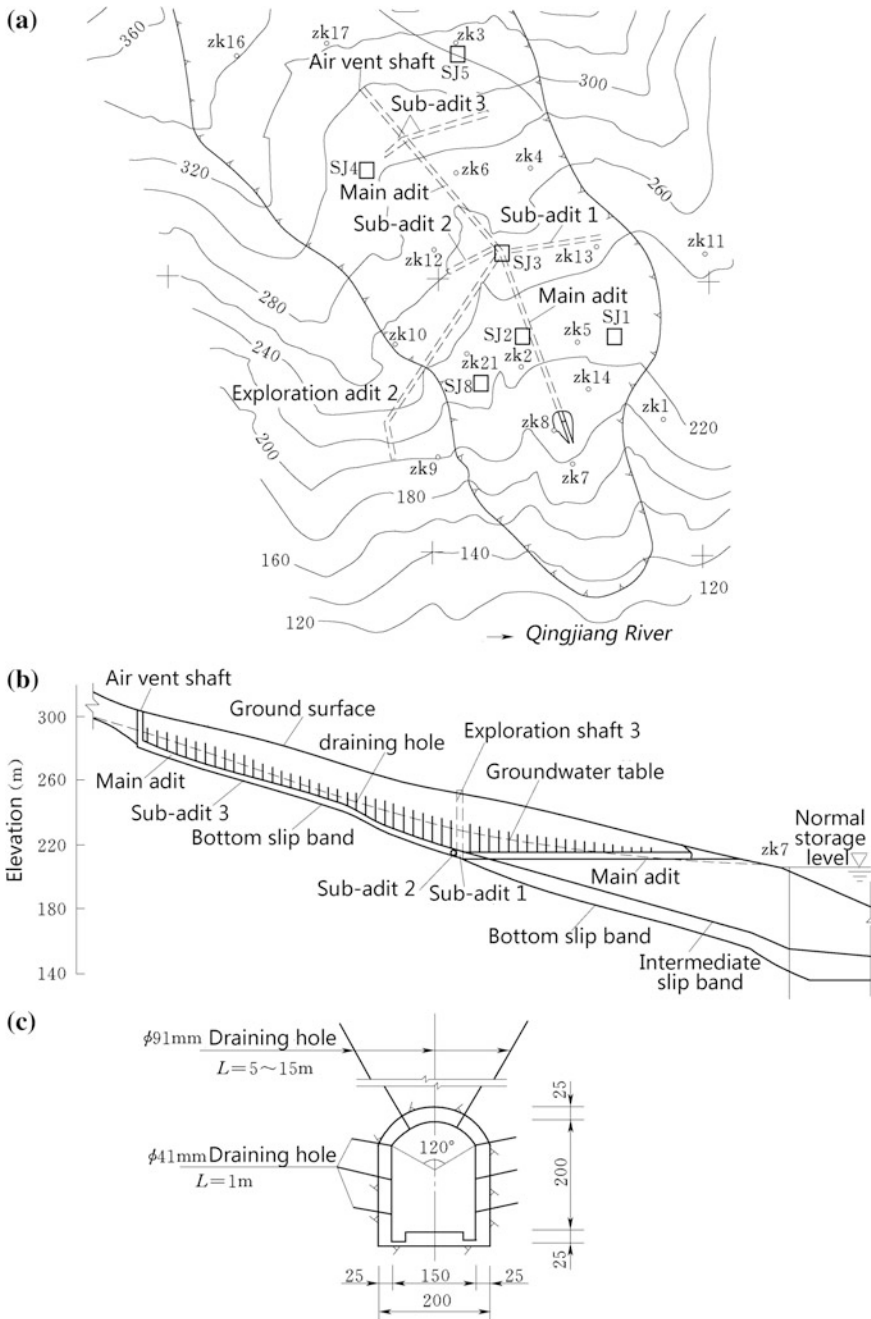


Fig. 14.17 Subsurface drainage layout for the Yangjiachao Landslide—the Shuibuya Project, China. **a** Plan; **b** vertical section; **c** section of main drainage adit

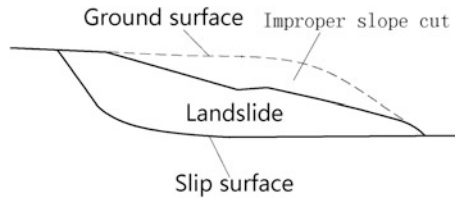
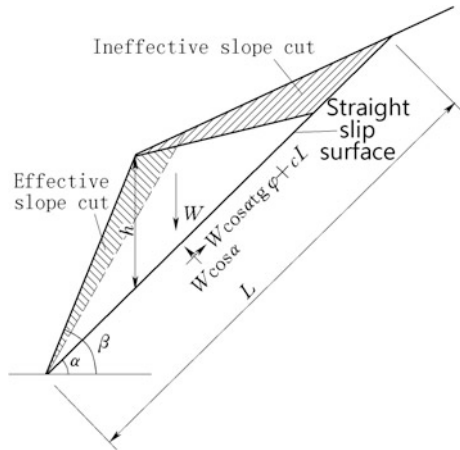


Fig. 14.18 Improper excavation of slope (curvilinear slip)

Fig. 14.19 Effectiveness of the excavation of slope (straight slip)

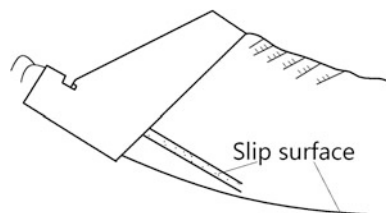


back analyzing the rock mass strength parameters. This information can then be used to design the required reduction in slope angle and/or height that will produce the expected factor of safety.

4. Retaining wall

A concrete or masonry retaining wall at the toe provides external support to the slope (Fig. 14.20). Entailed by the height and size, retaining wall has limited effect in raise the overall stability for a large slope, hence its major function in the slope stabilization is to improve the local stability near slope toe, which is indispensable to prevent the progressive failure of slope.

Fig. 14.20 Retaining wall



Requirements in the design of retaining walls are (Huntington 1957; Jones 1979; Wei and Zhou 2004) the sliding stability, overturning stability, deformation, and bearing capacity, which have been discussed in the Chap. 11. The pressure on the retaining wall is the residual thrust force from the landslide, which is usually assumed in a rectangular distribution from the wall top to the outcrop of slip surface on slope.

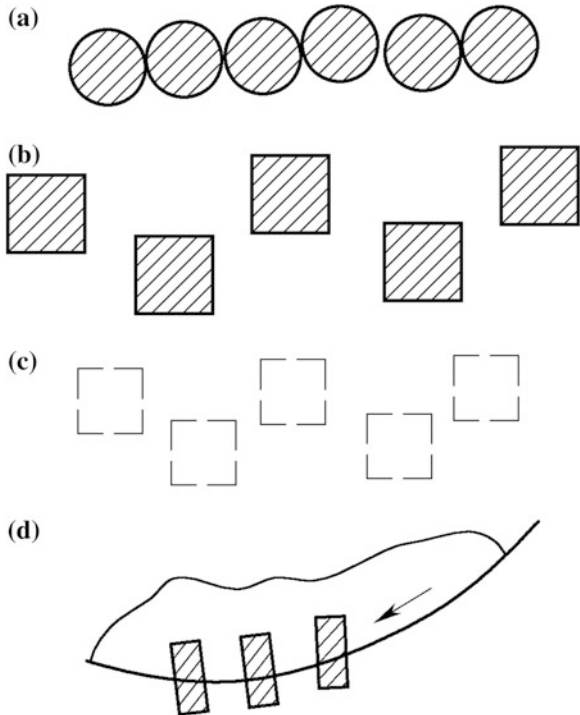
5. Stabilization piles

Stabilization piles are preferable for landslides with obvious slip surface and good bedrock underneath. The stabilization of slope by placing passive piles is one of the important stabilization techniques due to their advantages of high shear resistance, flexibility arrangement, less field disturbance, small amount of engineering and investment, direct supplement, and check of geologic exploration data for optimal design (Broms 1964; Davissou and Prakash 1963; Ito et al. 1982; Poulos and Davis 1974, 1980). Figure 14.21 shows the layout of stabilization piles in a slope.

(a) Types of stabilization piles

By the construction methods, there are displacement (driven pile) and non-displacement piles (cast-in situ bored pile, dug pile); by materials, there are steel piles, concrete piles, and timber piles; by cross-sectional shape, there are H-piles,

Fig. 14.21 Layout of stabilization piles in a slope



pipe piles, and rectangular piles; by relative stiffness of pile and rock, there are rigid piles and elastic piles; by structural type, there are single-rowed piles, multi-rowed piles, bracket piles, and prestress anchor-hold piles. Attributable to the lower labor cost and rich experiences, dug piles had been widely exercised in China, particularly in the railroad engineering and hydraulic engineering.

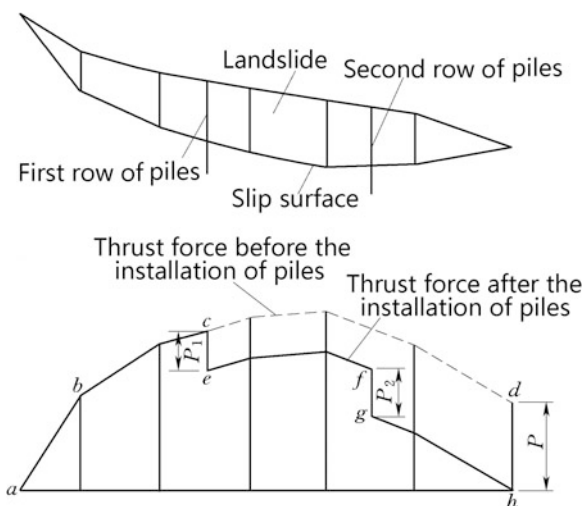
(b) Requirements for the design of stabilization piles

- That the stability safety factor of the stabilized slope against sliding should meet the allowable factor;
- That the cross-sectional and steel bar amount should be sufficient to resist the inner forces in plies;
- That the fixed sectional area of piles and foundation resistance should be sufficient, and the deformation of piles and slope also should be permissible;
- That the cross-sectional area, spacing, depth of embedment, should be appropriate; and
- That the design should be convenient in construction and has smallest engineering amount.

(c) Design thrust forces for piles

After the preliminary selection of piling rows and positions, the thrust force curve corresponding to the design stability safety factor may be computed which is in turn, employed to estimate the design thrust forces for stabilization piles needed to raise the safety factor up to the desired value. As shown in Fig. 14.22, where two rows of piles are layout, the curve $a-b-c-d$ represents the sliding driven force before the installation of piles, and the residual thrust force is P ; the curve $a-b-c-e-f-g-h$ represents the sliding driven force after the piling, where the residual thrust force is zero. It is obvious that P_1 is the sliding driven force shared by the first row

Fig. 14.22 Design sliding driven force for piles



of piles, P_2 is the sliding driven force shared by the second row of piles, and $P = P_1 + P_2$. The thrust force P is often termed as the lateral resisting force (RF) of piles.

(d) Positioning of piles

The positioning of piles should be based on the topographic and geologic conditions, quantity of residual thrust forces, and construction conditions.

The stabilization piles are usually layout in the areas near the middle portion or toe of slope as the resistance portion of slide body, where the slide thickness is not excessive large and the bedrock is solid. The purpose of such consideration is to reduce the bending moment and the cross section of piles. For single-rowed piles, on the one hand, the exerted thrust force corresponding to allowable stability is unchanged where ever the piles are coordinated; on the other hand, the thinner of the slope body, the smaller of the bending moment in the piles will be. However, it also should be emphasized that the thickness of slope where the piles are located should not be too thin, otherwise a portion of slide body may slip over the top of the piles, leading to the failure in the slope stabilization.

(e) Length and cross-sectional area of piles

Piles should be so designed to be capable of offering the required RF and to raise the safety factor of slope up to a prescribed level. Rectangular section is usually employed for dug piles with conventional size of 2.0 m \times 2.0 m, 2.0 m \times 3.0 m, 2.5 m \times 2.5 m, 3.0 m \times 4.0 m, 3.5 m \times 4.5 m, etc. The length of piles depends on the slide thickness and bedrock condition. The piles are keyed into bedrock with 1/3 \sim 1/2 of pile length. The construction difficulties and safety requirements often limit the maximum length within 35 m. However, there are fairly a number of exceptional cases, if necessary. In the Xiangyang-Chongqing railway engineering, the dug stabilization piles reached a cross section of 3.5 m \times 7.0 m and a length of 48 m; in the Xiaowan Project, the 3 m \times 5 m dug stabilization piles have been installed with the maximum length of 80 m.

(f) Detailed structural behavior of pile-slope systems

After the positioning and sizing the piles, the structural behavior is to be studied on which the reinforcement design for piles is carried out considering the deformation and stress of pile-slope system.

There are numerous methods for designing laterally stabilizing piles. They generally fall into two different categories as pressure- and displacement-based methods and numerical method (e.g., finite element method).

The first category of method is based on the analysis of passive piles subjected to lateral soil pressure or lateral soil movements. Usually, these methods are formulated on the assumptions of rigid piles with infinite length fixed in rigid and perfectly plastic soil. Therefore, they are not rigorous in representing the real pile-slope

system due to the overlooking of the actual behavior of finite flexible piles (e.g., soil arching). The corresponding lateral soil movements may be estimated using either measured inclinometer data, analytical result using the finite element approach, or empirical correlations based on similar case histories.

The second category of method investigates the pile-slope system simultaneously, which is analyzed as a continuous elastic or elasto-plastic medium using either finite element or finite difference approaches. The methods may provide a coupled solution in which the pile response and slope stability are obtained synchronously. However, it is computationally expensive and demands extensive training due to its three-dimensional and nonlinear nature.

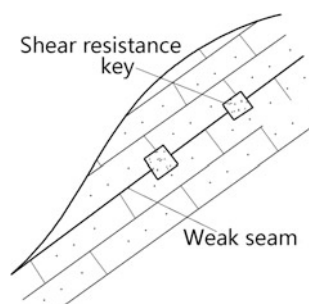
6. Shear keys

Shear keys exercised in slope engineering are similar to that have been discussed in the stabilization issue of dam foundations and abutments (vide Chap. 7). Tunnels (adits) are driven along a distinctly defined shear zone, with the excavation extending into sound rock on either side of the tunnels. They are then backfilled with reinforced concrete to create a high strength inclusion along the slip surface (Fig. 14.23). The exploration adits are sometimes reused for the construction of such shear keys.

7. Bolt reinforcement

Bolt reinforcement is effective and prevalent for slope stabilization, which comprises the installation of tensioned (prestressed) anchor cables or fully grouted and untensioned dowels (bolts) (Aydan et al. 1987; Bjurstrom 1974; Ceng et al. 2003; Chen and Egger 1999; Chen et al. 2009; Hanna 1982; Jalalifar et al. 2006; Littlejohn and Bruce 1977; Ma and Chang 2007; Post-Tensioning Institute 2004; Spang and Egger 1990; Xanthakos 1991). Factors that will influence the selection of an appropriate reinforcement system for the slope include the site geology, the required capacity of the reinforcement force, drilling equipment availability and access, and time permitted for the installation. Untensioned dowels are less expensive to install, but they only provide lower and shallow reinforcement. One technical factor dominating the reinforcement selection is that if a slope has been

Fig. 14.23 Layout of shear keys in a slope



relaxed and loss of interlock has taken place on the slip plane, then it is advisable to install tensioned anchors to directly apply normal and anti-shear forces as quick as possible. However, if the reinforcement can be installed prior to the excavation, then fully grouted dowels are preferable to prevent the relaxation on potential slip surface. Untensioned dowels also can be used where the rock is randomly jointed and there is a need to reinforce the whole slope exposure face, rather than a particular slip surface.

The aforementioned dowel bolts and anchors are commonly combined with piles, slope face concrete lattice frames, retaining walls, and slope face shotcrete.

A tensioned anchor installation involves drilling a hole extending below the slip surface, installing a rock bolt or strand cable that is bonded into the stable portion of slope, and then tensioning the bolt or anchor against the face (Fig. 14.24). The tension force T_j in the anchor modifies the normal and anti-shear forces exerting on the slip surface. Take the Sweden Arc Method as example, the factor of safety of the anchored slope is given by the moment equilibrium condition around the center (O):

$$R \cdot \sum \left(\frac{c'_i l_i + N_i \tan \phi'_i}{K} \right) + R \cdot \sum \left(T_j \cos \beta_j + T_j \sin \beta_j \cdot \frac{\tan \phi'_j}{K} \right) = R \cdot \sum W_i \sin \alpha_i + \sum Q_{iz_i} \tag{14.5}$$

where W_i = vertical load of the slice i ; Q_i = horizontal load of the slice i ; U_i = uplift on the slip surface of the slice i ; and T_j = design tension in the anchor j . Equation (14.5) may be re-arranged as follows:

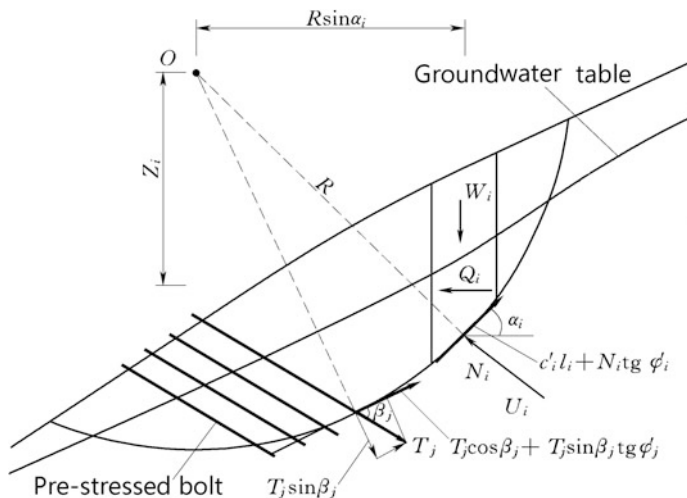


Fig. 14.24 Diagram to the calculation of prestress bolt using the Sweden arc method

$$\begin{aligned}
 K &= \frac{R \cdot \sum (c'_i l_i + N_i \tan \phi'_i) + R \cdot \sum T_j \sin \beta_j \tan \phi'_j}{R \cdot \sum W_i \sin \alpha_i + \sum Q_i Z_i - R \cdot \sum T_j \cos \beta_j} \\
 &= \frac{R \cdot \sum [c'_i l_i + (W_i \cos \alpha_i - Q_i \sin \alpha_i - U_i) \tan \phi'_i] + R \cdot \sum T_j \sin \beta_j \tan \phi'_j}{R \cdot \sum W_i \sin \alpha_i + \sum Q_i Z_i - R \cdot \sum T_j \cos \beta_j}
 \end{aligned}
 \tag{14.6}$$

where K = safety factor against sliding.

Equation (14.6) shows that the normal component of the anchor tension ($T_j \sin \beta_j$) is added to the normal force exerting on the slip surface, which has the effect of increasing the shear resistance against sliding. In addition, the driving forces are subtracted by the anti-shear component of the anchor tension ($T_j \cos \beta_j$).

If the RTM is employed in the stability analysis, the design anchor tension is

$$T = P / \cos \theta \tag{14.7}$$

where T = design anchor tension, kN; P = horizontal component of the residual thrust force under design safety factor, kN; and θ = inclination angle of anchor.

The factor of safety for a slope reinforced with tensioned anchors varies with the inclination of the anchors. The most optimal inclination should be decided by the minimum length of the anchors to obtain the required reinforcement effects.

As shown in Fig. 14.25, the total length of a tensioned anchor is

$$L = L_w + L_z + L_m \tag{14.8}$$

where L = total length of tensioned anchor, m; L_w = out-laid anchorage length, m; L_z = free length, m; and L_m = length of bonded inside anchorage head, m.

For a definite anchor cable, lengths of out-laid anchor head and bonded inside anchorage head have only small variation, and

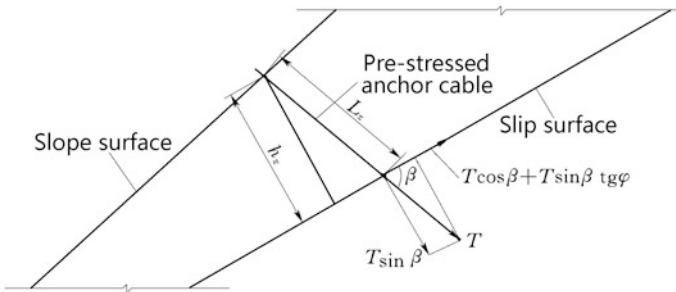


Fig. 14.25 Optimal reinforcement angle

- L_w = thickness of anchorage pier + working length of jack + thickness of anchorage + ΔL ($\Delta L \approx 0.1$ m). For the wire strand cable of 2000–3000 kN, $L_w \approx 1.8$ m;
- For soft rock, L_m is dependent on the shear strength of the interface of grout/rock;
- For hard rock, L_m is dependent on the strength of the interface of strand wire/grout;
- For the wire strand cable of 2000–3000 kN, $L_m \approx 6$ –8 m.

Therefore, the total length of cable is mainly dominated by the free length, which varies along with the inclination angle of cable.

Denote n as the ratio of shear resistance to the free length of cable, i.e.,

$$\begin{aligned} n &= \frac{T \cos \beta + T \sin \beta \tan \varphi}{L_z} = T \cdot (\cos \beta + \sin \beta \tan \varphi) \cdot \frac{\sin \beta}{h_z} \\ &= \frac{T}{h_z} \cdot \left(\sin^2 \beta \tan \varphi + \frac{1}{2} \sin 2\beta \right) \end{aligned} \quad (14.9)$$

where h_z = perpendicular distance from the daylight point of the cable borehole to the slip surface (Fig. 14.25). Let $\frac{\partial n}{\partial \beta} = 0$, we have

$$\beta = 45^\circ + \frac{\varphi}{2} \quad (14.10)$$

Since $\frac{\partial^2 n}{\partial \beta^2} < 0$, therefore the maximum of n will be reached when $\beta = 45^\circ + \frac{\varphi}{2}$, i.e., this angle gives rise to maximum sliding resistance ability using shortest cable length. β is therefore termed as “economical installation angle” or “optimal installation angle” of anchor cable. The relationship of Eq. (14.10) shows that the optimum installation angle for a tensioned anchor cable is more flat than the normal to the sliding plane. In practice, cement grouted anchors may be installed at about 10° – 15° below the horizontal, while resin grouted anchors are installed in up-holes.

The spacing of prestressed anchor cables is 4 m ~ 10 m, and a minimum spacing of 4 m is demanded to avoid anchor group effect. Theoretically, the minimum spacing also may be estimated by

$$D = \ln \frac{T}{L} \quad (14.11)$$

where D = minimum spacing between cables, m; T = design tension force, kN; and L = length of cable, m.

Restrained by the construction condition, the length of anchor cable is usually shorter than 50 m. In addition, for loosen or fragment rock slopes, attributable to the difficulties with the borehole drilling and grouting operation, the prestress anchor cable was seldom employed. However, this restraint is less rigorous nowadays attributable to the breakthrough of construction techniques. For example, altogether

1380 prestressed anchor cables had been installed for the Yingshuigou ancient landslide in the Xiaowan project by the “casing while drilling technique,” the average depth of borehole is 65 m, of which the maximum one is 92 m.

References

- Abramson LW, Lee TS, Sharma S, Boyce GM (2002) Slope stability and stabilization methods, 2nd edn. Wiley, New York
- Aydan O, Kyoya T, Ichikawa Y, Kawamoto T (1987) Anchorage performance and reinforcement effects of fully grouted rock bolts on rock excavations. In: Proceedings of the 6th ISRM Congress. ISRM, Montreal, pp 757–760
- Baker RF, Marshall HC (1958) Control and correction. In: Eckel EB (ed) Landslides and engineering practice (Highway research board special report 29. Highway Research Board, Washington, DC, pp 150–188
- Barton NR (1986) Deformation phenomena in jointed rock. *Geotechnique* 36(2):147–167
- Barton NR (1990) Scale effects or sampling bias? In: Proceedings of the 1st international workshop on scale effects in rock masses, Loen (Norway). Balkema AA, Rotterdam, pp 31–55
- Barton NR, Bandis S, Bakhtar K (1985) Strength, deformation and conductivity coupling of rock joints. *Int J Rock Mech Min Sci Geomech Abstr* 22(3):121–140
- Bieniawski ZT (1989) Engineering rock mass classifications. Wiley, New York
- Bjurstrom S (1974) Shear strength of hard rock joints reinforced by grouted untensioned bolts. In: Proceedings of the 3rd ISRM Congress. ISRM, Denver, pp 1194–1199
- Broms BB (1964) Lateral resistance of piles in cohesive soils. *J Soil Mech Found ASCE* 90(SM2):27–63
- Cedergren HR (1973) Seepage, drainage, and flow nets, 3rd edn. Wiley, New York
- Ceng LK, Fan JL, Han J, Xu JP (2003) Rock and soil reinforcement. China Building Industry Press, Beijing (in Chinese)
- Chang SB (2006) Handbook of engineering geology, 4th edn. China Construction Industry Press, Beijing (in Chinese)
- Chen SH (2006) Computational rock mechanics and engineering. China WaterPower Press, Beijing (in Chinese)
- Chen SH, Chen SF, Shahrou I, Egger P (2001) The feedback analysis of excavated rock slope. *Rock Mech Rock Eng* 34(1):39–56
- Chen SH, Egger P (1999) Three dimensional elasto-viscoplastic finite element analysis of reinforced rock masses and its application. *Int J Num Anal Meth Geomech* 23(1):61–78
- Chen SH, Feng XM, Shahrou I (2008) Numerical estimation of REV and permeability tensor for fractured rock masses by composite element method. *Int J Numer Anal Meth Geomech* 32(12):1459–1477
- Chen SH, Fu CH, Shahrou I (2009) Finite element analysis of jointed rock masses reinforced by fully-grouted bolts and shotcrete lining. *Int J Rock Mech Min Sci* 46(1):19–30
- Chen SH, He J, Shahrou I (2012) Estimation of elastic compliance matrix for fractured rock masses by composite element method. *Int J Rock Mech Min Sci* 49(1):156–164
- Chen SH, Shahrou I, Egger P, Wang WM (2002) Elasto-viscoplastic block element method and its application to arch dam abutment slopes. *Rock Mech Rock Eng* 35(3):171–193
- Chen SH, Xu MY, Shahrou I, Egger P (2003) Analysis of arch dams using coupled trial load and block element methods. *J Geotech Geoenviron Eng ASCE* 129(11):977–986
- Chen ZA, Sun ZL, Peng TB, Xi QX (eds) (2000) Hydropower engineering in China—Engineering geology. China Electric Power Press, Beijing (in Chinese)
- Chen ZY (2003) Soil slope stability analysis—theory, method, programs. China WaterPower Press, Beijing (in Chinese)

- Chen ZY, Wang XG, Yang J et al (2005) Rock slope stability analysis—theory, method, programs. China WaterPower Press, Beijing (in Chinese)
- Ching RKH, Fredlund DG (1983) Some difficulties associated with the limit equilibrium method of slices. *Can Geotech J* 20(4):661–672
- Davissou MT, Prakash S (1963) A review of soil-pile behavior. *Highway Res Rec* 1(39):25–48
- Dawson EM, Roth WH, Drescher A (1999) Slope stability analysis by strength reduction. *Géotechnique* 49(6):835–840
- Duncan JM (1996) State of the art: limit equilibrium and finite element analysis of slopes. *J Geotech Eng* 122(7):557–596
- Duncan JM, Wright SG (1980) The accuracy of equilibrium methods of slope stability analysis. *Eng Geol* 16(1/2):5–17
- Duncan JM, Wright SG, Wong KS (1990) Slope stability during rapid drawdown. In: Proceedings of the H. Bolton seed memorial symposium, vol 2. BiTech Publishers, Vancouver, pp 253–272
- Dunncliff J (1988) *Geotechnical Instrumentation for monitoring field performance*. Wiley, New York
- Einstein HH, Veneziano D, Baecher GB, O'Reilly KJ (1983) The effect of discontinuity persistence on slope stability. *Int J Rock Mech Min Sci Geomech Abstr* 20(5):227–236
- Fredlund DG, Khran J (1977) Comparison of slope stability methods of analysis. *Can Geotech J* 14(4):429–439
- Freeze RA, Cherry JA (1979) *Groundwater*. Prentice Hall, New Jersey
- Goodman RE (1989) *Introduction to rock mechanics*, 2nd edn. Wiley, New York
- Haar ME (1962) *Ground water and seepage*. McGraw Hill, New York
- Hanna TH (1982) *Foundations in tension—ground anchors*. Transactions Tech Publications/McGraw Hill, Clausthal-Zellerfeld
- Hanna TH (1985) *Field instrumentation in geotechnical engineering*. Trans Tech Publications, Clausthal-Zellerfeld
- Hencher SR, Richards LR (1989) Laboratory direct shear testing of rock discontinuities. *Ground Eng* 22(2):24–31
- Hoek E (1983) Strength of jointed rock masses (rankine lecture). *Geotechnique* 33(3):187–223
- Hoek E, Bray JW (1981) *Rock slope engineering*, 3rd edn. The Institution of Mining and Metallurgy, London
- Huntington WC (1957) *Earth pressures and retaining walls*. Wiley, New York
- Hudson JA, Harrison JP (1997) *Engineering rock mechanics—an introduction to the principles*. Elsevier Science Ltd, Oxford
- ICOLD (2002) *Reservoir landslides: investigation and management—guidelines and case histories* (Bulletin 124). ICOLD, Paris
- Ikegawa Y, Hudson JA (1992) A novel automatic identification system for three-dimensional multi-block systems. *Engineering Computations* 9(2):169–179
- Ito T, Matsui T, Hong WP (1982) Extended design method for multi-row stabilizing piles against landslide. *Soils Found* 22(1):1–13
- Jalalifar H, Aziz N, Hadi MSN (2006) The effect of surface profile, rock strength and pretension load on bending behaviour of fully grouted bolts. *Geotech Geol Eng* 24(5):1203–1227
- Jaeger JC, Cook NGW, Zimmerman R (2007) *Fundamentals of rock mechanics*, 4th edn. Wiley-Blackwell, Hoboken
- Jing LR, Hudson JA (2002) Numerical methods in rock mechanics. *Int J Rock Mech Min Sci* 39(4):409–427
- Jones CJFP (1979) Current practice in designing earth retaining structures. *Ground Eng* 12(6):40–45
- Kaiser PK, Hewitt KJ (1982) The effect of groundwater flow on the stability and design of retained excavations. *Can Geotech J* 19(2):139–153
- Kiersch GA (1963) Vajont reservoir disaster. *Civil Eng* 34(3):32–39
- Krahn J (2003) The 2001 RM Hardy lecture: the limits of limit equilibrium analyses. *Can Geotech J* 40(3):643–660

- Ling HI, Cheng AHD (1997) Rock sliding induced by seismic forces. *Int J Rock Mech Mining Sci* 34(6):1021–1029
- Littlejohn GS, Bruce DA (1977) Rock anchors—state of the art. Foundation Publications Ltd, Essex
- Lorig L (1999) Lessons learned from slope stability studies. In: Proceedings International of FLAC symposium on numerical modeling in geomechanics. Balkema, Leiden, pp 17–21
- Louis C, Maini YN (1970) Determination of in-situ hydraulic parameters in jointed rock. In: Proceedings of the 2nd international congress. ISRM, Belgrade, pp 235–245
- Ma GY, Chang ZH (2007) Theory and practice of grouting drainage and anchorage of rock mass. China WaterPower Press, Beijing (in Chinese)
- Meyerhof GG (1984) Safety factors and limit states analysis in geotechnical engineering. *Can Geotech J* 21(1):1–7
- Min KB, Jing LR (2003) Numerical determination of the equivalent elastic compliance tensor for fractured rock masses using the distinct element method. *Int J Rock Mech Min Sci* 40(6): 795–816
- Min KB, Rutqvist J, Tsang CF, Jing LR (2004) Stress-dependent permeability of fractured rock masses: a numerical study. *Int J Rock Mech Min Sci* 41(7):1191–1210
- Ministry of Water Resources of the People's Republic of China (2007) SL386-2007 “Design Code for Engineering Slopes in Water Resources and Hydropower Projects”. China WaterPower Press, Beijing (in Chinese)
- Morgenstern N (1963) Stability charts for earth slopes during rapid drawdown. *Geotechnique* 13(2):121–131
- National Reform and Development Commission of the People's Republic of China (2006) DL/T 5353-2006 “Design Specification for Engineering Slopes in Water Resources and Hydropower Projects”. China Electric Power Press, Beijing (in Chinese)
- Naylor DJ, Pande GN (1981) Finite elements in geotechnical engineering. Pineridge Press Ltd, Swansea
- Oriard LL (1971) Blasting effects and their control in open pit mining. In: Proceedings 2nd international conference on stability in open pit mining. AIME, New York, pp 197–222
- Pahl PJ (1981) Estimating the mean length of discontinuity traces. *Int J Rock Mech Min Sci Geomech Abstr* 18(3):221–228
- Peck RB (1969) Advantages and limitations of the observational method in applied soil mechanics (ninth rankine lecture). *Geotechnique* 19(2):171–187
- Piteau DR, Jennings JE (1970) The effects of plan geometry on the stability of natural slopes in rock in the Kimberley area of South Africa. In: Proceedings of the 2nd congress of the ISRM, Vol 3. ISRM, Belgrade, Paper 7–4
- Post-Tensioning Institute (2004) Recommendations for prestressed rock and soil anchors, 4th edn. Post-Tensioning Institute, Phoenix
- Poulos HG, Davis EH (1974) Elastic solutions for soil and rock mechanics. Wiley, New York
- Poulos HG, Davis EH (1980) Pile foundation analysis and design. Wiley, New York
- Price DG (ed) (2009) Engineering geology—principles and practice. Springer, Berlin
- Serafim JL (1968) Influence of interstitial water on the behaviour of rock masses. In: Stagg KG, Zienkiewicz OC (eds) Rock mechanics in engineering practice. Wiley, New York, pp 55–97
- Spang K, Egger P (1990) Action of fully-grouted bolts in jointed rock and factors of influence. *Rock Mech Rock Eng* 23(2):201–229
- Stagg KG, Zienkiewicz OC (eds) (1968) Rock mechanics in engineering practice. Wiley, New York
- Wei XC, Zhou ML (2004) Handbook of retaining structure design, 2nd edn. China Building Industry Press, Beijing (in Chinese)
- Wei ZQ, Egger P, Descoeders F (1995) Permeability prediction for jointed rock masses. *Int J Rock Mech Min Sci Geomech Abstr* 32(3):251–261
- Xanthakos PP (1991) Ground anchorages and anchored structures. Wiley, New York
- Yan TZ, Yang SA, Fang YL (2000) Landslidologies. China University of Geosciences Press, Wuhan (in Chinese)

- Zaruba Q, Mencl V (1969) *Landslide and their control*. Elsevier, Amsterdam
- Zhang X, Sanderson DJ, Harkness RM, Last NC (1996) Evaluation of the 2D permeability tensor for fractured rock masses. *Int J Rock Mech Min Sci Geomech Abstr* 33(1):17–37
- Zhou WY, Yang Q et al (2007) *Numerical computational methods for rock mechanics*. China Electric Power Press, Beijing (in Chinese)

Chapter 15

Hydraulic Steel Gates

15.1 General

15.1.1 Functions and Components

Almost every hydraulic project needs a reservoir (or pool) to control flood as well as to store water for irrigation, power generation, domestic, and/or industrial water supply. A spillway or headwork with control devices such as gates or shutters is almost invariably demanded for releasing excessive flood inflow, or diverting water into canal system (Mayer and Bowman 1969; Zuo et al. 1987; Ministry of Construction of the People's Republic of China 2006; Ministry of Water Resources of the People's Republic of China 1995; Ministry of Water Resources of the People's Republic of China, Electric Power Industry Ministry of the People's Republic of China 1995). Delivery of water also may be undertaken by hydraulic gates installed in tunnels and dam body conduits. However, control of flow in closed pipes such as penstocks conveying water for turbines is done by valves, which are different from gates in the sense that they come together with the driving equipment, whereas gates require separate driving (hoisting) equipments.

A hydraulic gate normally consists of movable member, stationary member, and mechanical equipment (Fig. 15.1).

The moveable member is also termed as “gate leaf” and used to shut the opening of the hydraulic work, to control discharge, to pass boats, and to flush silt. It consists of skin plate, frame, support and travel member, hanger, and water tightness (Fig. 15.2).

The stationary member is embedded into the pier or sidewall structure and intended to guide the gate, to carry loads imposed on gate support, to provide water tightness in areas of gate-to-structure contacts, to warm up these contacts, and to prevent concrete surface and edge from crushing.

The mechanical equipment is hoist and/or handle mechanism, for operating the gates during erection and shutdown.

Fig. 15.1 Components of hydraulic gate. 1 moveable structure; 2 stationary members; 3 mechanical equipment

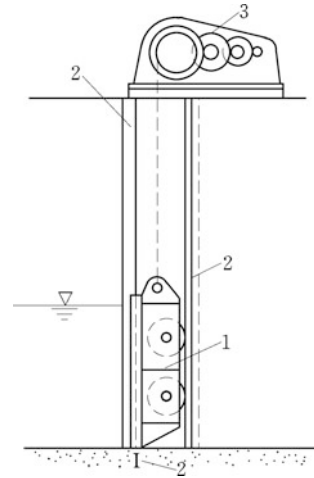
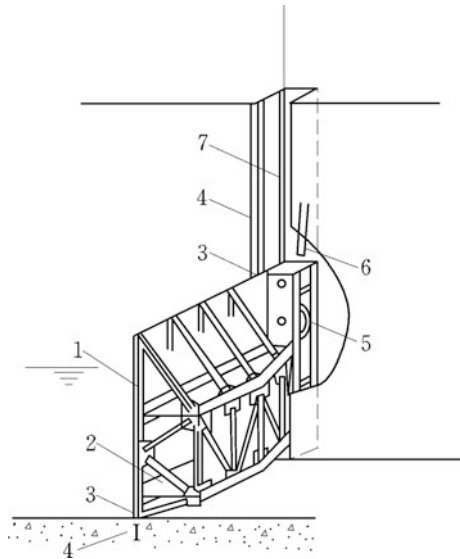


Fig. 15.2 Leaf components of plate gate. 1 skin plate; 2 framework; 3 water tightness; 4 embedded water tightness; 5 support and travel member (wheel); 6 embedded support and travel member; 7 hanger



15.1.2 Classification of Gates

Different types of hydraulic gate and hoist working on different principles and mechanism are used in spillways, sluices, and tunnels, etc. (Cai and Qu 1988; Chen and Chen 2014; Erbisti 2004; Fan 2000; Grishin 1982; Lewin 1995; Mayer and Bowman 1969).

By operational purpose, hydraulic gates fall into service (main) gate used for routine operation, bulkhead gate providing temporary damming surface to enable

the dewatering of a lock chamber or gate bay between dam piers, and emergency gate to close the opening in case of accident fraught with dangerous consequences.

By material used, hydraulic gates are distinguished as steel gate, reinforced concrete gate, wooden gate, etc., of which the steel gate is the most prevalent due to its high strength of material, high impact resistance, and durability.

By the location of opening with respect to headwater, hydraulic gates are divided into crest (surface) gate intended to close overflow openings (e.g., overflow dam monolith, sluice, and shore spillway) and submerged gate to close bottom orifices, which may be installed at position in the conduit between inlet and outlet. Hydraulic gates operating under heads up to and in excess of 50 m are conventionally referred to as “high-pressure gates.”

The prevalent classification of hydraulic gate is based on their structure and operation feature as shown in Fig. 15.3.

1. Stoplog gates

Stoplogs are smaller beam or girder structures that span the opening and are stacked to a desired damming height. A number of stacked stoplogs make up a stoplog gate, which is usually used in small sluices or culverts (Fig. 15.3a).

2. Vertical lift plate gates

Vertical lift plate (plain) gates have been widely employed in locks and spillways (Fig. 15.3b). They are raised and lowered vertically to open or close a lock chamber or a spillway vent. They are essentially a stiffened plate structure that transmits the water load exerting on the skin plate along horizontal girders into the sidewalls of the lock monolith or spillway piers. Vertical lift gates can be operated under moderate heads, but not be applicable under reverse head conditions.

3. Roller gates

They are mostly used at the exit of pumping station which may be further divided as flap gate (Fig. 15.3c), pivot leaf gate (Fig. 15.3d), and cover board gate (Fig. 15.3e).

4. Floating pontoon gates

They are similar to empty cases floating on water (Fig. 15.3f) and used as bulkhead gates by floating to the position and sinking down after the filling of water.

5. Radial gates

Radial (or Tainter) gate is a segment of cylinder mounted on radial arms, or struts, that rotate on trunnions anchored to the sidewalls or piers (Fig. 15.3g). Although numerous types of framing exist, yet the most common type comprises two or three frames, each of which consists of a horizontal girder that is supported at each end by a strut. Each frame lies in a radial plane with the struts joining at the trunnions. The girder supports the stiffened skin plate assembly that forms the damming surface.

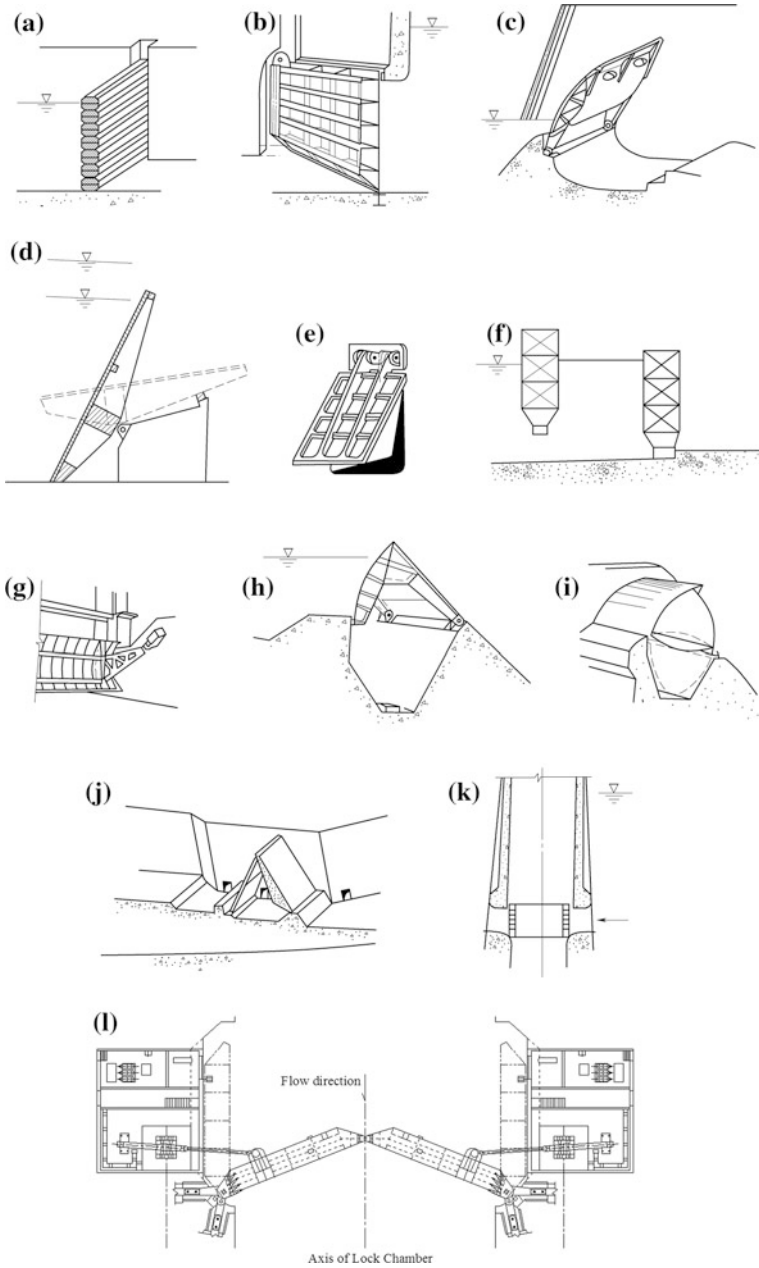


Fig. 15.3 Types of hydraulic gate. **a** Stoplog gate; **b** plate gate; **c–e** roller gate; **f** floating pontoon gate; **g** radial gate; **h** sector gate; **i** drum gate; **j** roof gate; **k** cylinder gate; **l** miter gate

6. Sector gates

They are framed similar to radial gates. Depending on the position of their axis, sector gates may be further divided as vertical axis sector gate and horizontal sector gate. The latter is actually a pair of arc gates hinged on vertical axis, which are commonly installed in navigation locks. The former usually has sealed top roof skin, and by feeling or emptying of the room inside, the gate may be moved up or down (Fig. 15.3h). Traditionally, sector gates have been used in the tidal reaches of river or canal where the dam may be subject to head reversal. Sector gates are generally limited to lifts of 3 m or less. Where the pivot trunnion is at the upstream side, it is also named as drum gates (Fig. 15.3i).

7. Roof (bear-trap) gates

They consist of two wickets turning about horizontal axes, which are also named as floating gates in China (Fig. 15.3j).

8. Ring gates

Ring gate is a cylindrical drum which moves vertically in an annular hydraulic chamber so as to control the peripheral flow of water from reservoir through a vertical shaft (Fig. 15.3k).

9. Miter gates

Miter gates are customarily used to close off the entrance and exit of a navigation lock to allow the passage of vessels between different water levels in a canal or river system. A miter gate consists of two leaves that provide a closure at one end of the lock. The miter gate derives its name from the fact that the two leaves meet at an angle pointing upstream to resemble a miter joint (Fig. 15.3l).

10. Valves

Valve is a device installed in various pipes (e.g., penstocks) that regulates, directs, or controls the flow of water by opening, closing, or partially obstructing. Valves are different from gates by their way of operation as they remain in the water both in the closed and open positions. Valves in hydraulic engineering are mostly intended to control flow in the high-pressure conduits such as penstocks conveying water to turbines for the generation of hydroelectricity.

15.1.3 Brief History of Hydraulic Gates

The manufacture of hydraulic gates is closely related with the development of irrigation and river navigation system (Erbisti 2004).

The first canal for transporting of goods is believed to appear in China, in an attempt to handle boats in the region of river rapids by building dikes with slopes on the banks of the canal. Around 987, the Chinese constructed two wood or stone

piers a certain distance apart on each side of the canal, to create a pool. Vertical grooves (slots) were cut into the opposite sides of the piers, and tree trunks were fitted horizontally into or out the grooves as stoplogs. In this way, boats could enter or exit the pool and the water level could be slowly raised or brought down. Later, the tree trunks were linked, forming an integral gate that could be lifted up or lowered down like a guillotine blade.

The development of hydraulic gates in the Netherlands followed a way similar to that of China where locks were very common at the end of the fourteenth century. The gates, still of the guillotine type, were provided with lead counterweights and equipped with drains.

In 1795, the Little Falls canal lock was put into operation. Two wood swinging gates were placed at each end of the lock. Instead of closing to a flat plate, the gates closed to form an angle pointing upstream, facing the current. This may be looked at as the initiation of miter gates. The miter gates designed with cast-iron structure and steel plate shielding were firstly laid in 1828 on the Nivernais Canal in France.

With the turn of the century, inventions with respect to hydraulic gates were booming.

The oldest known application of a radial gate was in 1853, on the Seine River in Paris (France), at 8.75 m wide and 1.0 m high. Around 1870, Parker in the USA invented the radial gate in parallel, who sold his invention to Tainer. In 1886, Tainer patented the radial gate in his name.

The sector gate was invented in the USA by Cooley and used for the first time in 1907 in the Lockport Dam on the Chicago Drainage Canal.

Carstanjen in Germany invented the roller gate in 1898. Its first application was on the Sau River.

Chittenden of the US Army Corps of Engineers invented the drum gate in 1896. Its first application was at the No. 1 Dam on the Osage River (USA) in 1911.

In 1818, White constructed the first roof (bear-trap) gate in the Mauch Chunk Creek, on the Lehigh River, USA.

The ring gate was developed by the USBR for the use in morning-glory spillways. It was firstly applied in 1936 in the Owyhee Dam, with a diameter of 18 m and a height of 3.6 m and then followed by the Hungry Horse Dam in 1953, with a diameter of 19.5 m and a height of 3.6 m.

In 1883, according to Stoney's patent, wrought-iron gates at 8.9 m wide and 4.4 m high installed with rollers sliding in cast-iron grooves fixed in the piers was first constructed at Belleek, Ireland. This type of gate was widely applied in Europe, USA, Egypt, and India at the beginning of the twentieth century.

15.2 Basic Requirements for the Layout of Gates

Most existing lock gates are miter gates and vertical lift gates, with a small percentage being sector gates (Buzzell 1958). Spillway gates installed on the crest to provide a moveable damming surface and to allow for the spillway crest being

located below a given water level are generally radial gates or vertical lift gates, but occasionally roller gates.

Right selection of gates and their hoists is the first step to ensure the effective control and safety of the project. A designer has to plan the gate and hoisting equipment together since separate planning of gates or hoists, sometimes will lead to unsatisfactory installation. Although the choice for the gates and hoists for spillways and outlets depends on various factors such as head, gate size, and river flow operational criteria, yet primarily the safety and convenience in operation as well as maintenance and economy, are the governing requirements in the same importance.

Gates should be installed at position where water flow is smooth. The conditions being disadvantageous for gate operation, such as the cross and swirl flow in front of gate, and the submerged flow and backflow at the back of gate, should be avoided as far as possible.

Specifically, selection of gates should take into account of following factors:

- Requirements of the project for the gate operation;
- Position of gates in the hydraulic structure, size of openings, head and tail water level, and operational head;
- Silt and floating debris;
- Type and capacity of hoists, hanger manners;
- Manufacture, transportation, installation, and maintenance; and
- Techno-economic indices.

To facilitate manufacture, transportation, and installation of gates, following requirements should be met in the design:

- Specific conditions of manufacture and installation;
- Sufficient rigid, adequate outer dimension, and self weight of the transportable unit;
- Standardized and patternized products for reducing the variety and specification of components and members;
- Less welding work for connecting structural members as far as possible; and
- Controlled assembly distortion using pins or blots for gate section joint, if possible.

Hereinafter in this chapter, an introduction is provided on the radial and plate gates, with respect to the specific purposes they may be met, the possible locations in which they may be installed, and the suitable hoists with which they are operated.

15.3 Plate Steel Gates

These are gates that move within vertical grooves (slots) incised between sidewalls or piers. The vertical lift gates for controlling flow over the crest of a hydraulic structure are ordinarily equipped with wheels. Nowadays, this type of gates is

commonly used for barrages but is rarely used for dam. Instead, the radial gates (discussed later) are more and more prevalent for dam spillways.

15.3.1 Types of Plate Gates

They may be vertical lift (Fig. 15.4) and lift flap (Fig. 15.5).

1. Vertical lift gate

The vertical lift gate, with wheels (rollers) at each end, moves vertically in slots and consists of a skin plate and horizontal girders that transmit the horizontal water thrust into the piers. Like the radial gate, it must be hoisted at both ends, and the entire weight is suspended from the hoisting chains or cables (cables are generally desirable). Piers must be extended to a considerable height above water in order to provide guide slots for the gate in a fully raised position. Vertical lift gates have been designed for spans in excess of 25 m. Historically, gantry cranes traveling on the barrage/spillway deck or working platform have been the standard equipment for operating vertical lift gates. However, fixed hoists may be justified as advantageous over gantry cranes, especially if the operating speed is important or remote control is desired. Dogging devices are sometimes provided on the gate to hold it at

Fig. 15.4 Vertical lift gate.
1 hoist; 2 operating bridge;
3 access bridge; 4 bulkhead
gate slot; 5 vertical lift gate

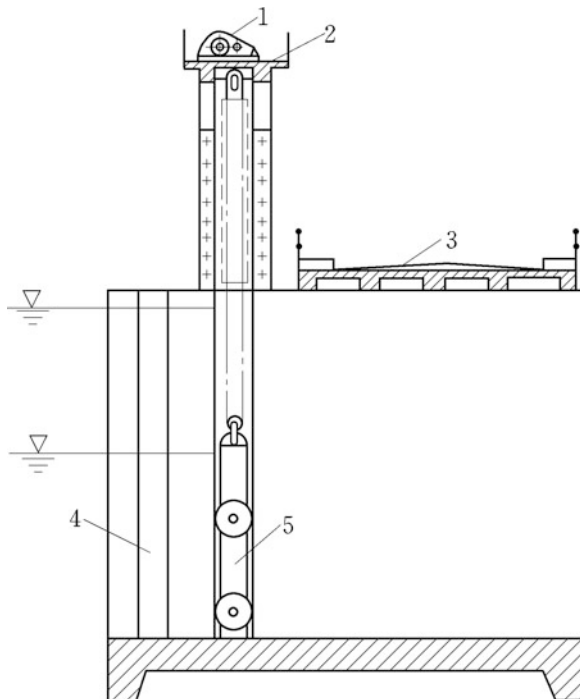
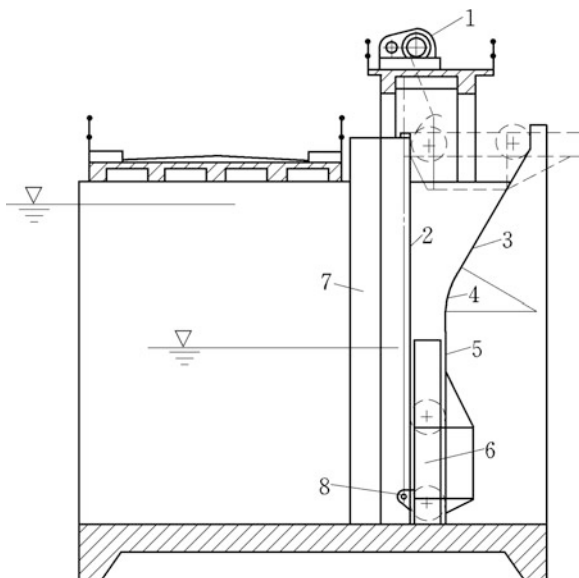


Fig. 15.5 Lift flap gate.
 1 hoist; 2 guide track;
 3 inclined track; 4 circular
 track; 5 straight track; 6 plate
 gate; 7 bulkhead gate slot;
 8 hanger



the proper elevation. In some cases, it may be advantageous to mount the dogs in the gate and provide a dogging ladder in the gate slot.

Some of the main advantages of vertical lift gates over radial gates are ease of fabrication, considerably shorter of erection time, and in most cases, shorter supporting piers. The load from the gate to the supporting piers or sidewalls is in one direction, which simplifies the design of supports. Some of the main disadvantages of using vertical lift gates are heavier lifting effort which requires greater hoist capacity, more labor intensive operation, greater time required for gate operation if only one gantry crane is provided, gate slots can lead to cavitation and debris collection, and fatigue under constant cyclic loading since the main load resisting frame relies on a tension flange.

Vertical lift gates would be preferred to radial gates when the elevation of the maximum controlled pool is far above the sill that excessively long piers would be demanded for radial gates, flood discharges, or drift conditions are such that any obstruction to the flow below the spillway bridge is impermissible.

2. Lift flap gate

With the lift flap gate, the track of wheel support is divided into three parts: vertical, circular, and inclined. The hanger is mounted at the upstream bottom of the leaf near the lower main girder. The gate is flapped gradually as its lifting until horizontal position. Lift flap gate may lower down the height of operating bridge or platform to obtain higher seismic resistance. Some of the main disadvantages of lift flap gate are the hanger on upstream side resulting in its corrosion; the horizontal position of lifted gate is inconvenient for repairing; and during the operation when it

is in the position of inclination, the gate is vulnerable to the flow and wave actions which give rise to strong swing and vibration.

15.3.2 Layout and Structure of the Leaf of Plate Gate

Leaf is the main body of a gate consisting of skin plate, stiffeners (tiers), horizontal girders, and end girders (Fig. 15.6).

Vertical lift gates may be framed of plate girders or horizontal trusses, and economy index normally indicates which frame system will be preferred. Support and travel members are intended to permit the traveling of gate and transfer pressure through slot and guide members to the embedded facilities. To limit the lateral displacement, misalignment, and vibration of gate, uses are made of side and reverse subsidiary supports and guide means (wheel, struts). Seals overlap the gaps between the movable gate structure and slot and guide members. Hangers connect the gate to the hoist.

The size of plate gate is dependent on the vent size of waterway. Although the crest gate permits overtopping of wave, yet its upper edge should be at least 0.3 m higher above the maximum level (inclusive of wind-wave pileup) maintained by the gate.

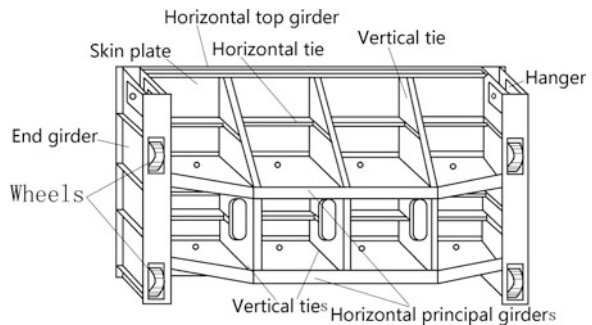
High vertical lift gates may be fabricated of two or more segments in order to facilitate storage, to reduce hoist capacity, or to facilitate passing of ice and debris, and they are termed as “two-tier gates” which can be operated separately, but when fully closed, they act as monolithic gates (Fig. 15.7). However, this does increase operating difficulties because the top leaf has to be removed and placed in another gate slot.

1. Layout of framework

The gate framework structure may be distinguished as simple crossbar, crossbar and vertical stiffener grid, and complex crossbar and stiffener grid (Fig. 15.8).

The framework structure selected will depend on the span, hydrostatic head, and lift requirements. Horizontal girders (crossbars) are the principal structural members

Fig. 15.6 Structural layout of an unitary vertical lift gate



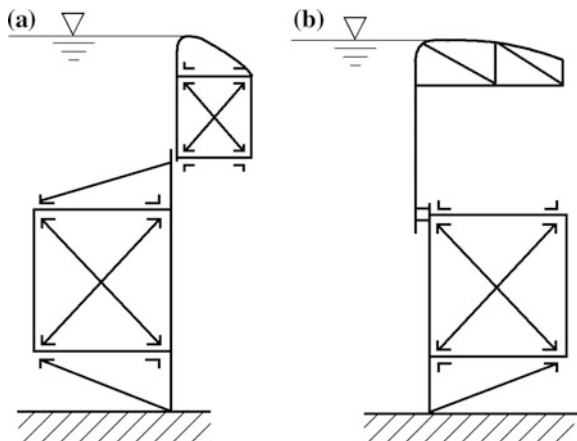


Fig. 15.7 Two-tier gates

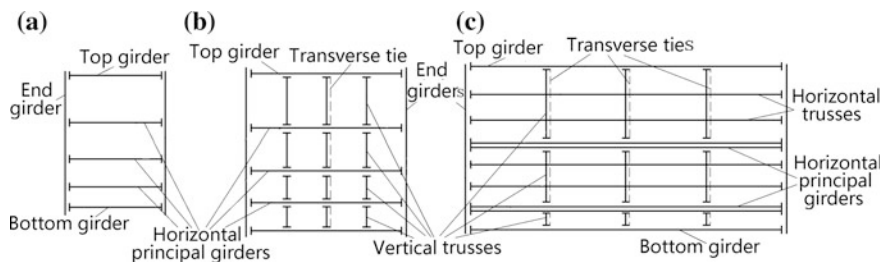


Fig. 15.8 Typical layout of frameworks for plate gates. **a** Simple crossbar; **b** crossbar and vertical stiffener grid; **c** complex crossbar and stiffener grid

of gate, to transfer the water pressure from the skin plate and vertical stiffeners (if any) to the end girders or end arms of the gate. Vertical stiffeners (also called as vertical tiers or vertical beams) are the structural members spanning vertically across horizontal girders to support the skin plate.

(a) Simple crossbar

The skin plate is supported on the crossbars (also called as horizontal girders), to which the hydrostatic pressure of water is transferred directly. This type is generally applied to small span gates.

(b) Crossbar and vertical stiffener grid

To reduce the thickness of skin plate, vertical stiffeners may be installed. This type is generally applied to medium span gates.

(c) Complex crossbar and stiffener grid

For a larger span plate gate, water exerts pressure on the skin plate which transfers it to the structural stand consisting of horizontal beams (strings) and vertical beams (stiffeners) before transfers it further to the crossbars.

2. Connection of framework with skin plate

There are three types of framework connecting with skin plate: inbuilt structural stand, lower stand, and extended (outside) stand (Fig. 15.9).

(a) Inbuilt stand

Horizontal and vertical beams and crossbars are included in its arrangement and linked directly with skin plate. The major advantage of this type lies in its higher stiffness of the framework; therefore, the amount of steel consumption may be reduced. The major disadvantage of this type is the inconvenience in manufacture—the horizontal beams are cut first and then connected to the vertical beams, the same occurs at the connection of vertical beams with the crossbars. This may be partially improved by using diaphragm plates as vertical beams, and the holes may be made through these diaphragms to let the horizontal beams pass through the holes directly, in this way they may be continuous. This is widely exercised for the connection of framework with skin plate.

(b) Lower stand

The crossbars and horizontal beams are connected directly with the skin plate, while the vertical beams are located to the downstream face of horizontal beams. In this way, the horizontal beams are kept continuous.

(c) Extended (outside) stand

The horizontal and vertical beams are located between the skin plate and crossbars. This design is simpler, but the sharing proportion of skin plate in the operation of

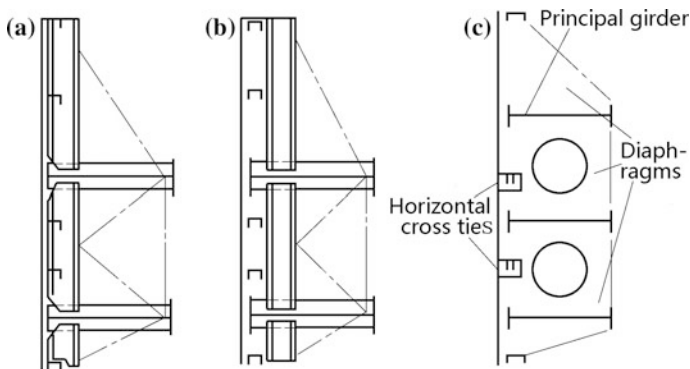


Fig. 15.9 Connection of framework with skin plate. **a** Inbuilt stand; **b** lower stand; **c** extended stand

the entire gate structure is rather small, let alone the augment in the gate thickness. This type is seldom practiced nowadays.

3. Layout of crossbars

The number of crossbars is depending on the size of gate. Where the span L of gate is smaller than the height (i.e., $L \leq H$), the number of crossbars is more than two, which is named as multi-crossbar gate. On the contrary, with a large ratio of span to height (e.g., $L \geq 1.5H$), two-crossbar gate is commonly employed. Most often, crest gates possess two crossbars rather than three crossbars. Crossbars are equal-loaded by positioning them at an equal distance from the resultant of water thrust exerting on the skin plate.

4. Layout of end girders

End girders (also called as support beams) can be single-walled or double-walled (Fig. 15.10).

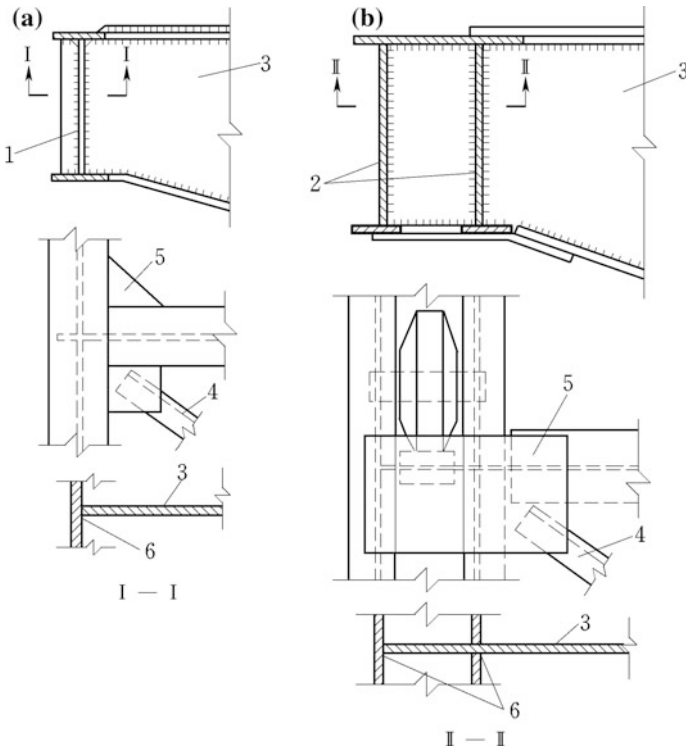


Fig. 15.10 Types of support beams. **a** Single-walled support beam; **b** double-walled support beam. 1 single-walled support beam; 2 double-walled support beam; 3 crossbar web; 4 cross-tie of truss for hanger; 5 strengthened plate of node; 6 k-type welding line

Single-walled support beam is simple and convenient to be connected to crossbars, but it has low stiffness against torsion. It is suitable for the gate with slide support, or for the fixed wheel support of small size. In the latter case, an additional support plate should be installed at the inner side of the web of support beam.

Double-walled support beam has high stiffness against torsion and is convenient for the installation of support wheels and hanger, but it is complex in structure and high in steel consumption. It is suitable for the large gate with fixed wheel support.

5. End supports

End supports are intended to transfer the loads to gate guides. The basic types of supports are slides and wheels, and the latter may be further divided as fixed, tractor (caterpillar), and Stoney. Structural steel guide members, such as guide rollers, should be provided to restrict the lateral and/or transverse movements of gate, either in the upstream or lateral direction (Fig. 15.11).

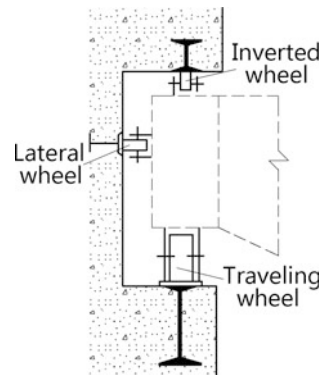
(a) Slide supports

Slide gate, as the name implies, is the gate in which the gate leaf slides on the sealing surfaces provided on the frame. In most cases, the sealing surfaces are also the load-bearing surfaces. Slide gates may be with or without top seal depending on whether they are used in a close conduit or as on a free flow crest. A typical installation of slide gate consists of a gate leaf and embedded parts (Fig. 15.12), and the latter serves the following purposes:

- Transmit water load on the gate leaf to the supporting concrete (sidewalls or piers);
- Guide the gate leaf during operation; and
- Provide sealing surface.

Slide gates use face-to-face contact for end support. A machined surface that is mounted to the front face of gate bears directly against a machined guide surface in the gate slot. The two bearing surfaces also serve as the gate seal. Materials for the

Fig. 15.11 Guide rollers on the sides of a gate



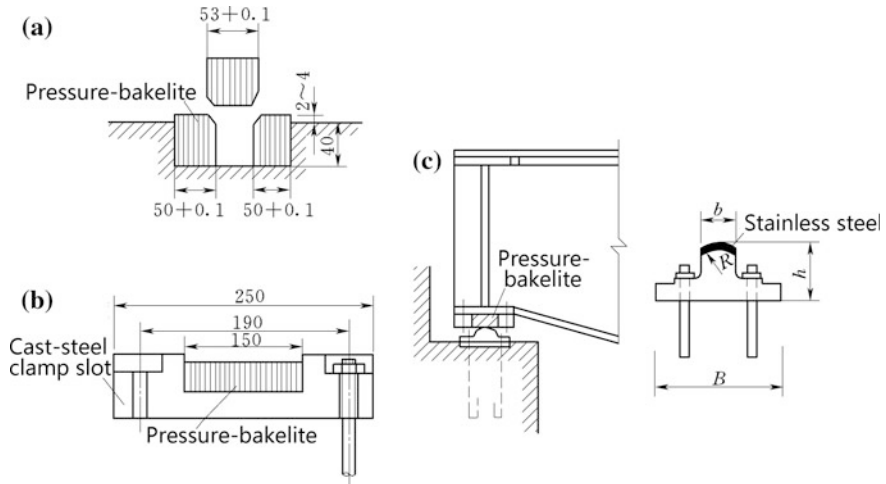


Fig. 15.12 Structure of pressure-bakelite slides (unit: mm)

gate seal surface may be aluminum, bronze, stainless steel, or pressure-bakelite. The last one is the most prevalent attributable to its high mechanism performance, low friction, and good processability. Under definite lateral confined stress, the bearing capacity of pressure-bakelit slides may reach up to 160 MPa and the friction coefficient between the pressure-bakelit slide and the smooth steel track may be as low as 0.09–0.13. The top of steel track is generally in a shape of circular. To control the slide friction, 3–5 mm thick stainless steel is coated on the track top and is polished at least up to 6–7 degree of finish (Fig. 15.12).

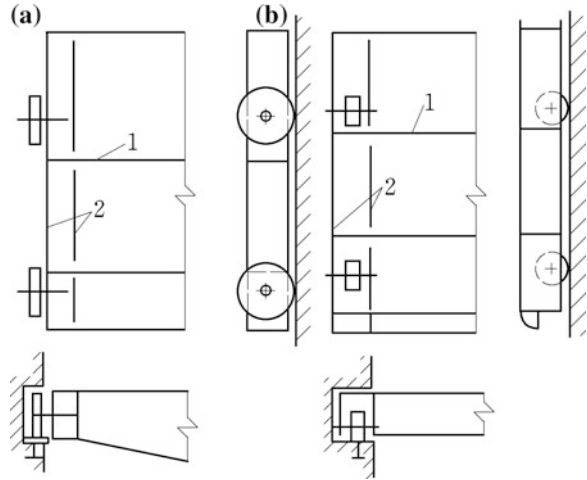
This type of gate may be employed for the intake/outlet of tunnels under high heads, where a head cover (bonnet) is used to seal off the guide slot from the gate operator for submerged flow installations.

(b) Wheel support

With this type of end support, the wheels revolve on fixed axes, which are customarily supported by the web of end girders attached to the gate framework. The wheels also may be mounted by pairs in trucks that carry the wheel loads through center pins to end girders. When the gate is operated without static head, this type of end support will be most economical.

In some cases such as where the gate moves on the tracks provided on the face of dam, skin plate is customarily installed on the downstream side, or skin plates are provided on both downstream side and upstream side if the downstream water is above sill. Under the latter circumstances, the gate may be fully or partially buoyant. This buoyancy should be taken into account in determining the net balance of vertical forces and addition of ballast, to ensure the closure without difficulty. The bottom of gate should be so shaped that satisfactory performance and

Fig. 15.13 Typical layout of wheels. **a** Cantilevered axis wheel; **b** simply pin-supported wheel. 1 crossbar; 2 side girder



freedom from harmful vibrations are attained under all conditions of operation in addition to minimum down-pull.

The wheel support permits the use of a smaller hoist capacity for gate operating, which is preferable to large size and high-head gates, particularly where the gate should be shut down by its self weight.

The unitary gate is the simplest type of wheel gates with four wheels on cantilevered pins or pins fixed between the walls of end girders (Fig. 15.13). Wheels on cantilevered pins need shallower gate slots and are convenient in installation and repair, but the outside web of the side girder in torsion and the cantilevered pins in bending entail them only be applicable for the gates of small size and under low head.

Pins fixed between the walls of side girder are mainly employed for the gates of large size and under high head.

The larger head and size of opening, the greater diameter and/or number of wheels will be, and it in turn deepens and widens the slots. Since the rigid support of a great number of wheels fails to ensure a uniform distribution of load on these wheels, use is often made of two-wheeled carriages. Hinges are provided between the carriages and end girders.

For small gates, cast iron is a commonly used wheel material. However, where the wheel pressure is in excessive of 200 kN, carbon steel or alloy steel should be alternatives.

6. Seals

Seal is a device for preventing the leakage of water around the periphery of hydraulic gate—a bottom seal is provided at its bottom, whereas side seals are fixed to its vertical ends, and a top seal (if any) is one that is installed at its top. As the pressure downstream of the gate drops, the seal, under the actions of head pressure, moves toward the seal plate.

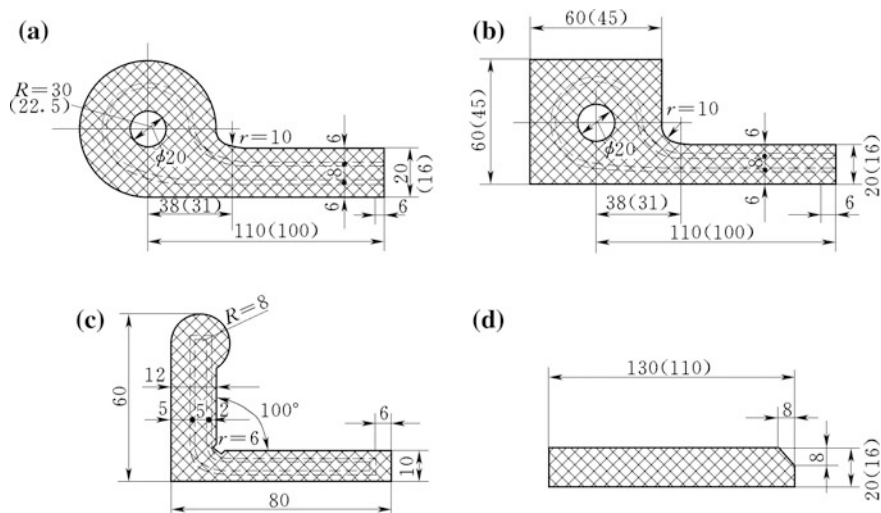


Fig. 15.14 Rubber seals (unit: mm). **a** J-type (or P-type) seal with circular bulb; **b** J-type (or P-type) seal with square bulb; **c** L-type (or angle-shaped type) seal; **d** rectangular seal

Rubber is almost universally employed for seals owing to its ability to form a watertight contact against any reasonably smooth surface. Seal types, sizes, and available molds are listed in their catalogs of major rubber seal manufacturers. J-type (or P-type, music note type) seal of circular bulb is mainly applied to seal the gate top and sides (Fig. 15.14a), while J-type seal of square bulb (Fig. 15.14b) is mainly employed for the sealing of gate top and sides of submerged radial gate. For crest radial gates, L-type (or angle-shaped type) (Fig. 15.14c) is commonly adopted as the side seal. Rectangular seal (Fig. 15.14d) is merely used for bottom seals.

For low- and moderate-head installations, the most frequently exercised side and top seals is the J-type with a 45 mm bulb and a 15 mm stem. The J-type seal of circular bulb or square bulb mounted on either the upstream or downstream side is most suitable for vertical lift gates, which is commonly employed as top and side seals of lower head gates (Fig. 15.14).

J-type seals are available with both hollow and solid bulbs. Hollow bulb seals provide a greater contact area with seal plates, thus aiding water tightness in low-head gates.

To allow greater flexibility for the seal and permit it to deflect toward the seal plate, the seal stem should be attached to the gate on the outer edge by the clamp bars. Seal mounting details should be carefully considered to prevent damage to the rubber under all conditions of operation.

All top seals should be fluorocarbon-clad to help prevent the bulb from rolling during the operation of gate. The bottom seal is normally a wedged rubber that relies on the weight of gate to provide the seal compression for sealing.

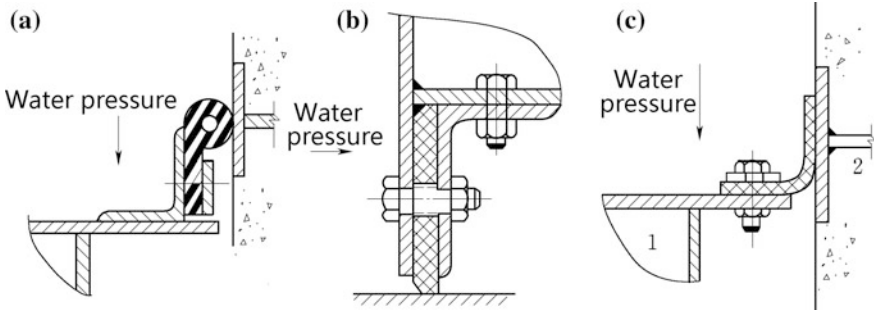


Fig. 15.15 Typical side seal layouts for crest gates. 1 gate leaf; 2 cushion of seal

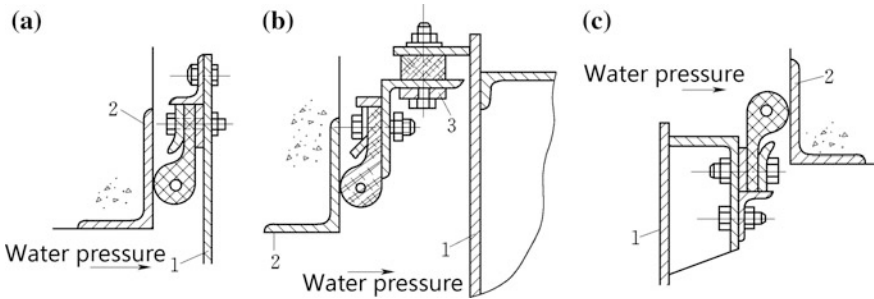


Fig. 15.16 Typical side seal layouts for submerged gates. 1 gate leaf; 2 seal cushion; 3 circular cushion

Figure 15.15 shows typical side seal layouts for crest gates, and Fig. 15.16 shows typical seal layouts for submerged gates.

15.3.3 Raising and Lowering Efforts and Hoists

1. Computation of hoisting force

Hydraulic down-pull or uplift is the net force exerting on a gate in vertically downward or upward direction under hydrodynamic condition (Sagar 1977a, b, c; Sagar and Tullis 1979).

(a) Lowering effort F_W

$$F_W = n_T(T_{zc} + T_{zs}) - n_G G + P_t \tag{15.1}$$

where n_T = revision coefficient with regard to the friction due to the reverse and side supports, and the inaccuracy in the calculation of frictional forces

($n_T = 1.2$); n_G = factor of under load against possible departure from the design weight of the gate ($n_G = 0.9-1.0$); T_{zc} = friction resistance of supports, kN; T_{zs} = friction resistance of seals, kN; G = gate weight of movable portion, kN; and P_t = uplift from bottom seal and bottom edge, the latter is related to the bottom shape of the gate, kN.

The negative result of F_W means the gate may be lowered down to shut the opening by its self weight. Where the calculated result is positive, pressure should be applied to help the closure of gate, i.e., the gate lowering needs assisting by down-pull which may be cared for by the use of a down-pull gear, a clamp beam, or a ballast to increase the weight of gate.

(b) Hoisting effort F_Q

$$F_Q = n_T(T_{zc} + T_{zs}) + P_X + n'_G G + G_j + W_s \quad (15.2)$$

where n'_G = factor of over-load against possible departure from the design weight of the gate ($n'_G = 1.0-1.1$); W_s = water column pressure on the top of the gate, kN; P_X = downward suction force due to ingress, which may be neglected for crest gate or submerged gate of open flow under good flow pattern and vented sufficiently, kN; and G_j = weight of ballast, kN.

2. Hoists

Hoists are the mechanical installations used for operating the gates, which are distinguished as mechanical hoists and hydraulic hoists.

Mechanical hoists fall into screw-operated type, rope-drum type (winch, chain-pulley block, monorail crane, gantry crane, etc.), and hydraulic cylinder type.

Screw-operated hoists are simple and reliable and able to provide both lowering effort and hoisting effort, but their capacities are smaller compared to the other types therefore applicable ordinarily for small gates.

Rope-drum hoists may be employed to spillway crests, outlets, and navigation locks. They are more preferable for gates that have deep submergence, where hydraulic cylinders above the deck is not allowed for, or when hoisting loads are too large and economics makes hydraulic cylinders impractical.

A hydraulic cylinder hoist system generally possesses two cylinders located at each side of the gate framework. The hoist cylinder normally consists of pump, reservoir, control, and piping. More recent applications use telescoping cylinders to accommodate deep submergence gates.

Where there is a fairly large number of gates and there are no requirements for simultaneous operation, instead of fixed hoists, movable hoists such as gantry cranes may be advisable.

15.4 Radial Gates

These are hinged gates, with the leaf (or skin) in the form of a circular arc whose center of curvature is at the hinge or trunnion. Radial gates have unique advantages over other gate types as follows:

- The radial shape provides efficient transfer of hydrostatic loads through the trunnion;
- A lower hoist capacity is demanded;
- They have a relatively fast operating speed; and
- Gate slots are not required, and favorable hydraulic conditions of discharge flowing are provided, by which problems associated with slot cavitation, and buildup of floating debris and ice, are avoided or alleviated.

The disadvantages brought about by the installation of radial gates are given as follows:

- To accommodate trunnions, the pier and foundation will likely be longer in the downstream direction than would be necessary for vertical gates;
- The hoisting arrangement may require taller piers, especially where the wire rope hoist system is employed. However, radial gates with hydraulic cylinder hoists generally demand lower piers than with wire rope hoists;
- Due to greater height of larger piers, seismic resistance will be lower;
- End frame members may encroach on water passage. This is more critical with inclined end frames; and
- Long strut arms are often demanded where flood levels are high, to allow for a clearance of the opened gate from the water surface.

15.4.1 Leaf Structure and Layout of Radial Gate

A radial gate has an upstream skin plate bent to an arc with its convex surface on the upstream side. The center of the arc is at the trunnion pins around which the gate rotates. The skin plate is supported by properly spaced stiffeners either horizontal or vertical or both. If horizontal stiffeners are adopted, they are supported by properly spaced vertical diaphragms which are connected together by horizontal girders (crossbars) transferring the load to the two vertical end diaphragms (end girders). The end diaphragms are supported by radial arms. If vertical stiffeners are adopted, they are supported by properly spaced horizontal girders (crossbars) which are supported by radial arms. The arms transmit the water load to the trunnions. Suitable seals are provided along the curved edges of the gate and along the bottom. If it is employed as a regulating gate in the tunnel or conduit, a horizontal seal fixed to the headroom structure seals the top edge of the gate in its closed position. Guide rollers are also necessitated to limit the swing of the gate during hoisting or lowering operation.

1. Layout of framework

The layout of crossbars gives rise to two basic types of framework for radial gates, which is mainly dependent on the ratio of width to height of the gate.

For wide gates with large ratio of width to height, horizontal girder framework is commonly employed. Structurally, the skin plate acts compositely with the ribs to form the skin plate assembly, which is, in turn, supported by the horizontal crossbars (girders) that span the gate width. The horizontal girders are supported by the end frames, which consist of radial struts or strut arms and bracing members that converge at the trunnions which are anchored to the piers. Structural bracing members (e.g., horizontal girder lateral bracing, downstream vertical truss, end frame bracing, and trunnion tie) are incorporated to resist specific loads and/or to brace compression members.

Where the horizontal girder framework is employed, three types of arms arrangements may be adopted: permitted by the support condition, the type shown in Fig. 15.17a is desirable; if the support is on the sidewalls, the type in Fig. 15.17b may be applied; and the type in Fig. 15.17c is applicable if the vent clearance is not sufficient.

Types in Fig. 15.17a, b are advantageous to reduce the bending moment at the middle portion of girders, which in turn reduce the amount of steel consumption. However, the type in Fig. 15.17a requires definite structure condition, and the type of Fig. 15.17b complicated the structure of trunnion. The type in Fig. 15.17c is advantages in simple structure and in convenient installation and manufacturing, but has higher steel consumption.

For tall gates with small ratio of width to height, vertical girders have to be used to simplify the end frame configuration. Curved vertical girders (crossbars) are employed to support several horizontal girders. Each vertical girder is supported by the corresponding end frame that may include two or more struts (Fig. 15.18).

2. Location of trunnion

Although it is sometimes practical to allow for submergence in the events of flood, especially on navigation dams, yet it is normally desirable to locate the trunnion above the maximum water surface, to prevent it from contacting with floating ice and debris, and to avoid the submergence of the operating parts. Trunnion is generally located on the position of $(1/2-3/4)H$, $(2/3-1)H$, and $1.1H$, above sill

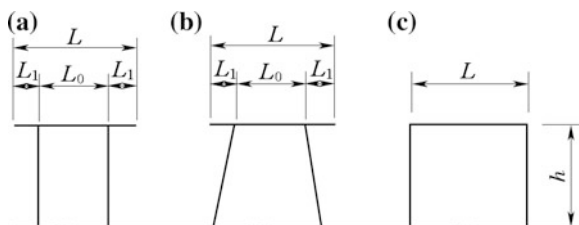


Fig. 15.17 Horizontal girders framework—arrangement of arms (plan)

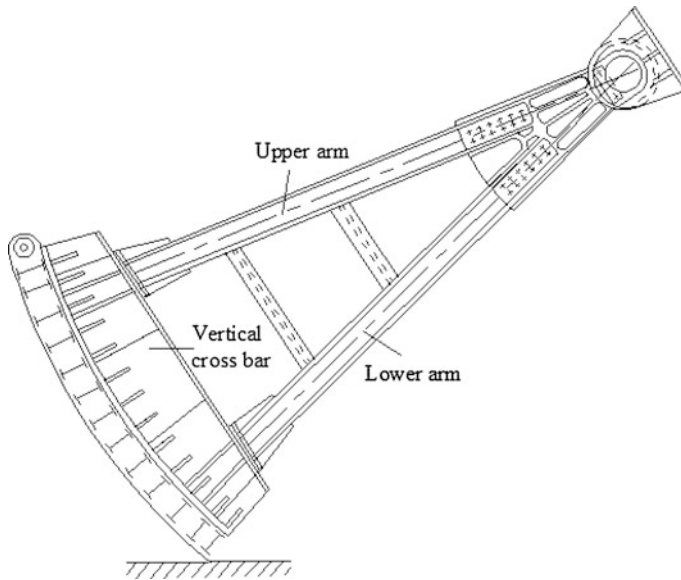


Fig. 15.18 Vertical girder framework—arrangement of arms (elevations)

(H = height of gate), for the crest gates of spillway, the crest gates of barrage, and the submerged deep gates, respectively.

If other considerations do not control, it will be desirable to so locate the trunnion as the maximum reaction is approximately horizontal. This will allow for simplified design and construction, where the trunnion post-tensioned anchorage may be placed in horizontal layers.

3. Seals

The standard side seals provide increased sealing force in proportion to the increased head, and seals usually tend to leak under low heads rather than high heads. Therefore, the J-type or L-type side seal arrangement is demanded for crest radial gates (Fig. 15.19). The seals may have a hollow bulb to increase flexibility under low-head applications. The seals are available with the rubbing surface coated with fluorocarbon (Teflon) to reduce friction. The seal attachment plate must have slotted bolt holes to allow for field adjustment of the seals. Bottom seal is laid by direct contact between the skin plate edge and the sill plate. The lip of the radial gate should form a sharp edge, and the downstream side of the lip should be perpendicular to the sill. It is not recommended to use rubber seals on the gate bottom unless normal leakage cannot be tolerated. If the leakage is critical, a narrow rubber bar seal attached rigidly to the back side of the gate lip should be installed.

For submerged radial gate, top seals should be installed on the upstream of skin plate (Fig. 15.20). Since the side seals of submerged gate cannot be located on the upstream, therefore the J-type of square head rubber may be employed as side seals to obtain their good connection with the top seal (Fig. 15.19c).

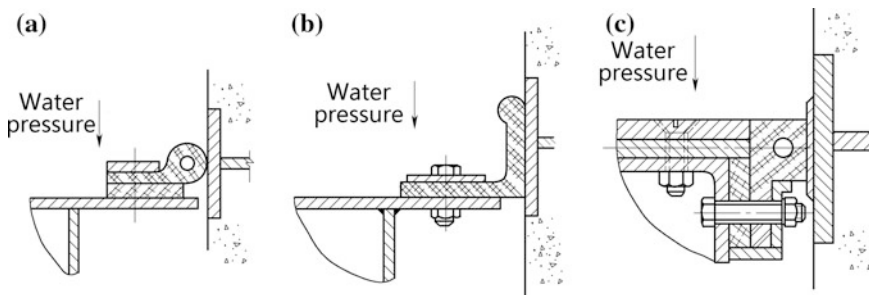


Fig. 15.19 Side seals of crest radial gate

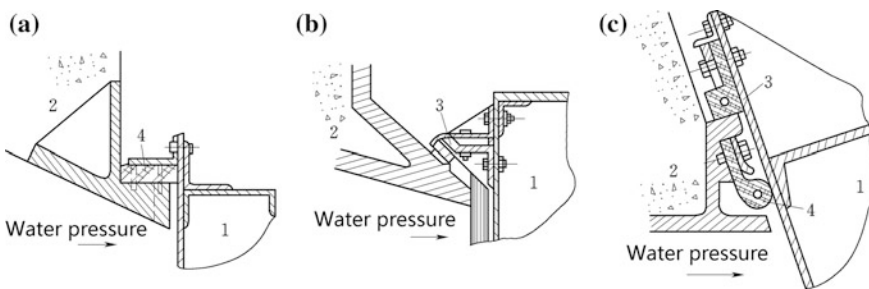


Fig. 15.20 Side seals of submerged radial gate. 1 gate leaf; 2 parapet wall; 3 seals for gate leaf; 4 seals for parapet

15.4.2 Raising and Lowering Efforts and Hoists

1. Computation of hoisting force

(a) Lowering effort F_W

$$F_W = \frac{1}{R_1} [1.2(T_{zd}r_0 + T_{zs}r_1) + P_l r_3 - 0.9Gr_2] \quad (15.3)$$

where T_{zd} = rotation resistance of trunnion hinges, kN; r_0 = radius of T_{zd} , m; T_{zs} = friction resistance of seals, kN; r_1 = radius of T_{zs} with respect to the rotation center of the gate, m; G_2 = gate weight of movable portion, kN; r_2 = radius of G_2 with respect to the rotation center of the gate, m; P_l = percolation force on lower seal, kN; r_3 = radius of P_l with respect to the rotation center of the gate, m; and R_1 = radius of lowering effort F_W with respect to the rotation center of the gate, m.

Where the calculated effort F_W is positive, gate lowering operation needs assisting.

(b) Hoisting effort F_Q

To raise a radial gate turning about its axis, it is necessary to apply a moment to overcome the moments of self weight and friction attributable to seals and support hinges. This condition can be expressed as

$$F_Q = \frac{1}{R_2} [1.2(T_{zd}r_0 + T_{zs}r_1) + P_t r_3 + 1.1Gr_2 + P_X r_4] \quad (15.4)$$

where P_X = downward suction force due to ingress, kN; r_4 = radius of P_X force with respect to the rotation center of the gate, m; and R_2 = radius of hoist effort F_Q with respect to the rotation center of the gate, m.

2. Hoists

Close coordination with mechanical engineer is necessitated to optimize the hoisting system. Rope-drum type (winch, chain-pulley block, monorail crane, gantry crane, etc.) may only be employed for the gate whose lowering operation does not need assisting, otherwise screw-operated type or hydraulic cylinder hoists are demanded. Many new gate designs utilize hydraulic cylinder hoist system, which generally possesses two cylinders located at each side of the gate. Each cylinder pivots on a trunnion mounted on the adjacent pier, and the piston rod is attached to the gate. The force magnitude and orientation of the cylinder will change continually throughout the range of motion. In determining the optimum cylinder position, the location of the cylinder trunnion and piston rod connection to the gate are closely related. Generally, the piston rod connection position is selected first, and then, the cylinder trunnion position is determined to minimize effects of lifting forces. For preliminary design, it is often assumed that the cylinder will be at a 45° inclination angle when the gate is closed, although optimization studies may indicate a slight adjustment. Generally, the most suitable location for the piston rod connection is on the gate end frame at or near the intersection of a bracing member and strut. It is preferable to have the piston rod connection above tail water elevations, but partial submergence may be acceptable for navigation structures.

15.5 Deep Gates**15.5.1 General**

Deep gates are commonly installed at the intake or exit of tunnel, the orifice in concrete dam, and the lock culvert. Covering a similar sectional area, they are exposed to heavier loads and operated in flows of high velocities.

1. Classification of deep gates

There are different classifications depending on the criteria based.

According to the head exerted, deep gates may be classified into low (below 25 m), medium (25–50 m), high (50–80 m), and particular high-pressure (above 80 m) gates.

According to the installation position, deep gates may be distinguished as intake gate, middle position gate, and exit gate, of spillways.

According to the flow pattern after the gates, deep gates fall into those of pressure flow behind and of free flow behind.

According to the structure, deep gates may be in the form of plate and radial.

2. Hydraulic features of deep gates

With the orifice partially opened, the velocities below and downstream the gate may reach 40 m³/s or even higher. Any alteration in the flow boundary induced by gate or walls of the conduit (e.g., gate slots) will bring about an abrupt change of pressure and the formation of eddies. These would give rise to pressure pulsation and oscillation exerted on the gate, and result in localized pressure drop immediately downstream, which may induce cavitation damage to the gate slots, gate leaf, embedded facilities, rod of hoist, etc., if the pressure drop is strong enough. Therefore, requirements for high-pressure gates on the manufacture workmanship and accuracy of assembly in situ are more rigorous than that for crest gates. This is especially significant for projects that operate at high heads with small gate openings, which should be carefully studied in the design of the slot position and shape, the concrete lining surrounding the gate chamber, and the gate itself as well.

15.5.2 Deep Plate Gates

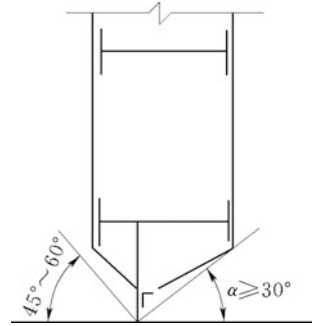
Since it requires larger hoisting capacity, deep plate gate is conventionally employed as medium—to small gate in medium to lower head projects—and often plays the role of bulkhead gate which only operated in still water.

Similar to crest gates, deep plate gates ordinarily adopt a horizontal framing system, for higher structurally efficient and easier to accommodate roller guides.

Deep plate gates may be framed with plate girders as has been described in crest and navigation lock gates. The main difference in framing is that the former requires a inclined bottom or flat bottom with lip extension on the downstream side, to reduce down-pull forces while operating with water flowing (Fig. 15.21).

Hoisting effort greatly depends on the position of the sealing contour. If the sealing contour is arranged in the upstream plane, the vertical force components of atmospheric pressure exerting on the gate are in fact balanced. Whereas if the sealing contour is arranged in the downstream plane which is the common case, the gate is exposed, from top, to a downward force of the water thrust created in the shaft, and from bottom, to a vertical force of a water load whose direction depends on the extent of gate opening. Cautions should be exercised that a check should be made with the seal manufacturer before using a seal for a particular application. To allow for the seal to move toward the seal plate, the stem should be compressed only on the

Fig. 15.21 Bottom edge of a deep plate gate



outer edge by the clamp bars. Observations of rubber seals indicate that the rubber could become extruded into the space between the clamp bar and the seal plate. To prevent this, brass-clad, or more recently fluorocarbon-clad with lower coefficient of friction (0.1) and greater flexibility and resiliency, may be employed. The lower coefficient of friction reduces the capacity of hoisting equipment. The bottom rubber seal is normally wedge-shaped that relies on the weight of the gate to provide the seal compression.

The majority of deep plate gates use slide support, which is advantageous in the reduction of cavitation and vibration. The wheeled versus slide gates need a smaller hoisting effort and are widely exercised in emergency-guard gates. The disadvantage of this type lies in the difficulty associated with protecting the wheel bosses and roller bearings against trash and liming. Where the principle hydrostatic load is considerably high, it is hardly possible to arrange wheels in numbers required by strength consideration. In this case, wheels are replaced by rollers joined by either a frame (roller supports) or a crawler belt (caterpillar supports). Control of gates with roller and caterpillar types of support demands smaller hoist efforts than with other types of support.

15.5.3 Deep Radial Gates

Radial gates are normally used as service (main) gates of large open size under high head. Their major advantage over plate gates lies in that they need considerably smaller hoisting capacities. In addition to a good flow boundary attributable to its arc gate skin, this type of gates does not necessarily need slots (grooves) and possesses support members protected against the direct actions of water and siltation. High structural stiffness reduces the vibration intensity of gate under the action of pulsating loads. The disadvantage of radial gate is a complicated design of supports whose cost is higher.

The curvature radius of deep radial gate skin is larger than that of crest one, whose proportion to the gate height may be the upper bound stipulated in the design codes, for reducing hoisting capacities and adapting the flow pattern. The

framework and arms of a radial deep gate is in the form of a conventional two-cantilever portal, as shown in Fig. 15.17a. Where the pressure is high, more than two arms on each side may be installed, and they are welded and box-shaped in cross-section by bracings and ties between arms. Frameworks of either horizontal girders or vertical girders may be adopted depending on the shape of the conduit, and the latter is preferable for square or tall and narrow conduits.

Effective closing orifice of deep gate may be accomplished by reverse radial gate hinged on the upstream side. Such a gate, if incorporated at the end of a conduit, has its arms and hinges located outside, a feature which improves gate operational conditions. This type is widely applied in the ship lock culverts. By placing the trunnions upstream and with the convex surface of the skin plate facing downstream and by sealing against the downstream end of the valve well, air may be prevented from entering the culvert at the gate recess.

Sealing of high-pressure gates should be well guaranteed that:

- No leakage will manifest when the conduit is shut down;
- No contacts of sealing—slot member at the time of raising, with a view to reduce frictional force and, consequently, hoisting and lowering efforts;
- Protection of sealing elements against the actions of flow at the partial opening of gate.

Due to high pressure, the friction force attributable to rotation resistance of trunnion hinges and seals is considerably large. The gate is ordinarily cannot be lowered down only by its self weight, and an additional lowering force shall be exerted. Hydraulic cylinder hoists therefore are commonly equipped for the operation of deep radial gates. Mechanical hoists of screw-operated type, where the hoisting capacity is permitted small, also may be applied.

References

- Buzzell DA (1958) Trends in hydraulic gate design. *Trans ASCE* 123(1):40–42
- Cai ZK, Qu ER (1988) Gate and operation, 2nd edn. Water Resources and Electric Power Press, Beijing (in Chinese)
- Chen SH, Chen ML (2014) Hydraulic structures, 2nd edn. China WaterPower Press, Beijing (in Chinese)
- Erbisti PCF (2004) Design of hydraulic gates. AA Bulkema, Lisse
- Fan CR (2000) Design of steel structures in hydraulic engineering. China WaterPower Press, Beijing (in Chinese)
- Grishin MM (ed) (1982) Hydraulic structures. Mir Publishers, Moscow
- Lewin J (1995) Hydraulic gates and valves in free surface flow and submerged outlets. Thomas Telford Publications, London
- Mayer PR, Bowman JR (1969) Spillway crest gates. In: Davis CV, Sorenson KE (eds) Handbook of applied hydraulics (Sect. 21), 3rd edn. McGraw-Hill, New York
- Ministry of Construction of the People's Republic of China. GB 50017-2003 (2006) Code for design of steel structures. China Architecture & Building Press, Beijing (in Chinese)

- Ministry of Water Resources of the People's Republic of China. SL74-95 (1995) Hydraulic and hydroelectric engineering specification for design of steel gate. China WaterPower Press, Beijing (in Chinese)
- Ministry of Water Resources of the People's Republic of China, Electric Power Industry Ministry of the People's Republic of China. DL/T5039-95 (1995) Specification for design of steel gate in hydraulic and hydroelectric engineering. China Electric Power Press, Beijing
- Sagar BTA (1977a) Downpull in high-head gate installations (Part I). *Int J Water Power Dam Constr* 29(3):38-39
- Sagar BTA (1977b) Downpull in high-head gate installations (Part II). *Int J Water Power Dam Constr* 29(4):52-55
- Sagar BTA (1977c) Downpull in high-head gate installations (Part III). *Int J Water Power Dam Constr* 29(5):29-35
- Sagar BTA, Tullis JP (1979) Downpull on vertical lift gates. *Int J Water Power Dam Constr* 31 (12):35-41
- Zuo DQ, Gu ZX, Wang WX (eds) (1987) Barrages, spillways and control works. Handbook of hydraulic structure design, vol 6. Water Resources and Electric Power Press, Beijing (in Chinese)

Chapter 16

Irrigation and Drainage Works

16.1 General

Irrigation and drainage engineering measures are required to control damage from draught, water logging, saline, and alkali, which are accomplished by construction corresponding works of water diversion and distribution. These works are customarily termed as “hydraulic structures in irrigation and drainage engineering,” or abbreviated as “irrigation and drainage works” (Chen and Chen 2014; Iqbal 1993; Novak et al. 1990).

There are various irrigation and drainage works, including water intakes from water sources, canals for water conveyance, regulating sluices for water-level controlling, diversion sluices and check gates (delivery gates) for discharge controlling, flumes and weirs for discharge measuring, protection works such as release sluices (escape sluices) and over-chutes for the normal and safe operating of canals, cross-drainage works (e.g., aqueducts, bridges, inverted siphons, and culverts) for conveying water across a natural depression or under a road and canal, and drop structures (chutes and drops) for conveying water from a higher elevation to a lower elevation and to dissipate excess energy resulting from the drops. In addition, special structures, such as dams, pumping stations, and navigation locks, also may be integrated in an irrigation and drainage engineering system (Aisenbrey et al. 1974; Economic and Social Commission for Asia and the Pacific, United Nations Office of Technical Co-operation 1973; USBR 1978; Varshney et al. 1979; Zuo et al. 1984). Some of the aforementioned structures have been introduced in the previous chapters of this book, and in this chapter, the interesting is directed merely to several typical irrigation and drainage works such as intakes, aqueducts, inverted siphons and culverts, and water measuring flumes.

Irrigation and drainage works in hydraulic projects have a large category with considerable differences: Some have small quantities but demand large unit investment; some need small unit investment but have large number and total investment. Therefore, it is important to select allowable design criteria based on

the rational classification of irrigation and drainage projects and canal systems. In the selection of irrigation and drainage project grade, the GB50288-99 “code for design of irrigation and drainage engineering” (Ministry of Water Resources of the People’s Republic of China 1999) shall be observed.

16.2 Water Intake Works

16.2.1 *Types and Features of Water Intake Works and Their Positions*

1. Functions and types of water intake works

Hydraulic projects designed to draw water from a water body or stream for consumptive uses, i.e., hydropower generation, irrigation, water supply for domestic comfort, and industrial purpose, are known as water intake works or intakes. The water intake works at near the entrance of canal is also named as diversion or headworks (Song 1989), and they are intended to provide a nonstop water delivery of proper quality in specified amount according to a water consumption planning and allowing no bed loads or suspended debris into the off-take structures (e.g., channel and pipelines). River training would be necessary to ensure the intake be located near the mainstream and to secure the stability of river.

2. Circulating flow in river bend

Natural river bends can be distinguished as forced (deformed), limited (entrenched), and free associated with the ratio of the curvature radius to the width ranging from about 3 (forced) to about 7.5 (limited), while 5 is for free bends. In free and limited bends, the depth gradually increases to a maximum downstream of the bend apex (Brandon 1987).

River bends are featured by spiral flow and triangular sections, with the maximum depth and velocity at the concave bank, and with the maximum sediment transportation at the convex bank, as well as talweg deviating from the river centerline, this phenomenon is attributable to spiral flow.

Water flowing through a river bend must follow curved streamlines for remaining within the banks of the river. The primary flow around the bend is vortex flow—the fastest velocity where the curvature radius is the smallest and the slowest velocity where the radius is the largest. The higher pressure near the concave bank is accompanied by slower water velocity, the lower pressure near the convex bank is accompanied by faster water velocity, and all this is consistent with Bernoulli’s principle. As a result, at any cross section within the river, the water pressure is slightly higher near the concave bank than near the convex bank as shown in the water column *db* (Fig. 16.1b), creating a pressure gradient from the concave bank toward the convex bank. Along a curved path, centripetal forces are demanded for each parcel of water to balance the pressure gradient, which are proportion to the square of velocity; therefore, they are larger on the surface and smaller at bottom

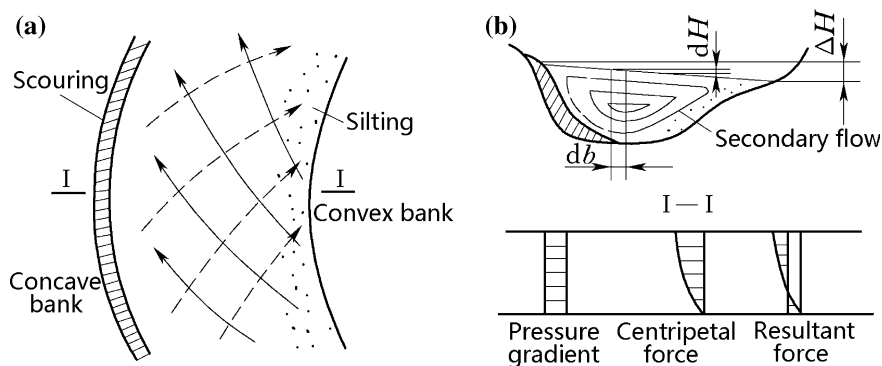


Fig. 16.1 Schematic of circulating flow in a river bend. **a** Plan; **b** horizontal force of water column

(Fig. 16.1b). As a result, there is a secondary flow near the floor of the riverbed across the stream from the concave bank toward the convex bank, which is driven by the unbalanced pressure gradient. Near the convex bank, this secondary flow moves up toward the water surface where it mixes with the primary flow back toward the concave bank. This motion is called circulating flow. The primary flow along the river bend and the secondary circulating flow around the river section form spiral flow.

On the floor of the riverbed, the secondary flow sweeps sand, silt, and gravel across the river and deposits them near the convex bank. This is why river bends often possess a convex bank which is shallow and made up of sand, silt, and gravel and a concave bank which is steep and heavily eroded. This process can lead to the formation of a meander or a point bar or, eventually, an oxbow lake (Brandt 2000; Garcia 2008; Ma and Zhou 2001; Morris and Fan 1998; Morris and Wiggert 1972; Petersen 1986).

Natural river bends can be employed as a silt excluding device by locating the barrage on the bend and the canal regulator on concave bank. The heavy bed load is swept toward the convex bank, and in this way, the sediment concentration on the concave bank is lower.

3. Features of water intake works

The water intake works from a natural river may be conventionally classified according to the presence or absence of dam as undammed and dammed (with barrage).

(a) Undammed intakes

Undammed intakes can be further distinguished as the surface type and submerged type. The former would take-off water by free flowing from surface layers of a river, whereas the latter from a certain depth by a closed conduit. Any large amount off-taking from a river disturbs its hydrological regime. The changes of water level, flow velocities, and sedimentation, in turn, influence the off-taking. An

example is the Dongfeng Canal, Henan Province, China, where serious silting due to the Yellow River swing finally blocked the headworks. In the designing of an intake, care should be exercised over the provision of the entry of bed loads and floating debris into the canal, to ensure the delivery of water according to the water consumption chart regardless any changes in the water level or possible riverbed deformation. Therefore, for headworks located at unstable river section, the river training works are customarily installed.

Lateral intake in straight river section will give rise to strong flow bending in front of the headwork, which in turn results in strong lateral secondary flow. As a result, a large quantity of bed loads may enter the canal following the bottom flow. Where the diversion ratio (proportion of the take-off to the river runoff) reaches 50 %, the bed loads almost all enter the canal. According to the rules of river training, special countermeasures for keeping off the bed loads are always demanded whenever more than 50 % of the water is diverted from the river.

(b) Dammed (barrage) intakes

A water intake system with dam comprises a dam or barrage, an upstream and a downstream regulator, control works, and sediment excluders or ejectors. In some instances, desilting basin to control primarily suspended loads and partly bed loads, and trash removal devices, is provided.

In silt-laden river, dams may lose their capacity due to siltation processes. Without any mitigating measures, the long-term viability of reservoir and water diversion is questionable, as the impacts and losses are not balanced by the profits. The modification of flow and sediment regime by a dam also has important influence on downstream reach: In the initial stage of operation, the released flow is clear and has large capacity of scouring; however, after a period when the reservoir is unviable, the silt loads are increased again, which lead to the resiltting of downstream stream, and in very serious case, this resiltting may bury the whole dam within. In the design of project, this procedure should be studied and corresponding countermeasures should be taken.

Instead of dams, barrages are advantageous because it does not change natural river stream significantly. By both the ability of water retaining and silt flushing through under sluices and flushing sluices, barrages possess better adaptability for desilting and regulating of water level. The proper operation of gates also may adjust the direction of main stream, to secure the head regulator being under good diversion condition. However, barrages demand higher expenditure and are complicated in management.

Rubber dams are more and more prevalent for medium and small headworks.

4. Location of water intake works

With the discharge, each river entrains solid matter in the form of suspended loads or as bed loads. The location of an intake structure must be so positioned that the largest possible portion of the bed loads remains in the river and does not enter into the diversion canal following the diverted water. However, a satisfactory arrangement of intake structure does not remove the suspended loads—actually this

is the task of a sand trap arranged downstream the canal. In the selection of headworks, the geological condition of banks, flood characteristics, silt content, and riverbed evolution (river morphological change) are to be considered, and the following requirements are to be met:

- The altitude of headworks should meet the requirements for gravity irrigation, water convey, and non-silting;
- If at all possible, intakes should be arranged on the concave bank of river bend, in order to be able to profit from circulating flow;
- If the intakes are arranged on a straight river segment, they should be located at the section with stable banks and near to stable main river stream with higher water level and velocities. In order to prevent bed loads from being transported into the canal, the river flow in front of the intake structures must be deflected;
- Wandering reach should be shunned, for provision headworks from blocking due to the river swinging;
- Branch afflux is avoided, for provision its influence on the water diversion and sand excluding;
- The dam or barrage should be located at the river section of well shaped, with its axis be perpendicular to the river, and a smooth flow through the dam or barrage is provided;
- Competent geologic conditions are desired; and
- Appropriate construction site is required for the construction, management, transportation, etc.

16.2.2 Layout of Undammed Intakes

An undammed intake comprises water intake sluice, silt flushing sluice, sedimentation basin, and river training works. Undammed intakes may be of single-headed or multi-headed.

Undammed intakes are widely exercised in China attributable to their simpler structure, lower cost, smaller detrimental effect on the natural river and less contradiction with other economic departments related to navigation, wood drifting, and fishing industry.

In most cases, lateral intake without damming is applicable only for the diverting of small amount of water. The discharge into the intake structure which is arranged laterally is directly related to the water level in the river. Dependent on the minimum regime of the river, the diverted inflow is thus limited.

In many cases, it is nevertheless advantageous to dispense without damming in order to avoid an encroachment on the discharge where insufficient knowledge is available of the hydrological phenomena, to avoid generating detrimental back-water to the upstream reach and having to construct expensive jetties.

The disadvantages of leaving the river undammed may be compensated by engineering measures, such as the water may be fed into the intake area with the aid of repelling groin (diversion dyke).

The optimization of the position and the angle of off-taking are very important to control sediment from entering into the canal. The angle of off-taking α is defined as the included angle of the off-taking direction and main stream direction (Fig. 16.2). According to the principle of circulating flow, the position of undammed intake must be laid on the concave bank behind the apex of the bend, where the water level is relatively high, the flow velocity is relatively large, and the bed load content is relatively low.

An off-taking at 90° is the least desirable one, whereas an off-taking angle of around $30^\circ\text{--}45^\circ$ is ordinarily recommended. Based on the experience from the Yellow River basin for irrigation, if the off-taking angle is selected between 40° and 50° , the amount of sediment entering into the canal might be largely reduced.

1. Single-headed water intake

Single-headed water intake must always be situated on the concave bank (Fig. 16.2). The intake is normally composed of sand guide sill, approach channel, water intake sluice, and silt excluder. The most favorable site for the intake structure is somewhat downstream of the apex of the bend where the spiral flow is strongest, by which the most of bed loads may be transported toward the convex bank. The circumference distance L from the intake to the starting of the bend along the axis of river is related to the curvature radius R of the bended river axis and the width b of the river bend (Fig. 16.3), which may be estimated by Eq. (16.1)

$$L = 2ks = kb\sqrt{4\frac{R}{b} + 1} \tag{16.1}$$

where s = normal distance from the starting sectional center to the concave bank, m ; k = experimental coefficient ranged within $0.5\text{--}1.0$ (usually $k = 0.8$).

In front of intake sluice (head regulator), it is customarily installed with sand guide sill in a shape of “T” or trapezoid. The sill top is usually $0.5\text{--}1.0$ m higher than the canal sill. Sand guide sill may enlarge surface water diversion and reduce

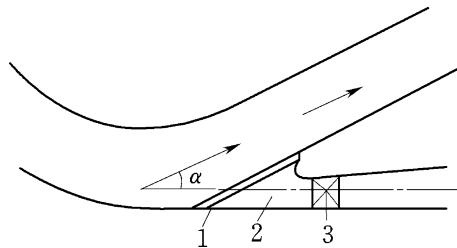
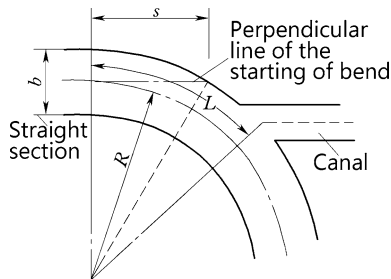


Fig. 16.2 Layout of single-headed water intake. 1 sand guide sill; 2 approach channel; 3 water intake sluice

Fig. 16.3 Positioning of water intake



bottom flow passage; in this way, the bed loads are largely prevented from entering the canal. The sill of intake floor is normally identical to or a bit of higher than that of the canal. Settling basin is a device placed on the canal downstream of its head regulator, for the purpose of removing sediment loads which cannot be trapped by the conventional excluders or ejectors. It consists of an enlarged section of the channel on the canal bed. The settled sediment is removed by flushing or dredging.

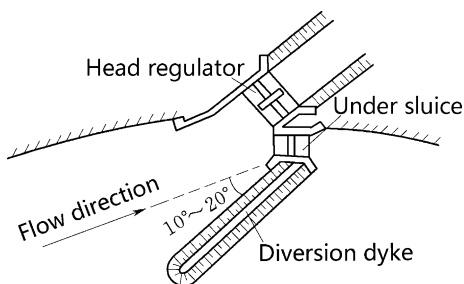
In unstable mountain torrents, apart from intake sluice, diversion dike as well as release and flushing sluice is usually installed. The diversion dike extended from the head regulator to the upstream direction until it is near the main stream. The axis of diversion dike forms an included angle of 10° – 20° with the mainstream (Fig. 16.4).

Where the river bank stability against flow scouring is not secured, approach channel may be installed in front of head regulator (Fig. 16.5).

2. Multi-headed water intake

In unstable and silt-laden river, single-headed water intake is easy to be blocked giving rise to insufficient off-taking in canal. Multi-headed water intake may improve the situation under such circumstances, by installing 2–3 approach channels spaced at 1–2 km or even 3–4 km apart. The intakes are installed for each channel, or just one intake at the junction of channels (Fig. 16.6). In dry season, the channels work together to ensure the diversion discharge; in flood season, only one channel works, while the others are desilting. This type is disadvantageous because it is easy to weed if inoperative for long time and demands high maintenance cost due to large amount of desilting.

Fig. 16.4 Intake with diversion dyke



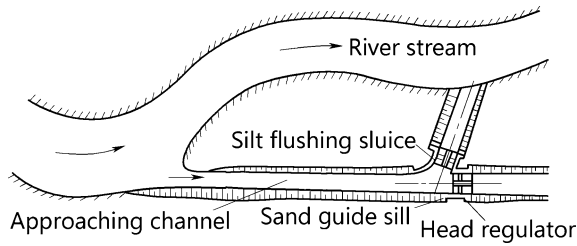
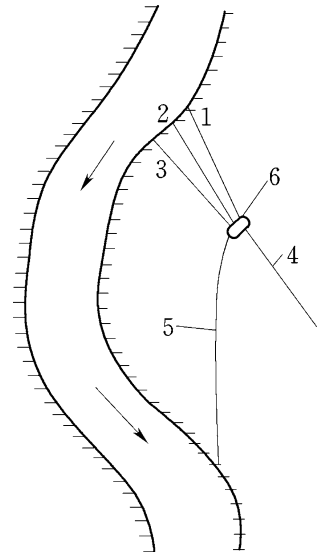


Fig. 16.5 Layout of a headwork with approach channel

Fig. 16.6 Schematic of multi-headed water intake. 1, 2, 3 approach channels; 4 main canal; 5 escape and flushing channel; 6 water intake sluice



16.2.3 Layout of Lateral Intakes with Water Damming by Barrage

Lateral intake with water damming usually comprises barrage or dam, head regulator, and silt prevention structures. Barrage/dam is intended to control the river level and to ensure the diversion discharge for canal. In the projects with requirements for the other departments (e.g., navigation, hydropower generation, log transportation, and fishery), ship lock, hydropower station, raft sluice, and fish ways are installed.

In sediment-laden river, featured by silt excluder and flushing sluice, headwork layouts are patternized into the intake with under sluice pocket, the intake with artificial bend, the bottom grating intake, the two-storeyed intake, etc.

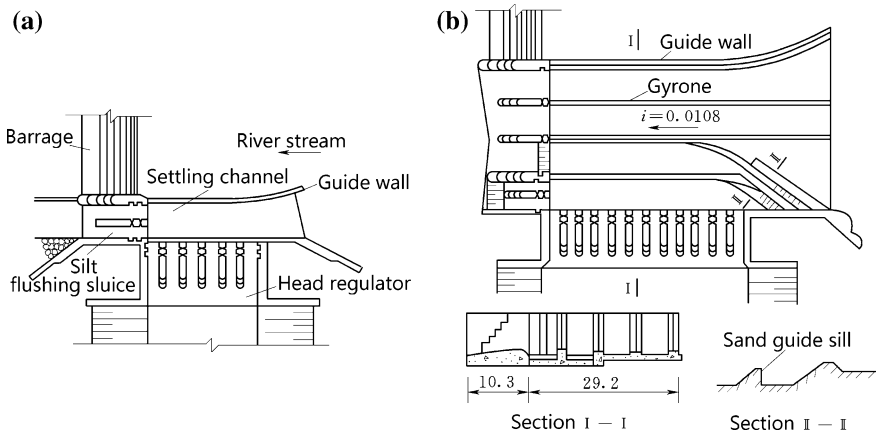


Fig. 16.7 An intake with under sluice pocket (*unit: m*)

1. Intake with under sluice pocket

An intake with under sluice pocket is composed of barrage/dam, flushing sluice, desilting channel, guide wall and off-taking sluice (head regulator), whose design principle is off-taking at lateral and silt excluding in front (Fig. 16.7). It is also termed as “Indian headwork” attributable to its origin from India where rivers in her northern and eastern territory are originated from the Himalayas—geologically quite young mountains, which flow quite fast in the upper reaches and carry with them heavy sediment loads due to the comparatively soft hill formations. In the lower reach plains, their velocities are reduced following the sudden changes of riverbed slope, and as a result, the sediment loads get deposited.

With an Indian headwork, sediment excluding device is provided as a part of the under sluice bays of the barrage floor in the river pocket adjacent to the head regulator, to minimize sediment entry into the canal. Generally, gravels and boulders are excluded by keeping the crest of spillway bays low, while the suspended loads and bed loads are removed through special silt excluding structures.

The intake structure is accomplished with the help of divide wall which creates a quite zone (referred to as pocket) in front of the canal. The angle of off-taking was used to be 90° , but nowadays, it is normally 30° – 60° , for reducing the secondary flow and sediment entry into canal. The pocket performs like a pond area of low velocity which allows much of the sediment to get deposited instead of entry into the canal. The sediment deposited is flushed through the sediment excluders which are a series of tunnels made of reinforced concrete at the riverbed level laid in front of the head regulator and ending at the under sluice bays. There are, generally, two common types of layout for sediment excluders. The first one possesses staggered tunnel mouths and is sometimes called the “Khanki type,” the name is derived from the first project built by Nicholson for the Lower Chenab Canal at the Khanki headworks. The other type of excluder arranges all the tunnel mouths along an

angled line in plan, which is called the “Kalabagh type” or “Trimmu type,” due to the first application at Trimmu on the Heveli Canal headworks. The tunnel mouths of the Khanki type being staggered may be extended to any length, each being independent of the other. Hence, this type of excluder possesses a greater flexibility in tunnel arrangement, but is more complicated to construct, as compared to the Kalabagh type. The Kalabagh type of excluders is more sensitive to the river approach conditions, and their performance may be deteriorated if the river morphology keeps changing with time.

The elevation of the bottom floor of intake sluice (head regulator) should be 1.0–2.0 m higher than that of the pocket. There is guide wall between the flushing sluice and barrage, which entails pocket together with the wing wall of the head regulator.

In mountainous regions, large-sized boulders may roll down the rivers. To remove them away from the head regulator, a structure in the form of a sediment excluder without the top slab called sediment deflector has to be provided. The crest level of head regulator should be higher than the top of the deflector by at least 0.5–1 m so as to prevent the entry of coarse silt into the head regulator.

Intake with under sluice pocket is advantageous attributable to its simplicity in construction and low in expenditure. It is widely employed in the northwestern China. The main disadvantages experienced from the Chinese practices are as follows:

- Since the axes of the head regulator and the river form a right included angle, the diverted flow turning an angle of 90° into canal induces secondary flow near the inlet and carries a part of silt into canal;
- To operate the flushing sluice, the head regulator should be shut down to prevent the silt from entering into the canal; and
- The reservoir formed by barrage is vulnerable to silting.

2. Intake with artificial bend

Intake with artificial bend uses principle of circulating flow in river bend to off-take clear water and to flush the silt laterally. The intake is located at a natural bending river segment after the river training into a regular bend, which comprises artificial bend, head regulator, flushing sluice, escape sluice, and downstream silt release chute (Fig. 16.8). Intakes with artificial bend are originated from the Fergana district in Uzbekistan; therefore, they are also termed as “Fergana headworks.” They entered Xinjiang Uygur Autonomous Regions of China in 1950s and are prevalent in this district so far.

The head regulator is located at the concave side and layout along the axial direction of the bend to form front diversion flow. The bottom level is 1.0–1.5 m higher than that of flushing sluice. In front of the head regulator, a sand guide sill of cantilever type is installed. Flushing sluice is located at the convex bank whose flow forms an included angle of 36° – 45° with the flow of head regulator. The escape sluice is normally located at the entrance of the bend, whose central axis forms an

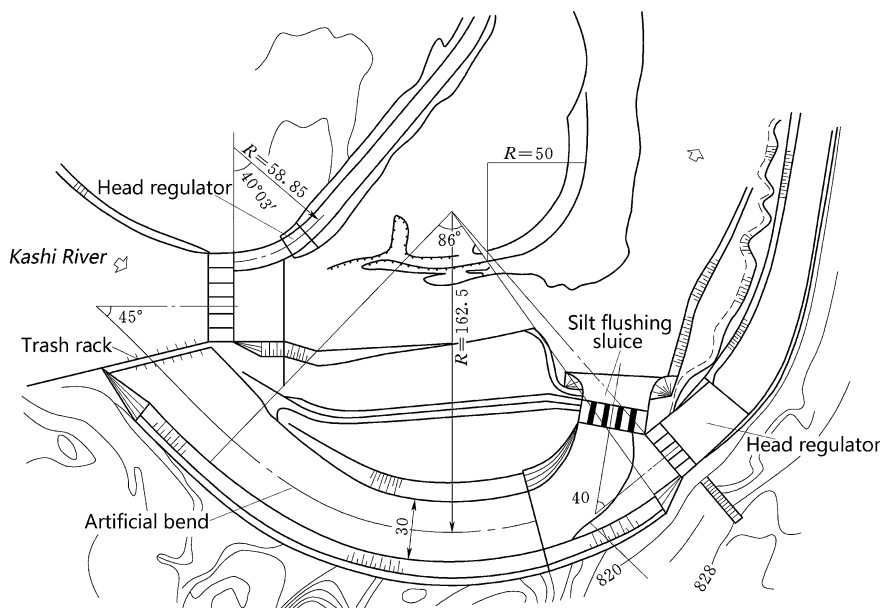


Fig. 16.8 Intake with artificial bend at the Kashi River, Xinjiang Uygur Autonomous Regions, China (unit: m)

included angle of 40° – 45° with the central line of the bend. The level of escape sluice bottom floor is 1.0–1.5 m lower than that of the bend entrance and beneficial for flood releasing and silt flushing.

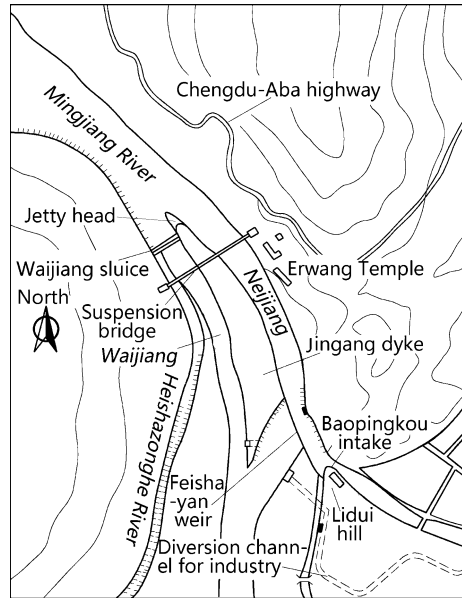
The key issue in the design of intake with artificial bend is how to ensure sufficiently strong circulating flow during flood season. In recent 30 years, this issue has been well studied and handled. Intake with artificial bend at the Kashi River, Xinjiang Uygur Autonomous Regions, China (Fig. 16.8), is an successful example. The world famous water diversion project of the Dujiangyan, Sichuan Province, China, also makes use of artificial bend principle (Fig. 16.9).

Intake with artificial bend is disadvantageous in large engineering amount, decentralized layout of the project, and inconvenient management. This type of headworks is suitable for large-to-medium projects in mountainous area with natural river bend, where the bed loads are high with large grain variation.

3. Bottom trash rack intake

Water intakes in mountainous rapids are vulnerable and expensive structural elements in river-fed canal systems. They are easily damaged by floods and suffered from the buildup of sediment or rubbish in the water. Bottom grating (trash rack) intake provides a more reliable and cheaper alternative, which is an inlet structure in which water is abstracted from the mainstream through the screen over a gutter. The gutter is usually made of concrete and built into the riverbed. The bars of the screen

Fig. 16.9 Water diversion project of the Dujiangyan, Sichuan Province, China



are laid in the direction of the current and inclined at an angle of 15° – 30° in the downstream direction, so that coarse bed loads are kept away from the collection canal and transported further downstream, instead of blocking the screen. The bottom intake can be constructed at the same level of the riverbed or in the form of a sill. Particles which are smaller than the space between the screen bars are introduced into the collection canal or pipeline together with the water, and these must later on be separated from the water for power generation by suitable flushing devices. From the gutter, water enters a canal or pipeline, which drains into a sedimentation tank and then flows by gravity into the rest of the system (Fig. 16.10). This type of intake is originated from the Tyrol district of Austria, which gives rise to the name of “Tyrolean type water intake.”

Tyrolean intakes are simple in structure, reliable and cheap in operation, and facilitated in construction and management. They are preferable in small permanent rivers and streams where the gravel and pebble content are higher, and sediment content and bed load transportation are low. The disadvantages are that the silt is easy to enter the canal and the gutter is easy to be blocked. Several site visits per year are demanded for inspection, cleaning, and minor repairs, particularly during and after storm periods.

4. Two-storeyed intake

This type of intake with damming water surface makes use of the non-uniformity distribution principle of sediment along flow depth, whose intake sluice is located at the upper layer to fetch surface clean water, while the flushing gallery is installed at

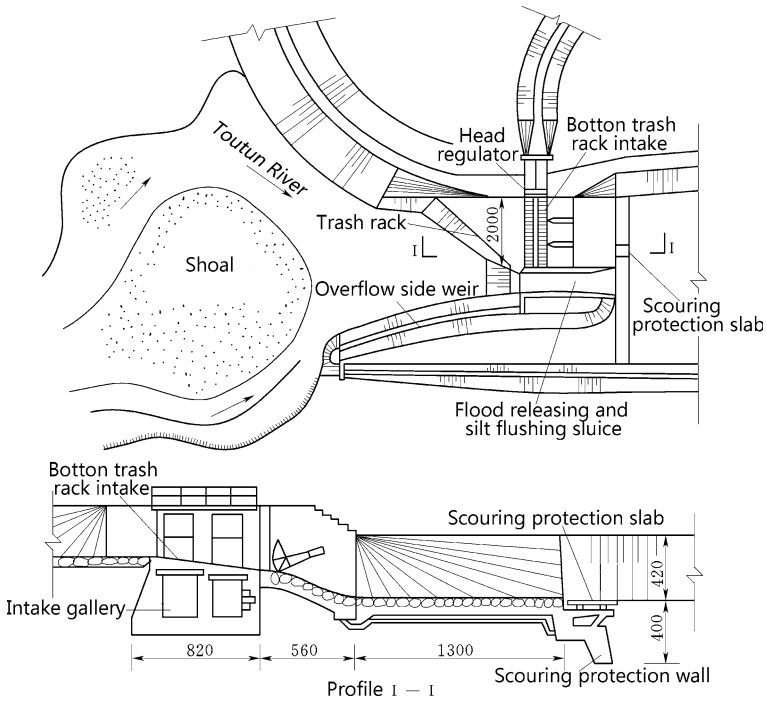


Fig. 16.10 Layout of the bottom grating (trash rack) intake—the Toutunhe River Headworks, Xingjiang Uygur Autonomous Regions, China (*unit: cm*)

the bottom layer to release the bottom flow containing bed loads. According to the position of head regulator, lateral intake and front intake may be distinguished (Fig. 16.11).

In the lateral two-storeyed intake, its axis is somehow parallel to the direction of the flow with an acute off-taking angle and is set up at the river bank, while the flushing galleries are built at the riverbed or beneath the bottom board of the intake sluice. As water is drawn, the gate of escape is closed and the flow turns an acute angle near 90° and runs into the intake sluice above the hanging board. When the sediment has deposited in front of the sluice, it will be removed away by the operation of flushing galleries. Due to the circulating flow near the intake, more silt will be deposited near the upstream lip of the entrance. The flushing galleries, therefore, are layout in a manner of non-uniform: near the upstream lip of the entrance, there are dense galleries, while near the barrage abutment, there are sparse galleries.

Front two-storeyed intake has not circulating flow effect, which is advantageous in reducing the silt from entry into canal. The flushing galleries are installed under the bottom floor of head regulator, which is able to flushing silt without the interrupting of water diverting. Since the silt flushing and water off-taking are

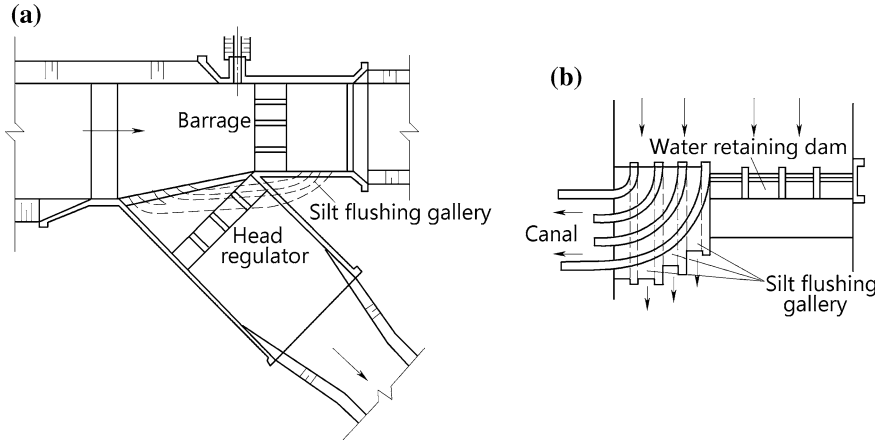


Fig. 16.11 Typical two-storeyed intakes. **a** Lateral two-storeyed intake; **b** front two-storeyed intake

carried out simultaneously, sufficient head and flow discharge are necessitated, which means this is applicable only for the river of large afflux and runoff.

The disadvantage of two-storeyed intake is complex in structure, easy abrasion damage to galleries, and difficult for repairing.

In the southern China, the headworks are usually integrated into comprehensive hydraulic projects to meet the multi-purposes of irrigation, navigation, log passage, power generating, etc. Figure 16.12 shows the layout of such a project located in the Shaoshan County, Hunan Province, China.

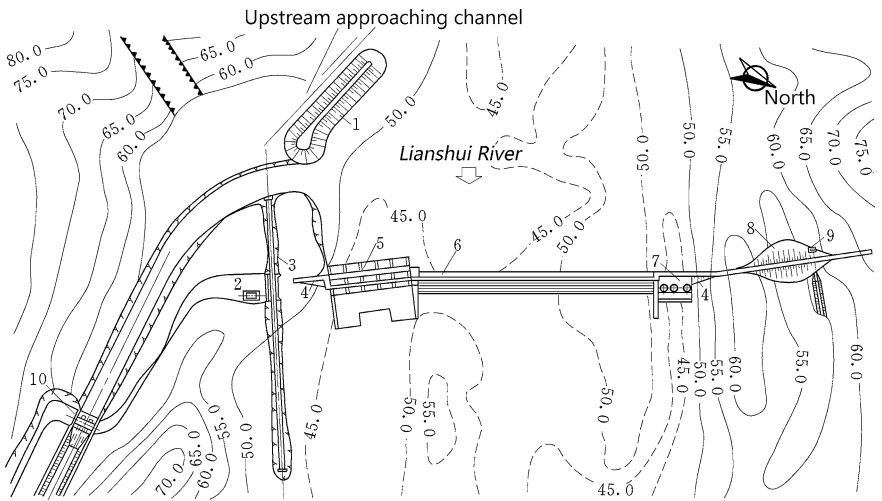


Fig. 16.12 Layout of the headwork (unit: m)—the Shaoshan Hydraulic Project, China. 1 diversion dike; 2 machinery chamber; 3 inclined ship lift; 4 gravity dam; 5 under sluice; 6 barrage; 7 hydropower plant; 8 earthfill dam; 9 intake culvert

16.3 Aqueducts

In the layout of a canal, it is usually necessary to cross a number of channels, varying from small and shallow depressions to large rivers (Leliavsky 1979; Zhao et al. 1989). In general, the solution for all the conditions possible for conveying an canal across a natural stream or depression is by providing a cross-drainage work which may:

- Carry the canal over the natural stream;
- Carry the canal beneath the natural stream; or
- Carry the canal at the same level of the natural stream.

Conveying a canal over a natural stream or depression may be accomplished in the form of a bridge resting on piers and foundations which is called aqueduct. Else, when the canal passes below the trough as a pressure flow, then it is termed as a siphon or a canal siphon.

Around the year 500 AD, the Romans built a system of aqueducts to bring fresh water from the hills around Rome into the city to supply the million or so people who lived there. The aqueducts were, for the most part, open masonry channels in which water flowed under the impetus of gravity. However, nowadays aqueducts are less and less exercised because of associated maintenance problems, environmental considerations, and aesthetics, and because of the availability of precast concrete pressure pipe with rubber gasket joints that can commonly be more economically constructed under natural drainage channels or depressions.

1. Functions, composition, and types of aqueducts

An aqueduct comprises flume, supports, foundation, inlet, and outlet (Fig. 16.13).

There are different classifications for aqueducts. According to the materials used, they may be of timber, brick and stone, concrete, and reinforced concrete. According to the construction methods employed, they fall into the types of precast and cast in situ. According to the cross-sectional shapes adopted, they are distinguished as the types of rectangular shaped, semicircular shaped (U-shaped), trapezoidal shaped, ellipse shaped, and circular piped. According to the supporting manners, they are divided into the types of girder, arch, truss, suspension, or cable

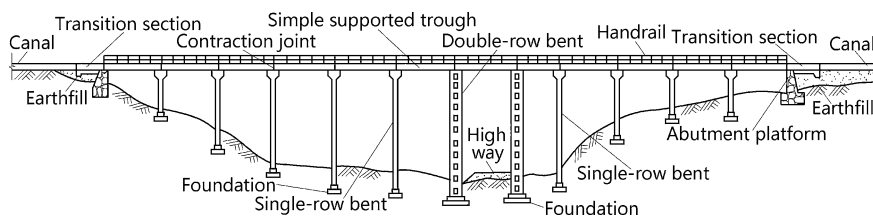


Fig. 16.13 Girder aqueduct

stayed. The classification according to supporting is widely employed because it may better reflect the structure feature, bearing situation, load transfer mechanism, and design method.

(a) Beam-type aqueducts

Beam aqueducts are constructed in a form of flumes structurally similar to beam bridges spanning between trestle supports (Parry and Jones 1993). According to the supporting type, it may be further divided as simply supported beam, cantilever beam, continuous beam, etc.

By simply supported type, the beams only connect across a single span, and the vertical loads on the aqueduct give rise to shear and flexural inner forces in the beam which is transferred down to the piers on either side. Simply supported beam aqueduct is advantageous in reliable and simple with respect to structure and joint water stops, and is convenient for construction, but its large flexural in the middle of span results in strong tensile at its bottom floor, which is unfavorable for the prevention of cracking and leaking.

Cantilever aqueducts are built using horizontal beams supported on only one end, and their spans may be longer than that of simply supported. However, they are sensitive to the pier foundation settlement, which may lead to the failure of joint water stops.

By continuous type, the beams are connected monolithically across two or more spans, which is advantageous in higher bearing capacity but disadvantageous in very sensitive to the pier foundation settlement. Continuous type is seldom exercised in aqueducts.

Spans are the most important characteristic size of beam-type aqueducts. By engineering experiences, the commonly used span for simply supported aqueduct is 8–12 m, whereas cantilever aqueduct may possess span of 25–35 m. The application of prestressed reinforced concrete structure may further increase the aqueduct span.

The supports of beam aqueducts are usually provided by gravity piers, hollow gravity piers, and bents, etc.

(b) Arch aqueducts

An arch aqueduct has abutments (pier platforms) at each end and is shaped as an arch bridge, which transfers the self weight and other loads partially through main arch rings into a horizontal thrust restrained by the abutments. The upper structure joins the flume with the main arch rings, which may be either solid spandrel type (Fig. 16.14) or open spandrel type (Fig. 16.15).

Solid spandrel type is material consuming and heavy; therefore, it is ordinarily applied to small span aqueduct, on which the flume is commonly in the shape of rectangular, below which the main arch rings may be single or double curvature. The whole solid spandrel-type aqueduct may be made of brick, stone, or masonry.

Open spandrel type may be employed for larger span aqueduct attributable to its light structure, which may be further distinguished as vertical wall type (Fig. 16.15) and bent frame type. The former is actually a transformed solid spandrel type by the

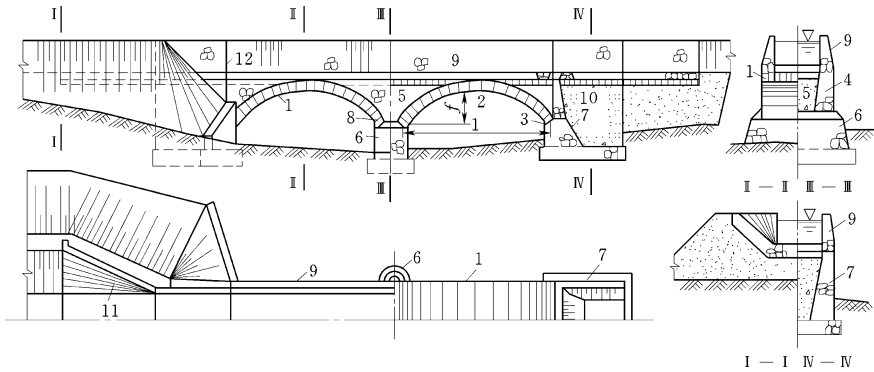


Fig. 16.14 Solid spandrel arch masonry aqueduct. 1 main arch ring; 2 arch crown; 3 arch support; 4 sidewall; 5 backfill on arch; 6 aqueduct pier; 7 aqueduct pier platform; 8 draining pipe; 9 aqueduct flume; 10 cushion; 11 transition; 12 deformation joint

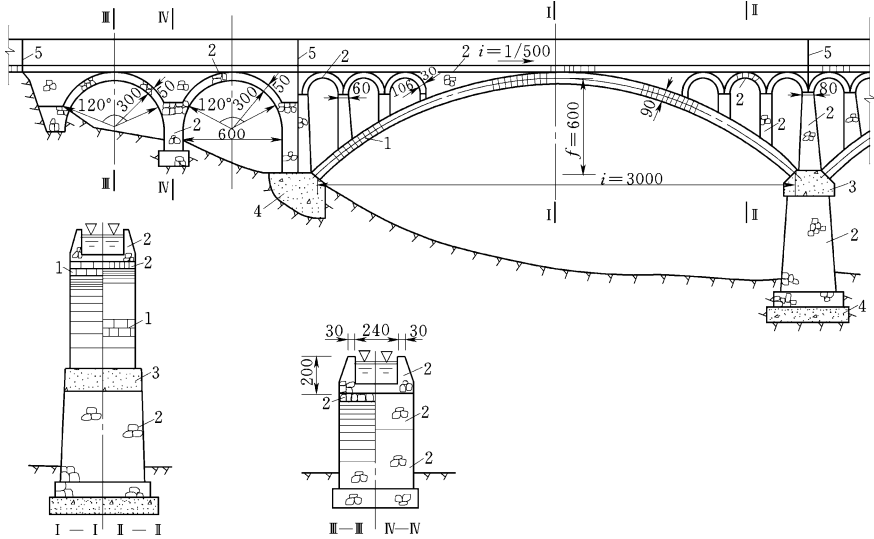


Fig. 16.15 Spandrel-braced arch masonry aqueduct with web (*unit: cm*). 1 cement-rubble masonry; 2 stone masonry; 3 C20 concrete; 4 C10 concrete; 5 deformation joint

installation of city-gate-shaped holes; the latter uses bent frame as upper structure to support the flume on the main arch rings.

2. Layout of aqueducts

Tasks of layout for an aqueduct are accomplished by the selection of its axis, the coordination of its starting, and ending extremities. For a small and short aqueduct, its position has been fixed according to the overall layout of the canal system, and

few alternatives leave for the designer. However, for a large aqueduct located under complex topographic and geological conditions, the position should be selected by the comparison of possible schemes with regard to the following aspects:

- Make full advantages of competent topographic and geologic conditions, to achieve a design of short flume length and to reduce foundation works as well as pier engineering amount. The inlet and outlet are better to be on the excavated foundation;
- Axis of flume normally follows the canal. Although an axis normal to the river is shorter and more economical, a skewed alignment sometimes has to be employed, to prevent the continuation canal from detrimental flowing pattern;
- The aqueduct should be on the river section of reliable stability for the piers against river scour and debris impaction. The curved river section, steep, and unstable bank are shunned;
- For the purposes of repairing aqueduct and downstream canal, or of the upstream diversion, a head regulator is commonly installed at the inlet or outlet of the aqueduct incorporative with escape sluice, and in this way, the canal water may be released into creek or river; and
- Clearance should be assured for navigating river.

3. Hydraulic computation of aqueducts

The inlet transition, flume trough, and outlet transition compose the flow conveying channel (Hinds 1928). The task of hydraulic design for aqueducts is to decide the layout, size, and elevation of the components related to flow conditions. In the following, the longitudinal slope i , net depth h , net width b , and the elevations ∇_1 and ∇_2 of the flume bottom at the starting and ending sections will be discussed.

The maximum flow discharge Q_{\max} is commonly used to get initial estimation of i, h , and b ; then, the designed flow discharge Q is employed to calculate the total loss Δz through the flume, which is required being equal to or a bit of smaller than the allowable loss. Next, the corresponding elevations of the flume are calculated by the values of i, h , and Δz .

Usually, flowing velocities in flume are greater than that in canal, which results in additional drag and transition losses (King and Brater 1976). Where the flume length $l < (15 \sim 20)H$ (H = water depth in the flume), the flow discharge through the flume may be calculated as the free flow of submerged broad crested weir. Where $l > (15 \sim 20)H$, the flow discharge through the flume should be calculated as the open channel uniform flow (Fig. 16.16), in which the surface drop in the inlet is z_0 , the drag loss in the flume body is $z_1 = il$, and the surface rise in the outlet is z_2 .

The total loss Δz is calculated by Eq. (16.2), i.e.,

$$\Delta z = (z_0 - z_2) + z_1 \quad (16.2)$$

In the total loss Δz , the component $(z_0 - z_2)$ has small variation within 0.1–0.3 m; therefore, the loss Δz of long aqueduct is mainly associated with the longitudinal

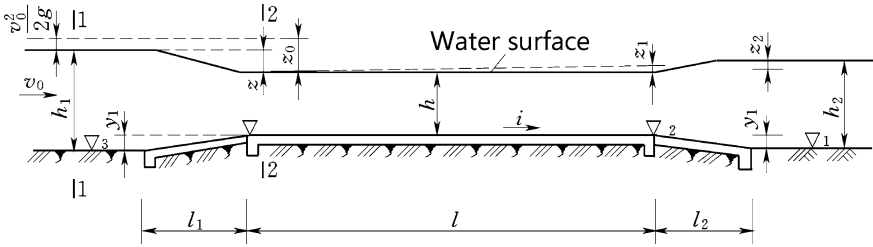


Fig. 16.16 Diagram to the aqueduct hydraulic computation

slope i , which is a key parameter in the aqueduct hydraulic computation. Generally, larger i reduces engineering amount of aqueduct. However, as the velocities in flume increases, the total loss will be increased, and as a result, the gravity irrigation area would be reduced, too.

Ratio h/b is another important parameter in the aqueduct hydraulic computation. The most hydraulically efficient and other considerations such as structural requirements may suggest that the flume should be narrower or wider. A study of h/b ratio with regard to hydraulic efficiency and construction expenditure indicates that an acceptable ratio is in the range of 1.0–0.3. For any ratio in this range, the respective values of area, velocity, and wetted perimeter are nearly identical for a longitudinal slope i between 0.0001 and 0.100. Therefore, the structure requirements are usually predominant in the selection of flume slope i and the ratio h/b . Where the conditions are permitted, the preliminary selection of i may be made in the range of 1/500–1/1500, provided be smaller than critical slope. The preliminary selection of h/b may be made in the range of 0.6–1.0, usually $h/b = 0.6–0.8$ for rectangular flume, and $h/b = 0.7–0.9$ for U-shaped flume.

16.4 Inverted Siphons and Culverts

Siphons and culverts, together with aqueducts, are three major cross-drainage works.

16.4.1 Inverted Siphons

In the building of aqueduct system to bring fresh water into the city of Roman around the year 500 AD, deep depressions posed a serious problem, since the bridging ability of the ancient Roman was limited. To get the water across a deep depression, they utilized what is today termed as “inverted siphon” consisting of a fee tank at the upstream end, a pipe, or series of pipes supplied with water from the feed tank, which carried the water down into the depression and up the other side,

where a receiver tank at the pipe outlet collected the outflow and fed it into a continuation of the canal (open channel), to continue its journey to Rome.

1. Functions, applicability, and structures of inverted siphons

An inverted siphon for canal may be employed across a depression (valley or river), road, and railway line where conditions such as the depth and length of the depression are suitable (Leliavsky 1979; McBirney 1958; Yu et al. 1988). The siphon structure usually consists of an inlet structure, an outlet structure, and a closed conduit being able to withstand the load of coverage and wheels from outside and the hydrostatic pressure from inside. Transitions for changing cross sections are demanded at the inlet and outlet of a siphon, to reduce head losses and to prevent erosion in unlined canals.

The inverted siphon is applicable where:

- The water in the canal is about at the same level of the obstruction;
- The wide and deep river valley is not economical spanned by the alternatives such as aqueduct; or
- The head loss requirements are not strict.

The inlet and outlet are ordinarily constructed using reinforced concrete, whereas the conduit generally consists of cast-in-place or precast concrete pressure pipe or box, or even steel pipe. The annular section is most convenient for construction, and most economical and efficient in withstanding internal pressure. More recently, cast-in-place or precast concrete pressure pipes have been prevalent, particularly for siphons with flow discharge smaller than 30 m³/s. When the internal pressure is small and the external load is high, the large flow discharge inverted siphon is commonly made in the shape of a box or ellipse. Multiple-barrel siphons are frequently found to be rectangular in cross section and are customarily exercised in the plain area of China. For lower head small siphon, plain concrete or masonry construction may be applicable. Reinforced concrete is commonly employed for the conduit of medium head (below 50–60 m). For higher head, the prestressed concrete is more preferable. Where the head is very high, steel pipe or prestressed concrete penstock with steel lining may be suggestable.

2. Layout of inverted siphons

(a) Layout of conduit pipe

The conduit pipe layout should meet the requirements for covering, conduit pipe slope, bend angle, and submergence of inlet and outlet.

Where topographic and geologic conditions are permitted, conduit type of inverted siphon is preferably straight and perpendicular to the depression or road. The inlet and outlet are located on the excavated canal segments, for reducing settlement and seepage, and for preventing collapse. If a backfill foundation is inevitable, effective compaction and seepage prevention measures are secured. The conduit pipe should be located on a stable stratum and easy for construction. The conduit pipe is usually layout along the ground slope, and any curve in plan and change in vertical slope are avoided as far as possible to reduce the head loss and

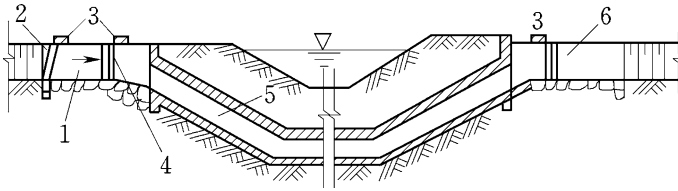


Fig. 16.17 Layout of an inclined inverted siphon. 1 inlet; 2 trash rack; 3 operating bridge; 4 slot for bulkhead gate; 5 conduit pipe; 6 outlet

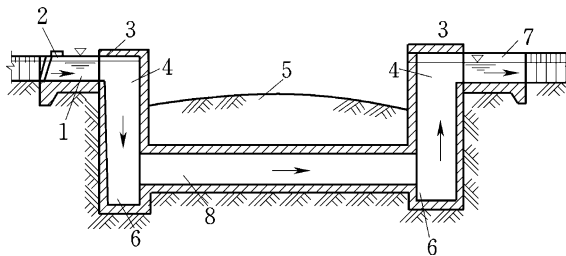


Fig. 16.18 Layout of a shaft inverted siphon. 1 inlet; 2 operating bridge; 3 cover plate; 4 shaft; 5 road; 6 silt collection pit; 7 outlet; 8 horizontal conduit pipe

number of anchor blocks. At the low point of the conduit, a pipe equipped with a valve is customarily provided for the purposes of seasonal draining, silt flushing, inspection, and maintenance.

Two types of conduit pipe layout may be adopted according to the topography and flow discharge. Where the canal intersects with road or other canal and their elevation difference is small, inclined conduit pipe (Fig. 16.17) or shaft conduit pipe (Fig. 16.18) may be employed. Inclined conduit pipe is widely employed in small and short inverted siphon, where the pipe slope should not be steeper than 2:1. Shaft conduit pipe is applicable for small flow discharge and low head at 3–5 m. The latter is simple in construction but worse in flow pattern.

For a work site topography with large altitude variation, conduit pipe is usually laid in open air or shallow embedded (Fig. 16.19). Open-air pipe is advantageous in small engineering amount and easy for construction and inspection, but it will be strongly influenced by sunshine and ambient temperature. Since the larger temperature variation of the pipe wall will induce longitudinal cracks, it is recommended only for small siphon in areas of mild climate. Shallow embedded layout may reduce temperature variation effectively. Since the benefit for temperature variation control will not be further significantly strengthened if the overburden

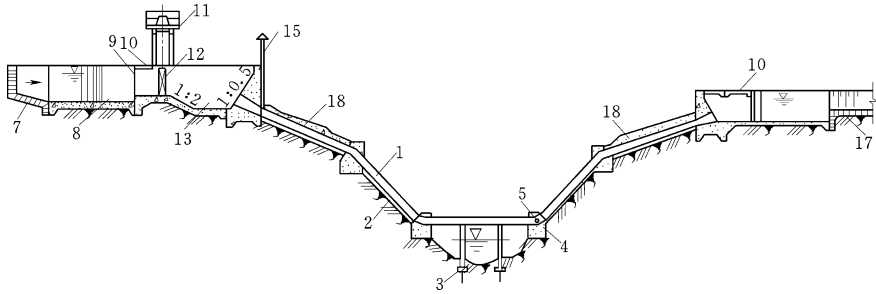


Fig. 16.19 Ground surface and suspension combined layout of an inverted siphon. 1 conduit pipe; 2 continuous support; 3 bent; 4 anchor block; 5 flushing hole; 6 access hole (manhole); 7 transition; 8 settling basin; 9 trash rack; 10 access bridge; 11 hoist; 12 regulator; 13 stilling basin; 14 parapet; 15 air vent; 16 escape and flushing sluice; 17 canal; 18 backfilled earth

depth exceeds 0.8 m, the overburden depth at 0.5–1.0 m is suggestible. The requirements for the pipe covering with respect to the other factors are as follows:

- For a siphon crossing farmland, a minimum earth cover provided should ensure that it is under the plow depth;
- In chilly areas, the top of siphon pipe should be under the freezing zone;
- Traffic roads require at least 0.7 m of overburden; and
- If ditches exist and are extended over the siphon pipe, the minimum distance from the ditch to the top of the siphon pipe should be 0.5–0.7 m.

In the vertical profile, where the slope along siphon has to be changed obligatorily due to topographic condition, circular transition and anchor blocks are installed to bear the centrifuge force from the bending flow and to maintain the stability of the siphon. However, such slope change should be limited as far as possible in the siphon layout. If the inclined section of conduit pipe is long, anchor blocks are installed to prevent the slip of conduit pipe along the slope, whose spacing is dependent on the topographic and geologic conditions. For a long inverted siphon, blow off structure is provided at or near its lowest point to permit draining the pipe for inspection and maintenance or wintertime shutdown. Essentially, the blow off structure consists of a valved steel pipe which is tapped into the siphon barrel. The blow off also may be employed in an emergency in conjunction with waste ways for evacuating water from canals. When necessary, short siphons are ordinarily dewatered by pumping from either end of the siphon. If winter time draining is not needed, the breaking into pipe smaller than 60 cm in diameter for emergency draining is an economical alternative instead of the blow off structure.

(b) Layout of inlet and outlet

Generally, inlet and outlet should be so layout to meet the requirements for good hydraulic conditions, reliable operation, sufficient resistance against sliding and scouring, etc., of the inverted siphon.

Transitions are nearly always necessitated for the inlet and outlet of a siphon to reduce head losses and to prevent erosion in unlined canals from scouring, by gradual velocity change between the canal and conduit pipe. Trash racks at the inlet are required. Gates are provided at both the inlet and outlet to control water flow and to facilitate repairs of any pipe of the multi-barrels without interrupting the operation of the entire siphon. For trash clearance and gate operation, service bridge or operation platform for hoists may be installed. Where the siphon is relatively short, such as that used for crossing roads, it is frequently more economical to neglect transitions even though the length and size of the pipe and protection may increase.

With respect to the expenditure, the flow velocity or pipe size of a long siphon is of particular importance. Generally, velocities in siphon are ranged in 2–4 m/s, depending on available head and economic considerations.

Head losses should be taken into account by adequate layout to ensure good and smooth transition from inlet to conduit entrance under various flow discharges. For the large inverted siphon, the inlet is commonly in a shape of morning glory, by which the entrance section is enlarged up to $1.3\text{--}1.5D$, where D is the diameter of the conduit pipe. Such enlargement may be for all four directions, or for up- and lateral sides solely. The entrance section is curved to join the conduit pipe, and the curvature radius is commonly $2.5\text{--}4D$ (Fig. 16.20). Sometimes, small siphons neglect entrance section of morning glory and curved transition, whose pipe is embedded directly in the retaining wall. Obviously, it exhibits poor flow pattern. The bottom of inlet is generally lower than the canal, which is decided by hydraulic computation.

In silt-laden canals, the inverted siphon should possess the corresponding silt transporting capacity to prevent the pipe from blocking, by maintain adequate flow velocities. In this case, the double- or multi-barreled layout is preferable—the number of pipes in operation may be adjusted to ensure a flow velocity larger than silt deposit velocities. Coarse sand passing pipes may cause abrasion damages; therefore, it should be prevented by installing a settling basin ahead of inlet, which may be cleared manually or by flushing laterally through the escape and flushing sluice installed at the end of the settling basin.

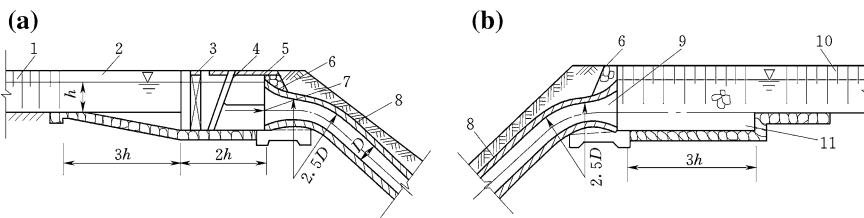


Fig. 16.20 Inlet and outlet of inverted siphons. 1 upstream canal; 2 transition; 3 gate; 4 trash rack; 5 operating bridge; 6 water retaining wall; 7 inlet; 8 conduit; 9 outlet; 10 downstream canal; 11 stilling basin

The outlet of inverted siphon normally comprises exit, gate and operating platform (or bridge), stilling basin, and transition. For small inverted siphons with low flow velocities, stilling basins may be neglected. After the stilling basin, a transition section is installed to adjoin the canal, whose layout is similar to that of aqueducts.

16.4.2 Culverts

Culvert is a covered channel of relatively short length designed for a variety of purposes such as water conveying under backfill channels and traffic roads and draining for release storm water from river and creeks through under embankments (e.g., canal, highway, railroad, dam, and levee), (Guan et al. 1983; Portland Cement Association 1941; Spangler 1948; Young et al. 1974; Ministry of Communications of the People’s Republic of China 2007). Its design requires a hydrological study of the upstream catchment to estimate the maximum (design) discharge and the risks of exceptional (emergency) floods. Structurally, culverts are ranging from 0.3 m pipes to larger reinforced concrete boxes, which are typically surrounded by soil. A culvert normally comprises inlet, outlet, and conduit (Fig. 16.21). Usually, referred culverts are not equipped with gates, otherwise they are termed as “culvert-type sluices.”

1. Types, features, and structures of culverts

Culvert is normally either under condition of full flow or partially full flow (either uniform flow or non-uniform).

Water conveying culvert has small cross-head; therefore, it is customarily designed as partially full flow with flow velocity around 2 m/s, whose flow type is

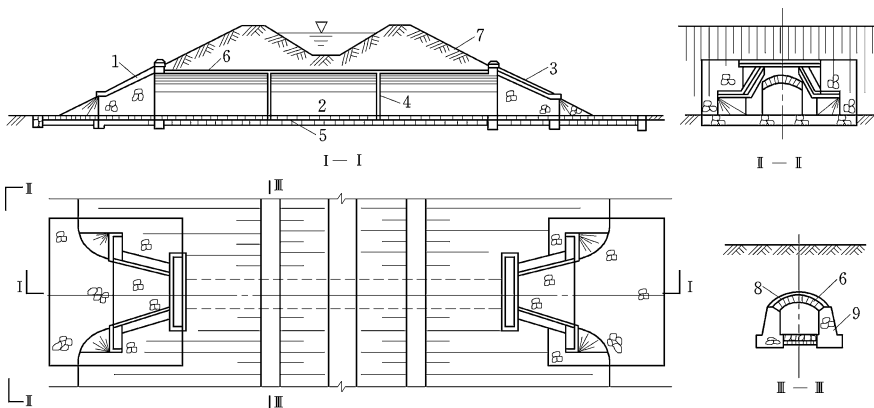


Fig. 16.21 Masonry arch culvert under a backfilled channel. 1 inlet; 2 conduit; 3 outlet; 4 settlement joint; 5 sand cushion; 6 water proof layer; 7 backfilled channel; 8 arch ring; 9 lateral wall

similar to that of free-flowing water convey tunnels. Anti-seepage, drainage, and outlet energy dissipation are normally not required. Drainage culvert may be designed as full flow or partially full flow, and energy dissipation and scouring protection should be installed if the cross-head and outlet velocity are high (Bradley and Peterka 1957a, b, c; Chang 1990; Escarameia 1998; Maynard et al. 1989). Since the duration of flood in small rivers and creeks is short, the necessity for the installation of anti-seepage and drainage devices is selective based on the studies for particular case under consideration.

A culverts conduit may be the precast reinforced concrete pressure pipe, the precast reinforced concrete culvert pipe, the asbestos-cement pressure pipe, the reinforced plastic mortar pressure pipe, and the rectangular concrete box. Pipe is the most preferable due to its good hydraulic and structural performances. Pipe culverts may be single or multi-barreled dependent on the flow discharge.

Rectangular concrete box is usually reinforced. Good at the adaptability to foundation settlement, it is applicable for free-flowing or low pressure culverts with large discharge, thick overburden, large span, and poor foundation. Concrete box may be founded on sandy foundation, cushion of masonry, or pure concrete.

Arch or multi-arch roof provides good bearing capacity, which enables it to be installed over free-flowing culverts of large span and thick overburden. In the areas of the Sichuan and Xingjiang, China, dry sand and cobble pitched arch culverts have been traditionally constructed in a long history, where the flat arch and round arch are commonly employed. The ratio of rise to span is generally $1/3-1/8$, to exploit merits of bearing capacity and saving of materials, but rather large of horizontal thrust from arch springing demands thick vertical walls. The round arch has small horizontal thrust; therefore, it needs thick arch, but the thickness of the vertical walls may be reduced.

In case of a slab culvert, the top slab is supported over the vertical walls (abutments/piers) but has no monolithic connection between them. The bottom floor and vertical walls may be made of masonry or concrete, while top slab is generally of reinforced concrete or stone if the span is small. The slab culvert may be recommended where the top slab is not required to withstand too large vertical loads, or the culvert span is small.

Several types of transitions used for culvert inlet and outlet are shown in Fig. 16.22. The best choice for any particular situation is dependent upon the hydraulics, the topographic characteristics of the work site, and the relative elevations of the embankment and drainage channel.

2. Layout of culverts

The sizing of a culvert is based on hydraulic, structural, and geotechnical considerations. Actually, the culvert height and width affect the size and cost of the embankment (or drainage channel). The impact of culvert on the environment also must be taken into account. A detailed analysis must be conducted, and the engineers should ask if their design responds to the objectives. The major tasks of culvert layout are accomplished by:

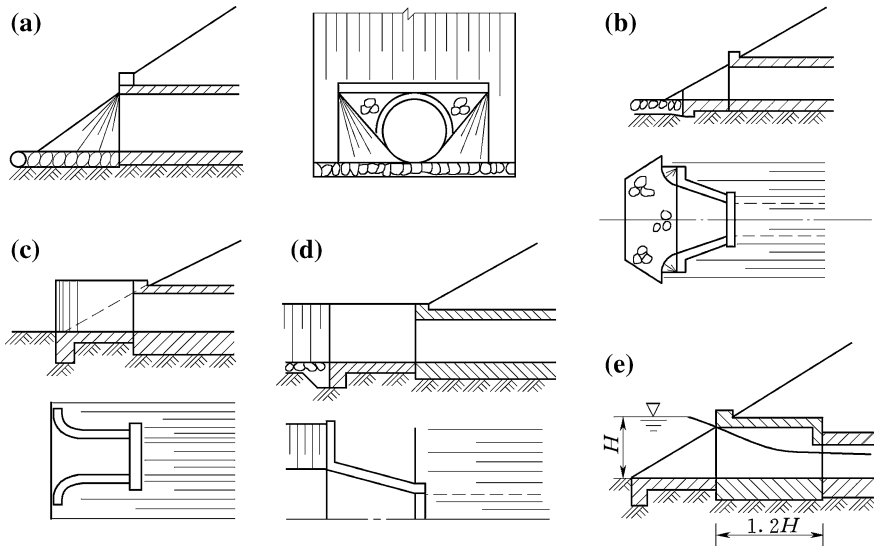


Fig. 16.22 Types of transitions for culvert inlet and outlet. **a** Double curvature wing wall; **b** splayed wing wall; **c** return wing wall; **d** splayed wing wall; **e** risen crown

- Location of culvert;
- Selection of flow pattern;
- Selection of the structure types for inlet, outlet, and conduit;
- The sizing and positioning of inlet and outlet; and
- The sizing and longitudinal grading of conduit.

Ideally, a culvert should be placed in the natural channel and be layout with smooth flow, little excavation, and channel works at the inlet and outlet, especially where the culvert is short.

Most longitudinal culvert profiles have a slope grading ranged in 1–3 %, which are desirable to approximate the natural stream bed. Other profiles may be chosen with respect to either economic or hydraulic reasons. Modified culvert slope, or a slope other than that of the natural stream, can be used for the purposes to prevent stream from degradation, to minimize sedimentation, to improve the hydraulic performance of the culvert, to shorten the culvert, or to meet the structural requirements. However, the modified slope also can lead to stream erosion and deposition.

Where the permeability of backfill earth is high, the anti-seepage measures for the conduit top should be provided. At chilly areas, the conduit should be laid at least 0.3–0.5 m deep under the freezing zone.

16.5 Water Measuring

Effective irrigation water management depends on reliable water measuring for determining both total volumes of water and flow rates. Measuring of volumes will verify that the proper amount of water is supplied to each receiver area and that amounts permitted by water management districts are not exceeded, whereas flow rate measuring helps to control whether the irrigation system is operating properly. The canal discharge measuring may be realized by:

- Discharge measuring through the average velocity in canal;
- Discharge measuring by the rating curve of canal; and
- Discharge measuring by the special facilities or equipments.

In a typical irrigation system, water is customarily measured at the storage reservoir outlet, the canal headworks, and at lateral and farm turnouts. There are many different types of water measuring structures practiced in the Chinese irrigation systems. The type of measuring structure selected depends on availability of head, adaptability to site, economy of installation, and ease of operation (Bos et al. 1984; Clemmens et al. 2001; Leliavsky 1979; Replogle et al. 1999). Measuring by existed hydraulic structures is the most convenient and economic, which should be primarily considered. Particular measuring devices, such as flumes and weirs, have higher measuring accuracy, but additional investment and management cost are required, which are usually employed under the circumstances of in short of adequate hydraulic structures or if their accuracy is not satisfied. Modern facilities such as the acoustic velocity meters and the magnetic flow meters are able to offer a reliable way for the flow measuring in irrigation systems, but they are not included hereinafter.

16.5.1 Particular Measuring Devices

Weirs are identified by the shape of their openings, which can be either sharp crested or broad crested, of which the former is most frequently used for water measuring and is built across open canals. The sharp crested weirs are easy to construct and able to accurately measure the discharge when correctly installed. However, it is demanded that the downstream water level should always be below the weir crest, otherwise the discharge reading will be incorrect. The water-level upstream of the weir is measured using a measuring gauge. The discharge corresponding to that water level is then read from a table which is specified with regard to the size and type of the weir being used, or the gauge post can show the discharge directly.

1. Thin plate weir (sharp crested weir)

Sharp crested weir is made from thin metal plate by cut nick on its top. Examples of three well-known thin plate weir types are the rectangular weir, the Cipoletti trapezoidal weir, and the 90° V-notch weir. The rectangular weir has a rectangular opening. The Cipoletti trapezoidal weir is in fact an improved rectangular weir, with a slightly higher capacity for the same crest length, whose opening is trapezoidal with the sides inclining at a slope of 4 (vertical): 1 (horizontal). The Cipoletti type is very commonly applied in China. Triangular weir normally possess a 90° V-notch opening and is well suited to measuring small flows with high accuracy. The angle other than 90° also may be adopted, depending on the variation range of flow discharge.

To obtain a reliable measuring of the flow over the weir, certain dimensions must be respected because they are critical to correct operation. These are the level of the weir crest relative to the channel bottom; the horizontal distance between the measuring gauge and the weir; the downstream water level being always below the weir crest; the minimum width of approach flume; and the level of the gauge relative to the level of the weir crest.

2. Measuring flume

Other well-known structure for discharge measuring is flume, which consists of a narrowed canal section with a particular, well-defined shape. When used to measure the flow of water in open channels, the flume is designed as a specially shaped hydraulic structure under free flowing, which forces flow to accelerate in such a manner that the flow rate through the flume can be characterized by a level-to-flow relationship. Acceleration is accomplished through either a convergence of the sidewalls, or a change in floor elevation, or a combination of both. A flow measuring flume typically consists of a converging section, a throat section, and a diverging section. Not all sections, however, need to be present. In the case of the cut-throat flume for example, the converging section directly joins the diverging section, forming a throat section without length. The advantage of flumes over weirs is the small drop in water level (head loss); therefore, they are preferable in shallow canals with flat slopes. The drop in water level is only one quarter of the drop needed to be able to use a weir, for the same discharge under similar conditions. In addition, smaller flumes can easily be used as transportable measuring devices. A disadvantage of flumes is that they are relatively expensive and they cannot easily be combined with other structures.

If the canal flow passes in a subcritical state through the flume, for measuring discharge, two gauges—one at upstream and another at the throat (narrowest cross section)—are required. On the contrary, if the flume is so designed as the flow will transfer from subcritical to supercritical state while passing through the flume, a single measuring at the throat is sufficient for the computation of discharge.

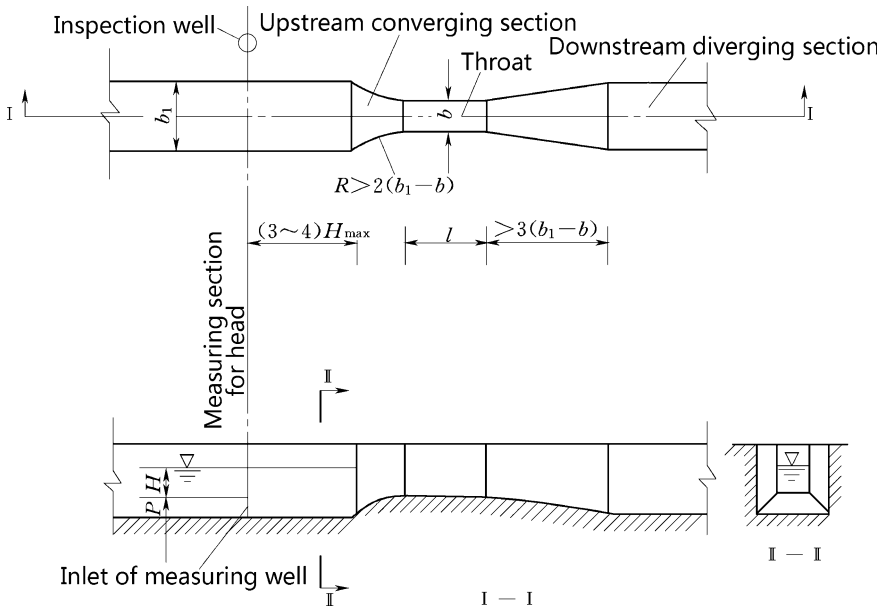


Fig. 16.23 Rectangular long-throated flume

To ensure the occurrence of critical depth at the throat, the flumes are designed in such a manner as to form a hydraulic jump on the downstream side of the structure. These flumes are called “standing wave flumes.”

A variety of flumes are available in measuring water flow for a larger canal, of which the long-throated flume and the short-throated flume are most prevalent.

(a) Long-throated flume

It possesses long throat manifesting small curvature of free surface nearly parallel to the bottom of flume. Long-throated flumes can exhibit nearly any desired cross-sectional shape including rectangular, trapezoidal, U-shaped, and triangular. For rectangular long-throated flume, it may be side contractions only, or bottom contraction only, or the combination of both (Fig. 16.23).

Long-throated flumes are more accurate, lower cost, and better performance and can be computer designed and calibrated. The cross-sectional flexibility of the long-throated flumes allows them to fit various channel shapes more conveniently than short-throated flumes. As a result, the construction of the long-throated flume is normally facilitated. The long-throated flume has transitions of more gradual; therefore, floating debris gives rise to fewer detrimental problems. In addition, field observations have shown that the flume can be designed to pass sediment entrained in channels with subcritical flow.

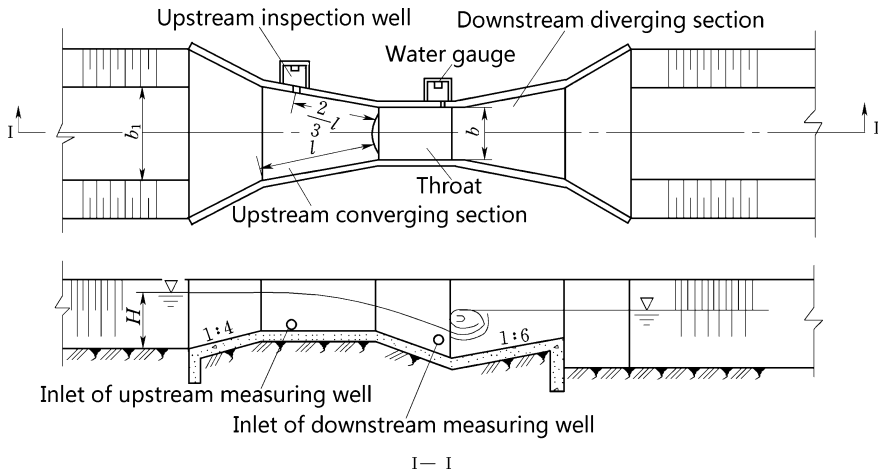


Fig. 16.24 Parshall flume

(b) Short-throated flume

Short-throated flume, by its name, is a kind of critical depth flume with short throat, whose measuring principle is the same as that of long-throated flume. Because of its short throat, the flow surface has larger curvature and is no longer parallel to the bottom floor. Therefore, the rating curve can not be computed theoretically, but only can be rated by in situ or laboratory tests. There are various subtypes of short-throated flumes, including the Khafagi flume, the Parshall flume, the cut-throat flume, and the H flume. The Khafagi flume is mainly used in the European countries, while the last three are mainly employed in USA. The Parshall flume was invented in USA in 1920 (Skogerboe and Hyatt 1967) and is still prevalent in China nowadays, which consists of three principal sections: a converging section at the upstream end, a constricted section or throat in the middle, and a diverging section downstream (Fig. 16.24). The floor of the throat inclines in the direction of downstream, and the diverging section has a slope toward upstream. The Parshall flume has standard dimensions which must be followed closely in order to obtain accurate measurements.

Various factors influence the type selection of measuring flumes, which should be studied comprehensively:

- Variation range of the up- and downstream water levels;
- Requirement for the head;
- Discharge and its variation range;
- Requirement for the measuring accuracy;
- Shape and size of the canal section, and the approach flow condition; and
- Silt-laden situation in the measured canal.

16.5.2 Measuring by Existing Hydraulic Structures

Using of barrages and sluices, culverts, aqueducts, chutes, drops, etc., for the purpose of water measuring is the most economical and simple and is preferable where the conditions are permitted. To do so, level gauges at up- and downstream are set to measure the level difference. According to the type, shape, and size of the structure or/and intake, as well as the flow pattern, the flow discharge may be computed based on hydraulics (Chow 1959). The structures employed for the measuring should be located on the straight segment of the measured canal without obstacles, where the water flow is smooth and accordance with the hydraulic principles employed. In addition, the measuring operation should have minor disturbance on the normal operation of the canal, and it is convenient for the management.

References

- Aisenbrey AJ, Hayes RB, Warren HJ, Winsett DL, Young RB (1974) Design of small canal structures. United States Department of the Interior Bureau of Reclamation, Denver
- Bos MG, Replogle JA, Clemmens AJ (1984) Flow measuring flumes for open channel systems. Wiley, New York
- Bradley JN, Peterka AJ (1957a) The hydraulic design of stilling basins: hydraulic jumps on a horizontal apron (basin I). *J Hydraul Div, ASCE* 83(HY5): paper 1401-1-24
- Bradley JN, Peterka AJ (1957b) The hydraulic design of stilling basins: short stilling basin for canal structures, small outlet works, and small spillways (basin III). *J Hydraul Div, ASCE* 83 (HY5): paper 1403-1-22
- Bradley JN, Peterka AJ (1957c) The hydraulic design of stilling basins: small basins for pipe or open channel outlets—no tail water required (basin VI). *J Hydraul Div, ASCE* 83(HY5): paper 1406-1-17
- Brandon TW (ed) (1987) River engineering. Part 1, design principles, vol 7. Institution of Water and Environmental Management, London
- Brandt SA (2000) A review on reservoir desiltation. *Int J Sedim Res* 15(3):321–342
- Chang HH (1990) Hydraulic design of erodible bed channels. *J Hydraul Div, ASCE* 116(1):87–101
- Chen SH, Chen ML (2014) Hydraulic structures, 2nd edn. China WaterPower Press, Beijing (in Chinese)
- Chow VT (1959) Open channel hydraulics. McGraw-Hill, New York
- Clemmens AJ, Wahl TL, Bos MG, Replogle JA (2001) Water measurement with flumes and weirs (ILRI Publication 58). International Institute for Land Reclamation and Improvement, Wageningen
- Economic and Social Commission for Asia and the Pacific, United Nations Office of Technical Co-Operation (1973) Design of low-head hydraulic structures (Water Resources Series No. 45). United Nations Publication, New York
- Escarameia M (1998) Design manual on river and channel revetments. Thomas Telford, London
- Garcia MH (2008) Sediment transport and morphodynamics. In: Garcia MH (ed) ASCE manual of practice 110—sedimentation engineering: processes, measurements, modeling and practice. ASCE, Reston, pp 21–163
- Guan FN et al (1983) Culverts. Water Resources and Electric Power Press of China, Beijing (in Chinese)

- Hinds J (1928) The hydraulic design of flume and siphon transitions. *Trans ASCE* 92(1):1433–1459
- Iqbal A (1993) *Irrigation and hydraulic structures—theory, design and practice*. Institute of Environmental Engineering & Research, NED University of Engineering & Technology, Karachi
- King HW, Brater EF (1976) *Handbook of hydraulics*, 6th edn. McGraw-Hill, New York
- Leliavsky S (1979) *Irrigation engineering: siphons, weirs and locks*. Chapman and Hall Ltd, New Delhi
- Ma YG, Zhou SZ (2001) Sediment control for irrigation intakes. *J Hydrodyn Ser B* 13(1):122–126 (in Chinese)
- Maynard ST, Ruff JF, Abt SR (1989) Riprap design. *J Hydraul Div, ASCE* 115(7):937–949
- McBirney WB (1958) Some experiments with emergency siphon spillways. *J Hydraul Div, ASCE* 84(5):1–24
- Ministry of Communications of the People's Republic of China (2007) JTG/T D65-04-2007. <<Guidelines for Design of Highway Culvert>>. People's Transportation Press, Beijing (in Chinese)
- Ministry of Water Resources of the People's Republic of China (1999) GB50288-99 <<Code for Design of Irrigation and Drainage Engineering>>. China WaterPower Press, Beijing (in Chinese)
- Morris GL, Fan J (1998) *Reservoir sedimentation handbook*. McGraw-Hill, New York
- Novak P, Moffat AIB, Nalluri C, Narayanan R (1990) *Hydraulic structures*. The Academic Division of Unwin Hyman, London
- Morris HM, Wiggert JM (1972) *Applied hydraulics in engineering*. Wiley, New York
- Pary JD, Jones TE (1993) A design manual for small bridges. *REAAA J* 1(2):27–31
- Petersen MS (1986) *River engineering*. Prentice Hall, New Jersey
- Portland Cement Association (1941) *Concrete culverts and conduits: concrete for permanence*. Portland Cement Association, Chicago
- Replogle JA, Clemmens AJ, Pugh CA (1999) Hydraulic design of flow measuring structures. In: Mays LW (ed) *Hydraulic design handbook*. McGraw-Hill, New York
- Skogerboe VB, Hyatt ML (1967) Design and calibration of submerged open channel flow in measurement structures—Part 2 Parshall Flumes. Utah State University, Logan
- Spangler MG (1948) Underground conduits—an appraisal of modern research. *Trans ASCE* 113(1):316–345
- Song ZZ (1989) *Head works*. Water Resources and Electric Power Press of China, Beijing (in Chinese)
- USBR (1978) *Design of small canal structures*. US Government Print office, Denver
- Varshney RS, Gupta SC, Gupta RL (1979) *Theory and design of irrigation structures*. Nem Chand & Bros, Roorkee
- Young G, Childrey M, Trent R (1974) Optimal design for highway drainage culverts. *J Hydraul Div, ASCE* 100(HY7):971–993
- Yu JK et al (1988) *Inverted siphons*. Water Resources and Electric Power Press of China, Beijing (in Chinese)
- Zhao WH et al (1989) *Aqueducts*. Water Resources and Electric Power Press of China, Beijing (in Chinese)
- Zuo DQ, Gu ZX, Wang WX (eds) (1984) *Irrigation projects*. In: *Handbook of hydraulic structure design* (vol 8). Water Resources and Electric Power Press of China, Beijing (in Chinese)

Chapter 17

Appurtenant Works

17.1 General

For the purposes of power generation, flood control, navigation, irrigation, water supply, etc., dams are constructed to collect water head by raising the upstream water level. The rise of the upstream water level submerges the upstream critical bars, increases the navigable river channel depth, and brings down the flow velocity. The navigable conditions of downstream reach are also greatly improved by the control and regulation of releasing flow. However, the construction of dams cuts off the natural river streams. Structures allow for the safe and quick pass of vessel, fish, and log, between the up- and downstream, have to be built up in order to overcome the concentrated head and keep the whole river navigable. They are important components of multi-purposed hydraulic projects intended to serve various other purposes of economic significance and are named as the appurtenant works. For example, the navigation structures in the Gezhouba Project and the Three Gorges Project play crucial roles in the inland waterway transportation of the Yangtze River.

Appurtenant works may be grouped according to their functions into navigation structures, log pass structures, fish pass structures, floating debris discharging structures, etc.

17.2 Navigation Structures

17.2.1 Classification of Navigation Structures

Waterway navigation played a paramount role in the human history and continuously makes up an ever-important component in the modern transportation system. Compared to the other means of transportation, waterway transportation has the following features:

- Transportation by water can cover any distance by boats, ships, sailboats, or barges, over oceans and lakes, through rivers and canals. Virtually any materials that are able to be moved may be transported over water. Shipping may be for commerce, recreation, or the military, whose transportation capacity is commonly much higher than that of the railways and airplanes.
- Transportation by water is cheaper. Small motor powers than for trains and airplanes attributable to the low friction resistance of water are required; the construct and management of special infrastructures such as port also have lower expenditure compared to the special infrastructures such as railway roads/stations and airports.
- Transportation by water possesses high load-carrying capacity.
- Due to its weight, the transportation by water is slow and could become impractical when material delivery is highly time-critical.

The purpose of navigation works is to assist navigation on dammed rivers. Therefore, the navigation structures are constructed under the circumstances such as:

- Concentrated heads on rivers due to damming are to overcome, for the passage of vessels over the dams;
- In the canalization of natural rivers with torrent and riffle sections, cascade barrage projects are ordinarily erected to improve the navigation canal, in which navigation structures are installed.
- In the canalization of natural rivers, navigation structures also may be demanded for the river sections of large topographically altitude difference or sloping.

Navigation works are commonly distinguished as ship locks and lifts (Leliavsky 1979; Niu and Song 2007; Zuo et al. 1987). A ship lock depending on raised or lowered water level works as a portion of the dam and must be designed with respect to structural stability under the same loading conditions. A lift is basically a machinery equipment employing chamber with a ship therein that is raised or lowered, to pass the ship over the dam.

17.2.2 Ship Locks

1. Composition of ship locks

Ship lock consists of a lock chamber, upstream and downstream lock bays, water conveyance system, and up- and downstream approach channels (Ministry of Communications of the People's Republic of China 2001a, b). Figure 17.1 shows the layout of the No. 2 ship lock in the Gezhouba Barrage Project.movable longitudinal log conveyer;

(a) Lock chamber

Lock chamber is for harboring ships during lockage, which ordinarily has the configuration of a prismatic trough with vertical walls and a solid bottom, whose up- and downstream is enclosed by the upper and lower gate bays.

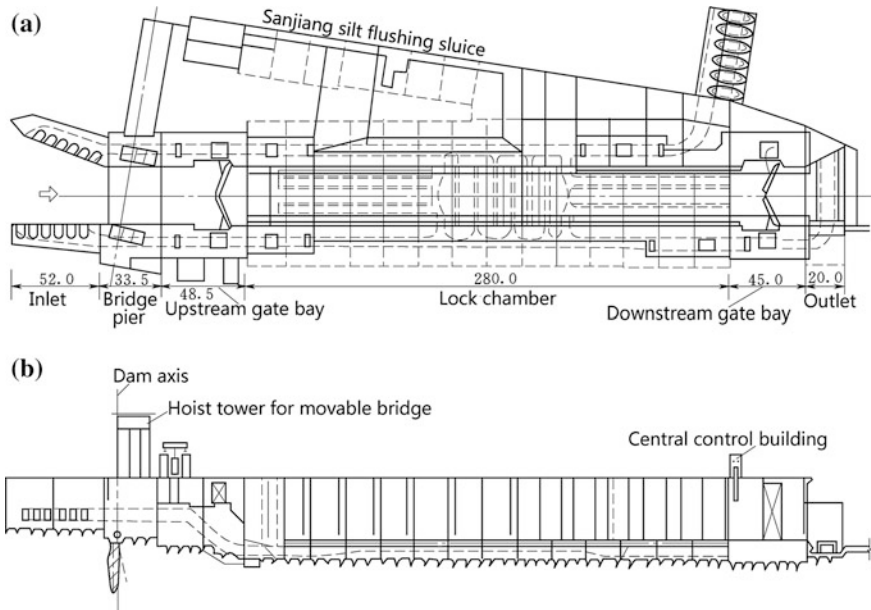


Fig. 17.1 No. 2 ship lock (unit: m)—the Gezhouba Barrage Project, China. **a** Plan; **b** longitudinal profile

To keep the ships under control and stationary while the lock chamber is being filled or emptied, 4–8 floating mooring bits (bollards) are commonly provided in each chamber wall, depending on the length of the lock chamber, with a variable spacing to fit tows of different size barges. On these floating mooring bits, mooring rings may be moved up and down freely. The ships tied to the mooring rings may move up and down, too, but their horizontal movement is restricted.

The lock chamber wall may be in the form of mass concrete (gravity), reinforced concrete, tied-back concrete, steel sheet piling, and earth (chamber walls) construction, of which the gravity is very commonly employed. Usually, the floors in mass concrete locks are not constructed integrally with the walls and are not used as structural members to resist flexural forces. When the walls are founded on sound bedrock, the lock chamber floor can be separated from walls and laid on competent excavated rock surface without any additional treatment. Where the individual mass concrete wall monoliths cannot resist lateral forces to maintain the required stability against sliding, reinforced concrete struts may be installed to transfer the lateral forces to the opposing wall.

(b) Upper and lower gate bays and gates

The gate bay monoliths are water-retaining structures and intended to accommodate the gate recesses, gate anchorages, gate machinery, and sometimes culvert valves and culvert bulkheads. They enclose the lock chamber from the up- and

downstream approach channels, and maintain and regulate the water level within the chamber, for the passing of ships.

The gate bay comprises floor and sidewalls, too, which may be monolithic or separated. Service-gate slot is usually installed at the entrance or exit of the bay. To reduce the height of gate where the head is large, curtain (parapet) wall may be installed for the upper gate bay.

The primary function of service gates is to form a damming surface across the lock chamber. Depending on the specific gate type and the conditions at a particular project, lock gates can be used to fill and empty the lock chamber and to pass ice and debris. These gates can also be employed to dewater the lock chamber and to provide access from one lock wall to the other by means of walkways laid on the top of gate. Various types of gate structures have been invented as lock service gates, including miter gates, submergible vertical liftgates, overhead vertical liftgates, submergible radial gate, vertical axis sector gates, rolling gates, and tumbler gates. Although the use of any of these gates may be preferable under specific project conditions and requirements, the horizontally framed miter gates have been proven to be the most prevailing lock gates attributable to their high operational efficiency and lower maintenance requirements.

(c) Lock filling and emptying system

Lock filling system composed of culverts (or pipes) and valves fills and empties lock to lift or lower down ships (Nelson and Johnson 1964). In the course of filling and emptying the lock, a complex unsteady flow manifests, not only in the lock itself but also in its approach channels (or basins). This flow exerts considerable forces on the ships which must be not exceed a permissible limit, and their detrimental effects must be alleviated or even eliminated by the tying of the ships with mooring rings in the lock chamber or in its approach channels (or basins). However, during emptying of the locks, the ships are normally affected by smaller forces than during filling, due to the greater initial depth of water in the lock.

The layout of water conveyance system should secure the flow forces on the ships be not in excessive of permissible limit during the filling and emptying. For the lock with medium head (5–12 m), indirect filling by means of short culverts may be employed (Fig. 17.2) to simplify the structure of lock chamber, but energy dissipation devices are demanded for the concentrated outflow energy. In the case of high-head locks, indirect filling by means of long culverts situated either in the lateral lock walls or in its bottom, and connected with the lock chamber through suitable designed outlets (Fig. 17.3a, b), is a better choice. By the long culvert arrangement, the outflow energy is not so concentrated and its actions on the ships are smaller, but the structure of lock chamber is complex. In the case of low-head (below 4–5 m) and small size locks, direct filling and emptying through service gates also may be employed. The size of water conveyance system should be adequate to meet the requirement for lockage time.

Valves in the lock filling system are usually vertical lift, butterfly, or cylindrical types.

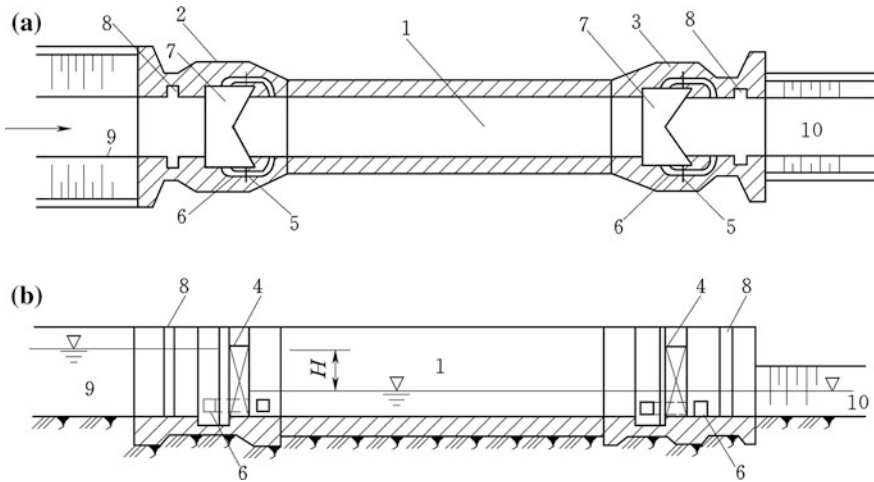


Fig. 17.2 Indirect filling by means of short culverts. **a** Plan; **b** longitudinal profile. *1* lock chamber; *2* upper gate bay; *3* lower gate bay; *4* gate; *5* valve; *6* culvert; *7* gate recess; *8* bulkhead slot; *9* upstream approach channel; *10* downstream approach channel

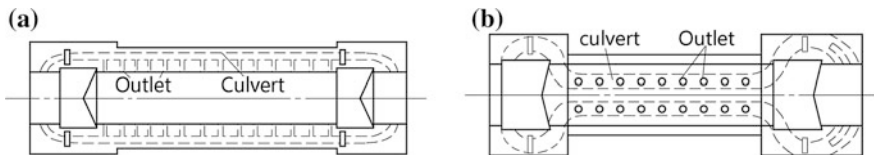


Fig. 17.3 Indirect filling by means of long culverts. **a** Culverts situated in the lateral lock walls; **b** culverts situated in the bottom floor

(d) Lock approaching

Lock approaching provides the transition between the navigable river and the lock. It must be designed to secure a safe and speedy entry into the approach basin (channel) and the lock and to permit the mooring of ships waiting lockage while this is operating to pass other ships down-or upstream.

The hydraulic characteristics of the waterway in the vicinity of the up- and downstream lock approaches and the nature of the traffic dictate what type of special structures (e.g., approach walls) are needed to facilitate the entrance to and the exit from locks as well as to alleviate hazards caused by detrimental currents. Ships large enough to nearly occupy the whole width of a lock chamber must carefully approach the lock. During adverse current or wind conditions, an approach wall offers a long and safe target as the operator initiates alignment for entry into the lock. The wall also helps the operator to check the progress of a tow by using check posts or line hooks to correct the alignment.

Approach walls also provide mooring spaces for the separated part of tows which are too long to pass the lock in one lockage.

2. Types of ship locks

The classification may be based either on steps, lanes, or structures.

(a) Single chamber and tandem chamber locks

Where the site conditions permit, it will probably be more economical to provide the total lift in one chamber (Fig. 17.1). It will certainly be less expensive to the users and will entail less maintenance and operation costs, but the design will be more complicated. Locks have been constructed in China with the maximum lift up to 32.5 m in a single chamber. Single chamber locks have several variations such as shaft locks and locks with middle gate bay.

Figure 17.4 shows a high single-lift lock of shaft type. To reduce the gate height, at the upstream a curtain wall and at the downstream a parapet wall are installed. The lock of Ust-Kamenogorsk (former USSR) with maximum lift of 42 m is a shaft lock.

Figure 17.5 shows a lock chamber with middle gate bay, which divides the chamber into two segments. The chamber may be used as a whole for the lockage

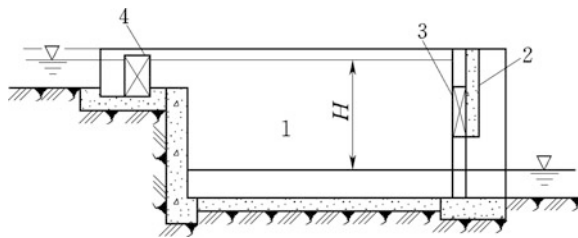


Fig. 17.4 A shaft lock. 1 lock chamber; 2 parapet wall; 3 vertical lift plate gate; 4 miter gate

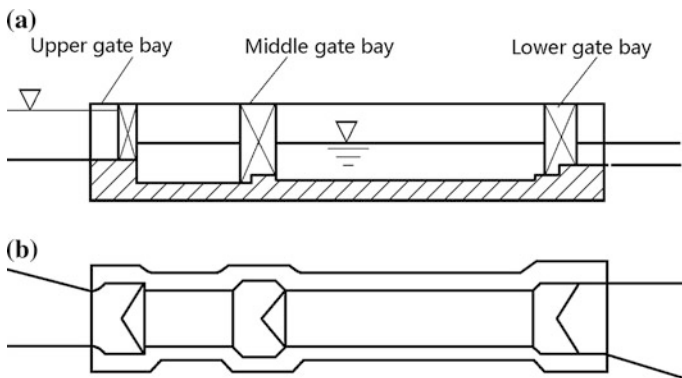


Fig. 17.5 A lock with middle gate bay. a Longitudinal profile; b plan

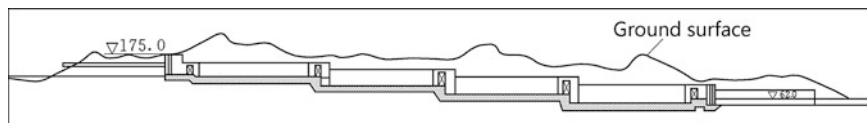


Fig. 17.6 Dual-lane and five tandem locks—the Three Gorges Project, China

of large or more ships; where the boats are small or few, only the front or rear portion of the chamber is operated, to save the water consumption and lockage time.

If the required lift exceeds the limit for a single lock, or foundation conditions are not permitted, tandem (stepped) locks may be constructed (Zhou and Xie 2011). These may be in a continuous flight or they may be separated by short approach channels (Fig. 17.6).

(b) Number of lock lanes

Generally, a single-lane lock on a waterway system with sufficient dimensions to handle the standard size ships will have enough capacity to handle the tonnage capacity. In fact, a large lock may be more economical to construct and operate than equivalent two smaller locks.

On the other hand, traffic departments may require dual-lane locks or even multi-lane locks to handle the projected tonnage. If an auxiliary lock with smaller capacity (shorter length) than the main lock is provided, the auxiliary lock should have the same width as the main lock. This will allow the interchange of spare gates, emergency closures, maintenance bulkheads, and operating equipments between the two locks. In addition, this arrangement enables us to handle the standard width of tow configurations on the waterway but composed of fewer barges. As a further consideration, the smaller auxiliary lock can be used to handle the most small tows and recreational craft, and the main lock can be used to handle the larger tows which should maximize the tonnage capacity of the lock project. The examples are triple-lane locks of single lift in the Gezhouba Project (China), the dual-lane and five tandem locks in the Three Gorges Project in the Yangtze River.

If a navigation project is designed using dual-lane locks of equal size, the alternatives for non-separated locks (sharing a common intermediate wall) and separated locks should be studied with regard to operational efficiency, capacity, cost, and safety. Separated locks will allow for the placement of one or two spillway gates between the locks to provide flow between the locks to align navigation flows and to pass ice. Separated locks also can provide improved traffic handling efficiency and greater capacity, since the tows can make simultaneous approaches and departures. In addition, the separated locks possess benefits from staged construction by putting one lock in operation at an earlier time. The disadvantages of separated locks are higher first expenditure and the requirement for suitable work site conditions.

3. Process of ship handling (lockage)

From upstream to downstream, there are a number of successive operations of passing ships through a ship lock. At first, close the lock bays by gates. Secondly, the lock chamber is filled with headwater through the water conveyance system. Thirdly, the upstream lock bay is opened, and the ship enters the chamber. Fourthly, the upstream lock bay and sluice of water conveyance system are closed. Then, the downstream sluice of water conveyance system is opened, and the water is released so that the water level in the lock chamber drops to the tailwater level. At last, the downstream lock bay is opened, and the ship goes out of the chamber.

Similarly, from downstream to upstream, there are also a number of successive operations in the reverse order.

4. Lock size

The lock should be large enough to accommodate the traffic vessels which can reasonably be anticipated during the service life of the project, taking into account any restrictions on size of tows due to sharp bends, narrow channels, or shallow depths, whose correction is not feasible. The sizes of a lock chamber are determined by a balance with respect to economy for the construction and the average or probable number and size of vessels likely to be transported. The basic sizes of lock are width, length, effective depth over sill, and width and length of approach channels (Bloor 1951).

The ship size is described by its length L , width B , and draught T . The displacement is defined as $W = \delta LBT$, in which δ is the displacement coefficient. The tonnage is defined as $D = \gamma_w W$, i.e., $D = \gamma_w \delta LBT$, in which γ_w is the unit weight of water.

Lock design and vessel design influence each other to such an extent that the size of each generally corresponds to the other. Data on the width, length, capacity, power, and number of barges and tugboats, including the years in which they were built and operated on existing similar waterways, can be obtained from various transportation administration departments and shipping line operators. These data can help to determine which group of barges and their tow formations are the prevalent configuration for the waterway system being studied.

(a) Effective length L_k of lock chamber

The effective length of lock chamber L_k is defined as the distance from the downstream side of the upper gate bay where it joins the lock wall to the upstream side of the lower gate bay when it is in the recessed position Fig. 17.7a. If the direct filling without culverts is adopted (filling from the holes on the gates), the effective length of lock chamber L_k is defined as the distance from the upstream edge of the lower gate bay to the downstream edge of the energy dissipation section Fig. 17.7b.

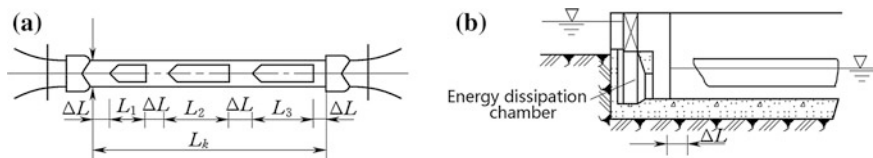


Fig. 17.7 Group of barges and their tow formation. **a** Plan; **b** longitudinal profile

The effective length L_k of lock chamber may be estimated by Eq. (17.1):

$$L_k = L_1 + n_1 L_2 + (n_1 + 2)\Delta L \quad (17.1)$$

where L_1 = length of tugboat, m; L_2 = length of barge, m; n_1 = number of barges; and ΔL = distance between two barges or the barge and the head of lock (generally $\Delta L = 1\text{--}3$ m or more), m.

(b) Effective width B_k of lock chamber

The effective width B_k of lock chamber is defined as the minimum distance between the chamber walls or gate bay walls and is obtained by Eq. (17.2) or (17.3)

$$B_k = n_2 B_c + 2\Delta B \quad (17.2)$$

$$B_k = (1.10\text{--}1.15)n_2 B_c \quad (17.3)$$

where B_c = maximum width of ship or fleet, m; n_2 = rows of the passing ships or fleets; and ΔB = headroom between ship and the most extruded part of lock chamber (generally $\Delta B = 0.4\text{--}1.5$ m), m.

(c) Effective depth h_k of the lock chamber

The effective depth h_k of a lock chamber is measured from the top of sill to the water surface of the respective pool, to which it connects. It may be obtained by Eq. (17.4) or (17.5)

$$h_k = T_c + \Delta T \quad (17.4)$$

$$h_k = (1.25\text{--}1.50)T_c \quad (17.5)$$

where T_c = existing or projected maximum draft of the ships using the lock, m; ΔT = minimum depth over the sills (at least 0.9 m), m.

(d) Size of gate bay

Type and size of gate bay are mainly dependent on the gate type, filling and emptying system, geologic conditions, and the elevation of up- and downstream approach channels.

(e) Headroom under bridge (or parapet wall) h_b

Headroom under bridge (or parapet wall) h_b is defined as the difference between the maximum design navigation level and the bottom of fixed bridge (or parapet wall), which is identical to the requirement on the bridges in the waterway.

(f) Length and width of approach channel

The design of lock approach can manifest a significant impact on lock capacity, depending on the volume and bunch of traffic to be handled within a given time period. The purpose of approach walls is to align the approach currents parallel to the lock and to provide a smooth surface for the tows in order to make a parallel approach into the lock chamber. To achieve optimum lock approach conditions, measures must be provided such as controlling the direction of current in the approach channel and providing maneuver room to allow for strong crosswinds. The approach channel is straight whose length is normally 3.3–4.0 times of the longest tows. The width of approach channel is asymmetrically and gradually expanded (Fig. 17.8), for facilitating entrance and exit. The length of transition section is customarily 0.5–0.8 times of the longest tows. The width of approach channel is usually 2.5–3.0 times of the widest tows, for the permission of exchanging two tows where one is moored.

The term “guide walls” refer to the long extensions of the lock walls, in either the upstream or downstream direction, that are parallel to the lock walls. These walls serve primarily to guide the long tows into the lock and to provide mooring facilities for tows of too long to pass in a single lockage. The guide wall is straight whose length is normally 1.2–1.5 times of the longest tows.

Nowadays, many countries classify waterway into definite grades; tabulated data on barge and tugboat sizes are provided for these graded waterways. The selection for a lock size will be made from the standard grade.

5. Navigation capacity

By navigation capacity P_t , it means the total cargo tonnages per year passing the lock and may be estimated by

$$P_t = N \cdot n \cdot m \cdot W \tag{17.6}$$

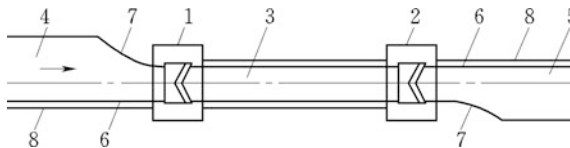


Fig. 17.8 Schematic of approach channel. 1 upper gate bay; 2 lower gate bay; 3 lock chamber; 4 upstream approach channel; 5 downstream approach channel; 6 major approaches; 7 auxiliary approaches; 8 mooring structures

where N = annual shipping days, d ; $n = \frac{1440}{T}$, lockage frequency per day and night; T = transit time for tows, min; m = number of tows per each lockage; and W = average carrying tonnage of fleets, kN.

Taking into account of factors associated with month traffic variation, under load of boat, non-cargo boat, and incident and repair of navigation facilities, the effective navigation capacity is computed by

$$P_a = (n - n_0) \frac{NmW\alpha\tau}{24\beta} \quad (17.7)$$

where n_0 = non-cargo lockage frequency per day and night; $\alpha = 0.7-0.8$, cargo tonnage utilization factor; $\beta = 1.25-1.75$, non-equilibrium factor of cargo; and τ = average operation time per one day and night, h .

6. Water consumption

A sufficient supply of water is required to maintain navigation pools at or above planned normal pool elevations, which is affected by factors such as available water supply, leakage, seepage, multi-purpose (e.g., hydropower generation) consumption, pumpage or diversion, and return flow (where applicable), evaporation, etc., apart from lockage.

Water consumption for lockage comprises the water consumption directly for lockage and indirectly due to leaking from gates and valves, which is a very important economic technical index in the design of ship lock. For a single-lift lock, a one-way lockage operation consumes water amount V which may be estimated by

$$V = (1.15-1.20)L_k B_k H \quad (17.8)$$

where H = design head of single-lift lock, m; L_k = effective length of lock chamber; and B_k = effective width of lock chamber, m.

Bidirectional lockage operation also consumes water amount V , of which one-way lockage operation consumes water amount $0.5 V$. Suppose the chance of one-way and bidirectional lockage is equal, then the average water consumption for each lockage is $0.75 V$.

7. Development of ship lock

China has earliest experiences in the building of navigation structures. In 987, Qiao Weiyue invented the earliest ship lock in the world, in the Lingqu Canal, Guangxi Province.

The navigation structures in China have developed greatly since the 1950s, from then more than 900 ship locks have been built. The effective length and width of the No. 1 and No. 2 ship locks in the Gezhouba Project are 280 m and 34 m, respectively, and the designed head is 27 m. They were two of the world's biggest ship locks (on continental rivers). Though the lock chamber of the No. 3 ship lock in the Gezhouba Project is smaller (120 m \times 18 m), the mean lift velocity 4.40 m/s of water surface is similar to that of the French Donzelei Ship Lock (its quickest

mean lift velocity of water surface is 4.64 m/min). With a head of 32.5 m, the ship lock in the Wan'an Project constructed in 1988 was one of the highest head of single-lift locks in the world. Since the 1990s, a batch of tandem ship locks has been successively constructed such as the Shuikou Project in the Minjiang River (Fujian Province) and the Wuqiangxi Project in the Yuanshui River (Hunan Province) with total heads of 59.0 m and 60.9 m, respectively. The dual-lane and five tandem ship locks in the Three Gorges Project (Fig. 17.6), with total crosshead of 113 m, record the largest construction scales in the world.

The longest ship lock in the world so far is the Cannelton Lock of USA (effective width of lock chamber = 33.6 m, effective length of lock chamber = 366 m, and effective depth = 5 m); the Ust-Kamenogorsk Lock on the Ertix River (Kazakhstan) has single lift height of 42 m, which is the highest single-lift lock in the world.

The lower miter gate of the Wilson Ship Lock on the Tennessee River (USA) has height of 36 m and width of 18.9 m, which is ranked at the largest in the world. With height of 27.8 m and width of 26.2 m and weight of 700 t, the world's largest overhead vertical liftgate is in the Ice Harbour Ship Lock (USA).

17.2.3 Ship Lifts

Ship lifts are machinery equipments to move ships across dams or barrages (David 1984; Uhlemann 2002). As a rule, a ship lift consists of horizontal and water-filled trough provided at both ends with gates; the trough also may be dry (National Reform and Development Commission of the People's Republic of China 2007). Ship lifts are employed at medium to high-head hydraulic projects. Their advantage over ship locks is saving both water and handling time needed for raising and lowering ships at high heads. By the manner of operation, ship lifts are divided into mechanical, hydraulic, and buoyant; by the travel direction of ship handling chamber, ship lifts can be either vertical or inclined.

1. Vertical lifts

According to the principle used for balancing and traveling the ship handling chamber, vertical lifts employ pistons, floats, counterweight balances, or other special mechanisms.

(a) Vertically hoisted ship lift

A vertically hoisted ship lift is similar to overhead traveling crane: After the entering of ship into the handling chamber, the crane raises the chamber to a level higher than the dam crest and the chamber travels horizontally of certain distance across the dam, before it is lowered down to the river or reservoir water. This type of lift needs large power and is mainly operated for medium to small ships.

Figure 17.9 shows the vertical ship lift of the Danjiangkou Project (Hubei Province, China), which has lift capacity of 4500 kN and lift height of 45 m, provided by 4 @ 500 kW electric motors. The ship handling chamber may be a

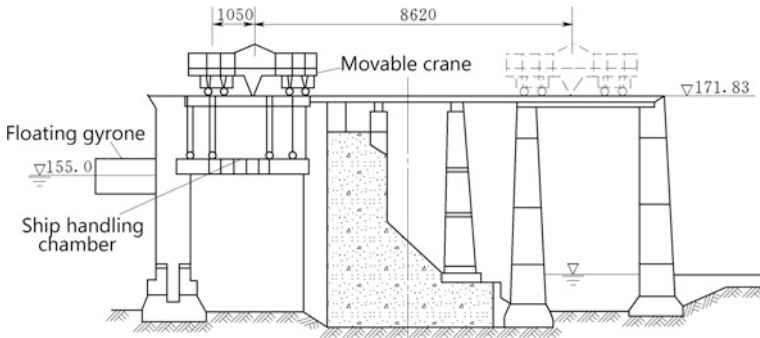


Fig. 17.9 Vertical ship lift (unit: cm)—the Danjiangkou Project, China

water-filled carrying 150 t or be dry carrying 300 t and be lifted at a maximum speed of 11.2 m/min. The size of ship handling chamber (length \times width) is 33.24 m \times 10.70 m for dry carriage and 24.00 m \times 10.70 m for water-filled carriage.

(b) Balanced vertical ship lift

A balanced vertical ship lift uses counterbalance by a suspended weight traveling on a track below the undercarriage of the handling chamber (Fig. 17.10). The power capacity required is smaller compared to the conventional vertically hoisted one because it is only necessary for overcome the unbalanced forces and the motion resistance as well as the inertia. However, balanced vertical ship lift is disadvantageous in complex technology and high steel consumption.

(c) Floating piston ship lift

Figure 17.11 shows a floating piston ship lift. Metal floats are installed in shafts filled with water; the buoyant is used for counterbalancing the weight of movable parts of the lift (including ship handling chamber, floats, and frame for floats). The power is mainly used to overcome motion resistance as well as the inertia of the system.

Floating piston ship lift is reliable, but the lift height is restrained by the construction of shafts.

2. Inclined ship lifts

Inclined ship lifts normally have a ship handling chamber mounted on a special undercarriage which travels along an inclined plane with tracks, either in the direction of the longitudinal trough axis or normal to it, of which the former is more prevalent. As a rule, the chamber is counterbalanced by a suspended weight traveling along an inclined plane with tracks below the undercarriage of the ship handling chamber. According to the operation manner, they are operated either by pull type or self-propelled, of which the former is more prevalent.

Figure 17.12 shows the inclined ship lifts of the Jingshuitan Project (Zhejiang Province, China).

Fig. 17.10 A balanced vertical ship lift (unit: m)

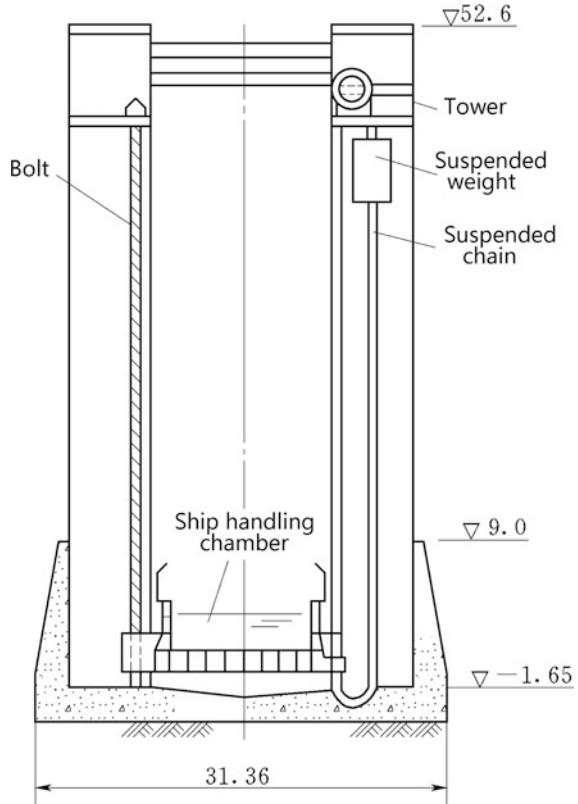


Figure 17.13 shows a schematic drawing of the ship lift with the greatest lift capability at present—the Krasnoyarsk in Russia, with a lift chamber size of 90 m × 18 m × 2.2 m and weight of 8100 t (with water inside) and the pass capacity for ship is 2000 t.

3. Pass capacity

A comprehensive study of present and projected future traffic requirements, with particular emphasis upon the lift size and time required for pass capacity of the ship lift, can indicate that whether one ship lift is sufficient to meet the requirement for economic capacity. Since the transported goods are spatial–time unevenly distributed, sometimes the volume ratio of up- and downstream traffic is 1–3, or even higher. Therefore, the one-way pass capacity is a controlled factor in the estimation of passing capacity.

The annual number of ship passing is computed as follows:

$$Z = \frac{60NT}{t} \tag{17.9}$$

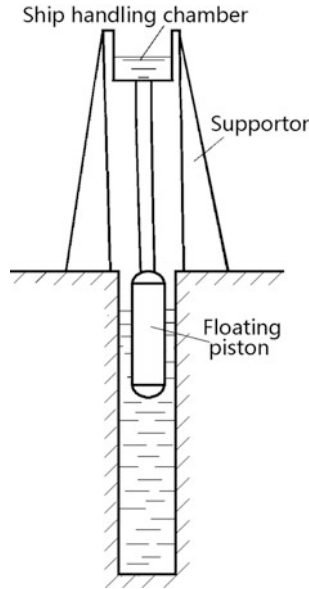


Fig. 17.11 A floating piston ship lift

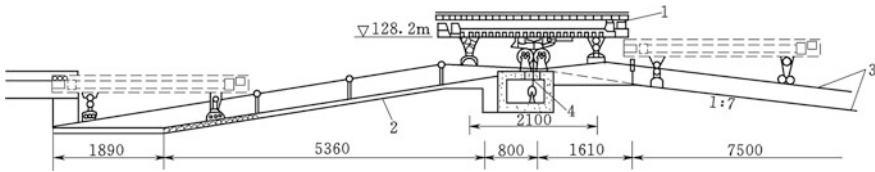


Fig. 17.12 Inclined ship lifts (unit: cm)—the Jingshuitan Project, China. 1 ship handling chamber; 2 inclined slope; 3 high- and low tracks; 4 wire cable

where N = annual shipping days, d ; T = transit time per one day and night, h ; and t = average transit time for one ship passing, min.

The one-way pass capacities Q_1 and Q_2 with respect to present and anticipated future are calculated by:

$$\text{Present } Q_1 = \frac{PZbd_1}{2a} \geq \text{Max (upstream pass capacity, downstream pass capacity)} \tag{17.10}$$

$$\text{Future } Q_2 = \frac{PZbd_2}{2a} \geq \text{Max (upstream pass capacity, downstream pass capacity)} \tag{17.11}$$

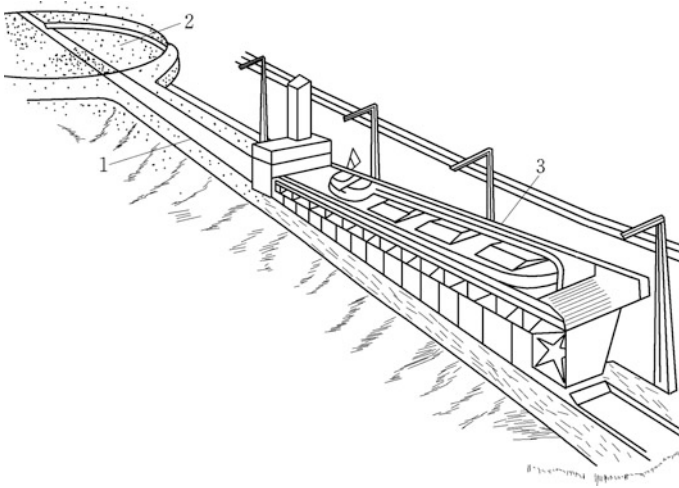


Fig. 17.13 Inclined ship lift of self-propelled—the Krasnoyarsk Project, Russia. 1 track; 2 rotator; 3 ship handling chamber

where P = design cargo capacity of ships, kN; $b = 0.7-0.85$, vessel load factor; $a = 1.2-1.6$, vessel uneven coefficient; $d_1 = 0.5-0.6$, present uneven coefficient of tonnage; and $d_2 = 0.75-0.85$, anticipated future uneven coefficient of tonnage.

The present and anticipated pass capacities Q_n and Q_L are then calculated by:

$$\begin{aligned} Q_n &= 2Q_1e \\ Q_L &= 2Q_2e \end{aligned} \quad (17.12)$$

where $e = 0.7-0.8$, direction uneven coefficient of goods flow.

4. Development of ship lift

The history of ship lift construction in China can be traced back to the period of the Three Kingdoms, when the Chinese solved the problem of transportation in the region of river rapids by building dikes with slopes on the canal. The boats were then manually hoisted up and down the slope. However, the development of modern ship lifts in China lags behind. The ship lifts constructed before 1980 are all small with capability lower than 50 tons. The largest constructed ship lift in China is the vertically inclined type in the Danjiangkou Project, Hubei Province (Fig. 17.9). The ship lift of the Zhexi Project may lift boat of 300 t passing the dam, which is the largest inclined ship lift in China. Although China has constructed more than 60 ship lifts so far, yet due to the lack of good balancing systems and powerful operation equipments, there is a large gap in the ship lift manufacturing technology compared to the world level. However, the situation is changing. A group of vertical ship lifts with advanced technologies in the world, such as the

Geheyan, the Shuikou, and the Yantan, are under the construction or will be put into operation soon. The construction of the Three Gorges Vertical Ship Lift, with the highest lift (113 m) and the maximum lift capability in the world (total lift weight of 11,800 t containing ship of 3000 t), will be started soon.

There are few inclined ship lifts compared to the vertical ones before the 1940s. Since the 1950s, ship lift construction has been boosted to meet the requirement for passing high-head dams. The Henrichenburg ship lift constructed in 1960s in Germany may carry ship at weight of 1350 t, which is the largest floating piston vertical ship lift. The Lueneburg Ship Lift of Germany is the largest balanced vertical ship lift with lift height of 37.8 m. It has double handling chambers, each of them is 100 m long, 12 m wide, and 3.5 m deep, by which the 1350 t vessel may be lifted. The world's largest inclined ship lift is one of self-propelled in the Krasnoyarsk Project, with a lift capacity of 2000 t and maximum lift height of 118 m.

17.2.4 Selection of Navigation Structures

The selection of navigation structures is mainly associated with the operative head. The attention also should be called at the conditions with regard to technology and economy, topography and geology, management and transportation capacity, etc.

Ship locks have advantages of high reliability, large passing capacity, lower operative cost, and versatile in construction and management. However, their construction and operation cost are increased remarkably as the rise of work head. The advantages of ship lifts are less water consumption and less restricted by work head. However, they require complex machinery facilities of higher requirements, and ship tonnage is also more tightly restrained. The inclined ship lifts are more economical and easy in construction and management, compared to the vertical ones, but they demand competent topographic condition, longer route, and transit time. Generally, where the head is lower than 10 m, ship lock is desirable; for the head between 10 and 40 m, single-lift ship lock or ship lift may be all possible; if the head is above 40 m, tandem locks or ship lift may be alternatives. In medium or small rivers with few ships of small tonnage, inclined ship lifts are normally economical; if the transportation capacity and management requirements are high-, dual-, or multi-lane ship locks integrated with ship lift may be configured.

17.2.5 Location of Navigation Structures

In identifying the structure location, the criteria should be evaluated are topographic and geologic conditions, traffic capacity, navigation efficiency and safety, visibility and straight approaches for vessels, foundation conditions, relative cost of structure, existence of public utilities, required relocations, lands available and suitable for

construction, esplanade and general operations, and any other advantages for a particular work site.

For coordinating the navigation structures, an integrated engineering and economic planning study needs to be performed, for determining the number, size, capacity, and layout of the various alternatives (e.g., single- or multi-lane locks). The number and size of navigation structures for the desired capacity depend on the challenges involved in selecting the most efficient work site. Different sites and configuration of navigation structures may have different capacities due to specific site conditions such as navigation approaches, lock separation, incorporation into an existing structure, complete replacement, location in a canal or open river, and associated expenditures of the structures.

The major factors should be considered during the coordination of navigation structures are as follows:

① When conditions permit, there may be an advantage in locating the lock or lift in a side canal or cutoff to take advantage of natural river formations, reduce cofferdam staging, or bypass undesirable features. For a dam construction in rivers, the incorporated lock is usually located against one bank of the stream adjacent to the abutment of the dam, while in canals, the lock often forms the damming surface to maintain pool.

② Locks and lifts should be located in straight stretches of river/canal with approaches aligned along the currents. For example, a location which gives rise to crosscurrents or shoaling in the approaches would be undesirable unless modified by dike work or channel relocation. The entrance of downstream approach channel should keep a distance from spillways as far as possible.

③ Locks are usually located at the downstream side of dam or barrage, to provide access for operation, and to avoid adverse load condition of the gate bay and lock chamber.

④ Horizontal and vertical navigation clearances under bridges at or near the lock are required, which is easier to meet if the bridges are installed on the lower gate bay. Where the bridges are installed at the upper gate bay and the clearances are difficult to meet, the movable bridge may be employed.

⑤ River morphological evolution and sediment accumulation around the exit and entrance of approaches are to be studied. Most locks should be equipped with recesses to trap sediment and to prevent it from interfering with gate operation. If the waterway is sediment laden, a number of countermeasures may be required to keep the sediment moving through the lock, involving various procedures which make use of water jetting and air bubbler systems to dislodge and to move the sediment.

⑥ From the tugboat pilot's standpoint, adequate visibility and ease of approach must be incorporated in the lock and lift design. A clear visible distance up- and downstream of several kilometers is preferable.

17.3 Timber Passing Structures

Timber may be floated one by one, or in form of raft. Ship locks, if exit, are often employed on navigable rivers to pass timber rafts. However, in order to reduce water consumption and achieve maximum use of the handling capacity of locks, special timber pass structures may be advisable which comprises log way, log slide, log lift, etc. (Hänninen 2009).

17.3.1 Log Ways

Log ways are inclined chutes made of wood, concrete, or reinforced concrete with rectangular cross section. A fast gate, usually segmented, is installed at the entrance of the chute. Floating bollards articulated with the chute are installed to reduce the impact when the raft emerges from the chute into the lower water. Water flows through the chute at a velocity of 2–4 m/s. The water flow and raft velocity can be reduced by artificially increasing the roughness of the chute bed or by building in zigzag-shaped outcrops (cutoffs) or brushwood barriers. Much water may be saved by installing a second gate in the chute to form a sluice chamber in the head part of the chute to hold rafts, which will float with the chamber's water after the second gate is opened.

1. Approaches

The width and the depth of up- and downstream approach channels are 1.2–2.0 times of the raft width and 1.2–1.5 times of the raft thickness, respectively. According to the topographic conditions, approaches may be either straight or curved, on which guide facilities are installed.

2. Entrance

The entrance of log way should be adaptive to the reservoir levels and has ability to adjust discharge in log way, for the purpose of safe pass and saving water. There are two types of entrance for log way distinguished as movable and fixed. The former is employed with respect to large reservoir level fluctuations, the latter is suitable for a reservoir level variation smaller than 2 m.

(a) Movable entrance

Movable entrance consists of movable raft trough and stoplog gate. The stoplog gate at the upstream end of movable raft trough is operated to retain water and to adjust discharge in chute. The upstream end of the movable chute may be moved up and down according to the reservoir level, whereas its downstream end joins the fixed chute. This type is applicable where the reservoir level variation is 2–10 m. Engineering practices show that this kind of log way is safe under the circumstances

of unit flow discharge within 1–3 m³/s.m and flow velocities within 3–4 m/s, no matter if rafts are self-floated or man operated passing the dam or barrage.

Figure 17.14 shows the entrance layout of the Chentianhe Log Way (Hunan province, China) with the maximum working head of 34.5 m, and with the length and width of 342 and 6.5 m, respectively. The variation of reservoir level is 10.3 m. A 66 m-long steel structure is employed for the movable chute to adjust entrance water depth. The weight of the movable chute is over 600 t, which is operated by two hoists of 25 t in capacity. The log way may pass 3–5 × 10⁵ m³ timber through the dam per year, with a water consumption of 100 m³ per cubic meters of log passing. This is one of the largest log ways in China.

(b) Fixed entrance

A conventional fixed entrance is similar to that of ship lock, which has two gates, as shown in Fig. 17.15. To pass rafts, the lower gate is closed and the upper gate is opened firstly; after the entering of rafts, the upper gate is closed and

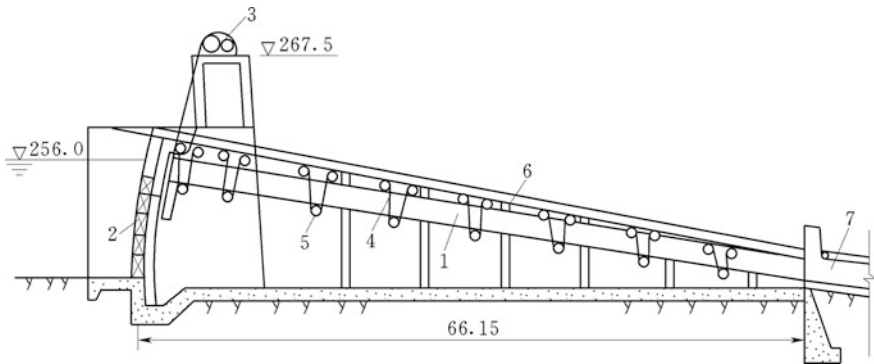


Fig. 17.14 Entrance to the log way—the Chentianhe Project, China. 1 movable chute; 2 stoplog gate; 3 hoist; 4 steel rope; 5 pulley block; 6 support frame; 7 fixed chute

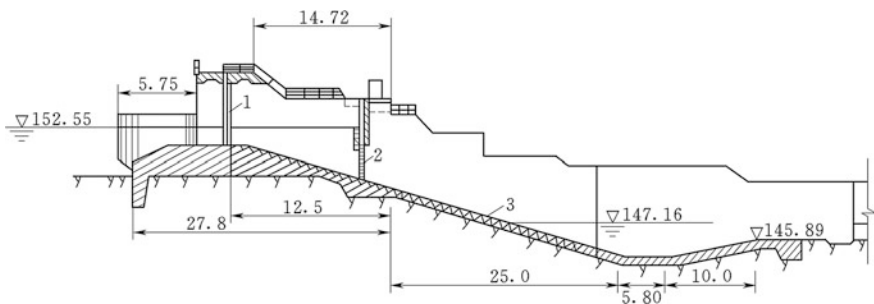


Fig. 17.15 Entrance to a log way (unit: m). 1 upper gate; 2 lower gate; 3 log way

followed by the opening of the lower gate, the emptying of raft chamber lowering down the rafts on the inclined floor of the chamber; finally, the upper gate is opened a bit to release a quantity of water to flush the rafts into downstream. This type is advantageous in simple structure and low water consumption, but it is disadvantageous in lower passing efficient and inevitable impaction of rafts on the floor.

Another fixed entrance is to join the reservoir directly; pull log gate is used to maintain the water depth in the entrance. This type is advantageous in continuous passing of raft and avoiding impaction of rafts on the floor, but it is disadvantageous in higher consumption of water.

3. Chute (trough)

Chute is a straight trough of wide and shallow rectangular in cross section. The width is dependent on the raft width, which is usually selected as the width of raft plus a margin of 0.3–0.5 m. Too wide of trough would result in transverse floating and impaction on the sidewalls. The depth is $\frac{2}{3}$ of the thickness of raft and should be deeper than 0.6 m.

The longitudinal layout of trough may be uniformly sloping, sectional sloping, or sectional step-down, of which the last two are preferable from the standpoint of hydraulic condition, engineering amount, and safe management.

To maintain appropriate depth and velocity in the chute, selection of grading in a range of 0.03–0.06 or installation of baffles on floor may be considered and the latter scheme conventionally makes use of dental sills.

4. Exit

The exit should be near the mainstream and be secured that the rafts will float in the range of tailwater variation.

The level of exit is customarily 1.5–2.5 m lower than the minimum tailwater level. At the end of chute exit, energy dissipation by the surface current is commonly desirable. If the bottom flow (jump) energy dissipation has to be employed, the depth in the stilling basin is better to near critical depth for preventing submerged jump, to safeguard the raft floating out of the stilling basin smoothly.

Where the tailwater level has large variation, the sectional step-down floor or movable exit may be employed.

5. Layout

The entrance and exit should be so located as to avoid the detrimental influence of crosscurrents, shoaling, and wave and to prevent rafts from being sucked by spillways or the other water intake structures. A straight layout is the most desirable. Where a curved layout is inevitable, the radius of curvature should be not smaller than 150–200 m. Berthage spaces are necessary at the up- and downstream of the log way.

17.3.2 Timber Slides

Timber slides (or log slides) are chutes of triangular or trapezoidal in cross section installed to pass loose-floating timber. Depending on the manner of water fed into the timber chutes, the timber slides are distinguished as floating, semi-floating, or wet. Floating timber slides are used to float timber when the water level is within 0.7–0.9 fraction of the log diameter, and their gradings usually lie within the range of 0.001–0.01. In semi-floating timber slides, the timber is transported in a semi-suspended state sliding along the slide bottom. This greatly reduces water consumption. Wet timber slides have steep slopes, and the little water (with water depth of 0.5–1.5 cm) they use serves only as a lubricant to move the logs along the chute.

Generally, the design of log slides is similar to that of log ways. To save the water consumption, movable gates are customarily employed to adapt the reservoir level variation, of which the commonly practiced are sector gates, lowering radial gates, and lowering plate gates, of which the first one is the most prevalent (Fig. 17.16) attributable to its good adjustment ability of water depth within the slide. However, it is vulnerable to be blocked in sediment-laden river.

Log slides with lowering radial gates also may be exercised for flood release by lifting the gate above water surface, which is preferable for the log slides of lower head barrage project. Figure 17.17 shows the log slide with lowering radial gate in the Yingxiuwan Project (Sichuan Province, China); the width of the gate is 12 m.

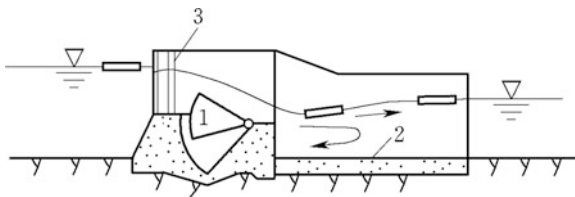


Fig. 17.16 Log slide with sector gate. 1 sector gate; 2 apron; 3 bulkhead gate

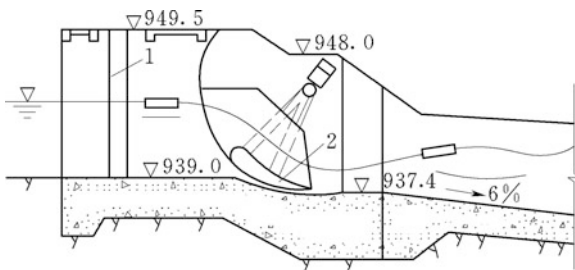


Fig. 17.17 Log slide with lowering radial gate—the Yingxiuwan Project. 1 bulkhead gate; 2 lowering radial gate

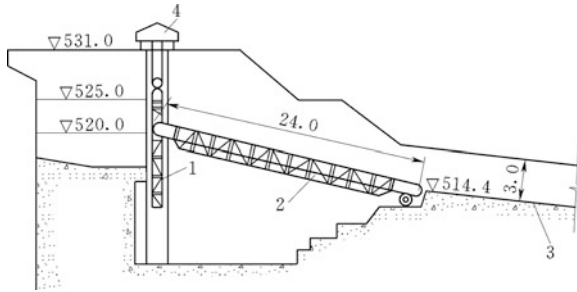


Fig. 17.18 Log slide with lowering plate gate (unit: m)—the Gongzui Project, China. 1 plate gate; 2 movable trough; 3 fixed trough; 4 hoist chamber

Figure 17.18 shows the log slide with lowering plate gate in the Gongzui Project (Sichuan Province, China) with a working head of 40–50 m and an average grading of 13%. The movable trough is 24 m long with a longitudinal grading of 1:7.

The entrance is usually a layout in a shape of morning-glory mouth. Apart from guiding facilities, mechanical or hydraulic accelerators may be installed to prevent the log from blocking near the entrance. The minimum velocity at the entrance is generally 1 m/s and in chute is 2–4 m/s or a bit of higher. The smooth exit of log to downstream water should be secured, but the requirement could be a bit lower than that of log ways.

17.3.3 Log and Raft Conveyers

Log and raft conveyers are machinery facilities for transferring logs or rafts from reservoir to a lower position downstream. There are large varieties of log and raft conveyers including chain conveyers, vertical or inclined lifts, gin pole derricks, stacker cranes, cable cars, etc. Log and raft conveyers are advantageous in less restriction on working head and layout, but they are disadvantageous in lower traffic capacity compared to the log ways and log slides, higher construction expenditure, and higher maintenance and operation cost of electric and machinery equipments.

Figure 17.19 shows the log and raft conveyer in the Bikou Project (China) with three tracks spaced 6 m apart, each has capacity of 900 m³/per machine team; the move velocity of the chain is 0.8 m/s. The length of log conveyer is 419.952 m.

17.3.4 Selection of Timber Passing Structures

The selection of timber passing structures is based on the consideration of floating amount, method, working head of the project, reservoir level variation, discharge layout, topographic condition, and requirement from forest department.

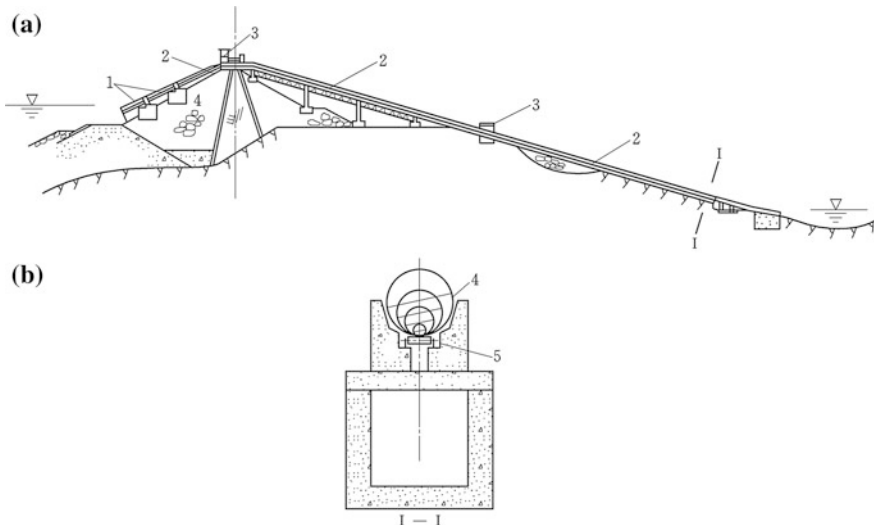


Fig. 17.19 Log and raft conveyor—the Bikou Project, China. **a** Longitudinal section; **b** transverse section. 1 movable longitudinal log conveyor; 2 fixed longitudinal log conveyor; 3 machinery room; 4 log; 5 tumbling cylinder; 6 dam body

Log ways and log slides have merits of high passing capacity, easy management, and low requirement on facilitates and structures, but they consume fairly amount of water for operation. Log ways and log slides are generally employed for projects with low to medium head and small reservoir level variation. Log and raft conveyers are generally applied in high-head projects, where there are difficulties in technical or economical aspects to install log ways and log slides.

17.4 Fish-Passing Structures

There are about 8000 potamodromous species of fish which live in freshwater and a further 12,000 oceanodromous species which live in the sea, and there are about 120 diadromous species which move regularly between the two. Fish populations are highly dependent upon the characteristics of the aquatic habitat which supports all their biological functions. This dependence is mostly marked in migratory fish that require different environments for the different phases of their life cycle including reproduction, production of juveniles, growth, and sexual maturation.

It has become customary to classify fishes according to their capacity to cope with waters of differing salinities during certain stages of their life cycle. The entire life cycle of the potamodromous species occurs within freshwaters of a river system, whose reproduction and feeding zones may be separated by distances that may vary from a few meters to hundreds of kilometers. The life cycle of the diadromous species takes place partly in fresh and partly in marine waters, with distances of up

to several thousands of kilometers between the reproduction zones and the feeding zones. Two different groups can be further distinguished in the category of diadromous species:

- Anadromous species (e.g., salmon), whose reproduction takes place in freshwater with the growing phase in the sea. Migration back to freshwater is for the purpose of breeding.
- Catadromous species (e.g., eel) have the reverse life cycle. Migration to the sea serves the purpose of breeding, and migration back to freshwater is a colonization for trophic purpose.

The construction of a dam within the river environment should be done with the concerns over the impacts on the fish and wildlife populations. These considerations often involve complex problems of feeding patterns and mobility, and where possible, an expert in this field should be consulted (Luo et al. 1992). It should be remembered that dams can be highly advantageous in that they provide a year-round supply spawning areas for fish. At the time of design, although as many benefits as possible to fish should be included, provisions also should be made for the future protection of fish population (Clay 1995; Katopodis et al. 2001; Parasiewicz et al. 1998).

Fish may move through sluices with low-head and low-flow velocity safely, but when these are closed, fish will seek out turbines and attempt to swim through them. Also, some fish will be unable to escape the current near a turbine and will be sucked through (Cada 1990). Even with the most fish-friendly turbine design, fish mortality per pass is high (above 15 %) due to pressure drop, contact with blades, cavitation, etc.

Fish life assisting measures associated with hydraulic projects are basically confined to provision for raising and lowering fish-passing through dams during the migration period, and for this purpose, fish-passing works are to be built.

17.4.1 Classification of Fish-Passing Structures

Written reports of rough fish-passing structures date to the seventeenth-century France, where bundles of branches were used to create steps in steep channels for fish to bypass river obstructions. A version was patented in 1837 by Richard McFarlan of Bathurst, New Brunswick, Canada, who designed a fishway to bypass a dam at his water-powered lumber mill. In 1852–1854, the Ballisodare Fish Pass was built in County Sligo (Ireland), to draw salmon into a river that had not supported a fishery. In 1880, the first fish ladder was built in Rhode Island (USA), on the Pawtuxet Falls Dam. Starting from the twentieth century, as the hydraulic engineering advanced, dams and other river obstructions became larger and higher, leading to the need for more effective fishways (Adam and Schwevers 1998; Godinho et al. 1991; ICOLD 1999; Orsborn 1987).

By purpose, the fish-passing structures designed to assist migratory fish are divided into fish passes and fish protection facilities or fish guarding enclosures. By mode of operation and design features, fish-passing structures would fall into fishways (fish ladders) in which fish are able to climb up the head, fish sluices, and fish lifts (Washburn and Gillis 1985). By the type of fish species, the fish-passing structures would be distinguished as the upstream and the downstream fish passages, of which the former is considered to be well-developed for certain anadromous species including mainly salmonids (e.g., salmon, trout) and clupeids (e.g., shad, alewives), whereas the latter involving juveniles of anadromous species and adults of catadromous species is much less sophisticated.

The general design principle of upstream fish-passing structures (or fish passes) is to attract migrants to a specified position in the river downstream of the obstruction and to induce them actively, or even make them passively, passing upstream by an opening waterway on/around dam or by trapping them in a tank (Larinier 1998).

In the first stages of dam development, engineers and fishery biologists were preoccupied with providing upstream fish passage facilities, while downstream passage through hydraulic turbines and over spillways was not considered to be a particularly important. However, experience has shown that problems associated with downstream migration can be significant factors that affect diadromous fish stocks.

17.4.2 Fish Ladders

A fish ladder, also known as fishway, fish pass, or fish steps, is a structure on or around dams and barrages, to facilitate natural migration for anadromous fishes. Most fishways enable fish to pass around the obstructions up to head of 20 m by swimming and leaping up a series of relatively low steps (hence the term ladder) into the waters on the other side. The velocity of water falling over the steps has to be great enough to attract the fish to the ladder, but it cannot be too great to wash fish back downstream or to exhaust them to the point of unable to continue their upriver journey. Sometimes an auxiliary water supply is also provided to attract fish to the downstream entrance.

The most common method to allow fish for passing dams is the fish ladder, for its good flow condition, simple structure, and easy operation. Fish ladders may be divided into several types as follows.

1. Fish chute type

A fish chute (trough) is an artificial channel of inclined or stepped. It is the simplest fishway and rectangular in cross section with a floor bed sloping so as to provide velocities acceptable for fish to climb up. Fish chutes are primarily con-

structured at small hydraulic works with heads under 2–3 m. As an improvement, baffle fish chutes use a series of symmetrically close-spaced baffles in the channel to redirect the flow of water, allowing fish to swim around the barrier. Baffle fishways need not have resting areas, although pools can be installed to provide resting areas or to reduce the velocity of the flow. Such fishways can be built with switchbacks to minimize the space needed for their construction. Baffles come in variety of designs. The original design for the Denil-type fishway was developed in 1909 and named by the Belgian scientist, which has since been adjusted and revised in many ways (Rajaratnam and Katopodis 1984; Slatick and Basham 1985). The Alaskan steep pass, for example, is a modular prefabricated Denil fishway variant originally designed for remote areas of Alaska (USA). The baffle fishway has stronger turbulence and aeration, which restricts its application only to lower head and strong fishes.

Incomplete transverse baffles shown in Fig. 17.20 may also be used to reduce flow velocities down to 0.8–2 m/s. These fishways are allowed to possess grading of 1:10–1:1.7 of floor bed and head drops of 5–7 m.

2. Pool and weir type

A pool and weir type is one of the oldest styles of fish ladders. It uses a series of small dams and pools to create a long, sloping channel for fish to travel around the obstruction. The channel performs as a fixed lock to gradually step down the water level. To head upstream, fish must jump over from pool to pool in the ladder (Fig. 17.21). According to the statistics of existing fish ladder, the allowable head difference between pools is 0.5–1.5 m, the applicable total head is 3–22 m, the depth of pool is 0.5–0.76 m, and the number of pools is 7–44. This type is usually laid out on the excavated bank round the dam or barrage, in a way similar to natural rivers.

Fig. 17.20 Fish chutes with incomplete transverse baffles

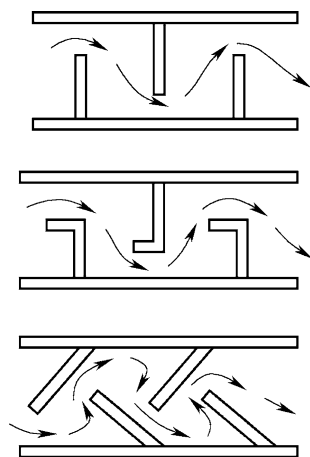
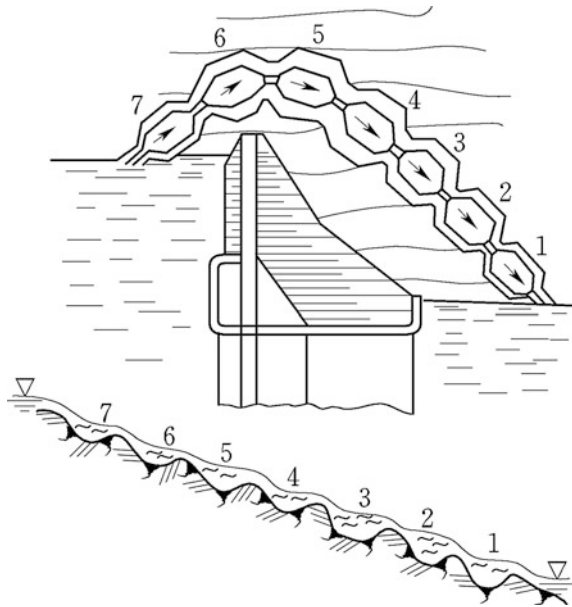


Fig. 17.21 A pool and weir type fishway



3. Rock ramp type

It uses large rocks and timbers to create pools and small falls that mimic natural rivers. Such structures are most appropriate for relatively short dams. They have a significant advantage in that they can provide fish spawning habitat.

4. Hole or vertical-slot type

A hole or vertical-slot fish ladder is similar to a pool and weir system, except that each “weir” has a narrow slot or holes in it near the channel wall. This allows fish for swimming upstream without leaping over an obstacle. Vertical-slot fish ladders also tend to handle reasonably well the seasonal fluctuation in water levels on each side of the barrier; therefore, they are more prevalent.

The main design parameters are the dimensions of the pools and the geometric features of the weirs creating the pools (e.g., heights, notches, slots, and orifices). These, together with water levels up- and downstream of the facility, determine the hydraulic conditions of the fish ladder, i.e., the flow discharge, the difference in water level from one pool to another, and the flow pattern within the pools.

Figure 17.22 shows such a fishway in the Doulonggang Project completed in 1967 (Jiangsu Province, China). The fish ladder is located at the right abutment and is built using reinforced concrete, whose length and width are 50 and 2 m, respectively. The design working head is 1.5 m, where the water depth in ladder is 1 m. The gradient of floor is 1:33.2, the maximum velocity is 0.8–1.0 m/s, and 36 baffles with narrow slots (0.16 m in width) on two sides are installed at the space of 1.17 m.

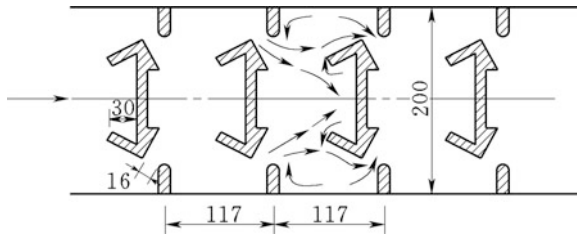


Fig. 17.22 Fish ladder (unit: cm)—the Doulonggang Project, China

5. Combined type

Figure 17.23 shows a combined fish ladder of pool and weir type and vertical-slot type completed in 1973, which is situated at the Taiping Project (Jiangsu Province, China); the sidewalls are in the form of multi-arch and the weirs are made of masonry; the design working head is 3 m and design velocities are 0.5–0.8 m/s; and the water depth in the chute is 1.8 m.

6. Design criteria for fish ladders

Design criteria are based on the swimming capacities and performances of the migratory fish species involved, as well as hydraulic models and field experiences. Different types of fishes have different active water depth, some like to live near surface and the others are used to stay in medium to bottom of the water. The flow

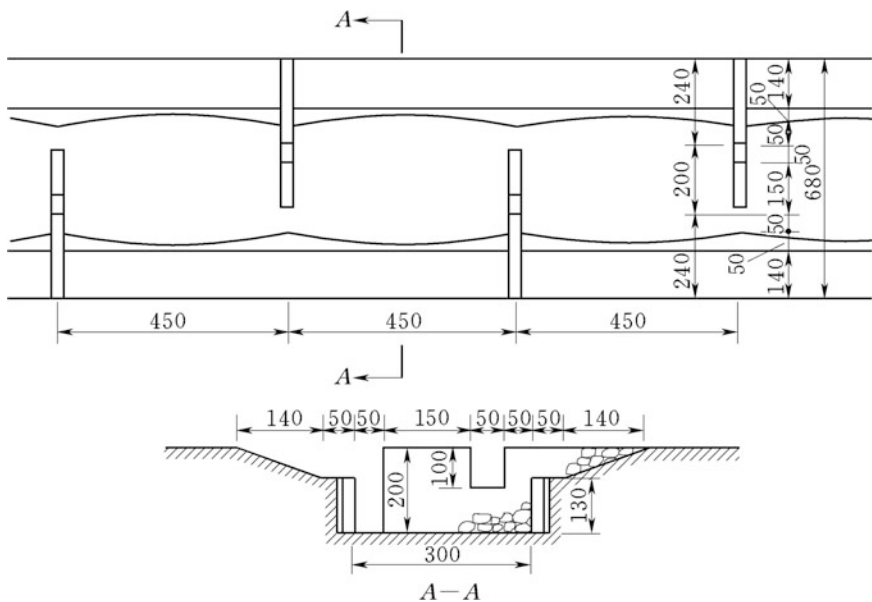


Fig. 17.23 Combined fish ladder (unit: cm)—the Taiping Project, China

velocities in the fish pass must be compatible with the swimming capacity and behavior of the species concerned. Some species are very strong which may overcome a current velocity of 0.4–0.8 m/s, while the common ones are only used to the flow velocities of 0.15–0.4 m/s. The drop between pools varies from 0.10 m to more than 0.4 m according to the migratory species, most frequently around 0.30 m, to obtain good compromise between economical length of the ladder and the preferable velocities for fish. Pool volume is determined from a maximum energy dissipation in the pools which limits turbulence and aeration. Although the aforementioned criteria seem to be commonly accepted nowadays, they must be adaptively employed for different fish species. Where the total crosshead is high for passing the dams or barrages, it is advisable to install restrooms at head interval of 2.5–4.0 m.

17.4.3 Fish Locks

A fish lock consists of a large holding chamber located at the downstream of dam linked to an upstream chamber at the forebay level by an inclined or vertical shaft. Automated control gates are installed at the extremities of the upstream and downstream chambers.

The operating principle of fish lock is very similar to a navigation lock. Figure 17.24 shows a vertical shaft fish lock, and Fig. 17.25 shows an inclined shaft fish lock. At up- and downstream, there are approach channels. Fish are attracted into the downstream holding pool which is enclosed and filled along with the shaft. Then, they exit the upstream chamber through the opened gate. A downstream flow is established within the shaft through a bypass tube located in the downstream chamber to encourage the fish to leave the lock.

The efficiency of fish lock depends mainly on the behavior of fish which must remain in the downstream pool during the whole phase of attraction, follow the rising water level during the filling stage, and leave the lock before it empties.

In this respect, it is demanded that the velocity and turbulence in the downstream holding pool be acceptable for the fish. On the other hand, the lock should not be filled up too quickly during the lifting phase, to prevent excess turbulence and aeration which might force the fish to remain in the lower chamber. The fish should have sufficient time to leave the lock in order to prevent any chance of being swept back downstream when the lock empties.

It is obviously impossible to determine a priori the optimum hydraulic conditions for migrating fish. In addition, the optimum characteristics of the operating cycle are closely linked to the fish species concerned. This is why the lock must be designed to have maximum flexibility in its operation (the duration of each phase of the cycle, the time and extent of the opening of the upstream and downstream sluices, etc.). However, it is a sad fact that in spite of these precautions, numerous fish locks have experienced either not very efficient, or even totally invalid.

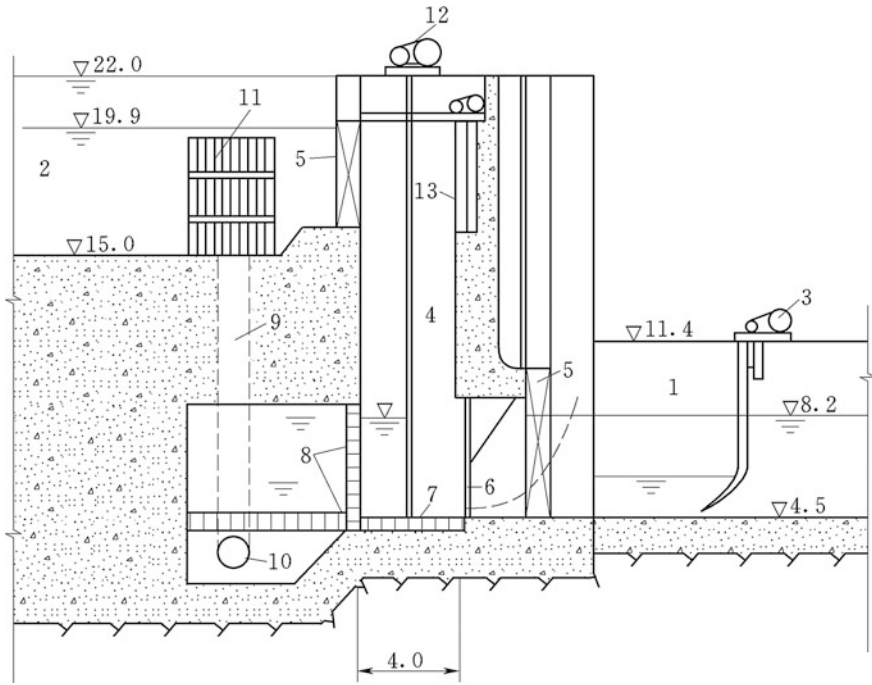


Fig. 17.24 A vertical shaft fish lock (unit: m). 1 downstream approach channel; 2 upstream approach channel; 3 fish driving fence of downstream approach; 4 shaft; 5 gate; 6 rotating fence; 7 lift fence; 8 vertical and horizontal energy dissipation fences; 9 bypass tube; 10 valve of bypass; 11 trash rack, 12 hoist; 13 fish driving fence

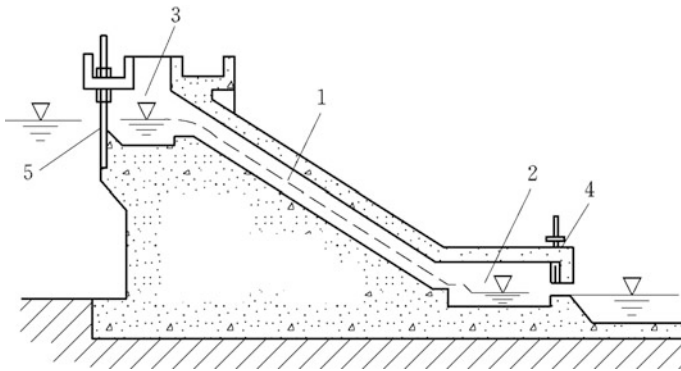


Fig. 17.25 An inclined shaft fish sluice. 1 inclined shaft; 2 lower gate bay; 3 upper gate bay; 4 lower gate; 5 upper gate

The main drawback of the fish lock is that it has a limited capacity (in terms of the number of fish it can handle) compared to that of a traditional fish pass. This is due to the discontinuous nature of its operation and the restricted volume of the lower chamber. The fish attracted into the lock also may leave the downstream chamber before the end of the trapping stage.

17.4.4 Fish Elevators

A fish elevator or fish lift, as its name implies, breaks with the ladder design by providing a sort of elevator to carry fish over a dam/barrage. With fish lift, fish are directly captured in a trap with a V-shaped entrance. When the trap is raised, fish and a small quantity of water in the lower part of the trap are lifted up until it reaches the top of the dam. At this point, the lower part of the trap tips forward and empties its contents into the upstream forebay.

Fish lift has similar operative principle of ship lift which is distinguished as wet and dry types. The former moves fish by a trough full of water and the latter moves fish by a kind of fishing net.

The main advantages of fish lifts compared to other types of fish-passing facilities lie in that their cost being practically independent on the height of dam, in their small overall volume, and in their low sensitivity to the variations of the upstream water level. They are also considered to be more efficient for some species, such as shad, which have difficulty with traditional fish passes. The main disadvantages lie in the higher cost of operation and maintenance. In addition, the efficiency of lifts for small fish species (e.g., eel) is generally low due to the fact that sufficiently fine screens cannot be used, attributable to operational reasons.

On the Connecticut River (USA), for example, a fish elevator may lift up to 500 fish at one run, 15.85 m, to clear the Holyoke Dam. In its first year (1955) of operation, the Holyoke fish lift carried 4,899 shad over the dam; by 2004, the typical annual amount of fish lifted had mounted more than 500,000.

17.4.5 Downstream Fish-Passing Facilities

Downstream fish-passing technologies are much less advanced than those concerning upstream ones and are the areas most in need of research. This is partially due to the fact that efforts toward re-establishing free movement for migrating fish began with the construction of upstream fish-passing facilities and that downstream migration problems have only more recently been addressed. This is also partially attributable to the much more difficult with and complex in the development of effective facilities for downstream fish migration. As yet, no country has found a satisfactory solution to downstream fish migration problems, especially where large dams are involved. Although problems concerning downstream migration have

been well examined in Europe and North America with regard to anadromous species, and more particularly to salmonids, comparatively little information is available on other migratory species.

Fish-passing through hydraulic turbines are subject to various forms of stress likely to cause high mortality, e.g., probability of shocks from moving or stationary parts of the turbine, sudden acceleration or deceleration, strong fluctuation in pressure, and cavitation. The mortality rate for juvenile salmonids in Francis and Kaplan turbines varies greatly; depending on the properties of the wheel (diameter, speed of rotation, etc.), their conditions of operation, the head, and the species and size of the fish concerned.

Fish-passing through spillways may be a direct cause of injury or mortality due to shearing effects, abrasion against spillway surfaces, turbulence in the stilling basin, sudden variations in velocity and pressure as the fish hits the water, and physical impact against energy dissipaters. Experiments have shown that significant damage to fish takes place when the impact velocity of the fish on the water surface exceeds 16 m/s, whatever its size.

For dams of low heights ($H < 10$ m), spillways are most often considered to be the safest passage for downstream migrating fish; on condition, there is sufficient tailwater depth and no over-aggressive baffles (pre-cast blocks, riprap, etc.).

One solution to prevent fish from passing through the turbines involves stopping them physically in front of water intakes using screens which must have a sufficiently small mesh. These screens have to guide fish toward a bypass (e.g., spillway), which is done most effectively by placing them diagonally to the flow, with the bypass in the downstream part of the screen. Surface bypasses associated with existing conventional trash racks or angled bar racks of close spacing have become one of the most frequently prescribed fish protection systems for small hydroelectric power projects.

Visual, auditory, electrical, and hydrodynamic stimuli give rise to a large number of experimental barriers including bubble screens, sound screens, fixed and movable chain screens, attractive or repellent light screens, electrical screens, and hydrodynamic ('louver') screens. Results obtained in particular cases with various screens have not been of any wide application because of their specificity, low reliability, and their susceptibility to local conditions.

17.4.6 Layout of Fish-Passing Facilities

Fish-passing design involves a multi-disciplinary approach. Engineers, biologists, and managers must closely work together. Fish-passing facilities must be systematically evaluated based on the knowledge on migratory fish species, their swimming capacities, and their migratory behaviors. It should be remembered that the fish-passing technique is empirical in the original meaning of the term.

Type of fish pass is generally selected for the major fish species. They are suitably sized and particularly tailor made for the rivers concerned. The advantages

of fishways are reliable and have continuous operative ability, which is commonly applied in barrage projects or low embankment dams with low head, huge amount of migration fish, and sufficient water consumption for fish-passing. However, where the head is high, the investment of fishways is high, too, which even account for 10 % of the whole project. The high head also lowers the passing effectiveness due to high mortality of fish. Therefore, for high dams, when there are numerous species of poorly known variable swimming abilities, migratory behaviors, and population sizes, it is advisable to initially concentrate mitigation efforts on the lower part of the fish pass, i.e., to construct and optimize the fish collection system including the entrance, the complementary attraction flow, and a holding pool which can be used to capture fish to subsequently transport them upstream, at least in an initial stage. This was the policy adopted by European and USA, as well as in China (Three Gorges Project, for example).

For a fish-passing structure to be configured efficient, the entrance must be so designed that fish find it with a minimum of delay. Since the width of entrance is small in proportion to the overall width of obstacle and its flow represents only a limited fraction of total river flow, the only active stimulus used to guide the fish toward the entrance is its location and the hydraulic conditions in the vicinity of the entrance. The latter must neither be masked by the turbulence due to the turbines or the spillway, nor by recirculating zones or static water.

In a case with wide river, it may be necessary to provide more than one fish-passing structures because a single one cannot guarantee to attract certain species from the opposite bank. Migrating fish may arrive either at the bank where the powerhouse is located or at the opposite bank where the spillway is discharging; therefore, it is advisable to design two separate fish-passes, each with one or more entrances.

The upstream exit should keep enough distance from the intakes of spillway and hydropower plant, for prevention of passing fish from being sucked back downstream. To understanding the number of fish-passing the dams, counting chamber should be installed.

It should be indicated that fish-passing technologies such as fish ladders and fish lifts have so far failed for tidal barrages, either offering extremely expensive solutions, or being used by a small fraction of fish only. Recently, a run of the river type turbine has been developed in France. This is a very large and slowly rotating Kaplan-type turbine mounted on an angle. Testing has indicated a fish mortality ratio to be lower than 5 %. This concept also seems very attractive for marine current/tidal turbines.

Apart from the fish-passing technologies discussed foregoing, the other provisions for protecting diadromous fishes are as follows:

- Artificial fish-breeding by re-establishing special fish hatcheries and fish farms;
- Reclamation of fish habitat within the river lower reaches, e.g., artificial desalination of estuary water, provision of spawning beds instead of those lost to the reservoir flood mitigation.

17.5 Floating Debris Discharging Structures

Considerable amounts of debris comprised of trees, brush, and other floating material such as ices and logs can collect and obstruct a spillway or plant entrance, resulting in significant loss of discharge capacity and hinderance of plant operation and delay of navigation. For example, the Gezhouba Hydropower Plant stopped operation twice in 1982 due to the blockage by floating debris. In 1984, the outburst flood of a tributary (Huangbaihe River) of the Yangtze River flushed a wood farm, as a result, 12,000 m³ log floated to the intake front of the plant, which again led to its outages. Therefore, design of spillways and hydropower plants must consider the requirements for the pass of debris and ice during flood events.

To prevent the blockage by floating debris, discharging structures are installed to release the floating debris from upstream reach, which can be achieved by the configuration of the spillway entrance, by the use of a floating debris boom and trash sluices, and by routine maintenance such as reservoir clearance. Since there are numerous types, quantities, and sizes of poorly known variable floating debris, it is advisable to design floating debris discharging structures as flexible as possible and being open to modifications.

Generally, the layout of floating debris discharging structures is combined with the spillways in concrete dam or barrage projects. A good example is the Three Gorges Project: Two floating debris channels are arranged at the left guide walls and longitudinal cofferdam of the spillway dam monolith, respectively, and another additional one is arranged at the section of the erection bay of the right power station. This layout is finally determined by hydraulic model tests associated with operation conditions.

Basically, there are two types of floating debris discharging structures: free overflow and pressure. The former is commonly combined with flood release structures such as overflow spillway dam monoliths and the latter is similar to pressure outlet in concrete dams. Figure 17.26 shows the floating debris discharging outlet of the Gezhouba Project, which is installed in the right erecting yard monolith of mainstream power station. The outlet is composed of double-decked pressure conduits; each is 3 m high and 6.5 m wide. The flow discharge for floating debris is 180–295 m³/s.

Booms are often provided in front of spillways, power intakes, or screening structures, for public safety and to collect large debris before it can reach the gates, trash racks, or screens. Booms are also used to guide the floating debris to the entrance of floating debris discharging structures. Timber boom sticks connected by chains are the most prevalent.

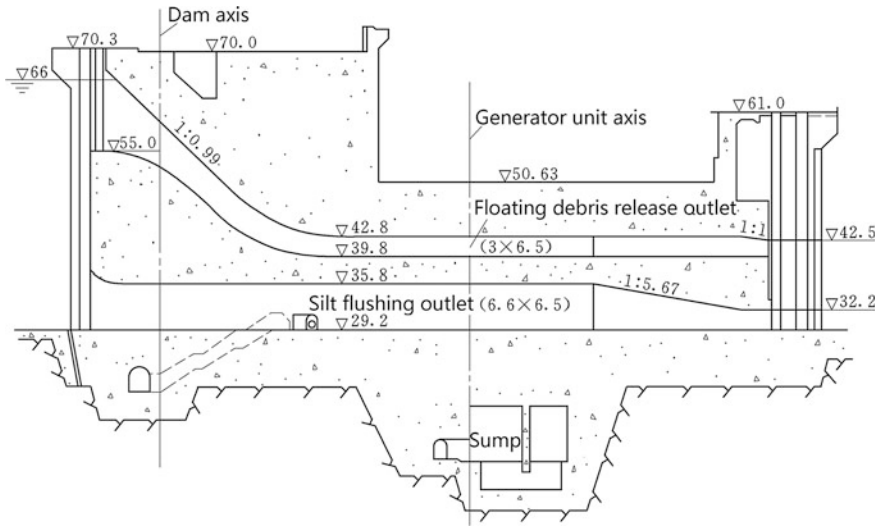


Fig. 17.26 Floating debris discharging outlet of the power plant (unit: m)—the Gezhouba Project

References

- Adam B, Schwevers U (1998) Monitoring of a prototype collection gallery on the Lahn River (Chap. 21). In: Jungwirth M, Schmutz S, Weiss S (eds) *Fish migration and fish bypasses: fishing news books*. Blackwell Science, Oxford, pp 246–256
- Bloor RW (1951) Design characteristics of lock systems in the United States: a symposium: lock sizes for inland waterways. *Trans ASCE* 116(1):864–888
- Cada GF (1990) A review of studies relating to effects of propeller-type turbine passage on fish early life stages. *North Am J Fish Manag* 10(1):418–426
- Clay CH (1995) *Design of fishways and other fish facilities*. CRC Press, Florida
- David T (1984) *Canal inclines and lifts*. Sutton Books, Gloucester
- Godinho HP, Godinho AL, Formagio PS, Torquato VC (1991) Fish ladder efficiency in a southeastern Brazilian river. *Cienc e Cultura* 43(1):63–67
- Hänninen N (2009) Hydropower build-up and the timber floating in northern Finland after the second world war. In: Paukkeri A, YläMella J, Pongrácz E (eds) *Energy research at the University of Oulu, Proceedings of the EnePro Conference*. Kaleva, University of Oulu, pp 94–97
- Hans-Joachim U (2002) *Canal lifts and inclines of the world* (trans: Clarke M). Internat, Somerset
- ICOLD (1999) *Dams and fishes—review and recommendations (Bulletin 116)*. Paris (France)
- Katopodis C, Kells JA, Acharya M (2001) Nature-like and conventional fishways: alternative concepts? *Can Water Resour J* 26(2):211–232
- Larinier M (1998) Upstream and downstream fish passage experience in France. In: Jungwirth M, Schmutz S, Weiss S (eds) *Fish migration and fish bypasses: fishing news books*. Blackwell Science, Oxford
- Leliavsky S (1979) *Irrigation engineering: syphons, weirs and locks*. Chapman and Hall Ltd, New Delhi
- Luo B, Xue P, Lu J, Huang S (1992) Impact of the three gorges project on the fishery of the Changjiang River estuary and adjacent waters. *Stud Mar Sin* 33(1):341–351 (in Chinese)

- Ministry of Communications of the People's Republic of China (2001a) JTJ305-2001 "Code for master design of shiplocks". People's Transportation Press, Beijing (in Chinese)
- Ministry of Communications of the People's Republic of China (2001b) JTJ307-2001 "Code for design of hydraulic structures of shiplocks". People's Transportation Press, Beijing (in Chinese)
- National Reform and Development Commission of the People's Republic of China (2007) DL/T5399-2007 "Design guide for vertical shiplift in hydropower and water resources projects". China Electric Power Press, Beijing (in Chinese)
- Nelson ME, Johnson HJ (1964) Navigation locks: filling and emptying systems for locks. *J Waterways Harbors Div ASCE* 90(1):47-59
- Niu XQ, Song WB (2007) Design of ship locks and lifts. China Water Power Press, Beijing (in Chinese)
- Orsborn JF (1987) Fishways—historical assessment and design practices. In: Common strategies of anadromous and catadromous fishes. American Fisheries Society, Maryland
- Parasiewicz P, Eberstaller J, Weiss S, Schmutz S (1998) Conceptual guidelines for natural-like bypass channels. In: Jungwirth M, Schmutz S, Weiss S (eds) Fish migration and fish bypasses: fishing news books. Blackwell Science, Oxford
- Rajaratnam N, Katopodis C (1984) Hydraulics of denil fishways. *J Hydraulics Div ASCE* 110(9):1219-1233
- Slatick E, Basham LR (1985) The effect of Denil fishway length on passage of some non-salmonid fishes. *Mar Fish Rev* 47(1):83-85
- Washburn BS, Gillis GF (1985) Upstream fish passage. Canadian Electrical Association Publishers, Montréal
- Zhou SD, Xie HB (2011) The design of three gorges hydropower station. *Eng Sci* 9(3):66-73 (in Chinese)
- Zuo DQ, Gu ZX, Wang WX (1987) Barrages, spillways and control works. In: Handbook of hydraulic structure design, vol 6. Water Resources and Electric Power Press of China, Beijing (in Chinese)

Chapter 18

Operation and Maintenance of Hydraulic Structures

18.1 General

Accident or failure of hydraulic structures in hydraulic projects may give rise to significant consequences ranging from losses of life, injury to economy, and damage to properties and environment. These highlight the necessity and importance of safe operation and maintenance for hydraulic structures. In China, responsibility for the safety of a hydraulic project rests with its owner as well as the local and state government (Electric Power Industry Ministry of the People's Republic of China 1998). It is routine to establish special management agency committed to the safety according to an effective management program for the hydraulic structures, particularly dam, to minimize the risk of failure and to protect the life and properties.

The major tasks in the operation and maintenance of hydraulic structures addressed in this chapter are as follows:

- Hydrologic observation and forecasting;
- Safety surveillance of hydraulic structures;
- Instrumentation of hydraulic structures;
- Remedial actions;
- Detection and mitigation of aging for hydraulic structures.

18.2 Hydrologic Observation and Forecasting

Safe operation of hydraulic project is based primarily on hydrologic forecasting, which is, in turn, dependent on water regime observation and prediction (Becker and Yeh 1974; Can and Houcks 1984; Eschenbach et al. 1999; Windsor 1973).

forecasting. It plays an important role in the safe construction and operation of hydraulic projects.

Hydrologic forecasting must provide the forecasting value and forecasting period with competent accuracy. According to the forecasting period, the hydrologic forecasting may be generally distinguished as follows:

- Short-term flood forecasting of several days, whose theoretical base is the theory of runoff yield and flow concentration and mainly serves the purpose for the flood-control operation;
- Mid- and long-term hydrologic forecasting, which is generally developed in the way of meteorology or statistics and mainly serves the purpose for the electric generation operation.

The study on the short-term flood forecasting operation commenced in the early 1950s in China, which concerns the following three basic issues:

- The flood forecasting for a river reach, by which the water regime of downstream section is forecasted;
- The watershed rainfall–runoff forecasting, by which the flood hydrograph at watershed outlet is forecasted using rainfall over the watershed;
- The flood forecasting of stream watershed.

China started to use the stream hydrologic forecasting system to make flood forecasting in the late 1970s. Insofar, a number of stream hydrology forecasting systems have been developed successfully, such as the flood online and real-time forecasting system of the Yangtze River, the Yellow River, the Huaihe River, etc. The combination of these systems with the real-time information processing system and operation system may quickly provide the results of forecasting as long as the information can be received.

It should be indicated that the forecasting accuracy would deteriorated with longer forecasting period due to the presence of chaos. Therefore, methods of mid- and long-term hydrologic forecasting are generally different from those of short-term flood forecasting. At present, there are three types of mid- and long-term hydrologic forecasting methods employed in China:

- Meteorology methods. Based on the relationship between the long-term change of runoff and large-scale climatic change, the long-term change rule of hydrologic elements is forecasted using antecedent atmospheric circulation characteristics;
- Statistic methods. Based on analyzing a lot of long-term historical hydrologic and meteorologic data, and the statistic relationship between the forecasted objective and factors, the mid- and long-term change of hydrologic elements is forecasted;
- Space–earth physics methods. The relationship between the change of space–earth physical factors and the long-term change of hydrologic elements in the regions concerned is founded as the basis for the mid- and long-term hydrologic forecasting.

18.2.3 Reservoir Operation

The reservoir operation is accomplished by normal operation and optimum operation. The normal operation applies the runoff regulation theory and the hydroenergy computation method to determine the reservoir storage–draft process satisfying the task defined by the reservoir operation policy. The optimum operation is firstly to set up the objective function and constraints for hydroelectric system, and then, the systematic equations consisting of the objective function and the constraint conditions are solved using the optimal method, and the control operation manner of the reservoir with maximum/minimum objective function value is obtained.

Reservoir operation concerns aspects of flood-control operation and beneficial operation. China is one of the countries where flood disasters frequently take place. Therefore, the emphasis of reservoir management is commonly on the flood-control operation. However, the development of an operation policy for a multi-purpose reservoir, particularly when the beneficial purposes are combined with flood control, is a complex task attributable to the conflicting nature of the different purposes: A full reservoir is needed to maximize returns from beneficial uses, while an empty reservoir gives rise to maximum benefits from flood control. Therefore, the operative study should be able to optimally resolve the conflicts among the various purposes.

The optimal operation of a single reservoir was realized firstly in USA in the 1940s, which was later introduced into China in the 1960s. The study and application were based on a variety of mathematical tools such as the dynamic programming and the Markov process theory, the countermeasure theory and the practical tactic iteration method, the nonlinear programming model and the multi-dimension dynamic programming model, the multi-purpose dynamic programming model and the flood-control real-time optimal operation model.

In the recent 20 years, real-time flood forecasting and operation of reservoir becomes more and more prevalent, which consists of the following three parts:

- The real-time rain and water regime information sub-system;
- The real-time flood forecasting sub-system; and
- The real-time reservoir operation sub-system.

18.3 Safety Surveillance for Hydraulic Structures

For a hydraulic structure such as a dam, safety management program begins with the initial investigation of the dam foundation and continues through its design, construction, and operation (Dunncliff 1988, 1990; Gu and Wu 2006; ICOLD 1988a, b, 1989, 2014; Iida et al. 1979; Luzi et al. 2010; Malakhanov 1990; Merkler et al. 1985; Wu 2003; Wu and Gu 1997). While many problems may emerge and

need to be handled during these phases, there is always a risk that not all problems have manifested themselves or been detected by the time the dam has been completed.

Surveillance is the continuous examination of the physical condition and operation of hydraulic structures such as dams. Surveillance program should be capable of detecting problems related to unsafe factors at an early stage so that remedy measures can be taken on time to secure the structure safety without compromise. To obtain a historical context for defects, surveillance should commence as early as possible in the whole life cycle of the structure, to detect the development of any unsafe trends and to provide full background information on a structure's performance. Any unusual behaviors, regardless of how seemingly insignificant, should be identified and documented because this may be the forewarning of a newly developed unsafe scenario.

Each hydraulic structure should have its own surveillance program, whose scope should be appropriate to the size of the dam and the storage of the reservoir, the population at risk and other consequences of dam failure, and of course the value of the structure to the owner.

The surveillance program should comprise a range of inspection activities from routine inspections by operational staff through to comprehensive inspections by experts; a system of comprehensive monitoring by instrumentation for collecting information or data relating to structural performance; and a series of safety evaluation (safety review or safety appraisal) based on the interpretation of the collected data.

In the following, dams will be taken as example to elucidate the principles of the surveillance program for hydraulic structures.

18.3.1 Safety Inspection for Dams

One of the most important activities in a surveillance program for hydraulic structure, particularly dam, is the frequent and regular safety inspection for its abnormalities and deteriorations, and for determining its status and features related to the structural and operational safety (Duscha and Jansen 1988). Different types of safety inspections should be undertaken for different purposes such as routine inspections, periodic inspections, and special inspections.

1. Routine inspections

The purpose of routine inspections is to identify physical deficiencies of the dam, which are commonly undertaken by the dam owner, as a part of their normal duties at the dam. Routine inspections are best carried out by someone involved in the day-to-day running of the dam such as the field and operating personnel, because much of the inspection and observation should be incorporated in the daily work. The standing operating procedures (SOP) should outline the guidelines with regard to the time and frequency of the inspections, who should be involved, and the

inspection reporting requirements. However, there is no report standard for these inspections as they can vary from a short weekly check for a small farm dam to a twice-daily check for a large dam. Routine inspections are generally carried out on one-weekly basis during construction period, on 1–2 daily bases during impounding period, and one-monthly basis during normal operation. In flood season or high-storage-level situations, the inspection frequency should be raised.

For concrete dams, the inspection checklist may comprise an advisable content in the following:

- Dam body. Differential movement between adjacent dam monoliths; expansion of joints and water stops; external surface cracking and leaking; damage and erosion and leaching of concrete; state of draining holes; seeping discharge and its chemical composition; etc.
- Dam foundation and abutments. Squashing, shearing, loosening, spalling, etc., in rock; shearing, cracking, and leaking, at the contact surface of dam and foundation; cracking, sliding, leaching, and bypass seeping, at the abutment rock mass; draining devices; seepage discharge and transparency (chemical composition).
- Diversion and flood releasing works. Silting and blocking and damage of intake inlets; cracking and damage of flood releasing works; scouring and abrasion of energy dissipaters; silting and scouring of downstream riverbed.
- Others. Outcrop variation of groundwater around dam site; cracking variation in bank slopes; situation of gate, slot, support, and sealing; hoist, electricity control system, and backup electric sources.

For embankment dams, the checklist may comprise an advisable content in the following:

- Dam cracking, sliding, collapsing, scouring, slope toe heaving.
- Downstream slope dispersed saturation, mechanical piping, pop-off, swamping; abnormal variation of pressure relief devices (relief wells, drain ditch, filters, etc.).
- Abnormality of slope protection.
- Damage and silting of surface draining.
- Activity of harmful insects (e.g., termite) and animals (e.g., rats and badger).

2. Periodic inspections

Periodic inspections are generally carried out by engineers for the purpose of identifying physical deficiencies of the dam by visual examination and analysis of monitoring data against prevalent knowledge. The inspection report should fully document the status of the dam and all deficiencies or unsafe factors and outline a strategy for taking remedial action. These inspections are generally carried out on 2–3 yearly bases.

The time of periodic inspection depends on the regional weather pattern. For example, if a distinct wet season exists, inspections are advisable to be carried out

immediately after the wet season, to allow for remedial work to be planned and undertaken prior to the next wet season.

3. Special inspections

The purpose of special inspection is for a particular physical feature or operational aspect of a dam due to some special reasons, which, for example, has been identified as having a possible deficiency or has been subject to abnormal loading conditions (e.g., earthquake and check flood). Special inspection is undertaken by specialists in dam engineering. The inspection report should fully document the status of the particular physical feature or operational aspect of the dam as well as any other deficiencies or unsafe conditions and outline a strategy for taking remedial action. Special inspection is often carried out with a degree of urgency, which will merely address issues that relate to the subject feature, and in addition to the routine and periodic inspections.

18.3.2 Monitoring for Dams

Monitoring is the collection, presentation, and evaluation of information by instrumentation devices installed at/in the hydraulic structures, which is intended to detect deterioration with respect to the actual performance of the structure, to detect structural trends or behaviors for establishing compliance with design expectations or providing some confirmation of the validity of design assumptions, to rectify structure design issues which could not be resolved to high reliability during the design and construction stages, and also to establish an initial datum pattern of performance against which subsequent observation can be assessed.

Today, the provision of monitoring instruments is accepted well for all new major hydraulic structures in large-to-medium projects. Instruments must cover known critical features of the dam, but for the purpose of comparison, some of them also should be placed at locations where normal behavior is anticipated. The planning and specification of a comprehensive suite of instruments involves a logical sequence of decisions, and it is good practice to draft an ideal instrumentation plan in the first instance, and then to progressively eliminate the less essential provisions until an adequate, balanced, and affordable plan is determined.

In addition, a basic level of instrumentation is now frequently installed retrospectively to monitor existing major hydraulic structures of large-to-medium projects.

1. Parameters in monitoring

The scope and degree of sophistication of individual suites of instruments varies greatly. The designer, review engineer, or inspection engineer should identify the issues that need to be monitored and incorporate appropriate instrumentation into the dam. For instance, for a farm dam, it may be concluded that there is no need for

any instrumentation. For the hydraulic structures of grades 1 and 2, the most significant parameters in monitoring are grouped as follows:

- Work condition monitoring (environmental factor monitoring). Including up- and downstream water levels, reservoir water temperature, ambient temperature, silting in front of dam, and downstream silting and scouring.
- Seepage and leakage monitoring. Including discharges of under seepage, bypass, transparency and chemical analysis of seeping water, uplift in concrete dam body, phreatic line in embankment dam body, and uplift in foundation.
- External and internal deformation. Including horizontal and vertical displacements, open and shear of joints and cracks, flexural and inclined deformation of concrete dam, and consolidation of embankment dam.
- Stress/strain and temperature. Including stress and strain within concrete dam, stress of steel bar, stress of the steel plate of penstocks and spiral case, temperature in concrete and foundation rock, pore pressure in embankment dam, and earth pressure.
- Others. Including bank slope stability of dam site, seismic response of dam, and hydraulic items.

2. Frequency of monitoring

The preferable frequency of monitoring varies over time and is related to the factors with respect to the nature of the performance being monitored, the stage of maturity of the dam, and the existence of any problems or events.

The first impounding and the following five years, usually once of monitoring is demanded for each ten days or each month, of which the first impounding period requires once of monitoring for each day or ten days. After the five years of service, usually once of monitoring is required for each month or quarter. The headwater level and tailwater level and ambient temperature should be taken every day. The internal monitoring frequency should be concentrated from the embed time within one month, in a series of 4 h, 8 h, 24 h, 5 d, until routine interval. Special events, such as record floods and earthquakes, will demand more intensive monitoring. Frequency of monitoring is subject to adjustment after long period of service.

18.3.3 Safety Review for Dams

The safety review of a dam is to assess its safety based on data obtained from safety inspections and monitoring, which can be quite complex and personnel engaged. Safety review is generally undertaken by the safety agency belonging to the water resources administration of the state. Where necessary, the services of suitably experienced geologists, hydrologists, and other specialists should be provided. Consideration should also be given to independent review by engineers other than those who carried out the original design of the dam.

The frequency of safety reviews is generally based on the age of the structure and the appropriateness of the technology used on that structure—usually within 3–5 years firstly from the starting of service. After the first safety review, the safety review is carried out at interval of 5–10 years (USA 5–6 years, France 5–10 years). For dams having served over 30 years, comprehensive checking and safety review is demanded, since the natural conditions (such as silting, scouring) and operation mode could be changed greatly after long service, problems of aging of appurtenance structures and materials are exposed obviously, and the same generation of experts concerning the dam design, construction, and management, are still living, which enable to reveal incipient faults.

Following the safety review, a safety review report should be documented by experienced dam engineers familiar with the entire history of the dam. A safety review report should comprise the following:

- Statement on the safety indicating whether or not the dam is in a satisfactory condition and capable of meeting current design criteria;
- Report on comprehensive inspection;
- Parameters adopted and assumptions made (and their bases for review analyses);
- Methods of review analysis and results (numerical and physical);
- Identification of any deficiencies in the dam including criticality ratings for these deficiencies;
- Recommendations for remedial work, emergency action, and/or further studies which should be undertaken and schedules for these activities.

By the safety review, dams are classified into three groups as dangerous dam, defective dam, and normal dam. Anomalies and concerning trends identified in the report should be considered as deficiencies. It is the responsibility of the dam owner to ensure that appropriate remedial actions are taken and documented.

18.4 Instrumentation for Hydraulic Structures

18.4.1 Deformation Monitoring

All structures move as the effects of exerted actions. The structural movements can be divided into three types: surface movement, internal movement, and crack or joint movement. Surface movement is defined as horizontal or vertical deflection of a point on the structure surface relative to a fixed point off the structure. Internal movement is defined as horizontal or vertical deflection within the structure relative to some points on the structure or in the foundation. Joint or crack movement is defined as slip, opening, or compressing of one part relative to another part, of a structure.

Movements in response to actions are usually normal and acceptable, provided that they are within tolerable ranges and do not cause structural damage. Embankments are less brittle than concrete structures and can undergo larger movements without distress. As a result, measuring of surface movements of

embankment dams is typically less precise than that for concrete structures. Sudden or unexpected direction, magnitude, or trend of surface movement could indicate developing deficiencies.

Measuring points for all movement should be so installed that they are not subject to the movement from freezing/thaw or traffic actions.

1. Horizontal displacement and deflection monitoring

Conventional methods prevalent are alignment surveys covering an extremely wide spectrum of engineering applications, and each of them may require specialized equipment. They have been used in the past and will surely continue to be used for many years. Alignment surveys are accomplished using a "line of sight" as reference line (or benchmark line) by optical or mechanical ways (Williams 1993). Mechanical alignment employs a reference line established by stretched wire (e.g., steel, nylon), such as the plumb line and tension wire. Direct optical alignment (collimation line method) employs optical line of sight or a laser beam to build the reference line. In diffraction alignment, the reference line is created by projecting a pattern of diffraction slits (laser alignment). Geodetic measuring techniques, combined network of triangulation and trilateration, etc., are also widely exercised. For concrete dam foundations and embankment dams, the internal horizontal displacement also may be measured by extensometers, inclinometers, etc.

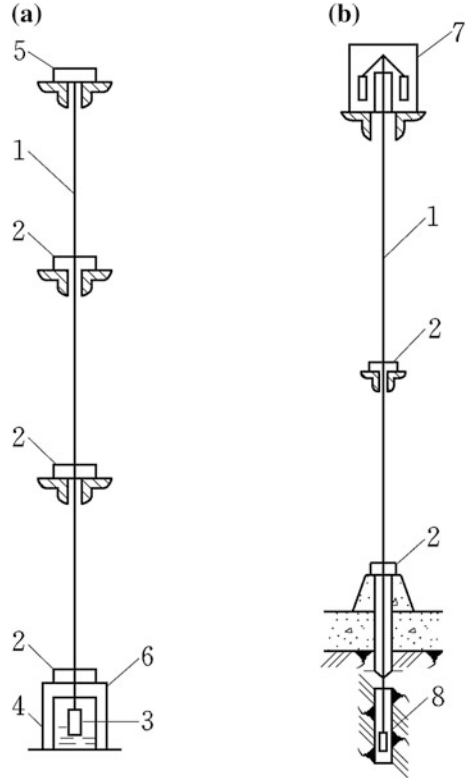
(a) Plumb lines

Plumb lines, inverted plumb lines, and optical plummets are designed to measure bending, tilting, or deflecting, of concrete structures resulting from external loads, temperature changes, sliding, or deformation of the foundation. Through the measurement operation, they will provide information with regard to the general elastic behavior of the entire structure including foundation.

The plumb line consists of a plumb bob suspended from a wire in a vertical shaft within the structure. Measurements for the location of the wire relative to the suspension point are taken at one or more elevations along the shaft by a micrometer or microscope. Plumb lines are simple, inexpensive, accurate, and reliable. These instruments should be located in the structure where unusual structural deflections are anticipated or where information on deflection is required. They should be located in the highest monoliths of the structure and at locations where reading stations will be easily accessible. These reading points are customarily provided in one or more of the galleries in the lower portion of the structure and at other elevations, if practicable. Plumb bob systems based on an inverted pendulum or deflectometer may be installed in structures where a reading station cannot be constructed near the base of the structure, or where it is desired to extend the reference points into the foundation.

Two kinds of mechanical plumbing are prevalent, i.e., suspended plumb line (Fig. 18.2a) and floating or inverted plumb line (Fig. 18.2b). The former installs the fix end near the dam crest, tensions the lowest end with plumb bob; the latter consists of an anchor at the base or in the foundation, a plumb wire, and a floating assembly at the top end of the plumb line which moves freely in a container of oil

Fig. 18.2 Schematic diagram of plumb lines. **a** Suspended plumb line; **b** floating or inverted plumb line. 1 plumb line; 2 measuring instrument; 3 plumb bob; 4 oil container; 5 fixed end; 6 measuring pier; 7 floating assembly; 8 anchor point



and establishes the plumb of its wire from being perpendicular to the surface of the oil. Inverted plumb lines are used in conjunction with conventional plumb lines to extend the length of measurable plumb path and to make reading of a long path easier since both reading stations can be combined in the same shaft. Inverted plumb lines have an advantage over suspended plumb lines in the possibility of monitoring absolute displacements of structures with respect to deeply anchored points in the foundation rock that may be considered as fixed. In the case of dams, the depth of the anchors must be 50 m or even deeper below the dam foundation in order to obtain absolute displacements of the surface points. If invar wire is used for the inverted plumb line, vertical movements of the structure with respect to the bedrock can also be determined.

The number of plumb lines is related to the engineering scale, dam type, and monitoring requirements, and usually, it is no less than 3 for large dams and 2 for medium dams. For a dam with special structure features, it may be divided into 2–3 sections along the height, for each section a plumb line is installed. For each plumb line, no less than 3 observing points should be arranged.

Several types of recording devices that measure displacements of structural points with respect to the vertical plumb lines are available from different companies. The simplest are mechanical or electromechanical micrometers. With these,

the plumb wire can be positioned with respect to reference lines of a recording (coordinating) table to the accuracy of ± 0.1 mm or better. Traveling microscopes may present a same accuracy. The microscope or micrometer slide is precision instrument designed for precise laboratory work and should be used in a manner conforming to good laboratory practice. So far as practicable, all microscope readings should be made by the same individual personnel who is thoroughly familiar with procedures prescribed herein. Whenever it becomes necessary to change observers, either for a short period of time or permanently, the recommended step-by-step operations to be followed in making readings should be carefully explained and demonstrated to the new observer. A written instruction sheet often will be found indispensable.

Automatic sensing and recording is possible, for instance, with a telecoordinator (Huggenberger, Switzerland) and with a telependulum (Telemac, France).

Two sources of error that may sometimes be overlooked by users are the influence of air currents and the spiral shape of the wires. Therefore, the plumb line should be protected within a pipe (e.g., PVC tube) with openings only at the reading tables to reduce the influence of the air currents.

The reading station should be located in the lower portion of the structure in the case of a conventional plumb bob system, as a recess in one of the galleries. There are two measuring methods for the plumb line:

- One-point support and multi-point measurement. This is exercised both for suspended plumb lines and for inverted plumb lines. The measured data of suspended plumb lines are the relative horizontal displacement of the suspended point with regard to the measuring point, denoted as S in Fig. 18.3a, while the deflection at the measuring point N is $S_N = S_0 - S$. The measured data of

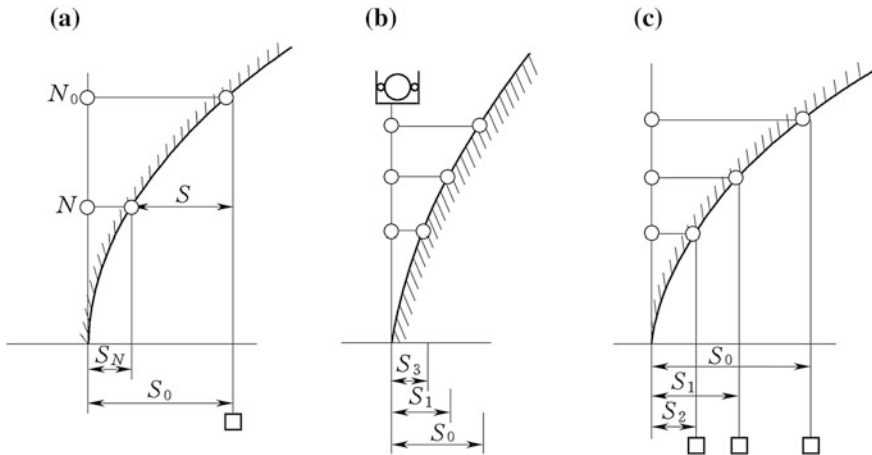


Fig. 18.3 Diagram to the measuring principles of plumb line. **a** One-point support and multi-point measuring (suspended plumb line); **b** one-point support and multi-point measuring (inverted plumb line); **c** multi-point support and one-point measuring (suspended plumb line)

inverted plumb lines are the relative horizontal displacement of the measuring point with regard to the anchored point in deep foundation, as shown in Fig. 18.3b.

- Multi-point support and one-point measurement (Fig. 18.3c). This is only exercised for suspended plumb lines. Supporter is installed at each measuring point, which clamps the plumb line in sequence during the measuring operation. The instrument is installed at the bottom of the plumb line, to obtain the relative horizontal displacement with regard to the measuring instrument.

(b) Tension wire alignment

Tension wire alignment belongs to mechanical alignment methods, where tensioned wires of 0.8–1.2 mm in diameter using stainless steel are installed as the reference lines. It has found many applications including dam deformation surveys, attributable to its simplicity, high accuracy, and easy adaptability to continuous monitoring of structural deformations using inductive sensors applicable over distances up to several hundred meters. Accuracies of 0.1 mm are achievable using mechanical alignment method.

Tension wire alignment comprises benchmark monument piers, reading points, stainless steel wire, and protecting pipe of wire. Tension wire is commonly installed at the dam crest or at longitudinal galleries of different altitudes, while the benchmark monuments are installed on the banks. Where restrained by topographic conditions, monuments also may be installed on dam, and under such circumstances, the displacements of monuments should be measured by the other methods, to obtain absolute horizontal displacement.

Monument piers are constructed using reinforced concrete, on which tension disk, pulley, and plumb bob are installed. On the reading point, there is a floating box and a staff gauge, as shown in Fig. 18.4. The protect pipe for wire is ordinarily transparent PVC tube of 10 cm in diameter.

Tension wire alignment is widely exercised in gravity dams, such as the Gezhouba Project ($H = 53.8$ m, China) and the Danjiangkou Project ($H = 97$ m,

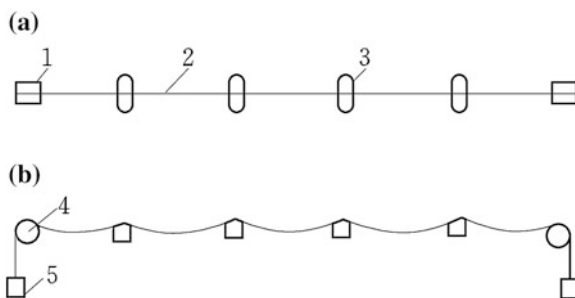


Fig. 18.4 Schematic diagram of tension wire alignment. **a** Plan; **b** elevations. 1 end; 2 tension wire; 3 displacement reading point and floating box; 4 pulley; 5 plumb bob

China). Automatic remote sensing and recording are also possible to improve its monitoring accuracy and efficiency.

(c) Collimation line

Collimation line belongs to direct optical methods utilizing either an optical telescope and movable targets with micrometric sliding devices or a collimated laser beam (projected through the telescope) and movable photo-centering targets. In addition to the aforementioned influence of atmospheric refraction, pointing and focusing are the main sources of error when using optical telescopes.

Horizontal surface movements are conventionally measured as offsets from a baseline. The measuring points for the level surveys are normally used for alignment surveys, too. The methods and equipments depend on the type of dam and the desired accuracy.

For embankment dams, one or more lines of measuring points are established along the crest and on the slopes parallel to the crest. Instrument and target monuments are set at the ends of the lines on the abutments far beyond the dam. To measure the dam movement, a theodolite is laid on the instrument monument on one abutment and sighted to the target monument on the opposite abutment. Offsets from the line of sight are then measured for each measuring point using a plumb bob and tape. Typically, survey methods and equipments should be sufficiently accurate to discern a movement on the order of 30 mm.

For concrete dams, a similar procedure is employed, but with refinements to raise the measuring accuracy. Measuring points are established along straight lines on the crest and, in some cases, along the face of the dam. The measuring points are markers set in the dam concrete. Instrument and target monuments are established outside the dam at the baseline ends on the banks. The monuments are customarily 0.2–0.25 cm diameter concrete-filled pipes buried at least 3 m into the ground. The top of the instrument monument is fitted with a threaded plate to accommodate a theodolite. The target monument is fitted with a threaded plate to accommodate a target. The line of sight is established using a high-precision theodolite set on the instrument monument and sighted to the target on the target monument. Offsets from the baseline are measured with a micrometer attached to a moveable target leveled over each measuring point. Typically, survey methods and equipments should be sufficiently accurate to discern a movement on the order of 3 mm.

Alignment surveys are the simplest for determining horizontal movement in straight dams. However, their application is restricted in cases of curved dams, irregularly shaped dams, or where the line of sight is limited and the number of measurement points along any line is insufficient. Another limitation of alignment surveys is the labor cost, although modern surveying equipments have reduced the time needed to perform a survey.

Collimation line using theodolite is convenient, but its accuracy is not competent for long-distance observation, due to the influence of telescope amplification and refraction of the theodolite. Therefore, the collimation line for concrete dams has a tendency of being replaced by the plumb line and tension wire alignment.

(d) Laser alignment

Laser alignment belongs to diffraction alignment methods, in which the pinhole source of monochromatic (laser) light, the center of a plate with diffraction slits, and the center of an optical or photoelectric sensor, establish three basic points, as shown in Fig. 18.5. If two of the three points are fixed, then the third may be aligned by centering the reticule on the interference pattern created by the diffraction grating.

As shown in Fig. 18.6, the pinhole source of monochromatic (laser) light is located at position A, and the zone plate is located at position i . If the point i moves toward j by a deflection l_i , the deflection is L_i on the sensor. According to the principle of similar triangles, we have

$$l_i/L_i = S_{Ai}/S_{AB} \tag{18.1}$$

where S_{Ai} and S_{AB} = distance from the point A to the points i and B, respectively.

Let

$$S_{Ai}/S_{AB} = K_i \tag{18.2}$$

where K_i = correction coefficient of the deflection at B with respect to the reading point i .

Therefore, Eq. (18.1) may be rewritten as

$$l_i = K_i L_i \tag{18.3}$$

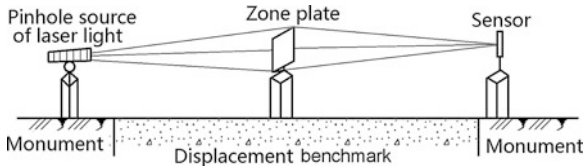


Fig. 18.5 Laser collimation with zone plate

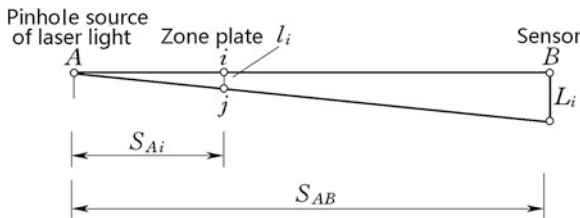


Fig. 18.6 Diagram to the deflection computation of laser collimation with zone plate

It should be pointed out that the movements of the laser and of its output do not influence the accuracy of this method because the laser serves merely as a source of monochromatic light placed behind the pinhole and not as the reference line. Therefore, any kind of laser may be employed in this method, even the simplest and least expensive ones, as long as the output power requirements are met. Various patterns of diffraction slits are used in engineering practice. The highest accuracy and the longest range are obtained with the so-called Fresnel zone plates that perform as focusing lenses.

The influences of the thermal turbulence of air in the open atmosphere may be reduced by vacuum pipe. Laser collimation with airless pipe in a vacuum, rectangular Fresnel zone plates with an electro-optical centering device was used in the deformation measurements of a 3-km-long nuclear accelerator giving relative error of 10^{-7} with respect to the distance measured. The key issue in the laser collimation with airless pipe is the rational value of the vacuity in tube.

The laser diffraction alignment has been successfully performed in the monitoring of both the straight and curved (arched) dams using self-centering targets with automatic data recording. In December 1978, the first laser collimation with airless pipe was installed in the Fengman Gravity Dam ($H = 90.5$ m) in China, which is 194 long and possesses 4 reading points. Until 1984, altogether 999.4 m-long laser collimation using airless pipes and with 52 reading points had been installed on the crest of the same dam and in its galleries, and automation measuring was accomplished in 1986. So far, more than 2000 laser collimations with airless pipes have been installed for the displacement monitoring in the Three Gorges Project ($H = 175$ m, China).

(e) Borehole inclinometer

Inclinometers are commonly installed in vertically drilled holes in dams and foundations/abutments. They are instruments ideally suited to long-term and precise monitoring of the position of a borehole over its entire length.

An inclinometer consists of specially shaped plastic casing with four longitudinal grooves cut in the inside wall, a probe that is lowered down the casing on an electrical cable with graduated depth markings (Fig. 18.7) and readout device.

The probe contains two accelerometers detecting the inclination angle of gravity acceleration g at the relative plane of their axis by measuring the tilt of the probe in two mutually perpendicular directions. The probe is also equipped with a pair of wheels that run in the grooves in the casing and maintain the rotational stability of the probe. Inclination of the casing is measured using the probe at regular intervals by which the lateral movement with respect to the bottom of the casing is calculated. By making a series of readings over time, it is also possible to monitor the rate of movement.

The primary requirement for accurate measurement is to extend the borehole below the depth of movement so that readings made from the end of the hole are referenced to as a stable base. Precautions are also needed during the installation of the casing to maintain the vertical alignment of the grooves and to prevent spiraling. Readings are made by lowering a probe to the end of the hole and then raising it in

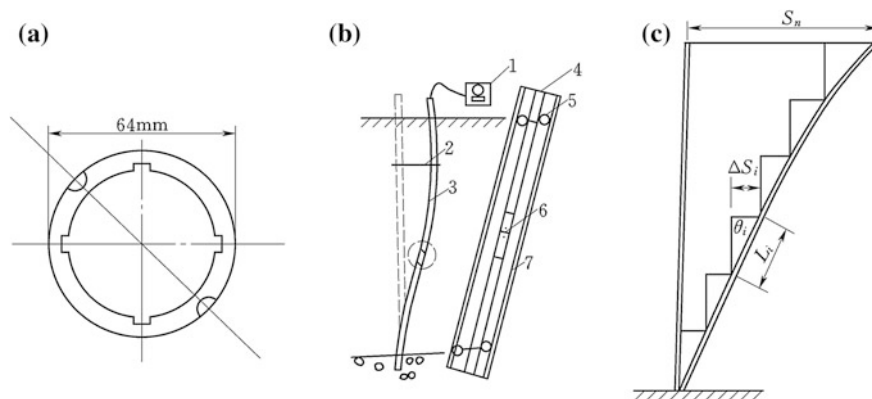


Fig. 18.7 Schematic diagram of inclinometer

increments equal to the length of the wheelbase L ($=0.5$ or 1 m) of the probe. At each depth increment, the tilt θ_i is measured, and then, the displacement ($L \sin \theta_i$) for each increment and the total displacement at the top of the hole ($\sum_i L \sin \theta_i$) are calculated. A check of the results is conventionally made by rotating the probe by 180° and taking a second set of readings. Another precaution is to allow time during the readings for the probe to reach temperature equilibrium in the borehole.

2. Vertical movement and inclination monitoring

Vertical surface movements are commonly measured by differential leveling techniques including geometric leveling and hydrostatic leveling (Unguendoli 1984). Reading points are established on the crest or slopes of the dam. Reading points for embankment are commonly materialized using steel bars embedded in concrete placed in the fill, whereas reading points for concrete dam are commonly materialized using bronze markers set in the concrete or scratch marks. Typically, survey methods and equipments for embankments should be sufficiently accurate to discern a movement on the order of 30 mm, whereas survey methods and equipments for concrete structures should be sufficiently accurate to discern a movement on the order of 3 mm. Level surveys are simplest and most accurate for determining vertical movement of a hydraulic structure.

(a) Geometric leveling

Geometric leveling is an old method of geodetic surveying employed to measure elevation difference between two points at the structure surface. Two types may be distinguished as geometric (or direct) leveling and trigonometric (or indirect) leveling. The geometric leveling is featured of highly precise, lighter monument, less expensive in equipment and fieldwork, and easier in operation procedures.

In geometric leveling, the difference of height between two points is determined by the difference of readings to the staffs placed on those points. The readings are made with a leveling instrument such as optical level.

An optical level consists of a telescope fitted with crosshairs and rotating around a vertical axis, with a very sensitive spirit level or other device fixed to it that enables the line of sight to become horizontal. The reading on a graduated vertical staff is measured through the telescope. If staffs are placed on successive ground points, and the telescope is truly leveled, the difference between the readings at the crosshairs will be equal to the altitude difference between the points.

The points in a leveling line fall into three categories:

- Object points, i.e., points that are to be measured;
- Reference points;
- Benchmark points.

Under certain circumstances, auxiliary points also may be installed.

Benchmark points are the basis of absolute vertical displacement leveling. They should be located at a proper distance from the structure without the influence of its displacement and with solid foundation. For medium-to small project, one or two benchmark points are sufficient, whereas for large project, two or three benchmark points may be needed; for particular large project, fine leveling network system is demanded, which includes all benchmark points and reference points.

When the reference points are located in the area to be controlled (and therefore might undergo displacements), only relative displacements can be determined. Where reference points are located outside of that area, tied to bedrock or other non-moving structure, absolute displacements can be determined. Although theoretically only one reference point is needed in leveling lines, the experience advises to place at least three reference points, to identify unstable reference points. Auxiliary points are placed, for instance, to avoid too long distances between level and staffs or to link sectors of a leveling line that, otherwise, would be independent.

For concrete dams, object points in rows should be layout both on the dam crest and in foundation gallery, while another row of object points is advisable to be installed in a gallery at middle elevation. Each dam monolith ordinarily possesses one object point, while additional point may be set for important portion. For embankment dams, the object points are ranged along transverse sections located in controlling profiles. The monitoring sections are spaced 50–100 m apart, and at least 4 object points should be set for each monitoring section. Figure 18.8 shows the layout for the vertical movement measurement of dams.

Object points are usually materialized by pegs sealed on the floor or, less usually, by metal pieces, sealed on a wall. The first one is used to place staffs with inferior support, and the second one is to place hung measuring rules. All points must be well tied to the structure concerned. Sometimes, it is necessary to place the points in protected places to prevent them from damage.

Automatic levels, i.e., optical levels with a built-in compensator that employs an extremely sensitive pendulum device, which automatically makes the line of sight horizontal, could be employed. To improve the accuracy, a parallel plate

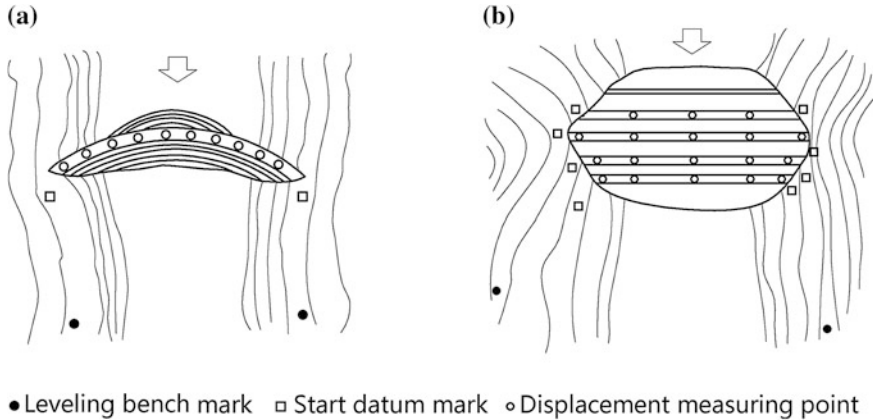


Fig. 18.8 Layout for vertical movement monitoring of dams. **a** Arch dam; **b** embankment dam

micrometer must be fitted over the telescope objective, which permits direct readings on a centimeter graduated staff, to 0.1 mm, and estimated readings, to 0.01 mm. Digital levels are automatic ones with a built-in digital image processing system that permits automatic reading of special staffs (coded bar) and electronic recording. Errors caused by manual reading and recording are eliminated, and the speed of leveling can be raised (by about 30 %).

Rigid invar staffs with scales engraved directly into the paint coat on an invar strip are made of nickel steel alloy that has a linear thermal expansion coefficient of $0.7 \times 10^{-6} \text{ }^\circ\text{C}$ (about 15 times smaller than steel)—a quite important characteristic since the measurements would be undertaken in extreme temperature conditions.

For transferring elevation to the gallery, the shafts for plumb lines or vertical galleries may be employed as shown in Fig. 18.9, where A is a point on the dam with elevation H_A . To measure the elevation of B within the gallery, invar steel rule is hung in shaft, under which the rule plumb bob is submerged in floating box filled with transformer oil for the stability of the rule. Theodolites are installed both on the dam surface and in gallery, and invar staffs are installed at both A and B . The altitude at B is determined by the readings a_1, b_1, a_2, b_2 as follows:

$$H_B = H_A + a_1 - (b_1 - a_2) - b_2 \quad (18.4)$$

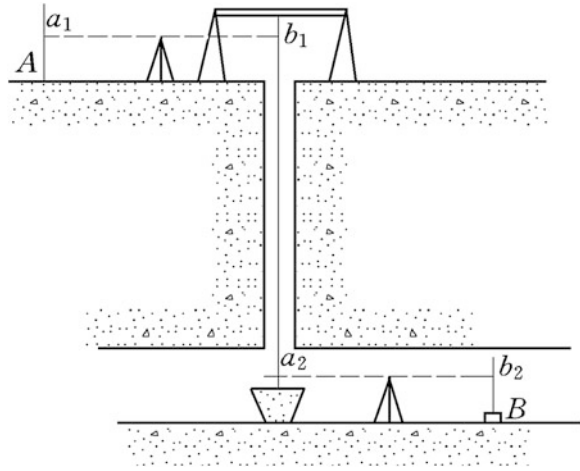
in which the readings b_1 and a_2 of invar steel rule should be revised according to the temperature and rule length.

(a) Hydrostatic leveling

Hydrostatic leveling may be employed to measure differential settlements of floors, footings, columns, walls, and galleries in dams or any structures.

If two connected containers are partially filled with a liquid, then the heights h_1 and h_2 of the liquid in the containers are related through the hydrostatic equation.

Fig. 18.9 Elevation transferring by shaft



Hydrostatic leveling is frequently exercised in the form with a network of permanently installed instruments filled with a liquid and connected by hosepipes to monitor the change in height differences of large structures. The height differences of the liquid levels are automatically recorded. The accuracy ranges from 0.1 to 0.01 mm over a few tens of meters depending on the types of instruments. The main factor affecting the survey accuracy is the temperature. To reduce this effect, either the instrument must be installed in a place with minor temperature variations, or the temperature along the pipes must be measured and corrections applied, or a double liquid (e.g., water and mercury) is employed to derive the correction for temperature effect. Liquid of a constant temperature is pumped into the system just before taking the readings for the highest accuracy applications. The instruments with direct measurement of the liquid levels are restricted in the vertical range by the height of the containers. This problem may be overcome if liquid pressures are measured instead of the changes in its levels, where pneumatic pressure cells or pressure transducer cells may be installed.

3. Crack and joint measuring

In both new and existing structures, the development of cracks and the movement of joints are indications of stresses on the structure that are probably abnormal. In some cases, these conditions can be anticipated beforehand, while in others, the situation arises spontaneously. Measurement of these areas is provided through the displacement indicators that can be either installed in predetermined locations to monitor expected cracks, or placed at the location of a known crack or joint as the need arises for its monitoring.

(a) Crack measuring

These instruments are either manual or electrical, and the latter is adaptable to displacement measurement (Morrison 1984; Raphael and Carlson 1965; Seippel 1983;

Sheingold 1980). The monolith joint displacement indicator, relative movement indicator, multi-position strain gauge, dial gauge, “L”-shaped gauge, and scratch gauge are all manual gauges requiring periodic reading to determine the displacements. The Carlson joint meter and the multiple position borehole extensometer are electrical instruments utilizing the change in electric resistance of a stretching wire as a measure of strain.

Reference points can be scratch marks in the concrete, metal pins, or metal plates on opposite sides of a joint or crack. The distance between the scratch marks is measured with a micrometer or dial gauge to determine the movement. Sometimes, three points are used in a triangle to measure both horizontal and vertical movements.

(b) Joint measuring

Movement of one side of a crack or joint in a concrete structure relative to the other side is commonly measured with reference points or crack meters. Grout or plaster patches can be used to evaluate whether or not a movement is occurring. Crack meters are commercially available devices that allow for the measurement of the movements in two directions. A common device consists of two plastic plates: One is opaque containing a grid, and the other is translucent containing a set of crosshairs. The plates are fixed on each side of the crack or joint with the crosshairs set over the center of the grid. Movement is measured by noting the location of the crosshairs with respect to the grid. In addition, a variety of other crack meters, including Carlson and vibrating wire sensors, dial gauges, and mechanics feeler gauges, may be employed to measure the movement of crack or joint.

Figures 18.10 and 18.11 show the configuration of the horizontal and vertical deformations measured by means of joint meter.

Conventional surveys, however, require “line of sight” and do not lend themselves to unattended, continuous field operations. Their instruments are also restricted in range and do not offer connection to an absolute reference frame. All these make it exceedingly difficult to assess how the dam might have moved with respect to surrounding bedrock.

Monitoring the integrity of a hydraulic structure demands very high precision displacement measurements from a robust system with real-time response. Continuous data recorded from the GPS satellites, using ground-based receivers and robust telemetry, are now more and more prevalent for the safe and health monitoring of hydraulic structures (Colesanti et al. 2003; Wang et al. 2004). Attributable to much less complex, robust automation of highly precise GPS analysis is now reasonably routine (Featherstone et al. 1998; Li et al. 1996).

4. Rock slope movement monitoring

Many rock slopes move to some degrees during the course of their service life. Such movement normally indicates that the slope is in a quasi-stable state, but this condition may continue for many years, or even centuries, without the occurrence of failure. However, in other cases, initial minor slope movement may be a precursor for accelerating movement followed by landslide or collapse. Because of the

Fig. 18.10 Horizontal deformation measuring

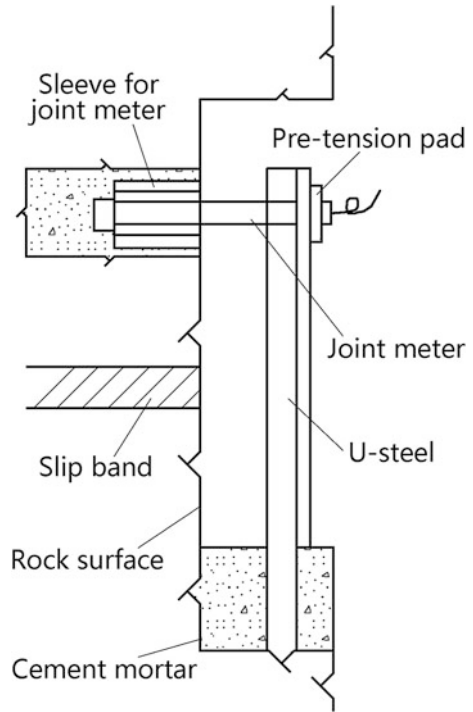
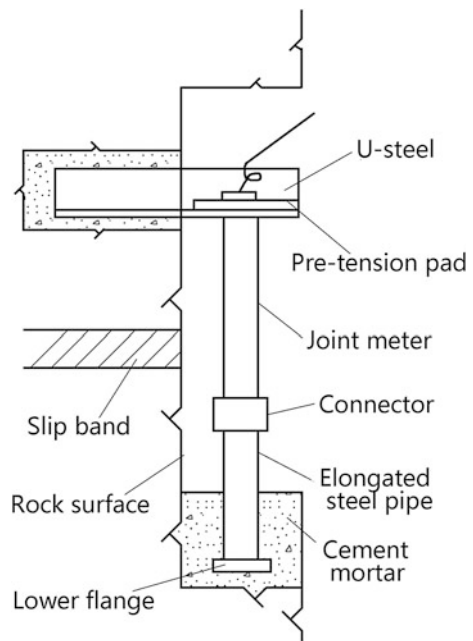


Fig. 18.11 Vertical deformation measuring



strong uncertainty of slope's behavior, movement monitoring programs can be of crucial value in managing slope hazards, which also provide information that is useful for the design of remedial or stabilization works (Dunncliff 1988; Hanna 1985; Peck 1969).

(a) Surface monitoring

In general, monitoring of a slope surface is likely to be less costly to set up and maintain than subsurface monitoring that will demand drilling holes to install the instruments. However, surface monitoring can only be exercised where the surface movement accurately represents the overall movement of the slope. For example, it would not be appropriate to make surface monitoring where loose rock blocks on the surface were toppling and rotating independently of the main slope movement. Other factors to consider in the selection of a monitoring system include the time available to set up the instruments, the rate of movement, and safe access to the site.

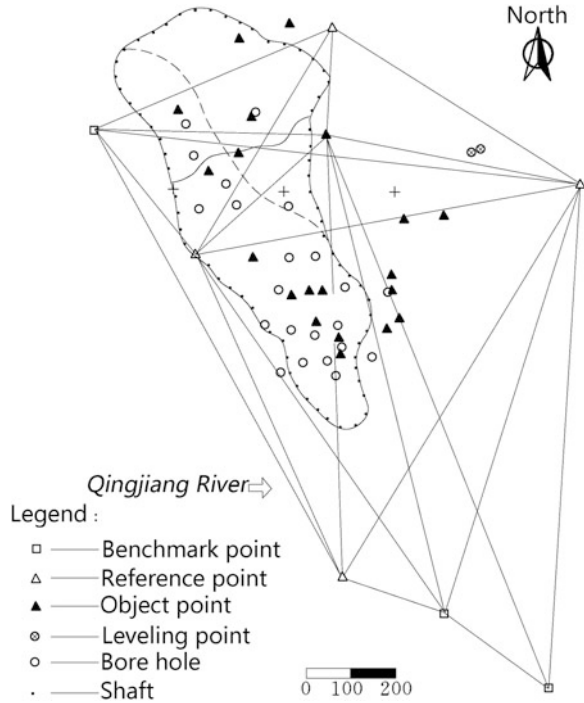
Options for monitoring equipment comprise automation for collecting data at preset intervals on loggers and using telemetry to transmit these results to another location for analysis and plotting. The system can also incorporate alarms that are triggered if preset movement thresholds are exceeded. An important consideration of such automated systems is the cost of installation and maintenance, which normally restrain their use to high hazard locations, and for temporary situations while longer-term stabilization is implemented.

Surface monitoring for slopes comprises monitoring on land surface deformation, surface crack, etc.

Land surface deformation is a routine item in the slope mentoring, which makes use of theodolite, water level gauge, tiltmeters, electronic total station, and the Global Positioning System (GPS). Figure 18.12 is the layout of the land surface deformation monitoring of the Yangjiacao Landslide (Hubei Province, China).

Since tension cracks are an almost universal feature of slope movement, crack width measuring is often a reliable and inexpensive means of movement monitoring. The simplest procedure is to install a pair of pins on either side of the crack and measure the distance between them with a steel tape. If there are two pins on either side of the crack, then the diagonal distance can also be measured to check the transverse (shear) displacement. The maximum practical distance between the pins is ordinarily 2 m. The wire extensometer can be employed to measure the total movement across a series of cracks over a distance as far as 20 m. The measurement station is located on stable ground beyond the cracks, and the cable extends to a pin located on the crest of the slope. The cable is tensioned by the weight, and the movement is measured by the position of the steel block threaded on the cable. The wire extensometer also can incorporate a warning system comprising a second steel block threaded on the cable that is set at a selected distance from a trip switch. If the movement exceeds this preset limit, the trip switch is triggered and an alarm is activated. The main requirements for the crack width monitoring are that the upslope pin or reference point must be on stable ground and that people should access the crest of the slope to make the measurements. This monitoring work could be hazardous where the slope is moving rapidly. Under such circumstances, it

Fig. 18.12 Layout of the surface deformation monitoring—the Yangjiacao Landslide, China



should be replaced by automated system using vibrating wire strain gauges and data loggers, to read and record the measured results from a remote location.

(b) Subsurface monitoring

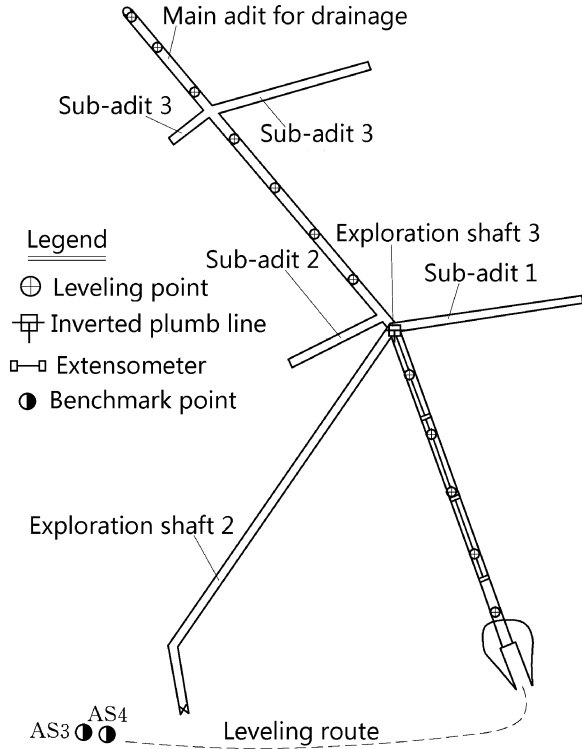
Figure 18.13 shows the layout of the subsurface monitoring of the Yangjiacao Landslide.

Subsurface monitoring of slope movement is often an important task of the monitoring program in order to provide a more complete image of the slope behavior. The main purpose of the measurement is to locate the slip surface or surfaces and to monitor the rate of movement. Inclined meters are commonly employed in the subsurface monitoring. In some cases, the holes (shafts) are used for monitoring both the movements and water pressures. When the slip surface is revealed by the shaft or adit, joint meter or time-domain reflectometry may be employed to monitor the slip deformation.

(c) Shear deformation measuring

The shear deformation measuring usually makes use of joint meter, as shown in Figs. 18.10 and 18.11.

Fig. 18.13 Layout of the subsurface deformation monitoring—the Yangjiacao Landslide, China



(d) Time-domain reflectometry

Time-domain reflectometry is another means of locating a slip surface, which is also able to monitor the rate of movement. This involves grouting into a borehole a coaxial cable comprising inner and outer metallic conductors separated by an insulating material. When a voltage pulse wave is sent down the cable, it will be reflected at any point where there is a change in the distance between the conductors. The reflection takes place due to the change in distance that alters the characteristic impedance of the cable. Movement of a slip surface that gives rise to a crimp or kink in the cable will be sufficient to change the impedance, and in this way, the location of the slip surface can be detected.

The primary advantage of time-domain reflectometry compared to inclinometers is that the cable is inexpensive so that it can be sacrificed in a rapidly moving landslide. In addition, the readings can be made in a few minutes from a remote location either by extending the cable to a safe place off the slide, or by telemetry, to reduce travel time and to directly show the movement without the need to download and plot the results.

18.4.2 Seepage Monitoring

1. Uplift pressure

(a) Uplift pressure under concrete dams

Monitoring of uplift pressure under concrete dams is made to check the validity and accuracy of the design assumptions pertaining to uplift and to provide information for the future designs with regard to the exerting surface and magnitude of uplift pressure.

The measuring points are layout according to the importance, type, size, foundation geology, seepage prevention and draining devices, etc., of the dam concerned. Customarily, several sections perpendicular to the dam axis are set for uplift monitoring, and they are commonly located at the monoliths with maximum dam height, on main river stream, with poor foundation bedrock, and where the stability analysis is conducted in design. In addition, it is advisable that they are at the positions with transverse galleries, to facilitate the measuring operation. The section number is normally 2–7 and mostly 3–4. The point layout in a monitoring section is dependent on the section size and structural and geological features along creep line and within foundation, for the purpose of good representation of uplift distribution and variation. Generally, the following principles are to be observed in the layout:

- To understand the effects of anti-seepage devices, one point on the downstream side of grout curtain, cutoff wall, dental wall, sheet pile, etc., is desirable;
- To understand the effects of seepage pressure relief, one point on the downstream side of draining curtain is desirable;
- One point at the base of structure and at the vicinity of downstream toe is desirable.

Apart from the above transverse sections, additional longitudinal section is also commonly established, which is along the dam axis, at which 1–2 points are located for each dam monolith. An illustrative instrumentation layout for the uplift pressure of a new concrete dam is shown in Fig. 18.14.

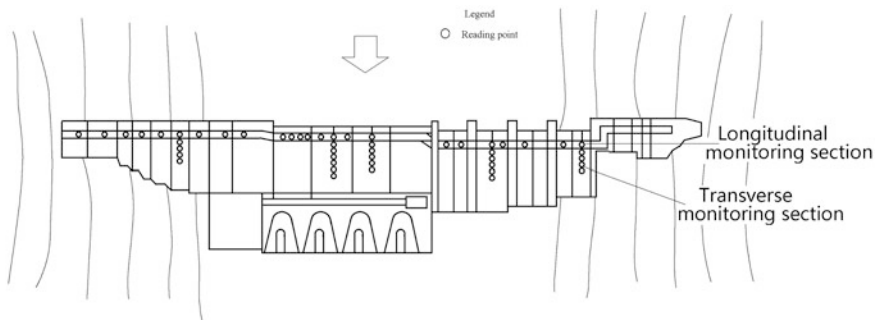


Fig. 18.14 Instrumentation layout of the uplift pressure in a concrete dam

(b) Uplift pressure in embankment dams

Measuring of uplift in embankment dams is accomplished according to the importance and scale of the reservoir, the type and size of the dam, foundation stratum, seepage prevention and relief devices, etc. The monitoring sections are usually the most important and the most representative ones in the design of seepage control, and they are generally spaced 100–200 m apart. For medium-height dam or above, at least 3 monitoring sections are demanded, whereas for small dam, at least 2 sections are required.

The measuring points in each monitoring section are adequate to illustrate the seepage regime such as the phreatic line and the working situation of important components (anti-seepage device, seepage pressure relief, and filter). Figure 18.15 shows the minimum number of monitoring points in different types of embankment dams.

(c) Uplift pressure under embankment dams

The typical monitoring layout for uplift pressure under embankment dams is shown in Fig. 18.16.

(d) Bypass seepage and groundwater at the vicinity of dams

Bypass seepage monitoring is mainly intended to obtain sufficient observed data available for isopotential line plotting, whose basic requirements are as follows:

- At least two rows, each of them consisting of at least 3 points, are laid out along the anticipated streamline;
- At mesa terrace along the main stream, 2–3 rows, each of them consisting of at least 3 points, are laid out perpendicular to the anticipated streamline;
- 1–2 rows of measuring points may be laid out at the permeable stratum with potentially concentrated seepage;
- The points for phreatic line observation should be embedded at least deeper than the water table before the dam impounding.

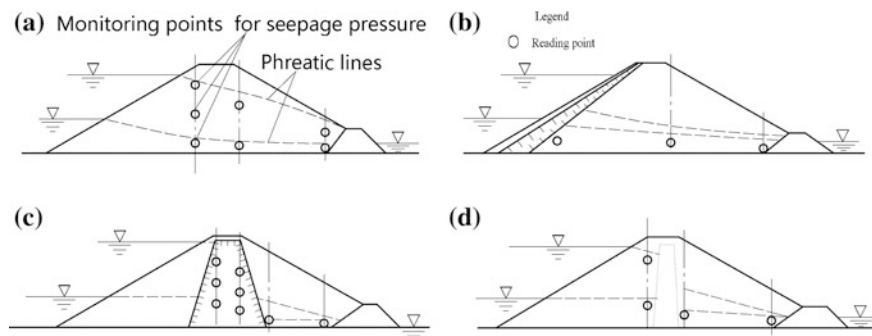


Fig. 18.15 Instrumentation layout of the uplift pressure in embankment dams. **a** Homogeneous; **b** sloping core; **c** broad central core; **d** narrow central core

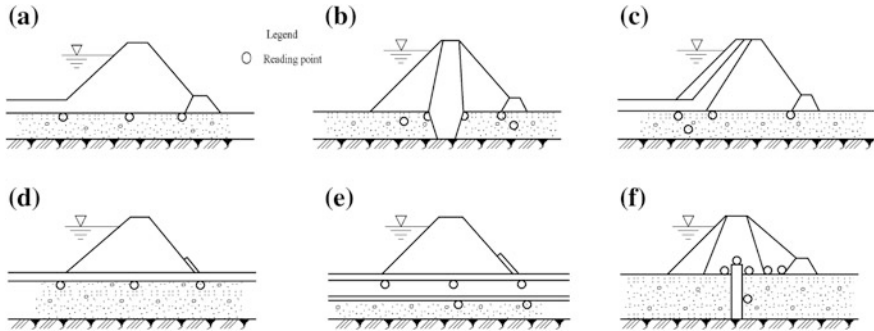


Fig. 18.16 Instrumentation layout of the uplift pressure under embankment dam

Figure 18.17 shows the layout of bypass seepage and groundwater monitoring.

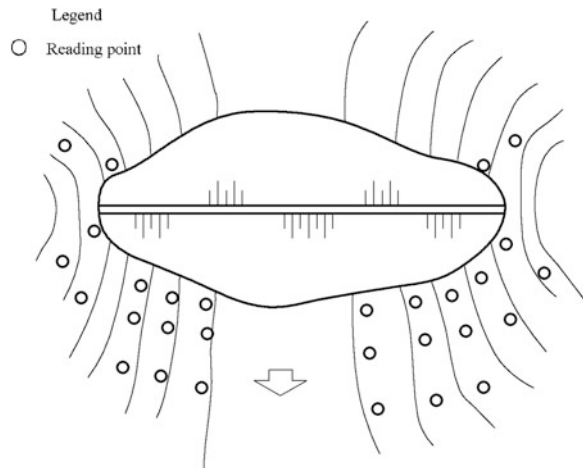
(e) Seepage pressure in rock slopes

The importance of seepage pressure to the slope stability has been well emphasized (Vide Chap. 14). If a reliable design concerning slope stability is guaranteed, it is essential that seepage pressure within the slope should be well monitored. It is most conveniently carried out by the observation of groundwater table directly in borehole, or of seepage pressure using piezometers that are devices sealed within the ground, generally in boreholes, which respond only to seepage pressure in the immediate vicinity.

(f) Instruments for uplift (seepage) pressure measurement

Being simple, reliable, inexpensive, and easy to operate, open standpipe piezometers are standard against which all other piezometers are calibrated. Open

Fig. 18.17 Layout for the bypass seepage and groundwater monitoring in an embankment dam



standpipe piezometers are also known as Casagrande-type piezometers and, in concrete dams, as pore pressure cells. They are observation wells with subsurface seals that isolate the strata to be measured. The seals are usually made of bentonite clay or cement grout, and care must be taken during the installation to ensure a good seal. Riser pipe joints should be watertight to prevent the leakage into or out of the pipe, which could deviate the water level in the pipe.

A common version of the open standpipe piezometer is a well point, which is a prefabricated screened section and riser pipe that is pushed into place. If the screened section is not adequately sealed, it will perform like an observation well rather than a piezometer.

The sensing zone (screened length or porous tip) of observation wells and open standpipe piezometers is susceptible to clogging, which can give rise to time lag or result in failure of the instrument. This can be diminished by a properly designed filter pack that meets filter criteria with the surrounding soil and properly sized perforations that are compatible with the filter pack.

The other evolved types of the piezometers available from various manufacturers are that of closed standpipe, twin-tube hydraulic, pneumatic, vibrating wire, bonded resistance strain gauge, hydraulic pore water pressure cell, etc.

2. Seepage discharge

The amount of seepage or leakage is directly proportional to the material permeability and seepage pressure. Periodic monitoring of the outflow from foundation drains, joint drains, and face drains serves as an indication of the adequacy with respect to foundation grout curtain and good functioning with regard to drains and reveals when and where remedial measures could be undertaken. Observations of leakage flow from contraction joints, lift joints, and cracks provide a means for judging the quality of construction, as well as for disclosing the necessity for remedial actions to preserve the integrity of the structure.

The main drainage sump may be utilized as a collecting and gauging point for all flows. Two types of gauges, namely V-notch weirs and critical depth meters, are available for the discharge measuring.

(a) Layout

For embankment dams, the commonly used configuration is to collect the seeping water from dam body or foundation into downstream gutter, and the measuring operation is undertaken at the exit of the gutter. For concrete dams, both the total discharge collection, and, the measuring operation, may be made at the sump in dam body.

(b) Instruments

Seepage and leakage are commonly measured with calibrated containers and weirs. Other flow measuring devices such as flowmeters also may be appropriate under special circumstances.

- Calibrated containers. They are preferable for the discharge smaller than 1 L/s, or where it is not permissible to use devices of long-term seepage collection and releasing. The collection time for seeping water into the container should be not shorter than 10 s;
- Weirs. They are applicable for the discharge of 1–300 L/s. Thin-plate weirs, such as rectangular weir, Cipolletti trapezoidal weir, and 90° V-notch weir, may be installed at the straight section of a gutter for the purpose of measuring, as is illustrated in Chap. 16 of this book.
- Flowmeters. They are suitable for measuring larger flow discharge.

18.4.3 Strain/Stress and Temperature Monitoring

A variety of mechanical and electrical strain gauges may be employed to measure the strains in concrete dams. Some of the instruments are designed to be embedded in the dam during the construction, and the others are surface-mounted following the construction. Strain gauges are often installed in groups so that the three-dimensional state of the strain can be evaluated.

Stress in concrete structures can be directly measured with total pressure cells or Carlson-type cells designed to have stiffness similar to the concrete. It also can be measured indirectly by overcoring.

For indirect stress measured via strain, the Young's modulus, creep coefficient, and Poisson's ratio of the concrete should be determined by the laboratory tests using concrete cylindrical samples from prototype dams.

In mass concrete, temperature variation is the primary cause of volumetric change and stress. In order to determine the effect of temperature on the stress and volumetric change, temperatures should be measured at a number of points within the structure, as well as at the boundaries. The resistance thermometer and thermocouple are normally employed to measure the temperature in concrete (Baker et al. 1953). Thermocouples are preferable for measuring temperature under certain conditions and at several locations. However, resistance thermometers are advantageous over thermocouples because they are more reliable, highly precise, and less complicated in measuring operation.

1. Strain/stress monitoring

The general requirements with regard to monitoring monoliths, sections, levels, and points should be met as follows:

- Be able to detect the maximum stress (quantity and direction);
- Be convenient for the validation among observation, design, and experiment;
- Be conforming to the other monitoring facilities for comprehensive analyses of the structure;

- Be allowable of certain repeated installations of monitoring points to secure the reliable monitoring for important positions;
- Be facilitated for the installation construction and monitoring operation.

(a) Gravity dams

- Monitoring monoliths. Usually, at least one observation monolith is, respectively, selected from non-overflow and overflow dam monoliths, and additional monoliths may be desirable for important dams on complicated foundation;
- Observation sections. 1–2 monitoring sections may be set for each observed monolith;
- Observed levels. Apart from the level near foundation (lower than 5 m above base), several observation levels may be selected taking into account dam height and structure feature;
- Reading points. 3–5 strain meter groups or stress meters are commonly laid out for each observation level. The minimum distance of the points from dam surface is 3 m. Two additional points may be positioned at a distance of 1.5–2.0 m from the longitudinal joints. Additional points also may be laid out near the dam surface for measuring the surface stress, if necessary.

As the advancement in the understanding of stress state, in recent years, the stress monitoring for concrete gravity dams has been greatly simplified, and some low-gravity dams even neglect the stress instrumentation totally.

(b) Arch dams

- Observation sections. The crown cantilever section, and the abutment cantilever sections, may be selected for monitoring. For important dam, radial cantilever sections located at 1/4 crest length from the central line may be additionally selected for monitoring;
- Observed levels. Apart from the level near foundation (lower than 5 m above base), several levels may be observed taking into account dam height and structure feature;
- Reading points. Two points from up- and downstream surface in a depth around 1 m should be monitored, with additional point at the center. Denser points are desirable for thick dams or where the temperature monitoring is demanded.

(c) Instruments for concrete dams

Single strain meters, strain meter groups, or stress meters are prevalent in the strain/stress monitoring of concrete dams. To obtain both the quantity and direction of strain/stress, strain meters are often integrated into groups of multi-directional meters as “strain meter spider” (Carlson 1975) as shown in Fig. 18.18. For the purpose of measuring independently the volumetric effects due to temperature and moisture changes and chemical actions within a large structure, “no-stress” strain

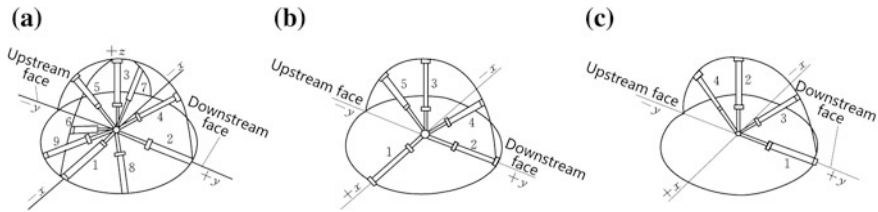


Fig. 18.18 Schematic of strain meter groups. **a** 9 directional meters; **b** 5 directional meters; **c** 4 directional meters

meters are installed in conjunction with strain meter groups. This can be accomplished by embedding an ordinary strain meter in typical mass concrete which is isolated from the deformations due to loading, but is responsive to the temperature, moisture, and growth volume changes in the structure.

The installation of multi-directional meters is usually carried out under the following circumstances:

- Gravity dams. 5 directional meters are commonly used, of which 4 strain meters are in the sectional plane, while the rest one is perpendicular to the section;
- Arch dams. 9 directional meters or 5 directional meters are commonly used, of which the latter has 4 meters in the sectional plane, while the rest one is perpendicular to the section;
- Near the dam base. Where the compression stress is the maximum, single stress meter may be installed;
- Boundary groups. They consist of several meters (from three to six) and may be placed at a depth of 0.1–1 m from a surface of structure, with each meter arranged in a plane parallel to the surface concerned;
- At the toe/heel of dam/foundation contact face, single strain meter, single joint meter, and reinforced concrete meter (R-C meter) may be installed, to check the real stress state in these areas.

(d) Embankment dams

Normally, 1–2 transverse sections may be selected for monitoring, and on each of them, 2–3 levels with reading points may be arranged. The points may be within anti-seepage device, downstream shell, contact face of anti-seepage device/dam shell, etc., as illustrated in Fig. 18.19.

Earth pressure cells are commonly employed in the stress monitoring for embankment dams. To obtain both the quantity and direction of stress, earth pressure cells are often integrated into group of multi-directional meters (2–3 for each group).

(e) Concrete faced rockfill dams

Typical face slab slices, such as the slab slices at portions of the mainstream, abutments, and in between (1/4 of crest length), are selected for monitoring, as

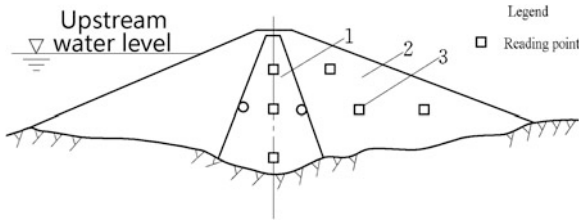


Fig. 18.19 Monitoring layout for the stress in an embankment dam. 1 core; 2 dam shell

shown in Fig. 18.20. The highest slab slice shall replace the middle one where they are not coincidence. The first and second abutment slab slices in close vicinity to the banks are not appropriate to be monitored. The strain sensors and reinforcement meters are laid out at portions lower than the normal storage level, which may be sparse at the upper portion and denser at the lower portion.

(f) Slopes

- ① Prestressed wire strand anchor cables. Dynamometers are customarily set to monitor the prestress. Conventional dynamometers for prestressed anchor are pressure transducer, vibrating wire pressure cell, strain gauge pressure cell, and liquid pressure cell. The Chinese design codes stipulate that the number of long-term observed anchors should be no less than 5 % than that of the total anchors installed.
- ② Stabilization piles and shear keys. Pressure cells are normally applied, which have various types according to their working principles. In the type selection of pressure cells, the major factors to be taken into account are the measuring range and precision, earthquake and impact resistance, tightness, etc.

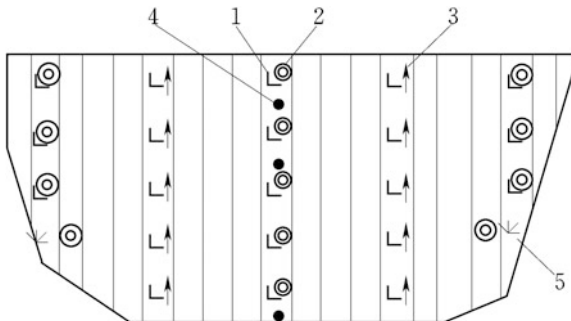


Fig. 18.20 Stress monitoring layout for a CFRD. 1 2 directional meters; 2 “no-stress” strain meter; 3 reinforcement meter; 4 temperature sensor; 5 4 directional meters

(g) Others

Reinforcement meters are required in the area of galleries, penstocks, and piers, for monitoring the stress in steel bars.

Earth pressures within fill against concrete structures are commonly measured with earth pressure cells. These are also known as total pressure cell consisting of two flexible diaphragms sealed around the periphery and with a fluid in the annular space between the diaphragms. Pressure is determined by measuring the incremental fluid pressure behind the diaphragm with pneumatic or vibrating wire sensors. Earth pressure cells should have similar stiffness as the surrounding soil to avoid error due to arching. Soil pressures against structures can also be measured with a Carlson-type cell, which consists of a chamber with a diaphragm on the end, and the deflection of diaphragm is measured by a Carlson-type transducer and converted to pressure.

2. Temperature monitoring

Temperature monitoring of dam and foundation is frequently demanded for reducing data from instruments, raising precision, or interpreting results. For example, movements and leakage changes of concrete dams are commonly related to the changes in temperature. Temperature is also commonly measured in the concrete dams under construction to evaluate the placement design (e.g., mix, rate, block, and lift size), to schedule grouting of construction joints, and to provide thermal loads. Temperature measured from seeping water may indicate the sources of seepage.

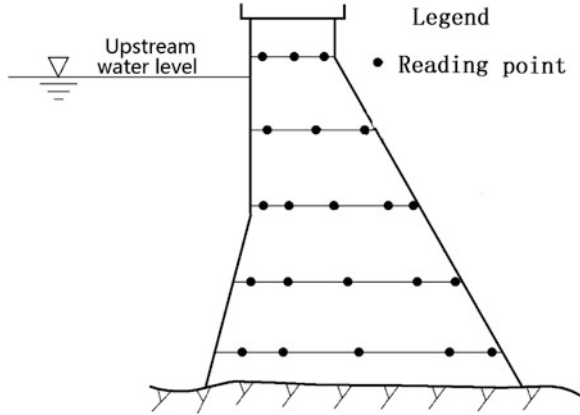
One of the common layouts would be to place thermometers spaced about every 8–15 m apart along an elevation in the monolith. For a small structure, a denser spacing may be desirable. A few thermometers should be placed near the structure faces to evaluate the daily and weekly temperature fluctuations. Another layout commonly exercised is to configure observation lines of thermometers parallel and transverse to the structure axis and in a vertical direction as well. The space of the reading points may be very small near the exposed surfaces and quite large in the interior regime with more uniform temperature. Near or crossing construction joints, it is conventional to position reading points close to the joint surface for temperature monitoring.

(a) Internal temperature

The monoliths, sections, and levels, for internal temperature monitoring, are commonly identical to that for strain/stress monitoring.

The temperature monitoring points for a gravity dam on one level are laid out at the space of 8–15 m, which is subject to be more concentrated around holes and near boundaries and less concentrated in the central portion of dam. Monitoring sections perpendicular to the penstocks are demanded. To facilitate the construction, the monitoring points are ordinarily laid out on the surface of lift joint. Figure 18.21 is a schematic layout of the temperature monitoring for a gravity dam.

Fig. 18.21 Layout of the temperature monitoring for a gravity dam



For monitoring the crown cantilever section of an arch dam, 3–7 monitoring levels are normally laid out, and on each level, at least 3 monitoring points are set. The portions near crest and abutment are subject to more concentrated points. Figure 18.22 is a schematic layout of the temperature monitoring for an arch dam.

(b) Boundary temperature

Points for boundary temperature monitoring may be laid out at a distance of 5–10 cm from upstream surface and is commonly $1/10 \sim 1/15$ of the dam height but may be doubled below the inactive storage level. On the downstream surface, temperature sensors are also laid out to evaluate the influence of sunshine.

(c) Foundation temperature

Temperature transducers should be laid out along the contact face of dam/foundation on the monitoring section. To understand the heat dispersion procedure, at the mid of contact face, a vertical monitoring line may be installed using several sensors, as shown in Fig. 18.23.

Fig. 18.22 Layout of the temperature monitoring for an arch dam. **a** Cantilever section; **b** arch section

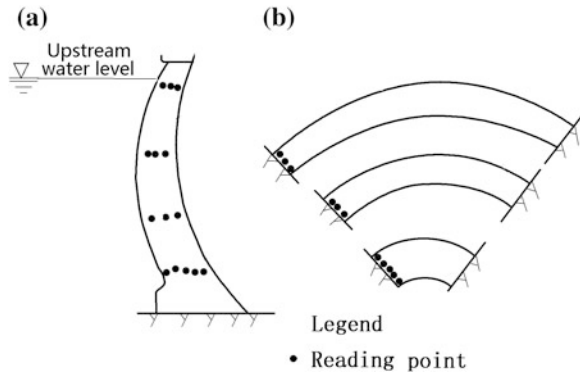
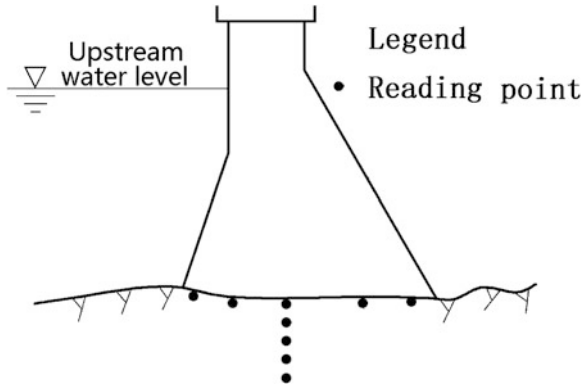


Fig. 18.23 Layout of the foundation temperature monitoring for a gravity dam



3. Internal monitoring system

For a medium-to-large hydraulic project, the internal monitoring system should be established which covers strain/stress, temperature, crack/joint movement, seepage/leakage, uplift, etc., for the purpose of overall safety surveillance and management. Figure 18.24 schematically shows such a system.

The process of breaking down the physical phenomena into their fundamental quantities of length, time, mass, and temperature enables engineer to better define the desirable types of measuring components (transducers) for the instrumentation system. In other words, the engineer should explicitly define and examine the non-electrical quantities that must be converted into usable electrical signals. Ultimately, these electrical signals must reliably and accurately represent the values of physical quantities being monitored.

A measurement is made by an element or transducer which produces a voltage, current, or frequency that represents the quantity or property being measured. This

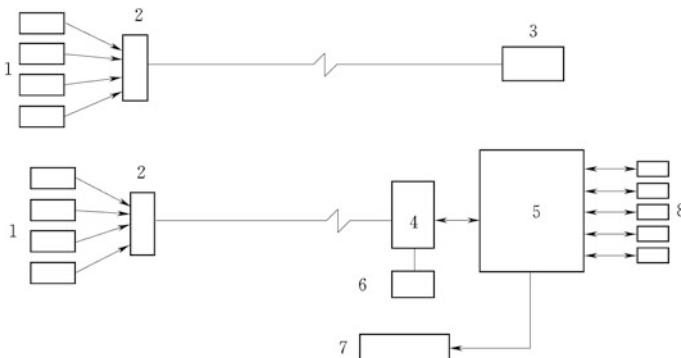


Fig. 18.24 Schematic of internal monitoring system. 1 transducer; 2 remote-controlled collective line box; 3 receiving instrument; 4 monitoring instrument; 5 computer; 6,7,8 peripheral equipments (e.g., power and power conditioning equipments)

is accomplished by varying inductance, light, capacitance, or resistance. The output must be digitized for the use by the computer system. It may be digitized at the source before transmission or later in the instrumentation system. Care must be exercised in the transmission of the signals if they are properly digitized at the system. Transmission of digital signals may give rise to high noise immunity and should be checked to assure that what is transmitted is what is received.

Distribution and acquisition of electronic signals from numerous sensors and instruments demand competent system architectures. A centralized acquisition system is generally recommended if the application is small, with signal sources close together. Larger application, typical of large dams, where instruments are geographically dispersed, may demand remote processing or distributed intelligence architecture of the data acquisition system. Wiring costs can be a large factor in determining the proper type of the system.

Most data acquisition system (DAS) manufacturers offer signal conditioning with multi-channel analog-to-digital (A/D) converters. Depending upon the type of input device, signal conditioning consists of amplification, bridge completion networks, thermocouple compensation, excitation voltage and current supplies, as well as filtering. The higher accuracy and precision are required, the higher of the system expenditure will be accompanied by the cost rise in maintenance and calibration.

18.4.4 Automated Measurement Techniques and Data Acquisition for Dams

The dam owner is responsible for the collection, storage, and presentation of all data associated with its operation and maintenance. There are two types of such data:

- Static data that do not change with time. They will normally be stored in the data books, dam safety reviews, and reports. Static data usually encompass all design and construction investigations. As much of the static data will never be changed, it may be reduced and stored on microfilm or electronic storage medium. Sufficient, easily accessible information should be kept on hand in data books to provide information for any situations which could arise.
- Dynamic data that change with time. They comprise data derived from dam safety inspection, monitoring, and operation and maintenance activities, which are accumulated in the corresponding reports. Most of the dynamic data are suitable for computer storage and presentation, particularly those arising from monitoring.

For data collection and management purposes, it should be well aware that

- The power and limitation of computer storage and retrieval systems (e.g., ease of access for the retrieval of information)
- Issues associated with compatibility of computer systems.

It should be made certain that the system used to collect and process the data has facilities to detect the occurrence of “obviously different” data, which can be resulted from the following:

- Data recording and transferring errors;
- Instrumentation malfunction;
- Abnormal behavior of the dam.

Instrumentation automation is increasingly becoming a valuable means of collecting monitored data (Choquet et al. 1998; Huang et al. 2004; ICOLD 2000b). Automation permits a greater volume of data to be collected in a given period of time. Where an instrumentation reading staff may take 4–6 h to read a set of plumb lines, the same readings can be taken in less than 10 min when collected by automated plumb line equipment. Therefore, it is now more economical, in terms of overall cost, to automate the reading of certain types of instrumentation than to continue reading them manually.

Automated data acquisition systems (ADAS) have evolved significantly since the 1990s and are currently installed on hundreds of dams in China. Figure 18.25 shows a schematic flowchart of the ADAS for dam safety monitoring, which can handle various tasks ranging from simple use of a data logger to collect data from a few instruments, to computer-based system that collect, deduce, present, and interpret data of a network with hundreds of different instruments. Most types of water level, water pressure, seepage, leakage, stress, strain, and temperature can be readily monitored and analyzed. However, some types of instrumentation such as probe inclinometers cannot be automated insofar.

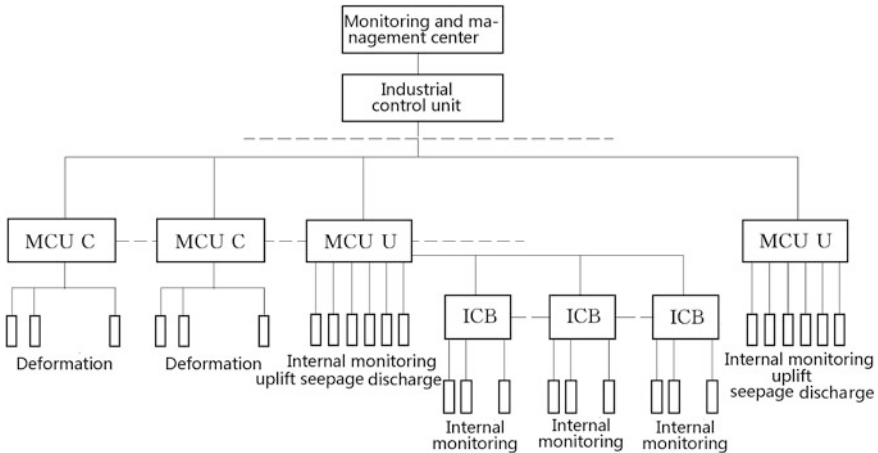


Fig. 18.25 Schematic flowchart of ADAS for dam safety monitoring. *MCU C* measure and control unit for capacitor equipments; *MCU U* measure and control unit for usual equipments; *ICB* intelligent conversion box

Advantages of ADAS are rapid notification of potentially hazardous performance and increased frequency of measurements being taken on demand. Disadvantages of ADAS are high initial expenditure and complex equipment, and the visual observations normally undertaken during the routine manual data collection will not be made.

18.5 Remedial Action

18.5.1 The Need for Remedial Action

There are a number of situations that may demand remedial actions for a dam, which can vary from a minor deficiency in the dam, to a moderate incident or major accident, or even dam failure.

Deficiencies threaten the safety of the dam and may be detected by surveillance, which are probably resulted from inappropriateness or deficiency in design or construction, changes to design criteria, time-based deterioration or breakdown of materials, maintenance-related problems, deficiencies in the dam operation and safety management program, and environmental impacts (e.g., landslide, erosion, earthquake, aging).

Incident is an event, which may evolve to a very serious situation endangering the dam. Examples of incidents are rapid change in seepage, overtopping of earth embankment, excessive beaching, excessive embankment erosion, spillway erosion or blockage, excessive cracking or deflection in the concrete dam and spillway, sliding or settlement of the dam, and malfunction of gates.

The failure of the dam means the physical collapse of whole or a part of the dam, or the uncontrolled release of any of its contents. Scenarios of failure include overtopping of embankment dams, collapse or erosion of spillways, internal erosion or piping through earth embankments or abutments, failure of release conduits, and overturning of concrete dams.

18.5.2 Requirements for Remedial Action

Remedial action is required in response to any deficiency, incident, or dam failure. The type of remedial actions necessitated and its urgency is determined by the nature of the event, which may be distinguished as follows:

- Preventative measures to stop situations worsening;
- Short-term actions such as activation of emergency action plans (EAP) inclusive evacuations and operation of warning systems, modification of operating procedures inclusive lowering of reservoir level and strengthening surveillance;
- Long-term actions such as structural changes and reinforcements, changes to operating procedures, and decommissioning.

A remedial action review should be undertaken which methodically evaluates the various options, covering the determination of the failure risk, the preparation of a failure impact assessment to determine the current population at risk and a consequence assessment to determine the other consequences, the development of possible solutions with respect to the benefits and implementation costs of each solution, and the justification for the adoption of the preferred remedial action.

18.5.3 Emergency Action Plans (EAP) for Dams

The standards and specifications used for design, construction, operation, maintenance, and inspection are intended to minimize the risk of dam failure (ICOLD 1987, 1995). However, as unusual circumstances may appear, the dam owner needs to identify conditions which could lead to failure situations and which may require emergency plans.

Emergency plan takes place at two levels: to prescribe the activities at the dam—known as the emergency action plan (EAP), which is prepared and operated by the dam owner, and to prescribe the activities below or beyond the dam—known as the counter disaster plan (CDP), which is prepared and operated by the appropriate local or central government departments with significant input from the dam owner (Cox 2007).

An EAP or CDP should indicate who is responsible for undertaking particular actions under emergency circumstances and must be tailor worked out to the conditions for each dam.

In the following text, the flood defense for embankment dams or river levees intended to provide temporary flood mitigation until permanent mitigation is taken as an example for a brief illustration of EAP.

During flood seasons, the embankment shall be patrolled continuously, to make it be certain that

- There are no indications of developing slides or sloughs;
- Wave wash or scouring action is not taking place;
- Overtopping action does not give rise to;
- No other conditions exist which might endanger the structure.

The problems that may arise during a flood season are varied and innumerable. It is impossible to enumerate all the categories of problems that field personnel must handle. The most valuable asset of field personnel under emergency conditions is their common sense and sensitivity to human relations, by which many problems can be solved quickly and efficiently. Physical problems with the embankment and related infrastructure can be identified early if a patrol team equipped with a good communication system has been well organized.

1. Overtopping

Overtopping of an embankment manifests after the water level exceeding its crest elevation, which will generally be resulted from

- Unusual hydrologic phenomena such as heavy rainfall that lead to a much higher water level than anticipated;
- Insufficient time in which to complete the embankment; or
- Unexpected settlement or failure of the embankment.

Overtopping should be prevented at any cost. Generally, emergency barriers are built about 0.5 m above the predicted water level. On an existing or completed barrier, predictions concerning water levels or settlements of the barrier will call for some form of capping to raise the barrier. Capping should be done with earth fill or sandbag.

2. Seepage

Seepage through the embankment is generally not a problem unless

- The downstream embankment slope becomes saturated over a large area;
- Seeping water is washing out solid material from the embankment.

Seepage is almost impossible to eliminate totally, and any attempt to do so may create a much more severe condition. If seepage gives rise to saturation and sloughing on the downstream slope, the embankment section should be flattened (Fig. 18.26). Material for flattening should be at least as pervious as the existing embankment shell, to avoid a pressure buildup.

3. Sand boil

A sand boil is the rupture of the top foundation stratum due to uplift pressure in the substratum. Even when an embankment is properly constructed and of such mass to resist the destructive action of flood water, water still may seep through a sand or gravel stratum under the embankment and break through the ground surface in the form of bubbling springs.

All sand boils should be watched closely. A sand boil that discharges clear water in a steady flow normally does not endanger the embankment. However, if the flow of water increases and the sand boil begins to discharge material, remedial actions should be undertaken immediately. One of the prevalent remedial actions for

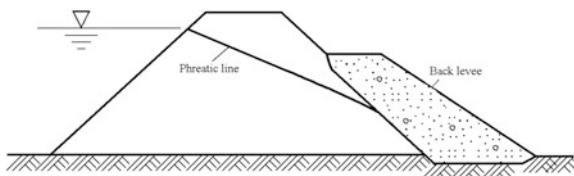


Fig. 18.26 Flattening of an embankment section

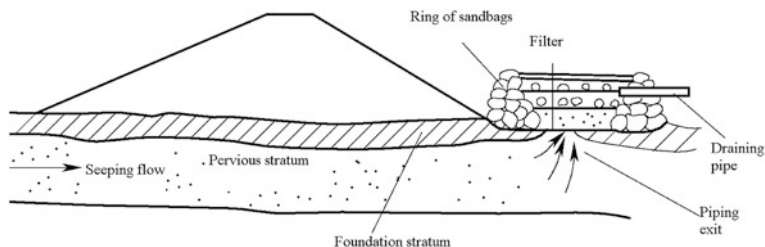


Fig. 18.27 Ring of sandbags around a sand boil

treating sand boils is to construct a ring of sandbags around the boil (Fig. 18.27), in this manner to build up a counter head of water within the ring sufficient to check the velocity of flow, thereby to prevent sand and silt from further moving. In general, the following principles may be observed in the construction of sandbag ring:

- The base width of the sandbag section on each side of the ring should be 1–0.5 times greater than the contemplated height;
- Weak soils near the boil should be enclosed within the ring, thereby preventing a breakthrough later; and
- The ring should be sufficient in size to permit sacking operations.

The height of the ring should only be that necessary to just stop the movement of soil in the water, and be not so high as to completely eliminate seepage—otherwise beyond the ring a new boil may erupt suddenly. Where many boils are found to exist in a given area, a ring levee of sandbags should be constructed around the entire area, and if necessary, water should be pumped into the area to provide sufficient water weight to counterbalance the upward pressure.

4. Erosion

Erosion of the embankment slope is one of the most severe problems that will be encountered during a flood fight. Emergency operations to control such erosion include the use of polyethylene sheeting and sandbag anchors.

18.6 Aging of Hydraulic Structures

There are already more than 86,000 reservoirs and 200,000 km river dikes in China, whose aging or deterioration is of great concern to personnel involved in their design, construction, and operation. These concerns extend throughout their entire life cycle until safe abandonment or decommission (ICOLD 1994).

The damages to hydraulic structures (incident and accident) may be generally classified into two categories: damages related to unusual events (flood and

earthquake) and damages related to the environmental factors during service. The latter are regarded as aging after at least five years of operation. The aging of dams, as defined herein, is due to time-related changes in the properties of the materials of which the structure and its foundation are composed.

Good design may mitigate the effects of aging. Vigilance during construction may correct conditions contributing to aging. Surveillance during operation may identify aging processes which could have impact on dam safety.

For an understanding of aging, it is necessary to establish the relationship between causes and effects leading to the degradation in structural properties of the dam and/or foundation. These processes are referred to as “scenarios.” The causes originate actions on the dam and/or foundation and may affect the material’s properties. The consequences of deterioration may sometimes only be observed after several years of operation.

18.6.1 Nondestructive Examination

Each dam site and its environment are unique, with different characteristics governing its performance; therefore, it is important to establish and to maintain a strong database to assess the impact of aging scenarios on dam safety.

An up-to-date knowledge concerning the dam status is documented so that the anomalous behavior is detected in time to allow for appropriate intervention correcting the situation and avoid severe consequences. Indirect evaluation should be accomplished by monitoring the effects and consequences of aging, whereas direct evaluation of aging is realized by inspecting and testing data in structural properties.

Laboratory and in situ experiments, as an important direct evaluation method to obtain the knowledge concerning the dam status for the study of the anomalous behavior due to aging, will be discussed in the text hereinafter.

By laboratory tests, the physical and mechanical properties of rock, soil, and concrete may be studied on the samples extracted from prototype dams. These tests usually belong to destructive examination and have scale effects.

In situ tests may be destructive or nondestructive. Destructive examination comprises a large category including

- Hydraulic tests such as packer or pumping tests for porosity and permeability;
- Borehole sampling, borehole camera, and TV inspection;
- Leakage detection, chemical and physical test of water (reservoir and leakage), and other materials.

Nondestructive examination (NDE), also known as nondestructive testing (NDT), is intended to examine materials for flaws without harming the tested object (Bray and McBride 1992; Prassianakis and Grum 2011). As a widely applied industrial test technique, NDT provides an effective means for detection, while it protects the object’s usability. NDT uses several methods including visual inspection, seismic exploration, and radiography.

To successfully apply NDT, a clear understanding of its limitations and manipulations of recorded data is essential, since experience has taught us that dependence on any one particular technique often leads to unacceptable mistakes.

1. Acoustic method

Sudden application of a point force to the surface of a homogeneous elastic body generates body waves and surface waves. The body waves are distinguished as compressive (P) and shear (S). There are two types of shear waves as vertically polarized (SV) and horizontally polarized (SH). In a homogeneous isotropic body, the velocities of these two waves are identical. In concrete, velocity V_p of P -waves is related to the Young's modulus, density, and Poisson's ratio, while velocity V_s of S -waves is related to the shear modulus and density. Where there are material boundaries or flaws affecting the wave transmission from the source, the waveforms are converted: Along boundaries, they are called "love" waves and those responding to the boreholes are called "tube" waves.

If the point force source is within the medium, the waves generated will depend upon the characteristic of the motion at the source. A pure spherical expanding source will generate P -waves, but any non-spherically symmetric disturbance will generate both P and S -waves. In reality, the necessity for finite source dimensions complicates the type of waves produced. Furthermore, inhomogeneities give rise to wave conversions, whether the source is at the surface or at the depth.

Acoustic method is based on the generation of elastic waves in the structure and the measurement of the time taken by the waves to travel from the source, through the materials to a series of geophones, which are usually laid out spaced one to ten meters apart along a straight line from the source (Li et al. 1998). Seismic technique involves frequencies in the range of 100–500 Hz generated by explosives and other energy sources (in rock mass or dam concrete), higher frequencies in the range of 10–30 kHz are used in "acoustic" technique with piezoelectric sources, whereas ultrasonic technique employs a frequency range in 0.5–25 MHz. With lower frequencies, the interaction effects of the waves with internal flaws would be so small that detection accuracy is poor. However, with lower frequencies, the damp would be lower which enables the waves to penetrate deeper into the structures.

Seismic tomography technique (ST) enables to obtain the wave distribution at the dam section, and in this way, the dynamic elastic properties and integrity of the dam may be evaluated. ST was used in Italy for the exploration of 27 concrete dams and 10 embankment dams, as early as the year of the 1990s.

2. Electromagnetic method

Electromagnetic method employs higher-frequency waves for detection, including electromagnetic induction and ground-penetrating radar (GPR), and the latter will be illustrated herein.

GPR is a prevalent geophysical method (Bertacchi et al. 1985; Butler et al. 1991; Daniels et al. 1997; McDowell et al. 2002; Xiao 2000) that generates and receives radar pulses to image the subsurface. This nondestructive method employs

electromagnetic radiation in the microwave band (UHF/VHF frequencies) of the radio spectrum and detects the reflected signals from subsurface structures. GPR has been successfully exercised in a very wide range of tasks from mapping geological structure, to identifying defects (voids and cracks) in concrete.

High-frequency (usually polarized) radio waves transmit into the ground by antenna (T). When the waves hit a buried object or a boundary with different dielectric constants, the receiving antenna (R) records the variation in the reflected return signal (Fig. 18.28). The principles involved are similar to reflection seismology, except that electromagnetic energy is used instead of acoustic energy, and reflections appear at boundaries with different dielectric constants instead of acoustic impedances (Daniels 2004; Goodman 1994; Guo 2000; Hanssen 2001; Kamps 2006).

Travel time of an electromagnetic pulse may be calculated by

$$t = \sqrt{4z^2 + x^2}/v \quad (18.5)$$

where t = time for the travel, ns ($1 \text{ ns} = 10^{-9} \text{ s}$), and v = electromagnetic pulse velocity in the ground medium, m/ns.

The survey line spacing varies according to target type, size, and depth. It is typically ranged in 0.25–1.0 m as a standard for civil engineering targets, but may be increased up to 10–20 m for mapping geological layers. The measuring interval between individual GPR waveforms is normally set between 1 cm and 1 m, depending on the size of the target and the resolution required. As an empirical rule, to define discrete targets, it is necessary to record a minimum of 2.5 waveform traces in the distance that the dimension of the target occupies. Additional survey lines, or a multi-line grid, may be demanded to detect small or multiple targets, or in cases where a high degree of spatial accuracy in data analysis is necessary. Taking the ordinate as t (ns) and the abscissa as distance x (m), a GPR log obtained is shown in Fig. 18.29.

Cross-borehole GPR has been developed within the field of hydrogeophysics to be a valuable means for assessing the presence and amount of soil water.

The detected depth of GPR is restrained by the electrical conductivity of the ground, the transmitted center frequency, and the radiated power. As conductivity increases, the penetration depth decreases. This is because the electromagnetic

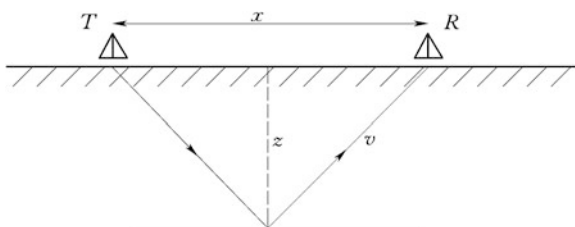
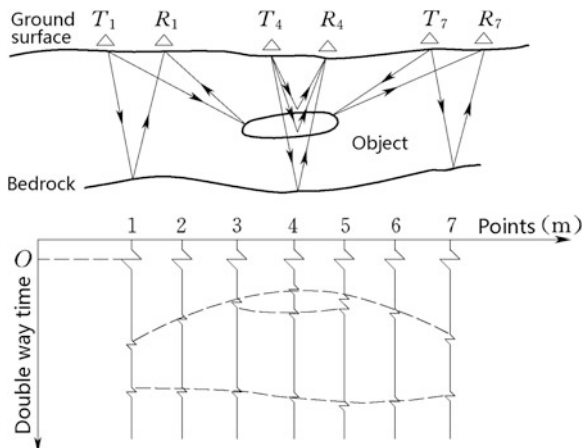


Fig. 18.28 Schematic diagram of ground-penetrating radar

Fig. 18.29 A ground-penetrating radar log



energy will be more quickly dissipated into heat, resulting in a loss in signal strength at depth. Therefore, the most significant restraint of GPR is imposed by high-conductivity materials such as clay soils and soils that are salt-contaminated. Good penetration is achieved in dry sandy soils or massive dry materials such as granite, limestone, and concrete where the depth of penetration could be up to 15 m. In moist and/or clay-laden soils and soils with high electrical conductivity, penetration depth is sometimes only a few centimeters. Higher frequencies do not penetrate as far as lower frequencies, but give better resolution. Performance of GPR is also limited by signal scattering in heterogeneous conditions (e.g., rocky soils).

Disadvantages of currently available GPR systems are as follows: Interpretation of radargrams is generally non-intuitive to the novice; considerable expertise is necessary to effectively design, conduct, and interpret GPR surveys; and relatively high energy consumption can be problematic for extensive field surveys. However, recent advances in GPR hardware and software have done much to ameliorate these disadvantages, and further improvement can be expected with the ongoing innovations.

3. Spontaneous potential (SP) method

It is also termed as “self-potential method,” which measures the natural or spontaneous potential difference that exists between the borehole and the surface in the absence of any artificially applied electric current, by an electrode relative to a fixed reference electrode. SP is usually caused by charge separation in clay or other minerals, due to the presence of semipermeable interface impeding the diffusion of ions through the pore space of materials, or by natural flow of a conducting fluid through the materials. SP is often measured down boreholes for formation evaluation in the oil and gas industry, and they also may be undertaken along the earth’s surface for mineral exploration or groundwater investigation.

The measuring network is usually laid out along the flow direction of groundwater, and the probes of Cu–CuSO₄ are embedded. The potential difference of every dual points measured enables to draw potential profiles or potential contours. The leakage zone has low potential, while the exit area of seepage flow has higher potential. Accordingly, the incipient fault of leakage may be analyzed concerning the position, embedding depth, development tendency, etc. Quantitatively, the relative abnormal value η of the potential curve may be used in the judgment, which is defined as the ratio of abnormal value to normal value: When $\eta = 1.3$ – 1.5 , concentrated leakage has formulated, whereas $\eta > 1.5$ indicates the occurrence of piping.

4. Resistivity method

The method is employed for the study of discontinuities, by utilizing direct currents or low-frequency alternating currents to investigate the electrical properties (resistivity) of subsurface materials (Edwards 1977; Johansson and Dahlin 1996). Resistivity measuring operation uses two current electrodes and two potential electrodes.

Electrical resistivity method is an excellent tool for groundwater exploration. Electric current is injected into ground through two electrodes, and the resultant potential is measured through another pair of electrodes. These electrodes are placed on ground at predefined locations. The data are then interpreted with available software, and the results are in the form of resistivity and the thickness of different layers. In the application to dams, the exploration network may be laid out parallel to the dam axis, and the results may be interpreted in a manner of deep resistivity profiling or resistivity contours.

Figure 18.30 shows the resistivity contours of the Baicaoping Embankment Dam ($H = 42$ m, China) along the dam axis. Above the altitude of 25 m, the contours are nearly horizontal, which means homogeneity of the core material along the horizontal direction. This had been verified by 5 borehole samplings with $\gamma_d = 1.2$ – 1.4 t/m³. Vertically, the contours may be divided into three groups:

- Above the altitude of 14 m enclosed by the contour of 50 Ω m, they are on the high side of resistivity, which means that the construction quality is good with dry density $\gamma_d = 1.5$ – 1.6 t/m³ by borehole samplings;
- From the altitude of 14 m to the dam base limited by 50 Ω m, there are two lower resistivity areas. The right one has the lowest resistivity at a depth of 25 m, which is the dam closure portion with poor construction compaction; the left one is at a depth of 15 m, which is mainly induced by the filling of frozen soil according to the construction log. The boreholes of 4, 7, and 8 all obtained over saturated soil samples;
- The zone under the resistivity 50 Ω m, where the density of contours increases at a faster rate, reflects the characteristics of sand–gravel foundation. The borehole 9 also revealed that the contour line 50 Ω m is the boundary of dam and foundation.

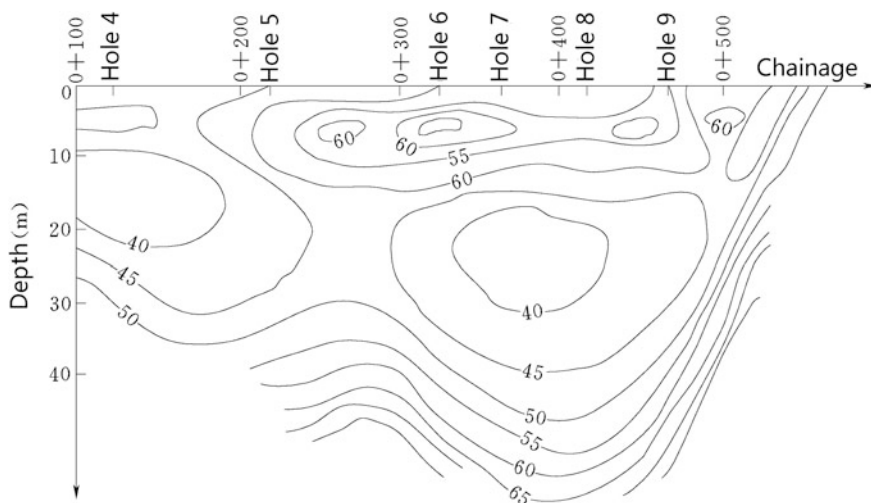


Fig. 18.30 Resistivity contours of the Baicaoping Embankment Dam, China, $H = 42$ m

5. Induced polarization method

Induced polarization (IP) means electrical surveying using geophysical imaging technique to identify the subsurface materials (Edwards 1977). The method is similar to electrical resistivity tomography, in that an electric current is induced into the subsurface through two electrodes, and voltage is monitored through two other electrodes. The method makes use of the capacitive action of the subsurface to locate zones where clay and conductive minerals are disseminated within their host rock: Under the similar target body condition, the higher the water content, the slower the decay of the induced polarization field. In the application to dams, a measuring network should be laid out along the dam axis, to detect the distribution of soft stratum within foundation or dam body.

Time-domain IP method measures the voltage decay or chargeability over a specified time interval after the induced voltage is removed. The integrated voltage is employed for the measuring operation.

Frequency-domain IP method uses alternating currents (AC) to induce electric charges in the subsurface, and the apparent resistivity is measured at different AC frequencies.

18.6.2 Aging Diseases of Hydraulic Structures

Aging of hydraulic structures should be examined from two aspects (Combelles 1991; ICOLD 1983, 1994; Jansen 1988; Sinniger et al. 1991):

- As an objective process of exhaustion of given properties over the course of time with respect to a set of factors including aesthetic, functional, physical, technoeconomic, environmental, social;
- As a process of accumulation over the course of time with respect to irreversible physicochemical changes in materials composing the object, which ultimately lead to the deterioration of the object and exhaustion of its given properties.

1. Aging of foundation rock and soil

Three scenarios of foundation rock and soil aging may be summarized in the following (Lin et al. 2009; Unal and Unver 2004).

(a) Loss of strength

It is a phenomenon associated with mechanical failure by shear leading to the progressive deterioration of the foundation. Loss of strength generally takes place in clay soils due to saturation and excessive strain. When clay soils are strained over their peak strength, they manifest a significant loss of strength.

(b) Deformation

When the foundation consists of very weak rocks or deformable soils, they are ordinarily removed or measures are taken to improve the material left in place. Otherwise, differential settlements due to consolidation may appear, resulting in the cracking of the dam body. In areas of dry climates, dry and low-density soils collapse when they become wetted, which also may lead to dam cracking.

(c) Uplift pressure

Uplift pressure builds up where the steady-state seepage is obstructed or where a sudden excess in seepage cannot be accommodated. In rock with erodible or soluble joint infilling under reservoir pressure, water penetrates the joints and progressively builds up the uplift pressure. Water seeping under the dam may transport fine grains which may progressively clog the draining filter or draining holes and build up the pressure at the downstream toe. Water seeping through poorly graded material may move material grains (internal erosion or piping) leading to subsidence or sinkholes.

2. Aging of concrete structure

The durability of concrete depends on the durability of its constituents, cement paste, and aggregates. A concrete with strong paste may not be durable if combined with poor aggregate and vice versa. One of the most important parameters is the “porosity” of the paste, which is a function of the amount of water relative to the cementitious materials. Excessive water can dilute the cement paste leaving a medium more porous, which is more vulnerable to deleterious substances and physical processes (Dolen 2005; Dolen 2006; Durcheva and Puchkova 1995; Tsulukidze 1962). The climate is a significant environmental factor influencing the long-term durability of concrete structures. One of the reasons that the ancient

structures have survived is because they were constructed in areas of relatively dry and mild climates.

The four primary scenarios of concrete deterioration in concrete dams may be summarized in the following:

- Sulfate attack (SA). The chemical and physical destruction of the cement paste by aggressive, sulfate-laden waters;
- Alkali–aggregate reaction (AAR). The chemical reaction between alkali compounds in cement with certain amorphous silica-bearing aggregates, responsible for concrete “growth” by expanding silica gel;
- Freezing/thawing deterioration (FT). The physical destruction of primarily cement paste by ice formation within the cement pores;
- Corrosion of reinforcing steel. Primarily related to structures constructed accidentally with insufficient cover. However, when other mechanisms deteriorate surrounding concrete, corrosion may ultimately become the primary means of deterioration.

(a) Sulfate attack

Effects of erosion water environment include internal sulfate attack (SA), acid attack, and chloride (corrosion) attack (Neville 2004). SA is a chemical degradation of cement paste caused by high concentrations of sulfates in soils and groundwater, which is attributable to chemical interactions between sulfate ions and constituents of the cement paste. The disintegration appears to be resulted from chemical reactions with cement hydration products and the formation of a secondary compound, ettringite, accompanied by a large volumetric expansion and cracking of the concrete. SA was also known as “cement corrosion” in the early 1900s and is very common in the white “alkali flats.” Early observations in these scenarios identified certain cement brands as being more resistant to deterioration than others.

(b) Alkali–aggregate reaction (AAR)

Alkali–aggregate reaction is a chemical reaction between certain specific mineralogical types of aggregates (either sand or gravel) and the alkali compounds (generally lower than 2 % of the cement composition) of cement in the presence of moisture (Pacheco-Torgal et al. 2008; ICOLD 1991a, b; Roy and Morrison 2000). Typical manifestations of concrete deterioration through AAR are expansion, cracking, exudations of jellylike or hard beads on surfaces, reaction rims on affected aggregate particles within the concrete, and sometimes pop-outs. The cracking may allow for moisture being more readily absorbed by the silica gel, which in turn accelerates AAR or further freezing–thawing damage.

Many new cases of expansion instances are being identified worldwide including that caused by alkalies in cement reacting with certain “glassy” siliceous aggregates such as opals, chalcedony, cherts, andesites, basalts, and some quartz, which is termed as “alkali-silica reaction (ASR),” and with certain specific carbonate aggregates, which is termed as “alkali-carbonate reaction (ACR),” as well as that

caused by internal sulfate attack (SA). In these ongoing expansion cases, it appears that the alkalis are also supplied by certain minerals, such as feldspars in the aggregates, and the reaction and associated expansion may possibly continue indefinitely.

An ICOLD paper stated that nearly 10 % of concrete and masonry dams suffered from the damages due to aging undergo expansion. Recent studies suggest that this figure is higher, as many cases of dam expansion have been reported recently and it also should be noted that the phenomenon can manifest even if it is not directly apparent (ICOLD 1991a, b). Over 100 cases found to be seriously affected by AAR in terms of dam safety, and operations were discussed at the “USCOLD Conference on Alkali Aggregate Reactions in Hydroelectric Projects and Dams” in 1995.

(c) Freezing/thawing (FT) deterioration

Freezing/thawing deterioration was identified early in USBR history under the general term of durability of concrete without specific causes or solutions. It is the deleterious expansion of water within the cement paste leading to the destruction of the concrete matrix, which appears in the chilly regions solely.

Water present in the cement paste expands about 9 % upon freezing. When confined within a rigid, crystalline microstructure, the expanding ice crystals can exert pressures far exceeding the tensile strength of the paste, causing cracking and ultimately disintegration of the concrete (Shang and Song 2006). For this form of deterioration to take place, the concrete must be nearly saturated when it undergoes the freezing. Water conveyance structures are more likely suffered from repeated cycles of freezing/thawing actions. Areas subject to cyclic freezing, such as in spillways, and particularly those in fluctuating water surface levels, or in splash or spray zones, are the most susceptible to FT deterioration.

Freezing/thawing deterioration is most pronounced in highly porous concrete with a high W/C and those concretes without purposely entrained air bubbles, such as the concretes commonly used in the early twentieth-century construction.

(d) Corrosion of reinforcing steel

Corrosion of steel bars in concrete is an electrochemical process. The damages to reinforced concrete of thin hydraulic structures (e.g., buttress dams, aqueducts, embedded conduits, sluices, inverted siphons, culverts, tunnel linings, bridges) resulting from the corrosion of embedded steel bars manifest in the forms of expansion, cracking, and eventual spalling of the cover. In addition to the loss of cover, a reinforced concrete structures may suffer structural damages due to the loss of bond between steel and concrete and the loss of the cross-sectional area of reinforcement—sometimes to the extent that structural failure becomes inevitable (Bentur et al. 1997; Bertolini et al. 2014; Mehta and Monteiro 2006).

When designed, a concrete hydraulic structure is usual to state the minimum concrete cover for the reinforcement steel bars, which is normally stipulated by the corresponding design specifications. It is conventional to postulate that when the embedded steel is protected from air by an adequately thick cover of a low-permeability concrete, the corrosion of steel and other problems associated

with it would not arise. However, this may not be entirely true from the high-frequency evidences—even some properly built reinforced concrete structures show premature deterioration due to steel corrosion. For example, a 1995 investigation organized by the Ministry of Water Resources (China) reported that of 200 hydraulic structures investigated (including 50 aqueducts, 33 embedded conduits, 36 sluices, 9 inverted siphons, 32 culverts, 18 tunnels, 8 gates, 14 bridges) in China that suffered from aging deterioration and required immediate repair, corrosion of reinforcing steel is responsible for 74 (accounting for 37 % of the total) (Luo, Luo, 1995).

The corrosion types may be classified according to the deferent criteria related to the corrosion mechanisms, final damage appearances, environmental factors, etc.

By the corrosion mechanism, the electrochemical potentials to form the corrosion cells may be generated in two ways:

- Composition cells may be formed when two dissimilar metals are embedded in concrete, such as steel bars and aluminum conduit pipes, or when significant variations exist in surface characteristics of the steel bars;
- In the vicinity of reinforcing steel, concentration cells may be formed due to differences in the concentration of dissolved ions, such as alkalies and chlorides.

As a result of aforementioned mechanism, one of the two metals becomes anodic and the other cathodic, among them the fundamental chemical changes occur. The transformation of metallic iron to rust is accompanied by an increase in volume that, depending on the state of oxidation, may be as large as 600 % of the original steel. This volume increase is believed to be the principal cause of concrete expansion and cracking.

Although the corrosion processes are not induced by environmental factors directly, they may cause the deterioration of the cover concrete and accelerate the ingress of aggressive species, making the pore solution in contact with the steel more corrosive. Among all the environmental factors, chloride ions (Glass and Buenfeld 2000) and carbon dioxide (Yoon et al. 2007) are mainly responsible for most corrosion of steel in concrete structures.

Chlorides can promote the corrosion of embedded steel rebar if present in sufficiently high concentration. The pore solution in concrete is an electrolyte containing various ions (e.g., sodium, potassium, calcium, hydroxyl) and is physically absorbed in the pores of the concrete. The chemical composition of the pore solution influences the conductivity of the concrete and the corrosion process. As the pH value of the pore solution in a well-cured new concrete is about 13.5, any steel in contact with such a pore solution should be in a passive state, so there is no problem with a young reinforced concrete structure if there is no chloride. Unfortunately, this high pH value can not always be kept. Under some circumstances for example, when concrete has high permeability, alkalies and most of the calcium hydroxide have been either carbonated or leached away, the pH value of concrete in the vicinity of steel may be reduced lower than 9. As a result, the passive film on the steel in contact with the pore solution with low pH value

would no longer be stable, and rapid corrosion would occur on the surface of the “active steel.”

Carbonation, or neutralization, is a chemical reaction of carbon dioxide in the air with calcium hydroxide and hydrated calcium silicate in the concrete and is another main cause responsible for the corrosion of reinforcement steel bars. Atmospheric CO_2 dissolved in the pore solution will react with the alkali hydroxide and the $\text{Ca}(\text{OH})_2$. As a result, the pH value of the pore solution is brought down below 9, the passivity of steel is destroyed, and the corrosion reaction of steel in concrete is dramatically enhanced.

In addition to aforementioned two major factors—chloride and carbonation, temperature and moisture, as well as some other factors such as steel type, pore solution of concrete, and permeability of concrete, will influence the corrosion of reinforcement steel bars in concrete:

- Since the electrochemical reactions are mainly responsible for the reinforcement corrosion, moisture should be an essential substance in the corrosion. Normally, if there is no water in concrete, there should be no corrosion problem with the reinforcement.
- An increase in temperature will lead to the rate increase of all electrochemical processes, consequently the increase in corrosion rate, too (Pour-Ghaz et al. 2009).
- Stress corrosion cracking and hydrogen-induced embrittlement are caused by the combination of particular corrosion media and stresses for some types of steels (Villalba and Atrens 2008). Different types of steels possess different microstructures and compositions, so they usually exhibit different corrosion performances in concrete. Generally, high-strength steel is one of the materials that are sensitive to stress corrosion and hydrogen-induced embrittlement. Unfortunately, the reinforced concrete structures and rock slopes, particularly when the prestress technique is employed, demand high-strength steel.
- The pores can facilitate the ingress of Cl , CO_2 , O_2 , H_2O and some other detrimental species from the environment. Therefore, higher porosity and large pore sizes lead to more severe corrosion (Hussain and Ishida 2010).
- The permeability directly affects two of the basic corrosion processes: the supply of depolarization reagents and the removal or accumulation of corrosive products. Therefore, it has significant influence on the steel corrosion in concrete.

3. Aging of embankment fill

(a) Cored and homogenous embankment

The long-duration process of consolidation of the embankment material after the completion of construction and during the first filling is the main cause of continuing deformations. This consolidation process may be influenced by environmental and operational actions (temperature, precipitation, earthquake, blasting, crest traffic, water level fluctuations).

Embankment deformation depends upon the mineral type, shape, hardness, grain-size distribution, moisture, and density of the compacted material, which leads to

- Differential deformation in adjacent sections of embankment, which may give rise to fissures leading to the internal erosion;
- Settlement at the contact with a concrete structure, which may initiate cracking, leaking, and erosion;
- Loss of freeboard.

Harmful effects of deformations can be prevented by appropriate positioning, and using, placing, and compacting, of materials. Monitoring of vertical and horizontal displacements will allow for the evaluation of deformations.

Loss of strength of embankment materials is associated with

- Wetting of improperly compacted embankment soil. Materials compacted on dry side without sufficient compaction effort to reduce the void volume will experience considerable particle reorientation leading to the large settlement and/or differential settlement, which, in turn, may lead to cracking and piping and manifest high pore pressure.
- Reduction in cohesion when wetted of some specific soils. Reservoir seepage, abutment groundwater, and rainfall may affect downstream shell stability by wetting.
- Change in the state of stress. Embankment heightening may stress the existing material beyond its peak strength, and a lower residual strength is onset. Cycles of drying/wetting of high-plasticity clays may result in slope instability, which is usually in the form of shallow downstream sliding. As the clay dries, capillary stresses lead to tensile cracking. When water is again available to the crack, material sloughs off into the crack and there is a loss of strength in the swelling clay at the crack face. A progression of these events would reduce the effective dam width and manifest other detrimental scenarios such as
- Pore pressure mounting. It is generally associated with progressive opening of transverse cracks in the core or through the whole fill.
- Adverse deformation. It may be associated with differential foundation settlement, differential embankment compression, embankment arching, contact with concrete structures, or drying out of the upper portion of the core during prolonged dry periods (Hjeldnes and Lavania 1980; Lo and Kaniaru 1990). It also may be associated with dissolution of dispersive clays, a defective layer in the core, poor material placement, or low permeability in downstream dam shell.

Good design and construction practices may preclude excessive pore pressure mounting by eliminating foundation overhangs, by shaping the abutment and structure contact, by using ductile material in the upper part of the dam, and by adequate downstream draining and careful material placing. Periodic inspections and displacement measuring, supplemented by seepage and pore pressure monitoring, are appropriate for the detection of these scenarios.

Internal erosion may manifest within the embankment core or the downstream shell with soils susceptible to cracking, piping, or other types of erosion (Fry 1997). Quite frequently, it occurs at the embankment contact with the foundation. Internal erosion generally finds its origin in design and construction inadequacies, but may progress unnoticed for a long time.

Detection of internal erosion depends on visual inspection, water flow monitoring, pore pressure readings, and turbidity measuring. Drilling and geophysical investigations are helpful to capture the internal erosion.

(b) Upstream surface erosion

Surface erosion, although a very common aging scenario, has not yet been regarded as an important contributor to embankment failures. Erosion on the downstream slope and crest may be due to heavy rainfall directly or surface water runoff, brief crest overtopping, and wind-driven wave splash over a parapet wall. Erosion on the upstream slope may be attributable to wave action on the riprap with too small blocks or inadequate bedding, breakdown of riprap, or freezing/thawing displacement. Surface erosion is readily detected by routine visual inspection, and a timely repair is emphasized.

Seepage through CFRDs is the aging scenario that had been mostly reported for dams constructed of dumped rockfill with little or no roller compaction, whose excessive settlement led to the damage of slab joints and even slab buckling. The high permeability of rockfill leads to large leakage, although internal erosion was not an urgent problem. Remedial measures are only undertaken when the seepage became too large or limitations on operation are found to be too restrictive.

(c) Others

Analyses of data on the deterioration of earth- and rockfill dams revealed other aging scenarios concerning the behaviors and materials of some specific dam elements.

- ① Loss of bond between concrete structure and embankment. It is associated with differential movements in the bonding zone due to settlement of the embankment material attributable to inadequate compaction and/or foundation treatment, or internal erosion. Settlements may lead to arching in the fill and reduction of the effective stress. Seepage develops through cracks in the fill or along the concrete structure promoting internal erosion if the filter drainage system is not able to tackle the severe erosion actions.

This scenario may be detected by inspection with regard to vertical displacements and seepage.

- ② Aging of geosynthetic material. Geosynthetic materials are installed for the purpose of water barriers (geomembranes), material separators, filters (geotextiles), and drainage and stabilization (geogrids, geotextile wraps). The common aging agents for geosynthetic materials are ultraviolet light, stress, temperature, moisture extraction, oxidation, chemical and biologic substances.

The construction operation including the storing, handling, and installing can give rise to the most damaging (ICOLD 2010).

Monitoring of the aging process may be carried out by physical and mechanical tests on the test samples from a project field test section, from time to time.

- ③ Aging of asphalt concrete facing. The bituminous material coating and binding together the aggregates in asphalt concrete breaks down from exposure to oxygen and ultraviolet light. Abrasive debris and wave action remove the bituminous coating from aggregates, allowing the aggregates for weathering. These aging scenarios will deteriorate the asphalt concrete as water barrier. Flames used in contact with the asphalt concrete for heating previously placed material cause severe deterioration of the bituminous material. Asphalt concrete also has been used for construction of an internal water barrier (core). So far, no examples of aging have been found, apart from only a very poorly designed and constructed asphalt concrete core being suspicious of aging.
- ④ Aging of soil–cement. Soil–cement slope protection may be deteriorated, attributable to the effects of freezing/thawing, abrasive debris, and wave actions. These may be hastened due to insufficient cement in the mixture, poor mixing, insufficient compaction, or lack of bond between layers. Soil–cement placed in stair-step fashion is sufficiently massive that repairs would only be necessary if large segments of protection are lost. However, aging damage to the soil–cement placed by the plating method demands immediate repairs.

18.6.3 Mitigation of Aging

1. Analysis

The first step in the mitigation is the analysis of aging process and its consequences on dam safety and project operations (Bangert et al. 2003). In most cases of deterioration, the specific causative process can be identified by concrete materials' experts, with the help of petrographers augmented by field and laboratory testing. The role of nondestructive testing techniques accompanied by the analysis and presentation using tomography methods is a fast advancing field and can help to develop an "internal" view of the structural condition.

The effects of aging processes on structural integrity and dam safety can sometimes be obvious, whereas in other cases such as AAR, detailed modeling that comprises finite element analysis is necessitated identifying the mechanisms and forecasting the potential effects such as cracking in the future.

A related key aspect is the long-term susceptibility to the corrosion and performance of high-strength anchors. They are increasingly used to improve the stability of structures where construction joints are deteriorating or where criteria

have escalated. Corrosion of reinforcing steel is clearly a major problem although it is often more of a maintenance issue and not always related to dam safety.

Understanding the predominant processes at the work can provide a basis to plan an appropriate structural management program. In some of such cases, the process may have a finite lifetime, while in others, it will continue indefinitely. In the latter case, long-term budget provisions should be made accordingly rather than a one-time fix. Economic analysis for the options of remedial actions should thus be done on a “life cycle” basis (Yang 2007). In some cases, these considerations may indicate that there is only a finite economical remaining service life and plans need to be made for a replacement structure.

2. Prevention and mitigation

No material is inherently durable. As a result of interactions with its environment, the microstructures and consequently the properties of materials change with time. A material may be assumed to have reached its end of service life when its properties under given conditions have deteriorated to such an extent that the continuing utilization of the structure is unsafe or the costs of ongoing repairs make the structure uneconomical.

In addition to having to deal with the physical and chemical processes of deterioration, the determination of acceptability of such structures is often made more difficult by changing criteria such as escalation in design floods (PMFs) and earthquakes (MCEs) due to improved knowledge and society’s evolving demands for public safety.

The economic value of the structures for water supply, energy generation, or flood control is frequently substantial, and thus, life extension and rehabilitation of existing dams and appurtenant works is an important activity. It is vital that the industry community understands what is the process of aging, how to assess its extent, and which remedial actions can be taken, to cost-effectively extend the service life of these structures.

It is ideal that prevention and mitigation of aging may be achieved through the design, construction, and operation of high quality. A well-planned and well-performed surveillance program is crucial for the early detection of aging scenarios. Provisions of convenient access to all vital areas of the structure will enhance the surveillance and regular maintenance.

(a) Concrete structures

For a durable concrete, the following are the main contributions (in chronological order) (Ahmaruzzaman 2010; Saraswathy and Song 2007; Yoon et al. 2002):

- Development of special cements to improve concrete quality, such as low-heat and sulfate-resisting cements;
- Development of internal vibrator to consolidate concrete—this equipment significantly reduces the water content of concrete and makes it less permeable;

- Determining the causes of and the solutions to AAR and FT attack, using methods such as petrographic mineralogical examination and long-term testing to identify the parameters, which affects the durability of concrete under these conditions; and
- Incorporating fly ash in concrete construction—fly ash may improve concrete workability, reduce the porosity of the cement paste, and improve its resistance to ST and ASR.

Because water, oxygen, and chloride ions play important roles in the corrosion of embedded steel and the cracking of concrete, it is obvious that permeability of concrete is the key to control the various processes involved in the corrosion phenomena. The permeability of concrete is mainly determined by the porosity of concrete and its pore size distribution, which are dependent on the ratio of W/C. Sometimes, the permeability could vary by as much as two orders of magnitude as W/C increases from 0.4 to more than 0.7. Other factors such as hydration process and the mineral mixture can also significantly influence the porosity and permeability.

Corrosion inhibitors, such as calcium nitrite, also can be added to the water mix before pouring concrete (Soylev and Richardson 2008). The nitrite anion is a mild oxidizer that oxidizes the soluble and mobile ferrous ions present at the surface of the corroding steel and causes it to precipitate as an insoluble ferric hydroxide. This causes the passivation of steel at the anodic oxidation sites.

Coatings and cathodic protection for reinforcing bars provide common approaches to prevent corrosion (Manning 1996). The former comprise two types: anodic coatings (e.g., zinc-coated steel) and barrier coatings (e.g., epoxy-coated steel), and the latter involves the suppression of current flow in the corrosion cell, either by supplying externally a current flow in the opposite direction or by using sacrificial anodes. Due to their complexity, they are finding limited applications, and long-time performance of these protections is still under investigation in many countries. In addition, they are costlier than producing a low-permeability concrete through quality, design, and construction controls.

(b) Embankment dams

Excessive differential deformations may be prevented by the appropriate selection, zoning, and compaction, of materials.

Cracking of dam core may be avoided by

- Placing ductile material at locations subject to tensions;
- Shaping abutments with smooth transitions from area to area;
- Battering adjoining appurtenant structures to permit a full compacting and bonding of core;
- Adopting a zoning scheme that does not place materials with large differences in deformation modulus adjacent to each other;
- Widening excavations and flattening slopes to prevent arching;
- Flaring the core near and at the abutment interfaces.

Internal erosion may be prevented by installing an upstream self-healing transition zone and a downstream filter zone of the core, avoiding internally unstable materials, treating fissured bedrock, and dispersive soils.

If instrumentation is to be installed within the dam core, it should be so designed that it does not become an “Achilles heel” for future degradation of the dam.

Slope protection with riprap of appropriate durability, size, grading, thickness, slope inclination, and proper placement is required. The riprap thickness with lower-quality rock should be raised, and bedding layer to prevent the underlying embankment from erosion is installed.

Where the only available rockfill may experience excessive deformations, which could be unacceptable for a concrete face slab, alternative use of an asphalt concrete face slab, geomembrane face, or central asphalt core is recommended.

The use of asphalt concrete requires careful selection of bitumen and aggregates, complete mixing, temperature control, and compaction.

The use of geosynthetic materials requires careful studies on their composition and manufacture and characterization of the environment into which the materials will be installed and handled, to avoid accelerated aging (ICOLD 1991a, b). Periodic retrieval of coupon samples from a field test section for the aging testing and evaluation is demanded.

Soil–cement requires careful selection of the soil to be mixed with cement and water. Design mixes are tested in laboratory to assure its engineering properties.

3. Rehabilitation

Many methods of treating surface deterioration have been available (ICOLD 2000a), including chemical treatment of the upstream face; upstream concrete coating using epoxy/gunite/shotcrete/sealant materials; geomembranes attached to the upstream face to provide a waterproof; downstream drainage layers covered with gunite or shotcrete and reinforced to the downstream face; grouting or other internal treatment; and concrete buttresses on the downstream face.

Remedies for more invasive forms of deterioration such as AAR or other swelling or internal mechanisms tend to be more structural in nature since no complete “cure” is available once the structure has been constructed. Some solutions available are anchoring to improve shear strength on lift joints or as an attempt to restrain the structure against the aging, stress relief by slot cutting, or other structural modifications.

The repair and replacement costs associated with concrete damaged by the corrosion of reinforcing steel have become a major maintenance expense. It is now prevalent to provide a waterproof membrane, or a thick overlay of an impervious concrete mixture on newly constructed, or thoroughly repaired surfaces of reinforced concrete structures that are large and possess flat configuration, if possible. Typically, concrete mixtures used for the overlay are of low slump, very low water-to-cement ratio (made possible by adding a super-plasticizing admixture), and high cement content. Portland cement mortars containing polymer emulsion (latex) also show excellent impermeability and have been exercised for the overlay installations.

References

- Ahmaruzzaman M (2010) A review on the utilization of fly ash. *Prog Energy Combust Sci* 36 (2):327–363
- Baker HD, Ryder EA, Baker NH (1953) *Temperature measurement in engineering*. Wiley, New York
- Bangert F, Grasberger S, Kuhl D, Meschke G (2003) Environmentally induced deterioration of concrete: physical motivation and numerical modeling. *Eng Fract Mech* 70(7–8):891–910
- Becker L, Yeh W (1974) Optimization of real-time operation of multiple reservoir system. *Water Resour Res* 10(6):1107–1112
- Bentur A, Diamond S, Berke NS (1997) *Steel corrosion in concrete: fundamentals and civil engineering practice*. E & FN Spon, London
- Bertacchi P, Zaninetti A, Carabelli E, Superbo S (1985) Geophysical methods for the detection of ageing and effectiveness of repairs in dams. In: *Proceedings of the seventeenth international congress on large dams, vol II, Q65*. ICOLD, Vienna, pp 619–636
- Bertolini L, Elsener B, Pedferri P, Redaelli E, Polder R (2014) *Corrosion of steel in concrete: prevention, diagnosis, repair, 2nd edn*. Wiley-VCH, Weinheim
- Bray DE, McBride D (eds) (1992) *Non-destructive testing techniques*. Wiley, New York
- Butler DJ, Llopis JL, Dobecki TL, Wilt MJ, Coewin RF, Olhoef G (1991) Comprehensive geophysics investigation of an existing dam foundation. *Geophys Lead Edge* 9(9):44–53
- Can EK, Houcks MH (1984) Real time reservoir operations by goal programming. *J Water Resour Plan Manag ASCE* 110(3):297–307
- Carlson RW (1975) *Manual for the use of strain meters and other instruments for embedment in concrete structures, 4th edn*. Carlson Instruments, California
- Choquet P, Dupuis M, Dadoun F, Klebba JM (1998) Integrated automatic data acquisition systems for dam monitoring. In: *ICOLD proceedings of the 66th annual meeting*. ICOLD, New Delhi
- Colesanti C, Ferretti A, Novali F, Prati C, Rocca F (2003) SAR monitoring of progressive and seasonal ground deformation using the permanent scatterers technique. *IEEE Trans Geosci Remote Sens* 41(7):1685–1701
- Combelles J (1991) Ageing of dams and remedial measures, general report Q.65. In: *Proceedings of 17th ICOLD congress*. ICOLD, Vienna
- Cox CW (2007) Dam emergency response suggestions for a dam safety engineer's toolkit and checklist. In: *Annual conference from the ASDSO*. Association of State Dam Safety Officials, Boston
- Daniels DJ (2004) *Ground penetrating radar, 2nd edn*. The Institute of Electrical Engineers, London
- Daniels JJ, Grumman D, Vendl M (1997) Vertical incident three dimensional GPR. *J Environ Eng Geophys* 2(2):1–9
- Dolen TP (2005) *Materials properties model for aging concrete*. Bureau of Reclamation Dam Safety Program Report No. DSO-05-05. USBR, Colorado
- Dolen TP (2006) Long-term performance of roller compacted concrete at Upper Stillwater Dam, Utah, USA. In: Berga and Buil (eds) *Roller compacted concrete dams, Proceedings of the 4th international symposium on roller compacted concrete dams*. Taylor and Francis, London, pp 1117–1126
- Dunnicliff J (1988) *Geotechnical instrumentation for monitoring field performance*. Wiley, New York
- Dunnicliff J (1990) Twenty-five steps to successful performance monitoring of dams. *Hydro Rev* 9 (4):48–62
- Durcheva VN, Puchkova SM (1995) Main causes, signs, and consequences of aging of concrete dams. *Hydrotech Constr* 29(2):9–10
- Duscha LA, Jansen RB (1988) Surveillance. In: Jansen RB (ed) *Advanced dam engineering, for design, construction, and rehabilitation*. Van Nostrand Reinhold, New York, pp 777–797

- Edwards LS (1977) A modified pseudosection for resistivity and induced-polarization. *Geophysics* 42(5):1020–1036
- Electric Power Industry Ministry of the People's Republic of China (1998) GB 17621–1998 specification of reservoir operation for large & medium-scale hydropower stations. China Electric Power Press, Beijing (in Chinese)
- Eschenbach EA, Magee T, Zagona E, Goranflo M, Shane R (1999) Goal programming decision support system for multi objective operation of reservoir system. *J Water Resour Plan Manag ASCE* 127(2):108–120
- Featherstone WE, Dentith MC, Kirby JF (1998) Strategies for the accurate determination of orthometric heights from GPS. *Surv Rev* 34(267):278–296
- Fry JJ (1997) Internal erosion and surveillance. In: ICOLD 19th congress, vol V. ICOLD, Florence, pp 255–268
- Glass GK, Buenfeld NR (2000) The influence of chloride binding on the chloride induced corrosion risk in reinforced concrete. *Corros Sci* 42(2):329–344
- Goodman D (1994) Ground-penetrating radar simulation in engineering and archaeology. *Geophysics* 59(2):224–232
- Gu CS, Wu ZR (2006) Safety monitoring of dams and dam foundations: theories and methods and their application. Hohai University Press, Nanjing (in Chinese)
- Guo H (2000) Theory and application of earth observation with radar. Science Press, Beijing (in Chinese)
- Hanna TH (1985) Field instrumentation in geotechnical engineering. Trans Tech Publications, Clausthal-Zellerfeld
- Hanssen RF (2001) Radar interferometry data interpretation and error analysis. Kluwer Academic Publishers, Dordrecht
- Hjeldnes EI, Lavania VK (1980) Cracking, leakage and erosion of earth dam materials. *J Geotech Eng Div ASCE* 106(GT2):117–135
- Huang S, Yin H, Jiang Z (2004) Deformation monitoring data processing. Wuhan University Press, Wuhan
- Hussain RR, Ishida T (2010) Influence of connectivity of concrete pores and associated diffusion of oxygen on corrosion of steel under high humidity. *Constr Build Mater* 24(6):1014–1019
- ICOLD (1983) Deterioration of dams and reservoirs—examples and their analysis. ICOLD, Paris
- ICOLD (1987) Dam safety guidelines (Bulletin 59). ICOLD, Paris
- ICOLD (1988a) Dam monitoring—general considerations (Bulletin 60). ICOLD, Paris
- ICOLD (1988b) Monitoring of dams and their foundations—state of the art (Bulletin 68). ICOLD, Paris
- ICOLD (1989) Monitoring of dams and their foundations—state of the art (Bulletin 68). ICOLD, Paris
- ICOLD (1991a) Watertight geomembranes for dams—state of the art (Bulletin 78). ICOLD, Paris
- ICOLD (1991b) Alkali-aggregate reaction in concrete dams—review and recommendations (Bulletin 79). ICOLD, Paris
- ICOLD (1994) Ageing of dams and appurtenant works (Bulletin No. 93). ICOLD, Paris
- ICOLD (1995) Dam failures: statistical analysis (Bulletin No. 99). ICOLD, Paris
- ICOLD (2000a) Rehabilitation of dams and appurtenant works—state of the art and case histories (Bulletin 119). ICOLD, Paris
- ICOLD (2000b) Automated dam monitoring systems—guidelines and case histories (Bulletin 118). ICOLD, Paris
- ICOLD (2010) Geomembrane sealings systems for dams (Bulletin 135). ICOLD, Paris
- ICOLD (2014) Dam surveillance guide (Bulletin 158). ICOLD, Paris
- Iida R, Hoko K, Matsumoto N (1979) Safety monitoring of dams during first filling of reservoirs. In: Proceedings of international congress on large dams. ICOLD, New Delhi, pp 385–405
- Jansen RB (1988) Advanced dam engineering for design, construction, and rehabilitation. Van Nostrand Reinhold, New York
- Johansson S, Dahlin T (1996) Seepage monitoring in an earth embankment dam by repeated resistivity measurements. *Eur J Eng Geophys* 1(3):229–247

- Kampes BM (2006) Radar interferometry persistent scatterer technique. Springer, Dordrecht
- Keller GV, Frischknecht FC (1966) Electrical methods in geophysical prospecting. Pergamon Press, Oxford
- Li ZH, Liu ZZ, Wang ZM (1996) Study on monitoring dam deformation with GPS positioning. *J Wuhan Univ Hydraul Electr Eng* 29(6):26–29 (in Chinese)
- Li Z, Li F, Zdunek A, Landis E, Shah SP (1998) Application of acoustic emission technique to detection of reinforcing steel corrosion in concrete. *ACI Mat J* 95(1):68–81
- Lin QX, Liu YM, Tham LG, Tang CA, Lee PKK, Wang J (2009) Time-dependent strength degradation of granite. *Int J Rock Mech Min Sci* 46(7):1103–1114
- Lo KY, Kaniaru K (1990) Hydraulic fracture in earth and rock-fill dams. *Can Geotech J* 27(4):496–506
- Luo JQ, Luo JH (1995) Ageing diseases and mitigation of hydraulic concrete structures. China Agricultural Sciencetech Press, Beijing (China)
- Luzi G, Crossetto M, Monserrat O (2010) Advanced techniques for dam monitoring. Dam maintenance and rehabilitation II: Proceedings of the 2nd international congress on dam maintenance and rehabilitation. CRC Press/Balkema, Zaragoza/Leiden, pp 23–25
- Malakhanov VV (1990) Technical diagnosis of earth dams. Energoatomizdat, Moscow
- Manning DG (1996) Corrosion performance of epoxy-coated reinforcing steel: North American experience. *Constr Build Mater* 10(5):349–365
- McDowell PW, Barker RD, Butcher AP, Culshaw MG, Jackson PD, McCann DM, Skipp BO, Matthews SL, Arthur JCR (2002) Geophysics in engineering investigations. Ciria, London
- McLean FG, Pierce JP (1988) Comparison of joint shear strengths of conventional and roller compacted concrete. In: Hansen K, McLean F (eds) Roller compacted concrete II, Proceedings of the 2nd conference on RCC Dams. ASCE, New York, pp 151–169
- Mehta PK, Monteiro PJM (2006) Concrete: microstructure, properties, and materials, 3rd edn. McGraw-Hill, New York
- Merkler GP, Blinde A, Armbruster H, Döscher HD (1985) Field investigations for the assessment of permeability and identification of leakage in dams and dam foundations. In: Proceedings of ICOLD 15th congress, Q58, R7. ICOLD, Lausanne
- Ministry of Water Resources of the People's Republic of China (1994) SL60-94 «Technical criterion on Earth-Rockfill Dam safety monitoring». China WaterPower Press, Beijing (in Chinese)
- Morrison R (1984) Instrumentation fundamentals and applications. Wiley, New York
- National Reform and Development Commission of the People's Republic of China. DL/T5211-2005 «Technical specification for dam safety monitoring automation». China Electric Power Press, Beijing (in Chinese)
- Neville A (2004) The confused world of sulfate attack on concrete. *Cem Concr Res* 34(8):1275–1296
- Pacheco-Torgal F, Castro-Gomes J, Jalali S (2008) Alkali-activated binders: a review. Part 1. Historical background, terminology, reaction mechanisms and hydration products. *Constr Build Mater* 22(7):1305–1314
- Peck RB (1969) Advantages and limitations of the observational method in applied soil mechanics (ninth rankine lecture). *Geotechnique* 19(2):171–187
- Pour-Ghaz M, Isgor OB, Ghods P (2009) The effect of temperature on the corrosion of steel in concrete. Part 2: Model verification and parametric study. *Corros Sci* 51(2):426–433
- Prassianakis IN, Grum J (2011) Special issue: non-destructive testing and preventive technology. *Int J Mater Prod Technol* 41(1–4):1–4
- Raphael JM, Carlson RW (1965) Measurement of structural action in dams, 3rd edn. James J Gillick, California (USA)
- Roy STR, Morrison JA (2000) Experience with alkali-aggregate reaction in the Canadian Prairie Region. *Can J Civ Eng* 27(2):261–276
- Saraswathy V, Song HW (2007) Improving the durability of concrete by using inhibitors. *Build Environ* 42(1):464–472
- Seippel RG (1983) Transducers, sensors, and detectors. Reston Publishing Company, Reston

- Shang HS, Song YP (2006) Experimental study of strength and deformation of plain concrete under biaxial compression after freezing and thawing cycles. *Cem Concr Res* 36(10):1857–1864
- Sheingold DH (ed) (1980) *Transducer interfacing handbook*. Analog Devices, Norwood
- Sinniger R et al (1991) ageing of dams—Swiss experience. In: *Proceedings of 17th ICOLD congress*, Q.65-R.10. ICOLD, Vienna
- SÖylev TA, Richardson MG (2008) Corrosion inhibitors for steel in concrete: state-of-the-art report. *Constr Build Mater* 22(4):609–622
- Stanton TE (1942) Expansion of concrete through reaction between cement and aggregates. *Trans ASCE* 107(1):54–84
- State Economy & Trade Commission of the People's Republic of China (2003) DL/T5178-2003 «Technical specification for concrete dam safety monitoring». China Electric Power Press, Beijing (in Chinese)
- Tsulukidze PP (1962) Investigation of old concrete of hydraulic structures. Tbilisi, Moscow
- Unal M, Unver B (2004) Characterization of rock joint surface degradation under shear loads. *Int J Rock Mech Min Sci* 41(Supplement 1):145–150
- Unguendoli M (1984) Errors in precise levelling. In: Unguendoli M (ed) *High precision geodetic measurements*. CUSL, Bologna, pp 5–25
- Villalba E, Atrens A (2008) Metallurgical aspects of rock bolt stress corrosion cracking. *Mater Sci Eng* 49(1):8–18
- Wang C, Zhang H, Shan X, Ma J, Liu Z, Chen SZ, Lu GN, Tang YX, Guo ZQ (2004) Applying SAR interferometry for ground deformation detection in China. *Photogramm Eng Remote Sens* 70(10):1157–1166
- Williams DC (ed) (1993) *Optical methods in engineering metrology*. Chapman & Hall, Dordrecht
- Windsor JS (1973) Optimization model for the operation of flood control systems. *Water Resour Res* 9(5):1219–1225
- Wu ZR (2003) *Safety monitoring theory and its application of hydraulic structures*. Higher Education Press, Beijing (in Chinese)
- Wu ZR, Gu CS (1997) *Dam safety comprehensive appraisal expert system*. Beijing Science & Technology Press, Beijing (in Chinese)
- Xiao BX (2000) *Progress in engineering geophysics*. Wuhan University of Hydraulic and Electric Engineering Press, Wuhan (in Chinese)
- Yang GB (2007) *Life cycle reliability engineering*. Wiley, New Jersey
- Yoon YS, Won JP, Woo SK, Song YC (2002) Enhanced durability performance of fly ash concrete for concrete-faced rockfill dam application. *Cem Concr Res* 32(1):23–30
- Yoon IS, Copuroglu O, Park KB (2007) Effect of global climatic change on carbonation progress of concrete. *Atmos Environ* 41(34):7274–7285
- Zuo DQ, Gu ZX, Wang WX (eds) (1987) *Barrages, spillways and control works*. In: *Handbook of hydraulic structure design (vol 6)*. Water Resources and Electric Power Press of China, Beijing (in Chinese)